Infrared Spectra of Bis(L-serinato)nickel(II) Dihydrate by Using Metal Isotope Technique[1)]

Junichi ODO,[a] Masaki MIFUNE,[a] Akimasa IWADO,[a] Yutaka SAITO,*[,a] Yoshimasa TANAKA,[a,2)] Noriko MOTOHASHI,[b] and Katsunosuke MACHIDA[c]

Faculty of Pharmaceutical Sciences, Okayama University,[a] 1–1–1, Tsushima-naka, Okayama 700, Japan, Kobe Women's College of Pharmacy,[b] 4–19–1, Motoyamakita-machi, Higashinada-ku, Kobe 658, Japan and Faculty of Pharmaceutical Sciences, Kyoto University,[c] Sakyo-ku, Kyoto 606, Japan.
Received August 2, 1990

The infrared spectra of bis(L-serinato)nickel(II) dihydrate ($Ni(L\text{-}ser)_2 \cdot 2H_2O$) and their isotopic complexes containing ^{58}Ni, ^{62}Ni and deuterium have been measured in the region between 4000 and 200 cm^{-1}. The shifts caused by nickel and hydrogen isotopic substitutions indicate that three bands at 342, 297 and 222 cm^{-1} are Ni-ligand stretching vibrations complicatedly coupled with Ni–O and Ni–N stretching vibrations. The conformational differences between *gauche–anti* and *anti–gauche* serinates in metallo-serinate complexes are characterized by the COO deformation vibrations. A normal coordinate analysis on the basis of a complete molecular conformation of $Ni(L\text{-}ser)_2 \cdot 2H_2O$ and an intermolecular force field reproduced well the observed frequencies and isotope shifts. In addition, the calculated result is consistent with both the empirical assignments and the observed frequency differences caused from the conformational differences.

Keywords infrared spectra; bis(L-serinato)nickel(II) dihydrate; ^{58}Ni–^{62}Ni substitution; deuteration; L-serine; normal coordinate analysis; intermolecular force; intramolecular force; conformational difference

Since the biological activity *in vivo* of metallo-proteins and -enzymes is known to be associated with the conformation changes around active sites, the relationship between the activity and conformation change are of much interest.[3)] Metallo-amino acid complexes as models of metallo-proteins and -enzymes are suitable subjects for investigating the correlation between vibrational spectra and the conformation of amino acids. Previously, we analyzed the infrared (IR) spectra of bis(L-serinato)copper(II) and -zinc(II) and revealed that the conformational difference between *gauche–gauche* and *anti–gauche* serinates (Fig. 1) was particularly reflected in the COO deformation and the skeletal stretching vibrations.[4)]

In the present work, the IR spectra of bis(L-serinato)-nickel(II) dihydrate were investigated in order to clarify the spectral differences of *gauche–anti* serinates from *gauche–gauche* and *anti–gauche* serinates in metallo-serinate complexes (Fig. 1). The vibrational spectra have been assigned on the basis of the frequency shifts on metal-isotope substitution and *N,O*-deuteration. In order to confirm the assignments, normal coordinate analysis was carried out by using a complete molecular conformation and inter- and intramolecular force fields.

Experimental

Materials L-Serine (Ishizu Seiyaku Ltd., Japan) was purified by recrystallization from a mixture of water and ethanol. *N,O*-Deuterated L-serine was obtained from purified L-serine by an exchange reaction with heavy water (CEA, France, min. 99.85%). Bis(L-Serinato)nickel(II) dihydrate, $Ni(L\text{-}ser)_2 \cdot 2H_2O$, was prepared from purified L-serine and $NiCl_2 \cdot 6H_2O$ according to the method of van der Helm *et al.*[5)] For preparation of the *N,O*-deuterated complex, $Ni(L\text{-}ser\text{-}d_3)_2 \cdot 2D_2O$, $Ni(L\text{-}ser)_2 \cdot 2H_2O$ was recrystallized more than three times from a mixture of heavy water and ethanol-d_1. The crystal obtained was filtered, washed with a mixture of heavy water and ethanol-d_1 and dried over phosphorous pentoxide under reduced pressure. For preparation of the complexes containing metal isotopes, ^{58}Ni and ^{62}Ni (Oak Ridge National Lab., U.S.A.) were converted into their corresponding nickel chlorides by reaction with dilute hydrochloric acid on a milligram scale. $^{58}Ni(L\text{-}ser)_2 \cdot 2H_2O$ and $^{62}Ni(L\text{-}ser)_2 \cdot 2H_2O$ and their *N,O*-deuterated analogues were prepared from the corresponding nickel chloride in a similar method. The IR spectrum of each complex containing a metal isotope coincided with that of the complex containing the metal of natural abundance, except for the metal isotope shifts. The isotopic purities were 96.64% for ^{58}Ni and 99.76% for ^{62}Ni.

Measurements The IR spectra were recorded on a JASCO DS-403G IR spectrophotometer (4000—200 cm^{-1}). The measurements were made for the solid samples in Nujol and hexachlorobutadiene (Merck, AG., Uvasol) mulls. The frequencies were calibrated by the standard absorptions of polystyrene, indene and water vapor. For measuring small shifts of band centers on ^{58}Ni and $^{62}Ni(^{58}Ni\text{–}^{62}Ni)$ substitution, the frequency scale was expanded ten times over the desired frequency region. The measurements were repeated at least three times to check the reproducibility of the spectra. The IR spectra in the region above 400 cm^{-1} are shown in Fig. 2, and parts of the expanded spectra in Fig. 3.

Normal Coordinate Analysis

The X-ray analysis by van der Helm *et al.*[5)] shows that $Ni(L\text{-}ser)_2 \cdot 2H_2O$ takes a monomeric structure in which the Ni atom is on a 2-fold axis of symmetry. The normal vibrations of $Ni(L\text{-}ser)_2 \cdot 2H_2O$ are, therefore, classified into A and B. These IR and Raman active normal vibrations

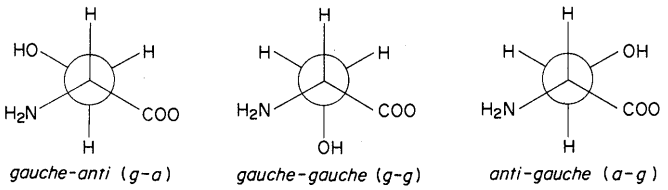

Fig. 1. Conformations of L-Serinate in $Me(L\text{-}ser)_2 \cdot nH_2O$ ($n=0$ or 2)

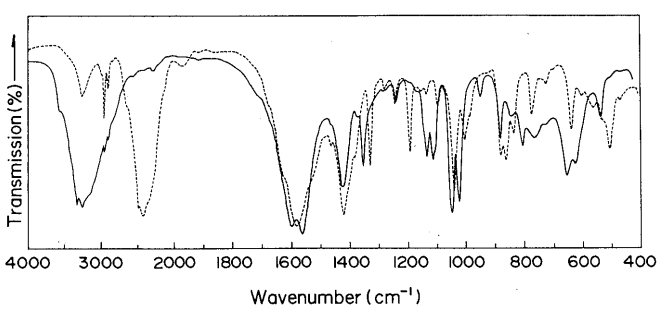

Fig. 2. IR Spectra of $Ni(L\text{-}ser)_2 \cdot 2H_2O$ and Its *N,O*-Deuterated Analogues in the Region between 4000 and 400 cm^{-1}

$Ni(L\text{-}Ser)_2 \cdot 2H_2O$ (—) and $Ni(L\text{-}ser\text{-}d_3)_2 \cdot 2D_2O$ (– – –).

TABLE I. Modified Urey–Bradley Type and Valence Type Force Constants

Modified Urey–Bradley type force constants[a] (mdyn/Å)									
K(C–O)	7.00	H(OC'O)	0.06	H(NiNC)	0.05	F(OC'O)	4.00	F(NiNC)	0.10
K(C–C')	2.13	H(OC'C)	0.35	H(OC''C)	0.45	F(OC'C)	0.70	F(OC''C)	0.761
K(C–H)	4.20	H(C'CN)	0.65	H(HC''H)	0.422	F(C'CN)	0.60	F(HC''H)	0.076
K(C–N)	2.67	H(C'CC'')	0.25	H(OC''H)	0.119	F(C'CC'')	0.30	F(OC''H)	0.637
K(N–H)	5.20	H(C''CN)	0.22	H(C''OH)	0.25	F(C''CN)	0.60	F(C''OH)	0.588
K(C–C'')	2.12	H(C'CH)	0.16	H(NiOC')	0.05	F(C'CH)	0.36	F(NiOC')	0.10
K(C''–O)	2.675	H(NCH)	0.25	H(NiO$_w$H)	0.15[d]	F(NCH)	0.54	F(NiO$_w$H)	0.11[d]
K(C''–H)	4.09	H(C''CH)	0.16	H(HO$_w$H)	0.60[d]	F(C''CH)	0.40	F(HO$_w$H)	0.10
K(O–H)	6.00	H(CNH)	0.34	H(ONiN)[b]	0.05	F(CNH)	0.50	F(ONiN)[b]	0.20[d]
K(O$_w$–H)	5.64	H(HNH)	0.50	H(ONiN)	0.05	F(HNH)	0.02	F(ONiN)	0.05
K(Ni–O)	0.80[d]	H(C'C''H)	0.245	H(O'NiN)	0.05	F(C'C''H)	0.502	F(O'NiN)	0.05
K(Ni–N)	1.00[d]	H(NiNH)	0.10			F(NiNH)	0.05		
K(Ni–O')	0.50[d]	κ(C')[c]	0.0	κ(C'')[c]	0.0	κ(N)[c]	−0.05		
Valence type force constants (mdyn·Å/rad^2)									
$f(\omega CO_2, \omega CO_2)$	1.50[d]	$f(\tau CC', \tau CC')$		0.05	$f(\tau H_2O, \tau H_2O)$	0.05[d]	$f(\tau CC'', \tau CC'')$		0.05
$f(\tau OH, \tau OH)$	0.004	$f(\omega H_2O, \omega H_2O)$		0.05[d]	$f(\tau CN, \tau CN)$	0.10			

a) C, C', C'' and O$_w$ denote the methine, carboxylate, methylene carbon and water oxygen atoms, respectively. b) Force constants concerned in the chelate ring. c) mdyn·Å. d) Refined value.

were calculated by using the same program as reported in the previous paper.[4] By assuming the bond-lengths $r_{CH}=1.08$, $r_{NH}=1.02$ and $r_{OH}=1.00$ Å, the structure parameters were constructed on the basis of the X-ray analysis of van der Helm *et al.*[5] A modified Urey-Bradley force field was used with a few valence-type constants for the torsional and out-of-plane bending coordinates. The force constants were initially transferred from those for Zn(L-ser)$_2$[4] and the water molecule.[6] To improve the frequency fit, $f(\omega CO_2, \omega CO_2)$ and some force constants concerned with the Ni atom and water molecule were adjusted. The force constants used in the final calculation are listed in Table I.

By analogy with the previous treatments,[7-10] the intermolecular forces were taken into account, and the intermolecular potential was assumed to be the sum of the exp-6 type non-bonded atom–atom interaction terms, the Lippincott-type hydrogen bond stretching terms and Coulomb interaction terms. In calculating the Coulomb interaction terms, the atomic charges of Ni(L-ser)$_2\cdot 2H_2O$ were estimated by CNDO/II calculation in which the Ni atom of Ni(L-ser)$_2\cdot 2H_2O$ was replaced by an Mg atom. The calculated frequencies in the final calculation are shown in Table II, together with the observed frequencies.

As can be seen in Table II, the agreement between the calculated and observed frequencies was satisfactory, despite using a crude approximation of the same force constants used for Zn(L-ser)$_2$[4], except for $f(\omega CO_2, \omega CO_2)$.

Discussion

The Region above 450 cm^{-1} Absence of appreciable frequency shifts on ^{58}Ni–^{62}Ni substitution indicates that all the bands in this region should be assigned to the vibrations of L-serinates and water molecules. According to the X-ray analyses,[5,11,12] L-serinates in Ni(L-ser)$_2\cdot 2H_2O$ takes a *gauche–anti* (*g–a*) conformation, and Cu- and Zn(L-ser)$_2$ include *gauche–gauche* (*g–g*) and both *gauche–gauche* (*g–g*) and *anti–gauche* (*a–g*) serinates, respectively. By comparing the IR spectrum of Ni(L-ser)$_2\cdot 2H_2O$ with those of Cu- and Zn(L-ser)$_2$, the vibrations due to *g–a* serinate can be distinguished from those due to *g–g* and *a–g* serinates. The IR spectra of Ni(L-ser)$_2\cdot 2H_2O$ are essentially the same as those of Cu- and Zn(L-ser)$_2$, and the vibrational assignments of Cu- and Zn(L-ser)$_2$ are transferable to those

TABLE II. Observed and Calculated Frequencies and Assignments for Ni(L-ser)$_2\cdot 2H_2O$ and its *N,O*-Deuterated Analogues in the Region between 4000 and 450 cm^{-1}

Ni(L-ser)$_2\cdot 2H_2O$		Ni(L-ser-d_3)$_2\cdot 2D_2O$		Assignments[c]
Obs.[a]	Calc.[b]	Obs.[a]	Calc.[b]	
3330 vs	3396	2490 sh	2465	νOH(OD)
3265 vs	3307	2440 vs	2421	ν_aH$_2$O(D$_2$O)
	3285	2415 vs	2367	ν_sH$_2$O(D$_2$O)
3160 sh	3184		2346	ν_aNH$_2$(ND$_2$)
	3128	2340 sh	2264	ν_sNH$_2$(ND$_2$)
2950 sh	2961	3050 m	2961	νCH
2905 sh	2947	3000 w	2948	ν_aCH$_2$
2890 sh	2920	2890 w	2920	ν_sCH$_2$
1595 vs	1612	1150 vw	1177	βH$_2$O(D$_2$O)
1595 vs	1608	1580 vs	1609	ν_aCO$_2$
1575 sh	1566	1131 vw	1156	βNH$_2$(ND$_2$)
1460 vw	1467	1464 vw	1466	βCH$_2$
1425 s	1420	1422 vs	1421	ν_sCO$_2$
1370 vw	1348	1328 s	1332	δ'CH
1354 s	1322	1275 w	1282	ωCH$_2$
1284 vw	1282	1000 m	1008	tNH$_2$(ND$_2$)
1270 vw	1246	945 vw	957	δOH(OD)
1236 w	1229	1242 w	1245	tCH$_2$
1164 vw	1197	860 s	867	ωNH$_2$(ND$_2$)
1132 m	1118	1190 s	1218	δCH
1110 m	1095	1094 w	1102	νskel
1047 s	1050	1038 s	1074	νskel
1021 s	1000	878 s	920	νskel
944 w	955	980 sh	999	νskel
876 m	860	834 m	832	ρCH$_2$
837 w	828	602 vw	606	ρH$_2$O(D$_2$O)
802 m	816	772 m	755	ωCO$_2$
760 w	758	506 m	490	ωH$_2$O(D$_2$O)
652 m	663	637 m	654	βCO$_2$
622 m	646	562 vw	582	ρNH$_2$(ND$_2$)
535 m	567	530 sh	550	ρCO$_2$
500 vw	517	468 vw	484	δskel
465 vw	437	430 vw	426	δskel

a) vs, very strong; s, strong; m, medium; w, weak; vw, very weak; sh, shoulder. b) Species A. c) ν, stretching; β, bending; δ, deformation; t, twisting; ω, wagging; ρ, rocking; skel, skeletal; s, symmetrical; a, asymmetrical.

of Ni(L-ser)$_2\cdot 2H_2O$. Thus, all the bands in this region can be assigned by referring to the frequency shifts on *N,O*-deuteration and the assignments for Cu- and Zn(L-ser)$_2$.[4] The assignments given are summarized in Table II.

As indicated in the previous work,[4] the COO deformation and the skeletal stretching vibrations were affected by the conformational difference between *a–g* and *g–g* serinates in Cu- and Zn(L-ser)$_2$. In the case of Ni(L-ser)$_2\cdot 2H_2O$, three bands at 802, 652 and 535 cm^{-1}, which show a small shift on *N,O*-deuteration, are assigned to the COO wagging, bending and rocking vibrations, respectively. These frequencies are midway between the corresponding frequencies of *a–g* and *g–g* serinates in Zn(L-ser)$_2$.[4] For example, the COO wagging frequency of *g–a* serinate is lower by 20 cm^{-1} than that of *g–g* serinate and higher by 38 cm^{-1} than that of *a–g* serinate. It should be noted that the frequency difference between *g–a* and *a–g* serinates amounts to 77 cm^{-1} for the COO bending band. From these results, it is apparent that the conformational differences of the serinates are reflected in three COO deformation frequencies. Four bands at 1110, 1047, 1021 and 944 cm^{-1} in Ni(L-ser)$_2\cdot 2H_2O$ are assigned to the skeletal stretching vibrations of the *g–a* serinate by referring to the calculated frequencies. Comparing *a–g* and *g–g* serinates in Zn(L-ser)$_2$,[4] the skeletal stretching frequencies of *g–a* serinates in Ni(L-ser)$_2\cdot 2H_2O$ are closer to those of the *g–g* serinate than those of the *a–g* serinate. The frequency differences observed between the corresponding bands of the serinate conforments studied in this work are summarized in Table III, together with the calculated differences. As a whole, the calculated frequency differences caused by the conformational difference reproduced well the trend of the observed frequencies. That is, large differences observed for the COO deformation, the skeletal stretching, the OH and the NH_2 deformation frequencies were all confirmed by calculation.

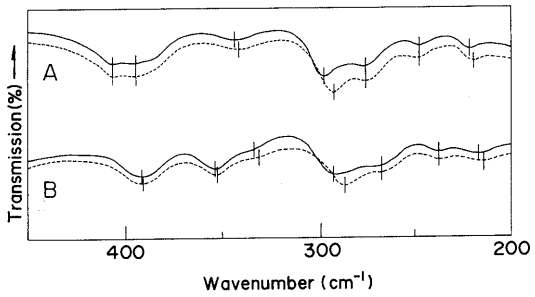

Fig. 3. IR Spectra of Ni(L-ser)$_2\cdot 2H_2O$ and Its *N,O*-Deuterated Analogues in the Region between 450 and 200 cm^{-1}

A, ^{58}Ni(L-ser)$_2\cdot 2H_2O$ (—) and ^{62}Ni(L-ser)$_2\cdot 2H_2O$ (– – –). B, ^{58}Ni(L-ser-d_3)$_2\cdot 2D_2O$ (—) and ^{62}Ni(L-ser-d_3)$_2\cdot 2D_2O$ (– – –).

The Region between 450 and 200 cm^{-1} According to X-ray analysis,[5] the coordination structure of Ni(L-ser)$_2\cdot 2H_2O$ is a distorted square-bipyramidal, comprising two amino nitrogen atoms and two carboxylic oxygen atoms with a *cis*-coordination, and two additional water molecules at apical positions. Since the central Ni atom occupies a symmetry site, C_2, in these environments, six metal-ligand stretching vibrations are all IR-active.

Three bands at 342, 297 and 222 cm^{-1} in this region show isotope shifts larger than 2 cm^{-1} on ^{58}Ni–^{62}Ni substitution, as shown in Fig. 3. The corresponding three bands of Ni(L-ser-d_3)$_2\cdot 2D_2O$ were observed at 330, 292 and 217 cm^{-1}. These bands can apparently be assigned to Ni-ligand stretching vibrations, including the displacement of the Ni atom. The shifts on *N,O*-deuteration by more than 5 cm^{-1} suggest that the Ni–OOC, the Ni–NH_2 and the Ni–OH_2 stretching vibrations couple complicatedly with one another. The calculated L matrices support this assignment. The remaining bands in this region are assigned to the skeletal deformation vibrations of serinate because

TABLE III. Observed and Calculated Frequency Differences Caused by the Conformations of Serinates in the Region between 1700 and 500 cm^{-1}

Me(L-ser)$_2\cdot nH_2O$				Me(L-ser-d_3)$_2\cdot nD_2O$				Bands[c]
$\Delta\nu_{g-g/g-a}$[a]		$\Delta\nu_{a-g/g-a}$[b]		$\Delta\nu_{g-g/g-a}$[a]		$\Delta\nu_{a-g/g-a}$[b]		
Obs.[d]	Calc.[d]	Obs.[d]	Calc.[d]	Obs.[d]	Calc.[d]	Obs.[d]	Calc.[d]	
−5	8	−37	−4	12	6	−22	−5	ν_aCO_2
−14	−8	−14	−5	−13	−9	−13	−5	ν_sCO_2
20	2	−38	−62	5	5	−10	−5	ωCO_2
−15	−1	76	82	−10	−14	77	72	βCO_2
−25	−41	21	−1	15	−3	19	0	ρCO_2
−40	−30	−45	−34	−14	−28	8	−9	$\beta NH_2(ND_2)$
35	35	67	54	48	29	48	53	$tNH_2(ND_2)$
−22	−49	−12	−41	2	5	−5	−11	$\omega NH_2(ND_2)$
32	27	32	8	−72	−103	−52	−56	$\rho NH_2(ND_2)$
−8	−2	12	23	−14	−1	8	24	βCH_2
−84	−48	−59	−28	38	14	22	5	ωCH_2
9	9	9	14	14	−3	33	15	tCH_2
−19	−8	12	18	−7	−37	10	−27	ρCH_2
−7	6	−19	−18	41	9	−4	−6	δ'CH
−12	−1	−34	−20	27	−19	−10	−31	δCH
−80	−53	−71	−30	−2	−8	2	0	δOH(OD)
−12	6	−58	−4	−4	−18	−4	−15	vskel
−8	−7	−24	−21	10	−16	−9	−55	vskel
−27	−5	−21	−3	69	43	116	67	vskel
−32	−23	50	24	−82	−96	−82	−116	vskel

a) Frequency differences = ν(*gauche–gauche*) − ν(*gauche–anti*). *b*) Frequency differences = ν(*anti–gauche*) − ν(*gauche–anti*). *c*) ν, stretching; δ, deformation; β, bending; ω, wagging; ρ rocking; t, twisting; skel, skeletal. *d*) Observed and calculated ν(*gauche–gauche*) and ν(*anti–gauche*) were taken from those for Zn(L-ser)$_2$.[3]

TABLE IV. Observed and Calculated Frequencies, Metal Isotope Shifts and Assignments for $Ni(L\text{-ser})_2 \cdot 2H_2O$ and Its *N,O*-Deuterated Analogues in the Region between 450 and 200 cm^{-1}

$Ni(L\text{-ser})_2 \cdot 2H_2O$						$Ni(L\text{-ser-}d_3)_2 \cdot 2D_2O$						
Obs.[a]	Calc.[b]		$\Delta\nu_m$[c]			Obs.[a]	Calc.[b]		$\Delta\nu_m$[c]			Assignments[d]
	A	B	Obs.	Calc.[b] A	Calc.[b] B		A	B	Obs.	Calc.[b] A	Calc.[b] B	
405 w	405	397	0	0.1	0.0	391 w	376	370	0.5	0.1	0.1	δskel
395 w	365	372	0	0.0	0.8	353 w	315	279	1.0	0.0	0.6	δskel
342 vw		310	2.0		2.0	330 sh		337	*ca.* 2		1.8	νNi-ligand
297 w	295		5.0	2.2		292 w	288		6.0	2.0		νNi-ligand
275 sh	273	285	0	0.0	0.2	267 sh	250	268	0	0.0	0.6	δskel
247 vw	264	269	0	0.0	0.4	237 vw	238	230	0	0.2	0.9	δskel
222 vw		256	2.0		3.0	217 vw		257	2.0		3.0	νNi-ligand

a) w, weak; vw, very weak; sh, shoulder. *b*) A, species A; B, species B. *c*) Shifts of band center on ^{58}Ni–^{62}Ni substitution. *d*) ν, stretching; δ, deformation; skel, skeletal.

of lack of any appreciable shifts on ^{58}Ni–^{62}Ni substitution. The assignments discussed above are summarized in Table IV, together with calculated frequencies and isotope shifts.

As shown in Table IV, the calculated frequencies and metal isotope shifts on ^{58}Ni–^{62}Ni substitution reproduced well the observed trend. The Ni-ligand stretching bands were observed in almost the same region as the Zn-ligand stretching bands of $Zn(L\text{-ser})_2$.[4] In order to reproduce the observed frequencies, however, the force constants for the Ni-ligand stretching modes should be more than twice as large as those for the Zn-ligand stretching modes. This result indicates that the Ni-ligand binding forces were much larger than the Zn-ligand bonds, in spite of the similarity of the corresponding frequencies. The calculated L matrices for $Zn(L\text{-ser})_2$[4] and $Ni(L\text{-ser})_2 \cdot 2H_2O$ indicate that the metal-ligand stretching vibrations of $Ni(L\text{-ser})_2 \cdot 2H_2O$ couple far more strongly with the metal-ligand deformation vibrations than the metal-ligand stretching vibrations of $Zn(L\text{-ser})_2$. The effect of the different degrees of vibrational coupling seems to cancel the effect of the difference of the force constant, which may be caused from the point that $Ni(L\text{-ser})_2 \cdot 2H_2O$ takes a six-coordinated square-bipyramidal structure, while $Zn(L\text{-ser})_2$ takes a five-coordinated square-pyramidal structure.

In conclusion, the conformational difference of serinate sensitively affects the frequencies of the COO deformation vibrations, which are easily distinguished from other vibrations in general.

Acknowledgments The calculations were carried out using an ACOS 1000 computer of the Okayama University Computer Center. This work was supported by a Grant-in-Aid for Scientific Research from the Ministry of Education, Science and Culture, Japan.

References and Notes

1) A part of this work was presented at the Symposium on Molecular Structure, Sendai, 1983.
2) Present address: *Department of Biochemistry, College of Sciences, Okayama University of Sciences, Ridai-cho, Okayama 700, Japan.*
3) J. F. Chlebowski and J. E. Coleman, "Metal Ions in Biological Systems," Vo. 6, ed. by H. Sigel, Marcel Dekker, Inc., New York, 1976, pp. 1—140.
4) J. Odo, M. Nishio, Y. Saito, Y. Tanaka, and K. Machida, *Chem. Pharm. Bull.*, **31**, 3802 (1983).
5) D. van der Helm and M. B. Hossain, *Acta Cryst.*, **B25**, 457 (1969).
6) Y. Kyogoku, *Nippon Kagaku Zasshi*, **81**, 1648 (1960).
7) K. Machida, A. Kagayama, Y. Saito, and Y. Kuroda, *Spectrochim. Acta*, **33A**, 569 (1977).
8) K. Machida, A. Kagayama, Y. Saito, and T. Uno, *Spectrochim. Acta*, **34A**, 909 (1978).
9) K. Machida, A. Kagayama, and Y. Saito, *J. Raman Spectrosc.*, **7**, 188 (1978).
10) K. Machida, A. Kagayama, and Y. Saito, *J. Raman Spectrosc.*, **8**, 133 (1978).
11) D. van der Helm and W. A. Franks, *Acta Cryst.*, **B25**, 451 (1969).
12) D. van der Helm, A. F. Nicholas, and C. G. Fisher, *Acta Cryst.*, **B26**, 1172 (1970).

Metal Isotope Effects on the Vibrational Spectra of [Bis(glycylglycinato)calcium Chloride]$_n$[1)]

Junichi ODO,*[,a] Marumi ARIMA,[a] Masaki MIFUNE,[a] Akimasa IWADO,[a] Noriko MOTOHASHI,[b] Yoshimasa TANAKA[a,2)] and Yutaka SAITO[a]

Faculty of Pharmaceutical Sciences, Okayama University,[a] 1–1, 1-chome, Tsushima-naka, Okayama 700, Japan and Kobe Women's College of Pharmacy,[b] 4–19–1, Motoyamakita-machi, Higashinada-ku, Kobe 658, Japan. *Received August 29, 1990*

The infrared and Raman spectra of [bis(glycylglycinato)calcium chloride]$_n$ and its isotopic complexes containing metal and hydrogen isotopes have been measured. A large isotope shift of more than 4 cm^{-1} on ^{40}Ca and ^{44}Ca substitution has been observed in the infrared-active bands at 345, 267 and 242 cm^{-1}. These bands have been assigned to Ca–O antisymmetric stretching vibrations. The Raman-active bands at 305, 158 and 111 cm^{-1} have been assigned to Ca–O symmetric stretching vibrations with no displacement of the calcium atom. The result of a normal coordinate analysis is consistent with both the empirical assignments and the experimental isotope shifts. These results indicate that Ca-ligand bond forces are almost similar to those of copper– and zinc–amino acid complexes.

Keywords infrared spectra; Raman spectra; metal isotope effect; [bis(glycylglycinato)calcium chloride]$_n$; normal coordinate analysis; ^{40}Ca–^{44}Ca substitution; amino acid; deuteration; glycylglycine, calcium complex

Calcium-binding proteins, such as calmodulin, troponin and parvalbumin, are of much interest because of their biological properties,[3–5)] and a relationship between their biological activities *in vivo* and a coordination structure of the calcium atom has been investigated by various methods.[6–8)] Calcium–amino acid complexes are suitable substances, as models of calcium–binding proteins, for investigating the coordination structure around the calcium atom. Although vibrational spectroscopy provides information about coordination of metal complexes, infrared (IR) and Raman spectra of calcium complexes have been investigated in less detail than X-ray analyses and nuclear magnetic resonance (NMR) spectra.[9–12)] It seems, however, rather difficult to analyze the vibrational spectra of calcium complexes, since they frequently have a complicated polymeric structure. Previously, it has been shown for complicated polymeric copper– and zinc–complexes that the metal isotope technique is very useful for assigning the vibrations involving displacement of the metal atom.[13–15)]

In the present work, the infrared and Raman spectra of a complicated polymeric [bis(glycylglycinato)calcium chloride]$_n$ (Ca-GG) were investigated by the metal isotope technique (^{40}Ca and ^{44}Ca substitution) in order to study the metal-ligand stretching vibrations. The metal isotope shifts observed indicate that the frequencies of the Ca-ligand stretching frequencies are relatively higher than those of the six-coordinated Ca–amino acid complexes. These frequencies are in almost the same region as those for the copper– and zinc–amino acid complexes, although the Ca-ligand bond-lengths of Ca-GG are longer than those of the copper– and zinc–amino acid complexes.

Experimental

Materials Commercially available glycylglycine (GG) was purified several times by recrystallization from a mixture of water and ethanol. *N,N'*-Deuterated glycylglycine (GG-d_4) was obtained from the purified GG by the usual exchange reaction with heavy water (Merck, AG., 99.8%). [Bis(glycylglycinato)calcium chloride]$_n$ was prepared from the purified GG and $CaCl_2 \cdot 2H_2O$ according to the method of Meulemans *et al.*[16)] For the preparation of the *N,N'*-deuterated complex (Ca-GG-d_8), $CaCl_2 \cdot 2D_2O$ was reacted with GG-d_4 in heavy water. The complex was precipitated by the addition of ethanol-d_1, filtered, washed with a mixture of heavy water and ethanol-d_1 and dried on phosphorous pentoxide under reduced pressure. For the preparation of the complexes containing ^{40}Ca and ^{44}Ca, $^{40}CaCO_3$ and $^{44}CaCO_3$ (Oak Ridge National Lab., U.S.A.) were converted into the corresponding calcium chloride dihydrate by

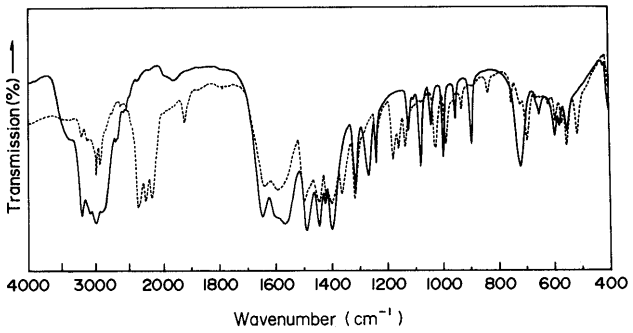

Fig. 1. IR Spectra of Ca-GG in the Region between 4000 and 400 cm^{-1}
Ca-GG (—) and Ca-GG-d_8 (– – –).

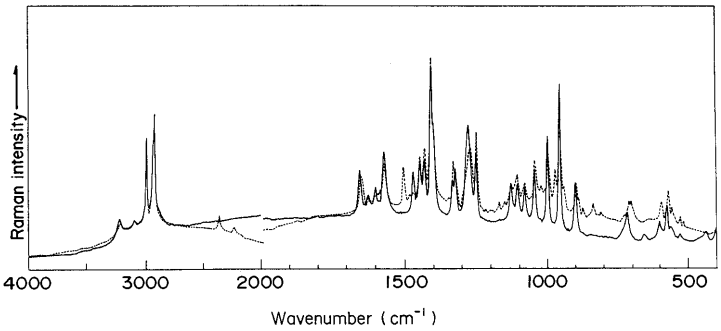

Fig. 2. Raman Spectra of Ca-GG in the Region between 4000 and 400 cm^{-1}
Ca-GG (—) and Ca-GG-d_8 (– – –).

reaction with dilute hydrochloric acid on a milligram scale. ^{40}Ca-GG and ^{44}Ca-GG were prepared from the corresponding calcium chloride dihydrate in a similar way. The infrared and Raman spectra of each complex containing a metal isotope coincided with that of the complex containing the metal of natural abundance except for the metal isotope shifts. The isotopic purities were more than 98% for $^{40}CaCO_3$ and $^{44}CaCO_3$.

Measurements The IR spectra were recorded on a JASCO DS-403G IR spectrophotometer (4000—200 cm^{-1}). Measurements of the solid samples were made in Nujol and hexachlorobutadiene (Merck, AG., Uvasol) mulls. The frequencies were calibrated by use of the standard absorptions of polystyrene, indene and water vapor. For measuring small shifts of band centers on ^{40}Ca and ^{44}Ca (^{40}Ca–^{44}Ca) substitution, the frequency scale was expanded ten times over the desired frequency region. The measurements were repeated at least three times to check the reproducibility of the frequencies. The IR spectra of Ca-GG and its *N,N'*-deuterated analog in the region above 400 cm^{-1} are shown in Fig. 1, and parts of the expanded spectra in the region between 420 and 200 cm^{-1} are shown in Fig. 3.

The Raman spectra were recorded for the solid samples in a glass capillary tube by using a JASCO NR-1000 Raman spectrophotometer and an NEC 3300 Ar^+ ion laser (514.5 nm). The frequencies were calibrated by use of the standard bands of indene. The Raman spectra of Ca-GG and its *N,N'*-deuterated analog in the region above 400 cm^{-1} and parts of the expanded spectra in the region between 450 and 50 cm^{-1} are shown in Figs. 2 and 4, respectively.

Normal Coordinate Analysis

According to X-ray analysis,[16] Ca-GG takes a complicated polymeric structure chained by the bonds between the calcium atom and carbonylic and carboxylic oxygens of the neighboring glycylglycinates. Since the complex belongs to the C_i point group, the normal vibrations of the complex are classified into Raman-active A_g and IR-active A_u species. The optical active normal frequencies of Ca-GG were calculated by using the same computer program as reported in the previous paper.[17] By assuming the bond-lengths, $r_{CH}=1.08$ and $r_{NH}=1.02$ Å, structure parameters were constructed on the basis of the X-ray data reported by Meulemans *et al.*[16] The calculation was carried out for a full chain molecule, neglecting the chloride atoms. A modified Urey–Bradley force field was used with a few valence-type force constants for the torsional and out-of-plane bending coordinates. The force constants for glycylglycinates were initially transferred from DL-serine,[18] and those concerning the calcium atom were transferred from Cu(DL-serinate)$_2$ reported by Inomata *et al.*[19] In this calculation, only the intramolecular forces were taken into account. The force constants used in the final calculation are listed in Table I.

The calculated frequencies in the final calculation are shown in Table II, together with the observed frequencies and the approximate intensities.

Vibrational Assignments and Discussion

The Region above 400 cm^{-1} All the bands of Ca-GG and Ca-GG-d_8 in this region showed no appreciable shift on ^{40}Ca–^{44}Ca substitution, and are accordingly assigned to the vibrations involving no displacement of the calcium atom. By referring to the frequency shifts on *N,N'*-deuteration and the assignments for GG by previous authors,[20,21] the bands in this region were assigned to the vibrations of glycylglycinates. As shown in Table II, the agreement of the calculated and the observed frequencies was satisfactory for the A_g and A_u species.

The Region below 400 cm^{-1} According to X-ray analysis,[16] the coordination structure around the calcium atom of Ca-GG is square-bipyramidal, including six oxygen atoms of the carbonyl and carboxyl groups, and the central calcium atom is on a center of symmetry. Consequently, three Ca-ligand antisymmetric stretching vibrations are IR-active (A_u species) and three Ca-ligand symmetric stretching vibrations are Raman-active (A_g species). The metal isotope effect on ^{40}Ca–^{44}Ca substitution is expected for only three Ca-ligand antisymmetric stretching vibrations (A_u species) involving displacement of the calcium atom.

For the IR spectra in the region between 400 and 200 cm^{-1}, five bands are observed at 391, 345, 309, 267 and 242 cm^{-1} as seen in Fig. 3. On ^{40}Ca–^{44}Ca substitution, the centers of the 345, 267 and 242 cm^{-1} bands shift to lower frequencies by 6.5, 5.4 and 4.3 cm^{-1}, respectively, and these

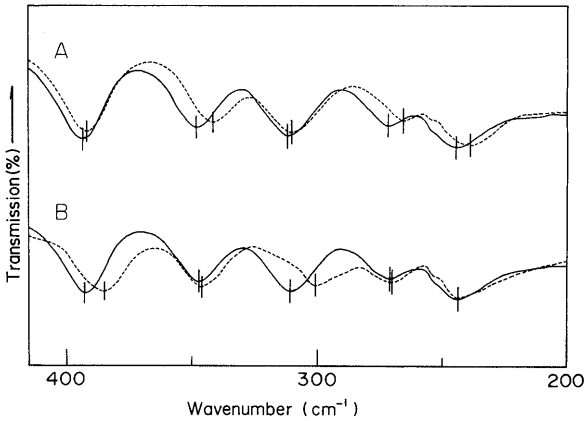

Fig. 3. IR Spectra of Ca-GG in the Region between 420 and 200 cm^{-1}
A, ^{40}Ca-GG (—) and ^{44}Ca-GG (– – –). B, Ca-GG (—) and Ca-GG-d_8 (– – –).

TABLE I. Modified Urey–Bradley Type and Valence Type Force Constants

Modified Urey–Bradley type force constants (mdyn/Å)							
K(C–O)	7.55	*H*(HCH)	0.422	*H*(OCaO)	0.0	*F*(CCN)	0.60
K(C–C)	1.95	*H*(NCH)	0.25	*H*(OCaO)	0.0	*F*(CNC)	0.50
K(C–N)	2.45	*H*(CCN)	0.55	κ(N)[a]	−0.05	*F*(CNH)	0.50
K(C–H)	4.00	*H*(CNC)	0.40	κ(C)[a]	0.01	*F*(NCO)	0.50
K(N–H)	5.45	*H*(CNH)	0.30	*F*(OCO)	2.52	*F*(CNH)	0.50
K(Ca–O)	0.50	*H*(NCO)	0.40	*F*(OCC)	0.70	*F*(HNH)	0.02
H(OCO)	0.10	*H*(CNH)	0.30	*F*(CCH)	0.40	*F*(CaOC)	0.10
H(OCC)	0.24	*H*(HNH)	0.55	*F*(HCH)	0.076	*F*(OCaO)	0.0
H(CCH)	0.16	*H*(CaOC)	0.05	*F*(NCH)	0.54	*F*(OCaO)	0.0
Valence type force constants (mdyn·Å/rad^2)							
$f(\omega CO_2, \omega CO_2)$	1.20		$f(\delta NH, \delta NH)$	0.50		$f(\delta C=O, \delta C=O)$	0.50
$f(\tau CC, \tau CC)$	0.15		$f(\tau CN, \tau CN)$	0.45		$f(\tau C=O, \tau C=O)$	0.50

a) mdyn·Å.

TABLE II. Observed and Calculated Frequencies and Assignments for Ca-GG and Its *N,N'*-Deuterated Analogues in the Region between 4000 and 50 cm^{-1}

A_u species (IR)				A_g species (Raman)				Assignments[b]
Ca-GG		Ca-GG-d_8		Ca-GG		Ca-GG-d_8		
Obs.[a]	Calc.	Obs.[a]	Calc.	Obs.[a]	Calc.	Obs.[a]	Calc.	
3215 s	3297 3242 3242	2370 s 2260 s	2408 2395 2393	3225 w	3297 3242 3242	2375 w	2408 2395 2393	νNH(ND) $\nu_d NH_3(ND_3)$ $\nu_d NH_3(ND_3)$
3080 s	3151	2170 s	2258	3105 w	3151	2250 vw	2258	$\nu_s NH_3(ND_3)$
3000 s	3030	2995 w	3030		3030	3105 vw	3030	$\nu_a CH_2$
2920 sh	2871	2940 w	2872	2995 s	2871	2998 s	2872	$\nu_a CH_2$
	2845	2930 sh	2845	2940 sh	2845	2940 sh	2845	$\nu_s CH_2$
	2845	2860 sh	2845	2927 s	2845	2928 s	2845	$\nu_s CH_2$
1647 s	1654	1638 m	1653	1662 m	1654	1652 m	1652	$\nu_a CO_2$
1607 sh	1631	1593 m	1597	1630 w	1631	1572 m	1596	$\nu C=O$
1595 sh	1626	1181 m	1167	1608 w	1626	1170 vw	1167	$\delta_d NH_3(ND_3)$
1568 s	1623		1163	1575 m	1623	1150 vw	1163	$\delta_d NH_3(ND_3)$
1493 s	1506	1138 m	1124	1470 m	1506	1126 w	1123	δNH(ND)in-plane
	1493	1160 m	1158	1446 w	1493	1105 w	1158	$\delta_s NH_3(ND_3)$
1447 s	1452	1502 s	1457	1430 m	1452	1503 m	1457	βCH_2
1424 w	1444	1447 s	1455	1405 s	1444	1446 m	1455	βCH_2
1402 s	1364	1402 s	1364	1395 sh	1364	1405 s	1362	$\nu_s CO_2$
1325 sh	1310	1367 s	1309	1330 sh	1310	1330 m	1308	ωCH_2
1317 m	1294	1319 s	1294	1320 m	1293	1322 sh	1294	ωCH_2
1269 m	1239		1287	1276 m	1238	1280 sh	1286	$\nu C=O$ in-plane
	1249	1242 m	1237		1249	1271 m	1236	tCH_2
1241 m	1231		1229	1248 m	1231	1249 m	1229	tCH_2
1123 m	1122	755 m	756	1126 m	1122	715 w	756	$\rho NH_3(ND_3)$
1105 w	1108	699 m	708	1102 m	1108	708 w	703	$\rho NH_3(ND_3)$
1081 m	1077	1027 m	1054	1077 w	1076	1044 m	1054	νskel
1042 m	1008		997	1044 m	1008	1021 vw	997	νskel
999 m	962	965 sh	945	998 m	962	972 w	943	νskel
953 m	947	991 m	955	952 s	947	997 m	955	ρCH_2
895 m	861	933 m	927	897 m	858	956 s	926	νskel
	860	892 w	915		860	899 m	915	ρCH_2
721 m	767	839 m	810	815 w	765	840 w	807	νskel
	694	480 w	444	710 m	694	520 vw	437	δNH(ND) out-of-plane
653 w	661	622 w	659	655 w	656	600 w	651	βCO_2
596 m	582	558 m	568	600 m	578	560 vw	561	ρCO_2
579 w	536	598 m	611	574 m	535	574 m	610	ωCO_2
551 m	524	520 m	513	557 sh	529	530 vw	501	$\delta C=O$ out-of-plane
500 w	494	480 w	408	520 w	485		408	δskel
391 w	367	383 w	363	386 w	362	384 w	354	δskel
346 w	327	344 w	325	—[d]	—[d]	—[d]	—[d]	ν_{as}Ca-O
—[d]	—[d]	—[d]	—[d]	305 w	301	302 w	296	ν_sCa-O
—[c]	353	287 sh	329	320 sh	329	320 w	307	δskel
309 w	250	299 w	245	212 m	237	210 w	231	δskel
267 vw	238	268 vw	235	—[d]	—[d]	—[d]	—[d]	ν_{as}Ca-O
—[d]	—[d]	—[d]	—[d]	158 m	169	156 m	167	ν_sCa-O
242 w	203	242 w	200	—[d]	—[d]	—[d]	—[d]	ν_{as}Ca-O
—[d]	—[d]	—[d]	—[d]	111 m	135	110 m	129	ν_sCa-O
—[e]	190	—[e]	184	135 vw	154	122 vw	148	δskel
—[e]	138	—[e]	132	115 sh	114	—[c]	108	δskel
—[e]	124	—[e]	117	89 m	79	88 m	78	δskel
—[e]	84	—[e]	81	75 m	76	75 w	73	δskel
—[e]	46	—[e]	44	53 m	41	53 m	40	δskel

a) s, Strong; m, medium; w, weak; vw, very weak; sh, shoulder. *b*) ν, Stretching; β, bending; δ, deformation; t, twisting; ω, wagging; ρ, rocking. *c*) Hidden by a neighboring band. *d*) Not expected. *e*) Not observed.

bands are undoubtedly assigned to the vibrations involving displacement of the calcium atom. Since these bands remain almost unshifted on *N,N'*-deuteration, these bands are clearly assigned to the Ca-ligand antisymmetric stretching vibrations. The remaining bands were assigned to the skeletal deformation vibrations of glycylglycinates because of small isotope shifts on ^{40}Ca–^{44}Ca substitution and large shifts on *N,N'*-deuteration.

In the Raman spectra, eleven bands are observed in the region between 400 and 50 cm^{-1}. Since three Ca-ligand symmetric stretching vibrations belong to the A_g species, these vibrations involve no displacement of the calcium atom, and are expected to show no metal isotope effect on ^{40}Ca–^{44}Ca substitution. Actually, all eleven bands showed no metal isotope shift on ^{40}Ca–^{44}Ca substitution, as shown in Fig. 4. By referring to the shifts on *N,N'*-deuteration and the result of the normal coordinate analysis, the relatively strong bands at 305, 158 and 111 cm^{-1} were assigned to

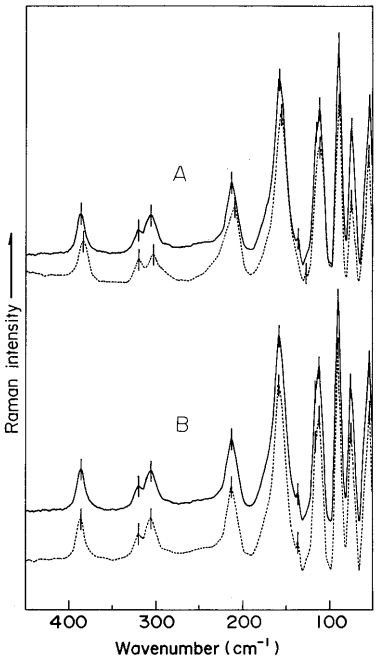

Fig. 4. Raman Spectra of Ca-GG in the Region between 450 and 50 cm^{-1}

A, Ca-GG (—) and Ca-GG-d_8 (– – –). B, ^{40}Ca-GG (—) and ^{44}Ca-GG (– – –).

the Ca-ligand symmetric stretching vibrations. The remaining bands in this region were assigned to the skeletal deformation vibrations of glycylglycinates. The bands corresponding to the Ca-ligand antisymmetric stretching vibrations were not observed in the Raman spectra, as expected from the mutual exclusion rule.

The observed and calculated isotope shifts for the vibrations of IR-active A_u species are summarized in Table III, together with their assignments. Table III indicates that the final calculation reproduced well the observed isotope shifts on ^{40}Ca–^{44}Ca substitution and *N,N'*-deuteration, although the calculated frequencies were generally lower than those observed. Small isotope shifts of the skeletal deformation vibrations on ^{40}Ca–^{44}Ca substitution may be caused by a small contribution of the Ca-ligand stretching vibrations. The calculated L matrices actually reveal that the Ca-ligand stretching vibrations couple with most of the skeletal deformation vibrations. The calculated frequencies for the A_g species also correspond well not only to the observed Ca-ligand stretching vibrations but also to the observed skeletal deformation vibrations, as shown in Table II. No frequency shifts on ^{40}Ca–^{44}Ca substitution were calculated for all the vibrations of the Raman-active A_g species, supporting the present assignments.

Previously, the metal-ligand stretching vibrations of copper– and zinc–amino acid complexes were comprehensively investigated by the metal isotope technique (^{63}Cu–^{65}Cu and ^{64}Zn–^{68}Zn substitution, respectively) and were observed in the region between 450 and 200 cm^{-1}.[13-15,17] Since the Ca-ligand bond-lengths of Ca-GG are longer than those of the copper– and zinc–amino acid complexes, the Ca-ligand stretching vibrations of Ca-GG are expected to be observed in the region below 200 cm^{-1}. However, the metal-isotope sensitive Ca-ligand stretching vibrations of Ca-GG were observed in almost the same region as those of copper– and zinc–amino acid complexes. The force constants for the metal-ligand stretching mode of Ca-GG used in this calculation were somewhat larger than those for Zn(L-serinate)$_2$.[17]

TABLE III. Observed and Calculated Infrared-Active Frequencies, Isotope Shifts and Assignments of Ca-GG in the Region between 400 and 200 cm^{-1} (A_u species)

Ca-GG		$\Delta\nu_m$[a]		$\Delta\nu_h$[b]		Assignments[c]
Obs.	Calc.	Obs.	Calc.	Obs.	Calc.	
391	367	1.6	1.1	7.2	4.4	δskel
345	327	6.5	3.0	0.9	2.3	ν_{as}Ca-O
—[d]	353	—[d]	1.8	*ca.* 20	23.3	δskel
309	250	1.5	1.9	9.7	5.8	δskel
267	238	5.4	5.0	0.2	2.4	ν_{as}Ca-O
242	203	4.3	3.2	*ca.* 0	2.9	ν_{as}Ca-O

a) Shift on ^{40}Ca and ^{44}Ca substitution for Ca-GG. *b*) Shift on *N,N'*-deuteration. *c*) δ, deformation; ν_{as}, antisymmetric stretching. *d*) Hidden by 309 cm^{-1} band.

In conclusion, the Ca-ligand stretching vibrations are observed around 300 cm^{-1}, which is higher than those expected from their bond-lengths. This result is useful for investigations of calcium–amino acids and –drugs as fundamental data.

Acknowledgments The authors are very grateful to Prof. Katsunosuke Machida, Faculty of Pharmaceutical Sciences, Kyoto University, for his kind offering of the computer program. The calculations were carried out using an ACOS 1000 computer of the Okayama University Computer Center. This study was supported by a Grant-in-Aid for Scientific Research from the Ministry of Education, Science and Culture, Japan.

References and Notes

1) This work was presented at the 25th Meeting of the Chugoku–Shikoku Branch, Pharmaceutical Society of Japan, Tottori, Japan, 1986.
2) Present address: *Department of Biochemistry, College of Science, Okayama University of Science, Ridai-cho, Okayama 700, Japan.*
3) S. Kakiuchi, *Taisha*, **17**, 1201 (1980).
4) W. Y. Cheung, *Science*, **207**, 19 (1980).
5) S. Ebashi, *Proc. R. Soc. London*, **B207**, 259 (1980).
6) J. R. Dedman, J. D. Potter and A. R. Means, *J. Biol. Chem.*, **252**, 2437 (1977).
7) R. H. Kretsinger, *Ann. Rev. Biochem.*, **45**, 239 (1976).
8) R. E. Reid and R. S. Hodges, *J. Theor. Biol.*, **84**, 401 (1980).
9) T. Takagi, T. Nemoto, K. Konishi, M. Yazawa and K. Yagi, *Biochem. Biophys. Res. Commun.*, **96**, 377 (1980).
10) J. H. Collins, J. D. Potter, M. J. Horn, G. Wilshire and N. Jackson, *FEBS Lett.*, **36**, 268 (1973).
11) P. C. Moews and R. H. Kretsinger, *J. Mol. Biol.*, **91**, 201 (1975).
12) B. A. Levine, R. J. P. Williams, C. S. Fullmer and R. H. Wasserman, "Calcium-Binding Proteins and Calcium Function, Proc. Int. Symp. 2nd," ed. by R. H. Wasserman, Elsevier N. Holland, New York, 1977, pp. 29—37.
13) Y. Saito, J. Odo and Y. Tanaka, *Chem. Pharm. Bull.*, **29**, 907 (1981).
14) J. Odo, M. Nishio, Y. Saito and Y. Tanaka, *Chem. Pharm. Bull.*, **30**, 2661 (1982).
15) J. Odo, M. Uematsu, Y. Saito and Y. Tanaka, *Chem. Pharm. Bull.*, **30**, 4512 (1982).
16) R. Meulemans, P. Piret and M. van Meerssche, *Bull. Soc. Chim. Belgs.*, **80**, 73 (1971).
17) J. Odo, M. Nishio, Y. Saito, Y. Tanaka and K. Machida, *Chem. Pharm. Bull.*, **31**, 3802 (1983).
18) K. Machida, M. Izumi and A. Kagayama, *Spectrochim. Acta*, **35A**, 1333 (1979).
19) Y. Inomata, T. Inomata and T. Moriwaki, *Bull. Chem. Soc. Jpn.*, **44**, 365 (1971).
20) P. Lagant, G. Vergoten, M. H. Loucheux-Lefebvre and G. Fleury, *Biopolymers*, **22**, 1267 (1983).
21) S. Alex, R. Savoie, M. C. Corbeil and A. L. Beauchamp, *Can. J. Chem.*, **64**, 148 (1986).

Studies on Glycosylation of the Mitomycins. Syntheses of 7-*N*-(4-*O*-Glycosylphenyl)-9a-methoxymitosanes[1)]

Kimio FURUHATA,[a] Kanki KOMIYAMA,[b] Haruo OGURA,*[,a] and Toju HATA[b]

School of Pharmaceutical Sciences, Kitasato University[a] and The Kitasato Institute,[b] Shirokane, Minato-ku, Tokyo 108, Japan. *Received May 1, 1990*

Two new derivatives of glycosyl mitomycin C, 7-*N*-{4-*O*-(β-D-glucopyranosyl and α-sialosyl)phenyl}-9a-methoxymitosanes, were synthesized, and their structures were elucidated by analysis of the nuclear magnetic resonance spectra. Field desorption mass spectrometry was successfully used for the confirmation of these structures. The cytotoxic, antibacterial, and antitumor activities of 7-*N*-(4-glycosylphenyl)-9a-methoxymitosanes were also examined.

Keywords mitomycin A; sialic acid; D-glucose; glycosylation; mitomycin C

Mitomycin C is a potent antitumor agent that is currently used clinically for cancer chemotherapy.[2,3)] Numerous analogs of the mitomycins have been prepared in the hope of obtaining derivatives with superior the therapeutic properties.[4,5)]

Glycosyl residues play important roles in various biological processes (masking of cell-surface antigens, mitogenic receptors for lectins in cell-to cell recognition and other behavior).[6-8)] In view of these facts, it is possible that glycoside derivatives of mitomycin may provide a degree of selectivity between normal cells and some cancer cells. In the previous paper,[9)] we reported on the syntheses of 7-*O*-glycosyl-9a-methoxymitosanes, and some of their biological activities. However, there still remains the problem of *O*-deacetylation of their constituent per-*O*-acetylated glycosides, because the glycoside bond of 7-*O*-glycosyl-9a-methoxymitosanes having an *O*-acetylated glycoside moiety is hydrolyzed more easily than their *O*-acetyl groups under mild basic conditions. In this paper, as a part of our program on the syntheses of glycoconjugates of mitomycins, we describe the synthesis of 7-*N*-{4-*O*-(glucopyranosyl and sialosyl)phenyl}-9a-methoxymitosanes having no hydroxy-protection. The structures of the glycosylation products were elucidated on the basis of the field desorption (FD) mass spectra (MS) and the nuclear magnetic resonance (NMR) spectra. Some of the biological activities of these derivatives were also investigated.

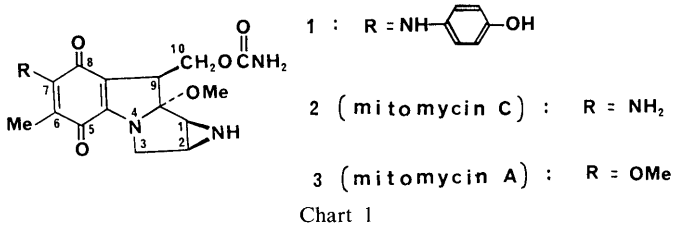

Chart 1

Results and Discussion

Chemistry 7-*N*-(4-Hydroxyphenyl)-9a-methoxymitosane sodium salt (**1**) is one of the most active mitomycin C (**2**) derivatives, showing higher antitumor activity than **2** against several murine tumor models and significantly lower bone marrow toxicity.[10)] Therefore, we investigated the glycosylation of mitomycin A (**3**) using 4-aminophenol as a spacer.

4-Aminophenyl 2,3,4,6-tetra-*O*-acetyl-β-D-glucopyranoside (**4**) was prepared by utilizing the conditions reported by Ekborg *et al.*[11)] Treatment of **3** and **4** in anhydrous methanol gave 7-*N*-{4-*O*-(2,3,4,6-tetra-*O*-acetyl-β-D-glucopyranosyl)phenyl}-9a-methoxymitosane (**5**) in 69% yield.[12)] *O*-Deacetylation of **5** with sodium methoxide in methanol at 20 °C for 30 min gave two major products.[13)] The reaction mixture was separated by column chromatography on silica gel to give 7-*N*-{4-*O*-(β-D-glucopyranosyl)phenyl}-9a-methoxymitosane (**6**) and its 6-*O*-monoacetyl derivative (**7**). Their structures were elucidated on the basis of the ^{1}H-NMR spectra (Tables I and II). Proton assignments for these compounds were made by two-dimensional (2-D) ^{1}H-^{1}H correlation spectroscopy (COSY). Consistent patterns were noted in the ^{1}H-NMR spectra for **7**, suggesting the presence of 9a-methoxymitosane and a 4-aminophenyl 2,3,4,6-tetra-*O*-acetyl-β-D-glucopyranoside moiety. The *O*-

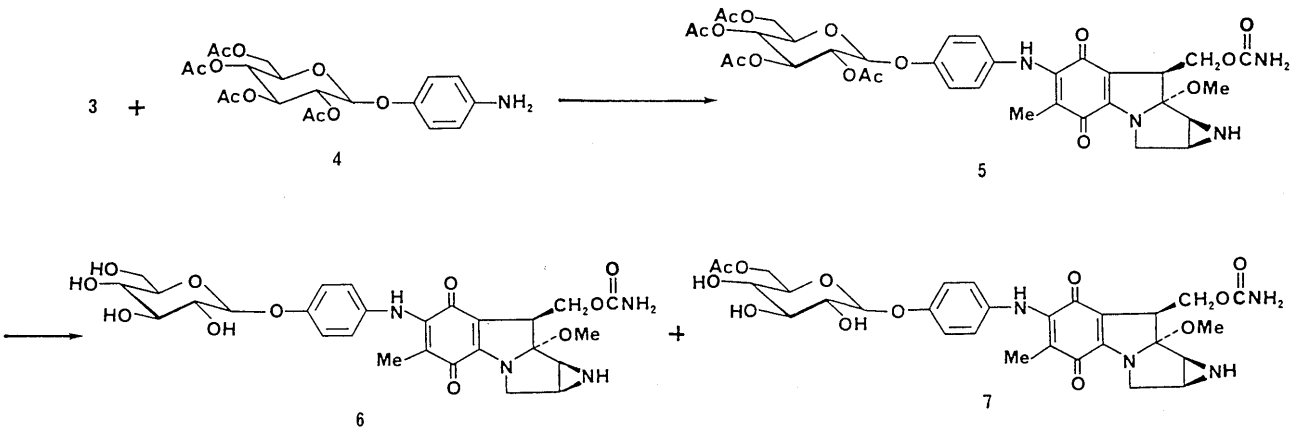

Chart 2

TABLE I. ^{1}H-NMR Data for the Glucosyl Moiety in **5**, **6**, and **7**

Hydrogen number	Compound		
	5	**6**	**7**
1-H	5.03 d (8.0)	5.50 d (7.0)	5.44 d (7.2)
2-H	5.15 t (9.5)		4.15—4.26 (2H)
3-H	5.24 t (9.5)	4.15—4.30 (3H)	
4-H	5.29 t (9.5)		3.98—4.14 (2H)
5-H	3.86 ddd (2.5, 5.5, 10.0)	4.02 m	
6-H	4.36 dd (2.5, 10.0)	4.26 dd (5.0, 12.0)	4.46 dd (6.0, 11.5)
6′-H	4.27 dd (5.0, 12.5)	4.44 dd (2.0, 12.0)	4.83 dd (1.5, 11.5)
OAc	2.02 s, 2.04 s, 2.06 s, 2.07 s		1.83 s
Phenyl group	6.90 d (9.0) 6.95 d (9.0)	6.87 d (9.0) 7.20 d (9.0)	6.96 d (9.0) 7.19 d (9.0)

Spectra were measured in $CDCl_3$ for **5** and in C_5D_5N for **6** and **7**. Chemical shifts are given in δ (ppm). Coupling constans (Hz) are given in parentheses.

TABLE II. ^{1}H-NMR Data for the Mitosane Moiety in **5**, **6**, and **7**

Hydrogen number	Compound		
	5	**6**	**7**
1-H	2.91 br s	3.04 br s	3.04 br d (4.0)
2-H	2.83 br s	2.65 br s	2.65 br d (2.5)
3-H	3.51 br d (13.5)	3.48 br d (13.0)	3.49 br d (12.0)
3-H′	4.24 d (13.5)	4.39 d (13.0)	4.38 d (12.5)
6-Me	1.42 s	1.40 s	1.46 s
7-NH	7.70 s	8.10 s	8.94 s
9-H	3.63 dd (4.7, 10.5)	3.93 dd (4.5, 11.0)	3.93 dd (4.5, 11.0)
9a-OMe	3.22 s	3.16 s	3.12 s
10-H	4.53 br t (10.5)	5.02 br t (11.0)	4.99 br t (10.5)
10-H′	4.70 dd (4.5, 10.5)	5.28 dd (4.5, 10.5)	5.28 dd (4.5, 10.5)
NH_2	4.89 br s		

Spectra were measured in $CDCl_3$ for **5** and in C_5D_5N for **6** and **7**. Chemical shifts are given in δ (ppm). Coupling constans (Hz) are given in parentheses.

acetylated position of **7** was elucidated to be at C-6 on the basis of the fact that two deshielded signals for 6-H and 6-H′ appeared at δ 4.46 and δ 4.83 in the ^{1}H-NMR spectrum. The structure of the deacetylation product **6** was also in full agreement with the ^{1}H-NMR data.

Recently, many kinds of biological functions of sialosylglycoconjugates have been reported.[14-16] As a further step in these investigations, we have synthesized 7-*N*-(4-*O*-sialosylphenyl)-9a-methoxymitosanes.

Methyl (4-nitrophenyl 5-acetamido-4,7,8,9-tetra-*O*-acetyl-3,5-dideoxy-α-D-*glycero*-D-*galacto*-2-nonulopyranosid)onate (**8**) was prepared by glycosylation of 4-nitrophenol with methyl (5-acetamido-4,7,8,9-tetra-*O*-acetyl-3,5-dideoxy-α-D-*glycero*-D-*galacto*-2-nonulopyranosyl chlorid)onate as described by Eschenfelder and Brossmer.[17] The nitro group of **8** was reduced to an amino group by catalytic hydrogenation to give the intermediate **9**, whose ^{1}H-NMR spectrum was consistent with the assigned structure.

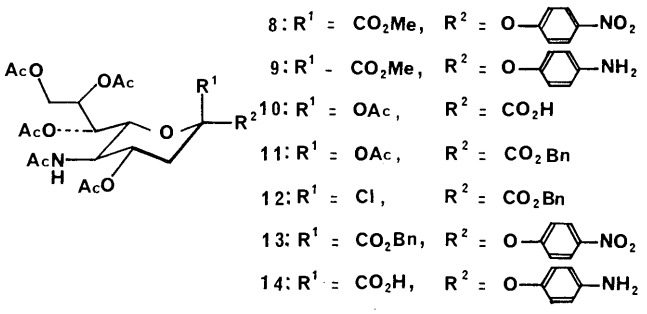

Chart 3

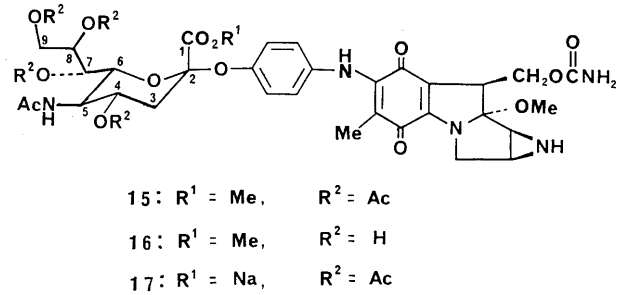

Chart 4

The intermediate 4-aminophenyl 5-acetamido-4,7,8,9-tetra-*O*-acetyl-3,5-dideoxy-α-D-*glycero*-D-*galacto*-2-nonulopyranosidonic acid (**14**) was obtained by the following route.[18] Esterification[19] of the cesium salt **10** with benzyl bromide (BnBr) in *N*,*N*-dimethylformamide (DMF) followed by treatment of the resulting benzyl ester **11** with excess hydrogen chloride gas gave the chloride **12**, which was submitted to the next glycosylation step. Glycosylation of **12** with 4-nitrophenol in DMF afforded benzyl (4-nitrophenyl 5-acetamido-4,7,8,9-tetra-*O*-acetyl-3,5-dideoxy-α-D-*glycero*-D-*galacto*-2-nonulopyranosid)onate (**13**) as pale-yellow crystals in 20% yield. The structure of **13** was unambiguously assigned from the ^{1}H-NMR spectrum. The anomeric configuration of **13** was also elucidated from the ^{1}H-NMR spectrum. The observed chemical shifts of δ 2.75 for 3-H and δ 4.96 for 4-H of **13** are characteristic[20] of the α-glycosidic linkage of *N*-acetylneuraminic acid. The nitro group was reduced to an amino group and the benzyl group was hydrogenolyzed by with a PtO_2 catalyst to give crystalline **14**.

In the same manner as described for the preparation of **5**, the treatment of **3** in methanol with **9** gave 7-*N*-{4-*O*-(methyl 5-acetamido-4,7,8,9-tetra-*O*-acetyl-3,5-dideoxy-α-D-*glycero*-D-*galacto*-2-nonulopyranosylonate)phenyl}-9a-methoxymitosane (**15**) in good yield. Removal of the *O*-acetyl group of **15** was carried out by treatment of **15** with sodium methoxide in methanol to give 7-*N*-{4-*O*-(methyl 5-acetamido-3,5-dideoxy-α-D-*glycero*-D-*galacto*-2-nonulopyranosylonate)phenyl}-9a-methoxymitosane (**16**) in 75% yield.

Moreover, treatment of **3** with **14** in methanol in the presence of triethylamine gave 7-*N*-{4-*O*-(5-acetamido-

TABLE III. ^{1}H-NMR Data for the Sialosyl Moiety in **15**, **16**, and **17**

Hydrogen number	Compound		
	15	**16**	**17**
3-H_{ax}	2.21 t (12.5)	2.46 br t (12.5)	1.91 t (12.5)
3-H_{eq}	2.72 dd (4.5, 13.0)	3.20 dd (4.5, 12.5)	2.65 dd (4.5, 12.5)
4-H	4.93 ddd (4.5, 10.5, 12.5)	4.18—4.50 m	5.02 dd (4.5, 10.5)
5-H	4.10 br q (10.0)	3.37—3.45 m	3.91 t (10.0)
6-H	4.38 dd (1.0, 10.5)	4.18—4.50 m	4.55—4.65 m
7-H	5.34—5.37 (2H)	4.54—4.81 (2H)	5.27 br d (6.0)
8-H			5.33 m
9-H	4.13 dd (1.0, 12.0)	4.18—4.50 (2H)	4.11 dd (6.5, 13.0)
9-H′	4.28 dd (2.0, 12.0)		4.15 d (13.0)
COOMe	3.60 s	3.42 s	—
NAc	1.90 s	1.85 s	1.85 s
OAc	2.04, 2, 2.12 2.14		1.97, 1.98 2.01, 2.08
NH	5.32 d (10.0)		
Phenyl group	6.90 d (9.0) 7.20 d (9.0)	6.62 d (9.0) 7.31 d (9.0)	6.82 d (9.0) 7.05 d (9.0)

Spectra were measured in $CDCl_3$ for **5** and in C_5D_5N for **6** and **7**. Chemical shifts are given in δ (ppm). Coupling constants (Hz) are given in parentheses.

TABLE IV. ^{1}H-NMR Data for the Mitosane Moiety in **15**, **16**, and **17**

Hydrogen number	Compound		
	15	**16**	**17**
1-H	2.92 br s	3.04 d (4.5)	2.86 d (4.5)
2-H	2.83 br s	2.65 br d (4.5)	2.78 br d (4.5)
3-H	3.52 br d (13.0)	3.50 br d (13.0)	3.46 br d (12.0)
3-H′	4.24 d (13.0)	4.36 d (13.0)	4.33 br d (12.0)
6-Me	1.41 s	1.37 s	1.37 s
7-NH	7.68 br s	7.50 br s	
9-H	3.56 dd (4.5, 10.5)	3.94 dd (4.5, 10.5)	3.56 dd (4.5, 10.5)
9a-OMe	3.23 s	3.14 s	3.18 s
10-H	4.56 br t (10.5)	4.99 br t (10.5)	4.38 br t (10.5)
10-H′	4.73 dd (4.5, 10.5)	5.29 dd (4.5, 10.5)	4.55—4.65
NH_2	4.80 br s	5.70 br s	

Spectra were measured in $CDCl_3$ for **5** and in C_5D_5N for **6** and **7**. Chemical shifts are given in δ (ppm). Coupling constants (Hz) are given in parentheses.

4,7,8,9-tetra-*O*-acetyl-3,5-dideoxy-α-D-*glycero*-D-*galacto*-2-nonulopyranosylonic acid)phenyl}-9a-methoxymitosane, and its sodium salt (**17**) was prepared by treatment with an equimolar amount of sodium hydrogen carbonate in 60% yield.

Biological Activity These derivatives of **2**, 7-*N*-(4-*O*-glycosylphenyl)-9a-methoxymitosanes were examined for cytotoxic, anti-*Escherichia coli* (*E. coli*) and antitumor activities.

TABLE V. Growth Inhibitory Concentration of Derivatives of **2** against Tumor Cells and *E. coli in Vitro*

Compound number	IC_{50} value (μg/ml)[a]		
	P388/ADM	P388	*E. coli*[b]
1	1.01	0.108	18.6
2	0.92	0.105	40.1
5	0.48	0.084	16.3
6	1.02	0.108	±
15	0.78	0.112	13.9
16	2.21	0.740	10.0
17	5.63	5.01	—

a) Cells were exposed to the agents for 72 h. *b*) Inhibitory zone (mm) obtained by the paper disc method at a dose of 10 μg/ml.

TABLE VI. Antitumor Activity of Derivatives of **2** against P388/ADM Leukemia

Total dose (mg/kg)	Percent in increase of life span						
	1	**2**	**5**	**6**	**15**	**16**	**17**
160	Toxic	—	Toxic	—	58.3	Toxic	0
40	91.6	Toxic	16.1	Toxic	25.0	25.0	0
10	25.0	75.0	16.6	0	0	8.3	0

Tumor: P388/ADM 1×10^5 cell/mouse, i.p. Treatment: Days 1, 5, 9, i.p. Toxic: A percent ILS value of −15% or a larger negative value was taken to indicate toxicity.

The cytotoxic effect of the derivatives of **2** was examined against P388 and P388/ADM leukemic cells cultured *in vitro*. As shown in Table V, cytotoxic activities of **5**, **6**, and **15** were similar to that of **2**. In contrast, the derivatives showed weaker antibacterial activity than that of **2**.

The antitumor activity of the derivatives of **2** was examined against P388/ADM as shown in Table VI. Though **15** showed 58.3% ILS which is the highest activity among the derivatives, this activity is still less than that of **1** or **2**.

Experimental

Melting points were measured with a Yamato melting point apparatus and are uncorrected. Optical rotations were measured with a JASCO DIP-181 digital polarimeter. Thin layer chromatography (TLC) was performed on silica gel GF-254 (Merck) plates. FD-MS, ultraviolet (UV), and infrared (IR) spectra were measured with JEOL JMA-3100, Hitachi 340, and JASCO IR-A2 instruments, respectively. The NMR spectra were measured in chloroform-d_3 ($CDCl_3$) or pyridine-d_5 (C_5D_5N) with tetramethylsilane (TMS) as an internal standard, with a Varian VXR-300 spectrometer. Column chromatography was conducted on Silica gel 60 (70—230 mesh, Merck).

7-*N*-{4-*O*-(2,3,4,6-Tetra-*O*-acetyl-β-D-glucopyranosyl)phenyl}-9a-methoxymitosane (5) A solution of **3** (100 mg, 0.29 mmol) in methanol was treated with **4** (660 mg, 1.37 mmol). The reaction mixture was stirred for 5 h at room temperature, and evaporated to dryness under reduced pressure. The residue was purified by column chromatography on silica gel with chloroform–methanol (20 : 1) to give **5** (150 mg, yield 69%) as a dark green amorphous powder. *Anal.* Calcd for, $C_{35}H_{40}N_4O_{15}$: C, 55.55; H, 5.32; N, 7.40. Found: C, 55.21; H, 5.46; N, 7.11. FD-MS *m/z*: 758 ($M^+ + 1$), 779 ($M^+ + Na$). IR ν_{max}^{KBr} cm^{-1}: 1750, 1635, 1560, 1505. UV λ_{max}^{MeOH} nm (log ε): 375 (4.23), 255 (4.32), 215 (4.44). ^{1}H-NMR data are given in Tables I and II.

7-*N*-{4-*O*-(β-D-Glycopyranosyl and 6-*O*-Acetyl-β-D-glucopyranosyl)-phenyl}-9a-methoxymitosane (6 and 7) A solution of **5** (80 mg, 0.11 mmol) in methanol (15 ml) was treated with 28% sodium methoxide–methanol (20 mg). The reaction mixture was stirred for 30 min at 20 °C. Sodium methoxide in the reaction mixture was removed by using a small amount of Dowex 50 (H^+, 80 mg) in methanol and the solvent was evaporated off under reduced pressure. The residue was chromatographed on a column

of silica gel with chloroform–methanol (5:1) to give two fractions. The faster-eluting fraction gave 6 (46 mg, yield 75%) as a dark green amorphous powder. The second fraction gave **7** (7 mg, yield 10%) as a dark green amorphous powder.

6: *Anal.* Calcd for $C_{27}H_{32}N_4O_{11}$: C, 55.09; H, 5.47; N, 9.51. Found: C, 54.87; H, 5.45; N, 9.32. FD-MS *m/z*: 589 ($M^+ + 1$), 612 ($M^+ + Na$). IR ν_{max}^{KBr} cm^{-1}: 1710, 1630, 1560, 1505. UV λ_{max}^{MeOH} (log ε): 375 (3.85), 355 (3.99), 215 (4.13). ^{1}H-NMR data are given in Tables I and II.

7: *Anal.* Calcd for $C_{29}H_{34}N_4O_{12}$: C, 55.23; H, 5.43; N, 8.88. Found: C, 55.15; H, 5.42; N, 8.79. FD-MS *m/z*: 631 ($M^+ + 1$), 653 ($M^+ + Na$). IR ν_{max}^{KBr} cm^{-1}: 3400, 1720, 1638, 1560, 1510. UV λ_{max}^{MeOH} (log ε): 378 (4.07), 255 (4.20), 215 (4.32). ^{1}H-NMR data are given in Tables I and II.

Methyl (4-Aminophenyl 5-Acetamido-4,7,8,9-tetra-*O*-acetyl-3,5-dideoxy-α-D-*glycero*-D-*galacto*-2-nonulopyranosid)onate (9) A solution of **8** (307 mg, 0.50 mmol) in ethyl acetate (20 ml) was treated with hydrogen over PtO_2 (100 mg) for 2 h at room temperature. The solution was filtered through Celite and evaporated to dryness at 20 °C to give **9** (251 mg, yield 84%) as an amorphous powder. $[\alpha]_D^{22}$ +30° (*c*=1, MeOH). *Anal.* Calcd for $C_{27}H_{34}N_2O_{13}$: C, 54.54; H, 5.76; N, 4.71. Found: C, 54.85; H, 5.65; N, 4.40. IR ν_{max}^{KBr} cm^{-1}: 3360, 1745, 1675, 1510. ^{1}H-NMR ($CDCl_3$): 1.88 (3H, s, NAc), 2.01 (3H, s, OAc), 2.04 (3H, s, OAc), 2.10 (3H, s, OAc), 2.12 (3H, s, OAc), 2.03 (1H, t, *J*=13.0 Hz, 3-H_{ax}), 2.66 (1H, dd, *J*=4.8, 13.0 Hz, 3-H_{eq}), 3.66 (3H, s, –COOH), 4.04 (1H, br q, *J*=10.5 Hz, 5-H), 4.18 (1H, dd, *J*=5.0, 12.5 Hz, 9-H), 4.20 (1H, br d, *J*=10.5 Hz, 6-H), 4.34 (1H, dd, *J*=2.0, 12.5 Hz, 9-H'), 4.92 (1H, ddd, *J*=4.8, 10.5, 12.0 Hz, 4-H), 5.30 (1H, d, *J*=10.0 Hz, NH), 5.34 (2H, br s, 7-H and 8-H), 6.57 (2H, d, *J*=9.0 Hz, phenyl group), 6.87 (2H, d, *J*=9.0 Hz, phenyl group).

Benzyl (4-Nitrophenyl 5-Acetamido-4,7,8,9-tetra-*O*-acetyl-3,5-dideoxy-α-D-*glycero*-D-*galacto*-2-nonulopyranosid)onate (13) A suspension of **10** (1.02 g, 1.96 mmol), Cs_2CO_3 (0.5 g, 1.54 mmol), and BnBr (0.5 g, 2.92 mmol) in DMF (5 ml) was stirred for 3 h at room temperature, then poured into water (20 ml) and extracted with chloroform. The extract was washed with water, dried over sodium sulfate, and evaporated to dryness to give **11** as an amorphous material. A solution of **11** in acetic acid (20 ml) and acetyl chloride (5 ml) was cooled in ice bath and saturated with dry hydrogen chloride gas. The reaction mixture was kept at room temperature for 16 h, then evaporated to a syrup. This was dissolved in dry benzene and the solution was evaporated to dryness at 20 °C. This was repeated twice to give **12** as a colorless solid.

A solution of **12** and sodium 4-nitrophenol (1.0 g, 7.19 mmol) in DMF (10 ml) was stirred at room temperature for 16 h. The reaction mixture was poured into water (50 ml) and extracted with chloroform. The extract was dried over sodium sulfate then evaporated to dryness. The residual oil was purified by column chromatography on silica gel. 4-Nitrophenol was eluted with ether and **13** was eluted with ethyl acetate. The fractions containing only **13** were combined and concentrated. The residue was crystallized from ether–hexane to give **13** (270 mg, yield 20%) as pale-yellow needles. mp 88—90 °C. $[\alpha]_D^{22}$ +20° (*c*=1, MeOH). *Anal.* Calcd for $C_{32}H_{36}N_2O_{15}$: C, 55.81; H, 5.27; N. 4.07. Found: C, 55.50; H, 5.44; N, 3.96. IR ν_{max}^{KBr} cm^{-1}: 1750, 1665, 1615, 1595, 1515. ^{1}H-NMR ($CDCl_3$): 1.91 (3H, s, NAc), 2.03 (3H, s, OAc), 2.04 (3H, s, OAc), 2.10 (3H, s, OAc), 2.18 (3H, s, OAc), 2.30 (1H, br t, *J*=13.0 Hz, 3-H_{ax}), 2.75 (1H, dd, *J*=4.5, 13.0 Hz, 3-H_{eq}), 4.08 (1H, dd, *J*=4.5, 12.0 Hz, 9-H), 4.14 (1H, br q, *J*=10.5 Hz, 5-H), 4.21 (1H, dd, *J*=2.5, 12.0 Hz, 9-H'), 4.67 (1H, br d, *J*=11.0 Hz, 6-H), 4.92 (1H, d, *J*=11.5 Hz, –CHPh), 4.96 (1H, ddd, *J*=4.5, 10.0, 12.0 Hz, 4-H), 5.17 (1H, d, *J*=11.5 Hz, –CHPh), 5.35 (2H, br s, 7-H and 8-H), 5.38 (1H, d, *J*=10.0 Hz, NH), 7.00 (2H, d, *J*=9.0 Hz, phenyl group), 7.12—7.25 (4H, m, phenyl group), 7.32—7.38 (1H, m, phenyl group), 7.96 (2H, d, *J*=9.0 Hz, phenyl group).

4-Aminophenyl 5-Acetamido-4,7,8,9-tetra-*O*-acetyl-3,5-dideoxy-α-D-*glycero*-D-*galacto*-2-nonulopyranosidonic Acid (14) A solution of **13** (230 mg, 0.33 mmol) in ethyl acetate (20 ml) was treated with hydrogen over PtO_2 (100 mg) for 3 h at room temperature. The solution was filtered through Celite and evaporated to dryness at 20 °C. The residue was crystallized from chloroform–methanol to give **14** (163 mg, yield 86%) as colorless needles. mp 128 °C (dec.). $[\alpha]_D^{22}$ +248° (*c*=1, MeOH). *Anal.* Calcd for $C_{25}H_{32}N_2O_{13}$: C, 53.79; H, 5.56; N, 4.83. Found: C, 53.99; H, 5.74; N, 4.46. IR ν_{max}^{KBr} cm^{-1}: 350, 1740, 1660, 1515. ^{1}H-NMR ($CDCl_3$:CD_3OD=1:1): 1.78 (3H, s, NAc), 1.91 (3H, s, OAc), 1.99 (3H, s, OAc), 2.02 (3H, s, OAc), 1.93 (1H, t, *J*=12.5 Hz, 3-H_{ax}), 2.58 (1H, dd, *J*=4.5, 12.5 Hz, 3-H_{eq}), 3.90 (1H, br t, *J*=10.5 Hz, 5-H), 4.05 (1H, dd, *J*=4.5, 12.5 Hz, 9-H), 4.25 (1H, dd, *J*=2.0, 12.5 Hz, 9-H'), 4.28 (1H, br d, *J*=10.5 Hz, 6-H), 4.92 (1H, ddd, *J*=4.5, 10.5, 12.0 Hz, 4-H), 5.23 (2H, br s, 7-H and 8-H), 6.61 (2H, d, *J*=9.0 Hz, phenyl group), 6.84 (2H, d, *J*=9.0 Hz, phenyl group).

7-*N*-{4-*O*-(Methyl 5-Acetamido-4,7,8,9-tetra-*O*-acetyl-3,5-dideoxy-α-D-*glycero*-D-*galacto*-2-nonulopyranosylonate)phenyl}-9a-methoxymitosane (15) A solution of **3** (100 mg, 0.27 mmol) in methanol (40 ml) was treated with **9** (800 mg, 1.35 mmol). The reaction mixture was stirred at room temperature for 5 d. The residue was purified by column chromatography on silica gel with chloroform–methanol (20:1) to give **15** (131 mg, yield 51%) as dark bluish purple amorphous powder. *Anal.* Calcd for $C_{41}H_{49}N_5O_{18}$: C, 54.73; H, 5.49; N, 7.78. Found: C, 54.65; H, 5.49; N, 7.76. FD-MS *m/z*: 900 ($M^+ + 1$), 922 ($M^+ + Na$). IR ν_{max}^{KBr} cm^{-1}: 1735, 1635, 1560, 1500. UV λ_{max}^{MeOH} nm (log ε): 375 (4.08), sh 250 (4.27), 215 (4.34). ^{1}H-NMR data are given in Tables III and IV.

7-*N*-{4-*O*-(Methyl 5-Acetamido-3,5-dideoxy-α-D-*glycero*-D-*galacto*-2-nonuropyranosylonate)phenyl}-9a-methoxymitosane (16) A solution of **15** (20 mg, 0.022 mmol) in methanol (15 ml) was treated with 28% sodium methoxide–methanol (20 mg). The reaction mixture was stirred at room temperature for 25 min and the progress of the reaction was monitored by TLC with chloroform–methanol (10:1). Then sodium methoxide in the reaction mixture was removed by column chromatography on silica gel with methanol and the eluate was evaporated under reduced pressure. The residue was extracted with ethyl acetate (30 ml) and filtered, and the filtrate was evaporated to dryness to give **16** (12 mg, yield 75%) as a dark green amorphous powder. *Anal.* Calcd for $C_{33}H_{41}N_5O_4$: C, 69.33; H, 7.23; N, 12.25. Found: C, 69.29; H, 7.15; N, 12.22. FD-MS *m/z*: 732 ($M^+ + 1$), 754 ($M^+ + Na$). IR ν_{max}^{KBr} cm^{-1}: 1730, 1635, 1560, 1505. UV λ_{max}^{MeOH} nm (log ε): 375 (4.20), sh 250 (4.25), 215 (4.50). ^{1}H-NMR data are given in Tables III and IV.

7-*N*-{4-*O*-(Sodium 5-Acetamido-4,7,8,9-tetra-*O*-acetyl-3,5-dideoxy-α-D-*glycero*-D-*galacto*-2-nonulopyranosylonate)phenyl}-9a-methoxymitosane (17) A solution of **3** (100 mg, 0.27 mmol) in pyridine (1 ml) and methanol (30 ml) was treated with **14** (500 mg, 0.88 mmol). The reaction mixture was stirred for 12 h at room temperature and evaporated to dryness under reduced pressure. The residue was purified by column chromatography on silica gel (after quenching with pyridine) with chloroform–methanol (10:1) and the eluate was evaporated to dryness under reduced pressure. The resulting powder was dissolved in 3% $NaHCO_3$, and chromatographed on Diaion HP20 with 75% methanol. The eluent was evaporated under reduced pressure. Lyophilization of the residue gave **17** (156 mg, yield 60%) as a dark green amorphous powder. *Anal.* Calcd for $C_{40}H_{46}N_5NaO_{18}$: C, 52.92; H, 5.10; N, 7.71. Found: C, 52.88; H, 5.10; N, 7.67. FD-MS *m/z*: 930 ($M^+ + Na$). IR ν_{max}^{KBr} cm^{-1}: 1730, 1630, 1560, 1505. UV λ_{max}^{MeOH} nm (log ε): 395 (3.98), 230 (4.35). ^{1}H-NMR data are given in Tables III and IV.

Cytotoxicity Tumor cells were maintained in plastic dishes in RPMI 1640 medium supplemented with 10% fetal calf serum and kanamycin (60 μg/ml). For the drug treatment, tumor cells (4×10^3 P388 or P388/ADM) were incubated at 37 °C for 24 h in a 96-well microplate containing 200 μl/ml of growth medium in a humidified atmosphere of 5% CO_2. Drug solution (5 μl) was added to each well and incubation was continued for 72 h. After the incubation, 20 μl of tetrazolium (MTT) stock solution (5 mg/ml) was added to each well and the plate was incubated at 37 °C for 4 h. After aspiration of the medium, dimethyl sulfoxide (100 μl) was added to each well and mixed. The plate was read on a microplate reader, using a test wavelength of 570 nm (reference wavelength at 630 nm) as described by Alley *et al.*[21] The IC_{50} values were determined by plotting the logarithm of the drug concentration versus the growth rate of the treated cells.

Antibacterial Activity *E. coli* NIHJ was cultured in peptone broth (polypeptone 1%, NaCl 0.5%) at 37 °C for 24 h. Nutrient agar (Difco Lab., Michigan) medium was mixed with the culture solution of *E. coli* to produce a final concentration of 0.1%. Anti-*E. coli* activities of derivatives of **2** were determined by the paper disc (6 mm in diameter, thin type) method.

Antitumor Activity For evalution of antitumor activity of derivatives of **2**, P388/ADM (1×10^5) cells were inoculated i.p. into CDF1 mice on day 0, and derivatives were administered i.p. on days 1, 5, and 9 after tumor inoculation. Antitumor activity was expressed as the percent increase in life span (ILS).

Acknowledgements We are indebted to Dr. Takashi Nara and Mr. Akio Fujinuma of Kyowa Hakko Kogyo Co., Ltd., for a generous supply of mitomycin A and C. This work was supported in part by a Grant-in-Aid for Scientific Research (63470129) from the Ministry of Education, Science and Culture, and by grants from Morimura Gakuen and the Waksman Foundation of Japan.

References

1) This contitutes Part XXIII in the series entitled "Studies on Sialic Acids."
2) W. A. Remers, "The Chemistry of Antitumor Antibiotics," John Wiley and Sons, Inc., New York, 1979, pp. 221—276.
3) S. K. Carter and S. T. Crooke, "Mitomycin C. Current Status and New Developments," Academic Press, New York, 1979.
4) S. M. Sami, B. S. Iyengar, W. A. Remers, and W. T. Bradner, *J. Med. Chem.*, **30**, 168 (1987).
5) Y. Tokunaga, T. Iwase, J. Fujisaki, S. Sawai, and A. Kawayama, *Chem. Pharm. Bull.*, **36**, 3557 (1988).
6) R. Schauer, A. K. Shukia, C. Schroder, and E. Miller, *Pure Appl. Chem.*, **56**, 907 (1984).
7) S. Hakomori, *Chem. Phys. Lipids*, **42**, 209 (1986).
8) R. R. Schmidt, *Pure Appl. Chem.*, **61**, 1257 (1989).
9) K. Furuhata, K. Komiyama, K. Takeda, H. Takayanagi, K. Torii, K. Mishima, H. Ogura, and T. Hata, *Chem. Pharm. Bull.*, **37**, 2651 (1989).
10) R. Imai, K. Komatsu, C. Urakawa, M. Morimoto, and N. Nakamura, *Gann*, **71**, 560 (1980).
11) G. Ekborg, P. J. Garegg, and B. Gotthamar, *Acta. Chem. Scand.*, **B29**, 765 (1975).
12) S. M. Sami, B. S. Iyengar, S. E. Tarnow, W. A. Remers, W. T. Bradner, and J. E. Schuring, *J. Med. Chem.*, **27**, 701 (1984).
13) A. Thompson and M. L. Wolfrom, "Methods in Carbohydrate Chemistry," Vol. II, R. L. Whistler and M. L. Wolfron, Eds, Academic Press, New York and London, 1963, pp. 215—220.
14) "Sialic Acid 1988," Proceeding of the Japan–German Symposium on Sialic Acids, R. Schauer and T. Yamakawa, Eds, Barbel Mende, Kiel, 1988.
15) S. Tuji, T. Yamakawa, M. Tanaka, and Y. Nagai, *J. Neurochem.*, **50**, 414 (1988).
16) I. Kijima-Suda, T. Miyazawa, M. Itoh, S. Toyoshima, and T. Osawa, *Cancer Res.*, **48**, 3728 (1988).
17) V. Eschenfelder and R. Brossmer, *Carbohydr. Res.*, **162**, 294 (1987).
18) P. Meindl and H. Tuppy, *Monatsch. Chem.*, **96**, 802 (1965).
19) K. Furuhata and H. Ogura, *Chem. Pharm. Bull.*, **37**, 2037 (1989).
20) H. Paulsen and H. Tietz, *Carbohydr. Res.*, **125**, 47 (1984).
21) M. C. Alley, D. A. Scudiero, A. Monks, M. L. Hursey, M. J. Shoemaker, and M. R. Boyd, *Cancer Res.*, **48**, 589 (1988).

The Remarkable Effect of Titanium Tetraisopropoxide in Diastereoselective Reaction of Carbaldehydes with Chiral Benzenesulfonamide Lithium Complexes

Hiroshi TAKAHASHI,* Takeshi TSUBUKI, and Kimio HIGASHIYAMA

Faculty of Pharmaceutical Science, Hoshi University, 2–4–41, Ebara, Shinagawa, Tokyo 142, Japan. *Received June 12, 1990*

Chiral benzenesulfonamide titanium ate-complexes (4 and 8) were prepared from the lithium complexes (2 and 6) by treatment with titanium tetraisopropoxide. The diastereoselective reactions of aromatic carbaldehydes with 4 and 8 were performed, and the chiral *o*-(1-aryl-1-hydroxymethyl)benzenesulfonamides (3a—d and 7a—e) were obtained in 80—87% yields. The diastereomeric excesses (d.e.) of these products were evaluated as 62—82%. These compounds were also prepared from the lithium complexes (2 and 6), but the d.e. values were only 6—14% in this case.

Keywords chiral benzenesulfonamide; chiral benzenesulfonylpyrrolidine; chiral *ortho*-lithiated benzamide; diastereoselective reaction; (*S*)-*N*-methylvalinol; organolithium complex; organotitanium ate-complex; (*S*)-prolinol; titanium tetraisopropoxide; transmetalation

The utility of *ortho*-metalation in the regiospecific synthesis of aromatic compounds has been the subject of a number of reviews,[1-3] and several papers have appeared on the preparation of phthalides *via* the *ortho*-lithiated benzamides[4] or phenyloxazolines.[5,6] Meyers and co-workers[7] reported that chiral 2-(*o*-lithiophenyl)-4-methoxymethyl-5-phenyloxazoline could be condensed with various carbonyl compounds to afford the chiral imino lactones in 60—70% yields, though with rather poor stereoselectivity (2—28% diastereoselectivities). In this paper, we wish to describe the stereoselective reaction of chiral *ortho*-metalated benzenesulfonamides with various carbaldehydes and the key role of titanium tetraisopropoxide in this reaction.

The synthesis of (*S*)-*N*-(2′-hydroxy-1′-isopropylethyl)-*N*-methylbenzenesulfonamide (**1**) was achieved by condensation of (*S*)-*N*-methylvalinol with benzenesulfonyl chloride in 75% yield, and the lithium 2-(*o*-lithiobenzenesulfonamido)-2-isopropylethoxide (**2**) was prepared from (*S*)-**1** by treatment with two equimolar amounts of *n*-butyllithium. The reaction of aromatic carbaldehydes such as benzaldehyde, *p*-tolualdehyde, *p*-anisaldehyde, and 1-naphthaldehyde with **2** gave diastereomeric mixtures of *o*-(1′-aryl-1′-hydroxymethyl)-*N*-(2-hydroxy-1-isopropylethyl)-*N*-methylbenzenesulfonamides (**3a—d**) in 79—84% yields. Two diastereomeric forms could be considered, depending on the configuration of the newly created asymmetric carbon atom of the 1′-aryl-1′-hydroxymethyl groups. The ratios of the two isomers were estimated by proton nuclear magnetic resonance (^{1}H-NMR) spectrometry, and the diastereomeric excesses (d.e.) of these products were evaluated to be 6—10%.

Recent work has demonstrated the utility of exchanging lithium for copper, magnesium, zinc,[8] and titanium,[9] and we have reported that lithium complexes are easily converted into titanium ate-complexes by treatment with titanium tetraisopropoxide.[9] Thus, the chiral benzenesulfonamide lithium complex (**2**) was converted into the chiral benzenesulfonamide titanium ate-complex (**4**) by treatment of an equimolar amount of titanium tetraisopropoxide. The diastereoselective reaction of aromatic carbaldehydes with **4** was performed in a similar manner to that employed for the reaction with **2** to give **3a—d** in 80—87% yields. The d.e. values of these products were estimated as 66—80% by ^{1}H-NMR spectrometry. A great improvement in the diastereoselectivity was thus achieved with the aid of titanium tetraisopropoxide. The major products of **3a—d**

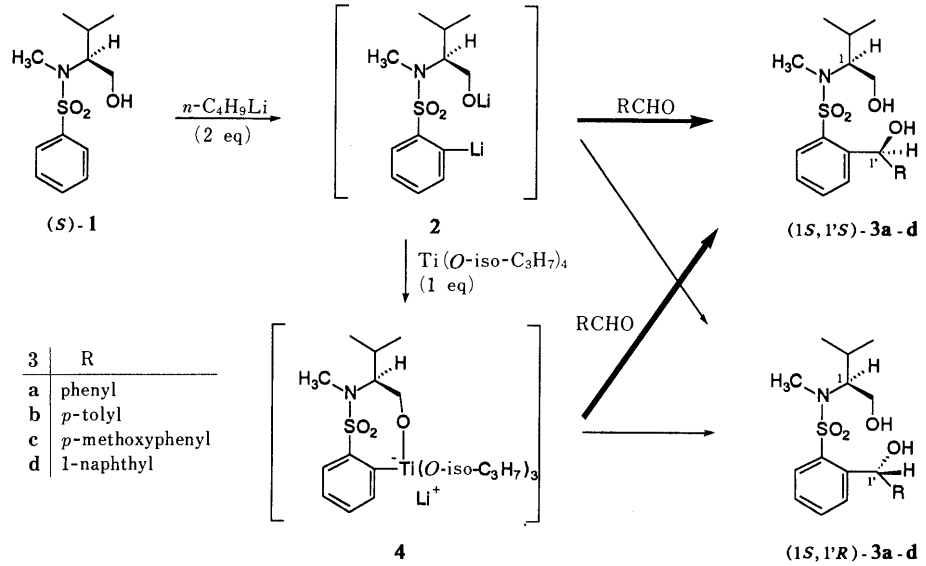

Chart 1

TABLE I. Reaction of Carbaldehydes with Chiral Benzenesulfonamide Metal Complexes

Carbaldehyde	Product	Lithium complex 2[a] 6[b]			Titanium complex 4[a] 8[b]		
		Complex	Yield[c] (%)	Ratio of isomers[d] (1′S) : (1′R)	Complex	Yield[c] (%)	Ratio of isomers[d] (1′S) : (1′R)
Phenyl	**3a**	**2**	82	54 : 46	**4**	85	83 : 17
p-Tolyl	**3b**	**2**	84	54 : 46	**4**	82	87 : 13
p-Methoxyphenyl	**3c**	**2**	81	53 : 47	**4**	80	90 : 10
1-Naphthyl	**3d**	**2**	79	55 : 45	**4**	87	89 : 11
Phenyl	**7a**	**6**	75	57 : 43	**8**	85	83 : 17
p-Tolyl	**7b**	**6**	82	56 : 44	**8**	80	84 : 16
p-Methoxyphenyl	**7c**	**6**	80	55 : 45	**8**	82	88 : 12
1-Naphthyl	**7d**	**6**	80	57 : 43	**8**	84	91 : 9
2-Furyl	**7e**	**6**	75	53 : 47	**8**	85	81 : 19

a) Run at −50°C for 4 h. *b*) Run at 0°C for 3 h. *c*) Isolated yield. *d*) Estimated by ^{1}H-NMR (270 MHz) spectral analysis.

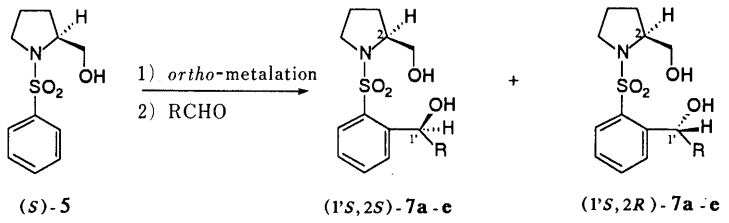

(*S*)-**5** (1′*S*,2*S*)-**7a-e** (1′*S*,2*R*)-**7a-e**

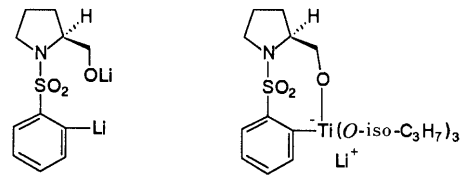

6 **8**

7	R
a	phenyl
b	*p*-tolyl
c	*p*-methoxyphenyl
d	1-naphthyl
e	2-furyl

Chart 2

prepared from **2** coincided with the major products prepared from **4** on the basis of ^{1}H-NMR spectral comparison, and the former minor products also coincided with the later minor products. The optically active compounds, *i.e.*, (1*S*,1′*S*)-**3a—d** (major products) and (1*S*,1′*R*)-**3a—d** (minor products), were isolated from the diastereomeric mixtures by recrystallization.

The preparation of (*S*)-*N*-benzenesulfonyl-2-hydroxymethylpyrrolidine (**5**) was achieved by condensation of (*S*)-prolinol with benzenesulfonyl chloride in 90% yield, and the reaction of **5** with two equimolar amounts of *n*-butyllithium gave chiral lithium *N*-(*o*-lithiobenzenesulfonyl)-pyrrolidinyl-2-methoxide (**6**). The condensation of aromatic carbaldehydes such as benzaldehyde, *p*-tolualdehyde, *p*-anisaldehyde, 1-naphthaldehyde, and 2-furaldehyde with **6** gave diastereomeric mixtures of *N*-[*o*-(1′-aryl-1′-hydroxymethyl)benzenesulfonyl]-2-hydroxymethylpyrrolidines (**7a—e**) in 75—82% yields. The d.e. values of these products were estimated as 6—14% by ^{1}H-NMR spectrometry. The chiral lithium complex (**6**) was converted into the chiral benzenesulfonylpyrrolidine titanium ate-complex (**8**) by treatment with an equimolar amount of titanium tetraisopropoxide, and the reaction of aromatic carbaldehydes with **8** was performed to give diastereomeric mixtures of **7a—e** in 80—85% yields. The d.e. values of these products were

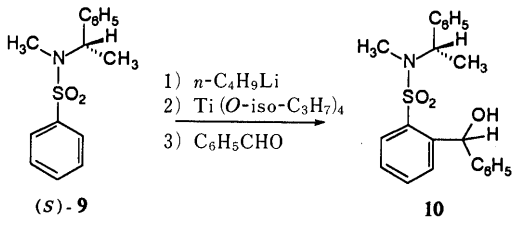

(*S*)-**9** **10**

Chart 3

estimated as 62—82% by ^{1}H-NMR spectrometry. The major products of **7a—e** prepared from **6** coincided with the major products produced from **8** on the basis of ^{1}H-NMR spectral comparison, and the former minor products coincided with the later minor products. The major component of *N*-[*o*-(1′-hydroxy-1′-(α-naphthyl)methyl)benzenesulfonyl]-2-hydroxymethylpyrrolidine [(1′*S*,2*S*)-**7d**] was a solid, which was isolated by recrystallization from the isomeric mixture, but diastereomerically pure compounds could not be isolated from the oily diastereomeric mixtures (**7a—c** and **7e**).

The diastereoselective reactions of (*S*)-*N*-methyl-*N*-(1-phenylethyl)benzenesulfonamide (**9**) lacking the hydroxymethyl group at the chiral center were examined. Benzaldehyde was condensed with the corresponding lith-

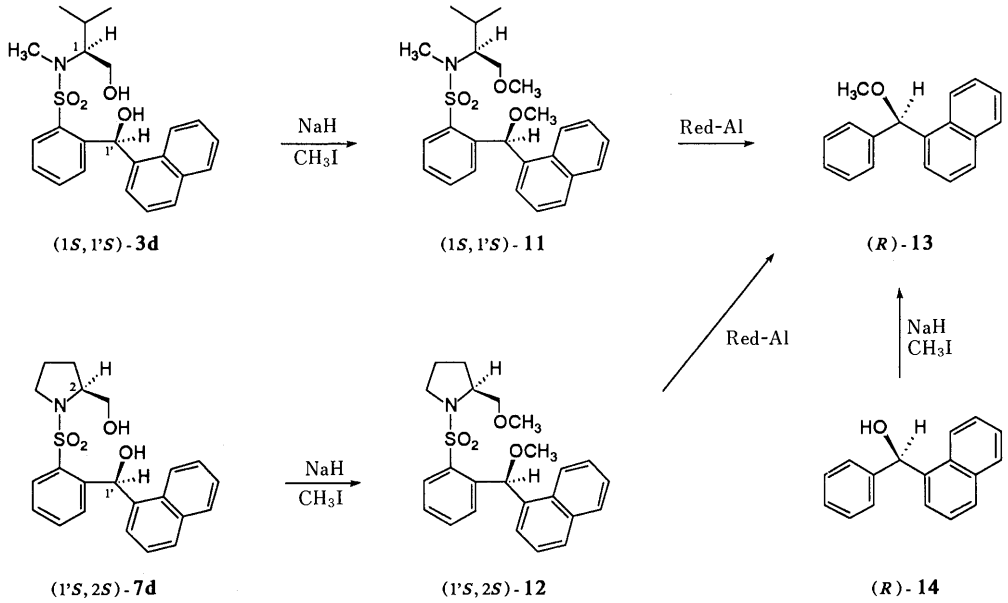

Chart 4

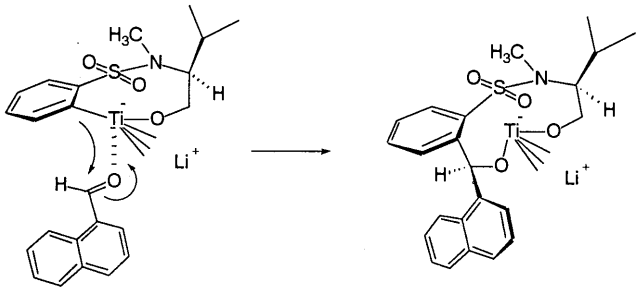

(a) (b)

Chart 5

ium and titanium complexes to give a mixture of *o*-(1-hydroxy-1-phenylmethyl)-*N*-methyl-*N*-(1-phenylethyl)-benzenesulfonamide (**10**) in 85% and 82% yields, and the d.e. values of these products were estimated as 9% and 6% by ^{1}H-NMR spectrometry. It was suggested that the hydroxymethyl group is important for increasing the diastereoselectivity, because the titanium could be linked between the oxygen atom of the chiral hydroxymethyl group and the carbon atom at the *ortho*-position of the benzene ring.

The absolute configurations at the 1'-positions of **3d** and **7d** were elucidated as follows: The major products of **3d** and **7d** gave (1*S*,1'*S*)-*N*-(2-methoxy-1-isopropylethyl)-*o*-[1'-methoxy-1'-(α-naphthyl)methyl]-*N*-methylbenzenesulfonamide (**11**) and (1'*S*,2*S*)-*N*-[*o*-(1'-methoxy-1'-(α-naphthyl)-methyl)benzenesulfonyl]-2-methoxymethylpyrrolidine (**12**), respectively, upon *O*-methylation with sodium hydride and methyl iodide. The removal of the sulfonamide groups was performed by hydrogenolysis with sodium bis(2-methoxyethoxy)aluminum hydride (Red-Al) to give (*R*)-1-methoxy-1-(α-naphthyl)-1-phenylmethane (**13**). On the other hand, (*R*)-**13** was synthesized by *O*-methylation of (*R*)-1-(α-naphthyl)-1-phenylmethanol (**14**)[10,11] and the identical with the compounds prepared from **11** and **12**. Consequently, the absolute configurations of **3d** and **7d** were determined as (1*S*,1'*S*) and (1'*S*,2*S*), and those of **3a**—**c**, **7a**—**c**, and **7e** may be assumed to have the same configurations because these compounds are expected to be formed through a similar reaction mechanism.

It was found that the reaction of carbaldehydes with chiral benzenesulfonamide titanium ate-complexes by means of 1,6-asymmetric induction proceeds with high diastereoselectivity. Consequently, we propose a reaction mechanism in which the chiral benzenesulfonamide titanium ate-complex approaches the carbonyl carbon atom (a), and a chelated dialcoholatotitanium ate-complex intermediate (b) is formed, as shown in Chart 5.

Experimental

The ^{1}H-NMR spectra were obtained with a JEOL JNM-GSX270 spectrometer and the mass spectra (MS) were recorded with a JEOL JMS-D300 spectrometer by using the electron impact (EI) and the chemical ionization (CI) (isobutane) methods. The melting points were measured with a Yanagimoto micromelting-point apparatus and are uncorrected. The optical rotations were measured with a JASCO DIP-360 digital polarimeter.

(*S*)-*N*-(2'-Hydroxy-1'-isopropylethyl)-*N*-methylbenzenesulfonamide (1) Benzenesulfonyl chloride (17.7 g, 100 mmol) was added dropwise to a stirred solution of (*S*)-*N*-methylvalinol (12.3 g, 105 mmol) and Et_3N (11.1 g, 110 mmol) in CH_2Cl_2 (100 ml) at 0 °C, and stirring was continued at room temperature for 2 h. The reaction mixture was concentrated under reduced pressure. The orange oily residue was dissolved in AcOEt (120 ml) and passed through a short column of silica gel. The solvent was evaporated off under reduced pressure to give a colorless solid (19.3 g, 75%). Colorless plates, mp 72—73 °C (pentane–CH_2Cl_2). $[\alpha]_D^{20}$ −16.9° (*c*=1.04, $CHCl_3$). *Anal.* Calcd for $C_{12}H_{19}NO_3S$: C, 56.00; H, 7.44; N, 5.44. Found: C, 56.14; H, 7.54; N, 5.36. MS *m/z*: EI, 226 ($M^+ - CH_2OH$, 100%), 214 ($M^+ - C_3H_7$, 35%), 141 ($PhSO_2^+$, 50%); CI, 258 ($M^+ + 1$, 100%), 226 ($M^+ - CH_2OH$, 24%). ^{1}H-NMR ($CDCl_3$) δ: 0.74 (3H, d, *J*=6.7 Hz, $CHC\underline{H}_3$), 0.94 (3H, d, *J*=6.7 Hz, $CHC\underline{H}_3$), 1.53 (1H, dd, *J*=4.9, 6.1 Hz, $CH_2O\underline{H}$), 1.72 (1H, double septet, *J*=6.7, 8.6 Hz, $CHC\underline{H}(CH_3)_2$), 2.79 (3H, s, NCH_3), 3.53 (1H, ddd, *J*=4.9, 8.6, 11.0 Hz, $NCHC\underline{H}_2OH$), 3.64 (1H, dt, *J*=3.1, 8.6 Hz, $NC\underline{H}CH_2OH$), 3.74 (1H, ddd, *J*=3.1, 6.1, 11.0 Hz, $NCHC\underline{H}_2OH$), 7.47—7.89 (5H, m, aromatic H).

Reaction of Carbaldehydes with Lithium Complex (2) *n*-BuLi (12.5 mmol, 7.8 ml of 1.6 M solution of hexane) was added dropwise to a stirred solution of (*S*)-**1** (1.29 g, 5 mmol) in tetrahydrofuran (THF) (25 ml) at 0 °C under a nitrogen atmosphere, and stirring was continued for 10 min. The resulting solution was placed on a cold bath at −50 °C and stirred for 20 min to form a lithium complex (**2**). A solution of a carbaldehyde

(benzaldehyde, *p*-tolualdehyde, *p*-anisaldehyde, or 1-naphthaldehyde, 6.5 mmol) in THF (8 ml) was slowly added dropwise to a stirred solution of **2** using an infusion pump at −50 °C, and stirring was continued for 4 h. The reaction mixture was treated with NH_4Cl saturated aqueous solution (1 ml) and dried over $MgSO_4$. The resulting white precipitate was filtered off, and the filtrate was concentrated under reduced pressure. The d.e. value of the residue thus obtained was estimated by ^{1}H-NMR spectrometry. The residue was subjected to column chromatography on silica gel with a solution of hexane–ether (2:3) to give the corresponding diastereomeric mixture (**3a—d**). The experimental data are summarized in Table I.

Reaction of Carbaldehydes with Titanium Complex (4) Ti(*O*-iso-C_3H_7)$_4$ (1.8 ml, 6 mmol) was added dropwise to a stirred solution of **2** prepared form (*S*)-**1** (5 mmol), and stirring was continued at −50 °C for 30 min to from a titanium complex (**4**). A solution of a carbaldehyde (6.5 mmol) in THF (8 ml) was slowly added dropwise to the stirred solution of **4** using an infusion pump at −50 °C, and stirring was continued for 4 h. The reaction mixture was worked up as described for the reaction of **2** to give the corresponding diastereomeric mixture (**3a—d**). The experimental data are summarized in Table I.

(1*S*,1′*S*)-*N*-(2-Hydroxy-1-isopropylethyl)-*o*-(1′-hydroxy-1′-phenylmethyl)-*N*-methylbenzenesulfonamide (**3a**) [Major Product]: This compound was isolated from the diastereomeric mixture (ratio, 83:17) by recrystallization from hexane–CH_2Cl_2 solution. Colorless plates, mp 105—106 °C (hexane–CH_2Cl_2). $[\alpha]_D^{22}$ −236.7° (*c*=0.39, $CHCl_3$). *Anal.* Calcd for $C_{19}H_{25}NO_4S$: C, 62.78; H, 6.93; N, 3.85. Found: C, 63.02; H, 7.03; N, 3.79. MS *m/z*: EI, 345 ($M^+ - H_2O$, 0.1%), 332 ($M^+ - CH_2OH$, 12%); CI, 364 ($M^+ + 1$, 0.4%), 346 ($M^+ - OH$, 100%), 332 ($M^+ - CH_2OH$, 5%). ^{1}H-NMR ($CDCl_3$) δ: 0.97 (3H, d, *J*=6.7 Hz, $CHCH_3$), 1.03 (3H, d, *J*=6.7 Hz, $CHCH_3$), 1.78 (1H, double septet, *J*=6.7, 8.5 Hz, $CHCH(CH_3)_2$), 2.15 (1H, br, OH), 2.75 (3H, s, NCH_3), 3.47—3.56 (1H, m, $NCHCH_2OH$), 3.82—3.92 (2H, m, $NCHCH_2OH$), 4.15 (1H, br, OH), 6.88 (1H, s, PhCHOH), 7.20—8.01 (9H, m, aromatic H).

(1*S*,1′*R*)-**3a** [Minor Product]: This compound was isolated from the diastereomeric mixture (ratio, 54:46) by recrystallization from ether–hexane solution. Colorless plates, mp 139—140 °C (hexane–benzene). $[\alpha]_D^{21}$ +189.2° (*c*=0.25, $CHCl_3$). *Anal.* Calcd for $C_{19}H_{25}NO_4S$: C, 62.78; H, 6.93; N, 3.85. Found: C, 62.91; H, 7.01; N, 3.85. MS *m/z*: EI, 345 ($M^+ - H_2O$, 0.1%), 332 ($M^+ - CH_2OH$, 16%); CI, 364 ($M^+ + 1$, 3%), 346 ($M^+ - OH$, 100%), 332 ($M^+ - CH_2OH$, 9%). ^{1}H-NMR ($CDCl_3$) δ: 0.95 (3H, d, *J*=6.7 Hz, $CHCH_3$), 0.98 (3H, d, *J*=6.7 Hz, $CHCH_3$), 1.60 (1H, br, OH), 1.83 (1H, double septet, *J*=6.7, 9.2 Hz, $CHCH(CH_3)_2$), 3.01 (3H, s, NCH_3), 3.41 (1H, dt, *J*=3.7, 9.2 Hz, $NCHCH_2OH$), 3.58 (1H, dd, *J*=9.2, 12.2 Hz, $NCHCH_2OH$), 3.72 (1H, dd, *J*=3.7, 12.2 Hz, $NCHCH_2OH$), 3.95 (1H, br, OH), 6.66 (1H, s, PhCHOH), 7.20—8.08 (9H, m, aromatic H).

(1*S*,1′*S*)-*N*-(2-Hydroxy-1-isopropylethyl)-*o*-[1′-hydroxy-1′-(*p*-tolyl)-methyl]-*N*-methylbenzenesulfonamide (**3b**) [Major Product]: This compound was isolated from the diastereomeric mixture (ratio, 87:13) by recrystallization from hexane–CH_2Cl_2 solution. Colorless plates, mp 68.5—69.5 °C (hexane–CH_2Cl_2). $[\alpha]_D^{23}$ −191.8° (*c*=0.60, $CHCl_3$). *Anal.* Calcd for $C_{20}H_{27}NO_4S$: C, 63.63; H, 7.21; N, 3.71. Found: C, 63.73; H, 7.36; N, 3.46. MS *m/z*: EI, 359 ($M^+ - H_2O$, 12%), 346 ($M^+ - CH_2OH$, 8%); CI, 378 ($M^+ + 1$, 0.7%), 360 ($M^+ - OH$, 100%), 346 (M^+ -CH_2OH, 2%). ^{1}H-NMR ($CDCl_3$) δ: 0.97 (3H, d, *J*=6.7 Hz, $CHCH_3$), 1.02 (3H, d, *J*=6.7 Hz, $CHCH_3$), 1.78 (1H, double septet, *J*=6.7, 8.6 Hz, $CHCH(CH_3)_2$), 2.09 (1H, br, OH), 2.32 (3H, s, $PhCH_3$), 2.76 (3H, s, NCH_3), 3.47—3.56 (1H, m, $NCHCH_2OH$), 3.81—3.90 (2H, m, $NCHCH_2OH$), 3.98 (1H, br, OH), 6.84 (1H, s, PhCHOH), 7.13—8.00 (8H, m, aromatic H).

(1*S*,1′*R*)-**3b** [Minor Product]: This compound was isolated from the diastereomeric mixture (ratio, 54:46) by recrystallization from ether. Colorless needles, mp 153.5—154.5 °C (ether). $[\alpha]_D^{24}$ +175.6° (*c*=0.52, $CHCl_3$). *Anal.* Calcd for $C_{20}H_{27}NO_4S$: C, 63.63; H, 7.21; N, 3.71. Found: C, 63.87; H, 7.33: N, 3.66. MS *m/z*: EI, 359 ($M^+ - H_2O$, 7%), 346 ($M^+ - CH_2OH$, 8%); CI, 378 ($M^+ + 1$, 0.6%), 360 ($M^+ - OH$, 100%), 346 ($M^+ - CH_2OH$, 4%). ^{1}H-NMR ($CDCl_3$) δ: 0.95 (3H, d, *J*=6.7 Hz, $CHCH_3$), 0.96 (3H, d, *J*=6.7 Hz, $CHCH_3$), 1.71 (1H, t, *J*=5.5 Hz, CH_2OH), 1.82 (1H, double septet, *J*=6.7, 9.2 Hz, $CHCH(CH_3)_2$), 2.35 (3H, s, $PhCH_3$), 3.00 (3H, s, NCH_3), 3.41 (1H, dt, *J*=3.7 9.2 Hz, $NCHCH_2OH$), 3.58 (1H, ddd, *J*=5.5, 9.2, 11.6 Hz, $NCHCH_2OH$), 3.71 (1H, ddd, *J*=3.7, 5.5, 11.6 Hz, $NCHCH_2OH$), 3.82 (1H, d, *J*=3.1 Hz, CHOH), 6.63 (1H, d, *J*=3.1 Hz, PhCHOH), 7.17—8.07 (8H, m, aromatic H).

(1*S*,1′*S*)-*N*-(2-Hydroxy-1-isopropylethyl)-*o*-[1′-hydroxy-1′-(*p*-methoxyphenyl)methyl]-*N*-methylbenzenesulfonamide (**3c**) [Major Product]: This compound was isolated from the diastereomeric mixture (ratio, 90:10) by recrystallization from ether. Colorless plates, mp 111.5—112.5 °C (benzene). $[\alpha]_D^{22}$ −225.9° (*c*=0.65, $CHCl_3$). *Anal.* Calcd for $C_{20}H_{27}NO_5S$: C, 61.05; H, 6.92; N, 3.56. Found: C, 61.33; H, 7.13; N, 3.45. MS *m/z*: EI, 375 ($M^+ - H_2O$, 0.4%), 362 ($M^+ - CH_2OH$, 9%); CI, 394 ($M^+ + 1$, 0.2%), 376 ($M^+ - OH$, 100%), 362 ($M^+ - CH_2OH$, 3%). ^{1}H-NMR ($CDCl_3$) δ: 0.97 (3H, d, *J*=6.7 Hz, $CHCH_3$), 1.01 (3H, d, *J*=6.7 Hz, $CHCH_3$), 1.77 (1H, double septet, *J*=6.7, 9.2 Hz, $CHCH(CH_3)_2$), 2.16 (1H, br, OH), 2.74 (3H, s, NCH_3), 3.50 (1H, dd, *J*=10.4, 12.8 Hz, $NCHCH_2OH$), 3.78 (3H, s, OCH_3), 3.80—3.89 (2H, m, $NCHCH_2OH$), 4.01 (1H, br, OH), 6.81 (1H, s, PhCHOH), 6.83—7.99 (8H, m, aromatic H).

(1*S*,1′*R*)-**3c** [Minor Product]: This compound was isolated from the diastereomeric mixture (ratio, 53:47) by recrystallization in hexane–CH_2Cl_2 solution. Colorless needles, mp 149.5—150.5 °C (pentane–CH_2Cl_2). $[\alpha]_D^{25}$ +172.4° (*c*=0.41, $CHCl_3$). *Anal.* Calcd for $C_{20}H_{27}NO_5S$: C, 61.05; H, 6.92; N, 3.56. Found: C, 61.28; H, 7.05; N, 3.48. MS *m/z*: EI, 375 ($M^+ - H_2O$, 2%), 362 ($M^+ - CH_2OH$, 5%); CI, 394 ($M^+ + 1$, 0.3%), 376 ($M^+ - OH$, 100%), 362 ($M^+ - CH_2OH$, 1%). ^{1}H-NMR ($CDCl_3$) δ: 0.95 (3H, d, *J*=6.7 Hz, $CHCH_3$), 0.96 (3H, d, *J*=6.7 Hz, $CHCH_3$), 1.69 (1H, t, *J*=6.1 Hz, CH_2OH), 1.82 (1H, double septet, *J*=6.7, 9.2 Hz, $CHCH(CH_3)_2$), 3.00 (3H, s, NCH_3), 3.41 (1H, dt, *J*=3.7, 9.2 Hz, $NCHCH_2OH$), 3.58 (1H, ddd, *J*=6.1, 9.2, 12.2 Hz, $NCHCH_2OH$), 3.73 (1H, ddd, *J*=3.7, 6.1, 12.2 Hz, $NCHCH_2OH$), 3.81 (3H, s, OCH_3), 3.83 (1H, d, *J*=3.1 Hz, CHOH), 6.61 (1H, d, *J*=3.1 Hz, PhCHOH), 6.87—8.07 (8H, m, aromatic H).

(1*S*,1′*S*)-*N*-(2-Hydroxy-1-isopropylethyl)-*o*-[1′-hydroxy-1′-(α-naphthyl)methyl]-*N*-methylbenzenesulfonamide (**3d**) [Major Product]: This compound was isolated from the diastereomeric mixture (ratio, 89:11) by recrystallization from benzene. Colorless plates, mp 172—173 °C (benzene). $[\alpha]_D^{27}$ −215.1° (*c*=0.45, $CHCl_3$). *Anal.* Calcd for $C_{23}H_{27}NO_4S$: C, 66.80; H, 6.58; N, 3.39. Found: C, 66.89; H, 6.57; N, 3.24. MS *m/z*: EI, 395 ($M^+ - H_2O$, 0.2%), 382 ($M^+ - CH_2OH$, 6%); CI, 414 ($M^+ + 1$, 0.4%), 396 ($M^+ - OH$, 100%), 382 ($M^+ - CH_2OH$, 2%). ^{1}H-NMR ($CDCl_3$) δ: 0.99 (3H, d, *J*=6.7 Hz, $CHCH_3$), 1.06 (3H, d, *J*=6.7 Hz, $CHCH_3$), 1.88 (1H, double septet, *J*=6.7, 8.5 Hz, $CHCH(CH_3)_2$), 2.51 (1H, dd, *J*=4.3, 6.7 Hz, CH_2OH), 2.83 (3H, s, NCH_3), 3.56 (1H, ddd, *J*=6.7, 9.8, 11.6 Hz, $NCHCH_2OH$), 3.88 (1H, dt, *J*=4.3, 11.6 Hz, $NCHCH_2OH$), 3.98 (1H, ddd, *J*=4.3, 8.5, 9.8 Hz, $NCHCH_2OH$), 4.34 (1H, d, *J*=4.3 Hz, CHOH), 7.10—8.08 (12H, m, NaphCHOH, and aromatic H).

(1*S*,1′*R*)-**3d** [Minor Product]: This compound was isolated from the diastereomeric mixture (ratio, 55:45) by recrystallization from hexane–CH_2Cl_2 solution. Colorless needles, mp 140—140.5 °C (CH_2Cl_2). $[\alpha]_D^{26}$ +211.6° (*c*=0.17, $CHCl_3$). *Anal.* Calcd for $C_{23}H_{27}NO_4S$: C, 66.80; H, 6.58; N, 3.39. Found: C, 66.54; H, 6.64; N, 3.28. MS *m/z*: EI, 395 ($M^+ - H_2O$, 1%), 382 ($M^+ - CH_2OH$, 3%); CI, 414 ($M^+ + 1$, 0.8%), 396 ($M^+ - OH$, 100%), 382 ($M^+ - CH_2OH$, 4%). ^{1}H-NMR ($CDCl_3$) δ: 1.00 (3H, d, *J*=6.7 Hz, $CHCH_3$), 1.11 (3H, d, *J*=6.7 Hz, $CHCH_3$), 1.82 (1H, t, *J*=5.5 Hz, CH_2OH), 1.89 (1H, double septet, *J*=6.7, 8.6 Hz, $CHCH(CH_3)_2$), 3.08 (3H, s, NCH_3), 3.54—3.80 (3H, m, $NCHCH_2OH$), 4.17 (1H, d, *J*=2.4 Hz, CHOH), 7.07—8.19 (12H, m, NaphCHOH and aromatic H).

(*S*)-*N*-Benzenesulfonyl-2-hydroxymethylpyrrolidine (5) Benzenesulfonyl chloride (17.9 g, 101 mmol) was added dropwise to a stirred solution of (*S*)-prolinol (11.1 g, 110 mmol) and Et_3N (13.2 g, 130 mmol) in CH_2Cl_2 (100 ml) at 0°C, and strring was continued at room temperature for 2 h. The reaction mixture was worked up as described for the preparation of (*S*)-**1** to give a colorless oil (21.7 g, 90%). bp 160—162 °C (0.25 mmHg). $[\alpha]_D^{27}$ −58.8° (*c*=1.08, $CHCl_3$). *Anal.* Calcd for $C_{11}H_{15}NO_3S$: C, 54.75; H, 6.27; N, 5.80. Found: C, 54.87; H, 6.39; N, 5.74. MS *m/z*: EI, 223 ($M^+ - H_2O$, 25%), 210 ($M^+ - CH_2OH$, 100%), 141 ($PhSO_2^+$, 51%); CI, 242 ($M^+ + 1$, 100%), 224 ($M^+ - OH$, 53%), 210 ($M^+ - CH_2OH$, 18%). ^{1}H-NMR ($CDCl_3$) δ: 1.40—1.52 (1H, m, CH_2CH_2), 1.63—1.89 (3H, m, CH_2CH_2), 2.79 (1H, br, OH), 3.28 (1H, dt, *J*=6.7, 10.4 Hz, NCH_2), 3.48 (1H, dt, *J*=6.1, 10.4 Hz, NCH_2), 3.61—3.75 (3H, m, $NCHCH_2OH$), 7.52—7.89 (5H, m, aromatic H).

Reaction of Carbaldehydes with Lithium Complex (6) *n*-BuLi (2.4 mmol, 1.5 ml of 1.6 M solution of hexane) was added dropwise to a stirred solution of (*S*)-**5** (0.24 g, 1 mmol) in THF (5 ml) at 0 °C under a nitrogen atmosphere and the reaction mixture was stirred for 30 min to form a lithium complex (**6**). A solution of a carbaldehyde (benzaldehyde, *p*-tolualdehyde, *p*-anisaldehyde, 1-naphthaldehyde, or 2-furaldehyde, 1.3 mmol) in THF (1 ml) was slowly added dropwise to the stirred solution of **6** at 0 °C, and stirring was continued for 3 h. The reaction mixture was worked up as

described for the reaction of **2**. The d.e. value of the residue was estimated by ^{1}H-NMR spectrometry, and the residue was subjected to column chromatography on silica gel with the appropriate eluent to give the corresponding diastereomeric mixture (**7a—e**). The experimental data are summarized in Table I.

Reaction of Carbaldehydes with Titanium Complex (8) Ti(*O*-iso-C_3H_7)$_4$ (0.35 ml, 1.2 mmol) was added dropwise to a stirred solution of **6** prepared from (*S*)-**5** (1 mmol), and stirring was continued at 0 °C for 30 min to form the titanium complex (**8**). A solution of a carbaldehyde (1.3 mmol) in THF (1 ml) was slowly added dropwise to the stirred solution of **8** at 0 °C, and stirring was continued for 3 h. The reaction mixture was worked up as described for the reaction of **6** to give the corresponding diastereomeric mixture (**7a—e**). The experimental data are summarized in Table I.

N-[*o*-(1′-Hydroxy-1′-phenylmethyl)benzenesulfonyl]-2-hydroxymethylpyrrolidine (**7a**): Eluent, CH_2Cl_2–ether (10 : 1). MS *m/z*: EI, 329 ($M^+ - H_2O$, 0.1%), 316 ($M^+ - CH_2OH$, 43%); CI, 348 ($M^+ + 1$, 3%), 330 ($M^+ - OH$, 100%), 316 ($M^+ - CH_2OH$, 6%). ^{1}H-NMR ($CDCl_3$) δ: (1′*S*,2*S*)-**7a** (Major component); 1.77—2.02 (4H, m, CH_2CH_2), 2.48 (1H, t, J=4.3 Hz, CH_2OH), 3.16 (1H, dt, J=6.1, 9.8 Hz, NCH_2), 3.37 (1H, dt, J=6.7, 9.8 Hz, NCH_2), 3.58 (1H, dt, J=11.6, 4.3 Hz, $NCHCH_2OH$), 3.77 (1H, d, J=4.9 Hz, CHOH), 3.83 (1H, dt, J=11.6, 4.3 Hz, $NCHCH_2OH$), 4.09 (1H, dq, J=8.5, 4.3 Hz, $NCHCH_2OH$), 6.93 (1H, d, J=4.9 Hz, PhCHOH), 7.24—8.00 (9H, m, aromatic H). (1′*S*,2*R*)-**7a** (Minor component); 1.72—2.10 (4H, m, CH_2CH_2), 2.56 (1H, br, OH), 3.20—3.30 (1H, m, $NCHCH_2OH$), 3.34—3.47 (2H, m, NCH_2 and $NCHCH_2OH$), 3.70—3.80 (1H, m, NCH_2), 3.87—3.96 (1H, m, $NCHCH_2OH$), 3.90 (1H, br, OH), 6.86 (1H, s, PhCHOH), 7.20—8.07 (9H, m, aromatic H).

N-[*o*-(1′-Hydroxy-1′-(*p*-tolyl)methyl)benzenesulfonyl]-2-hydroxymethylpyrrolidine (**7b**): Eluent, CH_2Cl_2–AcOEt (5 : 1). MS *m/z*: EI, 343 ($M^+ - H_2O$, 0.03%), 330 ($M^+ - CH_2OH$, 16%); CI, 362 ($M^+ + 1$, 0.8%), 344 ($M^+ - OH$, 100%), 330 ($M^+ - CH_2OH$, 8%). ^{1}H-NMR ($CDCl_3$) δ: (1′*S*,2*S*)-**7b** (Major component); 1.78—2.01 (4H, m, CH_2CH_2), 2.34 (3H, s, $PhCH_3$), 2.45 (1H, t, J=4.3 Hz, CH_2OH), 3.17 (1H, dt, J=6.1, 9.8 Hz, NCH_2), 3.36 (1H, dt, J=6.7, 9.8 Hz, NCH_2), 3.57 (1H, dt, J=11.6, 4.3 Hz, $NCHCH_2OH$), 3.63 (1H, d, J=4.9 Hz, CHOH), 3.82 (1H, dt, J=11.6, 4.3 Hz, $NCHCH_2OH$), 4.07 (1H, dq, J=8.5, 4.3 Hz, $NCHCH_2OH$), 6.89 (1H, d, J=4.9 Hz, PhCHOH), 7.15 (2H, d, J=7.9 Hz, aromatic H), 7.31 (2H, d, J=7.9 Hz, aromatic H), 7.36—7.99 (4H, m, aromatic H). (1′*S*,2*R*)-**7b** (Minor component); 1.70—2.05 (4H, m, CH_2CH_2), 2.34 (3H, s, $PhCH_3$), 2.60 (1H, br, OH), 3.15—3.75 (5H, m, NCH_2, $NCHCH_2OH$, and PhCHOH), 3.85—3.95 (1H, m, $NCHCH_2OH$), 6.83 (1H, s, PhCHOH), 7.10—8.05 (8H, m, aromatic H).

N-[*o*-(1′-Hydroxy-1′-(*p*-methoxyphenyl)methyl)benzenesulfonyl]-2-hydroxymethylpyrrolidine (**7c**): Eluent, hexane–AcOEt (1 : 1). MS *m/z*: EI, 359 ($M^+ - H_2O$, 0.5%), 346 ($M^+ - CH_2OH$, 14%); CI, 378 ($M^+ + 1$, 1%), 360 ($M^+ - OH$, 100%), 346 ($M^+ - CH_2OH$, 2%). ^{1}H-NMR ($CDCl_3$) δ: (1′*S*,2*S*)-**7c** (Major component); 1.81—2.04 (4H, m, CH_2CH_2), 2.38 (1H, t, J=6.1 Hz, CH_2OH), 3.18 (1H, dt, J=9.8, 6.1 Hz, NCH_2), 3.37 (1H, dt, J=9.8, 6.7 Hz, NCH_2), 3.56 (1H, d, J=4.9 Hz, CHOH), 3.58 (1H, ddd, J=4.3, 6.1, 11.0 Hz, $NCHCH_2OH$), 3.80 (3H, s, OCH_3), 3.83 (1H, ddd, J=4.3, 6.1, 11.0 Hz, $NCHCH_2OH$), 4.07 (1H, dq, J=8.5, 4.3 Hz, $NCHCH_2OH$), 6.87 (1H, d, J=4.9, PhCHOH), 6.88 (2H, d, J=7.4 Hz, aromatic H), 7.35 (2H, d, J=7.4 Hz, aromatic H), 7.37—7.99 (4H, m, aromatic H). (1′*S*,2*R*)-**7c** (Minor component); 1.83—2.10 (4H, m, CH_2CH_2), 2.38 (1H, br, OH), 3.15—3.90 (5H, m, NCH_2, $NCHCH_2OH$, and PhCHOH), 3.80 (3H, s, OCH_3), 3.94 (1H, dq, J=8.5, 4.3 Hz, $NCHCH_2OH$), 6.80 (1H, s, PhCHOH), 6.87—8.03 (8H, m, aromaric H).

N-[*o*-(1′-Hydroxy-1′-(α-naphthyl)methyl)benzenesulfonyl]-2-hydroxymethylpyrrolidine (**7d**): Eluent, CH_2Cl_2–ether (10 : 1). MS *m/z*: EI, 379 ($M^+ - H_2O$, 0.4%), 366 ($M^+ - CH_2OH$, 15%); CI, 398 ($M^+ + 1$, 1%), 380 ($M^+ - OH$, 30%), 366 ($M^+ - CH_2OH$, 4%). The major product [(1′*S*,2*S*)-**7d**] was isolated from a diastereomeric mixture (ratio, 91 : 9) by recrystallization in benzene. Colorless needles, mp 113.5—114.5 °C (benzene). $[\alpha]_D^{20}$ −236.7° (c=1.04, $CHCl_3$). *Anal.* Calcd for $C_{22}H_{23}NO_4S$: C, 66.50; H, 5.79; N, 3.46. Found: C, 66.48; H, 5.83; N, 3.52. ^{1}H-NMR ($CDCl_3$) δ: 1.90—2.12 (4H, m, CH_2CH_2), 2.40 (1H, t, J=5.2 Hz, CH_2OH), 3.18 (1H, dt, J=10.4, 6.1 Hz, NCH_2), 3.41 (1H, dt, J=10.4, 6.7 Hz, NCH_2), 3.65 (1H, ddd, J=4.0, 5.2, 11.6 Hz, $NCHCH_2OH$), 4.02 (1H, ddd, J=4.0, 5.2, 11.6 Hz, $NCHCH_2OH$), 4.31 (1H, dq, J=7.9, 4.0 Hz, $NCHCH_2OH$), 4.44 (1H, d, J=5.5 Hz, NaphCHOH), 7.08—7.44 (5H, m, aromatic H), 7.47 (1H, d, J=5.5 Hz, NaphCHOH), 7.58—8.08 (6H, m, aromatic H). (1′*S*,2*R*)-**7d** (Minor component); ^{1}H-NMR ($CDCl_3$) δ: 1.90—2.12 (4H, m, CH_2CH_2), 2.72 (1H, br, CH_2OH), 3.27 (1H, dt, J=9.8, 6.7 Hz, NCH_2), 3.45—3.70 (3H, m, $NCHCH_2OH$ and NaphCHOH), 3.81 (1H, dt, J=6.7, 9.8 Hz, NCH_2), 4.15 (1H, dq, J=8.5, 4.3 Hz, $NCHCH_2OH$), 7.05—8.12 (12H, m, NaphCHOH and aromatic H).

N-[*o*-(1′-(α-Furyl)-1′-hydroxymethyl)benzenesulfonyl]-2-hydroxymethylpyrrolidine (**7e**): Eluent, CH_2Cl_2–ether (1 : 1). MS *m/z*: EI, 319 ($M^+ - H_2O$, 0.1%), 306 ($M^+ - CH_2OH$, 9%); CI, 338 ($M^+ + 1$, 1%), 320 ($M^+ - OH$, 100%), 306 ($M^+ - CH_2OH$, 2%). ^{1}H-NMR ($CDCl_3$) δ: (1′*S*,2*S*)-**7e** (Major component); 1.74—1.90 (4H, m, CH_2CH_2), 2.25 (1H, t, J=6.1 Hz, CH_2OH), 3.22—3.28 (2H, m, NCH_2), 3.41 (1H, d, J=4.9 Hz, CHOH), 3.53 (1H, ddd, J=4.3, 6.1, 11.6 Hz, $NCHCH_2OH$), 3.69 (1H, ddd, J=4.3, 6.1, 11.6 Hz, $NCHCH_2OH$), 3.98 (1H, dq, J=8.5, 4.3 Hz, $NCHCH_2OH$), 6.31 (1H, d, J=3.7 Hz, furyl H), 6.37 (1H, dd, J=1.8, 3.7 Hz, furyl H), 6.88 (1H, d, J=4.9 Hz, CHOH), 7.40 (1H, d, J=1.8 Hz, furyl H), 7.44—8.02 (4H, m, aromatic H). (1′*S*,2*R*)-**7e** (Minor component); 1.72—2.04 (4H, m, CH_2CH_2), 2.58 (1H, brs, CH_2OH), 3.20—3.30 (1H, m, NCH_2), 3.30—3.45 (1H, m, NCH_2), 3.47 (1H, brs, CHOH), 3.50—3.60 (1H, m, $NCHCH_2OH$), 3.64—3.75 (1H, m, $NCHCH_2OH$), 3.90 (1H, dq, J=8.5, 4.3 Hz, $NCHCH_2OH$), 6.27 (1H, dd, J=1.8, 3.1 Hz, furyl H), 6.35—6.36 (1H, m, furyl H), 6.83 (1H, s, CHOH), 7.40—8.04 (5H, m, aromatic H).

(*S*)-*N*-Methyl-*N*-(1-phenylethyl)benzenesulfonamide (9) A solution of benzenesulfonyl chloride (3.54 g, 20 mmol) in CH_2Cl_2 (8 ml) was added dropwise to a stirred solution of (*S*)-*N*-methyl-1-phenylethylamine (2.74 g, 20.3 mmol) and Et_2N (2.98 g, 29.4 mmol) in CH_2Cl_2 (30 ml) at room temperature. The reaction mixture was refluxed for 20 min, then concentrated. The residue was dissolved in AcOEt (40 ml) and the solution was passed through a short column of silica gel. The solvent was evaporated off under reduced pressure to give a colorless solid (4.60 g, 84%). Colorless prisms, mp 71—72 °C (benzene–hexane). $[\alpha]_D^{25}$ −28.7° (c=1.51, $CHCl_3$). *Anal.* Calcd for $C_{15}H_{17}NO_2S$: C, 65.43; H, 6.22; N, 5.09. Found: C, 65.36; H, 6.26; N, 5.04. MS *m/z*: EI, 275 (M^+, 1%), 260 ($M^+ - CH_3$, 26%), 141 ($PhSO_2^+$, 31%); CI, 276 ($M^+ + 1$, 100%), 260 ($M^+ - CH_3$, 12%). ^{1}H-NMR ($CDCl_3$) δ: 1.30 (3H, d, J=6.7 Hz, $CHCH_3$), 2.59 (3H, s, NCH_3), 5.30 (1H, q, J=6.7 Hz, $CHCH_3$), 7.22—7.89 (10H, m, aromatic H).

Reaction of Benzaldehyde with Lithium Complex of (*S*)-9 *n*-BuLi (1.3 mmol, 0.81 ml of 1.6 M solution of hexane) was added dropwise to a stirred solution of (*S*)-**9** (0.28 g, 1 mmol) in toluene (30 ml) at −20 °C under a nitrogen atmosphere, and stirring was continued for 30 min to form the lithium complex of (*S*)-**9**. A solution of benzaldehyde (0.14 g, 1.3 mmol) in toluene (1 ml) was added dropwise to stirred suspension of the lithium complex, and stirring was continued at −20 °C for 3 h. The reaction mixture was worked up as described for the reaction of (*S*)-**2**. The d.e. value was estimated as 9% by ^{1}H-NMR spectrometry. The residue was subjected to column chromatography on silica gel with a solution of hexane–ether (3 : 1) to give a diastereomeric mixture of (*S*)-*o*-(1-hydroxy-1-phenylmethyl)-*N*-methyl-*N*-(1-phenylethyl)benzenesulfonamide (**10**) (0.32 g, 85%) as a colorless oil. This product decomposed during distillation *in vacuo*. MS *m/z*: EI, 366 ($M^+ - CH_3$, 0.1%); CI, 382 ($M^+ + 1$, 0.2%), 366 ($M^+ - CH_3$, 1%). ^{1}H-NMR ($CDCl_3$) δ: 1.57 and 1.58 (3H, d, J=7.3 Hz, $CHCH_3$), 2.67 and 2.71 (3H, s, NCH_3), 3.17 and 3.41 (1H, d, J=4.3 Hz, CHOH), 5.26 and 5.31 (1H, q, J=7.3 Hz, $CHCH_3$), 6.64 and 6.72 (1H, d, J=4.3 Hz, PhCHOH), 7.16—8.00 (14H, m, aromatic H).

Reaction of Benzaldehyde with Titanium Complex of (*S*)-9 Ti(*O*-iso-C_3H_7)$_4$ (0.38 ml, 1.3 mmol) was added dropwise to a stirred suspension of the lithium complex (1 mmol) prepared from (*S*)-**9**, and stirring was continued at −20 °C for 30 min to form the titanium complex. A solution of benzaldehyde (0.14 g, 1.3 mmol) in toluene (1 ml) was added dropwise to the stirred solution of the titanium complex, and stirring was continued at −20 °C for 3 h. The reaction mixture was worked up as described for the reaction with the lithium complex to give a diastereomeric mixture of **10** (0.31 g, 82%). The d.e. value was estimated as 6% by ^{1}H-NMR spectrometry.

(1*S*,1′*S*)-*N*-(2-Methoxy-1-isopropylethyl)-*o*-[1′-methoxy-1′-(α-naphthyl)-methyl]-*N*-methylbenzenesulfonamide (11) NaH (17 mmol, 0.68 g of 60% NaH in liquid paraffin) was added to a stirred solution of (1*S*,1′*S*)-**3d** (2.01 g, 4.86 mmol) in THF (20 ml), and CH_3I (1.5 ml, 23 mmol) was added dropwise to the mixture. The reaction mixture was refluxed for 10 min, then treated with NH_4Cl aqueous solution, and the whole was extracted with ether. The organic layer was dried over $MgSO_4$ and evaporated. The residue was subjected to column chromatography on silica gel with a solution of hexane–ether (3 : 1) to give a colorless solid (1.85 g, 86%). Colorless plates, mp 79—80 °C (hexane–benzene). $[\alpha]_D^{22}$ −39.0° (c=0.76, $CHCl_3$). *Anal.* Calcd for $C_{25}H_{31}NO_4S$: C, 68.05; H, 7.08; N, 3.17. Found: C, 67.97; H, 7.15; N, 3.09. MS *m/z*: EI, 441 (M^+, 0.2%), 396 ($M^+ - CH_2OCH_3$, 12%), 311 ($M^+ - C_7H_{16}NO$, 55%). ^{1}H-NMR ($CDCl_3$) δ: 0.90 (3H, d, J=6.7 Hz, $CHCH_3$), 0.94 (3H, d, J=6.7 Hz, $CHCH_3$), 1.92 (1H, double septet, J=6.7, 9.8 Hz, $CHCH(CH_3)_2$), 2.69 (3H, s, NCH_3),

3.18 (3H, s, OCH_3), 3.32 (1H, dd, J=3.1, 10.4 Hz, $NCHC\underline{H}_2O$), 3.42 (1H, dd, J=6.1, 10.4 Hz, $NCHC\underline{H}_2O$), 3.54 (3H, s, OCH_3), 3.70 (1H, ddd, J=3.1, 6.1, 9.8 Hz, $NC\underline{H}CH_2O$), 7.23 (1H, s, $NaphC\underline{H}OCH_3$), 7.32—8.16 (11H, m, aromatic H).

(1′*S*,2*S*)-*N*-[*o*-(1′-Methoxy-1′-(α-naphthyl)methyl)benzenesulfonyl]-2-methoxymethylpyrrolidine (12) NaH (18.3 mmol, 0.73 g of 60% NaH in liquid paraffin) was added to a stirred solution of (1′*S*,2*S*)-**7d** (2.12 g, 5.33 mmol) in THF (20 ml), and CH_3I (1.3 ml, 20 mmol) was added dropwise to the mixture. The reaction mixture was refluxed for 10 min, then worked up as described for the preparation of (1*S*,1′*S*)-**11** to give a colorless solid (1.86 g, 82%). Colorless needles, mp 96—97 °C (hexane–benzene). $[\alpha]_D^{21}$ +14.1° (c=0.46, $CHCl_3$). *Anal.* Calcd for $C_{24}H_{27}NO_4S$: C, 67.74; H, 6.40; N, 3.29. Found: C, 67.97; H, 6.45; N, 3.58. MS m/z: 425 (M^+, 0.2%), 380 ($M^+ - CH_2OCH_3$, 20%), 311 ($M^+ - C_6H_{12}NO$, 60%). ^{1}H-NMR ($CDCl_3$) δ: 1.14—1.70 (4H, m, CH_2CH_2), 3.10 (2H, dd, J=6.1, 7.3 Hz, NCH_2), 3.16 (1H, dd, J=7.3, 9.8 Hz, $NCHC\underline{H}_2O$), 3.18 (3H, s, OCH_3), 3.26 (1H, dd, J=4.3, 9.8 Hz, $NCHC\underline{H}_2O$), 3.54 (3H, s, OCH_3), 3.66—3.75 (1H, m, $NC\underline{H}CH_2O$), 7.18 (1H, s, $NaphC\underline{H}OCH_3$), 7.08—8.21 (11H, m, aromatic H).

(*R*)-1-Methoxy-1-(α-naphthyl)-1-phenylmethane (13) i) From (1*S*,1′*S*)-**11**: Red-Al (20 mmol, 10 ml of 2 M solution in toluene) was added dropwise to a stirred solution of (1*S*, 1′*S*)-**11** (2.45 g, 5.55 mmol) in toluene (16 ml). The reaction mixture was refluxed for 15 h, then poured into a 0.5 N HCl aqueous solution, and the whole was extracted with ether. The organic layer was washed with 0.5 N HCl and 20% K_2CO_3 aqueous solutions, dried over $MgSO_4$, and evaporated. The residue was subjected to column chromatography on alumina with a solution of hexane–ether (25 : 1) to give a colorless oil (0.45 g, 33%), bp 160—165 °C (0.8 mmHg) (bulb-to-bulb distillation). $[\alpha]_D^{22}$ +93.5° (c=1.83, benzene). *Anal.* Calcd for $C_{18}H_{16}O$: C, 87.06; H, 6.49. Found: C, 87.02; H, 6.48. MS m/z: 248 (M^+, 100%), 217 ($M^+ - OCH_3$, 89%), 171 ($M^+ - C_6H_5$, 58%), 121 ($M^+ - C_{10}H_7$, 31%). ^{1}H-NMR ($CDCl_3$) δ: 3.46 (3H, s, OCH_3), 5.92 (1H, s, $PhC\underline{H}OCH_3$), 7.21—8.08 (12H, m, aromatic H).

ii) From (1′*S*,2*S*)-**12**: Red-Al (21 mmol, 10.5 ml of 2 M solution in toluene) was added dropwise to a stirred solution of (1′*S*,2*S*)-**12** (1.50 g, 3.52 mmol) in toluene (10 ml). The reaction mixture was refluxed for 9 h, then worked up as described for the reaction of (1*S*,1′*S*)-**11** to give a colorless oil (0.21 g, 24%). $[\alpha]_D^{28}$ +89.0° (c=0.41, benzene). This compound was identical with (*R*)-**13** prepared from (1*S*,1′*S*)-**11** on the basis of ^{1}H-NMR spectral comparison.

iii) From (*R*)-1-(α-Naphthyl)-1-phenylmethanol (**14**): NaH (2.5 mmol, 0.1 g of 60% NaH in liquid paraffin) was added to a stirred solution of (*R*)-**14** (73.4% e.e.)[11] (0.16 g, 0.68 mmol) in THF (6 ml), and CH_3I (0.5 ml) was added dropwise to the mixture. The reaction mixture was refluxed for 10 min, then worked up as described for the reaction of (1*S*,1′*S*)-**11**. The residue was subjected to column chromatography on silica gel with a solution of hexane–ether (25 : 1) to give a colorless oil (0.16 g, 93%). $[\alpha]_D^{22}$ +71.1° (c=1.45, benzene). This compound was identical with (*R*)-**13** on the basis of ^{1}H-NMR spectral comparison.

Acknowledgment We are grateful to Miss Y. Takahashi and Mrs. T. Ogata of Hoshi University for MS and elemental analysis.

References and Notes

1) V. Snieckus, *Heterocycles*, **14**, 1649 (1980).
2) P. Beak and V. Snieckus, *Acc. Chem. Res.*, **15**, 306 (1982).
3) M. Reuman and A. I. Meyers, *Tetrahedron*, **41**, 837 (1985).
4) P. Beak and R. A. Brown, *J. Org. Chem.*, **44**, 4463 (1979); *idem*, *ibid.*, **47**, 34 (1982).
5) A. M. Becker, R. W. Irvine, A. S. McCormick, R. A. Russell, and R. N. Warrener, *Tetrahedron Lett.*, **27**, 3431 (1986).
6) C. A. Boulet and G. A. Poulton, *Heterocycles*, **28**, 405 (1989).
7) A. I. Meyers, M. A. Hanagan, L. M. Trefonas, and R. J. Baker, *Tetrahedron*, **39**, 1991 (1983).
8) M. P. Sibi, M. A. J. Miah, and V. Snieckus, *J. Org. Chem.*, **49**, 737 (1984).
9) H. Takahashi, T. Tsubuki, and K. Higashiyama, *Synthesis*, **1988**, 238.
10) D. Seebach, A. K. Beck, S. Roggo, and A. Wonnacott, *Chem. Ber.*, **118**, 3673 (1985).
11) This compound showed $[\alpha]_D^{22}$ +43.7° (c=0.92, benzene) and the enantiomeric excess was estimated as 73.4% [lit.[10] $[\alpha]_D^{25}$ +59.5° (c=0.82, benzene)].

Partial Synthesis of *Rauwolfia* Alkaloids, Vomilenine and (19*Z*)-Vomilenine, and Their Relative Thermodynamic Stability as Revealed by Their Transformation into Perakine

Hiromitsu TAKAYAMA,[a] Chada PHISALAPHONG,[a] Mariko KITAJIMA,[a] Norio AIMI,[a] Shin-ichiro SAKAI*,[a] and Joachim STÖCKIGT[b]

Faculty of Pharmaceutical Sciences, Chiba University,[a] 1–33 Yayoi-cho, Chiba 260, Japan and Institute of Pharmaceutical Biology, Ludwig-Maximilian-University Munich,[b] Karlstrasse 29, D-8000 Munich 2, F.R.G. *Received July 10, 1990*

The geometry of the ethylidene side chain in vomilenine (1) was proven to be (19*E*) by the spectroscopic analysis of the synthetic intermediates from ajmaline (2) to vomilenine (1). The relative thermodynamic stability of vomilenine (1) and (19*Z*)-vomilenine (19), as revealed by their transformation into perakine (9), is discussed.

Keywords *Rauwolfia* alkaloid; indole alkaloid; ajmaline; vomilenine; (19*Z*)-vomilenine; perakine; partial synthesis; structure elucidation; differential NOE experiment; thermodynamic stability

Vomilenine (**1**) was first isolated from *Rauwolfia vomitoria* as a minor constituent[1] and later it was found in some New Caledonian *Rauwolfia* species.[2] Recently, the important role of vomilenine (**1**) in the biogenesis of some *Rauwolfia* alkaloids, such as ajmaline (**2**), raucaffricine (**8**), raucaffrinoline (**10**), *etc.*, has been revealed, as summarized in Chart 1.[3] The structure of **1** was determined by Taylor *et al.*[4] through the chemical correlation with ajmaline (**2**), as illustrated in Chart 2. The structure of **1** then proposed had a (19*Z*) ethylidene side chain, but later, without any chemical evidence, the geometry of the C-19 position was revised to (19*E*),[5] as in the common sarpagine class of indole alkaloids. However, several sarpagine-type indole alkaloids having a (19*Z*) ethylidene moiety were found in *Gardneria* and *Gelsemium* species.[6] Consequently, careful confirmation of the ethylidene configuration is needed. Meanwhile one of the *Rauwolfia* alkaloids, perakine (**9**), is considered to be an artifact derived from vomilenine (**1**) based on the fact that treatment of **1** with hot acetic acid gave perakine (**9**).[4] We were interested in the effect of the

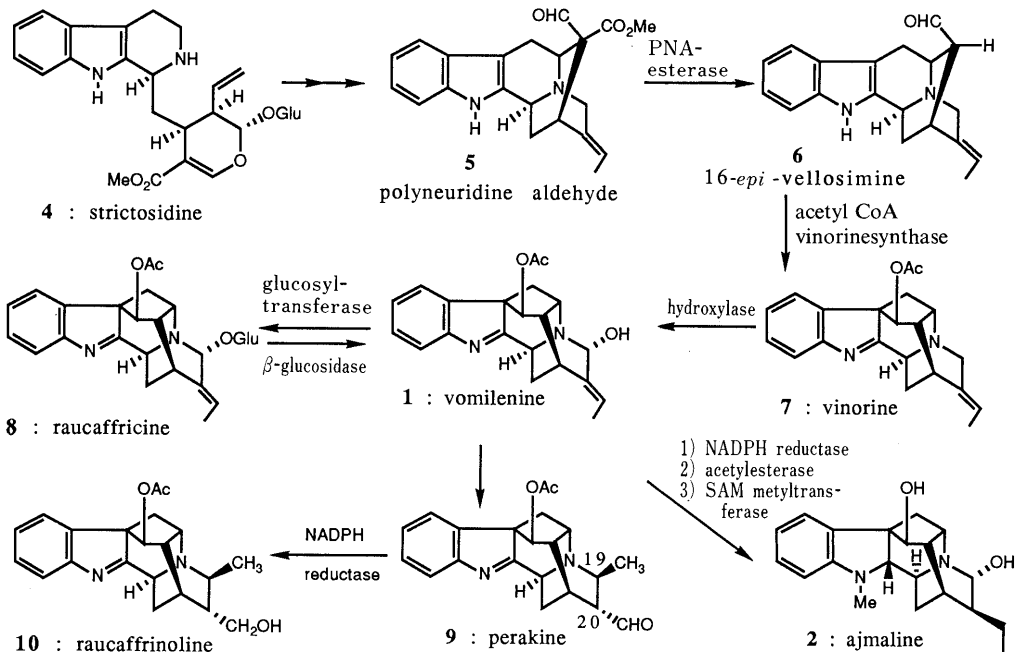

Chart 1. Proposed Biosynthetic Pathways of Sarpagine/Ajmaline Alkaloids[3]

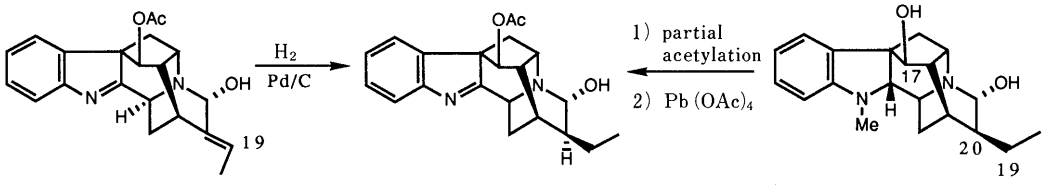

Chart 2

configuration of the ethylidene side chain on the facility of the transformation into perakine (**9**). In order to obtain chemical evidence of the configuration of the ethylidene side chain in **1** and to compare the thermodynamic stability of **1** and (19*Z*)-vomilenine (**19**), we planned the synthesis of vomilenine (**1**) and **19** from ajmaline (**2**).

Initially, ajmaline (**2**) was treated with *N*,*N*-dimethylhydrazine and a catalytic amount of H_2SO_4 to afford the secondary amine, that was directly converted to the carbamate (**11**) by using $\beta\beta\beta$-trichloroethyl chloroformate under Schotten–Baumann conditions in 70% overall yield. On hydrolysis of the hydrazone function in **11** with cupric chloride ($CuCl_2$) in aqueous tetrahydrofuran (THF) at pH 7,[7] the aldehyde (**12**) was obtained in 86% yield. After acetylation of the C-17 hydroxy group with acetic anhydride in pyridine, the N_a-methylindoline moiety was oxidized with lead tetraacetate [$Pb(OAc)_4$] in dry CH_2Cl_2 at $-70\,^{\circ}C$ to furnish the indolenine (**14**) in 88% yield. Compound **14** showed the characteristic ultraviolet (UV) absorption peaks at 210, 220, and 249 nm due to the indolenine chromophore. At this stage, we cleaved the protecting group on N_b in **14** with zinc (Zn) in AcOH at room temperature to afford 1-demethyl-Δ'-17-acetylajmaline (**3**) (mp 238—242 °C); its spectral properties [mass spectrum (MS), proton (^{1}H-) and carbon-13 nuclear magnetic resonance (^{13}C-NMR) spectra] were in accord with those of natural **3**.[2,8] This fact indicates that the configuration at the C-20 position did not epimerize under the reaction conditions of transformation from **2** to **3** *via* the hydrazone derivative. To introduce the double bond at the 19–20 position, a bromine atom or phenylselenyl group were introduced at the C-19 position through the silyl enol ether of the aldehyde function. Thus, **14** was treated successively with *tert*-butyldimethylsilyltriflate (TBSOTf) and triethylamine (Et_3N) in dry CH_2Cl_2 and then with phenylselenenyl chloride (PhSeCl) or *N*-bromosuccinimide (NBS) to provide the α-substituted aldehydes (**15** or **16**) in 53% and 71% yields, respectively. Oxidation of **15** using *m*-chloroperbenzoic acid (*m*CPBA) or sodium periodate ($NaIO_4$) resulted in the exclusive formation of the tetrasubstituted olefins, but dehydrobromination of **16** with lithium carbonate (Li_2CO_3) in dimethylformamide (DMF) at 80°C afforded the desired *E*-olefin (**17**) in 26% yield accompanied with the *Z*-olefin (**18**) (21%) and tetrasubstituted olefins (total 18%). The geometry of the olefins (**17** and **18**) was unambiguously determined by nuclear Overhauser effect (NOE) experiments. Thus, irradiation of the C-21 aldehyde proton (δ 9.39, 9.37)[9] in **17** led to enhancement (22.7%) of the C-19 olefinic proton signal (δ 6.62), while 9.5% enhancement was observed between the aldehyde proton (δ 10.21, 10.16) and C-18 methyl protons (δ 2.16, 2.17) in **18**. Finally, the protecting group on N_b in **17** was removed with Zn in AcOH at room temperature to give rise to vomilenine (**1**) in 68% yield. The ^{1}H- and ^{13}C-NMR spectra, infrared (IR) spectrum, MS and mp (189—191 °C) were identical with those of natural vomilenine (**1**). Therefore, the structure of vomilenine was concluded to be **1**. The *Z*-isomer (**18**) was also converted to the vomilenine-type compound (**19**) in 75% yield by removal of the carbamate group under the same reaction conditions.

Next, we compared the facility of the transformation of vomilenine (**1**) and (19*Z*)-vomilenine (**19**) into perakine (**9**). On standing of **19** in acetic acid at room temperature, 25% of the starting material had changed to perakine (**9**) after 17 h, and two weeks later **19** was completely converted to **9**. The synthetic compound (mp 179—183 °C) exhibited

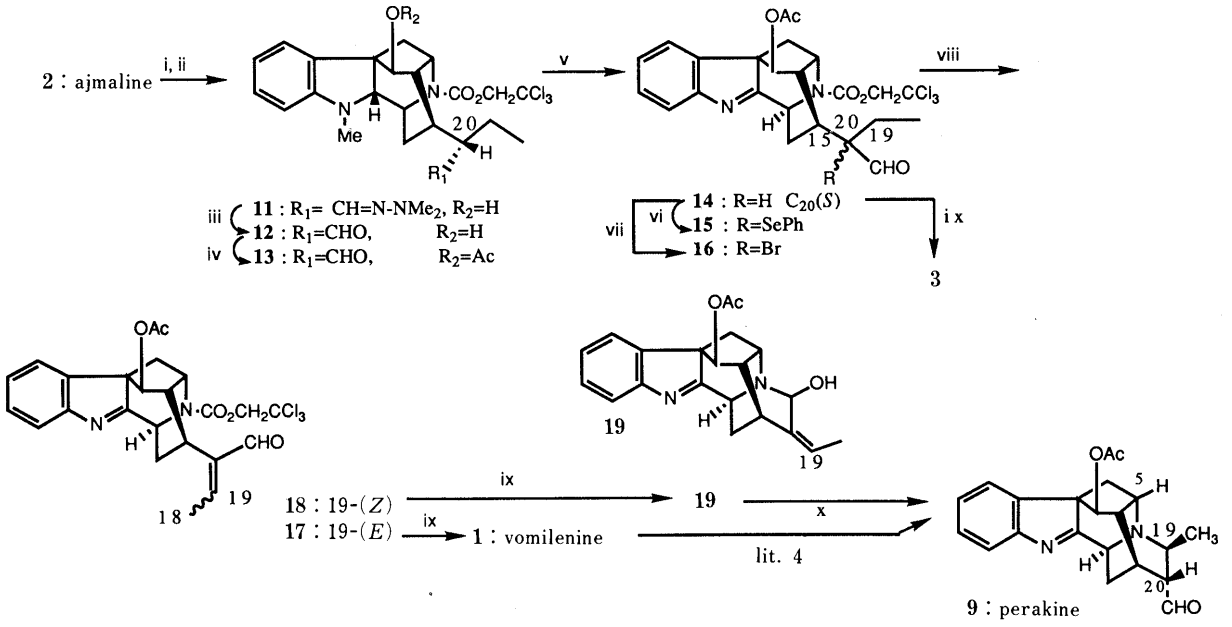

reagents and conditions : i, H_2N-NMe_2, cat. H_2SO_4, 3A-MS, EtOH, reflux, 2.5 h; ii, $ClCO_2CH_2CCl_3$, 1N NaOH/CH_2Cl_2, 0°C to r.t., 40 min; iii, $CuCl_2$, aq. THF, phosphate buffer (pH 7); iv, Ac_2O, pyridine, r.t., overnight; v, $Pb(OAc)_4$, dry CH_2Cl_2, -70°C to 0°C, 4 h; vi, TBSOTf, Et_3N, dry CH_2Cl_2, 0°C to r.t., then PhSeCl in dry CH_2Cl_2, r.t.; vii, TBSOTf, Et_3N, dry CH_2Cl_2, 0°C to r.t., then NBS, 0°C; viii, Li_2CO_3, DMF, 80°C, 4.5 h; ix, activated Zn, AcOH, r.t., 1.5—3.5 h; x, AcOH, r.t., 2 weeks

Chart 3

spectral properties (^{1}H- and ^{13}C-NMR, IR, and MS) in accord with those of authentic perakine (**9**). In contrast to the results obtained with **19**, **1** was quite stable in acetic acid at room temperature. For the conversion of vomilenine (**1**) to perakine (**9**), relatively severe conditions (reflux in AcOH)[4] were required. Interestingly, the two geometric isomers, vomilenine (**1**) and (19*Z*)-vomilenine (**19**), gave the same product, perakine (**9**). In the ^{13}C-NMR spectra, the signal of C-21 in **19** was observed at 1.5 ppm upfield from the corresponding signal of **1**. Therefore, probably due to the steric repulsion between the hydroxy group and/or the hydrogen on C-21 and the C_{18}-methyl group in **19**, cleavage of the amino-acetal function in **19** could proceed more readily than that of **1** and subsequent Michael-type ring closure between N_b and C-19 would furnish the thermodynamically controlled product, perakine (**9**), through epimerization at the C-20 position.

Experimental

All melting points were determined on a Yamato MP-21 apparatus and are uncorrected. The instruments used in this study were as follows; UV spectra, Hitachi U3400 spectrophotometer; IR spectra, Hitachi 260 spectrophotometer; MS, Hitachi RMU-6E and RMU-7M spectrometers; ^{1}H- and ^{13}C-NMR spectra, JEOL JNM GX270, JEOL GSX400, and JEOL GSX500 instruments (in $CDCl_3$ with tetramethylsilane as an internal standard; chemical shifts are recorded in δ values); optical rotation, JASCO DIP-140 polarimeter. Thin-layer chromatography was performed on Merck precoated Silicagel 60 F_{254} plates. Column chromatography was carried out on Merck Silica gel 60 (230—400 mesh for flash chromatography) and pre-packed columns [Kusano CPS-HS-221-05 (for medium-pressure column chromatography)].

Preparation of the Hydrazone (11) from Ajmaline (2) Concentrated H_2SO_4 (1 ml), *N,N*-dimethylhydrazine (6.8 ml, 89.5 mmol) and molecular sieves (3 Å, 12 g) were added to a stirred suspension of ajmaline (**2**) (6.0 g, 18.38 mmol) in dry ethanol (100 ml), and the mixture was heated under reflux for 2.5 h. After evaporation of the ethanol, the reaction mixture was poured into cold 10% aqueous Na_2CO_3 solution and the whole was extracted with $CHCl_3$. The organic extract was dried over $MgSO_4$ and evaporated to give 7.5 g of residue. The resulting crude hydrazone was dissolved in CH_2Cl_2 (240 ml) and 1 N NaOH solution (60 ml). Then $ClCO_2CH_2CCl_3$ (3.7 ml, 26.88 mmol) was added to the vigorously stirred solution during 2 min at 0 °C and the mixture was stirred at room temperature for 40 min. The reaction mixture was diluted with water (100 ml) and the organic layer was separated. The aqueous layer was extracted with CH_2Cl_2. The combined organic layer was washed with water, dried over $MgSO_4$ and evaporated. The residue was purified by flash column chromatography (AcOEt–hexane, 2 : 1) to give the carbamate (**11**) (7.00 g, 70%) as an amorphous powder. UV λ_{max}^{EtOH} nm: 247, 293. IR $\nu_{max}^{CHCl_3}$ cm^{-1}: 3350, 2950, 1750, 1300. ^{1}H-NMR (270 MHz) δ: 6.45, 6.40[9] (1H, each d, J=7.0 Hz, N=CH), 4.82, 4.79 (1H, each d, J=11.9 Hz, $CH_aH_bCCl_3$), 4.73, 4.69 (1H, each d, J=11.9 Hz, $CH_aH_bCCl_3$), 4.48, 4.40 (1H, each dd, J=7.3, 4.0 Hz, 5-H), 4.08, 4.07 (1H, each s, 17-H), 2.76, 2.75 [9H, each s, N_a-CH_3, $N(CH_3)_2$], 0.86, 0.84 (3H, each t, J=7.3 Hz, 18-CH_3). MS *m/z* (%): 544 (M^++2, 24), 542 (M^+, 25), 144 (100), 113 (76).

The Aldehyde (12) $CuCl_2$ (139 mg, 0.103 mmol) was added to a solution of **11** (187 mg, 0.034 mmol) in THF (4.6 ml), phosphate buffer (pH 7, 0.24 ml) and water (2.2 ml). The mixture was stirred at room temperature for 36 h and then diluted with water (10 ml) and concentrated ammonia (5 ml). The whole was extracted with $CHCl_3$ and the organic layer was washed with water, and dried over $MgSO_4$. Evaporation of the solvent gave a residue (214 mg), which was separated by flash column chromatography (AcOEt–hexane, 2 : 1) to afford the aldehyde (**12**) (149 mg, 86%) as an amorphous powder. UV λ_{max}^{EtOH} nm: 247, 291. IR $\nu_{max}^{CHCl_3}$ cm^{-1}: 3300, 2950, 1710, 1430, 1120. ^{1}H-NMR (270 MHz) δ: 9.64 (1H, d, J=3.7 Hz, CHO), 4.90, 4.76 (1H, each d, J=11.9 Hz) and 4.83, 4.65 (1H, each d, J=12.2 Hz) (CH_2CCl_3), 4.68 (1H, d, J=8.6 Hz, 3-H), 4.48—4.40 (1H, m, 5-H), 4.13 (1H, s, 17-H), 2.77, 2.76 (3H, each s, N_a-CH_3), 0.86 (3H, t, J=7.3 Hz, 18-CH_3). MS *m/z* (%): 502 (M^++2, 17), 500 (M^+, 18), 144 (100).

The 17-*O*-Acetate (13) A solution of **12** (618 mg, 1.23 mmol) in dry pyridine (10 ml) and acetic anhydride (4 ml) was stirred at room temperature overnight. After evaporation of the solvents, 5% aqueous Na_2CO_3 solution was added to the residue and the whole was extracted with $CHCl_3$. The organic extract was washed with water, dried over $MgSO_4$ and evaporated. The residue was purified with flash column chromatography (AcOEt–hexane, 2 : 1) to give the acetate (**13**) (623 mg, 93%) as an amorphous powder. UV λ_{max}^{EtOH} nm: 247, 293. IR $\nu_{max}^{CHCl_3}$ cm^{-1}: 2960, 1710, 1430, 1240, 1120. ^{1}H-NMR (270 MHz) δ: 9.51, 9.49 (1H, each d, J=3.4 Hz, CHO), 4.89 (1H, s, 17-H), 4.85, 4.70 (1H, each d, J=11.9 Hz) and 4.80 (1H, s) (CH_2CCl_3), 4.72 (1H, d, J=8.6 Hz, 3-H), 4.46—4.39 (1H, m, 5-H), 2.774, 2.768 (3H, each s, N_a-CH_3), 2.21, 2.19 (3H, each s, $OCOCH_3$), 0.87 (3H, t, J=7.4 Hz, 18-CH_3). MS *m/z* (%): 544 (M^++2, 20), 542 (M^+, 20), 144 (100).

Lead Tetraacetate Oxidation of the Indoline (13) $Pb(OAc)_4$ was added to a stirred solution of **13** (915 mg, 1.68 mmol) in dry CH_2Cl_2 (20 ml) at −70 °C in the following manner: 0 min, 746 mg (1.68 mmol); 60 min, 840 mg (1.89 mmol); 135 min, 650 mg (1.47 mmol). During this period, stirring was continued at the same temperature, and after the final addition of $Pb(OAc)_4$ the reaction temperature was gradually raised to 0 °C over 1 h. The reaction mixture was diluted with CH_2Cl_2 and washed successively with 5% aqueous Na_2CO_3 solution and water. The organic layer was dried over $MgSO_4$ and evaporated to give a residue, which was purified by flash column chromatography (AcOEt–hexane, 1 : 2) to yield the indolenine (**14**) (788 mg, 88%) as an amorphous powder. UV λ_{max}^{MeOH} nm: 210, 220, 249. IR $\nu_{max}^{CHCl_3}$ cm^{-1}: 2950, 1720, 1420, 1220, 1120. ^{1}H-NMR (270 MHz) δ: 9.544, 9.540 (1H, each d, J=4.4 Hz, CHO), 5.46, 5.43 (1H, each d, J=7.1 Hz, 3-H), 5.01, 4.84 (1H, each d, J=12.0 Hz, $CH_aH_bCCl_3$), 4.76, 4.57 (1H, each d, J=12.0 Hz, $CH_aH_bCCl_3$), 2.15, 2.14 (3H, each s, $COCH_3$), 0.88, 0.86 (3H, each t, J=7.2 Hz, 18-CH_3). MS *m/z* (%): 499 (M^++2−CHO, 11), 497 (M^+−CHO, 12), 167 (100).

1-Desmethyl-Δ^1-17-acetylajmaline (3) Zinc dust (99 mg) was added to a solution of **14** (49 mg, 0.093 mmol) in acetic acid (1 ml), and the mixture was stirred at room temperature for 30 min. The reaction mixture was filtered and the filtrate was concentrated *in vacuo* and then basified by the addition of chilled 5% aqueous $NaHCO_3$ solution. The whole was extracted with $CHCl_3$. The organic extract was washed with water, and dried over $MgSO_4$. Removal of the solvent gave a residue, which was subjected to medium-pressure liquid column chromatography (MPLC) (5% MeOH–$CHCl_3$) to afford 17 mg (52%) of **3** as colorless prisms, mp 238—242 °C (lit[8], 240—242 °C). UV λ_{max}^{MeOH} nm: 219, 257. IR ν_{max}^{KBr} cm^{-1}: 3300—3000, 2960, 1740, 1240. ^{1}H-NMR (500 MHz) δ: 5.37 (1H, br s, OH), 5.00 (1H, s, 17-H), 4.33 (1H, d-like, $J\approx$11 Hz, 3-H), 4.31 (1H, s, 21-H), 3.33 (1H, t, J=5.7 Hz, 5-H), 2.78 (1H, dd, J=12.0, 5.0 Hz, 6-H$_\beta$), 2.42 (1H, m, 15-H), 2.26 (1H, t, J=6.0 Hz, 16-H), 2.17 (3H, s, $COCH_3$), 1.89 (1H, dd, J=14.0, 10.1 Hz, 14-H$_\alpha$), 1.74 (1H, dd, J=14.0, 5.0 Hz, 14-H$_\beta$), 1.64 (1H, d, J=12.0 Hz, 6-H$_\alpha$), 1.50—1.40 (2H, m, 19-H_2), 0.98 (3H, t, J=6.6 Hz, 18-CH_3). ^{13}C-NMR (67.8 MHz) δ: 183.2 (C2), 54.8 (C3), 49.8 (C5)*, 37.7 (C6), 65.1 (C7), 136.5 (C8), 123.8 (C9), 125.5 (C10), 128.8 (C11), 121.1 (C12), 156.4 (C13), 27.8 (C14), 27.6 (C15), 47.0 (C16)*, 78.7 (C17), 11.9 (C18), 26.0 (C19), 42.0 (C20), 87.5 (C21), 169.9 (CO), 21.1 ($CO\underline{C}H_3$) (The assignments having a superscript may be interchanged). MS *m/z* (%): 352 (M^+, 100), 324 (24), 323 (26), 169 (95). Exact MS Calcd for $C_{21}H_{24}N_2O_3$: 352.1788. Found: 352.1787.

Preparation of the α-Phenylselenoaldehyde (15) Et_3N and TBSOTf were added to a stirred solution of **14** (318 mg, 0.60 mmol) in dry CH_2Cl_2 (5 ml) at 0 °C as follows: 0 min, Et_3N (125 μl, 0.90 mmol) and TBSOTf (200 μl, 0.87 mmol); 45 min, Et_3N (125 μl, 0.90 mmol) and TBSOTf (200 μl, 0.87 mmol); 180 min, TBSOTf (150 μl, 0.65 mmol). Stirring was continued at the same temperature for 4 h. To this reaction mixture containing silyl enol ether, a solution of PhSeCl (116 mg, 0.60 mmol) in dry CH_2Cl_2 (2 ml) was added at −20 °C. After 2 h, a solution of PhSeCl (89 mg, 0.46 mmol) in dry CH_2Cl_2 (0.6 ml) was added at −20 °C and then the mixture was stirred at room temperature for 30 min. The reaction mixture was diluted with CH_2Cl_2 and washed with 5% aqueous Na_2CO_3 solution. The aqueous layer was extracted with CH_2Cl_2 and the combined organic layer was washed with water and dried over $MgSO_4$. Evaporation of the solvent gave a residue, which was purified by flash column chromatography (AcOEt–hexane, 2 : 1) and then by MPLC (1% MeOH–$CHCl_3$) to give oily **15** (220 mg, 53%) as a diastereomeric mixture and the starting material **14** (31 mg, 10%). IR $\nu_{max}^{CHCl_3}$ cm^{-1}: 2970, 1720, 1420, 1320, 1220. ^{1}H-NMR (400 MHz) δ: 7.70—7.20 (9H, m, arm-H). MS *m/z* (%): 655 (M^++2−CO, 4), 653 (M^+−CO, 4), 345 (58), 343 (59), 169 (70), 168 (100), 167 (96).

Preparation of the α-Bromoaldehyde (16) Et_3N and TBSOTf were added to a stirred solution of **14** (92 mg, 0.174 mmol) in dry CH_2Cl_2 (1.5 ml) at 0 °C as follows: 0 min, Et_3N (37 ml, 0.27 mmol) and TBSOTf (58 ml, 0.25 mmol); 75 min, Et_3N (37 ml, 0.27 mmol) and TBSOTf (58 ml,

0.25 mmol); 180 min, TBSOTf (29 ml, 0.13 mmol). After the final addition of the reagent, the mixture was stirred at room temperature for 5 h. To this reaction mixture containing silyl enol ether, a solution of NBS (36 mg, 0.202 mmol) in dry CH_2Cl_2 (1.5 ml) was added at 0 °C, and the whole was stirred at the same temperature for 10 min. The reaction mixture was diluted with CH_2Cl_2 and washed with 5% aqueous $NaHCO_3$ solution. The aqueous layer was extracted with CH_2Cl_2 and the combined organic layer was washed with brine, dried over $MgSO_4$ and evaporated. The residue was purified by MPLC (AcOEt–hexane, 1 : 2) to afford 75 mg (71%) of oily **16** as a diastereomeric mixture. IR $\nu_{max}^{CHCl_3}$ cm^{-1}: 2950, 1720, 1700, 1220. ^{1}H-NMR (500 MHz) δ: 9.47, 9.45, 9.42 (1H, each s, CHO), 2.19, 2.18, 2.17, 2.16 (3H, each s, $COCH_3$). MS *m/z* (%): 525 ($M^+ + 2 - HBr$, 15), 523 ($M^+ - HBr$, 17), 345 (63), 343 (65), 169 (77), 168 (90), 167 (100), 156 (63).

Dehydrobromination of 16 with Li_2CO_3 A mixture of **16** (134 mg, 0.22 mmol) and Li_2CO_3 (50 mg, 0.68 mmol) in dry DMF (4 ml) was stirred at 80 °C for 4.5 h under an argon atmosphere. Then 5% aqueous $NaHCO_3$ solution was added to the reaction mixture and the whole was extracted with $CHCl_3$. The organic extract was washed with brine, dried over $MgSO_4$ and evaporated. DMF was removed in a Kugelrohr apparatus and the residue was purified by MPLC (AcOEt–hexane, 1 : 2) to give oily **17** (30 mg, 26%), oily **18** (25 mg, 21%), a more polar tetrasubstituted olefin (8 mg, 7%), and a less polar tetrasubstituted olefin (13 mg, 11%). **17**; UV λ_{max}^{EtOH} nm: 220.2. IR $\nu_{max}^{CHCl_3}$ cm^{-1}: 3000, 1710, 1430, 1220, 1130, 1040. ^{1}H-NMR (500 MHz) δ: 9.39, 9.37 (1H, each s, CHO), 6.62 (1H, q, J=7.2 Hz, 19-H), 5.52, 5.49 (1H, each d, J=8.5 Hz, 3-H), 5.06, 4.98 (1H, each m, 5-H), 4.85, 4.81 (1H, each d, J=11.8 Hz, $C\underline{H}_aH_bCCl_3$), 4.76, 4.63 (1H, each d, J=11.8 Hz $CH_a\underline{H}_bCCl_3$), 4.60, 4.59 (1H, each s, 17-H), 2.17, 2.16 (3H, each s, $COCH_3$), 2.05 (3H, d, J=6.9 Hz, 18-CH_3). MS *m/z* (%): 526 ($M^+ + 2$, 25), 524 (M^+, 24), 498 (13), 496 (13), 345 (54), 343 (53), 169 (69), 168 (76), 167 (100). **18**; UV λ_{max}^{EtOH} nm: 220.5. IR $\nu_{max}^{CHCl_3}$ cm^{-1}: 2940, 1715, 1680, 1430, 1220, 1130, 1040. ^{1}H-NMR (400 MHz) δ: 10.21, 10.16 (1H, each s, CHO), 6.79 (1H, qt, J=7.5, 1.3 Hz, 19-H), 5.46, 5.44 (1H, each d, J=8.5 Hz, 3-H), 4.96, 4.73 (1H, each d, J=11.9 Hz, $C\underline{H}_aH_bCCl_3$), 4.91, 4.80 (1H, each m, 5-H), 4.80 (1H, s, 17-H), 4.70, 4.53 (1H, each d, J=11.9 Hz, $CH_a\underline{H}_bCCl_3$), 2.17, 2.16 (3H, each s, $COCH_3$), 2.16, 2.14 (3H, each dd, J=7.5, 1.6 Hz, 18-CH_3). MS *m/z* (%): 526 ($M^+ + 2$, 24), 524 (M^+, 23), 498 (13), 496 (13), 168 (82), 167 (100).

Preparation of Vomilenine (1) Zinc dust (450 mg) was added to a solution of **17** (124 mg, 0.24 mmol) in acetic acid (4 ml), and the mixture was stirred at room temperature for 3 h, then filtered. The filtrate was concentrated and then basified with chilled 5% aqueous $NaHCO_3$ solution. The whole was extracted with $CHCl_3$ and the organic extract was washed with water and dried over $MgSO_4$. Evaporation of the solvent gave the residue, which was purified by MPLC (5% MeOH–$CHCl_3$) to afford 58 mg (68%) of vomilenine (**1**) as colorless prisms from AcOEt. mp 189—191 °C. $[\alpha]_D^{19}$ −71.6° (c=0.45, pyridine). UV λ_{max}^{MeOH} nm: 219, 260. IR ν_{max}^{KBr} cm^{-1}: 3300—3000, 2950, 1740, 1600, 1450, 1230. ^{1}H-NMR (500 MHz) δ: 6.06 (1H, br s, OH), 5.75 (1H, q, J=6.6 Hz, 19-H), 5.03 (1H, br s, 21-H), 4.98 (1H, s, 17-H), 4.31 (1H, dd, J=7.1, 2.8 Hz, 3-H), 3.92 (1H, t, J=5.8 Hz, 5-H), 3.28 (1H, m, 15-H), 2.77 (1H, dd, J=12.1, 4.7 Hz, 6-H_β), 2.17 (3H, s, $COCH_3$), 1.68 (3H, d, J=6.6 Hz, 18-CH_3). ^{13}C-NMR (67.8 MHz) δ: 182.3 (C_2), 54.4 (C3)*, 50.9 (C5)*, 36.4 (C6), 65.2 (C7), 136.3 (C8), 123.8 (C9), 125.7 (C10), 128.8 (C11), 121.1 (C12), 156.4 (C13), 26.4 (C14), 28.4 (C15), 49.2 (C16)*, 77.6 (C17), 13.0 (C18), 119.6 (C19), 139.2 (C20),[10] 82.4 (C21), 169.9 (CO), 21.1 ($CO\underline{C}H_3$) (The assignments having a superscript may be interchanged). MS *m/z* (%): 350 (M^+, 29), 169 (100), 43 (15). *Anal.* Calcd for $C_{21}H_{22}N_2O_3 \cdot 1/4H_2O$: C, 71.07; H, 6.39; N, 7.89. Found: C, 70.96; H, 6.27; N, 7.82. Exact MS Calcd for $C_{21}H_{22}N_2O_3$: 350.1629. Found: 350.1627.

Preparation of (19*Z*)-Vomilenine (19) Zinc dust (99 mg) was added to a solution of **18** (42 mg, 0.08 mmol) in acetic acid (2 ml), and the mixture was stirred at room temperature for 1.5 h. A residue obtained by work-up as described above was purified by MPLC (iso-PrOH–$CHCl_3$–hexane, 7 : 63 : 30) to give 21 mg (75%) of **19** as an amorphous solid and 3 mg (7%) of the starting material **18**. UV λ_{max}^{EtOH} nm: 219, 258. IR $\nu_{max}^{CHCl_3}$ cm^{-1}: 3600—3100, 2970, 1740, 1230. ^{1}H-NMR (500 MHz) δ: 7.65—7.20 (4H, m, arm-H), 5.54 (1H, q like, 19-H), 5.19 (1H, s, 21-H), 4.99 (1H, s, 17-H), 2.16 (3H, s, $COCH_3$), 1.8—1.6 (3H, 18-CH_3). ^{13}C-NMR (100 MHz) δ: 182.9 (C2), 55.5 (C3), 50.6 (C5), 37.0 (C6), 64.3 (C7), 136.3 (C8), 123.8 (C9), 125.5 (C10), 128.7 (C11), 121.1 (C12), 156.4 (C13), 26.4 (C14), 34.4 (C15), 48.6 (C16), 77.8 (C17), 13.0 (C18), 122.1 (C19), 139.4 (C20), 80.9 (C21), 169.9 (CO), 21.0 (OCH_3. MS *m/z* (%): 350 (M^+, 100), 321 (20), 196 (32), 169 (56), 168 (80), 43 (42). Exact MS Calcd for $C_{21}H_{22}N_2O_3$: 350.1629. Found: 350.1621.

Preparation of Perakine (9) from (19*Z*)-Vomilenine (19) A solution of **9** (6 mg, 0.017 mmol) in acetic acid (0.5 ml) was stirred at room temperature under an argon atmosphere. After 17 h, a small portion of the reaction mixture was neutralized with chilled ammonia water and extracted with $CHCl_3$. The organic extract was dried over $MgSO_4$ and evaporated. The crude residue was subjected to ^{1}H-NMR measurement. The ratio of (19*Z*)-vomilenine (**19**) and perakine (**9**) was calculated from the integrals of the signals of the olefinic proton (19-H) of **19** and the aldehyde proton (21-H) of **9**. The reaction mixture after 17 h contained 25% perakine (**9**) and 75% starting material **19**. The remaining reaction mixture was stirred at the same temperature for two weeks. The ^{1}H-NMR spectrum of the crude residue obtained by the same work-up procedure as above showed the exclusive presence of perakine (**9**). The residue was crystallized from acetone–hexane to give 4 mg of colorless prisms. mp 179—182 °C (lit.[4] 185 °C). The chromatographic behavior on TLC, as well as the IR, MS, Exact MS (Calcd for $C_{21}H_{22}N_2O_3$: 350.1629. Found: 350.1622), and ^{1}H- and ^{13}C-NMR spectra of the semisynthetic compound were identical with those of authentic perakine (**9**). The stereochemistry at the C-19 and C-20 positions was further confirmed by the differential NOE spectrum. Irradiation of 18-H_3 (δ 1.30) in **9** led to enhancement of the 5-H (16%) and H-20 (15%) signals.

Acknowledgment We thank Professor J. Poisson, Centre d'Etudes Pharmaceutiques-F, for providing a sample of natural vomilenine. Thanks are also due to Mrs. H. Seki, Miss R. Hara and Mr. T. Kuramochi in the Analytical Center of our University for measurements of spectral data (NMR and MS). Support of this research by the Ministry of Education, Science and Culture, Japan (International Scientific Research Program, Joint Research; No. 01044025) is gratefully acknowledged.

References and Notes

1) A. Hofmann and A. J. Frey, *Helv. Chim. Acta*, **40**, 1866 (1957).
2) F. Libot, N. Kunesch and J. Poisson, *Phytochemistry*, **19**, 989 (1980).
3) *a*) L. Polz, H. Schübel and J. Stöckigt, *Z. Naturforsch.*, **42c**, 333 (1987); *b*) C. M. Ruyter, H. Schübel and J. Stöckigt, *ibid.*, **43c**, 479 (1988); *c*) J. Stöckigt and H. Schübel, *NATO ASI Series*, **H18**, 251 (1988); *d*) H. Schübel, C. M. Ruyter and J. Stöckigt, *Phytochemistry*, **28**, 491 (1989).
4) W. I. Taylor, A. J. Frey and A. Hofmann, *Helv. Chim. Acta*, **45**, 611 (1962).
5) W. I. Taylor, "The Alkaloids," Vol. XI, ed. by R. H. F. Manske, Academic Press, New York, 1968, Chapter 2.
6) *a*) N. Aimi, S. Sakai, Y. Iitaka and A. Itai, *Tetrahedron Lett.*, **1971**, 2061; *b*) D. Ponglux, S. Wongseripipatana, S. Subhadhirasakul, H. Takayama, M. Yokota, K. Ogata, C. Phisalaphong, N. Aimi and S. Sakai, *Tetrahedron*, **44**, 5075 (1988).
7) *a*) H. Takayama, M. Kitajima, S. Wongseripipatana and S. Sakai, *J. Chem. Soc., Perkin Trans. 1*, **1989**, 1075; *b*) H. Takayama, M. Horigome, N. Aimi and S. Sakai, *Tetrahedron Lett.*, **31**, 1287 (1990).
8) M. F. Bartlett, B. F. Lambert and W. I. Taylor, *J. Am. Chem. Soc.*, **86**, 729 (1964).
9) Carbamate derivatives of ajmaline were often found from the ^{1}H-NMR spectra to occur as a mixture of rotational isomers in the ratio of approximately 1 : 1.
10) The chemical shift value at C_{20} (δ 131.0) of vomilenine in the literature[2] should be revised to δ 139.2 (personal correspondence with Professor J. Poisson).

Novel Annelations of Xanthines by the Reaction of 8-Aminoxanthines with Dimethyl Acetylenedicarboxylate

Taisei UEDA, Yoshinori KAWABATA, Nobutoshi MURAKAMI, Shin-ichi NAGAI, Jinsaku SAKAKIBARA,* and Masafumi GOTO

Faculty of Pharmaceutical Sciences, Nagoya City University, Tanabe-dori, Mizuho-ku, Nagoya 467, Japan. *Received July 18, 1990*

Annelations of xanthines by the reaction of dimethyl acetylenedicarboxylate (DMAD) with 7-alkyl-8-amino-1,3-dimethylxanthines (3) have been investigated. Treatment of 3 with DMAD in refluxing methanol gave 5-alkyl-1,3-dimethyl-9-methoxycarbonyl-1,2,3,4-tetrahydro-5*H*,7*H*-pyrimido[1,2-*e*]purine-2,4,7-triones (4) and 7-alkyl-1,2,3,6-tetrahydro-1,3-dimethyl-8-(1,2,4,5,6,7-hexamethoxycarbonyl-3-azatricyclo[2.2.1.0^{2,6}]heptyl)purine-2,6-diones (10). However, when the reaction was run in *N*,*N*-dimethylformamide, 5-alkyl-1,3-dimethyl-1,2,3,4-tetrahydro-7,8,11-tris(methoxycarbonyl)-5*H*,9*H*[1,3]-diazocino[1,2-*e*]purine-2,4,9-triones (11), 5-alkyl-1,3-dimethyl-7,8-bis(methoxycarbonyl)-1,2,3,4,9,10-hexahydro-10-(methoxycarbonyl)methylene-5*H*[1,3]-diazepino[1,2-*e*]purine-2,4,9-triones (12), and 5-alkyl-1,3-dimethyl-1,2,3,4,9,10-hexahydro-7,8,9,10-tetrakis(methoxycarbonyl)-5*H*[1,3]-diazepino[1,2-*e*]purine-2,4-diones (13) were formed.

Keywords annelation; 8-aminoxanthine; dimethyl acetylenedicarboxylate; purine; pyrimido[1,2-*e*]purine; diazocino[1,2-*e*]purine; diazepino[1,2-*e*]purine; X-ray crystallography

Xanthine derivatives such as caffeine, theophylline, and theobromine are widely distributed in nature and show some important biological activities. In the course of medicinal and chemical studies of xanthines in our laboratory,[1] we previously synthesized 2,4,7,9-tetramethylpurino[7,8-*g*]-6-azapteridine-1,3,8,10(2*H*,4*H*,7*H*,9*H*)tetrone[2] (**2**) from 7,8-diamino-1,3-dimethylxanthine (**1**), and biological testing showed that **2** was active against P-388 leukemia. In connection with that work we became interested in preparing pyrimido[1,2-*e*]purines.[3] Thus, the reaction of 7-alkyl-8-amino-1,3-dimethylxanthines (**3a—d**) with dimethyl acetylenedicarboxylate (DMAD) was examined and found to give pyrimido[1,2-*e*]purines (**4a—d**). Similar annelation reactions to form diazocino[1,2-*e*]purines (**11a—d**), and diazepino[1,2-*e*]purines (**12a—d**, **13a—d**) were also investigated.

The starting materials **3a—d** were prepared regioselectively by the reaction of 8-aminotheophylline[4] (**5**) with allyl or alkyl bromide in *N*,*N*-dimethylformamide (DMF) in the presence of sodium hydride at room temperature in 80—85% yields. However, when the reaction was carried out in an elevated temperature, for instance, the reaction of **5**

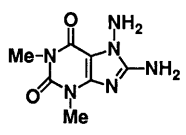

1

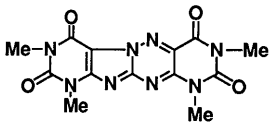

2

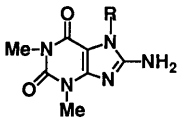

3a—d

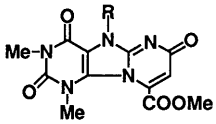

4a—d

a: R=allyl **b**: R=propyl **c**: R=butyl **d**: R=pentyl

Chart 1

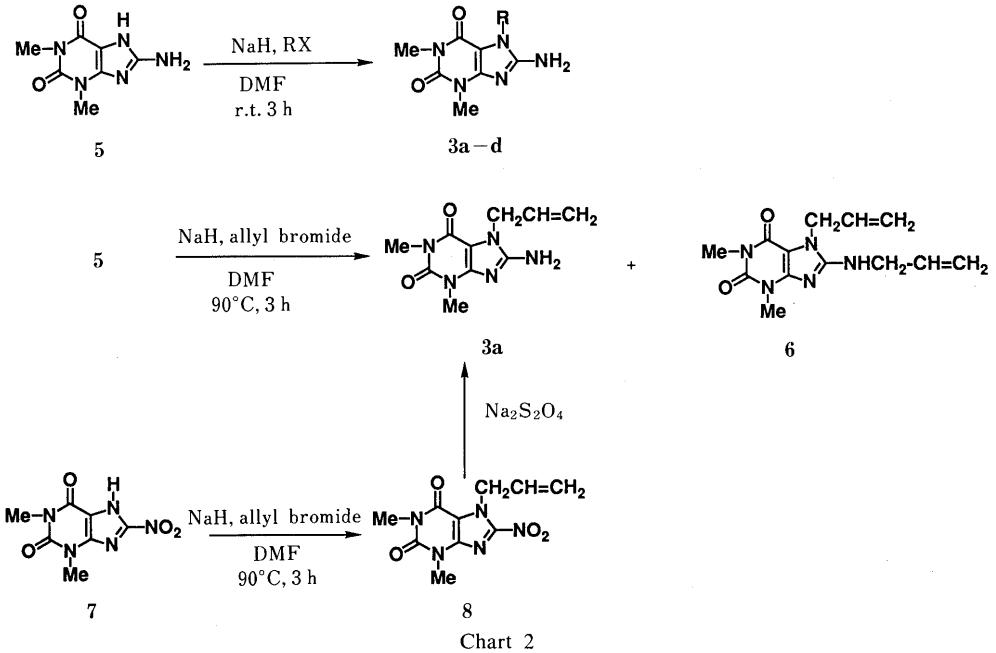

5 3a—d

5 3a 6

7 8

Chart 2

with allyl bromide at 90 °C for 3 h, 7-allyl-8-allylamino-1,3-dimethylxanthine (**6**) was afforded in 19% yield besides the objective product (**3a**). Compound **3a** was identical with the product derived from 8-nitrotheophylline[5] (**7**) *via* 7-allyl-1,3-dimethyl-8-nitroxanthine (**8**) and its reduction with sodium hydrosulfite (Chart 2). The reaction of **3a—d** with DMAD in refluxing methanol for 18—32 h afforded 5-alkyl-1,3-dimethyl-9-methoxycarbonyl-1,2,3,4-tetrahydro-5*H*,7*H*-pyrimido[1,2-*e*]purine-2,4,7-triones (**4a—d**) in 16—38% yields (Table I and Chart 3). When ethanol or propanol was used as a solvent, the 9-methoxycarbonyl group was converted partly to a 9-ethoxy (or propoxy) carbonyl function to give **9a, b**. The structures of **4a—d** and **9a, b** were assigned on the basis of the proton nuclear magnetic resonance (^{1}H-NMR) and infrared (IR) spectra and mass spectra (MS). Probably, the ring nitrogen at the 9-position of **3** is a nucleophilic site for the initial Michael addition and the reaction proceeds to give the 7-oxo structure (**4a—d**) rather than the 9-oxo structure (**4′**) as illustrated in Chart 4. Reports by Wade *et al.*[6] and Chan *et al.*[7] on the similar reactions of 2-amino-1-methylbenzoimidazol or 2-amino-benzothiazole with DMAD support the 7-oxo structure of the compounds (**4a—d**).

Compounds **10a, b** were also isolated from the resinous reaction products of **3a, b** and DMAD. The MS of these compounds indicated that they are the adducts of **3a, b** and 3 mol of DMAD. The ^{1}H-NMR spectra showed signals due to six methyl ester functions and two isolated methine protones at around 4 and 5 ppm. The final structural confirmation was carried out by the X-ray analysis of **10b** (Fig. 1). As far as we know, the azatricyclo[2.2.1.0^{2,6}]heptyl skeleton has not been reported yet, and appears to be a novel class of heterocycles. The mechanism of the formation of **10a, b** appears to proceed as illustrated in Chart 5.

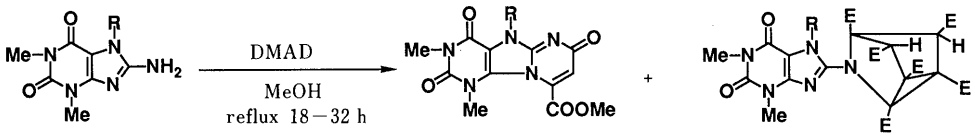

3a—d **4a—d**

10a : R=propyl
10b : R=butyl
E=CO_2Me

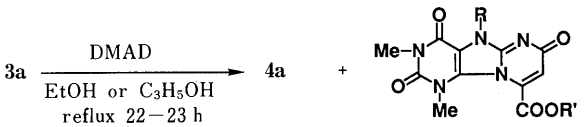

9a : R=allyl, R′=Et
9b : R=allyl, R′=*n*-propyl

Chart 3

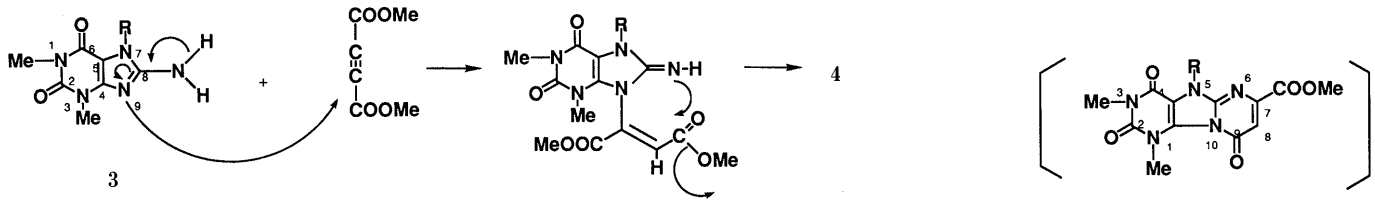

Chart 4

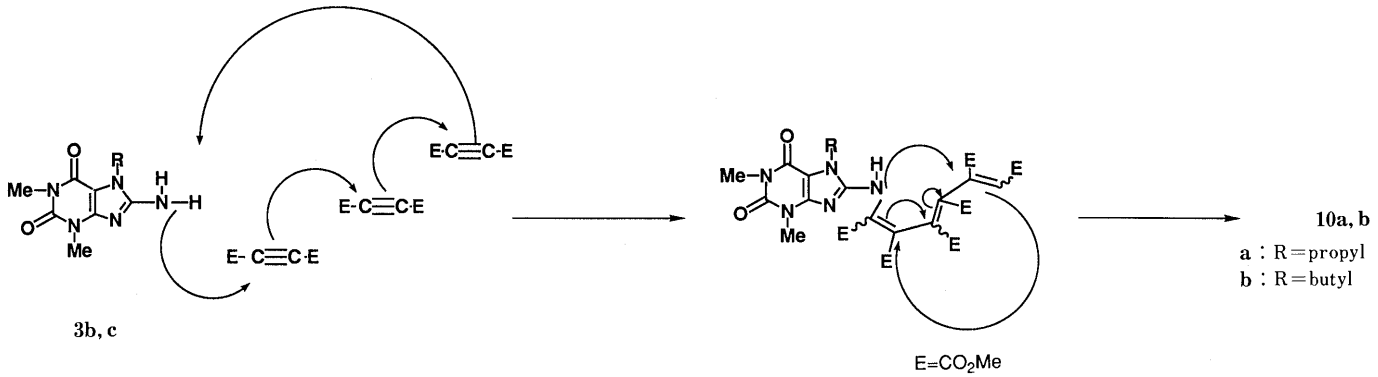

Chart 5

Michael addition of the 8-amino group of the xanthines to 3 mol of DMAD, followed by intramolecular cyclization, forms, the azatricyclo[2.2.1.$0^{2,6}$]heptyl skeleton.

Next we studied the above reaction in DMF as an aprotic solvent and found the formations of 5-alkyl-1,3-dimethyl-1,2,3,4-tetrahydro-7,8,11-tris(methoxycarbonyl)-5*H*,9*H*-[1,3]-diazocino[1,2-*e*]purine-2,4,9-triones (**11a—d**) (10—19%), 5-alkyl-1,3-dimethyl-7,8-bis(methoxycarbonyl)-1,2,3,4,9,10-hexahydro-10-methoxycarbonylmethylene-5*H*[1,3]-diazepino[1,2-*e*]purine-2,4,9-triones (**12a—d**) (10—13%), and 5-alkyl-1,3-dimethyl-1,2,3,4,9,10-hexahydro-7,8,9,10-tetrakis(methoxycarbonyl)-5*H*[1,3]-diazepino-[1,2-*e*]purine-2,4-diones (**13a—d**) (24—44%). Each of the ^{1}H-NMR spectra of **11a—d** showed three methylester signals at 3.71—3.97 ppm and an olefinic proton signal at 7.08—7.09 ppm. The MS and microanalyses were consistent with the assigned structures. Compound **12a** gave the same formula as **11a** and the ^{1}H-NMR spectrum disclosed signals due to three ester methyl groups at 3.81—3.88 ppm and an olefinic proton at 5.90 ppm. Acheson *et al.*[8] reported that methyl 2,3-dihydro-3-oxo-4*H*-benzo[*b*]-1,4-oxazine-2-methylenecarboxylate (A), which is structurally related to **12a**, showed one singlet proton signal at 5.97 ppm. The mechanism of the formation of **11**, **12**, and **13** by the reaction of **3** with DMAD probably involves the common intermediate B as illustrated in Chart 6. If the anion attacks one of the ester carbonyl groups *via* route a, diazocino[1,2-*e*]purines (**11**) may be afforded. Diazepino[1,2-*e*]purines (**12** and **13**) will be formed *via* routes b and c, respectively. Letcher and Sin[9] and Acheson *et al.*[10] reported similar reactions of indoles or benzimidazoles with DMAD to give azepines (compound **13** type). However, formations of compound **11** type and compound **12** type have not been reported. It appears that the reaction of **3** and DMAD in methanol, which is a good proton donor, gives **4** by protonation of the methoxycarbonyl group of the intermediate, followed by the elimination of methanol, as illustrated in Chart 4, whereas the reaction in an aprotic solvent gives rise to the further addition of DMAD to the 8-imino group to give the intermediate B as shown in Chart 6.

X-Ray Crystallography of 10b Compound **10b** consists of 7-*n*-butyl-1,3-dimethylxanthine and hexamethoxycarbonyl-3-azatricyclo[2.2.1.$0^{2,6}$]heptane moieties bonded between the 8-position of the former and the 3-aza nitrogen atom of the latter, as shown in Fig. 1. The xanthine moiety has normal bond lengths and angles, while its *n*-butyl group takes an extended *trans* structure. The dihedral angle between the plane of the xanthine moiety and the plane

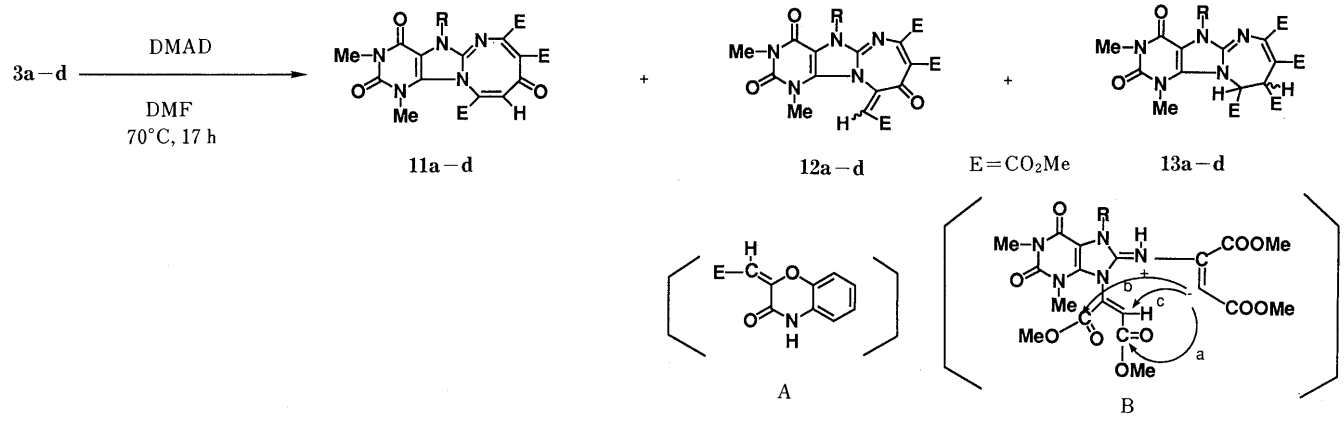

Chart 6

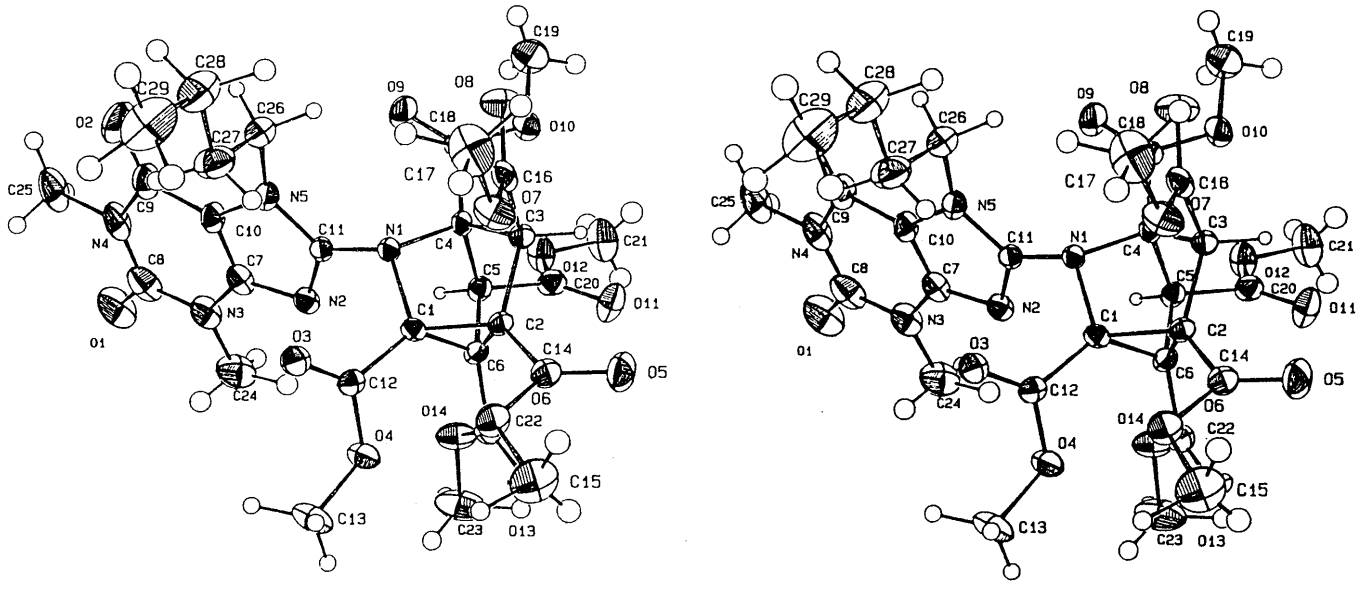

Fig. 1. Stereoscopic Drawing of **10b**

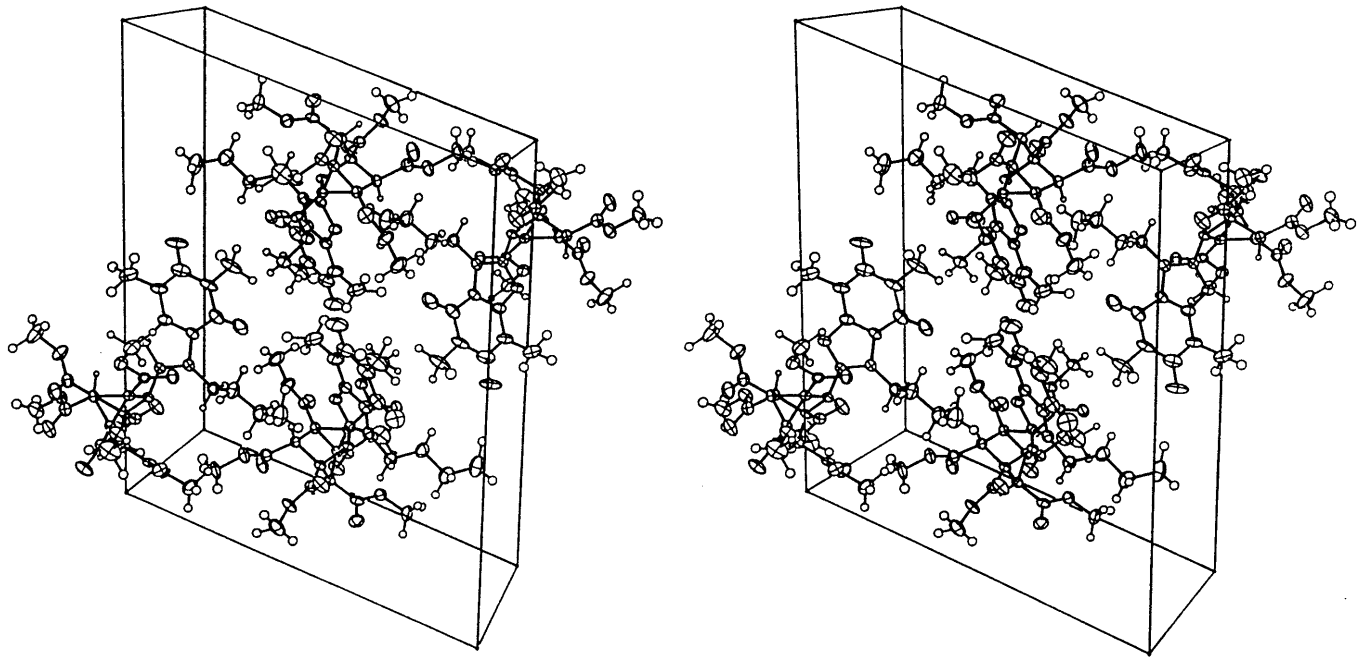

Fig. 2. Stereoscopic Drawing of the Molecular Packing of **10b**

defined by the N1, C3, C5 atoms is 37.5(2)°. The core of the hexamethoxycarbonylazatricycloheptane has an approximately C_3 axis which passes through the bridge-head C4 atoms and the center of the cyclopropane ring formed by the C1, C2, and C6 atoms. The bond lengths within the 3-azatricycloheptane are 1.510(5) Å (C1–C2), 1.527(5) Å (C1–C6), 1.516(5) Å (C2–C6) for the cyclopropane ring, 1.520(5) Å (C2–C6) and 1.528(5) Å (C5–C6) for the bridging carbon atoms and those included in the cyclopropane, and 1.542(5) Å (C3–C4) and 1.563(5) Å (C4–C5) for the bridge-head carbon (C4) and the bridging carbon atoms. The C–N bond length between C1 and N1 (1.471(4) Å) is shorter than that between N1 and C4 (1.499(4) Å). The interatomic angles of the cyclopropane moiety are close to 60.0°: 59.9(2)° for C2–C1–C6, 60.6(2)° for C1–C2–C6, and 59.5(2)° for C2–C6–C1. The bond angles around the bridging atoms are smaller than the tetrahedral value: 98.1(3)° for C4–N1–C1, 96.7(3)° for C4–C3–C2, and 95.4(3)° for C4–C5–C6. The bond angles around the C4 atom are smaller than those for 3-azatricycloheptane: 99.1(3)° for N1–C4–C3, 103.6(3)° for C5–C4–C3, and 103.6(3)° for N1–C4–C5. These structural characteristics are in close agreement with the results reported for nortricycloheptane included in an Ru complex.[11]

There is no distinct difference in the bond lengths and bond angles of the six methoxycarbonyl groups. But the arrangement of the six methoxycarbonyl groups does not follow the C_3 symmetry. One of them (–C16(O8)–O7–C17) is twisted and nearly parallel to the *n*-butyl group.

The molecules in the crystal are connected by hydrophobic interactions. The structure of the unit cell is shown in Fig. 2. The carbomethoxy groups are on both sides of the (1,0,0) plane and the *n*-butyl group fills a space formed by the molecule to which it belongs and the adjacent molecule extends approximately along the *c*-axis and in the direction parallel to the xanthine ring of the adjacent molecule.

Experimental

All melting points were determined with a Yanagimoto micro melting point apparatus and are uncorrected. The IR spectra were measured with a Jasco IR-810 spectrophotometer. The MS were measured with a JEOL JMS-DX 300 spectrometer. The ^{1}H-NMR spectra were recorded with a JEOL JNM-FX-100 spectrometer using tetramethylsilane as an internal standard. Abbreviations are as follows: s, singlet; d, doublet; q, quartet, br, broad; m, multiplet.

General Procedure for the Synthesis of 7-Alkyl-8-amino-1,3-dimethylxanthines (3a—d) 8-Aminotheophylline (**5**) (600 mg, 0.003 mol) was dissolved in 20 ml of DMF at 90 °C, and sodium hydride (60% mineral oil dispersion, 148 mg) was added with stirring. The mixture was allowed to cool to room temperature. Alkyl bromide (0.0036 mol) was added and stirring was continued for 3 h, then the reaction mixture was poured into water and extracted with chloroform. The extract was washed with water and dried over anhydrous magnesium sulfate. The solvent was distilled off and the crystalline residue was recrystallized from ethanol.

7-Allyl-8-amino-1,3-dimethylxanthine (**3a**): This compound was obtained as colorless prisms of mp 224—226 °C, yield 80%. IR (KBr): 3400, 3340 (NH_2), 1680, 1640 (amide C=O) cm^{-1}. ^{1}H-NMR ($CDCl_3$) δ: 3.35 (3H, s, N–CH_3), 3.45 (3H, s, N–CH_3), 4.65 (2H, s, NH_2), 4.80—5.35 (4H, m, –CH_2–CH=CH_2), 5.90 (1H, m, –CH_2–CH=CH_2). MS *m/z*: 235 (M^+). *Anal.* Calcd for $C_{10}H_{13}N_5O_2$: C, 51.06; H, 5.57; N, 29.77. Found: C, 51.8; H, 5.53; N, 29.54.

8-Amino-7-propyl-1,3-dimethylxanthine (**3b**): This compound was obtained as colorless prisms of mp 233—234 °C, yield 81%. IR (KBr): 3400, 3350 (NH_2), 1680, 1640 (amide C=O) cm^{-1}. ^{1}H-NMR ($CDCl_3$) δ: 0.98 (3H, t, J=8 Hz, –$CH_2CH_2CH_3$), 1.85 (2H, sextet, J=8 Hz, $CH_2CH_2CH_3$), 3.39 (3H, s, N–CH_3), 3.47 (3H, s, N–CH_3), 4.05 (2, t, J=8 Hz, –$CH_2CH_2CH_3$), 5.01 (2H, s, NH_2). MS *m/z*: 237 (M^+). *Anal.* Calcd for $C_{10}H_{15}N_5O_2$: C, 50.62; H, 6.37; N, 29.52. Found: C, 50.62; H, 6.44; N, 29.42.

8-Amino-7-butyl-1,3-dimethylxanthine (**3c**): This compound was obtained as colorless prisms of mp 202—203 °C, yield 84%. IR (KBr): 3380, 3300 (NH_2), 1680, 1640 (amide C=O) cm^{-1}. ^{1}H-NMR ($CDCl_3$) δ: 0.95 (3H, t, J=6 Hz, $CH_3CH_2CH_2CH_2$–), 1.35 (2H, m, $CH_3CH_2CH_2CH_2$–), 1.70 (2H, m, $CH_3CH_2CH_2CH_2$–), 3.35 (3H, s, N–CH_3), 3.48 (3H, s, N–CH_3), 4.09 (2H, t, J=8 Hz, $CH_3CH_2CH_2CH_2$–), 6.17 (2H, s, NH_2). MS *m/z*: 251 (M^+). *Anal.* Calcd for $C_{11}H_{17}N_5O_2$: C, 52.58; H, 6.82; N, 27.87. Found: C, 52.27; H, 6.64; N, 27.61.

8-Amino-7-pentyl-1,3-dimethylxanthine (**3d**): This compound was obtained as colorless prisms of mp 173—174 °C, yield 85%. IR (KBr): 3400, 3340 (NH_2), 1680, 1640 (amide C=O) cm^{-1}. ^{1}H-NMR ($CDCl_3$) δ: 0.92 (3H, t, J=7 Hz, $CH_3(CH_2)_4$–), 1.30—1.50 (4H, m, $CH_3CH_2CH_2CH_2CH_2$–), 1.75—1.90 (2H, m, $CH_3CH_2CH_2(CH_2)_2$–), 3.40 (3H, s, N–CH_3), 3.45

(3H, s, N–CH_3), 4.08 (2H, t, J=7 Hz, $CH_3(CH_2)_3C\underline{H}_2$–). MS m/z: 265 (M^+). *Anal.* Calcd for $C_{12}H_{19}N_5O_2$: C, 54.32; H, 7.22; N, 26.40. Found: C, 54.62; H, 7.15; N, 26.45.

7-Allyl-8-allylamino-1,3-dimethylxanthine (6) 8-Aminotheophylline (**5**) (600 mg, 0.003 mol) was dissolved in 20 ml of DMF at 90 °C, and sodium hydride (60% mineral oil dispersion, 148 mg) was added with stirring. Allyl bromide (436 mg, 0.0036 mol) was added to the above reaction mixture. Heating and stirring were continued for 3 h, then the reaction mixture was poured into water and extracted with chloroform. The extract was washed with water and dried over anhydrous magnesium sulfate. The solvent was distilled off and the residue was chromatographed on silica gel with chloroform–methanol (30 : 1). From the first eluate, compound **6** was obtained. Yield 156 mg (19%), colorless prisms of mp 164—165 °C (from AcOEt). IR (KBr): 3330 (NH), 1685, 1640 (amide C=O) cm^{-1}. ^{1}H-NMR ($CDCl_3$) δ: 3.35 (3H, s, N–CH_3), 3.50 (3H, s, N–CH_3), 4.00—6.10 (11H, m, CH_2–CH=CH_2 ×2, NH). MS m/z: 275 (M^+). *Anal.* Calcd for $C_{13}H_{17}N_5O_2$: C, 56.72; H, 6.22; N, 25.44. Found: C, 56.44; H, 6.12; N, 25.24.

The second eluate gave compound **3a** in 29% yield.

7-Allyl-8-nitro-1,3-dimethylxanthine (8) 2-Nitrotheophylline (**7**) (675 mg, 0.003 mol) was dissolved in 30 ml of DMF at 90 °C, and sodium hydride (60% mineral oil dispersion, 169 mg) was added with stirring. Allyl bromide (544 mg, 0.0045 mol) was added to the above reaction mixture. Heating and stirring were continued for 3 h, then the reaction mixture was poured into water and extracted with chloroform. The extract was washed with water and dried over anhydrous magnesium sulfate. The solvent was distilled off and the residue was chromatographed on silica gel with chloroform. The first eluate gave 476 mg (60%) of **8**, yellow prisms of mp 113—114 °C (from ethanol). IR (KBr): 1700, 1660 (amide C=O) cm^{-1}. ^{1}H-NMR ($CDCl_3$) δ: 3.42 (3H, s, N–CH_3), 3.60 (3H, s, N–CH_3), 5.25—3.20 (5H, m, CH_2–CH=CH_2). MS m/z: 265 (M^+). *Anal.* Calcd for $C_{10}H_{11}N_5O_4$: C, 45.29; H, 4.18; N, 26.41. Found: C, 45.33; H, 4.12, N, 26.30.

Preparation of 3a from 8 Compound **8** (210 mg, 0.00079 mol) was suspended in 3 ml of water, and a solution of sodium hydrosulfite (0.5 g) in 3 ml of water was added dropwise with stirring. The mixture was heated at 80—90 °C for 2 h. After cooling, the reaction mixture was extracted with chloroform. The extract was washed with water and dried over anhydrous magnesium sulfate. The solvent was distilled off to leave crystals, which were recrystallized from ethanol to give **3a** as colorless prisms of mp 224—226 °C, yield 64 mg (34%).

General Procedure for the Synthesis of 5-Alkyl-1,3-dimethyl-9-methoxycarbonyl-1,2,3,4-tetrahydro-5*H*,7*H*-pyrimido[1,2-*e*]purine-2,4,7-triones (4a—d) A mixture of 7-alkyl-8-amino-1,3-dimethylxanthines (**3a—d**) (0.00127 mol) and DMAD (1.81 g, 0.0127 mol) in 60 ml of methanol was refluxed for 18—32 h. The solvent was distilled off, and the residue was column-chromatographed on silica gel with a mixture of chloroform–methanol (50 : 1). From the first eluate, compounds **4a—d** were separated.

5-Allyl-1,3-dimethyl-9-methoxycarbonyl-1,2,3,4-tetrahydro-5*H*,7*H*-pyrimido[1,2-*e*]purine-2,4,7-trione (**4a**): This compound was obtained as colorless prisms of mp 193—194 °C (from isopropanol). IR (KBr): 1750 (ester C=O), 1700, 1670 (amide C=O) cm^{-1}. ^{1}H-NMR ($CDCl_3$) δ: 3.38 (3H, s, N–CH_3), 3.49 (3H, s, N–CH_3), 4.00 (3H, s, –OCH_3), 4.90—6.10 (5H, m, CH_2–CH=CH_2), 6.82 (1H, s, =CH–CO–). MS m/z: 345 (M^+). *Anal.* Calcd for $C_{15}H_{15}N_5O_5$: C, 52.17; H, 4.38; N, 20.28. Found: C, 52.24; H, 4.45; N, 20.38.

1,3-Dimethyl-5-propyl-9-methoxycarbonyl-1,2,3,4-tetrahydro-5*H*,7*H*-pyrimido[1,2-*e*]purine-2,4,7-trione (**4b**): This compound was obtained as colorless prisms of mp 178—179 °C (from ethanol). IR (KBr): 1740 (ester C=O), 1705, 1670 (amide C=O) cm^{-1}. ^{1}H-NMR ($CDCl_3$) δ: 0.94 (3H, t, J=7 Hz, $C\underline{H}_3CH_2CH_2$–), 1.84 (2H, sextet, J=7 Hz, $CH_3C\underline{H}_2CH_2$–), 3.30 (3H, N–CH_3), 3.42 (3H, s, N–CH_3), 4.01 (3H, s, O–CH_3), 4.42 (2H, t, J=7 Hz, $CH_3CH_2C\underline{H}_2$–), 6.77 (1H, s, =CH–CO–). MS m/z: 347 (M^+). *Anal.* Calcd for $C_{15}H_{17}N_5O_5$: C, 51.87; H, 4.93; N, 20.16. Found: C, 51.99; H, 4.81; N, 20.15.

5-Butyl-1,3-dimethyl-9-methoxycarbonyl-1,2,3,4-tetrahydro-5*H*,7*H*-pyrimido[1,2-*e*]purine-2,4,7-trione (**4c**): This compound was obtained as colorless prisms of mp 197—198 °C (from ethanol–hexane (1 : 1)). IR (KBr): 1740 (ester C=O), 1705, 1670 (amide C=O) cm^{-1}. ^{1}H-NMR ($CDCl_3$) δ: 1.00 (3H, t, J=7 Hz, –CH_2CH_2–$CH_2C\underline{H}_3$), 1.45 (2H, m, –$CH_2CH_2C\underline{H}_2CH_3$), 1.95 (2H, m, $CH_2C\underline{H}_2CH_2CH_3$), 3.37 (3H, s, N–$CH_3$), 3.48 (3H, s, N–$CH_3$), 4.44 (2H, t, J=7 Hz, $C\underline{H}_2CH_2CH_2CH_3$), 6.83 (1H, s, =CH–CO–). MS m/z: 361 (M^+). *Anal.* Calcd for $C_{16}H_{19}N_5O_5$: C, 53.18; H, 5.30; N, 19.38. Found: C, 53.20; H, 5.23; N, 19.47.

1,3-Dimethyl-9-methoxycarbonyl-5-pentyl-1,2,3,4-tetrahydro-5*H*,7*H*-pyrimido[1,2-*e*]purine-2,4,7-trione (**4d**): This compound was obtained as colorless prisms of mp 193—194 °C (from AcOEt–hexane (1 : 1)). IR (KBr): 1740 (ester C=O), 1706, 1680 (amide C=O) cm^{-1}. ^{1}H-NMR ($CDCl_3$) δ: 0.90 (3H, t, J=7 Hz, $C\underline{H}_3(CH_2)_4$–), 1.30—1.50 (4H, m, $CH_3(C\underline{H}_2)_2$–), 1.70—1.90 (2H, m, $CH_3(CH_2)_2C\underline{H}_2CH_2$–), 3.33 (3H, s, N–$CH_3$), 3.44 (3H, s, N–$CH_3$), 4.04 (3H, s, OCH_3), 4.40 (2H, t, J=7 Hz, $CH_3(CH_2)_3C\underline{H}_2$–), 6.80 (1H, s, =CH–CO–). MS m/z: 375 (M^+). *Anal.* Calcd for $C_{17}H_{21}N_5O_5$: C, 54.39; H, 5.64; N, 18.66. Found: C, 54.19; H, 5.36; N, 18.58.

5-Allyl-1,3-dimethyl-9-ethoxycarbonyl-1,2,3,4-tetrahydro-5*H*,7*H*-pyrimido[1,2-*e*]purine-2,4,7-trione (9a) A mixture of **3a** (100 mg, 0.43 mmol) and DMAD (600 mg, 4.3 mmol) in 30 ml of ethanol was refluxed for 22 h. The solvent was distilled off, and the residue was column-chromatographed on silica gel with chloroform. From the first eluate, **9a** (24 mg, 16%) was obtained. The second eluate gave **4a** in 18% yield.

9a: mp 165—167 °C (from ethanol). IR (KBr): 1730 (ester C=O), 1705, 1670 (amide C=O) cm^{-1}. ^{1}H-NMR ($CDCl_3$) δ: 1.45 (3H, t, J=7 Hz, $CH_2C\underline{H}_3$), 3.35 (3H, s, N–CH_3), 3.45 (3H, s, N–CH_3), 4.50 (2H, q, J=7 Hz, –$C\underline{H}_2CH_3$), 5.01—5.40 (4H, m, –$C\underline{H}_2CH$=$C\underline{H}_2$), 5.95 (1H, m, $CH_2C\underline{H}$=CH_2), 6.84 (1H, s, =CH–CO–). MS m/z: 359 (M^+). *Anal.* Calcd for $C_{16}H_{17}N_5O_5$: C, 53.48; H, 4.77; N, 19.49. Found: C, 53.29; H, 4.69; N, 19.24.

5-Allyl-1,3-dimethyl-9-propoxycarbonyl-1,2,3,4-tetrahydro-5*H*,7*H*-pyrimido[1,2-*e*]purine-2,4,7-trione (9b) A mixture of **3a** (186 mg, 0.79 mmol) and DMAD (1.124 g, 7.9 mmol) in 30 ml of *n*-propanol was refluxed for 23 h. The reaction mixture was treated by similar procedures to those described for **9a**.

9b: mp 177—179 °C (from hexane–*n*-propanol), yield 25 mg (9%). IR (KBr): 1750 (ester C=O), 1700, 1630 (amide C=O) cm^{-1}. ^{1}H-NMR ($CDCl_3$) δ: 1.04 (3H, t, J=8 Hz, $C\underline{H}_3CH_2CH_2$–), 1.50—1.90 (2H, sextet, J=8 Hz, $CH_3C\underline{H}_2CH_2$–), 3.32 (3H, s, N–CH_3), 3.44 (3H, s, N–CH_3), 3.70—3.90 (2H, m, $CH_3CH_2C\underline{H}_2$–), 5.05—5.50 (4H, m, –$C\underline{H}_2CH$=$C\underline{H}_2$), 5.95 (1H, m, –$CH_2C\underline{H}$=CH_2), 6.85 (1H, s, =CH–CO–). MS m/z: 373 (M^+). *Anal.* Calcd for $C_{17}H_{19}N_5O_5$: C, 54.69; H, 5.13; N, 18.76. Found: C, 54.78; H, 5.02; N, 18.52.

7-Propyl-1,3-dimethyl-1,2,3,6-tetrahydro-8-(1,2,4,5,6,7-hexamethoxycarbonyl-3-azatricyclo[2.2.1.0^{2,6}]heptyl)purine-2,6-dione (10a) After the removal of **4b** from the reaction mixture of **3b** and DMAD, the residue was chromatographed on silica gel and eluted with a mixture of chloroform–methanol (50 : 1). The eluate was concentrated and subjected to preparative thin layer chromatography (TLC) to give colorless prisms of mp 197—198 °C (from AcOEt–hexane), yield 7%. IR (KBr): 1750 (ester C=O), 1705, 1660 (amide C=O) cm^{-1}. ^{1}H-NMR ($CDCl_3$) δ: 0.98 (3H, t, J=7 Hz, –CH_2–$CH_2C\underline{H}_3$), 1.84—1.94 (2H, m, –$CH_2C\underline{H}_2CH_3$), 3.39 (3H, s, N–CH_3), 3.50 (3H, s, N–CH_3), 3.66 (3H, s, OCH_3), 3.70 (3H, s, OCH_3), 3.76 (3H, s, OCH_3), 3.77 (3H, s, OCH_3), 3.80 (3H, s, OCH_3), 3.88 (3H, s, OCH_3), 4.06—4.30 (2H, m, N–$C\underline{H}_2CH_2CH_3$), 4.35 (1H, s), 4.75 (1H, s). MS m/z: 663 (M^+).

7-Butyl-1,3-dimethyl-1,2,3,6-tetrahydro-8-(1,2,4,5,6,7-hexamethoxycarbonyl-3-azatricyclo[2.2.1.0^{2,6}]heptyl)purine-2,6-dione (10b) After the removal of **4c** from the reaction mixture of **3c** and DMAD, the residue was chromatographed on silica gel and eluted with a mixture of chloroform–methanol (50 : 1). The eluate was concentrated and subjected to preparative TLC to give colorless prisms of mp 225—226 °C (from AcOEt–hexane), yield 2%. IR (KBr): 1750 (ester C=O), 1705, 1660 (amide C=O) cm^{-1}. ^{1}H-NMR ($CDCl_3$) δ: 0.98 (3H, t, J=8 Hz, $C\underline{H}_3CH_2(CH_2)_2$–), 1.42 (2H, m, $CH_3C\underline{H}_2(CH_2)_2$–), 1.85 (2H, quintet, J=8 Hz, $CH_3CH_2C\underline{H}_2CH_2$–), 3.40 (3H, s, N–$CH_3$), 3.50 (3H, s, N–$CH_3$), 3.66 (3H, s, OCH_3), 3.70 (3H, s, OCH_3), 3.76 (6H, s, OCH_3 ×2), 3.80 (3H, s, OCH_3), 3.87 (3H, s, OCH_3), 4.11—4.33 (2H, m, –$C\underline{H}_2(CH_2)_2CH_3$), 4.34 (1H, s,), 4.76 (1H, s). MS m/z: 677 (M^+).

X-Ray Structure Determination of 10b Crystal Data: $C_{29}H_{35}N_5O_{14}$, Mr=677.63, monoclinic, space group $P2_1/c$, a=19.818(1) Å, b=11.027 Å (1), c=16.120(2) Å, β=109.3(4)°, V=3324(8) Å^3, Z=4, d_m=1.324 g

TABLE I. Yields (%) of **4**, **9** and **10**

R	Reaction condition	4	9	10
n-Propyl	Reflux for 19 h in MeOH	31		7
n-Butyl	Reflux for 21 h in MeOH	33		2
n-Pentyl	Reflux for 18 h in MeOH	16		
Allyl	Reflux for 32 h in MeOH	38		
Allyl	Reflux for 22 h in EtOH	18	16	
Allyl	Reflux for 23 h in *n*-propyl	17	9	

cm^{-3}, $d_c = 1.354\,g\,cm^{-3}$, Mo $K\alpha$ radiation of $\lambda = 0.7107$ Å, graphite filter, $T = 293 \pm 1$ K, $\mu_\varphi = 1.0\,cm^{-1}$

The crystal selected for intensity data collection measured $0.29 \times 0.29 \times 0.085$ mm. Accurate unit cell dimensions were derived from a least-squares fit for the setting angles of 18 reflections on a Nonius CAD-4 diffractometer. Intensity data were collected at 0.8° width, with variable speed, $\omega/2\theta$ scans to $\theta = 22.5°$ for $-19 \leqq h \leqq 19, 0 \leqq k \leqq 11, 0 \leqq l \leqq 17$. Lorentz and polarization corrections were made; no absorption corrections were required. There were small decreases in the intensities of three standard reflections monitored throughout the data collection and the intensity data were corrected on the bases of a linear decay with measurement time. After averaging, the intensity data set consisted on 3415 unique reflections.

The structure was solved by direct methods with MULTAN programs using those reflections of $F_O > 0.1$ for the input to the NORMAL program. Thirty three nonhydrogen atoms were located by the direct methods. Further refinement of atomic positions was done by full-matrix least-squares fits using 2439 reflections with $F_O/\sigma(|F_O|) > 3.0$. Non-hydrogen atoms were refined anisotropically and hydrogen atoms were included in positions obtained from difference Fourier maps, and their positions were refined with isotropical thermal factors fixed at the same value for those bonded to the same carbon atom. Final residuals were $R = 0.047$ and $R_w = 0.047$.

TABLE II. Positional Parameters with Their Estimated Standard Deviations in Parentheses

Atom	x	y	z	B(Å^2)
O(1)	0.5357 (2)	−0.3512 (4)	0.0655 (3)	8.0 (1)
O(2)	0.3984 (2)	−0.4106 (4)	0.2416 (3)	7.1 (1)
O(3)	0.3276 (2)	0.1175 (3)	0.1661 (2)	3.88 (8)
O(4)	0.3288 (2)	0.2143 (3)	0.0446 (2)	3.88 (8)
O(5)	0.0878 (2)	0.3042 (3)	−0.0388 (3)	5.5 (1)
O(6)	0.1975 (2)	0.3200 (3)	0.0604 (2)	4.37 (9)
O(7)	0.1111 (2)	0.1084 (3)	0.1270 (2)	4.46 (9)
O(8)	0.0668 (2)	−0.0768 (3)	0.0880 (2)	5.0 (1)
O(9)	0.1606 (2)	−0.2835 (3)	0.0193 (3)	5.3 (1)
O(10)	0.0651 (2)	−0.2078 (3)	−0.0846 (2)	4.56 (9)
O(11)	0.0772 (2)	0.0444 (3)	−0.2162 (2)	5.4 (1)
O(12)	0.1194 (2)	−0.1372 (3)	−0.2334 (2)	4.68 (9)
O(13)	0.2210 (2)	0.2834 (3)	−0.1273 (2)	5.0 (1)
O(14)	0.2737 (2)	0.1159 (4)	−0.1578 (2)	5.2 (1)
N(1)	0.2242 (2)	−0.0484 (3)	0.0544 (2)	2.53 (9)
N(2)	0.3308 (2)	−0.1160 (4)	0.0258 (3)	3.3 (1)
N(3)	0.4401 (2)	−0.2270 (4)	0.0430 (3)	4.8 (1)
N(4)	0.4678 (2)	−0.3771 (4)	0.1541 (3)	5.4 (1)
N(5)	0.3035 (2)	−0.2033 (4)	0.1367 (3)	3.3 (1)
C(1)	0.2369 (2)	0.0762 (4)	0.0304 (3)	2.5 (1)
C(2)	0.1638 (2)	0.1324 (4)	−0.0094 (3)	2.6 (1)
C(3)	0.1110 (2)	0.0317 (4)	−0.0110 (3)	2.8 (1)
C(4)	0.1581 (2)	−0.0743 (4)	−0.0220 (3)	2.5 (1)
C(5)	0.1792 (2)	−0.0354 (4)	−0.1034 (3)	2.9 (1)
C(6)	0.2046 (2)	0.0915 (4)	−0.0691 (3)	2.8 (1)
C(7)	0.3814 (3)	−0.1986 (5)	0.0671 (3)	3.8 (1)
C(8)	0.4844 (3)	−0.3193 (6)	0.0856 (4)	5.9 (2)
C(9)	0.4089 (3)	−0.3519 (5)	0.1834 (4)	5.1 (2)
C(10)	0.3671 (3)	−0.2540 (5)	0.1346 (3)	3.6 (1)
C(11)	0.2850 (2)	−0.1236 (4)	0.0702 (3)	2.6 (1)
C(12)	0.3026 (2)	0.1372 (4)	0.0898 (3)	2.8 (1)
C(13)	0.3874 (3)	0.2912 (6)	0.0955 (4)	5.1 (1)
C(14)	0.1447 (3)	0.2617 (4)	0.0008 (3)	3.5 (1)
C(15)	0.1847 (4)	0.4478 (5)	0.0730 (5)	7.4 (2)
C(16)	0.0941 (2)	0.0138 (4)	0.0736 (3)	3.3 (1)
C(17)	0.0983 (3)	0.0925 (7)	0.2105 (4)	6.2 (2)
C(18)	0.1291 (2)	−0.2022 (4)	−0.0245 (3)	3.2 (1)
C(19)	0.0312 (3)	−0.3278 (6)	−0.0963 (5)	6.4 (2)
C(20)	0.1192 (3)	−0.0353 (5)	−0.1891 (3)	3.7 (1)
C(21)	0.0600 (3)	−0.1550 (6)	−0.3148 (4)	6.2 (2)
C(22)	0.2336 (3)	0.1777 (5)	−0.1198 (3)	3.7 (1)
C(23)	0.3097 (4)	0.1912 (7)	−0.2066 (4)	7.8 (2)
C(24)	0.4533 (3)	−0.1656 (7)	−0.0310 (4)	7.0 (2)
C(25)	0.5144 (3)	−0.4784 (6)	0.1987 (5)	7.6 (2)
C(26)	0.2700 (3)	−0.2206 (5)	0.2043 (3)	4.1 (1)
C(27)	0.3031 (3)	−0.1333 (6)	0.2811 (4)	5.3 (2)
C(28)	0.2738 (4)	−0.1512 (6)	0.3548 (4)	6.3 (2)
C(29)	0.3052 (4)	−0.0614 (6)	0.4284 (4)	7.5 (2)

General Procedure for the Synthesis of 5-Alkyl-1,3-dimethyl-1,2,3,4-tetrahydro-7,8,11-tris(methoxycarbonyl)-5*H*,9*H*[1,3]-diazocino[1,2-*e*]-purine-2,4,9-triones (11a—d), 5-Alkyl-1,3-dimethyl-7,8-bis(methoxycarbonyl)-1,2,3,4,9,10-hexahydro-10-(methoxycarbonyl)methylene-5*H*[1,3]-diazepino[1,2-*e*]purine-2,4,9-triones (12a—d) and 5-Alkyl-1,3-dimethyl-1,2,3,4,9,10-hexahydro-7,8,9,10-tetrakis(methoxycarbonyl)-5*H*[1,3]-diazepino[1,2-*e*]purine-2,4-diones (13a—d) A mixture of 7-alkyl-8-amino-1,3-dimethylxanthines (**3a—d**) (0.00127 mol) and DMAD (1.81 g, 0.0127 mol) in 30 ml of DMF was heated at 70 °C for 17 h. The solvent was distilled off, and the residue was column-chromatographed on silica gel with a mixture of chloroform–methanol (30 : 1). From the first eluate, compounds **11a—d** were obtained. The second eluate gave **12a—d** and the third eluate gave **13a—d**.

5-Allyl-1,3-dimethyl-1,2,3,4-tetrahydro-7,8,11-tris(methoxycarbonyl)-5*H*,9*H*[1,3]-diazocino[1,2-*e*]purine-2,4,9-triones (**11a**): This compound was obtained as colorless prisms of mp 168—169 °C, yield 14%. IR (KBr): 1740 (ester C=O), 1700, 1640 (amide C=O). ^{1}H-NMR ($CDCl_3$) δ: 3.41 (3H, s, N–CH_3), 3.48 (3H, s, N–Me), 3.71 (3H, s, O–CH_3), 3.85 (3H, s, OCH_3), 3.92 (3H, s, OCH_3), 4.65—6.10 (5H, m, –$CH_2CH{=}CH_2$), 7.05 (1H, s, =CH–CO–). MS *m/z*: 487 (M^+). *Anal.* Calcd for $C_{21}H_{21}N_5O_9$: C, 51.75; H, 4.34; N, 14.37. Found: C, 52.01; H, 4.34; N, 14.15.

5-Propyl-1,3-dimethyl-1,2,3,4-tetrahydro-7,8,11-tris(methoxycarbonyl)-5*H*,9*H*[1,3]-diazocino[1,2-*e*]purine-2,4,9-triones (**11b**): This compound was obtained as colorless prisms of mp 202—203 °C, yield 10%. IR (KBr): 1740 (ester C=O), 1700, 1660 (amide C=O) cm^{-1}. ^{1}H-NMR ($CDCl_3$) δ: 0.99 (3H, t, J=8 Hz, $CH_3CH_2CH_2$–), 1.93 (2H, sextet, J=8 Hz, $CH_3CH_2CH_2$–), 3.43 (3H, s, N–CH_3), 3.49 (3H, s, N–CH_3), 3.72 (3H, s, OCH_3), 3.87 (3H, s, OCH_3), 3.95 (3H, s, OCH_3), 3.93—4.27 (2H, m, –$CH_2CH_2CH_3$), 7.08 (1H, s, =CH–CO–). MS *m/z*: 489 (M^+). *Anal.* Calcd for $C_{21}H_{23}N_5O_9$: C, 51.53; H, 4.74; N, 14.31. Found: C, 51.25; H, 4.72; N, 14.15.

5-Butyl-1,3-dimethyl-1,2,3,4-tetrahydro-7,8,11-tris(methoxycarbonyl)-5*H*,9*H*[1,3]-diazocino[1,2-*e*]purine-2,4,9-triones (**11c**): This compound was obtained as colorless prisms of mp 162—163 °C, yield 19%. IR (KBr): 1740 (ester C=O), 1700, 1660 (amide C=O) cm^{-1}. ^{1}H-NMR ($CDCl_3$) δ: 0.94 (3H, t, J=8 Hz, $CH_3(CH_2)_3$–), 1.40 (2H, m, $CH_3CH_2(CH_2)_2$–), 1.85 (2H, m, $CH_3CH_2CH_2CH_2$–), 3.43 (3H, s, N–CH_3), 3.49 (3H, s, N–CH_3), 3.72 (3H, s, OCH_3), 3.86 (3H, s, OCH_3), 3.94 (3H, s, OCH_3), 3.95—4.12 (2H, m, $CH_3(CH_2)_2CH_2$–), 7.08 (1H, s, =CH–CO–). MS *m/z*: 503 (M^+). *Anal.* Calcd for $C_{22}H_{25}N_5O_9$: C, 52.48; H, 5.00; N, 13.91. Found: C, 52.44; H, 4.79; N, 13.92.

5-Pentyl-1,3-dimethyl-1,2,3,4-tetrahydro-7,8,11-tris(methoxycarbonyl)-5*H*,9*H*[1,3]-diazocino[1,2-*e*]purine-2,4,9-triones (**11d**): This compound was obtained as colorless prisms of mp 171—172 °C, yield 17%. IR (KBr): 1740 (ester C=O), 1700, 1660 (amide C=O) cm^{-1}. ^{1}H-NMR ($CDCl_3$) δ: 0.89 (3H, t, J=8 Hz, $CH_3(CH_2)_4$–), 1.35 (4H, m, $CH_3(CH_2)_2$–), 1.90 (2H, m, $CH_3(CH_2)_2CH_2CH_2$–), 3.43 (3H, s, N–CH_3), 3.49 (3H, s, N–CH_3), 3.72 (3H, s, OCH_3), 3.87 (3H, s, OCH_3), 3.95 (3H, s, OCH_3), 3.96—4.25 (2H, m, $CH_2(CH_2)_3CH_3$), 7.26 (1H, s, =CH–CO–). *Anal.* Calcd for $C_{23}H_{27}N_5O_9$: C, 53.38; H, 5.26; N, 13.53. Found: C, 53.77; H, 5.18; N, 13.27.

5-Allyl-1,3-dimethyl-1,2,3,4-tetrahydro-7,8-bis(methoxycarbonyl)-1,2,3,4,9,10-hexahydro-10-(methoxycarbonyl)methylene-5*H*[1,3]-diazepino[1,2-*e*]purine-2,4,9-trione (**12a**): This compound was obtained as colorless prisms of mp 228—229.5 °C, yield 10%. IR (KBr): 1740 (ester C=O), 1700, 1660 (amide C=O) cm^{-1}. ^{1}H-NMR ($CDCl_3$) δ: 3.44 (3H, s, N–CH_3), 3.58 (3H, s, N–CH_3), 3.81 (3H, s, OCH_3), 3.83 (3H, s, OCH_3), 3.88 (3H, s, OCH_3), 4.99 (2H, d, J=6 Hz, –CH_2–CH=CH_2), 5.25—5.52 (2H, m, –CH_2–CH=CH_2), 5.80—6.05 (1H, m, CH=CH_2), 5.90 (1H, s, =CH–$COOCH_3$). MS *m/z*: 487 (M^+). *Anal.* Calcd for $C_{21}H_{21}N_5O_9$: C, 51.75; H, 4.34; N, 14.37. Found: C, 51.76; H, 4.25; N, 14.38.

5-Propyl-1,3-dimethyl-1,2,3,4-tetrahydro-7,8-bis(methoxycarbonyl)-1,2,3,4,9,10-hexahydro-10-(methoxycarbonyl)methylene-5*H*[1,3]diazepino[1,2-*e*]purine-2,4,9-trione (**12b**): This compound was obtained as colorless prisms of mp 266—267.5 °C, yield 13%. IR (KBr): 1740 (ester C=O), 1703, 1660 (amide C=O) cm^{-1}. ^{1}H-NMR ($CDCl_3$) δ: 0.95 (3H, t, J=8 Hz, $CH_3CH_2CH_2$–), 1.85 (2H, sextet, J=8 Hz, $CH_3CH_2CH_2$–), 3.42 (3H, s, N–CH_3), 3.59 (3H, s, N–CH_3), 3.80 (3H, s, OCH_3), 3.82 (3H, s, OCH_3), 3.88 (3H, s, OCH_3), 4.38 (2H, t, J=7 Hz, $CH_3CH_2CH_2$–), 5.90 (1H, s, =CH–$COOCH_3$). MS *m/z*: 489 (M^+). *Anal.* Calcd for $C_{21}H_{23}N_5O_9$: C, 51.53; H, 4.74; N, 14.31. Found: C, 51.46; H, 4.59; N, 14.08.

5-Butyl-1,3-dimethyl-1,2,3,4-tetrahydro-7,8-bis(methoxycarbonyl)-

1,2,3,4,9,10-hexahydro-10-(methoxycarbonyl)methylene-5*H*[1,3]-diazepino[1,2-*e*]purine-2,4,9-trione (**12c**): This compound was obtained as colorless prisms of mp 233—234 °C, yield 12%. IR (KBr): 1730 (ester C=O), 1704, 1680 (amide C=O) cm^{-1}. ^{1}H-NMR ($CDCl_3$) δ: 1.95 (3H, t, J=7 Hz, $C\underline{H}_3(CH_2)_3$–), 1.37 (2H, m, $CH_3C\underline{H}_2(CH_2)_2$–), 1.76 (2H, sextet, J=8 Hz, $CH_3CH_2C\underline{H}_2CH_2$–), 3.44 (3H, s, N–$CH_3$), 3.60 (3H, s, N–$CH_3$), 3.82 (3H, s, OCH_3), 3.84 (3H, s, OCH_3), 3.88 (3H, s, OCH_3), 4.40 (2H, m, $CH_3(CH_2)_2C\underline{H}_2$–), 5.88 (1H, s, =C<u>H</u>–$COOCH_3$). MS *m/z*: 503 (M^+). *Anal.* Calcd for $C_{22}H_{25}N_5O_9$: C, 52.48; H, 5.00; N, 13.91. Found: C, 52.17; H, 5.07; N, 13.81.

5-Pentyl-1,3-dimethyl-1,2,3,4-tetrahydro-7,8-bis(methoxycarbonyl)-1,2,3,4,9,10-hexahydro-10-(methoxycarbonyl)methylene-5*H*[1,3]-diazepino[1,2-*e*]purine-2,4,9-trione (**12d**): This compound was obtained as colorless prisms of mp 182—183 °C, 13%. IR (KBr): 1740 (ester C=O), 1700, 1660 (amide C=O) cm^{-1}. ^{1}H-NMR ($CDCl_3$) δ: 0.91 (3H, t, J=8 Hz, $C\underline{H}_3(CH_2)_4$–), 1.35 (4H, m, $CH_3C\underline{H}_2C\underline{H}_2(CH_2)_2$–), 1.81 (2H, quintet, J=8 Hz, $CH_3(CH_2)_2C\underline{H}_2CH_2$–), 3.44 (3H, s, N–$CH_3$), 3.60 (3H, s, N–$CH_3$), 3.82 (3H, s, OCH_3), 3.83 (3H, s, OCH_3), 3.89 (3H, s, OCH_3), 4.39 (2H, m, $CH_3(CH_2)_3C\underline{H}_2$–), 5.90 (1H, s, =C<u>H</u>–$COOCH_3$). *Anal.* Calcd for $C_{23}H_{27}N_5O_9$: C, 53.38; H, 5.26; N, 13.53. Found: C, 53.13; H, 5.16; N, 13.32.

5-Allyl-1,3-dimethyl-1,2,3,4,9,10-hexahydro-7,8,9,10-tetrakis(methoxycarbonyl)-5*H*[1,3]-diazepino[1,2-*e*]purine-2,4-dione (**13a**): This compound was obtained as colorless prisms of mp 211—212 °C, yield 24%. IR (KBr): 1750, 1710 (ester C=O), 1670 (amide C=O) cm^{-1}. ^{1}H-NMR ($CDCl_3$) δ: 3.38 (3H, s, N–CH_3), 3.63 (3H, s, N–CH_3), 3.73 (6H, s, $OCH_3\times2$), 3.79 (3H, s, OCH_3), 3.83 (3H, s, OCH_3), 4.80 (2H, d, J=4 Hz, N–$C\underline{H}_2$–CH=CH_2), 5.00—5.20 (2H, m, –CH=$C\underline{H}_2$), 5.80 (1H, m, –$C\underline{H}$=CH_2), 5.16 and 6.04 (each 1H, each d, J=6 Hz, –CH–CH–). MS *m/z*: 519 (M^+). *Anal.* Calcd for $C_{22}H_{25}N_5O_{10}$: C, 50.87; H, 4.85; N, 13.48. Found: C, 51.02; H, 4.83; N, 13.56.

5-Propyl-1,3-dimethyl-1,2,3,4,9,10-hexahydro-7,8,9,10-tetrakis(methoxycarbonyl)-5*H*[1,3]-diazepino[1,2-*e*]purine-2,4-dione (**13b**): This compound was obtained as colorless prisms of mp 209—210.5 °C, yield 44%. IR (KBr); 1750, 1710 (ester C=O), 1670 (amide C=O) cm^{-1}. ^{1}H-NMR ($CDCl_3$) δ: 0.86 (3H, t, J=8 Hz, $C\underline{H}_3CH_2CH_2$–), 1.70 (2H, sextet, J=8 Hz, $CH_3C\underline{H}_2CH_2$–), 3.41 (3H, s, N–CH_3), 3.64 (3H, s, N–CH_3), 3.75 (3H, s, OCH_3), 3.76 (3H, s, OCH_3), 3.81 (3H, s, OCH_3), 3.86 (3H, s, OCH_3), 4.20 (2H, t, J=8 Hz, $CH_3CH_2C\underline{H}_2$–), 5.16 and 6.04 (each 1H, each d, J=6 Hz, –CH–CH–). MS *m/z*: 521 (M^+). *Anal.* Calcd for $C_{22}H_{27}N_5O_{10}$: C, 50.67; H, 5.22; N, 13.43. Found: C, 50.45; H, 5.09; N, 13.23.

5-Butyl-1,3-dimethyl-1,2,3,4,9,10-hexahydro-7,8,9,10-tetrakis(methoxycarbonyl)-5*H*[1,3]-diazepino[1,2-*e*]purine-2,4-dione (**13c**): This compound was obtained as colorless prisms of mp 176—177 °C, yield 24%. IR (KBr): 1750, 1710 (ester C=O), 1670 (amide C=O) cm^{-1}. ^{1}H-NMR ($CDCl_3$) δ: 0.90 (3H, t, J=7 Hz, $C\underline{H}_3(CH_2)_3$–), 1.10—1.40 (2H, m, $CH_3C\underline{H}_2(CH_2)_2$–), 1.55—1.75 (2H, m, $CH_3CH_2C\underline{H}_2CH_2$–), 3.40 (3H, s, N–$CH_3$), 3.64 (3H, s, N–$CH_3$), 3.74 (3H, s, O–$CH_3$), 3.76 (3H, s, O–$CH_3$), 3.80 (3H, s, O–$CH_3$), 3.84 (3H, s, O–$CH_3$), 4.22 (2H, t, J=7 Hz, $C\underline{H}_2(CH_2)_2CH_3$), 5.19 and 6.06 (each 1H, each d, J=6 Hz, –CH–CH–). MS *m/z*: 535 (M^+). *Anal.* Calcd for $C_{23}H_{29}N_5O_{10}$: C, 51.59; H, 5.46; N, 13.08. Found: C, 51.48; H, 5.22; N, 12.96.

5-Pentyl-1,3-dimethyl-1,2,3,4,9,10-hexahydro-7,8,9,10-tetrakis(methoxycarbonyl)-5*H*[1,3]-diazepino[1,2-*e*]purine-2,4-dione (**13d**): This compound was obtained as colorless prisms of mp 180—190.5 °C, yield 32%. IR (KBr): 1730, 1720 (ester C=O), 1680 (amide C=O) cm^{-1}. ^{1}H-NMR ($CDCl_3$) δ: 0.87 (3H, t, J=7 Hz, $C\underline{H}_3(CH_2)_4$–), 1.20—1.37 (4H, m, $CH_3(C\underline{H}_2)_2(CH_2)_2$–), 1.69 (2H, m, $CH_3(CH_2)_2C\underline{H}_2CH_2$–), 3.40 (3H, s, N–$CH_3$), 3.64 (3H, s, N–$CH_3$), 3.74 (3H, s, O–$CH_3$), 3.76 (3H, s, O–$CH_3$), 3.80 (3H, s, O–$CH_3$), 3.84 (3H, s, O–$CH_3$), 4.20 (3H, t, J=7 Hz, $CH_3(CH_2)_3C\underline{H}_2$–), 5.18 and 6.06 (each 1H, each d, J=6 Hz, –CH–CH–). *Anal.* Calcd for $C_{24}H_{31}N_5O_{10}$: C, 52.46; H, 5.69; N, 12.74. Found: C, 52.47; H, 5.66; N, 13.02.

Acknowledgement The authors thank Misses T. Naito and S. Kato of this Faculty for elemental analyses and NMR measurements.

References and Notes

1) *a*) T. Ueda, N. Oda, J. Sakakibara, and K. Takeya, *Heterocycles*, **19**, 2291 (1982); *b*) J. Sakakibara, T. Ueda, T. Osaki, K. Takeya, and S. Ando, *Yakugaku Zasshi*, **105**, 730 (1985).
2) T. Ueda, T. Adachi, J. Sakakibara, K. Asano, and J. Nakagami, *Chem. Pharm. Bull.*, **35**, 4031 (1987).
3) No report on the synthesis of this ring system has been published except for the paper by Hino *et al.* They synthesized this ring system from 8-bromoadenine and hydroxypropylamine: *Chem. Pharm. Bull.*, **21**, 1696 (1975).
4) J. W. Jones and R. K. Robins, *J. Am. Chem. Soc.*, **82**, 3773 (1960).
5) B. F. Duesel, H. Berman, and R. J. Schachter, *J. Am. Pharm. Assoc.*, **49**, 453 (1954).
6) J. J. Wade, R. F. Hegel, and C. B. Toso, *J. Org. Chem.*, **44**, 1811 (1979).
7) C. Chan, J. C. N. Ma, and T. C. W. Mak, *J. Chem. Soc., Perkin Trans. 2*, **1977**, 1070.
8) R. M. Acheson, M. W. Foxton, and G. R. Miller, *J. Chem. Soc.*, **1965**, 3200.
9) R. M. Letcher and D. W. M. Sin, *Tetrahedron Lett.*, **28**, 3687 (1987).
10) R. M. Acheson, M. W. Foxton, P. J. Abbot, and K. R. Mills, *J. Chem. Soc. (C)*, **1967**, 882.
11) K. Itoh, N. Oshima, G. B. Jameson, H. C. Lewis, and J. A. Ibers, *J. Am. Chem. Soc.*, **103**, 3014 (1981).

Studies on Conjugated Nitriles. VI.[1] Reaction of 2-Methylquinoline and Related Compounds with Acyl Cyanides

Masanori SAKAMOTO,* Mitsuaki ABE, and Keitaro ISHII

Meiji College of Pharmacy, 1–35–23 Nozawa, Setagaya-ku, Tokyo 154, Japan. *Received July 23, 1990*

The reactions of 2-methylquinoline (7), 2-methylbenzothiazole (25), and related compounds 8—11 and 26—30 with benzoyl cyanide (1) or 4-nitrobenzoyl cyanide (2) proceeded *via* the cyanohydrin derivatives to afford the corresponding *C*-acylated products 12—17 and 31—36.

Keywords azine ring; azole ring; azoline ring; benzoyl cyanide; 4-nitrobenzoyl cyanide; *C*-acylation; cyanohydrin

The reaction of aldimines or ketimines with benzoyl cyanide (**1**) generally affords Reissert-type compounds.[2] Previously, we reported that the reaction of *N*-(1-phenylalkylidene)benzylamine **3a**, **b** and 1-alkyl-3,4-dihydroisoquinolines **5a**—**d** with 4-nitrobenzoyl cyanide (**2**) gave 4,5-dihydropyrrole derivatives **4a**, **b**[3] and **6a**—**d**,[4] respectively. The reactions presumably proceed initially by nucleophilic addition of **3** and **5** in the enamine form to **2**, affording the cyanohydrin intermediates, followed by cyclization to the adducts **4** and **6** (Chart 1).

Therefore, it is of interest to compare the reactivity of the imino moiety in a heteroaromatic system with that of compounds **3** and **5**. The subject of the present paper is the reaction of compounds **7**—**11**, possessing an imino moiety in a six-membered aromatic ring, with **1** and **2**.

The reaction of 2-methylquinoline (**7**) with **1** in refluxing xylene afforded a 22:1[5] mixture of (*Z*)-1,2-dihydro-2-benzoylmethylenequinoline (**12A**)[6] and 2-benzoylmethylquinoline (**12C**)[6] in 22% yield. Three tautomeric structures can be considered in the product **12**: the enamine form **12A**, the enol form **12B**, and the keto form **12C**. The structure of **12** was determined from a comparison of its ultraviolet (UV),[7] infrared (IR), and proton nuclear magnetic resonance (^{1}H-NMR) spectral data with literature values.[6a,b] The following key signals in the ^{13}C-NMR spectrum also supported these structures: a doublet at 89.9 ppm and a triplet at 48.8 ppm due to the carbon atom positioned α to the carbonyl group for **12A** and for **12C**, a singlet at 154.2 ppm due to the C-2 carbon atom, and two singlets at 184.1 and 195.6 ppm due to the carbonyl carbon atom for **12A** and for **12C**, respectively (Chart 2).

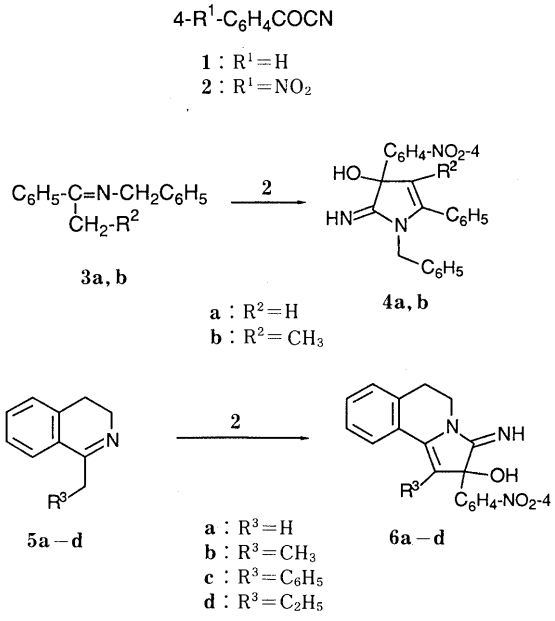

Chart 1

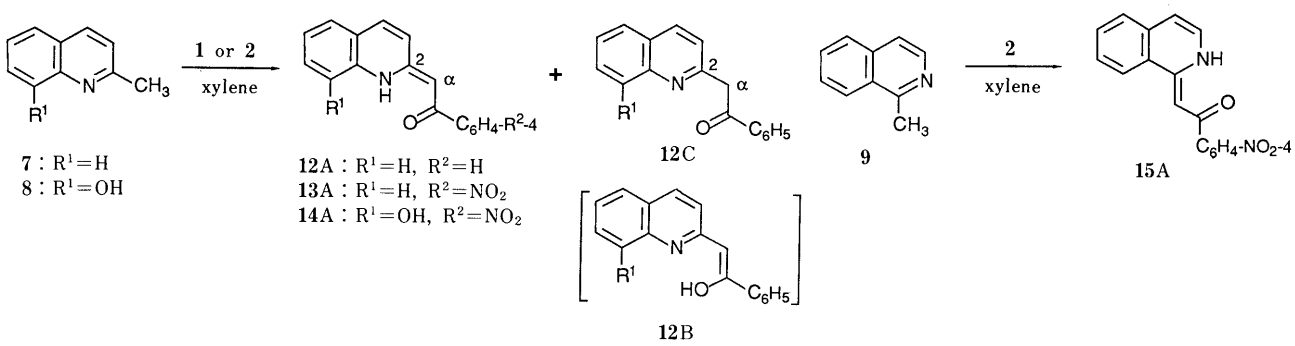

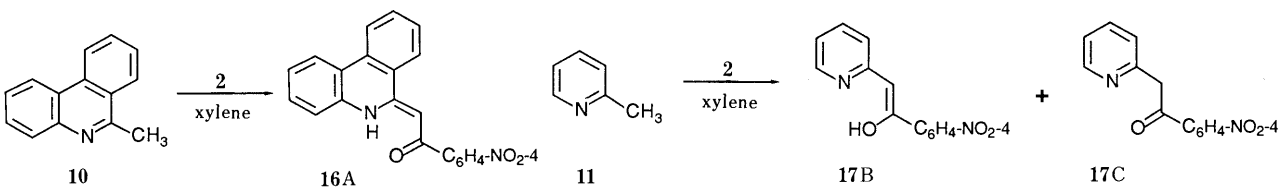

Chart 2

TABLE I. Results and Characterization for Compounds **12**—**17**

Substrate	Method[a]	Time (h)	Product	Yield (%)	mp (°C) (Solv.)[b]	Mol. Formula	Analysis (%) Found C	Found H	Found N	Calcd C	Calcd H	Calcd N
7	II	15	**12**	22	117—118 (PA) [116—117][c]	$C_{17}H_{13}NO$	82.36	5.05	5.63	82.57	5.30	5.66
7	I	15	**13**	48	210—211 (AC)	$C_{17}H_{12}N_2O_3$	70.13	3.84	9.59	69.85	4.14	9.59
8	I	6	**14**	7	293—294 (AC)	$C_{17}H_{12}N_2O_4$	66.16	3.71	9.09	66.23	3.92	9.09
9	I	12	**15**	48	239—240 (AC)	$C_{17}H_{12}N_2O_3$	69.55	3.96	9.73	69.85	4.14	9.59
10	I	15	**16**	34	254—255 (DMF)	$C_{21}H_{14}N_2O_3$	73.97	3.85	8.21	73.67	4.12	8.18
11	II	4	**17**	11	176—177 (BE)	$C_{13}H_{10}N_2O_3$	64.73	3.95	11.53	64.46	4.16	11.57

a) See the experimental section. *b*) PA = petroleum ether, AC = acetone, DMF = dimethylformamide, and BE = benzene. *c*) Ref. 6*b*.

TABLE II. Spectral Data for **12**—**17** and **20**—**22**

Compd.	UV $\lambda_{max}^{CHCl_3}$ nm (log ε)	IR ν_{max}^{KBr} cm^{-1} N–H	IR ν_{max}^{KBr} cm^{-1} C=O	^{1}H-NMR δ: ppm CαH (**A** or **B**)	^{1}H-NMR δ: ppm CαH$_2$ (**C**)	^{1}H-NMR δ: ppm NH or OH
12	439 (3.76), 456 (3.77)	3440	1634	6.07 (**A**)	4.84	15.7[f]
	427 (4.49), 453 (4.45)[a]		1636[d]			
	[428 (4.51), 453 (4.45)][a,b]		[1639][b,d]	[5.98][b]	[4.75][b,f]	
13	449 (4.41), 466 (4.40)	3440	1632	6.45 (**A**)	—[e]	15.8[g]
	455 (4.27), 476 (4.28)[c]					
14	460 sh (4.29), 476 (4.31)[c]	3450	1634	6.43 (**A**)	—[e]	15.7[h]
15	447 (4.39)	3460	1608	7.04 (**A**)	—[e]	16.1[i]
16	448 (4.39)	3460	1595	7.29 (**A**)	—[e]	—[e,h]
				6.81 (**A**)	—[e]	16.1[f]
17	380 (4.22)	3450 (O–H)	1627 (C=C)	6.19 (**B**)	4.67	15.7[f]
20	403 (4.13), 424 (4.16)	3450	1602	6.87 (**A**)	—[e]	15.1[f]
21	403 (4.09), 427 (4.14)	3440	1602	6.83 (**A**)	—[e]	14.8[f]
22	392 (3.75)	3450 (O–H)	1638 (C=C)	6.16 (**B**)	—[e]	15.5[f]

a) In EtOH. *b*) Ref. 6*b*. *c*) In DMSO. *d*) Nujol. *e*) Not detectable. *f*) In $CDCl_3$, r.t. *g*) In DMSO-d_6, 70 °C. *h*) In DMSO-d_6, r.t. *i*) In DMSO-d_6, 80 °C.

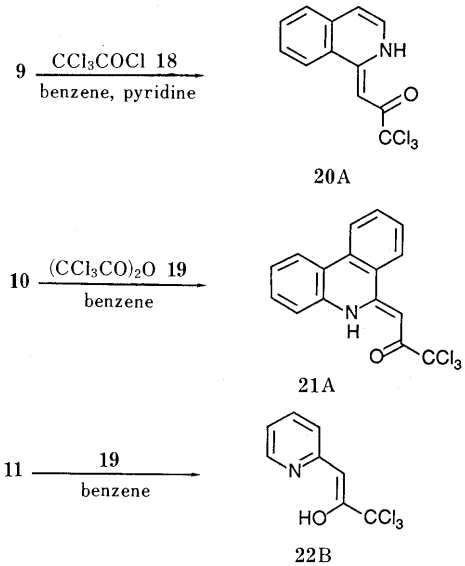

Chart 3

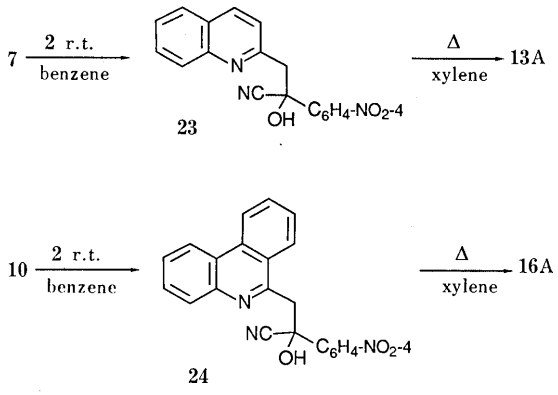

Chart 4

Similarly, the reactions of **7**, 8-hydroxy-2-methylquinoline (**8**), 1-methylisoquinoline (**9**), 6-methylphenanthridine (**10**), and 2-methylpyridine (**11**) with **2** afforded *C*-acylated compounds **13A**,[8] **14A**[8] **15A**,[8] **16A**,[8] and **17B** and **17C** (13 : 1),[5] respectively. The structures of the products **13**—**16** were deduced from a comparison of their spectral data with those of **12**. The structure of **17B** was confirmed by comparison of the spectral data with those of 2-phenacylpyridine.[6c,9] The results of the reaction, the characterization, and the relevant spectral data for **12**—**17** are summarized in Tables I and II.

Further evidence for the structures of **15**—**17** was obtained from their reactions with **9**—**11** and trichloracetyl chloride (**18**) or trichloroacetic anhydride (**19**), *C*-acylation agents for imines of this type,[10] which afforded **20A**[8] (2%), **21A**[8] (13%), and **22B**[8] (5%), respectively. The spectral data for **20**—**22** also supported the *C*-acylated structures of **15**—**17** (Chart 3). The relevant spectral data for **20**—**22** are listed in Table II.

On the other hand, the reactions of **7** and **10** with **2** in benzene at room temperature (r.t.) gave the cyanohydrins **23** (29%) and **24** (36%), which were transformed by

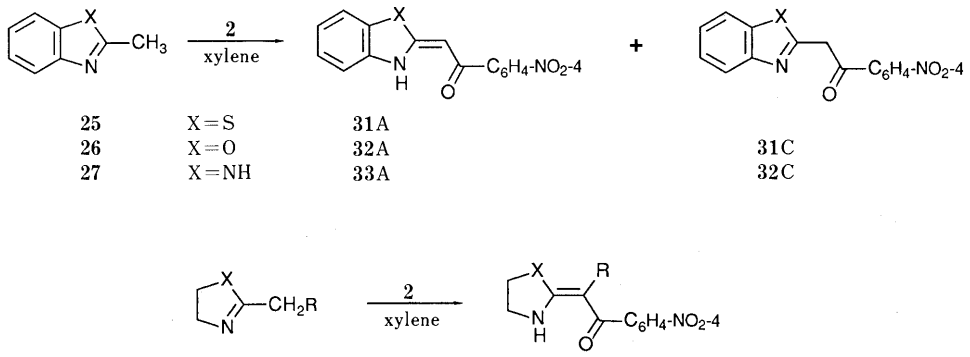

Chart 5

TABLE III. Results and Characterization for Compounds **31**—**36**

Substrate	Time (h)	Product	Yield (%)	mp (°C) (Solv.)[a]	Mol. Formula	Analysis (%) Found C	Found H	Found N	Calcd C	Calcd H	Calcd N
25	8	**31**	17	224—225 (AC)	$C_{15}H_{10}N_2O_3S$	60.31	3.22	9.38	60.39	3.38	9.39
26	25	**32**	20	248—249 (AC)	$C_{15}H_{10}N_2O_4$	63.92	3.35	9.93	63.83	3.57	9.93
27	6	**33**	9	165—166 (DMF)	$C_{15}H_{11}N_3O_3$	64.15	3.74	15.05	64.05	3.94	14.94
28	72	**34**	37	226—227 (AC)	$C_{11}H_{10}N_2O_3S$	52.59	4.00	11.13	52.80	4.03	11.20
29	12	**35**	39	263—264 (AC)	$C_{11}H_{10}N_2O_4$	56.27	4.20	12.05	56.41	4.30	11.96
30	72	**36**	30	179—180 (AC)	$C_{12}H_{12}N_2O_4$	57.89	4.84	11.28	58.06	4.87	11.29

a) See footnote to Table I.

TABLE IV. Spectral Data for **31**—**36**

Compd.	UV $\lambda_{max}^{CHCl_3}$ nm (log ε)	IR ν_{max}^{KBr} cm^{-1} N–H	IR C=O	^{1}H-NMR δ: ppm CαH (A)	CαH$_2$ (C)	NH or OH
31	302 (3.97), 387 (4.44)	3460	1626	6.88	5.12	—[b,c]
32	375 (4.35), 378 (4.17)[a]	3450	1637	6.70	4.96	—[b,d]
33	331 (4.18),[a] 412 (4.16)[a]	3440	1616	6.15	—[b]	—[b,e]
34	273 (4.00), 370 (4.00)	3460	1612	5.97	—[b]	10.73[f]
35	268 (4.26), 352 (4.07)	3450	1625	5.58	—[b]	9.87[d]
36	296 (4.73), 350 (3.38)	3440	1638			10.29[g]

a) In DMSO. *b*) Not detectable. *c*) In DMSO-d_6, 50 °C. *d*) In DMSO-d_6, 80 °C. *e*) In DMSO-d_6, 40 °C. *f*) In $CDCl_3$, r.t. *g*) In DMSO-d_6, r.t.

refluxing in xylene to **13A** and **16A**, respectively. The structures of **23** and **24** were determined from the spectral data. In particular, the ^{1}H-NMR spectra for **23** and **24** showed two doublets at 3.66 and 3.94 ppm and 3.96 and 4.58 ppm due to the methylene protons, respectively (Chart 4).

The reactions of the six-membered aromatic nitrogen ring system in **7**—**11** with **1** and **2** gave the corresponding *C*-acylated compounds. Furthermore, the investigated the reactions of the azole and azoline ring systems in **25**—**30**, bearing one heteroatom at the 3-position to the nitrogen atom, with **2**.

Compounds **25**—**30** were refluxed with **2** in xylene to afford the corresponding *C*-acylated compounds **31A** and **31C** (16 : 1),[5] **32A** and **32C** (1.8 : 1),[5] **33A**,[8] **34A**,[8] **35A**,[8] and **36A**,[8] respectively (Chart 5). The results, the characterization, and selected spectral data for the products **31**—**36** are summarized in Table III and IV. The tautomeric

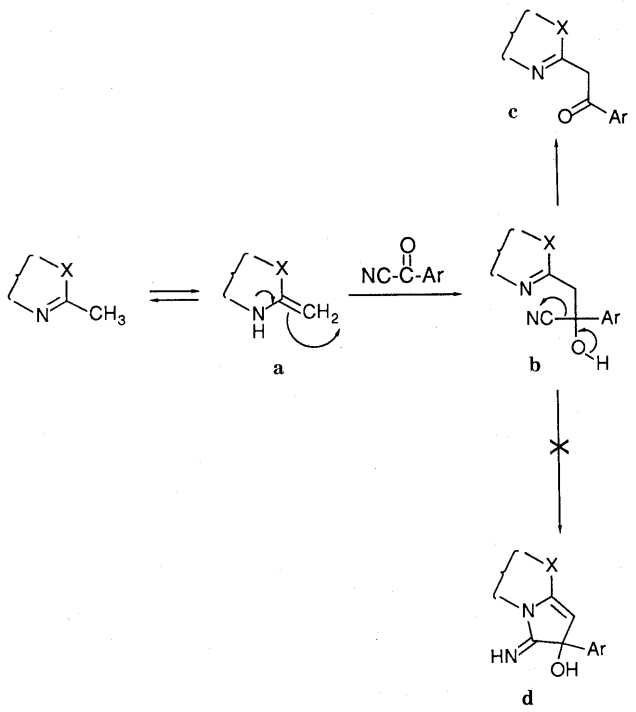

Chart 6

structure A and *E*/*Z*-configuration for the products **31**—**36** were deduced from a comparison of their spectral data with those of compounds **12**—**17**, 2-methylenebenzothiazoline,[11a] and 2-methylenethiazoline derivatives.[11b]

The proposed mechanism for the formation of *C*-acylated compounds is shown in Chart 6. The enamine form **a** of the imines undergoes addition to **1** and **2**, leading to the cyanohydrin intermediate **b**, followed by elimination of hydrogen cyanide to give the *C*-acylated compound **c**. In contrast to the reaction of **3**[3] and **5**[4] with **2**, the reaction of **7**—**11** and **25**—**30** with **2** did not afford the cyclic product **d**. The nucleophilicity of the imine nitrogen in **7**—**11** and **25**—**30** is not enough to permit attack on the cyano group, leading to **d**, since the nitrogen atom is incorporated into the aromatic system and/or may be influenced by the inductive effect of the heteroatom (X) (Chart 6).

Experimental

Melting points were measured with a Yanaco MP-3 apparatus and are uncorrected. UV spectra were recorded on a Hitachi 124 spectrometer and IR spectra on a Hitachi 215 spectrometer. ^{1}H-NMR spectra were obtained with a JEOL PS-100 (PS), a JEOL JNM-EX270 (EX), or a JEOL GX-400 (GX) spectrometer and ^{13}C-NMR spectra were run on an EX or a GX spectrometer using tetramethylsilane as the internal standard. Mass spectra (MS) were taken on a JEOL JMS-D300 spectrometer. Column chromatography (CC) was performed with Kanto silica gel, 80—100 mesh.

4-Nitrobenzoyl cyanide (**2**) was prepared by the method of Dornow and Grabhofer.[12]

General Procedure for the Reactions of the Azines 7—11 and Acyl Cyanides 1 and 2 A solution of an azine (2 mmol) and an acyl cyanide (2 mmol) in anhydrous xylene (30 ml) was heated under reflux for an appropriate time (Table I). Method I: After cooling, the resulting precipitates were collected by filtration. Method II: After removal of the solvent *in vacuo*, the residue was purified by CC ($CHCl_3$ as an eluent). In both cases, the crude product was purified was purified by recrystallization. The results, the characterization, and UV spectral data are summarized in Tables I and II.

(*Z*)-1,2-Dihydro-2-benzoylmethylenequinoline (**12A**) and 2-Benzoylmethylquinoline (**12C**)[6] (22 : 1)[5]: Yellow needles. ^{1}H-NMR ($CDCl_3$, r.t., GX) δ: 4.84 (2H, s, CH_2 for **12C**), 6.07 (1H, s, HC=C(2) for **12A**), 6.85 (1H, d, J=9.2 Hz, H-C(3)), 7.22—7.27, 7.42—7.53, 7.94—7.97 (9H, 3m, H-Ar), 7.63 (1H, d, J=9.2 Hz, H-C(4)), 15.7 (1H, br s, NH). ^{13}C-NMR ($CDCl_3$, r.t., GX) δ: 48.8 (t, CH_2 for **12C**), 89.9 (d, C=C(2) for **12A**), 118.2 (d, C(3)), 122.3, 123.7, 127.6, 130.4, 131.0 (5d, 4C in Ar, 1C in Ph), 123.3 (s, C(4a)), 126.7, 128.3 (2d, 4C in Ph), 136.2 (d, C(4)), 137.8 (s, 1C in Ph), 139.8 (s, C(8a)), 154.2 (s, C(2)), 184.1 (s, CO). MS *m/z*: 247 (M^+), 219 ($M^+ -28$), 105 ($PhCO^+$).

(*Z*)-1,2-Dihydro-2-(4′-nitrobenzoylmethylene)quinoline (**13A**): Red needles. IR (KBr): 3440 (N–H), 1630 (C=O), 1531, 1341 cm^{-1} (NO_2). ^{1}H-NMR (DMSO-d_6, 70°C, GX) δ: 6.45 (1H, s, HC=C(2), D_2O-erasable), 7.22 (1H, d, J=9.0 Hz, H-C(3)), 7.42 (1H, ddd, J_1=8, J_2=7.1, J_3=1.2 Hz, H-C(7)), 7.68 (1H, ddd, J_1=8.3, J_2=7.1, J_3=1.2 Hz, H-C(6)), 7.75 (1H, d, J= 8.3 Hz, H-C(5)), 7.80 (1H, dd, J_1=8, J_2=1.2 Hz, H-C(8)), 8.09 (1H, d, J=9.0 Hz, H-C(4)), 8.17, 8.29 (4H each, d, J=9.0 Hz, $C_6H_4NO_2$),15.8 (1H, br s, NH, D_2O-erasable). MS *m/z*: 292 (M^+), 170 ($M^+ -122$).

(*Z*)-1,2-Dihydro-8-hydroxy-2-(4′-nitrobenzoylmethylene)quinoline (**14A**): Orange needles. IR (KBr): 3450 (N–H), 1634 (C=O), 1524, 1340 cm^{-1} (NO_2). ^{1}H-NMR (DMSO-d_6, r.t., GX) δ: 6.43 (1H, s, HC=C(2), D_2O-erasable), 7.12—7.27 (4H, m, H-Ar), 8.02 (1H, d, J=9.3 Hz, H-C(4)), 8.18, 8.31 (4H each, d, J=9.0 Hz, $C_6H_4NO_2$), 10.89 (1H, br s, OH, D_2O-erasable), 15.7 (1H, br s, NH, D_2O-erasable). ^{13}C-NMR (DMSO-d_6, r.t., EX) δ: 89.9 (d, C=C(2)), 114.6, 117.9, 122.2, 124.4 (4d, 4C in Ar), 123.5, 127.5 (2d, 4C in $C_6H_4NO_2$), 124.1, 126.7, 145.5, 148.2 (5s, 2s at 145.5, 3C in Ar, 2C in $C_6H_4NO_2$), 152.7 (s, C(2)), 179.5 (s, CO). MS *m/z*: 308 (M^+), 158 ($M^+ -150$), 150 ($COC_6H_4NO_2^+$).

(*Z*)-1,2-Dihydro-1-(4′-nitrobenzoylmethylene)isoquinoline (**15A**): Red needles. IR (KBr): 3460 (N–H), 1608 (C=O), 1558, 1342 cm^{-1} (NO_2). ^{1}H-NMR (DMSO-d_6, 80°C, GX) δ: 7.04 (1H, s, HC=C(1), D_2O-erasable), 7.14 (1H, d, J=6.6 Hz, H-C(4)), 7.62—7.67 (1H, m, H-C(7)), 7.79—7.82 (3H, m, H-C(3), H-C(5), H-C(6)), 8.26, 8.31 (4H, each d, J=8.8 Hz, $C_6H_4NO_2$), 8.57 (1H, d, J=8.1 Hz, H-C(8)), 16.1 (1H, br s, NH, D_2O-erasable). MS *m/z*: 292 (M^+).

(*Z*)-5,6-Dihydro-6-(4′-nitrobenzoylmethylene)phenanthridine (**16A**): Red needles. IR (KBr): 3460 (N–H), 1595 (C=O), 1556, 1342 cm^{-1} (NO_2). ^{1}H-NMR (DMSO-d_6, r.t., EX) δ: 7.29 (1H, s, HC=C(6)), 7.54, 7.73 7.85, 8.03 (4H, 4m with t-character, J=8 Hz, H-C(2), H-C(3), H-C(8), H-C(9)), 7.75, 8.63, 8.76, 8.84 (4H, 4d, J=8 Hz, H-C(1), H-C(4), H-C(7), H-C(10)), 8.40, 8.49 (4H, each d, J=8.9 Hz, $C_6H_4NO_2$). ^{1}H-NMR ($CDCl_3$, r.t., GX) δ: 6.81 (1H, br s, HC=C(6)), 7.38—7.44 (1H, m), 7.52—7.62 (2H, m), 7.67, 7.85 (2H, 2m with t-character, J=7.5 Hz), 8.17 (2H, m with d-character), 8.28—8.34 (4H, m), 8.44 (1H, m with d-character), 16.1 (1H, br s, NH). MS *m/z*: 342 (M^+), 220 ($M^+ -122$).

(*Z*)-2-(2′-Hydroxy-2′-(4″-nitrophenyl)vinyl)pyridine (**17B**) and 2-(4′-Nitrobenzoylmethyl)pyridine (**17C**) (13 : 1)[5]: Yellow needles. IR (KBr): 3450 (O-H), 1627 (C=C), 1518, 1336 cm^{-1} (NO_2). ^{1}H-NMR ($CDCl_3$, r.t., EX) δ: 4.67 (2H, s, CH_2 for **17C**), 6.19 (1H, s, H-C(1′) for **17B**), 7.09 (1H, ddd, J_1=7.3, J_2=5.0, J_3=1.0 Hz, H-C(5)), 7.15 (1H, d, J=7.9 Hz, H-C(3)), 7.65—7.73 (1H, t with fine splitting, J=8 Hz, H-C(4)), 7.99, 8.26 (4H, each d, J=8.9 Hz, $C_6H_4NO_2$), 8.35 (1H, d, J=5.0 Hz, H-C(6)), 15.7 (1H, br s, OH). ^{13}C-NMR (DMSO-d_6, r.t., GX) δ: 47.8 (t, CH_2 for **17C**) 96.1 (d, C(1′) for **17B**), 119.4, 122.2 (2d, C(3), C(5)), 123.3, 126.0 (2d, 4C in $C_6H_4NO_2$), 138.0 (d, C(4)), 142.2, 147.5 (2s, 2C in $C_6H_4NO_2$), 143.8 (d, C(6)), 156.8 (s, C(2)), 161.2 (s, C(2′) for **17B**), 196.2 (s, CO for **17C**). MS *m/z*: 242 (M^+).

Reactions of the Azines 9—11 with Trichloroacetyl Chloride (18) or Trichloroacetic Anhydride (19) A solution of **18** (340 mg, 2.00 mmol) in anhydrous benzene (20 ml) was added dropwise to a stirred solution of **9** (286 mg, 2.00 mmol) in anhydrous benzene (20 ml) and pyridine (174 mg, 2.2 mmol). The reaction mixture was stirred for 24 h at room temperature. The resulting precipitates were filtered, and the filtrate was dried over $MgSO_4$. After removal of the solvent *in vacuo*, the residue was purified by CC (ethyl acetate). Recrystallization from benzene afforded 10 mg (2%) of (*Z*)-1,2-dihydro-1-trichloroacetylmethylenisoquinoline (**20A**) as yellow needles, mp 205—206 °C. *Anal.* Calcd for $C_{12}H_8Cl_3NO$: C, 49.95; H, 2.79; N, 4.85. Found: C, 49.74; H, 2.59; N, 4.83. IR (KBr): 3450 (N–H), 1602 cm^{-1} (C=O). ^{1}H-NMR ($CDCl_3$, r.t., GX) δ: 6.87 (1H, s, HC=C(1)), 7.03 (1H, d, J=6.7 Hz, H-C(4)), 7.46—7.52 (1H, m, $W_{1/2}$=13.5 Hz, H-C(3)), 7.63 (1H, t with fine splitting, J=8 Hz, H-C(7)), 7.69 (1H, d, J=7.3 Hz, H-C(5)), 7.78 (1H, t with fine splitting, J=7 Hz, H-C(6)), 8.22 (1H, d, J=8.5 Hz, H-C(8)), 15.1 (1H, br s, NH). MS *m/z*: 291 ($M^+ +4$), 289 ($M^+ +2$), 287 (M^+), 170 ($M^+ -117$).

A solution of **19** (618 mg, 2.00 mmol) in anhydrous benzene (20 ml) was added dropwise to a stirred solution of **10** (386 mg, 2.00 mmol) in anhydrous benzene (20 ml). The reaction mixture was stirred for 12 h at room temperature. The resulting precipitates were filtered and the filtrate was washed with saturated $NaHCO_3$ and dried over $MgSO_4$. After removal of the solvent *in vacuo*, recrystallization of the residue from benzene afforded 85 mg (13%) of (*Z*)-5,6-dihydro-6-trichloroacetylmethylenephenanthridine (**21A**) as yellow needles, mp 231—232 °C. *Anal.* Calcd for $C_{16}H_{10}Cl_3NO$: C, 56.78; H, 2.98; N, 4.14. Found: C, 56.83; H, 2.73; N, 4.09. IR (KBr): 3440 (N–H), 1602 cm^{-1} (C=O). ^{1}H-NMR ($CDCl_3$, r.t., GX) δ: 6.83 (1H, s, HC=C(6), D_2O-erasable), 7.39, 7.53, 7.61, 7.81 (4H, 4t, J=8 Hz, H-C(2), H-C(3), H-C(8), H-C(9)), 7.42, 8.17, 8.21 (3H, 3d, J=8 Hz, H-C(1), H-C(4), H-C(10)), 8.33 (1H, d, J=7.9 Hz, H-C(7)), 14.8 (1H, br s, NH, D_2O-erasable). ^{13}C-NMR ($CDCl_3$, r.t., GX) δ: 80.1 (d, HC=C(6)), 97.6 (s, CCl_3), 118.6, 122.7, 122.8, 125.1, 125.8, 128.5, 130.3, 133.1 (8d, 8C in Ar), 120.8, 123.8, 132.4, 133.6 (4s, 4C in Ar), 154.9 (s, C(6)), 180.2 (s, CO). MS *m/z*: 341 ($M^+ +4$), 339 ($M^+ +2$), 337 (M^+), 220 ($M^+ -117$).

2-Methylpyridine (**11**) (465 mg, 5.00 mmol) and **19** (1.55 g, 5.00 mmol) were allowed to react, and the reaction mixture was worked up as described above to afford 50 mg (5%) of (*Z*)-2-(2′-hydroxy-2′-trichloroacetylvinyl)-pyridine (**22B**) as yellow needles, mp 153.5—154.5 °C. *Anal.* Calcd for $C_8H_6Cl_3NO$: C, 40.29; H, 2.54; N, 5.87. Found: C, 40.41; H, 2.37; N, 5.86. IR (KBr): 3450 (O–H), 1638 cm^{-1} (C=C). ^{1}H-NMR ($CDCl_3$, r.t., EX) δ: 6.16 (1H, s, H-C(1′)), 6.92 (1H, ddd, J_1=7.3, J_2=5.9, J_3=1.3 Hz, H-C(5)), 7.10 (1H, d, J=8.9 Hz, H-C(3)), 7.64 (1H, ddd, J_1=8.9, J_2=7.3, J_3=1.3 Hz, H-C(4)), 7.91 (1H, d, J=5.9 Hz, H-C(6)), 15.5 (1H, br s, OH). ^{13}C-NMR ($CDCl_3$, r.t., GX) δ: 84.1 (d, C(1′)), 96.5 (s, CCl_3), 116.2, 123.1 (2d, C(3), C(5)), 136.3, 139.3 (2d, C(4), C(6)), 155.8 (s, C(2)), 174.2 (s, C(2′)). MS *m/z*: 241 ($M^+ +4$), 239 ($M^+ +2$), 237 (M^+), 120 ($M^+ -117$), 92 ($M^+ -145$).

Reactions of the Azines 7 and 10 with 2 at Room Temperature A solution of **7** (286 mg, 2.00 mmol) and **2** (344 mg, 2.00 mmol) in anhydrous benzene (30 ml) was stirred at room temperature for 12 h. The resulting precipitates were collected by filtration. Recrystallization from acetone yielded 286 mg (29%) of 2-(2′-cyano-2′-hydroxy-2′-(4″-nitrophenyl)ethyl)quinoline (**23**) as orange prisms, mp 209—210 °C. *Anal.* Calcd for $C_{18}H_{13}N_3O_3$: C, 67.70; H, 4.11; N, 13.16. Found: C, 67.74; H, 3.89; N, 13.19. UV $\lambda_{max}^{CHCl_3}$ nm (log ε): 265 (3.97), 305 (3.59), 318 (3.59). IR (KBr): 3440 (O–H), 1527, 1347 cm^{-1}

(NO_2).[13] ^{1}H-NMR (acetone-d_6, r.t., PS) δ: 3.66, 3.94 (2H, each d, J=17 Hz, 2H-C(1')), 7.4—8.5 (6H, m, H-Ar), 8.02, 8.35 (4H, each d, J=9 Hz, $C_6H_4NO_2$), 8.00—8.34 (1H, br, OH). MS m/z: 292 (M^+ −27).

A solution of **10** (386 mg, 2.00 mmol) and **2** (344 mg, 2.00 mmol) in anhydrous benzene (30 ml) was stirred and worked-up as described above. Recrystallization of the product from acetone yielded 247 mg (36%) of 6-(2'-cyano-2'-hydroxy-2'-(4''-nitrophenyl)ethyl)phenanthridine (**24**) as yellow needles, mp 253—254 °C. *Anal.* Calcd for $C_{22}H_{15}N_3O_3$: C, 71.53; H, 4.09; N, 11.38. Found: C, 71.58; H, 3.89; N, 11.43. UV $\lambda_{max}^{CHCl_3}$ nm (log ε): 256 (4.83), 334 (3.54), 349 (3.46). IR (KBr): 3440 (O–H), 1524, 1344 cm^{-1} (NO_2).[13] ^{1}H-NMR (acetone-d_6, r.t., PS) δ: 3.96, 4.58 (2H, each d, J=17 Hz, 2H-C(1')), 7.7—9.0 (9H, m, H-Ar and OH), 8.12, 8.37 (4H, each d, J=9 Hz, $C_6H_4NO_2$). MS m/z: 342 (M^+ −27), 220 (M^+ −149).

Transformations of the Cyanohydrins 23 and 24 to 12 and 16, Respectively A solution of **23** (31.8 mg, 0.100 mmol) in anhydrous xylene (1 ml) was stirred under reflux for 4 d. After cooling, the resulting precipitates were collected by filtration, yielding **12** quantitatively. A solution of **23** (31.8 mg, 0.100 mmol) in 20% aqueous NaOH (1 ml) was stirred for 12 h at room temperature. The resulting precipitates were collected by filtration, affording **12** quantitatively.

The cyanohydrin **24** (36.9 mg, 0.100 mmol) was treated as described above, affording **16** quantitatively.

General Procedure for the Reactions of the Azoles 25—27 and the Acyl Cyanide 2 A 0.10 M solution of an azole and 1 eq of **2** in anhydrous xylene was refluxed for an appropriate time (Table III). After cooling, the resulting precipitates were collected by filtration, and the crude product was purified by recrystallization. The results, the characterization, and UV spectral data are summarized in Table III and IV.

(*E*)-2-(4'-Nitrobenzoylmethylene)benzothiazoline (**31A**) and 2-(4'-Nitrobenzoylmethyl)benzothiazole (**31C**) (16 : 1)[5]: Orange prisms. IR (KBr): 3460 (N–H), 1626 (C=O), 1517, 1337 cm^{-1} (NO_2). ^{1}H-NMR (DMSO-d_6, 50 °C, EX) δ: 5.12 (2H, s, CH_2 for **31C**, D_2O-erasable), 6.88 (1H, s, HC=C(2) for **31A**, D_2O-erasable), 7.27, 7.44 (2H, each t, J=7.5 Hz, H-C(5), H-C(6)), 7.47—7.59 (1H, m, H-C(7)), 7.88 (1H, d, J=7.5 Hz, H-C(4)), 8.13, 8.31 (4H, each d, J=9 Hz, $C_6H_4NO_2$). MS m/z: 298 (M^+), 270 (M^+ −28), 167 (M^+ −122), 150 ($COC_6H_4NO_2^+$).

(*E*)-2-(4'-Nitrobenzoylmethylene)benzoxazoline (**32A**) and 2-(4'-Nitrobenzoylmethyl)benzoxazole (**32C**) (1.8 : 1)[5]: Yellow needles. IR (KBr): 3450 (N–H), 1637 (C=O), 1525, 1343 cm^{-1} (NO_2). ^{1}H-NMR (DMSO-d_6, 80 °C, GX) δ: 4.96 (2H, s, CH_2 for **32C**, D_2O-erasable), 6.70 (1H, s, HC=C(2) for **32A**, D_2O-erasable), 7.33—7.43, 7.65—7.72 (4H, m, H-Ar), 8.19, 8.30 (4H, each d, J=9.0 Hz, $C_6H_4NO_2$ for **32A**), 8.27, 8.35 (4H, each d, J=8.5 Hz, $C_6H_4NO_2$ for **32C**). MS m/z: 282 (M^+), 150 ($COC_6H_4NO_2^+$).

2-(4'-Nitrobenzoylmethylene)benzimidazoline (**33A**): Red prisms. IR (KBr): 3440 (N–H), 1616 (C=O), 1528, 1338 cm^{-1} (NO_2). ^{1}H-NMR (DMSO-d_6, 40 °C, GX) δ: 6.15 (1H, s, HC=C(2)), 7.17—7.24, 7.47—7.54 (4H, each m, H-Ar), 8.09, 8.29 (4H, each d, J=8.7 Hz, $C_6H_4NO_2$). MS m/z: 281 (M^+), 159 (M^+ −122), 150 ($COC_6H_4NO_2^+$).

General Procedure for the Reactions of the Azolines 28—30 and the Acyl Cyanide 2 A 0.050 M solution of an azoline and 1 eq of **2** in anhydrous ether was stirred at room temperature for an appropriate time (Table III). After removal of the solvent *in vacuo*, the crude product was purified by recrystallization from acetone. The results, the characterization, and UV spectral data are summarized in Tables III and IV.

(*E*)-2-(4'-Nitrobenzoylmethylene)thiazolidine (**34A**): Yellow needles. IR (KBr); 3460 (N–H), 1612 (C=O), 1524, 1343 cm^{-1} (NO_2). ^{1}H-NMR ($CDCl_3$, r.t., EX) δ: 3.33, 4.01 (4H, each t, J=7.6 Hz, 2H-C(4), 2H-C(5)), 5.97 (1H, br s, $W_{1/2}$=13 Hz, HC=C(2)), 7.98, 8.25 (4H, each d, J=8.9 Hz, $C_6H_4NO_2$), 10.73 (1H, br s, $W_{1/2}$=137 Hz, NH). ^{13}C-NMR ($CDCl_3$, r.t., GX) δ: 29.4 (t, C(5)), 49.9 (t, C(4)), 87.4 (d, HC=C(2)), 123.5, 128.0 (2d, 4C in Ph), 145.3, 149.1 (2s, 2C in Ph), 171.5 (s, C(2)), 183.5 (s, CO). MS m/z: 250 (M^+), 222 (M^+ −28).

(*E*)-2-(4'-Nitrobenzoylmethylen)oxazolidine (**35A**): Yellow needles. IR (KBr): 3450 (N–H), 1625 (C=O), 1540, 1341 cm^{-1} (NO_2). ^{1}H-NMR (DMSO-d_6, 80°C, GX) δ: 3.78 (2H, t, J=8.0 Hz, 2H-C(4)), 4.52 (2H, t, J=8.0 Hz, 2H-C(5)), 5.58 (1H, s, HC=C(2), D_2O-erasable), 8.03, 8.21 (4H, each d, J=8.9 Hz, $C_6H_4NO_2$), 9.87 (1H, br s, NH, D_2O-erasable). MS m/z: 234 (M^+), 233 (M^+ −1), 206 (M^+ −28), 112 (M^+ −122).

(*E*)-2-(1'-(4''-Nitrobenzoyl)ethyliden)oxazolidine (**36A**): Yellow needles. IR (KBr): 3440 (N–H), 1638 (C=O), 1542, 1350 cm^{-1} (NO_2). ^{1}H-NMR (DMSO-d_6, r.t., GX) δ: 1.70 (3H, s, Me), 3.80 (2H, td, J_1=8.5, J_2=2.6 Hz, 2H-C(4), J_2 disappeared upon addition of D_2O), 4.54 (2H, t, J=8.5 Hz, 2H-C(5)), 7.59, 8.23 (4H, each d, J=9.0 Hz, $C_6H_4NO_2$), 10.29 (1H, br s, NH, D_2O-erasable). ^{13}C-NMR (DMSO-d_6, r.t., GX) δ: 12.2 (q, Me), 43.8 (t, C(4)), 67.9 (t, C(5)), 81.5 (s, C(1')), 123.3, 128.1 (2d, 4C in $C_6H_4NO_2$), 147.1, 148.7 (2s, 2C in $C_6H_4NO_2$), 169.0 (s, C(2)), 186.7 (s, CO). MS m/z: 248 (M^+), 247 (M^+ −1), 220 (M^+ −28), 150 ($COC_6H_4NO_2^+$).

Acknowledgements The authors wish to thank the staff of the Analysis Center of Meiji College of Pharmacy for elemental analyses (Miss A. Koike), and measurements of NMR spectra (Miss Y. Takeuchi), and mass spectra (Mr. K. Satoh).

References and Notes

1) Part V: Y. Akiyama, J. Abe, T. Takano, T. Kawasaki, and M. Sakamoto, *Chem. Pharm. Bull.*, **32**, 2821 (1984).
2) A. Dornow and S. Lupfert, *Chem. Ber.*, **89**, 2718 (1956); *idem*, *ibid.*, **90**, 1780 (1957); M. J. Gardent and M. M. Delepine, *C. R. Acad. Sci.*, **247**, 2153 (1958); M. Rai, K. Krisham, and A. Singh, *Indian J. Chem., Sect. B*, **16**, 834 (1978).
3) M. Sakamoto, Y. Akiyama, N. Furumi, K. Ishii, Y. Tomimatsu, and T. Date, *Chem. Pharm. Bull.*, **31**, 2623 (1983).
4) M. Sakamoto, T. Akimoto, Y. Akiyama, K. Fukutomi, and K. Ishii, *Chem. Pharm. Bull.*, **32**, 1170 (1984).
5) The ratio was estimated from the ^{1}H-NMR spectrum.
6) *a*) T. Okamoto and H. Takayama, *Chem. Pharm. Bull.*, **11**, 514 (1963); *b*) M. Yamazaki, K. Noda, and M. Hamana, *ibid.*, **18**, 908 (1970); *c*) G. Fukata, C, O'Brien, and R. A. M. O'Ferrall, *J. Chem. Soc., Perkin Trans. 2*, **1979**, 792; *d*) A. R. E. Carey, G. Fukata, R. A. M. O'Ferrall, and M. G. Murphy, *ibid.*, **1985**, 1711.
7) The UV spectrum of **12A** was compared with that of 2-styrylquinoline (enol form B) and 1-methyl-2-phenacylidene-1,2-dihydroquinoline (enamine form A).
8) Only one tautomeric form was observed in the ^{1}H-NMR spectrum.
9) A. H. Beckett and K. A. Kerridge, *J. Chem. Soc.*, **1954**, 2948; R. F. Branch, A. H. Beckett, and D. B. Cowell, *Tetrahedron*, **19**, 401 (1963); A. R. Katritzky, H. Z. Kucharska, and J. D. Rowe, *J. Chem. Soc.*, **1965**, 3093; G. Klose and E. Uhlemann, *Tetrahedron*, **22**, 1373 (1966).
10) T. Morimoto and M. Sekiya, *Chem. Pharm. Bull.*, **25**, 1230 (1977).
11) *a*) Z.-T. Huang and X. Shi, *Chem. Ber.*, **123**, 541 (1990); *b*) *Idem*, *Synthesis*, **1990**, 162.
12) A. Dornow and H. Grabhofer, *Chem. Ber.*, **91**, 1824 (1958).
13) The C≡N band was absent. For example, see: Ref. 3 and R. E. Kitson and N. E. Griffith, *Anal. Chem.*, **24**, 334 (1952).

Ring Transformation of Condensed Pyrimidines by Enamines and Ynamines. Formation of Condensed Pyridines and Condensed Diazocines

Akira MIYASHITA,*,[a] Naokata TAIDO,[b] Susumu SATO,[b] Ken-ichi YAMAMOTO,[a] Hitoshi ISHIDA,[a] and Takeo HIGASHINO[a]

School of Pharmaceutical Sciences, University of Shizuoka,[a] 395 Yada, Shizuoka 422, Japan and Central Research Laboratories, S S Pharmaceutical Co.,[b] 1143 Nanpeidai, Narita 286, Japan. *Received July 23, 1990*

A [4+2]-cycloaddition of quinazoline (2) and the 3*H*-1,2,3-triazolo[4,5-*d*]pyrimidine 4 with enamines 1a—e resulted in ring transformation into the quinolines, 3a and 3c, and the 3*H*-1,2,3-triazolo[4,5-*b*]pyridines, 5a—e, respectively. Similarly, the ynamine 13a cycloadded to 2 and its 4-cyano derivative 6, giving the quinolines, 14a and 14b, respectively.

On the other hand, the 3*H*-1,2,3-triazolo[4,5-*d*]pyrimidines 4, 15, 8, 16, 17, 18, and 19 underwent [2+2]-cycloaddition with the ynamine 13a, resulting in ring transformation into the corresponding 3*H*-1,2,3-triazolo[4,5-*d*]-[1,3]diazocines 21a—27. The 7-methoxy derivative 20, the 4-methoxy- and 4-cyano-1*H*-pyrazolo[3,4-*d*]pyrimidines, 30 and 31, and the 6-cyano-9*H*-purine 36 also underwent [2+2]-cycloaddition with 13a to give the corresponding 3*H*-1,2,3-triazolo[4,5-*b*][1,5]diazocine 28, 1*H*-pyrazolo[3,4-b][1,5]diazocines, 32 and 33, and 3*H*-imidazo[4,5-*b*]-[1,5]diazocine 37, respectively.

The structures of the 1,3- and 1,5-diazocines, 21a and 28, were determined by X-ray crystallography.

Keywords condensed pyrimidine; enamine; ynamine; cycloaddition; condensed pyridine; condensed diazocine; X-ray analysis

It is well known that electron-deficient pyrimidines undergo an inverse-electron-demand Diels–Alder reaction with enamines (**1**) or ynamines (**13**) to afford pyridine products. Results on the inverse-electron-demand Diels–Alder reaction of monocyclic pyrimidines up to 1983 have been summarized in a comprehensive review.[1] To the best of our knowledge, no example of an inverse-electron-demand Diels–Alder reaction on the condensed pyrimidine ring has been reported so far. In the present paper we show that the condensed pyrimidine ring is able to undergo cycloaddition with electron-sufficient enamines **1** and ynamines **13**, resulting in ring transformation into the condensed pyridine and the condensed diazocine rings.

When a solution of quinazoline (**2**)[2] and enamines, **1a** and **1c**, in xylene was refluxed for a period described in Chart 1, an inverse-electron-demand Diels–Alder reaction proceeded, although in poor yields, resulting in the formation of the corresponding quinolines **3a**[3] and **3c**[4] together

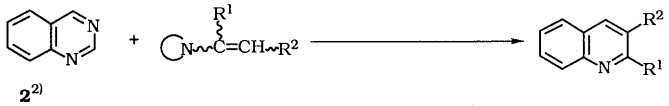

2[2]

1	N–	R^1	R^2	reaction time (h)	3	yield (%)
1a	piperidino	$(CH_2)_3$		24	3a[3]	9
1c	piperidino	Ph	H	48	3c[4]	4

4[5]

1	N–	R^1	R^2	reaction time (h)	5	yield (%)
1a	piperidino	$(CH_2)_3$		30	5a[6]	11
1b	piperidino	$(CH_2)_4$		48	5b[6]	5
1c	piperidino	Ph	H	22	5c[6]	16
1d	morpholino	Ph	Me	96	5d	3
1e	morpholino	Et	Me	40	5e	5

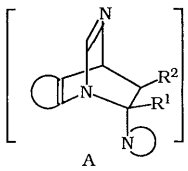

A

Chart 1

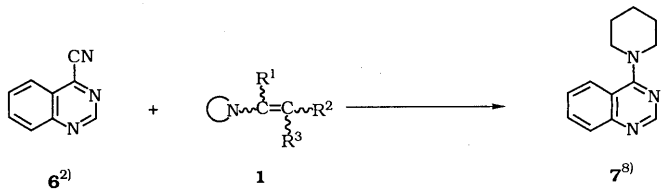

6[2] **1** **7**[8]

1	yield (%)
1a	87
1b	90

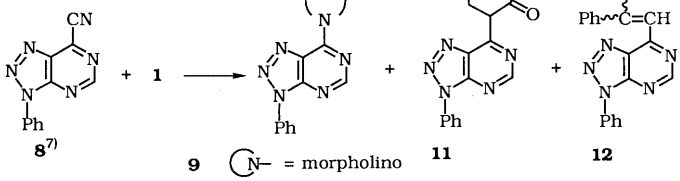

8[7] **9** N– = morpholino **10**[7] N– = NEt_2 **11** **12**

	products 9	10	yield (%) 11	12
1b	-	-	8	-
1c	-	-	-	35
1d	46	-	-	-
1e	63	-	-	-
1f	65	-	-	-
1h	67	-	-	-
1i	-	37	-	-

1	N–	R^1	R^2	R^3
1f	morpholino	$CHMe_2$	H	H
1h	morpholino	H	Me	Me
1i	NEt_2	H	COOMe	H

Chart 2

with recovery of the starting **2**. Similarly, the 3*H*-1,2,3-triazolo[4,5-*d*]pyrimidine **4**[5] reacted with enamines **1a—e** to give the corresponding 3*H*-1,2,3-triazolo[4,5-*b*]pyridines **5a—e**[6] together with recovery of the starting **4**. In each case, the electron-sufficient dienophile **1** adds selectively across the N^1/C^4 of the pyrimidine portion in **2** and **4**. Successive loss of hydrogen cyanide and the amine from the initial cycloadduct (A) affords the condensed pyridines **3** and **5**. The more electron-deficient 4-quinazolinecarbonitrile (**6**)[2] and 3-phenyl-3*H*-1,2,3-triazolo[4,5-*d*]pyrimidine-7-carbonitrile (**8**)[7] preferentially undergo nucleophilic substitution with **1a—e** rather than an inverse-electron-demand Diels–Alder reaction, and 4-piperidinoquinazoline (**7**),[8] 7-morpholino-, 7-diethylamino-, 7-(2-oxocyclohexyl)-, and 7-(2-phenyl-2-piperidinoethenyl)-3-phenyl-3*H*-1,2,3-triazolo[4,5-*d*]pyrimidines (**9**, **10**,[7] **11** and **12**) were obtained, as shown in Chart 2.

The inverse-electron-demand Diels–Alder reaction of **2** and **6** with ynamine **13a** proceeded, giving the corresponding quinolines **14a** and **14b** as shown in Chart 3.

On the other hand, the reaction of the triazolopyrimidine **4** with the ynamines **13a** and **13b** proceeded in a different way from the inverse-electron-demand Diels–Alder reaction of the quinazolines **2** and **6**, resulting in the formation of the corresponding 3*H*-1,2,3-triazolo[4,5-*d*][1,3]diazocines **21a** and **21b**. The structure of **21a** was determined by X-ray crystallography (Fig. 1 and Table I). The ORTEP view of the molecule **21a** in Fig. 1 shows that the molecule consists of a fully conjugated 1,3-diazocine ring condensed with a 1,2,3-triazole ring, and the conformation of the 1,3-diazocine ring can be drawn as a tub-shape.

In the proton nuclear magnetic resonance (^{1}H-NMR) spectrum of **21a**, the C^9-H at 6.40 ppm shows the characteristic long-range coupling ($J = 1.5$ Hz) with the C^8-CH_3 at 2.12 ppm, and the C^5-H resonated at the lowest field (7.89 ppm) as a singlet.

The formation of the 3*H*-1,2,3-triazolo[4,5-*d*][1,3]diazocine **21a** may be explained as follows. The ynamine **13a** adds selectively across the C^7/N^6 double bond in **4**, followed by isomerization of the resulting [2+2]-cycloadduct (B) into the 3*H*-1,2,3-triazolo[4,5-*d*][1,3]diazocine **21a**. Reports on a [2+2]-cycloaddition of an ynamine to the C=N double bond of heteroaromatics have appeared in the literature.[9-11] However, it is not yet clear why the 3*H*-1,2,3-triazolo[4,5-*d*]pyrimidine preferentially undergoes [2+2]-cycloaddition rather than [4+2]-cycloaddition with an ynamine.

Similarly, the 3*H*-1,2,3-triazolo[4,5-*d*]pyrimidines **15**,[5] **17**,[13] **18**,[13] and **19**,[13] in which the 7 position is free, reacted with the ynamine **13a**, and the corresponding 3*H*-1,2,3-triazolo[4,5-*d*][1,3]diazocines **22**, **25**, **26**, and **27** were obtained in moderate yields. As a matter of course, the more electron-deficient derivative **8** smoothly underwent [2+2]-cycloaddition with **13a** and **13b** to afford the corresponding 3*H*-1,2,3-triazolo[4,5-*d*][1,3]diazocinecarbonitriles **23a** and **23b**. A [2+2]-cycloaddition of the 7-methyl-3*H*-1,2,3-triazolo[4,5-*d*]pyrimidine **16**[12] with **13a** proceeded, resulting in the formation of the 9-methyl-3*H*-1,2,3-triazolo-[4,5-*d*][1,3]diazocine **24** in 29% yield. As described in the experimental section, the ^{1}H-NMR signals of the C^9-H and

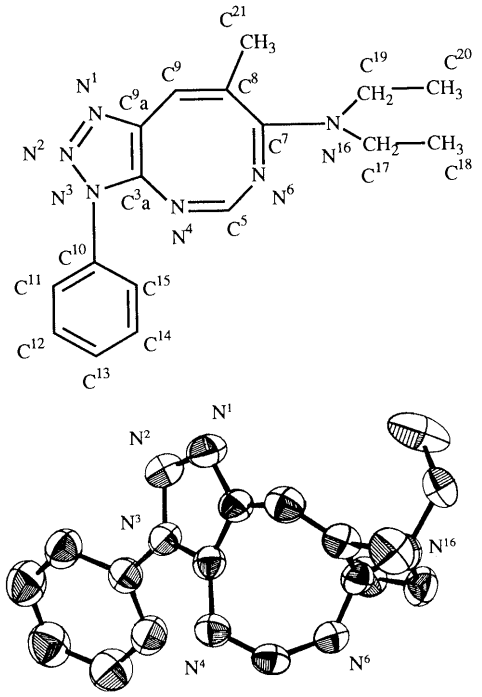

Fig. 1. Numbering and ORTEP Drawing for **21a**

TABLE I. Final Atomic Coordinates and Equivalent Isotropic Thermal Parameters for Non-hydrogen Atoms of **21a**[a]

No.	Atom	*x*	*y*	*z*	B_{eq}
1	N^1	0.7725 (4)	0.7635 (2)	0.5574 (3)	4.8
2	N^2	0.8582 (4)	0.7045 (2)	0.5135 (3)	4.8
3	N^3	0.7981 (0)	0.6725 (2)	0.4168 (0)	3.7
4	C^3a	0.6711 (4)	0.7112 (2)	0.3999 (3)	3.6
5	N^4	0.5939 (4)	0.7040 (2)	0.3002 (3)	4.0
6	C^5	0.4672 (4)	0.6806 (2)	0.3017 (3)	3.8
7	N^6	0.3991 (4)	0.6434 (2)	0.3861 (3)	3.8
8	C^7	0.3959 (4)	0.6825 (2)	0.4834 (3)	3.5
9	C^8	0.4115 (4)	0.7891 (2)	0.5018 (3)	4.0
10	C^9	0.5367 (5)	0.8277 (3)	0.5104 (4)	4.5
11	C^9a	0.6559 (4)	0.7682 (2)	0.4911 (3)	4.0
12	C^{10}	0.8659 (4)	0.6025 (2)	0.3524 (3)	3.7
13	C^{11}	1.0070 (4)	0.6040 (3)	0.3512 (4)	4.9
14	C^{12}	1.0713 (5)	0.5351 (4)	0.2910 (5)	6.3
15	C^{13}	0.9976 (5)	0.4660 (3)	0.2311 (4)	6.3
16	C^{14}	0.8574 (5)	0.4657 (3)	0.2337 (4)	5.4
17	C^{15}	0.7914 (5)	0.5341 (3)	0.2945 (4)	4.8
18	N^{16}	0.3649 (4)	0.6284 (2)	0.5703 (3)	3.7
19	C^{17}	0.3537 (5)	0.6666 (3)	0.6833 (4)	4.5
20	C^{18}	0.4678 (7)	0.6373 (5)	0.7612 (5)	7.8
21	C^{19}	0.3518 (4)	0.5240 (3)	0.5551 (4)	4.5
22	C^{20}	0.4866 (5)	0.4733 (3)	0.5471 (4)	5.0
23	C^{21}	0.2811 (5)	0.8457 (3)	0.5049 (5)	5.8

a) Estimated standard deviations are given in parentheses.

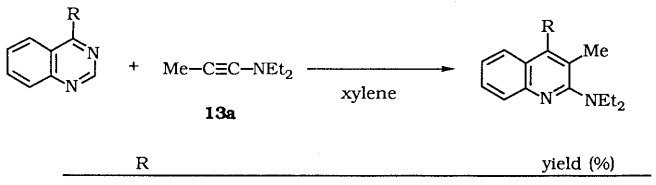

	R		yield (%)
2	H	**14a**	35
6	CN	**14b**	63

Chart 3

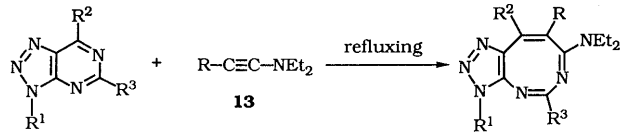

	R^1	R^2	R^3		R	reaction time (h)	product	yield (%)
4	Ph	H	H	**13a**	Me	7	**21a**	58
4 [5]	Ph	H	H	**13b**	Et	7	**21b**	67
15 [5]	Me	H	H	**13a**	Me	7	**22**	53
8	Ph	CN	H	**13b**	Et	5	**23a**	60
8 [12]	Ph	CN	H	**13a**	Me	5	**23b**	67
16 [13]	Ph	Me	H	**13a**	Me	7	**24**	29
17 [13]	Ph	H	Me	**13a**	Me	7	**25**	60
18 [13]	Ph	H	Ph	**13a**	Me	7	**26**	53
19 [13]	Ph	H	OMe	**13a**	Me	15	**27**	94

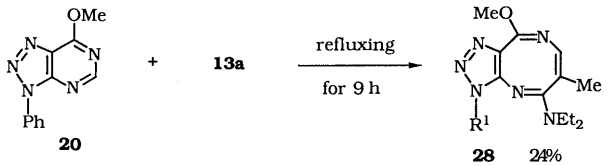

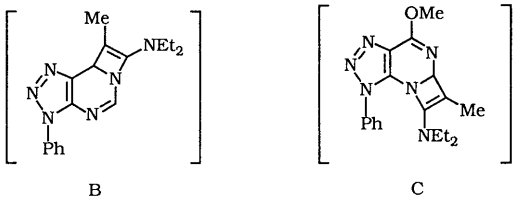

Chart 4

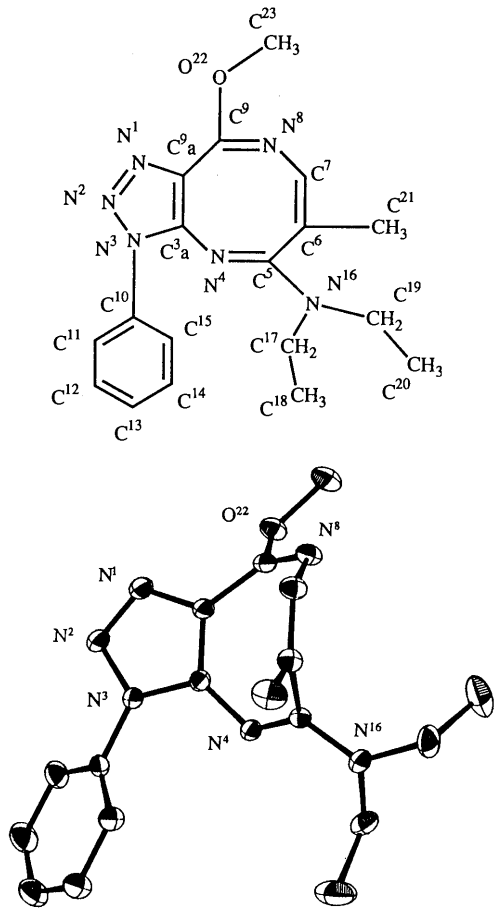

Fig. 2. Numbering and ORTEP Drawing for **28**

the C^8-CH_3 (or C^8-CH_2–) groups of the newly obtained compounds **22**—**27** agree well with those found for **21a**, indicating that the 3*H*-1,2,3-triazolo[4,5-*d*][1,3]diazocine ring is fully conjugated.

However, in the case of the reaction of the 7-methoxy derivative **20**,[7] the nucleophilic carbon of the ynamine **13a** selectively attacks the ring carbon at C^5 rather than at C^7, and eventually, the corresponding 3*H*-1,2,3-triazolo[4,5-*b*][1,5]diazocine **28** was obtained by way of an intermediate [2+2]-cycloadduct (C), as shown in Chart 4. The structure of **28** was determined by X-ray crystallography (Fig. 2 and Table II). The molecule **28** consists of a fully conjugated 1,5-diazocine ring condensed with a 1,2,3-triazole ring, and exists in a tub-shaped conformation. In the ^{1}H-NMR spectrum of **28** the C^7-H resonates at 6.38 ppm and shows a characteristic long-range coupling (J=1.5 Hz) with the C^6-CH_3 at 1.73 ppm.

In the case of the 1*H*-pyrazolo[3,4-*d*]pyrimidine ring, when ring transformation of the 1*H*-pyrazolo[3,4-*d*]pyrimidine **31**[14] with the ynamine **13a** to the pyrazolodiazocine ring was attempted, the desired product was not obtained. But the 4-methoxy- and 4-cyano derivatives, **30**[15] and **31**,[16]

Table II. Final Atomic Coordinates and Equivalent Isotropic Thermal Parameters for Non-hydrogen Atoms of **28**[a]

No.	Atom	x	y	z	B_{eq}
1	N^1	0.1997 (3)	0.4681 (3)	0.2196 (2)	3.0
2	N^2	0.3112 (3)	0.4297 (3)	0.2847 (2)	3.0
3	N^3	0.3838 (2)	0.5392 (2)	0.3235 (2)	2.4
4	C^3a	0.3161 (3)	0.6487 (3)	0.2835 (2)	2.1
5	N^4	0.3757 (2)	0.7686 (2)	0.3014 (2)	2.4
6	C^5	0.2984 (3)	0.8690 (3)	0.2956 (2)	2.1
7	C^6	0.1609 (3)	0.8584 (3)	0.2962 (2)	2.5
8	C^7	0.0463 (3)	0.8148 (3)	0.2335 (2)	2.7
9	N^8	0.0279 (3)	0.7758 (3)	0.1555 (2)	2.7
10	C^9	0.0918 (3)	0.6754 (3)	0.1498 (2)	2.5
11	C^9a	0.1981 (3)	0.6013 (3)	0.2174 (2)	2.4
12	C^{10}	0.5174 (3)	0.5248 (3)	0.3935 (2)	2.7
13	C^{11}	0.5609 (4)	0.6152 (4)	0.4558 (2)	3.3
14	C^{12}	0.6917 (4)	0.5999 (5)	0.5237 (2)	4.5
15	C^{13}	0.7720 (4)	0.4924 (5)	0.5270 (3)	5.0
16	C^{14}	0.7255 (4)	0.4025 (5)	0.4642 (3)	4.9
17	C^{15}	0.5962 (4)	0.4177 (4)	0.3950 (2)	3.7
18	N^{16}	0.3485 (3)	0.9895 (2)	0.2995 (2)	2.8
19	C^{17}	0.4949 (4)	1.0079 (4)	0.3163 (2)	3.3
20	C^{18}	0.5865 (5)	1.0250 (6)	0.4090 (3)	5.7
21	C^{19}	0.2587 (4)	1.1053 (3)	0.2755 (2)	3.5
22	C^{20}	0.2047 (6)	1.1338 (5)	0.1834 (3)	5.2
23	C^{21}	0.1649 (4)	0.8952 (4)	0.3776 (2)	3.5
24	C^{22}	0.0662 (2)	0.6256 (2)	0.0761 (1)	3.2
25	C^{23}	−0.0474 (4)	0.6828 (4)	0.0052 (2)	3.9

a) Estimated standard deviations are given in parentheses.

	R	yield (%)	
29	H	-	-
30	OMe	**32**	4
31	CN	**33**	9

Chart 5

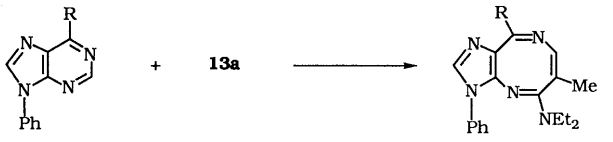

	R	yield (%)	
34	H	-	-
35	OMe	-	-
36	CN	**37**	65

Chart 6

underwent a [2+2]-cycloaddition with **13a**, although in poor yields, resulting in the formation of the corresponding 1*H*-pyrazolo[3,4-*b*][1,5]diazocines **32** and **33**. The structural elucidation of **32** and **33** was achieved as follows. The C^6-H resonates in a range of 6.60—6.43 ppm and shows a characteristic long-range coupling ($J=1.5$ Hz) with the C^7-CH_3 in the region of 1.86—1.82 in the ^{1}H-NMR spectra of **32** and **33**. These values agree well with those for the 1,5-diazocine portion of the 3*H*-1,2,3-triazolo[4,5-*b*][1,5]-diazocine **28**.

In the case of the 9*H*-purine ring, [2+2]-cycloaddition of 9-phenyl-9*H*-purine (**34**)[17] and its 6-methoxy derivatives (**35**)[18] with ynamine **13a** did not proceed, and the starting **34** and **35** were recovered. On the other hand, the 9*H*-purine-6-carbonitrile **36**[19] reacted with the ynamine **13a**, giving the 3*H*-imidazo[4,5-*b*][1,5]diazocinecarbonitrile **37** in moderate yield. The structure of **37** was determined by comparison of the ^{1}H-NMR spectrum with that of the 3*H*-1,2,3-triazolo[4,5-*b*][1,5]diazocine **28**.

The experimental results may be summarized as follows. i) Both quinazoline (**2**) and the 3*H*-1,2,3-triazolo[4,5-*d*]-pyrimidine **4** underwent a [4+2]-cycloaddition with enamines **1a**—**e**, resulting in ring transformation into the quinolines, **3a** and **3c**, and the 3*H*-1,2,3-triazolo[4,5-*b*]-pyridines, **5a**—**e**, respectively. Similarly, reaction of **2** and its 4-cyano derivative **6** with the ynamine **13a** gave the quinolines, **14a** and **14b**. ii) On the other hand, [2+2]-cycloaddition of the 3*H*-1,2,3-triazolo[4,5-*d*]pyrimidines **4**, **15**, **8**, **16**, **17**, **18**, and **19** with **13a** resulted in the formation of the corresponding 3*H*-1,2,3-triazolo[4,5-*d*]-[1,3]diazocines **21a**—**27**. The 7-methoxy derivative **20**, the 4-methoxy- and the 4-cyano-1*H*-pyrazolo[3,4-*d*]pyrimidines, **30** and **31**, and the 4-cyano-9*H*-purine **36** underwent [2+2]-cycloaddition with **13a** to give the corresponding 3*H*-1,2,3-triazolo[4,5-*b*][1,5]diazocine **28**, 1*H*-pyrazolo-[3,4-*b*][1,5]diazocines, **32** and **33**, and 3*H*-imidazo[4,5-*b*][1,5]diazocine **37**.

Experimental

All melting points are uncorrected. Infrared (IR) absorption spectra were recorded on a Jasco A-102 diffraction grating IR spectrometer. ^{1}H-NMR spectra were measured at 60 MHz on a Hitachi R-24B high-resolution NMR spectrometer, and ^{13}C-NMR spectra were obtained with a JEOL JNM-FX90Q FTNMR spectrometer operating at 22.5 MHz. Chemical shifts are quoted in parts per million (ppm) with tetramethylsilane as an internal standard, and coupling constants (J) are given in hertz (Hz). The following abbreviations are used: s=singlet, d=doublet, t=triplet, q=quartet, m=multiplet, Mass spectra (MS) were recorded on a JEOL JMS D-100 mass spectrometer. The exact mass measurements were made on a JEOL JMS-01SG-2 MS spectrometer combined with a JEC spectrum computer. Samples were vaporized in a direct inlet system. Unit-cell parameters and intensity data for X-ray crystallography were measured on a Rigaku AFC-5R automatic four-circle diffractometer with graphite-monochromated MoK_α radiation at room temperature. The intensities of all the reflections were measured by the ω–2θ scanning technique. The structure was solved by direct methods using the program SAPI 85,[20] a version of MULTAN 80.[21] The structure was refined by the full-matrix least-squares method with anisotropic thermal parameters for the non-hydrogen atoms and with isotropic thermal parameters for the hydrogen atoms. Column chromatography was carried out on SiO_2, Wakogel C-200 (200 mesh).

Reaction of Quinazoline (2) with Enamines (1) i) A solution of **2** (200 mg, 1.5 mmol) and 1-piperidinocyclopentene (**1a**, 3.1 mmol, 468 mg) in xylene (3 ml) was refluxed for 24 h. After cooling, the reaction mixture was poured into an excess of H_2O, and extracted with $CHCl_3$. The extract was washed with H_2O, dried over Na_2SO_4, and concentrated to dryness. The residue was chromatographed on a column of SiO_2 to remove impurities. The first fraction eluted with benzene gave **3a** as a yellow oil in 9% yield (24 mg). The picrate, yellow needles (from MeOH), mp 196—198 °C, showed no melting point depression on admixture with the picrate of 2,3-dihydro-1*H*-cyclopenta[*b*]quinoline prepared by another route.[3] The second fraction eluted with $CHCl_3$ gave unchanged **2** in 43% (86 mg) yield.

ii) A solution of **2** (200 mg, 1.5 mmol) and 1-phenyl-1-piperidinoethylene (**1c**, 3.1 mmol, 580 mg) in xylene (3 ml) was refluxed for 48 h. Work-up of the reaction mixture as described for **3a** gave 2-phenylquinoline (**3c**) as colorless needles (from petroleum benzin), mp 80—81 °C, in 4% yield (10 mg), and unchanged **2** in 25% (50 mg) yield. Compound **3c** showed no melting point depression on admixture with an authentic specimen prepared by another route.[4]

Reaction of 3-Phenyl-3*H*-1,2,3-triazolo[4,5-*d*]pyrimidine (4) with 1: General Procedure for the 5,6-Disubstituted 3-Phenyl-3*H*-1,2,3-triazolo[4,5-*b*]pyridines (5) A solution of **4** (200 mg, 1.0 mmol) and an enamine **1** (2.0 mmol) in xylene (3 ml) was refluxed for the period shown in Chart 1. After cooling, the reaction mixture was poured into an excess of H_2O, and extracted with $CHCl_3$. The extract was washed with H_2O, dried over Na_2SO_4, and concentrated to dryness. The residue was chromatographed on a column of SiO_2. The first fraction eluted with benzene afforded **5** as colorless needles on recrystallization from petroleum benzin. The second fraction provided a large amount of unchanged **4**.

Reaction of **4** with **1a** gave 3-phenyl-3,5,6,7-tetrahydrocyclopenta[*e*]-1,2,3-triazolo[4,5-*b*]pyridine (**5a**) as colorless needles, mp 117—118 °C, in 11% yield (26 mg). Compound **5a** showed no melting point depression on admixture with an authentic specimen prepared by another route.[6]

Reaction of **4** with 1-piperidinocyclohexene (**1b**) gave 3-phenyl-5,6,7,8-tetrahydro-3*H*-1,2,3-triazolo[4,5-*b*]quinoline (**5b**) as colorless needles, mp 110—112 °C, in 5% yield (17 mg). Compound **5b** showed no melting point depression on admixture with an authentic specimen prepared by another route.[6]

Reaction of **4** with **1c** gave 3,5-diphenyl-3*H*-1,2,3-triazolo[4,5-*d*]pyridine (**5c**) as colorless needles, mp 124—125 °C, in 16% yield (45 mg). Compound **5c** showed no melting point depression on admixture with an authentic specimen prepared by another route.[6]

Reaction of **4** with 1-morpholino-1-phenyl-1-propene (**1d**) gave 6-methyl-3,5-diphenyl-3*H*-1,2,3-triazolo[4,5-*b*]pyridine (**5d**) as colorless needles, mp 135—136 °C, in 3% yield (19 mg). *Anal.* Calcd for $C_{18}H_{14}N_4$: C, 75.50; H, 4.93; N, 19.57. Found: C, 75.52; H, 4.97; N, 19.66. MS *m/z*: 286 (M^+). ^{1}H-NMR ($CDCl_3$): 8.31 (1H, s, C^7-H), 8.40—7.14 (10H, m, N^3- and C^5-C_6H_5), 2.48 (3H, s, CH_3). ^{13}C-NMR ($CDCl_3$): 160.97 (s), 143.96 (s), 140.11 (s), 137.30 (s), 136.91 (s), 129.49 (d), 129.38 (d), 129.17 (d), 128.19 (d), 127.76 (d), 120.98 (d), 20.97 (q).

Reaction of **4** with 3-morpholino-2-pentene (**1e**) gave 5-ethyl-6-methyl-3-phenyl-3*H*-1,2,3-triazolo[4,5-*b*]pyridine (**5e**) as colorless needles, mp 108—109 °C, in 5% yield (12 mg). *Anal.* Calcd for $C_{14}H_{14}N_4$: C, 70.57; H, 5.92; N, 23.51. Found: C, 70.91; H, 6.20; N, 23.56. MS *m/z*: 238 (M^+). ^{1}H-NMR ($CDCl_3$): 8.10 (1H, s, C^7-H), 8.69—7.40 (5H, m, N^3-C_6H_5), 3.11 (2H, q, $J=8.0$, $\underline{CH_2}Me$), 2.60 (3H, s, CH_3), 1.54 (3H, t, $J=8.0$, $CH_2\underline{CH_3}$). ^{13}C-NMR ($CDCl_3$): 164.43 (s), 143.91 (s), 137.13 (s), 137.02 (s), 129.33 (d), 128.73 (s), 128.08 (d), 127.65 (d), 120.88 (d), 29.26 (t), 19.40 (q), 11.97 (q).

Reaction of 4-Quinazolinecarbonitrile (6) with 1 A solution of **6** (500 mg, 3.2 mmol) and **1** (6.4 mmol) in xylene (5 ml) was refluxed for 24 h. The reaction mixture was poured into an excess of H_2O, and extracted with $CHCl_3$. The extract was washed with H_2O, dried over Na_2SO_4, concentrated, and chromatographed on a column of SiO_2. The fraction eluted with $CHCl_3$ gave 4-piperidinoquinazoline (**7**) as a slightly yellow oil. The picrate of **7**, yellow needles (from MeOH), mp 193—194 °C,

showed no melting point depression on admixture with an authentic specimen prepared by another route.[8]

Reaction of **6** with **1a** gave **7** in 87% yield (600 mg), and the reaction with **1b** provided **7** in 90% yield (614 mg).

Reaction of 3-Phenyl-3*H*-1,2,3-triazolo[4,5-*d*]pyrimidine-7-carbonitrile (8) with 1: General Procedure A solution of **8** (200 mg, 0.9 mmol) and **1** (1.8 mmol) in xylene (3 ml) was refluxed for 20 h. The reaction mixture was poured into an excess of H_2O, and extracted with $CHCl_3$. The extract was washed with H_2O, dried over Na_2SO_4, and concentrated to dryness. The residue was chromatographed on a column of SiO_2 with appropriate solvent as an eluent, to give the reaction products.

In the case of the reaction of **8** with **1b**, the fraction eluted with benzene–$CHCl_3$ gave 2-(3-phenyl-3*H*-1,2,3-triazolo[4,5-*d*]pyrimidin-7-yl)-cyclohexanone (**11**) as slightly yellow needles (from petroleum benzin), mp 185—187 °C, in 8% yield (20 mg). *Anal.* Calcd for $C_{16}H_{15}N_5O$: C, 65.52; H, 5.15; N, 23.88. Found: C, 65.44; H, 5.16; N, 23.79. MS *m/z*: 293 (M^+). IR ν_{max}^{KBr} cm^{-1}: 1620 (C=O). ^{1}H-NMR ($CDCl_3$): 13.50 (1H, br s, enolic H, exchangeable with MeOD), 8.10—7.20 (6H, m, aromatic H), 3.27—3.28 (2H, m, CH_2), 2.57—2.26 (2H, m, CH_2), 1.97—1.50 (4H, m, $2\times CH_2$).

In the case of the reaction of **8** with **1c**, the fraction eluted with $CHCl_3$ gave 7-(2-phenyl-2-piperidinoethenyl)-3-phenyl-3*H*-1,2,3-triazolo[4,5-*d*]-pyrimidine (**12**) as yellow needles (from petroleum benzin), mp 147—149 °C, in 35% yield (120 mg). *Anal.* Calcd for $C_{23}H_{22}N_6$: C, 72.23; H, 5.80; N, 21.97. Found: C, 72.02; H, 5.83; N, 21.81. MS *m/z*: 382 (M^+). ^{1}H-NMR ($CDCl_3$): 8.26—7.10 (11H, m, aromatic H), 6.38 (1H, s, olefinic H), 3.52—3.09 (4H, m, $2\times CH_2$), 1.90—1.50 (6H, m, $3\times CH_2$). ^{13}C-NMR ($CDCl_3$): 162.81 (s), 159.40 (s), 155.88 (d), 147.86 (s), 136.54 (s), 133.23 (s), 129.44 (d), 129.22 (d), 128.57 (d), 127.89 (d), 121.37 (d), 92.70 (d), 49.85 (t), 26.06 (t), 24.38 (t). However, the stereoisomeric (*cis* or *trans*) form of **12** has not been determined yet.

In the cases of the reaction of **8** with **1d, e, f, h**, the fraction eluted with benzene provided the unchanged cyanide **8** in 3—15% yields, and the fraction eluted with $CHCl_3$ afforded 7-morpholino-3-phenyl-3*H*-1,2,3-triazolo[4,5-*d*]pyrimidine (**9**) as orange needles (from petroleum benzin), mp 140—142 °C, in 46, 63, 65, and 67% yields (118, 161, 165, and 171 mg). *Anal.* Calcd for $C_{14}H_{14}N_6O$: C, 59.56; H, 5.00; N, 29.77. Found: C, 59.65; H, 5.02; N, 29.66. MS *m/z*: 282 (M^+). ^{1}H-NMR ($CDCl_3$): 8.30 (1H, s, C^5-H), 8.21—7.14 (5H, m, N^3-C_6H_5), 4.87—3.42 (8H, m, morpholinic H).

In the case of the reaction of **8** with methyl *trans*-β-diethylaminoacrylate (**1i**) by refluxing for 50 h, the fraction eluted with benzene gave unchanged **8** in 21% yield (42 mg) and the fraction eluted with $CHCl_3$ gave 7-(diethylamino)-3-phenyl-3*H*-1,2,3-triazolo[4,5-*d*]pyrimidine (**10**) as colorless needles (from MeOH), mp 75—76 °C, in 37% yield (90 mg). Compound **10** showed no melting point depression on admixture with an authentic specimen prepared by another route.[7]

Reaction of 2 with 1-(Diethylamino)propyne (13a) A solution of **2** (200 mg, 1.5 mmol) and **13a** (344 mg, 3.1 mmol) in xylene (3 ml) was refluxed for 24 h. After cooling, the reaction mixture was poured into an excess of H_2O, and extracted with $CHCl_3$. The extract was washed with H_2O, dried over Na_2SO_4, and concentrated to dryness. The residue was chromatographed on a column of SiO_2. The fraction eluted with benzene gave 2-(diethylamino)-3-methlquinoline (**14a**) as a slightly yellow oil, in 35% yield (114 mg). MS *m/z*: 214 (M^+). ^{1}H-NMR ($CDCl_3$): 7.90—6.98 (4H, m, aromatic H), 7.44 (1H, s, C^4-H), 3.33 (4H, q, J=8.0, $N(\underline{CH_2}Me)_2$), 2.33 (3H, s, CH_3), 1.12 (6H, t, J=8.0, $2\times CH_2\underline{CH_3}$). ^{13}C-NMR ($CDCl_3$): 160.59 (s), 146.01 (s), 137.67 (d), 127.98 (d), 127.33 (d), 126.24 (d), 125.64 (s), 125.21 (s), 123.42 (d), 44.64 (t), 19.45 (q), 13.33 (q).

Reaction of 6 with 13a A solution of **6** (200 mg, 1.3 mmol) and **13a** (289 mg, 2.6 mmol) in xylene (3 ml) was refluxed for 22 h. Work-up of the reaction mixture as described for **14a** gave 2-(diethylamino)-3-methyl-4-quinolinecarbonitrile (**14b**) as yellow prisms (from petroleum benzin), mp 74—76 °C, in 63% yield (194 mg). *Anal.* Calcd for $C_{15}H_{17}N_3$: C, 75.28; H, 7.16; N, 17.56. Found: C, 75.18; H, 7.22; N, 17.28. MS *m/z*: 239 (M^+). IR ν_{max}^{KBr} cm^{-1}: 2224 (CN). ^{1}H-NMR ($CDCl_3$): 8.01—7.15 (4H, m, aromatic H), 3.45 (4H, q, J=7.0, $N(\underline{CH_2}Me)_2$), 2.61 (3H, s, CH_3), 1.19 (6H, t, J=7.0, $2\times CH_2\underline{CH_3}$). ^{13}C-NMR ($CDCl_3$): 159.88 (s), 145.47 (s), 131.71 (s), 129.65 (d), 127.98 (d), 125.54 (d), 124.13 (d), 122.67 (s), 120.01 (s), 115.57 (s), 44.92 (t), 18.53 (q), 13.17 (q).

Reaction of the 3*H*-1,2,3-Triazolo[4,5-*d*]pyrimidines with 13: General Procedure A solution of a 1,2,3-triazolo[4,5-*d*]pyrimidine (1 mmol) and **13** (2 mmol) in xylene (3 ml) was refluxed for the period shown in Chart 4. After cooling, the reaction mixture was poured into an excess of H_2O, and extracted with $CHCl_3$. The extract was washed with H_2O, dried over Na_2SO_4, concentrated to dryness. The residue was chromatographed on a column of SiO_2 to remove impurities. The fraction eluted with $CHCl_3$ gave the 3*H*-1,2,3-triazolo[4,5-*d*][1,3]diazocine.

Reaction of **4** with **13a** gave 7-(diethylamino)-8-methyl-3-phenyl-3*H*-1,2,3-triazolo[4,5-*d*][1,3]diazocine (**21a**) as slightly yellow needles (from petroleum benzin), mp 109—111 °C, in 58% yield (181 mg). *Anal.* Calcd for $C_{17}H_{20}N_6$: C, 66.21; H, 6.54; N, 27.25. Found: C, 66.22; H, 6.54; N, 26.91. MS *m/z*: 308 (M^+). ^{1}H-NMR ($CDCl_3$): 7.89 (1H, s, C^5-H), 7.80—7.28 (5H, m, N^3-C_6H_5), 6.40 (1H, q, J=1.5, C^9-H), 3.30 (4H, q, J=6.0, $N(\underline{CH_2}Me)_2$), 2.12 (3H, d, J=1.5, C^8-CH_3), 1.14 (6H, t, J=6.0, $2\times CH_2\underline{CH_3}$). ^{13}C-NMR ($CDCl_3$): 162.16 (s), 159.13 (d), 143.31 (s), 141.90 (s), 136.37 (s), 135.45 (s), 129.00 (d), 128.14 (d), 122.99 (d), 122.83 (d), 43.24 (t), 41.56 (t), 21.02 (q), 14.03 (q), 12.03 (q).

Reaction of **4** with 1-(diethylamino)butyne (**13b**) gave 7-(diethylamino)-8-ethyl-3-phenyl-3*H*-1,2,3-triazolo[4,5-*d*][1,3]diazocine (**21b**) as slightly yellow needles (from petroleum benzin), mp 125—127 °C, in 67% yield (218 mg). *Anal.* Calcd for $C_{18}H_{22}N_6$: C, 67.06; H, 6.88; N, 26.06. Found: C, 67.07; H, 6.93; N, 25.97. MS *m/z*: 322 (M^+). ^{1}H-NMR ($CDCl_3$): 7.78 (1H, s, C^5-H), 7.71—7.19 (5H, m, N^3-C_6H_5), 6.31 (1H, t, J=1.5, C^9-H), 3.53—2.83 (4H, m, $N(\underline{CH_2}Me)_2$), 2.54—1.83 (2H, m, $\underline{CH_2}Me$), 1.22 (3H, m, $CH_2\underline{CH_3}$), 1.05 (6H, t, J=6.0, $2\times CH_2\underline{CH_3}$). ^{13}C-NMR ($CDCl_3$): 161.56 (s), 159.29 (d), 150.03 (s), 141.90 (s), 136.43 (s), 135.40 (s), 129.00 (d), 128.14 (d), 122.93 (d), 121.20 (d), 43.40 (t), 41.50 (t), 28.39 (t), 13.27 (q), 13.98 (q), 12.03 (q).

Reaction of 3-methyl-3*H*-1,2,3-triazolo[4,5-*d*]pyrimidine (**15**) with **13a** gave 7-(diethylamino)-3,8-dimethyl-3*H*-1,2,3-triazolo[4,5-*d*][1,3]diazocine (**22**) as slightly yellow needles (from petroleum benzin), mp 111—112 °C, in 53% yield (130 mg). MS *m/z* Calcd for $C_{12}H_{18}N_6$: 246.1592 (M^+). Found: 246.1596. ^{1}H-NMR ($CDCl_3$): 7.93 (1H, s, C^5-H), 6.40 (1H, q, J=1.5, C^9-H), 3.91 (3H, s, N^3-CH_3), 3.16 (4H, m, $N(\underline{CH_2}Me)_2$), 2.08 (3H, d, J=1.5, C^8-CH_3), 1.11 (6H, m, $2\times CH_2\underline{CH_3}$).

Reaction of **8** with **13a** gave 7-(diethylamino)-8-methyl-3-phenyl-3*H*-1,2,3-triazolo[4,5-*d*][1,3]diazocine-9-carbonitrile (**23a**) as yellow needles (from benzene–petroleum benzin mixture), mp 181—183 °C, in 60% yield (200 mg). *Anal.* Calcd for $C_{18}H_{19}N_7$: C, 64.85; H, 5.74; N, 29.41. Found: C, 64.87; H, 5.78; N, 29.38. MS *m/z*: 333 (M^+). IR ν_{max}^{KBr} cm^{-1}: 2210 (CN). ^{1}H-NMR ($CDCl_3$): 7.76 (1H, s, C^5-H), 7.68—7.15 (5H, m, N^3-C_6H_5), 3.51—2.85 (4H, m, $N(\underline{CH_2}Me)_2$), 2.37 (3H, s, C^8-CH_3), 1.36—0.81 (6H, m, $2\times CH_2\underline{CH_3}$). ^{13}C-NMR ($CDCl_3$): 158.64 (s), 158.53 (d), 156.91 (s), 142.76 (s), 135.89 (s), 131.01 (s), 129.17 (d), 128.73 (d), 122.99 (d), 114.11 (s), 108.90 (s), 43.89 (t), 41.99 (t), 20.86 (q), 13.98 (q), 11.81 (q).

Reaction of **8** with **13b** gave 7-(diethylamino)-8-ethyl-3-phenyl-3*H*-1,2,3-triazolo[4,5-*d*][1,3]diazocine-9-carbonitrile (**23b**) as slightly yellow needles (from benzene–petroleum benzin mixture), mp 146—148 °C, in 67% yield (232 mg). *Anal.* Calcd for $C_{19}H_{21}N_7$: C, 65.69; H, 6.09; N, 28.22. Found: C, 65.78; H, 6.13; N, 28.03. MS *m/z*: 347 (M^+). IR ν_{max}^{KBr} cm^{-1}: 2200 (CN). ^{1}H-NMR ($CDCl_3$): 7.79 (1H, s, C^5-H), 7.78—7.20 (5H, m, N^3-C_6H_5), 3.64—2.79 (4H, m, $N(\underline{CH_2}Me)_2$), 2.69—2.01 (2H, m, $\underline{CH_2}Me$), 1.31 (3H, t, J=6.0, $CH_2\underline{CH_3}$), 1.05 (6H, m, $2\times CH_2\underline{CH_3}$). ^{13}C-NMR ($CDCl_3$): 163.46 (s), 158.75 (d), 157.18 (s), 142.87 (s), 135.94 (s), 130.95 (s), 129.22 (d), 128.73 (d), 122.99 (d), 114.00 (s), 107.98 (s), 43.89 (t), 41.94 (t), 28.66 (t), 14.20 (q), 13.92 (q), 11.81 (q).

Reaction of 7-methyl-3-phenyl-3*H*-1,2,3-triazolo[4,5-*d*]pyrimidine (**16**)[12] with **13a** gave 7-(diethylamino)-8,9-dimethyl-3-phenyl-3*H*-1,2,3-triazolo-[4,5-*d*][1,3]diazocine (**24**) as pale yellow needles (from petroleum benzin), mp 126—128 °C, in 29% yield (87 mg). *Anal.* Calcd for $C_{18}H_{22}N_6$: C, 67.06; H, 6.88; N, 26.06. Found: C, 66.90; H, 6.84; N, 25.87. MS *m/z*: 322 (M^+). ^{1}H-NMR ($CDCl_3$): 7.80 (1H, s, C^5-H), 7.75—7.13 (5H, m, N^3-C_6H_5), 3.50—2.89 (4H, m, $N(\underline{CH_2}Me)_2$), 2.05 (3H, s, CH_3), 2.00 (3H, s, CH_3), 1.33—0.69 (6H, m, $2\times CH_2\underline{CH_3}$). ^{13}C-NMR ($CDCl_3$): 163.90 (s), 159.08 (d), 140.92 (s), 139.79 (s), 136.48 (s), 135.02 (s), 130.03 (s), 128.95 (d), 128.08 (d), 122.99 (d), 43.51 (t), 41.56 (t), 17.77 (q), 17.61 (q), 13.87 (q), 11.87 (q).

Reaction of 5-methyl-3-phenyl-3*H*-1,2,3-triazolo[4,5-*d*]pyrimidine (**17**)[13] with **13a** gave 7-(diethylamino)-5,8-dimethyl-3-phenyl-3*H*-1,2,3-triazolo-[4,5-*d*][1,3]diazocine (**25**) as pale yellow needles (from petroleum benzin), mp 137—139 °C, in 60% yield (184 mg). *Anal.* Calcd for $C_{18}H_{22}N_6$: C, 67.06; H, 6.88; N, 26.06. Found: C, 66.81; H, 6.92; N, 25.81. MS *m/z*: 322 (M^+). ^{1}H-NMR ($CDCl_3$): 7.75—7.13 (5H, m, N^3-C_6H_5), 6.34 (1H, q, J=1.5, C^9-H), 3.42—2.93 (4H, q, J=7.0, $N(\underline{CH_2}Me)_2$), 2.22 (3H, s, C^5-CH_3), 2.03 (3H, d, J=1.5, C^8-CH_3), 1.05 (6H, t, J=7.0, $2\times CH_2\underline{CH_3}$).

Reaction of 3,5-diphenyl-3*H*-1,2,3-triazolo[4,5-*d*]pyrimidine (**18**) with **13a** gave 7-(diethylamino)-8-methyl-3,5-diphenyl-3*H*-1,2,3-triazolo[4,5-*d*][1,3]diazocine (**26**) as a slightly yellow powder (from benzene–petroleum benzin), mp 145—147 °C, in 53% yield (203 mg). *Anal.* Calcd for $C_{23}H_{24}N_6$: C, 71.85; H, 6.29; N, 21.86. Found: C, 72.07; H, 6.21; N,

21.72. MS *m/z*: 384 (M^+). ^{1}H-NMR ($CDCl_3$): 8.01—7.01 (10H, N^3- and C^5-C_6H_5), 6.28 (1H, q, J=1.5, C^9-H), 3.60—3.01 (4H, m, $N(\underline{CH_2}Me)_2$), 1.98 (3H, d, J=1.5, C^8-CH_3), 1.13 (6H, t, J=7.0, 2×$CH_2\underline{CH_3}$).

Reaction of 5-methoxy-3-phenyl-3*H*-1,2,3-triazolo[4,5-*d*]pyrimidine (**19**)[13] with **13a** gave 7-(diethylamino)-5-methoxy-3-phenyl-3*H*-1,2,3-triazolo[4,5-*d*][1,3]diazocine (**27**) as colorless prisms (from benzene–petroleum benzin), mp 158—160 °C, in 94% yield (317 mg). *Anal.* Calcd for $C_{18}H_{22}N_6O$: C, 63.89; H, 6.55; N, 24.83. Found: C, 63.89; H, 6.55; N, 24.65. MS *m/z*: 338 (M^+). ^{1}H-NMR ($CDCl_3$): 7.89—7.19 (5H, m, N^3-C_6H_5), 6.40 (1H, q, J=1.5, C^9-H), 3.80 (3H, s, OCH_3), 3.54—2.98 (4H, m, $N(\underline{CH_2}Me)_2$), 2.07 (3H, d, J=1.5, C^8-CH_3), 1.90—0.90 (6H, m, 2×$CH_2\underline{CH_3}$). ^{13}C-NMR ($CDCl_3$): 163.63 (s), 163.41 (s), 142.82 (s), 140.71 (s), 136.70 (s), 134.96 (s), 128.84 (d), 127.87 (d), 122.83 (d), 122.72 (d), 55.16 (q), 43.24 (t), 41.23 (t), 21.40 (q), 14.03 (q), 11.92 (q).

Reaction of 7-Methoxy-3-phenyl-3*H*-1,2,3-triazolo[4,5-*d*]pyrimidine (20) with 13a A solution of **20** (0.9 mmol, 200 mg) and **13a** (1.8 mmol, 200 mg) in xylene (3 ml) was refluxed for 9 h. Work-up of the reaction mixture as described for **21a** gave 5-(diethylamino)-9-methoxy-6-methyl-3-phenyl-3*H*-1,2,3-triazolro[4,5-*b*][1,5]diazocine (**28**) as colorless prisms (from benzene–peptroleum benzin), mp 179—181 °C, in 24% yield (70 mg). *Anal.* Calcd for $C_{18}H_{22}N_6O$: C, 63.89; H, 6.55; N, 24.83. Found: C, 63.87; H, 6.54; N, 24.84. MS *m/z*: 338 (M^+). ^{1}H-NMR ($CDCl_3$): 7.90—7.09 (5H, m, N^3-C_6H_5), 6.38 (1H, q, J=1.5, C^7-H), 3.81 (3H, s, OCH_3), 3.99—2.82 (4H, m, $N(\underline{CH_2}Me)_2$), 1.73 (3H, d, J=1.5, C^6-CH_3), 1.16 (6H, t, J=7.0, 2×$CH_2\underline{CH_3}$). ^{13}C-NMR ($CDCl_3$): 165.30 (s), 157.83 (s), 147.59 (s), 139.90 (d), 136.70 (s), 128.79 (d), 127.81 (d), 127.49 (s), 122.83 (d), 116.54 (s), 54.45 (q), 44.43 (t), 40.96 (t), 19.29 (q), 14.03 (q), 12.62 (q).

Crystal Data of 21a for X-Ray Crystallographic Analysis A crystal of **21a** for X-ray crystallographic analysis was obtained from a saturated solution of **21a** in MeOH. The crystal data are as follows: $C_{17}H_{20}N_6$, F.W. = 308.39, crystal dimensions 0.2×0.2×0.3 mm, monoclinic, space group *Cc*, a=9.831 (2), b=13.919 (4), c=12.084 (6) Å, β=93.17 (2)°, V=1651.0 (9) Å^3, D_{calcd}=1.24 g·cm^{-3} and Z=4. A total of 2128 independent reflections were measured, of which 1896 reflections with $|F_O|>3\sigma|F_O|$ were used for calculation.

The final residual values were R=0.042 and R_w=0.046.

Crystal Data of 28 for X-Ray Crystallographic Analysis A crystal of **28** for X-ray crystallographic analysis was obtained from a saturated solution of **28** in MeOH. The crystal data are as follows: $C_{18}H_{22}N_6O$, F.W. = 338.42, crystal dimensions 0.3×0.3×0.4 mm, monoclinic, space group $P2_1/c$, a=10.873 (1), b=10.290 (1), c=18.316 (2) Å, β=117.24 (8)°, V=1822.1 (4) Å^3, D_{calcd}=1.23 g·cm^{-3} and Z=4. A total of 4468 independent reflections were measured, of which 3264 reflections with $|F_O|>3\sigma|F_O|$ were used for calculation.

The final residual values were R=0.064 and R_w=0.072.

Reaction of the 1*H*-Pyrazolo[3,4-*d*]pyrimidines (30, 31) with 13a i) A solution of 4-methoxy-1-phenyl-1*H*-pyrazolo[3,4-*d*]pyrimidine (**30**, 226 mg, 1.0 mmol) and **13a** (222 mg, 2.0 mmol) in xylene (3 ml) was refluxed for 20 h. After cooling, the reaction mixture was poured into an excess of H_2O, and extracted with $CHCl_3$. The extract was washed with H_2O, dried over Na_2SO_4, and concentrated to dryness. The residue was chromatographed on a column of SiO_2 with $CHCl_3$ then benzene–ethyl acetate (20 : 1) as eluents. The fraction eluted with $CHCl_3$ gave 210 mg (93%) of unchanged **30**. The fraction with benzene–ethyl acetate gave 8-(diethylamino)-4-methoxy-7-methyl-1-phenyl-1*H*-pyrazolo[3,4-*b*][1,5]-diazocine (**32**), a slightly yellow oil, in 4% yield (11 mg). MS *m/z* Calcd for $C_{19}H_{23}N_6O$: 337.1903 (M^+). Found: 337.1912. ^{1}H-NMR ($CDCl_3$): 7.73—7.26 (5H, m, N^1-C_6H_5), 7.61 (1H, s, C^3-H), 6.43 (1H, q, J=1.5, C^6-H), 3.98 (3H, s, OCH_3), 3.84—2.90 (4H, m, $N(\underline{CH_2}Me)_2$), 1.82 (3H, d, J=1.5, C^7-CH_3), 1.24 (3H, t, J=7.0, $CH_2\underline{CH_3}$), 1.18 (3H, t, J=7.0, $CH_2\underline{CH_3}$).

ii) A solution of 1-phenyl-1*H*-pyrazolo[3,4-*d*]pyrimidine-4-carbonitrile (**31**, 200 mg, 0.9 mmol) and **13a** (200 mg, 1.8 mmol) in xylene (3 ml) was refluxed for 18 h. The reaction mixture was worked up as described for **32**, and chromatographed on a column of SiO_2. The fraction eluted with benzene gave 8-(diethylamino)-7-methyl-1-phenyl-1*H*-pyrazolo[3,4-*b*]-[1,5]diazocine-4-carbonitrile (**33**) as orange needles (from petroleum benzin), mp 125—126 °C, in 9% yield (27 mg). *Anal.* Calcd for $C_{19}H_{20}N_6$: C, 68.65; H, 6.07; N, 25.28. Found: C, 68.93; H, 6.09; N, 25.27. MS *m/z*: 332 (M^+). ^{1}H-NMR ($CDCl_3$): 7.72—7.01 (5H, m, N^1-C_6H_5), 7.47 (1H, s, C^3-H), 6.60 (1H, q, J=1.5, C^6-H), 3.90—2.80 (4H, m, $N(\underline{CH_2}Me)_2$), 1.86 (3H, d, J=1.5, C^7-CH_3), 1.41—0.91 (6H, m, 2×$CH_2\underline{CH_3}$). ^{13}C-NMR ($CDCl_3$): 164.33 (s), 151.92 (s), 142.76 (s), 141.41 (d), 139.30 (s), 138.32 (d), 128.57 (d), 126.68 (d), 122.88 (d), 120.93 (s), 116.06 (s), 106.19 (s), 44.32 (t), 41.29 (t), 19.67 (q), 13.76 (q), 12.79 (q).

Reaction of 9-Phenyl-9*H*-purine-6-carbonitrile (36) with 13a A solution of **36**[19] (200 mg, 0.9 mmol) and **13a** (200 mg, 1.8 mmol) in xylene (3 ml) was refluxed for 18 h. Work-up of the reaction mixture as described for **32** gave 5-(diethylamino)-6-methyl-3-phenyl-3*H*-imidazo[4,5-*b*][1,5]diazocine-9-carbonitrile (**37**) as pale yellow needles (from benzene–petroleum benzin), mp 157—158 °C, in 65% yield (194 mg). *Anal.* Calcd for $C_{19}H_{20}N_6$: C, 68.65; H, 6.07; N, 25.28. Found: C, 68.72; H, 6.08; N, 25.37. MS *m/z*: 332 (M^+). IR ν_{max}^{KBr} cm^{-1}: 2224 (CN). ^{1}H-NMR ($CDCl_3$): 8.28 (1H, s, C^2-H), 7.33—6.83 (5H, m, N^3-C_6H_5), 6.30 (1H, q, J=1.5, C^7-H), 3.70—3.15 (4H, q, J=7.0, $N(\underline{CH_2}Me)_2$), 1.93 (3H, d, J=1.5, C^6-CH_3), 1.43—1.06 (6H, t, J=7.0, 2×$CH_2\underline{CH_3}$). ^{13}C-NMR ($CDCl_3$): 163.95 (s), 158.75 (s), 149.97 (d). 142.06 (s), 140.92 (s), 135.40 (d), 134.59 (s), 129.11 (d), 123.75 (d), 123.15 (s), 118.66 (d), 116.06 (s), 42.91 (t), 17.45 (q), 13.33 (q).

Acknowledgement The authors are greatly indebted to the staff of the central analysis room of the University of Shizuoka for elemental analysis and mass spectral measurement.

References

1) D. L. Boger, *Tetrahedron*, **39**, 2869 (1983).
2) T. Higashino, *Yakugaku Zasshi*, **80**, 245 (1960).
3) W. Borsche, *Justus Liebigs Ann. Chem.*, **377**, 121 (1910).
4) O. Doebner and W. von Miller, *Ber.*, **16**, 1665 (1883).
5) T. Higashino, T. Katori, and E. Hayashi, *Chem. Pharm. Bull.*, **27**, 2431 (1979).
6) T. Higashino, T. Katori, and E. Hayashi, *Chem. Pharm. Bull.*, **27**, 2861 (1979).
7) T. Higashino, T. Katori, H. Kawaraya, and E. Hayashi, *Chem. Pharm. Bull.*, **28**, 337 (1980).
8) B. E. Christensen, B. Graham, and A. J. Tomisek, *J. Am. Chem. Soc.*, **68**, 1306 (1946).
9) R. A. Abramovitch, K. M. More, I. Shinkai, and P. C. Srinivasan, *Heterocycles*, **5**, 95 (1976).
10) R. Fuks and H. G. Viehe, *Chem. Ber.*, **103**, 573 (1976).
11) *a*) A. T. M. Marcelis, H. C. van der Plas, and S. Harkema, *J. Org. Chem.*, **50**, 270 (1985); *b*) A. T. M. Marcelis and H. C. van der Plas, *ibid.*, **51**, 67 (1986).
12) T. Higashino, T. Katori, S. Yoshida, and E. Hayashi, *Chem. Pharm. Bull.*, **27**, 3176 (1979).
13) K. Tanji, K. Yamamoto, and T. Higashino, *Chem. Pharm. Bull.*, **37**, 1731 (1989).
14) T. Higashino, Y. Iwai, and E. Hayashi, *Yakugaku Zasshi*, **94**, 666 (1974).
15) C. C. Cheng and R. K. Robins, *J. Org. Chem.*, **21**, 1240 (1956).
16) E. Hayashi, T. Higashino, and S. Suzuki, *Yakugaku Zasshi*, **98**, 89 (1978).
17) E. Hayashi, N. Shimada, and Y. Matsuoka, *Yakugaku Zasshi*, **99**, 114 (1979).
18) E. Hayashi and N. Shimada, *Yakugaku Zasshi*, **99**, 201 (1979).
19) E. Hayashi, N. Shimada, and A. Miyashita, *Yakugaku Zasshi*, **96**, 1370 (1976).
20) J. Yao, C. Zheng, J. Qian, F. Han, Y. Gu, and H. Fan, SAPI 85, "A Computer Program for Automatic Solution of Crystal Structures from X-Ray Diffraction Data," Institute of Physics, Academia Sinica, Beijing, China, 1985.
21) P. Main, S. J. Fiske, S. E. Hull, L. Lessinger, G. Germain, J. Declercq, and M. M. Woolfson, MULTAN 80, "A System of Computer Programs for the Automatic Solution of Crystal Structures from X-Ray Diffraction Data," Univ. of York, England, and Louvain, Belgium, 1980.

Lipid A and Related Compounds. XXIV.[1] Efficient Synthesis of Several Lipid as *via* Common Disaccharide Intermediates

Seijiro AKAMATSU, Kiyoshi IKEDA, and Kazuo ACHIWA*

School of Pharmaceutical Sciences, University of Shizuoka, Yada 395, Shizuoka 422, Japan. *Received August 3, 1990*

We describe the development of new common disaccharide intermediates bearing two amino and six hydroxyl groups that are chemically differentiated, and their application to syntheses of several lipid As.

Keywords total synthesis; *Proteus mirabilis* lipid A; *Salmonella* mutant lipid A; disaccharide intermediate; chemical differentiation

Lipid A is responsible for the expression of many biological activities of the lipopolysaccharide (LPS) of gram-negative bacteria, *e.g.*, endotoxicity, adjuvanticity, antitumor activity and so on.[2] Lipid A consists of a $\beta(1\rightarrow6)$-linked D-glucosamine disaccharide moiety which carries phosphate residues at positions 1 and 4′ as well as amide-bound and ester-bound D-3-hydroxy and/or acyloxy fatty acids as indicated in Chart 1.[3]

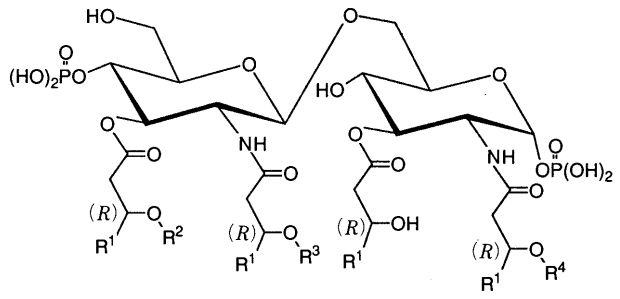

1a: R^1= $CH_3(CH_2)_{10}$-, R^2= R^3= R^4= H
(*Salmonella* mutant)
1b: R^1= $CH_3(CH_2)_{10}$-, R^2= $CH_3(CH_2)_{12}CO$-, R^3= $CH_3(CH_2)_{10}CO$-, R^4= H
(*Escherichia coli*)
1c: R^1= $CH_3(CH_2)_{10}$-, R^2= $CH_3(CH_2)_{12}CO$-, R^3= $CH_3(CH_2)_{10}CO$-, R^4= $CH_3(CH_2)_{14}CO$-
(*Salmonella minnesota*)
1d: R^1= $CH_3(CH_2)_{10}$-, R^2= $CH_3(CH_2)_{12}CO$-, R^3= $CH_3(CH_2)_{12}CO$-, R^4= H
(*Proteus mirabilis*)
1e: R^1= $CH_3(CH_2)_{10}$-, R^2= $CH_3(CH_2)_{12}CO$-, R^3= $CH_3(CH_2)_{12}CO$-, R^4= $CH_3(CH_2)_{14}CO$-
(*Proteus mirabilis*)

Chart 1

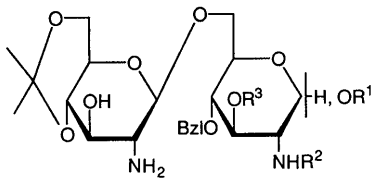

2a: R^1= allyl (β), R^2= R^3= TCBOC
2b: R^1= allyl (α), R^2= R^3= TCBOC
2c: R^1= allyl (α), R^2= TCEC, R^3= TCBOC
allyl: CH_2=$CHCH_2$-, TCEC : Cl_3CCH_2OCO-, TCBOC : $Cl_3C\overset{CH_3}{\underset{CH_3}{C}}OCO$-

Chart 2

Recently, Shiba's group has synthesized the biologically active constituents of LPS from *Salmonella* mutant (**1a**),[4] *Escherichia coli* (**1b**),[5] and *Salmonella minnesota* (**1c**)[6] by means of an elegant two-fragment condensation method. In this paper, we describe the development of the new common disaccharide intermediates **2a**,[7] **2b**,[8] **2c** bearing two amino and six hydroxyl groups that are chemically differentiated, and their application to syntheses of several lipid As.

We first describe the formal synthesis of *Salmonella* mutant lipid A (**1a**) *via* **2a** from the previously reported key intermediate[9] of lipid X, allyl 2-amino-2-deoxy-4,6-isopropylidene-β-D-glucopyranoside (**3**). The amino alcohol **3** was treated with 2,2,2-trichloro-*tert*-butoxycarbonyl chloride (TCBOC-Cl) in pyridine containing a catalytic amount of 4-dimethylaminopyridine (DMAP) to afford the diacylate **4** in 95% yield. The isopropylidene group of **4** was removed by treatment with 90% aqueous AcOH to afford the diol **5** in 90% yield and the primary alcohol of **5** was selectively protected with benzoyl chloride in pyridine–tetrahydrofuran (THF) to give the 6-*O*-benzoylated compound **6** in 75% yield. The remaining hydroxyl group of **6** was benzylated with benzyl 2,2,2-trichloroacetimidate in the presence of a catalytic amount of trifluoromethanesulfonic acid in CH_2Cl_2 to afford compound **7** in 49% yield, then the benzoyl group of **7** was removed with NH_4OH–MeOH (1 : 10) to give the reducing unit **8** in 74% yield. The neighboring group supported glycosylation of **8** with the suitably protected glycosyl donor **9** by using anhydrous $FeCl_3$, 1,1,3,3-tetramethylurea (TMU), and Molecular Sieves 4A (MS4A) in CH_2Cl_2[10] to give stereoselectively, as expected, the $\beta(1\rightarrow6)$-disaccharide **10** in 72% yield as a single isomer. The β-configuration of the newly formed glycosidic linkage was confirmed by the coupling constant value (8.0 Hz) of the signal due to the anomeric protons in the proton nuclear magnetic resonance (^{1}H-NMR) spectrum of **10**. The disaccharide **10** was deacetylated with NH_4OH–MeOH (1 : 10) to give the triol **11** in 86% yield, then **11** was converted into the 4′,6′-*O*-isopropylidene derivative **12** with 2,2-dimethoxypropane in the presence of a catalytic amount of *p*-toluenesulfonic acid (*p*-TsOH) in dimethylformamide (DMF) in 71% yield. Selective removal of the N-chloroacetyl group of **12** was carried out with thiourea and diisopropylethylamine in THF to give the common key intermediate **2a** in 92% yield.

The common key intermediate **2a** thus obtained was applied for the formal synthesis of *Salmonella* mutant lipid A as follows. The free amino and hydroxyl groups of **2a** were acylated with optically active (*R*)-3-benzyloxytetra-

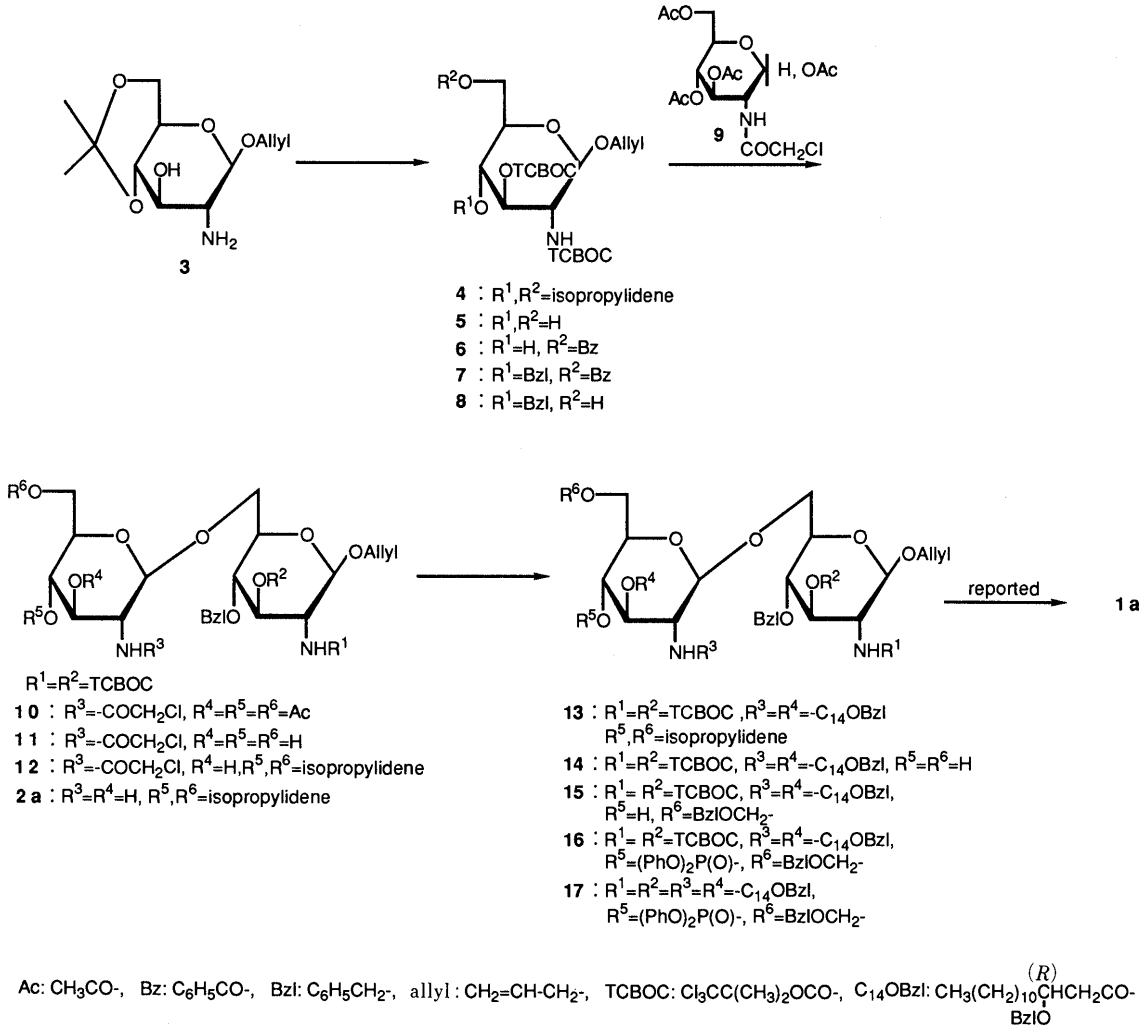

Chart 3

decanoic acid in the presence of dicyclohexylcarbodiimide (DCC) and a catalytic amount of DMAP in CH_2Cl_2 to give the diacylate **13** in 87% yield. Hydrolysis of the isopropylidene group of **13** with 90% AcOH gave the diol **14** in 94% yield. The 6′-*O*-hydroxyl group was selectively protected with benzyloxymethyl chloride and TMU in CH_2Cl_2, then the 4′-*O*-hydroxyl group was phosphorylated with diphenylphosphorochloridate in the presence of pyridine and DMAP in CH_2Cl_2 to afford the phosphorylated compound **16** in 55% yield. Replacement of the TCBOC group with an acyl group was carried out as follows. Treatment of **16** with activated Zn-dust in acetic acid at room temperature followed by acylation of free amino and hydroxyl groups with (*R*)-3-benzyloxytetradecanoic acid and DCC–DMAP in CH_2Cl_2 gave the fully protected compound **17** in 52% yield. Compound **17** is the intermediate for *Salmonella* mutant lipid A synthesis as reported by Shiba's group.[4] Accordingly we proved the availability of **2a** as a common key intermediate for the construction of lipid As.

Next, we describe a short preparation of the new disaccharide intermediate **2b** as a synthetic equivalent of **2a** and its application to the total synthesis of *Proteus mirabilis* lipid A (**1e**) as shown in Chart 4.

The selective protection of the amino group of D-glucosamine hydrochloride with TCBOC-Cl afforded the carbamate compound **18** in 87% yield. The glycosylation of **18** in 2% dry HCl in allyl alcohol at 100 °C gave the α-allyl glycoside **19** in 62% yield and its β-anomer in 7% yield. The configuration at C-1 of **19** was assigned as α on the basis of ^{1}H-NMR data (δ 4.89 with J=2.6 Hz for H-1). The α-glycoside **19** was then converted into the 4,6-*O*-isopropylidene derivative **20** with 2,2-dimethoxypropane in the presence of *p*-TsOH in DMF in 82% yield. Acylation of the free hydroxyl group of **20** with TCBOC-Cl in pyridine and DMAP gave **21** in 94% yield. Subsequently, cleavage of the isopropylidene group of **21**, followed by selective protection as the benzoyl ester, benzylation of the remaining hydroxyl group, and debenzoylation of **24** led to **25** in good overall yield. Coupling of the glycosyl donor **9** and the glycosyl acceptor **25** was achieved with $FeCl_3$ and TMU to give a sole disaccharide **26**, whose configuration of the glycosidic linkage at C-1′ was assigned as β from ^{13}C-NMR data (δ 100.2 with $^1J_{CH}$=161 Hz for C-1′). After cleavage of the acetyl group of **26**, 4′,6′-*O*-isopropylidenation of the resulting triol **27** and then deprotection of the chloroacetyl group of **28** were successively carried out by the same procedure as described for **2a**. The successful approach to the total synthesis of **1e** *via* **2b** is described below.

The free amino and hydroxyl groups of **2b** were simulta-

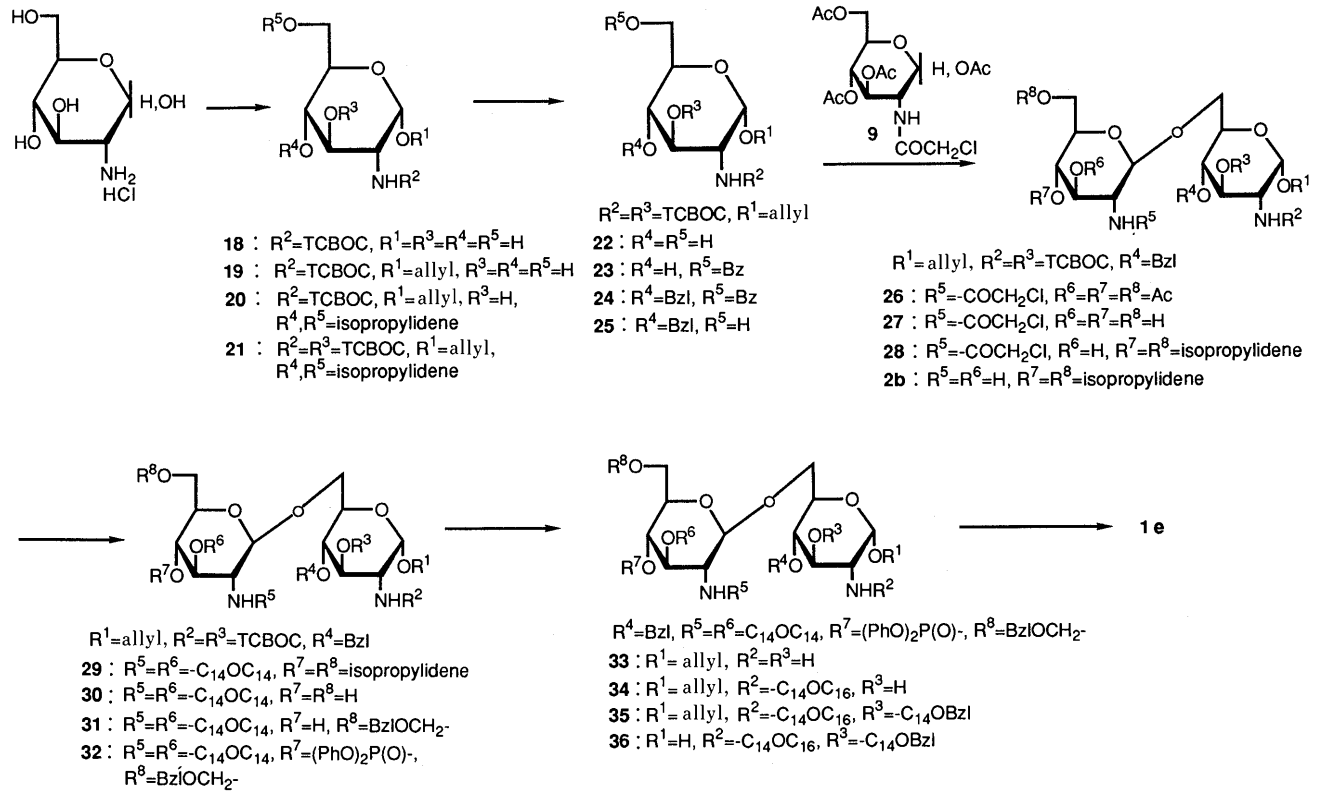

18 : R^2=TCBOC, R^1=R^3=R^4=R^5=H
19 : R^2=TCBOC, R^1=allyl, R^3=R^4=R^5=H
20 : R^2=TCBOC, R^1=allyl, R^3=H, R^4,R^5=isopropylidene
21 : R^2=R^3=TCBOC, R^1=allyl, R^4,R^5=isopropylidene

R^2=R^3=TCBOC, R^1=allyl
22 : R^4=R^5=H
23 : R^4=H, R^5=Bz
24 : R^4=Bzl, R^5=Bz
25 : R^4=Bzl, R^5=H

R^1=allyl, R^2=R^3=TCBOC, R^4=Bzl
26 : R^5=-$COCH_2Cl$, R^6=R^7=R^8=Ac
27 : R^5=-$COCH_2Cl$, R^6=R^7=R^8=H
28 : R^5=-$COCH_2Cl$, R^6=H, R^7=R^8=isopropylidene
2b : R^5=R^6=H, R^7=R^8=isopropylidene

R^1=allyl, R^2=R^3=TCBOC, R^4=Bzl
29 : R^5=R^6=-$C_{14}OC_{14}$, R^7=R^8=isopropylidene
30 : R^5=R^6=-$C_{14}OC_{14}$, R^7=R^8=H
31 : R^5=R^6=-$C_{14}OC_{14}$, R^7=H, R^8=$BzlOCH_2$-
32 : R^5=R^6=-$C_{14}OC_{14}$, R^7=$(PhO)_2P(O)$-, R^8=$BzlOCH_2$-

R^4=Bzl, R^5=R^6=$C_{14}OC_{14}$, R^7=$(PhO)_2P(O)$-, R^8=$BzlOCH_2$-
33 : R^1=allyl, R^2=R^3=H
34 : R^1=allyl, R^2=-$C_{14}OC_{16}$, R^3=H
35 : R^1=allyl, R^2=-$C_{14}OC_{16}$, R^3=-$C_{14}OBzl$
36 : R^1=H, R^2=-$C_{14}OC_{16}$, R^3=-$C_{14}OBzl$

Ac : CH_3CO-, Bz : C_6H_5CO-, Bzl : $C_6H_5CH_2$-, allyl : CH_2=CH-CH_2-, TCBOC : $Cl_3CC(CH_3)_2OCO$-

$C_{14}OBzl$: $CH_3(CH_2)_{10}\overset{(R)}{C}HCH_2CO$- (BzlO) ·$C_{14}OC_{16}$: $CH_3(CH_2)_{10}\overset{(R)}{C}HCH_2CO$- ($CH_3(CH_2)_{14}C(O)O$)

Chart 4

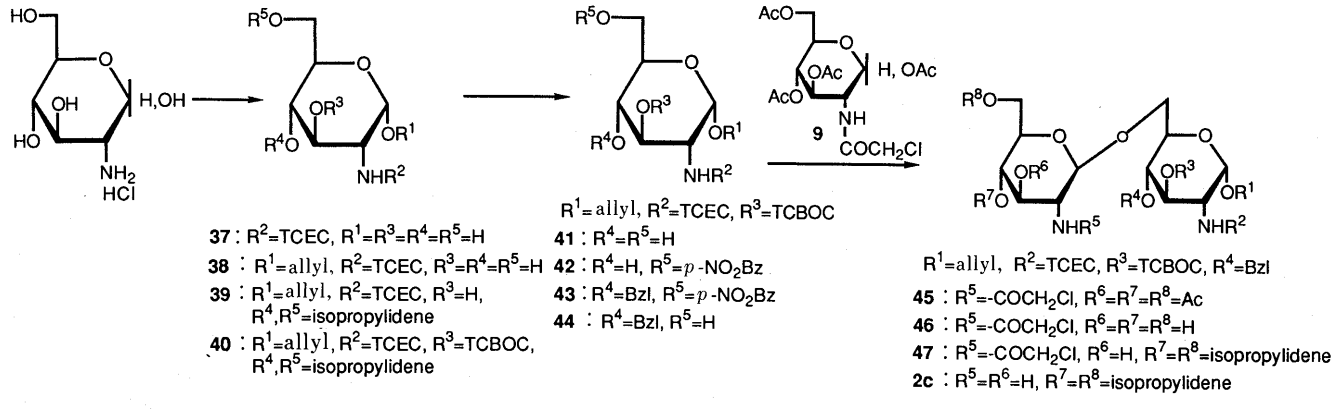

37 : R^2=TCEC, R^1=R^3=R^4=R^5=H
38 : R^1=allyl, R^2=TCEC, R^3=R^4=R^5=H
39 : R^1=allyl, R^2=TCEC, R^3=H, R^4,R^5=isopropylidene
40 : R^1=allyl, R^2=TCEC, R^3=TCBOC, R^4,R^5=isopropylidene

R^1=allyl, R^2=TCEC, R^3=TCBOC
41 : R^4=R^5=H
42 : R^4=H, R^5=p-NO_2Bz
43 : R^4=Bzl, R^5=p-NO_2Bz
44 : R^4=Bzl, R^5=H

R^1=allyl, R^2=TCEC, R^3=TCBOC, R^4=Bzl
45 : R^5=-$COCH_2Cl$, R^6=R^7=R^8=Ac
46 : R^5=-$COCH_2Cl$, R^6=R^7=R^8=H
47 : R^5=-$COCH_2Cl$, R^6=H, R^7=R^8=isopropylidene
2c : R^5=R^6=H, R^7=R^8=isopropylidene

Ac : CH_3CO-, Bz : C_6H_5CO-, Bzl : $C_6H_5CH_2$-, allyl : CH_2=CH-CH_2-, TCBOC : $Cl_3CC(CH_3)_2OCO$-, TCEC : Cl_3CCH_2OCO-

Chart 5

neously acylated with (*R*)-3-tetradecanoyloxytetradecanoic acid in the presence of DCC and a catalytic amount of DMAP in CH_2Cl_2 to give the diacylate **29** in 73% yield. Removal of the isopropylidene group of **29** with 90% acetic acid afforded the diol **30** in 75% yield. The 6′-*O*-hydroxyl group was selectively protected with benzyloxymethyl chloride and TMU in CH_2Cl_2 to give the benzyloxymethyl compound **31** in 63% yield. Then the phosphorylation of **31** with diphenylphosphoryl chloride in the presence of pyridine–DMAP in CH_2Cl_2 gave **32** in 76% yield. Treatment of **32** with Zn-dust in acetic acid gave the amino alcohol compound **33** in 89% yield. Then the free amino group of **33** was acylated with (*R*)-3-hexadecanoyloxytetradecanoic acid and DCC in CH_2Cl_2 to give the triacylated compound **34** in 67% yield. The remaining hydroxyl group of **34** was acylated with (*R*)-3-benzyloxytetradecanoic acid and DCC–DMAP in CH_2Cl_2 to give **35** in 72% yield. Selective removal of the glycosidic allyl group was followed by isomerization with iridium complex,[11] then the resultant 1-propenyl glycoside was treated with iodine[12] in aqueous THF to give **36** in 87% yield. α-Configuration of the hydroxyl group at C-1 of **36** was

assigned on the basis of ^{13}C-NMR data (C-1 signal at δ 91.3 with $^{1}J_{CH}=173$ Hz). The glycosidic hydroxyl group of **36** was phosphorylated with *n*-BuLi and dibenzylphosphoryl chloride in THF at $-70\,^{\circ}C$[13] and the product was immediately hydrogenolyzed. Stepwise removal of the benzyl group with Pd–C, H_2 and then phenyl esters of the 4′-*O*-phosphate group with PtO_2, H_2 afforded the final product **1e** in 10% yield from **36** after isolation by means of a silica gel column ($CHCl_3$–MeOH–H_2O–Et_3N, 20:5:1:0.05) and then acidic precipitation, and lyophilization from dioxane. The molecular weight of **1e** was confirmed by positive ion fast atom bombardment (FAB)-mass spectrometry, which showed an $(M+H+NEt_3)^+$ ion at *m/z* 2164.7, and an $(M+NEt_3+Na)^+$ ion at *m/z* 2186.8. Compound **1e** possesses a variety of biological activities of lipid A.[14] An improved synthesis of the key intermediate **2c** was developed as indicated in Chart 5. That is, the amino group of **37** was protected by a 2,2,2-trichloroethoxycarbonyl (TCEC) group in place of the expensive TCBOC group, and the protection of the 6-*O*-hydroxyl group of **41** was carried out with a *p*-nitrobenzoyl group. The overall yield of **2c** was 22.2% from D-glucosamine HCl in 12 steps, in contrast with the synthesis of **2b** in 5.0% yield from D-glucosamine HCl in 12 steps.

In this way, we have developed methods for the chemoselective protection and deprotection of the glucosamine, and demonstrated the utility of the new methodology for the efficient synthesis of lipid As, using key disaccharide intermediates.

Experimental

All melting points are uncorrected. ^{1}H-NMR spectra (90 MHz) and ^{13}C-NMR spectra (22.5 MHz) were taken on a JEOL JNM-FX90Q NMR spectrometer with tetramethylsilane (in $CDCl_3$) as an internal standard, and the chemical shifts are given in δ values. The abbreviations of signal patterns are as follows: s, singlet; br s, broad singlet; d, doublet; t, triplet; q, quartet; m, multiplet. Infrared (IR) spectra were recorded on a JASCO A-202 infrared spectrophotometer. Optical rotations were determined with a JASCO DIP-140 digital polarimeter.

Column chromatography was carried out on silica gel (Kiesel gel-60, 70—230 mesh, Merck). Thin-layer chromatography (TLC) on Kiesel gel 60-F_{254} (Merck) was used to monitor the reaction and to ascertain the purity of the reaction products. The spots were visualized by spraying with aqueous sulfuric acid and then heating.

Allyl 2-Deoxy-4,6-*O*-isopropylidene-3-*O*-(2,2,2-trichloro-*tert*-butoxycarbonyl)-2-*O*-(2,2,2-trichloro-*tert*-butoxycarbonylamino)-β-D-glucopyranoside (4) A solution of TCBOC-Cl (2.88 g, 12 mmol) in dry CH_2Cl_2 (2 ml) was added to a stirred solution of allyl 2-amino-2-deoxy-4,6-*O*-isopropylidene-β-D-glucopyranoside (**3**) (1.04 g, 4.0 mmol), prepared as previously described in the literature,[9] and DMAP (49 mg, 0.40 mmol) in dry pyridine (20 ml) at 0 °C under nitrogen. The mixture was stirred for 12 h at room temperature, then the insoluble materials were filtered off and the filtrate was evaporated. The residue was chromatographed on silica gel with $CHCl_3$–isopropyl ether (IPE) (20:1) to give **4** (2.56 g, 96%), mp 85—87 °C. $[\alpha]_D^{21}$ −18.1° (*c*=1.00, $CHCl_3$). IR (KBr): 3404 (NH), 1761 (carbonate), 1732 (carbamate), 858 cm^{-1} (Me_2C). ^{1}H-NMR ($CDCl_3$) δ: 1.39, 1.47 (each 3H, s, Me_2C), 1.91 (12H, s, $Cl_3CCMe_2\times2$), 4.77 (1H, d, *J*=8.1 Hz, H-1), 5.62—6.14 (1H, m, $-CH_2=$). *Anal.* Calcd for $C_{22}H_{31}Cl_6NO_9$: C, 39.66; H, 4.69; N, 1.80. Found: C, 40.17; H, 4.76; N, 2.06.

Allyl 2-Deoxy-3-*O*-(2,2,2-trichloro-*tert*-butoxycarbonyl)-2-(2,2,2-trichloro-*tert*-butoxycarbonylamino)-β-D-glucopyranoside (5) A solution of **4** (1.21 g, 1.82 mmol) in 90% aqueous AcOH (12 ml) was heated at 90 °C for 15 min. The mixture was cooled and the solvent was evaporated off *in vacuo*. The residue was chromatographed on silica gel with $CHCl_3$–MeOH (15:1) to give **5** (1.03 g, 90%) as prisms, mp 106 °C. $[\alpha]_D^{21}$ −10.7° (*c*=1.00, $CHCl_3$). IR (KBr): 3376 (OH, NH), 1760 (carbonate), 1725 cm^{-1} (carbamate). ^{1}H-NMR ($CDCl_3$) δ: 1.90 (12H, s, $Cl_3CCMe_2\times2$), 4.70 (1H, d, *J*=7.9 Hz, H-1), 5.64—6.15 (1H, m, $-CH=$). *Anal.* Calcd for $C_{19}H_{27}Cl_6NO_9$: C, 36.45; H, 4.35; N, 2.24. Found: C, 36.18; H, 4.26; N, 2.22.

Allyl 6-*O*-Benzoyl-2-deoxy-3-*O*-(2,2,2-trichloro-*tert*-butoxycarbonyl-2-(2,2,2-trichloro-*tert*-butoxycarbonylamino)-β-D-glucopyranoside (6) Benzoyl chloride (0.343 g, 2.44 mmol) was added to a stirred solution of **5** (1.02 g, 1.63 mmol) and pyridine (0.387 g, 4.89 mmol) in dry THF (15 ml) at 0 °C under nitrogen. The mixture was stirred for 2 h at 0 °C with addition of benzoyl chloride (0.343 g, 2.44 mmol) after 5 h at 0 °C, and then a small amount of water (1.0 ml) was added. The organic layer was dried and evaporated. After removal of the solvent, the residue was chromatographed on silica gel with $CHCl_3$–IPE (20:1) to give **6** (0.892 g, 75%) as white prisms, mp 84 °C. $[\alpha]_D^{23}$ −9.97° (*c*=1.00, $CHCl_3$). IR (KBr): 3404 (NH, OH), 1756 (carbonate), 1723 (carbamate, ester), 710 cm^{-1} (Ph). ^{1}H-NMR ($CDCl_3$) δ: 1.91 (12H, s, $Cl_3CCMe_2\times2$), 5.66—6.14 (1H, m, $-CH=$), 7.33—8.18 (5H, m, Ph). *Anal.* Calcd for $C_{26}H_{31}Cl_6NO_{10}$: C, 42.76; H, 4.28; N, 1.92. Found: C, 43.07; H, 4.37; N, 1.92.

Allyl 6-*O*-Benzoyl-4-*O*-benzyl-2-deoxy-3-*O*-(2,2,2-trichloro-*tert*-butoxycarbonyl)-2-(2,2,2-trichloro-*tert*-butoxycarbonylamino)-β-D-glucopyranoside (7) Trifluoromethanesulfonic acid (0.123 g, 0.82 mmol) was added to a stirred solution of **5** (2.00 g, 2.73 mmol) and benzyl 2,2,2-trichloroacetimidate (1.38 g, 5.46 mmol) in dry CH_2Cl_2 (30 ml) at 0 °C under nitrogen. After 12 h at room temperature, the reaction mixture was washed with saturated aqueous $NaHCO_3$, dried and concentrated. The residue was subjected to column chromatography on silica gel with $CHCl_3$–IPE (50:1) to give **7** (1.08 g, 49%), as white prisms, mp 69 °C. $[\alpha]_D^{23}$ +9.73° (*c*=1.04, $CHCl_3$). IR (KBr): 3420 (NH), 1759 (carbonate), 1730 (carbamate, ester), 712, 700 cm^{-1} (Ph). ^{1}H-NMR ($CDCl_3$) δ: 1.91 (12H, s, $Cl_3CCMe_2\times2$), 5.64—6.11 (1H, m, $-CH=$), 7.24 (5H, s, $PhCH_2$), 7.40—8.14 (5H, m, PhCO). *Anal.* Calcd for $C_{33}H_{37}Cl_6NO_{10}$: C, 48.32; H, 4.55; N, 1.71. Found: C, 48.08; H, 4.60; N, 1.70.

Allyl 4-*O*-Benzyl-2-deoxy-3-*O*-(2,2,2-trichloro-*tert*-butoxycarbonyl)-2-(2,2,2-trichloro-*tert*-butoxycarbonylamino)-β-D-glucopyranoside (8) Compound **6** (0.470 g, 0.58 mmol) was dissolved in a solution (20 ml) of NH_4OH–MeOH (1:10). The solution was stirred at room temperature for 48 h, then the solvent was evaporated off *in vacuo*. The residue was chromatographed on silica gel with $CHCl_3$–IPE (10:1) to give **8** (0.488 g, 74%), as white prisms, mp 75—77 °C. $[\alpha]_D^{24}$ −9.98° (*c*=1.04, $CHCl_3$). IR (KBr): 3412 (NH, OH), 1759 (carbonate), 1729 (carbamate), 698 cm^{-1} (Ph). ^{1}H-NMR ($CDCl_3$) δ: 1.90 (12H, s, $Cl_3CCMe_2\times2$), 4.68 (2H, s, $PhCH_2$), 5.64—6.13 (1H, m, $-CH=$), 7.29 (5H, s, $PhCH_2$). *Anal.* Calcd for $C_{26}H_{33}Cl_6NO_9$: C, 43.60; H, 4.64; N, 1.96. Found: C, 43.84; H, 4.66; N, 1.89.

Allyl 4-*O*-Benzyl-6-*O*-(3,4,6-tri-*O*-acetyl-2-chloroacetylamino-2-deoxy-β-D-glucopyranosyl)-2-deoxy-3-*O*-(2,2,2-trichloro-*tert*-butoxycarbonyl)-2-(2,2,2-trichloro-*tert*-butoxycarbonylamino)-β-D-glucopyranoside (10) A mixture of **8** (0.323 g, 0.46 mmol), 1,3,4,6-tetra-*O*-acetyl-2-chloroacetamido-2-deoxy-β-D-glucopyranose (**9**) (0.109 g, 0.92 mmol), TMU (0.390 g, 0.92 mmol) and pulverized MS 4A (1 g) in dry CH_2Cl_2 (10 ml) was stirred for 1 h, and anhydrous $FeCl_3$ (0.180 g, 1.1 mmol) was added at room temperature under nitrogen. After 24 h at room temperature, the same amounts of $FeCl_3$ and TMU were again added. Since the donor **9** was still present, more reagents (equivalent to the previous amounts) were added and stirring was continued for 24 h. The mixture was then poured into ice-cold, aqueous $NaHCO_3$. After the addition of $CHCl_3$ and mixing, the organic layer was filtered through Celite, and the filtrate and washings were combined, washed with saturated aqueous $NaHCO_3$ and then water, dried and concentrated. The crude product was purified by column chromatography with $CHCl_3$–acetone (30:1) to give **10** (0.351 g, 72%) as white prisms, mp 100—102 °C. $[\alpha]_D^{21}$ −6.97° (*c*=1.13, $CHCl_3$). IR (KBr): 3320 (NH), 1757 (carbonate, carbamate), 1657 (amide), 697 cm^{-1} (Ph). ^{1}H-NMR ($CDCl_3$) δ: 1.84, 1.88 (12H, s, $Cl_3CCMe_2\times2$), 2.03 (9H, s, $AcO\times3$), 3.92 (2H, s, $ClCH_2CO$), 4.62 (2H, s, $PhCH_2$), 4.83 (1H, d, *J*=8.0 Hz, H-1′), 5.63—6.12 (1H, m, $-CH=$), 6.76 (1H, d, *J*=9.3 Hz, $NHCOCH_2Cl$), 7.28 (5H, s, $PhCH_2$). *Anal.* Calcd for $C_{40}H_{51}Cl_7NO_{17}$: C, 44.48; H, 4.76; N, 2.59. Found: C, 44.36; H, 4.81; N, 2.46.

Allyl 4-*O*-Benzyl-6-*O*-(2-chloroacetylamino-2-deoxy-β-D-glucopyranosyl)-2-deoxy-3-*O*-(2,2,2-trichloro-*tert*-butoxycarbonyl)-2-(2,2,2-trichloro-*tert*-butoxycarbonylamino)-β-D-glucopyranoside (11) Compound **9** (0.300 g, 0.28 mmol) was dissolved in a solution of NH_4OH–MeOH (1:10) (3.0 ml). The mixture was stirred for 15 h at room temperature and concentrated *in vacuo*. The residue was chromatographed on silica gel with $CHCl_3$–MeOH (10:1) to give **11** (0.227 g, 86%) as a white powder, mp 174—175 °C. $[\alpha]_D^{24}$ −21.6° (*c*=1.00, $CHCl_3$). IR (KBr): 3372 br (NH, OH), 1762 (carbonate), 1740 (carbamate), 1683 (amide), 700 cm^{-1} (Ph). ^{1}H-NMR ($CDCl_3$) δ: 1.83, 1.89 (12H, s, $Cl_3CCMe_2\times2$), 4.05 (2H, s,

$ClCH_2CO$), 4.70 (2H, s, $PhCH_2$), 5.70—6.20 (1H, m, –CH=), 6.74 (1H, d, J=9.3 Hz, $NHCOCH_2Cl$), 7.33 (5H, s, Ph). *Anal.* Calcd for $C_{34}H_{45}Cl_7N_2O_{14}\cdot H_2O$: C, 42.02; H, 4.87; N, 2.88. Found: C, 42.11; H, 4.68; N, 2.79.

Allyl 4-*O*-Benzyl-6-*O*-(2-chloroacetylamino-2-deoxy-4,6-*O*-isopropylidene-β-D-glucopyranosyl)-2-deoxy-3-*O*-(2,2,2-trichloro-*tert*-butoxycarbonyl)-2-(2,2,2-trichloro-*tert*-butoxycarbonylamino)-β-D-glucopyranoside (12) *p*-TsOH (0.012 g, 0.07 mmol) was added to a stirred solution of **11** (0.225 g, 0.24 mmol) and 2,2-dimethoxypropane (0.075 g, 0.72 mmol) in DMF (2.0 ml) at room temperature under nitrogen. After 5 h, the reaction mixture was neutralized with ion exchange resin (Amberlite IRA-400) (0.282 g, 1.04 mg eq.) and then the resin was removed by filtration. The filtrate was evaporated to dryness and the residue was chromatographed on silica gel with $CHCl_3$–acetone (10 : 1) to give **12** (0.166 g, 71%) as white prisms, mp 126—128 °C. $[\alpha]_D^{26}$ −23.7° (c=0.27, $CHCl_3$). IR (KBr): 3400 br (NH, OH), 1761 (carbonate), 1737 (carbamate), 1673 (amide), 855 (Me_2C), 700 cm^{-1} (Ph). ^{1}H-NMR ($CDCl_3$) δ: 1.43, 1.52 (each 3H, s, Me_2C), 1.83, 1.88 (12H, s, $Cl_3CCMe_2\times2$), 3.99 (2H, s, $ClCH_2CO$), 4.61 (2H, s, $PhCH_2$), 5.68—6.18 (1H, m, –CH=), 6.75 (1H, d, J=9.0 Hz, $NHCOCH_2Cl$), 7.22 (5H, s, Ph). *Anal.* Calcd for $C_{37}H_{49}Cl_7N_2O_{14}$: C, 44.71; H, 4.79; N, 2.82. Found: C, 44.45; H, 4.92; N, 2.88.

Allyl 4-*O*-Benzyl-6-*O*-(2-amino-2-deoxy-4,6-*O*-isopropylidene-β-D-glucopyranosyl)-2-deoxy-3-*O*-(2,2,2-trichloro-*tert*-butoxycarbonyl)-2-(2,2,2-trichloro-*tert*-butoxycarbonylamino)-β-D-glucopyranoside (2a) A mixture of **12** (0.766 g, 0.77 mmol), thiourea (0.293 g, 3.85 mmol), diisopropylethylamine (0.498 g, 3.85 mmol), and pulverized MS 4A (1 g) was stirred at 55 °C for 12 h under nitrogen. The resulting suspension was filtered through Celite and the filtrate was concentrated *in vacuo*. The residue was subjected to silica gel chromatography with $CHCl_3$–MeOH (40 : 1) to give **2a** (0.648 g, 92%) as reddish prisms, mp 119—121 °C. $[\alpha]_D^{21}$ −20.0° (c=1.17, $CHCl_3$). IR (KBr): 3372 br (NH, OH), 1761 (carbonate), 1738 (carbamate), 854 (Me_2C), 700 cm^{-1} (Ph). ^{1}H-NMR ($CDCl_3$) δ: 1.43, 1.50 (each 3H, s, Me_2C), 1.84, 1.89 (12H, s, $Cl_3CCMe_2\times2$), 4.65, 4.69 (each 1H, d, J=11.2 Hz, $PhC\underline{H}_2$), 5.65—6.11 (1H, m, –CH=), 7.29 (5H, s, Ph). *Anal.* Calcd for $C_{35}H_{48}Cl_7N_2O_{13}$: C, 45.82; H, 5.27; N, 3.05. Found: C, 45.57; H, 5.30; N, 3.05.

Allyl 4-*O*-Benzyl-6-*O*-[3-*O*-[(*R*)-3-benzyloxytetradecanoyl]-2-[(*R*)-3-benzyloxytetradecanoylamino]-2-deoxy-4,6-*O*-isopropylidene-β-D-glucopyranosyl]-2-deoxy-3-*O*-(2,2,2-trichloro-*tert*-butoxycarbonyl)-2-(2,2,2-trichloro-*tert*-butoxycarbonylamino)-β-D-glucopyranoside (13) DCC (0.481 g, 2.3 mmol) was added to a stirred solution of **2a** (0.648 g, 0.71 mmol), (*R*)-3-benzyloxytetradecanoic acid (0.709 g, 2.1 mmol), and DMAP (0.009 g, 0.07 mmol) in dry CH_2Cl_2 (10 ml) at 0 °C under nitrogen. The mixture was stirred for 6 h at 0 °C, then at room temperature for 12 h. The resulting suspension was filtered through Celite and evaporated. The residue was chromatographed on silica gel with $CHCl_3$–IPE (10 : 1) to give **13** (0.948 g, 87%) as white prisms, mp 95—97 °C. $[\alpha]_D^{27}$ −13.0° (c=0.64, $CHCl_3$). IR (KBr): 3328 (NH), 1761 (carbonate), 1738 (carbamate), 1651 (amide), 859 (Me_2C), 700 cm^{-1} (Ph). ^{1}H-NMR ($CDCl_3$) δ: 0.88 (6H, t, J=5.8 Hz, $-(CH_2)_{10}C\underline{H}_3\times2$), 1.25 (40H, br s, $-(C\underline{H}_2)_{10}CH_3\times2$), 1.33, 1.38 (each 3H, s, Me_2C), 1.84, 1.88 (12H, s, $Cl_3CCMe_2\times2$), 2.27 (2H, d, J=4.7 Hz, $NCOCH_2$), 2.48 (2H, d, J=5.6 Hz, $OCOCH_2$), 4.50 (4H, br s, $PhCH_2\times2$), 4.58 (2H, br s, 4-position $PhCH_2$), 5.62—6.04 (1H, m, –CH=), 6.27 (1H, d, J=9.5 Hz, $NHCOCH_2$), 7.27, 7.31, 7.34 (15H, s, Ph×3). *Anal.* Calcd for $C_{77}H_{112}Cl_6N_2O_{17}$: C, 59.65; H, 7.28; N, 1.81. Found: C, 59.37; H, 7.21; N, 1.76.

Allyl 4-*O*-Benzyl-6-*O*-[3-*O*-[(*R*)-3-benzyloxytetradecanoyl]-2-[(*R*)-3-benzyloxytetradecanoylamino]-2-deoxy-β-D-glucopyranosyl]-2-deoxy-3-*O*-(2,2,2-trichloro-*tert*-butoxycarbonyl)-2-(2,2,2-trichloro-*tert*-butoxycarbonylamino)-β-D-glucopyranoside (14) A solution of **13** (0.412 g, 0.27 mmol) in 90% aqueous AcOH (5.0 ml) was heated at 90 °C for 15 min. After cooling, the solvent was evaporated off *in vacuo*. The residue was subjected to silica gel chromatography with $CHCl_3$–MeOH (20 : 1) to give **14** (0.376 g, 94%) as white prisms, mp 65—67 °C. $[\alpha]_D^{20}$ −13.3° (c=1.09, $CHCl_3$). IR (KBr): 3406 br (NH, OH), 1758 (carbonate), 1742 (carbamate, ester), 1664 (amide), 696 cm^{-1} (Ph). ^{1}H-NMR ($CDCl_3$) δ: 0.88 (6H, t, J=5.5 Hz, $-(CH_2)_{10}C\underline{H}_3\times2$), 1.25 (40H, br s, $-(C\underline{H}_2)_{10}CH_3\times2$), 1.84, 1.88 (each 6H, s, $Cl_3CCMe_2\times2$), 2.28 (2H, d, J=5.4 Hz, $NCOCH_3$), 2.56 (2H, d, J=4.9 Hz, $OCOCH_2$), 4.50 (4H, br s, $PhCH_2\times2$), 4.62 (2H, br s, 4-position $PhCH_2$), 5.62—6.11 (1H, m, –CH=), 6.29 (1H, d, J=9.5 Hz, $NHCOCH_2$), 7.28, 7.30, 7.33 (15H, s, Ph×3). *Anal.* Calcd for $C_{74}H_{108}Cl_6N_2O_{17}$: C, 58.85; H, 7.21; N, 1.85. Found: C, 58.80; H, 7.19; N, 1.93.

Allyl 4-*O*-Benzyl-6-*O*-[6-*O*-benzyloxymethyl-3-*O*-[(*R*)-3-benzyloxytetradecanoyl]-2-[(*R*)-3-benzyloxytetradecanoylamino]-2-deoxy-β-D-glucopyranosyl]-2-deoxy-3-*O*-(2,2,2-trichloro-*tert*-butoxycarbonyl)-2-(2,2,2-trichloro-*tert*-butoxycarbonylamino)-β-D-glucopyranoside (15) Benzyloxymethyl chloride (0.279 g, 1.78 mmol) was added to a stirred solution of **14** (0.538 g, 0.36 mmol), and TMU (0.207 g, 1.80 mmol), in dry CH_2Cl_2 (7.0 ml) at 0 °C under nitrogen. After 20 h at room temperature, the reaction mixture was washed with saturated aqueous $NaHCO_3$ and brine, and dried over $MgSO_4$. After removal of the solvent, the residue was chromatographed on silica gel with $CHCl_3$–acetone (10 : 1) to give **15** (0.424 g, 73%) as white prisms, mp 87—89 °C. $[\alpha]_D^{21}$ −11.5° (c=0.61, $CHCl_3$). IR (KBr): 3408 br (NH, OH), 1758 (carbonate), 1742 (carbamate, ester), 1653 (amide), 715, 698 cm^{-1} (Ph). ^{1}H-NMR ($CDCl_3$) δ: 0.88 (6H, t, J=5.6 Hz, $-(CH_2)_{10}C\underline{H}_3\times2$), 1.25 (40H, br s, $-(C\underline{H}_2)_{10}CH_3\times2$), 1.84, 1.88 (each 6H, s, $Cl_3CCMe_2\times2$), 2.28 (2H, d, J=5.2 Hz, $NCOCH_2$), 2.56 (2H, d, J=6.6 Hz, $OCOCH_2$), 4.51 (4H, br s, $PhCH_2\times2$), 4.57 (4H, br s, 4,6′-position $PhCH_2\times2$), 4.74 (2H, s, $OC\underline{H}_2OCH_2Ph$), 5.62—6.07 (1H, m, –CH=), 6.25 (1H, d, J=8.5 Hz, $NHCOCH_2$), 7.29, 7.32, 7.33 (20H, s, Ph×4). *Anal.* Calcd for $C_{82}H_{116}Cl_6N_2O_{18}\cdot H_2O$: C, 59.74; H, 7.21; N, 1.70. Found: C, 59.63; H, 6.97; N, 1.73.

Allyl 4-*O*-Benzyl-6-*O*-[6-*O*-benzyloxymethyl-3-*O*-[(*R*)-3-benzyloxytetradecanoyl]-2-[(*R*)-3-benzyloxytetradecanoylamino]-2-deoxy-4-*O*-diphenylphosphono-β-D-glucopyranosyl]-2-deoxy-3-*O*-(2,2,2-trichloro-*tert*-butoxycarbonyl)-2-(2,2,2-trichloro-*tert*-butoxycarbonylamino)-β-D-glucopyranoside (16) Diphenylphosphorochloridate (0.211 g, 0.75 mmol) was added to a stirred solution of **15** (0.250 g, 0.15 mmol), pyridine (0.059 g, 0.75 mmol) and DMAP (0.092 g, 0.75 mmol) at 0 °C under nitrogen. After 3 h at room temperature, the reaction mixture was washed with saturated aqueous $NaHCO_3$ and brine, dried over $MgSO_4$ and evaporated to dryness. The residue was chromatographed on silica gel with $CHCl_3$–acetone (30 : 1) to give **16** (0.211 g, 76%) as white prisms, mp 53—55 °C. $[\alpha]_D^{21}$ −4.72° (c=1.09, $CHCl_3$). IR (KBr): 3420 (NH), 1754 (carbonate), 1742 (carbamate, ester), 1670 (amide), 1215 (P=O), 958 (P–O–Ph), 695 cm^{-1} (Ph). ^{1}H-NMR ($CDCl_3$) δ: 0.88 (6H, t, J=5.4 Hz, $-(CH_2)_{10}C\underline{H}_3\times2$), 1.24 (40H, br s, $-(C\underline{H}_2)_{10}CH_3\times2$), 2.13 (2H, d, J=6.1 Hz, $NCOCH_2$), 2.43 (2H, d, J=6.6 Hz, $OCOCH_2$), 4.52 (8H, br s, $PhCH_2\times4$), 4.63 (2H, s, $OC\underline{H}_2OCH_2Ph$), 5.57—5.96 (1H, m, –CH=), 6.09 (1H, d, J=9.0 Hz, $NHCOCH_2$), 7.19, 7.25, 7.34 (30H, s, Ph×6). *Anal.* Calcd for $C_{94}H_{125}Cl_6N_2O_{21}P$: C, 60.61; H, 6.76; N, 1.50. Found: C, 60.61; H, 6.76; N, 1.29.

Allyl 4-*O*-Benzyl-6-*O*-[6-*O*-benzyloxymethyl-3-*O*-[(*R*)-3-benzyloxytetradecanoyl]-2-[(*R*)-3-benzyloxytetradecanoylamino]-2-deoxy-4-*O*-diphenylphosphono-β-D-glucopyranosyl]-2-deoxy-3-*O*-[(*R*)-3-benzyloxytetradecanoyl]-2-[(*R*)-3-benzyloxytetradecanoylamino]-β-D-glucopyranoside (17) Zinc powder (0.252 g, 3.9 mmol) was added to a stirred solution of **16** (0.120 g, 0.064 mmol) in AcOH (3.0 ml) and the mixture was stirred at room temperature for 12 h. After removal of the insoluble materials by filtration, the solvent was evaporated off *in vacuo*. The residue was again dissolved in CH_2Cl_2 (3.0 ml), and the solution was washed with saturated aqueous $NaHCO_3$, dried and concentrated. The residue was dissolved in dry CH_2Cl_2 (1.0 ml). To this solution, (*R*)-3-benzyloxytetradecanoic acid (0.048 g, 0.14 mmol) and DMAP (0.009 g, 0.07 mmol) were added, and then DCC (0.029 g, 0.14 mmol) was added at 0 °C and the whole was stirred for 5 h at the same temperature. After being stirring at room temperature for 12 h, the resulting suspension was filtered off and the filtrate was concentrated. The residue was dissolved in ethyl acetate (2.0 ml), the insoluble materials were filtered off, and the filtrate was evaporated *in vacuo*. After removal of the solvent, the residue was subjected to silica gel chromatography with $CHCl_3$–ether (10 : 1) to give **17** (0.070 g, 52%) as white prisms, mp 50—53 °C. $[\alpha]_D^{19}$ −1.67° (c=1.29, $CHCl_3$). IR (KBr): 3312 (NH), 1750, 1727 (ester), 1662 (amide), 1220 (P=O), 958 (P–O–Ph), 710, 697 cm^{-1} (Ph). ^{1}H-NMR ($CDCl_3$) δ: 0.88 (12H, t, J=5.6 Hz, $-(CH_2)_{10}C\underline{H}_3\times4$), 1.25 (80H, br s, $-(C\underline{H}_2)_{10}CH_3\times4$), 1.98—2.62 (8H, m, $COCH_2\times4$), 4.50 (12H, br s, $PhCH_2\times6$), 4.62 (2H, s, $OC\underline{H}_2OCH_2Ph$), 5.52—5.90 (1H, m, –CH=), 7.18, 7.25, 7.26, 7.32 (40H, s, Ph×8). *Anal.* Calcd for $C_{126}H_{179}N_2O_{21}P\cdot4H_2O$: C, 70.04; H, 8.72; N, 1.30. Found: C, 70.02; H, 8.53; N, 1.34.

2-Deoxy-2-(2,2,2-trichloro-*tert*-butoxycarbonylamino)-D-glucopyranose (18) A solution of TCBOC-Cl (21.6 g, 90.0 mmol) in ether (100 ml) was added portionwise to a stirred solution of D-glucosamine hydrochloride (19.4 g, 90.0 mmol) and $NaHCO_3$ (15.1 g, 180 mmol) in water (400 ml) at 0 °C for 1 h. The mixture was stirred for overnight at room temperature. The colorless precipitate was collected by filtration, and washed with ether to give **18** (29.8 g, 86.7%), mp 141—144 °C. $[\alpha]_D^{24}$ +37.0° (c=1.00, MeOH). *Anal.* Calcd for $C_{11}H_{18}Cl_3NO_7\cdot1/2H_2O$: C, 33.74; H, 4.89; N, 3.58. Found: C, 33.75; H, 5.02; N, 3.29.

Allyl 2-Deoxy-2-(2,2,2-trichloro-*tert*-butoxycarbonylamino)-α-D-gluco-

pyranoside (19) Compound **18** (23.2 g, 60.7 mmol) was heated with stirring at 100 °C in allyl alcohol (150 ml) containing 2% (w/v) dry HCl for 1.5 h. The mixture was cooled and the solvent was evaporated off *in vacuo*. The residue was chromatographed on silica gel with $CHCl_3$–MeOH (15 : 1) to give **5α** (15.8 g, 61.7%) and **5β** (1.86 g, 7.25%). **5α**: mp 143—146 °C. $[\alpha]_D^{25}$ +91.7° (c = 1.00, MeOH). IR (KBr): 3424 (NH, OH), 1743 (carbamate), 1640 cm^{-1} (allyl). ^{1}H-NMR (acetone-d_6) δ: 1.89 (6H, s, Cl_3CCMe_2), 4.89 (1H, d, J = 2.6 Hz, H-1), 5.02—5.54 (2H, m, =CH_2), 5.68—6.17 (1H, m, =CH–), 6.32 (1H, d, J = 6.9 Hz, NH). ^{13}C-NMR (acetone-d_6) δ: 21.9, 22.1 (q, CH_3), 55.7 (t, O$\underline{C}H_2$CH=), 88.3 (s, $Cl_3\underline{C}CMe_2$), 97.5 (d, C-1), 107.6 (s, $\underline{C}Cl_3$), 116.9 (t, =CH_2), 135.3 (d, =CH–), 155.6 (s, NHCO). *Anal.* Calcd for $C_{14}H_{22}Cl_3NO_7$: C, 39.78; H, 5.25; N, 3.31. Found: C, 39.91; H, 5.26; N, 3.20.

Allyl 2-Deoxy-4,6-*O*-isopropylidene-2-(2,2,2-trichloro-*tert*-butoxycarbonylamino)-α-D-glucopyranoside (20) 2,2-Dimethoxypropane (3.44 g, 33 mmol) and *p*-TsOH (0.48 g, 2.8 mmol) were added to a solution of compound **19** (4.67 g, 11.0 mmol) in DMF (50 ml) at room temperature. After 5 h, ethyl acetate–water (7 : 30) (925 ml) was added, and the mixture was neutralized by addition of 10% aqueous NaOH (25 ml). The organic layer was washed with brine, and dried over $MgSO_4$. After evaporation, the residue was chromatographed on silica gel with $CHCl_3$–acetone (15 : 1) to give **20** (4.17 g, 81.9%), mp 129—131 °C. $[\alpha]_D^{21}$ +63.9° (c = 1.34, $CHCl_3$). IR (KBr): 3480 (NH, OH), 1748 (carbamate), 1640 (allyl), 858 cm^{-1} (Me_2C). ^{1}H-NMR ($CDCl_3$) δ: 1.44, 1.52 (6H, s, Me_2C), 1.92 (6H, s, Cl_3CCMe_2), 4.88 (1H, d, J = 1.3 Hz, H-1), 5.11—5.44 (3H, m, =CH_2, H-3), 5.65—6.15 (1H, m, =CH–). ^{13}C-NMR ($CDCl_3$) δ: 19.2, 29.1 (q, Me_2C), 21.7 (q, $Cl_3CC\underline{Me}_2$), 55.6 (t, O$\underline{C}H_2$CH=), 88.6 (s, $NHCO_2\underline{C}$), 97.1 (d, C-1), 99.9 (s, $Me_2\underline{C}$), 106.4 (s, $NHCO_2C\underline{C}Cl_3$), 118.1 (t, =CH_2), 133.4 (d, =CH–), 154.4 (s, $NHCO_2$). *Anal.* Calcd for $C_{17}H_{26}Cl_3NO_7$: C, 44.12; H, 5.66; N, 3.03. Found: C, 44.37; H, 5.73; N, 2.88.

Allyl 2-Deoxy-4,6-*O*-isopropylidene-3-*O*-(2,2,2-trichloro-*tert*-butoxycarbonyl)-2-(2,2,2-trichloro-*tert*-butoxycarbonylamino)-α-D-glucopyranoside (21) A solution of TCBOC-Cl (9.0 g, 37.6 mmol) in dry CH_2Cl_2 (30 ml) was added to a stirred solution of **20** (11.6 g, 25.1 mmol) and DMAP (0.61 g, 5.0 mmol) in dry pyridine (60 ml) at 0 °C under nitrogen. The mixture was stirred for 12 h at room temperature, then the insoluble materials were filtered off and the filtrate was evaporated. The residue was chromatographed on silica gel with $CHCl_3$–IPE (20 : 1) to give **21** (15.7 g, 93.8%), mp 65—67 °C. $[\alpha]_D^{21}$ +50.4° (c = 1.01, $CHCl_3$). IR (KBr): 3360 (NH), 1760 (carbonate), 1740 (carbamate), 1655 (allyl), 859 cm^{-1} (Me_2C). ^{1}H-NMR ($CDCl_3$) δ: 1.40, 1.48 (6H, s, Me_2C), 1.89 (12H, s, Cl_3CCMe_2 × 2), 4.88 (1H, d, J = 3.6 Hz, H-1), 5.65—6.12 (1H, m, =CH–). ^{13}C-NMR ($CDCl_3$) δ: 19.1, 29.0 (q, Me_2C), 21.2, 21.6, 21.7 (q, $Cl_3CC\underline{Me}_2$), 54.1 (t, O$\underline{C}H_2$CH=), 88.5 (s, $NHCO_2\underline{C}$), 90.2 (s, $OCO_2\underline{C}$), 97.1 (d, C-1), 99.9 (s, $Me_2\underline{C}$), 105.5 (s, $OCO_2C\underline{C}Cl_3$), 106.3 (s, $NHCO_2C\underline{C}Cl_3$), 118.2 (t, =CH_2), 133.4 (d, =CH–), 152.4 (s, OCO_2), 153.4 (s, $NHCO_2$). *Anal.* Calcd for $C_{22}H_{31}Cl_6NO_9$: C, 39.66; H, 4.69; N, 2.10. Found: C, 39.64; H, 4.61; N, 2.05.

Allyl 2-Deoxy-3-*O*-(2,2,2-trichloro-*tert*-butoxycarbonyl)-2-(2,2,2-trichloro-*tert*-butoxycarbonylamino)-α-D-glucopyranoside (22) Compound **22** was obtained by a procedure similar to that described for **5**, and was recrystallized from IPE in 83% yield, mp 74—77 °C. $[\alpha]_D^{24}$ +55.3° (c = 1.00, $CHCl_3$). IR (KBr): 3440 br (NH, OH), 1757 (carbonate), 1740 (carbamate), 1650 cm^{-1} (allyl). ^{1}H-NMR ($CDCl_3$) δ: 1.89, 1.93 (12H, s, Cl_3CCMe_2 × 2), 4.91 (1H, d, J = 3.7 Hz, H-1), 5.12—5.44 (2H, m, =CH_2), 5.65—6.15 (1H, m, =CH–). ^{13}C-NMR ($CDCl_3$) δ: 21.3, 21.6, 21.7 (q, $Cl_3CC\underline{Me}_2$), 53.6 (t, O$\underline{C}H_2$CH=), 88.5 (s, $NHCO_2\underline{C}$), 90.5 (s, $OCO_2\underline{C}$), 96.7 (d, C-1), 105.4 (s, $OCO_2C\underline{C}Cl_3$), 106.3 (s, $NHCO_2C\underline{C}Cl_3$), 118.1 (t, =CH_2), 133.3 (d, =CH–), 152.8 (s, OCO_2), 153.4 (s, $NHCO_2$). *Anal.* Calcd for $C_{19}H_{27}Cl_6NO_9$: C, 36.45; H, 4.35; N, 2.24. Found: C, 35.99; H, 4.25; N, 2.13.

Allyl 6-*O*-Benzoyl-2-deoxy-3-*O*-(2,2,2-trichloro-*tert*-butoxycarbonyl)-2-(2,2,2-trichloro-*tert*-butoxycarbonylamino)-α-D-glucopyranoside (23) Compound **23** was obtained by a procedure similar to that described for **6**, and was chromatographed on silica gel with $CHCl_3$–IPE (10 : 1); 77% yield, mp 69—70 °C. $[\alpha]_D^{21}$ +52.0° (c = 1.01, $CHCl_3$). IR (KBr): 3440 (NH, OH), 1758 (carbonate), 1740 (carbamate), 1648 (allyl), 710 cm^{-1} (Ph). ^{1}H-NMR ($CDCl_3$) δ: 1.89, 1.93 (12H, s, Cl_3CCMe_2 × 2), 4.93 (1H, d, J = 3.4 Hz, H-1), 5.12—5.42 (2H, m, =CH_2), 5.67—6.14 (1H, m, =CH–), 7.32—8.11 (5H, m, PhCO). ^{13}C-NMR ($CDCl_3$) δ: 21.3, 21.6, 21.7 (q, $Cl_3CC\underline{Me}_2$), 53.7 (t, O$\underline{C}H_2$CH=), 88.9 (s, $NHCO_2\underline{C}$), 90.5 (s, $OCO_2\underline{C}$), 96.8 (d, C-1), 105.4 (s, $OCO_2C\underline{C}Cl_3$), 107.0 (s, $NHCO_2C\underline{C}Cl_3$), 118.2 (t, =CH_2), 128.5, 130.0 (d, Ph), 133.3 (d, =CH–), 152.9 (s, OCO_2), 153.5 (s, $NHCO_2$), 166.9 (s, OCOPh). *Anal.* Calcd for $C_{26}H_{31}Cl_6NO_{10}$: C, 42.76; H, 4.28; N, 1.92. Found: C, 42.31; H, 4.28; N, 1.94.

Allyl 6-*O*-Benzoyl-4-*O*-benzyl-2-deoxy-3-*O*-(2,2,2-trichloro-*tert*-butoxycarbonyl)-2-(2,2,2-trichloro-*tert*-butoxycarbonylamino)-α-D-glucopyranoside (24) Compound **24** was obtained by a procedure similar to that described for **7**, and was chromatographed on silica gel with $CHCl_3$–IPE (50 : 1); 83% yield, mp 50—51 °C. $[\alpha]_D^{19}$ +49.7° (c = 0.30, $CHCl_3$). IR (KBr): 3432 (NH), 1756 (carbonate), 1723 (carbamate), 1650 (allyl), 711, 697 cm^{-1} (Ph). ^{1}H-NMR ($CDCl_3$) δ: 1.90 (12H, s, Cl_3CCMe_2 × 2), 4.58, 4.78 (each 1H, d, J = 10.7 Hz, CH_2Ph), 4.92 (1H, d, J = 3.4 Hz, H-1), 5.65—6.13 (1H, m, =CH–), 7.25 (5H, s, $PhCH_2$), 7.30—8.08 (5H, m, PhCO). ^{13}C-NMR ($CDCl_3$) δ: 21.1, 21.6, 21.7 (q, $Cl_3CC\underline{Me}_2$), 53.8 (t, O$\underline{C}H_2$CH=), 88.5 (s, $NHCO_2\underline{C}$), 90.3 (s, $OCO_2\underline{C}$), 96.7 (d, C-1), 105.4 (s, $OCO_2C\underline{C}Cl_3$), 106.3 (s, $NHCO_2C\underline{C}Cl_3$), 118.2 (t, =CH_2), 128.1, 128.4, 129.6 (d, Ph), 133.1 (s, Ph), 133.1 (d, =CH–), 152.4 (s, OCO_2), 153.5 (s, $NHCO_2$), 166.0 (s, OCOPh). *Anal.* Calcd for $C_{33}H_{37}Cl_6NO_{10}$: C, 48.32; H, 4.55; N, 1.71. Found: C, 48.68; H, 5.10; N, 1.64.

Allyl 4-*O*-Benzyl-2-deoxy-3-*O*-(2,2,2-trichloro-*tert*-butoxycarbonyl)-2-(2,2,2-trichloro-*tert*-butyloxycarbonylamino)-α-D-glucopyranoside (25) Compound **25** was obtained by a procedure similar to that described for **8**, and was chromatographed on silica gel with $CHCl_3$–IPE (10 : 1); 57% yield, mp 41 °C. $[\alpha]_D^{21}$ +53.8° (c = 1.06, $CHCl_3$). IR (KBr): 3448 (NH, OH), 1758 (carbonate), 1740 (carbamate), 1650 (allyl), 715, 697 cm^{-1} (Ph). ^{1}H-NMR ($CDCl_3$) δ: 1.90 (12H, s, Cl_3CCMe_2 × 2), 4.69, 4.72 (each 1H, d, J = 10.7 Hz, CH_2Ph), 4.90 (1H, d, J = 3.4 Hz, H-1), 5.65—6.12 (1H, m, =CH–), 7.31 (5H, s, $PhCH_2$). ^{13}C-NMR ($CDCl_3$) δ: 21.1, 21.6 (q, $Cl_3CC\underline{Me}_2$), 53.9 (t, O$\underline{C}H_2$CH=), 88.4 (s, $NHCO_2\underline{C}$), 90.3 (s, $OCO_2\underline{C}$), 96.6 (d, C-1), 105.4 (s, $OCO_2C\underline{C}Cl_3$), 106.3 (s, $NHCO_2C\underline{C}Cl_3$), 118.0 (t, =CH_2), 127.5, 128.5 (d, Ph), 133.2 (d, =CH–), 137.5 (s, Ph), 152.5 (s, OCO_2), 153.6 (s, $NHCO_2$). *Anal.* Calcd for $C_{26}H_{33}Cl_6NO_9$: C, 43.60; H, 4.64; N, 1.94. Found: C, 43.39; H, 4.66; N, 1.99.

Allyl 4-*O*-Benzyl-6-*O*-(3,4,6-tri-*O*-acetyl-2-chloroacetylamino-2-deoxy-β-D-glucopyranosyl)-2-deoxy-3-*O*-(2,2,2-trichloro-*tert*-butoxycarbonyl)-2-(2,2,2-trichloro-*tert*-butoxycarbonylamino)-α-D-glucopyranoside (26) Compound **26** was obtained by a procedure similar to that described for **10**, and was chromatographed on silica gel with $CHCl_3$–acetone (20 : 1); 80% yield, mp 102—104 °C. $[\alpha]_D^{20}$ +32.8° (c = 1.41, $CHCl_3$). IR (KBr): 3444 (NH), 1753 (carbonyl), 1690 (amide), 696 cm^{-1} (Ph). ^{1}H-NMR ($CDCl_3$) δ: 1.89 (12H, s, Cl_3CCMe_2 × 2), 2.04, 2.05 (9H, s, CH_3CO × 3), 3.92 (2H, s, $NCOCH_2Cl$), 4.61, 4.67 (each 1H, d, J = 11.7 Hz, CH_2Ph), 5.65—6.12 (1H, m, =CH–), 6.71 (1H, d, J = 8.3 Hz, $NHCOCH_2Cl$), 7.35 (5H, s, $PhCH_2$). ^{13}C-NMR ($CDCl_3$) δ: 20.6 (q, CH_3CO), 21.1, 21.5, 21.6 (q, $Cl_3CC\underline{Me}_2$), 42.4 (t, $ClCH_2CO$), 53.5 (t, O$\underline{C}H_2$CH=), 88.4 (s, $NHCO_2\underline{C}$), 90.2 (s, $OCO_2\underline{C}$), 96.4 (d, C-1), 100.2 (C-1′), 105.3 (s, $OCO_2C\underline{C}Cl_3$), 106.3 (s, $NHCO_2C\underline{C}Cl_3$), 118.0 (t, =CH_2), 127.7, 128.0, 128.5 (d, Ph), 133.2 (d, =CH–), 137.5 (s, Ph), 152.3 (s, OCO_2), 153.3 (s, $NHCO_2$), 166.3 (s, $NH\underline{C}OCH_2Cl$), 169.3, 170.6 (s, CH_3CO). *Anal.* Calcd for $C_{40}H_{51}Cl_7N_2O_{17}$: C, 44.48; H, 4.76; N, 2.59. Found: C, 44.40; H, 4.57; N, 2.59.

Allyl 4-*O*-Benzyl-6-*O*-(2-chloroacetylamino-2-deoxy-β-D-glucopyranosyl)-2-deoxy-3-*O*-(2,2,2-trichloro-*tert*-butoxycarbonyl)-2-(2,2,2-trichloro-*tert*-butoxycarbonylamino)-α-D-glucopyranoside (27) Compound **27** was obtained by a procedure similar to that described for **11**, and was chromatographed on silica gel with $CHCl_3$–MeOH (10 : 1); 76% yield, mp 153—154 °C. $[\alpha]_D^{27}$ +31.6° (c = 1.00, $CHCl_3$). IR (KBr): 3440 br (NH, OH), 1757, 1734 (carbonyl), 1677 (amide), 696 cm^{-1} (Ph). ^{1}H-NMR (acetone-d_6) δ: 1.89 (12H, s, Cl_3CCMe_2 × 2), 4.06 (2H, s, $NCOCH_2Cl$), 4.71 (2H, s, CH_2Ph), 5.74—6.11 (1H, m, =CH–), 6.21 (1H, d, J = 10.1 Hz, $NHCOCH_2Cl$), 7.32 (5H, s, $PhCH_2$). ^{13}C-NMR (acetone-d_6) δ: 21.4, 21.9, 22.0 (q, $Cl_3CC\underline{Me}_2$), 43.5 (t, $ClCH_2CO$), 54.5 (t, O$\underline{C}H_2$CH=), 88.6 (s, $NHCO_2\underline{C}$), 90.5 (s, $OCO_2\underline{C}$), 97.4 (d, C-1), 101.9 (C-1′), 106.4 (s, $OCO_2C\underline{C}Cl_3$), 107.3 (s, $NHCO_2C\underline{C}Cl_3$), 117.4 (t, =CH_2), 126.8, 129.0 (d, Ph), 134.9 (d, =CH–), 139.2 (s, Ph), 153.1 (s, OCO_2), 154.5 (s, $NHCO_2$), 167.2 (s, $NH\underline{C}OCH_2Cl$). *Anal.* Calcd for $C_{34}H_{45}Cl_7N_2O_{14}\cdot 1/2H_2O$: C, 42.41; H, 4.81; N, 2.91. Found: C, 42.32; H, 4.68; N, 3.03.

Allyl 4-*O*-Benzyl-6-*O*-(2-chloroacetylamino-2-deoxy-4,6-*O*-isopropylidene-β-D-glucopyranosyl)-2-deoxy-3-*O*-(2,2,2-trichloro-*tert*-butoxycarbonyl)-2-(2,2,2-trichloro-*tert*-butoxycarbonylamino)-α-D-glucopyranoside (28) Compound **28** was obtained by a procedure similar to that described for **12**, and was chromatographed on silica gel with $CHCl_3$–acetone (10 : 1); 69% yield, mp 117—118 °C. $[\alpha]_D^{20}$ +17.7° (c = 0.550, $CHCl_3$). IR (KBr): 3480 (NH, OH), 1756, 1729 (carbonyl), 1669 (amide), 855 (Me_2C), 696 cm^{-1} (Ph). ^{1}H-NMR ($CDCl_3$) δ: 1.44, 1.52 (each 3H, s, Me_2C), 1.85, 1.88 (12H, s, Cl_3CCMe_2 × 2), 3.98 (2H, s, $NCOCH_2Cl$), 4.61, 4.68 (each 1H, d, J = 10.7 Hz, CH_2Ph), 4.89 (1H, d, J = 3.7 Hz, H-1), 5.64—6.13 (1H, m, =CH–), 6.89 (1H, d, J = 7.1 Hz, $NHCOCH_2Cl$), 7.30 (5H, s, $PhCH_2$).

^{13}C-NMR ($CDCl_3$) δ: 19.1, 29.0 (q, $\underline{Me}_2C$), 21.6, 22.2 (q, $Cl_3C\underline{Me}_2$), 42.6 (t, $Cl\underline{C}H_2CO$), 53.7 (t, $O\underline{C}H_2CH=$), 88.5 (s, $NHCO_2\underline{C}$), 90.3 (s, $OCO_2\underline{C}$), 97.0 (d, C-1), 99.9 (s, $Me_2\underline{C}$), 100.6 (d, C-1′), 105.4 (s, $OCO_2C\underline{C}Cl_3$), 106.4 (s, $NHCO_2C\underline{C}Cl_3$), 128.0, 128.5 (d, Ph), 137.6 (s, Ph), 152.4 (s, OCO_2), 153.4 (s, $NHCO_2$), 167.0 (s, $NHCOCH_2Cl$). *Anal.* Calcd for $C_{37}H_{49}Cl_7N_2O_{14}$: C, 44.71; H, 4.97; N, 2.82. Found: C, 44.60; H, 4.91; N, 2.76.

Allyl 4-*O*-Benzyl-6-*O*-(2-amino-2-deoxy-4,6-*O*-isopropylidene-β-D-glucopyranosyl)-2-deoxy-3-*O*-(2,2,2-trichloro-*tert*-butoxycarbonyl)-2-(2,2,2-trichloro-*tert*-butoxycarbonylamino)-α-D-glucopyranoside (2b) Compound **2b** was obtained by a procedure similar to that described for **2a**, and was chromatographed on silica gel with $CHCl_3$–MeOH (40:1); 95% yield, mp 88—89 °C. $[\alpha]_D^{20}$ +23.1° (c=0.308, $CHCl_3$). IR (KBr): 3424, 3384 (NH, OH), 1757 (carbonate), 1734 (carbamate), 853 (Me_2C), 696 cm^{-1} (Ph). ^{1}H-NMR ($CDCl_3$) δ: 1.43, 1.49 (each 3H, s, Me_2C), 1.85, 1.89 (12H, s, $Cl_3CCMe_2\times2$), 4.68, 4.72 (each 1H, d, J=11.0 Hz, CH_2Ph), 4.91 (1H, d, J=3.6 Hz, H-1), 5.66—6.13 (1H, m, =CH–), 7.30 (5H, s, $PhCH_2$). ^{13}C-NMR ($CDCl_3$) δ: 19.1, 29.0 (q, $\underline{Me}_2C$), 21.1, 21.6 (q, $Cl_3CC\underline{Me}_2$), 53.6 (t, $O\underline{C}H_2CH=$), 88.4 (s, $NHCO_2\underline{C}$), 90.2 (s, $OCO_2\underline{C}$), 96.6 (d, C-1), 99.8 (s, $Me_2\underline{C}$), 104.8 (d, C-1′), 105.3 (s, $OCO_2C\underline{C}Cl_3$), 127.7, 128.0, 128.5 (d, Ph), 133.2 (d, =CH), 137.6 (s, Ph), 152.4 (s, OCO_2), 153.4 (s, $NHCO_2$). *Anal.* Calcd for $C_{35}H_{48}Cl_6N_2O_{13}$: C, 45.82; H, 5.27; N, 3.05. Found: C, 45.25; H, 5.08; N, 2.92.

Allyl 4-*O*-Benzyl-2-deoxy-6-*O*-[2-deoxy-4,6-*O*-isopropylidene-3-*O*-[(*R*)-3-tetradecanoyloxytetradecanoyl]-2-[(*R*)-3-tetradecanoyloxytetradecanoylamino]-β-D-glucopyranosyl]-3-*O*-(2,2,2-trichloro-*tert*-butoxycarbonyl)-2-(2,2,2-trichloro-*tert*-butoxycarbonylamino)-α-D-glucopyranoside (29) DCC (0.155 g, 0.75 mmol) was added to a stirred solution of **2b** (0.223 g, 0.25 mmol), (*R*)-3-tetradecanoyloxytetradecanoic acid (0.341 g, 0.75 mmol) and DMAP (0.031 g, 0.25 mmol) in dry CH_2Cl_2 (5.0 ml) at 0 °C under nitrogen. The mixture was stirred for 4 h at 0 °C, then at room temperature for 12 h. The resulting suspension was filtered through Celite and evaporated. The residue was chromatographed on silica gel with $CHCl_3$–IPE (50:1) to give **29** (0.32 g, 73%), mp 132—134 °C. $[\alpha]_D^{19}$ +11.8° (c=1.41, $CHCl_3$). IR (KBr): 3392, 3300 (NH), 1759 (carbonate), 1743 (ester), 1721 (carbamate), 1655 (amide), 857 (acetonide), 751, 698 cm^{-1} (Ph). ^{1}H-NMR ($CDCl_3$) δ: 0.87 (12H, t, J=5.4 Hz, $(CH_2)_n\underline{CH}_3\times4$), 1.25 (88H, br s, $(CH_2)_n$), 1.35, 1.44 (each 3H, s, Me_2C), 1.84, 1.88 (each 6H, s, Cl_3CCMe_2), 2.15—2.40 (6H, m, $OCOCH_2$), 4.67, 4.71 (each 1H, d, J=10.6 Hz, CH_2Ph), 4.87 (1H, d, J=3.7 Hz, H-1), 5.01—5.40 (3H, m, $=CH_2$, H-1′), 5.56—6.15 (2H, m, =CH–, NH), 7.29 (5H, s, Ph). *Anal.* Calcd for $C_{91}H_{152}Cl_6N_2O_{19}$: C, 59.83; H, 8.61; N, 1.53. Found: C, 59.41; H, 8.10; N, 1.64.

Allyl 4-*O*-Benzyl-2-deoxy-6-*O*-[2-deoxy-3-*O*-[(*R*)-3-tetradecanoyloxytetradecanoyl]-2-[(*R*)-3-tetradecanoyloxytetradecanoylamino]-β-D-glucopyranosyl]-3-*O*-(2,2,2-trichloro-*tert*-butoxycarbonyl)-2-(2,2,2-trichloro-*tert*-butoxycarbonylamino)-α-D-glucopyranoside (30) A solution of **29** (0.32 g, 0.18 mmol) in 90% aqueous AcOH (40 ml) was heated at 85—90 °C for 15 min. After removal of the solvent, the residue was chromatographed on silica gel with $CHCl_3$–acetone (20:1) to give **30** (0.23 g, 75%), mp 88—90 °C. $[\alpha]_D^{20}$ +15.1° (c=0.68, $CHCl_3$) IR (KBr): 3296 (NH, OH), 1759 (carbonate), 1736 (ester), 1719 (carbamate), 1653 (amide), 751, 698 cm^{-1} (Ph). ^{1}H-NMR ($CDCl_3$) δ: 0.88 (12H, t, J=5.4 Hz, $(CH_2)_n\underline{CH}_3\times4$), 1.26 (88H, br s, $(CH_2)_n$), 1.86, 1.89 (each 6H, s, Cl_3CCMe_2), 2.16—2.50 (6H, m, $OCOCH_2$), 2.50—2.63 (2H, m, $NHCOCH_2$), 4.70, 4.72 (each 1H, d, J=11.0 Hz, CH_2Ph), 4.88 (1H, d, J=3.4 Hz, H-1), 4.81—5.42 (3H, m, $=CH_2$, H-1′), 5.60—6.16 (2H, m, =CH–, NH), 7.30 (5H, s, Ph). *Anal.* Calcd for $C_{88}H_{148}Cl_6N_2O_{19}$: C, 60.37; H, 8.52; N, 1.60. Found: C, 60.46; H, 8.42; N, 1.78.

Allyl 4-*O*-Benzyl-6-*O*-[6-*O*-benzyloxymethyl-2-deoxy-3-*O*-[(*R*)-3-tetradecanoyloxytetradecanoyl]-2-[(*R*)-3-tetradecanoyloxytetradecanoylamino]-β-D-glucopyranosyl]-2-deoxy-3-*O*-(2,2,2-trichloro-*tert*-butoxycarbonyl)-2-(2,2,2-trichloro-*tert*-butoxycarbonylamino)-α-D-glucopyranoside (31) Benzyloxymethyl chloride (0.454 g, 2.90 mmol) was added to a stirred solution of **30** (2.50 g, 1.45 mmol) and TMU (0.337 g, 2.90 mmol) in dry CH_2Cl_2 (30 ml) at 0 °C under nitrogen. After 20 h at room temperature, the reaction mixture was successively washed with saturated aqueous $NaHCO_3$ and brine, and dried over anhydrous $MgSO_4$. After removal of the solvent, the residue was chromatographed on silica gel with $CHCl_3$–ether (20:1) to give **31** (1.67 g, 62.5%), mp 94—96 °C. $[\alpha]_D^{20}$ +14.6° (c=1.28, $CHCl_3$). IR (KBr): 3376, 3280 (NH, OH), 1759 (carbonate), 1739 (ester), 1718 (carbamate), 1652 (amide), 740, 696 cm^{-1} (Ph). ^{1}H-NMR ($CDCl_3$) δ: 0.88 (12H, t, J=5.6 Hz, $(CH_2)_n\underline{CH}_3\times4$), 1.26 (88H, br s, $(CH_2)_n$), 1.84, 1.88 (each 6H, s, Cl_3CCMe_2), 2.21—2.37 (6H, m, $OCOCH_2$), 2.51—2.64 (2H, m, $NHCOCH_2$), 4.59—4.87 (7H, m, H-1, CH_2Ph at 4-*O*-position, CH_2OCH_2Ph at 6′-*O*-position), 4.93—5.41 (3H, m, $=CH_2$, H-1′), 5.62—6.13 (2H, m, =CH–, NH), 7.28, 7.32 (10H, s, Ph). *Anal.* Calcd for $C_{96}H_{154}Cl_6N_2O_{19}$: C, 61.63; H, 8.40; N, 1.50. Found: C, 61.56; H, 8.34; N, 1.56.

Allyl 4-*O*-Benzyl-6-*O*-[6-*O*-benzyloxymethyl-2-deoxy-4-*O*-diphenylphosphono-3-*O*-[(*R*)-3-tetradecanoyloxytetradecanoyl]-2-[(*R*)-3-tetradecanoyloxytetradecanoylamino]-β-D-glucopyranosyl]-2-deoxy-3-*O*-(2,2,2-trichloro-*tert*-butoxycarbonyl)-2-(2,2,2-trichloro-*tert*-butoxycarbonylamino)-α-D-glucopyranoside (32) Diphenylphosphorochloridate (1.26 g, 4.5 mmol) was added to a stirred solution of **31** (1.66 g, 0.90 mmol), pyridine (0.356 g, 4.5 mmol) and DMAP (0.55 g, 4.5 mmol) at 0 °C under nitrogen, and then the mixture was stirred for 12 h at room temperature. The reaction mixture was washed with saturated aqueous $NaHCO_3$ and brine, dried over anhydrous $MgSO_4$, and evaporated. The residue was chromatographed on silica gel with $CHCl_3$–IPE (20:1) to give **32** (1.42 g, 76%), syrup. $[\alpha]_D^{20}$ +20.8° (c=0.74, $CHCl_3$). IR (KBr): 3356 (NH), 1758 (carbonate), 1745 (ester, carbamate), 1652 (amide), 1270 (P=O), 962 (P–O–Ph), 690 cm^{-1} (Ph). ^{1}H-NMR ($CDCl_3$) δ: 0.88 (12H, t, J=5.5 Hz, $(CH_2)_n\underline{CH}_3\times4$), 1.25 (88H, br s, $(CH_2)_n$), 1.88 (12H, br s, Cl_3CCMe_2), 2.07—2.68 (8H, m, $OCOCH_2$, $NHCOCH_2$), 4.46—4.77 (6H, m, CH_2Ph at 4-*O*-position, CH_2OCH_2Ph at 6′-*O*-position), 4.85 (1H, d, J=3.7 Hz, H-1), 4.93—5.38 (3H, m, $=CH_2$, H-1′), 5.51—6.06 (2H, m, =CH–, NH), 6.39 (1H, br d, J=7.3 Hz, NH), 7.06—7.36 (20H, m, Ph). *Anal.* Calcd for $C_{108}H_{163}Cl_6N_2O_{22}P$: C, 62.21; H, 7.88; N, 1.34. Found: C, 61.92; H, 8.02; N, 1.50.

Allyl 4-*O*-Benzyl-6-*O*-[6-*O*-benzyloxymethyl-2-deoxy-4-*O*-diphenylphosphono-3-*O*-[(*R*)-3-tetradecanoyloxytetradecanoyl]-2-[(*R*)-3-tetradecanoyloxytetradecanoylamino]-β-D-glucopyranosyl]-2-deoxy-α-D-glucopyranoside (33) Zinc powder (0.44 g, 6.8 mmol) was added to a stirred solution of **32** (1.42 g, 0.68 mmol) in AcOH (25 ml) and the mixture was stirred at room temperature for 12 h. After removal of the insoluble materials by filtration, the solvent was evaporated off *in vacuo*. The residue was again dissolved in CH_2Cl_2 (30 ml), and the solution was washed with saturated aqueous $NaHCO_3$ and brine, and dried over anhydrous $MgSO_4$. After removal of the solvent, the residue was chromatographed on silica gel with $CHCl_3$–MeOH (20:1) to give **33** (1.01 g, 88.5%) as a syrup. $[\alpha]_D^{23}$ +22.9° (c=0.68, $CHCl_3$). ^{1}H-NMR ($CDCl_3$) δ: 0.87 (12H, t, J=5.7 Hz, $(CH_2)_n\underline{CH}_3\times4$), 1.25 (88H, br s, $(CH_2)_n$), 2.11—2.47 (8H, m, $OCOCH_2$, $NHCOCH_2$), 4.42—4.86 (6H, m, CH_2Ph at 4-*O*-position, CH_2OCH_2Ph at 6′-*O*-position), 4.94—5.24 (3H, m, $=CH_2$, H-1′), 5.38—6.04 (1H, m, =CH–), 6.14 (1H, br d, J=7.8 Hz, NH), 6.99—7.44 (20H, m, Ph).

Allyl 4-*O*-Benzyl-6-*O*-[6-*O*-benzyloxymethyl-2-deoxy-4-*O*-diphenylphosphono-3-*O*-[(*R*)-3-tetradecanoyloxytetradecanoyl]-2-[(*R*)-3-tetradecanoyloxytetradecanoylamino]-β-D-glucopyranosyl]-2-deoxy-2-[(*R*)-3-hexadecanoyloxytetradecanoylamino]-α-D-glucopyranoside (34) DCC (0.240 g, 1.14 mmol) was added to a stirred solution of **33** (0.96 g, 0.57 mmol) and (*R*)-3-hexadecanoyloxytetradecanoic acid (0.55 g, 1.14 mmol) in dry CH_2Cl_2 (30 ml) at 0 °C under nitrogen. The mixture was stirred for 4 h at 0 °C, then at room temperature for 12 h. The resulting suspension was filtered through Celite and the filtrate was evaporated *in vacuo*. The residue was chromatographed on silica gel with $CHCl_3$–acetone (20:1) to give **34** (0.83 g, 67%), mp 53—55 °C. $[\alpha]_D^{23}$ +15.0° (c=0.57, $CHCl_3$). IR (KBr): 3428, 3420 (NH, OH), 1735 (ester), 1665 (amide), 1289 (P=O), 954 (P–O–Ph), 750, 730, 690 cm^{-1} (Ph). ^{1}H-NMR ($CDCl_3$) δ: 0.88 (18H, t, J=5.7 Hz, $(CH_2)_n\underline{CH}_3\times4$), 1.25 (136H, br s, $(CH_2)_n$), 2.07—2.52 (12H, m, $OCOCH_2$, $NHCOCH_2$), 4.46—4.86 (6H, m, CH_2Ph at 4-*O*-position, CH_2OCH_2Ph at 6′-*O*-position), 4.89—5.27 (3H, m, $=CH_2$, H-1′), 5.39—6.11 (1H, m, =CH–), 6.18 (1H, br d, J=7.1 Hz, NH), 7.06—7.39 (20H, m, Ph). *Anal.* Calcd for $C_{128}H_{211}N_2O_{22}P$: C, 70.55; H, 9.85; N, 1.29. Found: C, 70.12; H, 9.74; N, 1.51.

Allyl 4-*O*-Benzyl-6-*O*-[6-*O*-benzyloxymethyl-2-deoxy-4-*O*-diphenylphosphono-3-*O*-[(*R*)-3-tetradecanoyloxytetradecanoyl]-2-[(*R*)-3-tetradecanoyloxytetradecanoylamino]-β-D-glucopyranosyl]-2-deoxy-3-*O*-[(*R*)-3-benzyloxytetradecanoyl]-2-[(*R*)-3-hexadecanoyloxytetradecanoylamino]-α-D-glucopyranoside (35) DCC (0.16 g, 0.76 mmol) was added to a stirred solution of **34** (0.83 g, 0.38 mmol), (*R*)-3-benzyloxytetradecanoic acid (0.25 g, 0.76 mmol), DMAP (0.023 g, 0.19 mmol) in dry CH_2Cl_2 (25 ml) at 0 °C under nitrogen. The mixture was stirred for 5 h at 0 °C, then at room temperature for 12 h. The resulting suspension was filtered through Celite and the filtrate was evaporated off *in vacuo*. The residue was chromatographed on silica gel with $CHCl_3$–acetone (40:1) to give **35** (0.72 g, 77%), mp 48—49 °C. $[\alpha]_D^{23}$ +18.9° (c=2.18, $CHCl_3$). IR (KBr): 3316 (NH), 1738 (ester), 1664 (amide), 1291 (P=O), 958 (P–O–Ph), 731, 639 cm^{-1} (Ph). ^{1}H-NMR ($CDCl_3$) δ: 0.88 (21H, t, J=6.8 Hz, $(CH_2)_n$-$\underline{CH}_3\times7$), 1.25 (156H, br s, $(CH_2)_n$), 1.97—2.53 (14H, m, $OCOCH_2\times5$,

$NHCOCH_2 \times 2$), 4.46—4.89 (8H, m, CH_2Ph at 4-*O*-position, CH_2Ph at 3′-*O*-position, CH_2OCH_2Ph at 6′-*O*-position), 5.10—5.29 (3H, m, $=CH_2$, H-1′), 5.38—6.02 (1H, m, =CH–), 6.32 (1H, br d, $J=7.3$ Hz, NH), 6.97—7.41 (25H, m, Ph). ^{13}C-NMR ($CDCl_3$) δ: 94.8 (t, $-OCH_2O-$), 96.3 (d, C-1), 100.0 (d, C-1′). *Anal.* Calcd for $C_{149}H_{243}N_2O_{24}P$: C, 72.23; H, 9.89; N, 1.13. Found: C, 71.78; H, 9.69; N, 1.20.

4-*O*-Benzyl-6-*O*-[6-*O*-benzyloxymethyl-2-deoxy-4-*O*-diphenylphosphono-3-*O*-[(*R*)-3-tetradecanoyloxytetradecanoyl]-2-[(*R*)-3-tetradecanoyloxytetradecanoylamino]-β-D-glucopyranosyl]-2-deoxy-3-*O*-[(*R*)-3-benzyloxytetradecanoyl]-2-[(*R*)-3-hexadecanoyloxytetradecanoylamino]-α-D-glucopyranose (36) Bis(methyldiphenylphosphine)cycloocta-1,5-diene iridium(I) hexafluorophosphate $[C_8H_{12}Ir(PMePh_2)_2]PF_4$ (3.8 mg, 4.5×10^{-6} mol) was added to a stirred solution of **35** (0.224 g, 9.0×10^{-5} mol) in peroxide-free THF (8.0 ml) (freshly distilled from sodium-benzophenone). The stirred solution was degassed, placed under dry and oxygen-free nitrogen, and degassed once more. The catalyst was activated by hydrogen, during which operation the slightlly red suspension became colorless. To effect isomerization, the solution was degassed once more, placed under dry and oxygen-free nitrogen and heated at 50 °C for 2 h. To this solution, water (0.8 ml) and then iodine (46 mg, 1.8×10^{-4} mol) and pyridine (28 mg, 3.6×10^{-4} mol) were added, and the mixture was stirred at room temperature for 15 min. After removal of the solvent, the residue was chromatographed on silica gel with $CHCl_3$–acetone (20 : 1) to give **36** (190 mg, 87%) as a syrup. $[\alpha]_D^{22}$ +12.6° ($c=0.89$, $CHCl_3$). ^{1}H-NMR ($CDCl_3$) δ: 1.25 (156H, br s, $(CH_2)_n$), 2.06—2.61 (14H, m, $OCOCH_2 \times 5$, $NHCOCH_2 \times 2$), 4.47—4.82 (8H, m, CH_2Ph at 4-*O*-position, CH_2Ph at 3′-*O*-position, CH_2OCH_2Ph at 6′-*O*-position), 5.96 (1H, br d, $J=8.1$ Hz, NH), 6.50 (1H, br d, $J=6.8$ Hz, NH), 7.11—7.36 (25H, m, Ph). ^{13}C-NMR ($CDCl_3$) δ: 91.3 (d, C-1), 94.9 (t, $-OCH_2O-$), 99.0 (d, C-1′).

***Proteus mirabilis* Lipid A (1e)** *n*-BuLi (1.6 mol in *n*-hexane) (0.654 ml, 8.7×10^{-5} mol) was added to a stirred solution of **36** (180 mg, 8.7×10^{-5} mol) in dry THF (6.0 ml) at −70 °C under dry nitrogen. After 3 min, dibenzylphosphorochloridate (32 mg, 1.13×10^{-4} mol) in dry THF (0.5 ml) was added and the mixture was stirred for a further 10 min. The whole mixture was immediately subjected to hydrogenolysis over Pd-black (100 mg) at 40—45 °C under slight pressure for 20 h, the reaction being monitored by TLC developed with $CHCl_3$–MeOH (10 : 1). The catalyst was filtered off and Adams' platinum catalyst (50 mg) was added to the filtrate. Hydrogenolysis was continued at 40—45 °C for 20 h, when TLC with $CHCl_3$–MeOH–H_2O–Et_3N (20 : 5 : 1 : 0.05) showed the reaction to be complete. The catalyst was filtered off and the filtrate was concentrated to dryness. The residue was purified on a column (10 ml) of silica gel with $CHCl_3$–MeOH–H_2O–Et_3N (20 : 5 : 1 : 0.05) followed by treatment with aqueous 0.1 N HCl at 0 °C, then lyophilization from dioxane to give the desired compound (**1e**), mp 60—62 °C. $[\alpha]_D^{23}$ +3.64° ($c=0.22$, $CHCl_3$). *Anal.* Calcd for $C_{112}H_{212}N_2O_{26}P$: C, 65.15; H, 10.35; N, 1.36. Found: C, 64.96; H, 9.98; N, 1.52. Positive ion FAB-mass spectrometry (triethanol amine, m/z 2164.7 $(M+H+NEt_3)^+$, m/z 2186.8 $(M+NEt_3+Na)^+$.

Allyl 2-Deoxy-4,6-*O*-isopropylidene-3-*O*-(2,2,2-trichloro-*tert*-butoxycarbonyl)-2-*O*-(2,2,2-trichloroethoxycarbonylamino)-α-D-glucopyranoside (40) Compound **40** was prepared from **39**[5] by a procedure similar to that described for **4**, and was chromatographed on silica gel with $CHCl_3$–IPE (20 : 1); 97.3% yield, mp 168—170 °C. $[\alpha]_D^{20}$ +62.2° ($c=0.99$, $CHCl_3$). IR (KBr): 3456 (NH), 1750 (carbonate), 1739 (carbamate), 1654 (allyl), 864 (Me_2C). ^{1}H-NMR ($CDCl_3$) δ: 1.40, 1.49 (6H, s, Me_2C), 1.91 (6H, s, Cl_3CCMe_2), 4.71 (2H, s, Cl_3CCH_2), 4.90 (1H, d, $J=3.7$ Hz, H-1), 5.19—5.38 (2H, m, $=CH_2$), 5.66—6.15 (1H, m, =CH). ^{13}C-NMR ($CDCl_3$) δ: 19.07, 28.99 (q, $\underline{Me}_2C$), 21.18 (q, $Cl_3CC\underline{Me}_2$), 54.51 (t, $O\underline{C}H_2CH=$), 90.27 (s, OCO_2C), 97.04 (d, C-1), 99.91 (s, $Me_2\underline{C}$), 108.02 (s, $OCO_2CC(Me)_2\underline{C}Cl_3$), 118.33 (t, $=CH_2$), 133.01 (d, =CH), 152.36 (s, OCO_2), 155.03 (s, $NHCO_2$). *Anal.* Calcd for $C_{20}H_{27}Cl_6NO_9$: C, 37.68; H, 4.26; N, 2.19. Found: C, 37.80; H, 4.05; N, 2.15.

Allyl 2-Deoxy-3-*O*-(2,2,2-trichloro-*tert*-butoxycarbonyl)-2-(2,2,2-trichloroethoxycarbonylamino)-α-D-glucopyranoside (41) Compound **41** was obtained by a procedure similar to that described for **5** and was chromatographed on silica gel with $CHCl_3$–acetone (10 : 1); 97.0% yield, mp 196—198 °C. $[\alpha]_D^{20}$ +57.4° ($c=1.00$, $CHCl_3$). IR (KBr): 3448 (OH), 3364 (NH), 1759 (carbonate), 1737 (carbamate), 1650 cm^{-1} (allyl). ^{1}H-NMR ($CDCl_3$) δ: 1.93 (6H, s, Cl_3CCMe_2), 4.69 (2H, s, Cl_3CCH_2), 4.92 (1H, d, $J=3.4$ Hz, H-1), 5.15—5.41 (2H, m, $=CH_2$), 5.75—6.17 (1H, m, =CH). ^{13}C-NMR ($CDCl_3$) δ: 21.40 (q, $Cl_3CC\underline{Me}_2$), 54.83 (t, $O\underline{C}H_2CH=$), 90.64 (s, $OCO_2\underline{C}$), 97.09 (d, C-1), 110.75 (s, $OCO_2CC(Me)_2\underline{C}Cl_3$), 118.01 (t, $=CH_2$), 134.15 (d, =CH), 155.38 (s, OCO_2), 155.50 (s, $NHCO_2$). *Anal.* Calcd for $C_{17}H_{23}Cl_6NO_9$: C, 34.14; H, 3.88; N, 2.34. Found: C, 33.60; H, 3.73; N, 2.22.

Allyl 2-Deoxy-6-*O*-(*p*-nitrobenzoyl)-3-*O*-(2,2,2-trichloro-*tert*-butoxycarbonyl)-2-(2,2,2-trichloroethoxycarbonylamino)-α-D-glucopyranoside (42) A solution of *p*-nitrobenzoyl chloride (5.57 g, 30 mmol) in CH_2Cl_2 (20 ml) was added to an ice-cooled solution of **41** (12.0 g, 20 mmol) and pyridine (4.75 g, 60 mmol) in CH_2Cl_2 (200 ml). The mixture was stirred at 0 °C for 1 h. The brine (50 ml) was added and the mixture was stirred at room temperature. The organic layer was dried over anhydrous $MgSO_4$. After removal of the solvent, the residue was chromatographed on silica gel with $CHCl_3$–acetone (20 : 1) to give **42** (13.99 g, 93.6%), mp 121—123 °C. $[\alpha]_D^{20}$ +47.2° ($c=1.00$, $CHCl_3$). IR (KBr): 3532 (OH), 3452 (NH), 1757 (carbonate), 1744 (carbamate), 1719 (ester), 1655 (allyl), 717 cm^{-1} (Ph). ^{1}H-NMR ($CDCl_3$) δ: 1.91 (6H, s, Cl_3CCMe_2), 4.69 (2H, s, Cl_3CCH_2), 4.95 (1H, d, $J=3.9$ Hz, H-1), 5.19—5.44 (2H, m, $=CH_2$), 5.69—6.18 (1H, m, =CH), 8.15—8.39 (4H, m, Ph). ^{13}C-NMR ($CDCl_3$) δ: 21.29 (q, $Cl_3CC\underline{Me}_2$), 54.13 (t, $O\underline{C}H_2CH=$), 90.64 (s, $OCO_2\underline{C}$), 96.60 (d, C-1), 105.27 (s, CCl_3), 118.44 (t, $=CH_2$), 123.64 (d, *p*-NO_2Ph), 133.01 (d, =CH), 135.02 (s, *p*-NO_2Ph), 150.78 (s, $PhCO_2$), 152.84 (s, OCO_2), 154.14 (s, $NHCO_2$). *Anal.* Calcd for $C_{24}H_{26}Cl_6N_2O_{12}$: C, 38.58; H, 3.51; N, 3.75. Found: C, 38.45; H, 3.35; N, 3.65.

Allyl 4-*O*-Benzyl-2-deoxy-6-*O*-(*p*-nitrobenzoyl)-3-*O*-(2,2,2-trichloro-*tert*-butoxycarbonyl)-2-(2,2,2-trichloroethoxycarbonylamino)-α-D-glucopyranoside (43) Compound **43** was obtained by a procedure similar to that described for **7** and was chromatographed on silica gel with $CHCl_3$–IPE (100 : 1); 86.1% yield, mp 159—161 °C. $[\alpha]_D^{23}$ +68.6° ($c=1.00$, $CHCl_3$). IR (KBr): 3444 (NH), 1745 (carbonate, carbamate, ester), 1655 (allyl), 718, 697 cm^{-1} (Ph). ^{1}H-NMR ($CDCl_3$) δ: 1.93 (6H, s, Cl_3CCMe_2), 4.68 (2H, s, Cl_3CCH_2), 4.94 (1H, d, $J=3.7$ Hz, H-1), 5.11—5.47 (2H, m, $=CH_2$), 5.70—6.13 (1H, m, =CH), 7.31 (5H, s, $PhCH_2$), 8.07—8.37 (4H, m, *p*-NO_2Ph). ^{13}C-NMR ($CDCl_3$) δ: 21.07 (q, $Cl_3CC\underline{Me}_2$), 54.29 (t, $O\underline{C}H_2CH=$), 90.53 (s, $OCO_2\underline{C}$), 96.49 (d, C-1), 105.30 (s, CCl_3), 118.44 (t, $=CH_2$), 123.58 (d, *p*-NO_2Ph), 128.52 (d, $PhCH_2$), 132.96 (d, =CH), 135.02 (s, *p*-NO_2Ph), 136.91 (s, $PhCH_2$), 150.38 (s, $PhCO_2$), 152.41 (s, OCO_2), 154.14 (s, $NHCO_2$). *Anal.* Calcd for $C_{31}H_{32}Cl_6N_2O_{12}$: C, 44.47; H, 3.85; N, 3.35. Found: C, 44.80; H, 3.83; N, 3.34.

Allyl 4-*O*-Benzyl-2-deoxy-3-*O*-(2,2,2-trichloro-*tert*-butoxycarbonyl)-2-(2,2,2-trichloroethoxycarbonylamino)-α-D-glucopyranoside (44) Compound **43** (15.0 g, 17.9 mmol) was dissolved in a solution of NH_4OH–MeOH–THF (1 : 9 : 1) (200 ml). The solution was stirred at room temperature for 4 h, then the solvent was evaporated off *in vacuo*. The residue was chromatographed on silica gel with $CHCl_3$–IPE (10 : 1) to give **44** (11.69 g, 95.0%), mp 121—123 °C. $[\alpha]_D^{23}$ +51.9° ($c=0.99$, $CHCl_3$). IR (KBr): 3456 (NH, OH), 1759 (carbonate), 1739 (carbamate), 1655 (allyl), 737, 698 cm^{-1} (Ph). ^{1}H-NMR ($CDCl_3$) δ: 1.89 (6H, s, Cl_3CCMe_2), 4.67 (2H, s, Cl_3CCH_2), 4.92 (1H, d, $J=3.7$ Hz, H-1), 5.16—5.39 (2H, m, $=CH_2$), 5.67—6.10 (1H, m, =CH), 7.31 (5H, s, $PhCH_2$). ^{13}C-NMR ($CDCl_3$) δ: 21.08 (q, $Cl_3CC\underline{Me}_2$), 54.45 (t, $O\underline{C}H_2CH=$), 90.37 (s, OCO_2C), 96.49 (d, C-1), 105.32 (s, CCl_3), 118.22 (t, $=CH_2$), 128.03, 128.46 (d, $PhCH_2$), 133.07 (d, =CH), 137.51 (s, $PhCH_2$), 152.57 (s, OCO_2), 154.14 (s, $NHCO_2$). *Anal.* Calcd for $C_{24}H_{29}Cl_6NO_9$: C, 41.89; H, 4.25; N, 2.04. Found: C, 41.50; H, 4.52; N, 1.97.

Allyl 4-*O*-Benzyl-2-deoxy-6-*O*-(3,4,6-tri-*O*-acetyl-2-chloroacetylamino-2-deoxy-β-D-glucopyranosyl)-3-*O*-(2,2,2-trichloro-*tert*-butoxycarbonyl)-2-(2,2,2-trichloroethoxycarbonylamino)-α-D-glucopyranoside (45) Compound **45** was obtained by a procedure similar to that described for **10** and was chromatographed on silica gel with $CHCl_3$–acetone (20 : 1); 84.1% yield, mp 213—215 °C. $[\alpha]_D^{23}$ +32.9° ($c=1.00$, $CHCl_3$). IR (KBr): 3452 (NH), 1755 (carbonyl), 1679 (amide), 738, 698 cm^{-1} (Ph). ^{1}H-NMR ($CDCl_3$) δ: 1.88 (6H, s, Cl_3CCMe_2), 2.03, 2.05 (9H, s, $COCH_3 \times 3$), 3.92 (2H, s, $NCOCH_2Cl$), 4.67 (2H, s, Cl_3CCH_2), 4.92 (1H, d, $J=3.4$ Hz, H-1), 5.65—6.13 (1H, m, =CH–), 6.80 (1H, d, $J=8.6$ Hz, $NHCOCH_2Cl$), 7.31 (5H, s, $PhCH_2$). ^{13}C-NMR ($CDCl_3$) δ: 20.59 (q, $CO\underline{C}H_3$), 21.08, 21.19 (q, $Cl_3CC\underline{Me}_2$), 42.37 (t, $CO\underline{C}H_2Cl$), 54.24 (t, $O\underline{C}H_2CH=$), 88.37 (s, $NCO_2\underline{C}$), 90.37 (s, $OCO_2\underline{C}$), 96.37 (d, C-1), 100.29 (d, C-1′), 105.38 (s, CCl_3), 118.22 (t, $=CH_2$), 127.70, 128.08, 128.52 (d, $PhCH_2$), 133.12 (d, =CH), 137.56 (s, $PhCH_2$), 152.41 (s, OCO_2), 154.14 (s, $NHCO_2$), 166.38 (s, $NHCOCH_2$), 169.13, 170.56 (s, CH_3CO). *Anal.* Calcd for $C_{38}H_{48}Cl_7N_2O_{17}$: C, 43.35; H, 4.59; N, 2.66. Found: C, 43.11; H, 4.41; N, 2.58.

Allyl 4-*O*-Benzyl-6-*O*-(2-chloroacetylamino-2-deoxy-β-D-glucopyranosyl)-2-deoxy-3-*O*-(2,2,2-trichloro-*tert*-butoxycarbonyl)-2-(2,2,2-trichloroethoxycarbonylamino)-α-D-glucopyranoside (46) Compound **46** was obtained by a procedure similar to that described for **11** and was chromatographed on silica gel with $CHCl_3$–MeOH (10 : 1); 95.2% yield, mp 169—170 °C. $[\alpha]_D^{23}$ +23.0° ($c=1.01$, $CHCl_3$). IR (KBr): 3433 (NH, OH), 1755 (carbonate), 1720 (carbamate), 1672 (amide), 736, 699 cm^{-1} (Ph). ^{1}H-NMR ($CDCl_3$)

δ: 1.87 (6H, s, Cl_3CCMe_2), 4.00 (2H, s, $NCOCH_2Cl$), 4.68 (2H, s, Cl_3CCH_2), 4.86 (1H, d, J=3.3 Hz, H-1), 5.72—6.25 (1H, m, =CH–), 6.71 (1H, d, J=9.5 Hz, $NHCOCH_2Cl$), 7.30 (5H, s, $PhCH_2$). ^{13}C-NMR ($CDCl_3$) δ: 21.62 (q, $Cl_3CC\underline{Me}_2$), 43.40 (t, $CO\underline{C}H_2Cl$), 55.48 (t, $O\underline{C}H_2CH=$), 88.60 (s, $NCO_2\underline{C}$), 91.18 (s, $OCO_2\underline{C}$), 97.74 (d, C-1), 102.29 (d, C-1'), 106.74 (s, CCl_3), 118.22 (t, $=CH_2$), 128.57, 128.73, 129.32 (d, $PhCH_2$), 135.02 (d, =CH), 139.41 (s, $PhCH_2$), 153.20 (s, OCO_2), 155.46 (s, $NHCO_2$), 167.15 (s, $NHCOCH_2$). *Anal.* Calcd for $C_{32}H_{42}Cl_7N_2O_{14}$: C, 41.47; H, 4.57; N, 3.02. Found: C, 40.84; H, 4.38; N, 3.03.

Allyl 4-*O*-Benzyl-6-*O*-(2-chloroacetylamino-2-deoxy-4,6-*O*-isopropylidene-β-D-glucopyranosyl)-2-deoxy-3-*O*-(2,2,2-trichloro-*tert*-butoxycarbonyl)-2-(2,2,2-trichloroethoxycarbonylamino)-α-D-glucopyranoside (47) Compound **47** was obtained by a procedure similar to that described for **12** and was chromatographed on silica gel with $CHCl_3$–MeOH (10:1); 95.4% yield, mp 155—156 °C. $[\alpha]_D^{20}$ +22.8° (c=1.00, $CHCl_3$). IR (KBr): 3435 (OH), 3334 (NH), 1755 (carbonate), 1721 (carbamate), 1665 (amide), 855 (Me_2C), 738, 700 cm^{-1} (Ph). ^{1}H-NMR ($CDCl_3$) δ: 1.43, 1.50 (6H, s, Me_2C), 1.84, 1.89 (6H, s, Cl_3CCMe_2), 3.96 (2H, s, $NCOCH_2Cl$), 4.64 (2H, s, Cl_3CCH_2), 4.91 (1H, d, J=3.4 Hz, H-1), 5.64—6.12 (1H, m, =CH–), 6.71 (1H, d, J=9.5 Hz, $NHCOCH_2Cl$), 7.30 (5H, s, $PhCH_2$). ^{13}C-NMR ($CDCl_3$) δ: 19.70, 28.99 (q, $\underline{Me}_2C$), 21.02, 21.13 (q, $Cl_3CC\underline{Me}_2$), 42.59 (t, $CO\underline{C}H_2Cl$), 54.18 (t, $O\underline{C}H_2CH=$), 88.48 (s, $NCO_2\underline{C}$), 90.32 (s, $OCO_2\underline{C}$), 96.39 (d, C-1), 99.80 (s, $Me_2\underline{C}$), 100.45 (d, C-1'), 105.81 (s, CCl_3), 118.11 (t, $=CH_2$), 127.59, 127.98, 128.46 (d, $PhCH_2$), 133.12 (d, =CH), 137.56 (s, $PhCH_2$), 152.41 (s, OCO_2), 154.31 (s, $NHCO_2$), 167.03 (s, $NHCOCH_2$). *Anal.* Calcd for $C_{35}H_{46}Cl_7N_2O_{14}$: C, 43.48; H, 4.79; N, 2.90. Found: C, 43.82; H, 4.69; N, 2.89.

Allyl 6-*O*-(2-Amino-2-deoxy-4,6-*O*-isopropylidene-β-D-glucopyranosyl)-4-*O*-benzyl-2-deoxy-3-*O*-(2,2,2-trichloro-*tert*-butoxycarbonyl)-2-(2,2,2-trichloroethoxycarbonylamino)-α-D-glucopyranoside (2c) Compound **2c** was obtained by a procedure similar to that described for **2a** and was chromatographed on silica gel with $CHCl_3$–MeOH (10:1); 84.6% yield, mp 142—143 °C. $[\alpha]_D^{20}$ +18.6° (c=1.00, $CHCl_3$). IR (KBr): 3437 (OH), 3332 (NH), 1755 (carbonate), 1724 (carbamate), 856 (Me_2C), 735, 699 cm^{-1} (Ph). ^{1}H-NMR ($CDCl_3$) δ: 1.43, 1.50 (6H, s, Me_2C), 1.86, 1.89 (6H, s, Cl_3CCMe_2), 4.66 (2H, s, Cl_3CCH_2), 4.93 (1H, d, J=3.4 Hz, H-1), 5.63—6.13 (1H, m, =CH–), 7.30 (5H, s, $PhCH_2$). ^{13}C-NMR ($CDCl_3$) δ: 19.13, 29.04 (q, $\underline{Me}_2C$), 21.02, 21.13 (q, $Cl_3CC\underline{Me}_2$), 54.18 (t, $O\underline{C}H_2CH=$), 88.48 (s, $NCO_2\underline{C}$), 90.32 (s, $OCO_2\underline{C}$), 96.39 (d, C-1), 99.75 (s, $Me_2\underline{C}$), 104.84 (d, C-1'), 105.33 (s, CCl_3), 118.17 (t, $=CH_2$), 127.65, 127.98, 128.46 (d, $PhCH_2$), 133.07 (d, =CH), 137.51 (s, $PhCH_2$), 152.41 (s, OCO_2), 154.31 (s, $NHCO_2$). *Anal.* Calcd for $C_{33}H_{45}Cl_6N_2O_{13}$: C, 44.51; H, 5.09; N, 3.15. Found: C, 44.92; H, 4.96; N, 3.33.

Acknowledgment We are grateful to Professor T. Shiba for providing the ^{1}H-NMR spectrum of **17**. We also thank Mr. Kazuo Tanaka of JEOL Ltd. for obtaining the FAB-mass spectrum.

References

1) Part XVII: S. Nakamoto and K. Achiwa, *Chem. Pharm. Bull.*, **36**, 202 (1988) and references cited therein; Part XVIII: T. Shimizu, T. Masuzawa, Y. Yanagihara, S. Nakamoto, H. Itoh, and K. Achiwa, *J. Pharmacobio-Dyn.*, **11**, 512 (1988); Part XVIX: K. Ikeda, S. Akamatsu, and K. Achiwa, *Carbohydr. Res.*, **189**, C1 (1989); Part XX: T. Shimizu, T. Masuzawa, Y. Yanagihara, H. Itoh, S. Nakamoto, and K. Achiwa, *Chem. Pharm. Bull.*, **37**, 2535 (1989); Part XXI: K. Ikeda, S. Akamatsu, and K. Achiwa, *Chem. Pharm. Bull.*, **38**, 279 (1990); Part XXII: T. Shimizu, Y. Ohtsuka, T. Masuzawa, Y. Yanagihara, H. Itoh, S. Nakamoto, and K. Achiwa, *Mol. Biother.*, **2**, 110 (1990); Part XXIII: K. Idegami, K. Ikeda, and K. Achiwa, *Chem. Pharm. Bull.*, **38**, 1766 (1990).
2) C. Galanos, O. Lüderitz, E. T. Rietschel, and O. Westphal, *Int. Rev. Biochem.*, **14**, 239 (1977); O. Lüderitz, C. Galanos, V. Lehmann, H. Mayer, E. T. Rietschel, and J. Wechesser, *Naturwissenschaften*, **65**, 578 (1978).
3) T. Shiba and S. Kusumoto, *Yuki Gosei Kagaku Kyokai Shi*, **42**, 507 (1984); *idem*, *Tanpakushitsu Kakusan Koso*, **31**, 353 (1986).
4) M. Imoto, H. Yoshimura, M. Yamamoto, T. Shimamoto, S. Kusumoto, and T. Shiba, *Tetrahedron Lett.*, **25**, 2667 (1984).
5) M. Imoto, H. Yoshimura, N. Sakaguchi, S. Kusumoto, and T. Shiba, *Tetrahedron Lett.*, **26**, 1545 (1985).
6) H. Yoshimura, M. Imoto, Y. Tsuji, S. Kusumoto and T. Shiba, Abstracts of Papers, 50th Annual Meeting of the Chemical Society of Japan, 1986, Part II, p. 971.
7) T. Takahashi, S. Nakamoto, K. Ikeda, and K. Achiwa, *Tetrahedron Lett.*, **27**, 1819 (1986).
8) K. Ikeda, T. Takahashi, H. Kondo, and K. Achiwa, *Chem. Pharm. Bull.*, **35**, 1311 (1987).
9) T. Takahashi, C. Shimizu, S. Nakamoto, K. Ikeda, and K. Achiwa, *Chem. Pharm. Bull.*, **33**, 1760 (1985); *idem*, *ibid.*, **35**, 1383 (1987).
10) M. Kiso and L. Anderson, *Carbohydr. Res.*, **72**, C12 (1979).
11) J. J. Oltvoort, C. A. A. van Boeckel, J. H. de Koning, and J. H. van Boom, *Synthesis*, **1981**, 305.
12) N. A. Nashed and L. Anderson, *J. Chem. Soc., Chem. Commun.*, **1982**, 1274.
13) M. Inage, H. Chaki, S. Kusumoto, and T. Shiba, *Chem. Lett.*, **1982**, 1281.
14) T. Shimizu, S. Akiyama, T. Masuzawa, Y. Yanagihara, K. Ikeda, T. Takahashi, H. Kondo, and K. Achiwa, *Microbiol. Immunol.*, **31**, 381 (1987).

Marine Sterols. XIX.[1] Polyhydroxysterols of the Soft Corals of the Andaman and Nicobar Coasts. (3). Isolation and Structures of Five New C_{28} Polyhydroxysterols from Two *Sclerophytum* sp. Soft Corals

Masaru KOBAYASHI,*[,a] Fuyuko KANDA,[a] Chunduri Venkata Lakshmana RAO,[b] Saridi Madhava Dileep KUMAR,[b] Desaraju Venkata RAO,[c] and Chaganti Bheemasankara RAO*[,b]

Faculty of Pharmaceutical Sciences, Hokkaido University,[a] Kita-ku, Sapporo 060, Japan, and School of Chemistry,[b] and Department of Pharmaceutical Sciences,[c] Andhra University, Visakhapatnam 530 003, India. *Received August 13, 1990*

Nine polyhydroxysterols were isolated from the lipid extract of two *Sclerophytum* sp. soft corals collected in the Andaman and Nicobar Islands. Of these, three compounds (7a, b, and 8) had previously been isolated from the southern Japan soft coral *Sarcophyton glaucum*. Compound 1 was identified as lobosterol having a novel 6-keto-A/B-*cis* ring juncture. The structures of the five new compounds were determined as 25-deacetyllobosterol (2), (24*S*)-24-methylcholest-7-ene-3β,5α,6β,25-tetrol 25-monoacetate (3), (24*S*)-24-methylcholest-22*E*-ene-3β,5α,6β,25-tetrol (4), (24*S*)-24-methylcholestane-3β,5α,25-triol-6-one 25-monoacetate (5a) and its C-25 deacetoxy analog (6), from the spectral data and by chemical conversion.

Keywords coelenterata; soft coral; *Sclerophytum* sp.; polyhydroxy C_{28} sterol; 25-deacetyllobosterol; 24-methylcholest-7-ene-3β,5α,6β,25-tetrol 25-monoacetate; 24-methylcholest-22*E*-ene-3β,5α,6β,25-tetrol; 24-methylcholestane-3β,5α,25-triol-6-one 25-monoacetate; 24-methylcholestane-3β,5α-diol-6-one

Soft corals contain a diversity of mono- and polyhydroxysterols, most of which are derivatives of (24*S*)-24-methylcholestane-type[2] C_{28} sterols.[3,4] As a continuation of our studies on the sterols of the soft corals of the Okinawa Islands, we have started to investigate those of the soft corals in the Andaman and Nicobar Islands in the Indian Ocean. Of the nine soft corals collected, eight organisms were identified at the genus level as *Sclerophytum* sp., which has not previously been studied chemically, and one as an *Alcyonium* sp., but further definition was not possible. Extraction and separation of their polar lipids resulted in the isolation of various known and unknown polyhydroxysterols.[5] All eight *Sclerophytum* sp. soft corals contained (24*S*)-24-methylcholestane-3β,5α,6β,25-tetrol 25-monoacetate (**7a**) or its 25-deacetyl derivative **7b**. The present paper deals with the structures of the C_{28} polyhydroxysterols, isolated from two of the *Sclerophytum* sp. soft corals, code names MF-CBR-25 and MF-CBR-27.[5a] Repeated chromatography of their polar lipid extracts afforded seven (**1**—**4**, **7a**, **b** and **8**) and three (**5a**, **6** and **7a**) polyhydroxysterols from MF-CBR-27 and MF-CBR-25, respectively. Of these, compounds **7a**, **b**, and (24*S*)-24-methylcholest-5-ene-3β,25-diol (**8**) were identical with authentic specimens that we had previously isolated from the soft coral *Sarcophyton glaucum*, collected at Ishigaki Island, Okinawa.[4]

Compound **1** was a C_{28} sterol having one ketone, one tertiary acetoxyl, one hydroxyl, and two secondary hydroxyl groups, as indicated by its proton and carbon-13 nuclear magnetic resonance (^{1}H- and ^{13}C-NMR) spectra (Experimental). The two secondary hydroxymethine protons (δ 4.43 and 4.65) were shown to be coupled to each other with small coupling constants (J=3.0—3.5 Hz). Most of the ^{13}C-NMR signals (C-6 to C-9, and C-11 to C-28) were found to be identical with those of previously synthesized (24*S*)-24-methylcholestane-5β,25-diol-3,6-dione 25-monoacetate.[5a] Heteronuclear multiple bond correlation spectroscopy (HMBC)[6] of **1** indicated the correlation of the 7β-H (in $CDCl_3$, δ 2.48, dd) with quaternary C-5, carrying an oxygen atom (δ 85.7). The chemical shifts of the protons and calculated values of the A-ring carbons,[7] suggested that compound **1** corresponds to the known

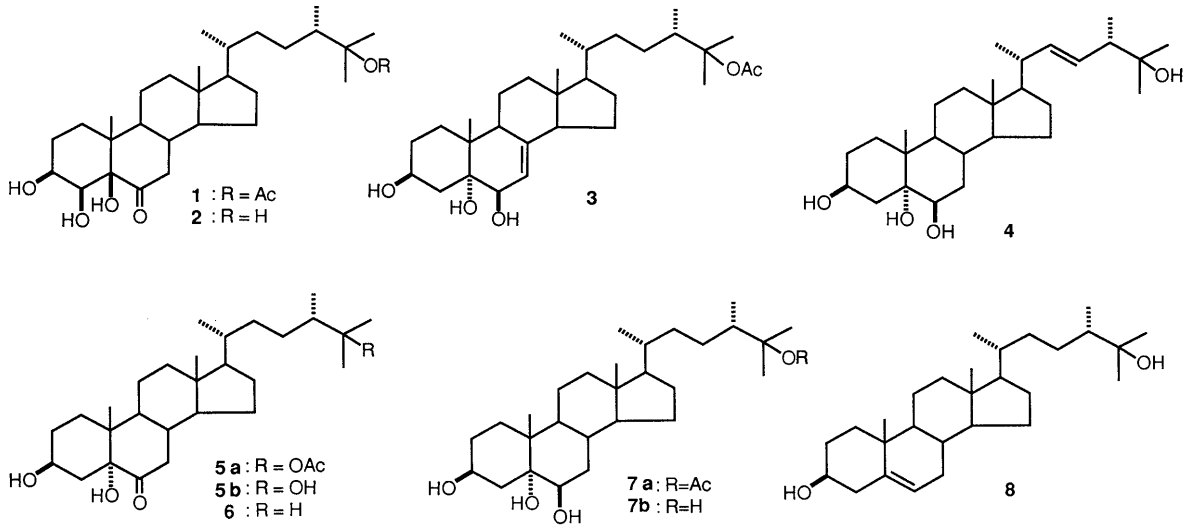

Chart 1

compound lobosterol,[8] having a 3β,4β,5β-trihydroxy-6-keto moiety. The structure of lobosterol has been established by X-ray crystallography. Direct comparison of compound **1** with an authentic specimen of lobosterol, provided by Daloze, confirmed their identity. Lobosterol is one of the earliest reported examples of marine polyhydroxysterols; its isolation from a soft coral, *Lobophytum pauciflorum*, was reported in 1976 by Tursch *et al.*, but to our knowledge isolation of this compound from other sources has not been reported since then. The characteristic feature of **1**, unlike other marine polyhydroxysterols, is that in $CDCl_3$, the ^{1}H-NMR signals of the three hydroxyl protons appear clearly (δ 2.77, d, J=11.0 Hz; δ 3.62, d, J=11.0 Hz; δ 4.49, s), possibly due to their tight internal hydrogen bondings.[9]

Compound **2** was shown to be 25-deacetyllobosterol; it had virtually the same ^{1}H- and ^{13}C-NMR chemical shifts (Experimental) as **1**, except for those of the side chain (^{1}H-NMR, δ 1.39, 1.41, each 3H, s; ^{13}C-NMR, δ 23.0, q, 23.5, q, 73.6, s). This identification was confirmed by mild alkaline hydrolysis of **1**, giving **2** as the sole product.

Compounds **3** and **4** are monounsaturated derivatives of **7a** and **7b**, respectively, having a 3β,5α,6β-trihydroxylated steroid nucleus. When studying polyhydroxysterols of *S. glaucum*,[4a] we pointed out that such a system could be readily recognized from the position and coupling pattern of the signals due to 3α-H (br m, $W_{1/2}$ = *ca.* 20 Hz), 4β-H (dd, J = *ca.* 13.0, 12.0 Hz), 6α-H (br s, $W_{1/2}$ = *ca.* 7 Hz), and 19-H_3. Because of the 1,3-*syn*-periplanar arrangement of hydroxyl groups (3α-H and 5α-OH, 4β-H and 6β-OH, 19-H_3 and 6β-OH), these protons are quite susceptible to the pyridine-induced deshielding effect,[10] and are shifted to unusually low field (**3**, 3α-H, δ 4.82, 4β-H, 3.04, 19-H_3, 1.55; **4**, 3α-H, δ 4.89, 4β-H, 2.97, 19-H_3, 1.67). This phenomenon is diagnostic for such a system and has been used subsequently by many workers in the structure elucidation of related polyhydroxysterols. The ^{1}H- and ^{13}C-NMR signals of the side chain of **3** (Experimental) were identical with those of **1** and **7a**,[11] so that the trisubstituted double bond (δ 5.75, 1H, m) was located in the steroid ring. The 18-H_3 signal (δ 0.59, taken in $CDCl_3$ solution) appeared at relatively high field, suggesting compound **3** to be a Δ^7 derivative.[12] Comparison of the ^{1}H- and ^{13}C-NMR signals with literature values revealed that they exactly coincide with those of the reference compound 24-methylcholesta-7,22-diene-3β,5α,6β-triol,[13] except for the side chain signals.

The ^{1}H- and ^{13}C-NMR signals due to the steroid nucleus of **4** (Experimental) were identical with those of **7b** reported previously,[4a] and those of the C-17 side chain were different. This indicated that the side chain is oxygenated at C-25 (δ 26.9, q, 28.7, q and 71.5, s) and bears one disubstituted double bond (δ 130.9, d and 137.2, d). From the vicinal coupling constant (15.5 Hz) of 22- and 23-H (δ 5.36 and 5.66, each 1H, dd) in the ^{1}H-NMR spectrum, the geometry at C-22 of **4** was concluded to be *E*. The mass spectrum of **4** did not give the molecular ion and the highest peak was observed at *m/z* 390. This ion could be attributed to the McLafferty-type cleavage at C-24 and C-25 with 1H transfer (Chart 2). From these results, compounds **3** and **4** were concluded to be (24*S*)-24-methylcholest-7-ene-3β,5α,6β,25-tetrol 25-monoacetate and (24*S*)-24-methylcholest-22*E*-ene-3β,5α,6β,25-tetrol, respectively. Assignment of 24*S* configuration to **4** is based only on the biogenetic analogy with other compounds simultaneously isolated.

Compounds **5a** and **6** were obtained as a crystalline mixture which was resistant to separation. The ^{1}H- and ^{13}C-NMR spectra of the mixture showed it to be composed of two compounds having 25-acetoxy-24-methylcholestane-type (major) and 24-methylcholestane-type C_{28} sterol structures, but the signals due to the steroid nucleus were common. A secondary (δ 67.3) and a tertiary hydroxyl group (δ 80.9), and one ketone moiety (δ 212.2) were present. The chemical shifts of C-12 to C-28 of the major component were identical with those of **1**, and the signals due to C-7 to C-9 and C-11 showed only small differences (less than 1.5 ppm). The ^{1}H-NMR (in $CDCl_3$) chemical shift of 3α-H (δ 3.98, m, $W_{1/2}$ = 20 Hz) and a signal at δ 2.72 (dd, J = 13.0, 12.5 Hz), which is assignable to 7α-H, showed, in pyridine-d_5, a significant pyridine-induced deshielding effect (Δδ, 3α-H, 0.70 ppm; 7α-H, 0.42 ppm) indicating the presence of a *syn*-periplanar 5α-hydroxyl group. Partial oxidation of **7a**, using 0.8 eq of pyridinium chlorochromate (PCC), afforded 3,6-diketo-(**9**), 3-monoketo-(**10**) and 6-monoketo-(**5a**) derivatives (Chart 3). Synthetic **5a** was shown to be identical with the major component of the natural mixture from the soft coral. Alkaline hydrolysis of this mixture afforded the deacetyl derivative (**5b**) and unchanged compound **6** having a 24-methylcholestane-type side chain. The ^{1}H-NMR chemical shifts of **6** due to 28-H (δ 0.775), and 26,27-H (δ 0.782 and 0.853) corresponded to those of the reference compound (24*S*)-24-methylcholesterol (22-dihydrobrassicasterol, δ 0.775, 0.783, 0.852),[14] and the signals corresponding to those of the (24*R*) isomer (campesterol, δ 0.773, 0.802, 0.850) were not observed.[14,15]

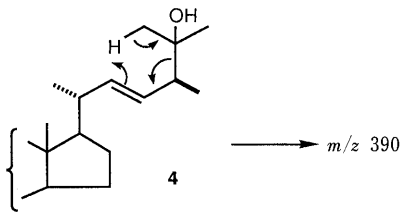

Chart 2

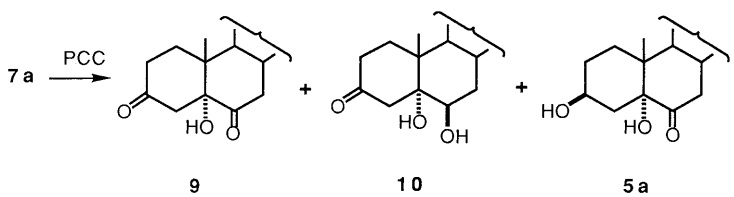

Chart 3

Experimental

Melting points were determined on a Kofler hot stage and are uncorrected. Optical rotations were determined on a JASCO DIP-370 digital polarimeter. Nuclear magnetic resonance (NMR) spectra were determined on a JEOL JMS GX-270 spectrometer at 270 MHz (^{1}H) and on a JEOL JNM FX-90Q spectrometer at 22.5 MHz (^{13}C) with tetramethylsilane as an internal standard. Mass spectra (MS) were determined on a JEOL JMS D 300 mass spectrometer. Chromatography was done by flash column chromatography[16] using silica gel (Wako gel C-300, 200—300 mesh, Wako Pure Chemical Industries).

Materials The collection locations and the code numbers of the soft corals, and details of the individual polyhydroxysterols and the general isolation process were reported in a previous paper.[5a] One soft coral sample, code name MF-CBR-25 (2.7 kg after extraction), gave the polyhydroxysterols MF-CBR-25-01 (**7a**, 220 mg) and MF-CBR-25-02 (mixture of **5a** and **6**, 72 mg). Another soft coral sample, code name MF-CBR-27 (2.2 kg after extraction) gave seven polyhydroxysterols MF-CBR-27-01 (**1**, 31 mg), -02 (**2**, 94 mg), -03 (**8**, 11 mg), -04 (**7a**, 2100 mg), -05 (mixture of **3**, **4** and **7b**, 97 mg). Attempted purification of MF-CBR-25-02 by chromatography using several solvent systems only gave the major compound **5a** having **6** as a persistent impurity. Chromatography of MF-CBR-27-05 (*ca.* 20 mg) with MeOH–$CHCl_3$ (1 : 10) gave compounds **3** (1.9 mg), **4** (4.2 mg) and **7b** (14.7 mg). The known compounds (**1**, **7a**, **b**, and **8**) were identified from the ^{1}H-NMR and MS, and by thin-layer chromatography (TLC) with authentic specimens.[4]

(24*S*)-24-Methylcholestane-3β,4β,5β,25-tetrol-6-one 25-Monoacetate (Lobosterol) (1) mp 220—222 °C, $[\alpha]_D^{29}$ −7° (*c* = 1.52, $CHCl_3$). ^{1}H-NMR (pyridine-d_5) δ: 1.51, 1.52, 2.04 (each 3H, s), 0.95, 1.00 (each 3H, d, *J* = 6.5 Hz). Other signals, see **2**. ^{13}C-NMR ($CDCl_3$) δ: C-24 (42.1), C-25 (86.0), C-26, 27 (23.0, 23.5), C-28 (14.6), OAc (22.6, 170.5). Other signals, see **2**.

(24*S*)-24-Methylcholestane-3β,4β,5β,25-tetrol-6-one (25-Deacetyllobosterol) (2) mp 220—225 °C, $[\alpha]_D^{29}$ −8° (*c* = 1.68, $CHCl_3$). ^{1}H-NMR (pyridine-d_5) δ: 0.61, 0.95, 1.39, 1.41 (each 3H, s), 1.03, 1.11 (each 3H, d, *J* = 6.5 Hz), 2.50 (1H, dd, *J* = 13.5, 5.0 Hz, 7β-H), 2.58 (1H, dd, *J* = 13.5, 12.5 Hz, 7α-H), 4.44 (1H, br q, *J* = 3.0 Hz, 3α-H), 4.66 (1H, br d, *J* = 3.0 Hz, 4α-H). ^{13}C-NMR ($CDCl_3$) δ: C-1 (27.0), C-2 (24.3), C-3 (69.6), C-4 (70.3), C-5 (85.7), C-6 (210.6), C-7 (41.6), C-8 (38.0), C-9 (43.1), C-10 (46.6), C-11 (21.8), C-12 (39.6), C-13 (43.3), C-14 (57.0), C-15 (24.1), C-16, 23 (27.9, 28.0), C-17 (56.0), C-18 (12.1), C-19 (17.0), C-20 (36.2), C-21 (19.0), C-22 (34.8), C-24 (45.2), C-25 (73.6), C-26, 27 (26.2, 27.4), C-28 (14.9). MS *m/z*: 464 (M^+), 446, 431, 377. High-resolution MS [Found (Calcd)] *m/z*: $C_{28}H_{48}O_5$ (M^+), 464.3480 (464.3502).

(24*S*)-24-Methylcholest-7-ene-3β,5α,6β,25-tetrol 25-Monoacetate (3) mp 225—230 °C, $[\alpha]_D^{29}$ −30° (*c* = 0.20, $CHCl_3$). ^{1}H-NMR ($CDCl_3$) δ: 0.59, 1.08, 1.97 (each 3H, s), 0.87, 0.95 (each 3H, d, *J* = 6.5 Hz), 1.39 (6H, s, 26, 27-H), 2.15 (1H, dd, *J* = 13.0, 11.5 Hz, 4β-H), 3.63 (1H, m, $W_{1/2}$ = 8 Hz, 6α-H), 4.08 (1H, m, $W_{1/2}$ = 18 Hz, 3α-H), 5.36 (1H, m, 7-H); (pyridine-d_5) δ: 0.66, 1.55, 2.02 (each 3H, s), 1.48 (6H, s), 0.92, 0.99 (each 3H, d, *J* = 6.5 Hz), 3.04 (1H, dd, *J* = 13.0, 11.5 Hz), 4.34 (1H, m), 4.82 (1H, m), 5.75 (1H, m). ^{13}C-NMR (pyridine-d_5) δ: C-1 (32.6), C-2 (33.9), C-3 (67.6), C-4 (41.9), C-5 (76.1), C-6 (74.2), C-7 (120.4), C-8 (141.6), C-9 (43.8), C-10 (38.0), C-11 (21.8), C-12 (40.0), C-13 (43.7), C-14 (55.1), C-15 (23.5), C-16, 23 (28.1), C-17 (56.3), C-18 (12.3), C-19 (18.8), C-20 (36.2), C-21 (19.3), C-22 (35.1), C-24 (42.4), C-25 (85.7), C-26, 27 (23.0, 23.5), OAc (22.5, 170.0). MS *m/z*: 472 ($M^+ - H_2O$), 439, 412, 394, 379, 303. High-resolution MS [Found (Calcd)] *m/z*: $C_{30}H_{48}O_4$ ($M^+ - H_2O$), 472.3531 (472.3553).

(24*S*)-24-Methylcholest-22*E*-ene-3β,5α,6β,25-tetrol (4) mp 241—244 °C, $[\alpha]_D^{29}$ −20° (*c* = 0.84, pyridine). ^{1}H-NMR (pyridine-d_5) δ: 0.76, 1.67 (each 3H, s), 1.09, 1.27 (each 3H, d, *J* = 6.5 Hz), 1.38, 1.42 (each 3H, s), 2.97 (1H, dd, *J* = 12.5, 11.5 Hz, 4β-H), 4.17 (1H, br s, $W_{1/2}$ = 7.0 Hz, 6α-H), 4.89 (1H, m, 3α-H), 5.36, 5.66 (each 1H, dd, *J* = 15.5, 8.5 Hz, 22,23-H). MS *m/z*: 390 ($M^+ - C_3H_6O$), 372, 354, 334, 316, 305, 271, 253. High-resolution MS [Found (Calcd)] *m/z*: $C_{25}H_{42}O_3$ ($M^+ - C_3H_6O$), 390.3146 (390.3134).

(24*S*)-24-Methylcholestane-3β,5α,25-triol-6-one 25-Monoacetate (5a) Data were derived from those of the mixture of **5a** and **6** by subtracting the data of **6**. ^{1}H-NMR (pyridine-d_5) δ: 0.65, 0.97, 1.50, 1.51 (each 3H, s), 0.84, 0.94 (each 3H, d, *J* = 7.0 Hz), 2.37 (1H, dd, *J* = 13.5, 12.0 Hz, 4β-H), 2.62 (1H, dd, *J* = 13.5, 4.0 Hz, 4α-H), 3.14 (1H, t, *J* = 12.5 Hz, 7α-H), 4.68 (1H, m, 3α-H); ($CDCl_3$) δ: 0.64, 0.81, 1.97 (each 3H, s), 1.39 (6H, s), 0.86, 0.92 (each 3H, d, *J* = 7.0 Hz), 2.12 (1H, dd, *J* = 13.0, 4.0 Hz, 4α-H), 2.72 (1H, dd, *J* = 13.0, 12.5 Hz, 7α-H), 3.98 (1H, m, 3α-H). MS, see synthetic **5a**. High-resolution MS [Found (Calcd)] *m/z*: $C_{30}H_{50}O_5$ (M^+), 490.3659 (490.3658).

Alkaline Hydrolysis of the Mixture of 5a and 6 Treatment of the mixture (*ca.* 5 mg) of **5a** and **6** with 10% KOH–MeOH, refluxing too long period (2 h), caused decomposition of 25-hydroxysterol **5b**. Column chromatography of the reaction product with ethyl acetate–hexane (1 : 1) gave **6** (1.2 mg) and a trace (0.45 mg) of **5b**.

(24*S*)-24-Methylcholestane-3β,5α,25-triol-6-one (5b) mp 257—260 °C, $[\alpha]_D^{29}$ −38° (*c* = 0.090, $CHCl_3$). ^{1}H-NMR ($CDCl_3$) δ: 0.64, 0.79 (each 3H, s), 0.89, 0.93 (each 3H, d, *J* = 6.5 Hz), 1.15, 1.16 (each 3H, s), 2.75 (1H, t, *J* = 12.5 Hz, 7α-H), 3.96 (1H, m, 3α-H). MS *m/z*: 448 (M^+), 430, 415, 390, 372, 305, 303, 287. High-resolution MS [Found (Calcd)] *m/z*: $C_{28}H_{48}O_4$ (M^+), 448.3526 (448.3553).

(24*S*)-24-Methylcholestane-3β,5α-diol-6-one (6) mp 251—253 °C, $[\alpha]_D^{29}$ −32° (*c* = 0.24, $CHCl_3$). ^{1}H-NMR ($CDCl_3$) δ: 0.64, 0.81 (each 3H, s), 0.775 (3H, d, *J* = 7.0 Hz, 28-H), 0.782, 0.853 (each 3H, d, *J* = 7.0 Hz, 26, 27-H), 0.912 (3H, d, *J* = 6.5 Hz, 21-H), 2.13 (1H, dd, *J* = 13.0, 4.5 Hz, 4α-H), 2.71 (1H, dd, *J* = 13.0, 12.0 Hz, 7α-H), 3.97 (1H, m, 3α-H). MS *m/z*: 432 (M^+), 414, 332, 303, 287. High-resolution MS [Found (Calcd)] *m/z*: $C_{28}H_{48}O_3$ (M^+), 432.3605 (432.3604).

PCC Oxidation of 7a A solution of **7a** (110 mg, 0.225 mmol) in 20 ml of CH_2Cl_2 was stirred with 26 mg (0.12 mmol) of PCC at room temperature for 20 min, then the mixture was diluted with Et_2O. The Et_2O layer was washed with H_2O and saturated NaCl solution and then the solvent was evaporated off. Column chromatography of the residue with 2.5% MeOH in $CHCl_3$ gave **9** (4.6 mg), **10** (15.1 mg) and **5a** (15.5 mg).

Compound 9 mp 255—256 °C, $[\alpha]_D^{26}$ −17° (*c* = 0.92, $CHCl_3$). ^{1}H-NMR ($CDCl_3$) δ: 0.67, 1.01, 1.97 (each 3H, s), 0.87, 0.93 (each 3H, d, *J* = 6.5 Hz), 1.39 (6H, s), 2.73 (1H, t, *J* = 12.5 Hz, 7α-H), 2.92 (1H, d, *J* = 15.5 Hz, 4-H). MS *m/z*: 488 (M^+), 470, 428, 410, 400, 385, 370, 301. High-resolution MS [Found (Calcd)] *m/z*: $C_{30}H_{48}O_5$ (M^+), 488.3519 (488.3502).

Compound 10 mp 215—220 °C, $[\alpha]_D^{26}$ +1° (*c* = 3.02, $CHCl_3$). ^{1}H-NMR ($CDCl_3$) δ: 0.71, 1.35, 1.97 (each 3H, s), 1.39 (6H, s), 0.87, 0.93 (each 3H, d, *J* = 6.5 Hz), 3.24 (1H, d, *J* = 15.0 Hz, 4-H), 3.54 (1H, br s, $W_{1/2}$ = 7 Hz, 6α-H). MS *m/z*: 490 (M^+), 472, 454, 430, 412, 303. High-resolution MS [Found (Calcd)] *m/z*: $C_{30}H_{50}O_5$ (M^+), 490.3682 (490.3658).

Compound 5a mp 240—242 °C, $[\alpha]_D^{24}$ −34° (*c* = 3.10, $CHCl_3$). ^{1}H-NMR: identical with natural **5a**. MS *m/z*: 490 (M^+), 430, 412, 397, 303. High-resolution MS [Found (Calcd)] *m/z*: $C_{30}H_{50}O_5$ (M^+), 490.3681 (490.3658).

Acknowledgement We are grateful to Dr. D. Daloze, Universite Libre de Bruxelles, for providing an authentic specimen of lobosterol, to the Zoological Survey of India, Calcutta for identification of the oragnisms, and to the Council of Scientific and Industrial Research, New Delhi, and the Department of Science and Technology, New Delhi, for financial support to C. B. R.

References and Notes

1) Rart XVIII: M. Kobayashi and F. Kanda, *J. Chem. Soc., Perkin Trans. 1*, in press.
2) According to the IUPAC convention rule, introduction of a double bond at C-22 changes the notation of the same chiral center to (24*R*).
3) *a*) F. J. Schmitz, "Marine Natural Products," Vol. 1, ed. by P. J. Scheuer, Academic Press, New York, 1978, p. 241; *b*) D. J. Faulkner, *Nat. Prod. Rep.*, **1**, 551 (1984); *c*) *Idem, ibid.*, **3**, 1 (1986); *d*) *Idem, ibid.*, **4**, 539 (1987); *e*) H. C. Krebs, "Progress in the Chemistry of Organic Natural Products," Vol. 49, ed. by W. Herz, H. Grisebach, G. W. Kirby, and C. Tamm, Springer-Verlag, Vienna, 1986, p. 151.
4) *a*) M. Kobayashi, T. Hayashi, F. Nakajima, and H. Mitsuhashi, *Steroids*, **34**, 285 (1979); *b*) M. Kobayashi, T. Hayashi, K. Hayashi, M. Tanabe, T. Nakagawa, and H. Mitsuhashi, *Chem. Pharm. Bull.*, **31**, 1848 (1983); *c*) M. Kobayashi and H. Mitsuhashi, *ibid.*, **31**, 4127 (1983).
5) *a*) M. Kobayashi, F. Kanda, S. M. C. Kumar, C. V. L. Rao, and C. B. Rao, *Chem. Pharm. Bull.*, **38**, 1724 (1990); *b*) M. Kobayashi, F. Kanda, D. S. Rao, D. V. Rao, and C. B. Rao, *ibid.*, **38**, 2400 (1990).
6) A. Bax, A. Aszalos, Z. Dinya, and S. Kubo, *J. Am. Chem. Soc.*, **108**, 8056 (1986).
7) H. Beierbeck, J. K. Saunders, and J. W. Apsimon, *Can. J. Chem.*, **55**, 2813 (1977). ^{13}C-NMR data for **1** were not reported in the original paper.[8] Application of the semiempirical derivation rule by Beierbeck *et al.* gave chemical shifts of δ 26.0 (C-1), 25.3 (C-2), 68.1 (C-3), 72.6 (C-4) and 42.7 (C-7) which are reasonably close to the values found here (see Experimental).

8) B. Tursch, C. Hootele, M. Kaishin, D. Losman, and R. Karlsson, *Steroids*, **27**, 137 (1976).
9) In the original paper on lobosterol,[8] the chemical shift of one of the hydroxymethine protons was reported as δ 4.5. This signal (singlet) is deuterium-exchangeable and should be assigned to the C-5 hydroxylic proton.
10) P. V. Demarco, E. Farkas, D. Dodderell, B. L. Mylari, and E. Wenkert, *J. Am. Chem. Soc.*, **90**, 5480 (1968).
11) Y. Yamada, S. Suzuki, K. Iguchi, H. Kikuchi, Y. Tsukitani, H. Horiai, and H. Nakanishi, *Chem. Pharm. Bull.*, **28**, 473 (1980).
12) R. F. Zurcher, *Helv. Chim. Acta*, **46**, 2054 (1963).
13) V. Picciali and D. Sica, *J. Nat. Prod.*, **50**, 915 (1987).
14) I. Rubinstein, L. J. Goad, A. D. H. Clague, and L. J. Mulheirn, *Phytochemistry*, **15**, 195 (1976).
15) Weak signals corresponding to cholestane-type derivatives[14] were observed (^{1}H-NMR, δ 0.907, 0.865, 0.860, each d, J=7.0 Hz).
16) W. C. Still, M. Kahn, and A. Mitra, *J. Org. Chem.*, **43**, 2923 (1978).

Purines. XLVIII.[1] Syntheses and Proton Nuclear Magnetic Resonance Study of 2-Deuterioadenines Substituted or Unsubstituted at the 9-Position and of Their *N*-Oxygenated Derivatives

Tozo FUJII,* Tohru SAITO, Kyoko KIZU, Hiromi HAYASHIBARA, Yukinari KUMAZAWA, Satoshi NAKAJIMA, and Tetsunori FUJISAWA

Faculty of Pharmaceutical Sciences, Kanazawa University, Takara-machi, Kanazawa 920, Japan. *Received August 17, 1990*

A detailed account is given of the syntheses of 9-alkyl-2-deuterioadenines (5b—d), adenosine-2-*d* (5e), and 2′-deoxyadenosine-2-*d* (5f) from the 9-substituted adenines 1b—f through cyclization of the aminoimidazolecarboxamidine salts 9 or the corresponding free bases 8 with formic-*d* acid-*d* or 1-(formyl-*d*)-2(1*H*)-pyridone. Glycosidic hydrolysis of 5e with boiling 0.5 N aqueous HCl afforded adenine-2-*d* (5a) in 77% yield. Peracid oxidation of 5a—e produced the corresponding 1-*N*-oxides (12a—e) in fair yields. Methylation of 9-methyl- (12b) and 9-benzyladenine-2-*d* 1-oxide (12d) and adenosine-2-*d* 1-oxide (12e) with MeI in $AcNMe_2$ gave the corresponding 1-methoxy derivatives (13b, d, e) in good yields. Dimroth rearrangements of 13b, 13d, and 13e *via* the free bases 14b, 14d, and 14e furnished the N^6-methoxy isomers 15b, 15d, and 15e, but their isotopic purities were unsatisfactory. Unambiguous assignments of the purine-ring proton signals in the proton nuclear magnetic resonance spectra of the unlabeled adenines (1a—f, 2a—e, 3b, d, and 10e) have been made by comparison with those of the labeled species (5a—f, 12a—e, 13b, d, and 14e).

Keywords 2-deuterioadenine; 9-substituted 2-deuterioadenine; adenine ring fission; aminoimidazolecarboxamidine cyclization; *N*-oxide; peracid oxidation; *N*-oxide *O*-methylation; Dimroth rearrangement; isotopic exchange; adenine ring proton NMR

The hydrogen at C(8) of purines can undergo isotopic exchange through an ionic process, providing, for example, a quick and convenient access to labeled adenine.[2] However, the exchange is reversible in H_2O,[2c,f,3] and this reversibility often limits the usefulness of C(8)-H labeled purines in biochemical, mechanistic, and spectroscopic studies. The more stable C(2)-H labeled purines[2c] may be secured by catalytic hydrogen exchange at both C(2) and C(8) and subsequent selective delabeling from C(8) in H_2O[3] or by isotopic hydrogenolysis of 2-halopurines.[4] Depending on the structures of the target purines, however, these C(2)-H labeling methods may frequently be inconvenient or difficult to carry out and may not always guarantee the correctness of the labeled position and/or the magnitude of labeling.[2i] A solution to this problem in the adenine series would be furnished by application of the "fission and reclosure" technology[5,6] developed in our laboratory for modification of the adenine ring. It was along this line that we were recently able to prepare some C(2)-deuterated adenine derivatives of usual and unusual structures.[6f,i,7] This paper describes a similar approach adopted originally for the synthesis of 2-deuterioadenines (type **5**) substituted or unsubstituted at the 9-position, together with their conversions into the corresponding 1-*N*-oxides (type **12**) and 1-methoxy and N^6-methoxy derivatives (types **13**, **14**, and **15**). The unlabeled species of most of these 2-deuterated derivatives have been awaiting unambiguous assignments of the purine-ring proton signals in their proton nuclear magnetic resonance (^{1}H-NMR) spectra. Brief accounts of the results reported here have been published in preliminary form.[8]

The first targets for synthesis in the present study were 9-substituted 2-deuterioadenines (**5b—f**), which we planned to prepare from the aminoimidazolecarboxamidines **8b—f** or their hydrochlorides (**9b—f**) by cyclization incorporating a deuterated C_1 unit. On the basis of our previous work,[5,6,9] the required monocycles **9b—f** should be available from 9-substituted adenines (**1b—f**) in four steps involving N(1)-oxidation to give the 1-*N*-oxides **2b—f**, *O*-alkylation to give the 1-alkoxy derivatives (type **3**), hydrolytic ring opening to give the *N*′-alkoxyimidazole-4-carboxamidines (type **4**), and hydrogenolytic dealkoxylation (Chart 1). Thus, **9b—e** were prepared according to the previously reported procedures,[9] and **9d** and **9e** were alternatively obtained in 75% and 54% overall yields, respectively, from the 1-methoxy analogues **3d**[10] and **10e**[11] (derived from **3e**[12]) through **4d** (82% yield from **3d**) and **4e** (57% yield from **10e**). Adenosine 1-oxide (**2e**),[13] the intermediate used for the preparation of **10e** from adenosine (**1e**), had previously been obtained in the form of the monohydrate[10] in 65% or 80% yield by oxidation of **1e** with 30% aqueous H_2O_2 in AcOH at 30 °C for 5 d[14] or at 50 °C overnight,[15] respectively. However, we found that the reaction proceeded much faster and with a higher yield (81%) of **2e**·H_2O when **1e** was oxidized with *m*-chloroperbenzoic acid in MeOH at 30 °C for 7 h.

A parallel sequence of reactions was applied to the synthesis of the 2-deoxyribofuranosyl analogue **9f**. Thus, the 1-oxide **2f**[16] was allowed to react with MeI in $AcNMe_2$ at 13—14 °C for 6.5 h. The methylated product (**3f**) was treated successively with Amberlite IRA-402 (HCO_3^-) and boiling aqueous NaOH (15 min), and the resulting *N*′-methoxycarboxamidine **4f** (64% overall yield from **2f**) was catalytically hydrogenolyzed in the usual manner to produce **9f**.

Cyclization of **9b—d** to give 9-alkyl-2-deuterioadenines (**5b—d**) through the deuterioformamido derivatives **6b—d** by incorporation of a deuterated C_1 unit was then effected in formic-*d* acid-*d* (of over 99% isotopic purity) at 70—75 °C for 16 h, affording **5b**, **5c**, and **5d** in 84%, 54%, and 56% yields, respectively. The use of a C_1 unit in the form of a formic acid in the cyclization of the aminoimidazolecarboxamidines **9b—d** was analogous to the procedures reported for the preparation of adenine-2-^{14}C[17] and some 2-deuterioadenine derivatives.[6f,7] An alternative deuterioformylation agent used for the same purpose was

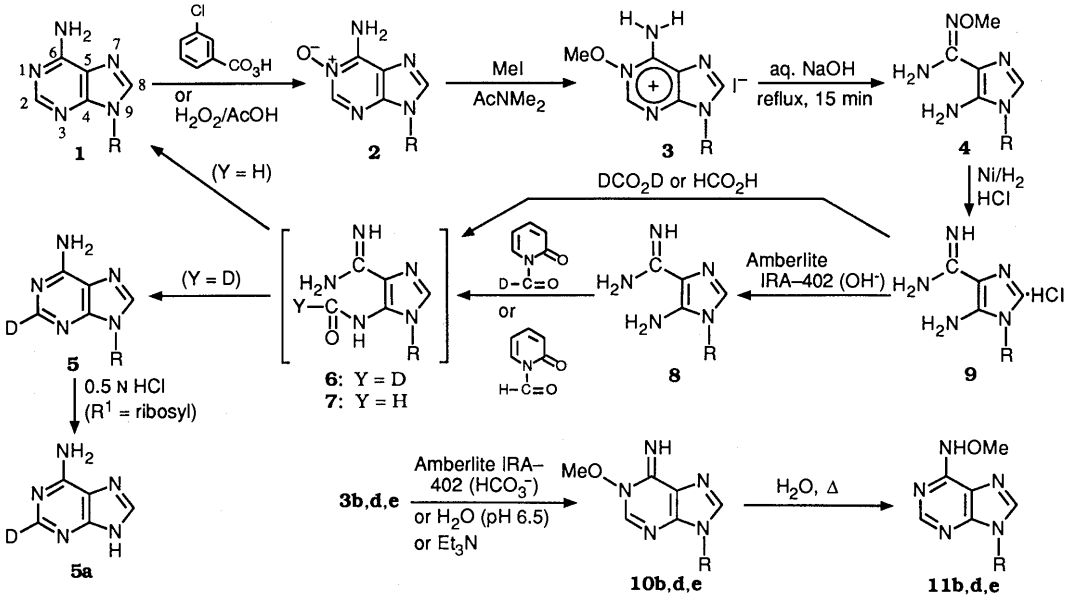

a: R = H **b**: R = Me **c**: R = Et

d: R = $PhCH_2$ **e**: R = 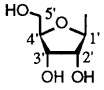 **f**: R = 

Chart 1

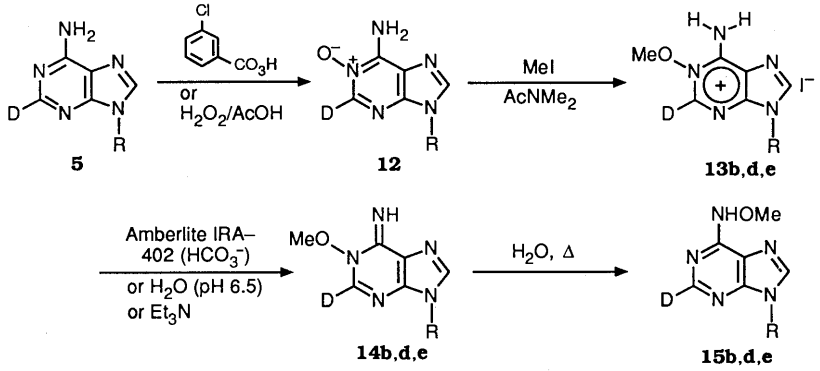

a: R = H **b**: R = Me **c**: R = Et

d: R = $PhCH_2$ **e**: R = 

Chart 2

1-(formyl-*d*)-2(1*H*)-pyridone, which we prepared from 2(1*H*)-pyridone by treatment with formic-*d* acid-*d* (of over 99% isotopic purity) and dicyclohexylcarbodiimide in CH_2Cl_2 at 0 °C for 2 h, the procedure being patterned after that reported[18] for the synthesis of 1-formyl-2(1*H*)-pyridone. Treatment of the free base **8b**, obtained from the hydrochloride **9b** by passing its aqueous solution through a column of Amberlite IRA-402 (OH^-), with 1-(formyl-*d*)-2(1*H*)-pyridone in boiling MeCN for 1.5 h produced 9-methyladenine-*2-d* (**5b**) in 62% yield. In view of the instability of the glycosidic bond under the former cyclization conditions, the latter cyclization method was then applied to the nucleoside **8e** with a slight modification. The hydrochloride **9e** was first converted into the free nucleoside **8e** by the use of Amberlite IRA-402 (OH^-). On treatment with 1-(formyl-*d*)-2(1*H*)-pyridone in $AcNMe_2$ at room temperature for 4.5 h, **8e** gave adenosine-*2-d* (**5e**) in 42% overall yield (from **4e**). 2′-Deoxyadenosine-*2-d* (**5f**) was likewise prepared from **9f** in 37% overall yield (from **4f**).

The correctness of the above synthetic outcome was supported by parallel cyclizations of **9b** with formic acid and of **8e** with 1-formyl-2(1*H*)-pyridone, which furnished 9-methyladenine (**1b**) and adenosine (**1e**) in 70% and 43% (from **4e**) yields, respectively. A similar cyclization of **8b** with 1-formyl-2(1*H*)-pyridone gave **1b** in 62% or 64% overall yield (from **9b** or **4b**, respectively). Finally, glycosidic hydrolysis of adenosine-*2-d* (**5e**) in boiling 0.5 N aqueous HCl for 2 h provided adenine-*2-d* (**5a**), another target unsubstituted at the 9-position, in 77% yield. All the 2-deuterioadenines **5a**—**f** thus obtained had deuterium

contents virtually equal in order of magnitude to that of the formic-*d* acid-*d* used in the cyclization step.

Next we synthesized the 1-*N*-oxides **12a—e** from the above 2-deuterioadenines (**5a—e**), together with some 1-methoxy (**13b, d** and **14e**) and N^6-methoxy derivatives (**15b, d, e**), as shown in Chart 2. The sequence of conversions adopted in these syntheses was essentially the same as that reported previously for the unlabeled series [**1**→**2**[10,13a,19]→**3**[10,11]→**10**[11,19]→**11**[7,12,20] (Chart 1)]. Thus, oxidation of **5a** with 30% aqueous H_2O_2 in AcOH at room temperature for 7 d gave the 1-*N*-oxide **12a**, which was isolated in 61% yield in the form of the monohydrate (**12a**·H_2O). Oxidations of **5b—e** with *m*-chloroperbenzoic acid in MeOH at room temperature or 30 °C for 4—4.5 h produced the corresponding 1-*N*-oxides, **12b**·H_2O (65% yield), **12c** (72%), **12d** (71%), and **12e**·H_2O (59%). In an attempt to prepare **12a** from **12e** by glycosidic hydrolysis, **12e**·H_2O was heated in 0.5 N aqueous HCl under reflux for 10 min or at 80 °C for 10—210 min. However, we were unable to isolate **12a**·H_2O from the reaction mixture. This lack of success was attributable to the instability of the adenine ring caused by the *N*-oxide function.[13b,21]

Among the 1-*N*-oxides thus obtained, **12b**·H_2O was treated with MeI in $AcNMe_2$ at 25 °C for 36 h, giving 1-methoxy-9-methyladenine-*2-d* hydriodide (**13b**) in 93% yield. A similar methylation of **12d** for 48 h afforded 9-benzyl-1-methoxyadenine-*2-d* hydriodide (**13d**) in 98% yield. Adenosine-*2-d* 1-oxide monohydrate (**12e**·H_2O) was likewise methylated for 24 h, and the product (presumed to be **13e**) was treated with Et_3N in EtOH, furnishing the free nucleoside **14e** in 66% yield. All the 1-*N*-oxides **12a—e** and the 1-methoxy derivatives **13b, d** had deuterium contents at the specified position equal to those of the starting 2-deuterioadenines **5a—e**, but the deuterium content in **14e** was only *ca.* 60%, as determined by ^{1}H-NMR spectroscopic analysis. The observed partial delabeling was probably due to isotopic exchange through an ionic process similar to that[2,3] proposed for isotopic exchange at C(8)-H of purines, and the electron-withdrawing 1-methoxy group might have facilitated the delabeling at C(2) when the crude **13e** was treated with Et_3N in EtOH.

The N^6-methoxy derivatives (**15b** and **15d**) of 9-methyl- and 9-benzyladenine-*2-d* were previously prepared by us from **4b** and **4d**, respectively, by cyclization using formic-*d* acid-*d* in MeCN.[7] However, the desired products were contaminated with the corresponding 2,8-dideuterated species to the extent of 16—50%. In the present study, we tried to prepare **15b, d** from **13b, d** through **14b, d** by Dimroth rearrangement. Thus, the hydriodide salt **13b** was converted into the free base **14b** by use of Amberlite IRA-402 (HCO_3^-) in H_2O, and treatment of **14b** with boiling H_2O for 3 h produced **15b**[7] in 51% yield. Treatment of **13d** with boiling 0.5 N phosphate buffer (pH 6.5) for 4 h provided **15d**[7] in 81% yield. A similar Dimroth rearrangement of **14e** in H_2O at 80—85 °C for 5 h gave **15e** in 41% yield. The deuterium contents in **15b**, **15d**, and **15e** at the 2-position as determined by ^{1}H-NMR and/or mass spectroscopic analysis were 82%, 77%, and *ca.* 60%, respectively.

Now that a series of 2-deuterioadenines substituted or unsubstituted at N(9) and their *N*-oxygenated derivatives were in hand, it was possible to compare their ^{1}H-NMR spectra with those of the unlabeled species. Table I assembles the chemical shifts for the protons of adenine-*2-d* (**5a**) and its 9-substituted derivatives (**5b—f**), together with those of the isotopically unmodified counterparts (**1a—f**). It may be seen that in adenine (**1a**) the C(2)-proton resonates at lower field than does the C(8)-proton, whereas the reverse is the case in 9-benzyladenine (**1d**), adenosine (**1e**), and 2′-deoxyadenosine (**1f**). This is in agreement with what has been reported.[22] However, the generalization[22b] that the C(2)-proton of a 9-substituted adenine resonates at higher field than the C(8)-proton does not hold true for 9-methyladenine (**1b**) and 9-ethyladenine (**1c**). In this series, the regions where the C(2)- and C(8)-protons resonate have a crossing at the N(9)-Et level. This emphasizes the importance of careful assignments of the ring-proton signals in the NMR spectra of 9-substituted adenines. It is also interesting that the C(8)-protons of the 9-benzyl

Table I. ^{1}H-NMR Data for Adenine and 9-Substituted Adenines

Compound			Chemical shift (δ)[a] in Me_2SO-d_6				
No.	N(9)-R[b]	Label at C(2)	C(2)-H	C(8)-H	NH_2	Other protons[c]	$\delta_{C(2)-H}-\delta_{C(8)-H}$
5a	H	D	—	8.07	7.05	—	—
1a	H	None	8.10	8.07	7.05	—	+0.03
5b	Me	D	—	8.08	7.16	3.72 (s, Me)	—
1b	Me	None	8.15	8.08	7.16	3.72 (s, Me)	+0.07
5c	Et	D	—	8.15	7.16	1.40 (t, $CH_2\underline{Me}$)[d] 4.17 (q, $C\underline{H}_2Me$)[d]	—
1c	Et	None	8.15	8.15	7.18	1.40 (t, $CH_2\underline{Me}$)[d] 4.18 (q, $C\underline{H}_2Me$)[d]	±0.00
5d	$PhCH_2$	D	—	8.24	7.21	5.37 (s, $C\underline{H}_2Ph$) 7.31 (s, $CH_2\underline{Ph}$)	—
1d	$PhCH_2$	None	8.14	8.24	7.22	5.37 (s, $C\underline{H}_2Ph$) 7.31 (s, $CH_2\underline{Ph}$)	−0.10
5e	Rib	D	—	8.34	7.34		—
1e	Rib	None	8.13	8.34	7.33		−0.21
5f	dRib	D	—	8.32	7.28		—
1f	dRib	None	8.13	8.32	7.28		−0.19

a) Measured at 20—80 mM concentration at 25 °C and expressed in ppm downfield from internal Me_4Si. The letter(s) in parentheses designate(s) the multiplicity or shape or assignment of the signal; the abbreviations are given in Experimental. *b*) Rib = β-D-ribofuranosyl; dRib = 2-deoxy-β-D-ribofuranosyl. *c*) Those of the sugar moiety are not included. *d*) With J = 7 Hz.

TABLE II. ^{1}H-NMR Data for N(1)-Oxygenated Adenines

Compound			Chemical shift (δ)[a] in Me_2SO-d_6					
No.	N(9)-R[b]	Label at C(2)	C(2)-H	C(8)-H	NH_2 or NH	OMe	Other protons[c]	$\delta_{C(2)-H}-\delta_{C(8)-H}$
12a·H_2O	H	D	—	8.28	—[d]	—	—	—
2a·H_2O	H	None	8.59	8.29	—[d]	—	—	+0.30
12b·H_2O	Me	D	—	8.27	—[d]	—	3.76 (Me)	—
2b	Me	None	8.65	8.29	—[d]	—	3.76 (Me)	+0.36
12c	Et	D	—	8.33	8.22 (br)	—	1.42 (t, CH_2Me)[e] 4.20 (q, CH_2Me)[e]	—
2c	Et	None	8.62	8.33	8.22 (br)	—	1.42 (t, CH_2Me)[e] 4.20 (q, CH_2Me)[e]	+0.29
12d	$PhCH_2$	D	—	8.43	—[d]	—	5.40 (s, CH_2Ph) 7.32 (s, CH_2Ph)	—
2d	$PhCH_2$	None	8.65	8.46	—[d]	—	5.41 (s, CH_2Ph) 7.33 (s, CH_2Ph)	+0.19
12e·H_2O	Rib	D	—	8.54	8.34 (br)	—		—
2e·H_2O	Rib	None	8.61	8.55	8.38 (br)	—		+0.06
13b	Me	D	—	8.52	9.67, 10.27	4.18	3.85 (Me)	—
3b	Me	None	9.17	8.52	9.66, 10.27	4.18	3.85 (Me)	+0.65
13d	$PhCH_2$	D	—	8.71	9.70, 10.30	4.16	5.50 (s, CH_2Ph) 7.37 (s, CH_2Ph)	—
3d	$PhCH_2$	None	9.15	8.71	9.4—10.6	4.16	5.50 (s, CH_2Ph) 7.37 (s, CH_2Ph)	+0.44
14e	Rib	D	(8.48)[f]	8.27	—[d]	4.02		(+0.21)
10e	Rib	None	8.42	8.23	6.8—7.8	4.02		+0.19

a) Measured at 7—41 mM concentration at 25 °C. The symbols and abbreviations are as defined in Table I. *b*) Rib = β-D-ribofuranosyl. *c*) Those of the sugar moiety are not included. *d*) No clear signal was observed. *e*) With J = 7 Hz. *f*) Found to contain the delabeled species (**10e**) to the extent of 40%. See the text for details.

(**1d**), 9-ribosyl (**1e**), and 9-(2-deoxyribosyl) (**1f**) analogues are somewhat less shielded than those of the other 9-alkyl analogues, paralleling our experience in similar structures.[6f,7]

Table II lists the chemical shifts for the protons of the N(1)-oxygenated 2-deuterioadenines (**12a—e**, **13b, d**, and **14e**) and those of the isotopically unmodified species (**2a—e**, **3b, d**, and **10e**).[23] It may be seen that in all 1-*N*-oxides (**2a—e**) the C(2)-proton resonates at lower field than does the C(8)-proton by 0.06—0.36 ppm, reflecting the dipolar structure of the *N*-oxide function in the pyrimidine moiety. This tendency is even more pronounced in the cases of the 1-methoxy derivatives **3b** and **3d**, where the positive charge and the electron-withdrawing methoxy group in the pyrimidine moiety lower the electron density at C(2). A similar effect of the 1-methoxy group may still be operative in the free nucleoside **10e**, in which the C(2)-proton is less shielded than the C(8)-proton by 0.19 ppm. Interestingly, the C(8)-protons of the 9-benzyl (**2d** and **3d**) and 9-ribosyl (**2e**) analogues are somewhat less shielded than those of the other 9-alkyl analogues, as in the cases of the above nonoxygenated series.

With the unambiguous assignments of the ring-proton signals made possible as described above, we then checked the selectivity in hydrogen exchange at C(2) and C(8) of a few adenine derivatives by means of ^{1}H-NMR spectroscopy. It is well known that adenine (**1a**) and 9-substituted adenines (type **1**) including adenosine (**1e**) undergo hydrogen exchange at C(8) much faster than at C(2).[2b,c,f,i] In our hands, adenosine-*8-d* (**16**), prepared from **1e** according to the reported deuterium-labeling procedure[24] (Chart 3), underwent delabeling in H_2O at 85 °C at a rate of 0.41 h^{-1} (half life 1.7 h). On the other hand, the label of adenosine-*2-d* (**5e**) was completely stable under similar conditions for at least 6 h. In order to investigate the effect of the 1-*N*-oxide

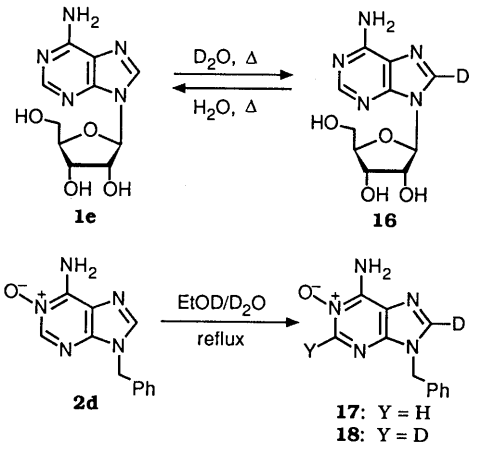

Chart 3

function on such selectivity, 9-benzyladenine 1-oxide (**2d**) was heated in a 10% (w/w) solution of EtOD in D_2O under reflux. Deuteration at C(8) (to form **17**) was 65% at 6 h; it was *ca.* 100% at C(8) at 24 h with 10% deuteration at C(2) (to form **18**). Further labeling in boiling CD_3CO_2D for 9 h did not complete hydrogen exchange at C(2). These results indicate that the effect of the 1-*N*-oxide function on isotopic exchange of C(2)-H is not significant.

In conclusion, the present work has established a general synthetic route to 2-deuterioadenines (type **5**), substituted or unsubstituted at the 9-position, and their N(1)-oxygenated derivatives (types **12** and **13**) of high isotopic purity. As a result of the syntheses of these 2-deuterated species, unambiguous assignments of the C(2)- and C(8)-proton signals in the NMR spectra of isotopically unmodified species (types **1**—**3**) have now become possible. These labeled compounds should be useful, because of their stability to isotopic exchange, as starting materials for

syntheses of a variety of adenine structures or as substrates for biochemical and spectroscopic investigations. Conversion of **13** into the N^6-methoxy isomer **15** was possible by Dimroth rearrangement, but the deuterium content of **15** was unsatisfactory.

Experimental

General Notes All melting points were determined by using a Yamato MP-1 capillary melting point apparatus and are corrected. See ref. 6*b* for details of instrumentation and measurements. The deuterium contents of deuterated samples were determined by ^{1}H-NMR spectroscopic analysis or mass spectroscopic analysis[25] in the usual manner. Elemental analyses were performed by Mr. Y. Itatani and his associates at Kanazawa University. The following abbreviations are used: br = broad, d = doublet, dd = doublet-of-doublets, m = multiplet, q = quartet, s = singlet, t = triplet.

Materials The known compounds used for the ^{1}H-NMR spectroscopic study were taken from stocks of commercial origin or which had been prepared according to published procedures: **1a**, **1e**, and **1f** (purchased from Seikagaku Kogyo Co.); **1b**—**d**[19,26]; **2a**—**d**[10,13a,19]; **2e**·H_2O[14]; **3b**[10]; **3d**[10]; **10e**.[11] Adenosine 1-oxide monohydrate (**2e**·H_2O) was alternatively prepared according to a new procedure developed in the present study, and other compounds were synthesized as described below.

Adenosine 1-Oxide Monohydrate (2e·H_2O) A mixture of adenosine (**1e**) (14.03 g, 52.5 mmol) and *m*-chloroperbenzoic acid (of 80% purity) (22.65 g, 105 mmol) in MeOH (1.5 l) was stirred at 30 °C for 7 h. After cooling, the reaction mixture was filtered to collect an insoluble solid, which was recrystallized from H_2O (160 ml) to yield colorless needles. The crystals were dried over P_2O_5 at 3 mmHg and 60 °C for 14 h and then kept in a closed vessel saturated with H_2O until they reached constant weight, giving a first crop (10.63 g, 67%) of **2e**·H_2O, mp 217—220 °C (dec.) [lit.[10,14] mp 224—225 °C (dec.)]. This sample was identical [by mixture melting point test and comparison of the infrared (IR) spectrum and thin-layer chromatographic (TLC) mobility] with authentic **2e**·H_2O.[10,14] The methanolic filtrate, obtained when the reaction mixture was filtered, was combined with activated carbon (15 g) and then stirred at room temperature for 4 h. The resulting mixture was filtered, and the filtrate was concentrated *in vacuo* to a volume of 400 ml, diluted with ether (400 ml), and kept in a refrigerator for 2 h. The precipitate that resulted was filtered off, recrystallized from H_2O (25 ml), and dried as described above for the first crop, yielding a second crop (2.18 g, 14%) of **2e**·H_2O. The total yield of **2e**·H_2O was 12.81 g (81%).

1-Methoxy-2′-deoxyadenosine Hydriodide (3f) A mixture of 2′-deoxyadenosine 1-oxide (**2f**)[16] (1.87 g, 7 mmol) and MeI (4.97 g, 35 mmol) in $AcNMe_2$ (14 ml) was stirred at 13—14 °C for 6.5 h. The resulting solution was diluted with ether (70 ml), and the solid that deposited was separated from the ethereal layer by decantation, washed with two 20-ml portions of ether, and dried to give crude **3f** (3.37 g) as a hygroscopic colorless solid. This sample was directly used in the next step without further purification.

5-Amino-1-benzyl-*N*′-methoxy-1*H*-imidazole-4-carboxamidine (4d) A stirred mixture of **3d**[10] (2.49 g, 6.5 mmol) and a solution of NaOH (1.60 g, 40 mmol) in H_2O (33 ml) was heated under reflux for 15 min. After cooling, the precipitate that resulted was filtered off, washed with H_2O, and dried to give **4d** (1.30 g, 82%), mp 117.5—119.5 °C. Recrystallization from H_2O yielded an analytical sample as slightly pinkish needles, mp 118.5—119.5 °C; UV $\lambda_{max}^{95\%\ EtOH}$ 264.5 nm (ε 11200); $\lambda_{max}^{H_2O}$ (pH 1) 280 (9700); $\lambda_{max}^{H_2O}$ (pH 7) 263 (10200); $\lambda_{max}^{H_2O}$ (pH 13) 263 (10200); ^{1}H-NMR (Me_2SO-d_6) δ: 3.64 (3H, s, OMe), 5.07 (2H, s, C$\underline{H}_2$Ph), 5.37 (2H, dull s, NH_2),[9] 5.49 (2H, dull s, amidine NH_2),[9] 7.1—7.45 (6H, m, Ph and imidazole protons). *Anal.* Calcd for $C_{12}H_{15}N_5O$: C, 58.76; H, 6.16; N, 28.55. Found: C, 58.49; H, 6.33; N, 28.49.

5-Amino-*N*′-methoxy-1-β-D-ribofuranosyl-1*H*-imidazole-4-carboxamidine (4e) A stirred mixture of **10e**[11] (892 mg, 3 mmol) and a solution of NaOH (0.90 g, 22.5 mmol) in H_2O (15 ml) was heated under reflux for 15 min. After cooling, the reaction mixture was brought to pH 4 with 10% aqueous HCl and then to pH 8 with saturated aqueous $NaHCO_3$ and concentrated *in vacuo*. The residue was dried and extracted with hot EtOH (4 × 10 ml). The ethanolic extracts were combined and concentrated *in vacuo* to leave a gum, which was chromatographed on a silica gel column using AcOEt–EtOH (4 : 1, v/v) as the eluent. Earlier fractions gave **4e** (491 mg, 57%) as a colorless solid, mp 131—135 °C. Recrystallization of the solid from MeCN yielded an analytical sample of **4e** as colorless prisms, mp 148.5—149.5 °C; MS *m/z*: 287 (M^+); UV $\lambda_{max}^{95\%\ EtOH}$ 222 nm (ε 10500), 262 (11000); $\lambda_{max}^{H_2O}$ (pH 1) 283 (9600); $\lambda_{max}^{H_2O}$ (pH 7) 222 (11000), 258 (10500); $\lambda_{max}^{H_2O}$ (pH 13) 259 (9500); ^{1}H-NMR (Me_2SO-d_6) δ: 3.59 [2H, br, C(5′)-H_2], 3.65 (3H, s, OMe), 3.8—4.4 [3H, m, C(4′)-H, C(3′)-H, and C(2′)-H], 5.0—7.0 [8H, m, NH_2's, OH's, and C(1′)-H], 7.33 [C(2)-H].[27] *Anal.* Calcd for $C_{10}H_{17}N_5O_5$: C, 41.81; H, 5.96; N, 24.38. Found: C, 41.91; H, 5.88; N, 24.34.

Later fractions in the above chromatography afforded N^6-methoxyadenosine hemihydrate (**11e**·1/2H_2O) (109 mg, 12%) as a colorless solid, mp 189—190 °C (dec.). This sample was identical (by comparison of the IR spectrum and TLC mobility) with authentic **11e**·1/2H_2O.[12]

5-Amino-1-(2-deoxy-β-D-ribofuranosyl)-*N*′-methoxy-1*H*-imidazole-4-carboxamidine (4f) A solution of the above crude **3f** (3.37 g) in H_2O (20 ml) was passed through a column of Amberlite IRA-402 (HCO_3^-) (17 ml), and the column was eluted with H_2O. The eluate (100 ml) was concentrated *in vacuo* to leave the free nucleoside **10f** as a yellowish oil. This oil was dissolved in a mixture of NaOH (1.77 g) and H_2O (35 ml), and the resulting solution was heated under reflux for 15 min. After cooling, the reaction mixture was first brought to pH 6 with 10% aqueous HCl and then to pH 8 with saturated aqueous $NaHCO_3$ and concentrated *in vacuo*. The residue was co-evaporated with three 10-ml portions of EtOH *in vacuo* and then extracted with boiling EtOH (3 × 25 ml). The ethanolic extracts were combined and concentrated *in vacuo* to leave a glass. The glass was chromatographed on a silica gel column [AcOEt–EtOH (7 : 1, v/v)] to furnish **4f** (1.21 g, 64% overall yield from **2f**), mp 138—139 °C. Recrystallization from AcOEt gave an analytical sample as colorless prisms, mp 138—139 °C; MS *m/z*: 271 (M^+); UV $\lambda_{max}^{95\%\ EtOH}$ 222 nm (ε 10800), 262 (11400); $\lambda_{max}^{H_2O}$ (pH 1) 282 (9900); $\lambda_{max}^{H_2O}$ (pH 7) 222 (10600), 259 (10000); $\lambda_{max}^{H_2O}$ (pH 13) 259 (10100); ^{1}H-NMR (Me_2SO-d_6) δ: 2.0—2.6 [2H, m, C(2′)-H_2], 3.53 [2H, m, C(5′)-H_2], 3.64 (3H, s, OMe), 3.79 [1H, m, C(4′)-H], 4.32 [1H, m, C(3′)-H], 5.07 [1H, t, J = 5 Hz, C(5′)-OH], 5.24 [1H, dd, J = 6, 8 Hz, C(1′)-H], 7.34 [1H, s, C(2)-H].[27] *Anal.* Calcd for $C_{10}H_{17}N_5O_4$: C, 44.28; H, 6.32; N, 25.82. Found: C, 44.18; H, 6.39; N, 25.61.

5-Amino-1-benzyl-1*H*-imidazole-4-carboxamidine Hydrochloride (9d) A solution of **4d** (1.10 g, 4.5 mmol) in a mixture of H_2O (90 ml) and 1 N aqueous HCl (4.5 ml) was hydrogenated over Raney Ni W-2 catalyst[28] (1.8 ml) at atmospheric pressure and 25 °C for 7 h. The catalyst was removed by filtration and washed with H_2O (30 ml). The filtrate and washings were combined and concentrated *in vacuo* to give **9d** (1.04 g, 92%). A small portion (25 mg) of this sample was converted into the monopicrate in a manner similar to that described previously,[9] giving yellow needles (34 mg, 71% from **4d**), mp 237.5—239.5 °C (dec.) [lit.[9] mp 237.5—239.5 °C (dec.)]. The picrate was identical (by comparison of the IR spectrum) with an authentic specimen.[9]

5-Amino-1-β-D-ribofuranosyl-1*H*-imidazole-4-carboxamidine Hydrochloride (9e) A solution of **4e** (861 mg, 3 mmol) in a mixture of H_2O (64 ml) and 1 N aqueous HCl (3 ml) was hydrogenated over Raney Ni W-2 catalyst[28] (0.9 ml) at atmospheric pressure and 26 °C for 2.5 h. The catalyst was removed by filtration and washed with H_2O (10 ml). The filtrate and washings were combined and concentrated *in vacuo*, and the residual reddish brown oil was dried to give crude **9e** (837 mg, 95%). A small portion of this sample was converted into the monopicrate monohydrate, mp 182.5—184 °C (dec.), in a manner similar to that described previously.[9] This picrate was identical (by comparison of the IR spectrum) with an authentic specimen.[9]

5-Amino-1-β-D-ribofuranosyl-1*H*-imidazole-4-carboxamidine (8e) A small amount (550 mg) of **9e** was dissolved in hot H_2O (10 ml), and the aqueous solution was immediately cooled in an ice bath. The cooled solution was passed through a column of Amberlite IRA-402 (OH^-) (4 ml), and the column was eluted with H_2O (150 ml). The eluate was concentrated *in vacuo*, and the residual oil (**8e**) was dried over P_2O_5 at 3 mmHg and room temperature for 12 h. The dried sample was directly used in the next cyclization step without purification.

5-Amino-1-(2-deoxy-β-D-ribofuranosyl)-1*H*-imidazole-4-carboxamidine (8f) A solution of **4f** (271 mg, 1 mmol) in a mixture of H_2O (20 ml) and 1 N aqueous HCl (1 ml) was hydrogenated over Raney Ni W-2 catalyst[28] (0.4 ml) at atmospheric pressure and room temperature for 4.5 h. The catalyst was removed by filtration and washed with a little H_2O. The filtrate and washings, presumed to contain **9f**, were combined and passed through a column of Amberlite IRA-402 (OH^-) (3 ml), and the column was eluted with H_2O (100 ml). The eluate was concentrated *in vacuo* to leave an oil (**8f**), which was dried over P_2O_5 at 3 mmHg and room temperature overnight and used directly in the next cyclization step without purification.

Cyclization of 5-Amino-1-methyl-1*H*-imidazole-4-carboxamidine Hy-

drochloride (9b) to 9-Methyladenine (1b) A stirred mixture of **9b**[9] (211 mg, 1.2 mmol) and formic acid (of over 98% purity) (2 ml, 53 mmol) was heated in an oil bath kept at 80—90 °C for 16 h. The reaction mixture was concentrated *in vacuo*, and the residue was co-evaporated with a mixture of H_2O and EtOH *in vacuo* to leave a pale yellowish solid. The solid was dissolved in H_2O (0.5 ml) by application of heat, and the resulting solution was brought to pH 8 with saturated aqueous $NaHCO_3$ and then kept in a refrigerator overnight. The crystals that deposited were filtered off, washed with a little H_2O, and dried to give **1b** (126 mg, 70%), mp > 300 °C. This sample was identical (by comparison of the IR spectrum and TLC mobility) with authentic **1b**.[19,26]

Cyclization of 5-Amino-1-methyl-1*H*-imidazole-4-carboxamidine (8b) to 9-Methyladenine (1b) i) In MeCN: A solution of **9b**[9] (176 mg, 1 mmol) in H_2O (3 ml) was passed through a column of Amberlite IRA-402 (OH^-) (2 ml), and the column was eluted with H_2O (20 ml). The eluate was concentrated *in vacuo* to leave **8b**, which was dried over P_2O_5 at 3 mmHg and 75 °C for 5 h. The crude **8b** was combined with 1-formyl-2(1*H*)-pyridone[18] (616 mg, 5 mmol) in MeCN (25 ml), and the resulting mixture was heated under reflux with stirring for 1.5 h. After addition of EtOH (1 ml), the reaction mixture was kept at room temperature overnight and then concentrated *in vacuo*. The residue was triturated with hot H_2O (20 ml), and an insoluble solid was removed by filtration while hot. Concentration of the aqueous filtrate under reduced pressure, trituration of the residue with EtOH (1 ml) under ice-cooling, and filtration of the resulting mixture left **1b** (92 mg, 62%) as a grayish solid, mp 298—300 °C. This sample was identical (by comparison of the IR spectrum and TLC mobility) with authentic **1b**.[19,26]

ii) In $HCONMe_2$: A solution of **4b**[20] (338 mg, 2 mmol) in H_2O (40 ml) containing 1 N aqueous HCl (2 ml) was hydrogenated over Raney Ni W-2 catalyst[28] (0.7 ml) at atmospheric pressure and room temperature for 2 h. The catalyst was removed by filtration and washed with H_2O (20 ml). The filtrate and washings were combined and concentrated *in vacuo* to leave crude **9b**, which was dissolved in H_2O (5 ml) by application of heat. The resulting solution was passed through a column of Amberlite IRA-402 (OH^-) (4 ml), and the column was eluted with H_2O (100 ml). The eluate was concentrated *in vacuo* to leave **8b**, which was dried over P_2O_5 at 3 mmHg and room temperature overnight. The crude **8b** was combined with 1-formyl-2(1*H*)-pyridone[18] (739 mg, 6 mmol) in $HCONMe_2$ (20 ml). The resulting mixture was stirred at room temperature for 4 h and then concentrated *in vacuo*. The residue was combined with 5% aqueous NH_3 (20 ml), and the mixture was stirred at room temperature for 1 h. Concentration of the ammoniacal mixture under reduced pressure left a solid, which was triturated with hot H_2O (15 ml). The insoluble material that resulted was removed by filtration, and the filtrate was concentrated to a volume of *ca.* 2 ml to give a first crop (128 mg, 43% overall yield from **4b**) of **1b**, mp 299—300 °C, identical (by comparison of the IR spectrum and TLC mobility) with an authentic sample.[19,26] The usual work-up of the mother liquor at this stage raised the total yield of **1b** to 192 mg (64% overall yield from **4b**).

Cyclization of 5-Amino-1-β-D-ribofuranosyl-1*H*-imidazole-4-carboxamidine (8e) to Adenosine (1e) A mixture of the total amount of the crude **8e** (*vide supra*), derived from **9e** (550 mg), and 1-formyl-2(1*H*)-pyridone[18] (1.85 g, 15 mmol) in $HCONMe_2$ (20 ml) was stirred at 24 °C for 4 h. The reaction mixture was filtered in order to remove an insoluble material, and the filtrate was concentrated *in vacuo* to leave a solid, which was stirred in 5% aqueous NH_3 (50 ml) at room temperature for 1 h. The ammoniacal mixture was filtered, and the filtrate was concentrated *in vacuo* to leave a solid. The solid was washed successively with boiling benzene (6 × 40 ml) and MeOH and then recrystallized from H_2O to give crude adenosine (**1e**) (225 mg, 43% overall yield from **4e**). Further recrystallization from H_2O yielded a pure sample as colorless needles, mp 231—233 °C, identical (by comparison of the IR spectrum and TLC behavior) with authentic adenosine.

1-(Formyl-*d*)-2(1*H*)-pyridone In following the procedure reported[18] for the synthesis of 1-formyl-2(1*H*)-pyridone from 2(1*H*)-pyridone and formic acid using *N*,*N*′-dicyclohexylcarbodiimide as a condensing agent, replacement of formic acid by formic-*d* acid-*d* (of over 99% isotopic purity) gave crude 1-(formyl-*d*)-2(1*H*)-pyridone in 63% yield as colorless needles, mp 63—65 °C. This sample was directly used for cyclizations of **8b**, **8e**, and **8f** without further purification.

Adenine-2-*d* (5a) A stirred solution of adenosine-2-*d* (**5e**) (*vide infra*) (107 mg, 0.4 mmol) in 0.5 N aqueous HCl (8 ml) was heated under reflux for 2 h. The reaction mixture was concentrated *in vacuo* to leave a pale yellowish residue, which was dissolved in H_2O (1 ml) by application of heat. The resulting solution was brought to pH 7 with saturated aqueous $NaHCO_3$ and kept at room temperature overnight. The slightly yellowish crystals that resulted were filtered off, washed with a little H_2O, and dried to give **5a** (42 mg, 77%), mp > 300 °C. Recrystallization from H_2O and drying over P_2O_5 at 3 mmHg and room temperature for 24 h yielded an analytical sample as slightly yellowish, minute crystals, mp > 300 °C; ^{1}H-NMR (Table I). *Anal.* Calcd for $C_5H_4DN_5 \cdot 1/8H_2O$[29]: C, 43.40; H, 3.82; N, 50.61. Found: C, 43.25; H, 3.74; N, 50.61.

9-Methyladenine-2-*d* (5b) i) From **9b**: A stirred mixture of **9b**[9] (1.40 g, 8 mmol) and formic-*d* acid-*d* (of over 99% isotopic purity) (4 ml, 104 mmol) was heated at 70—75 °C for 16 h. The reaction mixture was concentrated *in vacuo* to leave a grayish solid, which was dissolved in H_2O (1 ml) by application of heat. The resulting solution was brought to pH 8 with saturated aqueous $NaHCO_3$, and the colorless needles that deposited were filtered off, washed with a little H_2O, and dried to give **5b** (1.01 g, 84%), mp > 300 °C. Recrystallization from H_2O produced an analytical sample as colorless needles, mp > 300 °C; MS *m/z*: 150 (M^+); UV $\lambda_{max}^{95\%\ EtOH}$ 261 nm (ε 12900); $\lambda_{max}^{H_2O}$ (pH 1) 259 (14200); $\lambda_{max}^{H_2O}$ (pH 7) 261 (14500); $\lambda_{max}^{H_2O}$ (pH 13) 261 (14500); ^{1}H-NMR (Table I). *Anal.* Calcd for $C_6H_6DN_5$[29]: C, 47.99; H, 4.70; N, 46.63. Found: C, 48.23; H, 4.73; N, 46.41.

ii) From **8b**: A stirred mixture of crude **8b** (*vide supra*) (417 mg, 3 mmol) and 1-(formyl-*d*)-2(1*H*)-pyridone (*vide supra*) (1.85 g, 15 mmol) in MeCN (75 ml) was heated under reflux for 1.5 h. The reaction mixture was concentrated *in vacuo* to leave a solid, which was dissolved in hot H_2O (75 ml). The resulting solution was filtered in order to remove a small amount of an insoluble material. The filtrate was concentrated to a volume of *ca.* 20 ml, brought to pH 9 with 28% aqueous NH_3, and concentrated again to a volume of *ca.* 10 ml. The pH of the resulting solution was adjusted to 9 by addition of 28% aqueous NH_3, and the colorless needles that resulted were filtered off, washed with a little H_2O, and dried to give a first crop (239 mg, 53%) of **5b**, mp > 300 °C. This sample was identical (by comparison of the IR and ^{1}H-NMR spectra and TLC mobility) with the one prepared by method (i). The usual work-up of the mother liquor of the first crop raised the total yield of **5b** to 280 mg (62%).

9-Ethyladenine-2-*d* (5c) A stirred mixture of **9c**[9] (1.33 g, 7 mmol) and formic-*d* acid-*d* (of over 99% isotopic purity) (3.5 ml, 91 mmol) was heated at 70—75 °C for 16 h. The reaction mixture was concentrated *in vacuo*, and the residue was dissolved in a small amount of H_2O. The resulting solution was passed through a column of Amberlite IRA-402 (HCO_3^-) (50 ml), and the column was eluted with H_2O. Concentration of the eluate under reduced pressure left a reddish purple residue, which was dried and recrystallized twice from AcOEt to yield **5c** (618 mg, 54%) as slightly grayish needles, mp 194—196 °C. Further recrystallization from AcOEt furnished an analytical sample as colorless needles, mp 194—196 °C; MS *m/z*: 164 (M^+); ^{1}H-NMR (Table I). *Anal.* Calcd for $C_7H_8DN_5$[29]: C, 51.21; H, 5.52; N, 42.65. Found: C, 51.06; H, 5.55; N, 42.81.

9-Benzyladenine-2-*d* (5d) A solution of **9d** (*vide supra*) (1.01 g, 4 mmol) in formic-*d* acid-*d* (of over 99% isotopic purity) (2 ml, 52 mmol) was heated at 70—75 °C for 16 h. The reaction mixture was concentrated *in vacuo*, and the residual solid was suspended in H_2O (1 ml). The resulting suspension was neutralized with saturated aqueous $NaHCO_3$. The insoluble solid that resulted was filtered off, washed with H_2O, and dried to give a slightly reddish brown solid (751 mg). The solid was dissolved in boiling EtOH (50 ml), and the ethanolic solution was treated with activated carbon. The activated carbon was then removed by filtration, and the filtrate was concentrated to a volume of *ca.* 30 ml and kept in a refrigerator. The crystals that deposited were filtered off, washed with EtOH, and dried to give **5d** (513 mg, 56%) as colorless needles, mp 231—232 °C. Recrystallization from EtOH provided an analytical sample, mp 231.5—232.5 °C; MS *m/z*: 226 (M^+); UV $\lambda_{max}^{H_2O}$ (pH 1) 259 nm (ε 15100); $\lambda_{max}^{H_2O}$ (pH 7) 261 (15300); $\lambda_{max}^{H_2O}$ (pH 13) 261 (15400); ^{1}H-NMR (Table I). *Anal.* Calcd for $C_{12}H_{10}DN_5$[29]: C, 63.70; H, 4.90; N, 30.95. Found: C, 63.87; H, 4.68; N, 30.93.

Adenosine-2-*d* (5e) A mixture of the total amount of **8e**, prepared from **4e** (287 mg, 1 mmol) as described above for **9e** and **8e**, and 1-(formyl-*d*)-2(1*H*)-pyridone (*vide supra*) (745 mg, 6 mmol) in $AcNMe_2$ (10 ml) was stirred at room temperature for 4.5 h. The reaction mixture was concentrated *in vacuo*, and the residue was stirred in 5% aqueous NH_3 (20 ml) at room temperature for 1 h. The precipitate that resulted was removed by filtration, and the filtrate was chromatographed on a column packed with a mixture of Darco G-60 (activated carbon) (2.5 g) and Celite 535 (a filter aid) (5 g) by using H_2O, EtOH, and EtOH–$CHCl_3$ (2 : 1, v/v) in that order as the eluents. Fractions eluted with the first solvent gave 2(1*H*)-pyridone (derived from the deuterioformylating agent), and those eluted with the third solvent afforded crude **5e** (157 mg), which was

then recrystallized from H_2O (5 ml) to yield a pure sample (112 mg, 42% overall yield from **4e**), mp 233—234 °C. Further recrystallization from H_2O provided an analytical sample of **5e** as colorless needles, mp 233—234 °C; MS *m/z*: 268 (M^+); UV $\lambda_{max}^{H_2O}$ (pH 1) 257 nm (ε 14500); $\lambda_{max}^{H_2O}$ (pH 7) 259 (15000); $\lambda_{max}^{H_2O}$ (pH 13) 259.5 (15000); ^{1}H-NMR (Me_2SO-d_6) δ: 3.62 [2H, m, C(5′)-H_2], 3.96 [1H, m, C(4′)-H], 4.15 [1H, m, C(3′)-H], 4.61 [1H, m, C(2′)-H], 5.0—5.55 (3H, m, OH's), 5.89 [1H, d, J=6 Hz, C(1′)-H], other signals (see Table I). *Anal.* Calcd for $C_{10}H_{12}DN_5O_4$[29]: C, 44.78; H, 4.88; N, 26.11. Found: C, 44.71; H, 4.77; N, 26.06.

2′-Deoxyadenosine-2-*d* (5f) A mixture of the total amount of **8f**, obtained from **4f** (271 mg, 1 mmol) as described above under the name of **8f**, and 1-(formyl-*d*)-2(1*H*)-pyridone (*vide supra*) (745 mg, 6 mmol) in $AcNMe_2$ (10 ml) was stirred at room temperature for 4 h. The reaction mixture was worked up in a manner similar to that described above for **5e**, giving **5f**·H_2O (101 mg, 37% overall yield from **4f**), mp 188.5—190 °C (dec.). Recrystallization from H_2O and drying over P_2O_5 at 3 mmHg and room temperature for 24 h afforded an analytical sample as colorless scales, mp 189.5—191 °C (dec.); UV $\lambda_{max}^{95\%\ EtOH}$ 260 nm (ε 14600); $\lambda_{max}^{H_2O}$ (pH 1) 257 (14700); $\lambda_{max}^{H_2O}$ (pH 7) 259.5 (15200); $\lambda_{max}^{H_2O}$ (pH 13) 260 (15200); ^{1}H-NMR (Me_2SO-d_6) δ: 2.1—2.9 [2H, m, C(2′)-H_2], 3.58 [2H, m, C(5′)-H_2], 3.88 [1H, m, C(4′)-H], 4.41 [1H, m, C(3′)-H], 5.1—5.4 [2H, m, C(5′)-OH and C(3′)-OH], 6.34 [1H, dd, J=6, 8 Hz, C(1′)-H], other signals (see Table I). *Anal.* Calcd for $C_{10}H_{12}DN_5O_3 \cdot H_2O$[29]: C, 44.44; H, 5.59; N, 25.91. Found: C, 44.16; H, 5.63; N, 25.84.

Adenine-2-*d* 1-Oxide (12a) A hot solution of **5a**·1/8H_2O (65.7 mg, 0.483 mmol) in AcOH (0.39 ml) was cooled to room temperature, and 30% aqueous H_2O_2 (0.24 ml) was added. The resulting mixture was kept at room temperature for 7 d. The colorless crystals that deposited were filtered off, washed with cold H_2O (1 ml), and dried to yield a first crop (47.7 mg, 58%) of **12a**·H_2O, mp *ca.* 300 °C (dec.). The filtrate and washings were combined, neutralized with anhydrous Na_2CO_3, and kept in a refrigerator to deposit a second crop (2.8 mg, 3%) of **12a**·H_2O, mp 270—295 °C (dec.). The total yield of **12a**·H_2O was 50.5 mg (61%). Recrystallization of the above product from H_2O and drying over P_2O_5 at 3 mmHg and room temperature for 24 h afforded an analytical sample of **12a**·H_2O as colorless, minute prisms, mp >300 °C; MS *m/z*: 152 (M^+); ^{1}H-NMR (Table II). *Anal.* Calcd for $C_5H_4DN_5O \cdot H_2O$[29]: C, 35.30; H, 4.15; N, 41.16. Found: C, 35.29; H, 4.16; N, 41.30.

9-Methyladenine-2-*d* 1-Oxide (12b) A mixture of **5b** (120 mg, 0.8 mmol) and *m*-chloroperbenzoic acid (of 80% purity) (244 mg, 1.2 mmol) in MeOH (12 ml) was stirred at room temperature for 4 h. The precipitate that resulted was filtered off, washed with MeOH, and dried to give a first crop (83 mg, 56%) of **12b**·H_2O, mp 294.5—295.5 °C (dec.). The mother liquor was diluted with ether (10 ml), and the precipitate that resulted was filtered off, washed with ether, and dried to give a second crop (13 mg, 9%), mp 290.5—291.5 °C (dec.). The total yield of **12b**·H_2O was 96 mg (65%). Recrystallization of the first crop of **12b**·H_2O from H_2O and drying over P_2O_5 at 3 mmHg and room temperature for 24 h furnished an analytical sample as colorless prisms, mp >300 °C; MS *m/z*: 166 (M^+); UV $\lambda_{max}^{95\%\ EtOH}$ 235 nm (ε 42900), 263 (7600), 298 (2200); $\lambda_{max}^{H_2O}$ (pH 1) 213.5 (29100), 259 (12000); $\lambda_{max}^{H_2O}$ (pH 7) 232 (43600), 262 (8000), 291 (2200); $\lambda_{max}^{H_2O}$ (pH 13) 231 (29100), 267 (8300), 302 (3750); ^{1}H-NMR (Table II). *Anal.* Calcd for $C_6H_6DN_5O \cdot H_2O$[29]: C, 39.13; H, 4.93; N, 38.03. Found: C, 38.85; H, 5.05; N, 37.94.

9-Ethyladenine-2-*d* 1-Oxide (12c) A solution of **5c** (246 mg, 1.5 mmol) and *m*-chloroperbenzoic acid (of 80% purity) (486 mg, 2.25 mmol) in MeOH (22 ml) was stirred at room temperature for 4.5 h. The colorless solid (35 mg) that deposited was removed by filtration and washed with MeOH (2 ml). The filtrate and washings were combined, diluted with ether (100 ml), and kept in a refrigerator overnight. The precipitate that resulted was filtered off and dried to give **12c** (194 mg, 72%), mp 273.5—276 °C (dec.). Recrystallization from EtOH yielded an analytical sample as colorless, minute crystals, mp 281—284.5 °C (dec.); MS *m/z*: 180 (M^+); ^{1}H-NMR (Table II). *Anal.* Calcd for $C_7H_8DN_5O$[29]: C, 46.66; H, 5.03; N, 38.87. Found: C, 46.87; H, 5.10; N, 39.08.

9-Benzyladenine-2-*d* 1-Oxide (12d) A mixture of **5d** (226 mg, 1 mmol) and *m*-chloroperbenzoic acid (of 85% purity) (305 mg, 1.5 mmol) in MeOH (15 ml) was stirred at room temperature for 4 h. The precipitate that resulted was filtered off and recrystallized from 90% (v/v) aqueous EtOH to give **12d** (171 mg, 71%) as colorless needles, mp 271—272 °C (dec.). Repeated recrystallization from the same solvent afforded an analytical sample, mp 271—272 °C (dec.); MS *m/z*: 242 (M^+); UV $\lambda_{max}^{95\%\ EtOH}$ 235.5 nm (ε 44600), 263 (8300), 299 (2300); $\lambda_{max}^{H_2O}$ (pH 1) 212 (34200), 258.5 (12900); $\lambda_{max}^{H_2O}$ (pH 7) 232 (45600), 261 (8600), 291 (2400); $\lambda_{max}^{H_2O}$ (pH 13) 231 (28000), 268 (9000), 305 (4300); ^{1}H-NMR (Table II). *Anal.* Calcd for $C_{12}H_{10}DN_5O$[29]: C, 59.50; H, 4.58; N, 28.91. Found: C, 59.58; H, 4.63; N, 29.18.

Adenosine-2-*d* 1-Oxide (12e) A mixture of **5e** (150 mg, 0.56 mmol) and *m*-chloroperbenzoic acid (of 80% purity) (243 mg, 1.12 mmol) in MeOH (16 ml) was stirred at 30 °C for 4 h. The reaction mixture was worked up in a manner similar to that described above for **2e**·H_2O, giving **12e**·H_2O in 59% yield. Recrystallization from H_2O and drying over P_2O_5 at 3 mmHg and room temperature for 24 h provided an analytical sample as colorless cubes, mp 231 °C (dec.) (sintered at 220 °C); UV $\lambda_{max}^{95\%\ EtOH}$ 235 nm (ε 39200), 263 (8000), 303 (2200); $\lambda_{max}^{H_2O}$ (pH 1) 258 (12700); $\lambda_{max}^{H_2O}$ (pH 7) 232 (39400), 262 (8400), 294 (2000); $\lambda_{max}^{H_2O}$ (pH 13) 232 (24400), 268 (8900), 305 (4000); ^{1}H-NMR (Me_2SO-d_6) δ: 3.61 [2H, m, C(5′)-H_2], 3.95 [1H, m, C(4′)-H], 4.15 [1H, m, C(3′)-H], 4.53 [1H, m, C(2′)-H], 5.03 [1H, t, J=4 Hz, C(5′)-OH], 5.20 [1H, d, J=3.5 Hz, C(3′)-OH], 5.51 [1H, d, J=4 Hz, C(2′)-OH], 5.88 [1H, d, J=5.5 Hz, C(1′)-H], other signals (see Table II). *Anal.* Calcd for $C_{10}H_{12}DN_5O_5 \cdot H_2O$[29]: C, 39.74; H, 5.00; N, 23.17. Found: C, 39.90; H, 4.90; H, 23.02.

1-Methoxy-9-methyladenine-2-*d* Hydriodide (13b) A mixture of **12b**·H_2O (405 mg, 2.2 mmol) and MeI (1.25 g, 8.8 mmol) in $AcNMe_2$ (1.5 ml) was stirred at 25 °C for 36 h. The precipitate that resulted was filtered off, washed with a little EtOH, and dried to give **13b** (631 mg, 93%), mp 207—209 °C (dec.). Recrystallization from H_2O furnished an analytical sample as colorless prisms, mp 214 °C (dec.); ^{1}H-NMR (Table II). *Anal.* Calcd for $C_7H_8DN_5O \cdot HI$[29]: C, 27.29; H, 3.27; N, 22.73. Found: C, 27.08; H, 3.53; N, 22.67.

9-Benzyl-1-methoxyadenine-2-*d* Hydriodide (13d) A suspension of **12d** (80 mg, 0.33 mmol) in a mixture of MeI (187 mg, 1.32 mmol) and $AcNMe_2$ (0.22 ml) was stirred at room temperature for 48 h. The reaction mixture was diluted with ether (3 ml), and the precipitate that resulted was filtered off, washed with ether, and dried to give **13d** (124 mg, 98%) as a slightly yellowish solid, mp 192—196 °C (dec.). Recrystallization from H_2O yielded an analytical sample as colorless prisms, mp 194—196 °C (dec.); UV $\lambda_{max}^{95\%\ EtOH}$ 259 nm (ε 13200); $\lambda_{max}^{H_2O}$ (pH 1) 215 (38500), 259.5 (13700); $\lambda_{max}^{H_2O}$ (pH 7) 215 (37900), 259 (13500); $\lambda_{max}^{H_2O}$ (pH 13) unstable; ^{1}H-NMR (Table II). *Anal.* Calcd for $C_{13}H_{12}DN_5O \cdot HI$[29]: C, 40.64; H, 3.67; N, 18.23. Found: C, 40.55; H, 3.95; N, 18.21.

1-Methoxyadenosine-2-*d* (14e) A mixture of **12e**·H_2O (116 mg, 0.384 mmol) and MeI (276 mg, 1.94 mmol) in $AcNMe_2$ (1 ml) was stirred at room temperature for 24 h. The reaction mixture was concentrated *in vacuo* to leave a reddish brown oil (**13e**), which was dissolved in EtOH (0.2 ml). The resulting solution was kept in a refrigerator after addition of Et_3N (2 drops). The precipitate that resulted was filtered off, washed with EtOH, and dried to give **14e** (75 mg, 66%). Recrystallization from MeOH yielded an analytical sample as colorless crystals, mp 190—195 °C (dec.); UV $\lambda_{max}^{H_2O}$ (pH 1) 258 nm (ε 12600); $\lambda_{max}^{H_2O}$ (pH 7) 258 (12400); $\lambda_{max}^{H_2O}$ (pH 13) unstable; ^{1}H-NMR (Me_2SO-d_6) δ: 3.59 [2H, m, C(5′)-H_2], 3.93 [1H, m, C(4′)-H], 4.11 [1H, m, C(3′)-H], 4.44 [1H, m, C(2′)-H], 4.8—5.6 (3H, br, OH's), 5.77 [1H, d, J=5.5 Hz, C(1′)-H], other signals (see Table II). *Anal.* Calcd for $C_{11}H_{14}DN_5O_5$[29]: C, 44.29; H, 5.07; N, 23.48. Found: C, 44.11; H, 5.25; N, 23.15.

***N*^{6}-Methoxy-9-methyladenine-2-*d* (15b)** A solution of **13b** (616 mg, 2 mmol) in H_2O (25 ml) was passed through a column of Amberlite IRA-402 (HCO_3^-) (7 ml), and the column was eluted with H_2O (200 ml). The eluate was concentrated *in vacuo* to a volume of *ca.* 25 ml, heated under reflux for 3 h, concentrated again to a volume of *ca.* 5 ml, and then kept in a refrigerator for 2 h. The crystals that deposited were filtered off, washed with a little H_2O, and dried to give a first crop (123 mg, 34%) of **15b**, mp 243—244 °C (dec.). The filtrate and washings were combined and concentrated *in vacuo* to yield a second crop (61 mg, 17%) of **15b**, mp 243.5—244.5 °C (dec.). The total yield of **15b** was 184 mg (51%). Recrystallization of the crude **15b** from H_2O furnished an analytical sample as colorless prisms, mp 244—245 °C (dec.) [lit.[7] mp 244—245 °C (dec.)]; MS *m/z*: 180 (M^+) [d_1 (82%)], 179 [d_0 (18%)]. *Anal.* Calcd for $C_7H_8DN_5O$[29]: C, 46.66; H, 5.03; N, 38.87. Found: C, 46.84; H, 5.00; N, 39.00. This sample was identified by comparison of its ^{1}H-NMR spectrum in Me_2SO-d_6 with that reported previously.[7]

9-Benzyl-*N*^{6}-methoxyadenine-2-*d* (15d) A solution of **13d** (81 mg, 0.21 mmol) in 0.5 M phosphate buffer (pH 6.5) (1.5 ml) was heated under reflux for 4 h. After cooling, the precipitate that resulted was filtered off, washed with H_2O, and dried to give **15d** (44 mg, 81%), mp 218—220 °C (dec.). Recrystallization from EtOH yielded colorless prisms, mp 223.5—224.5 °C (dec.); MS *m/z*: 256 (M^+) [d_1 (76%)], 255 [d_0 (23%)]; UV $\lambda_{max}^{95\%\ EtOH}$ 269 nm (ε 14300); $\lambda_{max}^{H_2O}$ (pH 1) 268.5 (15500); $\lambda_{max}^{H_2O}$ (pH 7) 269 (15600); $\lambda_{max}^{H_2O}$ (pH 13) 286 (12400); ^{1}H-NMR (Me_2SO-d_6) δ: 3.76 (3H, s, OMe), 5.30 [2H, s, N(9)-CH_2], 7.31 (5H, m, Ph), 7.72 [*ca.* 0.23H, br, C(2)-H], 8.04 [1H, dull s, C(8)-H]. *Anal.* Calcd for $C_{13}H_{12}DN_5O$[29]: C,

60.93; H, 5.11; N, 27.33. Found: C, 60.98; H, 5.09; N, 27.19. The UV spectrum of this sample was virtually identical with that reported previously.[7]

N^6-Methoxyadenosine-2-*d* (15e) A stirred mixture of **14e** (22.3 mg, 0.075 mmol) and H_2O (2.5 ml) was heated in an oil bath kept at 80—85 °C for 5 h. The reaction mixture was concentrated to dryness *in vacuo*. The residual solid was triturated with a little H_2O under ice-cooling, and the insoluble solid was collected by filtration and dried to give **15e** (9.3 mg, 41%), mp 192—194 °C (dec.); ^{1}H-NMR (Me_2SO-d_6) (selected peaks) δ: 3.76 (3H, s, OMe), 7.58 [*ca.* 0.4H, br, C(2)-H], 8.11 [1H, dull s, C(8)-H].

Adenosine-8-*d* (16) A solution of adenosine (**1e**) (267 mg, 1 mmol) in D_2O (of over 99% isotopic purity) (10 ml) was heated under reflux for 4 h. Since ^{1}H-NMR spectroscopic analysis of the resulting solution (δ: 8.05 [1H, s, C(2)-H], 8.25 [0.02H, s, C(8)-H]) indicated that isotopic exchange of C(8)-H was still 98%, the reaction mixture was concentrated to dryness *in vacuo*, and the residual solid was dried over P_2O_5 at 3 mmHg and room temperature overnight and again heated in D_2O (*vide supra*) (10 ml) under reflux for 4 h. The resulting D_2O solution was concentrated *in vacuo* to leave a colorless solid, which was dissolved in H_2O (20 ml) at room temperature by ultrasonication. The aqueous solution was concentrated *in vacuo* to leave a colorless solid. This process for isotopic exchange at the N^6 and hydroxylic O atoms was repeated once more, and the resulting colorless solid was dried over P_2O_5 at 3 mmHg and room temperature for 48 h to give **16**, mp 233—234 °C; MS *m/z*: 268 (M^+); ^{1}H-NMR (Me_2SO-d_6) δ: 3.61 [2H, m, C(5')-H_2], 3.98 [1H, m, C(4')-H], 4.15 [1H, m, C(3')-H], 4.61 [1H, m, C(2')-H], 5.1—5.5 (3H, m, OH's), 5.88 [1H, d, J = 6 Hz, C(1')-H], 7.34 (2H, br, NH_2), 8.13 [1H, s, C(2)-H].

Kinetic Procedure i) Delabeling of **16** in H_2O: Adenosine-8-*d* (**16**) (35 mg) was dissolved in H_2O (35 ml) at room temperature by ultrasonication. Aliquots (5 ml) of the resulting solution were sealed in small ampules and placed in a thermoregulated constant-temperature bath kept at 85 °C (accurate to ±0.05 °C). At 30-min intervals, the ampules were removed, cooled, and broken, and the contents were concentrated *in vacuo*. The residual solids were separately dried over P_2O_5 at 3 mmHg and room temperature overnight, dissolved in Me_2SO-d_6 (0.4 ml), and analyzed by ^{1}H-NMR spectroscopy. The extent of delabeling of C(8)-D was determined by measuring the relative areas of the C(8)-H and C(2)-H signals at δ 8.34 and 8.13, respectively. Delabeling was followed for two half-lives with six measurements, and a good pseudo-first-order kinetics was obtained. The results are summarized in the text.

ii) Isotopic Stability of **5e** in H_2O: A solution of adenosine-2-*d* (**5e**) (5 mg) in H_2O (5 ml) was heated at 85 °C for 6 h and then worked up as described above under item (i). On ^{1}H-NMR spectroscopic analysis, the product did not show any signal at δ 8.13 [C(2)-H].

iii) Deuterium Labeling of **2d**: A stirred mixture of 9-benzyladenine 1-oxide (**2d**) (121 mg) and a 10% (w/w) EtOD solution in D_2O (5 g) was heated under reflux. At intervals, a portion of the reaction mixture was withdrawn, and the extent of labeling of C(8)-H and C(2)-H of the product was determined by ^{1}H-NMR spectroscopic analysis (Table II) in a manner similar to that described above under item (i). After having been refluxed for 24 h, the reaction mixture was concentrated *in vacuo* to leave a solid. A portion (50 mg) of the solid was dissolved in CD_3CO_2D (of over 99% isotopic purity) (1 ml), and the solution was heated under reflux for 9 h. The extent of labeling of the product from this reaction mixture was analyzed as described above. The results are summarized in the text.

Acknowledgment Financial support provided by the Ministry of Education, Science and Culture, Japan in the form of a Grant-in-Aid for Encouragement of Young Scientists (No. 57771456, to T. S.) and by the Japan Research Foundation for Optically Active Compounds is gratefully acknowledged.

References and Notes

1) Paper XLVII in this series, T. Fujii, T. Saito, H. Hisata, and K. Shinbo, *Chem. Pharm. Bull.*, **38**, 3326 (1990).
2) *a*) W. J. Wechter, *Collect. Czech. Chem. Commun.*, **35**, 2003 (1970); *b*) M. Maeda, M. Saneyoshi, and Y. Kawazoe, *Chem. Pharm. Bull.*, **19**, 1641 (1971); *c*) J. A. Elvidge, J. R. Jones, and C. O'Brien, *J. Chem. Soc., Chem. Commun.*, **1971**, 394; *d*) M. Tomasz, J. Olson, and C. M. Mercado, *Biochemistry*, **11**, 1235 (1972); *e*) D. Lichtenberg and F. Bergmann, *J. Chem. Soc., Perkin Trans. 1*, **1973**, 789; *f*) J. A. Elvidge, J. R. Jones, C. O'Brien, E. A. Evans, and H. C. Sheppard, *J. Chem. Soc., Perkin Trans. 2*, **1973**, 2138; *g*) *Idem*, *ibid.*, **1974**, 174; *h*) S. Mansy and R. S. Tobias, *J. Chem. Soc., Chem. Commun.*, **1974**, 957; *i*) J. L. Wong and J. H. Keck, Jr., *ibid.*, **1975**, 125.
3) M. Maeda and Y. Kawazoe, *Tetrahedron Lett.*, **1975**, 1643.
4) See, for example, *a*) W. C. Coburn, Jr., M. C. Thorpe, J. A. Montgomery, and K. Hewson, *J. Org. Chem.*, **30**, 1110 (1965); *b*) *Idem*, *ibid.*, **30**, 1114 (1965); *c*) T. Sugiyama, H. Iwasawa, and T. Hashizume, *Agric. Biol. Chem.*, **44**, 1057 (1980).
5) For a review, see T. Fujii, T. Itaya, and T. Saito, *Yuki Gosei Kagaku Kyokai Shi*, **41**, 1193 (1983).
6) *a*) T. Fujii, T. Saito, and T. Fujisawa, *Heterocycles*, **27**, 1163 (1988); *b*) T. Fujii, T. Itaya, T. Saito, K. Mohri, M. Kawanishi, and T. Nakasaka, *Chem. Pharm. Bull.*, **37**, 1504 (1989); *c*) T. Fujii, T. Saito, and T. Nakasaka, *ibid.*, **37**, 2601 (1989); *d*) T. Itaya, T. Saito, T. Harada, S. Kagatani, and T. Fujii, *ibid.*, **37**, 3200 (1989); *e*) T. Saito, Y. Asahi, S. Nakajima, and T. Fujii, *Heterocycles*, **30**, 329 (1990); *f*) T. Fujii, T. Saito, T. Nakasaka, and K. Kizu, *Chem. Pharm. Bull.*, **38**, 99 (1990); *g*) T. Fujii, T. Saito, T. Sakuma, M. Minami, and I. Inoue, *ibid.*, **38**, 652 (1990); *h*) T. Fujii, T. Saito, and Y. Kumazawa, *ibid.*, **38**, 1392 (1990); *i*) T. Saito, I. Inoue, and T. Fujii, *ibid.*, **38**, 1536 (1990); *j*) T. Fujii and T. Saito, *ibid.*, **38**, 1886 (1990).
7) T. Fujii, T. Saito, T. Itaya, K. Kizu, Y. Kumazawa, and S. Nakajima, *Chem. Pharm. Bull.*, **35**, 4482 (1987).
8) *a*) T. Fujii, T. Saito, K. Kizu, H. Hayashibara, Y. Kumazawa, and S. Nakajima, *Heterocycles*, **24**, 2449 (1986); *b*) T. Saito, H. Hayashibara, Y. Kumazawa, T. Fujisawa, and T. Fujii, *ibid.*, **31**, 1593 (1990).
9) T. Fujii, T. Itaya, T. Saito, ad M. Kawanishi, *Chem. Pharm. Bull.*, **26**, 1929 (1978).
10) T. Fujii, C. C. Wu, and T. Itaya, *Chem. Pharm. Bull.*, **19**, 1368 (1971).
11) T. Fujii, T. Itaya, F. Tanaka, T. Saito, K. Mohri, and K. Yamamoto, *Chem. Pharm. Bull.*, **31**, 3149 (1983).
12) T. Fujii, C. C. Wu, T. Itaya, S. Moro, and T. Saito, *Chem. Pharm. Bull.*, **21**, 1676 (1973).
13) *a*) M. A. Stevens, D. I. Magrath, H. W. Smith, and G. B. Brown, *J. Am. Chem. Soc.*, **80**, 2755 (1958); *b*) M. A. Stevens and G. B. Brown, *ibid.*, **80**, 2759 (1958).
14) T. Fujii, T. Saito, T. Itaya, and K. Yokoyama, *Chem. Pharm. Bull.*, **21**, 209 (1973).
15) K. Kikugawa, H. Suehiro, R. Yanase, and A. Aoki, *Chem. Pharm. Bull.*, **25**, 1959 (1977).
16) *a*) H. Klenow and S. Frederiksen, *Biochim. Biophys. Acta*, **52**, 384 (1961); *b*) J. A. Montgomery and H. J. Thomas, *J. Med. Chem.*, **15**, 182 (1972); *c*) T. Ueda, K. Miura, and T. Kasai, *Chem. Pharm. Bull.*, **26**, 2122 (1978); *d*) M. Saneyoshi, S. Nishimura, M. Okabe, and F. Fukuoka, *J. Pharmacobio-Dyn.*, **3**, 105 (1980).
17) A. R. P. Paterson and S. H. Zbarsky, *J. Am. Chem. Soc.*, **75**, 5753 (1953).
18) F. Effenberger, M. Keil, and E. Bessey, *Chem. Ber.*, **113**, 2110 (1980).
19) T. Fujii and T. Itaya, *Tetrahedron*, **27**, 351 (1971).
20) T. Fujii, T. Itaya, C. C. Wu, and F. Tanaka, *Tetrahedron*, **27**, 2415 (1971).
21) *a*) M. A. Stevens, H. W. Smith, and G. B. Brown, *J. Am. Chem. Soc.*, **81**, 1734 (1959); *b*) M. Sundaralingam, C. D. Stout, and S. M. Hecht, *Chem. Commun.*, **1971**, 240.
22) *a*) J. H. Keck, Jr., R. A. Simpson, and J. L. Wong, *J. Org. Chem.*, **43**, 2587 (1978), and references cited therein; *b*) M. Ishino, T. Sakaguchi, I. Morimoto, and T. Okitsu, *Chem. Pharm. Bull.*, **29**, 2403 (1981), and references cited therein.
23) See ref. 7 for the interpretation of the ^{1}H-NMR spectra of the N^6-methoxy derivatives **11b**, **11d**, and **11e**.
24) M. P. Schweizer, S. I. Chan, G. K. Helmkamp, and P. O. P. Ts'o, *J. Am. Chem. Soc.*, **86**, 696 (1964).
25) J. B. Lambert, H. F. Shurvell, L. Verbit, R. G. Cooks, and G. H. Stout, "Organic Structural Analysis," Macmillan, New York, 1976, pp. 446—448.
26) T. Fujii, S. Sakurai, and T. Uematsu, *Chem. Pharm. Bull.*, **20**, 1334 (1972).
27) For convenience, each carbon of the sugar moiety is indicated by a primed number.
28) R. Mozingo, "Organic Syntheses," Coll. Vol. III, ed. by E. C. Horning, John Wiley and Sons, New York, 1955, p. 181.
29) By H_2O/HDO gas volume analysis.

Stereocontrolled Synthesis of Exocyclic Olefins Using Arene Tricarbonyl Chromium Complex-Catalyzed Hydrogenation. I. Efficient Synthesis of Carbacyclin and Its Analogs

Mikiko SODEOKA,[a] Yuji OGAWA,[a] Yoshie KIRIO,[b] and Masakatsu SHIBASAKI*,[a]

Sagami Chemical Research Center,[a] Nishi-Ohnuma, Sagamihara, Kanagawa 229, Japan and Faculty of Pharmaceutical Sciences, Hokkaido University,[b] Sapporo 060, Japan. *Received August 20, 1990*

An efficient synthesis of carbacyclin and its analogs (2—7) is described in which the stereospecific 1,4-hydrogenation of a 1,3-diene to an internal monoene plays a key role. That is, arene·$Cr(CO)_3$ complex-catalyzed 1,4-hydrogenation of the dienes 13 and 58, obtainable from the Corey lactone in good yields, under high H_2 pressure afforded the exocyclic olefins 14 and 61 stereospecifically in excellent yields, and these intermediates were converted to therapeutically useful carbacyclin (2) and its analogs 3—7 in a usual way.

Keywords 1,3-diene; 1,4-hydrogenation; arene tricarbonyl chromium complex; Corey lactone; carbacyclin; prostacyclin; antiulcer drug; circulatory disease; exocyclic olefin

Carbacyclin (**2**) is one of the potent, chemically stable analogs of prostacyclin (PGI_2, **1**), which is a naturally occurring bioregulator having remarkable platelet aggregation-inhibiting activity. Some ω-chain derivatives **3** and **5** are being studied in clinical trials as therapeutic agents for cardiovascular and circulatory diseases. Although many groups have succeeded in the synthesis of these important compounds,[1] none of the syntheses has involved the completely stereocontrolled construction of a 5*E*-trisubstituted olefin (PG numbering).[2] Therefore, formation of a considerable amount of the biologically much less active 5*Z*-isomer and extremely troublesome separation of the stereoisomers were unavoidable, making the industrial-scale preparation of the carbacyclin analogs fairly difficult. We started our research with the aim of developing a practical synthetic route which would involve the completely stereocontrolled construction of an exocyclic olefin.[3]

Wittig reaction, semihydrogenation of alkynes, combination of hydro- or carbometalation of alkynes and cross-coupling reaction, and so on are known as methods for the stereocontrolled synthesis of olefins. These methods, however, could not be applied to carbacyclin synthesis involving the stereocontrolled construction of an exocyclic olefin. We gave attention to the 1,4-hydrogenation of conjugated dienes to *cis*-olefins catalyzed by arene·$Cr(CO)_3$ complex. This reaction was first reported in 1968.[4] Subsequent mechanistic studies using simple substrates suggested that the regio- and stereochemistry of the products were controlled by the bidentate coordination of a diene in *s-cis* conformation to the chromium atom.[5] However, few applications of this reaction to the syntheses of rather complex molecules have been reported.[6] Although the scope and limitations of this hydrogenation were not clear, we anticipated that this remarkable reaction could be used for the stereocontrolled synthesis of an exocyclic olefin moiety in carbacyclin and its analogs. That is, it was expected that the conjugate diene **9** would be stereospecifically converted to the exocyclic trisubstiuted olefin **10**, a key intermediate for the synthesis of carbacyclin and its analogs, by this 1,4-hydrogenation. Furthermore, application of this methodology to the cyano-substituted diene **58** would enable us to synthesize cyanocarbacyclins (**6** and **7**), new carbacyclin analogs which were expected to have a similar biological profile to that of nileprost (**8**). Nileprost (**8**) may be of therapeutic value for gastric ulcer because of its potent antiulcer effect with weak antiaggregatory and vasodilating

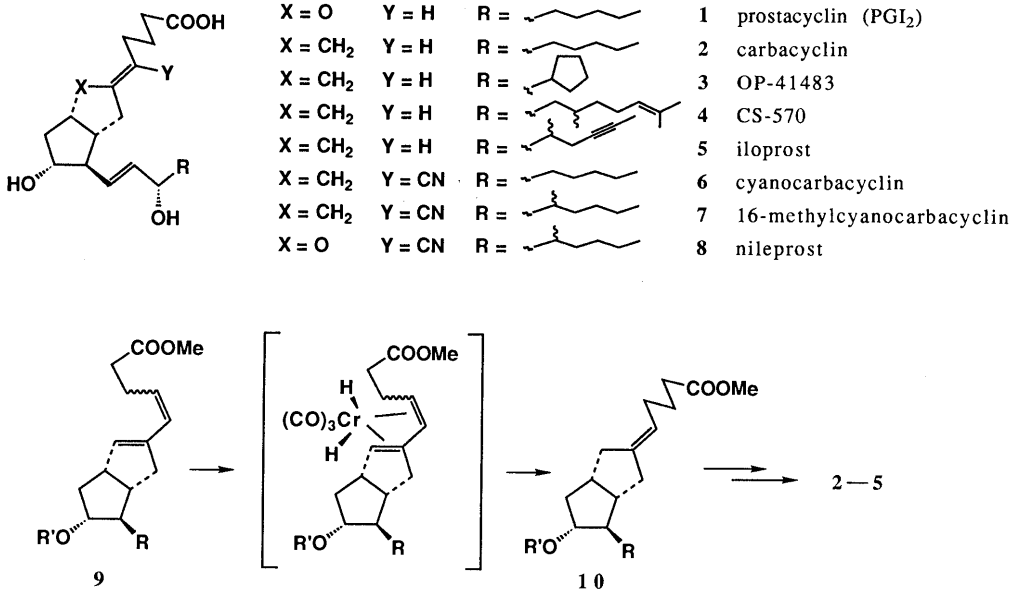

Chart 1

activities.

This account describes the stereospecific synthesis of carbacyclins (**2**—**5**) and cyanocarbacyclins (**6** and **7**).

Synthesis of Carbacyclin and Its Analogs It was well known that the most favorable stereochemistry of double bonds for the 1,4-hydrogenation was *E,E*.[5] Therefore, in the first place, the 1,4-hydrogenation of the conjugated diene **11** with an *E*-disubstituted olefin, which was stereospecifically synthesized from the well-known Corey lactone in *ca.* 27% overall yield by using an intramolecular thermal ene reaction as a key step,[7a,c] was undertaken. Hydrogenation of **11** in acetonitrile (70 kg/cm^2 of H_2 pressure, 130 °C, 12 h) using (methyl benzoate)$Cr(CO)_3$ as a catalyst (20 mol%) gave the desired *E*-exocyclic olefin **12** stereospecifically in 66% yield. None of the other possible products was observed except for the recovery of **11** (21%). The stereochemistry of **12** was unequivocally determined by comparison with an authentic sample[1] (gas liquid chromatography (GLC) analysis). Thus, the stereospecific synthesis of a 5*E*-trisubstituted olefin as found in carbacyclin (**2**) and its analogs **3**—**5** was realized for the first time. In order to improve the chemical yield, solvent effects were investigated, and acetone, which has weaker coordination ability to chromium than acetonitrile, was found to be an excellent solvent. That is, treatment of **11** with (methyl benzoate)$Cr(CO)_3$ (20 mol%) in acetone under 70 kg/cm^2 of H_2 pressure (120 °C, 15 h) provided **12** in nearly quantitative yield.

Next we turned our attention to the *Z*-rich 1,3-diene **13** (*Z*:*E*=2.2:1), which was prepared from the Corey lactone in much better overall yield (69%) by using an intramolecular aldol condensation as a key step.[7a,b] Hydrogenation of the *Z*-rich diene **13** in acetone (70 kg/cm^2 of H_2 pressure, 120 °C, 12 h) using (methyl benzoate)$Cr(CO)_3$ as a catalyst (20 mol%) gave the desired *E*-exocyclic olefin **14** in nearly quantitative yield. Careful GLC analysis of the hydrogenated product, however, indicated contamination with a trace amount of the regioisomer **15** (<2%). Treatment of **14** with tetrabutylammonium fluoride (TBAF) afforded the alcohol **16**, which was a versatile intermediate for the synthesis of carbacyclin and its analogs, in 95% yield, and at this stage the minor regioisomer **17** was found to be easily separated by silica gel chromatography (1.9%). Furthermore, when

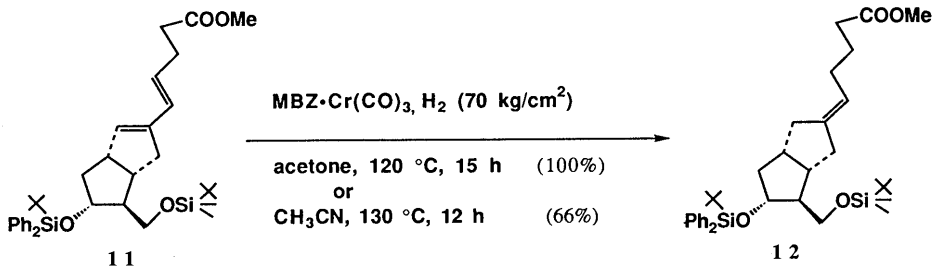

Chart 2

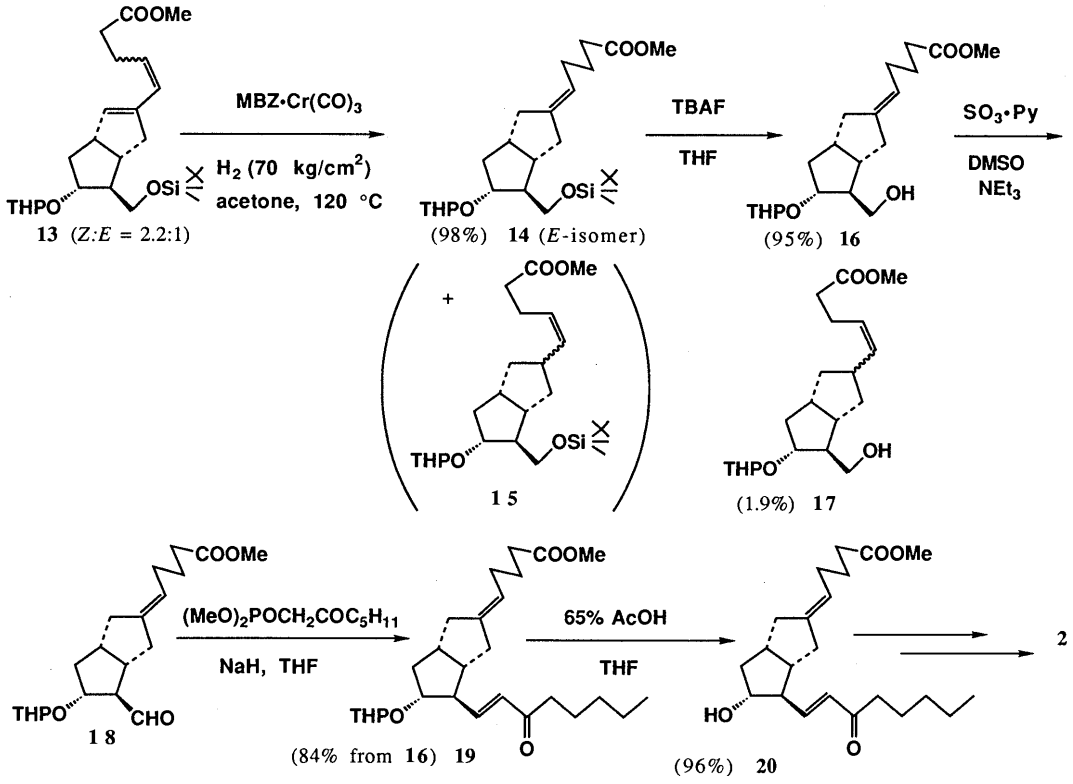

Chart 3

TABLE I. Hydrogenation of **13** ($Z:E=2.2:1$)

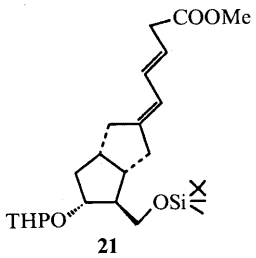

21

MBZ = methyl benzoate
NP = naphthalene
TOL = toluene
Ar = argon

Run	Catalyst[a]	Solvent	Pressure (kg/cm^2)	Temp. (°C)	Time (h)	Yield (%) 14	21	15	Recovery 13 Z	E
1	MBZ·$Cr(CO)_3$	Acetone	H_2 70	120	16	98	—	+[b]	—	—
2	NP·$Cr(CO)_3$	THF	H_2 70	45	23	95	—	+[b]	—	—
3	MBZ·$Cr(CO)_3$	CH_3CN	H_2 70	130	12	28	27	+[b]	37	—
4	MBZ·$Cr(CO)_3$	CH_3CN	H_2 130	120	24	83	—	+[b]	—	—
5	TOL·$Cr(CO)_3$	Acetone	H_2 70	130	13	81	4	+[b]	—	—
6	MBZ·$Cr(CO)_3$	CH_3CN	Ar 70	130	12	—	32	—	25	29
7	MBZ·$Cr(CO)_3$	Acetone	Ar 70	130	25	—	28	—	17	21

a) In each case, 20 mol% of catalyst was used. *b*) TLC analysis showed the presence of an extremely small amount of **15**.

naphthalene·$Cr(CO)_3$ complex was used as a catalyst in tetrahydrofuran (THF), the hydrogenation proceeded smoothly at 45 °C to give **14** stereospecifically in 95% yield. Thus, a highly efficient synthesis of the key intermediate for **2**—**5** was developed.

The alcohol **16** was then transformed to the enone **20** in a usual manner. Oxidation of **16** with SO_3·pyridine complex and triethylamine in dimethyl sulfoxide (DMSO) gave the aldehyde **18**, which was directly treated with the phosphonate carbanion derived from dimethyl (2-oxoheptyl)phosphonate and sodium hydride in THF to provide **19** in 84% overall yield. Deprotection of a 2-tetrahydropyranyl (THP) group in **19** afforded **20** in 96% yield, and **20** has been transformed to carbacyclin (**2**) in *ca.* 80% yield.[1k] The overall yield of carbacyclin (**2**) from the Corey lactone was *ca.* 40%, and using this route, the various ω-chain analogs **3**—**5** were also synthesized efficiently.

Reaction Pathway of the Hydrogenation Using 13 In contrast to the aforesaid successful results, hydrogenation of **13** in acetonitrile (70 kg/cm^2 of H_2 pressure, 130 °C, 12 h) using (methyl benzoate)$Cr(CO)_3$ as a catalyst (20 mol%) gave two main products (Table I, run 3). One was the desired 1,4-reduction product **14** (28%), and the other was the stereochemically homogeneous (3*E*, 5*E*) exocyclic conjugated diene **21** (27%), probably formed through a 1,5-hydrogen shift. In addition the starting diene containing only the 4*Z*-stereoisomer was recovered (37%). The exocyclic conjugated diene **21** was found to be formed just by heating **13** in the presence of a catalytic amount of (methyl benzoate)$Cr(CO)_3$ (20 mol%) in acetonitrile or acetone under an argon atmosphere in proportion to the consumption of the 4*Z*-isomer of **13** (runs 6 and 7). On the other hand, treatment of **21** with a catalytic amount of (methyl benzoate)$Cr(CO)_3$ in acetone under an argon atmosphere for 20 h at 130 °C afforded the 4*Z*-isomer of **13** (38%) together with **21** (62%). These results strongly implied that only one part (4*Z*) of the conjugated diene **13** and the exocyclic conjugated diene **21** were in a state of equilibrium through the η^5-pentadienylhydridochromium intermediate **22**. No other isomerized product was obtained in any case, showing that this 1,5-hydrogen shift catalyzed by (methyl benzoate)$Cr(CO)_3$ proceeded in a strictly stereocontrolled manner.[8] In marked contrast to the 4*Z*-isomer, no isomerization of the 4*E*-isomer having no readily abstractable hydrogen was found to occur.

It was of quite interest to understand why the exocyclic conjugated diene **21** or its 1,4-hydrogenated product **15** was scarcely formed from **13** under the reaction conditions mentioned above (runs 1 and 2). Even in the case of acetonitrile as the solvent, a simple increase in H_2 pressure to 130 kg/cm^2 afforded none of the exocyclic diene **21** (run 4). On the other hand, hydrogenation of **13** in acetone using toluene·$Cr(CO)_3$, a slightly less active catalyst compared with (methyl benzoate)$Cr(CO)_3$, also afforded a small amount of **21** (4%). We assumed the following mechanism (Chart 4). Under all the hydrogenation conditions used, while the 4*E*-isomer of **13** was exclusively hydrogenated to give the desired product **14**, the 4*Z*-isomer of **13** was isomerized very rapidly, being in a state of equilibrium between *Z*-**13** and **21**. However, owing to the extremely slow 1,4-hydrogenation of **21** to **15**, the 4*Z*-isomer of **13** was transformed into **14** in high yield. The reason why 1,4-hydrogenation of **21** to **15** was quite slow is not clear at present. Thus, the 5*E*-trisubstituted olefin **14** was formed in high yield under the well-suited hydrogenation conditions. This assumption was strongly supported by the experimental fact that hydrogenation of the exocyclic conjugated diene **21** in acetone using (methyl benzoate)-$Cr(CO)_3$ as a catalyst (20 mol%) (70 kg/cm^2 of H_2 pressure, 120 °C, 16 h) gave the 5*E*-trisubstituted olefin **14** in 94% yield accompanied with a trace amount of **15**.

1,4-Hydrogenation of the Dienes with an ω-Chain Next we turned our attention to the 1,4-hydrogenation of the conjugated dienes having an ω-chain **36**—**39**. As shown in Chart 5, the dienes **36**—**39** were synthesized from **13** in a usual manner. In the case of the dienes **36**—**38**, the stereospecific hydrogenation proceeded quite smoothly, and the desired exocyclic olefins **40**—**42** were obtained stereospecifically in nearly quantitative yields. The stereochemistry of the exocyclic olefins was unequivocally

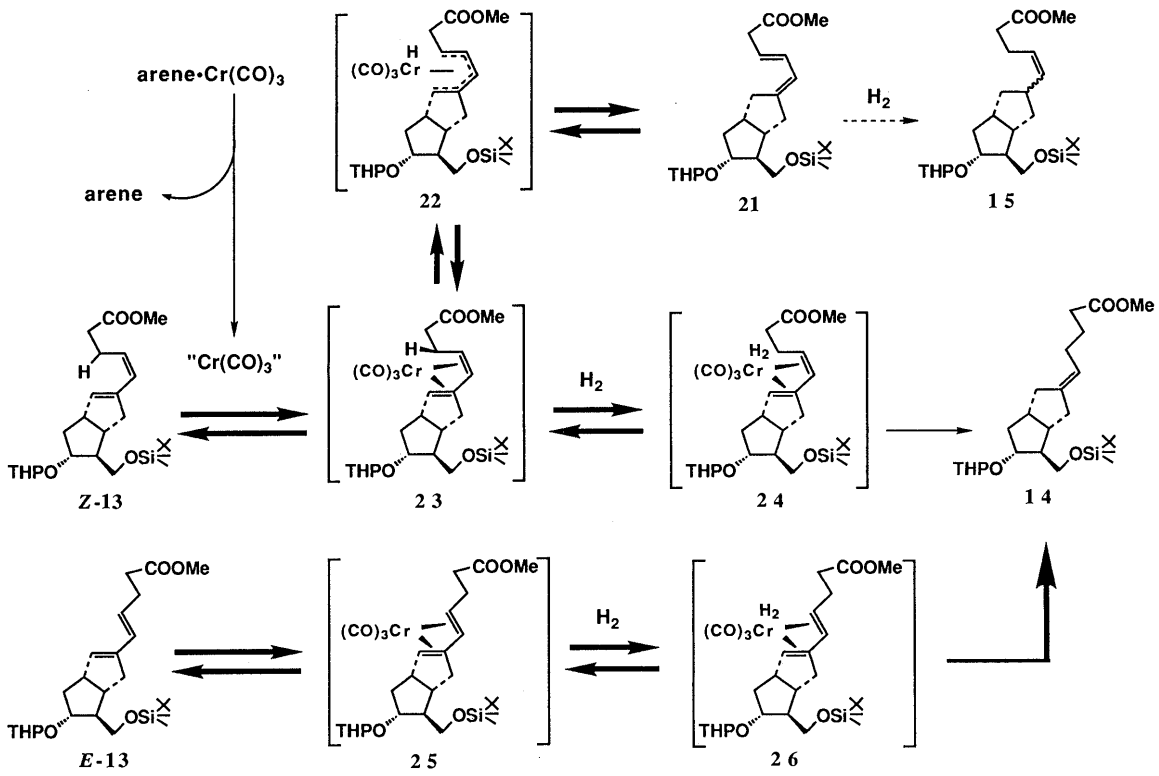

Chart 4

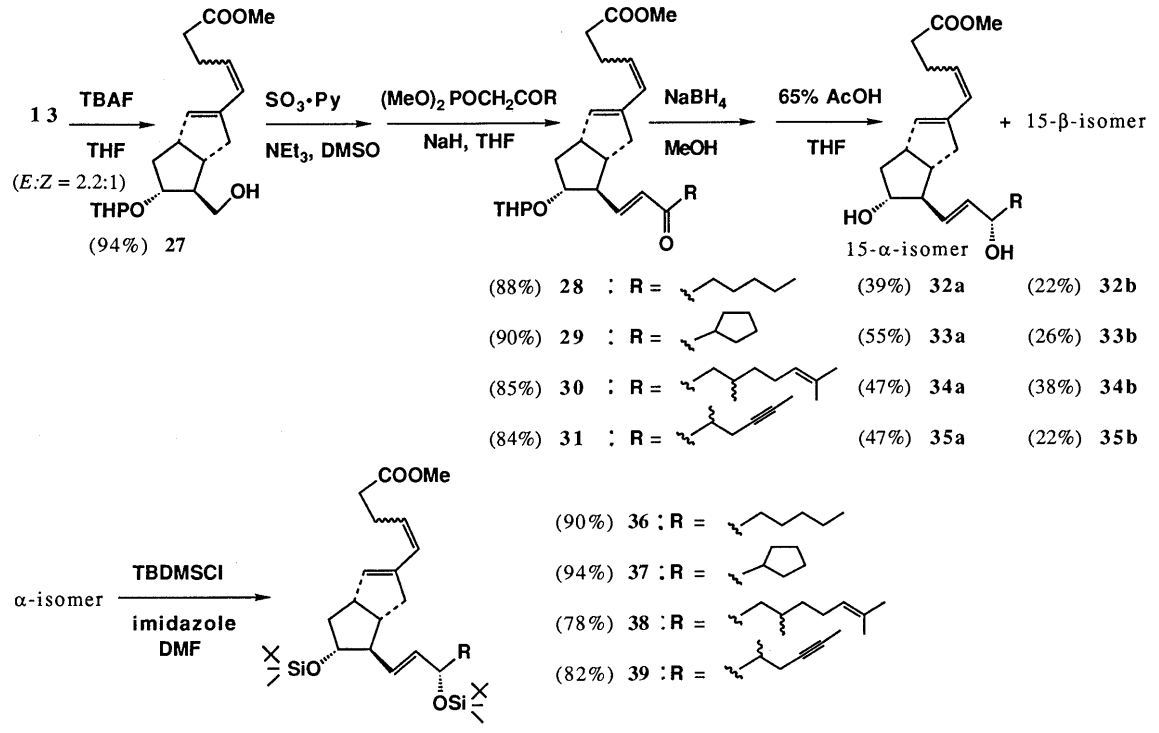

Chart 5

determined by comparison with authentic samples.[1] On the other hand, the hydrogenation of the diene **39** was complicated by the partial reduction of a triple bond. Namely, hydrogenation of the diene **39** in acetone (70 kg/cm^2 of H_2 pressure, 120 °C, 15 h) using (methyl benzoate)$Cr(CO)_3$ as a catalyst (20 mol%) gave the four products **43**—**46**. The yield of the desired product **43** was only 33%. Furthermore, the hydrogenation of the enone **29** was found to afford the saturated ketone **47** exclusively (100%). These new catalytic activities of arene·$Cr(CO)_3$ for the conversion of alkynes to *cis*-alkenes and enones to saturated ketones have already been reported in detail.[9]

The hydrogenation products **40**—**43** were then converted to the corresponding carbacyclin analogs **2**—**5** as shown in

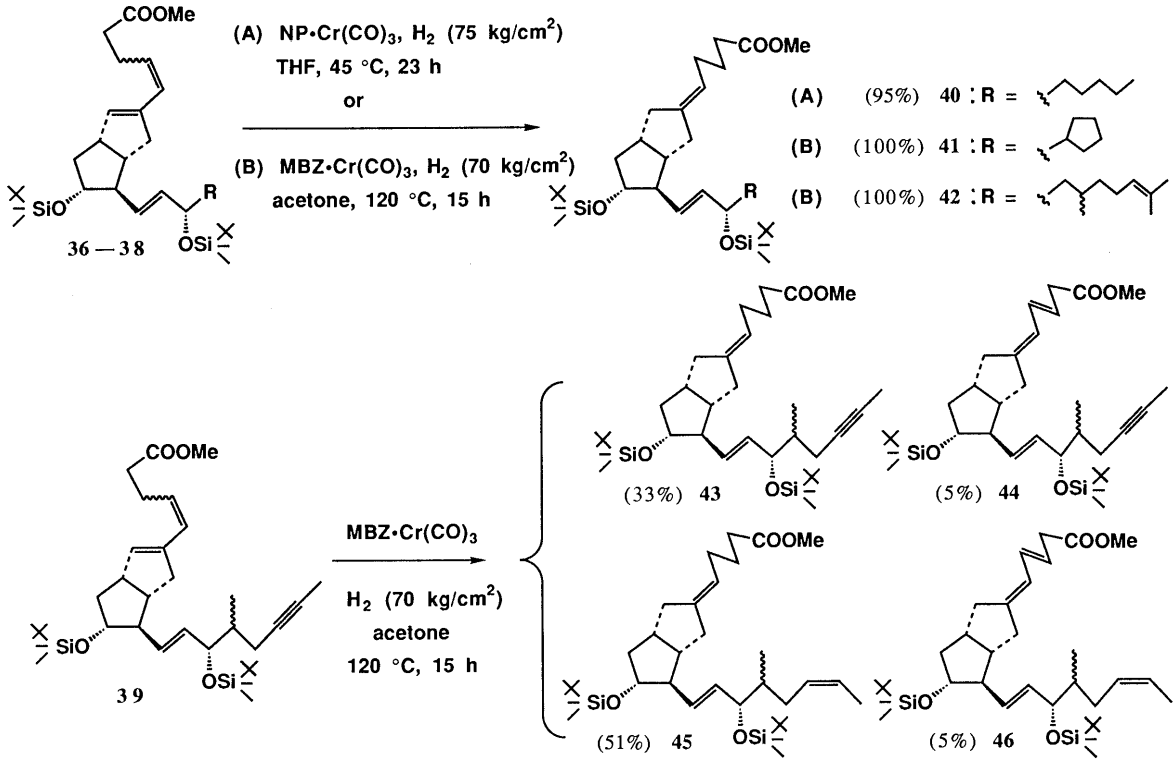

Chart 6

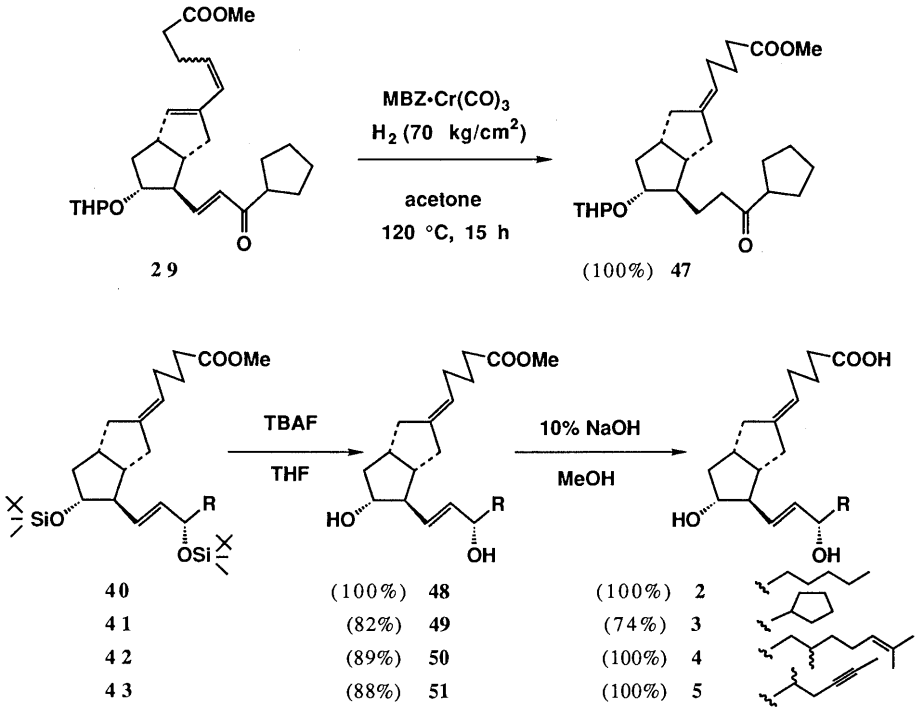

Chart 7

Chart 7. Since the synthetic routes to the conjugated dienes having an ω-chain from furfural or optically active 4-hydroxy-2-cyclopentenone were already established,[7a,10] the results described above should pave the way for the stereocontrolled synthesis of carbacyclin and its analogs from various starting materials.

Synthesis of Cyanocarbacyclin and Its Analogs Having established an efficient synthesis of carbacyclin and its analogs, we then turned our attention to the stereocontrolled synthesis of exocyclic tetrasubstituted olefins. Cyanocarbacyclins (**6** and **7**) were selected as target molecules with an exocyclic tetrasubstituted olefin moiety. In order to accomplish the stereocontrolled synthesis of cyanocarbacyclins (**6** and **7**) by using the 1,4-hydrogenation as a key step, the requisite conjugated diene **58** with a cyano functionality at the C-5 position was efficiently synthesized from **52** as

shown in Chart 8. The α,β-unsaturated aldehyde **52**, prepared from the Corey lactone in 73% overall yield,[7a,b] was first reduced to the allylic alcohol **53** diisobutyalminum hydride (DIBAH) in 98% yield. After conversion of **53** to the bromide **54** (PPh_3 and CBr_4 in CH_2Cl_2 at −60——−25 °C, 89% yield), **54** was treated with KCN and 18-crown-6 in CH_3CN to give the allylic cyanide **55** in 99% yield. The α-chain was regiospecifically introduced by the coupling reaction of **55** and the aldehyde **56**[11] (lithium diisopropylamide (LDA) in THF at −78 °C, then **56**), furnishing a diastereoisomeric mixture of the cyano-alcohols **57** in 82% yield. Subsequently these cyano-alcohols **57** were treated with methanesulfonyl chloride and triethylamine in CH_2Cl_2. Under these reaction conditions elimination occurred spontaneously to afford an easily separable mixture of the diene **58a** (83%) and **58b** (6%). The stereochemistry of both **58a** and **58b** was determined on the basis of the chemical shifts of the vinyl protons in their nuclear magentic resonance (NMR) spectra[12] (**58a**: δ 6.10 ppm, *trans* to nitrile, **58b**: δ 6.20, *cis* to nitrile). Furthermore, the chemical reactivity of **58a** and **58b** in the 1,4-hydrogenation reaction supported the above-mentioned stereochemistry.

The crucial 1,4-hydrogenation of **58a** proceeded smoothly *via* the transition state **60** by using (methyl benzoate)-$Cr(CO)_3$ (20 mol%) as a catalyst in acetone to afford the stereochemically homogeneous *Z*-tetrasubstituted olefin **61** in quantitative yield (70 kg/cm² of H_2 pressure, 120 °C,

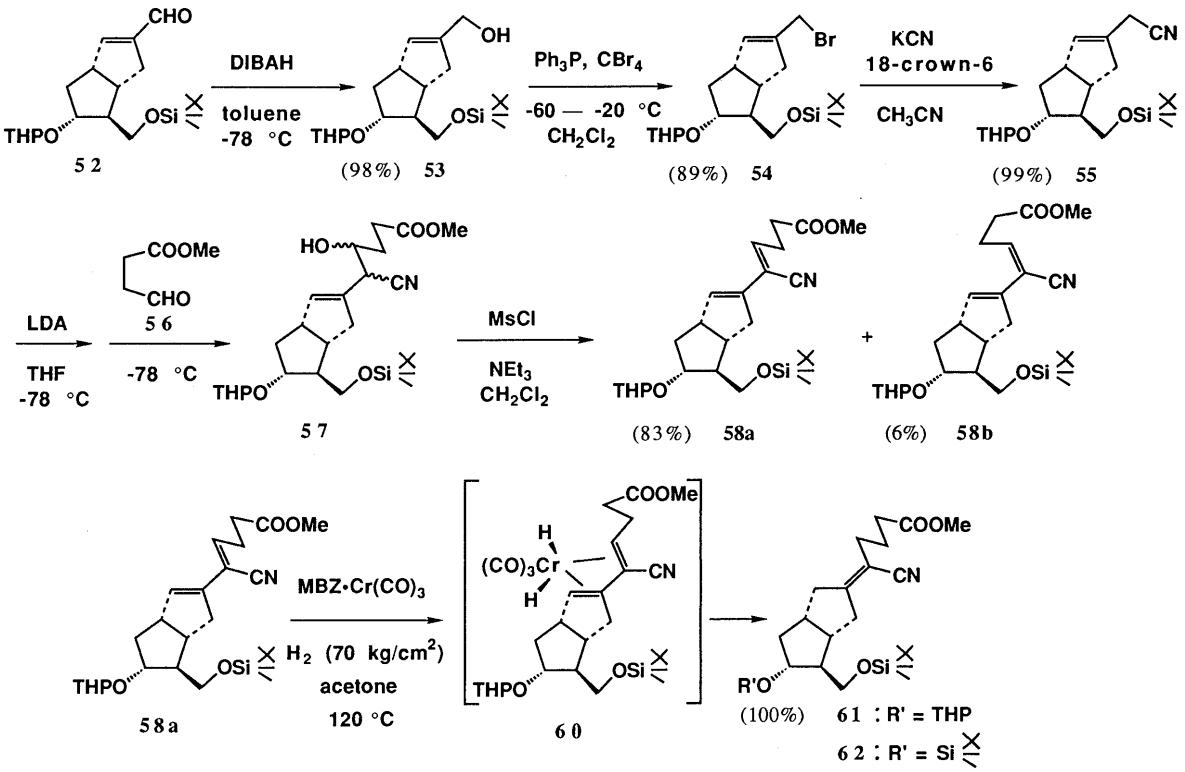

Chart 8

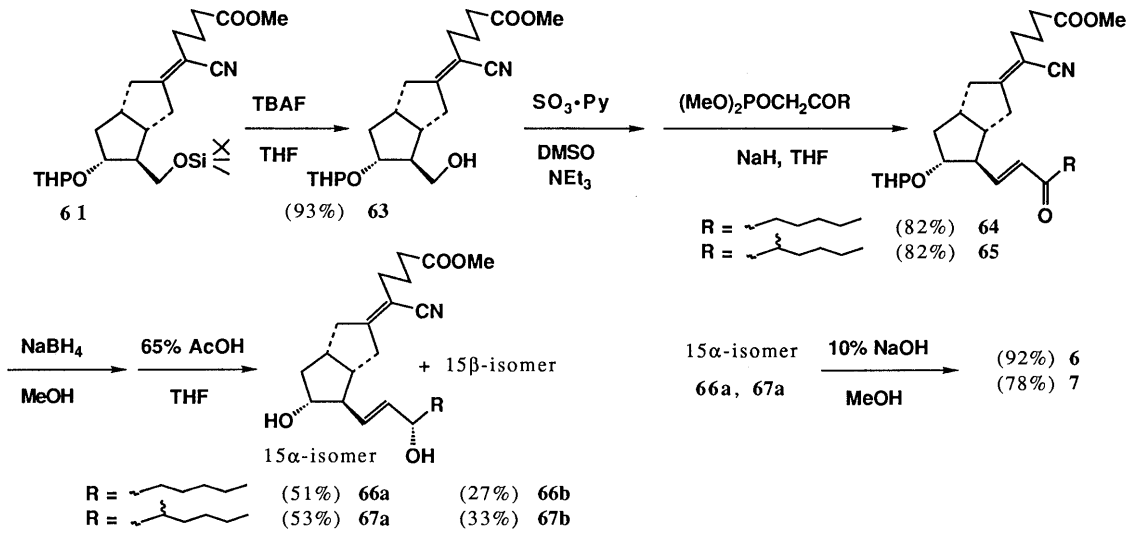

Chart 9

15 h). It was also found that the hydrogenation proceeded under milder conditions by the use of naphthalene·$Cr(CO)_3$ (20 mol%) as a catalyst in THF (70 kg/cm^2 of H_2 pressure, 45 °C, 21 h) to give **61** stereospecifically in 97% yield.[13] On the other hand, the 1,4-hydrogenation of **58b**, available in very low yield, remained unchanged under the various 1,4-hydrogenation conditions probably due to steric hindrance around the diene moiety.

Introduction of an ω-chain into the hydrogenation product **61** was accomplished according to the general procedure (Chart 9), and cyanocarbacyclin (**6**) and its 16-methyl analog **7** were obtained in 36 and 32% overall yields from **61**, respectively.

On the contrary, the stereoselective synthesis of the 5*E*-stereoisomer **68** was achieved by the Pd–C-catalyzed hydrogenation of **58**.[14] That is, treatment of **58** with 10% Pd–C in toluene (1 atm of hydrogen pressure, −40 °C) afforded **68** stereoselectively (**68**:**61** = 6.7:1) *via* reduction-isomerization. After desilylation, the 5*E*-isomer **72** was isolated from the alcohol derived from **70**. This selectivity might be explained by the steric effect and/or the intramolecular coordination of a cyano group to Pd in the π-allyl intermediate **71**. It is of particular interest that the stereoselectivity of the product can be reversed depending on the catalyst used. The stereochemistry of the newly formed double bonds of **61** and **68** was determined to be *Z* and *E*, respectively, from nuclear Overhauser effect (NOE) experiments on **62** derived from **61** (i. Et_2AlCl, ii. *tert*-butyldimethylchlorosilane (TBDMSCl), imidazole in dimethylformamide (DMF), 75% yield in two steps) and **69** derived from **72** (i. 65% AcOH, ii. TBDMSCl, imidazole, DMF, 45% in two steps) (Fig. 1 in the experimental section).

The absence of the 5*E*-stereoisomers **73** and **74** in the cyanocarbacyclins (**6**, **7**) was confirmed by the following experiments. Thus, **72** was transformed into 5*E*-cyanocarbacyclin (**73**, **74**) by a similar procedure to that described above (Chart 10). Careful thin layer chromatography (TLC) analysis of both **73**, **74** and **6**, **7** showed clearly that the cyanocarbacyclins (**6** and **7**) were stereochemically homogeneous, indicating that isomerization of an α,β-conjugated cyanide functionality did not occur during the ω-chain introduction. On the basis of the arguments present above, it was concluded that the 1,4-hydrogenation of 1,3-dienes bearing a cyano functionality at the C-2 position provides a useful method for the stereospecific construction of versatile exocyclic tetrasubstituted olefins.[15]

Biological Activity Preliminary results of the biological testing of cyanocarbacyclins **6** and **7**, and the dienecarbacyclin analogs **75**—**78** prepared by the hydrolysis of **32**—**35** are shown in Table II. Contrary to expectation, the platelet aggregation-inhibiting and cytoprotective effects of the cyanocarbacyclins **6** and **7** were both very weak. On the other hand, the new prostacyclin analogs 75—78 were as potent as the known carbacyclin analogs in inhibiting human platelet aggregation induced by adenosine diphosphate (ADP).[16] These new prostacyclin analogs might be of therapeutic value for occlusive peripheral vascular diseases.[17]

As described above, we have shown that the arene·$Cr(CO)_3$-catalyzed hydrogenation of conjugated dienes can

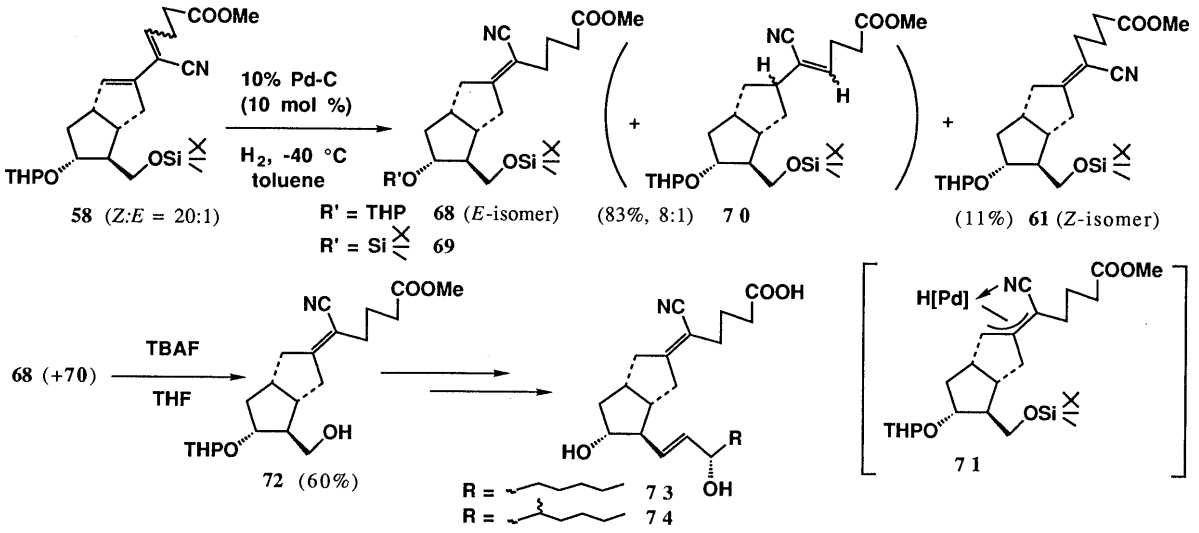

Chart 10

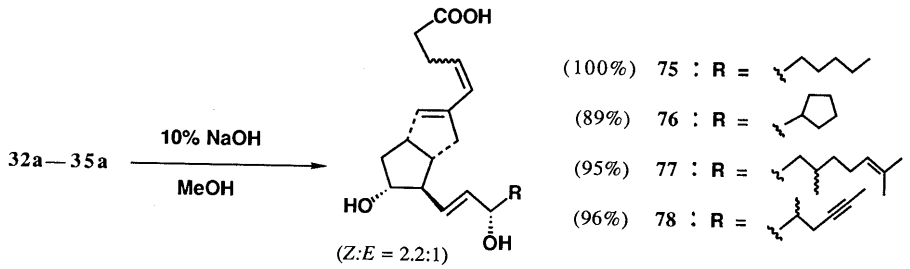

Chart 11

Table II. Biological Activities of Carbacyclin Analogs

Compound	ADP induced human platelet aggregation *in vitro* inhibition (%)						Cytoprotective effect[a] inhibition (%)	
	Drug concentration (M)						dose (μg/kg)	
	10^{-4}	10^{-5}	10^{-6}	10^{-7}	10^{-8}	10^{-9}	250	5
3				99	47	6		
5				99	89	35		
6	100	0					20	
7		91	15				27	
75				100	44			
76				100	64	16		
77				100	25	13		
78					100	59		77

a) Cytoprotective effects on HCl-induced gastric mucosal lesion in rats.

be an excellent method for the stereocontrolled synthesis of exocyclic olefins. The synthesis presented in this paper offers the most efficient synthetic route to carbacyclins. Carbacyclins and several synthetic intermediates are now being produced on a commercial basis.[18]

Experimental

General Methods Infrared (IR) spectra were measured on a JASCO A-202 diffraction grating infrared spectrophotometer. ^{1}H-NMR spectra were recorded with a Varian EM 390 NMR spectrometer or a Hitachi R-90H Fourier-transform NMR spectrometer or a Bruker ASX-500 spectrometer with tetramethylsilane as an internal standard. Low-resolution mass spectra (MS) were obtained with a Hitachi RUM-6MG mass spectrometer. Optical rotation was measured on a Horiba SEPA-200 high-sensitivity polarimeter. In general, reactions were carried out in dry solvents under an argon atmosphere unless otherwise mentioned.

In a similar manner to the previously reported[7a] intramolecular ene reaction route, the diene **11** was synthesized from methyl (*Z*)-7-[(1*R*,2*S*,3*R*)-2-*tert*-butyldimethylsilyloxymethyl-5-methylene-3-tetrahydropyranyloxycyclopentyl]hept-5-enoate. Yield and spectral data of the intermediates were as follows.

Methyl (*Z*)-7-[(1*R*,2*S*,3*R*)-2-*tert*-Butyldimethylsilyloxymethyl-3-*tert*-butyldiphenylsilyloxy-5-methylenecyclopentyl]hept-5-enoate Yield from methyl (*Z*)-7-[(1*R*,2*S*,3*R*)-2-*tert*-butyldimethylsilyloxymethyl-5-methylene-3-tetrahydropyranyloxycyclopentyl]hept-5-enoate was 87%. IR (neat): 1743, 1660 cm^{-1}. ^{1}H-NMR ($CDCl_3$) δ: 0.05 (s, 6H), 0.86 (s, 9H), 1.10 (s, 9H), 1.20—2.60 (m, 12H), 3.50 (d, J=6 Hz, 2H), 3.68 (s, 3H), 4.12 (m, 1H), 4.83 (br s, 2H), 5.50 (m, 2H), 7.20—7.60 (m, 6H), 7.60—7.90 (m, 4H). MS *m/z*: 563 ($M^+ - tert$-Bu), 296, 295, 294, 293, 255, 240, 239 (base peak), 237, 215. HR-MS *m/z*: (M^+ − Me) Calcd for $C_{36}H_{53}O_4Si_2$ 605.3479, Found 605.3475. $[\alpha]_D^{20}$: −22° (c=1.50, MeOH).

Methyl (*Z*)-7-[(1*S*,2*S*,3*R*,5*S*)-2-*tert*-Butyldimethylsilyloxymethyl-3-*tert*-butyldiphenylsilyloxy-5-hydroxymethylcyclopentyl]hept-5-enoate Yield was 78%. IR (neat): 3475, 1745, 740, 705 cm^{-1}. ^{1}H-NMR ($CDCl_3$) δ: 0.14 (s, 6H), 0.85 (s, 9H), 1.17 (s, 9H), 1.50—2.50 (m, 13H), 3.00—3.50 (m, 3H), 3.70 (s, 3H), 3.75 (m, 2H), 4.18 (m, 1H), 5.42 (m, 2H), 7.20—7.50 (m, 6H), 7.50—7.90 (m, 4H). MS *m/z*: 581 ($M^+ - tert$-Bu), 365, 271, 251, 234, 233, 221, 219, 209, 201, 73 (base peak). HR-MS *m/z*: (M^+) Calcd for $C_{37}H_{58}O_5Si_2$ 638.3820, Found 638.3847. $[\alpha]_D^{20}$: +16° (c=1.98, MeOH).

Methyl (*Z*)-7-[(1*S*,2*S*,3*R*,5*S*)]-2-*tert*-Butyldimethylsilyloxymethyl-3-*tert*-butyldiphenylsilyloxy-5-formylcyclopentyl]hept-5-enoate Yield was 100%. IR (neat): 1740, 1720, 740, 700 cm^{-1}. ^{1}H-NMR ($CDCl_3$) δ: 0.07 (s, 6H), 0.88 (s, 9H), 1.14 (s, 9H), 1.30—2.50 (m, 12H), 2.70 (m, 1H), 3.50 (m, 2H), 3.74 (s, 3H), 4.20 (m, 1H), 5.47 (m, 2H), 7.20—7.60 (m, 6H), 7.60—7.90 (m, 4H), 10.05 (d, J=3 Hz, 1H). MS *m/z*: 580, 579 ($M^+ - tert$-Bu), 368, 313, 272, 271, 249, 235, 231, 217, 211, 210, 209, 200, 73 (base peak). HR-MS *m/z*: ($M^+ - tert$-Bu) Calcd for $C_{33}H_{47}O_5Si_2$ 579.2959, Found 579.2931. $[\alpha]_D^{20}$: +7° (c=1.34, MeOH).

Methyl (1*R*,5*S*,6*S*,7*R*)-6-*tert*-Butyldimethylsilyloxymethyl-7-*tert*-butyldiphenylsilyloxybicyclo[3.3.0]oct-2-ene-3-γ-pentenoate (11) Yield from methyl (*Z*)-7-[(1*S*,2*S*,3*R*,5*S*)-2-*tert*-butyldimethylsilyloxymethyl-3-*tert*-butyldiphenylsilyloxy-5-formylcyclopentyl]hept-5-enoate was 57%. IR (neat): 1745, 740, 700 cm^{-1}. ^{1}H-NMR ($CDCl_3$) δ: 0.05 (s, 6H), 0.90 (s, 9H), 1.07 (s, 9H), 1.50—2.00 (m, 2H), 2.00—2.70 (m, 8H), 2.90 (m, 1H), 3.30—4.20 (m, 3H), 3.70 (s, 3H), 5.50 (m, 2H), 6.25 (d, J=16.5 Hz, 1H), 7.25—7.50 (m, 6H), 7.50—7.80 (m, 4H). MS *m/z*: 561 ($M^+ - tert$-Bu), 271, 231, 209, 205 (base peak). HR-MS *m/z*: ($M^+ - tert$-Bu) Calcd for $C_{33}H_{45}O_4Si_2$ 561.2854, Found 561.2871.

Methyl (1*S*,5*S*,6*S*,7*R*)-6-*tert*-Butyldimethylsilyloxymethyl-7-tetrahydropyranyloxybicyclo[3.3.0]octane-*E*-Δ$^{3,\delta}$pentanoate (14) The diene **13** (495 mg, 1.07 mmol) and (methyl benzoate)$Cr(CO)_3$ (58 mg, 0.21 mmol) were dissolved in acetone (15 ml). The solution was degassed by three freeze-pump-thaw cycles, and then transferred into an autoclave with glass insert (100 ml) under an argon atmosphere. The autoclave was purged repeatedly with hydrogen. The solution was stirred at 120 °C for 16 h under 70 kg/cm^2 of hydrogen pressure. After cooling to room temperature, the reaction mixture was exposed to air and light to decompose the catalyst. Removal of the solvent gave a dark green residue, which was purified by silica gel column chromatography (ether–hexane, 1 : 10—1 : 5) to afford the desired exocyclic olefin **14** (486 mg, 98%) as a colorless oil. The GLC analysis (OV-1, 1.5%, 1.5 m, 228 °C, 1.0 kg/cm^2 of N_2 pressure) of the product showed the absence of the 5*Z*-isomer of **14**, starting material and exocyclic conjugated diene, but revealed contamination with a trace amount of regioisomer **15** (retention time: 5*E*-isomer **14**, 6.5 min; 5*Z*-isomer, 5.9 min; regioisomer **15**, 5.3 min; starting material **13**, 4*Z*-isomer, 6.2 min; 4*E*-isomer, 7.5 min; exocyclic conjugated diene **21**, 8.1 min). Spectral data of **14**: IR (neat): 2970, 2880, 1747, 840 cm^{-1}. ^{1}H-NMR ($CDCl_3$) δ: 0.05 (s, 6H), 0.90 (s, 9H), 1.30—2.60 (m, 21H), 3.30—4.10 (m, 5H), 3.70 (s, 3H), 4.66 (m, 1H), 5.23 (t, J=7 Hz, 1H). MS *m/z*: 466 (M^+), 325, 233, 201, 159, 131, 117, 105, 91, 89, 86, 85 (base peak), 75, 73, 67, 57, 43, 41. HR-MS *m/z*: (M^+) Calcd for $C_{26}H_{46}O_5Si$ 466.3112, Found 466.3138.

In a similar manner, the hydrogenations described in Chart 2 and Table I were carried out. The spectral data of **12** and **21** were as follows.

Methyl (1*S*,5*S*,6*S*,7*R*)-6-*tert*-Butyldimethylsilyloxymethyl-7-*tert*-butyldiphenylsilyloxybicyclo[3.3.0]octane-*E*-Δ$^{3,\delta}$-pentanoate (12) IR (neat): 1745, 740, 703 cm^{-1}. ^{1}H-NMR ($CDCl_3$) δ: 0.04 (s, 6H), 0.90 (s, 9H), 1.08 (s, 9H), 1.20—2.60 (m, 15H), 3.20—3.80 (m, 2H), 3.68 (s, 3H), 3.80—4.10 (m, 1H), 5.25 (br t, J=7 Hz, 1H), 7.30—7.60 (m, 6H), 7.60—7.80 (m, 4H). MS *m/z*: 564, 563 ($M^+ - tert$-Bu), 531, 313, 307, 273, 272, 271, 235, 234, 233 (base peak). HR-MS *m/z*: ($M^+ - tert$-Bu) Calcd for $C_{33}H_{47}O_4Si_2$ 563.3009, Found 563.2998. $[\alpha]_D^{20}$: −17° (c=1.32, $CHCl_3$).

Methyl (1*S*,5*S*,6*S*,7*R*)-6-*tert*-Butyldimethylsilyloxymethyl-7-tetrahydropyranyloxybicyclo[3.3.0]octane-*E*-Δ$^{3,\delta}$-*E*-β-pentenoate (21) IR (neat): 2960, 1745, 840 cm^{-1}. ^{1}H-NMR ($CDCl_3$) δ: 0.05 (s, 6H), 0.90 (s, 9H), 1.20—2.00 (m, 8H), 2.00—2.80 (m, 7H), 3.13 (d, J=7 Hz, 2H), 3.30—4.10 (m, 5H), 3.71 (s, 3H), 4.63 (m, 1H), 5.64 (dt, J=15.5, 7 Hz, 1H), 5.96 (d, J=11 Hz, 1H), 6.25 (dd, J=15.5, 11 Hz, 1H), MS *m/z*: 464 (M^+), 323, 305, 231, 159, 157, 89, 85 (base peak), 75, 73. HR-MS *m/z*: (M^+) Calcd for $C_{26}H_{44}O_5Si$ 464.2956, Found 464.2973.

Methyl (1*S*,5*S*,6*S*,7*R*)-6-Hydroxymethyl-7-tetrahydropyranyloxybicyclo[3.3.0]octane-*E*-Δ$^{3,\delta}$-pentanoate (16) Tetrabutylammonium fluoride (1 M solution in THF, 1.56 ml) was added to a solution of **14** (486 mg, 1.04 mmol) in THF (5 ml), and the mixture was stirred for 11.5 h at 23 °C. The reaction was quenched by the addition of brine, followed by extraction with ether. The combined organic layers were dried over $MgSO_4$, and concentrated. The residue was purified by silica gel column chromatography (ether–hexane, 3 : 2) to give the alcohol (**16**) (349 mg, 95%) and the more polar regioisomer **17** (7 mg, 1.9%). Spectral data of **16**: IR (neat): 3480, 2950, 1741 cm^{-1}. ^{1}H-NMR ($CDCl_3$) δ: 1.00—2.60 (m, 21H), 2.60—3.30 (m, 1H), 3.30—4.20 (m, 5H), 3.65 (s, 3H), 4.65 (m, 1H), 5.22 (br t, J=7 Hz, 1H). MS *m/z*: 352 (M^+), 334 ($M^+ - H_2O$), 268 (M^+ − DHP), 250, 232, 219, 91, 86, 85 (base peak), 79, 67, 57, 55, 43, 41. HR-MS *m/z*: (M^+) Calcd for $C_{20}H_{32}O_5$ 352.2247, Found 352.2225. Spectral data of **17**: IR (neat): 3480, 2950, 1740 cm^{-1}. ^{1}H-NMR ($CDCl_3$) δ: 0.80—3.10 (m, 21H), 3.30—4.30 (m, 5H), 3.68 (s, 3H), 4.68 (m, 1H), 5.32 (m, 2H). MS *m/z*: 352 (M^+), 334 ($M^+ - H_2O$), 268 (M^+ − DHP), 250, 233, 219, 201, 173, 159, 149, 105, 91, 86, 85 (base peak), 84, 79, 67, 57, 55, 43, 41. HR-MS *m/z*: (M^+) Calcd for $C_{20}H_{32}O_5$ 352. 2247, Found 352.2252.

Methyl (1*S*,5*S*,6*R*,7*R*)-6-(3-Oxo-*E*-1-octenyl)-7-tetrahydropyranyloxybicyclo[3.3.0]octane-*E*-Δ$^{3,\delta}$-pentanoate (19) A solution of SO_3–pyridine complex (201 mg, 1.26 mmol) in DMSO (3 ml) was added to a stirred solution of the alcohol **16** (49 mg, 0.14 mmol) and triethylamine (0.36 ml) in DMSO (1.5 ml), and the mixture was stirred at 23 °C for 2.5 h. The reaction mixture was poured into ice-water, and extracted with ether. The ether extracts were washed with water and brine, and dried over $MgSO_4$. Removal of the solvent gave the crude aldehyde **18**. Sodium hydride (60%

in oil, 8 mg, 0.20 mmol) was washed with pentane, and suspended in THF (1.4 ml). A solution of dimethyl (2-oxoheptyl)phosphonate (47 mg, 0.21 mmol) in THF (0.2 ml) was added to the suspension, and the mixture was stirred at 23 °C for 30 min. Then, a solution of the crude aldehyde **18** in THF (0.6 ml) was dropped into a solution of the phosphonate carbanion, and the whole mixture was stirred for 30 min. The reaction was quenched by the addition of saturated aqueous NH_4Cl, followed by extraction with ether. The combined ether extracts were washed with brine, and dried over $MgSO_4$. Removal of the solvent and purification by silica gel column chromatography (ether–hexane, 2 : 5) afforded the enone **19** (52 mg, 84%) as a colorless oil. IR (neat): 2950, 1740, 1700, 1675, 1630 cm^{-1}. ^{1}H-NMR ($CDCl_3$) δ: 0.90 (t, J=6 Hz, 3H), 1.00—2.70 (m, 29H), 3.30—4.20 (m, 3H), 3.68 (s, 3H), 4.55, 4.65 (each br s, total 1H), 5.25 (t, J=7 Hz, 1H), 6.13, 6.17 (each d, J=16 Hz, total 1H), 6.75 (m, 1H). MS m/z: 362 (M^+ − DHP), 344 (M^+ − THPOH), 318, 279, 205, 167, 149, 85 (base peak), 74, 73, 61, 59, 57, 45 (base peak), 43. HR-MS m/z: (M^+ − DHP) Calcd for $C_{22}H_{34}O_4$ 362.2455, Found 362.2462.

Methyl (1*R*,5*S*,6*R*,7*R*)-7-Hydroxy-6-(3-oxo-*E*-1-octenyl)bicyclo[3.3.0]-octane-*E*-$\Delta^{3,\delta}$-pentanoate (20) A 65% aqueous solution of acetic acid (0.9 ml) was added to a solution of **19** (50 mg, 0.11 mmol) in THF (0.9 ml), and the mixture was stirred at 50 °C for 2 h, then poured into saturated aqueous $NaHCO_3$, and extracted with ether. The ether extracts were washed with brine, and dried over $MgSO_4$. Removal of the solvent and purification by silica gel column chromatography (ether–hexane, 3 : 2) afforded the alcohol **20** (39 mg, 96%) as a colorless oil. IR (neat): 3450, 2950, 1740, 1695, 1675, 1625 cm^{-1}. ^{1}H-NMR ($CDCl_3$) δ: 0.90 (t, J=7 Hz, 3H), 1.00—2.70 (m, 24H), 3.70 (s, 3H), 3.92 (m, 1H), 5.28 (br t, J=7 Hz, 1H), 6.22 (d, J=15 Hz, 1H), 6.76 (dd, J=15, 7 Hz, 1H). MS m/z: 362 (M^+), 344 ($M^+ - H_2O$), 318, 273 (base peak), 119, 105, 99, 91, 79, 71, 55, 43, 4. $[\alpha]_D^{20}$: +53° (c=0.77, MeOH). The spectral data of **20** were identical with those of an authentic sample prepared by the known method.[1)]

Methyl (1*R*,5*S*,6*S*,7*R*)-6-Hydroxymethyl-7-tetrahydropyranyloxybicyclo[3.3.0]oct-2-ene-3-γ-pentenoate (27) Tetrabutylammonium fluoride (1 M solution in THF, 0.32 ml) was added to a solution of **13** (100 mg, 0.22 mmol), and the mixture was stirred at 23 °C for 13 h. The reaction was quenched by the addition of brine, followed by extraction of the mixture with ether. The combined organic layers were dried over $MgSO_4$, and concentrated. The residue was purified by silica gel column chromatography (ether–hexane, 3 : 2) to give the alcohol **27** (71 mg, 94%) as a colorless oil. IR (neat): 3480, 2950, 1740 cm^{-1}. ^{1}H-NMR ($CDCl_3$) δ: 1.00—2.00 (m, 8H), 2.00—2.80 (m, 8H), 3.00 (m, 2H), 3.00—4.30 (m, 5H), 3.68 (s, 3H), 4.62 (m, 1H), 5.35 (m, 1H), 5.58 (br s, 1H), 6.00 (d, J=12 Hz, 2.2/3.2H), 6.26 (d, J=15 Hz, 1/3.2H). MS m/z: 350 (M^+), 266 (M^+-DHP), 248, 230, 217, 177, 117, 91, 85 (base peak). HR-MS m/z: (M^+) Calcd for $C_{20}H_{30}O_5$ 350.2090, Found 350.2081.

Methyl (1*R*,5*S*,6*R*,7*R*)-6-(3-Oxo-*E*-1-octenyl)-7-tetrahydropyranyloxybicyclo[3.3.0]oct-2-ene-3-γ-pentenoate (28) A solution of SO_3–pyridine complex (94 mg, 0.59 mmol) in DMSO (1.6 ml) was added to a stirred solution of the alcohol **27** (69 mg, 0.2 mmol) and triethylamine (0.16 ml) in DMSO (2.3 ml), and the mixture was stirred at 23 °C for 30 min. The reaction mixture was poured into ice-water, and extracted with ether. The ether extracts were washed with water and brine, and dried over $MgSO_4$. Removal of the solvent gave the crude aldehyde. Sodium hydride (60% in oil, 10 mg, 0.25 mmol) was washed with pentane, and suspended in THF (2 ml). A solution of dimethyl (2-oxoheptyl)phosphonate (47 mg, 0.21 mmol) in THF (0.3 ml) was added to the suspension, and the mixture was stirred at 23 °C for 30 min. Then, a solution of the crude aldehyde in THF (1 ml) was dropped into the solution of the phosphonate carbanion, and the whole mixture was stirred at 23 °C for 40 min. The reaction was quenched by the addition of saturated aqueous NH_4Cl, followed by extraction of the mixture with ether. The combined ether extracts were washed with brine, and dried over $MgSO_4$. Removal of the solvent and purification of the residue by silica gel column chromatography (ether–hexane, 2 : 5) afforded the enone **28** (77 mg, 88%) as a colorless oil. IR (neat): 2950, 1740, 1680, 1625 cm^{-1}. ^{1}H-NMR ($CDCl_3$) δ: 0.90 (t, J=6 Hz, 3H), 1.00—2.00 (m, 12H), 2.00—3.00 (m, 12H), 3.10 (m, 1H), 3.30—4.20 (m, 3H), 3.67 (s, 3H), 4.60 (m, 1H), 5.00—5.70 (m, 2H), 5.80—6.40 (m, 2H), 6.75 (m, 1H). MS m/z: 444 (M^+), 360 (M^+ − DHP), 342 (M^+ − THPOH), 316, 246, 99, 85 (base peak), 67, 57, 43, 41, HR-MS m/z: (M^+) Calcd for $C_{27}H_{40}O_5$ 444.2873, Found 444.2873.

In a similar manner, **29**—**31** were synthesized from **27** and the corresponding ketophosphonates. The spectral data were as follows.

Methyl (1*R*,5*S*,6*R*,7*R*)-6-(3-Cyclopentyl-3-oxo-*E*-1-propenyl)-7-tetrahydropyranyloxybicyclo[3.3.0]oct-2-ene-3-γ-pentenoate (29) IR (neat): 2960, 1740, 1700, 1670, 1630 cm^{-1}. ^{1}H-NMR ($CDCl_3$) δ: 1.20—2.00 (m, 14H), 2.00—2.90 (m, 10H), 3.10 (m, 2H), 3.30—4.20 (m, 3H), 3.68 (s, 3H), 4.60 (m, 1H), 5.00—5.70 (m, 2H), 5.80—6.50 (m, 2H), 6.80 (m, 1H). MS m/z: 442 (M^+), 411 (M^+ − MeO), 358 (M^+ − DHP), 340 (M^+ − THPOH), 244, 97, 85 (base peak), 69, 67, 57, 55, 43, 41. HR-MS m/z: (M^+) Calcd for $C_{27}H_{38}O_5$ 442.2716, Found 442.2713.

Methyl (1*R*,5*S*,6*R*,7*R*)-6-(5,9-Dimethyl-3-oxo-*E*-1,8-decadienyl)-7-tetrahydropyranyloxybicyclo[3.3.0]oct-2-ene-3-γ-pentenoate (30) IR (neat): 2950, 1740, 1695, 1680, 1625 cm^{-1}. ^{1}H-NMR ($CDCl_3$) δ: 0.93 (d, J=6 Hz, 3H), 1.00—1.80 (m, 15H), 1.80—2.90 (m, 14H), 3.10 (m, 1H), 3.30—4.20 (m, 3H), 3.70 (s, 3H), 4.65 (m, 1H), 4.90—5.70 (m, 3H), 5.80—6.50 (m, 2H), 6.80 (m, 1H). MS m/z: 498 (M^+), 414 (M^+ − DHP), 396 (M^+ − THPOH), 246, 230, 178, 153, 131, 129, 117, 109, 85 (base peak), 69, 67. HR-MS m/z: (M^+) Calcd for $C_{31}H_{46}O_5$ 498.3342, Found 498.3335.

Methyl (1*R*,5*S*,6*R*,7*R*)-6-(4-Methyl-3-oxo-*E*-1-octen-6-ynyl)-7-tetrahydropyranyloxybicyclo[3.3.0]oct-2-ene-3-γ-pentenoate (31) IR (neat): 2950, 1740, 1695, 1680, 1625 cm^{-1}. ^{1}H-NMR ($CDCl_3$) δ: 1.20 (d, J=7 Hz, 3H), 1.30—1.70 (m, 6H), 1.75 (t, J=2 Hz, 3H), 1.90—2.80 (m, 12H), 3.00 (m, 2H), 3.30—4.20 (m, 3H), 3.68 (s, 3H), 4.60 (m, 1H), 5.00—5.70 (m, 2H), 5.80—6.50 (m, 2H), 6.65—7.15 (m, 1H). MS m/z: 454 (M^+), 370 (M^+ − DHP), 352 (M^+ − THPOH), 326, 246, 202, 178, 169, 161, 155, 143, 129, 124, 117, 109, 105, 91, 85 (base peak). HR-MS m/z: (M^+) Calcd for $C_{28}H_{38}O_5$ 454.2717, Found 454.2723.

Methyl (1*R*,5*S*,6*R*,7*R*)-6-(3-Hydroxy-*E*-1-octenyl)-7-tetrahydropyranyloxybicyclo[3.3.0]oct-2-ene-3-γ-pentenoate An excess amount of sodium borohydride was added to a stirred solution of the enone **28** (73 mg, 0.16 mmol) in methanol (2.6 ml) at −25 °C, and the mixture was stirred at the same temperature for 40 min. The reaction was quenched by the addition of acetone, and then saturated aqueous NH_4Cl was added to the reaction mixture. After evaporation of the organic solvents, the water layer was extracted with ether. The combined ether extracts were dried over $MgSO_4$, and concentrated to give the alcohol as an epimeric mixture (81 mg). Spectral data of the alcohol: IR (neat): 3470, 2950, 1745 cm^{-1}. ^{1}H-NMR ($CDCl_3$) δ: 0.90 (m, 3H), 1.00—2.90 (m, 24H), 3.00 (m, 1H), 3.30—4.30 (m, 5H), 3.70 (s, 3H), 4.67 (m, 1H), 5.10—5.75 (m, 4H), 6.00 (d, J=11 Hz, 2.2/3.2H), 6.28 (d, J=16 Hz, 1/3.2H). MS m/z: 446 (M^+), 230, 217, 157, 156, 143, 129, 128, 117, 115, 91, 79, 78 (base peak), 77, 52. HR-MS m/z:(M^+) Calcd for $C_{27}H_{42}O_5$ 446.3029, Found 446.3006.

Methyl (1*R*,5*S*,6*R*,7*R*)-7-Hydroxy-6-[3(*S*)-hydroxy-*E*-1-octenyl]bicyclo[3.3.0]oct-2-ene-3-γ-pentenoate (32a) The crude alcohol (epimeric mixture, 80 mg) was dissolved in a mixture of 65% aqueous acetic acid (1.3 ml) and THF (0.13 ml), and the mixture was stirred at 50 °C for 2 h, then poured into saturated aqueous $NaHCO_3$, and extracted with ether. The ether extracts were washed with brine, dried over $MgSO_4$, and concentrated. The residue was purified by silica gel column chromatography (ether–hexane, 3 : 1→ether) to afford the desired 15α-diol (**32a**) (23 mg, 39%) as a more polar fraction and the 15β-diol (**32b**) (13 mg, 22%) as a less polar fraction. Spectral data of **32a**: IR (neat): 3400, 2950, 1742 cm^{-1}. ^{1}H-NMR ($CDCl_3$) δ: 0.90 (m, 3H), 1.10—2.95 (m, 20H), 3.02 (m, 1H), 3.70 (s, 3H), 3.70 (m, 1H), 4.10 (m, 1H), 5.00—5.70 (m, 4H), 6.02 (d, J=11 Hz, 2.2/3.2 H), 6.30 (d, J=15 Hz, 1/3.2H). MS m/z: 362 (M^+), 344, 300, 273, 230, 220, 192, 191, 178, 167, 149, 143, 131, 129, 128, 119, 118, 117, 105, 99, 91, 79, 71, 67, 57, 55, 43 (base peak), 41. HR-MS m/z: (M^+) Calcd For $C_{22}H_{34}O_4$ 362.2454, Found 362.2451. $[\alpha]_D^{20}$: −35° (c=0.466, MeOH). The spectral data of **32b** were nearly identical with those of **31a** except for the optical rotation.

In a similar manner, **29**—**31** were converted to the corresponding diols **33a**—**35a**. The spectral data were as follows.

Methyl (1*R*,5*S*,6*R*,7*R*)-6-(3-Cyclopentyl-3-hydroxy-*E*-1-propenyl)-7-tetrahydropyranyloxybicyclo[3.3.0]oct-2-ene-3-γ-pentenoate IR (neat): 3500, 2970, 1742 cm^{-1}. ^{1}H-NMR ($CDCl_3$) δ: 1.00—2.90 (m, 23H), 3.02 (m, 1H), 3.30—4.10 (m, 7H), 3.70 (s, 3H), 4.70 (m, 1H), 5.10—5.80 (m, 4H), 6.00 (d, J=11 Hz, 2.2/3.2H), 6.28 (d, J=16 Hz, 1/3.2H). MS m/z: 444 (M^+), 342, 298, 220, 178, 85 (base peak), 69, 67, 57. HR-MS m/z: (M^+) Calcd for $C_{27}H_{40}O_5$ 444.2873, Found 444.2885.

Methyl (1*R*,5*S*,6*R*,7*R*)-6-[3(*R*)-Cyclopentyl-3-hydroxy-*E*-1-propenyl]-7-hydrobicyclo[3.3.0]oct-2-ene-3-γ-pentenoate (33a) IR (neat): 3400, 2950, 1740 cm^{-1}. ^{1}H-NMR ($CDCl_3$) δ: 1.10—2.80 (m, 21H), 3.02 (m, 1H), 3.40—4.00 (m, 2H), 3.65 (s, 3H), 5.17—5.75 (m, 4H), 5.95 (d, J=11 Hz, 2.2/3.2H), 6.22 (d, J=15 Hz, 1/3.2H). MS m/z: 360 (M^+), 342, 324, 298, 273, 220, 178, 131, 117, 105, 97, 91, 79, 69 (base peak), 67, 41. HR-MS m/z: (M^+) Calcd for $C_{22}H_{32}O_4$ 360.2298, Found 360.2293. $[\alpha]_D^{20}$: −30° (c=1.16, MeOH).

Methyl (1*R*,5*S*,6*R*,7*R*)-6-(3-Hydroxy-5,9-dimethyl-*E*-1,8-decadienyl)-7-tetrahydropyranyloxybicyclo[3.3.0]oct-2-ene-3-γ-pentenoate IR (neat):

3500, 2950, 1745 cm^{-1}. ^{1}H-NMR ($CDCl_3$) δ: 0.90 (d, J=6 Hz, 3H), 1.10—2.80 (m, 30H), 3.04 (m, 1H), 3.50—4.05 (m, 3H), 3.69 (s, 3H), 4.20 (m, 1H), 4.68 (m, 1H), 5.00—5.50 (m, 2H), 5.62 (m, 3H), 6.00 (d, J=11 Hz, 2.2/3.2H), 6.26 (d, J=15 Hz, 1/3.2H). MS m/z: 500 (M^+), 482, 416 (M^+ − DHP), 399, 398 (M^+ − THPOH), 380, 232, 231, 230, 131, 117, 109, 105, 95, 91, 86, 85 (base peak), 81, 79, 69, 67, 57, 55. HR-MS m/z: (M^+) Calcd for $C_{31}H_{48}O_5$ 500.3499, Found 500. 3539.

Methyl (1*R*,5*S*,6*R*,7*R*)-7-Hydroxy-6-[3-(*S*)-hydroxy-5,9-dimethyl-*E*-1,8-decadienyl]bicyclo[3.3.0]oct-2-ene-3-γ-pentenoate (34a) IR (neat): 3400, 2920, 1740 cm^{-1}. ^{1}H-NMR ($CDCl_3$) δ: 0.95 (d, J=6 Hz, 3H), 1.10—1.60 (m, 6H), 1.62 (s, 3H), 1.70 (s, 3H), 1.80—2.80 (m, 1H), 2.80—3.50 (m, 3H), 3.70 (s, 3H), 3.70 (m, 1H), 4.14 (m, 1H), 5.12 (t, J=7 Hz, 1H), 5.20—5.80 (m, 4H), 6.00 (d, J=12 Hz, 2.2/3.2H), 6.25 (d, J=15 Hz, 1/3.2H). MS m/z: 416 (M^+), 398 ($M^+ - H_2O$), 380 ($M^+ - 2H_2O$), 313, 230, 178, 143, 131, 129, 117, 109, 105, 95, 91, 81, 79, 68, 67, 55, 43, 41 (base peak). HR-MS m/z: (M^+) Calcd for $C_{26}H_{40}O_4$ 416.2923, Found 416.2909.

Methyl (1*R*,5*S*,6*R*,7*R*)-6-(3-Hydroxy-4-methyl-*E*-1-octen-6-ynyl)-7-tetrahydropyranyloxybicyclo[3.3.0]oct-2-ene-3-γ-pentenoate IR (neat): 3500, 2950, 1745 cm^{-1}. ^{1}H-NMR ($CDCl_3$) δ: 1.00 (m, 3H), 1.10—2.80 (m, 23H), 3.04 (m, 1H), 3.60—4.40 (m, 4H), 3.71 (s, 3H), 4.60 (m, 1H), 5.20—5.80 (m, 4H), 6.02 (d, J=12 Hz, 2.2/3.2H), 6.30 (d, J=16 Hz, 1/3.2H). MS m/z: 372 (M^+ − DHP), 354 (M^+ − THPOH), 310, 301, 220, 143, 117, 105, 91, 86, 85 (base peak), 81, 79, 77, 67, 57, 55, 53. HR-MS m/z: (M^+ − DHP) Calcd for $C_{23}H_{32}O_4$ 372.2298, Found 372.2285.

Methyl (1*R*,5*S*,6*R*,7*R*)-7-Hydroxy-6-[3(*R*)-hydroxy-4-methyl-*E*-1-octen-6-ynyl]bicyclo[3.3.0]oct-2-ene-3-γ-pentenoate (35a) IR (neat): 3400, 2940, 1740 cm^{-1}. ^{1}H-NMR ($CDCl_3$) δ: 0.98 (m, 3H), 1.10—2.80 (m, 16H), 1.78 (t, J=2 Hz, 3H), 3.03 (m, 1H), 3.30—4.30 (m, 2H), 3.68 (s, 3H), 5.00—5.70 (m, 3H), 6.00 (d, J=12 Hz, 2.2/3.2H), 6.25 (d, J=16 Hz, 1/3.2H). MS m/z: 372 (M^+), 354 ($M^+ - H_2O$), 336 ($M^+ - 2H_2O$), 310, 220, 178, 155, 145, 143, 131, 129, 119, 118, 117, 105, 91, 81 (base peak), 79, 77, 67, 55, 53. HR-MS m/z: (M^+) Calcd for $C_{23}H_{32}O_4$ 372.2299, Found 372.2302.

Methyl (1*R*,5*S*,6*R*,7*R*)-7-*tert*-Butyldimethylsilyloxy-6-[3(*S*)-*tert*-butyldimethylsilyloxy-*E*-1-octenyl]bicyclo[3.3.0]oct-2-ene-3-γ-pentenoate (36) Imidazole (12 mg, 0.18 mmol) and *tert*-butyldimethylsilyl chloride (27 mg, 0.18 mmol) were added to a stirred solution of the diol **32a** (21 mg, 0.06 mmol) in DMF (0.08 ml) at 0 °C. The mixture was stirred at 23 °C for 1 h, and then saturated aqueous NH_4Cl was added. The reaction mixture was extracted with ether, washed with brine, and dried over $MgSO_4$. Removal of the solvent and purification of the residue by silica gel column chromatography (ether–hexane, 1 : 10) afforded **36** (31 mg, 90%) as a colorless oil. IR (neat): 2950, 1750, 840 cm^{-1}. ^{1}H-NMR ($CDCl_3$) δ: 0.03 (s, 12H), 0.87 (t, J=7 Hz, 3H), 0.90 (s, 18H), 1.10—2.80 (m, 18H), 2.97 (m, 1H), 3.69 (s, 3H), 3.70 (m, 1H), 4.07 (m, 1H), 5.51 (m, 4H), 6.02 (d, J=12 Hz, 2.2/3.2H), 6.27 (d, J=16 Hz, 1/3.2H). MS m/z: 590 (M^+), 533 (M^+ − *tert*-Bu), 519, 458, 427, 401, 301, 75, 73 (base peak). HR-MS m/z: (M^+ − *tert*-Bu) Calcd for $C_{30}H_{53}O_4Si_2$ 533.3484, Found 533.3490.

In a similar manner, **33a**—**35a** were converted to the corresponding silyl ether **37**—**39**. The spectral data were as follows.

Methyl (1*R*,5*S*,6*R*,7*R*)-7-*tert*-Butyldimethylsilyloxy-6-[3(*R*)-*tert*-butyldimethylsilyloxy-3-cyclopentyl-*E*-1-propenyl]bicyclo[3.3.0]oct-2-ene-3-γ-pentenoate (37) IR (neat): 2960, 1745, 838 cm^{-1}. ^{1}H-NMR ($CDCl_3$) δ: 0.00 (s, 12H), 0.90 (s, 9H), 0.95 (s, 9H), 1.00—2.75 (m, 19H), 3.00 (m, 1H), 3.65—4.00 (m, 2H), 3.68 (s, 3H), 5.05—5.80 (m, 4H), 6.01 (d, J=11 Hz, 2.2/3.2H), 6.25 (d, J=16 Hz, 1/3.2H). MS m/z: 588 (M^+), 573.531 (M^+ − *tert*-Bu), 519, 387, 361, 299, 171, 147, 117, 105, 91, 79, 75, 73 (base peak), 67. HR-MS m/z: (M^+) Calcd for $C_{34}H_{60}O_4Si_2$ 588.4030, Found 588.4020.

Methyl (1*R*,5*S*,6*R*,7*R*)-7-*tert*-Butyldimethylsilyloxy-6-[3(*S*)-*tert*-butyldimethylsilyloxy-5,9-dimethyl-*E*-1,8-decadienyl]bicyclo[3.3.0]oct-2-ene-3-γ-pentenoate (38) IR (neat): 2960, 2940, 1745, 835 cm^{-1}. ^{1}H-NMR ($CDCl_3$) δ: 0.00 (s, 12H), 0.91 (m, 21H), 1.00—1.75 (m, 6H), 1.60 (s, 3H), 1.66 (s, 3H), 1.75—2.80 (m, 11H), 3.00 (m, 1H), 3.55—3.90 (m, 1H), 3.68 (s, 3H), 5.10 (t, J=7 Hz, 1H), 5.15—5.60 (m, 4H), 5.90 (d, J=11 Hz, 2.2/3.2H), 6.20 (d, J=15 Hz, 1/3.2H). MS m/z: 644 (M^+), 587 (M^+ − *tert*-Bu), 588, 519, 455, 387, 381, 361, 355, 217, 177, 147, 117, 109, 81, 75, 73 (base peak), 69. HR-MS m/z: (M^+) Calcd for $C_{38}H_{68}O_4Si_2$ 644.4652, Found 644.4621.

Methyl (1*R*,5*S*,6*R*,7*R*)-7-*tert*-Butyldimethylsilyloxy-6-[3(*R*)-*tert*-butyldimethylsilyloxy-4-methyl-*E*-1-octen-6-ynyl]bicyclo[3.3.0]oct-2-ene-3-γ-pentenoate (39) IR (neat): 2960, 2940, 1745, 840 cm^{-1}. ^{1}H-NMR ($CDCl_3$) δ: 0.00 (s, 12H), 0.90 (m, 21H), 1.05—2.70 (m, 13H), 1.75 (t, J=2 Hz, 3H), 3.00 (m, 1H), 3.25—4.20 (m, 2H), 3.65 (s, 3H), 5.05—5.70 (m, 4H), 5.97 (d, J=11 Hz, 2.2/3.2H), 6.23 (d, J=15 Hz, 1/3.2H). MS m/z: 600 (M^+), 543 (M^+ − *tert*-Bu), 519, 387, 361, 171, 155, 147, 131, 119, 117, 105, 91, 89, 81, 79, 75, 73 (base peak), 59. HR-MS m/z: (M^+) Calcd for $C_{35}H_{60}O_4Si_2$ 600.4027, Found 600.4052.

The 1,4-hydrogenations of **36**—**39** and **29** were carried out in a similar manner to that described in the case of the diene **13**. The spectral data were as follows.

Methyl (1*S*,5*S*,6*R*,7*R*)-7-*tert*-Butyldimethylsilyloxy-6-[3(*S*)-*tert*-butyldimethylsilyloxy-*E*-1-octenyl]bicyclo[3.3.0]octane-*E*-$\Delta^{3,\delta}$-pentanoate (40) IR (neat): 2950, 1745, 835, 755 cm^{-1}. ^{1}H-NMR ($CDCl_3$) δ: 0.00 (s, 12H), 0.88 (s, 9H), 0.90 (s, 9H), 1.00—2.50 (m, 26H), 3.40—3.80 (m, 1H), 3.65 (s, 3H), 4.02 (m, 1H), 5.18 (br t, J=7 Hz, 1H), 5.40 (m, 2H). MS m/z: 535 (M^+ − *tert*-Bu), 503, 460, 403, 389, 329, 297, 215, 201, 179, 171, 149, 147, 117, 105, 91, 79, 75, 73 (base peak), 67. HR-MS m/z: (M^+ − *tert*-Bu) Calcd for $C_{30}H_{51}O_4Si_2$ 535.3639, Found 535.3642.

Methyl (1*S*,5*S*,6*R*,7*R*)-7-*tert*-Butyldimethylsilyloxy-6-[3(*R*)-*tert*-butyldimethylsilyloxy-3-cyclopentyl-*E*-1-propenyl]bicyclo[3.3.0]octane-*E*-$\Delta^{3,\delta}$-pentanoate (41) IR (neat): 2950, 1745, 835, 775 cm^{-1}. ^{1}H-NMR ($CDCl_3$) δ: 0.00 (s, 6H), 0.03 (s, 6H), 0.88 (s, 9H), 0.98 (s, 9H), 1.00—2.70 (m, 24H), 3.50—4.00 (m, 2H), 3.68 (s, 3H), 5.23 (t, J=7 Hz, 1H), 5.50 (m, 2H). MS m/z: 533 (M^+ − *tert*-Bu), 521, 458, 389, 363, 327, 213, 201, 179, 171, 147, 133, 131, 129, 119, 117, 105, 91, 79, 75, 73 (base peak), 67. HR-MS m/z: (M^+ − *tert*-Bu) Calcd for $C_{30}H_{53}O_4Si_2$ 533.3479, Found 533.3477.

Methyl (1*S*,5*S*,6*R*,7*R*)-7-*tert*-Butyldimethylsilyloxy-6-[3(*S*)-*tert*-butyldimethylsilyloxy-5,9-dimethyl-*E*-1,8-decadienyl]bicyclo[3.3.0]octane-*E*-$\Delta^{3,\delta}$-pentanoate (42) IR (neat): 2960, 2940, 1745, 835, 775 cm^{-1}. ^{1}H-NMR ($CDCl_3$) δ: 0.00 (s, 12H), 0.90 (m, 21H), 1.00—2.70 (m, 22H), 1.63 (s, 3H), 1.74 (s, 3H), 3.75 (m, 1H), 3.70 (s, 3H), 4.18 (m, 1H), 5.18 (m, 2H), 5.50 (m, 2H). MS m/z: 631 (M^+ − Me), 590, 589 (M^+ − *tert*-Bu), 514, 457, 389, 384, 363, 201, 179, 171, 147, 109, 105, 95, 81, 75, 73 (base peak), 69, 41. HR-MS m/z: (M^+ − *tert*-Bu) Calcd for $C_{34}H_{61}O_4Si_2$ 589.4105, Found 589.4137.

Methyl (1*S*,5*S*,6*R*,7*R*)-7-*tert*-Butyldimethylsilyloxy-6-[3(*R*)-*tert*-butyldimethylsilyloxy-4-methyl-*E*-1-octen-6-ynyl]bicyclo[3.3.0]octane-*E*-$\Delta^{3,\delta}$-pentanoate (43) Spectral data of **43**: IR (neat): 2960, 2940, 1745, 840, 780 cm^{-1}. ^{1}H-NMR ($CDCl_3$) δ: 0.00 (s, 12H), 0.87 (m, 21H), 1.00—2.80 (m, 9H), 1.74 (t, J=2 Hz, 3H), 3.60—4.20 (m, 2H), 3.62 (s, 3H), 5.20 (br t, J=7 Hz, 1H), 5.45 (m, 2H). MS m/z: 602 (M^+), 546, 545 (M^+ − *tert*-Bu), 521, 470, 389, 363, 225, 171, 147, 117, 105, 91, 79, 75, 73 (base peak). HR-MS m/z: (M^+ − *tert*-Bu) Calcd for $C_{31}H_{53}O_4Si_2$ 545.3480, Found 545.3498. Spectral data of **44**: IR (neat): 2960, 2940, 1745, 840, 780 cm^{-1}. ^{1}H-NMR ($CDCl_3$) δ: 0.00 (s, 12H), 0.90 (m, 21H), 1.00—2.70 (m, 18H), 1.78 (t, J=2 Hz, 3H), 3.12 (d, J=7 Hz, 2H), 3.50—4.30 (m, 2H), 3.71 (s, 3H), 5.40—5.80 (m, 3H), 5.95 (d, J=11 Hz, 1H), 6.25 (dd, J=15, 11 Hz, 1H). MS m/z: 600 (M^+), 585 (M^+ − Me), 559, 543 (M^+ − *tert*-Bu), 468, 177, 171, 147, 117, 75, 73 (base peak). HR-MS m/z: (M^+) Calcd for $C_{35}H_{60}O_4Si_2$ 600.4030, Found 600.4039. Spectral data of **45**: IR (neat): 2960, 2950, 1745, 840, 780 cm^{-1}. ^{1}H-NMR ($CDCl_3$) δ: 0.00 (s, 12H), 0.90 (m, 21H), 1.00—2.60 (m, 18H), 1.60 (t, J=6 Hz, 3H), 3.65 (s, 3H), 3.70 (m, 1H), 3.95 (m, 1H), 5.20 (br t, J=7 Hz, 1H), 5.48 (m, 4H). MS m/z: 589 (M^+ − Me), 547 (M^+ − *tert*-Bu), 521, 515, 389, 363, 309, 257, 225, 201, 171, 147, 105, 75, 73 (base peak), 55. HR-MS m/z: (M^+ − *tert*-Bu) Calcd for $C_{31}H_{55}O_4Si_2$ 547.3635, Found 547.3629. Only NMR data of **46** are shown, because **46** was inseparable from **45**: ^{1}H-NMR ($CDCl_3$) δ: 0.00 (s, 12H), 0.90 (m, 21H), 1.00—2.70 (m, 15H), 3.08 (d, J=8 Hz, 2H), 3.60—4.20 (m, 2H), 3.62 (s, 3H), 5.00—6.50 (m, 7H).

Methyl (1*S*,5*S*,6*R*,7*R*)-6-(3-Cyclopentyl-3-oxopropyl)-7-tetrahydropyranyloxybicyclo[3.3.0]octane-*E*-$\Delta^{3,\delta}$-pentanoate (47) IR (neat): 2960, 1742, 1715 cm^{-1}. ^{1}H-NMR ($CDCl_3$) δ: 1.00—3.10 (m, 34H), 3.20—4.10 (m, 3H), 3.66 (s, 3H), 4.62 (br s, 1H), 5.20 (br t, J=7 Hz, 1H). MS m/z: 362 (M^+ − DHP), 344 (M^+ − THPOH), 233, 232, 179, 149, 145, 131, 85 (base peak), 69, 67, 57, 43, 41. HR-MS m/z: (M^+ − DHP) Calcd for $C_{22}H_{34}O_4$ 362.2454, Found 362.2449.

Methyl (1*S*,5*S*,6*R*,7*R*)-7-Hydroxy-6-[3(*S*)-hydroxy-*E*-1-octenyl]bicyclo[3.3.0]octane-*E*-$\Delta^{3,\delta}$-pentanoate (48) Tetrabutylammonium fluoride (1 M solution in THF, 0.39 ml) was added to a solution of **40** (80 mg, 0.13 mmol) in THF (1 ml), and the mixture was stirred at 23 °C for 13 h. The reaction was quenched by the addition of brine, followed by extraction with ethyl acetate. The combined organic layers were dried over $MgSO_4$, and concentrated. The residue was purified by silica gel column chromatography (ether) to give the diol **48** (59 mg, 100%) as a colorless oil. The spectral data of **48** thus obtained were identical with those of an authentic sample.[1k] In a similar manner, **41**—**43** were converted to the corresponding diols **49**—**51**.

Methyl (1*S*,5*S*,6*R*,7*R*)-6-[3(*R*)-Cyclopentyl-3-hydroxy-*E*-1-propenyl]-7-hydroxybicyclo[3.3.0]octane-*E*-$\Delta^{3,\delta}$-pentanoate (49) IR (neat): 3400, 2960, 1742 cm^{-1}. ^{1}H-NMR ($CDCl_3$) δ: 1.00—2.50 (m, 24H), 2.72 (s, 2H), 3.50—3.90 (m, 2H), 3.67 (s, 3H), 5.20 (t, J=7 Hz, 1H), 5.50 (m, 2H). MS m/z: 344 (M^+-H_2O), 326 (M^+-2H_2O), 300, 275, 257, 247, 179, 149, 145, 131, 119, 117, 105, 97, 95, 91, 81, 79, 77, 69 (base peak), 67, 57, 55. HR-MS m/z: (M^+-H_2O) Calcd for $C_{22}H_{32}O_3$ 344.2349, Found 344.2366.

Methyl (1*S*,5*S*,6*R*,7*R*)-7-Hydroxy-6-[3(*S*)-hydroxy-5,9-dimethyl-*E*-1,8-decadienyl]bicyclo[3.3.0]octane-*E*-$\Delta^{3,\delta}$-pentanoate (50) IR (neat): 3400, 2940, 1745 cm^{-1}. ^{1}H-NMR ($CDCl_3$) δ: 0.92 (d, J=6 Hz, 3H), 1.00—2.60 (m, 22H), 1.60 (s, 3H), 1.68 (s, 3H), 2.90 (br s, 2H), 3.68 (m, 1H), 3.68 (s, 3H), 4.15 (m, 1H), 5.26 (m, 2H), 5.50 (m, 2H). MS m/z: 400 (M^+-H_2O), 382 (M^+-2H_2O), 339, 315, 247, 246, 245, 233, 232, 219, 201, 179, 147, 131, 119, 117, 109, 105, 93, 91, 81, 79, 69 (base peak), 55, 41. HR-MS m/z: (M^+-H_2O) Calcd for $C_{26}H_{40}O_3$ 400.2975, Found 400.2978.

Methyl (1*S*,5*S*,6*R*,7*R*)-7-Hydroxy-6-[3(*R*)-hydroxy-4-methyl-*E*-1-octen-6-ynyl]bicyclo[3.3.0]octane-*E*-$\Delta^{3,\delta}$-pentanoate (51) IR (neat): 3400, 2940, 1742 cm^{-1}. ^{1}H-NMR ($CDCl_3$) δ: 0.98 (m, 3H), 1.06—2.70 (m, 20H), 1.78 (t, J=2 Hz, 3H), 3.66 (s, 3H), 3.67 (m, 1H), 4.06 (m, 1H), 5.24 (t, J=7 Hz, 1H), 5.55 (m, 2H). MS m/z: 374 (M^+), 356 (M^+-H_2O), 338 (M^+-2H_2O), 312, 205, 167, 150, 149 (base peak), 105, 104, 83, 76, 71, 70, 69, 57, 56, 55, 43, 41. HR-MS m/z: (M^+) Calcd for $C_{23}H_{34}O_4$ 374.2478, Found 374.2478.

(1*S*,5*S*,6*R*,7*R*)-7-Hydroxy-6-[3(*S*)-hydroxy-*E*-1-octenyl]bicyclo[3.3.0]-octane-*E*-$\Delta^{3,\delta}$-pentanoic Acid (2) A 10% NaOH aqueous solution (1.0 ml, 2.5 mmol) was added to a stirred solution of the diol **48** (45 mg, 0.12 mmol) in methanol (1 ml) at 0 °C, and the mixture was stirred at the same temperature for 13 h. The reaction mixture was diluted with ether, and neutralized by adding 10% aqueous HCl, followed by evaporation of the organic solvents. Then the remaining water layer was acidified to pH 3—4 by adding 10% aqueous HCl, followed by extraction with ethyl acetate. The combined organic layers were washed with brine, and dried over $MgSO_4$. Removal of the solvent afforded carbacyclin (**2**) (43 mg, 100%). The spectal data of **2** thus obtained were identical with those of an authentic sample.[1k] In a similar manner, the diols **49**—**51** and **32a**—**35a** were hydrolyzed to the carboxylic acids **3**—**5 and 75**—**78**. The IR and NMR data were as follows.

(1*S*,5*S*,6*R*,7*R*)-6-[3(*R*)-Cyclopentyl-3-hydroxy-*E*-1-propenyl]-7-hydroxybicyclo[3.3.0]octane-*E*-$\Delta^{3,\delta}$-pentenoic Acid (3) IR (neat): 3350, 2940, 1705 cm^{-1}. ^{1}H-NMR ($CDCl_3$) δ: 1.00—2.52 (m, 24H), 3.28—3.96 (m, 5H), 5.22 (br t, J=7 Hz, 1H), 5.42 (m, 2H).

(1*S*,5*S*,6*R*,7*R*)-7-Hydroxy-6-[3(*S*)-hydroxy-5,9-dimethyl-*E*-1,8-decadienyl]bicyclo[3.3.0]octane-*E*-$\Delta^{3,\delta}$-pentanoic Acid (4) IR (neat): 3400, 2940, 1712 cm^{-1}. ^{1}H-NMR ($CDCl_3$) δ: 0.92 (d, J=6 Hz, 3H), 1.00—2.70 (m, 22H), 1.60 (s, 3H), 1.68 (s, 3H), 3.70 (m, 1H), 4.15 (m, 1H), 4.90—5.40 (m, 2H), 5.40—5.90 (m, 4H).

(1*S*,5*S*,6*R*,7*R*)-7-Hydroxy-6-[3(*R*)-hydroxy-4-methyl-*E*-1-octen-6-ynyl]-bicyclo[3.3.0]octane-*E*-$\Delta^{3,\delta}$-pentanoic Acid (5) IR (neat): 3400, 2950, 1712 cm^{-1}. ^{1}H-NMR ($CDCl_3$) δ: 0.96, 1.00 (each d, J=7 Hz, total 3H), 1.10—2.70 (m, 18H), 1.80 (t, J=2 Hz, 3H), 3.15 (m, 3H), 3.76 (m, 1H), 4.10 (m, 1H), 5.26 (t, J=7 Hz, 1H), 5.60 (m, 2H).

(1*R*,5*S*,6*R*,7*R*)-7-Hydroxy-6-[3(*S*)-hydroxy-*E*-1-octenyl]bicyclo[3.3.0]-oct-2-ene-3-γ-pentenoic Acid (75) IR (neat): 3350, 2950, 1715 cm^{-1}. ^{1}H-NMR ($CDCl_3$) δ: 0.90 (m, 3H), 1.10—2.90 (m, 19H), 3.10 (m, 1H), 3.70—4.40 (m, 3H), 5.45 (m, 1H), 5.65 (m, 3H), 6.06 (d, J=11 Hz, 2.2/3.2H), 6.34 (d, J=16 Hz, 1/3.2H).

(1*R*,5*S*,6*R*,7*R*)-6-[3(*R*)-Cyclopentyl-3-hydroxy-*E*-1-propenyl]-7-hydroxybicyclo[3.3.0]oct-2-ene-3-γ-pentenoic Acid (76) IR (neat): 3350, 2950, 1715 cm^{-1}. ^{1}H-NMR ($CDCl_3$) δ: 1.10—2.90 (m, 20H), 3.10 (m, 1H), 3.65—4.60 (m, 3H), 5.43 (m, 1H), 5.54 (m, 3H), 6.04 (d, J=12 Hz, 2.2/3.2 H), 6.32 (d, J=16 Hz, 1/3.2H).

(1*R*,5*S*,6*R*,7*R*)-7-Hydroxy-6-[3(*S*)-hydroxy-5,9-dimethyl-*E*-1,8-decadienyl]bicyclo[3.3.0]oct-2-ene-3-γ-pentenoic Acid (77) IR (neat): 3350, 2950, 1715 cm^{-1}. ^{1}H-NMR ($CDCl_3$) δ: 0.93 (d, J=6 Hz, 3H), 1.00—3.30 (m, 23H), 1.61 (s, 3H), 1.68 (s, 3H), 3.82 (m, 1H), 4.24 (m, 1H), 5.12 (t, J=7 Hz, 1H), 5.28—5.72 (m, 4H), 6.02 (d, J=11 Hz, 2.2/3.2H), 6.30 (d, J=16 Hz, 1/3.2H).

(1*R*,5*S*,6*R*,7*R*)-7-Hydroxy-6-[3(*R*)-hydroxy-4-methyl-*E*-1-octen-6-ynyl]-bicyclo[3.3.0]oct-2-ene-3-γ-pentenoic Acid (78) IR (neat): 3350, 2950, 1715 cm^{-1}. ^{1}H-NMR ($CDCl_3$) δ: 0.98, 1.01 (each d, J=7 Hz, total 3H), 1.60—3.30 (m, 19H), 1.81 (t, J=2 Hz, 3H), 3.70—4.30 (m, 2H), 5.20—5.90 (m, 4H), 6.04 (d, J=11 Hz, 2.2/3.2H), 6.32 (d, J=16 Hz, 1/3.2H).

(1*R*,5*S*,6*S*,7*R*)-6-*tert*-Butyldimethylsilyloxymethyl-3-hydroxymethyl-7-tetrahydropyranyloxybicyclo[3.3.0]oct-2-ene (53) A solution of diisobutylaluminum hydride in hexane (1.76 M, 2.9 ml, 5.17 mmol) was added to a stirred solution of the aldehyde **52**[7a] (1.66 g, 4.36 mmol) in toluene (8 ml) at −70 °C. Stirring was continued at the same temperature for 45 min, and the reaction was quenched by the addition of methanol. After dilution of the mixture with ether, saturated aqueous NaCl was added. Stirring was continued at 23 °C until the organic layer became clear. The aqueous layer was extracted with ether, and the organic layers were combined and dried over $MgSO_4$. Removal of the solvent afforded the alcohol **53** (1.64 g, 98%) as a colorless oil. IR (neat): 3430, 2950, 838, 778 cm^{-1}. ^{1}H-NMR ($CDCl_3$) δ: 0.05 (s, 6H), 0.90 (s, 9H), 1.00—2.00 (m, 9H), 2.00—2.80 (m, 4H), 3.00 (m, 1H), 3.25—4.05 (m, 5H), 4.12 (s, 2H), 4.62 (m, 1H), 5.56 (br s, 1H). MS m/z: 382 (M^+), 298 (M^+−DHP), 241, 223, 159, 149, 131, 91, 85, (base peak), 75. HR-MS m/z: (M^+−DHP) Calcd for $C_{16}H_{30}O_3Si$ 298.1962, Found 298.1946.

(1*R*,5*S*,6*S*,7*R*)-3-Bromomethyl-6-*tert*-butyldimethylsilyloxymethyl-7-tetrahydropyranyloxybicyclo[3.3.0]oct-2-ene (54) Carbon tetrabromide (1.57 g, 4.74 mmol) was added to a stirred solution of the alcohol **53** (1.48 g, 3.87 mmol) and triphenylphosphine (1.24 g, 4.74 mmol) in methylene chloride (25 ml) at −60 °C, and the mixture was stirred at −25 °C for 1 h. The reaction was quenched by the addition of saturated aqueous $NaHCO_3$, followed by extraction of the mixture with ether. The combined ether extracts were washed with brine, and dried over $MgSO_4$. Removal of the solvent and purification by silica gel column chromatography (ether–hexane, 1 : 20) afforded the bromide **54** (1.54 g, 89%) as a colorless oil. IR (neat): 2950, 838, 776 cm^{-1}. ^{1}H-NMR ($CDCl_3$) δ: 0.05 (s, 6H), 0.90 (s, 9H), 1.00—2.00 (m, 8H), 2.00—2.70 (m, 4H), 3.00 (m, 1H), 3.25—4.00 (m, 5H), 4.00 (s, 2H), 4.60 (m, 1H), 5.70 (br s, 1H), MS m/z: 362 (M^+−DHP), 360 (M^+−DHP), 345 (M^+−THPOH), 343 (M^+−THPOH), 281, 213, 211, 159, 149, 131, 91, 89, 85 (base peak), 75, 67, HR-MS m/z: (M^+−DHP) Calcd for $C_{16}H_{29}BrO_2Si$ 362.1099, 360.1118, Found 362.1107, 360.1094.

(1*R*,5*S*,6*S*,7*R*)-6-*tert*-Butyldimethylsilyloxymethyl-3-cyanomethyl-7-tetrahydropyranyloxybicyclo[3.3.0]oct-2-ene (55) Potassium cyanide (97%, 113 mg, 1.68 mmol) was added to a stirred solution of the bromide **53** (500 mg, 1.12 mmol) and 18-crown-6 (444 mg, 1.68 mmol) in acetonitrile (25 ml), and the mixture was stirred at 23°C for 2 h. After evaporation of the acetonitrile, saturated aqueous $NaHCO_3$ was added. The mixture was extracted with ether. The combined ether extracts were washed with brine, and dried over $MgSO_4$. Removal of the solvent and purification by silica gel column chromatography (ether–hexane, 1 : 3) afforded the cyanide **55** (435 mg, 99%) as a colorless oil. IR (neat): 2950, 2260, 1735, 1260, 840, 780 cm^{-1}. ^{1}H-NMR ($CDCl_3$) δ: 0.05 (s, 6H), 0.90 (s, 9H), 1.00—2.00 (m, 8H), 2.00—2.80 (m, 4H), 3.05 (s, 2H), 3.05 (m, 1H), 3.25—4.10 (m, 5H), 4.60 (m, 1H), 5.68 (br s, 1H). MS m/z: 307 (M^+−DHP), 290, 159, 158, 86, 85 (base peak), 75, 73. HR-MS m/z: (M^+−DHP) Calcd for $C_{17}H_{29}NO_2Si$ 307.1965, Found 307.1948.

Methyl (1*R*,5*S*,6*S*,7*R*)-6-*tert*-Butyldimethylsilyloxymethyl-7-tetrahydropyranyloxybicyclo[3.3.0]oct-2-ene-3-δ-cyano-γ-hydroxypentanoate (57) A solution of lithium diisopropylamide prepared from diisopropylamine (71 μl, 0.51 mmol), butyllithium (1.50 M, 0.3 ml, 0.46 mmol) and THF (0.63 ml) was added to a stirred solution of the cyanide **55** (100 mg, 0.26 mmol) in THF (2 ml) at −78 °C, and the mixture was stirred at the same temperature for 25 min. A solution of the aldehyde **56** (59 mg, 0.51 mmol, bp 39 °C/1.3 mmHg) in THF (3 ml) was added to this pale yellow solution at −78 °C, and the reaction mixture was stirred at the same temperature for 20 min. The reaction was quenched by the addition of saturated aqueous NH_4Cl, followed by extraction of the mixture with ether. The combined organic layers were washed with brine, and dried over $MgSO_4$. Removal of the solvent and purification by silica gel column chromatography (ether–hexane, 1 : 3–1 : 1) afforded the desired coupling products **57** (108 mg, 82%, mixture of the diastereomers) as a colorless oil. IR (neat): 3490, 2950, 2240, 1738, 835, 775 cm^{-1}. ^{1}H-NMR ($CDCl_3$) δ: 0.05 (s, 6H), 0.90 (s, 9H), 1.10—2.70 (m, 16H), 2.70—4.20 (m, 9H), 3.66 (s, 3H), 4.50 (m, 1H), 5.75 (m, 1H). MS m/z: 424 (M^++H–DHP), 406 (M^++H–THPOH), 392, 374, 348, 334, 316, 307, 242, 232, 201, 196, 160, 159, 158, 145, 117, 115, 89, 86, 85 (base peak), 75, 73, 67, 59, 57, 43, 41. HR-MS m/z: (M^++H–DHP) Calcd for $C_{22}H_{38}NO_5Si$ 424.2517, Found 424.2546.

Methyl (1*R*,5*S*,6*S*,7*R*)-6-*tert*-Butyldimethylsilyloxymethyl-7-tetrahydropyranyloxybicyclo[3.3.0]oct-2-ene-3-δ-cyano-γ-pentenoate (58) Mesyl chloride (0.19 ml, 2.45 mmol) was added to a stirred solution of **57** (300 mg, 0.16 mmol) and triethylamine (1.03 ml, 7.35 mmol) at 0 °C, and the mixture was stirred at 23 °C for 20 min. The reaction was quenched by the addition of brine, followed by extraction of the mixture with ether. The combined organic layers were dried over $MgSO_4$, and concentrated. The residue was purified by silica gel column chromatography (ether–hexane, 1 : 4) to give

the 4*Z*-diene **58a** (240 mg, 83%) as a less polar fraction and the 4*E*-diene **58b** (18 mg, 6%) as a more polar fraction. Spectral data of **58a**: IR (neat): 2930, 2220, 1735, 828, 770 cm^{-1}. ^{1}H-NMR ($CDCl_3$) δ: 0.05 (s, 6H), 0.90 (s, 9H), 1.00—2.10 (m, 8H), 2.10—2.90 (m, 8H), 3.10 (m, 1H), 3.25—4.15 (m, 5H), 3.70 (s, 3H), 4.60 (m, 1H), 6.05 (br s, 1H), 6.10 (t, J=7 Hz, 1H). MS m/z: 458 (M^+ −MeO), 406 (M^+ +H−DHP), 388 (M^+ +H−THPOH), 349, 348, 330, 256, 224, 196, 159, 85 (base peak), 75, 73. HR-MS m/z: (M^+ +H−DHP) Calcd for $C_{22}H_{36}NO_4Si$ 406.2412, Found 406.2412. Spectral data of **58b**: IR (neat): 2950, 2230, 1740, 1620, 840, 780 cm^{-1}. ^{1}H-NMR ($CDCl_3$) δ: 0.05 (s, 6H), 0.90 (s, 9H), 1.10—2.10 (m, 8H), 2.10—2.90 (m, 8H), 3.06 (m, 1H), 3.30—4.30 (m, 5H), 3.68 (s, 3H), 4.60 (m, 1H), 5.98 (bs, 1H), 6.20 (t, J=7 Hz, 1H). MS m/z: 458 (M^+ −MeO), 406 (M^+ +H−DHP), 388 (M^+ +H−THPOH), 349, 348, 256, 196, 159, 85 (base peak), 75, 73. HR-MS m/z: (M^+ +H−DHP) Calcd for $C_{22}H_{36}NO_4Si$ 406.2412, Found 406.2423.

Methyl (1*S*,5*S*,6*S*,7*R*)-6-*tert*-Butyldimethylsilyloxymethyl-7-tetrahydropyranyloxybicyclo[3.3.0]octane-*Z*-$\Delta^{3,\delta}$-δ-cyanopentanoate (61) The diene **58a** (85 mg, 0.17 mmol) and (methyl benzoate)$Cr(CO)_3$ (10 mg, 0.035 mmol) were dissolved in acetone (10 ml). The solution was degassed by three free-pump-thaw cycles, and then transferred into an autoclave with glass insert (100 ml) under an argon atmosphere. The autoclave was purged repeatedly with hydrogen. The solution was stirred at 120 °C for 15 h under 70 kg/cm^2 of hydrogen pressure. After cooling to room temperature, the reaction mixture was exposed to air and light to decompose the catalyst. Removal of the solvent gave a dark green residue, which was purified by silica gel column chromatography (ether–hexane, 2 : 3) to afford the desired exocyclic olefin **61** (86 mg, 100%) as a colorless oil. IR (neat): 2950, 2200, 1740, 1640, 835, 775 cm^{-1}. ^{1}H-NMR ($CDCl_3$) δ: 0.05 (s, 6H), 0.90 (s, 9H), 1.10—2.00 (m, 10H), 2.00—2.80 (m, 11H), 3.30—4.10 (m, 5H), 3.66 (s, 3H), 4.60 (m, 1H). MS m/z: 434 (M^+ −*tert*-Bu), 390 (M^+ −THPO), 389 (M^+ −THPOH), 350, 332, 226, 159, 85 (base peak), 75, 73. HR-MS m/z: (M^+ −*tert*-Bu) Calcd for $C_{23}H_{36}NO_5Si$ 434.2361, Found 434.2365. TLC (ether–hexane, 4 : 1, silica gel, two times development): *Rf* **61** (*Z*-isomer) 0.29, **68** (*E*-isomer) 0.26.

Methyl (1*S*,5*S*,6*S*,7*R*)-6-Hydroxymethyl-7-tetrahydropyranyloxybicyclo[3.3.0]octane-*Z*-$\Delta^{3,\delta}$-δ-cyanopentanoate (63) Tetrabutylammonium fluoride (1 M solution in THF, 0.41 ml) was added to a solution of **61** (133 mg, 0.27 mmol) in THF (2 ml), and the mixture was stirred at 23 °C for 3 h. The reaction was quenched by the addition of brine, followed by extraction of the mixture with ether. The combined organic layers were dried over $MgSO_4$, and concentrated. The residue was purified by silica gel column chromatography (ether–hexane, 1 : 4) to give the alcohol **63** (95 mg, 93%) as a colorless oil. IR (neat): 3500, 2950, 2350, 2210, 1740, 1642 cm^{-1}. ^{1}H-NMR ($CDCl_3$) δ: 1.00—3.10 (m, 22H), 3.10—4.10 (m, 5H), 3.68 (s, 3H), 4.60 (m, 1H). MS m/z: 293 (M^+ −DHP), 275 (M^+ −THPOH), 257, 244, 243, 226, 225, 135, 117, 105, 91, 86, 85 (base peak), 84, 79, 77, 67, 57, 55, 43, 41. HR-MS m/z: (M^+ −DHP) Calcd for $C_{16}H_{23}NO_4$ 293.1625, Found 293.1622.

Methyl (1*S*,5*S*,6*S*,7*R*)-6-Hydroxymethyl-7-tetrahydropyranyloxybicyclo[3.3.0]octane-*E*-$\Delta^{3,\delta}$-δ-cyano-γ-pentanoate (72) A suspension of 10% Pd on C (241 mg, 10 mol%) in toluene (40 ml) was stirred at 23 °C for 1 h under a hydrogen atmosphere (1 atm). A solution of the diene **58** (1.11 g, 2.27 mmol), in toluene (40 ml) was added at −40 °C, and the mixture was stirred at the same temperature for 6 h. After filtration through a silica gel pad to remove the catalyst, the filtrate was concentrated and purified by silica gel column chromatography (ethyl acetate–hexane, 1 : 7) to afford a mixture of the 5*E*-exocyclic olefin **68** and the regioisomer **70** (929 mg, 83%, **68** : **70** = 8 : 1) and the 5*Z*-exocyclic olefin **61** (118 mg, 11%) as a colorless oil. Tetrabutylammonium fluoride (1 M solution in THF, 2.77 ml) was added to a solution of the mixture of **68** and **70** (906 mg) in THF (8 ml), and the mixture was stirred at 23 °C for 1.5 h. The reaction was quenched by the addition of saturated aqueous NH_4Cl, followed by extraction of the mixture with ethyl acetate. The combined organic layers were dried over Na_2SO_4, and concentrated. The residue was purified by silica gel column chromatography (ethyl acetate–hexane, 3 : 1) to give the alcohol **72** (428 mg, 62%) as a colorless oil. IR (neat): 3460, 2940, 2200, 1740, 1640 cm^{-1}. ^{1}H-NMR ($CDCl_3$) δ: 1.16—3.04 (m, 22H), 3.32—4.21 (m, 5H), 3.68 (s, 3H), 4.60 (m, 1H). MS m/z: 293 (M^+ −DHP), 275 (M^+ −THPOH), 257, 244, 226, 117, 85, 67, 57, 43 (base peak). HR-MS m/z: (M^+ −DHP) Calcd for $C_{16}H_{23}NO_4$ 293.1627, Found 293.1647.

NMR (500 MHz) Data of 62 and 69 **62** (5*Z*-Stereoisomer): H_a 3.67 (s, 3H), H_b 2.34 (t, J=7.1 Hz, 2H), H_c 1.86 (tt, J=7.5, 7.1 Hz, 2H), H_d 2.21 (t, J=7.5 Hz, 2H), H_e 2.35 (m, 1H), H_f 2.60 (dd, J=18, 9.5 Hz, 1H), H_g 2.77 (dd, J=18, 8.5 Hz, 1H), H_h 2.67 (br d, J=18 Hz, 1H), H_i 2.50 (m, 1H), H_j 2.40 (td, J=8.5, 4 Hz, 1H), H_k 2.14 (ddd, J=13, 7.3, 7.3 Hz, 1H),

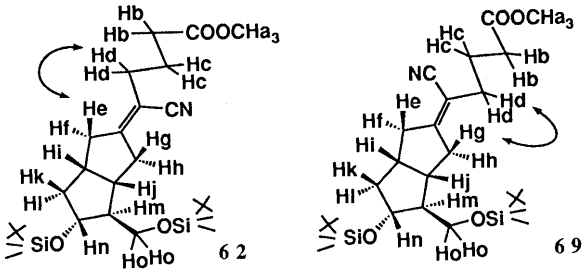

Fig. 1

H_l 1.30 (ddd, J=13, 7.1, 7.1 Hz, 1H), H_m 1.56 (ddt, J=7, 4, 4 Hz, 1H), H_n 3.98 (ddd, J=7.1, 7.1, 7.1 Hz, 1H), H_o 3.59 (d, J=4.4 Hz, 2H), *tert*-BuSi 0.89 (s, 9H), 0.85 (s, 9H), MeSi 0.04 (s, 6H), 0.03 (s, 3H), 0.02 (s, 3H).

69 (5*E*-Stereoisomer): H_a 3.67 (s, 3H), H_b 2.33 (t, J=7.3 Hz, 2H), H_c 1.85 (tt, J=7.3, 7.3 Hz, 2H), H_d 2.20 (t, J=7.3 Hz, 2H), H_e 2.82 (dd, J=17.9, 9.1 Hz, 1H), H_f 2.58 (dd, J=17.9, 4.2 Hz, 1H), H_g 2.42—2.48 (m, 1H), H_h 2.48—2.55 (m, 1H), H_i 2.43—2.52 (m, 1H), H_j 2.36—2.41 (m, 1H), H_k 2.13 (ddd, J=12.8, 7.0, 7.0 Hz, 1H), H_l 1.32 (ddd, J=12.8, 7.0, 7.0 Hz, 1H), H_m 1.52—1.57 (m, 1H), H_n 3.92 (ddd, J=7.0, 7.0, 7.0 Hz, 1H), H_o 3.55 (dd, J=10.8, 5.6 Hz, 1H), 3.61 (dd, J=10.8, 4.1 Hz, 1H), *tert*-BuSi 0.88 (s, 9H), 0.86 (s, 9H), MeSi 0.03 (s, 6H), 0.02 (s, 6H). Assignment of each signal was determined by correlated spectroscopy (COSY). The stereochemistry of the exocyclic olefin in **62** was assigned to be *Z* by nuclear Overhauser effect correlation spectroscopy (NOESY). Namely, strong NOE was observed between H_e and H_d, and no NOE was observed between H_g and H_d. On the other hand, no NOE was observed between H_e and H_d, and strong NOE was observed between H_g and H_d in the case of **69**.

Methyl (1*S*,5*S*,6*R*,7*R*)-6-(3-Oxo-*E*-1-octenyl)-7-tetrahydropyranyloxybicyclo[3.3.0]octane-*Z*-$\Delta^{3,\delta}$-δ-cyanopentanoate (64) A solution of SO_3-pyridine complex (104 mg, 0.65 mmol) in DMSO (1.6 ml) was added to a stirred solution of the alcohol **62** (82 mg, 0.22 mmol) and triethylamine (0.19 ml) in DMSO (2.4 ml), and the mixture was stirred at 23 °C for 40 min, then poured into ice-water, and extracted with ether. The ether extracts were washed with water and brine, and dried over $MgSO_4$. Removal of the solvent gave the crude aldehyde. Sodium hydride (60% in oil, 12 mg, 0.31 mmol) was washed with pentane, and suspended in THF (2.2 ml). A solution of dimethyl (2-oxoheptyl)phosphonate (73 mg, 0.33 mmol) in THF (1.4 ml) was added to this suspension, and the mixture was stirred at 23 °C for 50 min. Then, a solution of the crude aldehyde in THF (1 ml) was dropped into the solution of the sodium ketophosphonate, and the whole mixture was stirred at 23 °C for 30 min. The reaction was quenched by the addition of saturated aqueous NH_4Cl, followed by extraction of the mixture with ether. The combined ether extracts were washed with brine, and dried over $MgSO_4$. Removal of the solvent and purification by silica gel column chromatography (ether–hexane, 4 : 3) afforded the enone **64** (84 mg, 82%) as a colorless oil. IR (neat): 2950, 2350, 2210, 1740, 1699, 1675, 1628 cm^{-1}. ^{1}H-NMR ($CDCl_3$) δ: 0.90 (t, J=6 Hz, 3H), 1.00—2.05 (m, 16H), 2.05—3.00 (m, 13H), 3.45 (m, 1H), 3.69 (s, 3H), 3.80 (m, 2H), 4.51, 4.61 (each br s, total 1H), 6.17, 6.20 (each d, J=16 Hz, total 1H), 6.72, 6.78 (each dd, J=16, 7.5 Hz, total 1H). MS m/z: 440 (M^+ −MeO), 388, 387 (M^+ −DHP), 370, 369, 355, 343, 338, 327, 288, 256, 238, 151, 131, 130, 99, 91, 86, 85 (base peak), 71, 67, 57, 55, 43, 41. HR-MS m/z: (M^+ −DHP) Calcd for $C_{23}H_{33}NO_4$ 387.2407, Found 387.2402.

In a similar manner, the 5*E*-stereoisomer was synthesized from **72** in 64% yield. Spectral data of the 5*E*-stereoisomer of **64**: IR (neat): 2960, 2220, 1740, 1695, 1670, 1630 cm^{-1}. ^{1}H-NMR ($CDCl_3$) δ: 0.99 (t, J=6 Hz, 3H), 1.08—2.05 (m, 16H), 2.05—3.20 (m, 13H), 3.42 (m, 1H), 3.60—4.22 (m, 2H), 3.68 (s, 3H), 4.55, 4.64 (each br s, total 1H), 6.14, 6.17 (each d, J=16 Hz, total 1H), 6.72, 6.80 (each dd, J=16, 7.5 Hz, total 1H). MS m/z: 387 (M^+ −DHP), 369, 355, 338, 327, 288, 256, 229, 213, 165, 151, 99, 85 (base peak), 71, 67, 57, 43. HR-MS m/z: (M^+ −DHP) Calcd for $C_{23}H_{33}NO_4$ 387.2410, Found 387.2421. TLC (ether–hexane, 4 : 3, silica gel): *Rf* **64** (*Z*-isomer) 0.24, *E*-isomer of **64** 0.33.

Methyl (1*S*,5*S*,6*R*,7*R*)-7-Hydroxy-6-[3(*S*)-hydroxy-*E*-1-octenyl]bicyclo[3.3.0]octane-*Z*-$\Delta^{3,\delta}$-δ-cyanopentanoate (66a) An excess amount of sodium borohydride was added to a stirred solution of the enone **64** (83 mg, 0.18 mmol) in methanol (3 ml) at −20 °C, and the mixture was stirred at the same temperature for 1.5 h. The reaction was quenched by the addition of acetone, and then saturated aqueous NH_4Cl was added to the reaction mixture. After evaporation of the organic solvents, the water layer was extracted with ether. The combined ether extracts were dried over $MgSO_4$,

and concentrated to give the alcohol as an epimeric mixture (83 mg). Spectral data of the alcohol: IR (neat): 3480, 2940, 2210, 1738, 1641 cm^{-1}. ^{1}H-NMR ($CDCl_3$) δ: 0.89 (br t, J=6 Hz, 3H), 1.05—2.90 (m, 33H), 3.50 (m, 1H), 3.60—4.20 (m, 3H), 3.68 (s, 3H), 4.63 (br s, 1H), 5.56 (m, 2H). MS m/z: 371 (M^+ −THPOH), 353, 327, 117, 99, 86, 85 (base peak), 67, 57, 43, 41. HR-MS m/z: (M^+ −THPOH) Calcd for $C_{23}H_{33}O_3$ 371.2458, Found 371.2484. The alcohol thus obtained (epimeric mixture, 81 mg) was dissolved in a mixture of 65% aqueous acetic acid (1.3 ml) and THF (0.13 ml), and the mixture was stirred at 50 °C for 1 h, then poured into saturated aqueous $NaHCO_3$, and extracted with ether. The ether extracts were washed with brine, dried over $MgSO_4$, and concentrated. The residue was purified by silica gel column chromatography (ether) to afford the desired 15α-diol (**66a**) (34 mg, 51%) as a more polar fraction and the 15β-diol (**66b**) (28 mg, 42%) as a less polar fraction. Spectral data of **66a**: IR (neat): 3420, 2930, 2200, 1736, 1641 cm^{-1}. ^{1}H-NMR ($CDCl_3$) δ: 0.90 (br t, J=6 Hz, 3H), 1.05—1.65 (m, 10H), 1.65—3.10 (m, 15H), 3.68 (s, 3H), 3.70 (m, 1H), 4.02 (m, 1H), 5.50 (m, 2H). MS m/z: 371 ($M^+ - H_2O$), 354, 353 ($M^+ - 2H_2O$), 327, 300, 295, 268, 226, 225, 159, 149, 131, 130, 117, 99, 91, 81, 79, 71, 67, 57, 55, 43 (base peak), 41. HR-MS m/z: ($M^+ - H_2O$) Calcd for $C_{23}H_{33}NO_3$ 371.2458, Found 371.2439. $[\alpha]_D^{20}$: +1.4° (c=1.15, MeOH). Spectral data of **66b**: IR (neat): 3450, 2940, 2210, 1740, 1645 cm^{-1}. ^{1}H-NMR ($CDCl_3$) δ: 0.90 (br t, J=6 Hz, 3H), 1.05—1.65 (m, 10H), 1.65—2.80 (m, 15H), 3.68 (s, 3H), 3.83 (m, 1H), 4.10 (m, 1H), 5.60 (m, 2H). MS m/z: 371 ($M^+ - H_2O$), 353 ($M^+ - 2H_2O$), 327, 300, 295, 269, 268, 226, 225, 159, 131, 117, 99 (base peak), 91, 81, 79, 71, 67, 57, 55, 43, 41. HR-MS m/z: ($M^+ - H_2O$) Calcd for $C_{23}H_{33}NO_3$ 371.2458, Found 371.2484. $[\alpha]_D^{20}$: −12° (c=1.01, MeOH).

Methyl (1*S*,5*S*,6*R*,7*R*)-7-Hydroxy-6-[3(*S*)-hydroxy-*E*-1-octenyl]bicyclo-[3.3.0]octane-*E*-$\Delta^{3,\delta}$-δ-cyanopentanoate A 65% aqueous solution of acetic acid (2 ml) was added to a solution of the *E*-isomer of the enone **64** (122 mg, 0.26 mmol) in THF (1 ml), and the mixture was stirred at 65 °C for 10 h, then neutralized with saturated aqueous $NaHCO_3$, and extracted with ethyl acetate. The organic layers were washed with brine, and dried over Na_2SO_4. Removal of the solvent and purification of the residue by silica gel column chromatography (ethyl acetate–hexane, 1 : 1) afforded the alcohol (98 mg, 98%) as a colorless oil. IR (neat): 3450, 2950, 2220, 1740, 1690, 1665, 1625 cm^{-1}. ^{1}H-NMR ($CDCl_3$) δ: 0.89 (br t, J=6 Hz, 3H), 1.08—3.20 (m, 24H), 3.68 (s, 3H), 4.01 (ddd, J=9, 7, 7 Hz, 1H), 6.20 (dd, J=16, 1 Hz, 1H), 6.72 (dd, J=16, 8 Hz, 1H). MS m/z: 387 (M^+), 369 ($M^+ - H_2O$), 338, 298, 256, 99 (base peak), 71, 43. HR-MS m/z: (M^+) Calcd for $C_{23}H_{33}NO_4$ 387.2410, Found 387.2421. $[\alpha]_D^{20}$: +103° (c=0.46, $CHCl_3$). A solution of diisobutylaluminum hydride in toluene (1 M, 2.40 ml) was added to a stirred solution of 2,6-di-*tert*-butyl-4-methylphenol (726 mg, 3.43 mmol) in toluene (3 ml) at −10 °C, and the mixture was stirred at the same temperature for 1 h. To this solution was added a solution of the alcohol obtained above (86 mg, 0.22 mmol) in toluene (5 ml) at −78 °C, and the whole mixture was stirred at −78—−10 °C for 3 h. The raction was quenched by the addition of brine, followed by extraction with ethyl acetate. The combined organic layers were washed with brine, and dried over Na_2SO_4. Removal of the solvent and purification by silica gel column chromatography (ethyl acetate–hexane, 3 : 1) afforded the 15α-diol (61 mg, 71%) as a more polar fraction and the 15β-diol (11 mg, 13%) as a less polar fraction. Spectral data of 15α-diol (5*E*-isomer): IR (neat): 3420, 2950, 2240, 1745 cm^{-1}. ^{1}H-NMR ($CDCl_3$) δ: 0.83 (br t, J=6 Hz, 3H), 1.00—1.56 (m, 10H), 1.56—1.98 (m, 3H), 1.98—2.61 (m, 9H), 2.61—3.04 (m, 3H), 3.60—3.88 (m, 1H), 3.62 (s, 3H), 3.78—4.16 (m, 1H), 5.24—5.56 (m, 2H). MS m/z: 371 ($M^+ - H_2O$), 353 ($M^+ - 2H_2O$), 327, 300, 295, 268, 225, 99 (base peak), 71, 43. HR-MS m/z: ($M^+ - H_2O$) Calcd for $C_{23}H_{33}NO_3$ 371.2461, Found 371.2460. $[\alpha]_D^{20}$: +92° (c=0.60, $CHCl_3$). TLC (ether–methanol, 50 : 1, silica gel): *Rf* **66a** (*Z*-isomer) 0.29, *E*-isomer of **66a** 0.38, **66b** 0.42, *E*-isomer of **66b** 0.48.

(1*S*,5*S*,6*R*,7*R*)-7-Hydroxy-6-[3(*S*)-hydroxy-*E*-1-octenyl]bicyclo[3.3.0]-octane-*Z*-$\Delta^{3,\delta}$-δ-cyanopentanoic Acid (6) A 10% NaOH aqueous solution (0.4 ml, 1.0 mmol) was added to a stirred solution of the diol **66a** (20 mg, 0.05 mmol) in methanol (0.4 ml) at −5 °C, and the mixture was stirred at 0 °C for 12 h. The reaction mixture was diluted with ether, and neutralized by adding 10% aqueous HCl, followed by evaporation of the organic solvents. Then the remaining water layer was acidified to pH 3—4 by adding 10% aqueous HCl, followed by extraction with ethyl acetate. The combined organic layers were washed with brine, and dried over $MgSO_4$. Removal of the solvent afforded cyanocarbacyclin (**6**) (18 mg, 92%). IR (neat): 3400, 2950, 2210, 1700—1730, 1640 cm^{-1}. ^{1}H-NMR ($CDCl_3$) δ: 0.90 (br t, J=6 Hz, 3H), 1.05—1.75 (m, 10H), 1.75—2.80 (m, 13H), 3.02 (m, 3H), 3.82 (ddd, J=7, 7, 7 Hz, 1H), 4.10 (dt, J=6, 6 Hz, 1H), 5.56 (m, 2H). MS m/z: 375 (M^+), 357 ($M^+ - H_2O$), 339 ($M^+ - 2H_2O$), 286, 268, 243, 225, 183, 173, 159, 143, 131, 117, 105, 99 (base peak), 93, 91, 81, 79, 71, 67, 55, 43, 41. HR-MS m/z: ($M^+ - H_2O$) Calcd for $C_{22}H_{31}NO_3$ 357.2304, Found 357.2322. $[\alpha]_D^{20}$: −1.0° (c=0.348, MeOH).

In a similar manner, the 5*E*-stereoisomer **73** was synthesized from the corresponding ester in 45% yield. Spectral data of **73**: IR (neat): 3400, 2950, 2220, 1720, 1640 cm^{-1}. ^{1}H-NMR ($CDCl_3$) δ: 0.89 (br t, J=6.5 Hz, 3H), 1.02—1.71 (m, 10H), 1.71—2.10 (m, 3H), 2.10—2.70 (m, 9H), 2.76—2.93 (m, 1H), 3.30—4.40 (m, 5H), 5.48 (dd, J=15, 8 Hz, 1H), 5.58 (dd, J=15, 7 Hz, 1H). MS m/z: 357 ($M^+ - H_2O$), 339 ($M^+ - 2H_2O$), 268, 243, 225, 147, 117, 99, 91, 71, 43 (base peak). HR-MS m/z: ($M^+ - H_2O$) Calcd for $C_{22}H_{31}NO_3$ 357.2304, Found 357.2284. $[\alpha]_D^{20}$: +74° (c=0.39, $CHCl_3$). TLC (ether–methanol, 15 : 1, silica gel): *Rf* **6** (*Z*-isomer) 0.11, **73** (*E*-isomer) 0.45.

In a similar manner, 16-methylcyanocarbacyclin **7** and its 5*E*-stereoisomer **74** were synthesized from **63** and **72**. The spectral data were as follows.

Methyl (1*S*,5*S*,6*R*,7*R*)-6-(4-Methyl-3-oxo-*E*-1-octenyl)-7-tetrahydropyranyloxybicyclo[3.3.0]octane-*Z*-$\Delta^{3,\delta}$-δ-cyanopentanoate (65) Yield was 82%. IR (neat): 2935, 2250, 2210, 1740, 1695, 1670, 1622 cm^{-1}. ^{1}H-NMR ($CDCl_3$) δ: 0.89 (t, J=6 Hz, 3H), 1.10 (d, J=7 Hz, 3H), 1.10—2.10 (m, 16H), 2.10—3.00 (m, 12H), 3.20—4.30 (m, 3H), 3.68 (s, 3H), 4.51, 4.62 (each br s, total 1H), 6.18, 6.25 (each d, J=16 Hz, total 1H), 6.70 (m, 1H). MS m/z: 401 (M^+ −DHP), 383 (M^+ −THPOH), 288, 256, 113, 85 (base peak), 67, 57, 43, 41. HR-MS m/z: (M^+ −DHP) Calcd for $C_{24}H_{35}NO_4$ 401.2564, Found 401.2580.

Methyl (1*S*,5*S*,6*R*,7*R*)-6-(4-Methyl-3-oxo-*E*-1-octenyl)-7-tetrahydropyranyloxybicyclo[3.3.0]octane-*E*-$\Delta^{3,\delta}$-δ-cyanopentanoate Yield was 69%. IR (neat): 2950, 2210, 1740, 1695, 1625 cm^{-1}. ^{1}H-NMR ($CDCl_3$) δ: 0.86 (t, J=6 Hz, 3H), 1.10 (d, J=7 Hz, 3H), 1.10—2.04 (m, 16H), 2.04—3.14 (m, 12H), 3.22—4.22 (m, 3H), 3.66 (s, 3H), 4.53, 4.63 (each br s, total 1H), 6.28 6.32 (each d, J=16 Hz, total 1H), 6.78, 6.82 (each dd, J=16, 8 Hz, 1H). MS m/z: 401 (M^+ −DHP), 383 (M^+ −THPOH), 357, 288, 113, 85 (base peak). HR-MS m/z: (M^+ −DHP) Calcd for $C_{24}H_{35}NO_4$ 401.2566, Found 401.2573.

Methyl (1*S*,5*S*,6*R*,7*R*)-7-Hydroxy-6-[3(*S*)-hydroxy-4-methyl-*E*-1-octenyl]bicyclo[3.3.0]octane-*Z*-$\Delta^{3,\delta}$-δ-cyanopentanoate (67a) Yield: **66a**, 52%, **66b**, 43% (in two steps). Spectral data of **67a**: IR (neat): 3425, 2940, 2220, 1740, 1642 cm^{-1}. ^{1}H-NMR ($CDCl_3$) δ: 0.90 (m, 6H), 1.02—3.00 (m, 24H), 3.70 (s, 3H), 3.75—4.05 (m, 2H), 5.56 (m, 2H). MS m/z: 385 ($M^+ - H_2O$), 368, 367 ($M^+ - 2H_2O$), 318, 300, 269, 268 (base peak), 250, 242, 226, 225, 167, 159, 149, 113, 91, 85, 81, 79, 67, 57, 55, 43, 41. HR-MS m/z: ($M^+ - H_2O$) Calcd for $C_{24}H_{35}NO_3$ 385.2615, Found 385.2618. $[\alpha]_D^{20}$: +2.9° (c=0.90, MeOH). Spectral data of **67b**: IR (neat): 3450, 2950, 2220, 1740, 1640 cm^{-1}. ^{1}H-NMR ($CDCl_3$) δ: 0.90 (m, 6H), 1.00—3.00 (m, 24H), 3.70 (s, 3H), 3.80—4.10 (m, 2H), 5.62 (m, 2H). MS m/z: 385 ($M^+ - H_2O$), 367 ($M^+ - 2H_2O$), 318, 300, 269, 268 (base peak), 250, 242, 240, 226, 225, 159, 131, 130, 117, 112, 91, 85, 81, 79, 57, 55, 43, 41. HR-MS m/z: ($M^+ - H_2O$) Calcd for $C_{24}H_{35}NO_3$ 385.2615, Found 385.2629. $[\alpha]_D^{20}$: −16° (c=0.67, MeOH).

Methyl (1*S*,5*S*,6*R*,7*R*)-7-Hydroxy-6-[3(*S*)-hydroxy-4-methyl-*E*-1-octenyl]bicyclo[3.3.0]octane-*E*-$\Delta^{3,\delta}$-δ-cyanopentanoate Yield: 65% (in two steps). IR (neat): 3430, 2950, 2200, 1730, 1640 cm^{-1}. ^{1}H-NMR ($CDCl_3$) δ: 0.76—1.06 (m, 6H), 1.23—1.62 (m, 8H), 1.80—2.01 (m, 5H), 2.17—3.10 (m, 11H), 3.70 (s, 3H), 3.75—4.10 (m, 2H), 5.44—5.68 (m, 2H). MS m/z: 385 ($M^+ - H_2O$), 367 ($M^+ - 2H_2O$), 354, 341, 300, 268 (base peak), 159, 85, 43. HR-MS m/z: ($M^+ - H_2O$) Calcd for $C_{24}H_{35}NO_3$ 385.2617, Found 385.2623.

(1*S*,5*S*,6*R*,7*R*)-7-Hydroxy-6-[3(*S*)-hydroxy-4-methyl-*E*-1-octenyl]-bicyclo[3.3.0]octane-*Z*-$\Delta^{3,\delta}$-δ-cyanopentanoic Acid (7) Yield: 78%. IR (neat): 3400, 2980, 2220, 1720, 1650 cm^{-1}. ^{1}H-NMR ($CDCl_3$) δ: 0.90 (m, 6H), 1.05—3.20 (m, 25H), 3.90 (m, 1H), 5.55 (m, 2H). MS m/z: 389 (M^+), 371 ($M^+ - H_2O$), 353 ($M^+ - 2H_2O$), 286, 269, 268 (base peak), 250, 242, 159, 131, 113, 95, 85, 81, 67, 55, 43, 41. HR-MS m/z: ($M^+ - H_2O$) Calcd for $C_{23}H_{33}NO_3$ 371.2460, Found 371.2451. $[\alpha]_D^{20}$: +8° (c=0.22, MeOH).

(1*S*,5*S*,6*R*,7*R*)-7-Hydroxy-6-[3(*S*)-hydroxy-4-methyl-*E*-1-octenyl]-bicyclo[3.3.0]octane-*Z*-$\Delta^{3,\delta}$-δ-cyanopentanoic Acid (74) Yield: 100%. IR (neat): 3400, 2970, 2230, 1720, 1650 cm^{-1}. ^{1}H-NMR ($CDCl_3$) δ: 0.78—1.07 (m, 6H), 1.08—1.71 (m, 9H), 1.74—2.12 (m, 3H), 2.14—3.10 (m, 10H), 3.62—4.00 (m, 2H), 4.41—4.92 (m, 3H), 5.46—5.66 (m, 2H). MS m/z: 371 ($M^+ - H_2O$), 353 ($M^+ - 2H_2O$), 286, 268 (base peak), 159, 85, 43. HR-MS m/z: ($M^+ - H_2O$) Calcd for $C_{23}H_{33}NO_3$ 371.2460, Found 371.2442.

Acknowledgment We are grateful to Drs. K. Iseki, T. Kanayama and Y. Hayashi, Mitsubishi Kasei Corporation, for the tests of biological activity.

References and Notes

1) For nonstereoselective syntheses of carbacyclins, see: *a*) K. C. Nicolaou, W. J. Sipio, R. L. Magolda, S. Seitz, and W. E. Barnett, *J. Chem. Soc., Chem. Commun.*, **1978**, 1067; *b*) K. Kojima and K. Sakai, *Tetrahedron Lett.*, **1978**, 3743; *c*) M. Shibasaki, J. Ueda, and S. Ikagami, *ibid.*, **1979**, 433; *d*) D. R. Morton and F. C. Brokaw, *J. Org. Chem.*, **44**, 2880 (1979); *e*) Y. Konishi, M. Kawamura, Y. Arai, and M. Hayashi, *Chem. Lett.*, **1979**, 1437; *f*) A. Sugie, M. Shimomura, J. Katsube, and M. Yamamoto, *Tetrahedron Lett.*, **1979**, 2607; *g*) M. Shibasaki, K. Iseki, and S. Ikegami, *Chem. Lett.*, **1979**, 1299; h) A. Barco, S. Benetti, P. Pollini, P. G. Baraldi, and C. Gandolfi, *J. Org. Chem.*, **45**, 4776 (1980); *i*) M. Yamazaki, M. Shibasaki, and S. Ikegami, *Chem. Lett.*, **1981**, 1245; *j*) P. A. Aristoff, *J. Org. Chem.*, **46**, 1954 (1981); *k*) Y. Konishi, M. Kawamura, Y. Iguchi, Y. Arai, and M. Hayashi, *Tetrahedron*, **37**, 4391 (1981); *l*) W. Skuballa and H. Vorbrüggen, *Angew. Chem., Int. Ed. Engl.*, **20**, 1046 (1981); *m*) R. F. Newton and A. H. Wadsworth, *J. Chem. Soc., Perkin Trans. 1*, **1982**, 823; *n*) K. Kojima, S. Amemiya, K. Koyama, and K. Sakai, *Chem. Pharm. Bull.*, **31**, 3775 (1983); *o*) S. Amemiya, K. Kojima, and K. Sakai, *ibid.*, **32**, 4746 (1984); *p*) K. Ueno, H. Suemune, and K. Sakai, *ibid.*, **32**, 3768 (1984); *q*) B. Bennua, H. Dahl, and H. Vorbrüggen, *Synthesis*, **1985**, 41 ; *r*) W. Skuballa, E. Schillinger, and C.-St. Stürzebecher, *J. Med. Chem.*, **29**, 313 (1986); *s*) Y. Nagao, T. Nakamura, M. Ochiai, K. Fuji, and E. Fujita, *J. Chem. Soc., Chem. Commun.*, **1987**, 267; *t*) P. Magnus and D. P. Becker, *J. Am. Chem. Soc.*, **109**, 7495 (1987); For attempts to achieve stereocontrol, see: *u*) S. Amemiya, K. Kojima, and K. Sakai, *Chem. Pharm. Bull.*, **32**, 1349 (1984); *v*) H.-G. Gais, G. Schmiedl, A. Ball, J. Bund, G. Hellmann, and I. Erdelmeier, *Tetrahedron Lett.*, **29**, 1773 (1988); *w*) H. Rehwinkel, J. Skupsh, and H. Vorbrüggen, *ibid.*, **29**, 1775 (1988); For attempts to recycle the useless *Z*-isomer, see: *x*) H. Vorbrüggen and B. Bennua, *Synthesis*, **1985**, 925.

2) After our preliminary communication, two stereocontrolled syntheses were reported: *a*) D. K. Hutchinson and P. L. Fuchs, *J. Am. Chem. Soc.*, **109**, 4755 (1987); *b*) I. Erdelmeier and H.-J. Gais, *ibid.*, **111**, 1125 (1989).

3) Preliminary communications: *a*) M. Shibasaki, M. Sodeoka, and Y. Ogawa, *J. Org. Chem.*, **49**, 4096 (1984); *b*) M. Shibasaki and M. Sodeoka, *Tetrahedron Lett.*, **26**, 3491 (1985).

4) *a*) E. N. Frankel, E. Selke, and C. A. Grass, *J. Am. Chem. Soc.*, **90**, 2446 (1968); *b*) M. Cais, E. N. Frankel, and A. Rejoan, *Tetrahedron Lett.*, **1968**, 1919.

5) For review, see: *a*) M. F. Farona, "Organometallic Reactions and Syntheses," Vol. 6, ed. by E. N. Becker and M. Tsutsui, Plenum Press, New York and London, 1977, p. 246; *b*) M. Shibasaki and M. Sodeoka, *Yuki Gosei Kagaku Kyokai Shi*, **43**, 877 (1985) and references cited therein.

6) At nearly the same time, one application to the synthesis of rather complex molecules was reported. See: P. Rosenmund and M. Casutt, *Tetrahedron Lett.*, **24**, 1771 (1983).

7) *a*) M. Sodeoka, Y. Ogawa, T. Mase, and M. Shibasaki, *Chem. Pharm. Bull.*, **37**, 586 (1989); *b*) M. Sodeoka and M. Shibasaki, *Chem. Lett.*, **1984**, 579; *c*) Y. Ogawa and M. Shibasaki, *Tetrahedron Lett.*, **25**, 1067 (1984); *d*) T. Mase, M. Sodeoka, and M. Shibasaki, *ibid.*, **25**, 5087 (1984).

8) In the absence of the catalyst no isomerization was observed at 130 °C. This fact rules out the possibility of thermal 1,5-sigmatropic rearrangement. We found that this stereospecific isomerization of conjugated dienes occurred even at 20 °C in acetone or THF when naphthalene·$Cr(CO)_3$ was used as a catalyst. We also succeeded in the stereocontrolled synthesis of aryl-substituted exocyclic olefins and silyl dienol ethers using this unique isomerization. See *a*) M. Sodeoka, S. Satoh, and M. Shibasaki, *J. Am. Chem. Soc.*, **110**, 4823 (1988); *b*) M. Sodeoka, H. Yamada, and M. Shibasaki, *ibid.*, **112**, 4906 (1990).

9) M. Sodeoka and M. Shibasaki, *J. Org. Chem.*, **50**, 1147 (1985).

10) *a*) T. Bannai, T. Toru, A. Hazato, T. Oba, T. Tanaka, N. Okumura, K. Watanabe, and S. Kurozumi, *Chem. Pharm. Bull.*, **30**, 1102 (1982); *b*) A. Hazato, T. Tanaka, K. Watanabe, T. Bannai, T. Toru, N. Okumura, K. Manabe, A. Ohtsu, F. Kamimoto, and S. Kurozumi, *ibid.*, **33**, 1815 (1985).

11) The aldehyde **56** was synthesized by hydrogenation of 3-carbomethoxypropionyl chloride. See: A. W. Burgstahler, L. O. Weigdand, and C. G. Shaffer, *Synthesis*, **1976**, 767. Since **56** is rather unstable, it is necessary to use freshly prepared **56**.

12) R. M. Silverstein, G. C. Bassler, and T. C. Morrill, "Spectrometric Identification of Organic Compounds," John Wiley & Sons, Inc.

13) About 7% of the product was obtained as its chromium complex. Although the structure was not clear, this complex was transformed into **61** quantitatively under exposure to air and light.

14) A. Takahashi, Y. Kirio, M. Sodeoka, H. Sasai, and M. Shibasaki, *J. Am. Chem. Soc.*, **111**, 643 (1989).

15) The cyano group is easily converted to a variety of functional groups such as aldehyde, carboxylic acid, ester, alcohol, amine, *etc.*

16) The stereoisomers of **39** could be separated by $AgNO_3$-impregnated silica gel column chromatography. The 4*Z*-stereoisomer of **78** is approximately one hundred times as potent as the 4*E*-stereoisomer in inhibiting human platelet aggregation. See: K. Iseki, M. Shinoda, C. Ishiyama, Y. Hayashi, S. Yamada, and M. Shibasaki, *Chem. Lett.*, **1986**, 559.

17) For other diene-carbacyclins, see: *a*) K. Iseki, T. Katayama, Y. Hayashi, and M. Shibasaki, *Chem. Pharm. Bull.*, **38**, 1769 (1990); *b*) M. Shibasaki, A. Takahashi, T. Aoki, H. Sato, and S. Narita, *ibid.*, **37**, 1647 (1989).

18) Nissan Chemical Industries, Ltd., Tokyo, Japan

Stereocontrolled Synthesis of Exocyclic Olefins Using Arene Tricarbonyl Chromium Complex-Catalyzed Hydrogenation. II. A Catalytic Asymmetric Synthesis of an Anthracycline Intermediate

Mikiko SODEOKA, Takamasa IIMORI, and Masakatsu SHIBASAKI*

Sagami Chemical Research Center, Nishi-Ohnuma, Sagamihara, Kanagawa 229, Japan. *Received August 20, 1990*

A method for the stereospecific synthesis of trisubstituted exocyclic allylic alcohols is described. Using this methodology in combination with the Sharpless catalytic asymmetric epoxidation, an efficient synthesis of (*R*)-(−)-9, an important intermediate for anthracycline synthesis, has been accomplished in 36% overall yield from 14 with 93% ee.

Keywords dienol acetate; 1,4-hydrogenation; arene tricarbonyl chromium complex; exocyclic allylic alcohol; antineoplastic agent

The Sharpless asymmetric epoxidation is one of the most useful and versatile catalytic asymmetric reactions.[1] For the efficient use of this excellent reaction the olefin geometry of allylic alcohols has to be strictly controlled. Although a number of methods for the stereocontrolled synthesis of olefins are known, there is no methodology for the stereospecific synthesis of exocyclic allylic alcohols such as **4**. As described in the preceding paper,[2] we have exploited an extremely efficient method for the stereospecific synthesis of exocyclic tri- and tetrasubstituted olefins using the 1,4-hydrogenation of conjugated dienes catalyzed by arene·$Cr(CO)_3$ complex. This successful result led us to expect that extension of the 1,4-hydrogenation technique to dienol acetates **1** could produce exocyclic allylic alcohols **4** stereospecifically (Chart 1). To test the feasibility of this stereospecific synthesis of exocyclic allylic alcohols, the following asymmetric synthesis of the anthracycline intermediate **9** was undertaken (Chart 2).

4-Demethoxyadriamycin (**7**) and 4-demethoxydaunorubicin (**8**) are expected to be more clinically useful antineoplastic agents than the naturally occurring anthracyclines **5** and **6**.[3] Since these analogues are not available by the fermentation method, quite a number of synthetic studies on **7** and **8** have already been reported, and it has been established that (*R*)-(−)-2-acetyl-5,8-dimethoxy-1,2,3,4-tetrahydro-2-naphthol (**9**) is one of the most useful synthetic intermediates.[4] This account describes a synthesis of (*R*)-(−)-**9** using the above-mentioned methodology, which features a catalytic use of the chiral source.[5]

Regiocontrolled Synthesis of the Dienol Acetate The synthesis of the dienol acetate **13** started with the highly enolizable ketone **14**, which was prepared according to the reported procedure.[6] First we attempted to use the ethynyl-alcohol **16** as an intermediate, obtainable by the reaction of **14** with the ethynylcerium reagent[7] followed by desilylation (tetrabutylammonium fluoride (TBAF) in tetrahydrofuran (THF), 94%). Hydroboration of **16** with disiamylborane and subsequent oxidation[8] afforded the

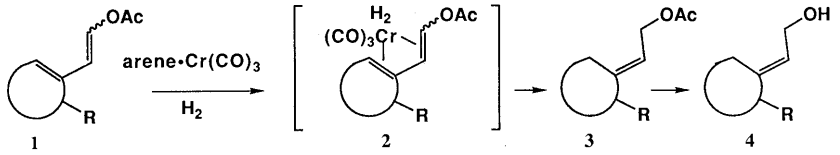

Chart 1

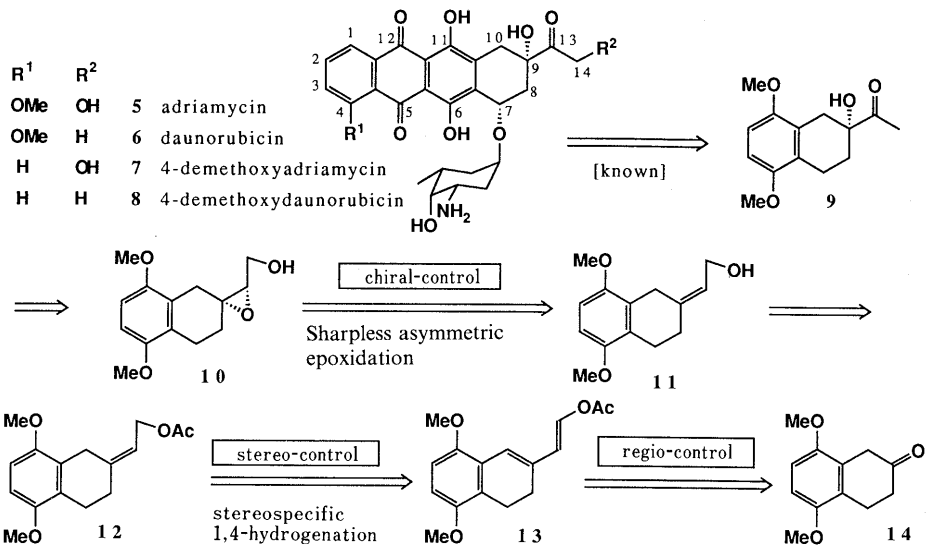

Chart 2

aldehydes **17** and **18**. These aldehydes could be converted to the desired dienol acetate **13** by treatment with acetic anhydride (3.6 eq) and triethylamine (4.0 eq) in toluene at 80 °C. The overall yield of **13** from **15**, however, was only 17% owing to instability of the aldehydes under the oxidation conditions. Furthermore, reproducibility of the reaction was poor.

Therefore, we next turned our attention to the allylic alcohol **19**, which was obtained efficiently from **14** according to the procedure reported by Hiyama *et al.*[9] Treatment of **19** with a catalytic amount of osmium tetroxide and 3 eq of sodium periodate in aqueous ether (ether–H_2O, 3 : 4) at 23 °C afforded the unstable aldehyde **17**, which, without purification, was converted to the dienol acetate **13** regio- and stereospecifically on exposure to acetic anhydride (5 eq), triethylamine (8 eq) and a catalytic amount of 4-dimethylaminopyridine (DMAP) in toluene at 80 °C for 40 min (60% overall yield from **19**).[10] A better overall yield was obtained by the following sequence. Acetylation of **19** (5 eq of Ac_2O, 5 eq of pyridine and a catalytic amount of DMAP in CH_2Cl_2) gave the acetate **20**, which was transformed into the dienol acetate **13** regio- and stereospecifically on exposure to the same reaction conditions as described above in 73% overall yield. The stereochemistry of the disubstituted double bond in the dienol acetate **13** was determined from the proton nuclear magnetic resonance (^{1}H-NMR) spectra. The coupling constant between H_a and H_b was 13 Hz, being in accord with those of *E*-enol acetates.[11]

1,4-Hydrogenation of the Dienol Acetate As expected, the crucial 1,4-hydrogenation of the dienol acetate **13** proceeded smoothly by using naphthalene·$Cr(CO)_3$ as a catalyst to afford the stereochemically homogeneous *Z*-allylic acetate **12** in 91% yield (20 mol% of the catalyst, acetone solvent, 140 kg/cm^2 of H_2 pressure, 45 °C, 13 h) together with recovery of **13** (9%). A part of **12** (4%) was isolated as its chromium complex (**21**), which was easily converted to **12** on exposure to $FeCl_3$/EtOH. The obtained allylic acetate **12** was then converted to the allylic alcohol **11** in quantitative yield by treatment with potassium carbonate in methanol.

Comparison of the ^{1}H-NMR spectra of **12** and **24** showed clearly that the 1,4-hydrogenation product was stereochemically homogeneous. The stereoisomer **24** was synthesized as shown in Chart 5. Furthermore, the stereochemistry of the desired exocyclic allylic alcohol **11** was unequivocally determined to be *Z* by the nuclear Overhauser effect (NOE) experiments.

Thus, we succeeded in the efficient and stereospecific synthesis of the exocyclic allylic alcohol **11**.

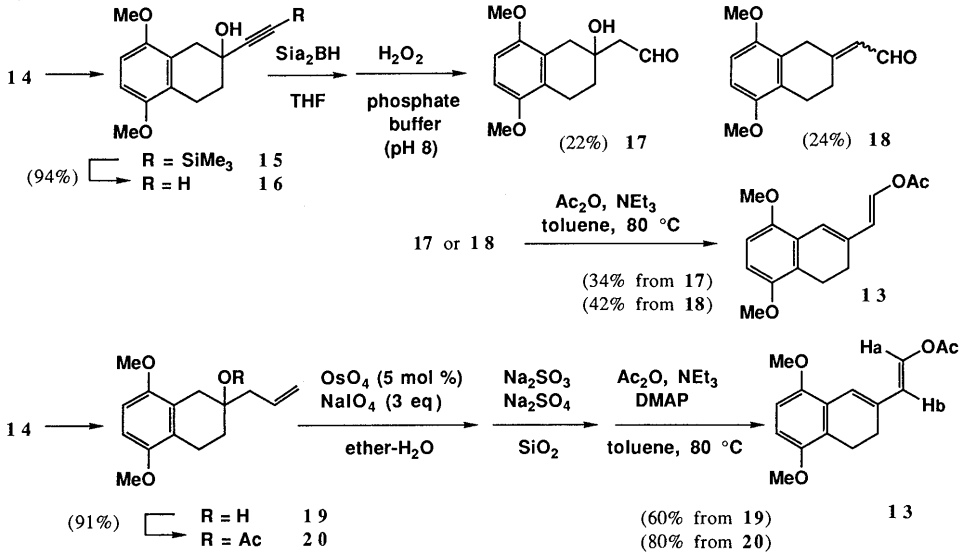

Chart 3

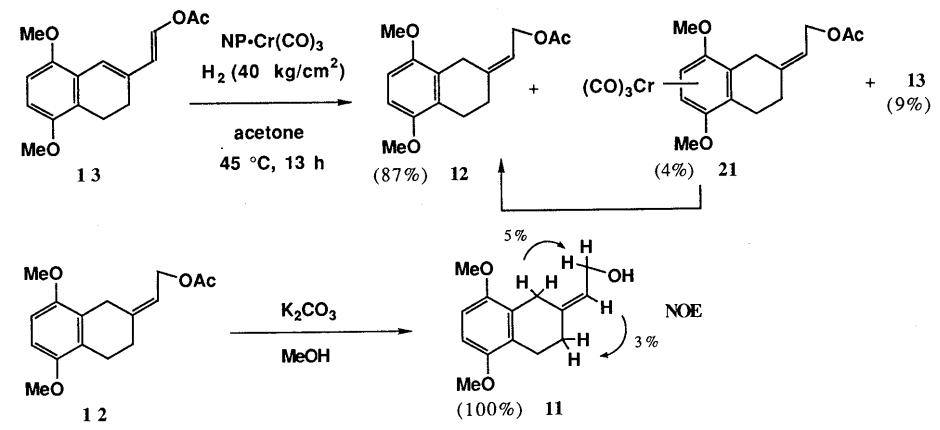

Chart 4

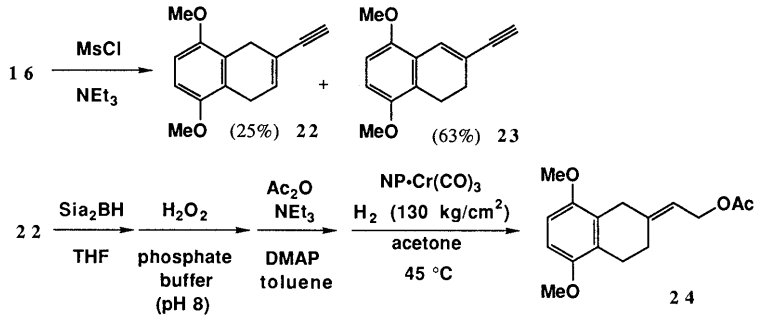

Chart 5

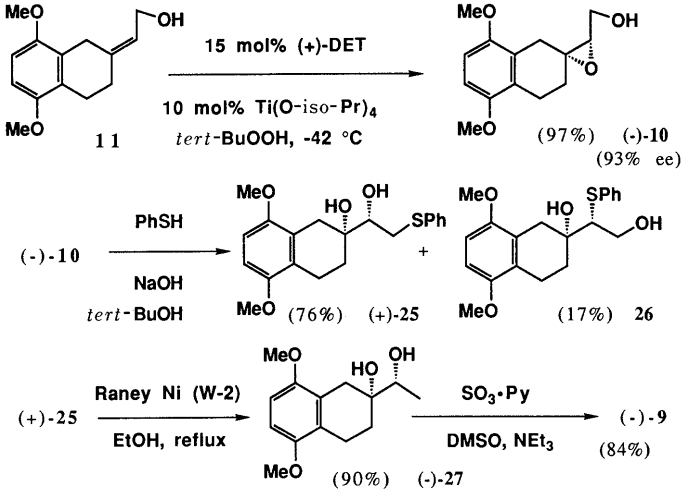

Chart 6

Asymmetric Synthesis of the Anthracycline Intermediate Next we turned our attention to the transformation of **11** into (*R*)-(−)-**9**. The Sharpless catalytic asymmetric epoxidation[1] of **11** proceeded smoothly (5 mol% of (+)-diethyl tartrate, 10 mol% of titanium(IV) isopropoxide, 2 eq of *tert*-butyl hydroperoxide, molecular sieves 4A, −42 °C, 2.5 h), providing the optically active and crystalline epoxy-alcohol **10** in 97% yield. The enantiomeric excess was determined to be 93% by ^{1}H-NMR analysis (400 MHz) of the corresponding MTPA ester.[12] Recrystallization of this sample from CH_2Cl_2–hexane gave optically pure (−)-**10** (yield, 43%).

Treatment of optically pure **10** with thiophenol under basic conditions (slow dropping of thiophenol into a solution of **10** in 0.5 N aqueous NaOH–*tert*-butanol (3 : 2) at 85—90 °C)[13] afforded the desired dihydroxy-sulfide **25** *via* Payne rearrangement[14] in 76% yield together with a small amount of the regioisomer **26** (17%). Hydrogenolysis of the carbon-sulfur bond of **25** was carried out with Raney Ni (W-2) in boiling ethanol, giving the diol **27** in 90% yield. Finally the diol **27** was converted to (*R*)-(−)-**9** in 84% yield on exposure to 10 eq of sulfur trioxide–pyridine complex and 30 eq of triethylamine in dimethyl sulfoxide (DMSO). The values of the optical rotation ($[\alpha]_D^{20}$ −48.7° (c=0.825, $CHCl_3$) and the melting point (128—129 °C) of **9** thus obtained were in good agreement with those reported in the literature (lit. 4*i* $[\alpha]_D^{20}$ −48.8° (c=1, $CHCl_3$), mp 128—129 °C, lit. 4*l* $[\alpha]_D^{20}$ −47.6° (c=1.02, $CHCl_3$), mp 129.5—130 °C, lit. 4*d* $[\alpha]_D^{20}$ −48.2° (c=0.982, $CHCl_3$), mp 128—129 °C).

In summary, we have accomplished an asymmetric synthesis of (*R*)-(−)-**9**, a well-known intermediate for the synthesis of anthracyclines, in 36% overall yield starting with **14**. The synthesis presented above involves a new and efficient method for the stereospecific synthesis of exocyclic allylic alcohols and a catalytic asymmetric induction process. The aforementioned methodology should be advantageous for synthesizing a variety of compounds.[15]

Experimental

General Methods Infrared (IR) spectra were measured on a JASCO A-202 diffraction grating infrared spectrophotometer. ^{1}H-NMR spectra were recorded with a Varian EM 390 NMR spectrometer or a Hitachi R-90H Fourier-transform NMR spectrometer or a Brucker AN-400 spectrometer with tetramethylsilane as an internal standard. Low-resolution mass spectra (MS) were obtained with a Hitachi RUM-6MG mass spectrometer. Optical rotation was measured on a Horiba SEPA-200 high-sensitivity polarimeter. In general, reactions were carried out in dry solvents under an argon atmosphere unless otherwise mentioned.

2-Ethynyl-2-hydroxy-5,8-dimethoxy-1,2,3,4-tetrahydronaphthalene (16) Tetrabutylammonium fluoride (1 M solution in THF, 3.59 ml) was added to a solution of **15**[7] (729 mg, 2.39 mmol) in THF (10 ml), and the mixture was stirred for 10 min at 23 °C. The reaction was quenched by the addition of saturated aqueous NH_4Cl, followed by extraction of the mixture with ether. The combined organic layers were washed with brine, dried over $MgSO_4$, and concentrated. The residue was purified by silica gel column chromatography (ether–hexane, 1 : 2) to give the alcohol **16** (522 mg, 94%) as colorless prisms. IR (KBr): 3310, 3260, 2110, 1605, 1258, 805 cm^{-1}. ^{1}H-NMR ($CDCl_3$) δ: 2.05 (t, J=7 Hz, 2H), 2.11 (s, 1H), 2.40 (s, 1H), 2.85 (t, J=7 Hz, 2H), 2.92 (d, J=16 Hz, 1H), 3.16 (d, J=16 Hz, 1H), 3.78 (s, 6H), 6.64 (s, 2H). MS m/z: 332 (base peak, M^+), 214 ($M^+ - H_2O$), 199, 183, 175, 164, 149, 165, 159, 121, 91, 77. *Anal.* Calcd for $C_{14}H_{16}O_3$: C, 72.39; H, 6.94. Found: C, 72.34; H, 6.92. mp 104—105 °C (recryst. from ether–CH_2Cl_2).

2-Acetoxy-2-allyl-5,8-dimethoxy-1,2,3,4-tetrahydronaphthalene (20) Pyridine (4.48 ml, 55 mmol), acetic anhydride (5.22 ml, 55 mmol) and a catalytic amount of DMAP were added to a stirred solution of the alcohol **19**[9] (2.75 g, 11 mmol) in methylene chloride (20 ml), and the mixture was stirred at 23 °C overnight. After evaporation of the solvent and the excess reagents, the residue was purified by silica gel column chromatography (ether–hexane, 1 : 5) to give **20** (2.91 g. 91%) as colorless prisms. IR (KBr): 1730, 1640, 1605, 1490, 1258 cm^{-1}. ^{1}H-NMR ($CDCl_3$) δ: 1.90 (s, 3H), 2.20—3.00 (m, 7H), 3.17 (d, J=17 Hz, 1H), 3.77 (s, 6H), 5.12 (m, 2H), 5.80 (m, 1H), 6.60 (s, 2H). MS m/z: 290 (M^+), 249 (M^+ − allyl), 230 (base peak), 215, 207, 199, 189, 174, 158, 115, 91, 43. *Anal.* Calcd for $C_{17}H_{22}O_4$: C, 70.32; H, 7.64. Found: C, 70.02; H, 7.48. mp 92—94 °C (recryst. from benzene–hexane).

2-(*E*-2-Acetoxyvinyl)-3,4-dihydro-5,8-dimethoxynaphthalene (13) From **16**: A solution of disiamylborane in THF (0.93 M, 1.11 ml, 1.03 mmol) was added to a stirred solution of **16** (100 mg, 0.43 mmol) in THF (1 ml) at 0 °C, and the mixture was stirred at 23 °C for 20 min. Then the reaction mixture was poured into a mixture of phosphate buffer (NaH_2PO_4 3.8 mmol, NaOH 3.3 mmol in 10 ml of H_2O, pH 8) and 30% H_2O_2 (0.351 ml, 3.10 mmol), and the whole reaction mixture was stirred at 23 °C for 40 min, then extracted with ether. The combined organic layers were washed with $Na_2S_2O_3$ and brine and dried over $MgSO_4$. Removal of the solvent gave the oily residue, which was purified by silica gel column

chromatography (ether–hexane, 1 : 1) to afford the aldehyde **17** (24 mg, 22%) and **18** (24 mg, 24%). Owing to the instability of these aldehydes, only the NMR spectra were measured. **17**: ^{1}H-NMR ($CDCl_3$) δ: 1.86 (m, 2H), 2.64 (d, J=2 Hz, 2H), 2.80 (m, 5H), 3.78 (s, 6H), 6.64 (s, 2H), 9.97 (t, J=2 Hz, 1H). **18**: ^{1}H-NMR ($CDCl_3$) δ: 2.30—3.20 (m, 6H), 6.02 (m, 1H), 3.78 (s, 6H), 6.65 (s, 2H), 10.10, 10.20 (each d, J=6 Hz, total 1H). Triethylamine (0.054 ml, 0.384 mmol), acetic anhydride (0.033 ml, 0.345 mmol) and a catalytic amount of DMAP were added to a stirred solution of the aldehyde **17** (24 mg, 0.096 mmol) in toluene (1.3 ml), and the mixture was stirred at 80 °C for 10 min, then allowed to cool to room temperature. The reaction was quenched by the addition of brine, followed by extraction of the mixture with ether. The combined ether extracts were dried over $MgSO_4$ and concentrated. The residue was purified by silica gel column chromatography (ether–hexane, 1 : 4) to afford the dienol acetate **13** (9 mg, 34%). In a similar manner, **18** was converted to **13** in 42% yield.

From **20**: A solution of osmium tetroxide in ether (0.1% (w/v), 1.8 ml, 0.7 mmol) was added to a solution of the acetate **20** (2.05 g, 7.0 mmol) in ether (26 ml). To this solution, an aqueous solution of $NaIO_4$ (4.49 g, 21 mmol in 35 ml of H_2O) was added over 5 min, and the mixture was stirred at 23 °C for 6.5 h. The separated ether layer was filtered through a pad of Na_2SO_4–Na_2SO_3–SiO_2. Removal of the solvent from the filtrate gave the crude aldehyde **17**. Triethylamine (7.8 ml, 56 mmol), acetic anhydride (3.3 ml, 35 mmol) and a catalytic amount of DMAP were added to a stirred solution of the crude aldehyde **17** in toluene (40 ml), and the mixture was stirred at 80 °C for 50 min, then allowed to cool to room temperature. The reaction was quenched by the addition of brine, followed by extraction of the mixture with ether. The combined ether extracts were washed with brine, dried over $MgSO_4$ and concentrated. The residue was purified by silica gel column chromatography (ether–hexane, 1 : 4) to afford the dienol acetate **13** (1.54 g, 80%) as colorless prisms. IR (KBr): 1757, 1640, 1618, 1598, 1490, 1215 cm^{-1}. ^{1}H-NMR ($CDCl_3$) δ: 2.18 (s, 3H), 2.33 (t, J=8 Hz, 2H), 2.83 (t, J=8 Hz, 2H), 3.80 (s, 6H), 6.29 (d, J=13 Hz, 1H), 6.66 (s, 2H), 6.76 (s, 1H), 7.52 (d, J=13 Hz, 1H). MS m/z: 274 (M^+), 232 (base peak), 43. *Anal.* Calcd for $C_{16}H_{18}O_4$: C, 70.06; H, 6.61. Found: C, 69.99; H, 6.67. mp 115—116 °C (recryst. from CH_2Cl_2–hexane).

(*Z*)-2-(2-Acetoxyethylidene)-5,8-dimethoxy-1,2,3,4-tetrahydronaphthalene (12) The dienol acetate **13** (410 mg, 1.49 mmol) and naphthalene·$Cr(CO)_3$ (80 mg, 0.3 mmol) were dissolved in acetone (10 ml). The solution was degassed by three freeze-pump-thaw cycles, and then transferred into an autoclave with a glass insert (100 ml) under an argon atmosphere. The autoclave was purged repeatedly with hydrogen. The solution was stirred at 45 °C for 13 h under 140 kg/cm^2 of hydrogen pressure. After cooling to room temperature, the reaction mixture was exposed to air and light to decompose the catalyst. Removal of the solvent gave a dark green residue, which was purified by silica gel column chromatography (ether–hexane, 1 : 5) to afford the desired exocyclic allylic acetate **12** (359 mg, 87%) as a more polar fraction and the starting material **13** (39 mg, 9%) as a less polar fraction. Furthermore, elution with ether afforded the unstable chromium complex **21** (28 mg, IR (KBr): 2940, 1952, 1865, 1735 cm^{-1}) as a yellow caramel. This complex was partially decomposed on exposure to air and light. A solution of $FeCl_3$ in wet ethanol was added to **21**, and the mixture was stirred at 23 °C for 1 h. Removal of the solvent and purification of the residue by silica gel column chromatography (ether–hexane, 1 : 5) afforded **12** (16 mg, 4%). Spectral data of **12**: IR (KBr): 2950, 1740, 1675, 1602, 1485, 1258, 1090 cm^{-1}. ^{1}H-NMR ($CDCl_3$) δ: 2.06 (s, 3H), 2.40 (t, J=7 Hz, 2H), 2.75 (t, J=7 Hz, 2H), 3.43 (br s, 2H), 3.75 (s, 3H), 3.78 (s, 3H), 4.68 (d, J=7 Hz, 2H), 5.48 (t, J=7 Hz, 1H), 6.62 (s, 2H). MS m/z: 276 (M^+), 218, 217, 216 (base peak), 201, 189, 175, 173, 115, 43. HR-MS m/z: (M^+) Calcd for $C_{16}H_{20}O_4$ 276.1359, Found 276.1357.

(*Z*)-2-(2-Hydroxyethylidene)-5,8-dimethoxy-1,2,3,4-tetrahydronaphthalene (11) Potassium carbonate (151 mg, 1.09 mmol) was added to a solution of the acetate **12** (151 mg, 0.55 mmol) in methanol (8 ml), and the mixture was stirred at 23 °C for 1 h. Evaporation of methanol, dilution of the residue with ether, and filtration through a silica gel pad afforded the desired alcohol **11** (128 mg, 100%) as a colorless solid. Recrystallization from ether–hexane gave colorless needles. IR (KBr): 3400, 1678, 1602, 1482, 1255, 1082, 790 cm^{-1}. ^{1}H-NMR ($CDCl_3$) δ: 1.38 (s, 1H), 2.39 (t, J=7 Hz, 2H), 2.77 (t, J=7 Hz, 2H), 3.43 (s, 2H), 3.76 (s, 3H), 3.80 (s, 3H), 4.26 (d, J=7 Hz, 2H), 5.55 (t, J=7 Hz, 1H), 6.63 (s, 2H). MS m/z: 234 (M^+), 217, 216 (base peak), 203, 201, 189, 188, 185, 173, 159, 128, 115, 91, 77, 61, 45, 43, 29. *Anal.* Calcd for $C_{14}H_{18}O_3$: C, 70.32; H, 7.64. Found: C, 70.02; H, 7.48. mp 63.5—65.0 °C (recryst. from ether–hexane).

2-Ethynyl-5,8-dimethoxy-1,4-dihydronaphthalene (22) Triethylamine (13.5 ml, 96.9 mmol) and mesyl chloride (2.5 ml, 32.3 mmol) were added to a solution of **16** (1.5 g, 6.46 mmol) in methylene chloride (40 ml) at 0 °C, and the mixture was stirred at 0—23 °C for 1.5 h. The reaction was quenched by the addition of brine, followed by extraction of the mixture wih ether. The combined ether extracts were washed with brine, dried over $MgSO_4$, and concentrated. The residue was purified by silica gel column chromatography (ether–hexane, 1 : 20) to give **22** (345 mg, 25%) as a less polar fraction and **23** (864 mg, 63%) as a more polar fraction. Spectral data of **22**: IR (neat): 3265, 2950, 2110, 1605 cm^{-1}. ^{1}H-NMR ($CDCl_3$) δ: 2.84 (s, 1H), 3.37 (s, 4H), 3.78 (s, 6H), 6.32 (br s, 1H), 6.62 (s, 2H). MS m/z: 214 (base peak, M^+), 199, 189, 183, 164, 149. HR-MS m/z: (M^+) Calcd for $C_{14}H_{14}O_2$ 214.0994, Found 214.0998. Spectral data of **23**: IR (neat): 3265, 2940, 2110, 1605 cm^{-1}. ^{1}H-NMR ($CDCl_3$) δ: 2.37 (br t, J=8 Hz, 2H), 2.80 (br t, J=8 Hz, 2H), 3.10 (s, 1H), 3.78 (s, 6H), 6.65 (s, 1H), 6.68 (s, 1H), 7.24 (s, 1H). MS m/z: 214 (base peak, M^+), 199, 189, 183. HR-MS m/z: (M^+) Calcd for $C_{14}H_{14}O_2$ 214.0994, Found 214.0982.

(*E*)-2-(2-Acetoxyethylidene)-5,8-dimethoxy-1,2,3,4-tetrahydronaphthalene (24) In a similar manner to that used for the synthesis of **12** from **16**, the stereoisomer of **12** (**24**) was synthesized. Spectral data of **24**: IR (neat): 2950, 1740, 1675, 1605 cm^{-1}. ^{1}H-NMR ($CDCl_3$) δ: 2.19 (s, 3H), 2.48 (t, J=7 Hz, 2H), 2.78 (t, J=7 Hz, 2H), 3.38 (br s, 2H), 3.75 (s, 6H), 4.65 (d, J=7 Hz, 2H), 5.55 (t, J=7 Hz, 1H), 6.61 (s, 2H). MS m/z: 276 (M^+), 217, 216 (base peak), 201, 175, 115, 43. HR-MS m/z: (M^+) Calcd for $C_{16}H_{20}O_4$ 276.1359, Found 276.1368.

(2*R*,3′*S*)-5,8-Dimethoxy-1,2,3,4-tetrahydronaphthalene-2-spiro-3′-hydroxymethyl-2′-oxirane (10) Titanium tetraisopropoxide (0.036 ml, 0.12 mmol) was added to a suspension of powdered molecular sieves 4A (60 mg, dried at 220 °C under vacuum) in methylene chloride (6 ml) at −22 °C, and the mixture was stirred at the same temperature for 10 min. L-(+)-Diethyl tartrate (0.033 ml, 0.19 mmol) was added, and this mixture was stirred at −22 °C for 15 min. A solution of *tert*-butyl hydroperoxide (6.1 M solution in CH_2Cl_2, 0.41 ml, 2.48 mmol) was added to this suspension, and the reaction mixture was stirred at the same temperature for 40 min. A solution of the allylic alcohol **11** (290 mg, 1.24 mmol) in methylene chloride (8 ml) was then added at −42 °C, and the whole mixture was stirred at −42 °C for 2.5 h. The reaction was quenched by addition of 10% aqueous sodium hydroxide solution saturated with sodium chloride (0.29 ml) at −42 °C, and the mixture was diluted with ether (5 ml), removed from the cold bath, allowed to warm to 10 °C with vigorous stirring, and filtered through a Celite pad. The clear filtrate was treated again with 10% aqueous sodium hydroxide solution saturated with sodium chloride (0.29 ml) at 23 °C for 10 min. A solution of phosphate buffer (0.2 ml) [Na_2HPO_4 (1.5 mol) and KH_2PO_4 (1.5 mol) were dissolved in H_2O (1 l), and the pH was adjusted to 7 by addition of NaOH], Celite (1 g), and $MgSO_4$ (1 g) were then added, and the whole mixture was filtered through a Celite pad. Evaporation of the solvent gave a pale yellow solid. Purification by silica gel column chromatography (ether–methylene chloride, 1 : 5) afforded the epoxy alcohol **10** (301 mg, 97%, $[\alpha]_D^{20}$ −18.1° (c=1.34, $CHCl_3$)) as a colorless solid. For analysis of the enantiomeric purity, **10** was converted to the corresponding methoxytrifluoromethylphenylacetate (MTPA ester). Thus, (−)-MTPA chloride (5 μl) was added to a solution of **10** (3 mg, 0.01 mmol) in pyridine (0.1 ml), and the mixture was stirred at 23 °C for 2 h. The reaction mixture was diluted with ether, followed by filtration through a silica gel pad. Purification by silica gel column chromatography provided the MTPA ester. Analysis was accomplished by the use of 400 MHz ^{1}H-NMR ($CDCl_3$). Diastereomeric excess was determined to be 93.2% from the ratio of the two peaks (δ 3.518 ppm, (−)-MTPA-(−)-**10**, and δ 3.543 ppm, (−)-MTPA-(+)-**10**, 96.6 : 3.4). Optically pure (−)-**10** (colorless fine needles, $[\alpha]_D^{20}$ −21.7° (c=0.725, $CHCl_3$), mp 145—146 °C) was obtained by single recrystallization from methylene chloride–hexane (recovery, 46%). The optical purity of this sample was determined to be >97% ee by ^{1}H-NMR (400 MHz) analysis of its MTPA ester. IR (KBr): 3390, 3310, 2960, 1605, 1485, 1255, 1085, 795, 715 cm^{-1}. ^{1}H-NMR ($CDCl_3$) δ: 1.78 (m, 2H), 2.02 (t, J=6 Hz, 1H), 2.50—3.00 (m, 4H), 3.01 (t, J=6 Hz, 1H), 3.50—4.00 (m, 2H), 3.74 (s, 3H), 3.76 (s, 3H), 6.62 (s, 2H). MS m/z: 250 (M^+, base peak), 232, 220, 219, 217, 206, 191, 190, 189, 177, 175, 174, 160, 159, 115, 91, 77. *Anal.* Calcd for $C_{14}H_{18}O_4$: C, 67.18; H, 7.25. Found: C, 67.05; H, 7.33.

(*R*)-2-[1(*S*)-Hydroxy-2-phenylthioethyl]-5,8-dimethoxy-1,2,3,4-tetrahydro-2-naphthol (25) A solution of thiophenol (0.092 ml, 0.9 mmol) in *tert*-butanol (6 ml) was added to a stirred solution of (−)-**10** (150 mg, 0.6 mmol) in *tert*-butanol (6 ml) and 0.5 N aqueous NaOH at 85—90 °C over 3.2 h. After cooling of the mixture to 23 °C, the reaction was quenched by the addition of water, followed by extraction with ether. The combined ether extracts were washed with brine, dried over $MgSO_4$, and con-

centrated. The residue was purified by silica gel column chromatography (ether–methylene chloride, 1:10) to give **25** (163 mg, 76%) as a less polar fraction and **26** (37 mg, 17%) as a more polar fraction. Recrystallization from chloroform–hexane gave colorless needles. Spectral data of **25**: IR (KBr): 3550, 3225, 2950, 1600, 1585, 1485, 1250, 1100, 1050, 802, 735 cm^{-1}. ^{1}H-NMR ($CDCl_3$) δ: 1.50—2.00 (m, 2H), 2.18 (s, 1H), 2.60—3.80 (m, 8H), 3.74 (s, 3H), 3.76 (s, 3H), 6.60 (s, 2H), 7.30 (m, 5H). MS *m/z*: 360 (M^+), 219, 218, 207, 206 (base peak), 191, 190, 189, 177, 175, 165, 164, 149, 91, 45. *Anal.* Calcd for $C_{20}H_{24}O_4S$: C, 66.64; H,6.71; S, 8.89. Found: C, 66.76; H, 6.80; S, 8.90. $[\alpha]_D^{20}$ +23.9° (*c*=0.750, $CHCl_3$). mp 135—136 °C (recryst. from chloroform–hexane). Spectral data of **26**: IR (KBr): 3350, 2940, 1605, 1585, 1482, 1262, 1115, 1070, 802 cm^{-1}. ^{1}H-NMR ($CDCl_3$) δ: 2.00 (m, 2H), 2.65—3.20 (m, 6H), 3.34 (t, *J*=6 Hz, 1H), 3.73 (s, 3H), 3.77 (s, 3H), 4.03 (d, *J*=6 Hz, 2H), 6.62 (s, 2H), 7.30 (m, 5H). MS *m/z*: 360 (M^+), 233, 207, 206 (base peak), 189, 164, 136. HR-MS *m/z*: (M^+) Calcd for $C_{20}H_{24}O_4S$ 360.1396, Found 360.1364.

(*R*)-2-[1(*R*)-Hydroxyethyl]-5,8-dimethoxy-1,2,3,4-tetrahydro-2-naphthol (27) A suspension of Raney Ni (W-2) in ethanol was added to a stirred solution of (+)-**25** (65 mg, 0.18 mmol) in ethanol (5 ml), and the mixture was stirred under reflux for 4.5 h. After disappearance of the starting material (determined by thin layer chromatography (TLC), SiO_2, ether–hexane, 3:2), the reaction mixture was filtered through a pad of Celite. Removal of the solvent and purification of the residue by silica gel column chromatography (ether–hexane, 3:1) afforded the diol **27** (41 mg, 90%) as a colorless caramel. IR (KBr): 3430, 2950, 1605, 1485, 1255, 1090, 795, 715 cm^{-1}. ^{1}H-NMR ($CDCl_3$) δ: 1.24 (d, *J*=6 Hz, 3H), 1.30—2.10 (m, 2H), 2.17 (s, 2H), 2.74 (m, 4H), 3.65 (m, 1H), 3.75 (s, 3H), 3.77 (s, 3H), 6.62 (s, 2H). MS *m/z*: 252 (M^+), 208, 207 (base peak), 206, 192, 190, 189, 177, 176, 175, 165, 164, 149. HR-MS *m/z*: (M^+) Calcd for $C_{14}H_{20}O_4$ 252.1359, Found 252.1342. $[\alpha]_D^{20}$ −43.2° (*c*=0.905, EtOH).

(*R*)-2-Acetyl-5,8-dimethoxy-1,2,3,4-tetrahydro-2-naphthol (9) A solution of SO_3–pyridine complex (223 mg, 1.4 mmol) in DMSO (0.8 ml) was added to a stirred solution of the diol **27** (36 mg, 0.14 mmol) and triethylamine (0.59 ml, 4.2 mmol) in DMSO (0.4 ml), and the mixture was stirred at 23 °C for 75 min. The reaction was quenched by the addition of 10% aqueous HCl (7 ml), followed by extraction with ether. The combined ether extracts were washed with water and brine, dried over $MgSO_4$, and concentrated. The residue was purified by silica gel column chromatography (ether–hexane, 5:6) to give the hydroxyketone **9** (30 mg, 84%) as a colorless solid. Recrystallization of this sample from ether–hexane afforded **9** as colorless prisms. The spectral data of **9** thus obtained were identical with those reported in the literature.[4] IR (KBr): 3500, 2950, 1705, 1605, 1485, 1260, 1105, 1090, 1080, 970, 810 cm^{-1}. ^{1}H-NMR ($CDCl_3$) δ: 1.70—2.10 (m, 2H), 2.31 (s, 3H), 2.60—3.10 (m, 4H), 3.44 (s, 1H), 3.75 (s, 3H), 3.77 (s, 3H), 6.64 (s, 2H). MS *m/z*: 250 (M^+), 232, 207 (base peak), 189, 176, 174, 164, 158, 147, 43. HR-MS *m/z*: (M^+) Calcd for $C_{14}H_{18}O_4$ 250.1205, Found 250.1180. $[\alpha]_D^{20}$ −48.7° (*c*=0.825, $CHCl_3$). mp 128—129 °C (recryst. from ether–hexane).

References and Notes

1) *a*) T. Katsuki and K. B. Sharpless, *J. Am. Chem. Soc.*, **102**, 5974 (1980); *b*) R. M. Hanson and K. B. Sharpless, *J. Org. Chem.*, **51**, 1922 (1986).
2) M. Sodeoka, Y. Ogawa, Y. Kirio, and M. Shibasaki, *Chem. Pharm. Bull.*, **39**, 309 (1991).
3) S. Neidel, *Nature* (London), **268**, 195 (1977).
4) *a*) F. Arcamone, L. Bernardi, P. Giardino, B. Patelli, A. DiMarco, A. M. Casazza, G. Pratesi, and P. Reggiani, *Cancer Treat. Rep.*, **60**, 829 (1976); *b*) F. Arcamone, L. Bernardi, B. Patelli, P. Giardino, A. DiMarco, A. M. Casazza, C. Soranzo, and G. Pratesi, *Experientia*, **34**, 1255 (1978); *c*) S. Terashima, S.-s. Jaw, and K. Koga, *Tetrahedron Lett.*, **1978**, 4937; *d*) S.-s. Jaw, S. Terashima, and K. Koga, *Chem. Pharm. Bull.*, **27**, 2351 (1979); *e*) S. Terashima, N. Tanno, and K. Koga, *Tetrahedron Lett.*, **21**, 2753 (1980); *f*) N. Tanno and S. Terashima, *Chem. Pharm. Bull.*, **31**, 811, 821 (1983); *g*) S. Terashima and K. Tamoto, *Tetrahedron Lett.*, **23**, 3715 (1982); *h*) K. Tamoto and S. Terashima, *Chem. Pharm. Bull.*, **32**, 4328 (1984); *i*) A. V. Rama Rao, J. S. Yadav, K. B. Reddy, and A. R. Mehendale, *J. Chem. Soc., Chem. Commun.*, **1983**, 453; *j*) *Idem*, *Tetrahedron*, **40**, 4643 (1984); *k*) K. Tamoto, M. Sugimori, and S. Terashima, *ibid.*, **40**, 4617 (1984); *l*) M. Suzuki, Y. Kimura, and S. Terashima, *Chem. Lett.*, **1985**, 367; *m*) *Idem*, *Bull. Chem. Soc. Jpn.*, **59**, 3559 (1986). For the synthesis of (±)-**9** see: *n*) C. M. Wong, D. Popien, R. Schwenk, and J. Te Raa, *Can J. Chem.*, **49**, 2712 (1971); *o*) C. M. Wong, R. Schwenk, D. Popien, and T.-L. Ho, *ibid.*, **51**, 466 (1973); *p*) T. H. Smith, A. N. Fujuwara, W. W. Lee, H. Y. Wu, and D. W. Henry, *J. Org. Chem.*, **42**, 3653 (1977); *q*) J. R. Wiseman, N. I. French, R. K. Hallmark, and K. G. Chiong, *Tetrahedron Lett.*, **1978**, 3765; *r*) R. J. Blade and P. Hodge, *J. Chem. Soc., Chem. Commun.*, **1979**, 85; *s*) S. Terashima, N. Tanno, and K. Koga, *Tetrahedron Lett.*, **21**, 2749 (1980); *t*) A. V. Rama Rao, V. H. Deshpande, and N. L. Reddy, *ibid.*, **21**, 2661 (1980); *u*) R. J. Ardecky, F. A. J. Kerdesky, and M. P. Cava, *J. Org. Chem.*, **46**, 1483 (1981); *v*) J. W. Lown, S. M. Sondhi, S. B. Sukhendu, and J. Murphy, *ibid.*, **47**, 4304 (1982); *w*) A. V. Rama Rao, V. H. Deshpande, and N. L. Reddy, *Tetrahedron Lett.*, **23**, 4373 (1982); *x*) J. F. Honeck, M. L. Mancini, and B. Belleau, *ibid.*, **24**, 257 (1983); *y*) S. Terashima, *Yuki Gosei Kagaku Kyokai Shi*, **40**, 20 (1982).
5) Preliminary communication; M. Sodeoka T. Iimori, and M. Shibasaki, *Tetrahedron Lett.*, **26**, 6497 (1985).
6) C. A. Grob and W. Jundt, *Helv. Chim. Acta*, **35**, 2111 (1952).
7) *a*) T. Imamoto, Y. Sugiura, and N. Takiyama, *Tetrahedron Lett.*, **25**, 4233 (1984); *b*) M. Suzuki, Y. Kimura, and S. Terashima, *Chem. Lett.*, **1984**, 1543; *c*) *Idem*, *Chem. Pharm. Bull.*, **34**, 1531 (1986).
8) *a*) H. C. Brown and G. Zweifel, *J. Am. Chem. Soc.*, **83**, 3834 (1961); *b*) H. C. Brown, C. G. Scouten, and R. Lotta, *ibid.*, **101**, 96 (1979).
9) T. Hiyama, M. Sawahata, and Y. Kusano, *Chem. Lett.*, **1985**, 611.
10) None of the desired product **17** was obtained by the ozonolysis of **19** owing to the oxidative cleavage of the aromatic ring.
11) Vicinal coupling constants of hydrogens in olefins having substituents such as halogen, alkoxy, and acyloxy groups are known to be smaller than those of alkyl substituted ones. See: P. Clerc and S. Simon, "Tabellen zur Strukturaufklärung Organischer Verbindungen mit Spektroskopischen Methoden," 2nd ed., Springer-Verlag, Berlin, Heidelberg, New York, 1981, p. H205.
12) J. A. Dole, L. D. Dull, and H. S. Mosher, *J. Org. Chem.*, **34**, 2543 (1969).
13) *a*) C. H. Behrens and K. B. Sharpless, *Aldrichimica Acta*, **16**, 67 (1983); *b*) K. B. Sharpless, C. H. Behrens, T. Katsuki, A. W. M. Lee, V. S. Martin, M. Takatani, S. M. Viti, F. J. Walker, and S. S. Woodward, *Pure & Appl. Chem.*, **55**, 589 (1983).
14) All attempts to reduce **10** with $NaBH_4$, $LiBH_4$ or $LiAlH(O\text{-}tert\text{-}Bu)_3$ *via* Payne rearrangement under basic conditions (aqueous NaOH–*tert*-BuOH, aqueous NaOH–DMSO or *tert*-BuOK–*tert*-BuOH) were unsuccessful. At the best, the yield of **27** was 36% ($NaBH_4$ in 0.5 N aqueous NaOH–*tert*-BuOH at reflux temperature).
15) We have accomplished a stereocontrolled synthesis of 3-oxacarbacyclin analogs using the 1,4-hydrogenation of the dienol acetate. See: A. Takahashi and M. Shibasaki, *J. Org. Chem.*, **53**, 1227 (1988).

Synthesis of Some Carbazolequinone Alkaloids and Their Analogues. Facile Palladium-Assisted Intramolecular Ring Closure of Arylamino-1,4-benzoquinones to Carbazole-1,4-quinones

Motoi YOGO, Chihiro ITO, and Hiroshi FURUKAWA*

Faculty of Pharmacy, Meijo University, Tempaku, Nagoya 468, Japan. *Received September 10, 1990*

Carbazolequinone alkaloids, murrayaquinone-A (1a), and pyrayaquinone-A (2) and -B (3), as well as pyrano[3,2-*b*]carbazolequinone 5, an isomer of 2 and 3, were prepared conveniently by the palladium-assisted intramolecular ring closure of the corresponding 2-arylamino-5-methyl-1,4-benzoquinones 9a and 9i—k. A series of their analogues, 6-, 7-, and 8-substituted 3-methylcarbazole-1,4-quinone derivatives 1b—g and 2-methylcarbazolequinones 6a—g corresponding to 1a—g, was also prepared in the same manner. Comparative analysis of the carbon-13 nuclear magnetic resonance spectra was found to provide useful information for the structural assignment of either 2- or 3-methylcarbazolequinones.

Keywords carbazolequinone alkaloid; murrayaquinone-A; pyrayaquinone-A; pyrayaquinone-B; palladium(II) acetate; carbazole-1,4-quinone; arylamino-1,4-benzoquinone; ^{13}C-NMR

The carbazolequinone alkaloids murrayaquinones-A through -D (**1a** and **1h—j**) and pyrayaquinones-A through -C (**2—4**), having a 3-methylcarbazole-1,4-quinone skeleton, are characteristic constituents of *Murraya euchrestifolia* HAYATA (Rutaceae).[1] Among these carbazolequinone alkaloids, murrayaquinone-A (**1a**) has been found to show a cardiotonic activity on guinea-pig papillary muscle.[2] Since their isolation, some synthetic studies of these alkaloids have been reported.[1a,b,3] However, most of these approaches do not allow easy access to various derivatives and thus there is still a need for a general and versatile synthetic procedure.

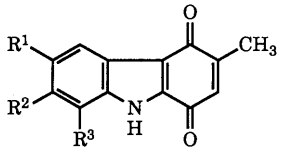

	R^1	R^2	R^3
1a:	H	H	H (murrayaquinone-A)
1b:	CH_3	H	H
1c:	Cl	H	H
1d:	F	H	H
1e:	OCH_3	H	H
1f:	H	OCH_3	H
1g:	H	H	OCH_3
1h:	H	OCH_3	prenyl (murrayaquinone-B)
1i:	H	OCH_3	geranyl (murrayaquinone-C)
1j:	H	OH	geranyl (murrayaquinone-D)

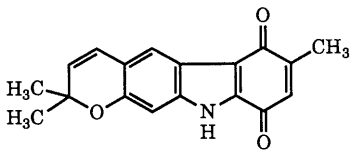

2 (pyrayaquinone-A)

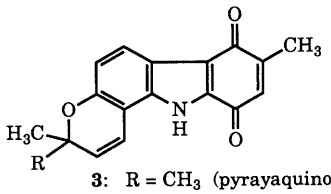

3: R = CH_3 (pyrayaquinone-B)
4: R = $CH_2CH_2CH{=}C(CH_3)_2$ (pyrayaquinone-C)

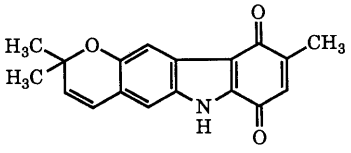

5

Recently, many palladium-assisted reactions have received considerable attention because of their versatile utilities in synthetic methodology.[4] For example, intramolecular cyclization of some diphenylamines by palladium(II) acetate [$Pd(OAc)_2$] is known to produce carbazole derivatives *via* a dehydrogenative coupling process.[5] The palladium-promoted oxidative coupling of 1,4-benzoquinone with aryl and heteroaryl compounds has been reported to give the corresponding aryl- and heteroaryl-1,4-benzoquinone derivatives, respectively.[6]

We have studied the palladium-assisted intramolecular ring closure of arylamino-1,4-benzoquinones as a facile alternative synthetic approach to carbazole-1,4-quinone derivatives. This paper describes the facile synthesis of the carbazolequinone alkaloids, murrayaquinone-A (**1a**), and pyrayaquinone-A (**2**) and -B (**3**), together with their analogues **1b—g**, **5**, and **6a—g**, which are of interest in connection with the biological activities of the parent compounds.[7]

Results and Discussion

Treatment of 2-anilino-5-methyl-1,4-benzoquinone (**9a**),[8,9]

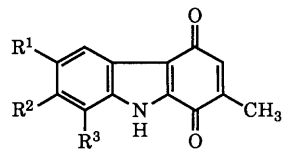

	R^1	R^2	R^3
6a:	H	H	H
6b:	CH_3	H	H
6c:	Cl	H	H
6d:	F	H	H
6e:	OCH_3	H	H
6f:	H	OCH_3	H
6g:	H	H	OCH_3

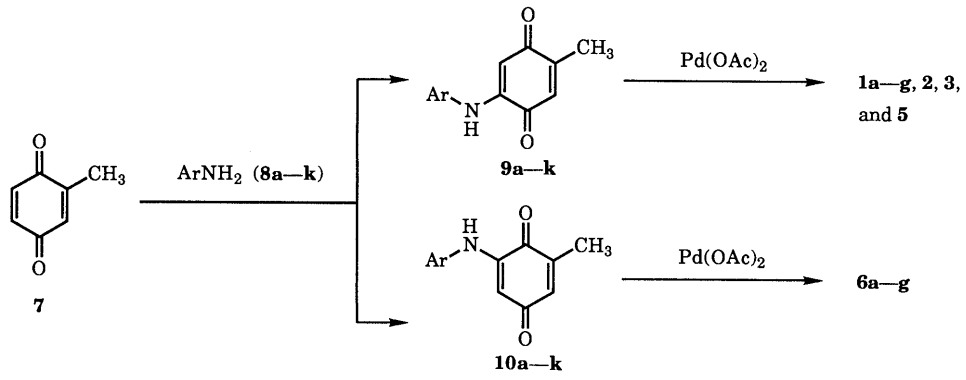

Ar =

	R^1	R^2	R^3
a:	H	H	H
b:	CH_3	H	H
c:	Cl	H	H
d:	F	H	H
e:	OCH_3	H	H
f:	H	OCH_3	H
g:	H	H	OCH_3
h:	OH	H	H

i: Ar =

j: Ar =

k: Ar =

Chart 1

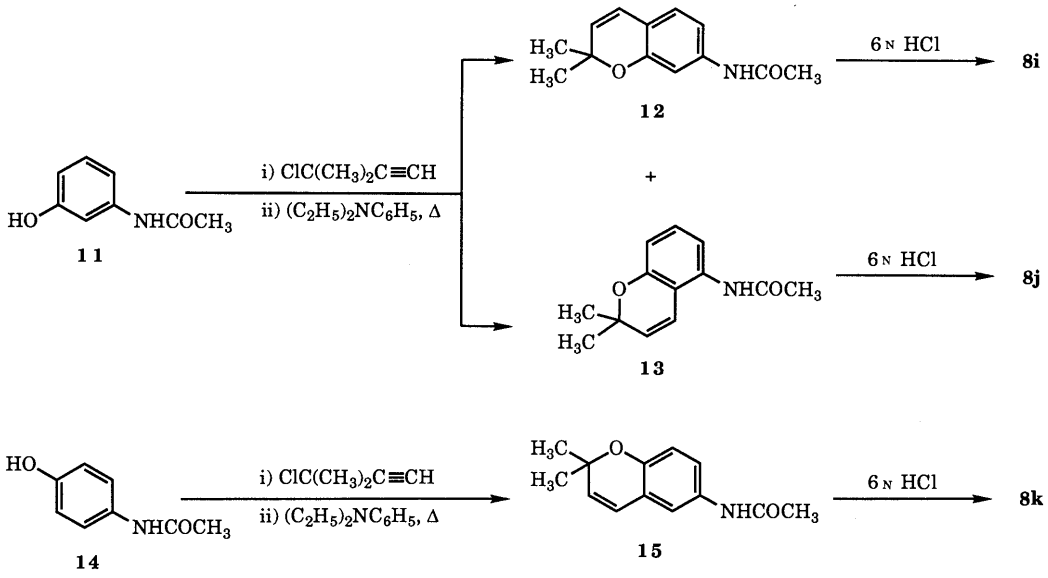

Chart 2

which was obtained together with 2-anilino-6-methyl-1,4-benzoquinone (**10a**) from methyl-1,4-benzoquinone (**7**) and aniline (**8a**),[10] with an equimolar amount of $Pd(OAc)_2$ in acetic acid (AcOH) at reflux temperature for 50 min under an argon atmosphere afforded 3-methylcarbazole-1,4-quinone (**1a**) in 64% yield. This product was found to be identical with natural murrayaquinone-A[1a,b] by spectrometric and co-thin layer chromatographic (TLC) comparisons. This synthetic method was then extended to the synthesis of pyrayaquinone-A (**2**) and -B (**3**).[1c] The starting materials, 7-amino- (**8i**) and 5-amino-2,2-dimethyl-2*H*-chromene (**8j**), were concurrently produced from 3-acetamidophenol (**11**) and 3-chloro-3-methyl-1-butyne[11] *via* etherification and a Claisen rearrangement followed by hydrolysis (Chart 2).[12] Condensation[10] of the aminochromenes **8i** and **8j** with the methylbenzoquinone **7** afforded 2-(2,2-dimethyl-2*H*-chromen-7-ylamino)- (**9i**) and 2-(2,2-dimethyl-2*H*-chromen-5-ylamino)-5-methyl-1,4-benzoquinone (**9j**) together with the corresponding 6-methyl isomers **10i** and **10j**, respectively.[13] Distinction between them was readily accomplished by analysis of the signals due to the substituted methylbenzoquinone moiety in the proton nuclear magnetic resonance (^{1}H-NMR) spectra (see Experimental).[8] Subsequent treatment of the benzoquinones **9i** and **9j** with $Pd(OAc)_2$ in AcOH under reflux for 4 min furnished 2,2,7-trimethyl-2*H*,10*H*-pyrano[2,3-*b*]-carbazole-6,9-quinone (**2**) and 3,3,8-trimethyl-3*H*,11*H*-pyrano[3,2-*a*]carbazole-7,10-quinone (**3**) in 78 and 50% yields, respectively. The pyranocarbazolequinones **2** and **3** were shown to be identical with natural specimens of

pyrayaquinone-A and -B, respectively.[1c] Similarly, the linear pyrano[3,2-*b*]carbazolequinone **5**, which has a regioisomer of pyrayaquinone-A, was prepared from 4-acetamidophenol (**14**) by way of 6-acetamidochromene **15**,[12,14] 6-aminochromene **8k**, and chromenylaminobenzoquinone **9k** as illustrated in Charts 2 and 1. The intramolecular cyclization of **9i** or **9k** gave the pyranocarbazolequinone **2** or **5**, respectively, as the sole isolated product, and no product cyclized in any other direction could be detected.

By means of the palladium-assisted intramolecular cyclization described above, benzenoid-ring-monosubstituted 3-methylcarbazole-1,4-quinone derivatives **1b**—**g** were obtained from 2-(substituted anilino)-5-methyl-1,4-benzoquinones **9b**—**g** in good yields. The cyclization of 6-methylated 2-anilino-1,4-benzoquinones **10a**—**g** with $Pd(OAc)_2$ also proceeded to furnish the corresponding 2-methylcarbazolequinones **6a**—**g** in good yields. In the cyclization of the 2-(3-methoxyanilino)benzoquinone **9f** or **10f**, the 7-methoxycarbazolequinone **1f** or **6f** was isolated as the sole product, respectively. Cyclization was not found to occur in any other direction.

Thus, the palladium-assisted intramolecular cyclization of the 5-methyl- and 6-methyl-2-arylamino-1,4-benzoquinones described here represents a useful synthetic method for 3-methyl- and 2-methylcarbazole-1,4-quinone derivatives. However, the present method can not be applied to the synthesis of the 5-substituted carbazolequinone derivatives in view of the results of the intramolecular cyclization of **9f**, **9i**, **9k**, and **10f** described above. Further, the reaction of anilinobenzoquinones **9h** and **10h** having a free hydroxy group resulted in the formation of a complex mixture, and attempts to isolate carbazolequinone derivatives were unsuccessful. Therefore, the protection of the hydroxy group is requisite for the synthesis of carbazolequinones bearing hydroxy groups.

During our structural elucidation of new carbazolequinones,[1a,b] one of the problems was the assignment of the location of the methyl group (at C-2 or C-3) on the 1,4-quinone moiety. The chemical shift of the olefinic proton at H-3 or H-2 has been reported to be useful as an indicator.[1a,b] In the ^{1}H-NMR spectrum of the 2-methylcarbazolequinone **6a**, the resonance of the olefinic proton (H-3) appeared at lower field than that (H-2) of the corresponding 3-methyl compound **1a** as deduced in a previous report,[1b] though the difference in chemical shift was small ($\Delta\delta_H$ 0.05 ppm). However, the olefinic proton signals of the 2-methyl derivatives **6b**—**e** appeared at rather higher field than those of the corresponding 3-methyl derivatives **1b**—**e**. These facts as well as comparison of the methyl proton resonances of **1a**—**g** with those of **6a**—**g** did not allow conclusive distinction between 2-methyl and 3-methyl derivatives on the basis of the ^{1}H-NMR spectra.

In the present studies of the carbon-13 nuclear magnetic resonance (^{13}C-NMR) spectra, we found that **1a**—**g** showed the allyl methyl carbon signals at δ_C 15.3—15.7, whereas in **6a**—**g** they appeared at slightly higher field, at δ_C 14.8—15.0. Further, the olefinic tertiary carbon (C-2) resonances in **1a**—**g** were observed at δ_C 131.5—131.7, whereas the C-3 signals in **6a**—**g** appeared in the region of δ_C 134.1—134.9. Thus the chemical shift value of the allyl methyl carbon and that of the olefinic tertiary carbon[15] may be used diagnostically for the determination of the location of the allyl methyl group in new carbazolequinone alkaloids.[16]

TABLE I. ^{1}H-NMR Data for the Olefinic Proton, and ^{13}C-NMR Data for the Allyl Methyl and Olefinic Tertiary Carbons of **1a**—**g** and **6a**—**g**[a]

Compd.	^{1}H-NMR δ_H		^{13}C-NMR δ_C		
	H-2	H-3	CH_3	C-2	C-3
1a	6.50		15.7	131.5	
1b	6.58		15.5	131.5	
1c	6.63		15.4	131.5	
1d	6.63		15.4	131.6	
1e	6.58		15.4	131.5	
1f	6.45		15.5	131.6	
1g	6.52		15.3	131.7	
6a		6.55	15.0		134.9
6b		6.53	14.8		134.7
6c		6.54	14.9		134.6
6d		6.53	14.9		134.8
6e		6.48	14.9		134.1
6f		6.51	14.9		134.8
6g		6.55	14.9		134.4

a) Solvents: see Experimental.

Experimental

All melting points were determined on a Yanagimoto hot-stage apparatus and are uncorrected. TLC was performed on Kieselgel 60 F_{254} precoated glass plates (Merck). Low-pressure column chromatography was performed by using 230—400 mesh Silica gel 60 (Nakarai) and a Kiriyama ILC-135-10 low-pressure pump system with typical flow pressure of 3 kg/cm^2. Mass spectra (MS) were recorded on a Hitachi M-52 spectrometer, and high-resolution MS on a Hitachi M-80 spectrometer. Infrared (IR) spectra were taken with a JASCO IR-810 spectrophotometer. ^{1}H-NMR spectra were recorded either on a JEOL JNM-FX-100 (100 MHz) or a JEOL JNM-GX-270 (270 MHz) spectrometer, and ^{13}C-NMR spectra on the former spectrometer operating at 25.00 MHz, with tetramethylsilane as an internal standard. Chemical shifts are quoted in δ (ppm).

Preparation of 2-Anilino-5-methyl-1,4-benzoquinones 9a—h and 2-Anilino-6-methyl-1,4-benzoquinones 10a—h The method of Jacini[10a] and Hanger *et al.*[10b] was used with slight modifications. A mixture of **7** (1780 mg, 14.6 mmol) and water (220 ml) was heated on a water-bath to dissolve **7** as much as possible. After the mixture had cooled to room temperature, a solution of an aniline **8a**—**h** (7.3 mmol) either in a mixture of AcOH (0.5 ml) and water (5 ml) (in the case of **8a**, **8b**, and **8e**—**g**) or in AcOH (17 ml) (in the case of **8c**, **8d**, and **8h**) was added to the resulting suspension, and the whole mixture was stirred at room temperature for 5 h. The reaction mixture was extracted with chloroform, and the extract was washed with water and dried over magnesium sulfate. The solvent was evaporated off under reduced pressure and the resulting residue was chromatographed under low pressure with benzene as an eluent. The earlier fractions yielded the corresponding **9a**—**h**, which were recrystallized from methanol. Compounds **10a**—**h** were isolated from the later fractions with the same solvent and recrystallized from methanol.[13]

2-Anilino-5-methyl-1,4-benzoquinone (**9a**): Yield 60%. Violet sticks, mp 155—157 °C (dec.) [lit.[8] mp 150—151 °C (dec.)]. *Anal.* Calcd for $C_{13}H_{11}NO_2$: C, 73.22; H, 5.20; N, 6.57. Found: C, 73.02; H, 5.16; N, 6.54. MS *m/z*: 213 (M^+). ^{1}H-NMR ($CDCl_3$) δ: 7.50—7.02 (6H, m, Ar-H + NH), 6.56 (1H, q, J = 1.7 Hz, H-6), 6.16 (1H, s, H-3), 2.10 (3H, d, J = 1.7 Hz, 5-CH_3).

2-Anilino-6-methyl-1,4-benzoquinone (**10a**): Yield 31%. Brown needles, mp 154—155 °C [lit.[8] mp 155—156 °C (dec.)]. *Anal.* Calcd for $C_{13}H_{11}NO_2$: C, 73.22; H, 5.20; N, 6.57. Found: C, 73.26; H, 5.10; N, 6.60. MS *m/z*: 213 (M^+). ^{1}H-NMR ($CDCl_3$) δ: 7.50—7.00 (6H, m, Ar-H + NH), 6.51 (1H, dq, J = 2.4, 1.7 Hz, H-5), 6.11 (1H, d, J = 2.4 Hz, H-3), 2.07 (3H, d, J = 1.7 Hz, 6-CH_3).

2-(4-Methylanilino)-5-methyl-1,4-benzoquinone (**9b**): Yield 64%. Violet needles, mp 122—123 °C. *Anal.* Calcd for $C_{14}H_{13}NO_2$: C, 73.99; H, 5.77; N, 6.16. Found: C, 73.89; H, 5.74; N, 6.01. MS *m/z*: 227 (M^+). ^{1}H-NMR ($CDCl_3$) δ: 7.50—6.80 (5H, m, Ar-H + NH), 6.52 (1H, q, J = 1.7 Hz, H-6), 6.07 (1H, s, H-3), 2.32 (3H, s, Ar-CH_3), 2.07 (3H, d, J = 1.7 Hz, 5-CH_3).

2-(4-Methylanilino)-6-methyl-1,4-benzoquinone (**10b**): Yield 30%. Reddish violet needles, mp 127—128 °C. *Anal.* Calcd for $C_{14}H_{13}NO_2$: C, 73.99; H, 5.77; N, 6.16. Found: C, 73.89; H, 5.74; N, 6.01. MS *m/z*: 227 (M^+). ^{1}H-NMR ($CDCl_3$) δ: 7.28—6.98 (5H, m, Ar-H + NH), 6.49 (1H, sextet, J=2.4, 1.7 Hz, H-5), 6.04 (1H, d, J=2.4 Hz, H-3), 2.33 (3H, s, Ar-CH_3), 2.07 (3H, d, J=1.7 Hz, 6-CH_3).

2-(4-Chloroanilino)-5-methyl-1,4-benzoquinone (**9c**): Yield 61%. Brown prisms, mp 157—158 °C. *Anal.* Calcd for $C_{13}H_{10}ClNO_2$: C, 63.04; H, 4.07; N, 5.66. Found: C, 63.06; H, 3.91; N, 5.52. MS *m/z*: 249 (M^+ +2), 247 (M^+). ^{1}H-NMR ($CDCl_3$) δ: 7.42—7.05 (5H, m, Ar-H + NH), 6.56 (1H, q, J=1.7 Hz, H-6), 6.09 (1H, s, H-3), 2.09 (3H, d, J=1.7 Hz, 5-CH_3).

2-(4-Chloroanilino)-6-methyl-1,4-benzoquinone (**10c**): Yield 27%. Violet needles, mp 168—170 °C. *Anal.* Calcd for $C_{13}H_{10}ClNO_2$: C, 63.04; H, 4.07; N, 5.66. Found: C, 62.95; H, 3.86; N, 5.60. MS *m/z*: 249 (M^+ +2), 247 (M^+). ^{1}H-NMR ($CDCl_3$) δ: 7.42—7.00 (5H, m, Ar-H + NH), 6.51 (1H, dq, J=2.4, 1.7 Hz, H-5), 6.05 (1H, d, J=2.4 Hz, H-3), 2.07 (3H, d, J=1.7 Hz, 6-CH_3).

2-(4-Fluoroanilino)-5-methyl-1,4-benzoquinone (**9d**): Yield 57%. Violet needles, mp 176—178 °C. *Anal.* Calcd for $C_{13}H_{10}FNO_2$: C, 67.53; H, 4.36; N, 6.06. Found: C, 67.51; H, 4.35; N, 5.97. MS *m/z*: 231 (M^+). ^{1}H-NMR ($CDCl_3$) δ: 7.22—6.96 (5H, m, Ar-H + NH), 6.55 (1H, q, J=1.7 Hz, H-6), 6.00 (1H, s, H-3), 2.09 (3H, d, J=1.7 Hz, 5-CH_3).

2-(4-Fluoroanilino)-6-methyl-1,4-benzoquinone (**10d**): Yield 29%. Violet prisms, mp 141—143 °C. *Anal.* Calcd for $C_{13}H_{10}FNO_2$: C, 67.53; H, 4.36; N, 6.06. Found: C, 67.57; H, 4.38; N, 6.07. MS *m/z*: 231 (M^+). ^{1}H-NMR ($CDCl_3$) δ: 7.30—6.90 (5H, m, Ar-H + NH), 6.51 (1H, sextet, J=2.4, 1.7 Hz, H-5), 5.95 (1H, d, J=2.4 Hz, H-3), 2.09 (3H, d, J=1.7 Hz, 6-CH_3).

2-(4-Methoxyanilino)-5-methyl-1,4-benzoquinone (**9e**): Yield 64%. Violet needles, mp 137—138 °C. *Anal.* Calcd for $C_{14}H_{13}NO_3$: C, 69.12; H, 5.39; N, 5.76. Found: C, 69.30; H, 5.34; N, 5.51. MS *m/z*: 243 (M^+). ^{1}H-NMR ($CDCl_3$) δ: 7.22—6.78 (5H, m, Ar-H + NH), 6.52 (1H, q, J=1.7 Hz, H-6), 5.96 (1H, s, H-3), 3.80 (3H, s, OCH_3), 2.09 (3H, d, J=1.7 Hz, 5-CH_3).

2-(4-Methoxyanilino)-6-methyl-1,4-benzoquinone (**10e**): Yield 32%. Violet needles, mp 141—143 °C. *Anal.* Calcd for $C_{14}H_{13}NO_3$: C, 69.12; H, 5.39; N, 5.76. Found: C, 69.05; H, 5.36; N, 5.82. MS *m/z*: 243 (M^+). ^{1}H-NMR ($CDCl_3$) δ: 7.22—6.78 (5H, m, Ar-H + NH), 6.48 (1H, sextet, J=2.4, 1.7 Hz, H-5), 5.91 (1H, d, J=2.4 Hz, H-3), 3.80 (3H, s, OCH_3), 2.06 (3H, d, J=1.7 Hz, 6-CH_3).

2-(3-Methoxyanilino)-5-methyl-1,4-benzoquinone (**9f**): Yield 50%. Reddish violet needles, mp 110—112 °C. *Anal.* Calcd for $C_{14}H_{13}NO_3$: C, 69.12; H, 5.39; N, 5.76. Found: C, 69.00; H, 5.32; N, 5.85. MS *m/z*: 243 (M^+). ^{1}H-NMR ($CDCl_3$) δ: 7.38—6.60 (5H, m, Ar-H + NH), 6.55 (1H, q, J=1.7 Hz, H-6), 6.19 (1H, s, H-3), 3.80 (3H, s, OCH_3), 2.09 (3H, d, J=1.7 Hz, 5-CH_3).

2-(3-Methoxyanilino)-6-methyl-1,4-benzoquinone (**10f**): Yield 26%. Violet needles, mp 96—98 °C. *Anal.* Calcd for $C_{14}H_{13}NO_3$: C, 69.12; H, 5.39; N, 5.76. Found: C, 69.21; H, 5.36; N, 5.75. MS *m/z*: 243 (M^+). ^{1}H-NMR ($CDCl_3$) δ: 7.38—6.60 (5H, m, Ar-H + NH), 6.50 (1H, dq, J=2.4, 1.7 Hz, H-5), 6.14 (1H, d, J=2.4 Hz, H-3), 3.80 (3H, s, OCH_3), 2.07 (3H, d, J=1.7 Hz, 6-CH_3).

2-(2-Methoxyanilino)-5-methyl-1,4-benzoquinone (**9g**): Yield 60%. Brown needles, mp 119—121 °C (lit.[10a] mp 138°C). *Anal.* Calcd for $C_{14}H_{13}NO_3$: C, 69.12; H, 5.39; N, 5.76. Found: C, 68.82; H, 5.32; N, 5.71. MS *m/z*: 243 (M^+). ^{1}H-NMR ($CDCl_3$) δ: 7.68 (1H, br s, NH), 7.36—6.84 (4H, m, Ar-H), 6.54 (1H, q, J=1.7 Hz, H-6), 6.21 (1H, s, H-3), 3.87 (3H, s, OCH_3), 2.09 (3H, d, J=1.7 Hz, 5-CH_3).

2-(2-Methoxyanilino)-6-methyl-1,4-benzoquinone (**10g**): Yield 31%. Violet sticks, mp 171—172 °C. *Anal.* Calcd for $C_{14}H_{13}NO_3$: C, 69.12; H, 5.39; N, 5.76. Found: C, 69.04; H, 5.31; N, 5.75. MS *m/z*: 243 (M^+). ^{1}H-NMR ($CDCl_3$) δ: 7.68 (1H, br s, NH), 7.34—6.83 (4H, m, Ar-H), 6.49 (1H, dq, J=2.4, 1.7 Hz, H-5), 6.16 (1H, d, J=2.4 Hz, H-3), 3.87 (3H, s, OCH_3), 2.07 (3H, d, J=1.7 Hz, 6-CH_3).

2-(4-Hydroxyanilino)-5-methyl-1,4-benzoquinone (**9h**): Yield 45%. Violet sticks, mp 146—148 °C. *Anal.* Calcd for $C_{13}H_{11}NO_3$: C, 68.11; H, 4.84; N, 6.11. Found: C, 68.19; H, 4.76; N, 6.03. MS *m/z*: 229 (M^+). ^{1}H-NMR (acetone-d_6) δ: 8.50 (1H, br s, OH or NH), 7.87 (1H, br s, NH or OH), 7.28—6.82 (4H, m, Ar-H), 6.57 (1H, q, J=1.7 Hz, H-6), 5.78 (1H, s, H-3), 2.01 (3H, d, J=1.7 Hz, 5-CH_3).

2-(4-Hydroxyanilino)-6-methyl-1,4-benzoquinone (**10h**): Yield 19%. Violet prisms, mp 210—212°C. *Anal.* Calcd for $C_{13}H_{11}NO_3$: C, 68.11; H, 4.84; N, 6.11. Found: C, 67.86; H, 4.79; N, 5.98. MS *m/z*: 229 (M^+). ^{1}H-NMR (DMSO-d_6) δ: 9.46 (1H, br s, OH or NH), 8.70 (1H, br s, NH or OH), 7.22—6.60 (4H, m, Ar-H), 6.49 (1H, br s, H-5), 5.57 (1H, d, J=2.4 Hz, H-3), 1.96 (3H, d, J=1.7 Hz, 6-CH_3).

Exclusive Preparation of 9a Method A: A mixture of 2-bromo-6-methyl-1,4-benzoquinone (**16**)[17] (800 mg, 4.0 mmol) and water (110 ml) was heated on a water-bath to dissolve **16** as much as possible. After the mixture had cooled to room temperature, a solution of **8a** (190 mg, 2.0 mmol) in a mixture of AcOH (0.5 ml) and water (5 ml) was added to the resulting suspension, and the whole mixture was stirred at room temperature for 16 h, then extracted with chloroform. The extract was washed with water and dried over magnesium sulfate. The solvent was evaporated off under reduced pressure and the resulting residue was chromatographed under low pressure. Elution with benzene followed by recrystallization from methanol gave 2-anilino-3-bromo-5-methyl-1,4-benzoquinone (**17**) (540 mg, 90%) as dark red flakes, mp 121—123 °C (dec.). *Anal.* Calcd for $C_{13}H_{10}BrNO_2 \cdot 1/10\ H_2O$: C, 53.12; H, 3.49; N, 4.77. Found: C, 52.89; H, 3.26; N, 4.47. MS *m/z*: 293 (M^+ +2), 291 (M^+). ^{1}H-NMR ($CDCl_3$) δ: 7.42—6.99 (6H, m, Ar-H + NH), 6.58 (1H, q, J=1.5 Hz, H-6), 2.15 (3H, d, J=1.5 Hz, CH_3).

A mixture of **17** (150 mg, 0.51 mmol) and methanol (30 ml) was hydrogenated catalytically in the presence of 10% palladium on charcoal (15 mg) at room temperature and 4 kg/cm^2 pressure for 1 h. The catalyst was filtered off and washed with a small amount of methanol. Powdered sodium hydrogencarbonate (80 mg) was added to the combined filtrate and washings, and the mixture was stirred at room temperature in a vessel open to the air for 2 h. The reaction mixture was diluted with water and extracted with chloroform. The extract was washed with water and dried over magnesium sulfate, and the solvent was evaporated off under reduced pressure. The resulting residue was purified by column chromatography under low pressure with benzene followed by recrystallization from methanol to give **9a** (70 mg, 64%).

Method B: A solution of butyllithium in hexane (4 mmol) was added dropwise to a stirred solution of **8a** (370 mg, 4 mmol) in anhydrous tetrahydrofuran (10 ml) at −78 °C under a nitrogen atmosphere. The mixture was stirred at the same temperature for 1 h and at room temperature for 1 h, then 4,4-dimethoxy-2-methylcyclohexa-2,5-dienone (**18**)[18] (500 mg, 4 mmol) was added to the mixture at −78 °C. The mixture

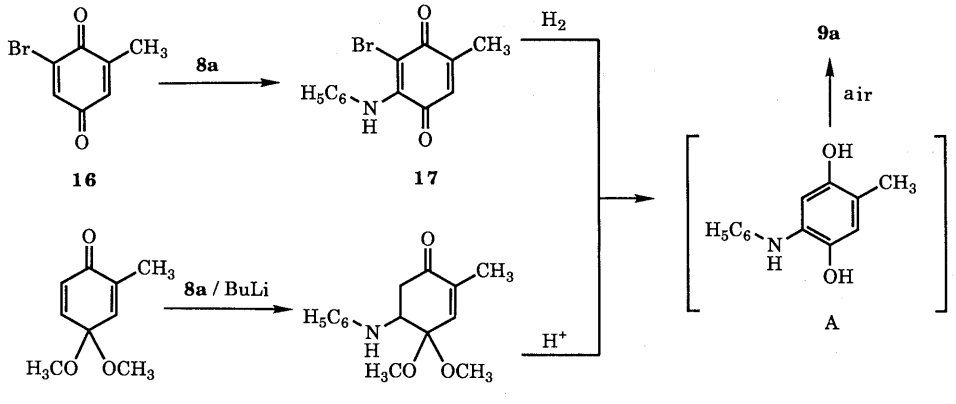

Chart 3

was stirred at the same temperature for 1 h, then at room temperature for 1 h. The reaction mixture was poured into water and extracted with dichloromethane. The extract was washed with water and dried over magnesium sulfate. Evaporation of the solvent gave the crude 5-anilino-4,4-dimethoxy-2-methylcyclohex-2-enone (**19**), which was purified by column chromatography with benzene followed by recrystallization from hexane to give pale yellow prisms (320 mg, 37%), mp 96—98 °C. *Anal.* Calcd for $C_{15}H_{19}NO_3$: C, 68.94; H, 7.33; N, 5.36. Found: C, 68.87; H, 7.36; N, 5.32. MS *m/z*: 261 (M^+). ^{1}H-NMR ($CDCl_3$) δ: 7.24—7.07 (2H, m, Ar-H), 6.77—6.50 (4H, m, Ar-H+H-3),[19] 4.04 (2H, br, NH+H-5),[20] 3.32 and 3.21 (each 3H, each s, $OCH_3 \times 2$), 2.84 (2H, br d, J=3.9 Hz, changed to sharp d on addition of D_2O, 6-CH_2), 1.86 (3H, d, J=1.5 Hz, CH_3).

A mixture of **19** (100 mg, 0.38 mmol), methanol (5 ml), water (5 ml), and AcOH (0.5 ml) was refluxed for 4 h, and then stirred at room temperature in a vessel open to the air for 27 h. The mixture was extracted with chloroform. The extract was washed with water and dried over magnesium sulfate. The solvent was evaporated off under reduced pressure and the resulting residue was purified by column chromatography under low pressure with benzene followed by recrystallization from methanol to give **9a** (70 mg, 82%).

In this procedure, the low isolation yield of **19** was ascribable to its instability toward chromatographic purification on silica gel. When the crude **19** was subjected to hydrolysis and subsequent aerial oxidation without purification, **9a** was obtained in 80% overall yield from **18**.

3-Methylcarbazole-1,4-quinones 1a—g A mixture of **9a—g** (0.5 mmol) and $Pd(OAc)_2$ (110 mg, 0.5 mmol) in AcOH (10 ml) was refluxed for 50 min under an argon atmosphere. The insoluble matter was filtered off and washed with acetone. The combined filtrate and washings were evaporated to dryness under reduced pressure, and the residue was chromatographed under low pressure with hexane–ethyl acetate (4 : 1, v/v) and recrystallized from acetone to give the corresponding **1a—g**. Compound **1a** was found to be identical (IR, ^{1}H- and ^{13}C-NMR, MS, and co-TLC) with natural murrayaquinone-A.[1a,b]

3-Methylcarbazole-1,4-quinone (murrayaquinone-A) (**1a**): Yield 64%. Red needles, mp 237—239 °C (dec.) [lit.[1a,b] mp 246—247 °C; lit.[3a,b] mp 240—241 °C; lit[3c] mp 241 °C (dec.)]. *Anal.* Calcd for $C_{13}H_9NO_2$: C, 73.92; H, 4.30; N, 6.63. Found: C, 73.95; H, 4.08; N, 6.32. IR ν_{max}^{KBr} cm^{-1}: 3220, 1665, 1640, 1605. MS *m/z*: 211 (M^+), 183, 168, 155, 154, 143, 115. ^{1}H-NMR ($CDCl_3$) δ: 9.02 (1H, br s, NH), 8.22 (1H, dt, J=5.0, 1.0 Hz, H-5), 7.60—7.30 (3H, m, H-6, -7, and -8), 6.50 (1H, q, J= 1.5 Hz, H-2), 2.18 (3H, d, J=1.5 Hz, 3-CH_3). ^{13}C-NMR ($CDCl_3$+DMSO-d_6) δ: 183.1 (s), 180.0 (s), 148.0 (s), 137.5 (s), 135.8 (s), 131.5 (d, C-2), 126.1 (d), 123.6 (s), 123.6 (d), 121.7 (d), 115.7 (s), 113.7 (d), 15.7 (q, 3-CH_3).

3,6-Dimethylcarbazole-1,4-quinone (**1b**): Yield 79%. Red needles, mp 228—230 °C (dec.). *Anal.* Calcd for $C_{14}H_{11}NO_2$: C, 74.65; H, 4.92; N, 6.22. Found: C, 74.47; H, 4.78; N, 5.88. MS *m/z*: 225 (M^+). ^{1}H-NMR (DMSO-d_6) δ: 12.67 (1H, br s, NH), 7.83 (1H, dd, J=1.5, 0.5 Hz, H-5), 7.43 (1H, d, J=8.5 Hz, H-8), 7.19 (1H, dd, J=8.5, 1.5 Hz, H-7), 6.58 (1H, q, J=1.7 Hz, H-2), 2.42 (3H, s, 6-CH_3), 2.06 (3H, d, J=1.7 Hz, 3-CH_3). ^{13}C-NMR (DMSO-d_6) δ: 182.8 (s), 179.8 (s), 147.8 (s), 135.8 (s), 133.0 (s), 131.5 (d, C-2), 127.9 (d), 123.9 (s), 120.9 (d), 114.9 (s), 113.4 (d), 21.2 (q), 15.5 (q, 3-CH_3).

6-Chloro-3-methylcarbazole-1,4-quinone (**1c**): Yield 46%. Orange needles, mp 253—254 °C (dec.). *Anal.* Calcd for $C_{13}H_8ClNO_2$: C, 63.56; H, 3.28; N, 5.70. Found: C, 63.55; H, 3.09; N, 5.60. MS *m/z*: 247 (M^+ +2), 245 (M^+). ^{1}N-NMR (DMSO-d_6) δ: 12.96 (1H, br s, NH), 7.97 (1H, dd, J=2.0, 0.7 Hz, H-5), 7.56 (1H, dd, J=8.8, 0.7 Hz, H-8), 7.38 (1H, dd, J=8.8, 2.0 Hz, H-7), 6.63 (1H, q, J=1.7 Hz, H-2), 2.07 (3H, d, J=1.7 Hz, 3-CH_3). ^{13}C-NMR (DMSO-d_6) δ: 182.2 (s), 179.5 (s), 147.7 (s), 136.5 (s), 135.7 (s), 131.5 (d, C-2), 128.2 (s), 126.1 (d), 124.1 (s), 120.3 (d), 115.3 (d), 114.5 (s), 15.4 (q, 3-CH_3).

6-Fluoro-3-methylcarbazole-1,4-quinone (**1d**): Yield 83%. Orange needles, mp 235—236 °C (dec.). *Anal.* Calcd for $C_{13}H_8FNO_2$: C, 68.12; H, 3.52; N, 6.11. Found: C, 67.91; H, 3.31; N, 5.97 . MS *m/z*: 229 (M^+). ^{1}H-NMR (DMSO-d_6) δ: 12.94 (1H, br s, NH), 7.67 (1H, ddd, J=9.3, 2.5, 0.5 Hz, H-5), 7.55 (1H, ddd, J=9.3, 4.6, 0.5 Hz, H-8), 7.24 (1H, td, J=9.3, 2.5 Hz, H-7), 6.63 (1H, q, J=1.7 Hz, H-2), 2.07 (3 H, d, J=1.7 Hz, 3-CH_3). ^{13}C-NMR (DMSO-d_6) δ: 182.4 (s), 179.5 (s), 164.1 and 154.6 (each s, fluorine-coupled carbon), 147.9 (s), 137.0 (s), 134.0 (s), 131.6 (d, C-2), 124.0 and 123.6 (each s, fluorine-coupled carbon), 115.5 and 115.2 (each d, fluorine-coupled carbon), 115.4 (s), 115.4 and 114.4 (each d, fluorine-coupled carbon), 106.3 and 105.3 (each d, fluorine-coupled carbon), 15.4 (q, 3-CH_3).

6-Methoxy-3-methylcarbazole-1,4-quinone (**1e**): Yield 52%. Red needles, mp 249—250 °C (dec.). *Anal.* Calcd for $C_{14}H_{11}NO_3$: C, 69.70; H, 4.59; N, 5.80. Found: C, 69.78; H, 4.43; N, 5.49. MS *m/z*: 241 (M^+). ^{1}H-NMR (DMSO-d_6) δ: 12.70 (1H, br s, NH), 7.44 (1H, d, J=2.5 Hz, H-5), 7.42 (1H, d, J=9.0 Hz, H-8), 7.00 (1H, dd, J=9.0, 2.5 Hz, H-7), 6.58 (1H, q, J=1.7 Hz, H-2), 3.81 (3H, s, 6-OCH_3), 2.06 (3H, d, J=1.7 Hz, 3-CH_3). ^{13}C-NMR (DMSO-d_6) δ: 183.1 (s), 179.3 (s), 158.7 (s), 147.0 (s), 138.8 (s), 134.8 (s), 131.5 (d, C-2), 122.3 (d), 117.7 (s), 115.8 (s), 114.9 (d), 95.0 (d), 55.2 (q), 15.4 (q, 3-CH_3).

7-Methoxy-3-methylcarbazole-1,4-quinone (**1f**): Yield 65%. Brown needles, mp 236—238 °C (dec.) [lit.[3a,b] mp 240 °C (dec.)]. *Anal.* Calcd for $C_{14}H_{11}NO_3 \cdot 1/10\ H_2O$: C, 69.18; H, 4.64; N, 5.76. Found: C, 69.13; H, 4.41; N, 5.79. High-resolution MS *m/z*: Calcd for $C_{14}H_{11}NO_3$: 241.0737. Found: 241.0730. ^{1}H-NMR ($CDCl_3$) δ: 8.90 (1H, br s, NH), 8.07 (1H, d, J=9.0 Hz, H-5), 6.98 (1H, dd, J=9.0, 2.2 Hz, H-6), 6.84 (1H, d, J=2.2 Hz, H-8), 6.45 (1H, q, J=1.7 Hz, H-2), 3.87 (3H, s, 7-OCH_3), 2.15 (3H, d, J=1.7 Hz, 3-CH_3). ^{13}C-NMR (DMSO-d_6) δ: 182.8 (s), 179.6 (s), 156.8 (s), 147.8 (s), 135.7 (s), 132.6 (s), 131.6 (d, C-2), 124.5 (s), 117.4 (d), 115.1 (s), 114.8 (d), 101.6 (d), 55.3 (q), 15.5 (q, 3-CH_3).

8-Methoxy-3-methylcarbazole-1,4-quinone (**1g**): Yield 55%. Dark red prisms, mp 220—221 °C (dec.). *Anal.* Calcd for $C_{14}H_{11}NO_3$: C, 69.70; H, 4.59; N, 5.80. Found: C, 69.49; H, 4.39; N, 5.84. MS *m/z*: 241 (M^+). ^{1}H-NMR (DMSO-d_6) δ: 12.97 (1H, br s, NH), 7.56 (1H, dd, J=8.1, 0.7 Hz, H-5), 7.18 (1H, t, J=8.1 Hz, H-6), 6.86 (1H, dd, J=8.1, 0.7 Hz, H-7), 6.52 (1H, q, J=1.5 Hz, H-2), 3.92 (3H, s, 8-OCH_3), 2.03 (3H, d, J=1.5 Hz, 3-CH_3). ^{13}C-NMR (DMSO-d_6) δ: 183.0 (s), 179.5 (s), 147.4 (s), 135.6 (s), 131.7 (d, C-2), 128.2 (s), 125.0 (s), 124.7 (d), 115.8 (s), 113.5 (d), 106.0 (d), 55.5 (q), 15.3 (q, 3-CH_3).

7-Acetamido-(12) and 5-Acetamido-2,2-dimethyl-2*H*-chromene (13) Potassium carbonate (600 mg, 4.4 mmol), potassium iodide (150 mg, 0.9 mmol), and water (2 drops) were added successively to a solution of **11** (1000 mg, 6.6 mmol) in acetone (15 ml), followed by addition of 3-chloro-3-methyl-1-butyne[11] (740 mg, 7.2 mmol). The mixture was refluxed with stirring for 2 d under a nitrogen atmosphere. More 3-chloro-3-methyl-1-butyne (740 mg, 7.2 mmol) in acetone (1 ml) was introduced and the refluxing was continued for a further 2d. Insoluble matter was filtered off and washed with acetone. The combined filtrate and washings were evaporated to dryness under reduced pressure. The residue was taken up in ether, washed successively with 3% aqueous sodium hydroxide and water, then dried over anhydrous potassium carbonate. Evaporation of the solvent gave the crude 1,1-dimethylpropargyl ether of **11** (870 mg) as an oil. The propargyl ether was dissolved in *N,N*-diethylaniline[21] (5 ml) and the mixture was refluxed for 2 h. After addition of ether, the mixture was washed successively with cold dilute hydrochloric acid and water, and dried over anhydrous potassium carbonate. The solvent was evaporated off and the resulting residue was chromatographed under low pressure with hexane–ethyl acetate (2 : 1, v/v) as an eluent. The earlier fractions yielded **12** (150 mg, 10%) as a viscous oil (lit.[22] mp 80—81 °C). High-resolution MS *m/z*: Calcd for $C_{13}H_{15}NO_2$: 217.1102. Found: 217.1120. ^{1}H-NMR ($CDCl_3$) δ: 7.98 (1H, br s, NH), 7.00 (1H, d, J=1.5 Hz, H-8), 6.88 (1H, dd, J=8.0, 1.5 Hz, H-6), 6.82 (1H, d, J=8.0 Hz, H-5), 6.23 (1H, d, J=10.0 Hz, H-4), 5.48 (1H, d, J=10.0 Hz, H-3), 2.09 (3H, s, $COCH_3$), 1.37 (6H, s, $CH_3 \times 2$).

Compound **13** was isolated from the later fractions with the same solvent and recrystallized from benzene–hexane to give colorless flakes (120 mg, 8%), mp 138—140 °C. *Anal.* Calcd for $C_{13}H_{15}NO_2 \cdot 1/10H_2O$: C, 71.27; H, 6.99; N, 6.39. Found: C, 71.40; H, 7.04; N, 6.45. High-resolution MS *m/z*: Calcd for $C_{13}H_{15}NO_2$: 217.1102. Found: 217.1110. ^{1}H-NMR (270 MHz, $CDCl_3$) δ: 7.14 (1H, d, J=8.0 Hz, H-6), 7.08 (1H, br s, NH), 7.09 (1H, t, J=8.0 Hz, H-7), 6.67 (1H, d, J=8.0 Hz, H-8), 6.35 (1H, d, J=9.7 Hz, H-4), 5.68 (1H, d, J=9.7 Hz, H-3), 2.18 (3H, s, $COCH_3$), 1.43 (6H, s, $CH_3 \times 2$).

6-Acetamido-2,2-dimethyl-2*H*-chromene (15) Procedures similar to those mentioned above for **12** and **13** starting from **14** (1000 mg, 6.6 mmol), followed by recrystallization from benzene–hexane, gave **15** (420 mg, 29%) as colorless flakes, mp 117—119 °C (lit.[14] mp 126—126.8 °C). *Anal.* Calcd for $C_{13}H_{15}NO_2$: C, 71.86; H, 6.96; N, 6.45. Found: C, 71.82; H, 6.91; N, 6.39. MS *m/z*: 217 (M^+). ^{1}H-NMR ($CDCl_3$) δ: 7.61 (1H, br s, NH), 7.22 (1H, d, J=2.4 Hz, H-5), 7.03 (1H, dd, J=8.5, 2.4 Hz, H-7), 6.67 (1H, d, J=8.5 Hz, H-8), 6.23 (1H, d, J=9.8 Hz, H-4), 5.59 (1H, d, J=9.8 Hz, H-3), 2.10 (3H, s, $COCH_3$), 1.39 (6H, s, $CH_3 \times 2$).

7-Amino- (8i), 5-Amino- (8j), and 6-Amino-2,2-dimethyl-2*H*-chromene (8k) A mixture of an acetamidochromene **12**, **13**, or **15** (110 mg, 0.5 mmol), 6 N hydrochloric acid (5 ml), and ethanol (5 ml) was refluxed for 2 h. After evaporation of the solvent, water was added to the residue, and the mixture was washed with ether. The aqueous solution was basified

with an aqueous ammonia solution and extracted with chloroform. The extract was dried over anhydrous potassium carbonate. In the case of the hydrolysis of **12**, evaporation of the extract under reduced pressure gave a viscous oil, which was subjected to silica gel column chromatography with benzene as an eluent to give **8i** (49%) as colorless crystals, mp 35—36 °C. High-resolution MS *m/z*: Calcd for $C_{11}H_{13}NO$: 175.0997. Found: 175.1008. ^{1}H-NMR ($CDCl_3$) δ: 6.74 (1H, d, J=8.0 Hz, H-5), 6.22 (1H, d, J=10.0 Hz, H-4), 6.14 (1H, dd, J=8.0, 1.5 Hz, H-6), 6.10 (1H, d, J=1.5 Hz, H-8), 5.38 (1H, d, J=10.0 Hz, H-3), 3.42 (2H, br s, NH_2), 1.38 (6H, s, $CH_3 \times 2$).

In the case of the hydrolysis of **13** or **15**, evaporation of the extract under reduced pressure gave **8j** or **8k** as a viscous oil, which was used in the subsequent step without further purification.

8j: Yield 99%. High-resolution MS *m/z*: Calcd for $C_{11}H_{13}NO$: 175.0997. Found: 175.1008. ^{1}H-NMR ($CDCl_3$) δ: 6.88 (1H, t, J=8.0 Hz, H-7), 6.33 (1H, d, J=10.0 Hz, H-4), 6.24 (1H, dt, J=8.0, 1.5 Hz, H-8), 6.20 (1H, dd, J=8.0, 1.5 Hz, H-6), 5.56 (1H, d, J=10.0 Hz, H-3), 3.60 (2H, br s, NH_2), 1.38 (6H, s, $CH_3 \times 2$).

8k[23]: Yield 97%. High-resolution MS *m/z*: Calcd for $C_{11}H_{13}NO$: 175.0997. Found: 175.0997. ^{1}H-NMR ($CDCl_3$) δ: 6.61 (1H, d, J=8.3 Hz, H-8), 6.44 (1H, dd, J=8.3, 2.7 Hz, H-7), 6.35 (1H, d, J=2.7 Hz, H-5), 6.21 (1H, d, J=9.8 Hz, H-4), 5.59 (1H, d, J=9.8 Hz, H-3), 3.10 (2H, br s, NH_2), 1.38 (6H, s, $CH_3 \times 2$).

Condensation of the 7-Amino-, 5-Amino-, and 6-Aminochromenes 8i, 8j, and 8k with Methyl-1,4-benzoquinone (7) A mixture of **7** (250 mg, 2 mmol) and water (50 ml) was heated on a water-bath to dissolve **7** as much as possible. After the mixture had cooled to room temperature, a mixture of an aminochromene **8i**, **8j**, or **8k** (180 mg, 1 mmol), AcOH (2 ml), and water (2 ml) was added to the resulting suspension, and the whole mixture was stirred at room temperature for 5 h, then extracted with ethyl acetate. The same work-up as described for the preparation of **9a—h** and **10a—h** gave the corresponding 2-chromenylamino-5-methylbenzoquinones **9i**, **9j**, and **9k** together with the 6-methyl isomers **10i**, **10j**, and **10k**.

2-(2,2-Dimethyl-2*H*-chromen-7-ylamino)-5-methyl-1,4-benzoquinone (**9i**): Yield 14%. Violet prisms from methanol, mp 134—135 °C. *Anal.* Calcd for $C_{18}H_{17}NO_3$: C, 73.20; H, 5.80; N, 4.74. Found: C, 73.31; H, 5.80; N, 4.31. MS *m/z*: 295 (M^+). ^{1}H-NMR ($CDCl_3$) δ: 7.22 (1H, br s, NH), 6.89 (1H, d, J=8.5 Hz, H-5′), 6.66 (1H, d, J=2.2 Hz, H-8′), 6.64 (1H, dd, J=8.5, 2.2 Hz, H-6′), 6.54 (1H, q, J=1.5 Hz, H-6), 6.27 (1H, d, J=9.8 Hz, H-4′), 6.24 (1H, s, H-3), 5.57 (1H, d, J=9.8 Hz, H-3′), 2.10 (3H, d, J=1.5 Hz, 5-CH_3), 1.43 (6H, s, 2′-$CH_3 \times 2$).

2-(2,2-Dimethyl-2*H*-chromen-7-ylamino)-6-methyl-1,4-benzoquinone (**10i**): Yield 12%. Violet prisms from hexane, mp 110—111 °C. *Anal.* Calcd for $C_{18}H_{17}NO_3$: C, 73.20; H, 5.80; N, 4.74. Found: C, 72.87; H, 5.76; N, 4.62. MS *m/z*: 295 (M^+). ^{1}H-NMR ($CDCl_3$) δ: 7.24 (1H, br s, NH), 6.95 (1H, d, J=8.5 Hz, H-5′), 6.64 (1H, d, J=2.2 Hz, H-8′), 6.63 (1H, dd, J=8.5, 2.2 Hz, H-6′), 6.50 (1H, sextet, J=2.5, 1.5 Hz, H-5), 6.28 (1H, d, J=9.8 Hz, H-4′), 6.18 (1H, d, J=2.5 Hz, H-3), 5.58 (1H, d, J=9.8 Hz, H-3′), 2.08 (3H, d, J=1.5 Hz, 6-CH_3), 1.42 (6H, s, 2′-$CH_3 \times 2$).

2-(2,2-Dimethyl-2*H*-chromen-5-ylamino)-5-methyl-1,4-benzoquinone (**9j**): Yield 18%. Reddish violet prisms from hexane, mp 114—116 °C. *Anal.* Calcd for $C_{18}H_{17}NO_3$: C, 73.20; H, 5.80; N, 4.74. Found: C, 73.22; H, 5.86; N, 4.36. MS *m/z*: 295 (M^+). ^{1}H-NMR ($CDCl_3$) δ: 7.11 (1H, t, J=8.0 Hz, H-7′), 7.00 (1H, br s, NH), 6.74 and 6.70 (each 1H, each br d, J=8.0 Hz, H-6′ and -8′), 6.55 (1H, q, J=1.5 Hz, H-6), 6.30 (1H, d, J=10.0 Hz, H-4′), 5.72 (1H, s, H-3), 5.67 (1H, d, J=10.0 Hz, H-3′), 2.08 (3H, d, J=1.5 Hz, 5-CH_3), 1.42 (6H, s, 2′-$CH_3 \times 2$).

2-(2,2-Dimethyl-2*H*-chromen-5-ylamino)-6-methyl-1,4-benzoquinone (**10j**): Yield 11%. Reddish violet prisms from methanol, mp 198—200 °C. *Anal.* Calcd for $C_{18}H_{17}NO_3$: C, 73.20; H, 5.80; N, 4.74. Found: C, 73.09; H, 5.72; N, 4.48. MS *m/z*: 295 (M^+). ^{1}H-NMR ($CDCl_3$) δ: 7.11 (1H, t, J=7.8 Hz, H-7′), 7.00 (1H, br s, NH), 6.72 and 6.70 (each 1H, each br d, J=7.8 Hz, H-6′ and -8′), 6.48 (1H, sextet, J=2.5, 1.5 Hz, H-5), 6.30 (1H, d, J=10.0 Hz, H-4′), 5.68 (1H, d, J=2.5 Hz, H-3), 5.67 (1H, d, J=10.0 Hz, H-3′), 2.08 (3H, d, J=1.5 Hz, 6-CH_3), 1.43 (6H, s, 2′-$CH_3 \times 2$).

2-(2,2-Dimethyl-2*H*-chromen-6-ylamino)-5-methyl-1,4-benzoquinone (**9k**): Yield 53%. Violet prisms from methanol, mp 148—150 °C. *Anal.* Calcd for $C_{18}H_{17}NO_3$: C, 73.20; H, 5.80; N, 4.74. Found: C, 73.50; H, 5.77; N, 4.69. MS *m/z*: 295 (M^+). ^{1}H-NMR ($CDCl_3$) δ: 7.08 (1H, br s, NH), 6.92 (1H, dd, J=8.3, 2.7 Hz, H-7′), 6.82 (1H, d, J=2.7 Hz, H-5′), 6.75 (1H, d, J=8.3 Hz, H-8′), 6.52 (1H, q, J=1.7 Hz, H-6), 6.26 (1H, d, J=9.8 Hz, H-4′), 5.98 (1H, s, H-3), 5.66 (1H, d, J=9.8 Hz, H-3′), 2.08 (3H, d, J=1.7 Hz, 5-CH_3), 1.44 (6H, s, 2′-$CH_3 \times 2$).

2-(2,2-Dimethyl-2*H*-chromen-6-ylamino)-6-methyl-1,4-benzoquinone (**10k**): Yield 31%. Violet needles from methanol, mp 117—118 °C. *Anal.* Calcd for $C_{18}H_{17}NO_3$: C, 73.20; H, 5.80; N, 4.74. Found: C, 73.19; H, 5.72; N, 4.65. MS *m/z*: 295 (M^+). ^{1}H-NMR ($CDCl_3$) δ: 7.09 (1H, br s, NH), 6.90 (1H, dd, J=8.3, 2.7 Hz, H-7′), 6.82 (1H, d, J=2.7 Hz, H-5′), 6.75 (1H, d, J=8.3 Hz, H-8′), 6.49 (1H, sextet, J=2.5, 1.5 Hz, H-5), 6.26 (1H, d, J=9.8 Hz, H-4′), 5.93 (1H, d, J=2.5 Hz, H-3), 5.65 (1H, d, J=9.8 Hz, H-3′), 2.06 (3H, d, J=1.5 Hz, 6-CH_3), 1.44 (6H, s, 2′-$CH_3 \times 2$).

Pyranocarbazolequinones 2, 3, and 5 A mixture of a chromenylaminobenzoquinone **9i**, **9j**, or **9k** (12 mg, 0.04 mmol) and $Pd(OAc)_2$ (9 mg, 0.04 mmol) in AcOH (5 ml) was refluxed for 4 min under an argon atmosphere. The same work-up as described above for **1a—g** afforded the corresponding **2**, **3**, and **5**. Compounds **2** and **3** were shown to be identical (IR, ^{1}H-NMR, MS, and co-TLC) with natural pyrayaquinone-A and -B,[1c] respectively.

2,2,7-Trimethyl-2*H*,10*H*-pyrano[2,3-*b*]carbazole-6,9-quinone (pyrayaquinone-A) (**2**): Yield 78%. Brown crystals, mp 228 °C (dec.) [lit.[1c] mp 222 °C (dec.); lit.[3a] mp 220—222 °C]. High-resolution MS *m/z*: Calcd for $C_{18}H_{15}NO_3$: 293.1051. Found: 293.1052. IR $\nu_{max}^{CHCl_3}$ cm^{-1}: 1660, 1645, 1630, 1605. MS *m/z*: 293 (M^+), 279, 278, 250, 236, 222, 210. ^{1}H-NMR ($CDCl_3$) δ: 8.98 (1H, br s, NH), 7.79 (1H, s, H-5), 6.81 (1H, s, H-11), 6.48 (1H, d, J=10.0 Hz, H-4), 6.46 (1H, q, J=1.5 Hz, H-8), 5.72 (1H, d, J=10.0 Hz, H-3), 2.16 (3H, d, J=1.5 Hz, 7-CH_3), 1.48 (6H, s, 2-$CH_3 \times 2$).

3,3,8-Trimethyl-3*H*,11*H*-pyrano[3,2-*a*]carbazole-7,10-quinone (pyrayaquinone-B) (**3**): Yield 50%. Brown crystals, mp 248 °C (dec.) [lit.[1c] mp 244 °C (dec.); lit.[3a,b] mp 242 °C]. High-resolution MS *m/z*: Calcd for $C_{18}H_{15}NO_3$: 293.1051. Found: 293.1052. IR $\nu_{max}^{CHCl_3}$ cm^{-1}: 1665, 1660, 1645, 1610. ^{1}H-NMR ($CDCl_3$) δ: 9.26 (1H, br s, NH), 7.94 (1H, d, J=8.8 Hz, H-6), 6.86 (1H, d, J=8.8 Hz, H-5), 6.60 (1H, d, J=9.8 Hz, H-1), 6.44 (1H, q, J=1.5 Hz, H-9), 5.70 (1H, d, J=9.8 Hz, H-2), 2.14 (3H, d, J=1.5 Hz, 8-CH_3), 1.48 (6H, s, 3-$CH_3 \times 2$).

2,2,9-Trimethyl-2*H*,6*H*-pyrano[3,2-*b*]carbazole-7,10-quinone (**5**): Yield 50%. Brown crystals, mp 252 °C (dec.). High-resolution MS *m/z*: Calcd for $C_{18}H_{15}NO_3$: 293.1051. Found: 293.1052. ^{1}H-NMR ($CDCl_3$) δ: 9.13 (1H, br s, NH), 7.59 (1H, s, H-11), 7.05 (1H, s, H-5), 6.46 (1H, q, J=1.7 Hz, H-8), 6.43 (1H, d, J=9.8 Hz, H-4), 5.81 (1H, d, J=9.8 Hz, H-3), 2.15 (3H, d, J=1.7 Hz, 9-CH_3), 1.45 (6H, s, 2-$CH_3 \times 2$).

2-Methylcarbazole-1,4-quinones 6a—g In the same manner as for **1a—g**, the $Pd(OAc)_2$ treatment of **10a—g** (0.5 mmol) afforded the corresponding **6a—g**.

2-Methylcarbazole-1,4-quinone (**6a**): Yield 64%. Red flakes, mp 237—239 °C (dec.). *Anal.* Calcd for $C_{13}H_9NO_2$: C, 73.92; H, 4.30; N, 6.63. Found: C, 73.99; H, 4.04; N, 6.45. MS *m/z*: 211 (M^+). ^{1}H-NMR (DMSO-d_6) δ: 9.08 (1H, br s, NH), 8.20 (1H, dt, J=5.0, 1.0 Hz, H-5), 7.54—7.22 (3H, m, H-6, -7, and -8), 6.55 (1H, q, J=1.7 Hz, H-3), 2.14 (3H, d, J=1.7 Hz, 2-CH_3). ^{13}C-NMR ($CDCl_3$+DMSO-d_6) δ: 183.3 (s), 180.2 (s), 143.9 (s), 137.8 (s), 135.6 (s), 134.9 (d, C-3), 126.2 (d), 123.7 (d), 123.3 (s), 121.8 (d), 115.8 (s), 113.7 (d), 15.0 (q, 2-CH_3).

2,6-Dimethylcarbazole-1,4-quinone (**6b**): Yield 61%. Red plates, mp 240—242 °C (dec.). *Anal.* Calcd for $C_{14}H_{11}NO_2$: C, 74.65; H, 4.92; N, 6.22. Found: C, 74.50; H, 4.78; N, 6.28. MS *m/z*: 255 (M^+). ^{1}H-NMR (DMSO-d_6) δ: 12.72 (1H, br s, NH), 7.76 (1H, dd, J=1.7, 0.5 Hz, H-5), 7.39 (1H, dd, J=8.5, 0.5 Hz, H-8), 7.18 (1H, dd, J=8.5, 1.7 Hz, H-7), 6.53 (1H, q, J=1.7 Hz, H-3), 2.40 (3H, s, 6-CH_3), 2.02 (3H, d, J=1.7 Hz, 2-CH_3). ^{13}C-NMR (DMSO-d_6) δ: 183.2 (s), 179.9 (s), 143.7 (s), 136.0 (s), 135.4 (s), 134.7 (d, C-3), 133.0 (s), 128.1 (d), 123.5 (s), 120.9 (d), 115.1 (s), 113.3 (d), 21.1 (q), 14.8 (q, 2-CH_3).

6-Chloro-2-methylcarbazole-1,4-quinone (**6c**): Yield 49%. Red prisms, mp 263—265 °C (dec.). *Anal.* Calcd for $C_{13}H_8ClNO_2$: C, 63.56; H, 3.28; N, 5.70. Found: C, 63.52; H, 3.29; N, 5.50. MS *m/z*: 247 (M^+ +2), 245 (M^+). ^{1}H-NMR (DMSO-d_6) δ: 12.97 (1H, br s, NH), 7.86 (1H, dd, J=2.0, 0.7 Hz, H-5), 7.50 (1H, dd, J=8.8, 0.7 Hz, H-8), 7.34 (1H, dd, J=8.8, 2.0 Hz, H-7), 6.54 (1H, q, J=1.7 Hz, H-3), 2.03 (3H, d, J=1.7 Hz, 2-CH_3). ^{13}C-NMR (DMSO-d_6) δ: 182.6 (s), 179.7 (s), 144.0 (s), 136.4 (s), 135.9 (s), 134.6 (d, C-3), 128.2 (s), 126.2 (d), 123.9 (s), 120.5 (d), 115.3 (d), 114.8 (s), 14.9 (q, 2-CH_3).

6-Fluoro-2-methylcarbazole-1,4-quinone (**6d**): Yield 83%. Orange flakes, mp 257—260 °C (dec.). *Anal.* Calcd for $C_{13}H_8FNO_2$: C, 68.12; H, 3.52; N, 6.11. Found: C, 68.07; H, 3.52; N, 6.11. MS *m/z*: 229 (M^+). ^{1}H-NMR (DMSO-d_6) δ: 12.94 (1H, br s, NH), 7.60 (1H, ddd, J=9.3, 2.4, 0.5 Hz, H-5), 7.52 (1H, ddd, J=9.3, 4.6, 0.5 Hz, H-8), 7.22 (1H, td, J=9.3, 2.4 Hz, H-7), 6.53 (1H, q, J=1.7 Hz, H-3), 2.03 (3H, d, J=1.7 Hz, 2-CH_3). ^{13}C-NMR ($CDCl_3$+DMSO-d_6) δ: 182.9 (s), 179.9 (s), 164.2 and 154.6 (each s, fluorine-coupled carbon), 144.2 (s), 136.9 (s), 134.8 (d, C-3), 134.3 (s), 123.7 and 123.2 (each s, fluorine-coupled carbon), 115.7 and 115.3 (each d, fluorine-coupled carbon), 115.7 (s), 115.7 and 114.6 (each d, fluorine-coupled carbon), 106.4 and 105.4 (each d, fluorine-coupled

carbon), 14.9 (q, 2-CH_3).

6-Methoxy-2-methylcarbazole-1,4-quinone (**6e**): Yield 46%. Orange needles, mp 280—281 °C (dec.). *Anal.* Calcd for $C_{14}H_{11}NO_3$: C, 69.70; H, 4.59; N, 5.80. Found: C, 69.67; H, 4.63; N, 5.70. MS *m/z*: 241 (M^+). ^{1}H-NMR (DMSO-d_6) δ: 12.70 (1H, br s, NH), 7.36 (1H, dd, J=9.0, 0.7 Hz, H-8), 7.34 (1H, d, J=2.4 Hz, H-5), 6.94 (1H, dd, J=9.0, 2.4 Hz, H-7), 6.48 (1H, q, J=1.5 Hz, H-3), 3.78 (3H, s, 6-OCH_3), 1.99 (3H, d, J=1.5 Hz, 2-CH_3). ^{13}C-NMR (DMSO-d_6) δ: 183.5 (s), 179.4 (s), 158.8 (s), 144.0 (s), 139.1 (s), 134.7 (s), 134.1 (d, C-3), 122.4 (d), 117.4 (s), 116.1 (s), 115.1 (d), 95.0 (d), 55.3 (q), 14.9 (q, 2-CH_3).

7-Methoxy-2-methylcarbazole-1,4-quinone (**6f**): Yield 42%. Brown needled, mp 250—252 °C (dec.). *Anal.* Calcd for $C_{14}H_{11}NO_3$: C, 69.70; H, 4.59; N, 5.80. Found: C, 69.68; H, 4.71; N, 5.65. MS *m/z*: 241 (M^+). ^{1}H-NMR (DMSO-d_6) δ: 12.63 (1H, br s, NH), 7.84 (1H, d, J=9.5 Hz, H-5), 6.93 (1H, dd, J=9.5, 2.2 Hz, H-6), 6.90 (1H, d, J=2.2 Hz, H-8), 6.51 (1H, q, J=1.7 Hz, H-3), 3.81 (3H, s, 7-OCH_3), 2.03 (3H, d, J=1.7 Hz, 2-CH_3). ^{13}C-NMR (DMSO-d_6) δ: 183.1 (s), 179.7 (s), 156.8 (s), 143.9 (s), 135.5 (s), 134.8 (d, C-3), 132.9 (s), 124.1 (s), 117.6 (d), 115.3 (s), 114.7 (d), 101.5 (d), 55.3 (q), 14.9 (q, 2-CH_3).

8-Methoxy-2-methylcarbazole-1,4-quinone (**6g**): Yield 58%. Brown needles, mp 212—214 °C. *Anal.* Calcd for $C_{14}H_{11}NO_3$: C, 69.70; H, 4.59; N, 5.80. Found: C, 69.64; H, 4.56; N, 5.50. MS *m/z*: 241 (M^+). ^{1}H-NMR (DMSO-d_6) δ: 12.98 (1H, br s, NH), 7.54 (1H, dd, J=7.8, 1.0 Hz, H-5), 7.19 (1H, t, J=7.8 Hz, H-6), 6.89 (1H, dd, J=7.8, 1.0 Hz, H-7), 6.55 (1H, q, J=1.7 Hz, H-3), 3.93 (3H, s, 8-OCH_3), 2.03 (3H, d, J=1.7 Hz, 2-CH_3). ^{13}C-NMR (DMSO-d_6) δ: 183.2 (s), 179.5 (s), 147.4 (s), 144.0 (s), 135.3 (s), 134.4 (d, C-3), 128.5 (s), 124.7 (s), 124.6 (d), 116.1 (s), 113.6 (d), 105.9 (d), 55.4 (q), 14.9 (q, 2-CH_3).

Acknowledgement We wish to thank Mr. Atsushi Takada for his assistance in the experimental work. We are also indebted to Mr. Katsuyoshi Masuda for measurement of the high-resolution MS and to Miss Tatsuko Sakai for elemental analyses.

References and Notes

1) *a*) T.-S. Wu, T. Ohta, and H. Furukawa, *Heterocycles*, **20**, 1267 (1983); *b*) H. Furukawa, T.-S. Wu, T. Ohta, and C.-S. Kuoh, *Chem. Pharm. Bull.*, **33**, 4132 (1985); *c*) H. Furukawa, M. Yogo, C. Ito, T.-S. Wu, and C.-S. Kuoh, *ibid.*, **33**, 1320 (1985); *d*) C. Ito, T.-S. Wu, and H. Furukawa, *ibid.*, **36**, 2377 (1988).
2) K. Takeya, M. Itoigawa, and H. Furukawa, *Eur. J. Pharmacol.*, **169**, 137 (1989).
3) *a*) K. Ramesh and R. S. Kapil, *J. Nat. Prod.*, **50**, 932 (1987); *b*) *Idem, Chem. Ind.* (London), **1986**, 614; *c*) T. Martin and C. J. Moody, *J. Chem. Soc., Perkin Trans. 1*, **1988**, 235; *d*) *Idem, J. Chem. Soc., Chem. Commun.*, **1985**, 1391; K. Ramesh and R. S. Kapil, *Indian J. Chem., Sect. B*, **25B**, 462 (1986); T. Martin and C. J. Moody, *J. Chem. Soc., Perkin Trans. 1*, **1988**, 241.
4) R. F. Heck, "Palladium Reagents in Organic Syntheses," Academic Press, Inc., London, 1985.
5) B. Åkermark, L. Eberson, E. Jonsson, and E. Perttersson, *J. Org. Chem.*, **40**, 1365 (1975).
6) T. Itahara, *J. Org. Chem.*, **50**, 5546 (1985).
7) A part of this study was reported as a preliminary communication.[1c]
8) S. C. Srivastava and U. Hornemann, *Angew, Chem., Int. Ed. Engl.*, **15**, 109 (1976).
9) The starting material **9a** was also synthesized by two alternative methods from **16**[17] and from **18**[18] *via* the hydroquinone intermediate A in 58 and 80% yields, respectively, as illustrated in Chart 3. The synthesis of **9a** by the methods reported previously[8,10] gave the corresponding regioisomer **10a** at the same time. However, the methods described here afforded exclusively **9a**.
10) *a*) G. Jacini, *Gazz. Chim. Ital.*, **77**, 252 (1947) [*Chem. Abstr.*, **42**, 1329*f* (1948)]; *b*) W. G. Hanger, W. C. Howell, and A. W. Johnson, *J. Chem. Soc.*, **1958**, 496.
11) I. E. Kopka, Z. A. Fataftah, and M. W. Rathke, *J. Org. Chem.*, **45**, 4616 (1980).
12) J. M. Evans, C. S. Fake, T. C. Hamilton, R. H. Poyser, and E. A. Watts, *J. Med. Chem.*, **26**, 1582 (1983).
13) Isolation and characterization of other minor compounds were not carried out.
14) J. A. Miller and H. C. S. Wood, Brit. Patent 1121307 (1968) [*Chem. Abstr.*, **69**, 96471*c* (1968)].
15) The assignments of these carbon resonances were easily confirmed by single-frequency selective proton-decoupling experiments: the mutual long-range coupling between the allyl methyl and the adjacent olefinic proton facilitated these assignments in the ^{1}H-NMR spectra.
16) In the ^{13}C-NMR spectra of murrayaquinone-B (**1h**) and -C (**1i**), the allyl methyl signals have been reported to appear at δ_C 16.1 and 16.0, respectively, and both C-2 signals at δ_C 131.5.[1a,b]
17) F. Kehrmann, *Ber.*, **48**, 2021 (1915).
18) A. McKillop, D. H. Perry, M. Edwards, S. Antus, L. Farkas, M. Nógrádi, and E. C. Taylor, *J. Org. Chem.*, **41**, 282 (1976).
19) The presence of the H-3 signal at about δ_H 6.50 overlapping with aromatic proton signals was supported by the decoupling experiment involving irradiation of the methyl signal at δ_H 1.86.
20) The signal was observed as a broad triplet on addition of deuterium oxide, and was changed to a sharp triplet (J=4.2 Hz) on additional irradiation of H-3.
21) J. Hlubucek, E. Ritchie, and W. C. Taylor, *Tetrahedron Lett.*, **1969**, 1369.
22) J. M. Evans, C. S. Fake, T. C. Hamilton, R. H. Poyser, and G. A. Showell, *J. Med. Chem.*, **27**, 1127 (1984).
23) Y. Yamagishi, K. Hamamura, and T. Fujimori, Japan. Kokai Tokkyo Koho JP 60197668 (1985) [*Chem. Abstr.*, **104**, 109474*z* (1986)].

Syntheses and Biological Properties of New 8-Fluorocarbapenem Derivatives

Azuma WATANABE, Michiko SAKAMOTO, Yasuo FUKAGAWA[1] and Takeo YOSHIOKA*

MERCIAN Corporation, Central Research Laboratories, 9–1 Johnan 4-chome, Fujisawa 251, Japan. *Received March 30, 1990*

8-Fluorocarbapenem derivatives having various C-3 side chains were synthesized to study for the structure–activity relationship of carbapenems by *in vitro* biological evaluation. The introduction of fluorine at C-8 of racemic PS-5 led to slight improvements of the antimicrobial activity and the stability to renal dehydropeptidase-I. When D-cysteine was additionally introduced to the C-3 position of (±)-8-fluorocarbapenem, the diastereomeric separation of the 8-fluorocarbapenems became feasible. As expected from penicillins and cephalosporins, (+)-8-fluoro-3-D-cysteinylcarbapenem (+)-7a was antimicrobially active, whereas (−)-7b was inactive. It is worth noting, however, that (+)-7a was significantly more sensitive to renal dehydropeptidase-I than (−)-7b. Irrespective of the presence of fluorine at C-8, basic S-side chains at C-3, such as the pyridyl and pyrrolidyl groups, significantly improved in antimicrobial activity and dehydropeptidase-I stability. The combination of 8-fluorination with C-3 basic side chains in 7c—g resulted in a marked improvement of antimicrobial activity and dehydropeptidase-I stability.

Keywords 8-fluorocarbapenem; carbapenem; PS-5; diastereomeric separation; sulfoxide displacement method; antimicrobial activity; dehydropeptidase-I stability

Since the isolation of PS-5 and related carbapenem compounds from streptomycetes,[2] we have continued development of a clinically acceptable carbapenem derivative which has improved physicochemical stability and is resistant to dehydropeptidase-I (DHP-I) *in vivo*. As a result, chemical modification of PS-5 at C-3 by displacement methods *via* sulfoxide provided a series of resistant carbapenem derivatives, but without practically satisfactory stability in mice to date.[3] Among these derivatives, the D-cysteinyl derivative **1** and the 4-pyridylthio derivative **2** were found to be most promising in antimicrobial activity and dehydropeptidase-I stability (Fig. 1).

Recently, imipenem has become available in the market as the first carbapenem drug, but it still has some inconveniences such as insufficient *in vivo* stability which requires coadministration of cilastatin; and also poor water solubility, which limits its clinical use to infusion only.[4] Mak and Fliri have reported the chemical synthesis of 8-fluorocarbapenem derivatives[5] as racemates through the Melillo lactone route.[6] Among them, the racemate of (5*R*,6*R*)-6-[(*R*)-1-fluoroethyl]-7-oxo-3-[(*N*,*N*,*N*′-trimethylcarbamimidoyl)methyl]thio-1-azabicyclo[3.2.0]hept-2-ene-2-carboxylic acid (88.617) showed excellent antimicrobial activity and a high resistance to renal DHP-I.[5] Starting from OA-6129B$_2$, a fermentation carbapenem product, we reported an efficient method of derivation of optically active 88.617 by stereoselective fluorination with DAST.[7] In due course, we thought that the combination of 8-fluorination with a suitable C-3 side chain might bring about a therapeutically more valuable carbapenem derivative which, unlike imipenem, is sufficiently stable *in vivo* without DHP-I inhibitors and is administrable by various routes in addition to infusion.

Using PS-5 as a starting compound, we showed that the chemical introduction of the D-cysteinyl and 4-pyridylthio groups at C-3 of PS-5 resulted in significantly improved antimicrobial activity and DHP-I stability.[3] Accordingly, we began this study with the derivation of the 8-fluoro-3-D-cysteinyl carbapenem derivative **7ab** from the racemic diazo compound (±)-**4**,[5] as illustrated in Fig. 2. In particular, the diazo group of (±)-**4** was treated with a catalytic amount of rhodium diacetate, resulting in the slective N–H insertion of carbenoid.[8] Without purification, the bicyclic keto-ester (±)-**5** was converted to a tris-protected 8-fluorocarbapenem

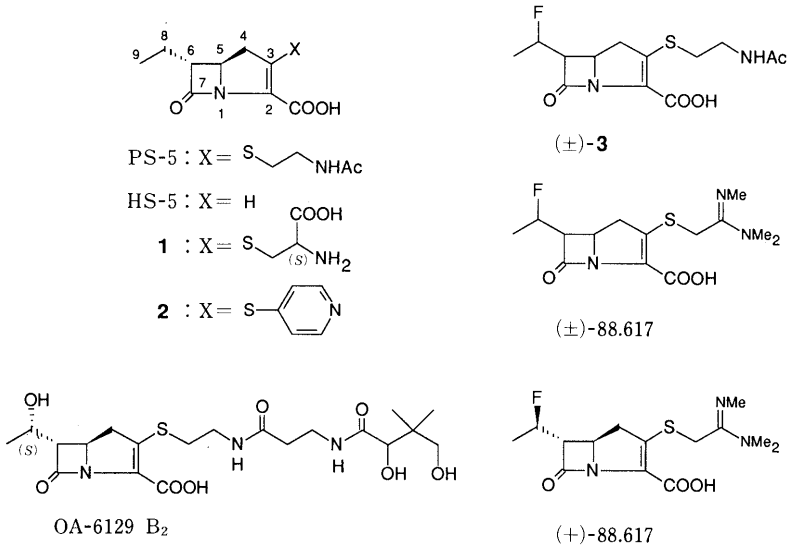

Fig. 1. PS-5 and Related Carbapenem Compounds

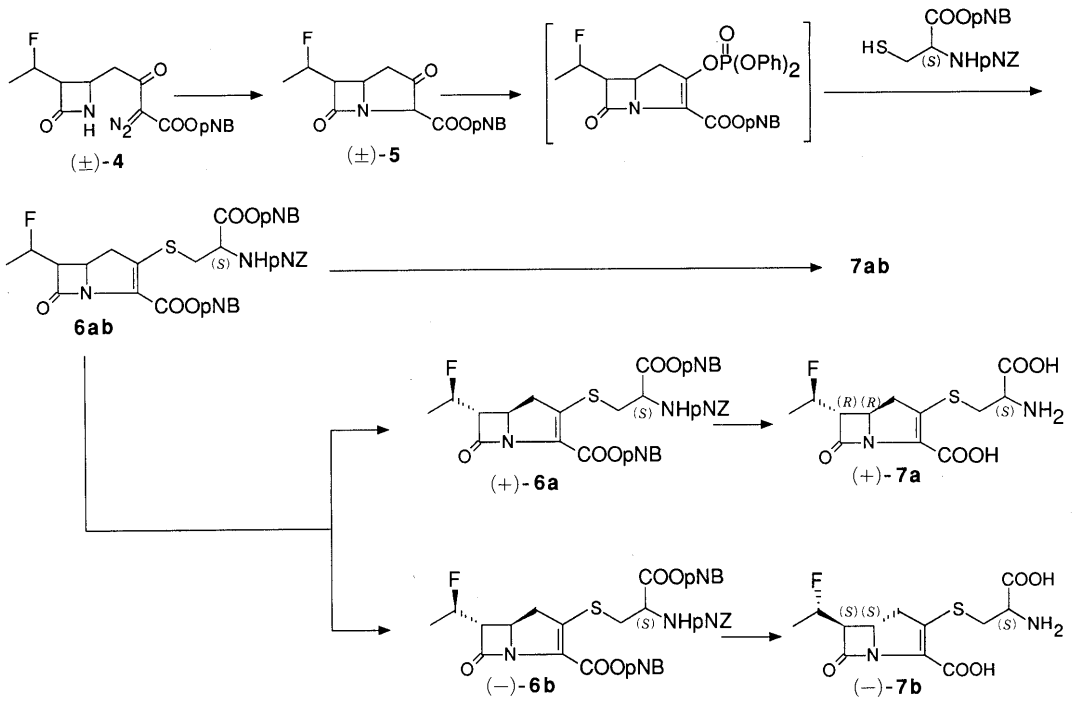

Fig. 2. Derivation and Diastereomeric Separation of **7ab**, (+)-**7a** and (−)-**7b**

TABLE I. Comparative Antimicrobial Activities of PS-5, 88.617 and Related Carbapenem Derivatives

Microorganism	CEZ	PS-5	(±)-**3**	**1**	**7ab**	(+)-**7a**	(−)-**7b**	**2**	**7c**	88.617
Gram-positive bacteria										
Bacillus subtilis ATCC6633	0.1	0.10	0.05	0.20	0.10	0.05	0.39	<0.007	<0.003	0.003
Micrococcus luteus ATCC9341	0.78	0.20	0.10	1.56	0.39	0.20	1.56	<0.007	<0.003	0.006
Staphylococcus aureus FDA209P	0.05	0.05	0.024	0.39	0.10	0.05	0.39	<0.007	<0.003	0.0008
Staphylococcus aureus SMITH	0.20	0.20	0.10	0.39	0.39	0.20	1.56	<0.007	0.006	0.006
Staphylococcus epidermidis	0.20	0.20	0.10	1.56	0.39	0.39	3.13	<0.007	—	—
Gram-negative bacteria										
Citrobacter freundii GN346[a]	>100	1.56	25	1.56	3.13	1.56	25	29.5	25	0.39
Comamonas terrigena B996	0.05	0.024	0.05	0.024	0.05	0.024	0.39	<0.007	<0.003	0.012
Enterobacter aerogenes E-19[a]	>100	1.56	6.25	0.39	0.78	0.78	6.25	7.4	0.78	0.78
Enterobacter cloacae 45[a]	>100	3.13	50	3.13	1.56	1.56	25	29.5	6.25	0.78
Escherichia coli K-12	0.78	1.56	0.78	0.024	0.39	0.20	1.56	0.92	0.10	0.39
Klebsiella pneumoniae 130[a]	50	6.25	1.56	0.39	0.39	0.39	3.13	14.8	1.56	0.78
Proteus vulgaris GN76[a]	>100	6.25	>100	0.78	1.56	1.56	25	29.5	3.13	3.13
Proteus sp. P-22[a]	>100	6.25	>100	1.56	1.56	1.56	25	29.5	1.56	1.56
Providencia sp. P-8	0.78	1.56	6.25	0.10	0.39	0.20	3.13	0.92	0.05	0.78
Pseudomonas aeruginosa IFO3445	>100	25	>100	3.13	25	12.5	>100	0.92	0.20	0.39
Pseudomonas aeruginosa NCTC10490	>100	25	50	6.25	50	50	>100	0.92	0.10	0.20
Serratia marcescens T55[a]	1.56	1.56	>100	3.13	3.13	1.56	25	29.5	12.5	1.56

a) Beta-lactamase producer. Diastereomeric purities of (+)-**7a** and (−)-**7b** were about 80% and 95%, respectively.

mixture **6ab** as a diastereomeric mixture with *N-p*-nitrobenzyloxycarbonyl-D-cysteine *p*-nitrobenzyl ester *via* an enol phosphate. After purification by silica gel column chromatography, the diastereomeric mixture **6ab** was subjected to fractional precipitation with chloroform to give (+)-**6a** and (−)-**6b** which contained small amounts of the corresponding diastereomers, respectively. After hydrogenation, diastereomerically about 80% pure (+)-**7a** and about 95% pure (−)-**7b** (by high performance liquid chromatography (HPLC) analysis) were produced for biological evaluation (Tables I and II).

Table I compares the antimicrobial activities of cefazolin (CEZ), PS-5,8-fluoro-PS-5 ((±)-**3**), 3-D-cysteinyl-HS-5 (**1**), **7ab**, (+)-**7a**, (−)-**7b**, 3-pyridyl-HS-5 (**2**), 8-fluoro-3-pyridyl-HS-5 (**7c**) and 88.617. Although the tested compounds (+)-**7a** and (−)-**7b** were not diastereomerically pure, it is still clear that (+)-**7a** is antimicrobially active, whereas (−)-**7b** seems to be inactive, as is the case in penicillins and cephalosporins. Retrospectively, the absolute configurations at C-5 of (+)-**7a** and (−)-**7b** are considered to be *R* and *S*, respectively. Furthermore, since the relative configuration of the beta-lactam hydrogens of (+)-**7a** and (−)-**7b** is *trans*, the full structures of (+)-**6a**, (−)-**6b**, (+)-**7a** and (−)-**7b** are concluded to be as shown in Fig. 2. Considering from the 95% diastereomeric purity of the (−)-**7b** preparation, it is reasonable to conclude that (−)-

diastereomers of carbapenems have no antimicrobial activity at all. In addition, as previously reported, the introduction of D-cysteine or 4-mercaptopyridines at C-3 of HS-5 leads to improved activity against the gram-positive pathogens,[3] while 8-fluorination has insignificant influence on the antimicrobial activity of PS-5 (Table I).

The currently inexplicably high susceptibility of carbapenems to DHP-I is a serious concern of organic chemists from the viewpoint of development of clinically useful carbapenem derivatives.[9] Figure 3 shows the comparative time courses of *in vitro* hydrolysis of the carbapenem derivatives, PS-5, **1**, **2** and (±)-**3**, by dog DHP-I.

TABLE II. Comparative DHP-I Stabilities of PS-5, 88.617 and Related Carbapenem Derivatives against Mouse, Dog and Man Dehydropeptidase-I

Animal	PS-5	(±)-3	1	7ab	2	7c	88.617
Mouse	1.0	3.1	7.7	8.7	21.6	8.3	25.9
Dog	1.0	1.0	1.7	5.4	—	15.8	4.6
Man	1.0	1.6	2.3	1.9	1.3	2.0	4.2

It is apparent that PS-5 is the most susceptible to mouse DHP-I *in vitro*; and that 8-fluorination, 3-cysteinylation or 3-pyridylthionylation of carbapenem results in significant stabilization of carbapenem to DHP-I.

As shown in Fig. 4, it is contrary to our expectations, (+)-**7a** in which the C-5 has the *R*-configuration is more susceptible to DHP-I than (−)-**7b** in which the C-5 has the *S*-configuration; also, the time course of hydrolysis of **7ab** is not the arithmetic mean of those of (+)-**7a** and (−)-**7b**. At present, our enzymological observations collected under various reaction conditions seem to suggest that, (−)-**7b** is a relatively poor DHP-I substrate, but acts as a kind of DHP-I inhibitor in **7ab** (unpublished results).

Based on the above-described findings, it is reasonable to conclude that racemic or diastereomeric mixtures of carbapenem derivatives should not be employed for biological evaluation of antimicrobial activity and DHP-I stability of carbapenems. So we have restricted the subsequent derivation of carbapenems to the optically active series starting from optically active (+)-**4** as follows (Fig. 5):

4-Mercaptopyridine and 4-mercaptopyrrolidines were se-

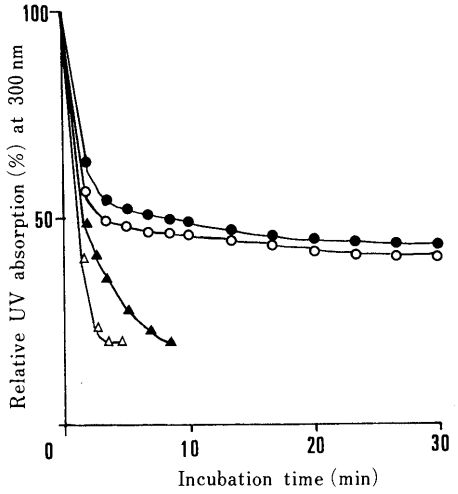

Fig. 3. Comparative Time Courses of Hydrolysis of PS-5 (△—△), **1** (●—●), **2** (○—○), and (±)-**3** (▲—▲) by Dehydropeptidase-I

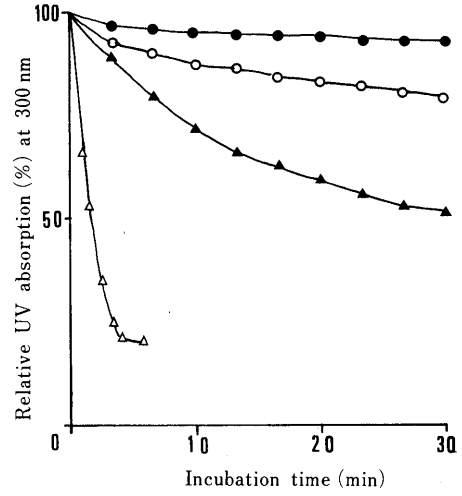

Fig. 4. Comparative Time Courses of Hydrolysis of PS-5 (△—△), **7ab** (○—○), (+)-**7a** (▲—▲) and (−)-**7b** (●—●) by Dehydropeptidase-I

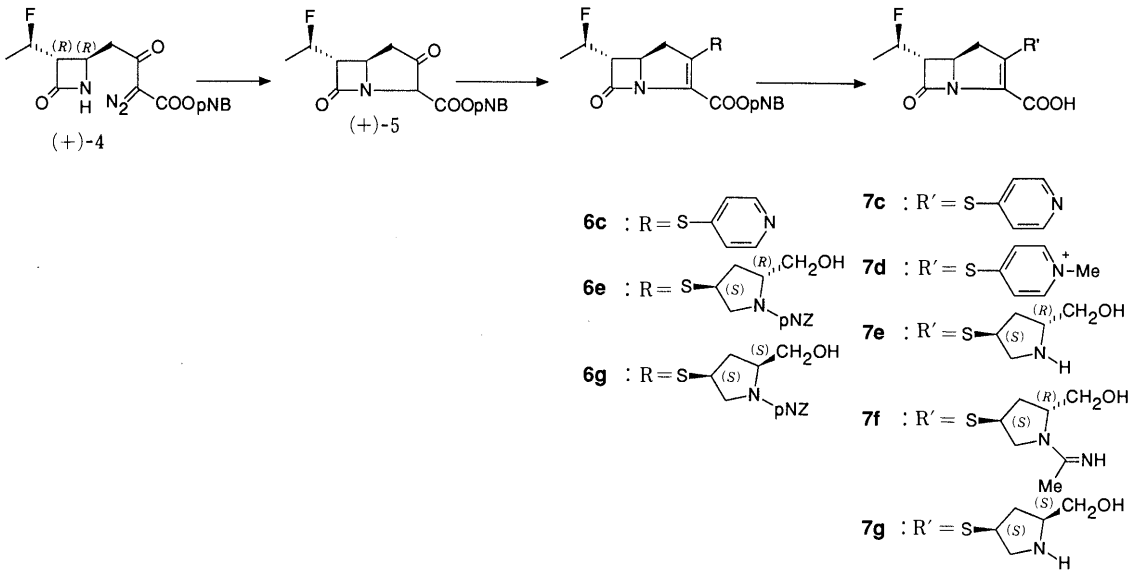

Fig. 5. Derivation of New 8-Fluorocarbapenem Derivatives

TABLE III. Antimicrobial Activities and Dehydropeptidase-I Stabilities of New 8-Fluorocarbapenem Derivatives

Microorganism	CEZ	PS-5	(±)-3	7c	7d	7e	7f	7g	88.617
Gram-positive bacteria									
Bacillus subtilis ATCC6633	0.10	0.10	0.05	<0.003	0.006	0.003	0.012	0.003	0.003
Micrococcus luteus ATCC9341	0.78	0.20	0.10	<0.003	0.003	0.012	0.012	0.006	0.006
Staphylococcus aureus FDA209P	0.05	0.05	0.024	<0.003	<0.003	0.0015	<0.0015	0.0015	0.0008
Staphylococcus aureus SMITH	0.20	0.20	0.10	0.006	0.006	0.012	0.006	0.003	0.006
Gram-negative bacteria									
Alcaligenes faecalis ATCC8750	12.5	1.56	0.39	0.012	0.006	0.39	0.20	0.20	0.78
Citrobacter freundii GN346[a]	>100	1.56	25	25	0.78	0.78	0.78	0.78	0.39
Comamonas terrigena B996	0.05	0.024	0.05	<0.003	0.006	0.012	0.012	0.003	0.012
Enterobacter aerogenes E-19[a]	>100	1.56	6.25	0.78	1.56	1.56	0.78	0.78	0.78
Enterobacter cloacae 45[a]	>100	3.13	50	6.25	3.13	1.56	1.56	1.56	0.78
Escherichia coli K-12	0.78	1.56	0.78	0.10	0.20	0.78	0.20	0.39	0.39
Escherichia coli RGN238[a]	1.56	1.56	1.56	0.10	0.39	0.78	0.39	0.78	0.78
Klebsiella pneumoniae 130[a]	50	6.25	0.78	1.56	0.78	0.78	0.78	0.78	0.78
Proteus morganii 111[a]	50	6.25	6.25	0.20	0.78	1.56	0.39	0.78	1.56
Proteus rettgeri P-48	50	3.13	12.5	0.78	3.13	1.56	0.78	1.56	1.56
Proteus vulgaris GN76[a]	>100	6.25	>100	3.13	3.13	3.13	3.13	3.13	3.13
Proteus sp. P-22[a]	>100	6.25	>100	1.56	3.13	3.13	3.13	3.13	1.56
Providencia sp. P-8	0.78	1.56	6.25	0.05	0.20	0.78	0.78	0.78	0.78
Pseudomonas aeruginosa IFO3445	>100	12.5	>100	0.20	0.39	0.20	0.39	0.39	0.39
Pseudomonas aeruginosa NCTC10490	>100	12.5	50	0.10	0.39	0.20	0.39	0.39	0.20
Pseudomonas aeruginosa E2[a]	>100	>100	>100	3.13	3.13	3.13	6.25	3.13	3.13
Salmonella gallinarum ATCC9184	0.78	1.56	1.56	0.10	0.20	0.78	0.39	0.78	0.39
Serratia marcescens IFO3736	>100	3.13	>100	6.25	1.56	3.13	0.78	1.56	1.56
Serratia marcescens T55[a]	1.56	6.25	>100	12.5	3.13	3.13	3.13	1.56	1.56
Shigella sonnei EW33	3.13	3.13	6.25	0.10	0.78	1.56	0.78	0.78	0.78
Dog dehydropeptidase-I (% activity after reaction[b])	//	21.1	—	88.7	93.9	91.8	84.5	90.0	97.1

a) Beta-lactamase producer. *b*) Incubation at 37 °C for 60 min.

lected as C-3 side chains for combination with 8-fluorination, as they seemed promising from the viewpoints of antimicrobial activity and DHP-I stability.[3]

Optically active (+)-**4**, which was prepared by a procedure including the resolution of the Melillo lactone,[10] was converted to a bicyclic ester (+)-**5** as described for (±)-**4**. The enol phosphate of (+)-**5** was then condensed with 4-mercaptopyridine to give **6c** in 58% yield, which was further led to **7c** by hydrogenation. **7d** was derived from **7c** by *N*-methylation with methyl iodide.

8-Fluorocarbapenem derivatives having pyrrolidine side chains at C-3,[11] **6e** and **6g**, were prepared by treating the enol phosphate of (+)-**5** with (2*R*,4*S*)-2-hydroxymethyl-4-mercapto-*N*-*p*-nitrobenzyloxycarbonylpyrrolidine.[12] Hydrogenation of **6e** resulted in **7e**. Treatment of **7e** with ethyl acetimidate hydrochloride at 0 °C under weakly alkaline conditions yielded the acetimidate **7f** in 72% yield. **6g**, a C-2′ epimer of **6e**, was hydrogenated to give **7g**.

Table III summarizes the antimicroial activities of new 8-fluorocarbapenem derivatives having pyridylthio and pyrrolidinylthio side chains at C-3. As in the case with thienamycin derivatives,[13] increased basicity of the C-3 side chains clearly resulted in significantly improved antimicrobial activity against both the gram-positive bacteria and the gram-negative. Table III also compares the *in vitro* dog DHP-I stability of the new carbapenem derivatives, which demonstrates that the pyridylthio and pyrrolidinylthio side chains at C-3 are more effective than 8-fluorination for stabilization of carbapenem toward DHP-I.

The results of *in vitro* biological evaluation in Tables I—III allow the following conclusions: 1) the *R*-configuration at C-5 is essential for antimicrobial activity, whereas the *S*-configuration at C-5 seems to be useful for DHP-I inhibition or resistance activity, but without antimicrobial activity (Table I and Fig. 4); 2) 8-fluorination slightly improves the antimicrobial activity and DHP-I stability, but also increases susceptibility to some beta-lactamases (Table I and Fig. 3); 3) basic side chains at C-3 lead to significant improvement in antimicrobial activity and DHP-I stability, but again make carbapenem somewhat more sensitive to beta-lactamases (Tables I and II); and 4) the combination of 8-fluorination with basic side chains at C-3 results in synergistic improvement of antimicrobial activity and DHP-I stability (Table III).

8-Fluorination shows another advantage by making markedly water-soluble generally least water-soluble 8-hydroxycarbapenem molecules with strong basic side chains at C-3.[4] For example, imipenem has a water-solubility as low as 1%, which limits the clinical use of imipenem to infusion only. In contrast, 8-fluorocarbapenem derivatives with a strong basic side chain at C-3, such as optically active 88.617, **7c**, **7e** and **7f**, show good water-solubility (over 30%). The new 8-fluorocarbapenem derivatives will be further evaluated by *in vivo* animal studies, including pharmacokinetics and toxicology, in a variety of animals including man.

Experimental

General Methodology Silica gel thin-layer chromatography (TLC) and column chromatography were carried out by using pre-coated TLC plate Silica gel 60 F_{254} (E. Merck) and silica gel 60 (70—230 mesh; E. Merck), respectively. Infrared (IR), ultraviolet (UV) and proton nuclear magnetic resonance (^{1}H-NMR) spectra were recorded with a Hitachi 260-30 infrared

spectrophotometer, a Hitachi 200-20 UV/visible spectrophotometer and a Varian EM-390 (90 MHz) spectrometer, respectively. Chemical shifts are given in ppm from internal tetramethylsilane (TMS) in $CDCl_3$ and pyridine-d_5 or sodium 3-(trimethylsilyl)-1-propanesulfonate (DSS) in D_2O. Optical rotations were measured with a JASCO DIP-181 digital polarimeter. Melting points were determined in a YANACO apparatus, and are uncorrected.

PS-5 This carbapenem was isolated from the fermentation broth of *Streptomyces cremeus* subsp. *auratilis* A271, a soil microorganism (ATCC 31358).[2a)]

(5*R*,6*R*)-3-[(2*S*)-2-Amino-2-carboxy]ethylthio-6-ethyl-7-oxo-1-azabicyclo[3.2.0]hept-2-ene-2-carboxylic Acid (3-D-Cysteinyl-HS-5: 1) and (5*R*,6*R*)-6-Ethyl-3-(pyridin-4-yl)thio-7-oxo-1-azabicyclo[3.2.0]hept-2-ene-2-carboxylic Acid (3-Pyridyl-HS-5: 2) 3-D-Cysteinyl-HS-5 (**1**) and 3-pyridyl-HS-5 (**2**) were prepared from the sulfoxide of PS-5 *p*-nitrobenzyl ester by the methods for displacing the C-3 sulfur side chains of carbapenems.[3c)]

(5*RS*,6*RS*)-3-Acetamidoethylthio-6-[(*RS*)-1-fluoroethyl]-7-oxo-1-azabicyclo[3.2.0]hept-2-ene-2-carboxylic Acid (8-Fluoro-PS-5: (±)-3) 8-Fluoro-PS-5 was prepared according to the method of Mak and Fliri.[5a)]

***p*-Nitrobenzyl (5*RS*,6*RS*)-3,7-Dioxo-6-[(*RS*)-1-fluoroethyl]-1-azabicyclo[3.2.0]heptane-2-carboxylate ((±)-5)** A suspension of 394 mg of *p*-nitrobenzyl 4-[(3*RS*,4*RS*)-3-[(*RS*)-1-fluoroethyl]-2-oxoazetidinin-4-yl]-2-diazo-3-oxobutyrate ((±-**4**) and 8.0 mg of rhodium (II) acetate dimer in 40 ml of benzene was heated at 80 °C for 1 h under a nitrogen atmosphere, cooled to room temperature and filtered. The filtrate was concentrated to dryness *in vacuo* to afford 356 mg (100% yield) of (±)-**5** which was employed in the next step without purification. IR (KBr): 1780 (shoulder), 1760, 1745 cm^{-1}. UV $\lambda_{max}^{CHCl_3}$ nm (ε): 266.5 (10200). ^{1}H-NMR ($CDCl_3$) δ: 1.52 (3H, dd, *J*=6.0, 24.0 Hz), 2.49 (1H, dd, *J*=8.0, 18.0 Hz), 2.98 (1H, dd, *J*=8.0, 18.0 Hz), 3.34 (1H, m), 4.20 (1H, dt, *J*=2.0, 8.0 Hz), 4.7—5.55 (1H, m), 4.80 (1H, s), 5.26 (1H, d, *J*=14.0 Hz), 5.40 (1H, d, *J*=14.0 Hz), 7.50 (2H, d, *J*=9.0 Hz), 8.25 (2H, d, *J*=9.0 Hz).

Optically active (+)-**5** was obtained from optically active (+)-**4** by the reaction procedure as described above for (±)-**5**. $[\alpha]_D^{20}$ +185.7° (*c*=1.0, $CHCl_3$).

***p*-Nitrobenzyl (5*RS*,6*RS*)-6-[(*RS*)-1-Fluoroethyl]-3-[(2*S*)-2-*p*-nitorobenzyloxycarbonyl-2-*p*-nitrobenzyloxycarbonylamino]ethylthio-7-oxo-1-azabicyclo[3.2.0]hept-2-ene-2-carboxylate (6ab) and Separation of the Two Diastereomers ((+)-6a and (−)-6b)** A racemic compound (±)-**5** (340 mg) was dissolved at −30 °C in 10 ml of *N*,*N*-dimethylformamide and then mixed with 0.253 ml of diisopropylethylamine and 0.243 ml of diphenylphosphoryl chloride at −30 °C. The mixture was stirred for 30 min at −30 °C. Diisopropylethylamine (0.202 ml) and a solution of 50.8 mg of *N*-*p*-nitrobenzyloxycarbonyl-D-cysteine *p*-nitrobenzyl ester in 2 ml of *N*,*N*-dimethylformamide were added dropwise to the reaction mixture and then stirred for 30 min. After mixed with 100 ml of dichloromethane, the dilution was washed with 70 ml each of 0.1 M phosphate buffers of pH 8.40, 6.90 and 8.40. The washed solution was dried over sodium sulfate and then evaporated to dryness *in vacuo* to provide an oil, which was subjected to silica gel (20 g) column chromatography using benzene–ethyl acetate (3:1) as an eluent. Eluate fractions containing the desired product were combined and concentrated to dryness *in vacuo* to afford a diastereomeric mixture **6ab** (520 mg, 70% yield) as a white precipitate. IR (KBr): 1780, 1735, 1690 cm^{-1}. UV $\lambda_{max}^{CHCl_3}$ nm (ε): 268.5 (35000). ^{1}H-NMR (pyridine-d_5) δ: 1.37 (3H, dd, *J*=6.0, 24.0 Hz), 3.3—4.05 (5H, m), 4.29 (1H, dt, *J*=2.5, 8.0 Hz), 4.45—5.65 (8H, m), 7.3—7.8 (6H, m), 8.10 (6H, d, *J*=9.0 Hz), 9.80 (1H, d, *J*=9.0 Hz). *Anal.* Calcd for $C_{34}H_{30}FN_5O_{13}S$: C, 54.32; H, 4.02; N, 24.23. Found: C, 54.59; H, 4.23; N, 23.95.

The precipitate was washed with 20 ml of chloroform, leaving (−)-**6b** 227 mg, $[\alpha]_D^{23}$ −27.7° (*c*=0.5, CH_2Cl_2) as a major diastereoisomer. The solid was further purified by precipitation from a mixture of CH_2Cl_2 and $CHCl_3$. The final preparation $[\alpha]_D^{23}$ −36.8° (*c*=0.5, CH_2Cl_2) of (−)-**6b** was found to be diastereomerically 80% pure.

The chloroform wash was concentrated to dryness under reduced pressure, yielding a (+)-**6a**-rich preparation $[\alpha]_D^{23}$ +17.5° (*c*=1.0, CH_2Cl_2). After repeated crystallization from chloroform, (+)-**6a** 44 mg, $[\alpha]_D^{23}$ +23.9° (*c*=0.25, CH_2Cl_2) was obtained as a 95%-pure preparation.

(5*RS*,6*RS*)-3-[(2*S*)-2-Amino-2-carboxy]ethylthio-6-[(*RS*)-1-fluoroethyl]-7-oxo-1-azabicyclo[3.2.0]hept-2-ene-2-caroxylic Acids (7ab) The diastereomer **6ab** (135 mg) was dissolved in a mixture of 4 ml of tetrahydrofuran, 3 ml of dioxane and 3 ml of 0.1 M phosphate buffer, pH 8.40; it was then hydrogenated in the presence of 100 mg of platinum dioxide at room temperature for 3.5 h at a hydrogen pressure of 4 kg/cm^2. After filtration, the filtrate was subjected to successive column chromatography on QAE-Sephadex A-25 (Pharmacia Fine Chemicals AB, Sweden) and Diaion CHP-20P (Mitsubishi Chemical Industries Ltd., Japan). Eluate fractions which showed a maximum UV absorption at 300 nm were combined and lyophilized to provide a white powder of diastereomer **7ab** (21.6 mg, 36% yield). IR (KBr): 1760 dm^{-1}. UV $\lambda_{max}^{0.001\,M\,PBS(pH\,7.0)}$ nm (ε): 298 (5600). ^{1}H-NMR (D_2O) δ: 1.41 (3H, dd, *J*=6.0, 25.0 Hz), 2.8—3.65 (5H, m), 3.75—4.0 (1H, m), 4.29 (1H, dt, *J*=2.5, 8.5 Hz), 5.11 (1H, ddd, *J*=6.0, 7.5, 48.4 Hz).

(5*R*,6*R*)-3-[(2*S*)-2-Amino-2-carboxy]ethylthio-6-[(*R*)-1-fluoroethyl]-7-oxo-1-azabicyclo[3.2.0]hept-2-ene-2-carboxylic Acid ((+)-7a) and (5*S*,6*S*)-3-[(2*S*)-2-Amino-2-carboxylethylthio-6-[(*S*)-1-fluoroethyl]-7-oxo-1-azabicyclo[3.2.0]hept-2-ene-2-carboxylic Acid ((−)-7b) Under the same reaction conditions as described for the diastereomeric mixture, (+)-**6a** and (−)-**6b** were hydrogenated to give (+)-**7a** and (−)-**7b**, respectively. The diastereomeric purities of (+)-**7a** and (−)-**7b** were determined by HPLC. The conditions for HPLC were as follows: column, μ-Bondapak C_{18} (3.7 i.d. × 300 mm, Waters Associates); solvent, MeOH–0.01 M phosphate buffer (pH 7.5) (1:9); flow rate, 2.0 ml/min; temperature, 25 °C; detection, UV 300 nm. The retention times of (+)-**7a** and (−)-**7b** were 22.5 and 21.0 min, respectively.

***p*-Nitrobenzyl (5*R*,6*R*)-6-[(*R*)-1-Fluoroethyl]-7-oxo-3-(pyridin-4-yl)thio-1-azabicyclo[3.2.0]hept-2-ene-2-carboxylate (6c)** Treatment of the enol phosphate of (+)-**5** (374 mg) with 4-mercaptopyridine sodium salt gave a mercaptopyridine derivative **6c** (277 mg, 58% yield) as an amorphous solid. IR (KBr): 1796, 1714 cm^{-1}. UV $\lambda_{max}^{CHCl_3}$ nm (ε): 321 (15000), 268 (15500). ^{1}H-NMR ($CDCl_3$) δ: 1.46 (3H, dd, *J*=6.0, 24.0 Hz), 2.86 (2H, d, *J*=9.0 Hz), 3.31 (1H, ddd, *J*=3.0, 7.5, 19.5 Hz), 4.21 (1H, dt, *J*=3.0, 9.0 Hz), 4.5—5.45 (1H, m), 5.28 (1H, d, *J*=13.5 Hz), 5.54 (1H, d, *J*=13.5 Hz), 7.40 (2H, d, *J*=5.0 Hz), 7.66 (2H, d, *J*=8.5 Hz), 8.22 (2H, d, *J*=8.5 Hz), 8.62 (2H, d, *J*=5.0 Hz). *Anal.* Calcd for $C_{21}H_{18}FN_3O_5S$: C, 56.87; H, 4.09; N, 9.48. Found: C, 57.13; H, 4.14; N, 9.58.

(5*R*,6*R*)-6-[(*R*)-1-Fluoroethyl]-7-oxo-3-(pyridin-4-yl)thio-1-azabicyclo[3.2.0]hept-2-ene-2-carboxylic Acid (7c) Under reaction conditions similar to those for **7ab**, 275 mg of *p*-nitrobenzyl ester **6c** was hydrogenated to afford 51.8 mg of **7c** (27% yield) as a colorless powder. IR (KBr): 1766 cm^{-1}. UV $\lambda_{max}^{0.001\,M\,PBS\,(pH\,7.0)}$ nm (ε): 303.5 (8800). ^{1}H-NMR (D_2O) δ: 1.39 (3H, dd, *J*=6.5, 24.5 Hz), 2.91 (2H, d, *J*=9.5 Hz), 3.4—3.85 (1H, m), 4.26 (1H, dt, *J*=3.0, 9.5 Hz), 4.65—5.55 (1H, m), 7.45 (2H, d, *J*=5.0 Hz), 8.40 (2H, d, *J*=5.0 Hz).

(5*R*,6*R*)-6-[(*R*)-1-Fluoroethyl]-3-(1-methyl-4-pyridinio)thio-7-oxo-1-azabicyclo[3.2.0]hept-2-ene-2-carboxylic Acid (7d) One milliliter of methyl iodide was added at 0 °C to a solution of 27.5 mg of **7c** in a mixture of 2.0 ml of a 0.01 M phosphate buffer, pH 8.3 and 2.0 ml of dioxane, and stirred for 12 h at room temperature. After being diluted with 10 ml of the phosphate buffer, the dilution was concentrated to about 5 ml *in vacuo*. The concentrate was again diluted with 10 ml of deionized water and washed twice, each time with 10 ml of ethyl acetate. The aqueous layer was recovered and subjected to column chromatography on Diaion CHP-20P using a linear concentration gradient of isopropyl alcohol from 0 to 50%. Active eluate fractions were combined and freeze-dried to produce 18.8 mg of **7d** (65% yield) as a colorless powder. IR (KBr): 1773 cm^{-1}. UV $\lambda_{max}^{0.001\,M\,PBS\,(pH\,7.0)}$ nm (ε): 305 (8000). ^{1}H-NMR (D_2O) δ: 1.43 (3H, dd, *J*=6.0, 24.5 Hz), 3.14 (2H, d, *J*=9.5 Hz), 3.83 (1H, ddd, *J*=3.0, 4.5, 28.5 Hz), 4.24 (3H, s), 4.48 (1H, dt, *J*=3.0, 9.5 Hz), 4.8—5.55 (1H, m), 7.80 (2H, d, *J*=6.0 Hz), 8.45 (2H, d, *J*=6.0 Hz).

***p*-Nitrobenzyl (5*R*,6*R*)-6-[(*R*)-1-Fluoroethyl]-3-[(2*R*,4*S*)-2-hydroxymethyl-1-*p*-nitrobenzyloxycarbonylpyrrolidin-4-yl]thio-7-oxo-1-azabicyclo[3.2.0]hept-2-ene-2-carboxylic Acid (6e)** Treatment of the enol phosphate of (+)-**5** (375 mg) with 401 mg of (2*R*,4*R*)-2-hydroxymethyl-4-mercapto-1-*p*-nitrobenzyloxycarbonylpyrrolidine yielded 499 mg of *p*-nitrobenzyl ester **6e** (72% yield) as an amorphous solid. IR ($CHCl_3$): 1785, 1700, 1670 cm^{-1}. UV $\lambda_{max}^{CHCl_3}$ nm (ε): 270 (21000), 318 (13000). ^{1}H-NMR ($CDCl_3$) δ: 1.50 (3H, dd, *J*=6.0, 23.0 Hz), 1.85—2.4 (2H, m), 3.27 (2H, d, *J*=9.5 Hz), 3.35—4.25 (8H, m), 4.28 (1H, dt, *J*=3.5, 9.5 Hz), 4.55—5.45 (1H, m), 5.21 (1H, d, *J*=13.5 Hz), 5.25 (2H, s), 5.52 (1H, d, *J*=13.5 Hz), 7.50 (2H, d, *J*=8.5 Hz), 7.67 (2H, d, *J*=8.5 Hz), 8.22 (2H, d, *J*=8.5 Hz). $[\alpha]_D^{24}$ +57.9° (*c*=1.0, $CHCl_3$). *Anal.* Calcd for $C_{29}H_{29}FN_4O_{10}S$: C, 54.02; H, 4.53; N, 8.69. Found: C, 53.79; H, 4.65; N, 8.74.

(5*R*,6*R*)-6-[(*R*)-1-Fluoroethyl]-3-[(2*R*,4*S*)-2-hydroxymethylpyrrolidin-4-yl]thio-7-oxo-1-azabicyclo[3.2.0]hept-2-ene-2-carboxylic Acid (7e) Under the same reaction conditions as for **7ab**, 456 mg of *p*-nitrobenzyl ester **6e** was hydrogenated to produce 97 mg of **7e** (42% yield) as a colorless powder. IR (KBr): 1768 cm^{-1}. UV $\lambda_{max}^{0.01\,M\,PBS\,(pH\,7.0)}$ nm (ε): 298.5 (10000). ^{1}H-NMR (D_2O) δ: 1.42 (3H, dd, *J*=6.0, 24.5 Hz), 2.05—2.45 (2H, m),

3.21 (2H, d, J=9.0 Hz), 3.3—4.15 (7H, m), 4.26 (1H, dt, J=3.0, 9.0 Hz), 4.7—5.5 (1H, m). $[\alpha]_D^{24}$ +55.6° (c=1.0, H_2O).

(5*R*,6*R*)-6-[(*R*)-1-Fluoroethyl]-3-[(2*R*,4*S*)-1-acetoimidoyl-2-hydoroxymethylpyrrolidin-4-yl]thio-7-oxo-1-azabicyclo[3.2.0]hept-2-ene-2-carboxylic Acid (7f) Ethyl acetimidate hydrochloride (72 mg) was slowly added at 0 °C to a solution of 38 mg of the pyrrolidine derivative **7e** in 15 ml of a 0.1 M phosphate buffer, pH 8.4, while the pH of the mixture was maintained in the range from 8.5 to 9.0 with 1 N NaOH. After stirring for 30 min, the pH of the reaction mixture was adjusted to 8.0 with 1 N HCl. The solution was subjected to column chromatography on Diaion CHP-20P, giving 31 mg of **7f** (72% yield) as a colorless powder. IR (KBr): 1768 cm^{-1}. UV $\lambda_{max}^{0.01\,M\,PBS\,(pH\,7.0)}$ nm (ε): 295.5 (11000). ^{1}H-NMR (D_2O) δ: 1.42 (3H, dd, J=6.0, 24.0 Hz), 1.95—2.55 (2H, m), 1.27 and 1.37 (total 3H, s and s), 3.22 (2H, d, J=9.0 Hz), 3.4—4.25 (7H, m), 4.27 (1H, dt, J=3.0, 9.0 Hz), 4.65—5.55 (1H, m). $[\alpha]_D^{24}$ +37.5° (c=1.0, H_2O).

(5*R*,6*R*)-6-[(*R*)-1-Fluoroethyl]-3-[(2*S*,4*S*)-2-hydroxymethylpyrrolidin-4-yl]thio-7-oxo-1-azabicyclo[3.2.0]hept-2-ene-2-carboxylic Acid (7g) Under reaction conditions similar to those for **7e**, **7g** was given as a colorless powder. IR (KBr): 1765 cm^{-1}. UV $\lambda_{max}^{0.01\,M\,PBS\,(pH\,7.0)}$ nm (ε): 298.5 (12000). ^{1}H-NMR (D_2O) δ: 1.40 (3H, dd, J=6.0, 25 Hz), 1.6—2.0 (1H, m), 2.4—4.05 (10H, m), 4.23 (1H, dt, J=3.0, 9.0 Hz), 4.65—5.4 (1H, m).

Biological Assays Antimicrobial activities against gram-positive and gram-negative bacteria were determined by the standard agar dilution technique using Mueller-Hinton agar (Difco Co.).[2]

Time course assay of relative DHP-I stability of a carbapenem derivative at 37 °C was run by UV-tracing the reaction mixture containing 0.2 ml of 100 μg/ml of PS-5 (reference carbapenem) (or a carbapenem derivative at the corresponding concentration) and 0.2 ml of a kidney homogenate (man, dog or mouse kidney homogenate) at 300 nm (for PS-5) or appropriate wavelengths (Table II).[3] Comparative DHP-I stability assay in Table III was carried out at 37 °C for 60 min by incubating 0.1 ml each of a test carbapenem solution (PS-5 at 100 μg/ml and other carbapenem derivatives at equivalent concentrations) and 0.1 ml of dog DHP-I homogenate in a 0.1 M Tris–HCl buffer, pH 7.0. After being heated at 100 °C for 15 s, the concentration of the carbapenem derivative remaining in the reaction mixture was bioassayed by the disc agar diffusion method using *Comamonas terrigena* B996.[3]

Acknowledgement The authors are grateful to Prof. Yasuji Yamada, Tokyo College of Pharmacy, for his valuable advice.

References and Notes

1) Present address: *Bristrol-Myers Research Institute, Ltd., Tokyo Research Center, 2–9–3 Shimo-meguro, Meguro-ku, Tokyo 153, Japan.*
2) *a*) K. Okamura, S. Hirata, Y. Okumura, Y. Fukagawa, Y. Shimauchi, K. Kouno, T. Ishikura and J. Lein, *J. Antibiot.*, **31**, 480 (1978); *b*) N. Shibamoto, A. Koki, M. Nishino, K. Nakamura, M. Okabe, R. Okamoto, Y. Fukagawa, Y. Shimauchi, T. Ishikura and J. Lein, *ibid.*, **33**, 1128 (1980); *c*) T. Yoshioka, I. Kojima, K. Isshiki, A. Watanabe, Y. Shimauchi, M. Okabe, Y. Fukagawa and T. Ishikura, *ibid.*, **36**, 1473 (1983).
3) *a*) M. Sakamoto, H. Iguchi, K. Okamura, S. Hori, Y. Fukagawa, T. Ishikura and J. Lein, *J. Antibiot.*, **32**, 272 (1979); *b*) M. Sakamoto, I. Kojima, M. Okabe, Y. Fukagawa and T. Ishikura, *ibid.*, **35**, 1264 (1982); *c*) K. Yamamoto, T. Yoshioka, Y. Kato, K. Isshiki, M. Nishino, F. Nakamura, Y. Shimauchi, and T. Ishikura, *ibid.*, **36**, 407 (1983); *d*) M. Sakamoto, K. Yamamoto, K. Isshiki, H. Tone, T. Ishikura, Y. Fukagawa and T. Yoshioka, *Chem. Pharm. Bull.*, **39**, 341 (1991).
4) F. M. Kahan, H. Kropp, J. G. Sundelof and J. Birnbaum, *J. Antimicrob. Chemother.*, **12**, Suppl. 1 (1983).
5) *a*) C. P. Mak and H. Fliri, U.S. Patent 4720490 (1988); *b*) C. P. Mak and K. Wagner, "Recent Advances in the Chemistry of Beta-Lactam Antibiotics," 3rd International Symposium 1984, ed. by A. G. Brown and S. M. Roberts, The Royal Society of Chemistry, 1984, pp. 366—370.
6) D. G. Melillo, I. Shinkai, T. Liu, K. Ryan and M. Sletzinger, *Tetrahedron Lett.*, **21**, 2783 (1980).
7) T. Yoshioka, A. Watanabe, N. Chida and Y. Fukagawa, *J. Antibiot.*, **42**, 1520 (1989).
8) R. W. Ratcliffe, T. N. Salzman and B. G. Christensen, *Tetrahedron Lett.*, **21**, 31 (1980).
9) A. Watanabe, Y. Fukagawa, T. Ishikura and T. Yoshioka, *Bull. Chem. Soc. Jpn.*, **60**, 2091 (1987).
10) Personal communication from C. P. Mak and H. Fliri.
11) T. Miyadera, Y. Sugimura, T. Hashimoto, T. Tanaka, K. Iino, T. Shibata and S. Sugawara, *J. Antibiot.*, **36**, 1034 (1983).
12) G. Emmer, P. Kneussel, J. Haselberandt, F. Turnowsky, A. Haselberger, A. Wenzel and P. Stutz, *J. Antibiot.*, **38**, 1371 (1985).
13) Y. Ueda and V. Vinet, *Can. J. Chem.*, **64**, 2186 (1986).

Kinetic Analysis of Dehydropeptidase-I and Comparative *in Vitro* and *in Vivo* Stabilities of PS-5 Derivatives Modified at the C-3 Side Chain

Michiko SAKAMOTO,* Ken-ichi YAMAMOTO, Kunio ISSHIKI, Hiroshi TONE, Tomoyuki ISHIKURA, Yasuo FUKAGAWA[1)] and Takeo YOSHIOKA

MERCIAN Corporation, Central Research Laboratories, 9–1 Johnan 4-chome, Fujisawa 251, Japan. *Received March 30, 1990*

With partially purified kidney dehydropeptidase-I (DHP-I) preparations, the hydrolysis kinetics of glycyldehydrophenylalanine (Gly-dPh) by DHP-I were found to be completely non-Michaelian, whereas those of PS-5 and imipenem were composed of at least two-phase reactions which were also observed using *Bacillus cereus* type II β-lactamase. Thus the DHP-I stabilities of 34 PS-5 carbapenem derivatives which were synthesized by chemical modification at the C-3 side chain of PS-5 were examined *in vitro* using fresh mouse, dog and human DHP-I preparations, and are tentatively expressed in reference to the DHP-I stabilities of PS-5. The *in vitro* DHP-I stability of PS-5 was significantly improved by introduction of basic side chains and cysteines at C-3. More particularly, the D-cysteinyl side chain was more stable relative to DHP-I than the L-cysteinyl. *In vivo*, however, the degree of improvement of the DHP-I-stability by chemical modification at C-3 was not sufficient enough to establish therapeutically effective levels of serum concentrations and urinary recoveries of the carbapenem derivatives after parenteral administration.

Keywords carbapenem antibiotic; PS-5; dehydropeptidase-I; glycyldehydrophenylalanine; Michaelis–Menten equation; enzyme kinetic; *B. cereus* type II β-lactamase

In a previous paper,[2)] the antimicrobial activities of 34 PS-5 carbapenem derivatives which possessed chemically-modified C-3 side chains were examined, revealing that the D-cysteinyl and 4-pyridylthio side chains were the best for the antibacterial activities against gram-negative and gram-positive bacteria, respectively. For these PS-5 carbapenem derivatives to be clinically useful, their *in vitro* and *in vivo* stabilities to dehydropeptidase-I (DHP-I)[3)] are also essential so that plasma levels may be kept satisfactorily high for a sufficient period of time after administration.

The present paper describes that the time course of hydrolysis of glycyldehydrophenylalanine (Gly-dPh)[4)] by DHP-I did not fit to the Michaelian kinetics; and that the hydrolysis of carbapenems by DHP-I showed at least a two-phase reaction pattern, indicating the conventional kinetic evaluation was inapplicable to DHP-I. *Bacillus cereus* type II β-lactamase was also found to hydrolyze benzylpenicillin, cephalothin, PS-5 and imipenem in two-phase reaction patterns. Accordingly the DHP-I stabilities of the 34 PS-5 carbapenem derivatives and related carbapenem compounds were determined *in vitro* relatively by using reference substrate PS-5 and fresh mouse, dog and human DHP-I preparations; and *in vivo* by pharmacokinetic studies in mice after intravenous or subcutaneous administration.

Materials and Methods

Gly-dPh, PS-5 Carbapenem Derivatives and Related Carbapenem Compounds Gly-dPh, the standard substrate for DHP-I, was prepared according to the procedure of Price.[4)] PS-5,[5)] thienamycin (THM)[6)] and the OA-6129 series of carbapenems[7)] were produced by fermentation. The C-3 side chain-modified PS-5 derivatives were described in a previous paper (for chemical structures see Table I). Imipenem (IPM)[8)] and 88617 (Fig. 7)[9)] were synthesized as reported in previous papers.

Fresh Kidney DHP-I Homogenates Fresh mouse, dog, hog, monkey (crab eating macaque), and human kidneys were homogenized in 5 volumes of buffer (1/100 M phosphate buffer saline (PBS), pH 7.0) with a Teflon Potter homogenizer. Refrigerated centrifugation at $8000 \times g$ for 20 min yielded the supernatant which was used as crude DHP-I or stored at −20 °C.

***In Vitro* DHP-I Stability Tests by DHP-I Homogenates** Because no theoretical base of objective comparison is available (see the text), PS-5 was included as reference carbapenem substrate for relative comparison of DHP-I stabilities in every run of the tests. Assay mixtures containing 0.1 ml of a test carbapenem solution (100 μg/ml) and 0.1 ml of a DHP-I homogenate were incubated at 37 °C for 60 min. Reaction was terminated by heating at 100 °C for 15 s. The concentration of the unreacted carbapenem in the assay mixture was bioassayed by the disc-agar diffusion method using *Comamonas terrigena* B-996 as assay organism. In numeric comparison, relative DHP-I stabilities of carbapenem compounds were expressed in relation to the DHP-I stability of PS-5 (1.0). Accordingly a ratio above 1.0 means that the carbapenem concerned is more stable than PS-5 to DHP-I and *vice versa*.

Solubilization of DHP-I from Kidney Acetone Powders The following kidney acetone powders were purchased from Sigma Chemical Co.: dog (K7625), horse (K7875), porcine type II (K7250), rat (K9125) and mouse (K7750). A kidney acetone powder (500 mg) was suspended in 50 ml of 1/20 M Tris–HCl buffer, pH 7.0, containing 20% *n*-BuOH, and stirred vigorously for 60 min at 5 °C. After dialysis in the same buffer without *n*-BuOH, the suspension was centrifuged at $10000 \times g$ for 20 min to give the supernatant or partially purified DHP-I preparation which was used for spectrophotometric enzyme kinetic studies.

Kinetic Analysis of DHP-I Computer-controlled ultraviolet (UV)-visible spectrophotometers (Hitachi double-beam UV-visible spectrophotometer 200-10 and Shimadzu UV-visible recording spectrophotometer UV-2100) equipped with thermostatted cuvette holders were employed. The assay was started by adding partially purified DHP-I to a substrate solution in a 3-ml cuvette; and the time course of absorbance (A) change at an assay wavelength was traced at preset time intervals. In this paper, the following differential molar extinction constants (ε) were employed: $8120\ M^{-1}cm^{-1}$ at 301 nm for PS-5, $14370\ M^{-1}cm^{-1}$ at 275 nm for Gly-dPh, $7600\ M^{-1}cm^{-1}$ at 300 nm for imipenem and 88617, $636\ M^{-1}cm^{-1}$ at 240 nm for benzylpenicillin, and $3840\ M^{-1}cm^{-1}$ at 280 nm for cephalothin. Absorbance readings collected were converted to molar substrate concentrations by the final-absorbance method that uses as zero the final absorbance reading at the completion of the assay.[10)] The time-molar substrate concentration data were combined by the constant-difference, constant-point or all-combination method for calculation of one set of K_m and V_{max} by the integrated form of the Lineweaver–Burk plot,[11)] Scatchard plot,[11)] Hanes–Woolf plot,[11)] direct linear plot,[12)] non-linear regression method[13)] or Bannister method.[14)]

***Bacillus cereus* Type II β-Lactamase** Type II β-lactamase of *B. cereus* 569 (ATCC 27348) was purified by the method of Davis *et al.*[15)]

Enzyme Kinetic Data 1. Dog DHP-I [Gly-dPh $\varepsilon = 14370\ M^{-1}cm^{-1}$ at 275 nm, 37 °C, 0.1 M MOPS, pH 7.0; A 2.6079 (10 s), 2.0194 (110), 1.7794 (210), 1.5722 (310), 1.3757 (410), 1.1712 (510), 0.9563 (610), 0.7415 (710), 0.5340 (810), 0.3475 (910), 0.2108 (1010), 0.1304 (1110), 0.0971 (1210), 0.0862 (1310), 0.0834 (1410); final $A = 0.0805$].

2. Dog DHP-I [PS-5 $\varepsilon = 8120\ M^{-1}cm^{-1}$ at 301 nm, 37 °C, 0.1 M MOPS, pH 7; A 0.5998 (10.5 s), 0.4730 (20.17), 0.3731 (30.32), 0.3025 (40.48), 0.2580 (50.15), 0.2276 (60.3), 0.2089 (70.45), 0.1991 (80.13), 0.1928 (90.28),

0.1900 (100.43), 0.1891 (110.1); final $A=0.1887$].

3. Dog DHP-I [IPM $\varepsilon=7600\,M^{-1}\,cm^{-1}$ at 300 nm, 37 °C, 0.1 M MOPS, pH 7; A 0.9442 (61.02 s), 0.8737 (180.43), 0.7992 (300.32), 0.7361 (420.22), 0.6737 (540.10), 0.5828 (780.38), 0.5579 (900.25), 0.5298 (1020.15), 0.5024 (1140.03), 0.4766 (1260.42), 0.4546 (1380.28), 0.4343 (1500.15), 0.4168 (1620.03), 0.4011 (1740.38), 0.3886 (1860.27), 0.3767 (1980.13), 0.3672 (2100.52), 0.3591 (2220.38), 0.3521 (2340.23), 0.3466 (2460.12), 0.3418 (2580.47), 0.3387 (2700.83), 0.3356 (2821.18), 0.3338 (2940.08); final $A=0.3298$].

4. *B. cereus* type II β-lactamase [benzylpenicillin $\varepsilon=636\,M^{-1}\,cm^{-1}$ at 240 nm, 30 °C, 0.1 M Tris–HCl, pH 7.0; A 0.8010 (30.08 s), 0.7407 (90.45), 0.6848 (150.32), 0.6319 (210.18), 0.5824 (270.05), 0.5358 (330.42), 0.4916 (390.30), 0.4524 (450.17), 0.4166 (511.00), 0.3840 (570.38), 0.3561 (630.27), 0.3324 (690.13), 0.3138 (750.48), 0.3001 (810.35), 0.2904 (870.23); final $A=0.2768$].

Comparative Time Course Assays of Relative DHP-I Stabilities of Carbapenem Derivatives As the routine application of the Michaelis–Menten equation to the kinetic DHP-I stability assay of carbapenem compounds was disapproved (see the text), the time course of absorbance change was graphically shown for ease of visual comparison of the relative DHP-I stability.

A carbapenem substrate in 0.1 M Tris–HCl, pH 7.0, and a partially purified DHP-I preparation were preincubated at 37 °C for 2 min, and then mixed at a ratio of 1 : 1 in a quartz cuvette of 1 mm lightpath. The time course of absorbance change at an assay wavelength was traced at 37 °C at the indicated time intervals in a UV-visible spectrophotometer. For convenience of visual comparison, several time courses of absorbance change were drawn on one sheet of graph paper, referring to the start absorbance readings as 100%.

Plasma Concentrations and Urinary Recoveries of Carbapenem Compounds in Mice A single dose of a carbapenem compound was given subcutaneously or intravenously to a group of 5 male ddY mice (aged 5 weeks, weighing 19—21 g). Blood specimens were collected from the retroorbital sinus at the indicated times with heparinized capillary tubes, and centrifuged at 5000 rpm for 5 min. At 6 h after drug administration, urine samples were recovered from the metabolic cages and bladders. The concentrations of the carbapenem compound in urine and plasma samples were disc-assayed for antimicrobial activity against *Comamonas terrigena* B-996.

Results and Discussion

Optimization of Reaction Conditions for Hydrolysis of PS-5 by DHP-I As previously reported,[16] DHP-I, which is a key enzyme in the renal metabolism of carbapenem compounds, opens the β-lactam ring of carbapenem by the same reaction mechanism as is known for β-lactamase with penicillins and cephalosporins.[17] For quantitative structure–activity relationship studies of carbapenem antibiotics, it is theoretically preferable to use the Michaelian parameters such as K_m, K_i and V_{max} for objective and precise comparison of their DHP-I stabilities. With this purpose in mind, the DHP-I assay conditions for PS-5 were optimized with respect to assay buffer and animal species. 1/10 M Tris–HCl, TES (*N*-tris[hydroxymethyl]methyl-2-aminoethanesulfonate), MOPS (3-[*N*-morpholino]propanesulfonate) and 1/100 M phosphate, pH 7.0, were compared by spectrophotometry, using PS-5 and partially purified hog DHP-I. Figure 1 shows that phosphate is clearly inferior to Tris–HCl, TES and MOPS. As zinc is the cofactor for DHP-I, it seems resonable that phosphate deprives DHP-I of zinc, resulting in the decreased DHP-I activity.

DHP-I enzymes were solubilized from acetone powders of dog, hog, mouse, rat and horse kidneys, and were comparatively assayed with PS-5 and IPM. The assay results revealed that the dog kidney acetone powder had the highest DHP-I activity among the tested preparations.

Reexamination of the Valid Applicability of the Michaelis–Menten Equation to the Kinetic Analysis of Hydrolysis of Gly-dPh by DHP-I DHP-I was discovered by Campbell *et al.*[18] and has been kinetically studied in details by the differential form of the Lineweaver–Burk plot. There are a variety of parameters of DHP-I's reported in the literature. For example, the K_m value of hog DHP-I for Gly-dPh scatters in a range from 0.6 to 2.0 mM,[19,20] and that for imipenem from 1.38 to 16.9 mM.[21,22]

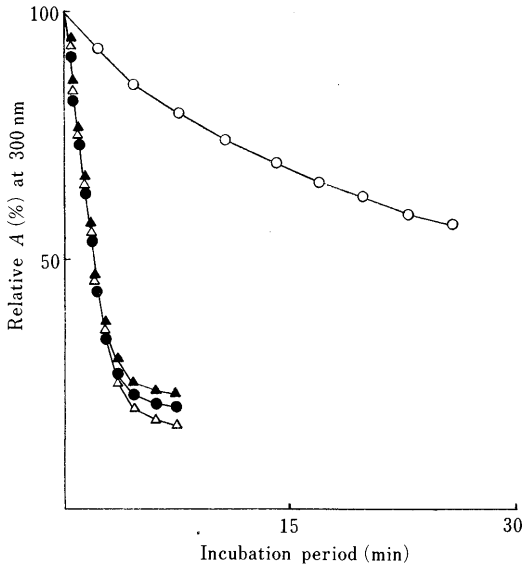

Fig. 1. Comparative Rates of PS-5 Hydrolysis by Hog DHP-I in PBS, Tris–HCl, TES and MOPS (pH 7.0).

—○—, PBS (1/100 M); —▲—, TES (1/10 M); —●—, Tris–HCl (1/10 M); —△—, MOPS (1/10 M).

Recently the present authors have devised a spectrophotometric progress curve assay of enzymes such as β-lactamase using a microcomputer.[12,23] As Gly-dPh is the standard substrate for DHP-I, the progress curve data of hydrolysis of Gly-dPh by hog DHP-I which was reported by Campbell *et al.*[24] was subjected to analysis by the integrated form of the Michaelis–Menten equation (Figs. 2C, C′). In addition, Gly-dPh was assayed by the computer-controlled spectrophotometric assay using mouse DHP-I (Fig. 2A) and dog DHP-I (data set 1; Fig. 2B). Figure 2 compares the Lineweaver–Burk plots of the four assays (Figs. 2A, B, C and D), where the kinetic data are combined at a constant difference of 1 by the constant-difference method. Figure 2A (mouse DHP-I; $S_0=0.12$ mM Gly-dPh) and Fig. 2B (dog DHP-I; $S_0=1.75$ mM Gly-dPh) apparently deny the application of the Michaelian kinetics, whereas Fig. 2C (hog DHP-I; $S_0=0.06$ mM Gly-dPh, Campbell *et al.*) and Fig. 2D (dog DHP-I, $S_0=0.88$ mM Gly-dPh) seemingly fit to the Michaelis–Menten equation. When the same kinetic data as employed in Figs. 2C and 2D are displayed in the −45°-rotated version of the Eadie-Hofstee space (unpublished work; Figs. 2C′ and 2D′) (less suitably, in the Scatchard space, too), the application of the Michaelian kinetics to these data sets is also unambiguously disapproved.

It is important to note that the single use of the Lineweaver–Burk plot sometimes results in the wrong conclusion on account of the error-concealing property of the Lineweaver–Burk transformation which is specifically ascribed to undue weighting on data points. As is the case with Figs. 2B and 2D, D′, the 2-fold difference in the initial

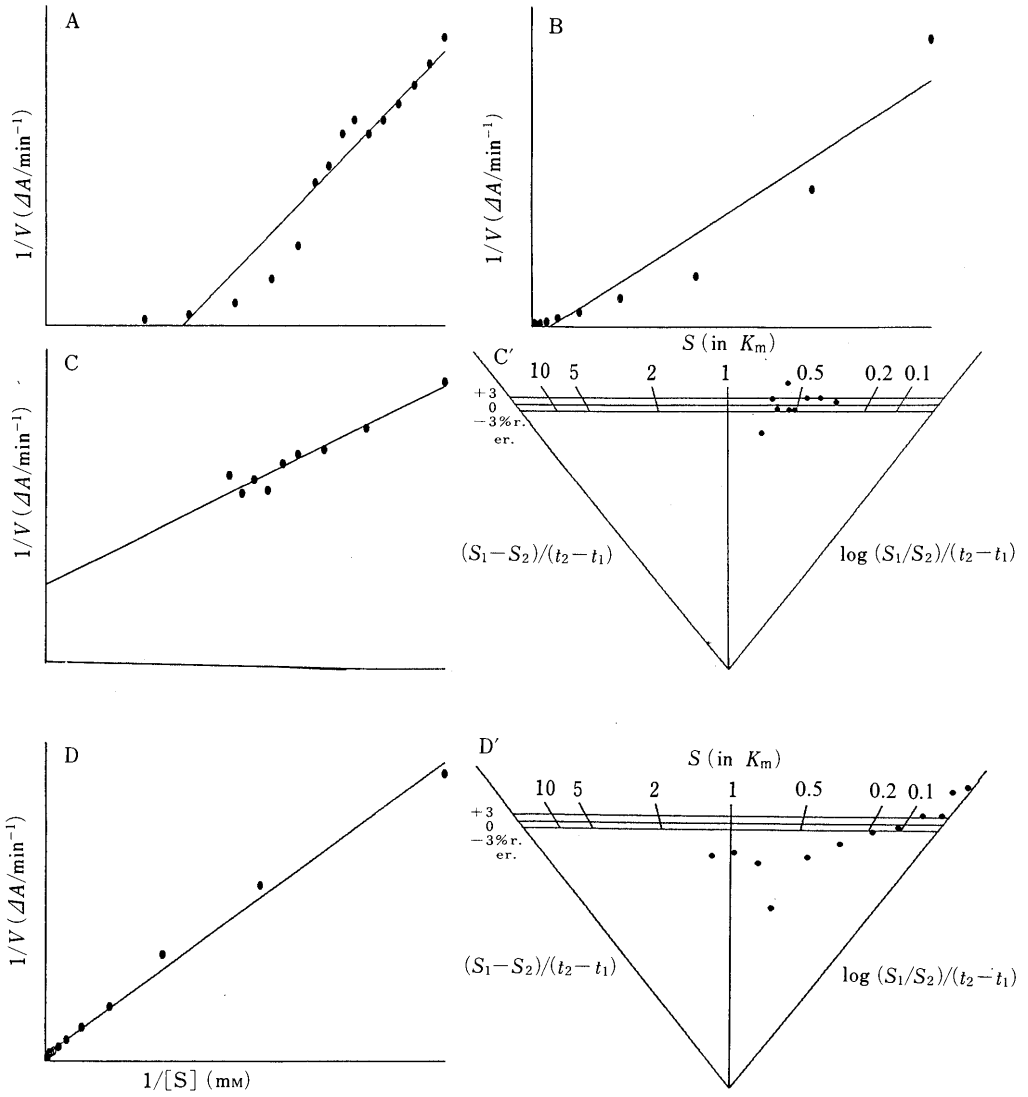

Fig. 2. Kinetic Analysis of Hydrolysis of Gly-dPh by Mouse, Dog and Hog DHP-I

A) Lineweaver–Burk: Constant difference = 1, $K_m = -72.44 \times 10^{-3}$, $V_{max} = -31.60 \times 10^{-6}$, $r = 96.54 \times 10^{-2}$. B) Lineweaver–Burk: Constant difference = 1, $K_m = -22.74 \times 10^{-2}$, $V_{max} = -14.47 \times 10^{-4}$, $r = 96.58 \times 10^{-2}$. C) Lineweaver–Burk: Constant difference = 1, $K_m = 67.66 \times 10^{-3}$, $V_{max} = 24.36 \times 10^{-6}$, $r = 96.56 \times 10^{-2}$. C') Eadie–Hofstee: Constant difference = 1, $K_m = 88.74 \times 10^{-3}$, $V_{max} = 28.92 \times 10^{-6}$, $r = -70.12 \times 10^{-2}$. D) Lineweaver–Burk: Constant difference = 1, $K_m = 13.09 \times 10^{-2}$, $V_{max} = 18.92 \times 10^{-4}$, $r = 99.69 \times 10^{-2}$. D') Eadie–Hofstee: Constant difference = 1, $K_m = 47.63 \times 10^{-2}$, $V_{max} = 54.60 \times 10^{-4}$, $r = -79.30 \times 10^{-2}$.

substrate concentration of Gly-dPh leads to the exactly opposite conclusion. There will be several plausible reasons for the complete deviation of DHP-I from the Michaelian kinetics. One reason which seems probable based on the concave progress line in Fig. 2B is that dehydrophenylalanine, one of the reaction products, is spontaneously converted to the secondary product, accompanied by concomitant inactivation of DHP-I.

Hydrolysis Curves of PS-5 and Imipenem by DHP-I Subsequently PS-5 (data set 3; $S_0 = 0.051$ mM) and IPM (data set 4; $S_0 = 0.081$ mM) were subjected to the spectrophotometric dog DHP-I assay, followed by the progress curve analysis. As is seen with Gly-dPh, the lineweaver–Burk plots (Figs. 3A and 3B) seem to show the valid applicability of the Michaelian kinetics to analysis, whereas the Eadie–Hofstee plots (Figs. 3A′ and 3B′) clearly reveal the invalidity.

Hydrolysis Curves of Benzylpenicillin and PS-5 by *B. cereus* Type II β-Lactamase *B. cereus* type II β-lactamase also requires zinc as the cofactor for enzyme activity, and hydrolyzes carbapenem by the same reaction mechanism as DHP-I. Comparative studies on this β-lactamase and DHP-I's are expected to shed light on the reaction specificity of DHP-I. Figure 4 compares the hydrolysis curves of benzylpenicillin ($S_0 = 0.82$ mM; data set 5; Figs. 4A and 4A′) and PS-5 ($S_0 = 0.07$ mM in 0.1 M MOPS, pH 7.0; Figs. 4B and 4B′) by the type II β-lactamase using the integrated forms of the Lineweaver–Burk and Eadie–Hofstee spaces. This β-lactamase was also concluded not to conform to the Michaelian kinetics.

There is no description available in the literature which indicates the possibility that *B. cereus* type II β-lactamase might not fit the Michaelis–Menten equation in kinetic analysis of hydrolysis of benzylpenicillin, cephalothin and other β-lactam compounds.

Insusceptibility of Gly-dPh to *B. cereus* Type II β-Lactamase Although the type II β-lactamase and DHP-I share several common properties, the finding that Gly-dPh is not susceptible to the β-lactamase suggests some critical difference in the detailed reaction mechanism between these

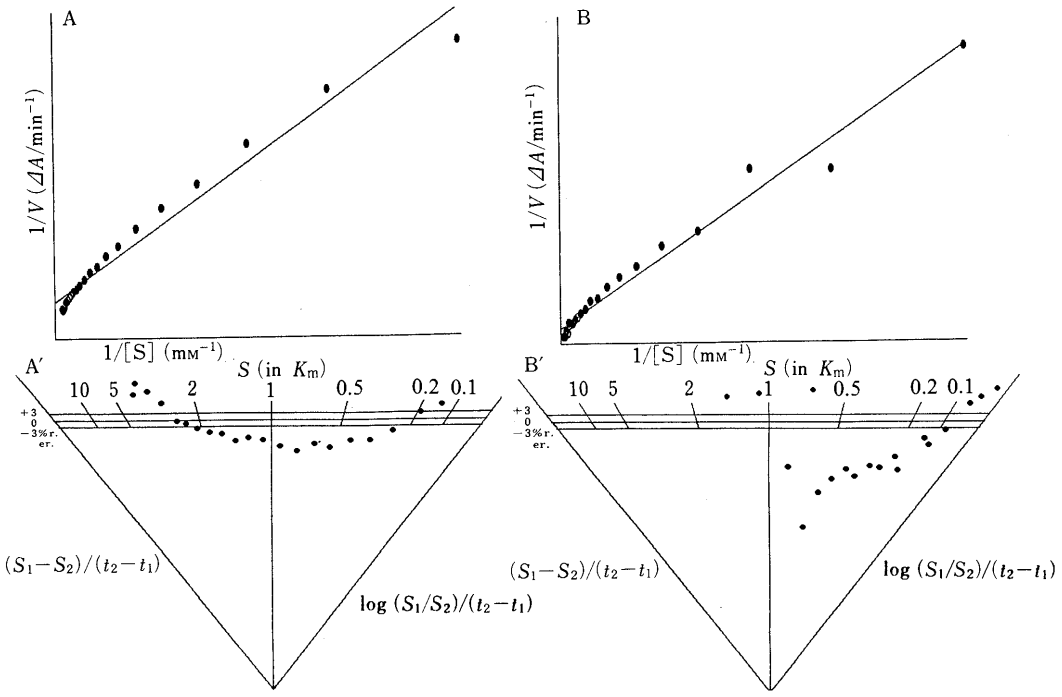

Fig. 3. Hydrolysis of PS-5 (A, A′) and Imipenem (B, B′) by Dog DHP-I

A) Lineweaver–Burk: Constant difference = 1, $K_m = 11.91 \times 10^{-3}$, $V_{max} = 90.33 \times 10^{-5}$, $r = 98.53 \times 10^{-2}$. A′) Eadie–Hofstee: Constant difference = 1, $K_m = 21.28 \times 10^{-3}$, $V_{max} = 12.57 \times 10^{-4}$, $r = -91.65 \times 10^{-2}$. B) Lineweaver–Burk: Constant difference = 1, $K_m = 12.51 \times 10^{-2}$, $V_{max} = 40.90 \times 10^{-5}$, $r = 98.81 \times 10^{-2}$. B′) Eadie–Hofstee: Constant difference = 1, $K_m = 53.18 \times 10^{-2}$, $V_{max} = 12.09 \times 10^{-4}$, $r = -67.05 \times 10^{-2}$.

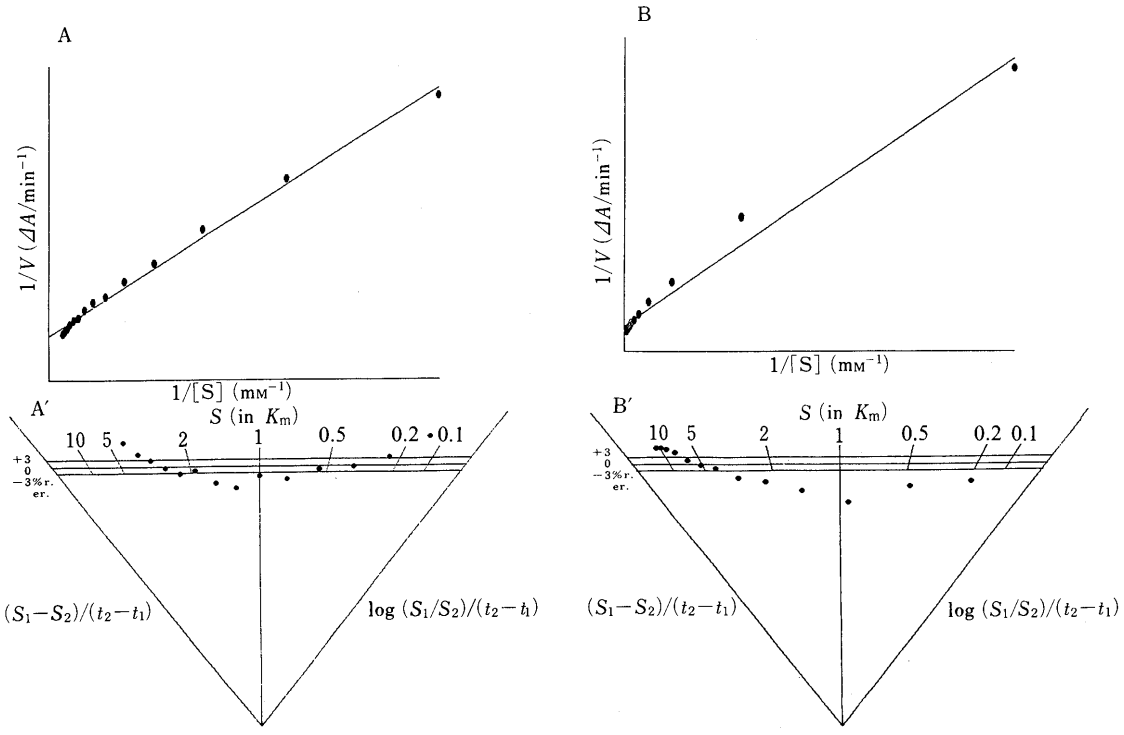

Fig. 4. Hydrolysis Curves of Benzylpenicillin (A, A′) and PS-5 (B, B′) by *B. cereus* Type II β-Lactamase

Lineweaver–Burk: Constant difference = 1, $K_m = 15.61 \times 10^{-2}$, $V_{max} = 16.10 \times 10^{-4}$, $r = 99.70 \times 10^{-2}$. A′) Eadie–Hofstee: Constant difference = 1, $K_m = 19.36 \times 10^{-2}$, $V_{max} = 17.97 \times 10^{-4}$, $r = -97.26 \times 10^{-2}$. B) Lineweaver–Burk: Constant difference = 1, $K_m = 38.00 \times 10^{-4}$, $V_{max} = 20.91 \times 10^{-5}$, $r = 99.07 \times 10^{-2}$. B′) Eadie–Hofstee: Constant difference = 1, $K_m = 61.92 \times 10^{-4}$, $V_{max} = 26.18 \times 10^{-5}$, $r = -94.34 \times 10^{-2}$.

enzymes.

Precise Analysis of the Reaction Progress Curves of PS-5 and Benzylpenicillin by DHP-I and *B. cereus* Type II β-Lactamase It seemed thus useful to comparatively analyze the reaction patterns of PS-5 and benzylpenicillin by these two types of enzymes in detail so that some reason for unapplicability of the Michaelian kinetics to the enzymes might hopefully be found. Figure 5 shows the results of pattern analysis of the four representative cases. The time courses of hydrolysis of PS-5 ($S_0 = 0.12$ and 0.74 mM in

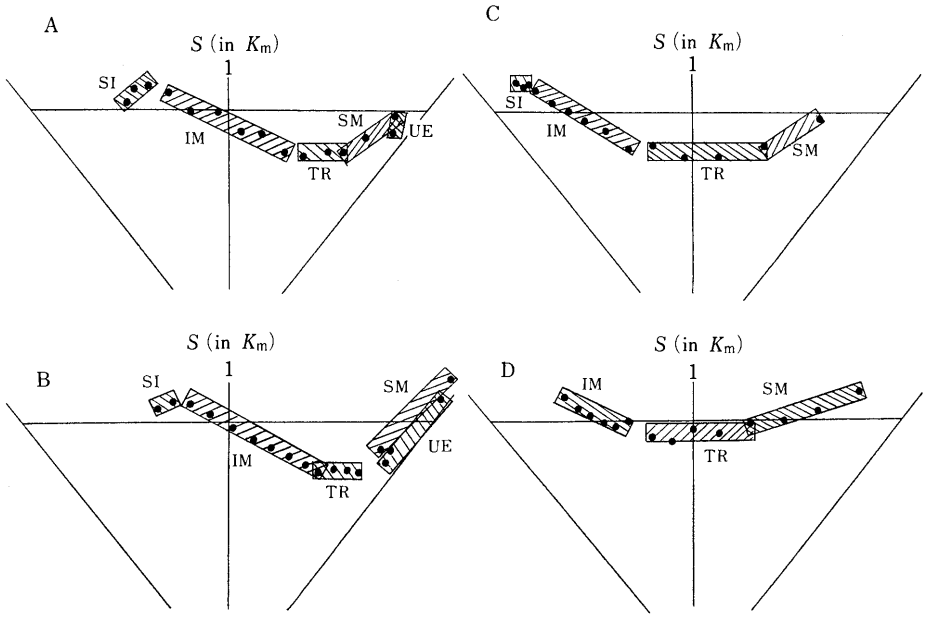

Fig. 5. Precise Analysis of the Reaction Progress Curves of DHP-I and *B. cereus* Type II β-Lactamase (−45°-Roated Version of the Eadie–Hofstee Plot)

A, PS-5: hog DHP-I; B, PS-5: dog DHP-I; C, PS-5: β-lactamase; D, PCG: β-lactamase. 5 Stages of a progress curve: Substrate inhibition (SI), initial Michaelian phase (IM), transition (TR), secondary Michaelian phase (SM) and unsaturated enzyme (UE).

Tris–HCl, pH 7.0, at 37 °C) by hog and dog DHP-I's are shown in Figs. 5A and 5B, and those of PS-5 ($S_0 = 0.067$ mM in 0.1 M TES, pH 7.0, containing 1 mM $ZnSO_4$, at 30 °C) and benzylpenicillin ($S_0 = 0.82$ mM in 0.1 M Tris–HCl, pH 7.0, at 30 °C) by the type II β-lactamase in Figs. 5C and 5D, by the −45°-rotated version of the Eadie–Hofstee plot using the constant-difference method (at a constant difference of 1). In general, each progress curve is divided into 5 stages of substrate inhibition (SI), initial Michaelian phase (IM), transition (TR), secondary Michaelian phase (SM) and unsaturated enzyme (UE). Of course, not all the five stages are always observed in every progress curve, depending on the assay conditions. It is possible that the transition stage be also regarded to be Michaelian, but the present authors prefer to think it non-Michaelian, based on the observation that some assays showed sudden fluctuations in absorbance change specifically only at this stage.

There remains much to be studied about the reaction patterns of DHP-I and *B. cereus* type II β-lactamase, particularly with reference to reaction conditions and the function of the zinc cofactor, because both enzymes are crucially important in metabolism and resistance expression of β-lactam compounds including cabapenems.

Relative Stabilities of Carbapenem Compounds to DHP-I's

Under the circumstances described above, the Michaelian analysis is meaningless to express the DHP-I stability of a carbapenem compound in an objective term such as K_m and K_i. For convenience of relative comparison in number, the DHP-I stability of a carbapenem derivative is expressed tentatively in relation to that of PS-5 as 1.0. The results of assays by mouse, dog and human fresh DHP-I homogenates are contained in Table I. The PS-5 derivatives were substantially inferior to THM and IPM in stability to mouse DHP-I; but the advantage of THM and IPM over PS-5 disappeared in stability to human DHP-I. Among the tested C-3 side chains, aminoethylthio (derivative **5**; NS-5) and 6-aminopenicillanyl (derivative **25**) were comparable to

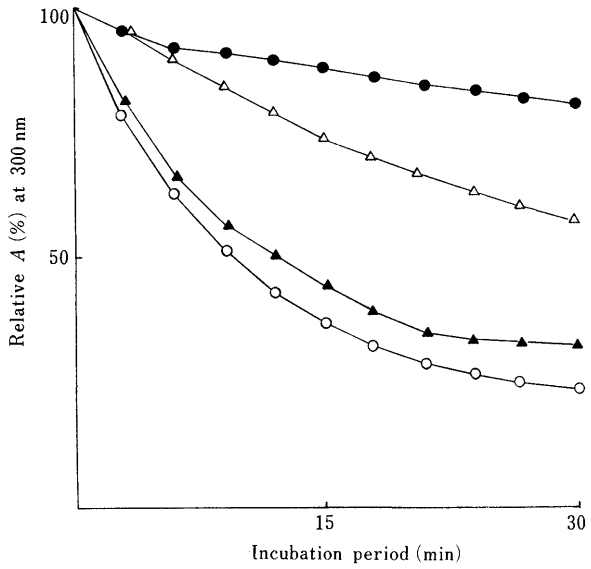

Fig. 6. Comparative Stabilities of PS-5 (—○—), OA-6129A (—▲—), OA-6129B_2 (—△—) and OA-6129C (—●—) to Dog DHP-I in 1/100 M PBS, pH 7.0

OA-6129 carbapenems

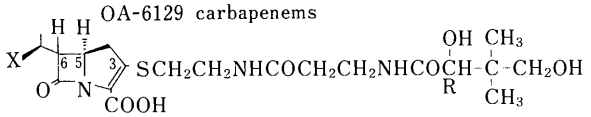

X	C_5–C_6	C_6	compound
H	*trans*	*R*	OA-6129A
OH	*trans*	*S*	OA-6129B_2
OSO_3H	*cis*	*R*	OA-6129C

THM and IPM in *in vitro* stability to human DHP-I. D-Cysteinyl side chain (**11**) was more stable to DHP-I than the L-cysteinyl side chain (**10**). As explained above, however, it is improbable that the *in vitro* DHP-I stability data of carbapenem derivatives can be extrapolated to predict their *in vivo* stabilities and clinical efficacy. Derivatives **11** and

TABLE I. Structures and Relative Stabilities of 35 *S*-Substituted Carbapenem Derivatives to Mouse, Dog. and Man DHP-I's Homogenates

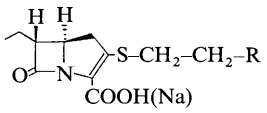

1—9

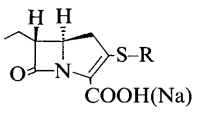

10—19, 27—35

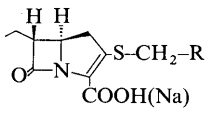

20—26

No.	R	Mouse	Dog	Man
1	$-NHCOCH_3$(=PS-5)	1.0	1.0	1.0
2	$-CH_2-CH_3$	—	—	—
3	$-OH$	0.0	—	—
4	$-COOH$	0.7	0.8	0.4
5	$-NH_2$	13.4	5.3	4.5
6	$-N(CH_3)_2$	0.0	—	—
7	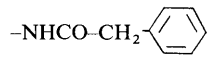	1.7	—	—
8	$-NHPO(OH)_2$	13.8	5.3	2.3
9		0.6	—	—
88617		25.9	4.6	4.2
THM		24.8	2.6	4.1
IPM		44.0	5.5	4.8
10	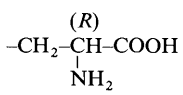	4.5	1.4	1.7
11	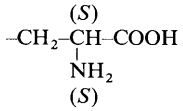	7.7	1.7	2.3
12	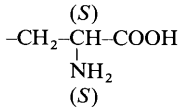	2.7	2.5	1.8
13	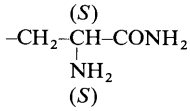	4.1	1.0	1.4
14	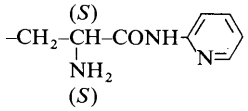	0.8	0.3	0.7
15	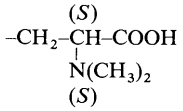	2.7	2.3	2.7
16	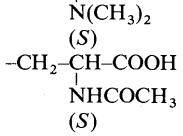	0.0	0.0	1.6
17	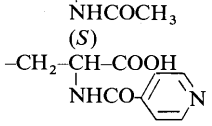	0.0	0.0	1.1
18	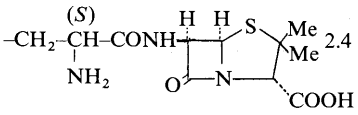	2.4	3.4	2.2
19	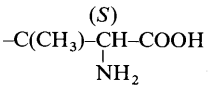	5.6	3.6	2.9
20		1.3	—	—
21		0.0	—	—
22		—	—	—
23	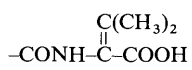	0.0	0.8	1.3
24	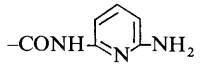	0.4	0.5	2.6
25	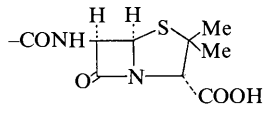	37.0	—	4.9
26	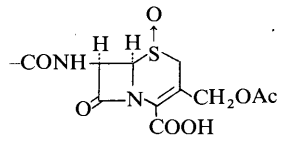	1.0	2.0	2.0
27		2.1	—	—
28		1.1	—	—
29		21.2	—	0.8
30		21.6	—	1.3
31	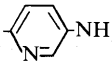	0.8	—	—
32		0.8	—	2.5
33	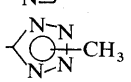	—	—	—
34	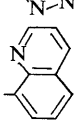	1.1	—	—
35	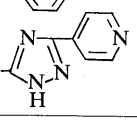	4.4	—	—

—: Not tested.

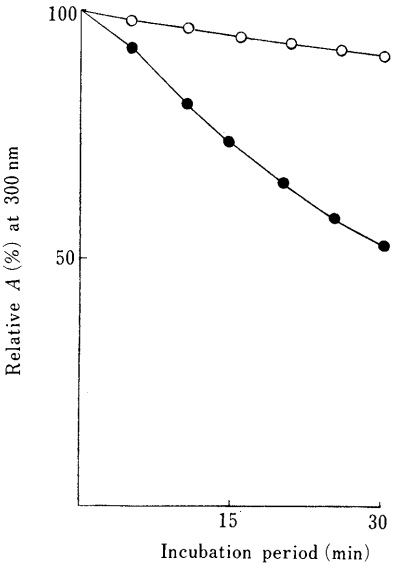

Fig. 7. Comparative Stabilities of 88617 (—○—) and Imipenem (—●—) to the Partially Purified Dog DHP-I Preparation in 1/10 M MOPS, pH 7.0

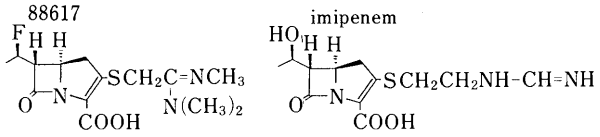

30 which seemed promising from the viewpoint of antimicrobial activity[2] were clearly concluded to be unsatisfactorily stable to DHP-I.

Figure 6 illustrates the effects of the C-6 side chains on DHP-I stability, revealing that, when the C-3 side chain was limited to pantetheinyl, sulfonylethyl (OA-6129C) was the most stable to DHP-I, and ethyl (OA-6129A) the least. Contrary to the authors' expectation, hydroxyethyl (OA-6129B$_2$) was significantly better than ethyl (OA-6129A). The importance of the C-6 side chain on the DHP-I stability is also demonstrated in Fig. 7, where the C-6 fluoroethyl group (carbapenem 88617) is compared with the C-6 hydroxyethyl group (IPM) by dog DHP-I, indicating that the stereospecific introduction of fluorine at C-8 was very effective to stabilize carbapenem to DHP-I, although they differed slightly in the C-3 side chain.

Plasma Levels and Urinary Recoveries of Carbapenem Derivatives in Mice The pharmacokinetic parameters and urinary recoveries of carbapenem derivatives which were determined in mice after subcutaneous or intravenous administration are summarized in Table II. Some of the C-3 side chain-modified PS-5 derivatives were not tested on account of no sample supply. Mice have very strong DHP-I activity and seem to significantly differ from human in the activity and substrate profile of the enzyme. Thus it seems difficult to reach by conjecture the therapeutic effects of carbapenem derivatives only from the results in Table II, but, in general, the PS-5 derivatives had shorter half lives than IPM after intravenous administration. IPM combined with cilastatin, a DHP-I inhibitor, is the sole carbapenem drug available on the market. It is probable, however, that carbapenem derivatives which are clinically useful must have better DHP-I stabilities and urinary recoveries than THM and IPM. The *in vivo* results in Table II, and the antibacterial evaluation[2] yield a conclusion that the 34 PS-5 derivatives having modified C-3 side chains are not clinically useful.

TABLE II. Plasma Levels and Urinary Recoveries of PS-5 and Related Derivatives after Single s.c. or i.v. Administration in Mice ($n=5$)

No.	Dose (mg/kg)	Route: s.c.		Route: i.v.		
		C_{max} (μg/ml)	U.R. (%)	C_{max} (μg/ml)	$T_{1/2}$ (min)	U.R. (%)
1 (=PS-5)	50	18.7	0.07			
	100	40.2	0.10	70.9	1.3	0.09
	200	56.6	0.10	149	1.5	0
3	200	73.8	0.04			
5	100	23.2	0	101.2	1.5	0.48
6	200	72.4	0.63			
7	100	2.8	0			
8	100	41.6	1.65	108	1.5	6.0
9	100	16.8	0.04			
11	100	21.6	0.6	62.4	1.0	3.6
12	100			263	1.5	1.25
13	100			56.9	1.0	0
14	100			90.8	1.2	0.11
15	100			45.9	1.2	0.2
16	200			69.4	1.0	0.13
17	200			282	1.8	0.2
21	100	42.0	0.02			
25	100			84.2	4.0	6.8
27	100	8.2	0.09			
28	100	11.3	0.2			
29	100	48.4	0.06	51.4	7.7	0.49
30	100	70.7	1.6			
32	100	23.6	0.2			
33	100	28.2	1.45			
34	100	0	0			
35	100	32.3	1.2			
THM	50	36.8	5.8			
IPM	20	19.6	N.T.	31.7	7.0	N.T.

C_{max}: maximum plasma level; $T_{1/2}$: plasma half life; U.R.: urinary recovery N.T.: not tested.

References and Notes

1) Present address: *Bristol-Meyers Research Institute, Ltd., Tokyo Research Center, 2-9-3 Shimo-meguro, Meguro-ku, Tokyo 153, Japan.*
2) M. Sakamoto, K. Yamamoto, K. Isshiki, T. Ishikura, Y. Fukagawa and T. Yoshioka, *J. Antibiot.*, **43**, 1254 (1990).
3) B. J. Campbell, "Method in Enzymology," Vol. 19, ed. by G. E. Perlman and L. Lorand, Academic Press, New York, 1970, pp. 722—729.
4) V. E. Price and J. P. Greenstein, *J. Biol. Chem.*, **171**, 477 (1947).
5) K. Okamura, A. Koki, M. Sakamoto, K. Kubo, Y. Mutoh, Y. Fukagawa, K. Kouno, Y. Shimauchi and T. Ishikura, *J. Ferm. Technol.*, **57**, 262 (1979).
6) J. S. Kahan, F. M. Kahan, R. Geogelman, S. A. Currie, M. Jackson, E. O. Stapley, T. W. Miller, A. K. Miller, D. Hendlin, S. Mochales, S. Hernandes, H. B. Woodruff and J. Birmbaum, *J. Antibiot.*, **32**, 1 (1979).
7) M. Okabe, S. Azuma, I. Kojima, K. Kouno, R. Okamoto, Y. Fukagawa and T. Ishikura, *J. Antibiot.*, **35**, 1255 (1982).
8) W. J. Leanza, K. J. Windonger, T. W. Miller and B. G. Christensen, *J. Med. Chem.*, **22**, 1435 (1979).
9) C. P. Mak and H. Fliri, U.S. Patent 4720490 (1988).
10) Y. Fukagawa, *Biochem. J.*, **185**, 186 (1980).
11) I. H. Seagel, "Enzyme Kinetics," John Wiley and Sons, Inc., New York, 1975, p. 44 and p. 208.
12) Y. Fukagawa, M. Sakamoto and T. Ishikura, *Agric. Biol. Chem.*, **49**, 835 (1985).
13) R. G. Duggleby, *Anal. Biochem.*, **110**, 9 (1981).
14) W. H. Bannister, A. Anastasi and J. V. Bannister, *FEBS Lett.*, **64**,

290 (1976).
15) R. B. Davis and E. P. Abraham, *Biochem. J.*, **143**, 129 (1974).
16) N. Shibamoto, M. Sakamoto, Y. Fukagawa and T. Ishikura, *J. Antibiot.*, **35**, 729 (1982).
17) N. Shibamoto, T. Yoshioka, M. Sakamoto, Y. Fukagawa and T. Ishikura, *J. Antibiot.*, **35**, 736 (1982).
18) B. J. Campbell and Y-C. Lin and E. Ballew, *J. Biol. Chem.*, **242**, 930 (1967).
19) D. W. Graham, W. T. Ashton, L. Barash, J. E. Brown, R. D. Brown, L. F. Canning, A. Chen, J. P. Springer and E. F. Rogers, *J. Med. Chem.*, **30**, 1074 (1987).
20) C. A. Farrell, N. J. Allegretto and M. J. M. Hitchkock, *Arch. Biochem. Biophys.*, **256**, 253 (1987).
21) H. S. Kim and B. J. Campbell, *Biochem. Biophys. Res. Commun.*, **29**, 1638 (1982).
22) H. Mikami, M. Ogashima, Y. Saino, M. Inoue and S. Mitsuhashi, *Antimicrob. Agents Chemother.*, **22**, 693 (1982).
23) Y. Fukagawa, M. Sakamoto and T. Ishikura, "Recent Advances in the Chemistry of β-Lactam Antibiotics," ed. by A. G. Brown and M. Roberts, The Royal Society of Chemistry, London, 1984, p. 381.
24) B. J. Campbell, W. H. Yudkin and I. M. Klotz, *Arch. Biochem. Biophys.*, **92**, 257 (1963).

Procedures on the Estimation of the Novel Quantitative Structure–Activity Relationship (QSAR) Descriptor σ_{s° for Poly-Substituted Benzene Series, and Their Polarizabilities

Yoshio SASAKI,[a] Hideko KAWAKI,[b] and Tatsuya TAKAGI*,[a]

Faculty of Pharmaceutical Sciences, Osaka University,[a] 1–6 Yamada-Oka, Suita, Osaka 565, Japan and Faculty of Pharmacy, Kinki University,[b] 3–4–1 Kowakae, Higashi-Osaka, Osaka 577, Japan. *Received June 13, 1990*

Procedures for the estimation of the novel quantitative structure–activity relationship (QSAR) descriptor σ_{s°, representing the contributions from both dispersion and repulsion interactions, have been presented for the poly-substituted benzene derivatives.

Observed values σ_{s° for $C_6H_{6-n}R_n$ (R=F, Cl, Me, Et: $n=2$—6) can be given by the equation $\sigma_{s^\circ}(R_n)=a\log n+b$, where the slope a and the intercept b are also linear against σ_{s°(mono). Consequently, the slope a and the intercept b estimated from σ_{s°(mono) and $\log n$ afford σ_{s° for poly-substituted benzene derivatives having an optional set of substituent groups. The values thus obtained agreed well with the observed ones, and were also found to be linear against $\Sigma\sigma_{s^\circ}$(mono), where the correction of the number of symmetry should be taken into account.

Furthermore, the net increases of polarizabilities $\Delta\alpha$ for the tetra-, penta-, and hexa-substituted benzene series from benzene reference are approved to be expressed by the linear relation against $\Sigma\Delta\alpha$(mono).

Keywords quantitative structure–activity relationship; entropy constant σ_{s°; poly-substituted benzene derivative; polarizability α; regression analysis

Introduction

In previous reports[1a–c] on the studies of the estimation of our novel quantitative structure–activity relationship (QSAR) descriptors σ_{s°, the authors determined those of mono-, di-, and tri-substituted benzene derivatives where linear relations among the observed or estimated descriptors σ_{s° and $\Sigma\sigma_{s^\circ}$(mono) were acknowledged.

In this work, in order to determine the values of σ_{s° for the poly-substituted benzene series, the authors have utilized the linear relations between $\sigma_{s^\circ}(R_n)$ ($n=2$—6, R=F, Cl, Me, Et) and $\log n$, where n denotes the number of the substituent. The slope and the intercept determined in the above four series were also found to be linear against σ_{s°(mono). The determination of the two factors written above enabled us to estimate the descriptor $\sigma_{s^\circ}(R_n)$.

In addition, the polarizabilities α for the polysubstituted benzene series have been approved as a linear function of $\Sigma\Delta\alpha$(mono) from benzene reference.

Experimental

Descriptor σ_{s° Observed data for mono- and poly-substituted benzene series were determined from S°_{298}(g) data sources[2a–e] by the usual way.

Polarizability α Polarizability/10^{-24} cm^3 was derived from the Clausius–Mossotti's equation $\alpha=n^2-(1/n^2)+2\cdot(M/d)\cdot\{3/(4N)\}$, where refractive index n and density d were cited from the references.[3a,b]

Regression Analyses Regression analyses were carried out on NEC PC-9801/M/VX and EPSON PC-286V personal computers using a program package for multi-variate analyses, MVA developed by Takagi *et al.*[4]

Results and Discussion

Descriptor σ_{s° for $C_6H_{6-n}R_n$ In the first step of this work, the two procedures written below were employed; (1) The parametrization of $\sigma_{s^\circ}(n)=\log a+b\log n+2.303cn$, supposing the curve-fitting on an equation expressed by $\sigma_{s^\circ}(n)=an^be^{cn}$, where n means the number of the substituent group. (2) The parametrization by $\sigma_{s^\circ}(n)=a=\log n$, $n\geq 2$, based on the relation $S^\circ_{298}(g)^{1/2}\propto n^{1/2}$, where the number $n=1$—6 could be regarded as a sort of entropy of information.

But, unfortunately the curve-fitting of process (1) failed. The results reproduced in the higher homologs were attended by inevitable deviations in the lower homologs, and the reverse situations were also observed. In addition, for process (2), the scattering of the plot is unavoidable in $C_6H_{6-n}X_n$ (X=F, Cl) because the slopes of $\sigma_{s^\circ}(n)$ against $\log n$ are gentle.

Under the above evidence, the authors examined the linear relations between $\sigma_{s^\circ}(n)$ and $\log n$ for $n=2$—6, rejecting the data of the monosubstituted benzene series, because the values of σ_{s° determined from the observed $S^\circ_{298}(g)$ were already proposed in our previous work.[1a]

Plots of the data against the logarithm of the number n of the substituent are linear, and after regression they are formulated as Eqs. 1—4 as given below:

$$\sigma_{s^\circ}(F_n)=0.1614(\pm0.0301)\log n+0.0221(\pm0.0161) \quad (1)$$
$$n=11,\ r=0.972,\ s=0.0069,\ d=2.103$$

$$\sigma_{s^\circ}(Cl_n)=0.2305(\pm0.0250)\log n+0.0307(\pm0.0133) \quad (2)$$
$$n=11,\ r=0.990,\ s=0.0057,\ d=2.659$$

$$\sigma_{s^\circ}(Me_n)=0.2375(\pm0.0229)\log n+0.0479(\pm0.0122) \quad (3)$$
$$n=11,\ r=0.992,\ s=0.0052,\ d=2.416$$

$$\sigma_{s^\circ}(Et_n)=0.4271(\pm0.0187)\log n+0.0786(\pm0.0100) \quad (4)$$
$$n=11,\ r=0.998,\ s=0.0043,\ d=2.023$$

TABLE I. Observed Descriptors σ_{s° (obs) for $C_6H_{6-n}R_n$ (R=F, Cl, Me, Et,: $n=1-6$) and Number n of Substituent R

n	$\log n$	Position	F	Cl	Me	Et
1	0.000	1	0.051	0.066	0.076	0.127
2	0.301	12	0.078	0.103	0.117	0.208
		13	0.076	0.106	0.123	0.213
		14	0.069	0.097	0.117	0.208
3	0.477	123	0.095	0.138	0.155	0.275
		124	0.109	0.145	0.167	0.284
		135	0.088	0.129	0.156	0.276
4	0.602	1234	0.115	0.169	0.196	0.333
		1235	0.122	0.172	0.196	0.338
		1245	0.119	0.165	0.192	0.335
5	0.699		0.144	0.199	0.217	0.381
6	0.778		0.153	0.209	0.225	0.413

TABLE II. Estimated Slopes and Intercepts for Typical Substituent Groups

		Slope	Intercept
1	NO_2	0.384	0.071
2	CN	0.251	0.042
3	COMe	0.473	0.090
4	COEt	0.606	0.119
5	CF_3	0.473	0.090
6	COOMe	0.623	0.123
7	COOEt	0.725	0.145
8	F	0.166	0.023
9	Cl	0.217	0.034
10	Br	0.260	0.047
11	I	0.310	0.058
12	Me	0.251	0.042
13	Et	0.425	0.080
14	OMe	0.425	0.080
15	OEt	0.572	0.112
16	OH	0.230	0.039
17	NH_2	0.240	0.043
18	NMe_2	0.450	0.088

TABLE III. Descriptors σ_{s°(obs) and Their Related Data for Poly-Substituted Benzene Derivatives

		Observed		Calculated			
		σ_{s°	S°	σ_{s°	S°	ΔS°	$\Sigma\sigma_{s^\circ}$ (mono)
1	1,2,3,4-Me_4	0.190	99.55	0.191	99.88	−0.33	0.304
2	-Et_4	0.333	138.45	0.336	139.47	−1.02	0.508
3	-F_4	0.115	83.45	0.121	85.01	−1.56	0.204
4	-Cl_4	0.169	94.91	0.169	94.95	−0.04	0.264
5	-$(COOMe)_4$	0.498[a]	202.53[a]	0.498[b]	202.53[b]		0.740
6	-$(COOEt)_4$	0.582[a]	245.74[a]	0.581[b]	245.18[b]		0.860
7	1,2,3,5-Me_4	0.196	100.99			1.11	
8	-Et_4	0.338	139.99			0.52	
9	-F_4	0.122	85.21			0.20	
10	-Cl_4	0.172	95.50			0.55	
11	-$(COOMe)_4$	0.502[a]	204.40[a]				
12	-$(COOEt)_4$	0.586[a]	248.02[a]				
13	1,2,4,5-Me_4	0.192	100.03			0.45	
14	-Et_4	0.335	139.03			−0.44	
15	F_4	0.119	84.62			−0.39	
16	-Cl_4	0.165	94.03			−0.92	
17	-$(COOMe)_4$	0.499[a]	202.99[a]				
18	-$(COOEt)_4$	0.584[a]	246.88[a]				
19	-Me_5	0.217	106.09	0.214	105.31	0.78	0.380
20	-Et_5	0.381	154.84	0.377	153.28	1.56	0.635
21	-F_5	0.144	89.64	0.137	88.20	1.44	0.255
22	-Cl_5	0.199	101.74	0.192	100.07	1.67	0.330
23	-$(COOMe)_5$	0.558[a]	232.53[a]	0.558[b]	232.53[b]		0.925
24	-$(COOEt)_5$	0.652[a]	288.72[a]	0.652[b]	288.72[b]		1.075
25	-Me_6	0.225	108.12	0.233	109.95	−1.83	0.456
26	-Et_6	0.413	166.62	0.411	165.72	0.90	0.762
27	-F_6	0.153	91.54	0.150	91.30	0.24	0.306
28	-Cl_6	0.209	104.13	0.210	102.68	1.45	0.396
29	-$(COOMe)_6$	0.608	260.90[a]	0.608[b]	260.90[b]		1.110
30	-$(COOEt)_6$	0.709	329.22[a]	0.709[b]	329.22[b]		1.290
31	-F_5, Me	0.186	98.74	0.196	101.00	−3.26	0.331
32	-F_5, Cl	0.182	97.83	0.191	99.77	−1.94	0.321
33	-F_5, Br	0.195	100.80	0.198	101.62	−0.82	0.336
34	-F_5, I	0.204	102.92	0.205	103.24	−0.32	0.349

a) The numerical values were obtained from Eqs. 7—11. *b*) The numerical values were obtained from Eqs. 5—6.

where the four kinds of slopes and intercepts thus determined are revealed to be linear against σ_{s°(mono) as below:

TABLE IV. Polarizabilities $\alpha/10^{-24}$ cm^3 and Their Related Quantities for Poly-Substituted Benzene Derivatives

		$\Delta\alpha$(obs)	$\Sigma\Delta\alpha$(mono)
1,2,3,4-Tetra-			
1	1,2,3,4-Me_4	7.491	7.716
2	1,2,3,4-Et_4	15.152	15.200
3	2-Et-1,3,4-Me_3	9.366	9.587
4	4-Et-1,2,3-Me_3	9.366	9.587
1,2,4,6-Tetra-			
1	1-COCl-2,4,6-Me_3	9.896	10.230
2	1,2,4,6-Me_4	7.580	7.716
3	2-Et-1,3,5-Me_3	9.441	9.589
4	6-Et-1,2,4-Me_3	9.435	9.589
5	5-Et-1,2,3-Me_3	9.455	9.589
6	1-*n*-Pr-2,4,6-Me_3	11.285	11.442
7	1-Cl-2,4,6-Me_3	7.684	7.848
8	1-Me-2-NO_2-4-iso-Pr-6-Cl	11.670	12.146
9	1-F-2,4,6-Cl_3	5.906	5.875
1,2,4,5-Tetra-			
1	1-iso-Pr-2,4,5-Me_3	11.367	11.432
2	1-CH=CH_2-2,4,5-Me_3	9.666	9.843
3	1-Et-2,4,5-Me_3	10.634	9.587
4	1-*n*-Pr-2,4,5-Me_3	11.293	11.442
5	1,2,4,5-F_4	−0.105	−0.176
6	1,2,4,5-Et_4	15.103	15.200
7	1-Br-*n*-Pr_3	20.057	20.057
8	1-NO_2-2,4,5-*n*-Pr_3	19.430	19.564
9	1-Me-2-F-4-NO_2-5-Cl	6.372	6.457
Penta-			
1	4-Br-2-C=CH-1,3,5-Me_3	12.212	12.573
2	3-CH_2Cl-1,2,4,6-Me_4	11.533	11.628
3	Me_5	9.358	9.645
4	3-C=CH-1,2,4,6-Me_4	10.932	11.412
Hexa-			
1	F_6	0.119	−0.264
2	F_5Cl	2.728	1.753
3	6-CF_3-2,3,4,5-F_4-1-Cl	4.031	3.616
4	F_5CF_3	2.260	1.599
5	Cl_5-CH=CH_2	12.791	13.921

$$\text{slope} = 3.4109(\pm 1.0274)\sigma_{s^\circ}(\text{mono}) - 0.0080(\pm 0.0087) \quad (5)$$
$$n=4,\ r=0.995,\ s=0.0136,\ d=3.212$$

$$\text{intercept} = 0.7454(\pm 0.3885)\sigma_{s^\circ}(\text{mono}) - 0.0148(\pm 0.0330) \quad (6)$$
$$n=4,\ r=0.986,\ s=0.0052,\ d=2.929$$

where script d means the Durbin–Watson ratio.[5] The slope and the intercept determined by the above procedures are all summarized in Table II, including the typical substituent groups. The data of observed σ_{s°(obs), as well as those of the calculated σ_{s°(cal) given by Eqs. 5—6, for the poly-substituted benzene series (n=4—6), including the additional data of CO_2R (R=Me, Et) are arranged in Table III, where the agreements within ±2 e.u. are accepted.

Furthermore, in the next step, we have expressed the values σ_{s°(obs) as a linear function of $\Sigma\sigma_{s^\circ}$(mono) as an independent variable, and regression analyses afforded Eqs. 7—11 as given below:

$$\sigma_{s^\circ}(\text{obs})/1234 = 0.7043(\pm 0.1128)\Sigma\sigma_{s^\circ}(\text{mono}) - 0.0236(\pm 0.0384) \quad (7)$$
$$n=4,\ r=0.9986,\ s=0.0060,\ F=720.6$$

$$\sigma_{s^\circ}(\text{obs})/1235 = 0.7017(\pm 0.0757)\Sigma\sigma_{s^\circ}(\text{mono}) - 0.0175(\pm 0.0257) \quad (8)$$
$$n=4,\ r=0.9994,\ s=0.0040,\ F=1590.0$$

$$\sigma_{s^\circ}(\text{obs})/1245 = 0.7063(\pm 0.0356)\Sigma\sigma_{s^\circ}(\text{mono}) - 0.0233(\pm 0.0121) \quad (9)$$
$$n=4,\ r=0.9999,\ s=0.0019,\ F=7284.7$$

$$\sigma_{s^\circ}(\text{obs})/n=5 \ = 0.6178(\pm 0.0993)\Sigma\sigma_{s^\circ}(\text{mono}) - 0.0119(\pm 0.0422) \quad (10)$$
$$n=4,\ r=0.9986,\ s=0.0066,\ F=717.4$$

$$\sigma_{s^\circ}(\text{obs})/n=6 \ = 0.5696(\pm 0.1209)\Sigma\sigma_{s^\circ}(\text{mono}) - 0.0234(\pm 0.0616) \quad (11)$$

They are, unfortunately, concerned with the homologs having the same substituent groups, and, when the loss of the symmetry number results from introducing different kinds of substituents, it is desirable to take into account correction due to the symmetry loss. The evidence is provided by the data of congeners 31—34, *e.g.* C_6F_5R (R = Me, Cl, Br, I)[2b-e] arranged in Table III, where the correction of 5Rln 2 e.u. is required from the reference value because the symmetry numbers inherent in $\Sigma\sigma_{s^\circ}$(mono) and C_6F_5R are 6 and 1, respectively.

Polarizability α and Poly-Substituted Benzene Series In this section, we have determined the net increase of polarizability $\Delta\alpha$ for the poly-substituted benzene series[3a,b] from benzene reference, as well as the sum of the excess amount of polarizability $\Sigma\Delta\alpha$(mono) determined individually from mono-substituted benzene derivatives,[6] respectively.

The results are all summarized in Table IV, where the two kinds of data are correlated successfully as given by Eqs. 12—16, and from which the values of $\Delta\alpha$ for the poly-substituted benzene series having optical kinds of substituent groups could be realized.

$$\Delta\alpha/1234 = 1.0260(\pm 0.0206)\Sigma\Delta\alpha(\text{mono}) - 0.4528(\pm 0.2240) \quad (12)$$
$$n=4,\ r=1.0000,\ s=0.0268,\ F=46065$$

$$\Delta\alpha/1235 = 0.9428(\pm 0.0404)\Sigma\Delta\alpha(\text{mono}) + 0.3464(\pm 0.3845) \quad (13)$$
$$n=9,\ r=0.9989,\ s=0.0938,\ F=3042.4$$

$$\Delta\alpha/1245 = 0.9890(\pm 0.0532)\Sigma\Delta\alpha(\text{mono}) + 0.1724(\pm 0.6892) \quad (14)$$
$$n=9,\ r=0.9982,\ s=0.4028,\ F=1929.5$$

$$\Delta\alpha/n=5 \ = 0.9884(\pm 0.4004)\Sigma\Delta\alpha(\text{mono}) - 0.1750(\pm 4.5504) \quad (15)$$
$$n=4,\ r=0.9913,\ s=0.1970,\ F=112.80$$

$$\Delta\alpha/n=6 \ = 0.8671(\pm 0.1018)\Sigma\Delta\alpha(\text{mono}) + 0.8090(\pm 0.6637) \quad (16)$$
$$n=5,\ r=0.9980,\ s=0.3612,\ F=734.8$$

Acknowledgement Financial assistance from the Fund of Hoan-sha is gratefully acknowledged.

References and Notes

1) *a*) Y. Sasaki, T. Takagi, and H. Kawaki, *Chem. Pharm. Bull.*, **36**, 3743 (1988); *b*) H. Kawaki, Y. Sasaki, T. Takagi, S. Fujii, and F. Masuda, *ibid.*, **37**, 3268 (1989); *c*) Y. Sasaki, H. Kawaki, and T. Takagi, *ibid.*, **38**, 2344 (1990).
2) *a*) D. R. Stull, E. F. Westrum, Jr., and G. C. Sinke, "The Chemical Thermodynamics of Organic Compounds," Wiley, New York, 1969; *b*) J. B. Butler and J. Lielmezs, *J. Chem. Eng. DATA*, **14**, 335 (1969); *c*) J. F. Counsell, J. L. Hales, and J. F. Martin, *J. Chem. Soc.* (*A*), **1968**, 2042; *d*) R. J. L. Andon, J. F. Counsell, J. L. Hales, E. B. Lees, and J. F. Martin, *ibid.*, **1968**, 2357; *e*) J. F. Counsell, J. L. Hales, E. B. Lees, and J. F. Martin, *ibid.*, **1968**, 2994.
3) *a*) Zvi Rappoport, "Handbook of Tables for Organic Compound Identification," 3rd Ed., Chemical Rubber Co., Ohio, 1969; *b*) Beilstein's "Handbuch der Organischen Chemie," Drittes Ergänzungswerke, Band. V, Springer Verlag, Berlin, 1963—1965.
4) T. Takagi, K. Tange, N. Iwata, Y. Shindo, A. Iwata, T. Katayama, H. Izaki, S. Fujii, and Y. Sasaki, "Proceedings of the 4th Software Conference," Osaka, 1988, p. 285.
5) J. Durbin and G. S. Watson, *Biometrika*, **58**, 1 (1971).
6) H. Kawaki, F. Masuda, and Y. Sasaki, *Chem. Pharm. Bull.*, **36**, 4814 (1988).

Studies on Cardiotonic Agents. VI.[1] Synthesis of Novel 4,5-Dihydro-3(2*H*)-pyridazinone Derivatives Carrying Some Benzoheterocycles at the 6-Position

Yuji NOMOTO,* Haruki TAKAI, Tetsuji OHNO and Kazuhiro KUBO

Pharmaceutical Research Laboratories, Fuji, Kyowa Hakko Kogyo Co., Ltd., Shimotogari 1188, Nagaizumicho, Shizuoka 411, Japan.
Recieved July 12, 1990

Several benzothiazolyl, imidazobenzothiazolyl, benzothienyl, benzothienopyrimidinyl and quinazolinyl 4,5-dihydro-3(2*H*)-pyridazinones were synthesized and examined for cardiotonic activity in anesthetized dogs after i.v. administration. Among them, 4-methylamino-7-(2,3,4,5-tetrahydro-5-methyl-3-oxo-6-pyridazinyl)quinazoline (36) showed potent and long-lasting inotropic activity (relative potency = 2.11, milrinone = 1). The activity of 36 was more potent than indolidan (2) (relative potency = 1.53) which is one of the most potent inotropic agents to date.

Keywords cardiotonic agent; structure–activity relationship; pyridazinone; quinazoline; benzothiazole; imidazobenzothiazole; benzothiophene; benzothienopyrimidine

As part of an ongoing project aimed at the development of new cardiotonic agents, we have recently reported the synthesis and biological activities of a new series of 6,7-dimethoxyquinazoline derivatives.[1] These compounds show combined inotropic-vasodilator properties, and may be useful for the treatment of congestive heart failure.

Several of these dual-activity cardiotonics have been described.[2] These include some 4,5-dihydro-3(2*H*)-pyridazinone derivatives (imazodan (**1**),[3] indolidan (**2**)[4] and pimobendan (**3**)[5]), which have closely related structures (Chart 1). All of these compounds possess a nitrogen atom on the phenyl ring at the *para*-position of the pyridazinone ring. We were interested in the inotropic activity of the 4,5-dihydro-3(2*H*)-pyridazinone derivatives having a carbon or sulfur atom at the *para*-position. Consequently, we synthesized sereval 5-benzothiazolyl (**7**—**15**, **17**), 6-imidazo-[2,1-*b*]benzothiazolyl (**16**), 1-benzothiophen-6-yl (**21**), 7-[1]benzothieno[3,2-*d*]pyrimidinyl (**23**—**25**) and 7-quinazolinyl (**28**—**31**, **35**—**36**) derivatives. The present paper describes the synthesis and pharmacological evaluation of these compounds.

Chemistry Previously, the Thomae group[6] obtained 4,5-dihydro-6-(2-dimethylamino-5-benzothiazolyl)-5-methyl-3(2*H*)-pyridazinone (**4**) by the reaction of 4,5-dihydro-6-(3-amino-4-mercaptophenyl)-5-methyl-3(2*H*)-pyridazinone with dimethyl carbamoylchloride. The Fujisawa group[7] synthesized 4,5-dihydro-6-(2-hydroxy-5-benzothiazolyl)-5-methyl-3(2*H*)-pyridazinone (**5**) from 2-hydroxy-5-propionylbenzothiazole in several steps.

We investigated the synthesis of the benzothiazolyl and the imidazobenzothiazolyl derivatives as outlined in Charts 2 and 3. Cyclization of butyric acid (**6**)[6] with CS_2 afforded 2-mercaptobenzothiazole, which, without isolation, was treated with hydrazine hydrate to afford 3(2*H*)-pyridazinone (**7**). Compound **7** was alkylated under alkaline conditions with MeI and iso-PrI to give **8** and **9**, respectively. Subsequently, oxidation of **8** with *m*-chloroperbenzoic acid afforded the sulfoxide (**10**), and with $KMnO_4$ in 70% AcOH afforded the sulfone (**11**).

Compound **11** was reacted with a large excess of ethylenediamine to give a 2-(2-aminoethyl)amino derivative (**12**). Cyclization of **12** with *N*,*N*′-carbonyldiimidazole (CDI) and CS_2 afforded 2-imidazolidinone (**13**) and 2-imidazolidinethione (**14**), respectively. The reaction of **11** with DL-valine in the presence of K_2CO_3 afforded **15**, followed by cyclization with Ac_2O to afford the imidazobenzothiazole (**16**). Treatment of **11** with NaSPh afforded thioether (**17**) (Chart 3).

Next, we attempted to synthesize benzothiophene and benzothienopyrimidine derivatives. Thus, the 4-bromo-3-nitrophenyl derivative (**19**) was prepared from 3-(4-bromo-3-nitrobenzoyl)butyric acid (**18**)[6] and hydrazine hydrate. The key intermediate, 4-cyano-3-nitrophenylpyridazinone (**20**), was obtained by the reaction of **19** with CuCN in *N*,*N*-dimethylformamide (DMF) at 100 °C under a N_2 atmosphere. A mixture of **20** and ethyl mercaptoacetate was treated with 2 N NaOH in DMF to afford the benzothiophene (**21**) in a 93% yield. Then, **21** was reacted with triethyl

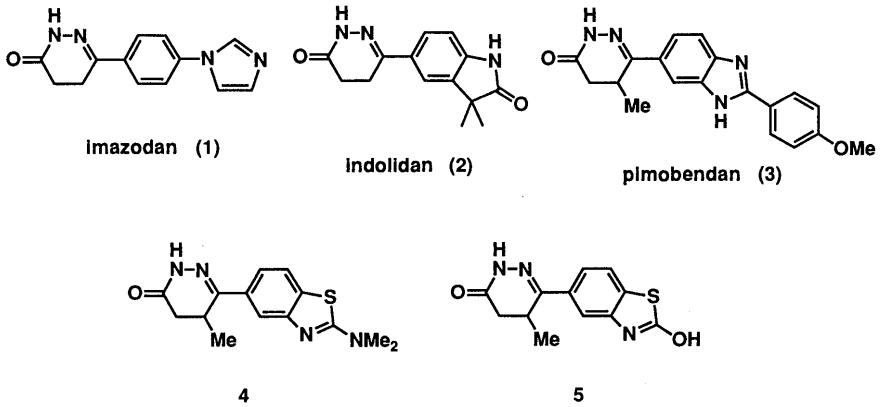

Chart 1

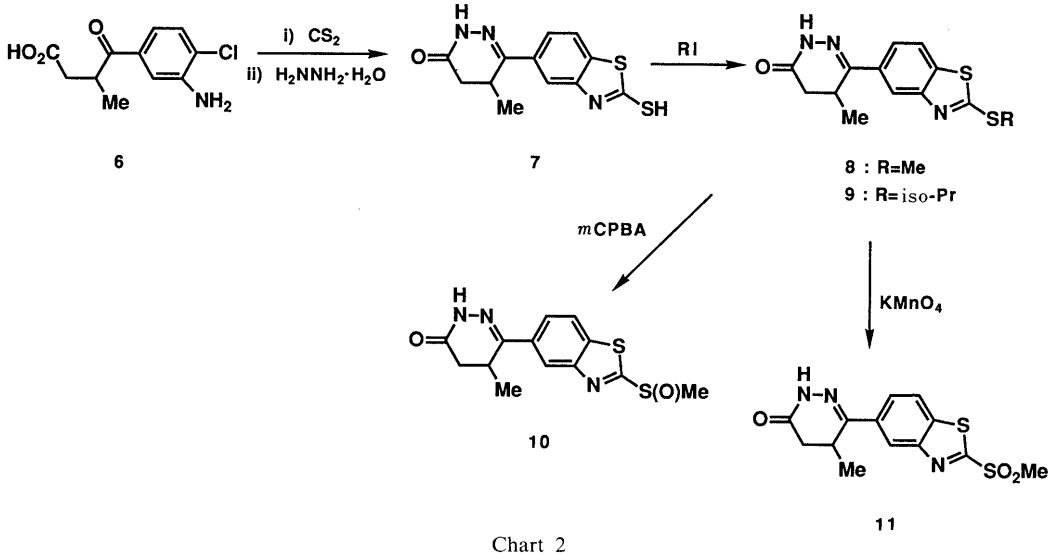

Chart 2

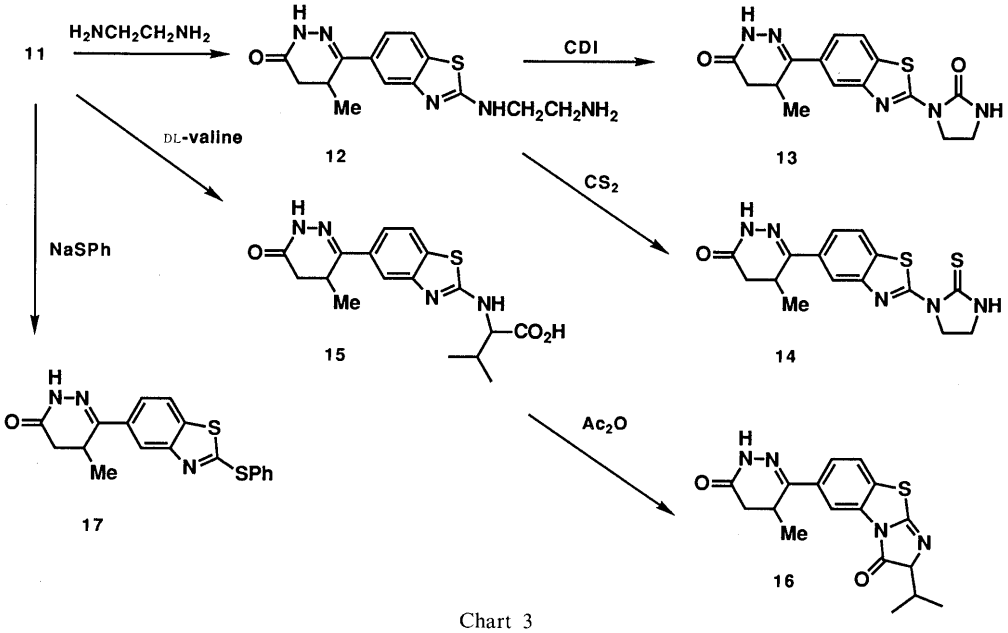

Chart 3

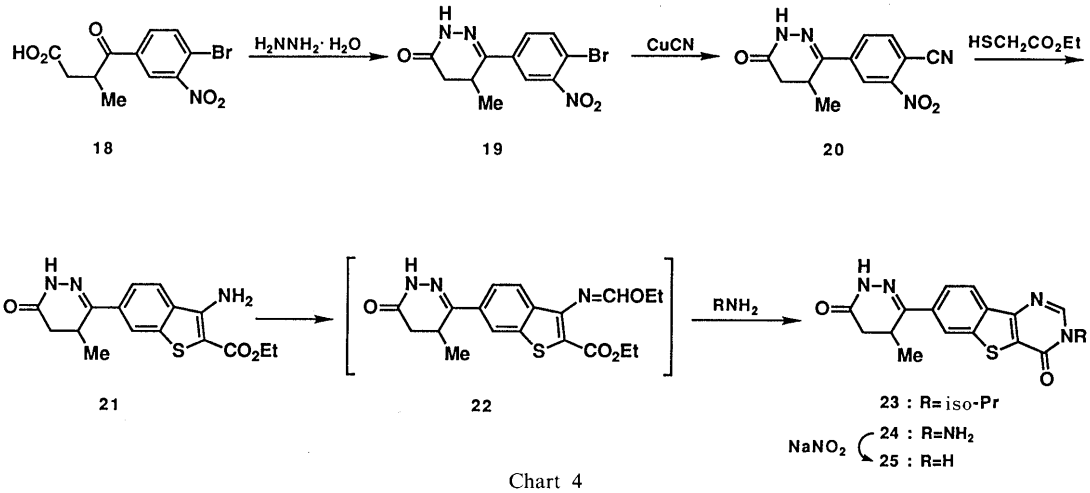

Chart 4

orthoformate, followed by treatment with isopropylamine and hydrazine hydrate, to give the benzothienopyrimidines **23** and **24**, respectively (Chart 4). Successive deamination of **24** with $NaNO_2$ afforded **25**.

Compound **20** was also converted to the quinazolines as outlined in Charts 5 and 6. Hydrolysis of **20** with H_2O_2

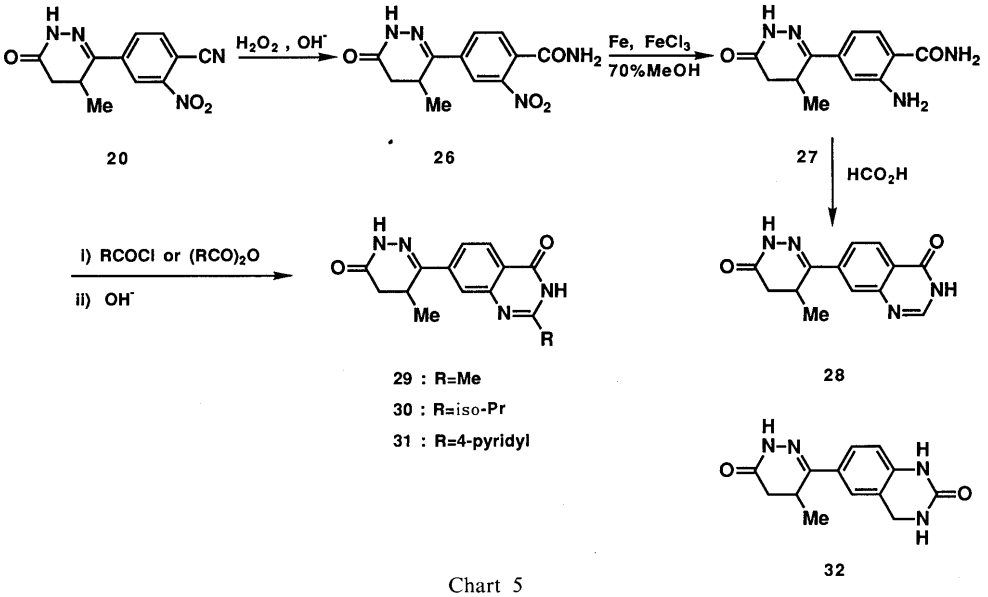

Chart 5

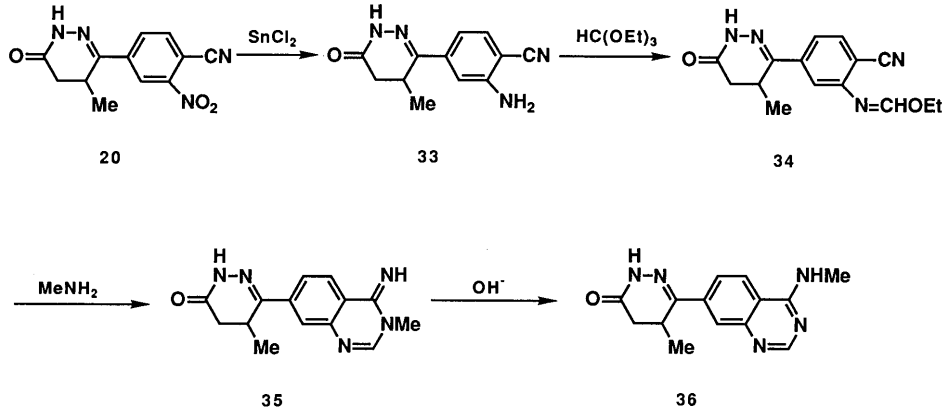

Chart 6

in 2N NaOH afforded the benzamide (**26**), and the subsequent reduction of **26** produced anthranilamide (**27**). Compound **27** was reacted with formic acid to give 4(3*H*)-quinazolinone (**28**). Other quinazolinone derivative (**29**—**31**) were synthesized by acylation of **27** with appropriate acid anhydrides or acid chlorides, followed by cyclization in 2N NaOH (Chart 5). When this work was complete, the Rorer group[8] reported the synthesis of 4,5-dihydro-5-methyl-6-(1,2,3,4-tetrahydro-2-oxo-6-quinazolinyl)-3(2*H*)-pyridazinone (**32**) *via* Fredel–Crafts acylation of 1,2-dihydro-2-quinazolinone.

Selective reduction of the nitro group of **20** with $SnCl_2$ in conc. HCl afforded anthranilonitrile (**33**). Catalytic hydrogenation of **20** gave only a complex mixture. Compound **33** reacted with triethyl orthoformate in the presence of CF_3CO_2H at 60 °C to give ethoxymethylenimine (**34**), and subsequent treatment with 40% methylamine in MeOH afforded a 3,4-dihydro-4-imino-3*H*-quinazoline derivative (**35**). In the reaction with triethyl orthoformate, the absence of CF_3CO_2H caused an increase in side products. The Dimroth rearrangement[9] of **35** under alkaline conditions afforded the 4-methylaminoquinazoline (**36**) (Chart 6). The proton nuclear magnetic resonance ^{1}H-NMR spectrum of **35** showed the methyl proton signal at δ 3.41 ppm as a singlet, while that of **36** showed it at δ 3.01 ppm as a doublet.

Biological Results

Cardiotonic activity of a novel series of the 4,5-dihydro-3(2*H*)-pyridazinones was evaluated in anesthetized open chest dogs using procedures previously described.[10] The results are shown in Table I. The positive cardiotonic activity of the compounds was determined by measuring the percentage increase in maximum dP/dt of left ventricular pressure (LVdP/dt max, Δ%) after i.v. administration (0.03 mg/kg) in anesthetized mongrel dogs of either sex (8—15 kg). The potency of cardiotonic activity of the test compounds was compared with milrinone[11] (0.03 mg/kg i.v.). Relative potency was calculated as the LVdP/dt max of each compound to that of milrinone (milrinone = 1) in the same dogs.

In a series of the benzothiazolyl derivatives, the cardiotonic activity depends upon the substituents at the 2-position. Thus, the methylthio derivative (**8**) exhibited potent activity, while isopropylthio (**9**) and 2-oxo-1-imidazolidinyl (**13**) derivatives resulted in a loss of activity. But **8** showed poor oral activity in anesthetized dogs, probably due to its low bioavailability (data not shown).

The imidazobenzothiazolyl (**16**), the benzothienyl (**21**) and the benzothienopyrimidinyl (**23**) derivatives showed

TABLE I. Cardiotonic Activity of Some Pyridazinone Derivatives in Anesthetized Dogs

Compd. No.	Cardiotonic activity		
	LVdP/dt max[a] (Δ%)	Relative[b] potency	Duration[c] (min)
7	19.1± 3.6	0.53	30
8	59.0± 8.5	1.64	40
9	12.8 (2)	0.33	20
10	35.9±12.1	0.88	40
11	7.9± 3.0	0.22	—
12	28.8± 4.6	0.69	60
13	8.9 (2)	0.26	—
14	8.5 (2)	—	—
16	23.0± 1.7	0.71	10
17	11.5 (2)	—	—
21	25.9± 1.7	0.81	10
23	29.2± 7.6	0.70	30
24	9.6 (2)	0.27	—
25	9.0 (2)	0.27	—
29	12.2 (2)	0.32	15
30	6.2 (2)	0.16	—
31	1.2 (2)	—	—
35	12.7 (2)	0.29	15
36	78.3± 2.5	2.11	>60
Indolidan (**2**)	70.2± 9.3	1.53	>60

a) Each value represents the mean ± standard error of triplicate experiments, except where otherwise noted in parentheses. *b*) Compared to the percentage increase in LVdP/dt max observed with milrinone (0.03 mg/kg i.v.) in the same dogs. *c*) Milrinone = 45—60 min.

moderate activity. In a series of the quinazolinyl derivatives, the 4-quinazolinone (**29**—**31**) and the 3,4-dihydro-4-imino-3-methyl-3*H*-quinazoline derivative (**35**) showed poor activity. In constrast, the 4-methylaminoquinazoline (**36**) was found to exhibit potent and long-lasting positive inotropic activity (relative potency = 2.11). In our test system, **36** was more potent than indolidan (**2**) (relative potency = 1.53), which has been one of the most potent and long-lasting inotropic agents to date. Compound **36** also demonstrated potent activity after *p.o.* administration (data not shown).

In summary, a novel series of 4,5-dihydro-2(3*H*)-pyridazinones was designed and synthesized. The attachment of a 4-methylaminoquinazolinyl group at the 6-position of the pyridazine resulted in significant enhancement of inotropic activity. Further modification and structure–activity relationship study of some quinazolinylpyridazinones are in progress and will be the subject of a forthcoming paper.

Experimental

All melting points were determined on a Büchi 510 micro melting point apparatus and are uncorrected. Infrared (IR) spectra were measured on a JASCO IR810 spectrophotometer. ^{1}H-NMR spectra were measured on a Hitachi R-90H and a JEOL JNM-GX-270 spectrometer using tetramethylsilane as an internal standard.

4,5-Dihydro-6-(2-mercapto-5-benzothiazolyl)-5-methyl-3(2*H*)-pyridazinone (7) A solution of **6** (4.8 g, 20 mmol) in DMF (50 ml) was basified to pH 11 with 2 N NaOH, and treated with CS_2 (10 ml) for 3 h at 60 °C. After cooling, the reaction mixture was acidified to pH 4 with 1 N HCl and extracted with $CHCl_3$. The extract was dried over $MgSO_4$ and concentrated. Hydrazine hydrate (5 ml) and AcOH (50 ml) were added to the residue, and everything was stirred for 3 h at 100 °C. The precipitated crystals were collected by filtration, successively washed with water and MeOH, and dried to give crude crystals of **7** (2.6 g, 47%) which were recrystallized from DMF–water for analysis, mp 301—303 °C. *Anal.* Calcd for $C_{12}H_{11}N_3OS_2$: C, 51.96; H, 4.00; N, 15.15. Found: C, 51.87; H, 4.30; N, 15.02. IR (KBr); 1640, 1600 cm^{-1}. NMR (DMSO-d_6) δ: 13.80 (1H, br, SH), 10.88 (1H, s, NH), 7.62 (1H, s, Ar-H), 7.42 (1H, d, J=8 Hz, Ar-H), 7.35 (1H, d, J=8 Hz, Ar-H), 3.45 (1H, m, CH), 2.70 (1H, dd, J=7, 17 Hz, CHC<u>H</u>'H), 2.22 (1H, d, J=17 Hz, CHCH'<u>H</u>), 1.10 (3H, d, J=7 Hz, CH_3).

4,5-Dihydro-5-methyl-6-(2-methylthio-5-benzothiazolyl)-3(2*H*)-pyridazinone (8) MeI (2.1 ml, 34 mmol) was added to a mixture of **7** (7.8 g, 28 mmol) in 2 N NaOH (30 ml) and MeOH (100 ml). The resulting mixture was stirred for 20 min at room temperature, then concentrated. Water was added to the residue, and the precipitated crystals were collected by filtration, washed with water and dried to give crude **8** (5.1 g, 62%), which was recrystallized from DMF–water for analysis, mp 170—173 °C. *Anal.* Calcd for $C_{13}H_{13}N_3OS_2$; C, 53.59; H, 4.50; N, 14.42. Found: C, 53.57; H, 4.41; N, 14.05. IR (KBr): 1680 cm^{-1}. NMR ($CDCl_3$) δ: 8.80 (1H, br, NH), 8.16 (1H, d, J=2 Hz), Ar-H, 7.84 (1H, dd, J=2, 8 Hz, Ar-H), 7.78 (1H, d, J=8 Hz, Ar-H), 3.45 (1H, m, C<u>H</u>CH$_3$), 2.82 (3H, s, SCH$_3$), 2.75 (1H, dd, J=7, 17 Hz, CHC<u>H</u>'H), 2.52 (1H, d, J=17 Hz, CHCH'<u>H</u>), 1.30 (3H, d, J=7 Hz, CH_3).

4,5-Dihydro-6-(2-isopropylthio-5-benzothiazolyl)-5-methyl-3(2*H*)-pyridazinone (9) The procedure described for **8** was followed, using iso-PrI (0.45 ml, 4.5 mmol) and **7** (1.0 g, 3.7 mmol) in 2 N NaOH (10 ml) and MeOH (30 ml). Crude **9** was recrystallized from DMF–water to give pure **9** (0.7 g, 62%), mp 177—178 °C. *Anal.* Calcd for $C_{15}H_{17}N_3OS_2$: C, 56.40; H, 5.36; N, 13.15. Found: C, 56.55; H, 5.34; N, 13.10. IR(KBr): 1680 cm^{-1}. NMR (DMSO-d_6) δ: 11.05 (1H, br, NH), 8.21 (1H, s, Ar-H), 8.04 (1H, d, J=8 Hz, Ar-H), 7.86 (1H, d, J=8 Hz, Ar-H), 4.08 (1H, m, C<u>H</u>(CH$_3$)$_2$), 3.55 (1H, m, C<u>H</u>CH$_3$), 2.75 (1H, dd, J=7, 17 Hz, CHC<u>H</u>'H), 2.28 (1H, d, J=17 Hz, CHCH'<u>H</u>), 1.48 (6H, d, J=7 Hz, CH(C<u>H</u>$_3$)$_2$), 1.10 (3H, d, J=7 Hz, CH_3).

4,5-Dihydro-5-methyl-6-(2-methylsulfinyl-5-benzothiazolyl)-3(2*H*)-pyridazinone (10) To a solution of **8** (0.80 g, 2.7 mmol) in AcOH (20 ml) was added *m*-chloroperbenzoic acid (0.60 g, 4.3 mmol) with stirring and ice-cooling. After additional stirring for 3 h at room temperature, the reaction mixture was basified to pH 10 with 2 N NaOH, and precipitated crystals were collected by filtration, washed with water and dried to give crude **10** (0.60 g, 71%), which was recrystallized from DMF–water for analysis, mp 228—230 °C. *Anal.* Calcd for $C_{13}H_{13}N_3O_2S_2$: C, 50.80; H, 4.26; N, 13.67. Found: C, 50.95; H, 4.06; N, 13.62. IR (KBr): 1670 cm^{-1}. NMR (DMSO-d_6) δ: 11.10 (1H, s, NH), 8.42 (1H, s, Ar-H), 8.30 (1H, d, J=8 Hz, Ar-H), 8.05 (1H, d, J=8 Hz, Ar-H), 3.58 (1H, m, C<u>H</u>CH$_3$), 3.10 (3H, s, S(O)CH$_3$), 2.75 (1H, dd, J=7, 17 Hz, CHC<u>H</u>'H), 2.30 (1H, d, J=17 Hz, CHCH'<u>H</u>), 1.12 (3H, d, J=8 Hz, CH_3).

4,5-Dihydro-5-methyl-6-(2-methylsulfonyl-5-benzothiazolyl)-3(2*H*)-pyridazinone (11) $KMnO_4$ (0.80 g, 5.1 mmol) was added to a suspension of **8** (1.0 g, 3.4 mmol) in 70% AcOH (50 ml) with ice-cooling, and the mixture was stirred for 3 h at the same temperature. In order to decompose excess $KMnO_4$, 30% H_2O_2 was added to the mixture until the mixture was colorless. The precipitated crystals were collected by filtration, washed with water and dried to give crude **11** (0.60 g, 54%), which was recrystallized with $CHCl_3$–Et_2O for analysis, mp 190—195 °C. *Anal.* Calcd for $C_{13}H_{13}N_3O_3S_2$: C, 48.28; H, 4.05; N, 12.99. Found: C, 47.93; H, 3.74; N, 12.59. IR(KBr): 1670 cm^{-1}. NMR (DMSO-d_6) δ: 11.15 (1H, s, NH), 8.58 (1H, s, Ar-H), 8.38 (1H, d, J=8 Hz, Ar-H), 8.18 (1H, d, J=8 Hz, Ar-H), 3.62 (3H, s, SO_2CH_3), 3.45 (1H, m, C<u>H</u>CH$_3$), 2.80 (1H, dd, J=7, 17 Hz, CHC<u>H</u>'H), 2.30 (1H, d, J=7 Hz, CH_3).

4,5-Dihydro-6-[2-(2-aminoethylamino)-5-benzothiazolyl]-5-methyl-3(2*H*)-pyridazinone (12) A suspension of **11** (1.5 g, 4.6 mmol) in ethylenediamine (5 ml) was stirred for 1 H at 100 °C, and concentrated under reduced pressure. Water was added to the residue, and the precipitated crystals were collected by filtration, washed with water and dried to give crude crystals of **12** (1.2 g, 87%), which were recrystallized from DMF–water for analysis. IR (KBr): 1660, 1620 cm^{-1}. NMR (DMSO-d_6) δ: 10.85 (1H, s, NH), 7.73 (1H, s, Ar-H), 7.68 (1H, d, J=8 Hz, Ar-H), 7.47 (1H, d, J=8 Hz, Ar-H), 3.50—2.90 (6H, br, NH$_2$, NH, CH$_2$, C<u>H</u>CH$_3$), 2.78 (2H, m, CH$_2$), 2.68 (1H, dd, J=7, 17 Hz, CHC<u>H</u>'H), 2.24 (1H, d, J=17 Hz, CHCH'<u>H</u>), 1.12 (3H, d, J=7 Hz, CH_3).

4,5-Dihydro-5-methyl-6-[2-(2-oxo-1-imidazolidinyl)-5-benzothiazolyl]-3(2*H*)-pyridazinone (13) CDI (0.62 g, 2.1 mmol) was added to a solution of **12** (0.62 g, 2.1 mmol) in CH_3CN (20 ml), and the resulting solution was stirred for 1 h at 100 °C. Precipitated crystals were collected by filtration, washed with water and dried to give crude **13** (0.52 g, 76%), which was recrystallized from DMF–water for analysis, mp >300 °C. *Anal.* Calcd for $C_{15}H_{15}N_5O_2S$: C, 54.70; H, 4.59; N, 21.26. Found: C, 54.48; H, 4.62; N, 21.51. IR(KBr): 1715, 1690, 1535 cm^{-1}. NMR (DMSO-d_6) δ: 10.88 (1H, s, NH), 7.98 (1H, d, J=8 Hz, Ar-H), 7.95 (1H, s, NH), 7.80 (1H, s,

Ar-H), 7.70 (1H, d, $J=8$ Hz, Ar-H), 4.17 (2H, t, $J=8$ Hz, CH_2), 3.57 (2H, t, $J=8$ Hz, CH_2), 3.50 (1H, m, C<u>H</u>CH_3), 2.75 (1H, dd, $J=7$, 17 Hz, CHC<u>H</u>'H), 2.28 (1H, d, $J=17$ Hz, CHCH'<u>H</u>), 1.15 (3H, d, $J=7$ Hz, CH_3).

4,5-Dihydro-5-methyl-6-[2-(2-thioxo-1-imidazolidinyl)-5-benzothiazolyl]-3-(2*H*)-pyridazinone (14) A solution of **12** (0.50 g, 1.7 mmol), Et_3N (1.0 ml, 7.2 mmol) and CS_2 (1.0 ml, 17 mmol) in DMF (10 ml) was stirred for 3 h at 100 °C, and concentrated. Water was added to the reaction mixture and precipitated crystals were collected by filtration, washed with water and dried to give **14** (0.31 g, 53%), which was recrystallized from DMF–water for analysis, mp > 300 °C. *Anal.* Calcd for $C_{15}H_{15}N_5OS_2$: C, 52.15; H, 4.38; N, 20.27. Found: C, 51.96; H, 4.52; N, 20.19. IR (KBr): 1680 cm^{-1}. NMR (DMSO-d_6) δ: 11.00 (1H, s, NH), 9.65 (1H, s, NH), 8.08 (1H, s, Ar-H), 7.98 (1H, d, $J=8$ Hz, Ar-H), 7.78 (1H, d, $J=8$ Hz, Ar-H), 4.48 (2H, t, $J=8$ Hz, CH_2), 3.75 (2H, t, $J=8$ Hz, CH_2), 3.52 (1H, m, C<u>H</u>CH_3), 2.75 (1H, dd, $J=7$, 17 Hz, CHC<u>H</u>'H), 2.28 (1H, d, $J=17$ Hz, CHCH'<u>H</u>), 1.15 (3H, d, $J=7$ Hz, CH_3).

2-[5-(2,3,4,5-Tetrahydro-5-methyl-3-oxo-6-pyridazinyl)-2-benzothiazolyl]amino-3-methylbutyric Acid (15) A mixture of **11** (1.5 g, 4.6 mmol), DL-valine (0.59 g, 5.0 mmol), K_2CO_3 (3.0 g) and DMSO (20 ml) was stirred for 5 h at 100 °C. After cooling, the reaction mixture was acidified with 1 N HCl to pH 4, and concentrated. The precipitated crystals were collected by filtration, washed with water and dried to give crude **15** (1.0 g, 60%), which was recrystallized from DMF–water for analysis, mp 240—244°C. *Anal.* Calcd for $C_{17}H_{20}N_4O_3S\cdot 1/2H_2O$: C, 55.26; H, 5.74; N, 15.16. Found: C, 55.43; H, 5.38; N, 15.20. IR(KBr): 1740, 1675, 1615 cm^{-1}. NMR (DMSO-d_6) δ: 12.70 (1H, br, CO_2H), 11.02 (1H, s, NH), 8.31 (1H, d, $J=8$ Hz, Ar-H), 7.74 (1H, s, NH), 7.70 (1H, s, Ar-H), 7.52 (1H, d, $J=8$ Hz, Ar-H), 4.40 (1H, m, C<u>H</u>CO_2H), 3.45 (1H, m, C<u>H</u>CH_3), 2.70 (1H, dd, $J=7$, 17 Hz, CHC<u>H</u>'H), 2.24 (1H, d, $J=17$ Hz, CHCH'<u>H</u>), 2.20 (1H, m, C<u>H</u> $(CH_3)_2$), 1.10 (3H, d, $J=7$ Hz, CH_3), 1.00 (6H, d, $J=7$ Hz, CH(C<u>H</u>$_3)_2$). 1.10 (3H, d, $J=7$ Hz, CH_3), 1.00 (6H, d, $J=7$ Hz, CH(C<u>H</u>$_3)_2$).

4,5-Dihydro-5-methyl-6-(2,3-dihydro-2-isopropyl-3-oxo-6-imidazo[2,1-*b*]benzothiazolyl)-3(2*H*)-pyridazinone (16) Compound **15** (1.5 g, 4.6 mmol) was dissolved in pyridine (20 ml) and Ac_2O (5 ml). The solution was stirred for 2 h at 60 °C, and concentrated. Water was added to the residue, and the precipitated crystals were collected by filtration, washed with water and dried to give **16** (0.51 g, 31%), which was recrystallized from DMF–water for analysis, mp 203 °C. *Anal.* calcd for $C_{17}H_{18}N_4O_2S$: C, 59.63; H, 5.30; N, 16.36. Found: C, 59.29; H, 5.10; N, 16.05. IR (KBr): 1730, 1680, 1600 cm^{-1}. NMR (DMSO-d_6) δ: 11.01 (1H, s, NH), 8.18 (1H, s, Ar-H), 7.80 (1H, d, $J=8$ Hz, Ar-H), 7.64 (1H, d, $J=8$ Hz, Ar-H), 4.53 (1H, d, $J=5$ Hz, C(O)CH), 3.40 (1H, m, C<u>H</u>CH_3), 2.72 (1H, dd, $J=7$, 17 Hz, CHC<u>H</u>'H), 2.28 (2H, m, C<u>H</u>$(CH_3)_2$, CHCH'<u>H</u>), 1.10 (6H, d, $J=7$ Hz, CH(C<u>H</u>$_3)_2$), 0.88 (3H, d, $J=7$ Hz, CH_3).

4,5-Dihydro-5-methyl-6-(2-phenylthio-5-benzothiazolyl)-3(2*H*)-pyridazinone (17) Compound **11** (0.5 g, 1.6 mmol) was added to a mixture of thiophenol (0.32 ml, 3.1 mmol), NaOMe (0.13 g, 2.4 mmol) and MeOH (20 ml), and everything was stirred for 1 h at room temperature. Water was added to the mixture, and the precipitated crystals were collected by filtration, washed with water and dried to give crude **17** (0.69 g, > 100%), which was purified by column chromatography (SiO_2, 2% MeOH–$CHCl_3$) to give pure **17** (0.34 g, 62%). The product was recrystallized from MeOH–$CHCl_3$, mp 198—200 °C. *Anal.* Calcd for $C_{18}H_{15}N_3OS_2$: C, 61.17; H, 4.28; N, 11.89. Found: C, 61.23; H, 4.12; N, 11.88. IR (KBr): 1670 cm^{-1}. NMR ($CDCl_3$) δ: 8.73 (1H, br s, NH), 8.16 (1H, s, Ar-H), 7.84—7.47 (7H, m, Ar-H), 3.42 (1H, m, C<u>H</u>CH_3), 2.76 (1H, dd, $J=7$, 17 Hz, CHC<u>H</u>'H), 2.53 (1H, d, $J=17$ Hz, CHCH'<u>H</u>), 1.29 (3H, d, $J=7$ Hz, CH_3).

6-(4-Bromo-3-nitrophenyl)-4,5-dihydro-5-methyl-3(2*H*)-pyridazinone (19) Compound **18**[6] (52.0 g, 0.17 mol) was added to a mixture of hydrazine hydrate (52.0 ml, 1.1 mol) and AcOH (300 ml), and the resulting solution was stirred for 3 h at 100 °C. The reaction mixture was concentrated to half volume and diluted with water (500 ml). The precipitated crystals were collected by filtration, washed with water and dried to give crude **19** (54.0 g, quant.), which was recrystallized from MeOH–water for analysis, mp 196 °C. *Anal.* Calcd for $C_{11}H_{10}BrN_3O_3$: C, 42.33; H, 3.23; N, 13.46. Found: C, 42.05; H, 2.96; N, 13.14. IR (KBr): 1715 cm^{-1}. NMR (DMSO-d_6) δ: 11.22 (1H, s, NH), 8.32 (1H, s, Ar-H), 7.98 (2H, s, Ar-H), 3.45 (1H, m, C<u>H</u>CH_3), 2.78 (1H, dd, $J=7$, 17 Hz, CHC<u>H</u>'H), 2.30 (1H, d, $J=17$ Hz, CHCH'<u>H</u>), 1.10 (3H, d, $J=7$ Hz, CH_3).

6-(4-Cyano-3-nitrophenyl)-4,5-dihydro-5-methyl-3(2*H*)-pyridazinone (20) A mixture of CuCN (50.0 g, 0.56 mol), **19** (73.0 g, 0.23 mol) and DMF (600 ml) was stirred for 2.5 h at 100 °C. After cooling, AcOEt (2.0 l) was added to the reaction mixture to form tarry precipitates. The precipitate was separated by decantation, and the AcOEt layer was washed with water, dried over $MgSO_4$ and evaporated under reduced pressure. The residue was diluted with water, and the precipitated crystals were collected by filtration, washed successively with water and MeOH, and dried to give crude **20** (35.1 g, 58%) which was recrystallized from DMF–water for analysis, mp 208—209 °C. *Anal.* Calcd for $C_{12}H_{10}N_4O_3$: C, 55.81; H, 3.90; N, 21.70. Found: C, 55.43; H, 3.75; N, 21.63. IR (KBr): 2210, 1680 cm^{-1}. NMR (DMSO-d_6) δ: 11.42 (1H, s, NH), 8.68 (1H, s, Ar-H), 8.28 (1H, d, $J=8$ Hz, Ar-H), 8.22 (1H, d, $J=8$ Hz, Ar-H), 3.55 (1H, m, C<u>H</u>CH_3), 2.82 (1H, dd, $J=7$, 17 Hz, CHC<u>H</u>'H), 2.35 (1H, d, $J=17$ Hz, CHCH'<u>H</u>), 1.12 (3H, d, $J=8$ Hz, CH_3).

3-Amino-2-ethoxycarbonyl-6-(2,3,4,5-tetrahydro-5-methyl-3-oxo-6-pyridazinyl)benzothiophene (21) To a solution of **20** (2.6 g, 10 mmol) and ethyl mercaptoacetate (1.2 g, 10 mmol) in DMF (20 ml) was added 2 N NaOH until the reaction mixture turned to deep red color. Water (60 ml) was added to the mixture, and precipitated crystals were collected by filtration, washed with water and dried to give crude **21** (3.1 g, 93%), which was recrystallized from DMF–water for analysis, mp 248 °C. *Anal.* Calcd for $C_{16}H_{17}N_3O_3S$: C, 57.99; H, 5.17; N, 12.68. Found: C, 57.70; H, 5.14; N, 12.66. IR (KBr): 1660, 1620 cm^{-1}. NMR (DMSO-d_6) δ: 11.08 (1H, s, NH), 8.66 (1H, s, Ar-H), 8.14 (1H, d, $J=8$ Hz, Ar-H), 7.85 (1H, d, $J=8$ Hz, Ar-H), 7.15 (2H, br, NH_2), 4.29 (2H, q, $J=8$ Hz, C<u>H</u>$_2$CH$_3$), 3.52 (1H, m, C<u>H</u>CH_3), 2.75 (1H, dd, $J=7$, 17 Hz, CHC<u>H</u>'H), 2.29 (1H, d, $J=17$ Hz, CHCH'<u>H</u>), 1.31 (3H, t, $J=8$ Hz, CH_2C<u>H</u>$_3$), 1.12 (3H, d, $J=8$ Hz, CH_3).

3,4-Dihydro-3-amino-4-oxo-7-(2,3,4,5-tetrahydro-5-methyl-3-oxo-6-pyridazinyl)[1]benzothieno[3,2-*d*]pyrimidine (24) A mixture of **21** (0.7 g, 2.1 mmol) and triethyl orthoformate (5 ml) was heated for 2.5 h under reflux, and the reaction mixture was concentrated. Hydrazine hydrate (5.0 ml) was added to the residue and everything was stirred for 1 h at 40°C. Water and MeOH were added to the reaction mixture, and the precipitated crystals were collected by filtration, washed and dried to give crude **24** (0.20 g, 29%), which was recrystallized from DMF–water for analysis, mp > 300 °C. *Anal.* Calcd for $C_{15}H_{13}N_5O_2S$: C, 55.03; H, 4.00; N, 21.39. Found: C, 54.76; H, 4.22: N, 21.19 IR (KBr): 1660 cm^{-1}. NMR (DMSO-d_6) δ: 11.15 (1H, s, NH), 8.63 (1H, s, Ar-H), 8.57 (1H, s, Ar-H), 8.24 (1H, d, $J=8$ Hz, Ar-H), 8.04 (1H, d, $J=8$ Hz, Ar-H), 6.08 (2H, br, NH_2), 3.58 (1H, m, C<u>H</u>CH_3), 2.78 (1H, dd, $J=7$, 17 Hz, CHC<u>H</u>'H), 2.32 (1H, d, $J=17$ Hz, CHCH'<u>H</u>), 1.15 (3H, d, $J=8$ Hz, CH_3).

3,4-Dihydro-3-isopropyl-4-oxo-7-(2,3,4,5-tetrahydro-5-methyl-3-oxo-6-pyridazinyl)[1]benzothieno[3,2-*d*]pyrimidine (23) A similar procedure as that described for **24** was carried out, except for the use of iso-$PrNH_2$ (10 ml) instead of hydrazine hydrate to give **23**, which was recrystallized from DMF–water to give pure **23** (0.19 g, 25%), mp 266—268 °C. *Anal.* Calcd for $C_{18}H_{18}N_4O_2S$: C, 61.00; H, 5.12; N, 15.81. Found: C, 60.83; H, 5.26; N, 15.83. IR (KBr): 1680, 1570 cm^{-1}. NMR (DMSO-d_6) δ: 11.14 (1H, s, NH), 8.66 (1H, s, Ar-H), 8.50 (1H, s, Ar-H), 8.21 (1H, d, $J=8$ Hz, Ar-H), 8.03 (1H, d, $J=8$ Hz, Ar-H), 4.20 (1H, m, C<u>H</u>$(CH_3)_2$), 3.50 (1H, m, C<u>H</u>CH_3), 2.75 (1H, dd, $J=7$, 17 Hz, CHC<u>H</u>'H), 2.28 (1H, d, $J=17$ Hz, CHCH'<u>H</u>), 1.47 (6H, d, $J=8$ Hz, CH(C<u>H</u>$_3)_2$), 1.14 (3H, d, $J=8$ Hz, CH_3).

3,4-Dihydro-4-oxo-7-(2,3,4,5-tetrahydro-5-methyl-3-oxo-6-pyridazinyl)-[1]benzothieno[3,2-*d*]pyrimidine (25) $NaNO_2$ (0.10 g, 1.4 mmol) was added to a suspension of **24** (0.30 g, 0.92 mmol) in 50% AcOH (20 ml), and the mixture was stirred for 30 min at room temperature. Water was added to the reaction mixture, and the precipitated crystals were collected by filtration, washed with water and dried to give crude **25** (0.25 g, 87%), which was recrystallized from DMF–water for analysis, mp > 300 °C. *Anal.* Calcd for $C_{15}H_{12}N_4O_2S$: C, 57.68; H, 3.87; N, 17.94. Found: C, 57.38; H, 3.68; N, 17.89. IR (KBr): 1680, 1650 cm^{-1}. NMR (DMSO-d_6) δ: 12.89 (1H, s, NH), 11.15 (1H, s, NH), 8.57 (1H, s, Ar-H), 8.35 (1H, s, Ar-H), 8.26 (1H, d, $J=8$ Hz, Ar-H), 8.08 (1H, d, $J=8$ Hz, Ar-H), 3.48 (1H, m, C<u>H</u>CH_3), 2.80 (1H, dd, $J=7$, 17 Hz, CHC<u>H</u>'H), 2.32 (1H, d, $J=17$ Hz, CHCH'<u>H</u>), 1.18 (3H, d, $J=8$ Hz, CH_3).

4-(2,3,4,5-Tetrahydro-5-methyl-3-oxo-6-pyridazinyl)-2-nitrobenzamide (26) To a suspension of **20** (8.3 g, 32 mmol) in 2 N NaOH (30 ml) and MeOH (30 ml), drops of 30% H_2O_2 (30 ml) were added during 30 min at 0 °C. The reaction mixture was neutralized with 1 N HCl and concentrated. The precipitated crystals were collected by filtration, washed with water dried to give crude **26** (5.5 g, 62%), which was recrystallized from DMF–water for analysis, mp 233—235 °C. *Anal.* Calcd for $C_{12}H_{12}N_4O_4$: C, 52.17; H, 4.38; N, 20.28. Found: C, 51.95; H, 4.16; N, 20.01. IR (KBr): 1720, 1670 cm^{-1}. NMR (DMSO-d_6) δ: 11.21 (1H, s, NH), 8.30 (1H, s, Ar-H), 8.20, 7.74 (each 1H, br s $CONH_2$), 8.11 (1H, d, $J=8$ Hz, Ar-H), 7.69 (1H, d, $J=8$ Hz, Ar-H), 3.49 (1H, m, C<u>H</u>CH_3), 2.78 (1H, dd, $J=7$, 17 Hz, CHC<u>H</u>'H), 2.31 (1H, d, $J=17$ Hz, CHCH'<u>H</u>), 1.12 (3H, d, $J=8$ Hz, CH_3).

2-Amino-4-(2,3,4,5-tetrahydro-5-methyl-3-oxo-6-pyridazinyl)-benzamide (27) A suspension of **26** (5.5 g, 20 mmol), iron powder (5.5 g) and $FeCl_3$ (0.30 g) in 70% MeOH (100 ml) was stirred for 1 h at 85 °C. The precipitate was removed by filtration, and the filtrate was concentrated. The crystalline residue was mixed with water, collected by filtration, washed with water and dried to give crude **27** (4.0 g, 81%), which was recrystallized from water for analysis, mp 221—223 °C. *Anal.* Calcd for $C_{12}H_{14}N_4O_2$: C, 58.52; H, 5.73; N, 22.75. Found: C, 58.19; H, 5.71; N, 22.55. IR (KBr): 1675 cm^{-1}. NMR (DMSO-d_6) δ: 10.97 (1H, s, NH), 7.78 (1H, s, Ar-H), 7.57 (1H, d, J=8 Hz, Ar-H), 7.14 (2H, br, NH_2), 6.90 (1H, d, J=8 Hz, Ar-H), 3.31 (1H, m, C<u>H</u>CH_3), 2.70 (1H, dd, J=7, 17 Hz, CHC<u>H</u>'H), 2.25 (1H, d, J=17 Hz, CHCH'<u>H</u>), 1.09 (3H, d, J=8 Hz, CH_3).

3,4-Dihydro-4-oxo-7-(2,3,4,5-tetrahydro-5-methyl-3-oxo-6-pyridazinyl)-quinazoline (28) A solution of **27** (1.1 g, 4.1 mmol) in HCO_2H (10 ml) was stirred for 3 h at 100 °C. Water was added to the reaction mixture and the precipitated ctystals were collected by filtration, washed with water and dried to give **28** (0.61 g, 58%), which was recrystallized from DMF–water for analysis, mp >300 °C. *Anal.* Calcd for $C_{13}H_{12}N_4O_2$: C, 60.93; H, 4.73; N, 21.86. Found: C, 60.72; H, 4.81; N, 21.90. IR (KBr): 1700, 1655, 1620 cm^{-1}. NMR (DMSO-d_6) δ: 12.28 (1H, br, NH), 11.21 (1H, s, NH), 8.14 (1H, s, Ar-H), 8.16 (1H, d, J=8 Hz, Ar-H), 7.98 (1H, s, Ar-H), 7.95 (1H, d, J=8 Hz, Ar-H), 3.52 (1H, m, C<u>H</u>CH_3), 2.68 (1H, dd, J=7, 17 Hz, CHC<u>H</u>'H), 2.29 (1H, d, J=17 Hz, CHCH'<u>H</u>), 1.13 (3H, d, J=8 Hz, CH_3).

3,4-Dihydro-2-methyl-4-oxo-7-(2,3,4,5-tetrahydro-5-methyl-3-oxo-6-pyridazinyl)quinazoline (29) A mixture of **27** (1.1 g, 4.1 mmol), Ac_2O (1.0 ml, 11 mmol) and pyridine (20 ml) was stirred for 30 min at 60°C, and concentrated. MeOH (50 ml) and 2 N NaOH (15 ml) was added to the residue, and everything was stirred for 2 h at 60 °C. The reaction mixture was neutralized with 1 N HCl, and concentrated. Water was added to the residue, and the precipitated crystals were collected by filtration, washed with water and dried to give **29** (0.80 g, 73%), which was recrystallized from DMF–water for analysis, mp 289—293 °C. *Anal.* Calcd for $C_{14}H_{14}N_4O_2$: C, 62.21; H, 5.22; N, 20.73. Found: C, 61.89; H, 5.19; N, 20.64. IR (KBr): 1680, 1620 cm^{-1}. NMR (DMSO-d_6) δ: 12.22 (1H, br, NH), 11.19 (1H, s, NH), 8.09 (1H, d, J=8 Hz, Ar-H), 7.89 (1H, d, J=8 Hz, Ar-H), 7.87 (1H, s, Ar-H), 3.52 (1H, m, C<u>H</u>CH_3), 2.78 (1H, dd, J=7, 17 Hz, CHC<u>H</u>'H), 2.38 (3H, s, CH_3), 2.30 (1H, d, J=17 Hz, CHCH'<u>H</u>), 1.13 (3H, d, J=8 Hz, CH_3).

3,4-Dihydro-2-isopropyl-4-oxo-7-(2,3,4,5-tetrahydro-5-methyl-3-oxo-6-pyridazinyl)quinazoline (30) A similar procedure to that described for **29** was carried out except for the use of 4-pyridinecarbonyl chloride instead to Ac_2O to give **30** (0.95 g, 78%), which was recrystallized from DMF–water for analysis, mp 283—285 °C (dec.). *Anal.* Calcd for $C_{16}H_{18}N_4O_2$: C, 64.41; H, 6.08; N, 18.78. Found: C, 64.47; H, 5.99; N, 18.80. IR (KBr): 1690, 1610 cm^{-1}. NMR (DMSO-d_6) δ: 12.21 (1H, br, NH), 11.18 (1H, s, NH), 8.12 (1H, d, J=7 Hz, Ar-H), 7.92 (1H, d, J=7 Hz, Ar-H), 7.90 (1H, s, Ar-H), 3.53 (1H, m, C<u>H</u>CH_3), 2.90 (1H, m, C<u>H</u>$(CH_3)_2$), 2.76 (1H, dd, J=7, 17 Hz, CHC<u>H</u>'H), 2.28 (1H, d, J=17 Hz, CHCH'<u>H</u>), 1.29 (6H, d, J=8 Hz, CH$(C\underline{H}_3)_2$), 1.12 (3H, d, J=8 Hz, CH_3).

3,4-Dihydro-4-oxo-2-(4-pyridyl)-7-(2,3,4,5-tetrahydro-5-methyl-3-oxo-6-pyridazinyl)quinazoline (31) A similar procedure to that described for **29** was carried out except (for the use of 4-pyridinecarbonyl chloride (1.6 g, 11 mmol) instead of Ac_2O to give **31** (1.3 g, 87%), which was recrystallized from DMF–water for analysis, mp > 300 °C. *Anal.* Calcd for $C_{18}H_{15}N_5O_2 \cdot H_2O$: C, 61.52; H, 4.89; N, 19.92. Found: C, 61.59; H, 4.65; N, 20.10. IR (KBr): 1680, 1660, 1600 cm^{-1}. NMR (DMSO-d_6) δ: 12.82 (1H, br, NH), 11.22 (1H, s, NH), 8.81 (2H, m, Ar-H), 8.22—8.00 (5H, m, Ar-H), 3.57 (1H, m, C<u>H</u>CH_3), 2.80 (1H, dd, J=7, 17 Hz, CHC<u>H</u>'H), 2.30 (1H, d, J=17 Hz, CHCH'<u>H</u>), 1.12 (3H, d, J=8 Hz, CH_3).

4,5-Dihydro-6-(3-amino-4-cyanophenyl)-5-methyl-3(2*H*)-pyridazinone (33) A solution of **20** (17.0 g, 66 mmol) in DMF (120 ml) was added dropwise to a solution of $SnCl_2 \cdot 2H_2O$ (46.0 g, 200 mmol) in conc. HCl (140 ml) for 30 min at 5—10 °C. The precipitated crystals were collected by filtration, washed with successive 50% DMF–conc. HCl and water. The resulting crystals were dissolved in DMSO and the mixture was neutralized with 2 N NaOH, then concentrated. The residue was mixed with water and the precipitated crystals were collected by filtration, washed successively with water and MeOH and dried to give crude **33** (10.0 g, 67%), which was recrystallized from DMSO–water for analysis, mp 208—209 °C. *Anal.* Calcd for $C_{12}H_{12}N_4O$: C, 63.14; H, 5.30; N, 24.55. Found: C, 62.78; H, 5.40; N, 24.49. IR(KBr): 2200, 1680, 1640 cm^{-1}. NMR (DMSO-d_6) δ: 11.01 (1H, s, NH), 7.38 (1H, d, J=8 Hz, Ar-H), 7.20 (1H, s, Ar-H), 6.96 (1H, d, J=8 Hz, Ar-H), 6.05 (2H, br, NH_2), 3.45 (1H, m, C<u>H</u>CH_3), 2.70 (1H, dd, J=7, 17 Hz, CHC<u>H</u>'H), 2.23 (1H, d, J=17 Hz, CHCH'<u>H</u>), 1.06 (3H, d, J=8 Hz, CH_3).

4,5-Dihydro-6-[4-cyano-3-(ethoxymethyleneamino)phenyl]-5-methyl-3(2*H*)-pyridazinone (34) A mixture of **33** (10.0 g, 44 mmol), CF_3CO_2H (0.5 ml) and triethyl orthoformate (100 ml) was stirred for 1 h at 80 °C. The precipitate was removed by filtration and the filtrate was concentrated. The residue was mixed with Et_2O, collected by filtration, washed with Et_2O, and dried to give crude **34** (10.2 g, 82%). The crystals were used in the next reaction without further purification because of their instability, even in the crystalline state. IR(KBr): 2210, 1680, 1630 cm^{-1}. NMR (DMSO-d_6) δ: 11.10 (1H, s, NH), 8.11 (1H, s, Ar-H), 7.72 (1H, d, J=8 Hz, Ar-H), 7.64 (1H, d, J=8 Hz, Ar-H), 7.49 (1H, s, Ar-H), 4.33 (2H, q, J=7 Hz, CH_2CH_3), 3.48 (1H, m, C<u>H</u>CH_3), 2.78 (1H, dd, J=7, 17 Hz, CHC<u>H</u>'H), 2.30 (1H, d, J=17 Hz, CHCH'<u>H</u>), 1.36 (3H, t, J=7 Hz, CH_2CH_3), 1.08 (3H, d, J=8 Hz, CH_3).

3,4-Dihydro-4-imino-3-methyl-7-(2,3,4,5-tetrahydro-5-methyl-3-oxo-6-pyridazinyl)quinazoline (35) A mixture of **34** (1.5 g, 5.3 mmol) and 40% $MeNH_2$–MeOH (40 ml) was stirred for 30 min at 50 °C. The precipitated crystals were collected by filtration, washed with MeOH and dried to give crude **35** (0.9 g, 63%), which was recrystallized from DMF–water for analysis, mp 253—255 °C. *Anal.* Calcd for $C_{14}H_{14}N_5O$: C, 62.44; H, 5.61; N, 26.01. Found: C, 62.39; H, 5.55; N, 25.83. IR (KBr): 1680, 1630, 1590 cm^{-1}. NMR (DMSO-d_6) δ: 10.05 (1H, s, NH), 8.40 (1H, br, NH), 8.23 (1H, d, J=8 Hz, Ar-H), 8.02 (1H, s, Ar-H), 7.78 (1H, d, J=8 Hz, Ar-H), 7.73 (1H, s, Ar-H), 3.47 (1H, m, C<u>H</u>CH_3), 3.41 (3H, s, NCH_3), 2.76 (1H, dd, J=7, 17 Hz, CHC<u>H</u>'H), 2.28 (1H, d, J=17 Hz, CHCH'<u>H</u>), 1.13 (3H, d, J=8 Hz, CH_3).

4-Methylamino-7-(2,3,4,5-tetrahydro-5-methyl-3-oxo-6-pyridazinyl)-quinazoline (36) A mixture of **35** (0.29 g, 1.1 mmol) and 2 N NaOH (10 ml) was stirred for 5 h at 100 °C. The reaction mixture was neutralized with 1 N HCl and the precipitated crystals were collected by filtration, washed with successive water and MeOH, and dried to give crude **36** (0.22 g, 76%), which was recrystallized from DMSO–water for analysis, mp 296—302 °C. *Anal.* Calcd for $C_{14}H_{15}N_5O$: C, 62.44; H, 5.61; N, 26.01. Found: C, 62.37; H, 5.62; N, 25.62. IR (KBr): 1680, 1620, 1580 cm^{-1}. NMR (DMSO-d_6) δ: 11.14 (1H, s, NH), 8.50 (1H, s, Ar-H), 8.33 (1H, br, NH), 8.18 (1H, d, J=8 Hz, Ar-H), 7.95 (1H, s, Ar-H), 7.92 (1H, d, J=8 Hz, Ar-H), 3.48 (1H, m, C<u>H</u>CH_3), 3.01 (3H, d, J=4 Hz, NHC<u>H</u>$_3$), 2.78 (1H, dd, J=7, 17 Hz, CHC<u>H</u>'H), 2.31 (1H, d, J=17 Hz, CHCH'<u>H</u>), 1.15 (3H, d, J=8 Hz, CH_3).

References and Notes

1) Part V: Y. Nomoto, H. Takai, T. Hirata, M. Teranishi, T. Ohno and K. Kubo, *Chem. Pharm. Bull.*, **39**, 86 (1991).
2) For a recent review; M. D. Taylor, I. Sircar and R. P. Steffen, *Annu. Rep. Med. Chem.*, **22**, 85 (1987).
3) J. A. Bristol, I. Sircar, W. H. Moos, D. B. Evans and R. E. Weishaar, *J. Med. Chem.*, **27**, 1099 (1984).
4) D. W. Robertson, J. H. Krushinski, E. E. Beedle, V. Wyss, G. Don Pollock, H. Wilson, R. F. Kauffman and J. S. Hayes, *J. Med. Chem.*, **29**, 1832 (1986).
5) V. Austel, J. Heider, W. Eberlein, W. Diederen and W. Haarmann, U. S. Patent 4361563 (1982) [*Chem. Abstr.*, **98**, 72123*p* (1983)].
6) N. Hauel, J. Heider, H. Stein, V. Austel, M. Riffen, W. Diederen and W. Haarmann, Ger. Patent 3006671 (1981) [*Chem. Abstr.*, **95**, 203981*e* (1981)].
7) I. Ueda, K. Taniguchi and Y. Katsura, Eur. Patent Appl. EP 132817 (1985) [*Chem. Abstr.*, **102**, 166768*f* (1985)].
8) D. E. Kuhla, H. F. Campbell, W. L. Studt, W. C. Faith and B. F. Molino, WO Patent 87 03201 [*Chem. Abstr.*, **108**, 6037*n* (1988)].
9) D. J. Brown and K. Ienaga, *J. Chem. Soc., Perkin Trans. 1*, **28**, 2182 (1975).
10) Part I: Y. Nomoto, H. Obase, H. Takai, T. Hirata, M. Teranishi, J. Nakamura and K. Kubo, *Chem. Pharm. Bull.*, **38**, 1591 (1990).
11) A. A. Alousi, J. M. Canter, M. J. Nontenaro, D. J. Fort and R. A. Ferrari, *Fed. Proc., Fed. Am. Soc. Exp. Biol.*, **410**, 663 (1981).

Basic Operating Characteristics of Neural Networks When Applied to Structure–Activity Studies[1)]

Tomoo AOYAMA[a] and Hiroshi ICHIKAWA*[,b]

Hitachi Computer Engineering Co., Ltd.,[a] Horiyamashita, Hadano, Kanagawa 259–13, Japan and Hoshi College of Pharmacy,[b] Shinagawa, Tokyo 142, Japan. *Received June 16, 1990*

This paper describes the basic operating characteristics in perceptron-type neural networks, especially when applied to structure–activity relationships (SAR). It was shown that the neural network has outstanding abilities in both classification and fitting. The operation of the neural network is basically carried out in a nonlinear manner. This nonlinearity brings forth merits as well as a small number of demerits. Problems with the operation of the neural network are pointed out and discussions are aimed at solutions.

Keywords neuro-computer; neural network; perceptron; multiregression analysis; graded classification; QSAR; SAR

The neural network (or so-called neuro-computer) is a data-processing method which was suggested by the neuron's operation in the brain.[2)] The basic idea of the neuro-computer goes back to the 1940s,[2)] the same era as that of the Neumann-type digital computer.[3)] Although the rapid development of the latter technique had made the study of neuro-computers less important, basic studies have been continued by a number of pioneering researchers. The operation of the neural network involves parallel-distributed processing and has recently attracted considerable attention, since this method may break through the bottleneck of the Neumann-type digital computer to jump to a new generation of computer architecture.

"Neural Network" is the name of the hardware structure, as compared to the usual serial processing unit. Fortunately, most of the operations of a neuro-computer can be simulated using a digital computer. Besides, such a simulation is more convenient in application studies than rigid hardware construction, since one can easily change the structure and the mode of operation.

There are several types of network connections such as the perceptron-type,[4)] the Hopfield type,[5)] and the Boltzmann-machine type (Fig. 1).[6)] Here we deal only with the perceptron-type connection. Perceptron was first proposed by Rosenblatt in 1957 as a model of self-organization, *i.e.* learning, in recognition.[4)] Although this method had attracted considerable attention and was studied by a number of researchers, in 1969 Minsky and Papert pointed out the limit of the perceptron's operation in linear separation[7)]: for example, even the simple Exclusive-OR function cannot be performed. This problem was solved recently by constructing a multi-layer network with a back-propagation algorithm.[8)] In addition, the perceptron-type neural network was found to perform far more functions than expected.[9)]

Recently, we have shown that a three-layer neural network works well in graded classification and multi-dimensional fitting. Therefore, it is a potential tool for studies of the structure–activity relationship (SAR) in developing drugs.[1b,10)] However, one may need to know the basic characteristics of the neural network's operation before adopting it. To this end, we have studied the operational characteristics of neural networks intended for use in SAR studies. To avoid complexity, we only deal with a three-layer network in this paper. In reality, the operation of a three-layer network is considered to be sufficient for practical application to SAR studies.

Mathematical Foundation of the Neural Network's Operation 1) Classification Shown in Fig. 2 is the perceptron-type three-layer network: The circles are neurons which are, in simulation, variables taking a value ranging from 0 to 1. The data is input to A and are output from B. Usually, the number of neurons in the input layer is set to be equal to that of the parameters (characteristics) plus 1, while that of the output layer is equal to the number of categories. The number of neurons in the second layer is arbitrary.

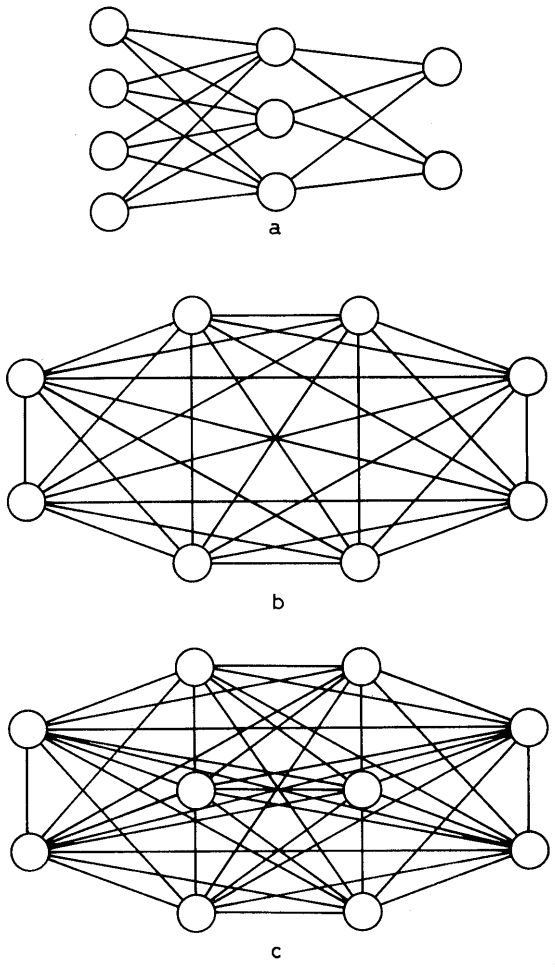

Fig. 1. Neural Network Connections

a, perceptron-type connection. This has a hiararchy structure. b, Hopfield-type connection in which the neurons are peripherally connected. c, Boltzmann machine-type connections in which the neurons are connected to all other neurons. Therefore, the perceptron-type and Hopfield-type connections are considered to be special cases of the Boltzmann machine-type connection.

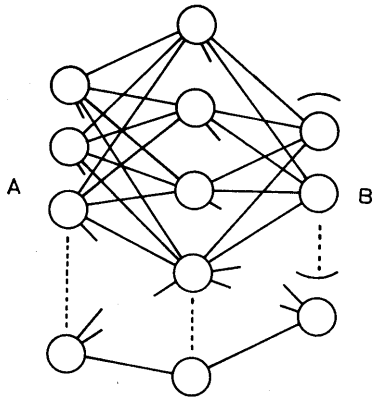

Fig. 2. A Three-Layer Perceptron-Type Neural Network Used in This Study

A, input side; B, output side. The number of neurons of the input (first) layer is the number of parameters plus 1 while that of the second layer is arbitrary. The number of neurons of the third (output) layer is set to be the number of categories in the classification or one in the fitting operation.

However, a small number reduces the resolution ability of the network whereas a large number consumes considerable time in the training phase. The recommended number is somewhere between the number of input neurons and double their number, unless the number of the input parameters is small (*e.g.* less than 5).

The value of a neuron (O_j) at the second or third layer can be expressed by Eq. 1,

$$O_j = 1/[1+\exp(-\alpha y_j)] \equiv f(y_j), \quad (1)$$

$$y_j = (\sum_i W_{ij} x_i) - \theta_j$$

where x_i is one of the values of a neuron at the first or second layer; W_{ij}, an element of the weight matrix, expresses the weight value of the connection between neurons i and j, and takes either a positive or a negative value; α is a parameter which expresses the nonlinearity of the neuron's operation; θ_j is a threshold value for neuron j. Usually, one needs not to set this value if constant 1 is always given to one of the neurons in the input layer. The reason is that the connection weights between the neuron with constant 1 and any of the neurons in the second layer are optimized during the learning (training) phase to play the same role as that of the optimized θ. The sigmoid function, $f(y)$, is not unique, and can be replaced by any function with an appropriate operation if it is differentiable (in the present study we used the sigmoid function). On feeding the input data, the value of each neuron expressed by Eq. 1 is synchronously renewed.

Given N neurons at the first layer. A set of the input data can be expressed by a vector with N elements for the input neurons, which is called here an "input pattern." Likewise, the output data can also be regarded as a vector and be called an "output pattern" (C_j). The vector which is compared with an output pattern to fix W_{ij} is called a "training pattern" (t_j).

The training of the network is based on the following equations.

$$\delta W_{ij} = -d_j x_i \varepsilon \quad (2)$$

$$d_j = (O_j - t_j) f'(y_j) \quad (3a)$$

$$d_j = \left(\sum_l W'_{jl} d'_l\right) f'(y_j) \quad (3b)$$

Here, ε is a parameter which determines the shift for correction in back-propagation. Equation 3a is used only to correct the connection between the second and third (output) layers while 3b is for another connection where W'_{jl} and d'_l at the second layer are W_{ij} and d_j at the third layer. If f is a sigmoid function, the derivative function, f', in Eq. 3 is,

$$f'(y_j) = f(y_j)[1 - f(y_j)] \cdot \alpha \quad (4)$$

In the above equations, both ε and α can be set independently of the layer.

Since the value of each neuron is defined between 0 and 1, the given data must be appropriately rescaled within the defined region. Here it should be noted that if the value of a neuron in the input layer is zero, the connections from such a neuron are always null, *i.e.*, the information from that neuron is not propagated to the second and the third layers. To avoid this difficulty, the smallest value should be set at slightly larger than zero, typically 0.1. We, therefore, used the following scaling equation,

$$\tilde{p} = ((q_{max} - q_{min})p + q_{min}p_{max} - q_{max}p_{min})/(p_{max} - p_{min}) \quad (5)$$

where q_{max} and q_{min} are the maximum and minimum values of scaling, p is the element of the input pattern to be scaled, p_{max} and p_{min} are the maximum and minimum values of the elements of the input patterns. Finally, each element of the training pattern should also be between 0 and 1.

There may be a number of ways to express the graded categories. For example, we simply used the pattern (0,0,0,0,1) for the first, and (1,0,0,0,0) for the fifth grade in the five-graded classification. By doing so, one can observe the degree of contamination in the determined class from other classes.

Training is carried out according to the above back-propagation algorithm until the error function,

$$E = \sum_j (O_j - t_j)^2 \quad (6)$$

becomes small enough. Even when M sets of the input and training patterns are given, all of the output patterns can be made close enough to the training patterns by iteration through Eqs. 1 and 2 owing to the convergence theorem of perceptron.[11] If convergence is attained, then the neural network has an ability to classify the input patterns into M groups.

2) Quantitative Structure–Activity Relationship (QSAR) Analysis Our previous paper showed that it is not only possible to let the neural network do similar work, such as multiregression analysis, but also that multiregression analysis is actually a special function of the neural network's operation.[1b] Namely, the fitting mode of multiregression analysis is linear while that of the neural network is nonlinear, including linear fitting as a special case.

The structure of the neural network used for the fitting operation is the same as that for graded classification except that the number of the neurons of the third layer is one. This neuron takes an analog value ranging from 0 to 1, so the training pattern consists of only one element with an

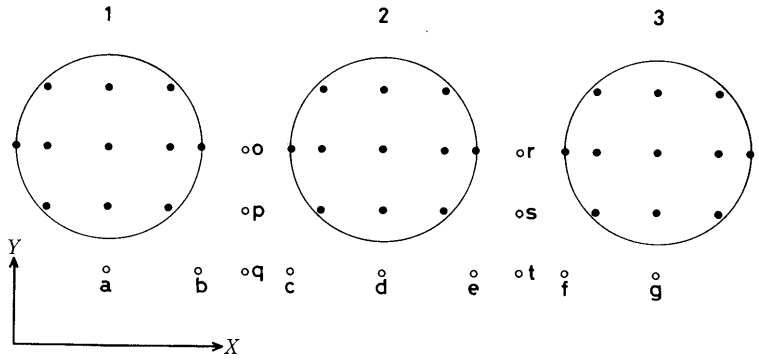

Fig. 3. Simple Classification and Prediction

The positional data in circles 1, 2, and 3 are used for training as classes 1, 2, and 3, respectively.

analog value scaled between 0 and 1.

Results and Discussion

Characteristics in Classification The neural network accepts any kind of data that is expressed numerically. In the learning (training) phase, information about the relationship between the input and training patterns are accumulated in the weight matrices. Once these matrices are fixed, the network predicts the categories of untrained data, even if they are out of defined regions. Generally, such a classification is carried out on a multi-dimensional scale. However, for simplicity, we show the characteristics of classification using a two-dimensional scale. The results are considered to stand in any dimensional space.

1) Simple Classification and Prediction Three circles in the x, y plane in Fig. 3 are the regions to which classified data should belong. The 11 symmetrical points of each circle are selected in terms of x, y coordinates as input data to form regions 1, 2, or 3. Points a—g are selected so we know how the network determined by those regions decides the points of undefined regions. Points o—t are on the center lines between regions 1 and 2 and regions 2 and 3.

It may also be interesting to know how the network judges them. The input data and the results of calculation are shown in Table I. Although it is better to scale not only the data used for training but also that for prediction, in practice, such a scaling may be difficult since both data may not be given at the same time. Therefore, p_{min} and p_{max} were determined for Eq. 5 using the data for training, and were used to scale the data both for training and prediction. The scaling range was arbitrary if the condition, $0<p\leqq 1$, is kept. In the present case, the range was set to be between 0.1 and 0.9. The number of the input parameter is 2, so that of the neurons in the first layer was 3. Since this number was too small to form the second layer, 10 neurons were incorporated in the second layer. The α, ε, and θ values in Eqs. 1 and 2 were set to be 1.0, 0.15, and 0.

From Table I, all points used for training were found to be correctly classified. It is also understood that the points of undefined regions were forced to belong to any in the nearest region. This is a remarkable character of the neural network: The network classifies the given data anyway. The input data of an undefined region may be classified by looking for a similar pattern experienced in the training phase.

One may see an asymmetric character in classification: the output patterns for points o, p, and q show that those

TABLE I. Input Data and Results for a Simple 3 Class Problem

	Input data			Result			
	x	y	Class	Output pattern			Decsn
Group A							
A1	0.0	10.0	1	1.000	0.000	0.000	1
A2	1.0	12.0	1	1.000	0.000	0.000	1
A3	1.0	10.0	1	1.000	0.000	0.000	1
A4	1.0	8.0	1	1.000	0.000	0.000	1
A5	3.0	12.0	1	1.000	0.000	0.000	1
A6	3.0	10.0	1	1.000	0.000	0.000	1
A7	3.0	8.0	1	1.000	0.000	0.000	1
A8	5.0	12.0	1	0.998	0.002	0.000	1
A9	5.0	10.0	1	0.997	0.003	0.000	1
A10	5.0	8.0	1	0.996	0.006	0.000	1
A11	6.0	10.0	1	0.973	0.033	0.000	1
Group B							
B1	9.0	10.0	2	0.028	0.996	0.000	2
B2	10.0	12.0	2	0.004	0.991	0.000	2
B3	10.0	10.0	2	0.003	0.993	0.000	2
B4	10.0	8.0	2	0.002	0.995	0.000	2
B5	12.0	12.0	2	0.000	0.998	0.000	2
B6	12.0	10.0	2	0.000	0.998	0.000	2
B7	12.0	8.0	2	0.000	0.998	0.000	2
B8	14.0	12.0	2	0.000	0.997	0.002	2
B9	14.0	10.0	2	0.000	0.995	0.004	2
B10	14.0	8.0	2	0.000	0.993	0.006	2
B11	15.0	10.0	2	0.000	0.973	0.031	2
Group C							
C1	18.0	10.0	3	0.000	0.030	0.971	3
C2	19.0	12.0	3	0.000	0.008	0.991	3
C3	19.0	10.0	3	0.000	0.006	0.994	3
C4	19.0	8.0	3	0.000	0.004	0.996	3
C5	21.0	12.0	3	0.000	0.001	0.999	3
C6	21.0	10.0	3	0.000	0.001	0.999	3
C7	21.0	8.0	3	0.000	0.001	0.999	3
C8	23.0	12.0	3	0.000	0.000	1.000	3
C9	23.0	10.0	3	0.000	0.000	1.000	3
C10	23.0	8.0	3	0.000	0.000	1.000	3
C11	24.0	10.0	3	0.000	0.000	1.000	3
a	3.0	6.0		1.000	0.000	0.000	1
b	6.0	6.0		0.950	0.092	0.000	1
c	9.0	6.0		0.015	0.984	0.000	1
d	12.0	6.0		0.000	0.998	0.000	2
e	15.0	6.0		0.000	0.916	0.113	2
f	18.0	6.0		0.000	0.012	0.990	3
g	21.0	6.0		0.000	0.001	0.999	3
o	7.5	10.0		0.493	0.551	0.000	2
p	7.5	8.0		0.411	0.671	0.000	2
q	7.5	6.0		0.335	0.773	0.000	2
r	16.5	10.0		0.000	0.502	0.553	3
s	16.5	8.0		0.000	0.341	0.715	3
t	16.5	6.0		0.000	0.215	0.834	3

points are unanimously shifted to region 2 and those for r, s, and t to region 3, the region with larger positional data.

To investigate the detailed characters of prediction, the following experiments were carried out: The lengths between 0 and 10 along the x and y axes were sectioned into 99 and 60 parts; therefore, 5940 ($=99\times60$) points were taken as the input data in which two points, (0,0) and (10,10) were used as the training patterns and were expressed by vectors, (1,0) and (0,1), respectively. The α value was 1.0. The number of neurons in the first and last layers were set at 3 and 2, while that of the second layer was set as high as 30 in order to avoid the influence of the neuron's number in this layer.

Figure 4 shows how the network predicts untrained points (5938 points). The numbers in the figure express the predicted neuron's values (O_j) which are approximately multiplied by 10 and integered, *i.e.*, the values 0, 1, $\cdots$9 express the ranges between *ca.* 0 and 0.09, 0.1 and 0.19$\cdots$, and 0.9 and 1.0, respectively.

Figure 4-a is the contour map thus obtained for the first element of the output pattern, which is designated by □ while Fig. 4-b, for the second elements, is designated by □. As already seen, an asymmetric character of prediction is observed: The network has a slight tendency to judge input points favorably to belong to the region with large positional values. The problem of this asymmetricity will be further discussed in a later section.

2) Nonlinear Classification Using the above data-generating procedure, 5940 points were taken as the input data. Among these, four points, (0,0), (10,10), (0,10), (10,0) were so trained that the first two points, designated by □, was for class 1 ((1,0) in terms of vector) and the others, designated by □, for class 2 (or (0,1)). This is the simplest

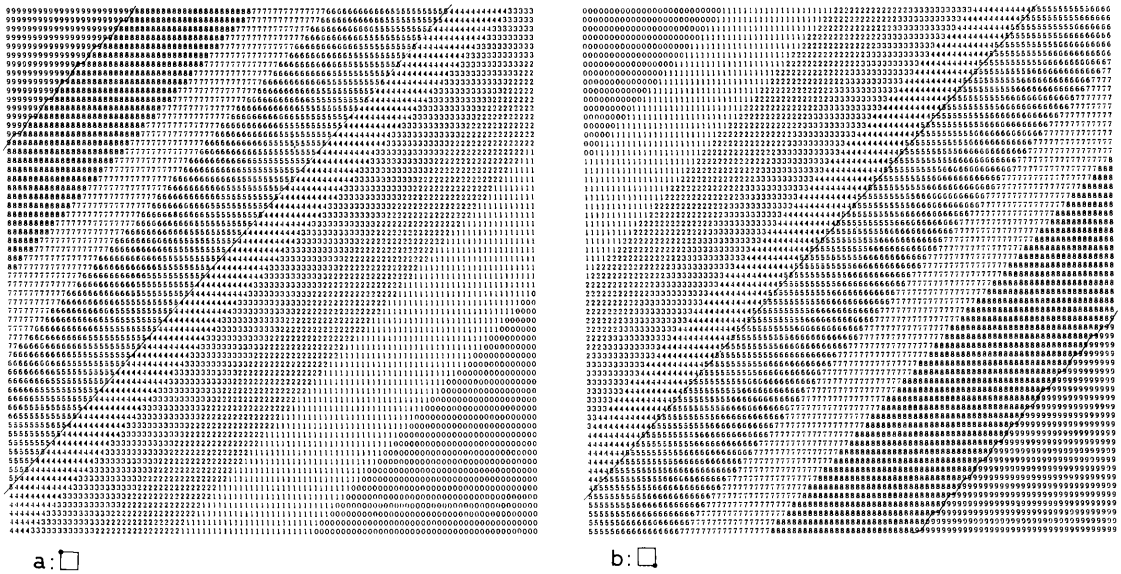

Fig. 4. Contour Maps of Output Vector

a, first element (□); b, second element (□). The numbers in the maps express the predicted values for 5940 points, which are approximately multiplied by 10 and integered.

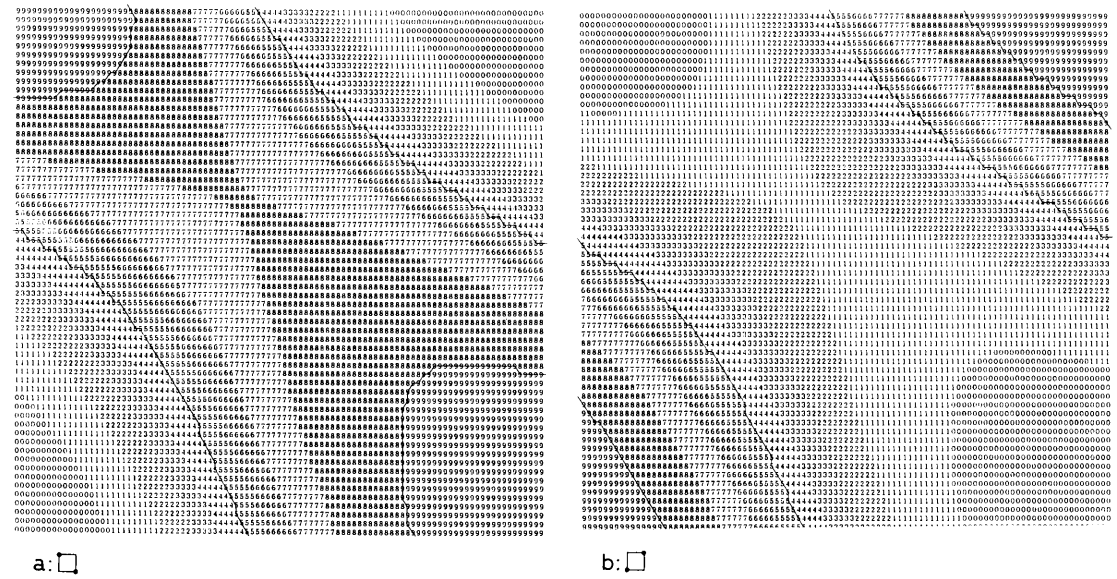

Fig. 5. Contour Maps of Nonlinear Separation

a, class 1 (□); b, class 2 (□).

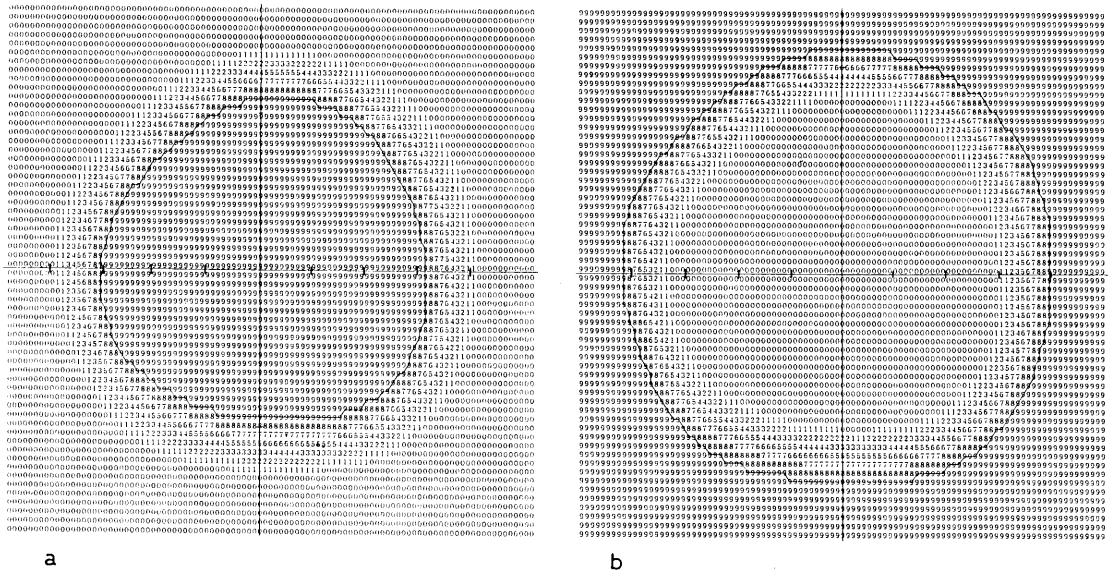

Fig. 6. Contour Maps of Concentric Two-Class Separation
a, class 1 (inner circle); b, class 2 (outer circle).

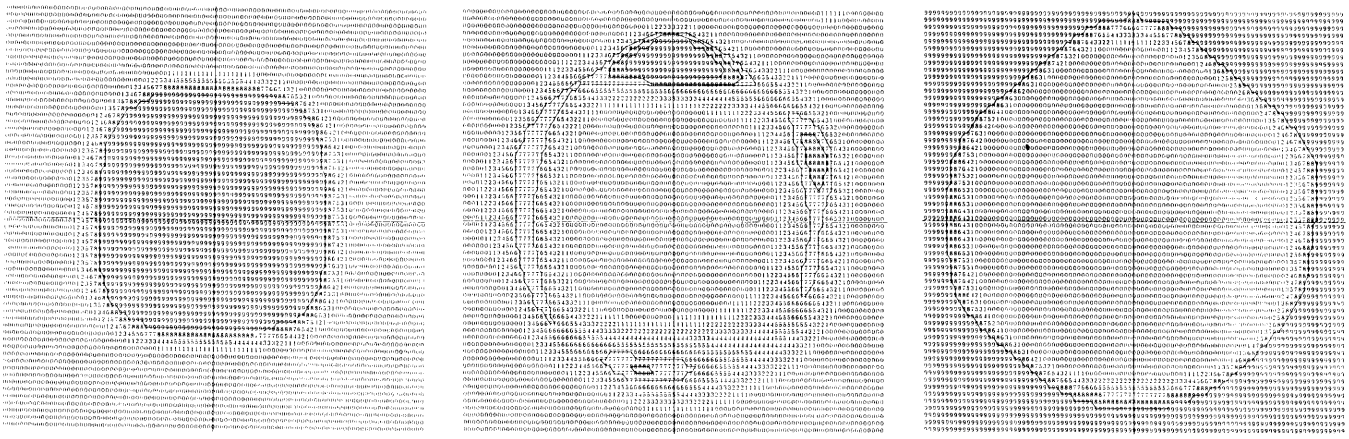

Fig. 7. Contour Maps of Concentric Three-Class Separation
a, class 1 (inner circle); b, class 2 (intermediate circle); c, class 3 (outer circle).

example of nonlinear classification, *i.e.*, an Exclusive OR function. The network structure is the same as that in Fig. 4. Figure 5 shows the results.

The classification is easily and correctly carried out. Again, the contour maps of prediction show asymmetric characters similar to those observed in the former cases.

3) Classification of Concentric Regions Although concentric classification may not appear in the SAR study, we used this problem to show the classification ability of the neural network. Again, we used two-dimension positional data. The concentric circles were defined by the diameters, 3, 4, and 5 (the scale is indicted in the figures). The circular region within diameter 3 was assigned as region 1 and the region surrounded by the circles with diameters 4 and 5 was assigned as region 2. The 28 points were so taken for each region as to become an even population in the regions and were used for training. The 5940 points were predicted by the network after training. The α, ε, and θ values are set to be 1.0, 0.15, and 0.

Figure 6-a shows the contour map for the first element of the output pattern, and Fig. 6-b for the second element. The classification worked nicely: All points used for training are correctly classified. As for prediction, all points in region 1 are completely assigned to class 1 with a vector element of more than 0.9. The points in both region 2 and the outer region are predicted to be class 2.

Next, simultaneous separation of regions 1, 2, and 3 were examined. The concentric circles in Fig. 7 have diameters of 1.85, 2.85, 3.35, 4.0, 4.4 and 5.0. The regions between 1.85 and 2.85, 3.35 and 4.0, and 4.4 and 5.0 are defined as regions 1, 2, and 3, respectively. The 28 training points are taken for each region. Again the 5940 points are input to produce the contour maps shown in Fig. 7.

This classification seemed to be difficult for the three-layer network: the error, E, did not become less than 0.15 at the give α value of 1.0. However, by increasing the α value to 5.0, the error value dropped to less than 0.02. Although contamination from other classes is included in the output patterns, all points were correctly classified even when $\alpha = 1.0$.

Characteristics of QSAR Analysis QSAR analysis was performed using multiregression analysis. As we already demonstrated,[11] one can allow the neural network do a job similar to that of multiregression analysis. In fact, the analysis by the network often gives better results. This stems from the basic difference between the two analytic methods, that is, multiregression analysis seeks linear dependence while the network uses nonlinear dependence including linear dependence. We show how linear/nonlinear fitting is carried out by the neural network. The α, ε, and θ values are set to be 4.0, 0.15, and 0. The influence of the α value on fitting performance will be mentioned. The number of neurons in the second layer was fixed to be 10.

1) Fitting in the Straight Line ($y=x$) This is a typical linear-fitting, in which regression analysis is most efficient. The input data and network training data are the same. We used 40 data as 0.0, 0.5, 1.0, $\cdots$ 18.5, 19.0, and 19.5. We examined the threshold values, 0.01, 0.001, and 0.0001 in terms of the scale unit, to see the influence of this value. The results are shown in Fig. 8, where the straight line is $y=x$ on which the input and training data are located. One may observe an interesting characteristic of the fitting performance: It becomes appearent at a large threshold value. Namely, at both ends (*i.e.*, 0.0 and 19.5) the difference between input and calculated values becomes substantial and the deviation appears sinusoidally along the straight line. If the α value is reduced to 1, the sinusoidal deviation becomes small. This is understandable because the α value in Eq. 1 can be regarded as a nonlinearity parameter.

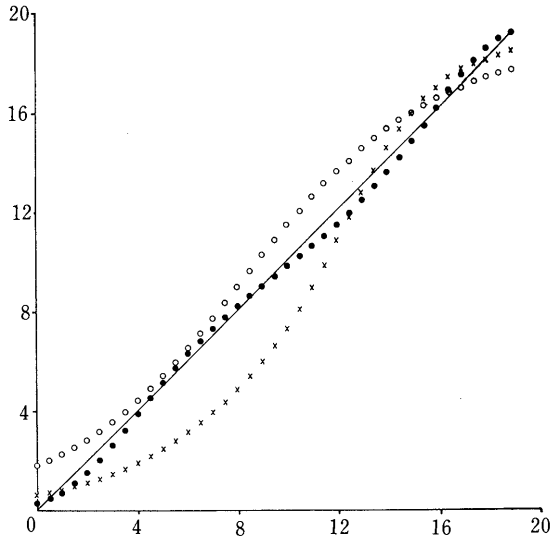

Fig. 8. Influence of the Threshold Value in Fitting in $y=x$
Open circles, 0.01; crosses, 0.001; filled circles, 0.0001.

To determine the prediction ability, we performed the following experiment. The numbers of input and training were are reduced to 10: they were taken in units of 2: 0.0, 2.0, 4.0, $\cdots$ 18.0. After training, we observed how the network predicted intermediate values. The input data and results are shown in Table II where the positional data used for training is underlined. The α, ε, and θ values are 4.0, 0.15, and 0. The threshold value was set to be 0.0001.

Again it is seen that the deviation appears sinusoidally. The points between the trained points are well interpolated. Another interesting character of prediction is also observed in the untrained region: the expected values in the high region are always smaller than those expected from the $y=x$ line. This situation appears very generally. The reason is that the network performs a nonlinear fitting to the given data; the data out of the training region cannot, therefore, be handled well resulting in estimating them to be near the highest value of the defined region. This is inevitable because of the network's nonlinear operation, and may be a defect of the neural network when used for the QSAR study, compared to multiregression analysis: In developing drugs, one may seek a stronger biological activity for a compound to be examined as compared to known drugs. However, it should be noticed that the network always predicts the values of the outer region as higher than the highest value of the defined region, *i.e.*, the compound with a stronger

TABLE II. Input Data[a] and Results for Linear Fitting

x	y	Δy	x	y	Δy
0.0	0.702	0.702	10.0	10.112	0.112
0.5	0.912	0.412	10.5	10.567	0.067
1.0	1.169	0.169	11.0	11.024	0.024
1.5	1.477	−0.023	11.5	11.492	−0.008
2.0	1.838	−0.162	12.0	11.974	−0.026
2.5	2.251	−0.249	12.5	12.474	−0.026
3.0	2.713	−0.287	13.0	12.996	−0.004
3.5	3.218	−0.282	13.5	13.537	0.037
4.0	3.757	−0.243	14.0	14.092	0.092
4.5	4.320	−0.180	14.5	14.652	0.152
5.0	4.897	−0.103	15.0	15.200	0.200
5.5	5.479	−0.021	15.5	15.720	0.220
6.0	6.057	0.057	16.0	16.193	0.193
6.5	6.623	0.123	16.5	16.606	0.106
7.0	7.174	0.174	17.0	16.950	−0.050
7.5	7.706	0.206	17.5	17.223	−0.177
8.0	8.219	0.219	18.0	17.433	−0.567
8.5	8.712	0.212	18.5	17.588	−0.912
9.0	9.190	0.190	19.0	17.700	−1.300
9.5	9.655	0.155	19.5	17.780	−1.720

a) The positional data with underline was used for training.

TABLE III. Fitting to the $y=x^2$ Function

x	x^2	x^2_{calcd}	Δ	x	x^2	x^2_{calcd}	Δ
−10.0	100.0	96.8	−3.2	0.5	0.3	1.9	1.5
−9.5	90.3	91.2	1.2	1.0	1.0	2.3	1.3
−9.0	81.0	82.1	1.1	1.5	2.3	3.1	0.8
−8.5	72.3	71.4	−0.9	2.0	4.0	4.3	0.3
−8.0	64.0	61.4	−2.6	2.5	6.3	6.1	−0.2
−7.5	56.3	53.0	−3.3	3.0	9.0	8.6	−0.4
−7.0	49.0	46.2	−2.8	3.5	12.3	11.8	−0.5
−6.5	42.3	40.5	−1.8	4.0	16.0	15.6	−0.4
−6.0	36.0	35.4	−0.6	4.5	20.3	19.9	−0.4
−5.5	30.3	30.5	0.2	5.0	25.0	24.6	−0.4
−5.0	25.0	25.6	0.6	5.5	30.0	29.6	−0.4
−4.5	20.3	20.7	0.4	6.0	36.0	35.0	−1.0
−4.0	16.0	15.9	−0.1	6.5	42.3	41.0	−1.3
−3.5	12.3	11.6	−0.7	7.0	49.0	47.6	−1.4
−3.0	9.0	8.0	−1.0	7.5	56.3	55.1	−1.2
−2.5	6.3	5.4	−0.9	8.0	64.0	63.3	−0.7
−2.0	4.0	3.6	−0.4	8.5	72.3	71.8	−0.5
−1.5	2.3	2.5	0.2	9.0	81.0	79.9	−0.1
−1.0	1.0	2.0	1.0	9.5	90.3	86.9	−3.4
−0.5	0.3	1.7	1.4	10.0	100.0	92.1	−7.9
−0.0	0.0	1.7	1.7	10.5	110.3	95.6	−14.7

The underlined data was used for training.

activity than the known drugs can be always calculated to be stronger. Therefore, we do not think that this problem emerges severely in practical use.

2) Fitting in $y=x^2$ and $y=\sqrt{x}$ Structural parameters (characteristics) used in the QSAR analysis do not always contribute to drug activity in a linear manner. To include such nonlinearity in the QSAR analysis, the squares and/or roots of some parameters are incorporated. The neural network is good at nonlinear fitting, and therefore, fitting in those functions is expected to be straightforward.

Results for $y=x^2$ and $y=\sqrt{x}$ are shown in Table III and IV, where the predicted values for untrained data are also shown to illustrate interpolation/extrapolation ability. Although sinusoidal deviations appear, the points between the trained points are well predicted in both cases. However, large errors are seen in the end region, as observed in the linearity fitting. Again, it should be noted that the network always predicts the values of the outer region higher than the highest value in the defined region.

3) Fitting in $y=|x-a|$ As an example of the functions which include an indifferentiable point, we tried fitting in $y=|x-10|$, although this kind of situation may not take place in QSAR analysis. The results are shown in Fig. 9, where the open circles are the points used for training. We considered the fitting to be fairly good, though a large error is found in the area larger than the turning point. To remove such an error one must impose a strict threshold on the iteration process. One may also observe an asymmetric character in the fitting.

Problems in Neural Networks As we have seen, the neural network has outstanding abilities in terms of classification and fitting. Such characteristics hold equally in any multi-dimensional space and are applicable in any field. In this section, we point out and discuss some problems of the neural network when applied to SAR studies.

1) Symmetric Operation It was observed that an asymmetric character generally appears in both classification

TABLE IV. Fitting to the $y=\sqrt{x}$ Function

x	$\sqrt{x}$	$\sqrt{x_{calcd}}$	Δ	x	$\sqrt{x}$	$\sqrt{x_{calcd}}$	Δ
0.0	0.00	0.37	0.37	52.5	7.25	7.20	−0.05
2.5	1.58	1.12	−0.46	55.0	7.42	7.38	−0.04
5.0	2.24	2.03	−0.21	57.5	7.58	7.56	−0.02
7.5	2.74	2.79	0.05	60.0	7.75	7.74	−0.01
10.0	3.16	3.34	0.18	62.5	7.91	7.91	0.00
12.5	3.54	3.75	0.21	65.0	8.06	8.08	0.02
15.0	3.87	4.07	0.20	67.5	8.22	8.25	0.03
17.5	4.18	4.35	0.17	70.0	8.37	8.41	0.04
20.0	4.47	4.59	0.12	72.5	8.51	8.57	0.06
22.5	4.74	4.83	0.09	75.0	8.66	8.73	0.07
25.0	5.00	5.05	0.05	77.5	8.80	8.86	0.06
27.5	5.24	5.26	0.02	80.0	8.94	9.00	0.06
30.0	5.48	5.47	−0.01	82.5	9.08	9.13	0.05
32.5	5.70	5.68	−0.02	85.0	9.22	9.24	0.02
35.0	5.92	5.88	−0.04	87.5	9.35	9.33	−0.02
37.5	6.12	6.08	−0.04	90.0	9.49	9.42	−0.07
40.0	6.32	6.27	−0.05	92.5	9.62	9.49	−0.13
42.5	6.51	6.46	−0.05	95.0	9.75	9.55	−0.20
45.0	6.71	6.65	−0.05	97.5	9.87	9.60	−0.27
47.5	6.89	6.83	−0.06	100.0	10.00	9.63	−0.37
50.0	7.07	7.02	−0.05	102.5	10.12	9.66	−0.46

The underlined data was used for training.

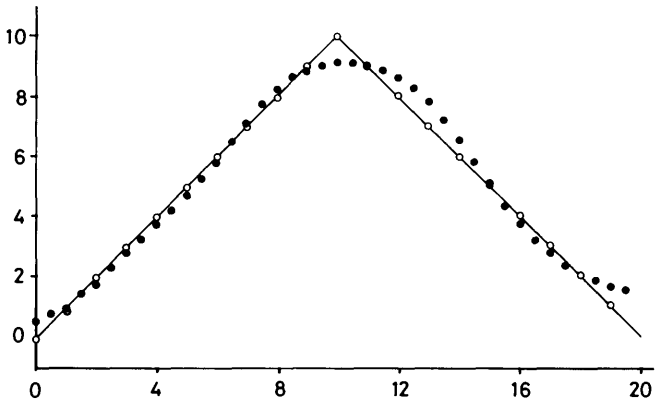

Fig. 9. Fitting Operation in the Function Which Has an Indifferentiable Point ($y=|x-10|$)

Open circles, points used for training; filled circles, predicted values.

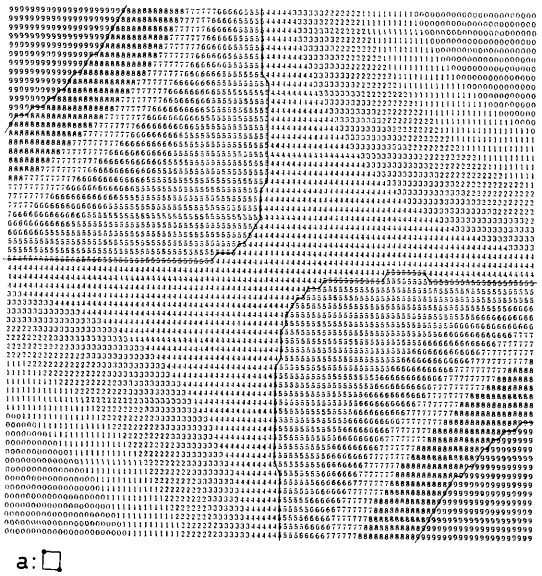

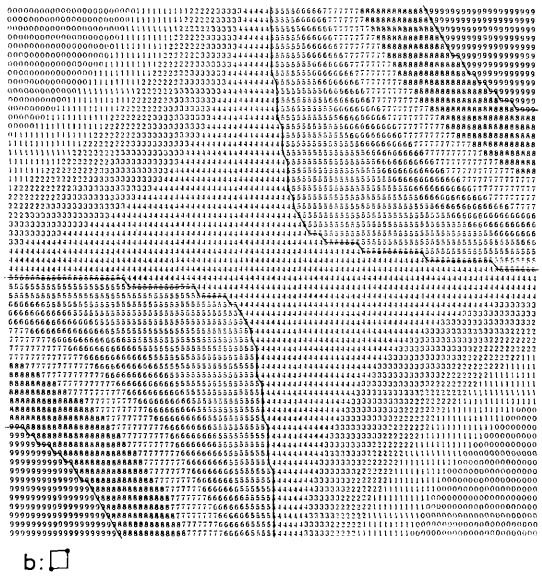

Fig. 10. An Example of Symmetrical Training

a, map for ( ); b, map for ( ).

and fitting. Here, we discuss this problem, although the degree is small and it is unnecessary to worry about in practical use. The asymmetric behavior stems from the asymmetric evaluation of the weight in Eq. 1. Namely, the information with a large value of the input element propagates strongly to the second layer through the weight matrix. It is, therefore, easily possible to make the network perform a symmetric operation by adopting a symmetric output function or simply by adopting a "symmetrical training" procedure. Let us explain the latter method.

Suppose that the input data, $\{p_i\}$, and training data, $\{t_i\}$, are scaled between 0 and 1. Then the reverse of $\{p_i\}$ and $\{t_i\}$ are defined as $\{\bar{p}_i\}(=1-p_i)$ and $\{\bar{t}_i\}(=1-t_i)$. Using these, the following four groups of back-propagation combinations are considered.

$$1:[\{p_i\},\{t_i\}],\quad 2:[\{\bar{p}_i\},\{t_i\}],\quad 3:[\{p_i\},\{\bar{t}_i\}],\quad 4:[\{\bar{p}_i\},\{\bar{t}_i\}]$$

Among those training sets, there may be plural combinations that are equivalent. Removing such redundancies, the effective number of combinations is determined to be N. After N number of trainings, the symmetric output pattern is derived by the following combination,

$$N^{-1}\left\{\sum_{i}^{\in 1,2} O_{1_i}+\sum_{i}^{\in 3,4}(1-O_{1_i})\right\} \tag{7}$$

where the first summation covers groups 1 and 2 while the second one, groups 3 and 4. By this procedure, one can obtain symmetric results. As an example, the result for nonlinear classification is shown in Fig. 10. As one may see, the contour maps are completely symmetric. However, we should say again that such a procedure may be unnecessary in practical use.

2) Convergence The learning process is continued until the sum of the squared errors falls within the present threshold value. When complete convergence is obtained, classification or fitting is completed. Such a convergence is possible according to the convergence theorem of perceptron.[12] In practice, however, it is in some cases very difficult to obtain a reasonable convergence, as we see in the problems of concentric three-class problem and fitting in $y=|x-a|$. Besides, it should be noted that the error function (Eq. 6) could have local minima and therefore, minimization by the back-propagation algorithm does not always give the smallest error.

TABLE V. Convergence Profile in Fitting in $y=|x-10|$

Iteration count	E
1	0.1295
101	0.1781
201	0.0337
301	0.0207
401	0.0174
501	0.0159
601	0.0147
701	0.0142
801	0.0136
901	0.0132
1001	0.0128
1201	0.0123
1401	0.0121
2001	0.0117
4001	0.0105

Table V shows how E changes according to the number of iterations on fittings in the $y=|x-10|$. The value rapidly converges into 0.03. However, after this point the convergence becomes slow. To increase the converging speed, increase of the ε value may be considered. However, such an increase often results in oscillation of the weight matrices. There are some techniques reported to correct this, such as the momentum method.[12] However, a fundamental solution needs to be found.

3) Linear *vs.* Nonlinear Operation It may be helpful in application to clarify the difference between the linear and

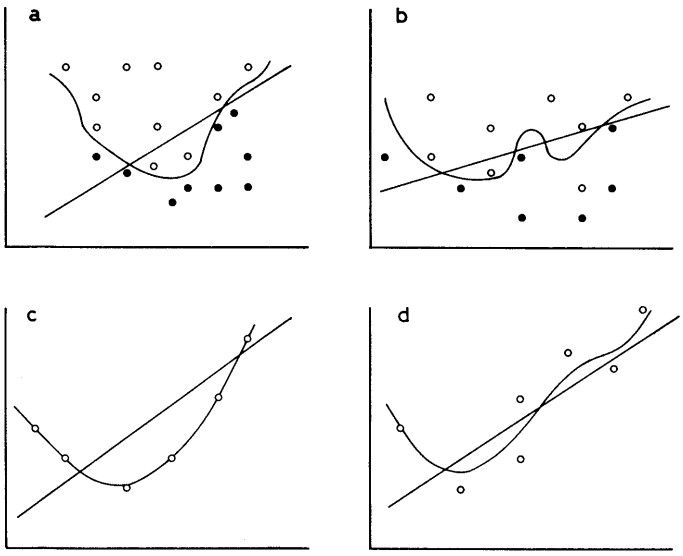

Fig. 11. Nonlinear *vs* Linear Separation and Fitting
a and c, data without contradiction; b and d, data with contradiction.

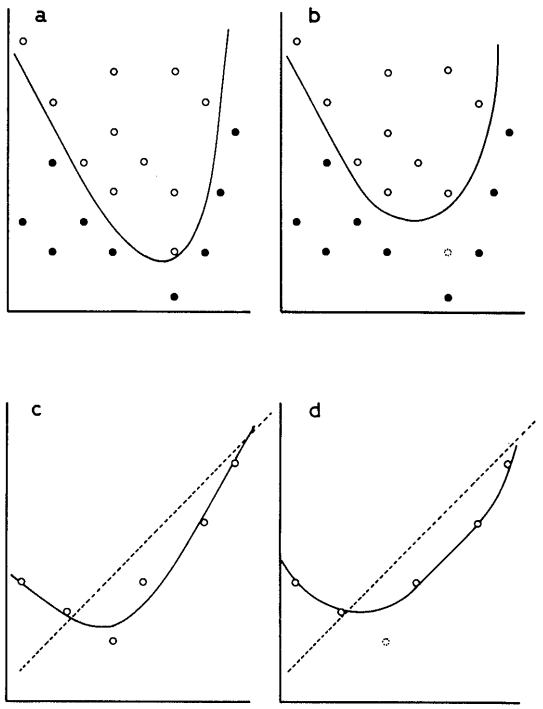

Fig. 12. Conceptual Diagrams of Separation and Fitting
a and b, nonlinear separation; c and d, nonlinear fitting. Diagrams b and d show that if any of the defined data (indicated by dotted circle) is taken out, the separation surface of the fitting line may be changed to give a wrong decision regarding the taken-out item.

nonlinear operations. There are two cases considered: the case in which there is no contradiction among the given data, and the case in which there is contradiction among the given data. The former case is already seen in this paper and the latter may appear in actual application.

Figure 11 shows conceptual diagrams of separation and fitting in the data with and without contradiction. It is apparent that in any case nonlinear operation is superior to linear operation since nonlinear operation includes linear operation as a special case. This is clearly illustrated in Fig. 11. However, the nonlinear operation is not always superior in prediction, for example, in the leave-one-out experiment. This is because "the separation surface or fitting line in a nonlinear operation is defined by the given data and does not assume any special relationship among given data beforehand," while a linear operation always assumes a linear relationship. Therefore, as Fig. 12 shows, if one of the given data is taken out, the separation surface or fitting line in the defined space is changed to give another one; regarding the taken-out item being submitted in this situation, the network naturally predicts it incorrectly. On the other hand, in linear operation, when one of the given data is removed, the separation or fitting line does not change much.

The nonlinear operation is not always superior to the linear operation. Therefore, it is sometimes necessary to incorporate linear operation in the network. This may be possible in several ways: by reducing α or by selecting the output function which behaves linearly *etc.* However, the most efficient method must be investigated.

4) Correlation Analysis A QSAR analysis requires knowledge about the degree of contribution of an input parameter compared to the strength of drug activity. This is easily done in the linear operation; for example, in multiregression analysis, such a factor can be obtained as a correlation coefficient. But because of nonlinear operation, the neural network cannot produce such simple coefficients. This problem will be solved by considering the derivatives of the output strength compared to the input parameter.[13]

Concluding Remarks The neural network method is a state-of-the-art technique which has recently and rapidly been developed. We showed in preceding papers that this method works well when applied to structure–activity studies.[1b,10,14] Here, we have shown the basic characteristics of the neural network's operation and pointed out some problems. However, the methodology is not established yet. We believe that the neural network will offer a far better method if the technique is refined. The apparent advantages are that the neural network accepts ambiguous data and a large number of structural parameters, whether or not they are independent. The operation of the neural network also suggests that there will be methods that remove contradictions included in the experimental data.[13]

Acknowledgment This research was financially supported by the Ministry of Education, Science and Culture (Grant-in-Aid for Developmental Scientific Research No. 02807197).

References

1) *a*) Neural Networks Applied to Pharmaceutical Problems. IV; *b*) For part III T. Aoyama, Y. Suzuki, and H. Ichikawa, *J. Med. Chem.*, **33**, 2583 (1990).
2) W. S. McCulloch and W. Pitts, *Bull. Math. Biophysics*, **5**, 115 (1943).
3) J. Von Neumann, "First Draft of a Report on the EDVAC," Contract No. W-670-Ord-4926, Univ. of Pennsylvania, Philadelphia, 1945.
4) F. Rosenblatt, "Principles of Neurodynamics: Perceptrons and the Theory of Brain Mechanics," Spartan Books, Rockelle Park, 1961.
5) J. J. Hopfield, *Proc. Natl. Sci. U.S.A.*, **79**, 2554 (1982).
6) *a*) D. H. Ackley, G. E. Hinton, and T. J. Sejnowski, *Cognitive Sciences*, **9**, 147 (1985); *b*) G. E. Hinton and T. J. Sejnowski, "Parallel Distributed Processing," Vol. 1, ed. by D. E. Rumelhart and J. L. McClelland, MIT Press, Cambridge, Ma., 1986, Chap. 7.
7) M. Minsky and S. Papert, "Perceptron-An Essay in Computational Geometry," MIT Press, Cambridge, Ma., 1969.
8) D. E. Rumelhart, G. E. Hinton, and R. J. Williams, *Nature* (London), **323**, 533 (1986).
9) *a*) T. J. Sejnowski and C. R. Rosenberg, The Johns Hopkins University Electrical Engineering and Computer Science Technical Report, JHU/EECS-86/01 (1986); *b*) T. J. Sejnowski and C. R. Rosenberg, *Complex Systems*, **1**, 145 (1987); *c*) R. P. Gorman and T. J. Sejnowski, *Neural Networks*, **1**, 75 (1988).
10) T. Aoyama, Y. Suzuki, and H. Ichikawa, *J. Med. Chem.*, **33**, 905 (1990).
11) N. Nilsson, "Learning Machines," McGraw-Hill, 1965.
12) S. E. Fahlman, "Proc. of the 1988 Connectionist Models," Carnegie-Mellon Univ., Pittsburgh, Pa., 1988, pp. 38—51.
13) The details of these methods will be reported in the near future.
14) T. Aoyama, Y. Suzuki, and H. Ichikawa, *Chem. Pharm. Bull.*, **37**, 2558 (1989).

Potential Nootropic Agents, 4-Alkoxy-2-(1-piperazinyl)quinazoline Derivatives[1)]

Manabu HORI,* Ryuichi IEMURA, Hideaki HARA, Takayuki SUKAMOTO, Keizo ITO and Hiroshi OHTAKA

Pharmaceuticals Research Center, Kanebo Ltd., 5–90, Tomobuchi-cho 1-chome, Miyakojima-ku, Osaka 534, Japan. *Received July 26, 1990*

A series of 4-alkoxy-2-(1-piperazinyl)quinazoline derivatives was synthesized and evaluated for its ability to reverse a scopolamine-induced learned impairment in a one-trial passive avoidance task (antiamnestic activity). 2-(4-Allyl-1-piperazinyl)-4-pentyloxyquinazoline (4) showed more potent antiamnestic activity than such reference compounds as aniracetam, idebenone and bifemelane at a wide dose range (1—30 mg/kg)). Compound 4 also exhibited potent anticonvulsive and antihypoxic activities, and was selected as the most promising nootropic candidate agent.

Keywords quinazoline; dementia; scopolamine; one-trial passive avoidance task; antiamnestic activity; nootropic agent

The treatment and prevention of dementia has been one of the most important targets in health science today. The symptoms of dementia include memory-cognitive disorder and affective disturbance.[2)] Drugs used for the treatment of dementia are called nootropic agents.[3)] Nootropic agents such as aniracetam, idebenone and bifemelane (Chart 1) are reported to improve the affective disturbance, but their effects on the memory-cognitive function are not satisfactory.[3)] Therefore, nootropic agents more effective than the existing agents are needed.

The main features of a desirable nootropic agent are (1) the enhancement of learned acquisitions, as well as the resistance of learned behaviors to agents that tend to impair them; (2) the partial enhancement of general resistance of the brain and, particularly, its resistance to physical injuries induced by convulsion, hypoxia and chemical toxicosis.[3,4)] The injuries also result in learned impairment.[5)] Although the existing nootropic agents improve the learned impairment (antiamnestic activity),[6–8)] their brain protective properties are not satisfactory: their antihypoxic activity is very weak,[8)] and there are no reports about their anticonvulsive activity. We considered that the existing nootropic agents could not prevent the progress of a memory-cognitive disorder because of their weak brain protective activity against physical injuries, and that in order to develop a potent nootropic agent, it was important to search for agents which show anticonvulsive and antihypoxic activities in addition to antiamnestic activity.

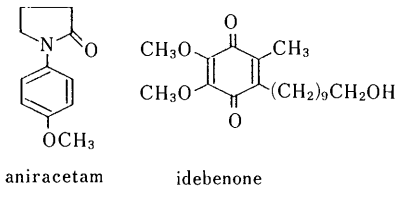

Chart 1

Recently, we reported anticonvulsive and antihypoxic activities of 4-phenoxy-, and 4-alkoxy-2-(1-piperazinyl)-quinazolines.[1,9)] Although the 4-alkoxyquinazolines showed potent anticonvulsive and antihypoxic activities, the antihypoxic activity of the 4-phenoxyquinazolines was negligible. If some compounds among the 4-alkoxyquinazolines showed antiamnestic activity, they would become desirable nootropic agents.

This paper deals with syntheses and evaluation of antiamnestic activity of the 4-alkoxyquinazolines. Structure–activity relationships are also discussed.

Chemistry Compounds for biological evaluation (Table I) were prepared as shown in Chart 2. The 4-alkoxy-2-(1-piperazinyl)quinazolines (**1**—**20**) were prepared by method

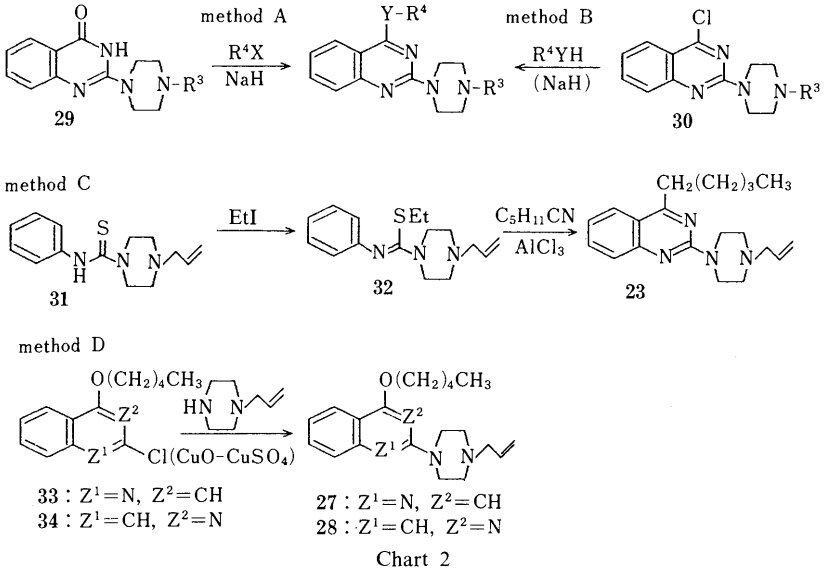

Chart 2

TABLE I. Reversal Activity of Scopolamine-Induced Learned Impairment

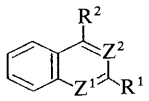

Compound					Mean latency[a] (30 mg/kg, i.p.) % of control
No.	R^1	R^2	Z^1	Z^2	
1[b]		$O(CH_2)_4CH_3$	N	N	117
2[b]		$O(CH_2)_4CH_3$	N	N	88
3[b]		$O(CH_2)_4CH_3$	N	N	125
4[b]		$O(CH_2)_4CH_3$	N	N	292[f]
5[b]		$O(CH_2)_4CH_3$	N	N	182
6[b]		$O(CH_2)_4CH_3$	N	N	91
7[b]		$O(CH_2)_4CH_3$	N	N	176
8[b]		$O(CH_2)_4CH_3$	N	N	167
9		OCH_3	N	N	221[e]
10[b]		$O(CH_2)_2CH_3$	N	N	209[e]
11[b]		$O(CH_2)_3CH_3$	N	N	224[e]
12[b]		$O(CH_2)_5CH_3$	N	N	106
13		$O(CH_2)_7CH_3$	N	N	132
14[b]		$OCH_2CHCH_2CH_2CH_3$ CH_3	N	N	173
15[b]		$OCHCH(CH_3)_2$ CH_2CH_3	N	N	124
16[c]		OPh	N	N	110
17		OCH_2Ph	N	N	100
18		$OCH_2CH_2OCH_2CH_3$	N	N	251[e]
19		$O(CH_2)_3NHCH_3$	N	N	89
20		$OCH_2COOCH_2CH_3$	N	N	164
21		$S(CH_2)_4CH_3$	N	N	154
22		$NH(CH_2)_4CH_3$	N	N	ND[d]
23		$(CH_2)_4CH_3$	N	N	147
24		$O(CH_2)_4CH_3$	N	N	227[e]
25		$O(CH_2)_4CH_3$	N	N	112
26		$O(CH_2)_4CH_3$	N	N	ND[d]
27		$O(CH_2)_4CH_3$	N	CH	180
28		$O(CH_2)_4CH_3$	CH	N	106

a) Statistical significance (Mann–Whitney U-test): *e*) $p<0.05$, *f*) $p<0.01$. *b*) Previously described in reference 1. *c*) Previously described in reference 5. *d*) Not detected because of toxicity.

A or method B, reported by us.[1)]

As compound **4** showed the most significant activity among the 4-alkoxy-2-(1-piperazinyl)quinazolines (**1**—**20**), we converted the 4-pentyloxy group, 1-piperazinyl moiety or quinazoline ring of **4** into other substituents or rings. The 4-pentylthio- and 4-pentylamino-quinazolines (**21** and **22**) were prepared by method B. We obtained 4-pentylquinazoline (**23**) by a reaction of hexanenitrile with **32** in the presence of Lewis acid (method C). A similar reaction to method C was reported by Meerwein and co-workers.[10)] The 2-(1-homopiperazinyl)- and 2-(2-aminoethylamino)-quinazolines (**24** and **25**) were prepared by method B. 2-(1-Allyl-4-piperidyl)-4-pentyloxyquinazoline (**26**) was obtained by method A with a concomitant formation of 2-(1-allyl-4-piperidyl)-3-pentyl-4(3*H*)-quinazolinone (**35**).[11)] Although the 2-chloroquinoline (**33**) readily reacted with *N*-allylpiperazine to give **27** (method D), the 3-chloroisoquinoline (**34**) did not react under a similar condition. The reaction of **34** with *N*-allylpiperazine proceeded when the CuO–$CuSO_4$ was added.[12)] The physicochemical properties are listed in Table II.

Pharmacological Results and Discussion

It is reported that learned behavior is closely related to the cholinergic system, and scopolamine (an anticholinergic agent)-induced learned impairment tests have been used to evaluate nootropic agents[6,7,13)] We evaluated antiamnestic activity as a reversal ability of learned impairment using a step-through type one-trial passive avoidance task[14)] at 30 mg/kg, i.p. The dose of administration of each compound was calculated as a free base, and the test was performed 24 h after administration. The result of the evaluation is listed in Table I.

Among the eight 4-pentyloxy-2-(1-piperazinyl)quinazolines with variously substituted 1-piperazinyl moiety (**1**—**8**), only the allyl derivative (**4**) showed significant antiamnestic activity. When the substituent at the 2-position was fixed with the 4-allyl-1-piperazinyl moiety, 4-methoxy, 4-propoxy, 4-butoxy and 4-pentyloxy derivatives (**9**—**11** and **4**) showed significant activity, but the compounds having a longer alkoxy than pentyloxy (**12** and **13**) were inactive. The 4-(branched alkoxy), 4-phenoxy and 4-benzyloxy derivatives (**14**—**17**) were also inactive. Introduction of hetero atoms into the 4-alkoxy chain (**18**—**20**) reduced activity.

The conversion of the 4-oxygen atom of **4** to others (**21**—**23**) diminished activity or enhanced toxicity. Replacement of the 1-piperazinyl moiety of **4** with a 1-homopiperazinyl, an aminoethylamino or a 4-piperidyl moiety (**24**—**26**) resulted in reduced activity or high toxicity. When the quinazoline ring of **4** was converted to a quinoline or an isoquinoline ring (**27** or **28**), the antiamnestic activity disappeared.

TABLE II. Physicochemical Data for the Quinazoline Derivatives

No.	Formula[a)]	Method	Yield[b)]	mp (Recryst. solvent)[c)]	Analysis (%) Calcd C	Calcd H	Calcd N	Found C	Found H	Found N
4[d)]	$C_{20}H_{28}N_4O \cdot Fu$	A	90	137.0—141.0 (C)	63.14	7.06	12.27	63.08	6.90	12.36
9	$C_{16}H_{20}N_4O \cdot Fu$	B	95	145.0—146.5 (B)	59.99	6.04	13.99	60.06	6.03	14.07
13	$C_{23}H_{34}H_4O \cdot Fu$	B	97	159.5—161.5 (A)	64.44	7.49	11.56	64.41	7.50	11.63
17	$C_{22}H_{24}N_4O$	B	96	86.5— 88.5 (E)	73.31	6.71	15.54	73.32	6.71	15.52
18	$C_{19}H_{26}N_4O_2 \cdot Fu \cdot 0.5H_2O$	B	65	126.0—128.5 (A)	59.09	6.68	11.98	59.40	6.60	12.02
19	$C_{19}H_{27}N_5O \cdot HCl \cdot H_2O$	A	45	161.5—163.5 (D)	57.64	7.64	17.69	57.29	7.30	17.59
20	$C_{19}H_{24}N_4O_3 \cdot Fu \cdot 0.5H_2O$	A	42	148.0—149.5 (A)	57.35	6.07	11.64	57.37	5.83	11.29
21	$C_{20}H_{28}N_4S \cdot Fu$	B	98	171.0—173.5 (B)	60.99	6.82	11.85	61.21	6.97	11.81
22	$C_{20}H_{29}N_5 \cdot 2Fu$	B	88	185.0—187.0 (B)	58.83	6.52	12.25	58.76	6.67	12.24
23	$C_{20}H_{28}N_4 \cdot Fu$	C	10	141.0—142.5 (A)	65.43	7.32	12.72	65.23	7.25	12.56
24	$C_{21}H_{30}N_4O \cdot 2.5Fu$	B	79	130.0—132.0 (B)	57.76	6.25	8.69	57.91	6.29	8.62
25	$C_{20}H_{30}N_4O \cdot Ox$	B	71	140.0—145.5 (B)	60.46	7.50	12.82	60.28	7.24	13.08
26	$C_{21}H_{29}N_3O \cdot 1.5Fu$	A	18	155.0—158.0 (A)	63.14	6.87	8.18	63.16	6.72	8.30
27	$C_{21}H_{29}N_3O \cdot 2Fu$	D	92	177.0—178.5 (A)	60.93	6.52	7.35	60.69	6.34	7.17
28	$C_{21}H_{29}N_3O \cdot 1.5Fu$	D	24	144.5—147.0 (A)	63.14	6.87	8.18	63.49	6.66	8.27

a) Abbreviations: Fu, fumaric acid; Ox, oxalic acid. *b*) Yield of free base. *c*) Solvents: A, EtOH; B, EtOH–AcOEt; C, CH_3CN–H_2O; D, CH_3CN; E, hexane. *d*) Previously described as 1.5 fumarate in reference 1. Monofumarate was obtained by a treatment with equivalent fumaric acid.

TABLE III. Pharmacological Properties of 4-Alkoxyquinazolines

No.	Amnest.[a)] % of control (30	10	3	1 mg/kg)	MES[b)] ED_{50} (mg/kg)	Hypoxic[c)] % of control (50 mg/kg)	Toxic[d)] LD_{50} (mg/kg)
4	292[h)]	283[h)]	386[h)]	215[g)]	13	185[i)]	>1000
9	221[g)]	164			46		
10	209[g)]	84			20	184[i)]	429
11	224[g)]	250[h)]	192[g)]	161	18	155[h)]	650
18	251[g)]	181			62		
24	227[g)]	92			48		
Idebenone	175[g)]	141			>100	125[e,g)]	>1000
Bifemelane	147	234[g)]	140		>100	129[f,h)]	1000

a) Antiamnestic activity was tested at 30, 10, 3 and 1 mg/kg, *p.o.* *b*) Anticonvulsive activity. See reference 1. *c*) Antihypoxic activity was tested at 50 mg/kg, *p.o.* Statistical significance (*T*-test): *g*) $p<0.05$, *h*) $p<0.01$, *i*) $p<0.001$. *d*) Acute toxicity. *e*) Tested at 300 mg/kg, *p.o.* *f*) Tested at 100 mg/kg, *p.o.*

For significant antiamnestic activity, the following structure–activity relationships are deduced: (1) both the quinazoline ring and 1-piperazinyl moiety are necessary; (2) the substituent of the 1-piperazinyl moiety is restricted to an allyl group; (3) the substituent at the 4-position of the quinazoline ring is restricted to a lower straight chain alkoxy group. From these considerations, it became clear that antiamnestic compounds were almost synthesized.

The nootropic properties (antiamnestic, anticonvulsive[15] and antihypoxic[15] activities) of the antiamnestic compounds (**4**, **9**, **10**, **11**, **18** and **24**) are listed in Table III.

The antiamnestic activity of idebenone was so weak that a statistical significance was barely obtained at 30 mg/kg. Bifemelane showed significant activity only at 10 mg/kg. Tobe and co-workers reported antiamnestic activity of bifemelane at 25—100 mg/kg, *p.o.* in mice[7]; however, we could not detect its activity at 30 mg/kg i.p. Although Cumin and co-workers reported antiamestic activity of aniracetam,[6] we could not detect its activity at 10—100 mg/kg. It is considered that the reason for these different results came from a difference in the strains of mice and/or a difference of experimental conditions.[16] However, another possible reason for this is that the potency of the existing nootropic agents was so weak that the results of the evaluation were sometimes inconsistent. Compound **4** showed more significant antiamnestic activity at 1—30 mg/kg than these reference compounds.

The reference compounds did not show anticonvulsive activity at 100 mg/kg, and showed weak antihypoxic activity. Because our quinazolines showed potent anticonvulsive and antihypoxic activities, they were expected to show more significant brain protective activity than these reference compounds. Among the six compounds, **4** showed the most potent anticonvulsive and antihypoxic activities. We selected **4** as the most promising nootropic candidate agent in this series.

It is reported that memory is usually classified into long-term memory and short-term memory, and that, in a study with antiamnestic agents, the effect is evaluated separately in impairment tests of the long-term and short-term memory.[13] The animal model described above was related to impariment of the long-term memory. Therefore, in order to confirm an improving effect of **4** on the impairment of short-term memory, we examined the effect of **4** in a delayed alternation task using the T-maze and rats.[13] As shown in Fig. 1, when the time interval was 30 s, correct responses decreased to 83% of that in the no-delay trial. Scopolamine decreased the no-delay correct responses to 53%. Although compound **4** alone did not affect the responses in the delayed trials, it significantly improved the scopolamine-induced decrease of correct responses.

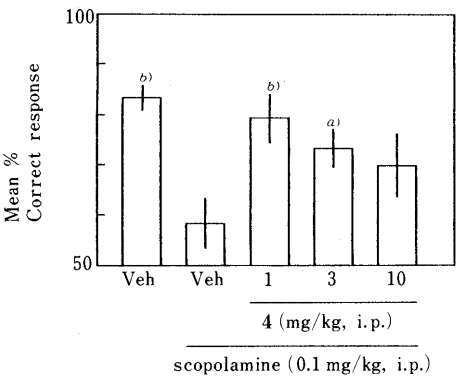

Fig. 1. Effect of **4** on the 30 s-Delayed Alternation Task in Rats Treated with Scopolamine

a) $p<0.05$, *b*) $p<0.01$ *vs.* vehicle control (Dunnet test).

Having an antagonistic effect against the scopolamine-induced learned impairments, compound **4** would have an affect on a cholinergic system.[17] We evaluated the cholinesterase-inhibiting activity of **4**, but it did not show activity at a concentration of 10^{-7}—10^{-3} M.[18] Studies on the mechanisms of the antiamnestic activity of **4** are in progress.

Experimental Section

Melting points were measured with a capillary melting point apparatus (Yamato MP-21) and are uncorrected. Infrared (IR) spectra were recorded on a Hitachi 270-50 spectrometer. Proton nuclear magnetic resonance (^{1}H-NMR) spectra were taken on a Hitachi R-24B NMR spectrometer with tetramethylsilane (TMS) as an internal standard. Chemical shifts are given as δ values (ppm): s, singlet; d, doublet; t, triplet; q, quartet; m, multiplet; br s, broad singlet. Elemental analyses were performed by the Analytical Department of Kanebo Research Center. For column chromatography, Silica gel 60 (Merck) was used.

2-(1-Acetyl-4-piperidyl)-4(3*H*)-quinazolinone (36) A mixture of *o*-aminobenzamide (8.2 g, 60 mmol), *N*-acetylisonipecotinic acid chloride (13.0 g, 60 mmol), triethylamine (8.0 g, 79 mmol) and $CHCl_3$ (80 ml) was refluxed for 1 h. The reaction mixture was washed with water, dried over $MgSO_4$, and concentrated. The resulting solid (10 g) and KOH (2.0 g) were dissolved in 20 ml of diglyme and stirred at 140 °C for 0.5 h. The reaction mixture was diluted with water and neutralized with diluted HCl. The precipitate was collected and recrystallized from EtOH to give **36** (6.0 g, 64%) as colorless needles, mp 240.0—242.0 °C. *Anal.* Calcd for $C_{15}H_{17}N_3O_2$: C, 66.40; H, 6.32; N, 15.49. Found: C, 66.39; H, 6.31; N, 15.51.

2-(1-Allyl-4-piperidyl)-4(3*H*)-quinazolinone (37) A suspension of **36** (6.0 g, 22 mmol) in 3 N HCl (50 ml) was refluxed for 2 h and neutralized with 20% NaOH. The precipitate was collected (4.0 g, 81%), and was added to a solution of triethylamine (2.0 g, 20 mmol), allyl bromide (2.4 g, 20 mmol) in *N*,*N*-dimethylformamide (DMF) (40 ml). The mixture was stirred at 70 °C for 1.5 h and diluted with water. The resulting solid was collected and recrystallized from EtOH to give **37** (2.6 g, 56%) as colorless needles, mp 209.0 °C (dec.). ^{1}H-NMR ($CDCl_3$) δ: 1.8—3.5 (11H), 5.0—5.4 (2H, m), 5.5—6.3 (1H, m), 7.3—8.3 (4H), 12.0 (1H, br s, –CONH–). *Anal.* Calcd for $C_{16}H_{19}N_3O$: C, 71.35; H, 7.11; N, 15.60. Found: C, 71.32; H, 7.10; N, 15.59.

***N*-Phenyl-1-(4-allyl-1-piperazine)carbothioamide (31)** *N*-Allylpiperazine (10.0 g, 74 mmol) was added to a solution of phenylisothiocyanate (10.0 g, 79 mmol) in CH_3CN (40 ml) at 0 °C, and the mixture was stirred at room temperature for 1 h. The precipitate was collected and washed with CH_3CN to give **31** (18 g, 93%) as colorless needles, mp 128.0—129.5 °C. *Anal.* Calcd for $C_{14}H_{19}N_3S$: C, 64.33; H, 7.33; N, 16.08. Found: C, 64.34; H, 7.28; N, 16.10.

Ethyl *N*-Phenyl-1-(4-allyl-1-piperazine)carbothioimidate (32) A mixture of **31** (10.0 g, 38 mmol), EtI (6.2 g, 40 mmol), K_2CO_3 (2.8 g, 20 mmol) and EtOH (50 ml) was stirred at 70 °C for 3.5 h. The reaction mixture was poured into water and extracted with AcOEt. The extract was washed with water, dried over $MgSO_4$, and concentrated. The residue was chromatographed on silica gel with hexane–AcOEt (2 : 1) to give **32** (9.3 g, 84%) as a colorless oil. *Anal.* Calcd for $C_{16}H_{23}N_3S$: C, 66.40; H, 8.01; N, 14.52. Found: C, 66.23; H, 7.90; N, 14.52.

2-Chloro-4-pentyloxyquinoline (33) A mixture of 2,4-quinolinediol monosodium salt (7.3 g, 40 mmol), 1-iodidopentane (8.0 g, 40 mmol) and DMF (30 ml) was stirred at 60 °C for 3 h. The reaction mixture was diluted with water and extracted with AcOEt. The extract was concentrated and the resulting solid was collected. The solid was recrystallized from EtOH to give 4-pentyloxy-2(1*H*)-quinolinone (**38**) (3.2 g, 35%) as yellow prisms, mp 149.0—150.5 °C. IR (KBr): 1650, 1615 cm^{-1}. ^{1}H-NMR ($CDCl_3$) δ: 0.95 (3H, t, J=7 Hz), 1.1—2.2 (6H), 4.12 (2H, t, J=6 Hz), 6.02 (1H, s), 7.0—8.0 (4H), 12.4 (1H, br s, –CONH–). *Anal.* Calcd for $C_{14}H_{17}NO_2$: C, 72.70; H, 7.41; N, 6.06. Found: C, 72.65; H, 7.33; N, 5.97. Compound **38** (2.3 g, 10 mmol) and $POCl_3$ (6 ml) was stirred at 90 °C for 30 min. The reaction

mixture was poured onto ice, neutralized with 3 N NaOH, and extracted with AcOEt. The extract was washed with water, dried over $MgSO_4$, and concentrated. The residue was recrystallized from CH_3CN to give **33** (1.9 g, 77%) as pale yellow needles, mp 80.0—81.5 °C. ^{1}H-NMR ($CDCl_3$) δ: 0.95 (3H, t, J=6 Hz), 1.3—2.3 (6H), 4.65 (2H, t, J=7 Hz), 6.70 (1H, s), 7.3—8.3 (4H). *Anal.* Calcd for $C_{14}H_{16}ClNO$: C, 67.33; H, 6.46; N, 5.61. Found: C, 67.43; H, 6.46; N, 5.60.

2-(1-Allyl-4-piperidyl)-4-pentyloxyquinazoline (26) (Method A) A mixture of 2-(1-allyl-4-piperidyl)-4(3*H*)-quinazolinone (**37**) (1.3 g, 4.8 mmol), 1-iodopentane (1.0 g, 5.0 mmol), NaH (in oil, 60%) (0.3 g, 7.5 mmol) and DMF (20 ml) was stirred at 70 °C for 5 h. The reaction mixture was diluted with water and extracted with AcOEt. The extract was washed with water, dried over $MgSO_4$, and concentrated. The residue was chromatographed on silica gel with $CHCl_3$–MeOH (30 : 1) to give **26** (0.3 g, 18%) as a colorless oil and **35** (0.1 g, 6%) as a colorless oil. **26**: Rf=0.49, $CHCl_3$–MeOH (15 : 1). ^{1}H-NMR ($CDCl_3$) δ: 4.55 (2H, t, J=7 Hz, O–C$\underline{H}_2$–). **35**: Rf=0.54, $CHCl_3$–MeOH (15 : 1). IR (neat): 1680 cm^{-1}. ^{1}H-NMR ($CDCl_3$) δ: 4.10 (2H, t, J=6 Hz, N–C$\underline{H}_2$–). *Anal.* Calcd for $C_{21}H_{29}N_3O$: C, 74.30; H, 8.61; N, 12.38. Found: C, 74.21; H, 8.73; N, 12.05. The oily compound **26** was crystallized as fumarate. The physicochemical properties of **26** are listed in Table II.

2-(4-Allyl-1-piperazinyl)-4-benzyloxyquinazoline (17) (Method B) A mixture of 2-(4-allyl-1-piperazinyl)-4-chloroquinazoline[9] (3.0 g, 10 mmol), benzyl alcohol (1.2 g, 11 mmol), NaH (0.6 g, 15 mmol) and DMF (30 ml) was stirred at 0 °C for 1 h. The reaction mixture was diluted with water and extracted with AcOEt. The extract was washed with water, dried over $MgSO_4$, and concentrated. The residue was recrystallized from hexane to give **17** (2.7 g, 71%) as pale yellow plates. ^{1}H-NMR ($CDCl_3$) δ: 2.51 (4H, t, J=5 Hz), 3.06 (2H, d, J=6 Hz), 3.97 (4H, t, J=5 Hz), 5.0—5.4 (2H, m), 5.50 (2H, s), 5.5—6.2 (1H, m), 6.9—8.1 (9H).

2-(4-Allyl-1-piperazinyl)-4-pentylquinazoline (23) (Method C) A mixture of **32** (14.0 g, 48 mmol), hexanenitrile (4.9 g, 50 mmol), $AlCl_3$ (13.4 g, 100 mmol) and 1,1,2,2-tetrachloroethane (100 ml) was stirred at 140 °C for 16 h. The reaction mixture was poured onto crushed ice, made basic with 20% NaOH and extracted with $CHCl_3$. The extract was washed with water, dried over $MgSO_4$, and concentrated. The residue was chromatographed on silica gel with hexane–AcOEt (2 : 1) to give **23** (1.7 g, 10%) as a yellowish oil. ^{1}H-NMR ($CDCl_3$) δ: 0.93 (3H, t, J=7 Hz), 1.2—2.2 (6H), 2.45 (4H, t, J=7 Hz), 2.95 (2H, d, J=6 Hz), 3.01 (2H, t, J=7 Hz), 3.92 (4H, t, J=7 Hz), 4.9—5.3 (2H, m), 5.6—6.3 (1H, m), 6.9—7.9 (4H).

3-(4-Allyl-1-piperazinyl)-1-pentyloxyisoquinoline (28) (Method D) 3-Chloro-1-pentyloxyisoquinoline (**34**) was prepared from 1,3-dichloroisoquinoline[19] with 1-pentanol by method B. **34**: colorless oil. *Anal.* Calcd for $C_{14}H_{16}ClNO$: C, 67.33; H, 6.45; N, 5.61. Found: C, 67.31; H, 6.54; N, 5.60. A mixture of **34** (3.0 g, 12 mmol), *N*-allylpiperazine (7.5 g, 60 mmol), CuO (1.0 g, 13 mmol) and $CuSO_4 \cdot 5H_2O$ (1.0 g, 4.0 mmol) was stirred at 180 °C for 4 h. The reaction mixture was diluted with water and $CHCl_3$, and the insoluble materials were filtered off. The organic layer was separated, washed with water, dried over $MgSO_4$, and concentrated. The residue was chromatographed on silica gel with $CHCl_3$–AcOEt (1 : 1) to give **28** (1.0 g, 24%) as a yellow oil. ^{1}H-NMR ($CDCl_3$) δ: 0.95 (3H, t, J=6 Hz), 1.2—2.1 (6H), 2.13 (4H, t, J=5 Hz), 3.07 (2H, d, J=7 Hz), 3.60 (4H, t, J=5 Hz), 4.46 (2H, t, J=6 Hz), 5.0—5.4 (2H, m), 5.5—6.2 (1H, m), 6.32 (1H, s), 7.0—8.2 (4H).

Biological Evaluation. Reversal of a Scopolamine-Induced Impairment of One-Trial Passive Avoidance Learning[14] A group of 10—20 male mice (ddY-strain, 20—28 g) was used for each dose of test compound. Each mouse was placed in a illuminated compartment (10 × 10 × 18 cm) equipped with a grid floor. As soon as the mouse entered the dark compartment, the door which separates the two compartments was closed, and footshock (0.5 mA, 2 s) was driven through the grid floor. In the retention test performed 24 h after the acquisition trial, the mouse was again placed in the illuminated compartment, and the response latency to enter the dark compartment was measured up to 300 s. Scopolamine hydrobromide (1 mg/kg, i.p.) was administered 20 min prior to the acquisition trial. Test compounds (dissolved in saline or suspended in 1% aqueous gum arabic) or the vehicle were administered (i.p.) immediately after the acquisition trial. Median response latency in the test trial was calculated, and a statistical analysis was performed using a two-tailed Mann–Whitney U-test.

Effect on a Scopolamine-Induced Impairment of Short-Term Memory in Rats[13] A group of 6—12 male Wister rats (260—270 g) was used for each dose of the test compound. Initially, rats were placed in a T-maze[13] and were allowed to freely run to learn that food pellets were placed in both of the two arms. Next, rats were trained using a forced run to one arm of the T-maze by closing another arm, which was followed by another free-choice run. A correct free-choice response was defined as a turn toward the arm opposite to that in the forced run and was rewarded with food pellets. The correct responses decreased according to how long a test of the free-choice run was delayed from the forced run. After repeated training of the 30 s-delayed alternation task, the effect of the test compounds was studied. Scopolamine hydrobromide was administered (0.1 mg/kg, i.p.) 20 min before the test trial and compound **4** was administered (i.p.) 30 min before the test trial. A statistical analysis was performed using the Dunnet test.

References and Notes

1) M. Hori, R. Iemura, H. Hara, A. Ozaki, T. Sukamoto and H. Ohtaka, *Chem. Pharm. Bull.*, **38**, 1286 (1990).
2) American Psychiatric Association "Diagnotic and Statistical Manual of Mental Disorders," Washington DC, 1980, pp. 107—113.
3) K. Sarai, *Rinsyo To Kenkyu*, **64**, 1138 (1987).
4) C. Giurgea and M. Salama, *Prog. Neuro.-Psychopharmacol.*, **1**, 235 (1977).
5) F. M. Hershenson and W. H. Moos, *J. Med. Chem.*, **29**, 1125 (1986).
6) R. Cumin, E. F. Bandle, E. Gamzu and W. E. Haefely, *Psychopharmacol.*, **78**, 104 (1982).
7) A. Tobe, T. Yamaguchi, R. Nagai and M. Egawa, *Jpn. J. Pharmacol.*, **39**, 153 (1985).
8) J. Nakaoka, Y. Kiyota, M. Miyamoto and A. Nagaoka, *Yakuri To Chiryo*, **16**, 1181 (1988).
9) M. Hori, R. Iemura, H. Hara, A. Ozaki, T. Sukamoto and H. Ohtaka, *Chem. Pharm. Bull.*, **38**, 681 (1990).
10) H. Meerwein, P. Laach, R. Mersch and J. Nentwig, *Chem. Ber.*, **89**, 224 (1956).
11) The effects of the 2-substituents on a ratio between the 3-*N*-alkylation and 4-*O*-alkylation were studied and will be reported separately.
12) T. Kametani, K. Kigasawa and M. Hiiragi, *Chem. Pharm. Bull.*, **15**, 704 (1967).
13) N. Yamazaki, A. Nagaoka and Y. Nagawa, *Jpn. J. Psychopharmacol.*, **5**, 321 (1985).
14) Z. Bohdancky and M. E. Jarnik, *Int. J. Neuropharmacol.*, **6**, 217 (1967).
15) Antihypoxic activity and anticonvulsive activity were evaluated according to reference 1.
16) H. Kuribara and S. Tadokoro, *Jpn. J. Pharmacol.*, **40**, 303 (1986).
17) K. Saito, S. Honda, A. Tobe and I. Yanagiya, *Jpn. J. Pharmacol.*, **38**, 375 (1985).
18) Modifying a following report, we evaluated an inhibiting activity of acetylcholinesterase: G. L. Ellman, K. D. Courtney, V. Andres Jr. and R. M. Featherstone, *Biochem. Pharmacol.*, **7**, 88 (1961).
19) G. Simchen, *Angew. Chem., Int. Ed. Engl.*, **5**, 663 (1966).

Obtaining the Correlation Indices between Drug Activity and Structural Parameters Using a Neural Network[1)]

Tomoo AOYAMA[a] and Hiroshi ICHIKAWA*,[b]

Hitachi Computer Engineering Co., Ltd.,[a] Horiyamashita, Hadano, Kanagawa 259–13, Japan and Hoshi College of Pharmacy,[b] Shinagawa, Tokyo 142, Japan. *Received August 2, 1990*

A linear operation was introduced to the neural network. We also studied a method that gives correlation coefficients between input parameters and outputs. It was difficult to obtain these coefficients. Instead, we proposed a new index, the divided difference of output intensity with respect to the input parameter ($\delta O/\delta x$). The divided differences were obtained using an unsaturated sigmoid function as an output function of neurons, where a new learning method with the concept of "neuron fatigue" is introduced. The new techniques were applied to quantitative structure–activity relationships (QSAR) studies in carboquinones and benzodiazepines to compare the results with those by multiregression analysis. It was found that the divided differences work well and can produce the equivalent partial differential coefficients that are obtained by multiregression analysis.

Keywords neural network; perceptron; graded classification; QSAR; correlation factor

Introduction

We have shown that neural network may be an efficient tool in developing drugs.[1b-4)] This method is itself a state-of-the-art technique which is recently and rapidly developing.[5)] As we have described in previous papers, the basic modes of operation of the neural network are nonlinear.[1b)] This offers outstanding capabilities in both classification and fitting. It also involves a few difficulties.[1b)] One of them is: because of its nonlinear operation, the neural network cannot give simple correlation coefficients like those in quantitative structure–activity relationships (QSAR) analysis using multiregression analysis.[6)] It was also pointed out that nonlinear operation is always superior to linear operation, neither in prediction nor in extra/interpolation, since the separation surface or fitting line is defined by the given data.[1b)] Therefore, it is sometimes necessary to incorporate a linear operation into the network. This paper describes solutions for those problems.

Theory

Introduction of Linear Operation into the Neural Network We deal only with a three-layer network in this paper. Figure 1 shows the diagram of a three-layer neural network: circles are neurons (or cells), which are variables taking a value between 0 and 1. The value of a neuron (O_j) at the second or third layer is determined by Eq. 1,

$$O_j = 1/[1+\exp(-\alpha y_j)] \equiv g(y)$$

$$y_j = (\sum_i W_{ij} x_i) - \theta_j \quad (1)$$

where x_i is one of the neuron's values at the first or second layer; W_{ij}, an element of the weight matrix, expresses the weight value of the connection between neurons, i and j; α is a parameter which expresses the nonlinearity of the neuron's operation; θ_j is a threshold value for neuron j (usually is set to be 0).

The neural network based on Eq. 1 performs a nonlinear operation. As we have shown in a previous paper, a nonlinear operation is not always convenient in practical application and therefore, it may be preferable if a linear operation is introduced into the neural network. This is possible to some extent by adopting a small α value. However, this method requires much time in the training phase. Instead we define a new output function as a combination of Eq. 1 and y_j as,

$$O_j = \beta/[(1+\exp(-\alpha y_j)] + (1-\beta) y_j \equiv f(y_j)$$

$$y_j = (\sum_i W_{ij} x_i) - \theta_j \quad (2)$$

Here, parameter β expresses the mixing degree of the linear operation to the nonlinear operation and therefore, by changing β, one can mix the linear operation into the network at any level. If β is set to be 0, the network can be expected to perform the linear operation correctly.

The training of the network is carried out until the sum of the squared errors, $\sum(O_j - t_j)^2$, becomes small enough based on the following equations,

$$\delta W_{ij} = -d_j x_i \varepsilon \quad (3)$$

$$d_j = (O_j - t_j) f'(y_j) \quad (4a)$$

$$d_j = (\sum_l W'_{lj} d'_l) f'(y_j) \quad (4b)$$

Here, ε is a parameter which determines a shift for correction in back-propagation. Equation 4a is used only to correct the connection between the second and third layers, while 4b is for another connection where W'_{lj} and d'_l at the second layer are W_{ij} and d_j at the third layer. If the new output function is adopted, the derivative function, f', in Eq. 4 is,

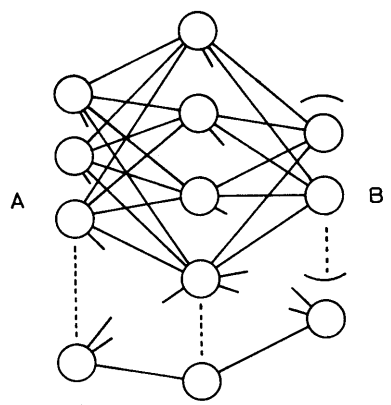

Fig. 1. Three-Layer Neural Network

$$f'(y_j)=\alpha\beta g(y_j)[1-g(y_j)]+1-\beta \tag{5}$$

In the above equations, both ε and α, and even β, can be set independently of the layer.

Partial Correlation Index in the Neural Network 1) Method 1 Suppose there is a relationship between output intensity and plural input parameters. The degree of influence of an input on an output depends on each item of the input parameters. The problem is how to seek such a degree *i.e.*, the partial correlation coefficient.

We express the input pattern, training pattern, and output data respectively as $\{x_K, i\}$, $\{t_i\}$, and $\{O_i\}$, where subscripts K and i describe the kind of parameters (characteristics) and the set of data. The partial correlation coefficient for parameter L may be defined and obtained by the following procedures.

Step 1: The training based on the back-propagation algorithm[8] is carried out using $\{t_i\}$ and $\{K(v\neq L), i\}$, the input patterns without data for parameter L. After training, $\{K(v\neq L), i\}$ is fed into the network to give the output $\{O_i\}$. The difference vector $\{\Delta_i\}(=O_i-t_i)$ is obtained.

Step 2: Using training patterns $\{x_{L,i}\}$ and input data without data for parameter $L\{K(v\neq L), i\}$, another training is carried out to give output $\{O_i'\}$ for $\{K(v\neq L), i\}$, which is used to obtain the difference vector $\{d_i\}(=O_i'-x_L, i)$.

Step 3: The correlation between $\{\Delta_i\}$ and $\{d_i\}$ is obtained as,

$$r=\sum(\Delta_i-\Delta)(d_i-d)/[\sum(\Delta_i-\Delta)^2\sum(d_i-d)^2]^{1/2} \tag{6}$$

where, Δ and d are averages of $\{\Delta_i\}$ and $\{d_i\}$.

Let us examine the relationship of correlation coefficients between multiregression analysis and the neural network with Eq. 2 under the following conditions: the α and β values are set to be 1 and 0, respectively, a large number of neurons is taken in the second layer, while that in the output layer is 1, and one of the neurons in the input layer is always taken as the constant 1.[7]

In the limit $\beta^{(2)}\to 0$ (where $\beta^{(2)}$ indicates the β value of the neurons in the second layer), a three-layer network is reduced to a network with a function similar to that of a two-layer network. Therefore, the back-propagation procedure in such a network is to seek the smallest sum of least-squares of error. This is theoretically equal to multiregression analysis. The difference in practice is, however, that multiregression analysis minimizes the sum of the least-squares errors for the total input data while the network minimizes least-squares errors of each input data. This results in possible discrepancies between the two. The differences may be more substantial as the number of input data becomes larger.

In the limit $\beta^{(2)}\to 1$, the linearity/nonlinearity operation of the network is determined by the α value. The neural network has an ability such that even a trivial difference in the input data $\{x_K, i\}$ is stressed to adapt to the difference in the training pattern. This fitting ability is increased as the α value is increased, and is called here "fitting ability."

The fitting ability of the neural network works well in classification or reproduction of the input data. Unfortunately, this causes difficulty in obtaining the partial coefficients as step 2 since the vector $\{d_i\}$ gradually comes close to the zero vector. Although all elements of $\{d_i\}$ do not become zeros, since a limited number of neurons is adopted in the second layer and the same α value is used for all neurons, the partial correlation coefficient, r, is dependent largely on the ways the network is trained. Namely, the calculation of r requires the training of two independent networks and therefore, unless the training method is the same for both, the calculated r values may fluctuate greatly. This may have an unfavorable effect.

2) Method 2 From the above discussion, it is clearly necessary to seek a method that gives the partial correlation index from a network determined by a single training procedure. One such procedure is to trace how an infinitesimal change of input data propagates into the second and third layers.

The infinitesimal change of the input data, $\{x_K, i+\delta x_L\}$, causes the neuron's value in the second layer to change by δy_j,

$$\delta y_j=W_{Lj}\delta x_L \tag{7}$$

where, L describes how the change δ takes place at parameter L. The change in the neuron's output is,

$$\delta O_j=\beta g'(y_j)\delta y_j+(1-\beta)\delta y_j \tag{8}$$

where, g' is the derivative of the sigmoid function (Eq. 1). Thus,

$$\delta O_j=\beta\alpha O(y_j)[1-O(y_j)]\delta y_j+(1-\beta)\delta y_i \tag{9}$$

Therefore, the ratio between the first and second layers is,

$$\delta O_j/\delta x_L=[\beta\alpha O(y_j)\{1-O(y_j)\}+(1-\beta)]W_{Lj} \tag{10}$$

Likewise, the ratio between the first and third layers is given by,

$$\begin{aligned}\delta O_k/\delta x_L=&\sum[\beta^{(3)}\alpha^{(3)}O(Z_k)\{1-O(Z_k)\}+(1-\beta^{(3)})]W_{jk}^{(2,3)}\\&\times[\beta^{(2)}\alpha^{(2)}O(y_j)\{1-O(y_j)\}+(1-\beta^{(2)})]W_{Lj}^{(1,2)}\end{aligned} \tag{11}$$

Here, $O(Z_k)$ is the output without the infinitesimal change of neuron $k(\delta x_L)$ in the third layer, and $O(y_j)$ is the output of j in the second layer. The superscripts on β, α, and W express the layer's order. The δO_k values of Eq. 11 must be averaged after calcultaion on each data. Thus,

$$(\delta O_k/\delta x_L)=N^{-1}\sum_i(\delta O_k/\delta x_i) \tag{12}$$

where N is the number of total input data. When $\beta\to 1$, the divided differences, $\delta O_k/\delta x_L$, approaches 0 as the output value nears 0 or 1. This character stems from the sigmoid function.

Since the strongest activity is referred to as 1, the character of the index given by Eq. 11 is not favorable. To remove this difficulty, one may use an unsaturated output function whose differential coefficient is not 0 even at the output being 1. However, such a function causes the neurons in the second layer to take a value out of the defined range, being unable to apply the back-propagation algorithm. We sloved this problem by adopting the following unsaturated output function.

$$f(y)=C/[a+\exp(-\alpha y)] \tag{13}$$

The parameters C and a are so determined as to give $f(1)=1$ and $f(0.5)=0.5$. A typical example is to set them as $\alpha=1$, $a=0.2642411$, and $C=0.6321206$.

As soon as a neuron's value exceeds 1, the learning between the neuron and any other neurons is disabled. But

it can be reactivated if its value becomes less than 1 by letting W_{ij} be small after a certain period of time. This procedure corresponds to having a "fatigue" effect on the neuron. The training procedures are, therefore, as follows.

The derivative for the back-propagation procedures for the above function is,

$$f'(y)=C\alpha h(y)[1-ah(y)] \tag{14}$$

using,

$$f(y)=C/[a+\exp(-\alpha y)]\equiv Ch(y) \tag{15}$$

As a neuron's value exceeds 1, the neuron is deactivated. Training is continued M times excluding the deactivated neuron. After M turns, the neuron is again activated by multiplying W_{ij} by 1/(neuron's value). Here, M is typically found to be 9.

Using the above procedures, one can calculate the divided difference, $\delta O_k/\delta x_L$. Here, it is recommended that the number of neurons in the second layer be set at three times as many as that in the usual sigmoid function, since, due to the unsaturated sigmoid function, the cognizability of neurons is lowered considerably.

Results and Discussion

Since the value of each neuron is defined between 0 and 1, the given data must be appropriately rescaled within the defined region. Further, it should be noted that if the value of a neuron in the input layer is zero, the connections from such a neuron are always null, *i.e.*, the information from that neuron is not propagated to the second and third layers.

TABLE I. Structural Parameters and Biological Intensities in Carboquinones[a)]

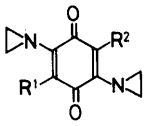

structure A

No.			MR_{12}	π_{12}	π_2	MR_1	F	R	Chron. inj. MED obsd.	Chron. inj. OD obsd.	Sing. inj. MED obsd.	Sing. inj. OD obsd.
1	CH_3	$COCH_3$	1.69	−0.05	−0.55	0.57	0.28	0.07			3.94	3.48
2	C_6H_5	C_6H_5	5.08	3.92	1.96	2.54	0.16	−0.16	4.33	4.14		3.53
3	CH_3	$(CH_2)_3C_6H_5$	4.50	3.66	3.16	0.57	−0.08	−0.26	4.47	4.21	3.93	3.60
4	C_5H_{11}	C_5H_{11}	4.86	5.00	2.50	2.43	−0.08	−0.26	4.63	4.52	4.07	3.62
5	$CH(CH_3)_2$	$CH(CH_3)_2$	3.00	2.60	1.30	1.50	−0.08	−0.26	4.77	4.59	4.36	4.14
6	CH_3	$CH_2C_6H_5$	3.57	2.51	2.01	0.57	−0.12	−0.14	4.85	4.69	4.74	4.26
7	C_3H_7	C_3H_7	3.00	3.00	1.50	1.50	−0.08	−0.26	4.92	4.44	4.32	4.14
8	CH_3	$CH_2OC_6H_5$	3.79	2.16	1.66	0.57	−0.04	−0.13	5.15	4.71	4.68	3.89
9	$R^1=R^2=CH_2CH_2OCON(CH_3)_2$		6.14	0.72	0.36	3.07	−0.08	−0.26	5.16	4.85		4.62
10	C_2H_5	C_2H_5	2.06	2.00	1.00	1.03	−0.08	−0.26	5.46	5.09	4.94	4.79
11	CH_3	$CH_2CH_2OCH_3$	2.28	1.03	0.53	0.57	−0.08	−0.26	5.57	5.42	5.19	5.12
12	OCH_3	OCH_3	1.58	−0.04	−0.02	0.79	0.52	−1.02	5.59	5.17	4.81	4.32
13	CH_3	$CH(CH_3)_2$	2.07	1.80	1.30	0.57	−0.08	−0.26	5.60	5.21	4.96	4.69
14	C_3H_7	$CH(OCH_3)CH_2OCONH_2$	4.24	0.98	−0.52	1.50	−0.04	−0.13	5.63	5.07	5.01	4.64
15	CH_3	$CH_2CH_2OCON(CH_3)_2$	3.64	0.86	0.36	0.57	−0.08	−0.26			5.09	4.84
16	CH_3	CH_3	1.14	1.00	0.50	0.57	−0.08	−0.26	5.66	5.36	5.36	4.79
17	H	$CH(CH_3)_2$	1.60	1.30	1.30	0.10	−0.04	−0.13	5.68	5.37	5.16	4.59
18	CH_3	$CH(OCH_3)C_2H_5$	2.75	1.53	1.03	0.57	−0.04	−0.13	5.68	5.33	5.26	4.84
19	C_3H_7	$CH_2CH_2OCONH_2$	3.56	1.45	−0.05	1.50	−0.08	−0.26	5.68	5.23	4.90	4.42
20	$R^1=R^2=CH_2CH_2OCH_3$		3.42	1.03	0.53	1.71	−0.08	−0.26	5.69	5.31	5.18	4.71
21	C_2H_5	$CH(OC_2H_5)CH_2OCONH_2$	4.23	0.98	−0.02	1.03	−0.04	−0.13	5.76	5.24	5.40	4.64
22	CH_3	$CH_2CH_2OCOCH_3$	2.78	1.23	0.73	0.57	−0.08	−0.26	5.78	5.78		
23	CH_3	$(CH_2)_3$-dimer	1.96	2.00	1.50	0.57	−0.08	−0.26	5.82	5.39		
24	CH_3	C_2H_5	1.60	1.50	1.00	0.57	−0.08	−0.26	5.86	5.37	5.16	4.52
25	CH_3	$CH(OCH_2CH_2OCH_3)$-CH_2OCONH_2	4.45	0.01	−0.49	0.57	−0.04	−0.13	6.03 6.14	5.39 5.79	5.45 5.86	4.96 5.18
26	CH_3	$CH_2CH(CH_3)OCONH_2$	3.09	0.75	0.25	0.57	−0.08	−0.26	6.16	5.22	5.62	4.92
27	C_2H_5	$CH(OCH_3)CH_2OCONH_2$	3.77	0.48	−0.52	1.03	−0.04	−0.13	6.18	5.66	6.03	5.20
28	CH_3	$CH(C_2H_5)CH_2OCONH_2$	3.55	1.25	0.75	0.57	−0.08	−0.26	6.18	5.22	5.53	4.62
29	CH_3	$CH(OC_2H_5)CH_2OCONH_2$	3.77	0.48	−0.02	0.57	−0.04	−0.13	6.18	5.93	5.55	5.48
30	CH_3	$(CH_2)_3OCONH_2$	3.09	0.95	0.45	0.57	−0.08	−0.26	6.21	5.75	5.83	5.46
31	CH_3	$(CH_2)_2OCONH_2$	2.63	0.45	−0.05	0.57	−0.08	−0.26	6.25	5.48	5.98	4.88
32	C_2H_5	$(CH_2)_2OCONH_2$	3.09	0.95	−0.05	1.03	−0.08	−0.26	6.39	5.79	5.89	5.25
33	CH_3	CH_2CH_2OH	1.78	0.34	−0.16	0.57	−0.08	−0.26	6.41	5.71	5.93	5.31
34	CH_3	$CH(CH_3)CH_2OCONH_2$	3.09	0.75	0.25	0.57	−0.08	−0.26	6.41	5.66	5.81	5.03
35	CH_3	$CH(OCH_3)CH_2OCONH_2$	3.31	−0.02	−0.52	0.57	−0.04	−0.13	6.45	6.19	6.02	5.74
36	H	$N(CH_2)_2$	1.66	0.18	0.18	0.10	0.10	−0.92	6.54	6.05	5.93	5.60
37	$R^1=R^2=CH_2CH_2OH$		2.42	−0.32	−0.16	1.21	−0.08	−0.26	6.77	6.21	6.54	5.69
38	CH_3	$N(CH_2)_2$	2.13	0.68	0.18	0.57	0.06	−1.05	6.90	5.75	6.05	5.27
39	CH_3	$CH(OCH_3)CH_2OH$	2.47	−0.13	−0.63	0.57	−0.04	−0.13				

a) The data was taken from literature (ref. 15). Chron. inj., chronic injection. Sing. inj., singular injection. MED, minimum effective dose. OD, optimal dose.

Therefore, the least value should be set at slightly larger than zero. We scaled the input data between 0.1 and 1 using the following equation,

$$\tilde{p}=[(q_{max}-q_{min})p+q_{min}p_{max}-q_{max}p_{min}]/(p_{max}-p_{min}) \quad (16)$$

where q_{max} and q_{min} are the maximum and minimum scaling values, *i.e.*, 1.0 and 0.1, p is the element of the input patterns to be scaled, and p_{max}, and p_{min} are the maximum and minimum values of the element of the input patterns. Finally, the analog value of the training pattern was also rescaled to between 0 and 1.

Application to QSAR Studies in Carboquinones To be fair with the adopted data, we used those well-known and well-studied by conventional methods. Carboquinones were synthesized by Nakao *et al.*[8,9] and other groups,[10-12] and were developed as an anti-carcinogenic drug for clinical use. A detailed QSAR study has been carried out by Yoshimoto *et al.*[13] We first applied our new technique to this problem.

The input data, the physicochemical parameters, are the molecular refractivity constant (MR), hydrophobicity constant (π), substituent constants (F and R), and $MR_{1,2}$ and $\pi_{1,2}$ used to estimate the steric effects of R^1 and R^2 and the total hydrophobicity. The biological data includes the minimum effective dose (MED) and the optimal dose (OD) on a chronic treatment schedule or in a single injection. MED is the dose which gives a 40% increase in lifespan compared to the controls. OD is the dose giving the maximum increase of lifespan. The input data are shown in Table I.

Since the number of input parameters is 6, that in the input layer is 7 (6+1),[7] and that in the second layer is 6, and 1 for the third layer. The θ values are unanimously set at zero. The back-propagation parameter, ε, was set at 0.06 for the correction between the first and second layers and 0.03 between the second and third layers. The maximum number of iterations was set at 15000. On obtaining the relationship between the α and β values and the decision coefficients, the numbers of neurons are set to be 7, 6, and 1 respectively in the first, second, and third layers. Other parameters are fixed to be the same as those in obtaining the partial correlation coefficients. The results are shown in Table II.

First let us examine the set the α and β values in various cases. If a nonlinearity operation of neurons is enforced by setting $\beta=1$ and $\alpha=5$, the decision coefficient is increased to show that the output of the network well fits the observed values. On the other hand, if the linearity operation of neurons is increased, the decision coefficient is decreased to resemble that of the multiregression analysis. The decision coefficient is further decreased by setting $\alpha=1$ and $\beta=0.2$. The reason is clearly given by the discussion in method 1.

A change in the output function of a neuron causes the partial correlation coefficients for π_2 and F to vary greatly. Partial correlation coefficients between variables are obtained by multiregression analysis and are shown in Table III. The table shows that π_2 and F correlate highly, respectively, with $\pi_{1,2}$ and R. Therefore, it is understood that changes in the operation function and the mode of training cause large variations in those correlation coefficients.

Divided Differences We have calculated the divided differences, $\delta O_k/\delta x_L$, using the same data. The number of neurons in the first, second, and third layers is 7, 18, 1. The output function for neurons in the second layer is,

$$f(y)=0.6321206/[0.2642411+\exp(-y)] \quad (17)$$

The ε and θ values are set to be 0.06 and 0. The deactivation cycle, M, is set to be 9.

TABLE II. Partial Correlation Coefficients Obtained by Various Sets of α and β in Carboquinones

α	5	2	1	1	1	MR
β	1	1	1	0.5	0.2	
$MR_{1,2}$	−0.01	−0.07	−0.09	−0.07	−0.11	−0.04
$\pi_{1,2}$	−0.35	−0.33	−0.22	−0.15	−0.27	−0.28
π_2	−0.18	−0.17	−0.35	−0.48	−0.30	−0.59
MR_1	−0.25	−0.38	−0.37	−0.42	−0.40	−0.29
F	0.06	−0.11	−0.43	−0.50	−0.45	−0.30
R	−0.38	−0.41	−0.45	−0.42	−0.48	−0.27
DC	0.924	0.889	0.883	0.851	0.850	0.853

MR, results by multiregression analysis. DC, decision coefficient.

TABLE III. Partial Correlation Coefficients between Variables Obtained by Multiregression Analysis

	$MR_{1,2}$	$\pi_{1,2}$	π_2	MR_1	F
$\pi_{1,2}$	−0.01				
π_2	−0.02	0.72			
MR_1	0.48	0.38	−0.55		
F	0.04	−0.09	−0.27	−0.16	
R	−0.28	0.07	−0.33	−0.30	−0.72

TABLE IV. Divided Differences ($\delta O_k/\delta x_L$) in Carboquinones

Variable	Chronic injection						Singular injection					
	MED			OD			MED			OD		
	N.N	SPRC	PRC	N.N	SPRC	PRC	N.N	SPRC	PRC	N.N	SPRC	PRC
MR_{12}	−6	−0.04	−0.02	−8	−0.13	−0.06	2	0.07	0.05	−2	−0.03	−0.01
π_{12}	−16	−0.18	−0.09	−24	−0.38	−0.17	−22	−0.46	−0.26	−29	−0.46	−0.23
π_2	−19	−0.59	−0.42	−6	−0.29	−0.17	−10	−0.35	−0.25	−5	−0.24	−0.16
MR_1	−11	−0.29	−0.27	−9	−0.19	−0.15	−10	−0.19	−0.26	−7	−0.10	−0.09
F	−16	−0.30	−1.77	−23	−0.43	−2.04	−35	−0.70	−3.85	−37	−0.65	−3.27
R	−8	−0.27	−0.75	−17	−0.43	−1.00	−20	−0.58	−1.59	−23	−0.54	−1.41
DC	0.868	0.853		0.858	0.822		0.854	0.839		0.893	0.844	

MED, minimum effective dose. OD, optimal dose. N.N, results by the neural network. SPRC, standard partial regression coefficient. PRC, partial regression coefficient. DC, decision coefficient.

TABLE V. Structural Parameters and Biological Intensities in Benzodiazepines[a)]

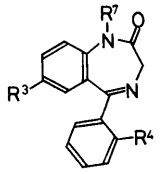

structure B

No.	Substituent	$MR-3$	$\pi-3$	$MR-7$	σ_m-3	$F-4$	$R-4$	$I-1$	Pent. obds.	Fight. obds.	Clined obsd.
1	3-Cl-7-iso-C_5H_{11}	0.60	0.71	2.42	0.37	0.0	0.0	0.0	4.99	3.53	2.83
2	3,4-F_2-7-CH_3	0.09	0.14	0.57	0.34	0.43	−0.34	0.0	3.33		2.85
3	3-SC_2H_5	1.84	1.07	0.10	0.15	0.0	0.0	1.0	3.57		
4	3-Cl-7-$CH_2CONHCH_3$	0.60	0.71	1.92	0.37	0.0	0.0	0.0	5.83	3.63	2.88
5	3-SC_4H_9	2.77	2.07	0.10	0.15	0.0	0.0	1.0	3.79		
6	3-NO_2-7-iso-C_5H_{11}	0.74	−0.28	2.42	0.71	0.0	0.0	0.0	4.80	3.77	2.94
7	3-$N(CH_3)_2$	1.56	0.18	0.10	−0.15	0.0	0.0	1.0	3.84		
8	3-Cl-4-OCH_3	0.60	0.71	0.10	0.37	0.26	−0.51	1.0	4.60	3.48	3.00
9	3-Cl-7-$(CH_2)_3N(CH_3)_2$	0.60	0.71	2.95	0.37	0.0	0.0	0.0	3.38		3.01
10	3-Cl-7-$(CH_2)_3OH$	0.60	0.71	1.65	0.37	0.0	0.0	0.0	4.34		3.04
11	3-NO_2-7-$CH_2CONHCH_3$	0.74	−0.28	1.92	0.71	0.0	0.0	0.0	5.29	4.55	3.07
12	3-Cl-7-$(CH_2)_2N(C_2H_5)_2$	0.60	0.71	3.41	0.37	0.0	0.0	0.0	5.06	3.57	3.09
13	3-Cl-7-$CH_2CON(CH_3)_2$	0.60	0.71	2.39	0.37	0.0	0.0	0.0	5.35	4.25	3.11
14	4-F-7-CH_3	0.10	0.0	0.57	0.0	0.43	−0.34	0.0	4.53	3.83	3.13
15	3-Cl-7-$CH_2C_6H_5$	0.60	0.71	3.00	0.37	0.0	0.0	0.0	4.64	3.56	
16	3-Cl-7-$(CH_2)_2N(CH_3)_2$	0.60	0.71	2.48	0.37	0.0	0.0	0.0	4.73	3.53	3.14
17	3-Cl-4-F-7-$(CH_2)_3N(CH_3)_2$	0.60	0.71	2.95	0.37	0.43	−0.34	0.0	4.76	3.97	3.17
18	H	0.10	0.00	0.10	0.00	0.00	0.00	1.0		3.37	3.20
19	3-CF_3-7-$CH_2CONHCH_3$	0.50	0.88	1.92	0.43	0.00	0.00	0.0	5.06	3.69	3.20
20	3-SCH_3	1.38	0.61	0.10	0.15	0.00	0.00	1.0	4.15	4.15	3.21
21	3-Cl-7-$(CH_2)_3OH$	0.60	0.71	1.65	0.37	0.00	0.00	0.0		3.61	
22	3-Cl-7-CH_2CONH_2	0.60	0.71	1.44	0.37	0.00	0.00	0.0	5.07	4.21	3.21
23	3-F	0.09	0.14	0.10	0.34	0.00	0.00	1.0		3.40	3.23
24	3-$SOCH_3$	1.37	−1.58	0.10	0.52	0.00	0.00	1.0	4.08		3.23
25	3-Cl-4-CH_3	0.60	0.71	0.10	0.37	−0.04	−0.13	1.0	4.57	3.45	3.28
26	3-$N(CH_3)_2$-7-CH_3	1.56	0.18	0.57	−0.15	0.00	0.00	0.0	4.69	3.86	3.29
27	3-Cl-4-F-7-$(CH_2)_2N(C_2H_5)_2$	0.60	0.71	3.41	0.37	0.43	−0.34	0.0	5.38	4.29	3.29
28	3-NO_2-7-$(CH_2)_3N(CH_3)_2$	1.56	0.18	0.57	0.37	0.41	−0.15	0.0	5.82	3.61	3.34
29	3-NO_2-7-$(CH_2)_3N(CH_3)_2$	0.74	−0.28	2.95	−0.15	0.00	0.00	0.0	4.28	3.96	3.35
30	3-NO_2-7-$(CH_2)_2N(CH_3)_2$	0.74	−0.28	2.48	0.71	0.00	0.00	0.0	4.70	4.25	3.37
31	3-Cl-4-Cl	0.60	0.71	0.10	0.37	0.41	−0.15	1.0	5.85	5.18	3.48
32	3-Cl-7-CH_2-cyclo-C_3H_5	0.60	0.71	1.82	0.37	0.00	0.00	0.0	4.90	4.51	3.51
33	3-CN	0.63	−0.57	0.10	0.56	0.00	0.00	1.0	5.30	3.81	3.54
34	3-NO_2-4-CF_3	0.74	−0.28	0.10	0.71	0.38	0.19	1.0	5.70	4.54	3.54
35	3-Cl	0.60	0.71	0.10	0.37	0.00	0.00	1.0	4.65	4.13	3.56
36	3-CN-4-F	0.63	−0.57	0.10	0.56	0.43	−0.34	1.0	5.63	4.75	3.57
37	3-Cl-7-C_2H_5	0.60	0.71	1.03	0.37	0.00	0.00	0.0	4.90	4.17	3.60
38	3-SCH_3-7-CH_3	1.38	0.61	0.57	0.15	0.00	0.00	0.0	3.60	3.87	3.77
39	3-Cl-7-CH_2COCH_3	0.60	0.71	1.51	0.37	0.00	0.00	0.0	5.28	4.21	3.82
40	3-Cl-4-Br	0.60	0.71	0.10	0.37	0.44	−0.17	1.0	5.77	4.85	3.85
41	3-Cl-4-F	0.60	0.71	0.10	0.37	0.43	−0.34	1.0	6.46	4.76	3.86
42	3-NO_2-4-CF_3-7-CH_3	0.74	−0.28	0.57	0.71	0.38	0.19	0.0	5.71	4.86	3.86
43	3-CF_3-7-$(CH_2)_2N(CH_3)_2$	0.50	0.88	2.48	0.43	0.00	0.00	0.0	4.76	4.27	3.88
44	3-Cl-7-$CH_2CH=CH_2$	0.60	0.71	1.45	0.37	0.00	0.00	0.0	5.35	4.49	3.89
45	3,4-Cl_2-7-CH_3	0.60	0.71	0.57	0.37	0.41	−0.15	0.0	6.03	4.50	3.90
46	3-Cl-7-CH_3	0.60	0.71	0.57	0.37	0.00	0.00	0.0	5.31	4.45	3.98
47	3-NO_2-4-Cl-7-CH_3	0.74	−0.28	0.57	0.71	0.41	−0.15	0.0	6.92	5.12	4.04
48	3-CF_3-4-CF_3	0.50	0.88	0.10	0.43	0.38	0.19	1.0	4.97	4.27	4.09
49	3-Br	0.89	0.86	0.10	0.39	0.00	0.00	1.0	5.20	4.20	4.10
50	3-CN-7-CH_3	0.63	−0.57	0.57	0.56	0.00	0.00	0.0	5.44	4.74	4.14
51	3-NO_2	0.74	−0.28	0.10	0.71	0.00	0.00	1.0	5.60	4.75	4.27
52	3-NO_2-7-CH_3	0.74	−0.28	0.57	0.71	0.00	0.00	0.0	5.62	5.07	4.47
53	3-CF_3	0.50	0.88	0.10	0.43	0.00	0.00	1.0	5.48	4.48	4.48
54	3-Cl-4-F-7-CH_3	0.60	0.71	0.57	0.37	0.00	−0.34	0.0	5.88	4.78	4.48
55	3-CF_3-7-$CH_2CH=CH_2$	0.50	0.88	1.45	0.43	0.00	0.00	0.0	5.03	4.54	4.54
56	3-NO_2-4-Cl	0.74	−0.28	0.10	0.71	0.41	−0.15	1.0	6.30	4.20	
57	3-NO_2-7-NH_2	0.74	−0.28	0.54	0.71	0.00	0.00	0.0	5.77	5.17	4.77
58	3-NO_2-4-NO_2	0.74	−0.28	0.10	0.71	0.67	0.16	1.0	5.97	3.91	
59	3-NO_2-4-F	0.74	−0.28	0.10	0.71	0.43	−0.34	1.0	6.00	5.17	4.88
60	3-NO_2-4-F-7-CH_3	0.74	−0.28	0.57	0.71	0.43	−0.34	0.0	6.50	5.80	5.50

a) The data was taken from literature (ref. 18). Pent., anti-pentylenetetrazole effect. Fight., anti-fighting behavior. Clined, clined screen test.

TABLE VI. Divided Differences ($\delta O_k/\delta x_L$) is Benzodiazepines

Variable	Anti-pentylenetetrazole effect			Anti-fighting effect			Clined screen test		
	N.N	SPRC	PRC	N.N	SPRC	PRC	N.N	SPRC	PRC
$MR-3$	11	−0.12	−0.22	−9	0.01	0.02	5	0.04	0.08
$\pi-3$	15	0.10	0.13	29	0.02	0.02	42	0.17	0.18
$MR-7$	−15	−0.27	−0.20	−20	−0.48	−0.26	−42	−0.63	−0.35
$\sigma-3$	17	0.51	1.85	32	0.46	1.22	28	0.45	1.26
$F-4$	17	0.29	1.13	16	0.13	0.36	−4	−0.05	−0.14
$R-4$	−12	−0.02	−0.12	−2	−0.16	−0.58	0	−0.09	−0.33
$I-1$	−5	−0.21	−0.34	−9	−0.41	−0.47	−9	−0.33	−0.40
DC	0.787	0.493		0.828	0.443		0.809	0.388	

N.N, results by the neural network. SPRC, standard partial regression coefficient. PRC, partial regression coefficient. DC, decision coefficient.

The output function in the third layer is,

$$f(y)=y \tag{18}$$

without deactivation, where the ε and θ values are set to be 0.03 and 0.

The input data into the first layer was scaled to between 0.1 and 1. Table IV shows the results at the iteration count of 30000, together with the standard partial regression coefficient (SPRC) and partial regression coefficient (PRC).

Since part of a sigmoid function is used as the output function of a neuron, the fitting ability as the full function is reduced to give poor decision coefficients in MED. The $\delta O_j/\delta x_L$ value should be considered as relative to others. The sign of this value is also important. The ratio and sign of $\delta O_j/\delta x_L$ between parameters shows a tendency similar to those of multiregression analysis: the strongest contribution to biological activity by the new method is also the strongest by the multiregression analysis.

To conclude, the following three points can be stated: (1) the quantity of the calculation for obtaining the $\delta O_j/\delta x_L$ value (method 2) is 1/20 smaller than that for the partial correlation coefficient by the neural network (method 1) in addition to the merit that method 2 does not require complicated training of two networks. (2) The decision coefficient is also obtained by the network which is used to give the $\delta O_j/\delta x_L$ value. (3) The ratio and sign of $\delta O_j/\delta x_L$ between parameters show a similarity to both partial correlation coefficients by method 1 and multiregression analysis, but shows a much stronger similarity to the latter method.

Application to the QSAR Study in Benzodiazepines Benzochlorodiazepoxide, a derivative of benzodiazepine, is introduced by Randall *et al.* as a minor tranquilizer.[14] The biological activities of 1,4-benzodiazepines have been extensively studied and play a major role as a minor tranquilizer.[6b] Kubota *et al.* have studied the QSAR of this series of compounds.[15] The same biological data and structural parameters were used as those in the literature.[15]

The input parameters are $MR-3$, $\pi-3$, $MR-7$, σ_m-3, $F-4$, $R-4$, and $I-1$. The parameters of the network were set to be the same as those in the former study, except for the number of neurons. The number of neurons in the first, second and third layers were set to be 8, 21, and 1, respectively. The maximum iteration count was set at 20000. The results are shown in Table V.

As we indicated in the previous paper,[1b] the biological data may include much error and/or nonlinearity. This is further ensured by the fact that the decision coefficients by multiregression analysis range from 0.388 to 0.493, too low to be reliable. Contrary to multiregression analysis, the neural network gives high decision coefficients because of its nonlinear operation.

The $\delta O_j/\delta x_L$ values show tendencies similar to the SPRC and PRC values by multiregression analysis. However, the matching degree is not as good as in the former study. The reason is simply because nonlinear fitting is adequately carried out in the neural network.

Conclusions

In this paper, we have proposed an equation that introduces a linear operation to the neural network at any level. We also studied a method which gives correlation coefficients between the input parameters and outputs. Since it was found difficult to obtain these coefficients, we proposed a new index: the divided difference of the output strength with respect to the input parameter ($\delta O/\delta x$). For the sake of linearity, the divided differences were obtained using the "unsaturated sigmoid function" as an output function of the neurons, where a new learning method with the concept of "neuron fatigue" is introduced. The new techniques were applied to QSAR studies in carboquinones and bezodiazepines to compare the results with those by multiregression analysis. It was found that the divided differences works well and can substitute for the partial differential coefficients obtained by multiregression analysis.

Acknowledgment This research was financially supported by the Ministry of Education, Science and Culture (Grant-in-Aid for Developmental Scientific Research No. 02807197).

References and Notes

1) *a*) Neural Networks Applied to Pharmaceutical Problems. V; *b*) For part IV, T. Aoyama and H. Ichikawa, *Chem. Pharm. Bull.*, **39**, 358 (1991).
2) T. Aoyama, Y. Suzuki and H. Ichikawa, *Chem. Pharm. Bull.*, **37**, 2558 (1989).
3) T. Aoyama, Y. Suzuki and H. Ichikawa, *J. Med. Chem.*, **33**, 905 (1990).
4) T. Aoyama, Y. Suzuki and H. Ichikawa, *J. Med. Chem.*, **33**, 2583 (1990).
5) *a*) For early review, see, "Parallel Distributed Processing Exploration in the Microstructure of Cognition, Vols. 1 and 2, ed. by D. E. Rumelhart and N. L. McClelland, MIT Press, Cambridge, MA, 1986; *b*) *Ibid.*, Vol. 1, Chap. 8.
6) *a*) For a review, see, for example, "Quantitative Structure–Activity

Relationship," ed. by J. G. Topliss, Academic Press, New York, 1983; *b*) L. H. Sternbach, L. O. Randall, R. Banziger and H. Lehr, "Medicinal Research Series 2. Drugs Affecting the Central Nervous System," ed. by A. Burger, Mercell Dekker, Inc., New York, 1968, p. 237.
7) The constant 1 is added to the input data: this effect is equivalent to the effect of having the parameter θ_j set to the best value.
8) H. Nakao, M. Arakawa, T. Nakamura and M. Fukushima, *Chem. Pharm. Bull.*, **20**, 1962 (1972).
9) H. Nakao and M. Arakawa, *Chem. Pharm Bull.*, **20**, 1968 (1972).
10) J. S. Discoll, G. F. Hazard Jr., H. B. Wood and A. Goldin, *Cancer Chemother. Rep. Part 2*, **4**, 1 (1976).
11) A. H. Khan and J. S. Discoll, *J. Med. Chem.*, **19**, 313 (1976).
12) F. Chou, A. H. Khan and J. S. Driscoll, *J. Med. Chem.*, **19**, 1302 (1976).
13) M. Yoshimoto, H. Miyazawa, H. Nakao, K. Shinkai and M. Arakawa, *J. Med. Chem.*, **22**, 491 (1979).
14) L. O. Randall, W. Schallek, G. A. Heise, E. F. Eith and R. E. Bagdon, *J. Pharmacol. Exp. Ther.*, **129**, 163 (1960).
15) T. Kubota, M. Yamakawa, H., Terada and H. Yoshimoto, "Structure–Activity Relationships–Quantitative Approaches," ed. by QSAR Research Group, Kagaku No Ryoiki Supl. ed., No. 122, Tokyo, 1979.

Studies on the Constituents of *Aconitum* Species. XII. Syntheses of Jesaconitine Derivatives and Their Analgesic and Toxic Activities

Takao MORI,[a] Mitsuo MURAYAMA,*,[a] Hideo BANDO[b] and Norio KAWAHARA[b]

Research Sections, Sanwa Shoyaku Co., Ltd.,[a] 6–1, Hiraide Kogyo Danchi, Utsunomiya 321, Japan and Hokkaido Institute of Pharmaceutical Sciences,[b] Katsuraoka-cho, Otaru 047–02, Japan. *Received June 21, 1990*

The role of the substituents at C3 and C8 of jesaconitine (1) on jesaconitine-induced analgesia and toxicity was examined. 3-*O*-Acetyljesaconitine (2), 3-*O*-anisoyljesaconitine (3), and 3-deoxyjesaconitine (6) showed dose-dependent analgesic action, and the potency of their compound-induced analgesia and toxicity was lower than those of 1. The most remarkable difference was found in the toxicity. The results indicate that the C3 hydroxy function of 1 participate in the induction of toxicity rather than of analgesia. 8-*O*-Linoleoyl-14-anisoylaconine (5), 8-*O*-methyl-14-anisoylaconine (7), 8-*O*-ethyl-14-anisoylaconine (8), 14-anisoylaconine (4) and 8-deoxy-14-anisoylaconine (9) showed lower activities than jesaconitine-induced analgesia and toxicity. The analgesic activity of 7 was almost the same as that of 8, but the toxicity of 7 was lower than that of 8. The analgesic activity of 9 was lower than that of 4, but the toxicities of both derivatives were not apparent. These facts indicate that the C8 function of 1 is important to the induction of analgesia and toxicity, and also that this function participates differently in the induction of the analgesia and toxicity. Subsequently, it was suggested that substituents at C3 and C8 of 1 played important roles of the induction of the analgesia and toxicity, and that the modes of this participation were not the same in analgesia and toxicity.

Keywords *Aconitum*; jesaconitine; analgesia; toxicity

The crude drug "bushi," prepared from roots of certain *Aconitum* spp. (Ranunclaceae) of Chinese and Japanese origin, is an indispensable material in oriental medicine. Traditionally, "bushi" had been thought to restore low metabolism in feeble patients and had been employed for such symptoms as pain, paralysis, atonia and coldness of the extremities. However, in modern clinical practice, processed aconite ("Kako-bushi" in Japanese), which is made by steaming raw aconite root under high pressure, is generally used, since the raw root has very strong toxicity. The toxicity has been found to be due to aconitine alkaloids, and the main alkaloids in *Aconitum* plants are aconitine, mesaconitine, hypaconitine and jesaconitine. These alkaloids not only have strong toxicity, but also potent analgesic action.[1,2] Accordingly, the pharmacological action of "bushi" can not be discussed without discussing the pharmacological action of aconitine alkaloids.

In some pharmacological studies on aconitine alkaloids, it has been reported that the mechanism of analgesic action of mesaconitine is related to the function of the noradrenergic neuron in the central nervous system[2]; that the sites of the analgesic action of mesaconitine are in the central nervous system; and that the nucleus reticularis gigantocellularis, the nucleus reticularis paragigantocellularis, the periaqueductal gray and the lumbar enlargement are involved in the sites of the analgesic action of mesaconitine.[3] Regarding toxicity, aconitine causes arrhythmia when a toxic dose is administered and is used as a tool for the induction of arrhythmia in experimental animals.[4,5] A consistent structure–activity relationship of aconitine alkaloids has not been reported. Investigation of the structure–activity relationship of aconitine alkaloids is important to elucidate the relation between its analgesic properties and its toxicity. In our preliminary experiment,[6] it was found that jesaconitine (**1**) among aconitine alkaloids has the most potent analgesic and toxic activities, and is one of the main alkaloids isolated from *Aconitum japonicum* native to Otaru, Hokkaido, Japan.[7] Accordingly, we concentrated on **1** among the aconitine alkaloids and studied the role of the oxygen-function attached to positions C3 and C8 of **1** and its derivatives in connection with the induction of toxicity and analgesia (Fig. 1). Regarding the method of measurement of analgesic activity, the acetic acid-induced writhing method was used.[2,8–10]

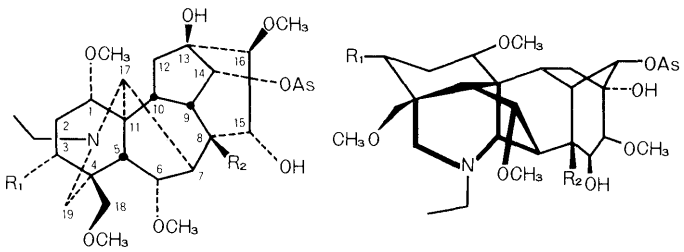

1 : R_1 = OH , R_2 = OAc : jesaconitine
2 : R_1 = OAc, R_2 = OAc : 3-*O*-acetyljesaconitine
3 : R_1 = OAs, R_2 = OAc : 3-*O*-anisoyljesaconitine
4 : R_1 = OH , R_2 = OH : 14-anisoylaconine
5 : R_1 = OH , R_2 = O-linoleoyl : 8-*O*-linoleoyl-14-anisoylaconine
6 : R_1 = H , R_2 = OAc : 3-deoxyjesaconitine
7 : R_1 = OH , R_2 = OCH_3 : 8-*O*-methyl-14-anisoylaconine
8 : R_1 = OH , R_2 = OCH_2CH_3 : 8-*O*-ethyl-14-anisoylaconine
9 : R_1 = OH , R_2 = H : 8-deoxy-14-anisoylaconine
Ac= $COCH_3$, As= COC_6H_4 (*p*-OCH_3)

Fig. 1. Structures of Jesaconitine and Its Derivatives

Results and Discussion

Chemistry 3-*O*-Acetyljesaconitine (**2**): Compound **1** was converted to **2** by treatment with acetic anhydride in a 92.5% yield. The ^{1}H-nuclear magnetic resonance (^{1}H-NMR) spectrum of **2** revealed the presence of two acetoxy groups. One of them at δ 1.43 was assigned to be in the C8 acetoxy group, which was shielded by the C14 anisoyl group. Another acetoxy group found a δ 2.06 was assigned to be at C3. The double doublet signal at δ 4.91 (1H, J=12.2, 5.3 Hz) was assigned to be C3-β-H. All of the signals in the ^{13}C-nuclear magnetic resonance (^{13}C-NMR) spectrum (Table I) of **2** are in agreement with the assigned structure.

3-*O*-Anisoyljesaconitine (**3**): Compound **1** was converted

to **3** by treatment with *p*-anisoyl chloride in a 27.6% yield. The ^{1}H-NMR spectrum of **3** revealed the presence of two anisoyl groups found at δ 7.99 (4H, d, J=8.9 Hz) and δ 6.93 (4H, d, J=8.9 Hz). The double doublet signal at δ 5.17 (1H, J=12.1, 5.4 Hz) was assigned to be C3-β-H. This structure was supported by the ^{13}C-NMR spectrum (Table I).

3-Deoxyjesaconitine (**6**): Compound **6** was synthesized in accordance with the method of a previous paper.[11]

14-Anisoylaconine (**4**): Compound **4** was also synthesized in accordance with the method of a previous paper.[12]

8-*O*-Linoleoyl-14-anisoylaconine (**5**): Treatment of **1** with linoleic acid in pyridine yielded **5** in a 79.9% yield. The ^{1}H-NMR spectrum was similar to that of **1** except for the disappearence of the acetyl group. A methyl group of linoleic acid residue attached at position C8 was seen at δ 0.97 (3H, t, J=7.6 Hz). The olefinic protons of linoleic acid residue at C8 were seen at δ 5.36 (4H, m). This structure was confirmed by the ^{13}C-NMR spectrum (Table I).

8-*O*-Methyl-14-anisoylaconine (**7**): Compound **7** was synthesized in accordance with the method of a previous paper.[7]

8-*O*-Ethyl-14-anisoylaconine (**8**): Compound **8** was synthesized in accordance with the method of a previous paper.[7]

8-Deoxy-14-anisoylaconine (**9**): Compound **1** was converted to pyrojesaconitine by heating at 200 °C under reduced pressure in a 65% yield.[12] Pyrojesaconitine was

TABLE I. ^{13}C-Chemical Shifts and Assignments for Jesaconitine (**1**), 3-*O*-Acetyljesaconitine (**2**), 3-*O*-Anisoyljesaconitine (**3**), 3-Deoxyjesaconitine (**6**), 14-Anisoylaconine (**4**), 8-*O*-Linoleoyl-14-anisoylaconine (**5**), 8-*O*-Methyl-14-anisoylaconine (**7**), 8-*O*-Ethyl-14-anisoylaconine (**8**) and 8-Deoxy-14-anisoylaconine (**9**)

Carbon	^{13}C-Chemical shifts (ppm)								
	1	**2**	**3**	**6**	**4**	**5**	**7**	**8**	**9**
1	82.3	81.9	83.5	85.2	82.4	82.3	82.2	82.5	83.7
2	33.6	31.9	32.1	26.4	33.0	33.4	32.8	33.2	33.8
3	70.6	71.4	71.6	35.2	71.9	71.5	71.5	71.6	72.0
4	43.1	42.2	42.7	39.4	43.0	43.0	43.0	42.9	43.2
5	46.6	45.9	45.9	49.2	47.6	46.4	45.4	45.5	47.2
6	83.3	83.5	82.0	83.3	83.5	83.4	83.1	83.4	85.2
7	44.6	45.2	44.7	45.2	46.2	44.7	45.0	45.2	39.2
8	91.1	91.8	91.9	92.1	78.6	91.7	82.2	82.1	40.7
9	44.2	44.6	45.3	44.1	46.0	44.3	42.2	42.9	37.5
10	40.8	40.5	40.5	41.0	42.0	40.9	41.4	41.3	41.6
11	49.9	47.1	49.7	49.9	50.4	50.1	50.3	50.5	50.6
12	35.8	36.3	36.5	36.6	36.0	35.7	36.1	36.2	36.6
13	74.0	74.1	74.1	74.2	74.8	74.0	74.7	74.2	75.1
14	78.6	78.5	78.5	78.7	75.9	73.6	79.4	79.2	80.2
15	78.8	78.7	78.7	78.8	81.9	78.9	76.9	77.3	72.4
16	90.0	90.2	90.1	90.2	90.7	90.0	93.3	93.3	94.3
17	60.9	61.0	60.7	61.4	61.7	61.3	61.3	61.1	62.4
18	75.8	71.4	71.6	80.3	77.3	75.7	77.4	76.8	77.4
19	46.9	49.7	47.4	53.2	48.9	47.0	47.6	43.7	47.3
N–CH_2	48.9	49.0	49.0	49.1	48.4	48.8	48.8	48.9	49.1
CH_3	13.3	13.4	13.4	13.4	13.5	13.3	13.0	13.2	13.4
1′	55.8	56.3	56.4	56.2	55.7	55.9	55.6	55.8	56.1
6′	57.9	58.2	58.3	58.0	58.0	58.1	58.8	58.5	57.9
16′	61.1	60.7	61.0	61.1	60.9	60.9	62.3	62.3	61.8
18′	59.0	58.7	58.7	59.1	59.1	59.0	59.0	59.0	59.1
C=O(C14)	165.7	165.7	165.6	165.8	165.9	165.6	165.7	165.8	165.9
C_6H_4	122.1	122.3	122.3	122.3	122.1	122.2	122.4	122.7	122.2
	131.6	131.6	131.6	131.2	131.8	131.7	131.6	131.6	131.8
	113.8	113.8	113.8	113.8	113.6	113.8	113.5	113.6	113.7
	163.5	163.4	163.4	163.4	163.5	163.5	163.2	163.1	163.6
p(OMe)	55.4	55.4	55.4	55.5	55.4	55.4	55.3	55.3	55.4
C=O(C8)	172.4	172.3	172.3	172.4	—	—	—	—	—
CH_3	21.5	21.4	21.5	21.5	—	—	—	—	—
8-O–$CH_{2(3)}$	—	—	—	—	—	—	49.8	57.1	—
CH_3	—	—	—	—	—	—	—	15.3	—
C=O(C3)	—	170.2	—	—	—	—	—	—	—
CH_3	—	21.1	—	—	—	—	—	—	—
C=O(C3)	—	—	165.2	—	—	—	—	—	—
C_6H_4	—	—	123.1	—	—	—	—	—	—
	—	—	113.5	—	—	—	—	—	—
	—	—	131.7	—	—	—	—	—	—
	—	—	163.2	—	—	—	—	—	—
p(OMe)	—	—	55.4	—	—	—	—	—	—
C=O(C8) lipo	—	—	—	—	—	175.1	—	—	—

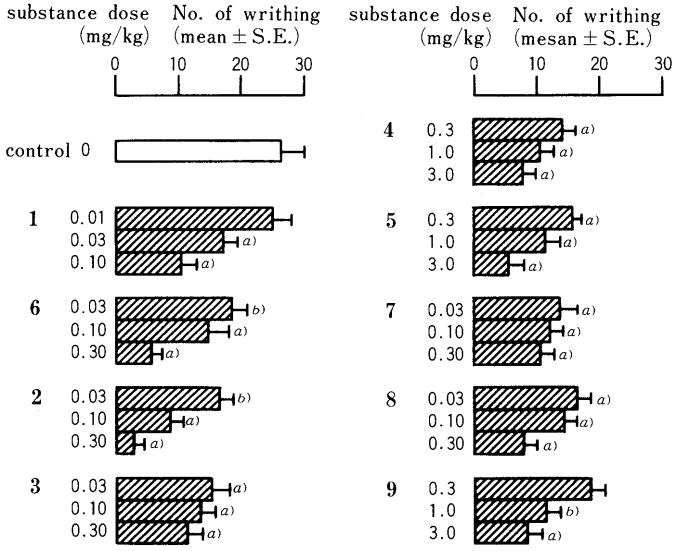

Fig. 2. Analgesic Effect of Jesaconitine and Its Derivatives

$n=7$, 8. Substances were administered s.c. 30 min before the injection i.p. of 0.7% acetic acid. Significantly different from the control, *a*) $p<0.01$ or *b*) $p<0.05$.

subsequently hydrogenated with $LiAl(OMe)_3H$ in tetrahydrofuran (THF) solution at $-70\,^{\circ}C$ to yield 8-deoxyaconine in a 96.8% yield. Next, treatment of 8-deoxyaconine with *p*-anisoyl chloride in a pyridine–dichloromethane solution at $-70\,^{\circ}C$ yielded **9** in a 64.3% yield. This structure was supported by both the ^1H-NMR and ^{13}C-NMR spectra (Table I).

Analgesic Activity To investigate the participation of the C3-hydroxy function in jesaconitine-induced analgesia and toxicity, the toxic and analgesic activities of **1** were compared with those of **2**, **3** and **6**. The compounds of **1**, **2**, **3** and **6** showed significant analgesic activity in a dose-dependent manner (Fig. 2). The toxic and analgesic activities of **6** were a little lower than those of **1**, and the decrease of the toxicity of **6** was found more marked than that of its analgesic activity (Table II). This result indicates that the hydroxy function at position C3 of **1** relates more closely to the induction of toxicity. Both the toxic and analgesic activities of 2 and 3 were lower than those of **1**. In particular, a more remarkable difference was found in the toxicity. The differences in the physical and chemical properties of the structures of **1** and **2**, **3** or **6** are present in the presence or absence of the substituents at position C3. From the stereo-models of **1**, **2**, **3** and **6**, the hydroxy function at position C3 of **1** may have hydrogen bonding or other binding to the active site of **1**, but the substituents at position C3 of **2**, **3** and **6** were not apt to cause such binding. Accordingly, it was considered that the hydroxy function at position C3 of **1** participates in the induction of toxicity. However, this participation seems only to assist in the induction of toxicity, since **6** still has the strong toxicity.

Next, to investigate the participation of the C8 O-function of **1** in toxicity and analgesia, the toxic and analgesic activities of **1** were compared with those of **4**, **5**, **7**, **8** and **9**. The compounds of **4**, **5**, **7**, **8** and **9** showed significant analgesic activity in a dose-dependent manner (Fig. 2). First, the analgesic activities of these compounds were observed. Compound **5** showed an analgesic activity about 1/15 lower

TABLE II. The Analgesic and Toxic Activity of Jesaconitine and Its Derivatives at the C3 Position in Mice

Substance	ED_{50} value in mg/kg, s.c. (95% confidence limits)	LD_{50} value in mg/kg, s.c. (95% confidence limits)
1	0.035 (0.019—0.064)	0.25 (0.19—0.33)
6	0.056 (0.039—0.080)	0.70 (0.63—0.78)
2	0.050 (0.027—0.093)	0.87 (0.78—0.97)
3	0.060 (0.022—0.164)	0.65 (0.44—0.96)

$n=7$, 8. Substances were administered s.c. 30 min before the injection i.p. of 0.7% acetic acid.

TABLE III. The Analgesic and Toxic Activity of Jesaconitine and Its Derivatives at the C8 Position in Mice

Substance	ED_{50} value in mg/kg, s.c. (95% confidence limits)	LD_{50} value in mg/kg, s.c. (95% confidence limits)
1	0.038 (0.018—0.080)	0.23 (0.18—0.29)
4	0.665 (0.388—1.140)	>100
5	0.580 (0.220—1.540)	>100
7	0.160 (0.039—0.653)	9.90 (9.11—10.76)
8	0.130 (0.058—0.269)	1.60 (1.26—2.04)
9	1.180 (0.468—2.974)	>100

$n=7$, 8. Substances were administered s.c. 30 min before the injection i.p. of 0.7% acetic acid.

than **1** (Table III). This result indicates that the 8-*O*-acetyl function of **1** participates in the induction of the analgesia. Compounds **7** and **8** showed lower activities than **1**, although differences between the activities of **7** and **8** were not apparent. The analgesic activity of **4** was lower than that of either **7** or **8** (Table III). These results demonstrate that the carbon atom of the carbonyl function at position C8 is important in inducing the analgesia by **1**. In addition, judging from the fact that the analgesic activity of **9** was lower than that of **4** (Table III), it was suggested that the oxygen atom binding to position C8 of **1** also participated in the induction of analgesia.

Secondly, the toxic activities of these compounds were observed. Compound **5** showed much lower toxicity than **1** (Table III). This fact indicates that the C8-acetyl function is important in inducing the toxicity by **1** and that the difference between the toxic activities of **5** and **1** may be due to the difference in size of the substituents at position C8. Compounds **4**, **7** and **8** showed lower toxicities than **1**; compound **8** had more potent toxicity than **7**, and compound **4** showed no toxicity (Table III). These results suggest that the two carbons and ketone of the acetyl function at position C8 of **1** more closely participate in the induction of toxicity. Additionally, from the fact that the toxicities of both **4** and **9** were not apparent, it was considered that the oxygen atom binding to position C8 is not essential in inducing toxicity. These facts indicate that for the induction of analgesia by **1**, the presence of a

C8-acetyl function is important, that two carbons in the C8-acetyl function participate in the induction of toxicity, and that the carbonyl carbon more closely participates in the induction of analgesia.

On the basis of the above evidence, it was demonstrated that the substituents at C3 and C8 of **1** play important roles in the induction of toxicity and analgesia. In addition, it was suggested that the C3 hydroxy function of **1** assists in the induction of toxicity rather than analgesia, that the acetyl function at position C8 plays a more important role in inducing toxicity and analgesia, and that the oxygen atom and carbonyl carbon at position C8 are more closely related to the induction of analgesia. Therefore, it was considered that the C3 and C8 substituents of **1** had participated differently in the induction of analgesia and toxicity.

Experimental

Optical rotations were measured with a JASCO DIP-4 polarimeter. Infrared (IR) spectra in KBr disks were taken with a JASCO IRA-2 spectrometer, and ultraviolet (UV) spectra were measured in an ethanol solution with a Shimadzu UV-240 spectrometer. Nuclear magnetic resonance (NMR) spectra were measured in a $CDCl_3$ solution with JEOL FX-100 and JEOL GX-270 spectrometers using tetramethylsilane as an internal standard. Mass spectra (MS) were measured with Shimadzu-LKB 9000B and Hitachi M-2000 spectrometers. Column chromatography was performed on Silica gel 60 (0.06—0.200 mm, Merck). Thin layer chromatography (TLC) was performed on Silica gel 60 F_{254} (Merck).

Jesaconitine (1) Compound **1** was isolated in accordance with the method of Mori *et al.*[11] Briefly, the dried aconite roots (1.31 kg) were extracted with ethanol (18 l). A suspension of ethanol extract (80 g) in water was partitioned with petroleum ether, and the water layer was adjusted to pH 9 with NH_4OH. The precipitate (5.7 g) was chromatographed over silica gel to give fractions A (170 mg), B (3.8 g) and C (1.2 g). Fraction B was subjected to column chromatography to give **1** (2.5 g). *Anal.* Calcd for $C_{35}H_{49}NO_{12}$: C, 62.21; H, 7.31; N, 2.07. Found: C, 62.16; H, 7.46; N, 1.98.

3-*O*-Acetyljesaconitine (2) A mixture of **1** (100 mg, 0.15 mmol), pyridine (2 ml) and acetic anhydride (8 ml) was stirred for 2 h at room temperature. The usual work up and purification was performed by column chromatography on silica gel with Et_2O saturated with 28% ammonia water : hexane = 3 : 2 as an eluting solvent to afford **2** (98 mg, 92.5%), amorphous powder, $[\alpha]_D^{19}$ +27.7° (c = 1.09, $CHCl_3$). HR-MS: Calcd for $C_{36}H_{47}NO_{11}$ (M^+ − AcOH): 657.3149. Found: 657.3152 and EI-MS *m/z*: 717 (M^+). UV λ_{max}^{EtOH} nm (log ε): 258 (3.95). IR ν_{max}^{KBr} cm^{-1}: 1710 (C=O). ^{1}H-NMR ($CDCl_3$) δ: 7.89 (2H, d, J = 9.2 Hz, anisoyl group), 6.93 (2H, d, J = 9.2 Hz, anisoyl group), 3.73 (3H, s, OCH_3), 3.25 (3H, s, OCH_3), 3.20 (6H, s, OCH_3), 3.87 (3H, s, OCH_3 of anisoyl group), 4.84 (1H, d, J = 4.9 Hz, C14-β-H), 4.46 (1H, dd, J = 5.3, 3.0 Hz, C15-β-H), 4.08 (1H, d, J = 6.6 Hz, C6-β-H), 1.43 (3H, s, CH_3 of acetoxy group at C8), 2.06 (3H, s, CH_3 of acetoxy group at C3), 1.10 (3H, t, J = 7.0 Hz, CH_3 of C_2H_5 at nitrogen atom), 4.91 (1H, dd, J = 12.2, 5.3 Hz, C3-β-H). MS *m/z*: 717 (M^+), 686 (M^+-OMe), 657 (M^+ − AcOH), 626 [M^+ − (OMe + AcOH)]. *Anal.* Calcd for $C_{37}H_{51}NO_{13}$: C, 61.91; H, 7.16; N, 1.95. Found: C, 62.18; H, 7.35; N, 2.08.

3-*O*-Anisoyljesaconitine (3) A mixture of **1** (150 mg, 0.22 mmol), pyridine (1 ml) and *p*-anisoyl chloride (40 mg, 0.24 mmol) was stirred for 1 h at 80 °C. After cooling, usual work up and purification by preparative TLC on SiO_2 with Et_2O saturated with 28% ammonia water : hexane = 5 : 1 as a developing solvent afforded **3** (49.7 mg, 27.6%), amorphous powder, $[\alpha]_D^{18}$ +24.0° (c = 0.3, $CHCl_3$). FD-MS *m/z*: 809 (M^+), UV λ_{max}^{EtOH} nm (log ε): 257 (4.49). IR ν_{max}^{KBr} cm^{-1}: 1705 (C=O). ^{1}H-NMR ($CDCl_3$) δ: 7.99 (4H, d, J = 8.9 Hz, anisoyl group, A_2B_2 pattern), 6.93 (4H, d, J = 8.9 Hz, anisoyl group, A_2B_2 pattern), 3.74 (3H, s, OCH_3), 3.26 (3H, s, OCH_3), 3.21 (3H, s, OCH_3), 3.12 (3H, s, OCH_3), 3.86 (6H, s, OCH_3 of anisoyl groups), 4.86 (1H, d, J = 5.3 Hz, C14-β-H), 1.44 (3H, s, CH_3 of acetoxy group), 1.14 (3H, t, J = 7.0 Hz, CH_3 of C_2H_5 at nitrogen atom), 5.17 (1H, dd, J = 12.1, 5.4 Hz, C3-β-H). *Anal.* Calcd for $C_{43}H_{55}NO_{14}$: C, 63.77; H, 6.84; N, 1.73. Found: C, 64.01; H, 6.73; N, 1.74.

14-Anisoylaconine (4) A mixture of **1** (100 mg, 0.15 mmol), dioxane (10 ml) and water (10 ml) was refluxed for 4 h. After cooling, the solvent was evaporized and the residue was purified by preparative TLC on SiO_2, with $CHCl_3$ saturated with 28% ammonia water : MeOH = 97 : 3 as a developing solvent to give **4** (75 mg, 80%). NMR and MS spectra of **4** were identical to those of an authentic sample reported by Mori *et al.*[12] *Anal.* Calcd for $C_{33}H_{47}NO_{11}$: C, 62.54; H, 7.47; N, 2.21. Found: C, 62.35; H, 7.29; N, 2.12.

8-*O*-Linoleoyl-14-anisoylaconine (5) A mixture of **1** (25 mg, 0.04 mmol), pyridine (0.09 ml) and linoleic acid (300 mg, 1.07 mmol) was stirred for 4 h at 70 °C. After cooling, ethyl acetate was added to the solution and washed with water, then dried over anhydrous sodium sulfate. The solvent was evaporized and the residue was purified by column chromatography on alumina with benzene : $CHCl_3$ = 3 : 1 as an eluting solvent to afford **5** (26.5 mg, 79.9%), oil, $[\alpha]_D^{23}$ +9.24° (c = 1.32, $CHCl_3$). UV λ_{max}^{EtOH} nm (log ε): 258 (4.00). FD-MS *m/z*: 895 (M^+). MS *m/z*: 615 ($M^+ - C_{18}H_{32}O_2$, 6%), 584 ($M^+ - C_{18}H_{32}O_2 - CH_3O$, base peak). ^{1}H-NMR ($CDCl_3$) δ: 7.97 (2H, d, J = 8.9 Hz, anisoyl group), 6.92 (2H, d, J = 8.9 Hz, anisoyl group), 3.75 (3H, s, OCH_3), 3.30 (3H, s, OCH_3), 3.26 (3H, s, OCH_3), 3.15 (3H, s, OCH_3), 3.85 (3H, s, OCH_3 of anisoyl groups), 4.06 (1H, d, J = 6.6 Hz, C6-β-H), 1.10 (3H, t, J = 7.0 Hz, CH_3 of C_2H_5 at nitrogen atom), 0.97 (3H, t, J = 7.6 Hz, CH_3 of a fatty acid residue), 5.36 (4H, m, olefinic protons of linoleic acid residue). *Anal.* Calcd for $C_{51}H_{77}NO_{12}$: C, 68.35; H, 8.66; N, 1.56. Found: C, 68.06; H, 8.37; N, 1.53.

3-Deoxyjesaconitine (6) A mixture of **1** (100 mg, 0.15 mmol) and thionyl chloride (1 ml) was refluxed for 3 h in an atmosphere of nitrogen. The reaction mixture was concentrated *in vacuo*, then the residue was added to ice water, which was made alkaline with a solution of 2 N sodium carbonate. The alkaline solution was extracted with $CHCl_3$. The $CHCl_3$ extract was purified by preparative TLC on SiO_2 with Et_2O saturated with 28% ammonia water : hexane = 4 : 1 as a developing solvent to yield a colorless amorphous powder (anhydrojesaconitine, 55 mg, 56%). Next, the solution of anhydrojesaconitine (54 mg, 0.08 mmol) in ethanol (5 ml) was subjected to hydrogen in the presence of platinic oxide (28 mg, 0.12 mmol) for 1.5 h. The solution was filtered and concentrated *in vacuo*. The resulting mixture was chromatographed on silica gel with Et_2O saturated with 28% ammonia water : hexane = 4 : 1 as an eluting solvent and crystallized from acetone to give **6** (25 mg, 45%). NMR and MS spectra of **6** were identical to those of an authentic sample reported by Mori *et al.*[11] *Anal.* Calcd for $C_{36}H_{49}NO_{11}$: C, 63.71; H, 7.49; N, 2.12. Found: C, 63.66; H, 7.49; N, 2.44.

8-*O*-Methyl-14-anisoylaconine (7) The solution of **1** (100 mg, 0.15 mmol) in methanol (30 ml) was stirred at 60 °C for 3 d. The solvent was evaporized and the residue was purified by preparative TLC on SiO_2 with $CHCl_3$ saturated with 28% ammonia water as a developing solvent to give **7** (83.3 mg, 82%). NMR and MS spectra of **7** were identical to those of an authentic sample reported by Bando *et al.*[7] *Anal.* Calcd for $C_{34}H_{49}NO_{11}$: C, 63.04; H, 7.62; N, 2.16. Found: C, 62.86; H, 7.47; N, 2.19.

8-*O*-Ethyl-14-anisoylaconine (8) The solution of **1** (100 mg, 0.15 mmol) in ethanol (30 ml) was stirred at 60 °C for 5 d. The solvent was evaporized and the residue was purified by preparative TLC on SiO_2 with $CHCl_3$ saturated with 28% ammonia water as a developing solvent to give **8** (72 mg, 72%). NMR and MS spectra of **8** were identical to those of an authentic sample reported by Bando *et al.*[7] *Anal.* Calcd for $C_{35}H_{51}NO_{11}$: C, 63.52; H, 7.76; N, 2.12. Found: C, 63.38; H, 7.95; N, 2.42.

8-Deoxy-14-anisoylaconine (9) Compound **1** (100 mg, 0.15 mmol) was heated at 200 °C for 30 min under reduced pressure (1.5—2.0 mmHg). The reaction mixture was separated with flash column chromatography (silica gel 5 g, 5% methanol–chloroform) to give pyrojesaconitine (60 mg, 65.9%). A THF solution (5 ml) of pyrojesaconitine (60 mg, 0.098 mmol) was added to a stirred suspension of $LiAl(OMe)_3H$, prepared from a dry-THF solution (5 ml) of $LiAlH_4$ (72 mg, 1.89 mmol) and dry methanol (0.23 ml) at 0 °C, and the reaction mixture was stirred for 1 h at −70 °C, and for an additional 1 h at room temperature. This solution was added to a wet-THF solution at 0 °C, and was filtered off. The filtrate was evaporized to give 8-deoxyaconine (45.6 mg, 96.8%). Next, *p*-anisoyl chloride (15 μl) was added to a mixture of 8-deoxyaconine (45 mg, 0.093 mmol), pyridine (5 ml) and dichloromethane (1 ml) at −70 °C. This reaction mixture was stirred and its temperature raised from −70 to −5 °C, which took 2 h. The reaction mixture was added to ice water and made alkaline with a solution of 5% sodium bicarbonate. The alkaline solution was extracted with chloroform, and the chloroform solution was washed with water, then dried over anhydrous sodium sulfate. The solvent was evaporized and the residue was purified by column chromatography on silica gel with Et_2O saturated with 28% ammonia water as an eluting solvent to yield **9** (37 mg, 64.3%), amorphous powder, $[\alpha]_D^{20}$ −5.2° (c = 1.46, $CHCl_3$). MS *m/z*: 617 (M^+). UV λ_{max}^{EtOH} nm (log ε): 257 (4.02). IR ν_{max}^{KBr} cm^{-1}: 1711 (C=O). ^{1}H-NMR ($CDCl_3$) δ: 7.99 (2H, d, J = 8.9 Hz, anisoyl group), 6.93 (2H, d, J = 8.9 Hz, anisoyl group), 3.69 (3H, s, OCH_3), 3.30 (3H, s, OCH_3), 3.28 (3H, s. OCH_3), 3.25 (3H, s, OCH_3), 3.87 (3H, s, OCH_3 of anisoyl

group), 4.43 (1H, d, $J=5.0$ Hz, C14-β-H), 4.51 (1H, dd, $J=10.2$, 6.6 Hz, C15-β-H), 1.11 (3H, t, $J=6.9$ Hz, CH_3 of C_2H_5 at nitrogen atom). *Anal.* Calcd for $C_{33}H_{47}NO_{10}$: C, 64.16; H, 7.67; N, 2.27. Found: C, 63.81; H, 7.32; N, 2.02.

Animals Male mice of the Std : ddY strain, weighing 20—24 g, were used. All mice were maintained at 24—25 °C on a 12 h light-dark cycle and were given food and water *ad libitum*.

Measurement of the Analgesic Activity of Jesaconitine (1) and Its Derivatives on the Acetic Acid-Induced Writhing in Mice Substances tested were used as 3% arabic gum suspensions and were administered s.c. 30 min before the i.p. injection of 0.7% acetic acid in a 0.9% physiological saline solution. The number of mice writhing for 10 min from 10 min after the injection of 0.7% acetic acid was counted. When the number of writhing mice was less than half the mean writhing-number of the control group, the analgesic effect of the substance was determined to be positive. The ED_{50} value and 95% confidence limits were calculated according to the method of Litchfield and Wilcoxon.[13]

Measurement of the Toxicity of Jesaconitine (1) and Its Derivatives in Mice Substances tested were administered s.c. and mortalities were observed 72 h after administration. The LD_{50} value and 95% confidence limits were calculated according to the method of Litchfield and Wilcoxon.[13]

References

1) H. Sato, C. Yamada, C. Konno, Y. Ohizumi, K. Endo and H. Hikino, *Tohoku J. Exp. Med.*, **128**, 175 (1979).
2) M. Murayama, T. Ito, C. Konno and H. Hikino, *Eur. J. Pharmacol.*, **101**, 29 (1984).
3) H. Hikino and M. Murayama, *Br. J. Pharmacol.*, **85**, 575 (1985).
4) G. Derouaux, *Ardr. Int. Pharmacodyn. The'r.*, **67**, 257 (1942).
5) D. Scherf, *Proc. Soc. Exp. Biol. Med.*, **64**, 233 (1947).
6) H. Bando, K. Wada, R. Wada and T. Amiya, Poster Abstract, the Japanese-United States Congress of Pharmaceutical Sciences in Hawaii, Dec. 1987, p. 195.
7) H. Bando, K. Wada, M. Watanabe, T. Mori and T. Amiya, *Chem. Pharm. Bull.*, **33**, 4717 (1985).
8) M. Murayama and H. Hikino, *Eur. J. Pharmacol.*, **108**, 19 (1985).
9) I. Kitagawa, Z. L. Chen, M. Yosihara, K. Kobayasi and M. Yoshikawa, *Yakugaku Zasshi*, **104**, 858 (1984).
10) K. Wada, H. Bando, R. Wada and T. Amiya, *Jpn. J. Pharmacognosy*, **43**, 50 (1989).
11) T. Mori, H. Bando, Y. Kanaiwa, K. Wada and T. Amiya, *Chem. Pharm. Bull.*, **31**, 2884 (1983).
12) T. Mori, T. Ohsawa, M. Murayama, H. Bando, K. Wada and T. Amiya, *Heterocycles*, **29**, 873 (1989).
13) J. T. Litchfield and F. Wilcoxon, *J. Parmacol. Exp. Ther.*, **96**, 99 (1949).

A New Monitoring System of Cultured Myocardial Cell Motion: Effect of Pilose Antler Extract and Cardioactive Agents on Spontaneous Beating of Myocardial Cell Sheets

Sheng-Lun HUANG, Nobuko KAKIUCHI,* Masao HATTORI and Tsuneo NAMBA

Research Institute for Wakan-yaku (Traditional Sino-Japanese Medicines), Toyama Medical and Pharmaceutical University, 2630 Sugitani, Toyama 930-01, Japan. *Received July 2, 1990*

Effects of various cardioactive agents and a water extract of the pilose antler of *Cervus nippon* var. *mantchuricus* on periodic beating of cultured myocardial cell sheets were examined by using an image analyzing system. Norepinephrine increased the beating rate and the beating amplitude, whereas digoxin and forskolin enlarged only the beating amplitude. Verapamil and propranolol decreased both the beating rate and the beating amplitude. The water extract of the pilose antler showed no remarkable effects in a standard medium (2.1 mM Ca^{2+}). However, it significantly increased the beating amplitude when the beating was suppressed by replacement with a low calcium medium (0.5 mM Ca^{2+}). A similar effect was found for 70% ethanol-soluble and -insoluble fractions of the extract.

Keywords *Cervus nippon* var. *mantchuricus*; chronotropic effect; inotropic effect; cultured myocardial cell; pilose antler; spontaneous beating

The heart cell in culture is a useful system for studying the actions of cardioactive agents.[1] Their actions can be detected sensitively as changes in beating rhythm, contraction force and other parameters. The magnitude of beating can be expressed by intracellular electrical depolarization or by the extent of displacement.[2,3] Though the electrical parameters give precise information, insertion of a microelectrode into a cell is not adequate to screen a large number of samples for a long period. Measurement of change in optical density caused by cell motion is a practical method, but the parameters do not necessarily correlate to the real motion and contractile force. We therefore developed a new monitoring system of myocardial cell motion using a microcomputer-driven image analyzing method. The system was applied to various cardioactive agents as well as a water extract of the pilose antler of *Cervus nippon* TEMMINCK var. *mantchuricus* SWINHOE, whose preventive activity against acute toxicity of doxorubicin in cultured myocardial cells was reported previously.[4]

Materials and Methods

Reagents and Media Calcium-containing and calcium-free Eagle's minimal essential medium (Eagle's MEM) and Dulbecco's calcium- and magnesium-free phosphate buffered saline (PBS(−)) were products of Nissui Laboratories (Tokyo, Japan), fetal calf serum (FCS) from Whittaker M&A Bioproducts (Walkersville, U.S.A.), *N*-2-hydroxyethylpiperadine-*N'*-2-ethane sulfonic acid (HEPES) from Dojin Laboratories (Kumamoto, Japan), verapamil hydrochloride, digoxin and norepinephrine from Wako Pure Chemicals (Osaka, Japan), and propranolol and forskolin from Sigma Co., Ltd. (St. Louis U.S.A.).

Measurement of Beating Rate and Beating Amplitude of Cultured Myocardial Cells Isolation and culture of mouse embryonic myocardial cells were performed as previously reported.[5] A cell sheet was prepared on a fibronectin-coated cover glass strip. The cell sheet attached to the cover glass was mounted upside-down on a small chamber in an acrylic plate (2 mm thick). The chamber was filled with a medium which was replaced continuously at a speed of 6—7 ml/h with a peristaltic pump. Cardioactive agents were dissolved in dimethyl sulfoxide (DMSO) and added to calcium-containing or calcium-free HEPES-buffered Eagle's MEM supplemented with 10% FCS. The final concentration of DMSO was 1% of the medium. The analyzing system for cell beating is schematized in Fig. 1. Cell images observed through a phase-contrast microscope (Olympus IMT-2) equipped with a thermostat system (Olympus IMT-2 IBS) maintained at 37±1 °C were monitored with a TV camera (Olympus FCD-10) and recorded with a videocamera cassette recorder (National AC-6300). The recorded images were displayed on a picture monitor (NEC PC-KD 854) and analyzed with a personal image analyzer (PIAS LA-500) equipped with a microcomputer (NEC PC-9801) using a newly developed

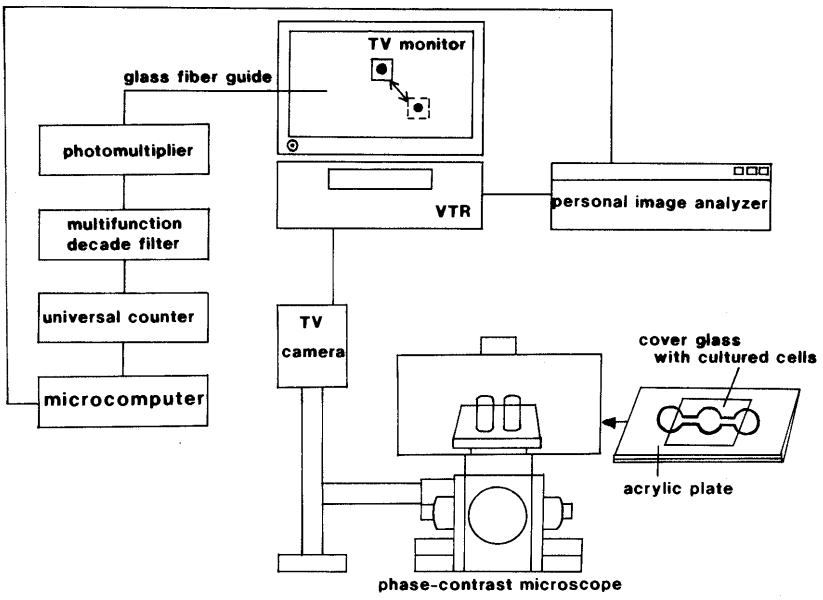

Fig. 1. Schematic Illustration of the Monitoring System Used for Analysis of Beating of Myocardial Cell Sheets

analysis program of cell beating. Several cell images with high light intensity were selected, and their central positions were recorded at 0.07 s intervals. Displacement of each central position, caused by periodic beating of the cell sheet, was followed (Fig. 2). The beating amplitude at the indicated time was expressed as the distance between peak and through in the oscillogram.

The relative beating amplitude after administration of samples was expressed as follows:

$$\frac{\text{beating amplitude after the perturbation}}{\text{beating amplitude before the perturbation}} \times 100$$

Similarly, the relative beating rate was expressed by the percentage of the beating rate (beats/min) to an initial beating rate observed just before administration of samples or medium replacement.

Preparation of a Water Extract of Pilose Antler The water extract of pilose antler and its 70% ethanol-soluble and -insoluble fractions were prepared as previously reported.[4]

Measurement of Inorganic Elements Portions of the extracts were burned with concentrated HNO_3, and their Ca^{2+}, K^+ and Na^+ contents were determined by atomic absorption spectrometry with a Shimadzu AA-640 spectrometer (Shimadzu Co., Ltd., Kyoto, Japan).

The water extract contained 5.4, 4.0 and 20.7×10^{-5} mol/g of Ca^{2+}, K^+ and Na^+, respectively. The 33% EtOH extract, 4.6, 5.2 and 15.7×10^{-5} mol/g of Ca^{2+}, K^+ and Na^+. The 99% EtOH extract, 0, 1.5 and 1.8×10^{-5} mol/g of Ca^{2+}, K^+ and Na^+.

Since the Ca^{2+}, K^+ and Na^+ contents of the three extracts were quite low, the respective ion concentrations in the medium were not appreciably changed by addition of the extracts.

Results

Using the image analyzing system, movement of a particular point on the cell sheet was followed. Monolayered cell sheets were used for assays since the beating amplitude (amplitude of displacement) was larger and more stable than that of single cells. Several points on the cell sheet were chosen, and the beating amplitude was expressed as the mean of values obtained at these pionts. During an assay of 30 min at 37 °C, a shift of the pacemaker of the cell sheet was rare. Therefore, the direction of contraction was assumed to be unchanged. Figure 2 shows typical osillograms of the periodic movement of a point on the cell sheet before and after treatment with either norepinephrine, digoxin or verapamil in a standard Eagle's MEM (2.1 mM Ca^{2+}). By addition of norepinephrine, the beating amplitude was slightly changed, and the beating rate became faster. On the other hand, the beating amplitude of the cell sheet treated with digoxin increased notably, although the beating rate was not altered. Both the beating rate and the beating amplitude of the cell sheet treated with verapamil changed appreciably. The time course of change in beating rate and beating amplitude in the presence of the above agents and propranolol and forskolin are shown in Figs. 3A and B. The beating amplitude of a control assay in a medium containing 1% DMSO tended to fall slightly for the first 15—20 min after the cell sheet was perfused with the medium, while the beating rate was unchanged within 30 min. Verapamil at a concentration of 10^{-7} M significantly suppressed both the beating rate and the beating amplitude up to approximately 40% of the initial values, soon after administration; the suppression continued for 30 min or longer (Fig. 3A). A similar finding was obtained in the case of 10^{-5} M propranolol. That is, the beating rate and the beating amplitude were suppressed to 80—85% and 65—80%, respectively, for 30 min (Fig. 3A). By contrast, 10^{-5} M

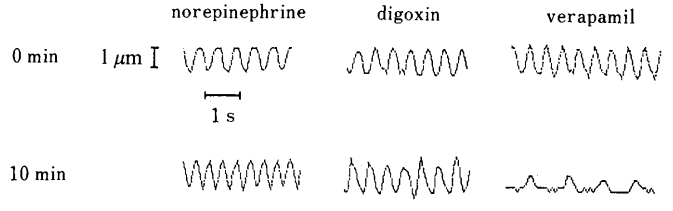

Fig. 2. Microcomputer Recordings of Periodic Movement of Points on Myocardial Cell Sheets before and 10 min after Administration of 10^{-5} M Norepinephrine, 10^{-5} M Digoxin or 10^{-7} M Verapamil

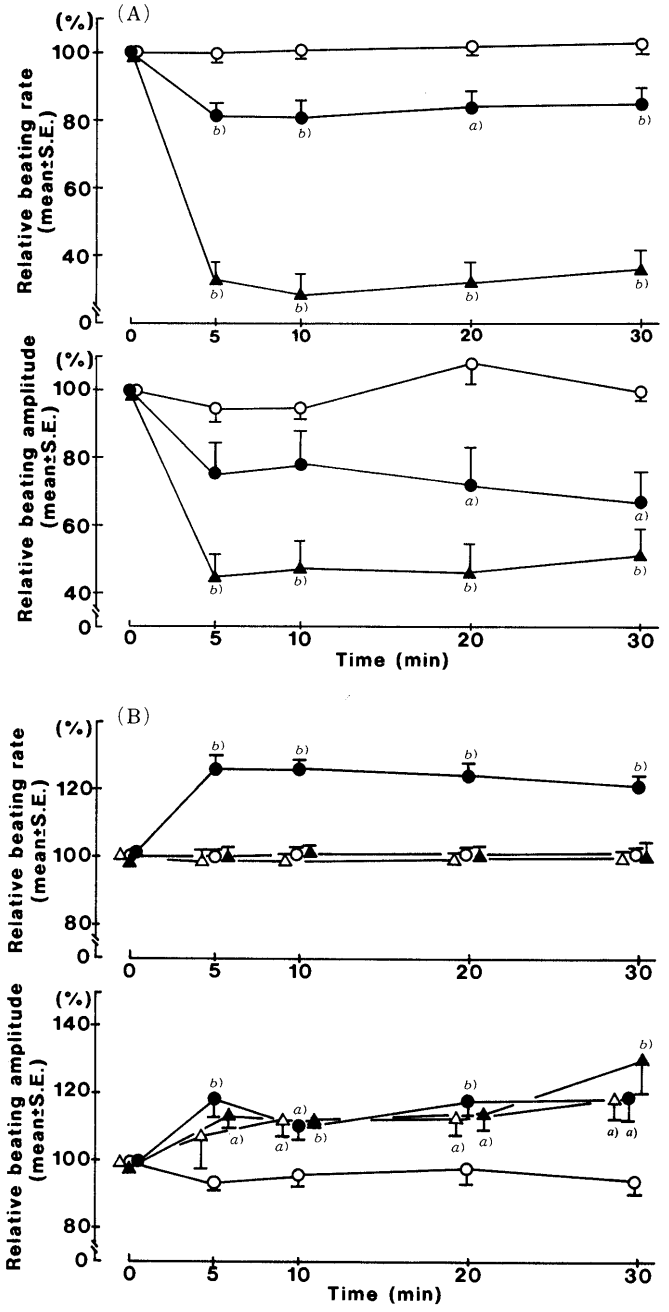

Fig. 3 (A). Time Courses of the Relative Beating Rate and the Relative Beating Amplitude of Myocardial Cell Sheets Treated with 1% DMSO (○), 10^{-5} M Propranolol (●) or 10^{-7} M Verapamil (▲)

Values stand for means ± S.E. of 3—4 independent assays. Statistical significance compared with the control values, *a*) $p<0.05$, *b*) $p<0.01$.

(B). Time Courses of the Relative Beating Rate and the Relative Beating Amplitude of Myocardial Cell Sheets Treated with 1% DMSO (○), 10^{-5} M Norepinephrine (●), 10^{-5} M Digoxin (△) or 10^{-9} M Forskolin (▲)

Values stand for means ± S.E. of 3—4 independent assays. Statistical significance compared with a control value with 1% DMSO, *a*) $p<0.05$, *b*) $p<0.01$.

norepinephrine accelerated the beating rate by 20—25%, and increased the beating amplitude significantly (Fig. 3B). Digoxin and forskolin at 10^{-5} and 10^{-9} M, respectively, did not affect the beating rates but increased the beating amplitude significantly (Fig. 3B). The latter compound gradually increased the beating amplitude, which eventually reached a level 30% higher than the initial value 30 min after administration.

Next, we tested a water extract of the pilose antler and its 70% ethanol-soluble and -insoluble fractions for effects on the beating of the myocardial cell sheet. The water extract and the two fractions induced no significant effect on the beating rate at concentrations of 0.01—0.1 mg/ml 10 min after administration, whereas the water extract and the 70% ethanol-soluble fraction were stimulated the beating amplitude at 0.1 mg/ml, but the effect was not significant (data not shown).

The contraction of myocardial cells is directly regulated by cytoplasmic Ca^{2+} concentrations, since coupling of troponin and Ca^{2+} triggered the sliding movement of actin and myosin. Further, in the automatically beating cells, the intracellular Ca^{2+} content greatly depended on Ca^{2+} concentrations of the outer fluid.[6] Figure 4 shows the effect of decreasing concentrations of Ca^{2+} in the medium on the beating rate and the beating amplitude at 10 min after replacement of the standard medium with media containing various concentrations of Ca^{2+}. Both the beating rate and the beating amplitude were reduced as the Ca^{2+} concentration decreased. At a concentration of 0.5 mM Ca^{2+}, these two indices fell to approximately 70—75% of those in the standard Ca^{2+} concentration of 2.1 mM. We examined the effects of the water extract of the pilose antler and its fractions on beating suppressed with 0.5 mM Ca^{2+}. Figure 5 shows the beating rate and the beating amplitude at 10 min after replacement of the standard medium to the low Ca^{2+} medium containing 0.1 mg/ml of the water extract, its fractions, 10^{-5} M digoxin or 10^{-9} M forskolin. Both digoxin and forskolin, as positive controls, enhanced the beating rate by approximately 10%, and increased the beating amplitude by approximately 15%. The extract and its fractions increased the beating amplitude by 10—15%, and the increasing values of the two fractions were slightly larger than that of the water extract. On the other hand, the beating rates tended to decrease in the presence of the water extract and its fractions.

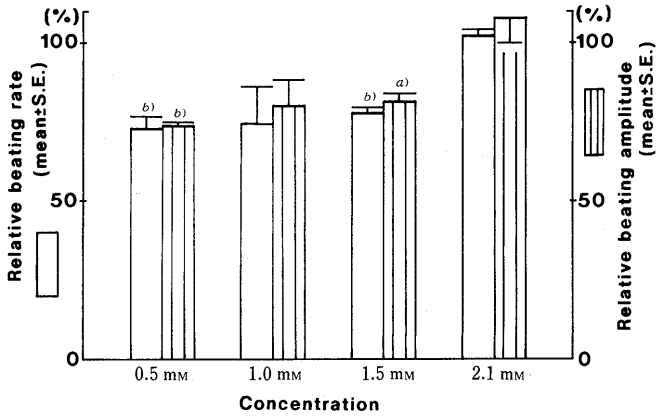

Fig. 4. Effect of Calcium Ion Concentrations in Media on the Relative Beating Rate and the Relative Beating Amplitude

Values stand for means ± S.E. of 3—4 independent assays 10 min after perturbation. Statistical significance compared with the value in the medium containing a standard calcium ion concentration, 2.1 mM, *a*) $p<0.05$, *b*) $p<0.01$.

Discussion

The method used in this paper is based on a micro-computer-driven image analyzing system which can analyze videotaped recordings of the movement of an object displayed on a TV monitor. One can measure intact cell movement under a microscope and no technical skill is necessary. Further, unlike the optical and electro-physiological measurements, no special laboratory room is needed to protect against optical or electronic noise from the

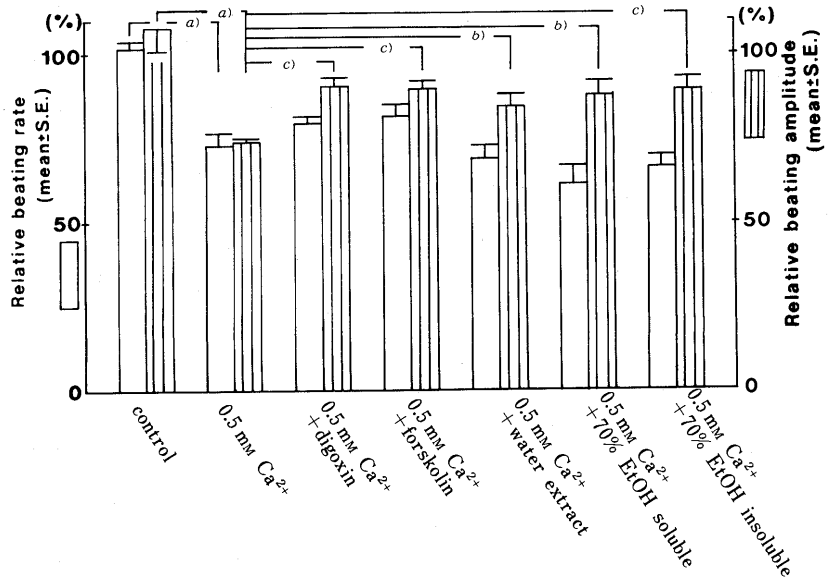

Fig. 5. Effects of Water Extract of the Pilose Antler and Its Fractions on the Relative Beating Rate and the Relative Beating Amplitude in the Medium Containing 0.5 mM Ca^{2+}

The concentration of water extract and its fractions was 0.1 mg/ml. The contractions of digoxin and forskolin were 10^{-5} and 10^{-9} M, respectively. Values stand for means ± S.E. of 3—4 independent assays 10 min after perturbation. Statistical significance compared with the control values, *a*) $p<0.01$, or the values at 0.5 mM Ca^{2+}, *b*) $p<0.05$, *c*) $p<0.01$.

environment.

By examining the beating rate and the beating amplitude of cultured myocardial cells, we could characterize a variety of cardioactive agents. Norepinephrine, one of the neurotransmitters which have been reported to increase the beating rate of myocardial cells,[7] was chronotropic and inotropic to the myocardial cell sheet. Further, beating embryonic myocardial cells have a character similar to pacemaker cells at the sinoatrial node,[8] which agreed with the effect of the neurotransmitter on pacemaker cells. Digoxin, one of the cardiac glycosides used for congestive heart failure, and forskolin, a diterpene which was reported as more inotropic than chronotropic to the isolated guinea pig heart,[9] were both positively inotropic to the myocardial cell sheet without a remarkable effect on the beating rate. Verapamil and propranolol suppressed both the beating rate and the beating amplitude to a similar extent. In the low Ca^{2+} medium, digoxin and forskolin increased both the beating rate and the beating amplitude.

The water extract of the pilose antler at concentrations of 0.01—0.1 mg/ml showed no significant effect on the beating rate and the beating amplitude in the standard medium. In the low Ca^{2+} medium, however, the extract and its fractions increased the beating amplitude significantly. However, they tended to decrease the beating rate. Thus, the extract and its fractions were inotropic rather than chronotropic when the spontaneous beating of the myocardial cell sheet was suppressed under low Ca^{2+} ion conditions.

References

1) O. F. Schanne and G. Bkaily, *Can J. Pharmacol.*, **59**, 443 (1981).
2) O. A. Bucher, *Exp. Cell Res.*, **13**, 109 (1957).
3) N. Sperelakis and D. Lehmkuhl, *Am. J. Physiol.*, **209**, 693 (1965).
4) S.-L. Huang, X.-W. Yang, N. Kakiuchi, M. Hattori, T. Namba and K. Takahashi, *Phytother. Res.*, **4**, 152 (1990).
5) T. Namba, O. Morita, S.-L. Huang, K. Goshima, M. Hattori and N. Kakiuchi, *Planta Med.*, **54**, 277 (1988).
6) S. Ringer, *J. Physiol.*, **4**, 29 (1883).
7) K. Goshima, *Exp. Cell Res.*, **84**, 223 (1974).
8) H. Irisawa, *Physiol. Rev.*, **58**, 461 (1978).
9) E. Linder, A. N. Dohadwalla and B. K. Bhattacharya, *Arzneim.-Forsch.*, **28**, 284 (1978).

Novel Acylated Saponins from *Tragopogon porrifolius* L. Isolation and the Structures of Tragopogonsaponins A—R

Tsutomu WARASHINA, Toshio MIYASE* and Akira UENO

School of Pharmaceutical Sciences, University of Shizuoka, 395, Yada, Shizuoka 422, Japan. *Received July 9, 1990*

Eighteen novel triterpenoid saponins, named tragopogonsaponins A—R, were isolated from the roots of *Tragopogon porrifolius* L. (Compositae). The structures of these saponins were determined on the basis of spectral and chemical evidence. Seventeen of the saponins contained phenyl propionic acid derivative as ester moiety. Their structures were elucidated as oleanane-type triterpene saponins which have echinocystic acid as the aglycone moiety.

Keywords *Tragopogon porrifolius*; Compositae; oleanane-type triterpene saponin; tragopogonsaponin; echinocystic acid; phenylpropanoid

Tragopogon porrifolius L. (Compositae) is indigenous to Europe and northern Asia and is widely cultivated as a vegetable. Since no phytochemical investigation has been reported on this plant, we have investigated its constituents in the course of our search for terpenic glycosides of Compositae plants. This paper describes the isolation and structural determination of tragopogonsaponins A—R.

The methanol extract of the roots was partitioned between ether and water and the water layer was passed through a Mitsubishi Diaion HP-20 column and the absorbed material was eluted with methanol. The methanol eluate was chromatographed on a silica gel column to give saponin fractions. These fractions were passed through an Amberlite IR-120 column and concentrated to give a residue which was then treated with diazomethane. From these fractions, eighteen new oleanane-type saponins have been isolated as their methyl ester. The methanol eluate of HP-20 gave echinocystic acid as an aglycone (**1**), and methyl ferulate, methyl *p*-coumarate, methyl *p*-hydroxyphenyl propionate and methyl 4-hydroxy-3-methoxyphenyl propionate as an ester by treatment with AcCl–MeOH (1 : 20).

The proton nuclear magnetic resonance (^{1}H-NMR) spectrum of **1** indicated the presence of oleanane-type triterpene, which was shown by seven methyl singlets [δ 0.95, 1.04, 1.07, 1.08, 1.20, 1.24, 1.86], an olefinic proton signal [δ 5.68 (1H, t, J=2.5 Hz)] and two carbinyl proton signals [δ 3.48 (1H, dd, J=11, 5 Hz); 5.27 (1H, br s)]. By comparison of these data with reported ones, **1** was determined to be echinocystic acid.[1)]

Tragopogonsaponin A methyl ester (**2a**) showed singlet signals of seven tertiary methyl groups at δ 0.85, 0.98, 1.03, 1.07, 1.19, 1.30, 1.87 and one anomeric proton signal at δ 5.01 (1H, d, J=8.5 Hz) in the ^{1}H-NMR spectrum. In the carbon-13 nuclear magnetic resonance (^{13}C-NMR) spectrum, one anomeric carbon signal was observed at δ 107.3 and the signal due to C-3 of the aglycone at δ 89.2 shifted down-field (Δ+11.1 ppm) by comparison with that of echinocystic acid (**1**). This was a glycosylation shift, indicating a sugar was attached at the C-3 position. This glycosylation shift was supported by the ^{13}C-NMR spectra of entada saponins.[2)] The positive ion fast atom bombardment mass (FAB-MS) spectrum of **2a** revealed the $[M+Na]^+$ ion peak at m/z 685, which was larger by 190 mass units than that of echinocystic acid (**1**), and acid hydrolysis followed by $NaBH_4$ reduction gave glucose as a sugar moiety (see Experimental). This difference was derived from the sugar moiety of **2a**, which was deduced to be a glucuronic acid methyl ester because of treatment with diazomethane. In the ^{1}H-NMR spectrum, the characteristic signal due to H-5 of glucuronic acid was exhibited at δ 4.61 (1H, d, J=9 Hz) and a signal due to a carbomethoxyl group was at δ 3.74 (3H, s). From these data, the structure of tragopogonsaponin A was determined to be **2**.

Acid hydrolysis of **3a** followed by $NaBH_4$ gave glucose and xylose as the sugar moiety. **3a** showed two anomeric proton signals at δ 4.96 (1H, d, J=8.5 Hz) and 6.17 (1H, d, J=8 Hz) in the ^{1}H-NMR spectrum. By comparison with that of **2a**, one signal at δ 4.96 was assigned to the anomeric proton of glucuronic acid methyl ester and another signal was assigned to that of xylopyranose. Moreover, **3a** gave a similar ^{13}C-NMR spectrum as that of **2a** in the glucuronic acid methyl ester and the aglycone moiety except for the signal due to C-28. The signal of C-28 in the aglycone moiety shifted up-field (Δ −4.1 ppm) in comparison with that of **2a**. Therefore, C-28 was esterized. In addition, the ^{1}H-NMR spectrum of **3a** exhibited AA′XX′-type signals at δ 6.61 (1H, d, J=16 Hz) and 7.92 (1H, d, J=16 Hz). The ^{13}C-NMR spectrum of **3a** showed twelve more signals than that of **2a**. They consisted of a carboxyl group signal (δ 166.9), two olefinic carbon ones (δ 114.9 and 146.4), four aromatic carbon ones (δ 116.9, 126.1, 131.2, 161.9) and five sugar carbon ones (δ 68.0, 71.0, 73.6, 76.1, 93.6). Thus, from these results, seven signals except for the sugar ones were deduced to be the signals of *p*-coumaric acid ester. In the ^{13}C-NMR spectrum, the anomeric carbon signal of xylopyranose appeared at δ 93.6, and in the ^{1}H-NMR spectrum, its anomeric proton signal appeared at δ 6.17 (1H, d, J=8 Hz). Therefore, xylopyranose was attached to C-28 as an ester-type glycoside. In the decoupling experiments, an irradiation on the anomeric proton signal of xylopyranose was effective in the signal due to H-2 of xylopyranose (δ 5.81). By comparison with 3-*O*-acetyl-28-*O*-β-D-xylopyranosyl oleanolic acid,[3)] an acylation shift was observed at the signals due to C-1 (Δ −2.6 ppm) and C-3 (Δ −2.1 ppm) of the xylopyranose moiety in **3a**. Thus, *p*-coumaric acid was attached to C-2 of xylopyranose, and the structure of tragopogonsaponin B was determined to be **3**.

Tragopogonsaponin C methyl ester (**4a**) showed a similar ^{13}C-NMR spectrum as that of **3a** except for the ester moiety. In the ester moiety, two signals for the carbons of the double bond were exhibited at δ 115.0 and 146.7, but being different from **3a**, **4a** showed six signals of the aromatic carbons and one methoxyl carbon (δ 111.9, 116.8, 124.7, 126.5, 149.3, 115.0, 56.3). The ^{1}H-NMR spectrum of **4a** also showed two

trans-olefinic proton signals at δ 6.66 (1H, d, $J=16$ Hz) and 7.94 (1H, d, $J=16$ Hz), ABC-type signals in the aromatic proton region [δ 7.17 (1H, dd, $J=8$, 1.5 Hz), 7.23 (1H, d, $J=8$ Hz), 7.26 (1H, d, $J=1.5$ Hz)] and one more methoxyl signal at δ 3.87 (3H, s) other than that of glucuronic acid methyl ester. In the difference nuclear Overhauser effect (NOE) spectrum of **4a**, the signal due to the methoxyl group showed a NOE to the signal due to H-2 of the aromatic protons (δ 7.26) in the ester moiety. Thus, the ester moiety of **4a** was determined to be ferulic acid and these results led us to conclude the structure of tragopogonsaponin C to be **4**.

The ^{1}H- and ^{13}C-NMR spectra of **5a** were similar to those of **4a**, but one more anomeric carbon and proton signals were seen at δ 102.3 and 5.63 (1H, d, $J=8.5$ Hz). In the ^{1}H-NMR spectrum, **5a** showed ABC-type signals in the aromatic proton region, two signals of the double bond and a signal due to the methoxyl group the same as **4a** did.

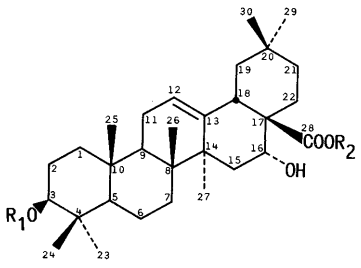

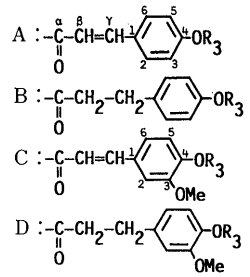

	R_1	R_2	R_3
1	-H	-H	
2	-glc·UA	-H	
2a	COOMe -glc·UA	-H	
3	-glc·UA	-xyl^{2}-A	-H
3a	COOMe -glc·UA	-xyl^{2}-A	-H
4	-glc·UA	-xyl^{2}-C	-H
4a	COOMe -glc·UA	-xyl^{2}-C	-H
5	-glc·UA	-xyl^{2}-C	-glc'
5a	COOMe -glc·UA	-xyl^{2}-C	-glc'
6	-glc·UA	-ara^{2}-C	-glc'
6a	COOMe -glc·UA	-ara^{2}-C	-glc'
7	-glc·UA	-xyl^{2}(-glc^{3})-A	-H
7a	COOMe -glc·UA	-xyl^{2}(-glc^{3})-A	-H
8	-glc·UA	-xyl^{2}(-glc^{3})-B	-H
8a	COOMe -glc·UA	-xyl^{2}(-glc^{3})-B	-H
9	-glc·UA	-ara^{2}(-glc^{3})-A	-H
9a	COOMe -glc·UA	-ara^{2}(-glc^{3})-A	-H
10	-glc·UA	-ara^{2}(-glc^{3})-B	-H
10a	COOMe -glc·UA	-ara^{2}(-glc^{3})-B	-H
11	-glc·UA	-ara^{2}(-glc^{3})-D	-H
11a	COOMe -glc·UA	-ara^{2}(-glc^{3})-D	-H
12	-H	-ara^{2}(-glc^{3})-A	-H
13	-H	-ara^{2}(-glc^{3})-B	-H
14	-H	-ara^{2}(-glc^{3})-D	-H
15	-glc·UA	-xyl^{2}(-glc^{3})-A	-glc'
15a	COOMe -glc·UA	-xyl^{2}(-glc^{3})-A	-glc'
16	-glc·UA	-xyl^{2}(-glc^{3})-B	-glc'
16a	COOMe -glc·UA	-xyl^{2}(-glc^{3})-B	-glc'
17	-glc·UA	-ara^{2}(-glc^{3})-B	-glc'
17a	COOMe -glc·UA	-ara^{2}(-glc^{3})-B	-glc'
18	-H	-ara^{2}(-glc^{3})-A	-glc'
19	-glc·UA	-ara^{2}(-glc^{3})-D	-glc'
19a	COOMe -glc·UA	-ara^{2}(-glc^{3})-D	-glc'

Chart 1

Accordingly, the ester moiety of **5a** was considered to be ferulic acid. In the difference NOE spectrum of **5a**, the proton signal due to a methoxyl group (δ 3.80) showed a NOE to the signal due to H-2 (δ 7.26) of the aromatic protons in the ester chain. That also supported that the ester moiety was ferulic acid. Secondly, irradiation on one more anomeric proton signal at δ 5.63 revealed a NOE to the signal due to H-5 (δ 7.60) in the ester moiety. This result suggested that thus another sugar was attached to the C_4-OH position in the aromatic carbons (δ 149.4) of the ester moiety. This sugar was determined by acid hydrolysis to be glucose. Based on the above evidence, the structure of tragopogonsaponin D was elucidated to be **5**.

Tragopogonsaponin E methyl ester (**6a**) consisted of a glucuronic acid methyl ester, glucose and arabinose as the sugar moiety from the result of acid hydrolysis, and showed ^{1}H- and ^{13}C-NMR spectra similar to those of **5a** except for the sugar which was attached to C-28. In the ^{13}C-NMR spectrum, **6a** showed an acylation shift at C-1 ($\Delta -2.5$ ppm) and C-3 ($\Delta -1.8$ ppm) compared with 3-*O*-acetyl-28-*O*-β-D-arabinopyranosyl oleanolic acid.[3] Moreover, the H-2 signal of arabinopyranose existed down-field at δ 6.10 (1H, d, $J=8$ Hz). These results suggested that ferulic acid was attached to C-2 of arabinopyranose, and then the structure of tragopogonsaponin E was determined to be **6**.

Tragopogonsaponin F methyl ester (**7a**) showed ^{1}H- and ^{13}C-NMR spectra similar to those of **3a**. In other words, the signals of xylopyranose and *p*-coumaric acid were shown, and in the decoupling experiments of xylopyranose

TABLE I. ^{13}C-NMR Spectral Data of Aglycone Moiety

Carbon No.	1	2a	3a	12
Aglycone moiety				
1	39.0	38.7	38.9	39.0
2	28.0	26.7	26.9	28.2
3	78.1	89.2	89.5	78.1
4	39.4	39.6	39.8	39.4
5	55.9	55.9	56.1	55.9
6	18.8	18.5	18.5	18.6
7	32.8	33.5	33.2	33.2
8	39.9	39.9	40.2	40.0
9	47.3	47.2	47.3	47.2
10	37.4	37.0	37.2	37.5
11	23.9	23.8	24.0	23.8
12	122.5	122.4	123.1	123.1
13	145.1	145.2	144.5	144.4
14	42.1	42.1	42.3	42.1
15	36.2	36.2	36.4	36.4
16	74.6	74.8	74.0	73.9
17	48.9	48.9	49.3	49.1
18	41.5	41.5	41.2	41.0
19	47.3	47.3	47.3	47.2
20	31.0	31.1	31.1	30.8
21	36.0	36.2	36.2	35.9
22	33.6	32.9	32.6	32.3
23	28.8	28.2	28.4	28.8
24	16.6	17.0	17.2	16.6
25	15.7	15.6	15.9	15.7
26	17.5	17.5	17.3	17.1
27	27.2	27.3	27.3	27.0
28	179.9	180.0	175.9	175.6
29	33.3	33.4	33.4	33.2
30	24.7	24.8	24.7	24.4

Run at 67.5 MHz in pyridine-d_5 solution. The spectral data of **4a**—**11a**, **15a**—**17a** and **19a** were almost the same as those of **3a**, and those of **13**, **14** and **18** were almost the same as those of **12**.

TABLE II. ^{13}C-NMR Spectral Data of Sugar and Ester Moieties

		2a	3a	4a	5a	6a	7a	8a	9a	10a	11a	12	13	14	15a	16a	17a	18	19a
Sugar moiety																			
glc·UA	1	107.3	107.3	107.3	107.3	107.2	107.3	107.3	107.3	107.3	107.3				107.2	107.3	107.3		107.2
	2	75.4	75.4	75.4	75.4	75.4	75.4	75.4	75.4	75.4	75.4				75.4	75.5	75.5		75.4
	3	77.9	77.9	77.9	77.9	77.9	77.9	77.9	77.9	77.9	77.9				77.9	77.9	77.9		77.9
	4	73.2	73.3	73.3	73.2	73.2	73.2	73.2	73.3	73.2	73.2				73.2	73.2	73.2		73.2
	5	77.2	77.3	77.3	77.2	77.2	77.1	77.2	77.2	77.2	77.2				77.2	77.2	77.2		77.2
	6	170.9	171.2	171.1	170.9	170.9	170.9	170.9	170.9	170.9	170.9				170.9	170.9	170.6		170.8
COOMe		52.0	52.4	52.4	52.0	52.0	52.0	52.1	52.2	52.1	52.1				52.0	52.0	52.1		52.0
xyl	1		93.6	94.0	93.8		93.5								93.5	93.4			
	2		73.6	73.6	73.6		71.1								71.3	71.5			
	3		76.1	76.1	76.1		85.5								85.8	86.0			
	4		71.0	71.0	70.9		69.4								69.4	69.3			
	5		68.0	68.0	67.9		67.1								67.1	67.2			
ara	1					93.4		93.3	93.7	93.4	93.4	93.6	93.5	93.5			93.4	93.6	93.4
	2					71.3		71.4	70.3	70.6	70.6	70.2	70.6	70.6			70.8	70.4	70.9
	3					72.3		86.1	80.7	80.6	80.6	80.6	80.7	80.7			80.3	80.6	80.1
	4					68.8		69.3	69.1	69.1	69.1	69.1	69.1	69.1			69.0	69.1	68.8
	5					67.1		67.1	68.1	68.1	68.1	68.0	68.1	68.1			67.9	68.0	67.8
glc	1						105.3	105.7	106.2	106.6	106.6	106.3	106.6	106.6	105.5	105.7	106.5	106.4	106.3
	2						74.7	74.6	74.6	74.5	74.5	74.6	74.5	74.5	74.8[a]	74.6[f]	75.0[j]	74.8[o]	74.9[t]
	3						78.7	78.6	78.6	78.5	78.5	78.6	78.6	78.6	78.7[b]	78.8	78.8[k]	79.2[p]	78.7[u]
	4						71.7	71.7	71.5	71.6	71.6	71.5	71.6	71.6	71.7[c]	71.7[g]	71.5[l]	71.5[q]	71.6[v]
	5						78.5	78.6	78.3	78.5	78.5	78.3	78.1	78.1	78.5[d]	78.5[h]	78.5[m]	78.5[r]	78.5[x]
	6						62.7	62.7	62.8	62.8	62.8	62.8	62.8	62.8	62.7[e]	62.7[i]	62.8[n]	62.8[s]	62.8[w]
glc′	1				102.3	102.2									102.3	102.4	102.3	102.2	102.6
	2				74.7	74.8									74.6[a]	75.0[f]	74.4[j]	74.6[o]	74.3[t]
	3				79.0	79.0									78.5[b]	78.8	78.5[k]	78.6[p]	78.5[u]
	4				71.3	71.7									71.3[c]	71.3[g]	71.3[l]	71.2[q]	71.3[v]
	5				78.5	78.5									78.4[d]	78.4[h]	78.4[m]	78.3[r]	78.4[x]
	6				62.5	62.4									62.4[e]	62.4[i]	62.4[n]	62.4[s]	62.5[w]
Ester moiety																			
	α		166.9	166.9	166.4	166.4	166.6	172.2	166.7	172.2	172.3	166.6	172.3	172.3	166.4	172.1	172.1	166.4	172.2
	β		114.9	115.0	116.1	116.1	115.1	36.7	115.3	36.8	36.8	114.7	36.8	36.8	116.8	36.4	36.5	117.0	36.5
	γ		146.4	146.7	145.8	145.7	145.9	30.3	145.7	30.4	30.4	145.6	30.4	30.4	145.1	30.3	30.4	144.8	30.8
	1		126.1	126.5	128.7	128.7	126.0	131.3	126.2	131.4	132.2	126.1	131.4	132.1	128.6	134.4	134.5	128.6	135.8
	2		131.2	111.9	111.8	111.8	131.0	129.9	131.0	129.9	113.0	130.9	129.9	112.9	130.5	129.9	129.7	130.4	113.8
	3		116.9	151.6	150.6	150.5	116.7	116.3	116.8	116.3	148.7	116.6	116.3	148.7	117.1	117.0	117.0	117.0	150.3
	4		161.9	149.3	149.4	149.1	161.7	157.4	161.7	157.4	146.7	161.6	157.4	146.8	160.6	157.2	157.2	160.4	146.7
	5		116.9	116.8	116.3	116.4	116.7	116.3	116.8	116.3	116.5	116.6	116.3	116.6	117.1	117.0	117.0	117.0	116.8
	6		131.2	124.7	124.2	124.0	131.0	129.9	131.0	129.9	121.4	130.9	129.9	121.4	130.5	129.9	129.7	130.4	121.1
OMe				56.3	56.1	56.1					56.0			56.0					56.3

Run at 67.5 MHz in pyridine-d_5 solution. *a*—*x*): Assignment may be interchanged in each column.

moiety, a H-2 signal existed at δ 5.82 (1H, t, J=8.5 Hz). Thus, *p*-coumaric acid was attached to C-2 of xylopyranose. This compound had one more sugar. In the ^{13}C-NMR spectrum, this anomeric carbon signal shifted down-field from that of **5a**, and in the ^{1}H-NMR spectrum, this proton signal shifted up-field from that of **5a**. Thus, it was deduced that this glucose was not attached to C_4-OH of the aromatic carbons in the ester chain as **5a**. In the ^{13}C-NMR spectrum, glycosylation shifts were observed at the xylopyranose moiety. That is to say, the signal of C-3 was shifted down-field (Δ+9.4 ppm), and the signals of C-2 and C-4 were shifted up-field (Δ−2.5 ppm and Δ−1.6 ppm) by comparison with those of **3a**. Therefore, in the difference NOE spectrum of **7a**, irradiation on the signal due to this anomeric proton (δ 5.07) of glucose brought a NOE to the signal due to H-3 of xylopyranose. Based on the above evidence, this glucose combined with C-3 of xylopyranose and the structure of tragopogonsaponin F was elucidated as **7**.

The ^{1}H- and ^{13}C-NMR spectra of tragopogonsaponin G methyl ester (**8a**) were much the same as those of **7a** except for the ester chain. In the ^{1}H-NMR spectrum, AA′BB′-type signals were observed at δ 7.08 (2H, d, J=8.5 Hz) and 7.18 (overlapped with C_5D_5N), but the signals of the olefinic protons disappeared and instead four multiplet signals which were not seen in the spectrum of **7a** appeared from δ 2.90 to 3.40. Similarly, in the ^{13}C-NMR spectrum, two signals were visible at δ 30.3 and 36.7 instead of the signals due to the olefinic carbons. In the FAB-MS spectrum, **8a** revealed the $[M+Na]^+$ ion peak at m/z 1127, which was larger by 2 mass units than that of **7a**. From these results, **8a** was considered to have a *p*-hydroxyphenyl propionic acid ester, and then the structure of tragopogonsaponin G was decided to be **8**.

Tragopogonsaponin H methyl ester (**9a**) showed similar NMR spectra to **7a**, three anomeric proton and carbon signals and the signals due to *p*-coumaric acid ester. But the signals of arabinopyranose were seen exchanging with those of xylopyranose. Especialy the characteristic signal due to H-4 of arabinopyranose was exhibited at δ 4.53 (1H, br s) in the ^{1}H-NMR spectrum. In the ^{13}C-NMR one, **9a** exhibited glycosylation shifts at C-2 (Δ−1.0 ppm),

C-3 (Δ +8.3 ppm) and C-4 (Δ +0.3 ppm) by comparison with **6a**. Accordingly, glucose was attached to C-3 of arabinopyranose and supported the above, that a NOE was observed at the signal due to H-3 of arabinopyranose by irradiation on the signal due to the anomeric proton of glucose (δ 5.14), and as a H-2 signal of arabinopyranose was observed at δ 6.28 (1H, d, J=9, 8.5 Hz), *p*-coumaric acid was attached to C-2 of arabinopyranose. These results led us to conclude that the structure of tragopogonsaponin H is **9**.

Tragopogonsaponin I methyl ester (**10a**) and J methyl ester (**11a**) could not be separated in any column we tried. The ^{1}H- and ^{13}C-NMR spectra were similar to those of **9a**. The NMR and FAB-MS spectra suggested that the ester moiety of **10a** and **11a** was *p*-hydroxyphenyl propionic acid and 4-hydroxy-3-methoxyphenyl propionic acid, respectively.

Tragopogonsaponin K (**12**) showed, in part, similar spectra to ^{1}H- and ^{13}C-NMR to those of **9a**. But the signals of glucuronic acid methyl ester were not visible and only two signals of the anomeric carbon and proton (δ 93.6 and 106.3; δ 6.13 and 5.17) due to arabinopyranose and glucose were observed compared to those of **9a**. The carbon signals due to C-2 and C-3 of the aglycone were much the same as those of echinocystic acid. In the arabinopyranose moiety, the ^{13}C-NMR spectrum of **12** showed a glycosylation shift

TABLE III. ^{1}H-NMR Spectral Data of Aglycone and Ester Moieties

Proton No.	1	2a	3a	4a	5a
Aglycone moiety					
3	3.48 (1H, dd, J=11, 5 Hz)	3.40 (1H, dd, J=12, 4 Hz)	3.34 (1H, dd, J=12, 4 Hz)	3.33 (1H, dd, J=12, 4 Hz)	3.33 (1H, dd, J=12, 4 Hz)
12	5.68 (1H, t, J=2.5 Hz)	5.64 (1H, t, J=3 Hz)	5.56 (1H, t, J=3 Hz)	5.56 (1H, t, J=3 Hz)	5.59 (1H, t, J=3 Hz)
16	5.27 (1H, br s)	5.26 (1H, br s)	5.25 (1H, br s)	5.24 (1H, br s)	5.20 (1H, br s)
18	3.65 (1H, dd, J=14, 3 Hz)	3.62 (1H, dd, J=14, 4 Hz)	3.45 (1H, dd, J=14, 4 Hz)	3.44 (1H, dd, J=14, 4 Hz)	3.45 (1H, dd, J=14, 4 Hz)
19α	2.86 (1H, t, J=14 Hz)	2.84 (1H, t, J=14 Hz)	2.75 (1H, t, J=14 Hz)	2.75 (1H, t, J=14 Hz)	2.76 (1H, t, J=14 Hz)
23	1.24 (3H, s)	1.30 (3H, s)	1.27 (3H, s)	1.26 (3H, s)	1.27 (3H, s)
24	1.04 (3H, s)	0.98 (3H, s)	0.95 (3H, s)	0.97 (3H, s)	0.93 (3H, s)
25	0.95 (3H, s)	0.85 (3H, s)	0.87 (3H, s)	0.88 (3H, s)	0.88 (3H, s)
26	1.08 (3H, s)	1.07 (3H, s)	1.02 (3H, s)	1.02 (3H, s)	1.02 (3H, s)
27	1.86 (3H, s)	1.87 (3H, s)	1.73 (3H, s)	1.74 (3H, s)	1.76 (3H, s)
29	1.07 (3H, s)	1.03 (3H, s)	0.99 (3H, s)	0.99 (3H, s)	1.01 (3H, s)
30	1.20 (3H, s)	1.19 (3H, s)	1.04 (3H, s)	1.05 (3H, s)	1.08 (3H, s)
Ester moiety					
β					
β'			6.61 (1H, d, J=16 Hz)	6.66 (1H, d, J=16 Hz)	6.68 (1H, d, J=16 Hz)
γ					
γ'			7.92 (1H, d, J=16 Hz)	7.94 (1H, d, J=16 Hz)	7.90 (1H, d, J=16 Hz)
2			7.55 (1H, d, J=8 Hz)	7.26 (1H, d, J=1.5 Hz)	7.26 (1H, d, J=1.5 Hz)
3			7.16 (1H, d, J=8 Hz)		
5			7.16 (1H, d, J=8 Hz)	7.23 (1H, d, J=8 Hz)	7.60 (1H, d, J=8 Hz)
6			7.55 (1H, d, J=8 Hz)	7.17 (1H, dd, J=8, 1.5 Hz)	7.15 (1H, dd, J=8, 1.5 Hz)
OMe				3.87 (3H, s)	3.80 (3H, s)

Proton No.	6a	7a	8a	9a	10a
Aglycone moiety					
3	3.34 (1H, dd, J=12, 4 Hz)	3.34 (1H, dd, J=12, 4 Hz)	3.39 (1H, dd, J=12, 4.5 Hz)	3.34 (1H, dd, J=12, 4 Hz)	3.39 (1H, dd, J=12, 4 Hz)
12	5.58 (1H, t, J=3 Hz)	5.58 (1H, t, J=3 Hz)	5.60 (1H, t, J=3 Hz)	5.57 (1H, t, J=3 Hz)	5.59 (1H, br s)
16	5.19 (1H, br s)	5.21 (1H, br s)	5.15 (1H, br s)	5.20 (1H, br s)	5.16 (1H, br s)
18	3.49 (1H, dd, J=14, 4.5 Hz)	3.44 (1H, dd, J=14, 4 Hz)	3.43 (1H, dd, J=14, 4 Hz)	3.44 (1H, dd, J=14, 4 Hz)	3.44 (1H, dd, J=14, 4 Hz)
19α	2.75 (1H, t, J=14 Hz)	2.75 (1H, t, J=14 Hz)	2.73 (1H, t, J=14 Hz)	2.74 (1H, t, J=14 Hz)	2.76 (1H, t, J=14 Hz)
23	1.27 (3H, s)	1.26 (3H, s)	1.28 (3H, s)	1.25 (3H, s)	1.28 (3H, s)
24	1.00 (3H, s)	1.00 (3H, s)	0.98 (3H, s)	0.99 (3H, s)	0.98 (3H, s)
25	0.88 (3H, s)	0.91 (3H, s)	0.92 (3H, s)	0.92 (3H, s)	0.92 (3H, s)
26	1.02 (3H, s)	1.00 (3H, s)	1.07 (3H, s)	1.02 (3H, s)	1.06 (3H, s)
27	1.75 (3H, s)	1.74 (3H, s)	1.83 (3H, s)	1.73 (3H, s)	1.82 (3H, s)
29	1.02 (3H, s)	1.01 (3H, s)	1.01 (3H, s)	1.01 (3H, s)	1.00 (3H, s)
30	1.03 (3H, s)	1.05 (3H, s)	1.07 (3H, s)	1.04 (3H, s)	1.09 (3H, s)
Ester moiety					
β			2.98 (1H, m)		2.93 (1H, m)
β'	6.64 (1H, d, J=16 Hz)	6.72 (1H, d, J=16 Hz)	3.30 (1H, m)	6.67 (1H, d, J=16 Hz)	3.26 (1H, m)
γ			3.14 (1H, m)		3.11 (1H, m)
γ'	7.85 (1H, d, J=16 Hz)	7.94 (1H, d, J=16 Hz)	3.21 (1H, m)	7.78 (1H, d, J=16 Hz)	3.20 (1H, m)
2	7.23 (1H, d, J=2 Hz)	7.49 (1H, d, J=8.5 Hz)	7.18[a]	7.45 (1H, d, J=8.5 Hz)	7.18 (1H, d, J=8.5 Hz)
3		7.11 (1H, d, J=8.5 Hz)	7.08 (1H, d, J=8.5 Hz)	7.09 (1H, d, J=8.5 Hz)	7.08 (1H, d, J=8.5 Hz)
5	7.59 (1H, d, J=8 Hz)	7.11 (1H, d, J=8.5 Hz)	7.08 (1H, d, J=8.5 Hz)	7.09 (1H, d, J=8.5 Hz)	7.08 (1H, d, J=8.5 Hz)
6	7.13 (1H, dd, J=8, 2 Hz)	7.49 (1H, d, J=8.5 Hz)	7.18[a]	7.45 (1H, d, J=8.5 Hz)	7.18 (1H, d, J=8.5 Hz)
OMe	3.79 (3H, s)				

TABLE III. (continued)

Proton No.	11a	12	13	14	15a
Aglycone moiety					
3	3.39 (1H, dd, J=12, 4 Hz)	3.41 (1H, br d, J=12 Hz)	3.46[a]	3.46[a]	3.33 (1H, dd, J=11, 4 Hz)
12	5.59 (1H, br s)	5.61 (1H, t, J=2.5 Hz)	5.63 (1H, br s)	5.63 (1H, br s)	5.59 (1H, t, J=2.5 Hz)
16	5.16 (1H, br s)	5.22 (1H, br s)	5.17 (1H, br s)	5.17 (1H, br s)	5.17 (1H, br s)
18	3.44 (1H, dd, J=14, 4 Hz)	3.47 (1H, dd, J=14, 4 Hz)	3.46[a]	3.46[a]	3.44 (1H, dd, J=14, 4 Hz)
19α	2.76 (1H, t, J=14 Hz)	2.76 (1H, t, J=14 Hz)	2.77 (1H, t, J=14 Hz)	2.77 (1H, t, J=14 Hz)	2.75 (1H, t, J=14 Hz)
23	1.29 (3H, s)	1.18 (3H, s)	1.21 (3H, s)	1.22 (3H, s)	1.26 (3H, s)
24	0.98 (3H, s)	1.01 (3H, s)	1.02 (3H, s)	1.02 (3H, s)	0.99 (3H, s)
25	0.92 (3H, s)	0.99 (3H, s)	1.00 (3H, s)	1.00 (3H, s)	0.91 (3H, s)
26	1.06 (3H, s)	1.05 (3H, s)	1.16 (3H, s)	1.16 (3H, s)	1.03 (3H, s)
27	1.82 (3H, s)	1.72 (3H, s)	1.81 (3H, s)	1.81 (3H, s)	1.74 (3H, s)
29	1.00 (3H, s)	1.05 (3H, s)	1.03 (3H, s)	1.04 (3H, s)	1.03 (3H, s)
30	1.09 (3H, s)	1.08 (3H, s)	1.14 (3H, s)	1.14 (3H, s)	1.06 (3H, s)
Ester moiety					
β	2.93 (1H, m)	6.70 (1H, d, J=16 Hz)	2.96 (1H, m)	2.96 (1H, m)	6.76 (1H, d, J=16 Hz)
β′	3.26 (1H, m)		3.25 (1H, m)	3.25 (1H, m)	
γ	3.11 (1H, m)	7.90 (1H, d, J=16 Hz)	3.12 (1H, m)	3.12 (1H, m)	7.86 (1H, d, J=16 Hz)
γ′	3.20 (1H, m)		3.20 (1H, m)	3.20 (1H, m)	
2	6.92 (1H, d, J=1.5 Hz)	7.48 (1H, d, J=8 Hz)	7.19 (1H, d, J=8 Hz)	6.93 (1H, br s)	7.45 (1H, d, J=8 Hz)
3		7.14 (1H, d, J=8 Hz)	7.10 (1H, d, J=8 Hz)		7.30 (1H, d, J=8 Hz)
5	7.11 (1H, d, J=8 Hz)	7.14 (1H, d, J=8 Hz)	7.10 (1H, d, J=8 Hz)	7.14 (1H, d, J=8 Hz)	7.30 (1H, d, J=8 Hz)
6	6.84 (1H, dd, J=8, 1.5 Hz)	7.48 (1H, d, J=8 Hz)	7.19 (1H, d, J=8 Hz)	6.85 (1H, br d, J=12 Hz)	7.45 (1H, d, J=8 Hz)
OMe	3.74 (3H, s)			3.75 (3H, s)	

Proton No.	16a	17a	18	19a
Aglycone moiety				
3	3.39 (1H, dd, J=12, 4 Hz)	3.38 (1H, dd, J=12, 4.5 Hz)	3.40 (1H, dd, J=11, 4.5 Hz)	3.38 (1H, dd, J=12, 4.5 Hz)
12	5.61 (1H, t, J=2.5 Hz)	5.59 (1H, t, J=2.5 Hz)	5.61 (1H, t, J=2 Hz)	5.60 (1H, t, J=2 Hz)
16	5.14 (1H, br s)	5.15 (1H, br s)	5.20 (1H, br s)	5.15 (1H, br s)
18	3.44 (1H, dd, J=14, 4 Hz)	3.44 (1H, dd, J=14, 4.5 Hz)	3.47 (1H, dd, J=14, 4 Hz)	3.45 (1H, dd, J=14, 4.5 Hz)
19α	2.77 (1H, t, J=14 Hz)	2.76 (1H, t, J=14 Hz)	2.76 (1H, t, J=14 Hz)	2.76 (1H, t, J=14 Hz)
23	1.30 (3H, s)	1.29 (3H, s)	1.24 (3H, s)	1.30 (3H, s)
24	0.99 (3H, s)	0.99 (3H, s)	1.02 (3H, s)	0.99 (3H, s)
25	0.92 (3H, s)	0.92 (3H, s)	0.99 (3H, s)	0.92 (3H, s)
26	1.09 (3H, s)	1.07 (3H, s)	1.11 (3H, s)	1.07 (3H, s)
27	1.83 (3H, s)	1.82 (3H, s)	1.72 (3H, s)	1.84 (3H, s)
29	1.02 (3H, s)	1.00 (3H, s)	1.06 (3H, s)	1.01 (3H, s)
30	1.09 (3H, s)	1.10 (3H, s)	1.12 (3H, s)	1.10 (3H, s)
Ester moiety				
β	2.97 (1H, m)	2.90 (1H, m)	6.72 (1H, d, J=16 Hz)	2.94 (1H, m)
β′	3.23 (1H, m)	3.10[a]		3.13[a]
γ	3.14[a]	3.10[a]	7.82 (1H, d, J=16 Hz)	3.13[a]
γ′	3.14[a]	3.10[a]		3.13[a]
2	7.18 (1H, d, J=8 Hz)	7.16 (1H, d, J=8.5 Hz)	4.44 (1H, d, J=8 Hz)	6.94 (1H, d, J=2 Hz)
3	7.26 (1H, d, J=8 Hz)	7.25 (1H, d, J=8.5 Hz)	7.32 (1H, d, J=8 Hz)	
5	7.26 (1H, d, J=8 Hz)	7.25 (1H, d, J=8.5 Hz)	7.32 (1H, d, J=8 Hz)	7.43 (1H, d, J=8 Hz)
6	7.18 (1H, d, J=8 Hz)	7.16 (1H, d, J=8.5 Hz)	7.44 (1H, d, J=8 Hz)	6.81 (1H, dd, J=8, 2 Hz)
OMe				3.75 (3H, s)

Run at 500.0 MHz in pyridine-d_5 solution. a) Obscured by other signals; therefore, could not be accurately determined. Assignments of 24, 26, 29 and 30 in all compounds may be interchanged in each column.

(C-2; Δ −1.1, C-3; Δ +8.3, C-4; Δ +0.3 ppm) by comparison with that of **6a** and in the ^{1}H-NMR spectrum, the H-2 signal of arabinopyranose appeared at δ 6.31. Thus, glucose was attached to C-3 of arabinopyranose and *p*-coumaric acid was at C-2. The structure of tragopogonsaponin K was determined to be **12**.

Tragopogonsaponins L (**13**) and M (**14**) were also inseparable. The ^{1}H-NMR spectrum was similar to that of **12** except for the ester chain and showed the presence of *p*-hydroxyphenyl propionic and 4-hydroxy-3-methoxyphenyl propionic acid ester, respectively.

Tragopogonsaponin N methyl ester (**15a**) showed four anomeric protons in the ^{1}H-NMR spectrum, that is to say, the signal at δ 4.93 (1H, d, J=8.5 Hz) was assigned to the anomeric proton of the glucuronic acid methyl ester, the one at δ 6.13 (1H, d, J=8.5 Hz) was the anomeric one of xylopyranose esterified to C-28 of the aglycone, the one at δ 5.05 (1H, d, J=8 Hz) was the anomeric one of glucose which was attached to C-3 of xylopyranose and that at δ 5.60 (1H, d, J=8.5 Hz) was the anomeric one of another glucose attached to C_4-OH of the aromatic carbons in the *p*-coumaric acid ester, because acid hydrolysis followed by $NaBH_4$ reduction gave glucose and xylose as the sugar moiety and the ^{1}H- and ^{13}C-NMR spectra of **15a** were

compared with those of **5a** and **7a**. The difference NOE spectrum also proved the attached position of sugar. Explained in detail, irradiation on a signal due to the anomeric proton of glucose (δ 5.05) showed an NOE to the signal due to H-3 of xylopyranose. An NOE was also exhibited between the signal due to the anomeric one of another glucose (δ 5.60) and the signal due to H-5 of the aromatic protons in *p*-coumaric acid ester (δ 7.30). Consequently, these results indicated the structure of tragopogonsaponin N to be **15**.

The ^{1}H-, ^{13}C-NMR and a difference NOE spectra of tragopogonsaponin O methyl ester (**16a**) were similar to those of **15a**. In the ester moiety, the spectra of **16a** showed two olefinic signals changed into two sp^3 carbon and proton signals much the same as those of **8a** and **10a** did. Thus, the ester moiety was determined to be *p*-hydroxyphenyl propionic acid, the FAB-MS spectrum supported that, and hence, the structure of tragopogonsaponin O was determined to be **16**.

Tragopogonsaponin P methyl ester (**17a**) showed four signals due to the anomeric protons and carbons and the ones of *p*-hydroxyphenyl propionic acid ester in the ^{1}H- and ^{13}C-NMR spectra, respectively. By comparison with the spectra of **10a** and **16a** and acid hydrolysis followed by $NaBH_4$ reduction, these sugars were determined to be an arabinopyranose, a glucuronic acid methyl ester and two glucoses, and the attached position of these sugars were deduced as **17a**. To confirm that, the difference NOE spectrum of **17a** was measured and NOEs were observed between the anomeric proton of glucuronic acid methyl ester (δ 4.97) and H-3 of the aglycone (δ 3.38), H-3 of arabinopyranose (δ 4.35) and H-1 of one glucose (δ 5.08), H-1 of another glucose (δ 5.55) and H-5 of the aromatic protons in *p*-hydroxyphenyl propionic acid ester (δ 7.25).

Tragopogonsaponin Q (**18**) showed three signals of the anomeric protons and carbons (one arabinopyranose and

TABLE IV. ^{1}H-NMR Spectral Data of Sugar Moiety

Proton No.		2a	3a	4a
Sugar moiety				
glc·UA	1	5.01 (1H, d, J=8.5 Hz)	4.96 (1H, d, J=8.5 Hz)	4.95 (1H, d, J=8.5 Hz)
	2	4.09 (1H, t, J=8.5 Hz)	4.05 (1H, t, J=8.5 Hz)	4.06 (1H, t, J=8.5 Hz)
	3	4.27 (1H, t, J=8.5 Hz)	4.23 (1H, t, J=8.5 Hz)	4.27 (1H, t, J=8.5 Hz)
	4	4.48 (1H, t, J=8.5 Hz)	4.44 (1H, t, J=8.5 Hz)	4.44 (1H, t, J=8.5 Hz)
	5	4.61 (1H, d, J=9 Hz)	4.57 (1H, d, J=9 Hz)	4.56 (1H, d, J=9 Hz)
	OMe	3.74 (3H, s)	3.73 (3H, s)	3.75 (3H, s)
xyl	1		6.17 (1H, d, J=8 Hz)	6.18 (1H, d, J=8.5 Hz)
	2		5.81 (1H, t, J=8 Hz)	5.81 (1H, t, J=8.5 Hz)
	3		4.30 (1H, t, J=8 Hz)	4.36 (1H, t, J=8.5 Hz)
	4		4.24[a]	4.30[a]
	5		3.85 (1H, t, J=11 Hz)	3.88 (1H, t, J=11 Hz)
	5′		4.33 (1H, dd, J=11, 5.5 Hz)	4.37 (1H, dd, J=11, 5 Hz)

Proton No.		5a	6a	7a	8a
Sugar moiety					
glc·UA	1	4.93 (1H, d, J=8.5 Hz)	4.93 (1H, d, J=8.5 Hz)	4.95 (1H, d, J=8.5 Hz)	4.97 (1H, d, J=8.5 Hz)
	2	4.04 (1H, t, J=8.5 Hz)	4.05 (1H, t, J=8.5 Hz)	4.06 (1H, t, J=8.5 Hz)	4.06 (1H, t, J=8.5 Hz)
	3	4.21 (1H, d, J=8.5 Hz)	4.22 (1H, t, J=8.5 Hz)	4.22 (1H, t, J=8.5 Hz)	4.23 (1H, t, J=8.5 Hz)
	4	4.43 (1H, t, J=8.5 Hz)	4.44 (1H, t, J=8.5 Hz)	4.43 (1H, t, J=8.5 Hz)	4.45 (1H, t, J=8.5 Hz)
	5	4.54 (1H, d, J=9 Hz)	4.55 (1H, t, J=9 Hz)	4.55 (1H, d, J=9 Hz)	4.57 (1H, d, J=9 Hz)
	OMe	3.72 (3H, s)	3.72 (3H, s)	3.72 (3H, s)	3.74 (3H, s)
xyl	1	6.18 (1H, d, J=8.5 Hz)		6.12 (1H, d, J=8.5 Hz)	6.06 (1H, d, J=8.5 Hz)
	2	5.80 (1H, t, J=8.5 Hz)		5.82 (1H, t, J=8.5 Hz)	5.70 (1H, t, J=8.5 Hz)
	3	4.31 (1H, t, J=8.5 Hz)		4.29 (1H, t, J=8.5 Hz)	4.16 (1H, t, J=8.5 Hz)
	4	4.24[a]		4.13[a]	4.08[a]
	5	3.85 (1H, t, J=11 Hz)		3.74 (1H, t, J=12 Hz)	3.72 (1H, t, J=11 Hz)
	5′	4.35[a]		4.27 (1H, dd, J=12, 6 Hz)	4.26 (1H, dd, J=11, 5.5 Hz)
ara	1		6.21 (1H, d, J=8 Hz)		
	2		6.10 (1H, t, J=8 Hz)		
	3		4.41[a]		
	4		4.38 (1H, br s)		
	5		3.96 (1H, d, J=10 Hz)		
	5′		4.42 (1H, br d, J=10 Hz)		
glc	1			5.07 (1H, d, J=8 Hz)	4.98 (1H, d, J=8 Hz)
	2			3.94 (1H, t, J=8 Hz)	3.93 (1H, t, J=8 Hz)
	3			4.12 (1H, t, J=8 Hz)	4.17 (1H, t, J=8 Hz)
	4			4.07 (1H, t, J=9 Hz)	4.06 (1H, t, J=8 Hz)
	5			4.03 (1H, m)	4.04[a]
	6			4.22 (1H, dd, J=12, 5.5 Hz)	4.23 (1H, dd, J=12, 5.5 Hz)
	6′			4.55 (1H, dd, J=12, 2.5 Hz)	4.53 (1H, dd, J=12, 1.5 Hz)
glc′	1	5.63 (1H, d, J=8.5 Hz)	5.65 (1H, d, J=8.5 Hz)		
	2	4.29 (1H, t, J=8.5 Hz)	4.32 (1H, t, J=8.5 Hz)		
	3	4.31 (1H, t, J=8.5 Hz)	4.32 (1H, t, J=8.5 Hz)		
	4	4.26 (1H, t, J=8.5 Hz)	4.27 (1H, t, J=8.5 Hz)		
	5	4.12 (1H, m)	4.12 (1H, m)		
	6	4.35 (1H, dd, J=12, 5 Hz)	4.35 (1H, dd, J=12, 5.5 Hz)		
	6′	4.52 (1H, dd, J=12, 2 Hz)	4.52 (1H, dd, J=12, 2 Hz)		

TABLE IV. (continued)

Proton No.		9a	10a	12	15a
Sugar moiety					
glc·UA	1	4.94 (1H, d, J=8.5 Hz)	4.97 (1H, d, J=8.5 Hz)		4.93 (1H, d, J=8.5 Hz)
	2	4.03 (1H, t, J=8.5 Hz)	4.06 (1H, t, J=8.5 Hz)		4.05 (1H, t, J=8.5 Hz)
	3	4.21 (1H, t, J=8.5 Hz)	4.23 (1H, t, J=8.5 Hz)		4.21 (1H, t, J=8.5 Hz)
	4	4.42 (1H, t, J=8.5 Hz)	4.44 (1H, t, J=8.5 Hz)		4.44 (1H, t, J=8.5 Hz)
	5	4.54 (1H, d, J=9 Hz)	4.57 (1H, d, J=9 Hz)		4.55 (1H, d, J=9 Hz)
	OMe	3.72 (3H, s)	3.74 (3H, s)		3.72 (3H, s)
xyl	1				6.13 (1H, d, J=8.5 Hz)
	2				5.82 (1H, t, J=8.5 Hz)
	3				4.27[a]
	4				4.12[a]
	5				3.76 (1H, t, J=10 Hz)
	5′				4.28[a]
ara	1	6.11 (1H, d, J=8.5 Hz)	6.04 (1H, d, J=8 Hz)	6.13 (1H, d, J=8 Hz)	
	2	6.28 (1H, dd, J=9, 8.5 Hz)	6.16 (1H, dd, J=9, 8 Hz)	6.31 (1H, dd, J=9.5, 8 Hz)	
	3	4.45 (1H, dd, J=9, 3 Hz)	4.34 (1H, dd, J=9, 3 Hz)	4.48 (1H, dd, J=9.5, 2.5 Hz)	
	4	4.53 (1H, br s)	4.50 (1H, br s)	4.56 (1H, br s)	
	5	3.82 (1H, d, J=12 Hz)	3.81 (1H, d, J=11.5 Hz)	3.84 (1H, d, J=12 Hz)	
	5′	4.17 (1H, d, J=12 Hz)	4.16[a]	4.19 (1H, d, J=12 Hz)	
glc	1	5.14 (1H, d, J=8 Hz)	5.08 (1H, d, J=8 Hz)	5.17 (1H, d, J=8 Hz)	5.05 (1H, d, J=8 Hz)
	2	3.87 (1H, t, J=8 Hz)	3.88 (1H, t, J=8 Hz)	3.90 (1H, t, J=8 Hz)	3.94 (1H, t, J=8 Hz)
	3	4.11[a]	4.17 (1H, t, J=8 Hz)	4.13[a]	4.11 (1H, t, J=8 Hz)
	4	4.11[a]	4.12 (1H, t, J=8 Hz)	4.13[a]	4.06 (1H, t, J=8 Hz)
	5	3.98 (1H, m)	3.98 (1H, m)	4.01 (1H, m)	4.05[a]
	6	4.32 (1H, dd, J=12, 5.5 Hz)	4.33 (1H, dd, J=12, 5.5 Hz)	4.33 (1H, dd, J=12, 4.5 Hz)	4.22 (1H, dd, J=12, 5 Hz)
	6′	4.52 (1H, dd, J=12, 2.5 Hz)	4.51 (1H, dd, J=12, 2 Hz)	4.56[a]	4.55 (1H, dd, J=12, 2 Hz)
glc′	1				5.60 (1H, d, J=8.5 Hz)
	2				4.27 (1H, t, J=8.5 Hz)
	3				4.32 (1H, t, J=8.5 Hz)
	4				4.30 (1H, t, J=8.5 Hz)
	5				4.11[a]
	6				4.39 (1H, dd, J=12, 5 Hz)
	6′				4.53 (1H, dd, J=12, 2 Hz)

Proton No.		16a	17a	18	19a
Sugar moiety					
glc·UA	1	4.97 (1H, d, J=8.5 Hz)	4.97 (1H, d, J=8.5 Hz)		4.97 (1H, d, J=8.5 Hz)
	2	4.07[a]	4.06 (1H, t, J=8.5 Hz)		4.07 (1H, t, J=8.5 Hz)
	3	4.24 (1H, t, J=8.5 Hz)	4.24 (1H, t, J=8.5 Hz)		4.24 (1H, t, J=8.5 Hz)
	4	4.46 (1H, t, J=8.5 Hz)	4.45 (1H, t, J=8.5 Hz)		4.46 (1H, t, J=8.5 Hz)
	5	4.58 (1H, d, J=9 Hz)	4.57 (1H, d, J=9 Hz)		4.58 (1H, d, J=9 Hz)
	OMe	3.74 (3H, s)	3.74 (3H, s)		3.74 (3H, s)
xyl	1	6.07 (1H, d, J=8.5 Hz)			
	2	5.70 (1H, t, J=8.5 Hz)			
	3	4.17 (1H, t, J=8.5 Hz)			
	4	4.07[a]			
	5	3.73[a]			
	5′	4.27 (1H, dd, J=11.5, 5.5 Hz)			
ara	1		6.07 (1H, d, J=8 Hz)	6.15 (1H, d, J=8 Hz)	6.07 (1H, d, J=8 Hz)
	2		6.14 (1H, dd, J=9.5, 8 Hz)	6.31 (1H, dd, J=9.5, 8 Hz)	6.15 (1H, dd, J=9, 8 Hz)
	3		4.35 (1H, dd, J=9.5, 3 Hz)	4.49 (1H, dd, J=9.5, 3 Hz)	4.38 (1H, dd, J=9, 3 Hz)
	4		4.49 (1H, br s)	4.57 (1H, br s)	4.49 (1H, br s)
	5		3.82 (1H, d, J=12 Hz)	3.86 (1H, d, J=12 Hz)	3.82 (1H, d, J=11.5 Hz)
	5′		4.16 (1H, dd, J=12, 2 Hz)	4.20 (1H, dd, J=12, 2 Hz)	4.16[a]
glc	1	4.96 (1H, d, J=8 Hz)	5.08 (1H, d, J=8 Hz)	5.17 (1H, d, J=8 Hz)	5.10 (1H, d, J=8.5 Hz)
	2	3.93 (1H, t, J=8 Hz)	3.88 (1H, t, J=8 Hz)	3.90 (1H, t, J=8 Hz)	3.89 (1H, t, J=8.5 Hz)
	3	4.15 (1H, t, J=8 Hz)	4.14 (1H, t, J=8 Hz)	4.13[a]	4.13 (1H, t, J=8.5 Hz)
	4	4.07[a]	4.13 (1H, t, J=8 Hz)	4.13[a]	4.12 (1H, t, J=8.5 Hz)
	5	4.07[a]	3.98 (1H, m)	4.00 (1H, m)	3.97 (1H, m)
	6	4.23 (1H, dd, J=12, 4.5 Hz)	4.35[a]	4.33 (1H, dd, J=12, 5 Hz)	4.33 (1H, dd, J=12, 4 Hz)
	6′	4.55 (1H, br d, J=12 Hz)	4.53 (1H, dd, J=12, 2 Hz)	4.54 (1H, dd, J=12, 2 Hz)	4.52 (1H, dd, J=12, 2 Hz)
glc′	1	5.55 (1H, d, J=8 Hz)	5.55 (1H, d, J=8.5 Hz)	5.63 (1H, d, J=8 Hz)	5.58 (1H, d, J=8 Hz)
	2	4.27 (1H, t, J=8 Hz)	4.26 (1H, t, J=8.5 Hz)	4.29 (1H, t, J=8 Hz)	4.30[a]
	3	4.32[a]	4.33 (1H, t, J=8.5 Hz)	4.35 (1H, t, J=8 Hz)	4.30[a]
	4	4.32[a]	4.31 (1H, t, J=8.5 Hz)	4.30 (1H, t, J=8 Hz)	4.30[a]
	5	4.07[a]	4.06 (1H, m)	4.13[a]	4.06[a]
	6	4.39 (1H, dd, J=12, 4.5 Hz)	4.38 (1H, dd, J=12, 5.5 Hz)	4.38 (1H, dd, J=12, 5.5 Hz)	4.37 (1H, dd, J=12, 4.5 Hz)
	6′	4.55 (1H, br d, J=12 Hz)	4.50 (1H, dd, J=12, 2 Hz)	4.56 (1H, dd, J=12, 2 Hz)	4.48 (1H, dd, J=12, 2 Hz)

Run at 500.0 MHz in pyridine-d_5 solution. *a*) Obscured by other signals; therefore, couplings could not be accurately determined.

TABLE V. Hydrolysis Products of Compounds **2a**—**11a**, **12**—**14**, **15a**—**17a**, **18** and **19**

Tragopogonsaponin	Ester	Sugar
A		Glucuronic acid
B	*p*-Coumaric acid	Glucuronic acid, xylose
C	Ferulic acid	Glucuronic acid, xylose
D	Ferulic acid	Glucuronic acid, glucose, xylose
E	Ferulic acid	Glucuronic acid, glucose, xylose
F	*p*-Coumaric acid	Glucuronic acid, glucose, xylose
G	*p*-Hydroxyphenyl propionic acid	Glucuronic acid, glucose, xylose
H	*p*-Coumaric acid	Glucuronic acid, glucose, arabinose
I, J	*p*-Hydroxyphenyl propionic acid 4-Hydroxy-3-methoxyphenyl propionic acid	Glucuronic acid, glucose, arabinose
K	*p*-Coumaric acid	Glucose, arabinose
L, M	*p*-Hydroxyphenyl propionic acid 4-Hydroxy-3-methoxyphenyl propionic acid	Glucose, arabinose
N	*p*-Coumaric acid	Glucuronic acid, glucose, xylose
O	*p*-Hydroxyphenyl propionic acid	Glucuronic acid, glucose, arabinose
P	*p*-Hydroxyphenyl propionic acid	Glucuronic acid, glucose, arabinose
Q	*p*-Coumaric acid	Glucose, arabinose
R	4-Hydroxy-3-methoxyphenyl propionic acid	Glucuronic acid, glucose, arabinose

two glucoses) and a *p*-coumaric acid ester in the ^{1}H- and ^{13}C-NMR spectra. But the signal of a glucuronic acid methyl ester was not visible and the signal due to C-3 of the aglycone was exhibited at δ 78.1. Thus, the structure of tragopogonsaponin Q was considered to be **18** in which glucuronic acid was not attached to the aglycone as **12** was.

The ^{1}H-, ^{13}C-NMR and the difference NOE spectra of tragopogonsaponin R methyl ester (**19a**) were very similar to those of **17a** except for the ester moiety. The ^{1}H-NMR spectrum indicated that this ester moiety was a 4-hydroxy-3-methoxyphenyl propionic acid ester because ABC-type signals of the aromatic protons and the signals of a methoxyl group and two sp^3 protons were seen in it, and in the difference NOE spectrum irradiation on the signal of the methoxyl protons showed an NOE to the signal due to H-2 of the aromatic protons in the ester moiety. Thus, the structure of tragopogonsaponin R was determined to be **19**.

Finally, to confirm the ester and sugar moieties, these compounds were treated with AcCl–MeOH (1:20) and reacted as follows. The ester moieties were compared with authentic samples by high performance liquid chromatography (HPLC) and the sugar moieties by gas chromatography (GC). These results were reported in Table V. From the results, we could confirm the presumptions of the sugar and ester moieties.

Experimental

The melting point was determined on a Yanaco MP-500 micromelting point apparatus. Optical rotations were determined with a JASCO-360 digital polarimeter. Ultraviolet (UV) spectra were taken on a Hitachi U-3410 spectrometer and FAB-MS spectra on a JEOL JMS-SX102 spectrometer. ^{1}H- and ^{13}C-NMR were recorded on JEOL GSX-500 (500 and 125.65 MHz, respectively) and JEOL GSX-270 (270 and 67.80 MHz, respectively) spectrometers. Chemical shifts were given on the δ (ppm) scale with tetramethylsilane as an internal standard (s, singlet; d, doublet; t, triplet; m, multiplet; br, broad). GC was run on a Hitachi G-3000 gas chromatograph. HPLC was run on a JASCO system 800 instrument.

Isolation The roots of *T. porrifolius* L. (2.5 kg) were extracted twice with MeOH under reflux. The extract was concentrated under reduced pressure and the residue was suspended in H_2O. This suspension was extracted with Et_2O. The H_2O layer was passed through a Mitsubishi Diaion HP-20 column and the MeOH eluate was concentrated under reduced pressure. The residue (22 g) was rechromatographed on a silica gel column with $CHCl_3$–MeOH (9:1) and semi-preparative HPLC [ODS: MeOH–H_2O (7:3—3:1); CH_3CN–H_2O (17:23), PhA: CH_3CN–H_2O (3:5—9:11)] to give compounds **2a** (9 mg), **3a** (38 mg), **4a** (18 mg), **5a** (48 mg), **6a** (66 mg), **7a** (348 mg), **8a** (29 mg), **9a** (532 mg), **10a**+**11a** (260 mg), **12** (17 mg), **13**+**14** (82 mg), **15a** (5 mg), **16a** (10 mg), **17a** (28 mg), **18** (6 mg) and **19a** (10 mg) after methylation with diazomethane.

Tragopogonsaponin A Methyl Ester (**2a**): Amorphous powder, $[\alpha]_D^{25}$ −8.2° (c=0.90, MeOH). *Anal.* Calcd for $C_{37}H_{58}O_{10}\cdot 5/4H_2O$: C, 64.84; H, 8.90. Found: C, 64.91; H, 8.83. FAB-MS m/z: 663 $(M+H)^+$, 685 $(M+Na)^+$. ^{1}H- and ^{13}C-NMR: Tables I—IV.

Tragopogonsaponin B Methyl Ester (**3a**): Amorphous powder, $[\alpha]_D^{25}$ +24.9° (c=1.27, MeOH). *Anal.* Calcd for $C_{51}H_{72}O_{16}\cdot 3H_2O$: C, 61.55; H, 7.90. Found: C, 61.54; H, 7.89. UV λ_{max}^{MeOH} nm (log ε): 212 (4.11), 229 (4.04), 301 (4.25), 317 (4.34). FAB-MS m/z: 963 $(M+Na)^+$. ^{1}H- and ^{13}C-NMR: Tables I—IV.

Tragopogonsaponin C Methyl Ester (**4a**): Amorphous powder, $[\alpha]_D^{25}$ +24.3° (c=0.90, MeOH). *Anal.* Calcd for $C_{52}H_{74}O_{17}\cdot 2H_2O$: C, 62.01; H, 7.81. Found: C, 61.96; H, 7.83. UV λ_{max}^{MeOH} nm (log ε) : 217 (4.10), 237 (3.98), 301 (4.08), 328 (4.25). FAB-MS m/z: 993 $(M+Na)^+$. ^{1}H- and ^{13}C-NMR: Tables I—IV.

Tragopogonsaponin D Methyl Ester (**5a**): Amorphous powder, $[\alpha]_D^{25}$ −4.4° (c=0.60, MeOH). *Anal.* Calcd for $C_{58}H_{84}O_{22}\cdot 3H_2O$: C, 58.67; H, 7.64. Found: C, 58.80; H, 7.70. UV λ_{max}^{MeOH} nm (log ε): 217 (4.12), 231 (4.02), 296 (4.20), 317 (4.20), 317 (4.22). FAB-MS m/z: 1155 $(M+Na)^+$. ^{1}H- and ^{13}C-NMR: Tables I—IV.

Tragopogonsaponin E Methyl Ester (**6a**): Amorphous powder, $[\alpha]_D^{25}$ +7.3° (c=1.10, MeOH). *Anal.* Calcd for $C_{58}H_{84}O_{22}\cdot 7/2H_2O$: C, 58.23; H, 7.67. Found: C, 58.16; H, 7.60. UV λ_{max}^{MeOH} nm (log ε): 215 (4.12), 235 (3.99), 296 (4.13), 321 (4.18). FAB-MS m/z: 1155 $(M+Na)^+$. ^{1}H- and ^{13}C-NMR: Tables I—IV.

Tragopogonsaponin F Methyl Ester (**7a**): Amorphous powder, $[\alpha]_D^{25}$ +20.9° (c=1.29, MeOH). *Anal.* Calcd for $C_{57}H_{82}O_{21}\cdot 4H_2O$: C, 58.25; H, 7.72. Found: C, 58.11; H, 7.72. UV λ_{max}^{MeOH} nm (log ε): 211 (4.05), 230 (3.98), 303 (4.22), 318 (4.32). FAB-MS m/z: 1125 $(M+Na)^+$. ^{1}H- and ^{13}C-NMR: Tables I—IV.

Tragopogonsaponin G Methyl Ester (**8a**): Amorphous powder, $[\alpha]_D^{25}$ −11.7° (c=0.95, MeOH). *Anal.* Calcd for $C_{57}H_{84}O_{21}\cdot 3H_2O$: C, 59.05; H, 7.82. Found: C, 58.95; H, 7.76. UV λ_{max}^{MeOH} nm (log ε): 223 (3.95), 283 (3.49), 317 (3.42). FAB-MS m/z: 1127 $(M+Na)^+$. ^{1}H- and ^{13}C-NMR: Tables I—IV.

Tragopogonsaponin H Methyl Ester (**9a**): Amorphous powder, $[\alpha]_D^{25}$ +7.2° (c=0.65, MeOH). *Anal.* Calcd for $C_{57}H_{82}O_{21}\cdot 5/2H_2O$: C, 59.62; H, 7.64. Found: C, 59.54; H, 7.71. UV λ_{max}^{MeOH} nm (log ε): 200 (4.16), 212 (4.08), 230 (4.01), 301 (4.22), 318 (4.33). FAB-MS m/z: 1125 $(M+Na)^+$. ^{1}H- and ^{13}C-NMR: Tables I—IV.

Tragopogonsaponin I Methyl Ester (**10a**): Amorphous powder, FAB-MS m/z: 1127 $(M+Na)^+$. ^{1}H- and ^{13}C-NMR: Tables I—IV.

Tragopogonsaponin J Methyl Ester (**11a**): Amorphous powder, FAB-MS m/z: 1157 $(M+Na)^+$. ^{1}H- and ^{13}C-NMR: Tables I—III.

Tragopogonsaponin K (**12**): Amorphous powder, $[\alpha]_D^{25}$ +59.4° (c=0.90, MeOH). *Anal.* Calcd for $C_{50}H_{72}O_{15}\cdot 3H_2O$: C, 62.09; H, 8.13. Found: C,

61.88; H, 8.03. UV λ_{max}^{MeOH} nm (log ε): 213 (4.09), 229 (4.00), 301 (4.20), 318 (4.30). FAB-MS *m/z*: 935 $(M+Na)^+$. ^{1}H- and ^{13}C-NMR: Tables I—IV.

Tragopogonsaponin L (**13**): Amorphous powder, FAB-MS *m/z*: 937 $(M+Na)^+$. ^{1}H- and ^{13}C-NMR: Tables I—III.

Tragopogonsaponin M (**14**): Amorphous powder, FAB-MS *m/z*: 967 $(M+Na)^+$. ^{1}H- and ^{13}C-NMR: Tables I—III.

Tragopogonsaponin N Methyl Ester (**15a**): Amorphous powder, $[\alpha]_D^{25}$ $-6.7°$ ($c=0.50$, MeOH). *Anal.* Calcd for $C_{63}H_{92}O_{26}\cdot 6H_2O$: C, 55.09; H, 7.63. Found: C, 64.98; H, 7.51. UV λ_{max}^{MeOH} nm (log ε): 225 (4.03), 299 (4.26), 308 (4.28). FAB-MS *m/z*: 1287 $(M+Na)^+$. ^{1}H- and ^{13}C-NMR: Tables I—IV.

Tragopogonsaponin O Methyl Ester (**16a**): Amorphous powder, $[\alpha]_D^{25}$ $0°$ ($c=0.40$, MeOH). *Anal.* Calcd for $C_{63}H_{94}O_{26}\cdot 11/2H_2O$: C, 55.37; H, 7.75. Found: C, 55.47; H, 7.62. UV λ_{max}^{MeOH} nm (log ε): 221 (4.06), 281 (3.56), 309 (3.64). FAB-MS *m/z*: 1289 $(M+Na)^+$. ^{1}H- and ^{13}C-NMR: Tables I—IV.

Tragopogonsaponin P Methyl Ester (**17a**): Amorphous powder, $[\alpha]_D^{25}$ $-7.2°$ ($c=0.90$, MeOH). *Anal.* Calcd for $C_{63}H_{94}O_{26}\cdot 11/2H_2O$: C, 55.37; H, 7.75. Found: C, 55.48; H, 7.68. UV λ_{max}^{MeOH} nm (log ε): 220 (4.07), 273 (3.29), 280 (3.26). FAB-MS *m/z*: 1289 $(M+Na)^+$. ^{1}H- and ^{13}C-NMR: Tables I—IV.

Tragopogonsaponin Q (**18**): Amorphous powder, $[\alpha]_D^{25}$ $+25.4°$ ($c=0.40$, MeOH). *Anal.* Calcd for $C_{56}H_{84}O_{20}\cdot 5H_2O$: C, 57.72; H, 7.96. Found: C, 57.63; H, 7.82. UV λ_{max}^{MeOH} nm (log ε): 224 (3.96), 299 (4.13), 307 (4.15). FAB-MS *m/z*: 1097 $(M+Na)^+$. ^{1}H- and ^{13}C-NMR: Tables I—IV.

Tragopogonsaponin R Methyl Ester (**19a**): Amorphous powder, $[\alpha]_D^{25}$ $-12.3°$ ($c=0.50$, MeOH). *Anal.* Calcd for $C_{64}H_{96}O_{27}\cdot 9/2H_2O$: C, 55.76; H, 7.68. Found: C, 55.87; H, 7.71. UV λ_{max}^{MeOH} nm (log ε): 219 (4.02), 275 (3.36), 280 (3.39), 310 (3.29). FAB-MS *m/z*: 1319 $(M+Na)^+$. ^{1}H- and ^{13}C-NMR: Tables I—IV.

Degradation of the Crude Saponin Fraction The crude saponin (*ca.* 30 mg) was refluxed in AcCl–MeOH (1 : 20) (5 ml) for 4 h. The reaction mixture was concentrated under reduced pressure to dryness and was partitioned between AcOEt and H_2O. The AcOEt layer was concentrated to dryness and the residue was chromatographed to give echinocystic acid (**1**) (6 mg), (Condition: column; ODS. flow rate; 6.0 ml/min. 70% CH_3CN + 0.05% trifluoroacetic acid) and this compound was recrystallized from MeOH to give colorless needles. mp 304—307 °C. $[\alpha]_D^{25}$ $+31.7°$ ($c=0.63$, MeOH) (lit. mp 308—309 °C. $[\alpha]_D^{19}$ $+39°$ ($c=1.0$, 95% EtOH)).[1] ^{1}H- and ^{13}C-NMR: Tables I and III. Moreover, phenyl propionic acid derivatives were analyzed with authentic samples by HPLC. (Condition: column; ODS. flow rate; 1.3 ml/min. 30% CH_3CN, t_R; methyl *p*-coumarate, 11.7 min, methyl ferulate, 12.8 min, methyl *p*-hydroxyphenyl propionate, 9.0 min, methyl 4-hydroxy-3-methoxyphenyl propionate, 9.8 min).

Degradation of Compounds 2a—19a with AcCl–MeOH (1 : 20) Compounds **2a—19a** (*ca.* 1 mg) were reduced with $NaBH_4$ (*ca.* 1 mg) for 12 h at room temperature. The reaction mixture was neutralized with 10% H_2SO_4 (2 drops) and passed through a Mitsubishi Diaion HP-20 column and the MeOH eluate was concentrated under reduced pressure. The residue was refluxed in AcCl–MeOH (1 : 20) (1 ml) for 1 h. After dryness, the reaction mixture was partitioned between AcOEt and H_2O. The AcOEt layer was concentrated to dryness, and the residue was analyzed by HPLC with authentic samples. (Conditions: column; ODS. flow rate; 1.3 ml/min. 30% CH_3CN, t_R; methyl *p*-coumarate, 11.7 min, methyl ferulate, 12.8 min, methyl *p*-hydroxyphenyl propionate, 9.0 min, methyl 4-hydroxy-3-methoxyphenyl propionate, 9.8 min. 70% CH_3CN, t_R; echinocystic acid, 8.0 min). The H_2O layer was also concentrated and the residue in 5—10% H_2SO_4 (2 drops) was heated in a boiling H_2O bath for 1 h. The solution was passed through an Amberlite IR-45 column and the eluate was concentrated to give a residue which was reduced with $NaBH_4$ (*ca.* 1 mg) for 1 h at room temperature. The reaction mixture was passed through an Amberlite IR-120 column and the eluate was concentrated to dryness. Boric acid was removed by co-distilation with MeOH and the residue was acetylated with acetic anhydride and pyridine (1 drop each) at 100 °C for 1 h. The reagents were evaporated off *in vacuo*. From each glycoside, glucitol acetate, xylitol acetate and arabinitol acetate were detected by GC. (Conditions: column, Spelco SP-2380 capillary column (0.25 mm × 30 m); column temperature, 250 °C; carrier gas, N_2; t_R, glucitol acetate, 12.0 min, xylitol acetate, 7.8 min, arabinitol acetate, 6.6 min).

Acknowledgement We thank the staff of the Central Analytical Laboratory of this university for elemental analysis and measurement of MS.

References and Notes

1) T. Konoshima, H. Fukushima, H. Inui, K. Sato and T. Sawada, *Phytochemistry*, **20**, 139 (1981).
2) Y. Okada, S. Shibata, T. Ikekawa, A. M. J. Javellana and O. Kamo, *Phytochemistry*, **26**, 2789 (1987).
3) K. Mizutani, K. Ohtani, R. Kasai, O. Tanaka and H. Matsuura, *Chem. Pharm. Bull.*, **33**, 2266 (1985).

Anti-5-hydroxytryptamine$_3$ Effect of Galanolactone, Diterpenoid Isolated from Ginger

Qirong HUANG,[a] Masatsugu IWAMOTO,[a] Shunji AOKI,[a] Naomi TANAKA,[a] Kiyoko TAJIMA,[a] Johji YAMAHARA,*[,a] Yoshihisa TAKAISHI,[b] Masaaki YOSHIDA,[b] Toshiaki TOMIMATSU[b] and Yoshin TAMAI[c]

Kyoto Pharmaceutical University,[a] Misasagi, Yamashina-ku, Kyoto 607, Japan, Faculty of Pharmaceutical Science, Tokushima University,[b] Shomachi 1–78, Tokushima 770, Japan and Kuraray Co., Ltd.,[c] NIC R & D Division, Nakajo-cho 2–28, Niigata 959–26, Japan. *Received July 30, 1990*

It has been reported that an acetone extract of ginger and its fractions have anti-5-HT (5-hydroxytryptamine; serotonin) effects. In the present study, guinea pig ileum, rat stomach fundus and rabbit aortic strips are used in order to determine the constituents of fraction 2 which are responsible for anti-5-HT effect and to examine their pharmacological properties.

The analysis of fraction 2—3 indicated that galanolactone, a diterpenoid, is one of the active constituents. In guinea pig ileum, galanolactone inhibited contractile responses to 5-HT with a pIC_{50} value 4.93. pIC_{50} value of galanolactone against the response to 2-methyl-5-HT, a selective 5-HT$_3$ agonist, in the presence of methysergide at 1×10^{-5} M was 5.10. pIC_{50} values of ICS 205-930, a selective 5-HT$_3$ antagonist, were 5.30 and 7.49, respectively. The concentration-response curve of 5-HT was shown as a biphasic curve and galanolactone caused a selective shift to the right of the second phase.

In the same preparations, the pIC_{50} value of galanolactone and ICS 205-930 against the response to carbamylcholine (CCh) was 4.45 and 4.46.

The inhibitory effect of galanolactone on the 5-HT response in the stomach fundus and aortic strips was less than that in the ileum.

In addition, in the thoracic aorta precontracted with 50 mM K^+, the relaxing effect of galanolactone was about 1/10 of that of papaverine.

These results suggest that the anti-5-HT effect of galanolactone, a diterpenoid isolated from ginger, is related to antagonism of 5-HT$_3$ receptors.

Keywords ginger; diterpenoid; galanolactone; anti-serotonergic action; 5-hydroxytryptamine$_3$ receptor

Introduction

We have already reported the inhibitory effect of acetone extract, and several constituents of ginger on the responses to serotonin (5-hydroxytryptamine, 5-HT).[1] In case of vomiting, ginger may be used singly or in combinated with the tubers of *Pinellia ternata* in China and Japan. The anti-emetic effects are generally held to reflect its dopamine D_2 receptor blocking activity, recent data has indicated that there is a good correlation between 5-HT$_3$ receptor antagonist potency and anti-emetic efficacy.[2] Further experiments were conducted to clarify the anti-5-HT constituents and the existence of anti-5-HT$_3$ antagonistic potency.

Experimental Methods

Fractionation Ginger was purchased from local market in Osaka and the roots, were coarsely cut, soaked in three times the volume of acetone for 2 d. The filtrate was concentrated under reduced pressure below 40 °C, dried and kept in a desiccator. Fractionation of the active constituents was carried out by our method, as shown Fig. 1. Fractions 2 and 3 significantly inhibited the contractile response induced by 5-HT. The active constituents of fraction 3 have been reported.[1] The present experiments were conducted in order to clarify the active constituents of fraction 2. Fraction 2 was further separated by silica gel column chromatography (Merck, Silica gel 60 F-254, elutional fluid; gradient, hexane : ethylacetate = 10 : 1 to 3 : 1), to obtain fractions 2-1 to 2-4. Fraction 2-3 was similarly purified by silica gel silanised column chromatography (Merck, silica gel silanisert, elution fluid, 50% methanol), comparison of mass spectrum (MS), proton nuclear magnetic resonance (^{1}H-NMR) and infrared spectrum (IR) with those of the standards indicated that the chief ingredient of fraction 2-3 was galanolactone[3] (Fig. 2).

Recording of Response Male Hartley guinea pigs (about 300 g) were bled to death by severing both arteries and the ileum removed and cut into strips (10—15 mm). Rat stomach fundus and rabbit thoracic aorta were also isolated with the same technique as the ileum. The fundus was cut into strips (1 × 5 mm) and the aorta was made the spiral cord and cut into strips (2 × 10 mm). Each ileum strip was placed in a tissue bath containing 25 ml of Tyrode solution, maintained at 37 °C and stomach fundus strips and aortic strips in the Krebs Henseleit solution.

The compositions of Tyrode solution and Krebs Henseleit solution were as follows (mM): Tyrode; NaCl 137.9, KCl 2.7, $CaCl_2$ 1.8, $MgCl_2$ NaH_2PO_4 1.1, $NaHCO_3$ 11.9, glucose 5.6. Krebs Henseleit; NaCl 118, KCl 4.7, $CaCl_2$ 2.5, KH_2PO_4 1.2, $NaHCO_3$ 25.0, $MgSO_4$ 1.2, glucose 10.0. It was aerated with a 95%O_2–5%CO_2 gas mixture and kept at pH 7.4. An initial stretch

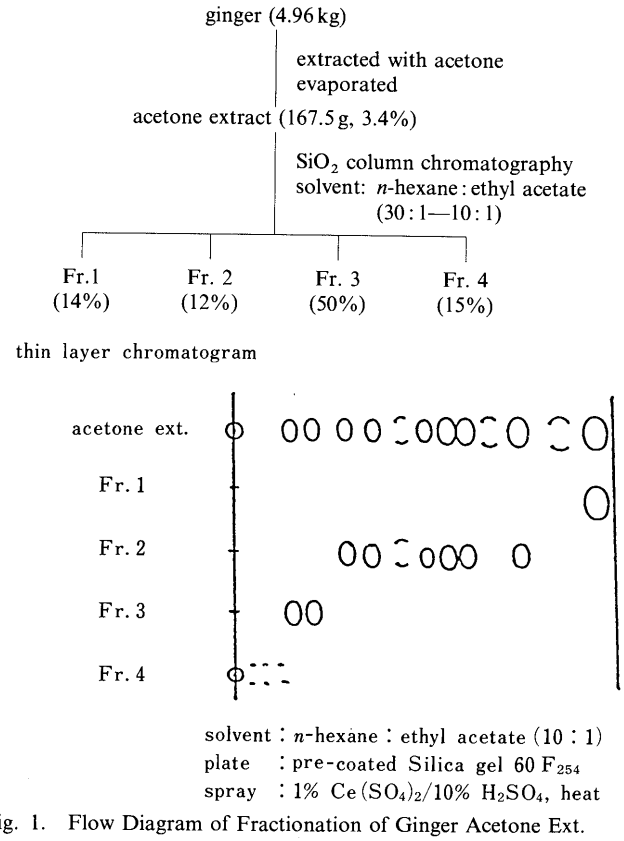

Fig. 1. Flow Diagram of Fractionation of Ginger Acetone Ext.

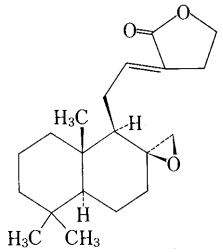

Fig. 2. Chemical Structure of Galanolactone

tension of 1 g was applied to each strip and at least 1 h was allowed before the start of the experiment. The contractile response of 5-HT was obtained by addition of 5-HT to the bath at concentrations of 10^{-5} M. Each tissue was then washed three times every 10 min. Thirty minutes thereafter, the contractile response of 5-HT (10^{-5} M) was again obtained 20 min after the application of test drugs. The contraction to 5-HT was compared to the response obtained in the first contraction of 5-HT taken as 100%. Non-cumulative concentration-response curve for 5-HT were established by adding increasing concentrations of the agonist to the organ bath at intervals of at least 15 min to avoid tachyphylaxis. Each concentration was left in contact with the tissue for 1 min. Antagonists were preequilibrated for 10 min prior to addition of 5-HT. The contraction expressed as percentage of the maximal response to 5-HT obtained from several preparations were plotted as mean value in order to obtain a log-concentration-response curve.

Contractions were measured with a force transducer (Nihon Denki San-ei: 45196A) and recorded on an oscillograph (Nihon Denki San-ei: 363).

Drugs Treatment Test samples were dissolved in ethanol or dimethyl sulfoxide (DMSO) and diluted in distilled water. The final bath concentration of ethanol and DMSO were less than 0.01%. Control experiments indicated that the concentration of ethanol and DMSO did not have any effect on the response of the ileum strips.

Drugs used were serotonin-creatinine sulfate (5-HT, Wako Pure Chemical Industries Ltd., Osaka), carbamylcholine (CCh, Aldrich Chemical Company, Inc. Milwaukee) methysergide (Sandoz, Switzerland) ketanserin and ICS 205-930 (Research Biochemical Inc. Massachusetts). 2-Methylserotonin was synthesized in our laboratory. Statistical analysis was performed by Dunnett's method.

Results

The Effect of Fractions on the Contraction of 5-HT in Guinea Pig Ileum It was shown that fraction 2, and fractions 2-1, 2-2, 2-3, 2-4 exhibited an anti-5-HT effect and fractions 2-1, 2-2 and 2-3 had nearly equal potency of inhibitory effects (Fig. 3).

The Effect of Galanolactone on the Concentration-Response Curve of 5-HT in Guinea Pig Ileum As shown in Fig. 4, the concentration-response curve of 5-HT was given as a biphasic curve. The effects of galanolactone (3×10^{-6} and 1×10^{-5} M) were found to possess an anti-5-HT effect and the first phase of the response curve was not affected by galanolactone (Fig. 4).

The Effect of Galanolactone on the Contraction to Cumulative Treatment of CCh in Guinea Pig Ileum As shown in Fig. 5, galanolactone (1×10^{-5} and 3×10^{-5} M) possessed a potency of anti-cholinergic effect, while the potency was weaker than that of anti-5-HT effect (Fig. 5).

The Relaxing Effect of Galanolactone on the High-concentration K^+ Contraction in Rabbit Thoracic Aorta As shown in Fig. 6, the relaxing effect of galanolactone was approximately 1/10 that of papaverine (Fig. 6).

Values of pIC_{50} of Galanolactone, Methysergide, Ketanserin and ICS 205-930 on the Contraction by 5-HT in Rat Stomach Fundus and Rabbit Thoracic Aorta and the Contraction by 2-Methyl-5-HT with Pretreatment of Methysergide in Guinea Pig Ileum In rat stomach fundus,

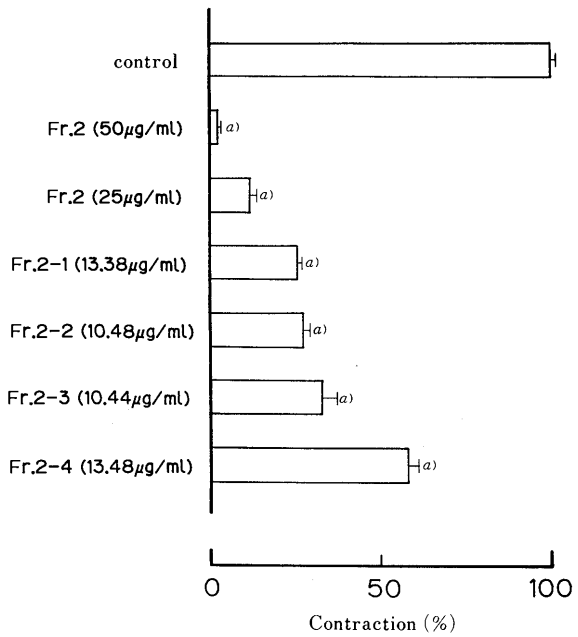

Fig. 3. Effects of Ginger Acetone Ext. Fraction on the Contractile Responses to 5-HT (1×10^{-5} M) in Guinea Pig Ileum

Each value represents mean S.E. of 4—9 experiments. *a)* $p<0.01$.

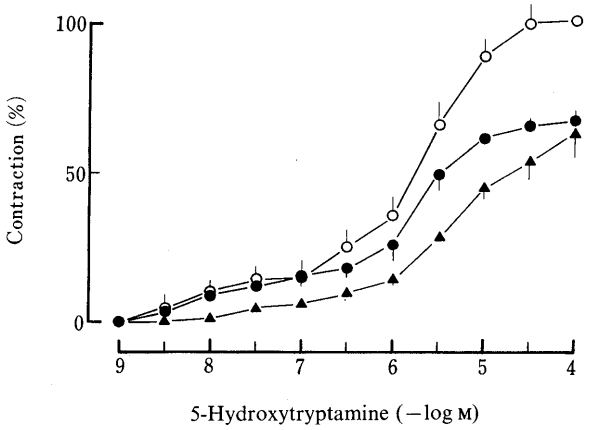

Fig. 4. Effect of Galanolactone on the Concentration-Response Curve of 5-HT in the Guinea Pig Ileum

○, control; ●, galanolactone 3×10^{-6} M; ▲, 1×10^{-5} M. Each point indicates the mean of six experiments. Vertical bars indicate the S.E. of the mean.

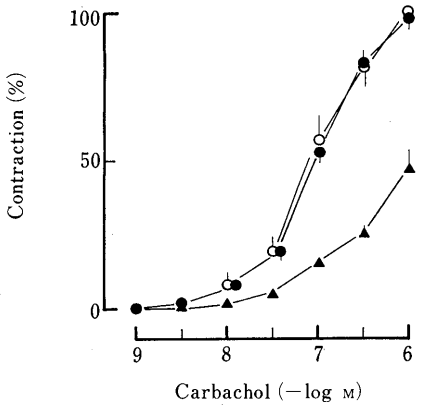

Fig. 5. Effect of Galanolactone on the Concentration-Response Curve of CCh in the Guinea Pig Ileum

○, control; ●, galanolactone 1×10^{-5} M; ▲, 3×10^{-5} M. Each point indicates the mean of six experiments. Vertical bars indicate the S.E. of the mean.

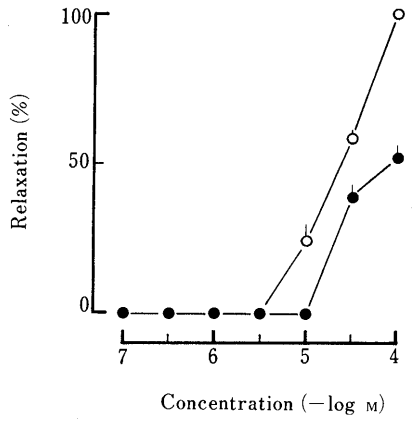

Fig. 6. The Relaxing Effect of Galanolactone (●) and Papaverine (○) on the High-concentration K^+ Contraction in the Rabbit Thoracic Aorta

Each point indicates the mean of six experiments. Vertical bars indicate the S.E. of the mean.

TABLE I. Inhibitory Effect of Galanolactone, Methysergide, Ketanserin and ICS 205-930 on the Contractile Responses of Isolated Guinea Pig Ileum Induced by 2-Methyl-5-HT and Rabbit Thoracic Aorta and Rat Stomach Fundus Induced by 5-HT

Compounds	n	pIC_{50}		
		Rat S.F.	Rabbit T.A.	G.P Ileum
Galanolactone	6	≫4.00	≫4.00	5.10
ICS 205-930	6	≫4.00	≫4.00	7.49
Methysergide	6	7.64	6.84	—
Ketanserin	6	≫4.00	6.71	≫4.00

The contractile response of guinea pig ileum was induced by 2-methyl-5-HT (1×10^{-5} M) and each drug was treated 5 min after the treatment of methysergide (1×10^{-5} M). The contractile response of rabbit T.A. and rat S.F. was induced by 5-HT (1×10^{-5} M). pIC_{50} is the negative logarithm of the concentration (M) of galanolactone, ICS 205-930, methysergide and ketanserin required to prevent 50% of contractile response elicited by 2-methyl-5-HT and 5-HT.

TABLE II. Inhibitory Effect of Galanolactone, ICS 205-930, Atropine and Ketanserin on the 2-Methyl-5-HT, 5-HT and CCh Induced Contraction of Isolated Guinea Pig Ileum

Compounds	n	pIC_{50}		
		2-Methyl-5-HT	5-HT	CCh
Galanolactone	6	5.10	4.93	4.45
ICS 205-930	6	7.49	5.30	4.46
Atropine	6	6.34	5.46	8.35
Ketanserin	6	4.74	5.15	4.13

On the contractile response induced by 2-methyl-5-HT, each drug was treated 5 min after the pretreatment of methysergide (1×10^{-5} M). pIC_{50} is the negative logarithm of the concentrations (M) of galanolactone, ICS 205-930, atropine and ketanserin required to prevent 50% of contractile response elicited by 2-methyl-5-HT (1×10^{-5} M), 5-HT (1×10^{-5} M) and CCh (3×10^{-7} M).

the value of pIC_{50} of galanolactone was more than 4.00 and was also ketanserin, while that of methysergide was 7.64. In rabbit thoracic aorta, the value of galanolactone was more than 4.00 and that of ketanserin was 6.71. In guinea pig ileum, the value of galanolactone was 5.10 and that of ICS 205-930 was 7.49 (Table I).

Comparison the Value of pIC50 of the Galanolactone between the Contraction by 2-Methyl-5-HT with Pretreatment of Methysergide and the Contraction by CCh in Guinea Pig Ileum The value of pIC50 of the galanolactone on the contraction by 2-methyl-5-HT was 5.10, while the value on the contraction by CCh was 4.45. Each value of ICS 205-930 and atropine were 7.94, 4.46 and 6.34, 8.35, respectively (Table II).

Discussion

Ginger is one of the important natural stomachics. Anti-emetic effect of ginger has also been known from ancient times. In recent years, the relationship between the 5-HT_3 receptor antagonist and anti-emetic and gastrointestinal motility enhancing effect has been largely recognized.[2] In the present study, one of the main aims was to determine the presence of 5-HT_3 antagonism in ginger constituents in order to substantiate the known medicinal efficacy. This is the first report which identified the anti-5-HT effect of galanolactone, a diterpenoid. Results indicated that anti-5-HT effect of galanolactone was much greater in a guinea pig ileum, which has mainly 5-HT_3 receptor,[4] than that in rat fundus strips, which are known for the much presence of 5-HT_1 receptors,[5] and rabbit aorta strips, which contain mainly 5-HT_2 receptors.[6] In addition, the effect of galanolactone was much greater in response to a selective 5-HT_3 agonist, 2-methyl-5-HT,[7] in the presence of a selective 5-HT_1 and 5-HT_2 antagonist, methysergide.[8]

Recently it was reported that at a low concentration (below 3×10^{-7} M), contractile response of 5-HT can be mediated by release of substance P which subsequently releases acetylcholine.[9] The value of pIC_{50} of galanolactone on the contraction of CCh was 4.45, while the value on the contraction of 2-methyl-5-HT with pretreatment of methysergide was 5.10. ICS 205-930 caused a selective shift to the right of the second phase of the 5-HT curve. Galanolactone also shifted to the right of the second phase of the concentration-response curve selectively. The results suggest that 5-HT_3 antagonism is involved in the anti-5-HT action of galanolactone.

The results in the present study not only substantiate the known medicinal efficacy of ginger but also may help to develop a new type of anti-5-HT_3. Further experiments are currently in progress to examine the *in vivo* effect of galanolactone and to determine the active constituent in other fractions of ginger.

References

1) J. Yamahara, Q. R. Huang, M. Iwamoto, G. Kobayashi, H. Matsuda and H. Fujimura, *Phytotherapy Research*, **3**, 70 (1989).
2) P. L. R. Andrews, W. G. Rapeport and G. J. Sanger, *Tips*, **9**, 334 (1988).
3) H. Morita and H. Itokawa, *Planata Med.*, **54**, 117 (1988).
4) P. B. Bradley, G. Engel, W. Feniuk, J. R. Fozard, P. P. A. Humphrey, D. N. Middelemiss, E. J. Mylecharane, B. P. Richardson and P. R. Saxena, *Neuropharmacology*, **25**, 563 (1986).
5) K. H. Buchheit, G. Engel, A. Hagenbach, D. Hoyer, H. O. Kalkman and M. P. Seiler, *Br. J. Pharmacol.*, **71**, 74 (1986).
6) B. P. Richardson and G. Engel, *Tins.*, **9**, 424 (1986).
7) B. P. Richardson, G. Engel, P. Donatsch and P. A. Stadler, *Nature* (London), **316**, 126 (1985).
8) N. W. Pedigo, H. J. Yamamura and D. L. Nelson, *J. Neurochem.*, **36**, 220 (1981).
9) K. H. Buchheit, G. Engel, E. Mutschler and B. Richadrson, *Naunyn-Schmied. Arch. Pharmacol.*, **329**, 36 (1985).

Studies on Absorption, Distribution, Excretion and Metabolism of Ginseng Saponins. VI.[1] The Decomposition Products of Ginsenoside Rb_2 in the Stomach of Rats

Masami KARIKURA,*,[a] Toshio MIYASE,[a] Hisayuki TANIZAWA,[a] Toshio TANIYAMA,[b] and Yoshio TAKINO[a]

School of Pharmaceutical Sciences, University of Shizuoka,[a] 395, Yada, Shizuoka 422, Japan and Koshiro Co., Ltd.,[b] 2–5–8, Dosho-machi, Chuo-ku, Osaka 541, Japan. *Received August 16, 1990*

The decomposition of ginsenoside Rb_2 (Rb_2) in rat stomach (*in vivo*) and in 0.1 N HCl solution (*in vitro*) was investigated in detail. By treating with 0.1 N HCl, the acidity of which is similar to that of gastric juice, a part of Rb_2 was hydrolyzed to 20(*R*,*S*)-ginsenoside Rg_3. On the other hand, Rb_2 was little decomposed in rat stomach and a small quantity of an unidentified metabolite, which was different from the hydrolyzed products in 0.1 N HCl, was observed. The metabolite was separated into four compounds, which were identified by ^1H- and ^{13}C-nuclear magnetic resonance and fast atom bombardment mass spectrometry. These compounds were determined to be 25-hydroxy-23-ene (IV), 24-hydroxy-25-ene (V), 25-hydroperoxy-23-ene (VI) and 24-hydroperoxy-25-ene (VII) derivative of Rb_2, respectively.

In this study, it is suggested that 20(*S*)-protopanaxatriol saponins undergo hydrolysis of the C-20 glycosyl moiety and hydration of the side chain, on the other hand, 20(*S*)-protopanaxadiol saponins undergo oxygenation of the side chain.

Keywords ginsenoside Rb_2; metabolism; rat stomach; hydroperoxide; ^1H-NMR; ^{13}C-NMR; FAB-MS; TLC; HPLC; ginseng saponin

In traditional Chinese medicine, the root of *Panax ginseng* C. A. MEYER (Araliaceae) is an important component in various prescriptions. Ginseng saponins, isolated from the root of *Panax ginseng*, have been regarded as the principal ingredients responsible for the pharmacological activities of the drug. Since few studies have been performed on the pharmacokinetics of ginseng saponins, further experiments are necessary for their evaluation. From this view point, we studied and reported on the pharmacokinetics of ginsenoside-Rg_1 (Rg_1) and -Rb_1 (Rb_1) in the rat gastrointestinal tract previously.[2] Continuously, we started the study on ginsenoside Rb_2 (Rb_2), one of the main 20(*S*)-protopanaxadiol saponins in Ginseng Radix, and already reported the decomposition products of Rb_2 in rat large intestine.[1] In that study, we have isolated five prosapogenins derived from Rb_2 in rat cecal contents, and discussed the decomposition pathway of Rb_2 in rat large intestine. In this paper, we describe the decomposition products of Rb_2 in rat stomach after oral administration and discuss the differences in decomposition of Rb_2 in 0.1 N HCl solution.

Experimental

Most of the materials were the same as described in our previous study.[1]

^1H- and ^{13}C-Nuclear Magnetic Resonance (^1H- and ^{13}C-NMR) ^1H-NMR spectra were measured with a JEOL model GSX-500 (500 MHz) spectrometer and ^{13}C-NMR spectra were measured with JEOL model FX-90Q (22.5 MHz) and GSX-270 (67.8 MHz) spectrometers. Chemical shifts are given on the δ scale (ppm) with tetramethylsilane as an internal standard (s, singlet; d, doublet; t, triplet; br s, broad singlet).

Fast Atom Bombardment Mass Spectrometry (FAB-MS) FAB-MS was measured with a JEOL JMS-SX102 mass spectrometer.

Thin-Layer Chromatography (TLC) Normal phase TLC was performed on Merck precoated Silica gel 60 F_{254} plates (0.25 mm thick). Reverse phase TLC was performed on Merck precoated RP-8 F_{254}s plates (0.25 mm thick). Developing solvents for normal and reverse phase TLC were a $CHCl_3$–MeOH–H_2O (65 : 35 : 10, v/v, lower phase) mixture and 35% aqueous CH_3CN, respectively. TLC spots were detected by spraying with 1% $Ce(SO_4)_2$–10% H_2SO_4 solution followed by heating (150 °C, 3—4 min).

Column Chromatography Silica gel 60 (230—400 mesh, Merck) and Bondapak C_{18} (Waters) were used for column chromatography.

High-Performance Liquid Chromatography (HPLC) HPLC was performed using a Shimadzu LC-6A liquid chromatograph with a Shimadzu SPD-6A ultraviolet detector, in a YMC-packed column AQ-312 (ODS, 5 μm, 6 × 150 mm, YMC) under the following conditions: 27% or 45% aqueous CH_3CN as the mobile phase, flow rate 1.0 ml/min, detection wavelength 202 nm. Compounds were isolated by a YMC-packed column SH-343-5 (ODS, 5 μm, 20 × 250 mm, YMC) under the following conditions: 35% or 80% aqueous CH_3CN as the mobile phase, flow rate 5.0 ml/min, detection wavelength 205 nm.

Chemical Decomposition of Rb_2 1) Hydrolysis of Rb_2 with 0.1 N HCl: Rb_2 (10 mg) was dissolved in 2 ml of 0.1 N HCl, and incubated at 37 °C for 24 h, then treated with a SEP-PAK® C_{18} cartridge (SEP-PAK) according to the procedure in Chart 1. The obtained decomposition products were subjected to TLC and HPLC.

2) Isolation of Hydrolysis Products of Rb_2: Rb_2 (200 mg) was dissolved in 0.1 N HCl (50 ml), incubated at 37 °C for 8 h, and chromatographed on a Bondapak C_{18} column (25 × 200 mm) pre-equilibrated with water. The column was washed with water (1 l) and 40% aqueous MeOH (2 l), and eluted with 80% aqueous MeOH which yielded two fractions after removal of the solvent under reduced pressure; fraction 1 (50 mg) and fraction 2 (130 mg). Fraction 1 was purified by HPLC (35% aqueous CH_3CN) to afford Rb_2 (40 mg). Fraction 2 was separated by HPLC (80% aqueous CH_3CN) into two fractions designated I (50 mg) and II (40 mg). The identifications of I and II were performed by comparison of ^{13}C-NMR spectral data with the reported values.[3]

Biological Decomposition of Rb_2 1) Decomposition of Rb_2 in Rat Stomach: Rb_2 (100 mg/kg, 2% aqueous solution) was administered orally to rats. After exsanguination from the abdominal artery under anesthesia with ether at 30, 60 or 90 min after administration, the stomach was isolated. The contents were flushed with MeOH and treated according to the procedure in Chart 1.

2) Isolation of Decomposition Products of Rb_2: a) Incubation of Rb_2 in Rat Cecal Content: The whole cecal contents of a normal rat were suspended in 50 ml of 0.9% saline. Rb_2 (20 mg) was added to the suspension and incubated at 37 °C for 3 h. 100 ml of MeOH was added, and the mixture was centrifuged (3000 rpm, 10 min). The supernatant was evaporated to dryness below 40 °C under reduced pressure, and the residue was treated with a SEP-PAK, and subjected to normal and reverse phase TLC. A spot identical to the decomposition product from rat stomach was detected in an incubation sample.

b) Isolation of Decomposition Products of Rb_2: The whole cecal contents of 3 normal rats were suspended in 0.9% saline (100 ml) containing 300 mg of Rb_2 and incubated at 37 °C for 8 h. MeOH (400 ml) was added, and the mixture was centrifuged (3000 rpm, 10 min). The supernatant was evaporated to dryness below 40 °C under reduced pressure. The residue was suspended in water (50 ml), and injected into a Bondapak C_{18} column (Waters, 25 × 200 mm) pre-equilibrated with water. After washing the column with water (1 l) and 40% aqueous MeOH (2 l), adsorbates were eluted with 80% aqueous MeOH (1 l). The solvent was removed under

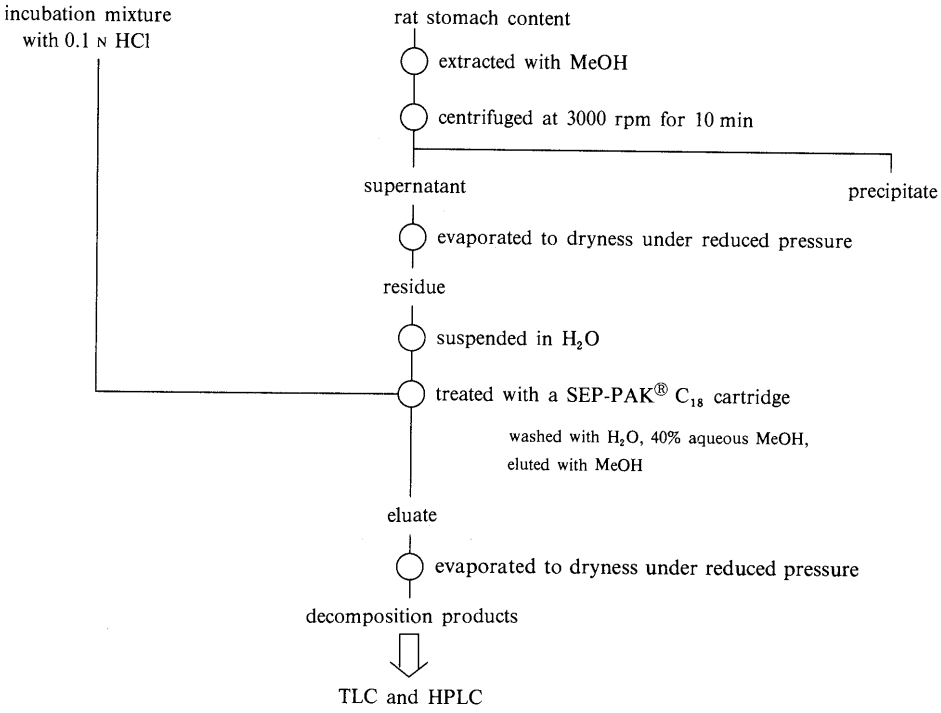

Chart 1. Procedure for Obtaining Decomposition Products of Ginsenoside Rb_2

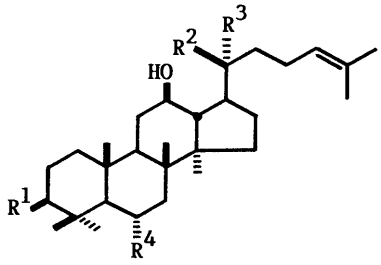

	R^1	R^2	R^3	R^4
Rb_2	-O-glc^2—glc	-O-glc^6—arap	$-CH_3$	-H
I	-O-glc^2—glc	-OH	$-CH_3$	-H
II	-O-glc^2—glc	$-CH_3$	-OH	-H
Rb_1	-O-glc^2—glc	-O-glc^6—glc	$-CH_3$	-H
Rg_1	-OH	-O-glc	$-CH_3$	-O-glc

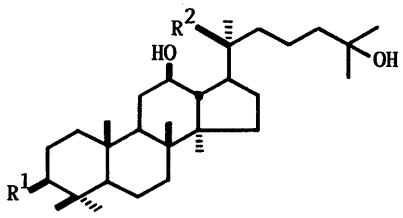

	R^1	R^2
III	-O-glc^2—glc	-O-glc^6—arap

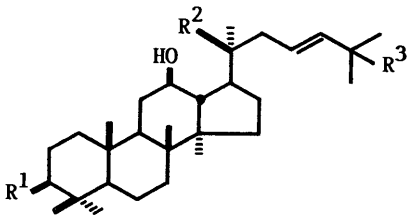

	R^1	R^2	R^3
IV	-O-glc^2—glc	-O-glc^6—arap	-OH
VI	-O-glc^2—glc	-O-glc^6—arap	-OOH

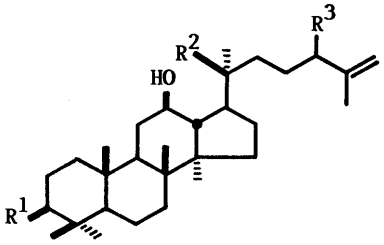

	R^1	R^2	R^3
V	-O-glc^2—glc	-O-glc^6—arap	-OH
VII	-O-glc^2—glc	-O-glc^6—arap	-OOH

Chart 2. Chemical Structures

glc; β-D-glucopyranosyl, arap; α-L-arabinopyranosyl.

TABLE I. ^{13}C-NMR Data for Rb_2, III, IV, V, VI, and VII[a)]

Carbon	Rb_2	III	IV	V	VI	VII
C-17	51.7	51.9	52.1	52.0	52.0	51.6
C-20	83.5	83.8	83.4	83.8	83.3	83.6
C-21	22.4	22.5	23.3	22.7	23.4	22.5
C-22	36.2	37.0	39.8	32.8	40.2	32.8
C-23	23.2	19.3	122.7	30.7	126.6	26.6
C-24	126.0	45.5	142.4	76.0	138.1	90.1
C-25	131.1	69.8	69.9	150.1	81.3	146.2
C-26	25.8	30.1	30.7	110.1	25.4	113.5
C-27	17.9	30.1	30.7	18.5	25.1	17.7
3-*O*-*β*-D-Glucopyranosyl						
C-1′	105.1	105.1	105.1	105.1	105.1	105.1
2′-*O*-*β*-D-Glucopyranosyl						
C-1″	106.1	106.1	106.1	106.1	106.1	105.8
20-*O*-*β*-D-Glucopyranosyl						
C-1‴	98.1	98.2	98.3	98.2	98.3	98.0
6‴-*O*-*α*-L-Arabinopyranosyl						
C-1⁗	104.6	104.4	104.2	104.4	104.3	104.6

a) Measured at 67.8 MHz in pyridine-d_5. Chemical shifts are in δc.

reduced pressure and the residue was subjected to silica gel column chromatography [silica gel 40 g, $CHCl_3$–MeOH–H_2O (65 : 35 : 10, v/v, lower phase)], followed by preparative HPLC (35% aqueous CH_3CN) to yield IV (3 mg), V (2 mg), VI (15 mg), VII (2 mg), and Rb_2 (100 mg). The identifications of these compounds were performed from their FAB-MS and by comparison of their ^{13}C-NMR spectral data with the reported values.[4,5] Their chemical structures and ^{13}C-NMR spectral data are shown in Chart 2 and Table I, respectively.

Rb_2: FAB-MS *m/z*: 1079 $(M+H)^+$, 1101 $(M+Na)^+$. ^{1}H-NMR (pyridine-d_5) δ: 0.82 (3H), 0.96 (6H), 1.11, 1.28, 1.65 (3H each) (all s, *tert*-$CH_3 \times 6$), 1.63, 1.67, (3H each, both s, vinyl. CH_3), 4.90, 5.00, 5.14, 5.38 (1H each, all d, $J=7.8$, 6.4, 7.8, 7.3 Hz, respectively, anomeric H × 4), 5.33 (1H, t, $J=6.4$ Hz, C_{24}-H). ^{13}C-NMR: shown in Table I.

IV: FAB-MS *m/z*: 1095 $(M+H)^+$, 1117 $(M+Na)^+$. ^{1}H-NMR (pyridine-d_5) δ: 0.84, 0.88, 1.01, 1.11, 1.29 (3H each), 1.56 (6H), 1.61 (3H) (all s, *tert*-$CH_3 \times 8$), 4.93, 5.00, 5.18, 5.38 (1H each, all d, $J=7.6$, 5.8, 7.6, 7.6 Hz, respectively, anomeric H × 4), 6.23 (1H, ddd, $J=7.0$, 8.2, 15.0 Hz, C_{23}-H), 6.08 (1H, d, $J=15.3$ Hz, C_{24}-H).

V: FAB-MS *m/z*: 1095 $(M+H)^+$, 1117 $(M+Na)^+$. ^{1}H-NMR (pyridine-d_5) δ: 0.80 (3H), 0.93 (6H), 1.10, 1.28, 1.64 (3H each) (all s, *tert*-$CH_3 \times 6$), 1.94 (3H) (s, vinyl. CH_3), 4.92, 5.04, 5.15, 5.37 (1H each, all d, $J=7.9$, 5.8, 7.6, 7.3 Hz, respectively, anomeric H × 4), 4.91, 5.26 (1H each, both br s, C_{26}-H_2).

VI: FAB-MS *m/z*: 1133 $(M+Na)^+$. ^{1}H-NMR (pyridine-d_5) δ: 0.84, 0.88, 1.02, 1.11, 1.29, 1.60 (3H each), 1.61 (6H) (all s, *tert*-$CH_3 \times 8$), 4.93, 5.02, 5.18, 5.38 (1H each, all d, $J=7.6$, 6.2, 7.6, 7.6 Hz, respectively, anomeric H × 4), 6.14 (2H, s, C_{23}-H and C_{24}-H).

VII: FAB-MS *m/z*: 1111 $(M+H)^+$, 1133 $(M+Na)^+$. ^{1}H-NMR (pyridine-d_5) δ: 0.79 (3H), 0.94 (6H), 1.10, 1.26, 1.62 (3H each) (all s, *tert*-$CH_3 \times 6$), 1.97 (3H) (s, vinyl. CH_3), 4.91, 5.00, 5.10, 5.39 (1H each, all d, $J=7.6$, 6.1, 7.9, 7.6Hz, respectively, anomeric H × 4), 5.06, 5.23 (1H each, both br s, C_{26}-H_2).

3) Identification of Decomposition Products in Rat Stomach: a) Synthesis of a C-25, 26 Hydrated Derivative of Rb_2 (III): Rb_2 (200 mg) was acetylated with Ac_2O–pyridine (1 : 1) (3 ml) at room temperature for 8 h. After dilution with water (20 ml), the reaction mixture was extracted with AcOEt (100 ml). After washing the AcOEt layer with 10% HCl, saturated aqueous $NaHCO_3$ and water, the AcOEt solution was dried with $MgSO_4$, and concentrated to dryness *in vacuo*. The residue was dissolved in CH_2Cl_2 (5 ml), and *m*-chloroperbenzoic acid (200 mg) was slowly added. The reaction mixture was stirred for 2 h at room temperature. After adding AcOEt (100 ml), the extract was washed with saturated aqueous $NaHCO_3$ followed by water, then dried with $MgSO_4$, and concentrated to dryness *in vacuo*. The residue was dissolved in 4 ml of absolute tetrahydrofurane (THF), and $LiAlH_4$ (400 mg)–THF suspension was added stepwise to the solution. The reaction mixture was stirred for 2 h at room temperature, then the reaction was stopped by adding Et_2O (50 ml) saturated with water. After adding 10% HCl (50 ml), the aqueous fraction was injected into a Bondapak C_{18} column (Waters, 25 × 200 mm) pre-equilibrated with water. The column was washed with water (1 l) and the adsorbates were eluted with 80% aqueous MeOH (1 l). The solvent was removed under reduced pressure and the residue was purified by column chromatography [silica gel 40 g, $CHCl_3$–MeOH–H_2O (65 : 35 : 10, v/v, lower phase)] to yield III (50 mg). The identification of III was performed from its FAB-MS and by comparing the ^{13}C-NMR spectral data with reported values.[2d,6)] Its chemical structure and ^{13}C-NMR spectrum are shown in Chart 2 and Table I, respectively.

III: FAB-MS *m/z*: 1120 $(M+Na)^+$. ^{1}H-NMR (pyridine-d_5) δ: 0.83, 0.93, 1.02, 1.11, 1.29 (3H each), 1.41 (6H), 1.61 (3H) (all s, *tert*-$CH_3 \times 8$), 4.92, 4.99, 5.14, 5.37 (1H each) (all d, anomeric H × 4, $J=8.2$, 5.5, 7.3, 7.3 Hz, respectively).

b) Photosensitized Oxygenation of Rb_2:A solution of Rb_2 (100 mg) and Rosebengal (5 mg) in MeOH–pyridine (1 : 1) (5 ml) was irradiated with a Hg lamp (250 W) under a stream of O_2 for 1.5 h. The reaction mixture was diluted with MeOH, passed through a column of active charcoal to remove the pigment, and concentrated to dryness *in vacuo*. The residue was immediately separated by preparative HPLC (35% aqueous CH_3CN) into compounds IV (4.1 mg), V (5.5 mg), VI (15.5 mg), and VII (3.5 mg). These compounds (IV—VII) were identical to decomposition products of Rb_2 found in rat stomach by normal and reverse phase TLC, HPLC (27% aqueous CH_3CN), FAB-MS, and ^{1}H- and ^{13}C-NMR.

Results and Discussion

As shown in Fig. 1, Rb_2 was little decomposed in rat stomach after oral administration. A small quantity of a decomposition product whose *Rf* value is lower than that of Rb_2 was observed on normal phase TLC. On the other hand, 0.1 N HCl treatment, the acidity of which is similar to that of gastric juice, resulted in TLC decomposition products with higher *Rf* values than that of Rb_2 or the rat stomach decomposition product.

Initially, we investigated the major TLC spot (*Rf* value, 0.54) of the decomposition products obtained by 0.1 N HCl treatment. This spot was separated into two peaks by HPLC (ODS, 45% aqueous CH_3CN, Fig. 2). The main products (I and II) were isolated and purified by preparative HPLC, and identified by ^{13}C-NMR. In the ^{13}C-NMR data for I and II, all of the carbon signals due to the aglycone moiety except for the C-20 signal appeared at virtually identical positions as those of Rb_2, and the ^{13}C-NMR spectrum of I was different from that of II in the signals arising from C-13, C-16, C-17, C-21 and C-22. Therefore, I and II were assumed to be prosapogenins of Rb_2, and C-20 epimeric pair. Based on these results, I and II were considered identical to 20(*S*)-ginsenoside Rg_3 and ginsenoside Rg_3,

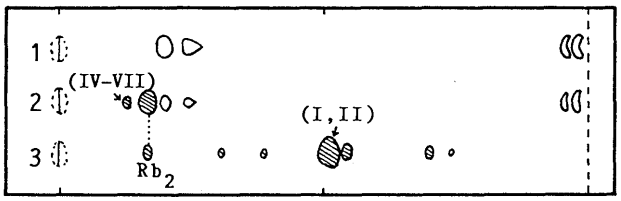

Fig. 1. Thin-Layer Chromatogram of Decomposition Products of Ginsenoside Rb_2 in Rat Stomach or in 0.1 N HCl

Developing solvent, $CHCl_3$–MeOH–H_2O (65:35:10, v/v, lower phase); plate, precoated Silica gel 60 F_{254} (Merck); detecting reagent, 1% of $Ce(SO_4)_2$–10% H_2SO_4 solution, with heated at 150 °C for 4 min. 1, normal rat; 2, Rb_2 (100 mg/kg, *p.o.*)-administered rat (1.5 h after treatment); 3, 0.1 N HCl (37 °C, 24 h).

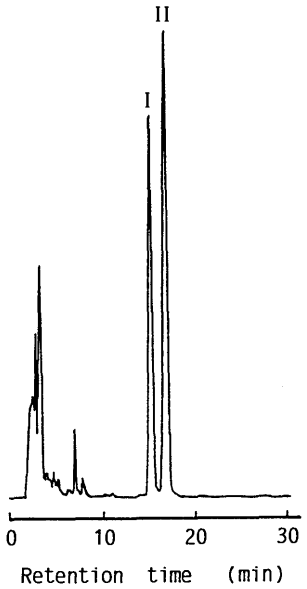

Fig. 2. HPLC Chromatogram of Decomposition Products of Ginsenoside Rb_2 in 0.1 N HCl

Column, YMC AQ-312 (ODS, 6 × 150 mm); mobile phase, 45% aqueous CH_3CN; flow rate, 1.0 ml/min; detection, UV 202 nm.

respectively, by comparison of the ^{13}C-NMR data for I and II with the reported values.[3)]

Next, we investigated an unidentified product in the rat stomach after oral administration, which was not found in 0.1 N HCl treated samples. From its TLC behavior, it was unlikely to be a hydrolysis product formed by elimination of O-glycosyl moieties from Rb_2. In our previous study,[2d)] C-25,26 hydrated ginsenoside Rh_1 was found as a metabolite of ginsenoside Rg_1 (Rg_1) in rat stomach. Therefore, we assumed the existence of a C-25, 26 hydrated derivative of Rb_2 (III), and attempted to synthesize as described in the experimental chapter. By comparing the ^1H- and ^{13}C-NMR spectra for III with those for Rb_2 and the reported values,[2d,6)] III was determined to be 3β,12β,20(*S*),25-tetrahydroxydammarane 3-*O*-[β-D-glucopyranosyl(1→2)-β-D-glucopyranoside]-20-*O*-[α-L-arabinopyranosyl(1→6)-β-D-glucopyranoside]. Comparison of the decomposition product of Rb_2 in the rat stomach with III was performed only by TLC method, and *Rf* value of the decomposition product was the same as that of III. However, further comparisons could not be done by either HPLC with a ultraviolet detector or ^{13}C-NMR, since III had no side chain double bond and the decomposition product was too low yield. Therefore, we attempted to incubate Rb_2 with rat

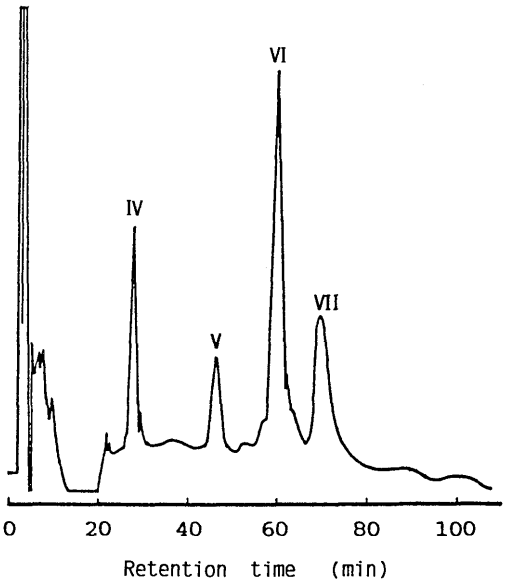

Fig. 3. HPLC Chromatogram of Biological Decomposition Products of Ginsenoside Rb_2

Column, YMC SH-343-5 (ODS, 20 × 250 mm); mobile phase, 32% aqueous CH_3CN; flow rate, 5.0 ml/min; detection, UV 205 nm.

cecal contents to yield the decomposition product in large quantities, since we have found a similar TLC spot in metabolites of Rb_2 in rat large intestine.[1)] We isolated the fraction whose *Rf* value was identical to that of the decomposition product by silica gel column chromatography, and subjected it to ^{13}C-NMR. Its ^{13}C-NMR data indicated that it was not yet pure and the double bonds (δ 113.5, 126.6, 138.1, and 146.2 ppm) existed in it. Therefore, it has become apparent that the decomposition product in the rat stomach was not III. Based on these results, this fraction was subjected to HPLC, and we found that although it appears to be one spot on TLC, it was separated into four peaks by HPLC (ODS, 27% aqueous CH_3CN). Therefore, this fraction was further isolated by preparative HPLC (Fig. 3) to yield four compounds (IV—VII). Comparison of their $(M+Na)^+$ ions in FAB-MS with that of Rb_2 led us to consider that a hydroxyl group exists in IV and V, and that a hydroperoxyl group exists in VI and VII. By comparison of the ^{13}C-NMR data for IV with those for chikusetsusaponin L_{9a}[4a)] and gypenoside LX,[4b)] the signals (δ 39.8, 122.7, 142.4, 69.9, 30.7 and 30.7 ppm) of IV were assignable to the side chain carbons. Consequently, IV was identified as 3β,12β,20(*S*),25-tetrahydroxydammar-23-ene 3-*O*-[β-D-glucopyranosyl(1→2)-β-D-glucopyranoside]-20-*O*-[α-L-arabinopyranosyl(1→6)-β-D-glucopyranoside]. By comparison of the ^{13}C-NMR data for V with those for ginsenoside M_{7cd}[5a)] and gypenoside LXXI,[5b)] the signals (δ 32.8, 30.7, 76.0, 150.1, 110.1 and 18.5 ppm) assignable to the side chain carbon led us to determine that V is 3β,12β,20(*S*),24(*S*)-tetrahydroxydammar-25-ene 3-*O*-[β-D-glucopyranosyl(1→2)-β-D-glucopyranoside]-20-*O*-[α-L-arabinopyranosyl(1→6)-β-D-glucopyranoside]. By referring to the reported papers,[7)] it was reasonable to consider that the ^{13}C-NMR signals of VI and VII (at δ 81.3 and 90.1 ppm, respectively) are assignable to that of the carbon attached to a hydroperoxyl group. In order to verify this presumption, Rb_2 was subjected to photosensitized oxygenation, and the products were identical to VI and VII.

Consequently, VI and VII were determined to be 3β,-12β,20(S)-trihydroxy-25-hydroperoxydammar-23-ene 3-O-[β-D-glucopyranosyl(1→2)-β-D-glucopyranoside]-20-O-[α-L-arabinopyranosyl(1→6)-β-D-glucopyranoside] and 3β,12β,20(S)-trihydroxy-24(S)-hydroperoxydammar-25-ene 3-O-[β-D-glucopyranosyl(1→2)-β-D-glucopyranoside]-20-O-[α-L-arabinopyranosyl(1→6)-β-D-glucopyranoside], respectively.

This study is the first report in which the presence of Rb_2 hydroperoxides is confirmed in rat stomach and cecum. The hydroperoxides of dammarane type saponins were predicted as intermediates in photosensitized oxidation followed by reduction.[4a,5a] However, the isolation and measurement of the ^{1}H- and ^{13}C-NMR spectra of Rb_2 hydroperoxides have not been reported in plants or animals until the present. It appears that production of Rb_2 hydroperoxides is due to the lipoxygenases, which are widely distributed *in vivo*. In our experiments, Rb_2 hydroperoxides were stable in the solid state, but decomposed gradually in aqueous and methanolic solutions into the corresponding hydroxides. It is not clear whether Rb_2 hydroperoxides are produced initially or together with the hydroxides in the rat stomach.

Han *et al.*[6] have reported that ginsenosides (Rg_1, Re and Rb_1) were hydrated easily in the side chain under mild acidic conditions (with 0.1 N HCl, at 37 °C). In our results so far, C-25,26 hydrated derivatives of Rg_1 were detected in both rat stomach and in 0.1 N HCl, but those of Rb_1 and Rb_2 were produced in neither media. This means that C-20 glucosyl moiety of Rg_1 is easily hydrolyzed and the side chain is easily hydrated, on the other hand, O-glycosyl moieties of Rb_1 and Rb_2 are fairly stable and the hydration does not occur in rat stomach.

The above facts led us to consider that the decomposition modes are different between 20(S)-protopanaxatriol saponins and 20(S)-protopanaxadiol saponins, and that 20(S)-protopanaxadiol saponins undergo oxygenation rather than hydration in the side chain. The decomposition pathway of Rb_2 in rat stomach or 0.1 N HCl is summarized in Chart 3. Hereafter, we also intend to investigate the oxygenation of Rb_1 in the sense of comparison with Rb_2.

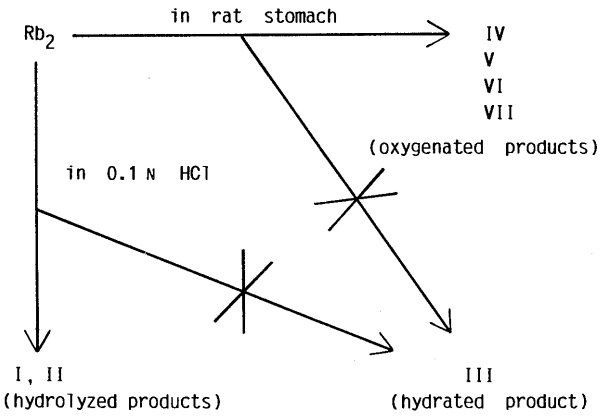

Chart 3. Decomposition Pathway of Ginsenoside Rb_2 in Rat Stomach or in 0.1 N HCl

Acknowledgment The authors are grateful to the Korea Ginseng and Tabako Research Institute and the Japan-Korea Red Ginseng Co., Ltd., for the supply of pure Rb_2. This work was supported in part by a grant from the Medical Society for Red Ginseng Research.

References

1) M. Karikura, T. Miyase, H. Hisayuki, Y. Takino, T. Taniyama, and T. Hayashi, *Chem. Pharm. Bull.*, **38**, 2859 (1990).
2) *a*) Y. Takino, T. Odani, H. Tanizawa, and T. Hayashi, *Chem. Pharm. Bull.*, **30**, 2196 (1982); *b*) T. Odani, H. Tanizawa, and Y. Takino, *ibid.*, **31**, 292 (1983); *c*) *Idem, ibid.*, **31**, 1059 (1983); *d*) *Idem, ibid.*, **31**, 3691 (1983).
3) *a*) I. Kitagawa, M. Yoshikawa, M. Yoshihara, T. Hayashi, and T. Taniyama, *Yakugaku Zasshi*, **103**, 612 (1983); *b*) R. Kasai, H. Besso, O. Tanaka, Y. Saruwatari, and T. Fuwa, *Chem. Pharm. Bull.*, **31**, 2120 (1983); *c*) J. Asakawa, R. Kasai, K. Yamasaki, and O. Tanaka, *Tetrahedron*, **33**, 1935 (1977).
4) *a*) S. Yahara, R. Kasai, and O. Tanaka, *Chem. Pharm. Bull.*, **25**, 2041 (1977); *b*) T. Takemoto, S. Arihara, and K. Yoshikawa, *Yakugaku Zasshi*, **106**, 664 (1986).
5) *a*) S. Yahara, K. Kaji, and O. Tanaka, *Chem. Pharm. Bull.*, **27**, 88 (1979); *b*) K. Yoshikawa, T. Takemoto, and S. Arihara, *Yakugaku Zasshi*, **107**, 262 (1987).
6) B. H. Han, M. H. Park, Y. N. Han, L. K. Woo, U. Sankawa, S. Yahara, and O. Tanaka, *Planta Medica*, **44**, 146 (1982).
7) *a*) I. Kitagawa, Z. Cui, B. W. Son, M. Kobayashi, and Y. Kyogoku, *Chem. Pharm. Bull.*, **35**, 124 (1987); *b*) M. Kobayashi, B. W. Son, Y. Kyogoku, and I. Kitagawa, *ibid.*, **32**, 1667 (1984).

Analgesic Principles from *Aralia cordata* THUNB.

Emi OKUYAMA, Satoshi NISHIMURA, and Mikio YAMAZAKI*

Faculty of Pharmaceutical Sciences, Chiba University, 1-33 Yayoi-cho, Chiba 260, Japan. *Received August 20, 1990*

The analgesic principles from *Aralia cordata* THUNB. were identified with (*ent*)-kaur-16-en-19-oic acid (KA) and (*ent*)-pimara-8(14),15-dien-19-oic acid (PA), respectively. Both compounds were significantly effective regarding analgesics, hypothermia, duration of pentobarbital-induced anesthesia, and depression of locomotor activity enhanced by methamphetamine at doses of 300 mg/kg (KA) and 500 mg/kg (PA) by oral administration.

Keywords *Aralia cordata*; Kyohkatsu; Dokukatsu; Qiang-huo; Du-huo; (*ent*)-kaur-16-en-19-oic acid; (*ent*)-pimara-8(14),15-dien-19-oic acid; pharmacologically active principle; analgesics

During our screening of neurotropic components from traditional medicinal plants, the methanol extract of *Aralia cordata* THUNB. (Araliaceae) showed hypothermic and analgesic effects and an elongation effect on pentobarbital-induced anesthesia in mice. Isolation of the pharmacologically active principles from this plant is described in this paper.

Traditional Chinese medicines named "Du-huo" and "Qiang-huo" in Chinese ("Dokukatsu" and "Kyohkatsu" in Japanese, respectively) have been used in remedies to produce analgesic effects. However, there is some confusion about their original plants.[1] Nowadays, in Japan, *A. cordata* is used as (Wa-)kyohkatsu or (Wa-)dokukatsu ("Wa" means Japanese in Japanese) with the same expectation.

The methanol extract of the roots of *A. cordata* showed a 66% inhibitory effect ($p<0.01$) on acetic acid-induced writhing at a dose of 2.0 g/kg, and 444% elongation ($p<0.001$) of pentobarbital-induced sleeping time, as well as $-1.0\,^{\circ}C$ ($p<0.01$) of ΔT_{max} (the maximum of body temperature differences) at a dose of 3.0 g/kg by oral administration (*p.o.*) in mice.

The extract was separated with the guidance of hypothermic effects in mice (Chart 1). Partition of the extract with *n*-butanol and water gave the hypothermic organic layer, which was then fractionated by LH-20 column chromatography. Fractions C and D, which were the most potent, were further purified by silica gel column chromatography to get frs. C-b and D-b (the total yield of combined frs. C-b and D-b: 10.8% from the extract) which appeared as a single spot on the silica gel thin-layer chromatography (TLC) plate, but as two spots on a reverse-phased plate. This fraction showed $-3.1\,^{\circ}C$ of ΔT_{max} at a dose of 500 mg/kg (*p.o.*) and seemed to contain the major components of *A. cordata*. The potency did not increase extensively during purification, perhaps due to the fact that purification caused less solubility and less absorption of the samples by the mice during the bioassay. The fraction also exhibited 69% inhibition ($p<0.001$) on acetic acid-induced writhing symptoms (500 mg/kg, *p.o.*) and 250% elongation ($p<0.001$) of pentobarbital-induced sleeping time (500 mg/kg, i.p.: intraperitoneal administration) in mice. By using reverse-phased medium pressure liquid chromatography (MPLC), the effective fraction was finally separated into compounds I and II (compds I and II).

Compd I was crystallized from *n*-hexane to give colorless needles, which have a melting point (mp) 164.5—166 °C and $[\alpha]_D^{16}$ $-120°$. Crystallization of compd II from methanol afforded colorless prisms, mp 178—180 °C. $[\alpha]_D^{16}$ $-110°$. The carbon-13 nuclear magnetic resonance (^{13}C-NMR) spectra of both compounds showed 20 carbon signals, one of which was assigned as carboxylic acid at δ 184.2 (compd I) and 184.6 (compd II) with relation to the absorptions at 1696 (compd I) and 1693 cm^{-1} (compd II) in the infrared (IR) spectra. In the proton nuclear magnetic resonance (^{1}H-NMR) spectra there were no OH signals except from the carboxylic acids assigned at δ 11.74 (compd I) and *ca.*

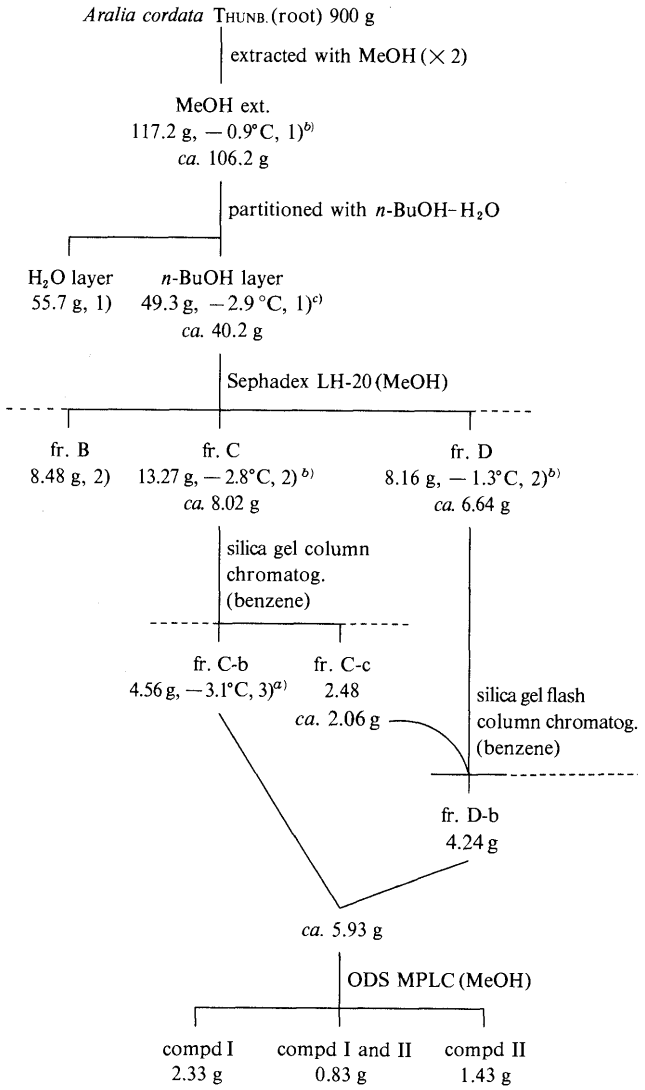

Chart 1. Isolation of Analgesic Principles from *A. cordata* THUNB.

1) 3.0 g/kg, 2) 2.0 g/kg, 3) 500 mg/kg. *a*) $p<0.05$, *b*) $p<0.01$, *c*) $p<0.001$, $n=3$—6.

11.58 (compd II). Compds I and II seemed to be diterpenoic acids with no hydroxyl group, because some diterpenoic acids have been isolated from *A. cordata*.[2b] Compd I was shown to have three methyl signals at δ 13.8, 29.1 and 29.3 in the ^{13}C-NMR, and δ 0.65, 1.26 and 1.00 (each 3H, s) in the ^{1}H-NMR, respectively. Two types of double bond moieties were also observed at δ 137.9 and 128.0 [δ 5.14 (1H, s) in the ^{1}H-NMR] and δ 147.2 and 112.9 [δ 5.71 (1H, dd, J=17.1 and 10.5 Hz), 4.91 (1H, dd, J=17.3 and 1.9 Hz) and 4.94 (1H, dd, J=10.7 and 1.9 Hz) in the ^{1}H-NMR] in the ^{13}C-NMR. These data and the other properties of compd I were quite similar to those of (*ent*)-pimara-8(14),15-dien-19-oic acid (PA), a major diterpenoic acid isolated from *A. cordata*[2] (Fig. 1). Compd I was directly identified with the authentic sample[3] by TLC (Merck HPTLC RP-18, methanol; Merck Kieselgel GF_{254}, benzene–acetone 10:1), IR and ^{1}H-NMR. The mp was not depressed by mixed fusion.

The ^{1}H- and ^{13}C-NMR of compd II revealed the presence of an *exo*-methylene by observing the signals at δ 155.9 and 103.0 in the ^{13}C-NMR and δ 4.78 and 4.80 (each 1H, s) in the ^{1}H-NMR, indicating a similarity of compd II to (*ent*)-kaur-16-en-19-oic acid (KA), another major component of *A. cordata*.[2] Compd II and the authentic sample were identical by TLC (Merck HPTLC RP-18, methanol; Merck Kieselgel GF_{254}, benzene–acetone 10:1), IR and ^{1}H-NMR. The mp was not depressed by mixed fusion.

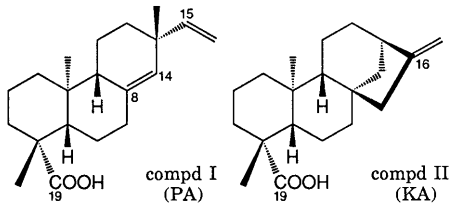

Fig. 1. Structures of Compds I (PA) and II (KA)

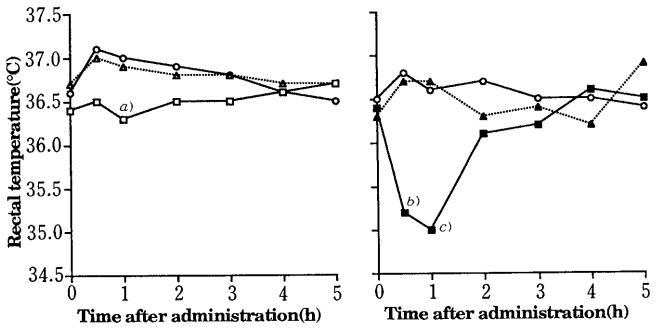

Fig. 2. Hypothermic Effects (*p.o.*) of Compds I (PA) and II (KA) in Mice

—○—, control; ---△---, PA 300 mg/kg; ---▲---, PA 500 mg/kg; —□—, KA 300 mg/kg; —■—, KA 500 mg/kg. *a*) $p<0.05$, *b*) $p<0.01$, *c*) $p<0.001$, $n=6$.

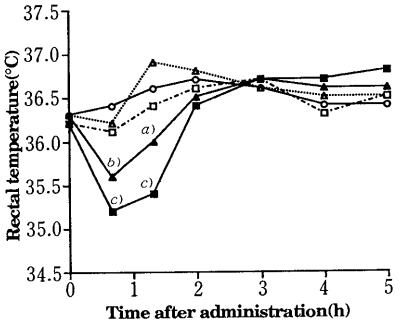

Fig. 3. Hypothermic Effects (i.p.) of Compds I (PA) and II (KA) in Mice

—○—, control; ---△---, PA 50 mg/kg; —▲—, PA 100 mg/kg; —·—□—·—, KA 50 mg/kg; —■—, KA 100 mg/kg. *a*) $p<0.05$, *b*) $p<0.01$, *c*) $p<0.001$, $n=6$.

The hypothermic effects of compds I(PA) and II(KA) in mice are shown in Fig. 2. (*p.o.*) and Fig. 3. (i.p.). Compd II(KA) caused hypothermia with -1.6 °C ($p<0.001$) and -0.7 °C ($p<0.05$) of ΔT_{max}'s at doses of 500 and 300 mg/kg, respectively by oral administration. Intraperitoneal injection of 100 mg/kg of compd I(PA) indicated -0.8 °C ($p<0.01$) of ΔT_{max}, although it did not show a significant effect at 500 mg/kg of oral administration.

The analgesic effects of both compounds in mice are

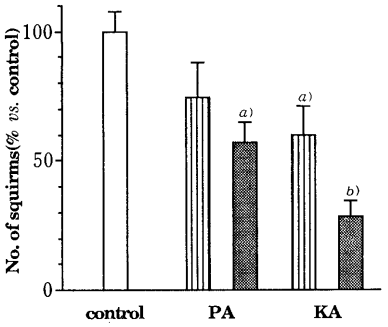

Fig. 4. Analgesic Activities of Compds I (PA) and II (KA) on Acetic Acid-Induced Writhing Symptoms in Mice

□, control; ▥, 300 mg/kg; ▩, 500 mg/kg. *a*) $p<0.01$, *b*) $p<0.001$. Each bar represents the mean ± S.D. n(samples) = 10, n(control) = 20.

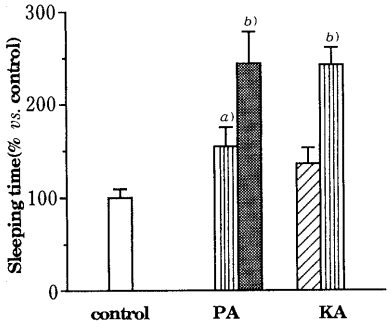

Fig. 5. Effects of Compds I (PA) and II (KA) on Duration of Anesthesia Induced by Sodium Pentobarbital in Mice

▨, 150 mg/kg; ▥, 300 mg/kg; ▩, 500 mg/kg. *a*) $p<0.05$, *b*) $p<0.001$. Each bar represents the mean ± S.D. n(samples) = 10, n(control) = 20.

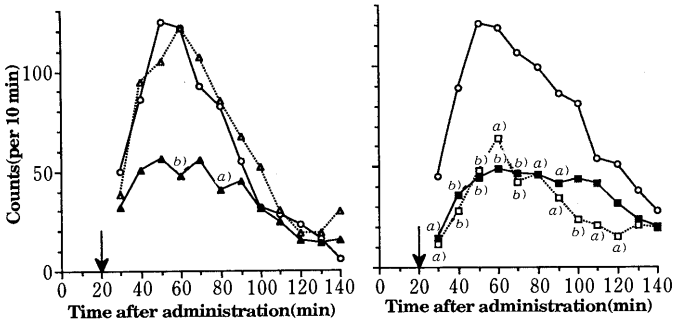

Fig. 6. Effects of Compds I (PA) and II (KA) on Locomotor Activity in Methamphetamine-Treated Mice

—○—, control; ---△---, PA 300 mg/kg; —▲—, PA 500 mg/kg; ---□---, KA 300 mg/kg; —■—, KA 500 mg/kg. *a*) $p<0.05$, *b*) $p<0.01$. 0 time, administration of test samples; ↓, methamphetamine-injection. n(control and KA) = 8, n(PA) = 6.

indicated in Fig. 4. Compds I(PA) and II (KA) reduced 43% ($p<0.01$) and 40% ($p<0.01$) of acetic acid-induced writhing by oral administration of 500 and 300 mg/kg, respectively. Both compounds also seemed to have dose-dependent effects on the duration of sleeping time induced by pentobarbital. The results are shown in Fig. 5.

Compds I(PA) and II(KA) produced sedative effects at oral doses of 500 and 300 mg/kg, respectively, on locomotor activity enhanced by methamphetamine (Fig. 6).

These results indicate that compds I and II, which were identified with (*ent*)-pimara-8(14),15-dien-19-oic acid (PA) and (*ent*)-kaur-16-en-19-oic acid (KA), respectively are pharmacologically active principles of *A. cordata*; however compd I was less effective in mice than compd II on analgesics, duration of pentobarbital-induced anesthesia, hypothermic effect and depression of locomotor activity enhanced by methamphetamine. Although the chemical structure of steviol (the 13-hydroxy derivative) was similar to that of KA, it did not show a hypothermic effect at the dose of 500 mg/kg (*p.o.*) in mice. This is the first report that a kaurenoic acid and a pimaradienoic acid contain pharmacological activities such as analgesic and sedative effects.

Experimental

Melting points were determined on a Yanagimoto melting point apparatus and are uncorrected. IR spectra were recorded on a Hitachi EPI-G3 spectrometer, and optical rotations were measured with a JASCO DIP-140 polarimeter. ^{1}H- and ^{13}C-NMR were recorded on JEOL GSX 400 and 500 spectrometers using tetramethylsilane as an internal standard. The following abbreviations are used: s = singlet, d = doublet, t = triplet, m = multiplet, br = broad. Column chromatographies were performed on Sephadex LH-20, Wakogel C-200 and Nakarai Silica gel 60. Two pre-packed columns (Kusano CPO-HS-221-20) connected in series were used for MPLC.

Isolation The dried plant was purchased by Kinokuniya Kan-yakkyoku Co., Ltd.

The material (900 g) was extracted with methanol at room temperature. The methanol extract (106.2 g) was partitioned with *n*-butanol and water to get a hypothermic *n*-butanol layer (49.3 g), which was chromatographed on Sephadex LH-20 (methanol). Fractions C and D containing activity were further separated independently by silica gel column chromatography eluted with benzene to give effective fractions, frs. C-b and D-b, respectively, which appeared as a single spot on silica gel TLC (Merck HPTLC, benzene–ethyl acetate 5 : 1). Both fractions were combined (12.7 g of the total yield calculated from the extract), and *ca.* 5.9 g of it was pursued by reverse-phased MPLC (methanol). Thus, the bioactive components, compds I (2.33 g) and II (1.43 g) were obtained.

Compd I Colorless needles from *n*-hexane, mp 164.5—166 °C, $[\alpha]_D^{16}$ −120° ($c=0.75$, $CHCl_3$). IR (KBr): 3425br, 2955, 1696, 1451, 1267, 920 cm^{-1}. ^{1}H-NMR ($CDCl_3$) δ: 0.65 (3H, s), 1.00 (3H, s), 1.05 (2H, td, 13.5, 3.9), 1.22 (1H, td, 13.5, 3.9), 1.26 (3H, s), 1.28 (1H, dd, 12.4, 2.8), 1.31—1.39 (1H, m), 1.44—1.48 (1H, m), 1.51—1.56 (1H, m), 1.54 (1H, br d, 10.2), 1.68 (1H, dd, 10.1, 6.2), 1.73 (1H, br d, 13.8), 1.78—1.90 (3H, m), 1.99 (1H, td, 13.7, 5.2), 2.17 (1H, br d, 13.5), 2.33 (1H, ddd, 13.8, 4.1, 2.3), 4.91 (1H, dd, 17.3, 1.9), 4.94 (1H, dd, 10.7, 1.9), 5.14 (1H, s), 5.71 (1H, dd, 17.1, 10.5), *ca.* 11.58 (1H, br). ^{13}C-NMR ($CDCl_3$) δ: 13.8, 19.2, 19.5, 24.1, 29.2, 29.3, 35.8, 36.4, 37.9, 38.5, 39.20, 39.23, 44.0, 50.5, 56.1, 112.9, 128.0, 137.9, 147.2, 184.2.

Compd II Colorless prisms from methanol, mp 178—180 °C, $[\alpha]_D^{16}$ −110° ($c=1.00$, $CHCl_3$). IR (KBr): 3430br, 2935, 1693, 1471, 1460, 1256, 877 cm^{-1}. ^{1}H-NMR ($CDCl_3$) δ: 0.81 (1H, td, 13.2, 3.5), 0.95 (3H, s), 1.01 (1H, td, 13.9, 4.4), *ca.* 1.06 (1H), 1.07 (1H, t-like, 7.4), 1.13 (1H, dd, 11.4, 4.9), 1.24 (3H, s), 1.40—1.48 (3H), 1.52 (1H, dt, 13.2, 3.3), 1.56—1.66 (3H), 1.83 (2H, td, 10.4, 3.3), 1.88—1.90 (2H), 1.99 (1H, br d, 11.1), 2.05 (2H, dd, 5.3, 2.7), 2.16 (1H, br d, 14.3), 2.64 (1H, br s), 4.74 and 4.80 (each 1H, s), 11.74 (1H, br). ^{13}C-NMR ($CDCl_3$) δ: 15.6, 18.4, 19.1, 21.8, 29.0, 33.1, 37.8, 39.67, 39.70, 40.7, 41.3, 43.7, 43.8, 44.2, 49.0, 55.1, 57.1, 103.0, 155.9, 184.6.

Pharmacological Assay Male ddY mice (5 weeks old, 22—32 g), propagated at Shizuoka Agricultural Cooperative Association (Hamamatsu, Japan) were used. Test samples were suspended in normal saline with 2% Tween 80 and 20—40% olive oil. Experiments were pursued under constant conditions at 23—25 °C.

Hypothermic Effect: Rectal temperatures were measured until 5 h after administration of the test samples by thermistor (Takara Instrumental Co., Ltd.).

Analgesic Activity: An acetic acid-induced writhing method[5] was used. At 30 min after administration of the test samples, 0.7% acetic acid (0.1 ml/10 g) was injected intraperitoneally. The number of squirms was counted in each mouse for 15 min beginning from 5 min after acetic acid injection.

Effect on Pentobarbital-Induced Anesthesia: Test samples were administered 30 min before i.p. injection of 50 mg/kg of sodium pentobarbital (Tanabe Pharmaceutical Co., Ltd.). The time required to regain the righting reflex was measured.

Effect on Locomotor Activity: Spontaneous motor activity was recorded by an Ambulatory Activity Analyzer (O'hara & Co., Ltd.). Test samples were administered at 20 min before subcutaneous injection of methamphetamin (Dainippon Pharmaceutical Co., Ltd.) at a dose of 2 mg/kg. The movements were counted for every 10 min up until 120 min.

Statistics: Statistical significance was evaluated by the Student's *t* test.

Acknowledgements This research was supported in part by a Grant-in-Aid (No. 1771901) from the Ministry of Education, Sciences and Culture. We are grateful to Professors O. Tanaka, K. Yamasaki and Kohda of Hiroshima University and Prof. Kuroyanagi of the University of Shizuoka for providing samples, and to Mr. S. Mitake for the medicinal plants. We thank Ms. L.-H. Gao and Mr. N. Iwase of this University for their technical assistance. We also thank the Chemical Analysis Center of this University for ^{1}H- and ^{13}C-NMR spectra.

References and Notes

1) H. Kohda and M. Satake, *Shoyakugaku Zasshi*, **37**, 165 (1983).
2) *a*) S. Shibata, S. Mihashi, and O. Tanaka, *Tetrahedron Lett.*, **1967**, 5241; *b*) M. Ozawa and O. Tanaka, *J. Traditional Sino-Japanese Medicine*, **8**, 69 (1987).
3) The authentic sample was used after crystallization from *n*-hexane.
4) C. A. Henrick and P. R. Jefferies, *Aust. J. Chem.*, **17**, 915 (1964).
5) B. A. Whittle, *Br. J. Pharmacol. Chemother.*, **22**, 246 (1964).

High Performance Liquid Chromatography of Bovine Serum Albumin–*cis*-Diaminedichloroplatinum(II) Complexes on *N*-Methylpyridinium Polymer Column

Atsushi SUGII,* Koichi NISHIMURA, Kumiko HARADA, Morio NAKAYAMA and Seiichi MASUDA

Faculty of Pharmaceutical Sciences, Kumamoto University, 5–1 Oe-honmachi, Kumamoto 862, Japan. *Received June 18, 1990*

***N*-Methylpyridinium polymer column, which had the ability for resolution of albumin components such as mercaptalbumin and non-mercaptalbumin, was applied to the study of reaction of *cis*-diaminedichloroplatinum(II) (DDP) with bovine serum albumin (BSA). The peak of BSA-DDP complex was resolved from other albumin component peaks and the participation of mercaptalbumin in this complex formation was elucidated. The participation of non-mercaptalbumin and disulphide type dimer in the complex formation with DDP were also investigated.**

Keywords albumin-*cis*-diaminedichloroplatinum(II) complex; bovine serum albumin; mercaptalbumin; *cis*-diaminedichloroplatinum; pyridinium polymer; HPLC

In the development of column packing for high performance liquid chromatography (HPLC) of proteins, high resolution that is able to recognize some small changes in the structure of solutes has been required. Recently we have reported that an *N*-methylpyridinium polymer (4VP-EG-Me)-based column had specific ability for the resolution of albumin components such as mercaptalbumin, non-mercaptalbumin *etc.*[1] This fact suggests that the column might be useful for the investigation of interaction between serum albumin and the compounds having high affinity for sulfhydryl groups of albumin. It is well known that *cis*-diaminedichloroplatinum(II) (DDP), an antineoplastic agent, reacts with various compounds and the reactions proceed by nucleophilic substitution for one or both of the coordinated chlorides.[2,3] Many proteins having a sulfhydryl group also respond to the platinum complex.[4–6] Gonias *et al.*[7] suggested that DDP had a strong affinity for the sulfhydryl group in mercaptalbumin from an experiment using albumins containing different numbers of sulfhydryl groups. However, they assayed only free DDP in the reaction system by spectrophotometry after deproteinization. In another investigation, albumin–DDP complex has been analyzed by reversed-phase HPLC, but the complex peak was not resolved from the unreacted albumin peak.[8]

In this paper, the reactivity of DDP with bovine serum albumin (BSA) used as a typical serum albumin was investigated by taking advantage of 4VP-EG-Me column. The characteristics of the column are capable to follow the reaction of DDP with each albumin component such as mercaptalbumin and non-mercaptalbumin.

Experimental

Materials Crystallized and liophilized BSA was obtained from Sigma (St. Louis, Mo., U.S.A.) and it was used as commercial BSA without further purification. Bovine mercaptalbumin (BMA) was prepared from the BSA (fraction V) by the use of DEAE–Sephadex column.[9] Bovine non-mercaptalbumin (BNA) was prepared by treatment of the BSA with a three fold molar excess of cystine.[10] Subsequently, the product was dialyzed and purified by DEAE–Sephadex column in a similar manner as BMA. Disulfide type dimer of BSA (BSA-dimer) was prepared by the method of Sogami *et al.*[10] DDP was kindly supplied by Nihon Kayaku Co. Ltd. (Tokyo, Japan).

Procedure DDP (3×10^{-4} M) was incubated at 37 °C with each albumin (3×10^{-4} M) in 0.05 M phosphate buffer (pH 7.4) containing 0.1 M sodium chloride. After incubation for 3, 6 and 18 h, each 5 μl was injected into the chromatographic system. When the sample solution incubated for 6 h was injected into the 4VP-EG-Me column, the eluate was fractionated. Determination of platinum in the fractions of HPLC eluate was carried out by using a Hitachi Z-8000 Zeeman-effect flameless atomic absorption spectrophotometer.

Chromatography The HPLC system consisted of a 655A-11 pump (Hitachi Ltd., Tokyo Japan), a Hitachi L-5000 low pressure gradient programmer and a Hitachi L-4000 variable wavelength ultraviolet (UV) monitor. The column packing material, an *N*-methylpyridinium polymer cross-linked with ethylene glycol dimethacrylate, was prepared as described previously.[11] A 250 × 4 mm (i.d.) column, packed with the polymer beads (10—15 μm) was used. Elution was accomplished by using a binary gradient from the initial starting buffer (solution A) of 0.05 M tris (hydroxy methyl) aminomethane (Tris)–HCl buffer (pH 7.0) to a final buffer (solution B) consisting of solution A containing 0.5 M sodium chloride at a flow rate of 0.5 ml/min (0—0.1 min, solution A from 100% to 95%; 0.1—20 min, solution A 95% to 70%; 20—20.1 min, solution A from 70% to 0%; 20.1—40 min, solution A 0%). The chromatography was performed at room temperature with detection at 280 nm for albumin and 205 nm for DDP.

Polyacrylamide Gel Electrophoresis Sodium dodecyl sulfate (SDS)-electrophoresis of peak fractions eluted from 4VP-EG-Me column was conducted on 10% gel slabs containing SDS as described by Laemmli,[12] but 2-mercaptoethanol was not employed for the sample preparation. Electrophoresis without SDS was also carried out in the same manner.

Results and Discussion

It was previously reported that buffer system of chromatographic eluent affected the peak resolution of albumin components.[1] Several gradient elution methods with increasing sodium chloride concentrations in Tris–HCl were examined. Good resolution of albumin components was achieved with the method which was presented in the experimental section. This method showed the peak resolution of mercaptalbumin and non-mercaptalbumin as well as did the method with a Tris–acetic acid buffer system reported previously[1] and was excellent in the resolution between monomeric fraction and oligomeric fraction. By

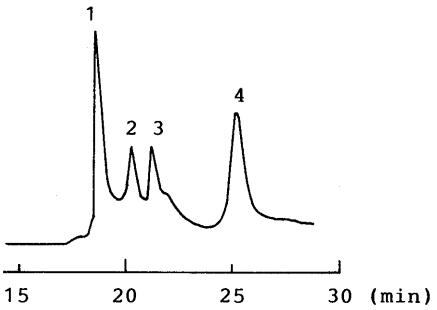

Fig. 1. Chromatogram of Commercial BSA

Peaks: (1) mercaptalbumin, (2) non-mercaptalbumin, (3) oxidized form, (4) oligomeric albumins. Detection: UV (280 nm). Other chromatographic conditions are in the text.

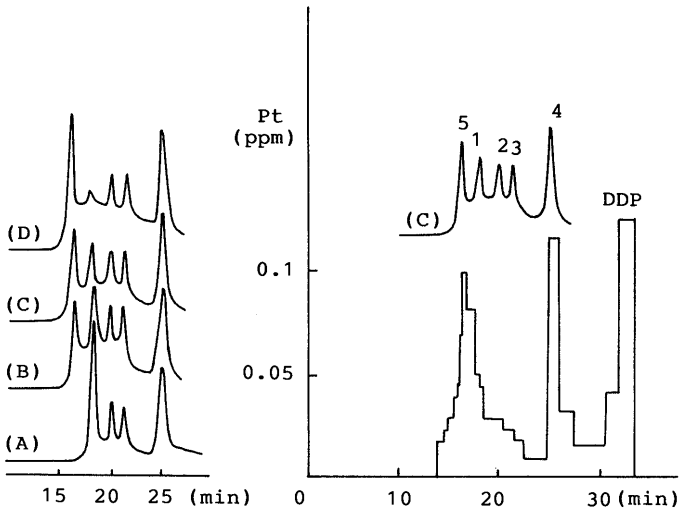

Fig. 2. Chromatograms of Commercial BSA Incubated with DDP for Various Periods of Time at 37 °C and Histogram of Platinum Concentration in the Eluent

Peaks: (1—4) are the same as those in Fig. 1, (5) new peak. Incubation time: (A) 0 h, (B) 3 h, (C) 6 h, (D) 18 h. Chromatographic conditions are in Fig. 1.

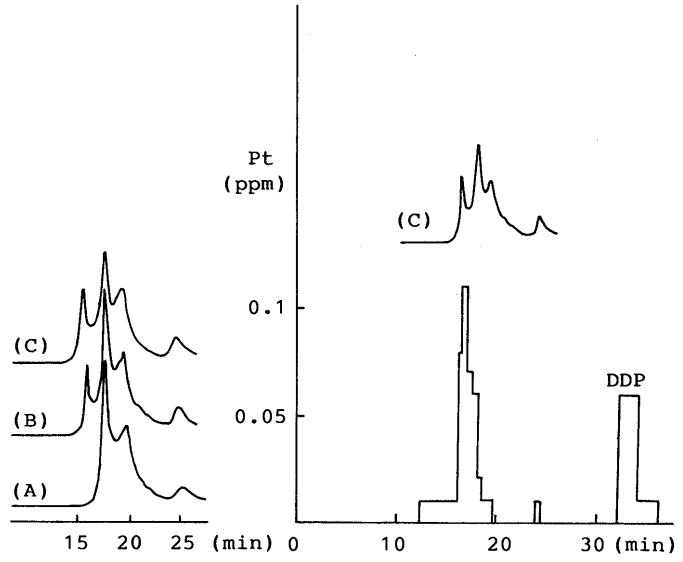

Fig. 3. Chromatograms of BMA Incubated with DDP for Various Periods of Time at 37 °C and Histogram of Platinum Concentration in the Eluent

Incubation time: (A) 0 h, (B) 3 h, (C) 6 h. Chromatographic conditions are in Fig. 1.

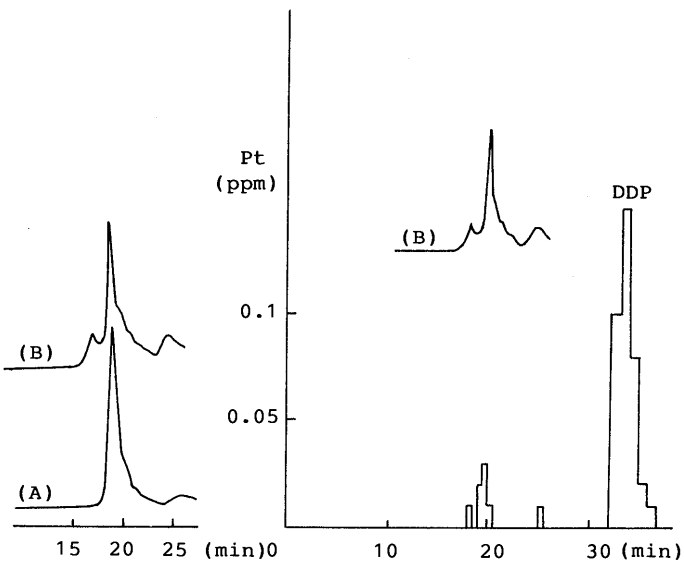

Fig. 4. Chromatograms of BNA Incubated with DDP for Various Periods of Time at 37 °C and Histogram of Platinum Concentration in the Eluent

Incubation time: (A) 0 h, (B) 6 h. Chromatographic conditions are in Fig. 1.

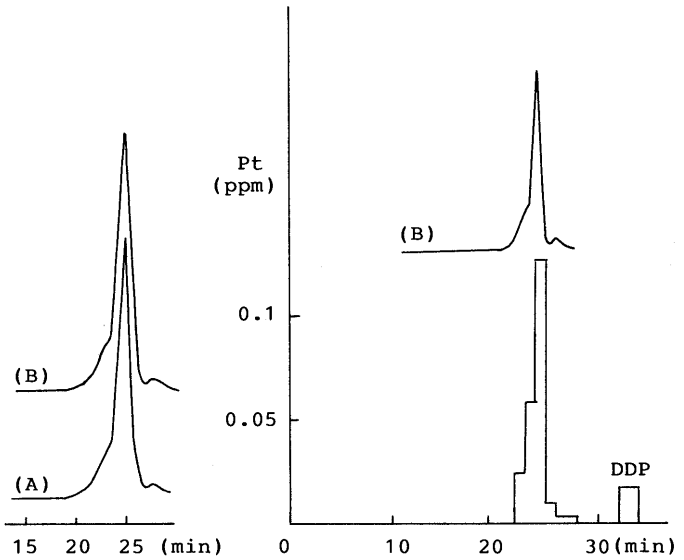

Fig. 5. Chromatograms of BSA-dimer Incubated with DDP for Various Periods of Time at 37 °C and Histogram of Platinum Concentration in the Eluent

Incubation time: (A) 0 h, (B) 6 h. Chromatographic conditions are in Fig. 1.

the use of this gradient method, BSA sample was chromatographed. As shown in Fig. 1, mercaptalbumin and non-mercaptalbumin (mixed disulfide with cysteine) eluted at 18 min and 20 min, respectively. The peak at 22 min is likely to be an oxidized form of mercaptalbumin containing a sulfinic acid/sulfonic acid group.[13] The peak eluted at 25 min contained oligomeric albumins such as dimer and trimer.

In the chromatograms of BSA incubated with DDP, a new peak, which was not observed in the case of BSA alone, appeared at 16 min (Fig. 2). This peak height increased with increasing incubation time, and the peak height of mercaptalbumin decreased. Non-mercaptalbumin peak, however, scarcely changed. High concentrations of platinum was observed in the new peak and the oligomeric albumin peak. When BSA was incubated in the presence of platinum ion($PtCl_6^{2+}$), the new peak didn't appear. Consequently, platinum existing in the new peak was regarded as arising from the albumin–DDP complex. These chromatographic changes suggest that DDP has a high reactivity for mercaptalbumin.

To examine in detail the reactivity of each component in albumin for DDP, BMA and BNA prepared separately were applied to the reaction. The time–course of the chromatogram of BMA incubated with DDP is shown in Fig. 3. A peak containing a high concentration of platinum appeared before the BMA peak and the peak height of BMA decreased with prolonged incubation. In the SDS-electrophoresis of this new peak fraction, the component showed the same migration as BSA-monomer. Therefore, it is expected that its molecular weight is similar to that of

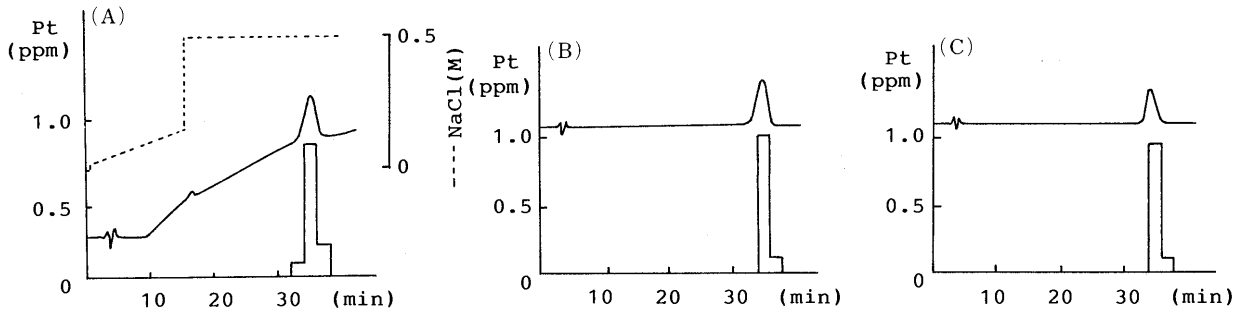

Fig. 6. Chromatograms of DDP and Histograms of Platinum Concentration in the Eluent

Elution: (A) gradient elution of NaCl as shown in the text, (B) isocratic elution of 0.05 M Tris–HCl buffer (pH 7.0), (C) isocratic elution of 0.5 M NaCl–0.05 M Tris–HCl buffer (pH 7.0). Detection: UV (205 nm).

a monomer of BSA. Furthermore, the molar ratio of albumin to platinum in the peak fraction was about 1 : 1. It is considered that mercaptalbumin–DDP (1 : 1) complex present in this peak. When the peak fraction was subjected to electrophoresis without SDS, the component showed slightly low migration compared with that of BMA. From the migration manner and the elution behavior on the 4VP-EG-Me column, it was suggested that mercaptalbumin–DDP (1 : 1) complex had a more positive charge than that of BMA.

Chromatograms of the reaction mixture of BNA and DDP are shown in Fig. 4. The low platinum incorporation into albumin fraction was observed and a large amount of unreacted DDP eluted at 35 min. This result clearly shows the low reactivity of BNA.

The presence of a high level of platinum in the oligomeric albumin fraction (contained mainly dimer) suggested that the oligomeric albumin also had a high affinity for DDP. In order to elucidate the affinity for DDP, the reactivity of dimer (disulfide type) with DDP was further investigated. Although this dimer, as well as non-mercaptalbumin, had no sulfhydryl group in the molecule, DDP reacted with the dimer (Fig. 5). In the chromatographic condition, the dimer–DDP complex eluted at the same retention time as that of the dimer. For the explanation of this fact, it was speculated that a conformational change occurred by dimerization, and might bring about the appearance of highly reactive functional group to DDP such as methionine or histidine moiety which is reactive with square planar platinum complex.[14]

Riley *et al.*[15] stated that retention of DDP by an anion exchange HPLC occurred with the ion–dipole interaction. In our system the retention of DDP was little affected by the salt concentrations in the eluent as shown in Fig. 6. Although albumin and albumin–DDP complex are mainly retained by ion exchange interaction, DDP is retained by the ion–dipole interaction. When DDP was incubated in water or a buffer solution containing chloride ions, the chromatograms of the DDP showed a new peak containing platinum at about 4 min for the monitoring at 205 nm and this peak height increased as decrease of that of DDP (t_R 35 min). The amount of the formation of this peak in water was larger than in the buffer at the same incubation time. The peak is probably an aquated complex produced by the hydrolysis of DDP.[16,17] Since the aquated complex has a positive charge, it was eluted at shorter retention times on this column.

In the inactivation of enzymes possessing cystine or methionine by DDP, it was considered that aquation of DDP was an important factor.[18] Bodenner *et al.*[4] also stated that hydrolysis of DDP was the rate-determining step in deoxyribonucleic acid (DNA) binding with DDP. The formation of albumin–DDP complex in the buffer system was rather slow. However, when DDP pre-incubated in water was used in the reaction, the complex peak appeared rapidly. From these results, it was considered that hydrolysis of DDP was the rate-determining step in the formation of albumin–DDP complex.

In conclusion, the high reactivity of mercaptalbumin with DDP was confirmed and the dimer of BSA also showed high affinity for DDP. These findings suggest that it will be necessary to take into account the contents of mercaptalbumin and dimer in the study using albumin preparations. We are currently evaluating the potential of this column for the investigation of albumin binding with other materials.

Acknowledgements We thank Miss T. Honjikawa for the technical assistance.

References

1) K. Nishimura, K. Harada, S. Masuda and A. Sugii, *J. Chromatogr.*, **525**, 176 (1990).
2) M. J. Cleare and J. D. Hoeshele, *Bioinorg. Chem.*, **2**, 187 (1973).
3) M. J. Cleare, *J. Clin. Hematol Oncol.*, **7**, 1 (1977).
4) D. L. Bodenner, P. C. Dedon, P. C. Keng and R. F. Borch, *Cancer Res.*, **46**, 2745 (1986).
5) P. T. Daley-Yates and D. C. H. McBrien, *Chem.-Biol. Interact.*, **40**, 325 (1982).
6) A. M. Guarino, D. S. Miller, S. T. Arnold, J. B. Pritchard, R. D. Davis, M. A. Urbanek, T. J. Miller and C. L. Litterst, *Cancer Treat. Rep.*, **63**, 1475 (1979).
7) S. L. Gonias and S. V. Pizzo, *J. Biol. Chem.*, **258**, 5764 (1983).
8) C. M. Riley, L. A. Sternson and A. J. Repta, *Anal. Biochem.*, **124**, 167 (1982).
9) J. Janatova, J. K. Fuller and M. J. Hunter, *J. Biol. Chem.*, **243**, 3612 (1968).
10) M. Sogami, S. Nagaoka, S. Era, M. Honda and K. Noguchi, *Int. J. Peptide Protein Res.*, **24**, 96 (1984).
11) A. Sugii, K. Harada, K. Nishimura, R. Hanaoka and S. Masuda, *J. Chromatogr.*, **472**, 357 (1989).
12) U. K. Laemmli, *Nature* (London), **227**, 680 (1970).
13) J. K. Fuller-Noel and M. J. Hunter, *J. Biol. Chem.*, **247**, 7391 (1972).
14) R. E. Dickerson, D. Eisenberg, J. Varnum and M. L. Kopka, *J. Mol. Biol.*, **45**, 77 (1969).
15) C. M. Riley, L. A. Sternson and A. J. Repta, *J. Chromatogr.*, **217**, 405 (1981).
16) R. J. Knox, F. Friedlos, D. A. Lydall and J. J. Roberts, *Cancer Res.*, **46**, 1972 (1986).
17) C. M. Riley, L. A. Sternson, A. J. Repta and S. A. Slyter, *Anal. Biochem.*, **130**, 203 (1983).
18) P. C. Dedon and R. F. Borch, *Biochem. Pharmac.*, **36**, 1955 (1987).

A New Chemiluminogenic Substrate for *N*-Acetyl-β-D-glucosaminidase, 4′-(6′-Diethylaminobenzofuranyl)phthalylhydrazido-*N*-acetyl-β-D-glucosaminide

Kazumi SASAMOTO*,[a] and Yosuke OHKURA[b]

Dojindo Laboratories,[a] Tabaru 2025-5, Mashiki-machi, Kamimashiki-gun, Kumamoto 861-22, Japan and Faculty of Pharmaceutical Sciences, Kyushu University 62,[b] Maidashi, Higashi-ku, Fukuoka 812, Japan. *Received July 13, 1990*

A new type of chemiluminogenic substrate for *N*-acetyl-β-D-glucosaminidase was synthesized. The substrate was obtained by incorporation of an enzyme-removable *N*-acetyl-D-glucosaminide group to the cyclic hydrazide moiety of an arylic hydrazide which contains a highly fluorescent benzofuran framework. Following enzyme-mediated hydrolysis, the substrate released the hydrazide that was subsequently subjected to chemiluminescent oxidation with hydrogen peroxide and a hemin catalyst in an alkaline buffer to generate light. The detection limit of the enzyme using this substrate was 0.6 I.U./l.

Keywords chemiluminogenic substrate; *N*-acetyl-β-D-glucosaminidase; 4′-(6′-diethylaminobenzofuranyl)phthalylhydrazido-*N*-acetyl-β-D-glucosaminide; chemiluminescence detection; enzyme assay

Since the enzymatic triggering of chemiluminescence was first realized by Schaap and co-workers[1] using an adamantyl dioxetane as a substrate, it has been gaining much attention for its extreme value in enzyme immunoassays.[2] Alkaline phosphatase or β-galactosidase are being utilized as enzyme labels which trigger the chemiluminescent decomposition of dioxetane in aqueous buffers without the addition of other co-reagents. In a previous paper,[3] we demonstrated through the synthesis of *o*-aminophthalylhydrazido-*N*-acetyl-β-D-glucosaminide that the enzyme-triggered chemiluminescence could also be achieved by substitution on the heterocyclic ring of luminol with an enzyme-removable group. Thus, the incorporation of an *N*-acetyl-D-glucosaminide group into the cyclic hydrazide moiety of luminol renders the compound nonluminescent; whereas enzymatic hydrolysis with *N*-acetyl-β-D-glucosaminidase (NAGase; EC 3.2.1.30) releases luminol, which is then detected chemiluminescently using hydrogen peroxide and a catalyst. The fact that the detection sensitivity of the enzyme by this method was insufficient under a detection limit of 5 I.U./l, which is approximately 10 times less sensitive compared to conventional spectrophotometric methods, led us to attempt to improve the chemiluminescent efficiency of the cyclic hydrazide. Although the observed efficiency of chemiluminescence is a result of: (1) the selectivity of the chemical reaction, (2) the efficiency of cross-over to the excited state of the light emitter (presumably the corresponding phthalate ion in the luminol system), and (3) the efficiency of fluorescence of the phthalate, the third factor is most important in various organic hydrazides.[4]

In order to exploit a substrate for sensitive detection of NAGase, we synthesized a new chemiluminogenic substrate, 4′-(6′-diethylaminobenzofuranyl)phthalylhydrazido-*N*-acetyl-β-D-glucosaminide (**1**, Chart 1) that covalently incorporates an arycyclic hydrazide having a highly fluorescent benzofuran skeleton, and herein report the synthesis and its chemiluminescent response to the enzyme.

Experimental

Apparatus Proton nuclear magnetic resonance (^{1}H-NMR) spectra and carbon-13 nuclear magnetic resonance (^{13}C-NMR) spectra were taken with a Bruker AC-200 spectrometer at 200 and 50 MHz, respectively, using tetramethylsilane as an internal standard. The splitting patterns are designated as follows: s, singlet; d, doublet; t, triplet; q, quartet; dd, doublet of doublets; m, multiplet; br, broad. Infrared (IR) spectra were measured in Nujol mull with a Hitachi 260-10 spectrometer. Chemiluminescence measurements were performed on a photon-counting computer-controlled Berthold Lumat LB-9501 luminometer (Wildbad, FRG); chemiluminescence reactions were carried out in 75 × 12 mm clear-polystyrene round-bottom tubes supplied by Sarstedt (Numbrecht, FRG). A Shimadzu LC-6A high-performance liquid chromatograph equipped with a Shimadzu SPD-6AV ultraviolet spectrometer operated at 254 nm was used. The column was a Nucleosil C18 (250 × 4.0 mm i.d., particle size 10 μm; Gasukuro Kogyo Inc., Tokyo, Japan). The column temperature was 40 °C and the flow rate of the mobile phase (aqueous 60% acetonitrile) was 1.0 ml/min. Uncorrected melting points were obtained on a Yamato MP-21 melting point apparatus. Fluorescence spectra were taken on a Hitachi 650-60 spectrometer in 10 × 10 mm quartz cells.

Materials NAGase from jack beans was purchased from Sigma (St. Louis, MO, U.S.A.) as a suspension of 0.8 mg of protein per ml in 2.5 M $(NH_4)_2SO_4$ solution (50 I.U./ml) and diluted with water prior to use. Other chemicals were of reagent grade. Stock solutions of substrate **1** and 4-(6-diethylaminobenzofuranyl)phthalhydrazide (**5**) were prepared in dimethylsulfoxide at 20 mM. Column chromatography was performed with silica gel (Kieselgel 60, E. Merck, Darmstadt, FRG).

Synthesis of Substrate 1 (Chart 1) 4-Methyl-*N*-phenylphthalimide (2) To a stirred solution of 4-methylphthalic anhydride (39.64 g, 0.244 mol) in 500 ml of ether was added aniline (22.3 ml, 0.245 mol), and the stirring was continued for 1 h at room temperature. A formed precipitate was collected and then heated with sodium acetate (8.35 g, 0.102 mol) in 90 ml of acetic anhydride at 90 °C for 30 min, during which time an initial suspension became clear and subsequently solidified. The solid was collected and recrystallized from benzene–hexane to give 40.0 g (69%) of compound **2** as a colorless crystalline solid, mp 163—164 °C. ^{1}H-NMR ($CDCl_3$) δ: 2.54 (s, 3H, CH_3), 7.39—7.51 (m, 5H, Ph), 7.57 (dd, J=8.2, 1.1 Hz, 1H, ArH), 7.75 (s, 1H, ArH), 7.83 (d, J=7.6 Hz, 1H, ArH). IR ν_{max} cm^{-1}: 1788 (phthalimide), 1713 (phthalimide), 1622 (aromatic).

4-Bromomethyl-*N*-phenylphthalimide (3) A solution containing compound **2** (10.0 g, 42.15 mmol), *N*-bromosuccinimide (8.50 g, 47.76 mmol), and benzoyl peroxide (250 mg, 1.03 mmol) in 200 ml of carbon tetrachloride was refluxed for 16 h. A formed precipitate was filtered off and the filtrate was concentrated *in vacuo* to give a slight yellow solid, which was purified by column chromatography (benzene). After recrystallization from benzene–petrolium ether, bromide **3** was obtained as an inseparable mixture with compound **2**; the purity was determined to be 89 mol% by ^{1}H-NMR analysis, yield 3.88 g (29%), mp 150—154 °C. ^{1}H-NMR ($CDCl_3$) δ: 4.59 (s, 2H, CH_2Br), 7.36–7.56 (m, 5H, Ph), 7.80 (dd, J=7.7, 1.3 Hz, 1H, ArH), 7.92 (s, 1H, ArH), 7.97 (d, J=5.1 Hz, 1H, ArH). IR ν_{max} cm^{-1}: 1791 (phthalimide), 1723 (phthalimide), 1628 (aromatic), 1609 (aromatic).

4-(6-Diethylaminobenzofuranyl)-*N*-phenylphthalimide (4) A mixture containing 4-diethylaminosalicylaldehyde (3.36 g, 17.39 mmol), bromide **3** (6.0 g, 17.37 mmol based on 89 mol% NMR purity), and K_2CO_3 (11.0 g, 79.59 mmol) in 120 ml of *N*,*N*-dimethylformamide was heated at 130 °C (bath temperature) for 1 h. The resulting brown-colored solution was diluted with ether and washed with aqueous $NaHCO_3$. After drying ($MgSO_4$) followed by concentration *in vacuo*, the crude product was obtained as a yellowish solid which was purified by column chro-

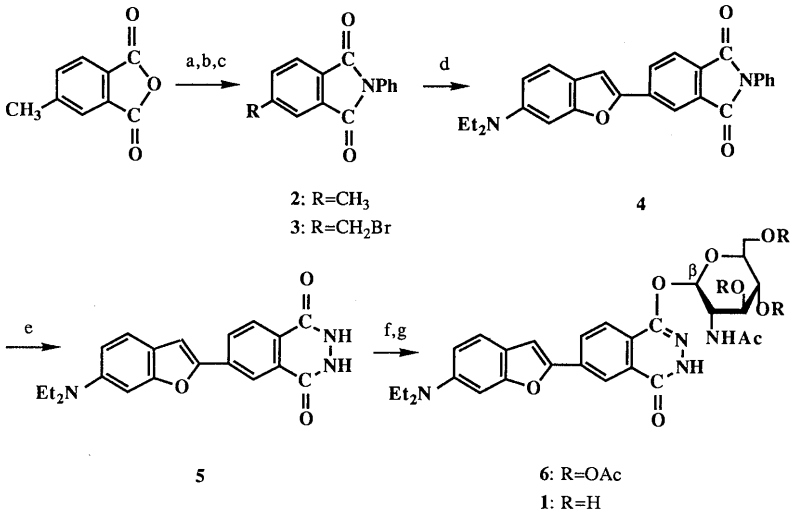

reagents: (a) aniline, Et_2O; (b) Ac_2O, AcONa; (c) NBS, CCl_4; (d) 4-diethylaminosalicylaldehyde, K_2CO_3, DMF; (e) hydrazine, EtOH: (f) 1-chloro-1-deoxy-2,3,4,6-tetraacetyl-α-D-glucosamine, NaH, DMF; (g) $NaOCH_3$, MeOH

Chart 1. Synthetic Route to 4′-(6′-Diethylaminobenzofuranyl)phthalylhydrazido-*N*-acetyl-β-D-glucosaminide (**1**)

matography (benzene) followed by recrystallization from benzene–petrolium ether, affording 1.06 g (15%) of compound **4** as red needles, mp 180–181 °C. ^{1}H-NMR ($CDCl_3$) δ: 1.23 (t, J=7.0 Hz, 6H, CH_3), 3.44 (q, J=7.0 Hz, 4H, CH_2), 6.72 (dd, J=8.8, 2.3 Hz, 1H, ArH), 6.78 (br s, 1H, ArH), 7.15 (s, 1H, ArH), 7.26 (s, 1H, furanyl H), 7.41—7.53 (m, 5H, Ph), 7.94(d, J=8.1 Hz, 1H, ArH), 8.13 (dd, J=7.8, 1.5 Hz, 1H, ArH), 8.30 (d, J=7.7 Hz, 1H, ArH). IR ν_{max} cm^{-1}: 1762 (phthalimide), 1710 (phthalimide), 1635 (aromatic), 1619 (aromatic).

4-(6-Diethylaminobenzofuranyl)phthalylhydrazide (5) A suspension of compound **4** (1.0 g, 2.44 mmol) and hydrazine hydrate (5.0 ml, 0.103 mol) in 25 ml of ethanol was refluxed for 30 min, during which time a light-yellow crystalline solid precipitated. The precipitate was collected and washed thoroughly with ethanol. Drying over P_2O_5 *in vacuo* overnight gave hydrazide **5** as a lemon-yellow crystalline solid, yield 0.70 g (82%), mp >269 °C (dec.). ^{1}H-NMR (DMSO-d_6) δ: 1.14 (t, J=6.8 Hz, 6H, CH_3), 3.42 (q, J=6.9 Hz, 4H, CH_2), 3.98 (br s, 2H, hydrazido H), 6.74 (dd, J=8.8, 1.5 Hz, 1H, ArH), 6.90 (s, 1H, ArH), 7.45 (d, J=8.6 Hz, 1H, ArH), 7.51 (s, 1H, ArH), 8.08 (d, J=8.4 Hz, 1H, ArH), 8.24 (d, J=8.3 Hz, 1H, ArH), 8.39 (s, 1H, ArH). ^{13}C-NMR (DMSO-d_6) δ: 12.31 (CH_3), 44.10 (CH_2), 93.04 (CH), 104.84 (CH), 109.80 (CH), 117.30, 119.00 (CH), 121.73 (CH), 125.00 (CH), 126.13, 127.07 (CH), 128.58, 133.51, 146.83, 150.62, 155.16, 155.39, 157.22. IR ν_{max} cm^{-1}: 1660, 1641, 1617 (hydrazide).

4′-(6′-Diethylaminobenzofuranyl)phthalylhydrazido-*N*-acetyl-β-D-glucosaminide Triacetate (6) To a stirred solution of hydrazide **5** (261 mg, 0.747 mmol) in 10 ml of *N*,*N*-dimethylformamide was added sodium hydride (60% oil dispersed, 30 mg, 0.75 mmol) at room temperature. After 10 min, solid 1-chloro-1-deoxy-2,3,4,6-tetraacetyl-α-D-glucosamine[6] (273 mg, 0.746 mmol) was added and the stirring was continued for 12 h at room temperature. The reaction was worked up by partitioning the reaction mixture between ethyl acetate and water, and the organic layer was washed (aqueous $NaHCO_3$), dried ($MgSO_4$), and concentrated *in vacuo* to leave a brown syrup. Column chromatography (5% methanol in chloroform) afforded compound **6** as a major product along with a more polar by-product (bis(2-acetamide-3,4,6-triacetyl-D-glucopyranosyl) substituted product) which appeared similar to compound **6** in thin layer chromatography (*Rf* values for compound **6** and this by-product are 0.30 and 0.26, respectively; 10% methanol in chloroform, Merck Silica gel 60) and also gave a similar NMR spectrum, yield 60 mg (12%), mp 183—185 °C (dec.). ^{1}H-NMR (DMSO-d_6) δ: 1.24 (t, J=6.8 Hz, 6H, CH_3), 2.03 (s, 9H, OAc), 2.12 (s, 3H, NHAc), 3.44 (q, J=7.0 Hz, 4H, CH_2), 3.98 (br s, 1H, hydrazido H), 4.25 (m, 2H, pyranosyl H), 4.73 (m, 1H, pyranosyl H), 5.25 (t, J=7.0 Hz, 2H, pyranosyl H), 5.85 (d, J=8.6 Hz, 1H, anomeric H), 6.53 (d, J=10.0 Hz, 1H, pyranosyl H), 6.74 (d, J=10.4 Hz, 1H, ArH), 7.02 (s, 1H, furanyl H), 7.28 (d, J=10.8 Hz, 1H, NHAc), 7.34 (d, J=8.6 Hz, 1H, ArH), 7.93 (m, 2H, ArH), 8.53 (s, 1H, ArH). IR ν_{max} cm^{-1}: 3300, 1750 (OAc), 1675 (hydrazide).

4′-(6′-Diethylaminobenzofuranyl)phthalylhydrazido-*N*-acetyl-β-D-glucosaminide (1) To a stirred solution of compound **6** (60 mg, 0.088 mmol) in 8 ml of methanol was added 1 M sodium methoxide in methanol (50 μl) and the solution was stored in refrigeration overnight. Deprotected product **1** precipitated out of the solution, which was collected, washed with cold methanol, and dried *in vacuo* over P_2O_5 overnight, yield 27 mg (55%), mp >200 °C (dec.). ^{1}H-NMR (DMSO-d_6) δ: 1.14 (t, J=6.9 Hz, 6H, CH_3), 1.74 (s, 3H, NHAc), 3.34 (m, 8H, OH and pyranosyl H), 3.42 (q, J=7.0 Hz, 4H, CH_2), 5.16 (t, J=5.3 Hz, 1H, pyranosyl H), 5.56 (d, J=8.7 Hz, 1H, anomeric H), 6.75 (dd, J=8.7, 1.5 Hz, 1H, ArH), 6.89 (s, 1H, ArH), 7.46 (d, J=8.7 Hz, 1H, ArH), 7.59 (s, 1H, furanyl H), 7.85 (d, J=7.3 Hz, 1H, NHAc), 7.89 (d, J=8.5 Hz, 1H, ArH), 8.36 (dd, J=8.4, 1.8 Hz, 1H, ArH), 8.50 (d, J=1.7 Hz, 1H, ArH). ^{13}C-NMR (DMSO-d_6) δ: 12.32 (CH_3), 44.10 (CH_2), 54.59 (CH_2), 61.00 (CH), 69.86 (CH), 74.00 (CH), 77.56 (CH), 92.93 (CH), 96.06 (CH), 105.08 (CH), 110.00 (CH), 117.21, 119.57 (CH), 121.87 (CH), 122.37 (CH), 124.13, 128.52 (CH), 129.45, 133.78, 146.99, 148.35, 150.16, 157.16, 157.34 (CO), 158.60 (CO), 169.41 (CONH). IR ν_{max} cm^{-1}: 3300 (OH), 1650 (hydrazide). *Anal.* Calcd for $C_{28}H_{32}N_4O_8$: C, 60.86; H, 5.84; N, 10.14. Found: C, 59.60; H, 5.87; N, 10.94.

Enzymatic Reaction A 10 μl of NAGase of a given concentration was added to a pre-incubated mixture (37 °C) of 0.5 ml of 0.1 M phosphate buffer (pH 6.5) and 0.5 ml of aqueous 1% (w/v) cetyltrimethylammonium bromide (CTMAB) containing the substrate (compound **1**, final concentration, 0.1 mM), and the mixture was incubated at 37 °C for 10 min in a tube. The reaction was then terminated by subsequent addition of 0.5 ml of 1 M KOH and 10 μl of 0.1 μM hemin (H_2O). The tube containing this mixture was placed in a luminometer and the chemiluminescent reaction was initiated by adding 10 μl of 0.05% H_2O_2. The resulting light emission was measured in the luminometer as a 10-min integral.

Results and Discussion

Synthesis The synthetic approach to substrate **1** involves the preparation of the arylic hydrazide **5** and its modification in the hydrazide portion with the enzyme-removable *N*-acetyl-D-glucosaminide group, as outlined in Chart 1. Since the red shifts at the emission maxima of the dialkylamino-substituted compounds relative to the corresponding unsubstituted ones were reported in 6-substituted benzofurans,[5b] we first aimed at the synthesis of the arylic hydrazide having a diethylamino group at 6-position. As a precursor to the corresponding hydrazide, an *N*-phenylphthalimide group was employed in the preparation of hydrazide **5** since chromatographic purification is not often applicable to hydrazide compounds because of their slight solubilities in most organic solvents; in addition, *N*-phenylphthalimides can be easily purified by recrystallization. Starting with 4-methylphthalic anhydride, *N*-phenylphthalimide (**2**) was readily obtained in good yield,

and was then subjected to benzylic bromination with *N*-bromosuccinimide to give bromide **3**. Construction of a benzofuran framework was effected by reacting bromide **3** with an equivalent of 4-diethylaminosalicylaldehyde in the presence of a base,[5] affording compound **4** in moderate yield. The conversion of compound **4** to hydrazide **5** proceeded smoothly and in quantitative yield with hydrazine in refluxing ethanol. Incorporation of an *N*-acetyl-D-glucosaminide group to the heterocyclic moiety of hydrazide **5** was achieved as described in the previous paper.[3] The reaction of hydrazide **5** with 1-chloro-1-deoxy-2,3,4,6-tetraacetyl-α-D-glucosamine,[6] readily obtained from commercially available *N*-acetyl-D-glucosamine, in the presence of sodium hydride in *N*,*N*-dimethylformamide yielded compound **6** as a major product. The structure of the coupling product (**6**) was corroborated by the ^{1}H-NMR spectrum data which appeared to be an overlap of the two independent spectra of glucosamine acetate and the benzofuran unit. The anomeric proton resonates at δ 5.85 as a doublet with a coupling constant of 8.6 Hz which is consistent for the vicinal diaxial coupling, thereby suggesting that the coupled product obtained was an α-anomer. The poor coupling yield (12%) is probably due to the heterogenity of the reaction. The coupling reaction also produced a minor by-product, which was not fully characterized because of its poor response to the enzyme. Subsequent removal of the acetyl groups in the sugar moiety performed in a usual manner with sodium methoxide in methanol gave substrate **1** as a highly fluorescent product. At this stage, it was difficult to fully assign the ring protons of the glucosamine unit in ^{1}H-NMR because of overlapping and broadening signals, except for the anomeric proton which appeared as a doublet (J=8.7 Hz) at δ 5.56.

The fluorescence spectra of compounds **1** and **5** are shown in Fig. 1, which indicates that the emission maximum of substrate **1** (λ_{em}=556 nm, excited at 420 nm) is red-shifted from that of hydrazide **5** (λ_{em}=540 nm, excited at 415 nm) and that, although we were unable to obtain it, hydrazide **5** is expected to exhibit similar chemiluminesence spectra upon an oxidative reaction with hydrogen peroxide and a catalyst. The reduction of the fluorescence intensity of substrate **1** is obviously due to the flexible sugar group.

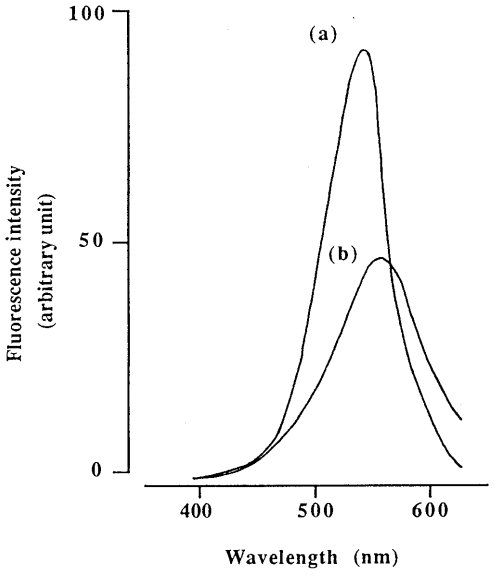

Fig. 1. Fluorescence Spectra of (a) Hydrazide **5** and (b) Substrate **1**
Both were measured in a DMSO solution.

^{1}H-NMR spectra of substrate **1** (Fig. 2a) shows two ABX patterns similar to those of hydrazide **5** (Fig. 2b), except for the H-2 proton that is shifted upfield. Since this shielding of the H-2 proton seems to favor an *O*-glycosylation at the carbonyl oxygen closer to the H-2 proton, the structure of substrate **1** was tentatively assigned as indicated in Chart 1. A nuclear Overhauser effect experiment failed to give any further information supporting the structure.

The acid susceptibility of substrate **1** due to its glycosidic bond was confirmed by high-performance liquid chromatography (HPLC) analysis based on monitoring the release of hydrazide **5** from substrate **1** following an acid treatment. When substrate **1** (5 mM) was incubated in 1 M hydrochloric acid at 37 °C, the complete disappearance of substrate **1** (retention time, 4.0 min) within 30 min resulting in hydrazide **5** (retention time, 6.7 min) was observed by HPLC.

Chemiluminescence Chart 2 illustrates the principle of the chemiluminescent detection of NAGase using compound **1** as the substrate. Substrate **1** can be regarded as a masked chemiluminescer in the sense that it is non-luminescent until the enzyme removes the sugar moiety. The released product (hydrazide **5**) is then subjected to chemiluminescent oxidation in an alkaline buffer with hydrogen peroxide and a catalyst to generate light and phthalate **7**. In this way the enzyme triggers the chemiluminescence of substrate **1** and a linear relationship is expected between the quantity of the enzyme and light production.

In order to attain this, we first investigated chemiluminescent reaction conditions for hydrazide **5**, the results of which are shown in Table I. Chemiluminescence of hydrazide **5** in a partly aqueous dimethylsulfoxide (DMSO) solution was found to be highly dependent on the ratio of DMSO to water; the presence of DMSO greatly enhanced the chemiluminescence. Since a similar enhancement effect by DMSO can be observed in the fluorescence of hydrazide **5**, the great loss of the chemiluminescence with an increasing water ratio can best be rationalized by an assumed

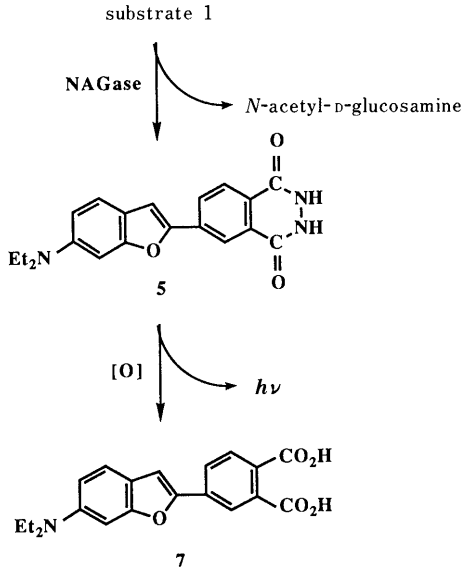

Chart 2. Principle of NAGase Detection Using Substrate **1**

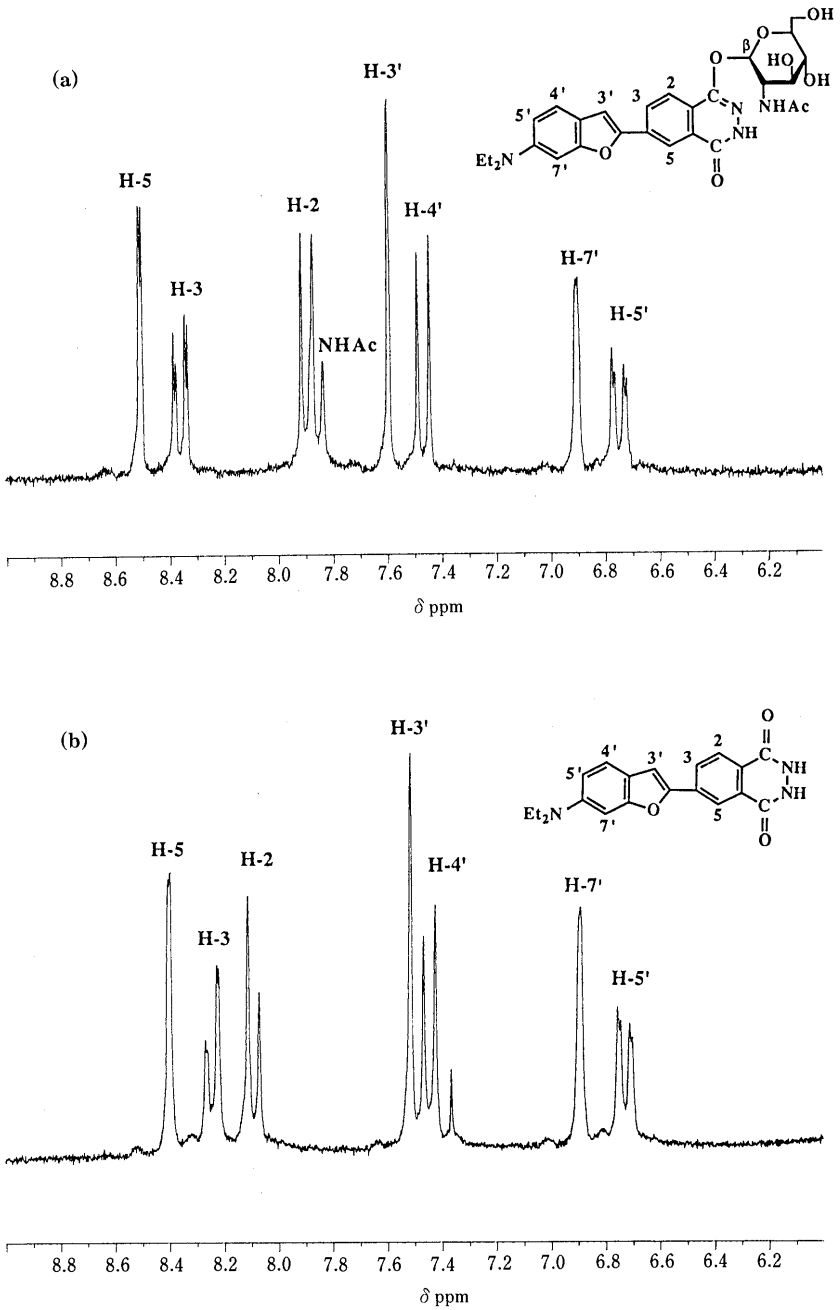

Fig. 2. ^{1}H-NMR Spectra of (a) Substrate **1** and (b) Hydrazide **5**

TABLE I. Chemiluminescence Intensities of Hydrazide **5** under Various Conditions

Reaction medium[a]		Chemiluminescence intensity[b]
DMSO + buffer	(3 : 1, v/v)	381
DMSO + buffer	(1 : 1, v/v)	80
DMSO + buffer	(1 : 3, v/v)	5.6
Buffer		1
Buffer + SDS	(1 : 1, v/v)	2.3
Buffer + Tween	(1 : 1, v/v)	0.4
Buffer + CTMAB	(1 : 1, v/v)	195

a) Buffer = 0.1 M boric acid–0.2 M KOH (1 : 1 (v/v), pH 12.6); SDS = aqueous 1% (w/v) sodium dodecyl sulfate; Tween = aqueous 1% (w/v) Tween 20; CTMAB = aqueous 1% (w/v) cetyltrimethylammonium bromide. *b*) Chemiluminescence reactions were initiated by adding 10 μl of hydrogen peroxide (0.05%) to a mixture containing 10 μl of hydrazide **5** (20 mM, DMSO) and 10 μl of hemin (0.1 μM) in 2.0 ml of the reaction media; the chemiluminescence intensities (arbitrary unit) were measured as a 10-min integral.

quenching of the fluorescence of the emitting species (presumably the corresponding phthalate (**7**)) by water. The solvation of the emitting species by an aprotic solvent such as DMSO prevents the fluorescence from being quenched, thereby enhancing the chemiluminescence. Hydrazide **5** is far more susceptible to aqueous quenching than luminol, whose chemiluminescence is, by contrast, insensitive to the ratio of DMSO under these conditions.

White and Bursey[7] reported the chemiluminescent behaviors of di- and tri-methoxysubstituted luminol analogs which were expected to chemiluminesce more efficiently than the parent luminol because of higher fluorescent quantum yields of the corresponding phthalates. These analogs, however, were found to be less efficient chemiluminescers than luminol in water, although they were more efficient in the DMSO system; they explained this as a hydrogen-

bonding effect, which is caused to a greater extent in these analogs than in luminol. Hydrazide **5** appears to be subject to this hydrogen bonding effect caused by the bulk of water, presumably because there are more sites for hydrogen bonding than in luminol. Compared to luminol in identical aqueous conditions (50% (v/v) DMSO), hydrazide **5** emits 4 times as much light.

The addition of CTMAB, a cationic surfactant, also enhances the chemiluminescence of hydrazide **5** by twice the magnitude. No significant increase in light production was observed either with non-ionic or anionic surfactants. The micellar-enhanced chemiluminescence by an alkylammonium salt surfactant in the luminol system has been well discussed based on a microenvironmental effect[8]; a microenvironment provides an effective surface for the chemiluminescent reaction, which leads to an acceleration of the reaction[9]; it also solubilizes the light emitter, thus increasing the fluorescent quantum yield.[10] Taking into account the fact that chemiluminescence enhancement is also observed by DMSO, the effect of the cationic surfactant can be better interpreted as an increase of the fluorescent efficiency of the phthalate, rather than that of the reaction rate.

In order to use CTMAB in the enzyme reaction of NAGase with substrate **1**, the effect of CTMAB over the enzyme activity was independently examined using *p*-nitrophenyl-*N*-acetyl-*β*-D-glucosaminide (PNP-NAG),[11] a commonly used substrate in NAGase assay (Fig. 3). NAGase activity with CTMAB, calculated from the slope in Fig. 3, is 56% higher than without CTMAB of the same enzyme solution.

Since the use of CTMAB was found to be beneficial in the sense that it enhances the chemiluminescence of hydrazide **5** and also activates the enzyme, we next investigated a chemiluminescent response of substrate **1** to an enzyme of different concentrations. Enzymatic reactions were carried out in a 0.1 M phosphate buffer (pH 6.5) in the presence of CTMAB (0.5% (w/v)) at 37 °C for 10 min and subsequently terminated by the addition of an alkali. Figure 4 shows the chemiluminescent intensities obtained from the enzymatic reactions *versus* NAGase activities determined by the PNP-NAG method.

A linear relationship between chemiluminescence and enzyme activity implies that the principle in Chart 2 is operative. The detection limit of 0.6 I.U./l might be satisfactory considering that a mean value of urinary NAGase activity in healthy adults is reportedly in the range of 3.0[12] to 4.6[13] I.U./l. The present method permits sensitivity of the assay of NAGase of less than 1 I.U./l, roughly 10-fold more sensitive compared to the previous method using *o*-aminophthalylhydrazido-*N*-acetyl-*β*-D-glucosaminide,[3] whose detection limit is 5 I.U./l and independent from the addition of CTMAB. However, the background emission is relatively high, which suggests a non-enzymatic hydrolysis of substrate **1**. This hydrolytic instability might be ascribed to a pH sensitivity of the diethylamino group at 6-position. A K_m value of 0.23 mM was calculated from the Lineweaver–Burk plot under these conditions.

In summary, we have synthesized both a new type of arylic hydrazide and, by introducing the enzyme-cleavable group, a new chemiluminogenic substrate for NAGase.

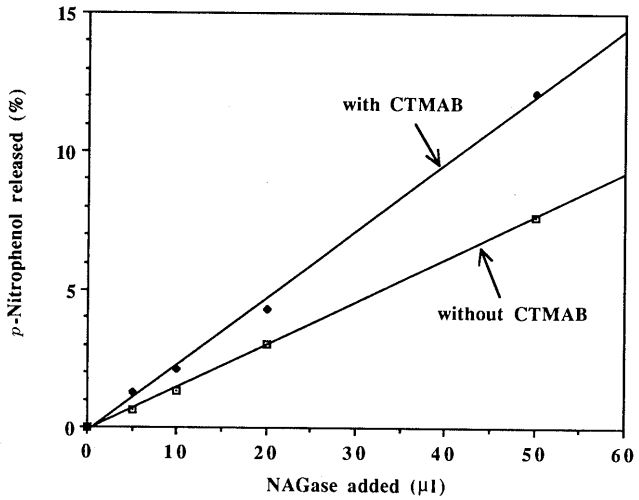

Fig. 3. Effect of the Addition of CTMAB on the NAGase Activity Using *p*-Nitrophenyl-*N*-acetyl-*β*-D-glucosaminide (PNP-NAG)

NAGase (55.6 I.U./ml) of a given amount (0—50 μl) was added to 1.0 ml of a pre-incubated 0.1 M citrate buffer (pH 5.0) containing PNP-NAG (4 mM), and the mixture was incubated at 37 °C for 5 min. Then 2.0 ml of 0.1 M bicarbonate buffer (pH 11.0) was added to terminate the enzymatic reaction and to measure the released *p*-nitrophenol at 400 nm. The same reaction was carried out in the presence of CTMAB (0.5% (w/v)).

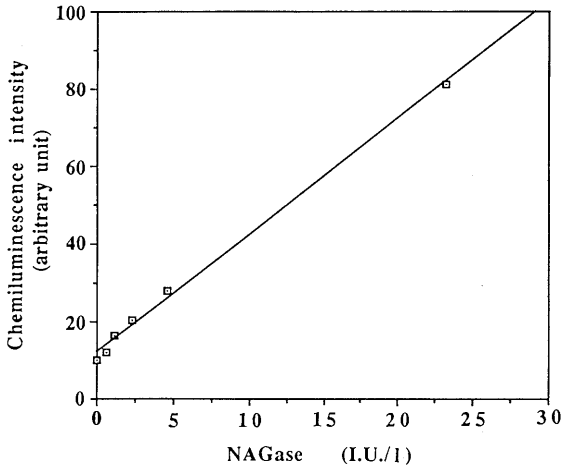

Fig. 4. Chemiluminescent Response of Substrate **1** to NAGase of Different Activities

NAGase solutions were treated according to the procedure described under Enzymatic Reaction.

Hydrazide **5** is more efficient than luminol, but more susceptible to aqueous quenching due to the hydrogen bonding effect. A number of arylic hydrazides have been synthesized in an effort to increase chemiluminescent efficiency, but only few are known to have a higher chemiluminescent quantum yield than luminol.[14] However, in an aprotic system, substitution of an electron-releasing group such as a methoxy or amino group on the phthalic hydrazide skeleton, for example, makes the parent luminol more efficient chemiluminescently because of an increase of the reaction rate and a higher fluorescence quantum yield of the corresponding phthalate.[4] In designing a highly efficient chemiluminescent compound, improving the fluorescence efficiency of a light emitter is a prerequisite. Most such compounds, however, suffer from substantial aqueous quenching, and sometimes lability to the oxidation or self-quenching of the fluorescence. The chemilumi-

nescence of hydrazide **5** is susceptible to aqueous quenching. However, it can be enhanced by cationic micelle through hydrophobic microenvironmental effects. Attaching a water-soluble substituent without affecting the chemiluminescene could offer an alternative solution to the problem of this aqueous quenching. In addition to chemiluminescent efficiency, the longer chemiluminescence wavelength of hydrazide **5** compared to luminol is another advantage because biological samples have less background emissions at longer wavelengths.

Regarding substrate **1**, because a chemiluminescence assay of enzymes being used currently involves multi-step enzymatic reactions to detect hydrogen peroxide as the final signal,[15] the approach using this substrate is straightforward in the sense that the substrate produces light directly on the action of the enzyme to be detected. Although sensitive detection of this enzyme of less than 0.5 I.U./l could be attainable by the conventional colorimetric[11,16] or fluorometric[17] methods, the present method offers an alternative to these spectrophotometric methods because of its simplicity and comparable sensitivity, and therefore it seems to have potential value in enzyme immunoassays. Furthermore, this kind of approach which involves incorporation of an enzyme-removable group into the hydrazide portion of an arycyclic hydrazide is not confined to a specific enzyme, basically being applicable to other enzymes such as those employed in enzyme immunoassays. In order to attain lower detection limits, however, the background emission caused by non-enzymatic hydrolysis should be minimized. Another factor that limits sensitivity and is inherent to this method is that the detection limit of the enzyme is restricted by the released amount of hydrazide **5**, rather than of the catalyst or hydrogen peroxide, which appears in a smaller amount than hydrazide **5** in this type of chemiluminescence reaction. We are currently working in this direction.

References

1) A. P. Schaap, M. D. Sandison and R. S. Handley, *Tetrahedron Lett.*, **28**, 1159 (1987).
2) I. Bronstein, B. Edwards and J. C. Voyta, *J. Bioluminescence and Chemiluminescence*, **4**, 99 (1989); J. C. Voyta, B. Edwards and I. Bronstein, *Clin. Chem.*, **34**, 1157 (1988); I. Bronstein, J. C. Voyta, G. H. G. Thorpe, L. J. Kricka and G. Armstrong, *ibid.*, **35**, 1441 (1989); I. Bronstein, J. C. Voyta and B. Edwards, *Anal. Biochem.*, **180**, 95 (1989).
3) K. Sasamoto and Y. Ohkura, *Chem. Pharm. Bull.*, **38**, 1323 (1990).
4) E. H. White and D. F. Roswell, *Acc. Chem. Res.*, **3**, 54 (1970) and references cited therein.
5) *a*) O. Dann, G. Bergen, E. Dermant and G. Voltz, *Justus Liebigs Ann. Chem.*, **749**, 68 (1971); *b*) S. Akiyama, H. Akimoto, S. Nakatsuji and K. Nakashima, *Bull. Chem. Soc. Jpn.*, **58**, 2192 (1985).
6) *Org. Synth. Coll. Vol.*, **V**, 1 (1973); D. H. Leabach, *Biological Preparations*, **10**, 118 (1963).
7) E. H. White and M. M. Bursey, *J. Org. Chem.*, **31**, 1912 (1966).
8) M. Yamada and S. Suzuki, *Anal. Lett.*, **17**, 251 (1984).
9) H. Karatani, *Bull. Chem. Soc. Jpn.*, **60**, 2023 (1987).
10) H. Karatani, *Chem. Lett.*, **1986**, 377.
11) E. Horak, S. M. Hopfer and F. W. Sunderman, Jr., *Clin. Chem.*, **27**, 1180 (1981).
12) P. H. Whiting, A. J. Nicholls and G. R. D. Catto, *Clin. Chim. Acta*, **108**, 1 (1980).
13) D. Maruhn, *Clin. Chim. Acta*, **73**, 453 (1976).
14) C. C. Wei and E. H. White, *Tetrahedron. Lett.*, **1971**, 3359; K. D. Gunderman, W. Horstmann and G. Bergmann, *Justus Liebigs Ann. Chem.*, **684**, 127 (1965).
15) S. Takayasu, M. Maeda and T. Tsuji, *J. Immunol. Methods*, **83**, 317 (1985).
16) A. Noto, Y. Ogawa, S. Mori, M. Yoshioka, T. Kitakaze, T. Hori, M. Nakamura and T. Miyake, *Clin. Chem.*, **29**, 1713 (1983).
17) D. H. Leabach and P. G. Walker, *Biochem. J.*, **78**, 151 (1961).

Post-translational Processing of Tumor Necrosis Factor Production

Namiko KITAHARA-TANABE, Yoshiyuki TANABE, Akinobu MORIKAWA, Den-Ichi MIZUNO, and Gen-Ichiro SOMA*

Biotechnology Research Center, Teikyo University, 907, Nogawa, Miyamae-ku, Kawasaki 216, Japan. *Received July 4, 1990*

To elucidate the mechanism of tumor necrosis factor (TNF) production, we analyzed proteins produced in macrophages sharing the epitope of TNF according to the priming and triggering of TNF production. Rabbit alveolar macrophages primed with Bacillus Calmette-Guerin (BCG) were isolated and cultured *in vitro* with ^{35}S-methionine, and the proteins produced were analyzed using anti-rabbit TNF monoclonal antibody. Primed with BCG, alveolar macrophages synthesized two proteins with molecular sizes of 50 and 17 kilodaltons (kDa) (p50 and p17) sharing the same epitope with mature TNF within the cells. These two proteins were released into the medium where other proteins were detected without TNF-activity. Cultured with lipopolysaccharide (LPS triggering), the primed alveolar macrophages released TNF-activity into the medium where p17 together with many larger proteins was detected by immunoprecipitation. *In vitro* translation of messenger ribonucleic acid (mRNA) from BCG-primed macrophages showed that primary TNF has a molecular size of 28 kDa (p28). These results suggest that active TNF of p17 is secreted when triggered *via* post-translational processing of the precursor molecules synthesized through priming with BCG.

Keywords macrophage; priming; triggering; tumor necrosis foctor production; post-translational regulation

A post-translational processing of cytokines derived from site-specific cleavage of the precursor has been reported for interleukin-1 (IL-1).[1-4] IL-1 is produced *via* post-translational processing of the precursor molecules; the process and products were reported in detail by Matsushima *et al.*[2] Like IL-1, the tumor necrosis factor (TNF) is a monokine produced by activated macrophages having a characteristic leader sequence different from the so-called signal peptide.[5,6] The present work presents evidence that active TNF, which has a molecular size of 17 kDa is produced and regulated by post-translational processing.

In the endogenous production of TNF, two steps of priming and triggering are known.[7] However, molecular machanisms of priming and triggering the production of TNF are still unknown. To learn the mechanism regulating TNF production at the molecular level, we analyzed the proteins produced in the stages from priming through triggering. Rabbit alveolar macrophages primed with Bacillus Calmette-Guerin (BCG) were isolated for the production of TNF with or without lipopolysaccharide (LPS) as a trigger. Their products were analyzed by anti-rabbit TNF monoclonal antibody, and their mRNAs were also examined in an *in vitro* translation system.

The results show that at the priming stage, mRNA, which encodes precursor TNF in *in vitro* protein synthesis, can be isolated within the cells, thus forming higher molecular sized TNFs called precursors which can be indentified by the monoclonal antibody. Triggered with LPS, the primed cells release a TNF molecule of 17 kDa which has TNF-activity.[7,8] This suggests that, on triggering, the post-translational processing of the precursor TNF might occur, which releases the TNF of 17 kDa.

Materials and Methods

Preparation of Alveolar Macrophages from Rabbit Japanese albino rabbits weighing 2.5—3.0 kg were injected intravenously (i.v.) with 18 mg lyophilized viable BCG (Japan BCG Ind., Tokyo, Japan). Ten days later they were anesthetized with Nembutal (Dainippon Pharmaceutical Co., Ltd., Osaka, Japan) containing 2000 units of heparin. Alveolar macrophages were prepared according to the procedure of Matthews.[9] The result of Giemsa staining revealed that more than 80% of the cells belonged to the macrophage population. Cells obtained in this way were used in the experiment as alveolar macrophages.

Monoclonal Antibody to Rabbit TNF Anti-rabbit TNF monoclonal antibody (Anti-TNF mAb) was prepared as described previously.[10]

Analysis of L-^{35}S-Methionine Labeled Proteins Synthesized in Primed Macrophages 1×10^7 cells of alveolar macrophages were suspended in 1 ml of Eagle's Minimal Essential Medium (MEM, minus methionine) containing L-^{35}S-methionine (New England Nuclear, Boston, MA., U.S.A., specific activity 1115 Ci/mmol, final concentration 100 μCi/ml) and incubated for 2 h at 37 °C under 5% CO_2 in air. Cells were washed twice in MEM and resuspended to reach the concentration of 2×10^5 cells/ml in MEM in the presence of lipopolysaccharide (LPS, from *Escherichia coli* 0127; B8, Difco Lab. Detroit, MI, U.S.A., final concentration 10 μg/ml) or in the absence of LPS. Then, the cells were cultured in 24 well multidishes (Nunc, Denmark) at 37 °C under 5% CO_2 in air. At 1, 2, 3 and 14 h after the incubation, the culture supernatant and cells were isolated. Cells were suspended in lysis buffer (50 mM Tris–HCl, pH 7.0, 25 mM KCl, 5 mM $MgCl_2$ and 0.1% Triton X-100) and placed on ice for 10 min. A cell extract was obtained by cetrifugation of the solution. Anti-rabbit TNF monoclonal antibody was added to each sample, which was then incubated overnight at 4 °C, followed by the addition of fixed *Staphylococcus aureus* cells (Cowan I strain).[11] The mixture was further incubated for 1 h at 30 °C. The immunoprecipitate was washed three times with 1 ml of 0.1% SDS, 10 mM Tris–HCl, pH 7.4, 2 mM EDTA dissociated with 0.1 M DTT, 2% SDS, 80 mM Tris–HCl, pH 6.8, 15% glycerol, 0.01% Bromophenol blue; and subjected to electrophoresis on 15% SDS-polyacrylamide gel. For fluorography, gels were treated with an autoradiography enhancer, EN^{3}HANCE (New England Nuclear, Boston, MA, U.S.A.), dried and exposed to XAR-5 film (Eastman Kodak Co., Rochester, NY, U.S.A.).

TNF Assay The TNF-activity of the cell extract and culture supernatant was measured by *in vitro* cytotoxicity assay with L929 cells as a target, according to the method of Ruff and Gifford,[12] with an internal standerd of rTNF-α (PAC-4D 2×10^6 U/mg, donated by Asahi Chem. Ind., Tokyo, Japan).

Isolation of Poly A RNA Poly A RNA of rabbit alveolar macrophages was prepared by the method previously reported.[13]

Cell Free Protein Synthesis and Product Analysis Cell free protein synthesis of poly A RNA isolated from rabbit alveolar macrophages primed with BCG was carried out with a nuclease-treated rabbit reticulocyte lysate system (Radiochemical Center, Amersham, U.K.). Analysis of translation products was carried out using the same methods as for the labeled proteins *in vitro*.

Results

Labeling and Chase of Alveolar Macrophage TNF BCG-primed alveolar macrophages were isolated and labeled with ^{35}S-methionine for 2 h, then washed and chased in a cold medium in the presence or absence of LPS as a trigger. The ^{35}S-radioactivity of the TCA-insoluble fraction in the supernatant of the medium was assayed.

As shown in Fig. 1, ^{35}S-radioactivity in the TCA-insoluble fraction was detected in media with the presence and absence

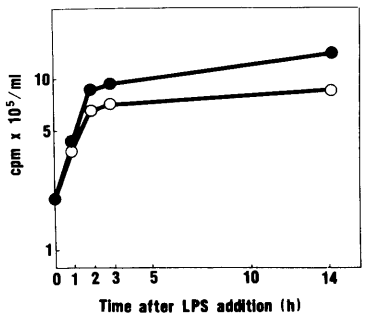

Fig. 1. ^{35}S-Radioactivity of TCA-Insoluble Fraction Released into the Culture Medium of BCG-Primed Macrophages with or without LPS

BCG-primed macrophages were labeled with ^{35}S-methionine for 2 h. After labeling, cells were washed, then cultured with LPS at 10 μg/ml (●) or without LPS (○). TCA-insoluble counts of aliquots of the supernatant at 0, 1, 2, 3, and 14 h, as indicated on the abscissa, were measured. The counts corresponding to the culture medium of 1×10^5 cells are indicated on the ordinate.

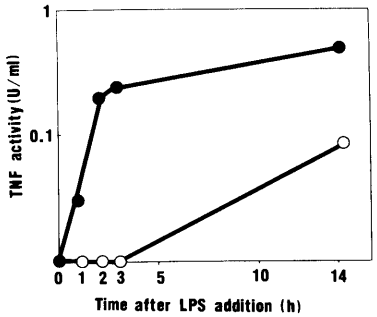

Fig. 2. TNF Cytotoxicity Assay on the Culture Supernatant of BCG-Primed Macrophages with or without LPS

TNF cytotoxicity assay was carried out on L929 cells as a target. Culture time (h) is indicated on the abscissa. Ordinate indicates the TNF activity in units/ml. Culture supernatant of the cells: with LPS (●), or without LPS (○).

of LPS at an early stage. Total activity detected in the medium with LPS was 30% higher than that without.

Cytotoxicity of TNF in the supernatant of the incubation medium was assayed with L929, and was revealed to run parallel to the radioactivity in the TCA-insoluble fraction only when LPS was added during the first 1—2 h of incubation (Fig. 2). During the same period, no cytotoxic activity was observed in the supernatant of the incubation medium that had no LPS, although slight activity was detected 14 h after the incubation.

Identification of Proteins Produced by Triggering with LPS Anti-TNF mAb was used to analyze and to identify the ^{35}S-proteins obtained as above. The supernatant of the incubation medium of BCG-primed rabbit alveolar macrophages labeled with ^{35}S-methionine and chased in the presence or absence of LPS was isolated, condensed and treated with anti-TNF mAb. Aggulutinates thus formed were then treated with staphylococcal bacterial cells, and the proteins bound to these cells were released and analyzed fluorographically on SDS-polyacrylamide gel. As shown in Fig. 3, a variety of bands were detected on the fluorogram, but the main bands were found at positions 65, 54, 50, 43, 39 and 17 kDa, regardless of whether or not the samples were from supernatant containing LPS. However, the 17 kDa band from the supernatant in the presence of LPS was slightly smaller than that in the absence of LPS, and the activity of TNF in the supernatant with LPS was significantly higher than that without.

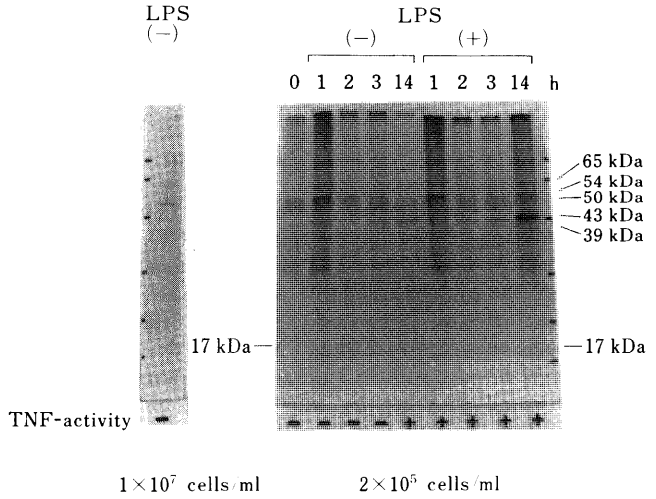

Fig. 3. Immunoprecipitation of Culture Supernatant of BCG-Primed Macrophages with or without LPS

^{35}S-Methionine labeled macrophages were cultures with (+) or without (−) LPS. The supernatant of the culture at the time indicated was treated with anti-rabbit TNF monoclonal antibody as described in Materials and Methods. Immunoprecipitate formed was subjected to 15% SDS-polyacrylamide gel electrophoresis followed by fluorography.

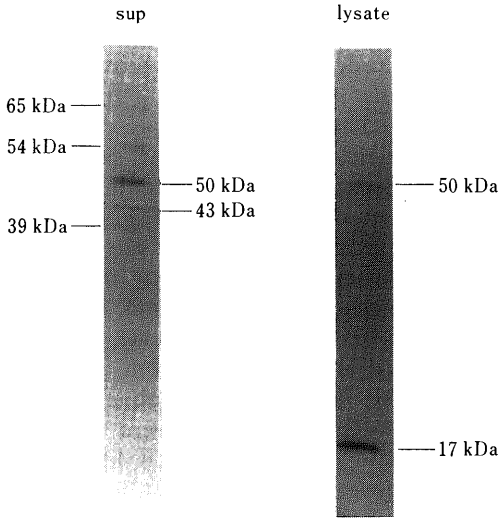

Fig. 4. Analysis of the Proteins in BCG-Primed Macrophages Cultured with ^{35}S-Methionine *in Vitro* by Using Immunoprecipitation Method

BCG-primed macrophages of 1×10^7 cells were isolated and cultured in 1 ml of MEM containing 100 μCi of ^{35}S-methionine for 2 h. Culture supernatant and cells were obtained and subjected to immunoprecipitation. Immunoprecipitates were then analyzed as described in the legend of Fig. 3 by SDS-polyacrylamide gel electrophoresis followed by fluorography. The left lane shows culture supernatant and the right shows cell lysate.

TNF-Like Proteins Isolated from Alveolar Macrophages Primed with BCG Rabbit alveolar macrophages primed with BCG (1.2×10^5 cells/well) were incubated for 2 h in a medium containing ^{35}S-methionine, then washed and lysed with a lysis buffer. Cell debris was discarded and anti-TNF mAb was added to the supernatant in which no TNF activity was detected. Agglutinates thus formed were further treated with staphylococcal bacterial cells. The proteins bound to the bacterial cells were released and analyzed fluorographically on SDS-polyacrylamide gel. The result of the analysis using anti-TNF mAb shows the existence of two marked bands corresponding to the sizes of 50 and 17 kDa on the fluorogram (Fig. 4), while no band was observed

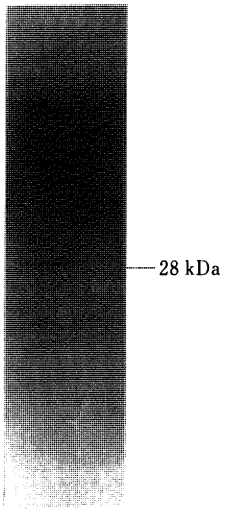

Fig. 5. Analysis of *in Vitro* Translation Product by Immunoprecipitation

0.5 μg of poly A RNA from BCG-primed rabbit macrophages was subjected to *in vitro* translation using a rabbit reticulocyte system. After translation, the reaction mixture was immunoprecipitated by monoclonal antibody. The proteins immunoprecipitated were analyzed as described in the legend of Fig. 3.

when unprimed alveolar macrophages were treated in the same way as the control (data not shown). These results indicate that TNF-like proteins (p50 and p17), which share the epitope with rabbit TNF having no TNF activity, are produced by priming with BCG.

***In Vitro* Translation Product with mRNA of Alveolar Macrophages** mRNA from alveolar macrophages primed with BCG was isolated as a poly A RNA. The mRNAs were translated in a rabbit reticulocyte lysate system. The proteins immunoprecipitated with anti-TNF mAb were analyzed fluorographically on SDS-polyacrylamide gel. As shown in Fig. 5, only one band of 28 kDa was observed on the fluorogram, indicating that in the reticulocyte lysate system, mRNA derived from primed macrophages encodes only one protein of 28 kDa, which is larger than TNF of 17 kDa and shares the epitope with the TNF of the latter.

Discussion

In this study we have examined post-translational processes of TNF production by using rabbit alveolar macrophages. The results obtained suggest that TNF-like proteins which have no TNF-activity are produced primarily within the primed cells; and, once triggered with LPS, they are subsequently processed and release active TNF of 17 kDa.

In the alveolar macrophages primed with BCG, no TNF-activity was detected, but the two proteins of p50 and p17, sharing the epitope of mature TNF, were identified (Fig. 4). On the other hand, mRNA derived from primed cells encodes in an *in vitro* translation system only the 28 kDa protein, which shares the epitope (Fig. 5). Since such proteins are not detected in unprimed macrophages, the priming process may involve a step which switches on mRNA transcription within the cells. Beutler and Cerami proposed that the mRNA present in primed mouse peritoneal macrophages does not produce a protein having the epitope of TNF (cachectin).[14] We do not know the reason for the discrepancy of their results with ours, but we should point out the existence of differences in the methods for detecting TNF molecules in the two groups: we used an immunoprecipitation method for radioisotope-labeled proteins, while they used immunoblotting. Therefore, this discrepancy may reside in a difference of sensitivity between the two methods. Moreover, different sources of macrophage preparations, *i.e.* alveolar macrophages and peritoneal macrophages, might bring about different mechanisms of TNF production.

p50 is quite interesting because its molecular size is larger than that of an *in vitro* translation product (Figs. 4 and 5). It is known that TNF has a trimeric form under native conditions.[15] However, it is quite unlikely that the assembly of TNF monomers or disulfide bridges may be formed in the TNF molecules under the conditions of SDS-polyacrylamide gel electrophoresis. Thus, at present we cannot explain the relationship between p50 and p17.

When the primed macrophages were labeled with ^{35}S-methionine and chased, a high level of redioactivity was detected during the first 2 h in the medium from which a variety of bands were observed on a fluorogram of SDS-polyacrylamide gel, irrespective of the presence or absence of a trigger (Figs. 1 and 3). These proteins may have the same epitope as that of TNF. However, no TNF-activity was detected in the incubation medium without triggering, whereas a significant amount was observed upon triggering with LPS (Fig. 2). After 14 h, a small amount of TNF-activity was observed even in the absence of a trigger. These facts suggest that during the first 2 h of incubation in the absence of a trigger, labeled proteins which shared the same epitope as that of TNF were processed automatically to convert into a variety of proteins, all of which have the same epitope but which lack the TNF-activity, and that triggering with LPS can produce active TNF molecules, probably of 17 kDa, in the primed cells, since a protein(s) showing TNF-activity cannot be detected until at least 14 h have elapsed in the case of no trigger.

Rabbit TNF as a monomer has been reported to have a molecular size of 17 kDa.[6,8] We were unable to separate or identify the two 17 kDa bands, one with and one without triggering, although they have slightly different mobilities. Recently, Cseh and Beutler reported an inactive TNF molecule of 18.5 kDa in mouse RAW264.7 cells.[16] This inactive TNF has 10 additional amino terminal residues as compared with mature TNF, suggesting an incomplete processing product. The two 17 kDa bands with slightly different mobilities observed in our experiments may also reflect a similar phenomenon. Obviously, proteins of these two bands are qualitatively different: one shows TNF-activity while the other does not, although they share the same TNF epitope. Such equivocal findings were also found by Spriggs *et al.*[17] They reported that the inactive 17 kDa molecule was found in tumor cells which were resistant to TNF, but they mentioned nothing more about it. The reason remains to be clarified.

The results we have obtained so far suggest that the priming switches on the transcription of mRNA which encode precursor TNFs and produce precursor proteins having no TNF-activity in the cells, and those which trigger these proteins are probably processed around the cell membranes to be converted into a variety of proteins which share the same epitope as that of TNF. Triggered with LPS,

TNF-activity can actually be preduced among these proteins. The mechanism of this process is ascribable to the perturbation of cells or lysosomal membranes, involving the activation of lysosomal enzyme by LPS, which is well known as a lysosome labilizer.

The integrated form of TNF was reported by Kriegler *et al.*[18] If we suppose that the primary product of 28 kDa is integrated into the cell membranes immediately after the synthesis of the primed macrophages, our result that the 28 kDa precursor was not detected in the cell lysate is explainable. In any event, it seems very likely that the triggering process is associated with membrane function, where some types of proteolytic processing of the precursor molecule can be expected.

References and Notes

1) Abbreviations: IL-1, interleukin-1; TNF, tumor necrosis factor; BCG, Bacillus Calmette-Guerin; LPS, lipopolysaccharide; mRNA, messenger ribonucleic acid; kDa, kilodalton; mAb, monoclonal antibody; MEM, minimal essential medium; SDS, sodium dodecyl sulfate; EDTA, ethylenediaminetetraacetic acid; DTT, dithiothreitol; rTNF, recombinant tumor necrosis factor; TCA, trichloroacetic acid; cpm, count per minute.
2) K. Matsushima, M. Taguchi, E. J. Kovacs, H. A. Young, and J. J. Oppenheim, *J. Immunol.*, **136**, 2883 (1986).
3) P. E. Auron, S. J. C. Warner, A. C. Webb, J. G. Cannon, H. A. Bernheim, K. J. P. W. McAdam, L. J. Rosenwasser, G. LoPreste, S. F. Mucci, and C. A. Dinarello, *J. Immunol.*, **138**, 1447 (1987).
4) M. J. Kostura, M. J. Tocci, G. L. Limjuco, J. Chin, P. Cameron, A. G. Hillman, N. A. Chartratin, and J. A. Schmidt, *Proc. Natl. Acad. Sci. U.S.A.*, **86**, 5227 (1989).
5) D. Pennica, G. E. Nedwin, J. S. Hayflick, P. H. Seeberg, R. Derynck, M. A. Palladino, W. J. Kohr, B. B. Aggarwal, and D. V. Goeddel, *Nature* (London), **312**, 724 (1984).
6) H. Ito, S. Yamamoto, S. Kuroda, H. Sakamoto, J. Kajihara, T. Kiyota, H. Hayashi, M. Kato, and M. Seno, *DNA*, **5**, 149 (1986).
7) E. A. Carswell, L. J. Old, R. L. Kassel, S. Green, N. Flore, and B. Williamson, *Proc. Natl. Acad. Sci. U.S.A.*, **72**, 3666 (1975).
8) S. Abe, T. Gatanaga, M. Yamazaki, G. Soma, and D. Mizuno, *FEBS Lett.*, **180**, 203 (1985).
9) N. Matthews, *Br. J. Cancer*, **44**, 418 (1981).
10) M. Nagai, T. Saigusa, Y. Shimada, H. Inagawa, H. Oshima, and M. Iriki, *Experientia*, **44**, 606 (1988).
11) S. W. Kassler, *J. Immunol.*, **115**, 1617 (1975).
12) M. R. Ruff and G. E. Gifford, *J. Immunol.*, **125**, 1671 (1980).
13) G. Soma, M. Obinata, and Y. Ikawa, *Biochemistry*, **19**, 3967 (1980).
14) B. Beutler and A. Cerami, *Nature* (London), **320**, 584 (1986).
15) R. A. Smith and C. Baglioni, *J. Biol. Chem.*, **262**, 6951 (1987).
16) K. Cseh and B. Beutler, *J. Biol. Chem.*, **264**, 16256 (1989).
17) D. Spriggs, K. Imamura, C. Rodriguez, J. Horiguchi, and D. W. Kufe, *Proc. Natl. Acad. Sci. U.S.A.*, **84**, 6563 (1987).
18) M. Kriegler, C. Perez, K. DeFay, I. Albert, and S. D. Lu, *Cell*, **53**, 45 (1988).

Structural and Functional Characterization of Calelectrins from Bovine Liver

Toshihiro FUJII,* Hirotada AKASHI, Yoshiro OGOMA and Yoshiyuki KONDO

Faculty of Textile Science and Technology, Shinshu University, 3–15–1, Tokida, Ueda, Nagano 386, Japan. *Received July 10, 1990*

Two Ca^{2+}-dependent membrane-binding proteins with apparent molecular weights of 70000 (calelectrin$_{70}$) and 32000 (calelectrin$_{32}$) were isolated from bovine liver using phenyl–Sepharose affinity chromatography followed by diethylaminoethyl (DEAE)–cellulose and Ultrogel AcA44 chromatographies. Limited proteolysis and immunological analyses indicated that calelectrin$_{32}$ was not a digested product from calelectrin$_{70}$. Both calelectrins bound to phosphatidylserine and to calmodulin in a Ca^{2+}-dependent manner. Circular dichroism studies showed that the apparent α-helical contents of calelectrin$_{70}$ and calelectrin$_{32}$ were 25 and 40%, respectively and they underwent Ca^{2+}-dependent conformational changes. When the calelectrins were incubated with a brain microtubule preparation, they were phosphorylated by endogenous kinase(s) and phosphorylation occurred on serine residues. Moreover, calelectrin$_{70}$ showed an inhibitory action on endogenous kinase activity in the presence of Ca^{2+}.

Keywords calelectrin; calmodulin; microtubule; phosphatidylserine; calcium; phosphorylation; circular dichroism

A new family of Ca^{2+}-binding proteins which interact with membranes and cytoskeletons has been established in a wide variety of animal tissues and termed annexin.[1] The family includes calelectrin,[2] lipocortin/calpactin,[3,4] calcimedin,[5] chromobindin,[6] and protein I—III.[7] The family of annexin is distinct from that of the EF-hand type Ca^{2+}-binding proteins.[8] These proteins can bind to acidic phospholipids and F-actin in a Ca^{2+}-dependent manner.[3,7,9] Lipocortins are physiological intracellular substrates for pp $60^{v\text{-}src}$[10] and the epidermal growth factor (EGF) receptor protein–tyrosine kinase,[11] indicating that these proteins participate in cell multiplication. Lipocortins have also been shown to inhibit phospholipase A_2 activity[12] and to act as anticoagulant factors.[13]

In this paper, we isolate calelectrins with molecular weights of 70000 and 32000 from bovine liver. We show their structural differences using specific antibodies and circular dichroism (CD), their affinity to bind phospholipids and calmodulin using affinity chromatography and their phosphorylation by endogenous kinase(s) in microtubule fractions.

Materials and Methods

Preparation of Proteins Calelectrins were prepared from frozen bovine liver by the method of Sudhof *et al.*[14] with some modifications. Briefly, about 150 g of liver was homogenized in 2 vol. of buffer A (10 mM *N*-2-hydroxyethylpiperazine-*N'*-2-ethanesulfonic acid (HEPES)–NaOH, pH 7.4, 150 mM NaCl and 0.05% NaN_3) containing 2 mM $CaCl_2$ in Polytron, and the homogenate was centrifuged at 27000 × *g* for 30 min at 4 °C. The pellets were washed twice by the above buffer. The final pellets were resuspended in buffer A containing 5 mM ethyleneglycol-bis(2-aminoethylether)*N*,*N*,*N'*,*N'*-tetraacetic acid (EGTA), and the suspension was centrifuged at 27000 × *g* for 30 min and 100000 × *g* for 60 min. The obtained supernatant was adjusted at 2 mM $CaCl_2$ and was applied to a phenyl–Sepharose 4B column (3 × 16 cm) which was equilibrated with buffer A containing 2 mM $CaCl_2$. The column was washed with the above buffer and the adsorbed proteins were eluted with 10 mM Tris–HCl buffer (pH 7.8) containing 10 mM EGTA. The eluate, which mainly consisted of 70000, 32000 and 17000 polypeptides on sodium dodecyl sulfate–polyacrylamide gel electrophoresis (SDS-PAGE), was dialyzed against buffer B (10 mM imidazole–HCl, pH 6.2, and 1 mM ethylenediaminetetraacetic acid (EDTA)). The dialyzate was then applied to a DEAE-cellulose column (1 × 18 cm) equilibrated with buffer B. After washing with the same buffer, the column was eluted with buffer B containing 50, 150 and 500 mM NaCl for obtaining 32000, 70000 and 17000 polypeptides, respectively. The 50 and 150 mM NaCl fractions were further purified on an Ultrogel AcA-44 column (3 × 85 cm) equilibrated with 20 mM Tris–HCl buffer (pH 7.5) containing 200 mM NaCl, 2 mM EDTA and 0.05% NaN_3. The yields of 70000 and 32000 polypeptides were about 2.4 and 4.2 mg, respectively.

Microtubule proteins were prepared from rat brain by three cycles of temperature-dependent polymerization and depolymerization as described previously.[15] Calmodulin was purified from porcine brain according to the method reported by Ishioka *et al.*[16]

SDS-PAGE SDS-PAGE was performed using the discontinuous buffer system of Laemmli[17] in 0.8 mm thick slab gels containing 10% acrylamide.

Immunochemical Experiments Antibodies against calelectrins were raised in female rats. Proteins separated by SDS-PAGE were electrophoretially transferred to a nitrocellulose membrane (Schleicher & Schüll) according to Towbin *et al.*[18] After blocking with 1% fetal calf serum in Tris-buffered saline (10 mM Tris–HCl, pH 7.5, and 150 mM NaCl) for 4 h at 25 °C, the filter was incubated with diluted antisera (1 : 500) to calelectrins for 2 h at 37 °C. For the dilution, 5% bovine serum albumin in Tris-buffered saline was used. The filter was then incubated with alkaline phosphatase-conjugated anti-rat immunoglobulin G (IgG) for 2 h at 37 °C. The immunoreactive bands were visualized by using nitro blue tetrazolium and 5-bromo-4-chloro-3-indolyl phosphate as a substrate for alkaline phosphatase.[19]

Protease Cleavage Calelectrins were digested with 1/25 (w/w) trypsin (Worthington), 1/25 chymotrypsin (Sigma) or 1/80 V8 protease (Miles). The buffer used was 20 mM Tris–HCl, pH 7.4, 1 mM EDTA and 0.2 mM dithiothreitol (DTT). After incubation for 2 h at 37 °C, reactions were terminated by the addition of a 5× electrophoresis buffer (155 mM Tris–HCl, pH 6.8, 5% SDS, 25% glycerol, 0.75% β-mercaptoethanol and 0.0025% pyronin Y).

CD CD spectra were measured with a Jasco J-40 spectropolarimeter at room temperature, approximately 23—24 °C. The CD measurement is performed in a 0.1 mm cylindrical quartz cell. The CD data is expressed in terms of mean residue ellipticity, $[\theta]$. The mean residue molecular weight of calelectrins was assumed to be 129 from the amino acid composition.[14]

Phosphorylation Analysis Phosphorylation was carried out at 37 °C in 30 μl of a kinase buffer consisting of 50 mM 2-(*N*-morpholino)ethanesulfonic acid (MES)–KOH, pH 6.5, 1 mM $Mg(CH_3COO)_2$, 1.5 mM EGTA (or 2 mM $CaCl_2$), 6 μM [γ-^{32}P] adenosine triphosphate (ATP) (5 μCi/nmol) and 10 μg of microtubule proteins. After 1 min incubation, the reaction was terminated by the addition of 12 μl of a 5× electrophoresis sample buffer. Samples were boiled at 100 °C for 1 min and applied quantitatively to SDS–polyacrylamide gels. The gels were stained with Coomassie Brilliant Blue, dried, and exposed for 5—15 h to X-Omat film (Kodak).

Phosphoamino Acid Analysis Phosphorylated calelectrin$_{70}$ was eluted from gels and dialyzed against 50 mM $NaHCO_3$, pH 8.0, to remove the electrode buffer. The protein was digested with trypsin for 16 h at 37 °C, and then subjected to acid hydrolysis in 6 N HCl for 2 h at 110 °C. The phosphoamino acids were resolved by electrophoresis on a cellulose thin layer plate in formic acid–acetic acid–water (44 : 156 : 1800) at pH 1.9, followed in acetic acid–pyridine–water (50 : 5 : 945) at pH 3.5 as described previously.[20]

Preparation of Affinity Column Phosphatidylserine (PS)- and phosphatidylcholine (PC)-conjugated polyacrylamide gels were prepared according to the procedure of Uchida and Filburn.[21] Calmodulin was coupled to cyanogen bromide (CNBr)–activated Sepharose 4B (Pharmacia) following the procedures outlined by Pharmacia. About 1 mg calmodulin was linked

to 0.3 ml Sepharose.

Results

Proteolytic Digestions of Calelectrins The structural relationships between calelectrin$_{70}$ and calelectrin$_{32}$ were examined using limited proteolysis and immunoblot. Figure 1 shows the digestion of calelectrins with trypsin, chymotrypsin and V8 protease. Calelectrins were not digested by trypsin. Chymotrypsin and V8 protease appeared to generate a group of fragments around 32000, so they did not attack to calelectrin$_{32}$. Immunoblotting with the polyclonal antibodies raised against calelectrin$_{70}$ and calelectrin$_{32}$ showed that calelectrin$_{70}$ and its fragments were strongly recognized by anti-calelectrin$_{70}$ antibodies, but barely by anti-calelectrin$_{32}$ antibodies, and *vice versa* for calelectrin$_{32}$. These results suggest that calelectrin$_{32}$ was not a digested product from calelectrin$_{70}$, and that both proteins showed differential reactivities with their antibodies.

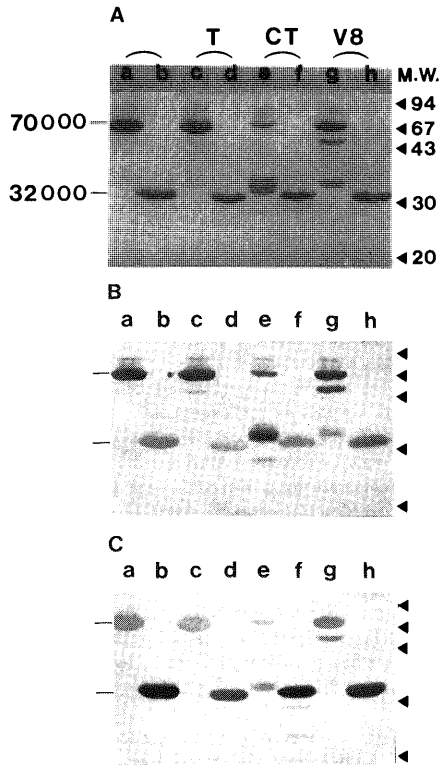

Fig. 1. Limited Digestion of Calelectrins by Trypsin (T), Chymotrypsin (CT) and V8 protease (V8), and Antibody Specificity

Samples were subjected to electrophoresis on 15% polyacrylamide gels. A, Coomassie Blue-stained SDS gels. B and C, Nitrocellulose transfer of gels with the same as in (A) and immunostained using anti-calelectrin$_{70}$ (B) and anti-calelectrin$_{32}$ (C). Calelectrin$_{70}$ (a, c, e, g); calelectrin$_{32}$ (b, d, f, h). The arrows indicate the position of molecular weight markers: phosphorylase b (94000), bovine serum albumin (67000), ovalbumin (43000), carbonic anhydrase (30000) and trypsin inhibitor (20000).

CD Spectra of Calelectrins The secondary structures of calelectrins in the absence and presence of Ca^{2+} were estimated from CD spectra (Fig. 2A and 2B). Calelectrins had two negative bands at 208 and 222 nm. In the absence of Ca^{2+} the α-helix contents of calelectrin$_{70}$ and calelectrin$_{32}$ were 25 and 40%, respectively (Fig. 2C). The addition of Ca^{2+} to the solutions decreased the content of the α-helix. At 2 mM Ca^{2+}, the contents were 9% in calelectrin$_{32}$ and 33% in calelectrin$_{70}$.

Interaction with Phospholipids and Calmodulin The binding of calelectrins to phospholipids was examined using columns of PS or PC immobilized by polyacrylamide gels. The fraction which was eluted by phenyl-Sepharose 4B consisted of calelectrin$_{70}$, calelectrin$_{32}$, calmodulin and a 68000 peptide. Ca^{2+} was added to 1 mM, and the sample was applied to a PS–polyacrylamide gel column equilibrared with buffer C (10 mM HEPES–NaOH, pH 7.4, 100 mM KCl and 0.05% NaN_3) containing 1 mM $CaCl_2$. The column was washed with the above buffer and the bound proteins were eluted by 10^{-6} and 10^{-7} M Ca^{2+} in buffer C (Fig. 3). Electrophoretic analysis showed that calelectrins were retained on the PS column at higher Ca^{2+} concentrations and released below 10^{-7} M Ca^{2+}. Calmodulin and a 68000 peptide were found in the unbound fraction. On the other hand, calelectrins did not bind to PC irrespective of the Ca^{2+} concentrations (data not shown).

We examined the interaction between calelectrins and calmodulin. As shown in Fig. 4, calelectrins were retained by calmodulin–Sepharose 4B in the presence of Ca^{2+} and eluted with EGTA.

Phosphorylation of Calelectrins by Microtubule Fraction The components of the annexin family have been

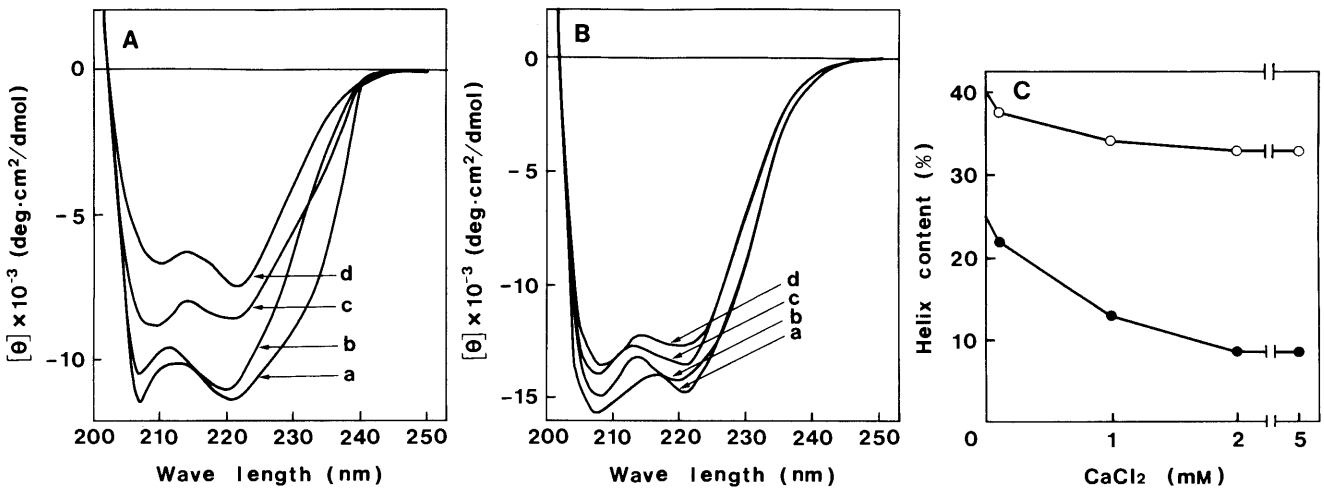

Fig. 2. Effects of Ca^{2+} on the CD Spectra of Calelectrins

The protein concentration was 0.34 mg/ml and the solvent was 20 mM Tris-HCl, pH 7.4, and 100 mM NaCl. Calelectrin$_{70}$ (A and ●); calelectrin$_{32}$ (B and ○). a, 1 mM EGTA; b, 0.1 mM $CaCl_2$; c, 1 mM $CaCl_2$; d, 2 mM $CaCl_2$.

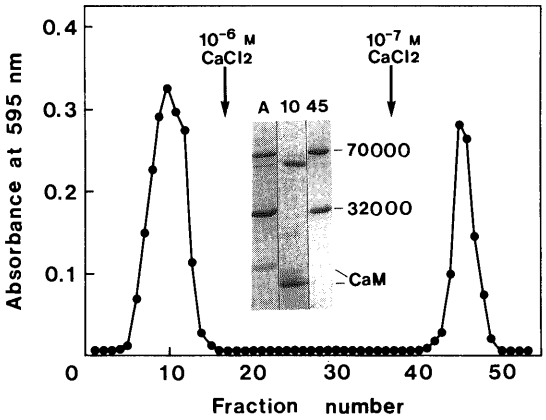

Fig. 3. Affinity Chromatography on the Polyacrylamide-Immobilized PS of Calelectrins

A fraction enriched in calelectrins obtained from Phenyl-Sepharose 4B was tested for the ability to bind to PS. The fraction was dialyzed against buffer C, Ca^{2+} was added to 1 mM, then the sample was applied to a PS-polyacrylamide gel column (1 × 8 cm) equilibrated with buffer C containing 1 mM $CaCl_2$. The column was washed with the same buffer, and at the points indicated by arrows, the bound protein was eluted with buffer C containing 10^{-7} M and 10^{-6} M $CaCl_2$. Fractions of 1 ml each were collected and analyzed for proteins using the Bradford assay. The inset shows the SDS-polyacrylamide gel profile, for the applied sample (A) and fractions 10 and 45. CaM, calmodulin.

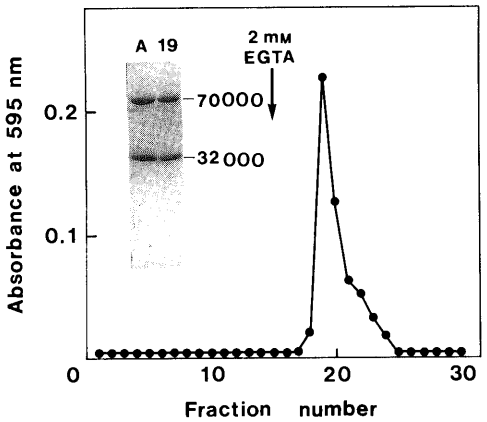

Fig. 4. Calmodulin-Sepharose 4B Affinity Chromatography of Calelectrins

Calelectrins were applied to a calmodulin-Sepharose column (0.9 × 8 cm) equilibrated with buffer C containing 1 mM $CaCl_2$. The column was washed with the same buffer, and at the point indicated by the arrow, the bound protein was eluted with 2 mM EGTA. Fractions (1 ml) were collected and analyzed for protein. The inset shows the applied sample (A) and fraction 19.

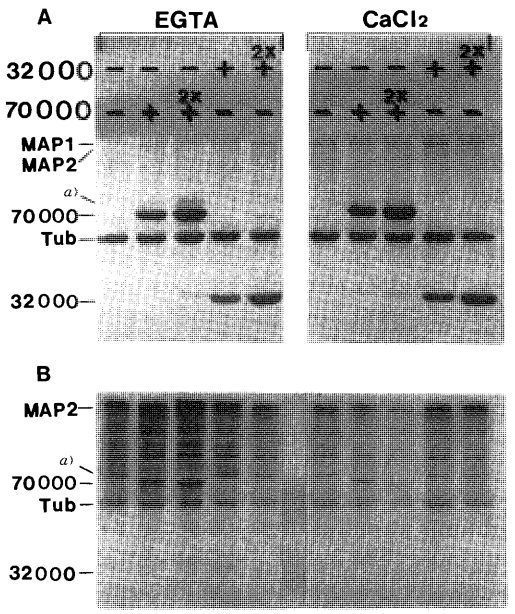

Fig. 5. Phosphorylation of Calelectrins by the Endogenous Kinases in Microtubule Fraction

The reaction mixtures contain 0.33 mg/ml of microtubule proteins, 0.16 mg/ml or 0.32 mg/ml (2×) of calelectrins either in the presence of 1.5 mM EGTA or 2 mM $CaCl_2$. The reaction products were separated by SDS-PAGE. A, Coomassie blue-stained gels; B, autoradiography. *a)* indicates the position of a 72000 peptide. Tub, tubulin.

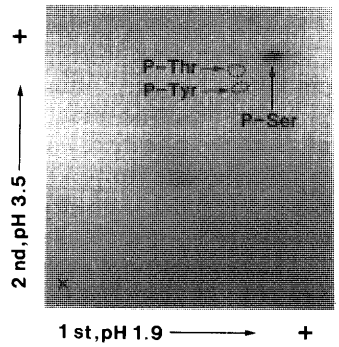

Fig. 6. Phosphoamino Acid Analysis of Phosphorylated $Calelectrin_{70}$

The positions for phosphoserine, phosphothreonine and phosphotyrosine are indicated.

shown to be phosphorylated by EGF receptor protein-tyrosine kinase, kinase C and oncogene products.[10,11,22] It has been reported that microtubule fraction from rat brain shows endogenous kinase activities.[23-25] We studied whether calelectrins were phosphorylated by the kinases in rat brain microtubule fraction. In the absence of calelectrins, microtubule-associated protein (MAP)2, which can regulate the assembly and disassembly of microtubules, was a preferential substrate for the kinases, and the phosphorylation of the protein bands including MAP2 was reduced in the presence of 2 mM Ca^{2+} (Fig. 5). When calelectrins were exogenously added to the solution, both proteins were phosphorylated in the absence and presence of Ca^{2+} and the extent was more prominent in $calelectrin_{70}$ than in $calelectrin_{32}$. In addition, $calelectrin_{70}$ reduced the phosphorylation of microtubule components, especially a 72000 peptide, in the presence of Ca^{2+}, but $calelectrin_{32}$ did not.

Phosphoamino acid content was analyzed by thin layer chromatography. $Calelectrin_{70}$ was phosphorylated by the kinases in microtubule fraction on serine residues (Fig. 6).

Discussion

We isolated two distinct forms of calelectrins (70000 and 32000) from bovine liver, which bound to PS and calmodulin in a Ca^{2+}-dependent fashion (Figs. 3 and 4). Recently, Sudhof *et al.*[26] reported the amino acid sequence of human $calelectrin_{67}$. Like other components of the annexin family, $calelectrin_{67}$ has a core domain consisting of an 8-fold repeat of the conserved 70-amino acid sequence, while $calelectrin_{32}$ contains a 4-fold repeat of the sequence. These results suggest that both are homologous proteins and belong to the annexin family. CD studies have indicated that $calelectrin_{34}$ from *Torpedo marmorata* has a 78% α-helix and the content is unchanged by the addition of Ca^{2+}.[27] More recently, Mani and Kay[28] have shown that the α-helix content (10—12%) of $calcimedin_{67}$ from chicken gizzard decreases by 6—8% in the presence of 0.5 mM Ca^{2+}. We

also observed a decrease in the α-helix contents of calelectrins by Ca^{2+}. Like the binding of calelectrins to F-actin, the Ca^{2+}-sensitivity was low compared to their binding to PS. The α-helix contents and Ca^{2+}-sensitivity were different among calelectrin$_{70}$, calelectrin$_{32}$ and calcimedin$_{67}$. Immunoblot analysis showed that the antibodies raised to calelectrin$_{32}$ weakly recognized calelectrin$_{70}$ (Fig. 2) and chicken gizzard calcimedin$_{67}$ (data not shown), while the antibodies to calelectrin$_{70}$ behaved *vice versa*. This data strongly suggests that calelectrins are distinctively different from each other in secondary structure and antigenicity, and may modulate distinct biological responses on the inner surface of the plasma membrane.

Lipocortins and calpactins have been shown to bind the F-actin from rabbit skeletal muscle at high concentrations of Ca^{2+} ($>10^{-4}$ M).[7,29] We observed that both subject calelectrins also interacted with F-actin when the KCl concentrations were less than 100 mM and Ca^{2+} concentrations were more than 2×10^{-4} M (data not shown). To study the possibility of F-actin being a physiological target protein for calelectrins, further experiments are necessary to determine whether phospholipids and phosphorylation modulate the binding under physiological conditions.

Microtubules have dynamic structures considered to play important roles in various cellular mechanisms including cell division, intracellular movements, pinocytosis and secretion processes. It has been reported that brain microtubule preparations contain endogenous protein kinases and that MAP2 is a major substrate for the kinase *in vitro*.[23,24] Cyclic adenosine monophosphate (AMP)-dependent protein kinase has been found to associate with microtubules.[24,25] We observed that addition of cyclic AMP (5 μM) stimulated the phosphorylation of MAP2 and calelectrins (data not shown). However, the phosphorylation of calelectrins remained considerably stable when *N*-[2-(methyl-amino)ethyl]-5-isoquinolinesulfonamide dihydrochloride (H-8), an inhibitor of cyclic AMP-dependent kinase, was added (0.5—20 μM). The kinase activity in the microtubule fraction was not affected by well-known kinase activators and inhibitors, such as cyclic guanosine monophosphate (GMP), Ca^{2+}/PS and heparin. The phosphorylation of calelectrin$_{70}$ occurred exclusively on serine residues (Fig. 6). These observations indicate the possibility that calelectrins are a substrate for independent serine–kinase(s) associated with microtubules, which is not characterized at present. Interestingly, calelectrin$_{70}$ exhibited an inhibitory effect on the kinase activity in microtubule fraction in the presence of Ca^{2+} and the effect was also observed in calelectrin$_{32}$ to a lesser extent (Fig. 5). Although the functions of calelectrins in living cells remain unknown, it is possible that calelectrins take part in the regulation of protein kinase activity.

Acknowledgments The authors are grateful to Dr. T. Arai, Science University of Tokyo, for his valuable suggestions and comments on this study. This work was supported in part by a Grant-in-Aid for Scientific Research from the Ministry of Education, Science and Culture of Japan and by a grant from the Research Foundation for Pharmaceutical Sciences.

References

1) M. J. Geisow, *FEBS Lett.*, **203**, 99 (1986).
2) J. H. Walker, *J. Neurochem.*, **39**, 815 (1982).
3) J. Glenney, *J. Biol. Chem.*, **261**, 7247 (1986).
4) R. B. Pepinsky and L. K. Sinclair, *Nature* (London), **321**, 81 (1986).
5) P. B. Moore and J. R. Dedman, *J. Biol. Chem.*, **257**, 9663 (1982).
6) C. E. Creutz, W. J. Zaks, H. C. Hamman, S. Crane, W. H. Martin, K. L. Gould, K. M. Oddie and S. J. Parsons, *J. Biol. Chem.*, **262**, 1860 (1987).
7) V. Gerke and K. Weber, *EMBO J.*, **3**, 227 (1984).
8) R. H. Kretsinger and C. D. Barry, *Biochim. Biophys. Acta*, **405**, 40 (1975); C. J. M. Saris, B. F. Tack, T. Kristensen, J. R., Jr. Glenney and T. Hunter, *Cell*, **46**, 201 (1986); T. Kristensen, C. J. M. Saris, T. Hunter, J. L. Hicks, D. J. Noonan, J. R. Glenney and B. F. Tack, *Biochemistry*, **25**, 4497 (1986); J. R., Jr. Glenney, B. Tack and M. A. Powell, *J. Cell Biol.*, **104**, 503 (1987); A. Frey, C. Hession, P. McGray, L. K. Sindair, E. P. Chow, J. L. Browing, K. L. Ramachandran, J. Tang, J. E. Smart and R. B. Pepinsky, *Cell*, **46**, 191 (1986).
9) C. E. Creutz, L. G. Dowling, J. J. Sando, C. Villar-Palasi, J. H. Whipple and W. J. Zaks, *J. Biol. Chem.*, **258**, 14664 (1983); W. F. Odenwald and S. J. Morris, *Biochem. Biophys. Res. Commun.*, **112**, 147 (1983); M. Geison, J. Child, B. Dash, A. Harris, G. Panayoton, T. Sudhof and J. H. Walker, *EMBO J.*, **3**, 2969 (1984); K. Takagi, H. Hotta and Y. Suketa, *Biochim. Biophys. Acta*, **930**, 320 (1987).
10) K. Radke and G. S. Martin, *Proc. Natl. Acad. Sci. U.S.A.*, **76**, 5212 (1979); K. Radke, T. Gilmore and G. S. Martin, *Cell*, **21**, 821 (1980); E. Ericckson, R. L. Cook, G. J. Miller and R. L. Erickson, *Mol. Cell Biol.*, **1**, 43 (1981).
11) R. A. Fava and S. Cohen, *J. Biol. Chem.*, **259**, 2636 (1984).
12) F. Hirata, *J. Biol. Chem.*, **256**, 7730 (1981).
13) R. J. Flower, J. N. Wood and L. Parente, *Adv. Inflamn. Res.*, **7**, 61 (1984); T. Funakoshi, L. E. Heindrickson, B. A. McMullen and K. Fujiwara, *Thromb. Res.*, **48**, 449 (1987); A. Iwasaki, M. Suda, T. Nagoya, Y. Saino, K. Arai, T. Mizoguchi, F. Sato, H. Yoshizaki, M. Hirata, T. Miyata, Y. Shidara, M. Murata and M. Maki, *J. Biochem.* (Tokyo), **102**, 1261 (1987).
14) T. C. Sudhof, M. Ebbecke, J. H. Walker, U. Fritsche and C. Boustead, *Biochemistry*, **23**, 1103 (1984).
15) T. Fujii, Y. Kondo, M. Kumasaka and K. Ohki, *J. Neurochem.*, **39**, 1587 (1982).
16) N. Ishioka, T. Isobe, T. Okuyama, Y. Numata and H. Wada, *Biochim. Biophys. Acta*, **625**, 281 (1980).
17) U. K. Laemmli, *Nature* (London), **227**, 680 (1970).
18) H. Towbin, T. H. Staehelin and J. Gordon, *Proc. Natl. Acad. Sci. U.S.A.*, **76**, 4350 (1979).
19) T. Fujii, M. Imai, G. C. Rosenfeld and J. Bryan, *J. Biol. Chem.*, **262**, 2757 (1987).
20) A. Magliaccio, A. Rotondi and F. Auricchio, *Proc. Natl. Acad. Sci. U.S.A.*, **81**, 5921 (1984).
21) T. Uchida and C. R. Filburn, *J. Biol. Chem.*, **259**, 12311 (1984).
22) K. L. Gould, J. R. Woodgett, C. M. Isacke and T. Hunter, *Mol. Cell Biol.*, **6**, 2738 (1986); N. C. Khanna, M. Tokuda and D. M. Waisman, *Biochem. Biophys. Res. Commun.*, **141**, 547 (1986); *idem*, *Cell Calcium*, **8**, 217 (1987).
23) R. D. Sloboda, S. A. Rudolph, J. L. Rosenbaum and P. Greengard, *Proc. Natl. Acad. Sci. U.S.A.*, **72**, 177 (1975); L. Jameson, T. Frey, B. Zeeberg, F. Dalldorf and M. Caplow, *Biochemistry*, **19**, 2472 (1980).
24) R. Vallee, *Proc. Natl. Acad. Sci. U.S.A.*, **77**, 3206 (1980).
25) W. E. Theurkauf and R. B. Vallee, *J. Biol. Chem.*, **257**, 3284 (1982).
26) T. C. Sudhof, C. A. Slaughter, I. Leznicki, P. Barjon and G. A. Reynolds, *Proc. Natl. Acad. Sci. U.S.A.*, **85**, 664 (1988).
27) U. Fritsche, A. V. Kieckebusch, M. Potschka, V. P. Whittaker and V. Witzemann, *Biochim. Biophys. Acta*, **957**, 122 (1988).
28) R. S. Mani and C. M. Kay, *Biochem. J.*, **259**, 799 (1989).
29) V. Gerke and K. Weber, *J. Biol. Chem.*, **260**, 1688 (1985).

Properties of Colony Promoting Activity in Procine Kidney Extract

Ikuo KASHIWAKURA,* Yukitoshi HAYASE, and Yoshinari TAKAGI

Hokkaido Institute of Pharmaceutical Sciences, 7–1, Katsuraoka-cho, Otaru 047–02, Japan. *Received July 12, 1990*

Aqueous extracts prepared from procine kidneys (PKE) possess colony-promoting activity (CPA) which increases the number of granulocyte and macrophage colonies in semi-solid cultures of mouse bone marrow cells (BMC) in the presence of colony-stimulating factor (GM-CSF).

PKE was totally inactivated by 15 mM *N*-ethylmaleimide, but was resistant to 5 mM dithiothreitol (DTT), 50 mM sodium metaperiodate and a mixture of diisopropylether–*n*-BuOH (3:2).

The proportion of deoxyribonucleic acid (DNA)-synthesizing cells of the PKE-responsive cells was about one-half in comparison to those of CSF-responsive cells, as estimated using the hydroxyurea (HU) suicide method.

Upon marrow preincubation with PKE in liquid culture for 24 h, the suicide rate of the colony forming unit in culture (CFU-C) by HU increased to 3 times compared to that of the control.

Since cyclophosphamide (CY) induces a change in the number of CFU-C, the effects of PKE on BMC obtained from CY injected mice were investigated. On day 1, the number of PKE-responsive cells significantly increased by about 2.3 times in comparison with that of control, whereas the number of CFU-C per 1×10^4 cells significantly decreased to about one-eighth of that of control.

These results suggest that a sulfhydryl group(s) is required for the appearance of the colony-promoting activity of PKE, and glycoproteins, glycopeptides or hydrophobic components are not required; they also suggest that PKE may act on immature granulocyte/macrophage progenitors, which are youger than CSF-responsive CFU-C.

Keywords colony promoting activity; CFU-C; kidney; kidney extract; bone marrow culture

Granulocyte-macrophage (GM) colony forming units in culture (CFU-C) proliferate and differentiate to form colonies in agar cultures containing colony-stimulating factors (CSF).[1,2] On the other hand, several factors have been reported, designated as colony-promoting activity (CPA) factors, which do not stimulate CFU-C colony formation by themselves, but can enhance colony formation in the presence of CSF. CPA was found in the lysates of erythrocytes,[3] post-endotoxin serum,[4] WEHI-3B cell conditioned medium,[5] leucocyte conditioned medium, and supernatants of murine long-term bone marrow cultures.[6,7]

Recently we found a CPA in the extracts of porcine kidney (PKE).[8] The CPA of PKE is a possible physiological factor in maintaining the number of CFU-GM by proliferating and differentiating pre-CFU-GM, since preincubation of bone marrow cells (BMC) with PKE causes an increase in the population of GM-CSF responsive cells.[8]

In this paper, we investigated the chemical properties of the CPA of PKE, and the characteristics of PKE-responsive cell populations were studied using the hydroxyurea (HU) suicide method as well as the PKE-responsiveness of BMC from cyclophosphamide (CY)-injected mice.

Experimental

Preparation of PKE Porcine kidneys were obtained immediately after the animals were sacrified from a slaughter house, and homogenized within 3 h with distilled water at a concentration of 12% (w/v) in a Waring blender at 0 °C. The homogenates were centrifuged at $1 \times 10^5 g$ (Hitachi rotor 42T) for 30 min at 4 °C and the clear supernatants thus obtained were lyophilized. The lyophilized material was dissolved in distilled water in a 1/10 volume of the $1 \times 10^5 g$ supernatants. To the solution, saturated ammonium sulfate solution was added. The precipitate from 50 to 65% saturation of ammonium sulfate was collected, dialyzed against 100 volumes of distilled water with a Visking tube three times, and lyophilized. The lyophilized material was dissolved in distilled water in a 1/50 volume of the $1 \times 10^5 g$ supernatants. Insoluble material was removed by centrifugation. The clear supernatant obtained was dialyzed against phosphate-buffered saline (PBS), passed through a membrane filter (0.45 μm pore size, Fuji Photo Film Co., Ltd.), and stored at −20 °C until use. The same preparation was used throughout the experiment. The results of repeated experiments showed good reproducibility on CPA of the preparations, and no detectable inactivation of CPA was observed during several months under the above storage condition.

Mice Male mice of ddY strain (Sankyo Labo Service Corporation, Sapporo) aged 6—10 weeks were used.

Preparation of GM-CSF Mouse abdominal walls were removed aseptically, washed with PBS, and incubated in 10 ml of an F-10 medium containing 20% horse serum (HS) (Gibco Laboratories, New York) at 37 °C in 5% CO_2. The conditioned medium was collected after 4 d of incubation, passed through a membrane filter (0.45 μm in pore size), and stored at −20 °C until use. This CSF stimulated granulocyte/macrophage colony formation, and the colony-stimulating activity of the preparation was stable for several months in the above storage condition.

Assay of CPA CPA was assayed in a semi-solid agar culture system by the modified method of Tsurusawa *et al.*[7] Briefly, 5×10^4 BMC from a mouse femur were cultured in 35 mm plastic Petri dishes (SH-S3512SW, Terumo, Tokyo) in 1 ml of nutrient mixture F-10 medium containing 0.32% Bacto-agar (Difco Laboratories, Detroit, MI), 20% HS, 20% mice abdominal wall conditioned medium as a CSF, and 5% PKE, for 7 d at 37 °C in 5% CO_2. Colonies with 50 or more cells were counted as CFU-GM.

The dose of PKE was determined from dose response curves of CPA in the range of 5 to 100 μl as described previously. PKE alone did not support colony formation, even at 100 μl.

CPA is expressed as the ratio of the colony number in the presence of PKE to the number in the absence of PKE.

Chemical Treatments of PKE Various chemical treatments were performed using the modified method of Brennan *et al.*[9]

Periodate Treatment: PKE was treated with 50 mM sodium metaperiodate (SMPI) (Wako Pure Chemical Industries, Ltd., Osaka) for 14 min at 4 °C, and the reaction was stopped by the addition of 1/10 volume of a 50% sucrose solution. The reaction mixture was dialyzed against PBS.

Reduction and Alkylation of PKE: PKE was treated with 5 mM dithiothreitol (DTT) (Nakarai Chemicals, Ltd., Kyoto) for 2 h at 23 °C, or with 15 mM *N*-ethylmaleimide (NEM) (Nakarai Chemicals, Ltd., Kyoto) for 2 h at 23 °C, and then dialyzed against distilled water.

Diisopropylether–*n*-BuOH Treatment: One volume of PKE was added to 2 volumes of diisopropylether–*n*-BuOH (3:2), and the mixture was shaken for 10 min at room temperature. After centrifugation, the aqueous phase was removed and lyophilized.

HU Suicide Experiments A modified method of Benestad *et al.*[10] and Kajigaya *et al.*[11] was applied.

HU Treatment of BMC Preincubated with PKE: BMC were incubated at a concentration of $8—9 \times 10^5$ cells/ml in a 25 cm^2 culture flask (MS-20050, Sumitomo, Tokyo) with 10 ml of F-10 medium containing 20% HS, with or without 5% PKE for 24 h at 37 °C in 5% CO_2. Non-adherent cells were collected, and washed three times with F-10

medium. The non-adherent cells thus obtained wrere treated with or without HU as described below and then assayed for CFU-GM in the absence of PKE.

Treatment of BMC with HU: BMC were incubated with or without 16 mM HU in F-10 medium for 60 min in a shaking water bath at 37 °C, washed three times with F-10 medium, resuspended with F-10 medium, counted, and then assayed for CFU-GM in the presence or absence of PKE. In the control cultures, PKE was replaced with PBS.

The HU suicide rate of the CFU-GM was calculated by the following formula:

$$\text{HU suicide rate } (\%) = [(X - Y)/X] \times 100$$

where X = means colony number of control cultures. Y = means colony number of the cultures of HU treated cells.

Preparation of Mouse BMC after Treatment with CY A modified method of Williams *et al.*[12] was applied. Mice received a single intraperitoneal injection of CY (Endoxan; Shionogi Co., Ltd., Osaka) (25 mg/ml) at a dose of 200 mg/kg of body weight. Control mice were treated with sterile saline instead of CY. One day or 4 d after injection, BMC were harvested, and the CPA of PKE on these cells was determined.

Results

Effect of Various Chemical Treatments on CPA of PKE As shown in Table I, the mean colony number was 63 in the control cultures, whereas in the cultures supplemented with PKE it was 117, showing an enhancement ratio of 1.86. Dialysis against distilled water or PBS did not affect the CPA of PKE. Inactivation of CPA was observed in the NEM-treated PKE; the colony number was less than halved. On the other hand, no significant decrease in CPA was observed after treatment of PKE with DTT or SMPI. And the CPA of PKE was retained in the aqueous phase after treatment with diisopropylether–*n*-BuOH.

Effect of PKE on Proportion of Deoxyribonucleic Acid (DNA) Synthesizing CFU-GM After BMC were incubated with PKE for 24 h, the proportion of DNA synthesizing CFU-GM was estimated using the HU suicide technique (Table II). The suicide rate of CFU-GM by HU was 60.6% in BMC preincubated with PKE, and that of the control without PKE was 20.2%. Consequently, the HU suicide rate was increased to 3 times normal by PKE treatment. It was also shown that CFU-GM which were enhanced by PKE were mostly in the DNA synthesizing period of the cell cycle.

The percentage of CFU-C in DNA synthesis in mouse BMC has been estimated at approximately 20—50%.[13-15] The suicide rate of the controls in this experiment is consistent with previous findings.

Effect of PKE on Colony Formation of HU Treated BMC PKE also enhanced colony formation in the cultures of HU-treated cells, and there was no difference between the increment of colony number on the cultures of HU-treated cells and that of HU-untreated cells. The suicide rate of CFU-GM in the absence and presence of PKE was 21.5 and 11.7%, respectively, so the suicide rate of PKE stimulated cells was lower than that of CSF responsive cells (Table III).

Effect of PKE on Colony Formation of BMC from CY-Injected Mice As shown in Table IV, the number of colonies per 1×10^4 BMC obtained from mice 1 d after CY injection was 2.1, about 1/8 of that of the control concentration. And the number of PKE responsive cells decreased from 15.7 to 7.2. The CPA of PKE on marrow cells one day after CY injection significantly increased to 4.43, while that of the control was 1.96.

On the other hand, the number of colonies per 1×10^4 BMC obtained from mice 4 d after CY injection was 56.5, which is 3.4 times larger than the control. The number of PKE responsive cells increased from 15.7 to 38.8. The CPA thereby decreased significantly from 1.96 to 1.69.

Discussion

Among BMC preincubated with PKE, both the number

TABLE I. Effect of Chemical Treatments on CPA of PKE

	Treatment	No. of colonies /1 × 10⁴ cells	CPA[a]
Experiment 1[b]	Control (without RKE)	63.0±2.6	1.00
	Untreated PKE	117.2±4.4	1.86
	PKE dialyzed against water	109.7±6.8	1.74
	PKE dialyzed against PBS	106.9±5.4	1.70
	DTT–PKE	109.8±3.6	1.74
	NEM–PKE	48.5±3.1	0.77
	SMPI–PKE	104.6±9.0	1.66
Experiment 2[c]	Control (without PKE)	41.0±2.6	1.00
	Untreated PKE	71.8±3.5	1.75
	Diisopropylether–*n*-BuOH extracted PKE	80.3±3.0	1.96

a) PKE(+)/PKE(−). *b*) Mean±S.E. of 6 dishes from two separate experiments. *c*) Mean±S.E. of 9 dishes from three separate experiments.

TABLE II. Percent of CFU-C in DNA Synthesis after Incubation with or without PKE in Liquid Culture

Preincubation	Treatment	No. of colonies[a] /1 × 10⁴ cells	Percent killed by HU
Control (PBS)	F-10 medium	33.2±1.6	
Control (PBS)	HU	26.5±1.8	20.2
PKE	F-10 medium	100.0±4.4	
PKE	HU	39.4±1.8	60.6

a) Mean±S.E. of 6 dishes from two separate experiments.

TABLE III. HU Suicide of CFU-C

Preincubation	Stimulus	No. of colonies[a] /1 × 10⁴ cells	Percent killed by HU
F-10 medium	AWCM	30.2±1.3	21.5
HU–F-10		23.7±1.2	
F-10 medium	AWCM+PKE	51.5±2.2	11.7[b]
HU–F-10		45.5±2.8	

a) Mean±S.E. of 6 dishes from two separate experiments. *b*) $p < 0.05$ by t test.

TABLE IV. Effect of PKE on Colony Formation of CY-Treated Mouse BMC

Cell	Number of mice	No. of colonies[d] PKE(−)	No. of colonies[d] PKE(+)	Pre-CFU-C[c]	CPA
Control BMC	5	16.4±0.9	32.1±1.7	15.7	1.96
1 d CY BMC[a]	6	2.1±0.6	9.3±2.3	7.2	4.43[e]
4 d CY BMC[b]	11	56.5±5.7	95.3±9.4	38.8	1.69[f]

a) BMC from mice 1 d after CY injection. 1×10^5 cells per plate. *b*) BMC from mice 4 d after CY injection. 1×10^4 cells per plate. *c*) [No. of colonies PKE(+)]−[No. of colonies PKE (−)]. *d*) Mean±S.E. of 9 dishes from three separate experiments. *e*) $p < 0.001$ by t test. *f*) $p < 0.05$ by t test.

and the suicide rate of CFU-GM by HU increased to 3 times that of the control (Table II). These results show that the proportion of DNA synthesizing CSF responsive cells was increased by preincubation with PKE; moreover, CFU-GM enhanced by PKE were mostly in an *S*-phase of the cell cycle, and those were reflected in the increment of the colony number.

PKE also enhanced colony formation in the cultures of HU-treated cells, but no difference was observed between the increment of colony number in HU-treated cells and HU-untreated cells. It seems that the target cells of PKE are little affected by HU. And the suicide rate of CSF responsive cells with PKE added to the culture after HU treatment was low in comparison to those with an absence of PKE (Table III).

The results of the HU suicide experiments indicate that the target cells of PKE are mostly in phases other than the *S*-phase, probably the G_o phase, and/or a slowly cycling cell population.

It is known that administration of CY causes a decrease in the number of blood leucocytes and BMC within a few hours after injection, and the number of CFU-GM of BMC decreased immediately after CY injection and then increased to several times larger than normal after 3—5 d.[12,16-18]

As shown in Table IV, the number of colonies obtained from the marrow cells one day after CY injection decreased to about 1/8 of that of the control. But the CPA significantly increased from 1.96 to 4.43. On the other hand, the number of colonies obtained from mice 4 d after CY injection increased to 3.4 times, and the number of PKE responsive cells increased to 2.5 times in comparison to that of the normal mice, and the CPA significantly decreased from 1.96 to 1.69. It seems that a change of CPA after CY injection is due to a variation of the relative proportion of the number of PKE responsive cells to the number of the CSF responsive cells.

A number of researchers have demonstrated that a population of primitive hemopoietic stem cells is capable of surviving either *in vitro* or *in vivo* exposure to chemotherapeutic agents such as 5-fluorouracil, 4-hydroxycyclophosphamide, HU and CY.[19-23] On the other hand, the percentage of hemopoietic progenitor cells in DNA synthesis have been estimated at 10%[24] in CFU-S, 22—52%[25,26] in BFU-E, 70%[25,26] in CFU-E and 20—50%[13-15] in CFU-GM, and these results suggest that the percentages of the cells in DNA synthesis decrease as differentiation progresses.

Accordingly, the results of the HU- and CY-experiments suggest that PKE may act on an immature granulocyte/macrophage progenitor younger than CSF-responsive CFU-GM and induce it to leave a G_0 state and enter a cell cycle, supporting our previous findings[8] that PKE stimulates pre-CFU.

Recently it has been reported that cytokines, such as IL-1, IL-3 and IL-6, stimulate the growth and development of hemopoietic progenitors at an early stage.[27-29] It is also known that IL-1 promotes colony formation indirectly through enhancing the production of GM-CSF, G-CSF, and IL-6.[30] IL-3 and IL-6 have a direct effect on undifferentiated hemopoietic progenitors. These cytokines are able to shorten the G_0 period of the progenitors and to stimulate CFU-C colony formation by themselves.[29,30]

The active factor(s) in PKE seems to differ between IL-1, IL-3 and IL-6, because the CPA of PKE has an apparent molecular weight of 140000 (on high-performance liquid chromatography) which is much larger than that of cytokines, and PKE had no detectable colony stimulating activity alone[8]; but PKE seems to enhance the effect of those cytokines (data not shown).

We described in the previous paper that the CPA of PKE was heat labile and trypsin sensitive.[8] In this study, we found that the CPA of PKE was totally inactivated by NEM but was resistant to DTT and periodate. Furthermore, the CPA of PKE was retained after treatment with diisopropylether–*n*-BuOH (Table I). These results suggest that the CPA of PKE does not depend on glycoproteins, glycopeptides or hydrophobic components, and that a sulfhydryl group(s) is required for the appearance of its activity.

References

1) M. Paran and L. Sachs, *J. Cell. Physiol.*, **72**, 247 (1968).
2) G. Pigoli, A. Waheed, and R. K. Shadduck, *Blood*, **59**, 408 (1982).
3) K. Tsuneoka, Y. Takagi, K. Hirashima, and M. Shikita, *Exp. Hematol.*, **6**, 445 (1978).
4) S. Bol and N. Williams, *J. Cell. Physiol.*, **102**, 233 (1980).
5) Y. Kajigaya, K. Ikuta, Y. Koiso, T. Funabiki, and S. Matsuyama, *ACTA Haematol. Jpn.*, **50**, 575 (1987).
6) H. Izumi, M. Tsurusawa, T. Miyanomae, K. Kumagai, and KJ. Mori, *Leuk. Res.*, **7**, 155 (1983).
7) M. Tsurusawa, T. Miyanomae, H. Izumi, and KJ. Mori, *Leuk. Res.*, **7**, 167 (1983).
8) I. Kashiwakura, Y. Hayase, and Y. Takagi, *Yakugaku Zasshi*, **108**, 984 (1988).
9) J. K. Brennan, C. N. Abboud, J. F. DiPersio, G. H. Barlow, and M. A. Lichtman, *Blood*, **58**, 803 (1981).
10) H. B. Benestad, K. Warhuus, and Å. Reikvam, *Exp. Hematol.*, **5**, 408 (1977).
11) Y. Kajigaya, K. Ikuta, H. Sasaki, Y. Koiso, T. Funabiki, and S. Matsuyama, *ACTA Haematol. Jpn.*, **51**, 832 (1988).
12) D. E. Williams, J. E. Straneva, R-N. Shen, and H. E. Broxmeyer, *Exp. Hematol.*, **15**, 243 (1987).
13) Y. Niho, *Saishin Igaku*, **28**, 1705 (1973).
14) V. S. Gallicchio and M. G. Chen, *Cell Tissue Kinet.*, **15**, 179 (1982).
15) N. Jacobsen, H. E. Broxmeyer, E. Grossbard, and M. A. S. Moore, *Blood*, **52**, 221 (1978).
16) S. H. Rosenoff, J. M. Bull, and R. C. Young, *Blood*, **45**, 107 (1975).
17) A. M. Yeager, F. C. Levin, and J. Levin, *J. Cell. Physiol.*, **112**, 222 (1982).
18) L. Stork, L. Barczuk, M. Kissinger, and W. Robinson, *Blood*, **73**, 938 (1989).
19) G. S. Hodgson and T. R. Bradley, *Nature* (London), **281**, 381 (1979).
20) T. Suda, J. Suda, and M. Ogawa, *Proc. Natl. Acad. Sci. U.S.A.*, **80**, 6689 (1983).
21) S. D. Roeley, O. M. Colvin, and R. K. Stuart, *Exp. Hematol.*, **13**, 295 (1985).
22) E. Necas, V. Znojil, and E. Frindel, *Exp. Hematol.*, **17**, 53 (1989).
23) H. E. Broxmeyer, D. E. Williams, S. Cooper, A. Waheed, and R. K. Shadduck, *Blood*, **69**, 913 (1987).
24) A. J. Becker, E. A. McCulloch, L. Siminovitch, and J. E. Till, *Blood*, **26**, 296 (1965).
25) N. N. Iscove, *Cell Tissue Kinet.*, **10**, 323 (1977).
26) C. J. Gregory and A. C. Eaves, *Blood*, **51**, 527 (1978).
27) L. C. Stork, V. M. Peterson, C. H. Rundus, and W. A. Robinson, *Exp. Hematol.*, **16**, 163 (1988).
28) K. Koike, E. R. Stanley, J. N. Ihle, and M. Ogawa, *Blood*, **67**, 859 (1986).
29) K. Ikebuchi, G. G. Wong, S. C. Clark, J. N. Ihle, Y. Hirai, and M. Ogawa, *Proc. Natl. Acad. Sci. U.S.A.*, **84**, 9035 (1987).
30) Y. C. Yang, S. Tsai, G. G. Wong, and S. C. Clark, *J. Cell. Physiol.*, **134**, 292 (1988).

Expression of a Restricted Fragment of Staphylococcal Tetracycline Resistance Determinant as a Fused Product in *Escherichia coli*

Takashi AOKI,* Keiko AMAUCHI and Hiroyuki WATABE

Department of Biochemistry, Faculty of Pharmaceutical Sciences, Higashi-Nippon-Gakuen University, Ishikari-Tobetsu, Hokkaido 061-02, Japan.
Received July 16, 1990

Tetracycline resistance (Tc^R) plasmid pNS1, a deletion derivative constructed from staphylococcal plasmid pTP5, carries a *tet* determinant which specifies a Tc^R protein (TET) with a molecular weight of 50 kilodaltons (kDa). In order to express the pNS1-encoded TET as a fused product, a 0.8 kilobase pairs fragment containing 57.1% of *tet* determinant was inserted into a chloramphenicol resistance determinant. From the nucleotide sequence, it is deduced that the fusion protein (designated CAT'-TET') is a 53 kDa protein composed of 472 amino acids in which the 199 and 262 amino acids are derived from CAT and TET, respectively. Although the molecular weight of CAT'-TET' obtained from the result of sodium dodecyl sulfate polyacrylamide gel electrophoresis (42 kDa) was not in agreement with its predicted weight (53 kDa), the ratio of TET' segment to the fusion protein (22 kDa/42 kDa) corresponded almost exactly to that deduced from the nucleotide sequence (29 kDa/53 kDa). The expression of CAT'-TET' in *Escherichia coli* caused a rapid decrease in growth rate and in the number of viable cells. This result is thought to be due to the toxic effect of CAT'-TET' on the cell membrane.

Keywords tetracycline resistance protein; recombinant plasmid; fusion protein; chloramphenicol acetyltransferase; immunoblotting

Tetracycline resistance (Tc^R) determinants have been found in a wide range of bacterial species and are mainly carried by plasmids. In members of the family *Enterobacteriaceae*, five Tc^R determinants have been defined: *tetA* through *tetE*.[1,2] The four classes (*tetA* through *tetD*) encode inner membrane Tc^R proteins (TETs) which mediate tetracycline efflux from the cell.[2,3] Nucleotide sequence analyses indicate that these TETs are related to each other and have probably been derived from a common origin.[4]

In *Staphylococcus aureus*,[5-7] *S. epidermidis*[8] and *Bacillus* spp.,[8-11] several plasmid-mediated Tc^R determinants have been described. The TETs encoded by these plasmids are probably also membrane-located proteins and display considerable homology, but they are clearly distinct from the proteins specified by the gram-negative determinants. These findings suggest that the Tc^R determinants of gram-positive bacteria have also been derived from a common origin, but that the gram-positive and -negative TETs appear to have evolved separately.[12]

The biochemical analysis of gram-positive TETs, however, lags behind that for gram-negative proteins. To examine the TETs in more detail, the establishment of an assay system or the preparation of an antibody reacting specifically with the TETs, and subsequent isolation of these proteins are necessary. We designed experiments to obtain an antibody reacting with the TET encoded by pNS1,[13,14] a deletion derivative constructed from a *S. aureus* Tc^R plasmid pTP5.[6] From the nucleotide sequence, it is deduced that the pNS1-encoded TET is a 50 kilodaltons (kDa) protein composed of 459 amino acids[14]; however, it is difficult to purify the protein effectively because the expression level in *B. subtilis* is very low and assay systems have not yet been established. In this paper, as a first step in isolating the pNS1-encoded TET, we report on its expression in *Escherichia coli* as a fusion protein related to chloramphenicol acetyltransferase (CAT) encoded by pTZ12,[15,16] a chloramphenicol resistance (Cm^R) plasmid in *Bacillus subtilis*.

Materials and Methods

Bacterial Strains and Plasmids The strain used as a recipient in the transformation was *E. coli* JM109, which is the *lac*-repressor overproducing strain. *B. subtilis* strains RM125 (pNS1) and RM125 (pTZ12) were kindly provided by Dr. M. Kono (Tokyo College of Pharmacy). Tc^R plasmid pNS1, a deletion derivative constructed from the staphylococcal plasmid pTP5, carries a *tet* determinant which specifies a 459-amino acid polypeptide with a molecular weight of 50 kDa.[13,14] Cm^R plasmid pTZ12 was derived from *Corynebacterium xerosis* and carries a *cat* determinant which specifies a 215-amino acid polypeptide (26 kDa).[15,16] The general cloning vector pUC18 and the expression vector pKK233-2, containing a hybrid *trp-lac* (*trc*) promoter, were obtained from Pharmacia LKB Biotechnology. These plasmids were maintained in *E. coli* JM109.

Media, Chemicals and Enzymes *E. coli* strains were grown in L broth or on agar. *B. subtilis* strains were grown in nutrient broth or on agar. Ampicillin, tetracycline and chloramphenicol were added to the growth media at concentrations of 50, 12.5 and 25 μg/ml, respectively. All antibiotics were purchased from Sigma Chemical Co. The *trc* promoter was induced with 1.0 mM isopropyl-β-D-thiogalactopyranoside (IPTG; Wako Pure Chemical Industries). Restriction endonucleases and T4 deoxyribonucleic acid (DNA) ligase were obtained from Bethesda Research Laboratories, New England Biolabs or Nippon Gene Co. T4 DNA polymerase and alkaline phosphatase were purchased from Boehringer Mannheim. Deoxynucleoside 5'-triphosphates and phosphorylated *Nco*I linker (12 mer) were purchased from Sigma Chemical Co. and Takara Shuzo Co., respectively.

Construction and Analysis of Plasmids Plasmids were prepared by the method of Birnboim and Doly,[17] with modifications. Enzyme reactions were performed as specified by the manufacturers. DNA was transformed into *E. coli* JM109 by the $CaCl_2$ procedure[18] and transformants were selected on L agar plates containing 50 μg/ml ampicillin. Agarose gel electrophoresis was performed to analyze the plasmids or to prepare the DNA fragments.

Preparation of Antibody against Chloramphenicol Acetyltransferase (CAT) The purification of CAT from *B. subtilis* RM125 (pTZ12) was performed according to the procedure described by Shaw *et al.*[19] CAT activity was assayed by the spectrophotometric method.[20] The purified CAT (100 μg/ml) was emulsified with an equal volume of Freund's complete adjuvant. Young male rabbits were given four weekly intramuscular injections of this emulsion. Two weeks following the final injection, antisera were collected.

Preparation of Cell Extract An overnight culture of bacteria was inoculated into fresh L broth and grown at 37 °C until mid-log phase. After induction by addition of 1.0 mM IPTG (final concentration) and further incubation for 2 h, cells were centrifuged at 10200 × *g* for 20 min and suspended in 20 mM Tris-HCl buffer, pH 7.5. In the case of the non-induced culture, IPTG was not added. The broken cells obtained by

sonic oscillation were centrifuged at 8600 × *g* for 20 min, and the supernatant fluid was used as a cell extract.

Gel Electrophoresis and Immunoblotting Proteins in the cell extract were separated on 0.1% sodium dodecyl sulfate (SDS)–14% polyacrylamide gel.[21] Prestained SDS-PAGE Standards (phosphorylase B, 110 kDa; bovine serum albumin, 84 kDa; ovalbumin, 47 kDa; carbonic anhydrase, 33 kDa; soybean trypsin inhibitor, 24 kDa; lysozyme, 16 kDa; Bio-Rad Laboratories) were used as molecular weight standards. The proteins separated by polyacrylamide gel were stained with 0.25% Coomassie brilliant blue R-250 or electroblotted onto nitrocellulose paper according to Towbin *et al.*[22] The paper was blocked with 5% skim milk solution and incubated with anti-CAT serum diluted 1:500 with TBS (50 mM Tris–HCl, 200 mM NaCl, pH 7.4) containing 3% bovine serum albumin. The bound antibody was visualized with horseradish peroxidase-labeled sheep anti-rabbit immunoglobulin G antibody and 3,3′-diaminobenzidine tetrahydrochloride (DAB; Sigma Chemical Co.) as described by Hawkes *et al.*[23]

Results and Discussion

Construction of pHTK354 Carrying a Fused *cat′-tet′* Determinant The construction of recombinant plasmids is shown in Fig. 1. A 0.8 kilobase pairs (kb) *Hpa*II-*Ssp*I fragment of pTZ12 was purified by agarose gel electrophoresis. The fragment was treated with T4 DNA polymerase and then ligated to *Nco*I linkers. The fragment with *Nco*I linkers attached to both ends was digested with *Nco*I and ligated into the *Nco*I site of pKK233-2. The resulting plasmid, pHTK113, carries 92.6% of the pTZ12 *cat* determinant (*cat′*), which specifies an incomplete CAT (designated CAT′). From the nucleotide sequence, the deduced N-terminal amino acid sequence of CAT′ shows that the first 16 N-terminal amino acids of CAT have been replaced by the three amino acids (Met, Ala and Asp) derived from the *Nco*I linker.

In a previous paper,[15] we reported that the pTZ12 *cat* determinant had the ability to express Cm resistance in *E. coli*. The strain bearing pHTK113, however, was Cm sensitive. This result indicates that as little as the first 16 N-terminal amino acids of the pTZ12-encoded CAT are necessary to confer Cm resistance.

A 0.8 kb *Kpn*I-*Dra*I fragment of pNS1, containing part of the *tet* determinant, was then ligated into the *Kpn*I-*Sma*I site of pUC18. The recombinant plasmid, pHTK312, carries 57.1% of the *tet* determinant (*tet′*) and the pUC18 *lacZ* determinant in the same translational frame. A 0.8 kb

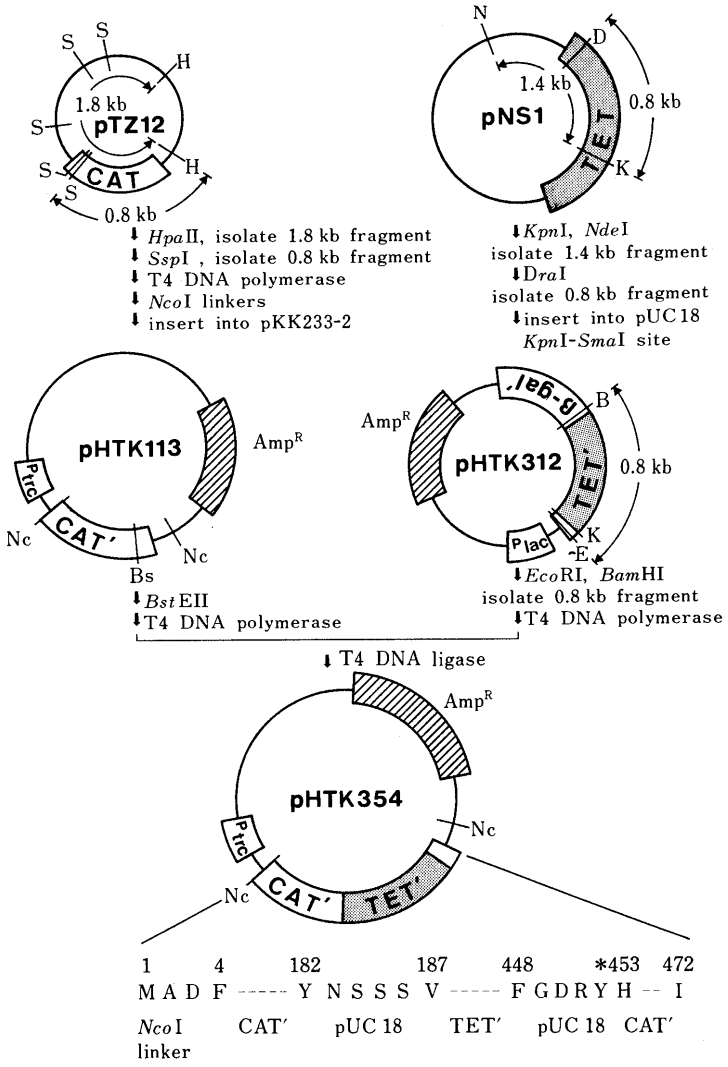

Fig. 1. Construction of Recombinant Plasmids pHTK113, pHTK312 and pHTK354

A 0.8 kb *Kpn*I-*Dra*I fragment of pNS1, containing 57.1% of *tet* determinant, was cloned into the *Kpn*I-*Sma*I site of pUC18. A 0.8 kb *Eco*RI-*Bam*HI fragment of the recombinant plasmid (pHTK312) was then cloned into the *Bst*EII site of pHTK113. The resulting plasmid, pHTK354, carries a fused *cat′-tet′* determinant downstream from the *trc* promoter in the same translational frame. Abbreviations: CAT, chloramphenicol acetyltransferase; TET, tetracycline resistance protein; CAT′, TET′ and β-gal′, incomplete derivatives of CAT, TET and β-galactosidase; P_{lac}, promoter for *lac*; P_{trc}, *trp-lac* hybrid promoter; Amp^R, ampicillin resistance; B, *Bam*HI; Bs, *Bst*EII; D, *Dra*I; E, *Eco*RI; H, *Hpa*II; K, *Kpn*I; N, *Nde*I; Nc, *Nco*I; S, *Ssp*I.

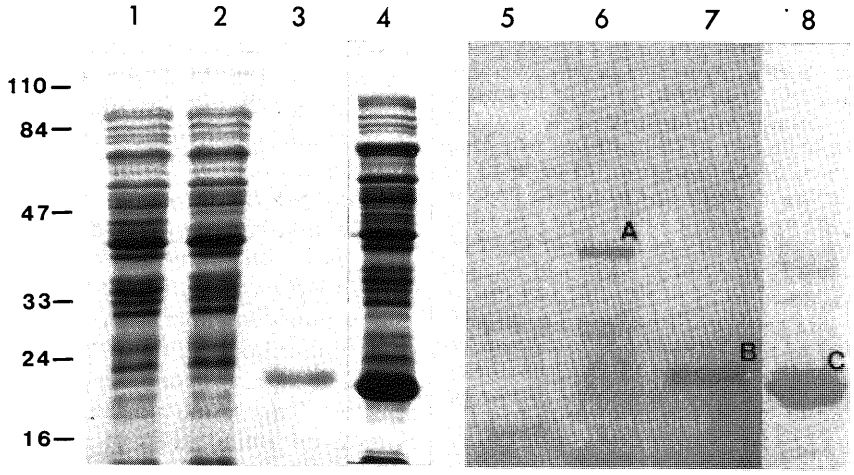

Fig. 2. Analysis of CAT′ and CAT′-TET′ by SDS-Polyacrylamide Gel Electrophoresis and Immunoblotting

The cell extracts prepared from IPTG-induced JM109 bearing pKK233-2 (lanes 1 and 5), pHTK354 (lanes 2 and 6) and pHTK113 (lanes 4 and 8) were analyzed on a SDS-14% polyacrylamide gel. Lanes 3 and 7, purified CAT. The separated-proteins were stained with Coomassie brilliant blue (lanes 1—4) or immunostained with anti-CAT antibody (lanes 5—8). Molecular weight markers (in kDa) are shown on the left side. A, CAT′-TET′ (42 kDa); B, CAT (22 kDa); C, CAT′ (19 kDa).

*Eco*RI-*Bam*HI fragment of pHTK312 treated with T4 DNA polymerase was then cloned into pHTK113 which had been digested with *Bst*EII and then treated with polymerase. The resulting plasmid, pHTK354, carries a fused *cat′-tet′* determinant specifying a fusion protein (designated CAT′-TET′; Fig. 1) downstream from the *trc* promoter in the same translational frame. The primary structure of CAT′-TET′ deduced from the nucleotide sequence is also shown in Fig. 1. As shown in Fig. 1, it is deduced that CAT′-TET′ is a 53 kDa protein composed of 472 amino acids, in which the 199 amino acids (Phe^{4}—Tyr^{182} and His^{453}—Ile^{472}) and the 262 amino acids (Val^{187}—Phe^{448}) are derived from CAT and TET, respectively. The duplicated sequence (filled-in *Bst*EII site of pHTK113) encodes the Tyr at position 452.

Expression of the Fusion Protein and Analysis by Immunoblotting The cell extracts prepared from *E. coli* JM109 strains bearing various plasmids were separated on 14% polyacrylamide gel and analyzed by immunoblotting using the anti-CAT antibody. In the cell extract prepared from the IPTG-induced strain bearing pHTK113, a major band was detected at the position which is approximately 19 kDa in molecular weight (Fig. 2, lane 4). Furthermore, only the 19 kDa protein reacted specifically with the antibody against CAT (Fig. 2, lane 8). These results showed clearly that the 19 kDa protein was CAT′ and about 10—20% of the cell extract prepared from IPTG-induced JM109 (pHTK113) corresponded to CAT′.

On the other hand, a major band resulting from IPTG induction (such as CAT′) was not detected from the strain bearing pHTK354 (Fig. 2, lane 2). However, a 42 kDa protein reacted specifically with the anti-CAT antibody by immunoblotting (Fig. 2, lane 6). Therefore, it seemed that the 42 kDa protein was the CAT′-TET′ fusion protein; but the expression level of CAT′-TET′ was far lower than that of CAT′. Although the molecular weights of CAT′ (19 kDa) and CAT′-TET′ (42 kDa) obtained from the results of SDS-PAGE were not in agreement with the molecular weights predicted (24 kDa of CAT′ and 53 kDa of CAT′-TET′), the ratio of TET′ segment to the fusion protein (22 kDa/42 kDa; 52%) corresponded almost exactly to that deduced from the nucleotide sequence (29 kDa/53 kDa; 55%).

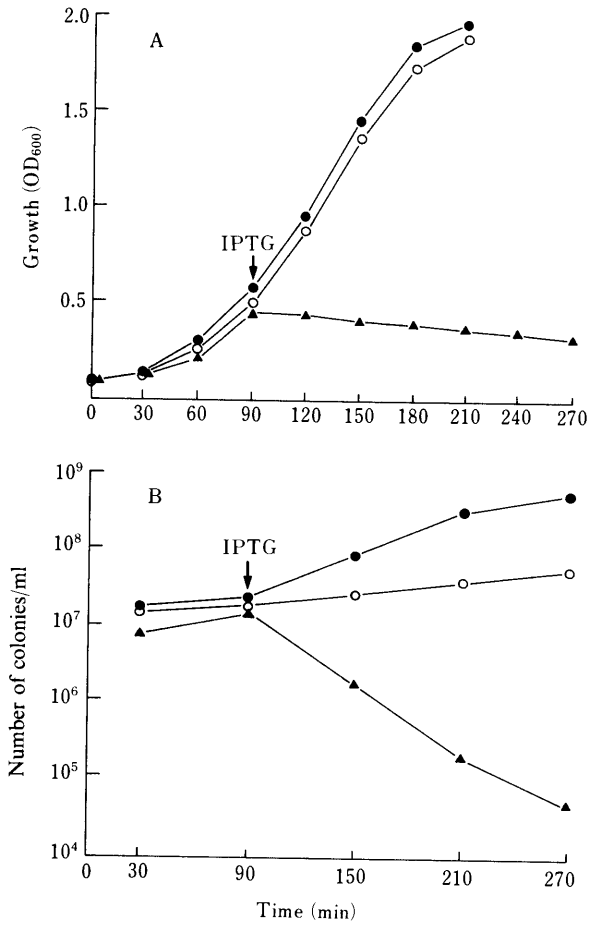

Fig. 3. Effects of CAT′ and CAT′-TET′ Expression on Cell Growth (A) and Viability (B)

Strains JM109 bearing pKK233-2 (●), pHTK113 (○) and pHTK354 (▲) were grown in L broth. IPTG (final concentration 1.0 mM) was added at the time indicated by the arrow. To test the viability, cells of each cultures were grown on L agar plates and the number of resulting colonies were counted.

The deduced amino acid sequence demonstrates that the pNS1-encoded TET is highly hydrophobic and is probably

a membrane-binding protein.[24] The localization of CAT′-TET′ has not yet been clarified but our recent studies suggested that it is membrane-located, since it was recovered from the cell envelope fraction (data not shown).

Effects of CAT′ and CAT′-TET′ Expression on Growth and Viability The effects of CAT′ and CAT′-TET′ expression on growth and viability were examined (Fig. 3). After the JM109 strains were grown until mid-log phase, the *trc* promoter was induced by the addition of 1.0 mM IPTG. No effect of induction on growth rate was detected in the strain bearing pHTK113 or in the control strain bearing pKK233-2, but the induction of CAT′ expression prevented an increase in the number of viable cells (Fig. 3B), probably owing to the overproduction of CAT′. Induction of CAT′-TET′ expression in JM109 (pHTK354) resulted in a rapid inhibition of growth (Fig. 3A) and a decrease in the number of viable cells (Fig. 3B). These results were thought to be due to the toxic effect of CAT′-TET′ on the cell membrane.

In gram-negative TETs, it has been reported that the overproduction of TET in *E. coli* caused the arrest of growth and killing of the cells.[25-28] The overproduced-TET molecules are believed to be inserted into the cell membrane in an abnormal conformation. The expression of CAT′-TET′ also caused the rapid decrease in growth rate and in the number of viable cells; however, the level of expression was very low. This result would be due to the properties of TET′ segment, originating from gram-positive bacteria.

The CAT′-TET′ fusion protein constructed in this work represents a minor component of the cell extract, but it is possible to purify it effectively using the anti-CAT antibody. Moreover, further preparation of antibody against the fusion protein could allow the isolation and analysis of the intact pNS1-encoded TET.

References

1) B. Mendez, C. Tachibana and S. B. Levy, *Plasmid*, **3**, 99 (1980).
2) B. Marshall, S. Morrissey, P. Flynn and S. B. Levy, *Gene*, **50**, 111 (1986).
3) S. B. Levy, *ASM News*, **54**, 418 (1988).
4) S. H. Waters, P. Regowsky, J. Grinsted, J. Altenbuchner and R. Schmitt, *Nucleic Acids Res.*, **11**, 6089 (1983).
5) A. Shafferman, Z. Shalita and I. Hertman, *J. Bacteriol.*, **134**, 345 (1978).
6) M. Kono, M. Sasatsu and H. Hamashima, *Microbios Lett.*, **5**, 55 (1978).
7) S. Iordanescu, M. Surdeanu, P. D. Latta and R. P. Novick, *Plasmid*, **1**, 468 (1978).
8) J. Polak and R. P. Novick, *Plasmid*, **7**, 152 (1982).
9) K. Bernhard, H. Schrempf and W. Goebel, *J. Bacteriol.*, **133**, 897 (1978).
10) K. Shishido, N. Noguchi, C. Kim and T. Ando, *Plasmid*, **10**, 224 (1983).
11) T. Hoshino, T. Ikeda, N. Tomizuka and K. Furukawa, *Gene*, **37**, 131 (1985).
12) I. Chopra, *J. Antimicrob. Chemother.*, **18**, *Suppl. C*, 51 (1986).
13) N. Noguchi, K. Shishido, T. Ando and M. Kono, *Gene*, **21**, 105 (1983).
14) N. Noguchi, T. Aoki, M. Sasatsu, M. Kono, K. Shishido and T. Ando, *FEMS Microbiol. Lett.*, **37**, 283 (1986).
15) M. Kono, T. Aoki, M. Sasatsu, N. Noguchi and K. O'hara, *Agric. Biol. Chem.*, **49**, 1429 (1985).
16) T. Aoki, N. Noguchi, M. Sasatsu and M. Kono, *Gene*, **51**, 107 (1987).
17) H. C. Birnboim and J. Doly, *Nucleic Acids Res.*, **7**, 1513 (1979).
18) M. Mandel and A. Higa, *J. Mol. Biol.*, **53**, 159 (1970).
19) W. V. Shaw, D. W. Bentley and L. Sands, *J. Bacteriol.*, **104**, 1095 (1970).
20) S. Iyobe, M. Kono, K. Ohara, H. Hashimoto and S. Mitsuhashi, *Antimicrob. Agents Chemother.*, **5**, 68 (1974).
21) U. K. Laemmli, *Nature* (London), **227**, 680 (1970).
22) H. Towbin, T. Staehelin and J. Gordon, *Proc. Natl. Acad. Sci. U.S.A.*, **76**, 4350 (1979).
23) R. Hawkes, E. Niday and J. Gordon, *Anal. Biochem.*, **119**, 142 (1982).
24) K. Shishido, R. Sakaguchi, N. Noguchi and M. Kono, *J. Protein Chem.*, **6**, 473 (1987).
25) I. Chopra, S. W. Shales, J. M. Ward and L. J. Wallace, *J. Gen. Microbiol.*, **126**, 45 (1981).
26) H. S. Moyed, T. T. Nguyen and K. P. Bertrand, *J. Bacteriol.*, **155**, 549 (1983).
27) H. S. Moyed and K. P. Bertrand, *J. Bacteriol.*, **155**, 557 (1983).
28) B. Eckert and C. F. Beck, *J. Bacteriol.*, **171**, 3557 (1989).

Functional and Structural Domains of the Sixth Component (C6) of Human Complement

Yasuko NAKANO,*[,a] Mizuko HASHIMOTO,[a] Nam-Ho CHOI,[a] Yuji SUGITA,[a] Takashi TOBE,[a] Toshio MAZDA[b] and Motowo TOMITA[a]

School of Pharmaceutical Sciences, Showa University,[a] Hatanodai, Shinagawa-ku, Tokyo 142, Japan and Japanese Red Cross Tokyo Blood Center,[b] Sakaiminami-cho, Musashino, Tokyo 180, Japan. *Received July 17, 1990*

The effects of serine protease inhibitors, diisopropyl fluorophosphate (DFP) and phenylmethanesulfonyl fluoride (PMSF), on hemolytic activity of C6 were reinvestigated. C6 was inactivated in a range of 1–10 mM by both of the inhibitors as previously reported. Limited proteolytic digestion was also studied to elucidate the functional and structural domains of C6. The major fragments produced by trypsin, plasmin, or lysyl endopeptidase could not be separated unless disulfide bonds were disrupted, but *Staphylococcus aureus* V8 protease yielded several fragments, each of which was not linked by disulfide bond. When C6 labeled with [^{3}H]DFP was subjected to limited digestion with V8 protease, a fragment with a molecular weight of 38 kilodaltons (kDa) was mainly labeled and other fragments of 53 kDa and 26.4 kDa were also faintly labeled, while fragment 35 kDa wasn't labeled, indicating specific domains reactive with DFP. On the other hand, when C6 with or without DFP treatment was digested with V8 protease and those fragments were incubated with C5 and subjected to sucrose density ultracentrifugation, fragments 53, 38, 35 and 27.5 kDa interacted with C5 in both cases. These results suggest that C6 modified by DFP can interact with C5, and the amino-terminal sequences of fragment 38 and 35 kDa suggest the binding domain of C6 with C5 takes place within the two short consensus repeats.

Keywords C6; diisopropyl fluorophosphate; functional domain; C5 binding; short consensus repeat

Introduction

Complement component C6 is one of the five proteins that assemble sequentially to form the membrane attack complex (MAC) of the complement system.[1] Activation of the complement through the classical or alternative pathway leads to the cleavage of C5 into C5b and C5a.[2] C5b has a metastable binding site for C6 and is capable of forming a bimolecular complex, C5b, 6, with C6.[3] The complex C5b, 6 binds to C7 and expresses a metastable binding site for the phospholipid bilayer. The resulting complex, C5b-7, binds sequentially to C8 and C9 to form MAC.[4,5]

C6 is a single-chain plasma protein of molecular weight 120000—125000 and contains 3.8% carbohydrate.[6-8] Recently, the complementary deoxyribonucleic acid (cDNA) sequence of C6 was reported.[9-11] Kolb *et al.*[7,12] reported that the hemolytic activity of C6 was inhibited by serine protease inhibitors, *i.e.* diisopropyl fluorophosphate (DFP), phenylmethanesulfonyl fluoride (PMSF), *p*-tosyl-L-lysyl chloromethyl ketone (TLCK) and dansyl fluoride, over a concentration range of 10—1 mM. Conversely, DiScipio and Gagnon[8] reported that C6 was not inactivated by 2 mM DFP or 0.2 mM PMSF. Since those two groups used different concentration ranges of the inhibitors, we tried to determine the concentration range of DFP and PMSF which influenced the hemolytic activity of C6. Indeed C6 hemolytic activity was inhibited by 4 mM PMSF and by 10 mM DFP. Therefore, we sought to identify the domains of C6 which reacted with DFP, because those domains might interact with C5.

Experimental

Materials K76-monocarboxylic acid was kindly provided by Dr. Miyazaki, Otsuka Pharmaceutical Co., Ltd. Molecular weight protein standard (MW-SDS-70 kit and MW-SDS-200 kit), TPCK–trypsin, soybean trypsin inhibitor (SBTI), *Staphylococcus aureus* V8 protease (V8 protease), plasmin, PMSF and DFP were purchased from Sigma Chemical Co. Lysyl endopeptidase from *Achromobacter Lyticus* was obtained from Wako Pure Chemical Industries, Ltd. [^{3}H]DFP (3.5 Ci/mmol; 5 mCi/ml) was from Amersham Japan Co., Ltd. Human C5 was purified from human outdated serum by a modification of the methods of Hammer *et al.*[13] and Dessauer and Rother.[14] Human C6 was purified by a modification of the methods of Hammer *et al.*[13] and Podack *et al.*[15] C5 and C6 were stored at −70 °C. An antiserum to human C6 was prepared from rabbit.

Buffers VB: 4.9 mM sodium barbital, pH 7.4. VBS: VB containing 145 mM NaCl. SGVB^{++}: VB containing 9.73% sucrose, 0.15 mM $CaCl_2$, 1 mM $MgCl_2$ and 0.1% gelatin. GVB: VB containing 145 mM NaCl and 0.1% gelatin. Ethylenediamine tetraacetic acid (EDTA)–saline: 145 mM NaCl containing 10 mM EDTA. PBS: 10 mM sodium phosphate pH 7.4 containing 145 mM NaCl.

C6 Hemolytic Assay A C6-depleted serum (R6) was prepared by passing human serum containing 10 mM EDTA through a rabbit anti-human C6 antibody–Sepharose column.[6] EAC1-3b,P was prepared according to the method of Hong *et al.*[16] using sheep erythrocytes and guinea pig serum treated with K76-monocarboxylic acid. The assay mixture (150 μl) consisting of 1×10^7 EAC1-3b,P, 20 μl of R6 and 10 μl of a C6-containing sample in SGVB^{++} was incubated for 30 min at 37 °C. The mixture was diluted to 3 ml with ice-cold EDTA–saline, and the absorbance of the supernatant at 413 nm was measured after centrifugation. The average number of hemolytic sites per cell (Z) was calculated, and C6 hemolytic activity was expressed as a Z value.

[^{3}H]DFP-Labeling A mixture of 120 μg C6 in PBS and 20 μl [^{3}H]DFP was incubated for 30 min at 37 °C, subsequently adjusted to 10 mM in DFP with unlabeled DFP, and again incubated for 30 min at 37°C. The sample was applied to a TSK gel Phenyl-5PW RP column (4.6 mm i.d. × 7.5 cm) equilibrated with solvent A, and eluted at a flow rate of 0.5 ml/min with a linear gradient from 0 to 100% of solvent B; solvent A was 5% acetonitrile/0.1% (v/v) trifluoroacetic acid (TFA) and solvent B was 80% acetonitrile/0.075% TFA. [^{3}H]DFP-labeled C6 was dissolved in 50 mM of an ammonium acetate buffer, pH 4.0, digested with V8 protease at 37 °C for 20 min and analyzed by sodium dodecyl sulfate–polyacrylamide gel electrophoresis (SDS-PAGE).

Sucrose Density Ultracentrifugation C5 (90 μg) and C6 (45 μg) in 150 μl were mixed and dialyzed against 5 mM of phosphate buffer, pH 8.0 at 4 °C. The solution was incubated for 10 min at room temperature. A linear 5 to 25% sucrose gradient in 5 mM of phosphate buffer of pH 8.0 was prepared with a Hitachi DGF-U density gradient fractionator. Ultracentrifugation was performed for 41 h at 25000 rpm at 4 °C with a swing rotor. Fractions of 0.5 ml were collected from the top of the tubes with the above device. SDS-PAGE of the fractions was performed by the method of Laemmli,[17] and the immunoblotting was done with an apparatus purchased from Marisol Co. and a Vectastain kit from Vector Co.

Protein Sequencing Partial sequence analyses of C6 peptides were carried out in an Applied Biosystems 470A protein sequencer.

Results

Inactivation of C6 by PMSF and DFP According to the method of Kolb *et al.*,[7] C6 was incubated with various

concentrations of DFP or PMSF at 37 °C for 3 h in VBS and assayed for the remaining hemolytic activity. As shown in Fig. 1, PMSF started inhibiting the hemolytic activity of C6 at 2 mM concentration and produced a plateau at more than 4 mM. DFP required a higher concentration for inhibition than PMSF; it started inhibiting the hemolytic activity of C6 at 6 mM and inhibited almost completely at 10 mM. The inhibition profiles suggest that there is a critical concentration needed for the inhibition of hemolytic activity of C6.

To deduce the mechanism of the inhibition by DFP or PMSF, C6 was incubated with [^{3}H]DFP. To devoid the conformational change of C6 by the [^{3}H]DFP solvent, propylene glycol, we used [^{3}H]DFP at a final concentration of 0.5 mM. This was much less than the satisfying concentration of 10 mM to which 19-fold of cold DFP should be added. Even at this concentration, as shown in Fig. 2, [^{3}H]DFP was certainly incorporated into C6. This incorporation was completely inhibited by the preincubation of C6 with PMSF (data not shown), indicating that DFP and PMSF were incorporated in the same sites of C6.

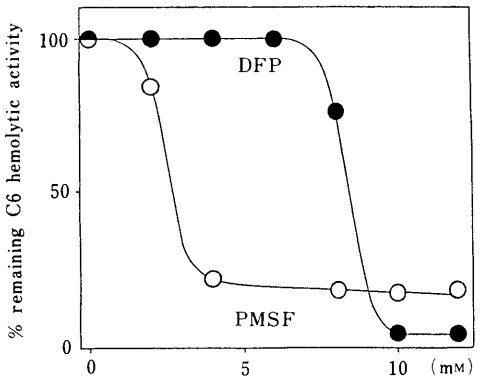

Fig. 1. The Effect of PMSF and DFP on the Hemolytic Activity of C6

C6 (4×10^{-7} M) was incubated with the indicated concentration of PMSF (○) or DFP (●) in VB, pH 7.4, at 37°C for 3 h. Each sample (10 μl) was diluted to 1 ml with ice-cold GVB and assayed for the remaining C6 hemolytic activity.

Chakravarti and Müller-Eberhard reported that neither DFP or PMSF inhibited the hemolytic activity of C6 at the concentration at which we observed the inhibition.[18] Presently, we have no clue to explain this apparently conflicting finding. Chakravarti and Müller-Eberhard suggested that the high concentration of DFP would make the solution pH acidic and induce the loss of the hemolytic activity of C6. Nevertheless, in our experiments, before and after DFP treatment of C6, no pH change was observed, and it is certain that DFP reacts with C6 as shown in Fig. 2.

Limited Proteolytic Digestion of C6 Proteins consist of several structural and functional domains. In some proteins, those domains can be released from the original protein by limited proteolytic digestion. Once the domains are obtained, they are very useful in elucidating the structure–function relationship of the original protein. Since the

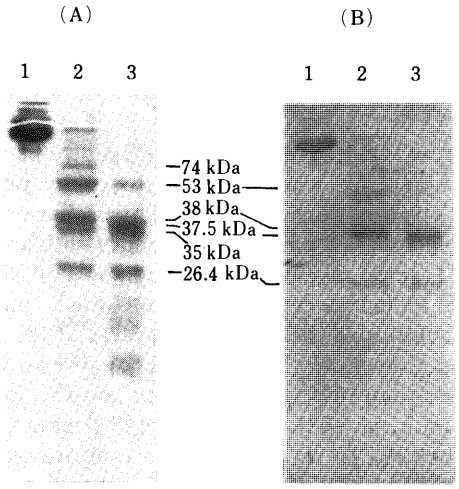

Fig. 2. Limited Proteolytic Digestion of [^{3}H]DFP-Labeled C6

Lanes 1, [^{3}H]DFP-labeled C6, Lanes 2 and 3, C6 digested with 1% (w/w) of V8 protease and with 10% (w/w) of V8 protease. 15% polyacrylamide gel electrophoresis was done as described in Experimental. (A) Coomassie blue stain of resulting gel. (B) Autoradiograph of the same gel.

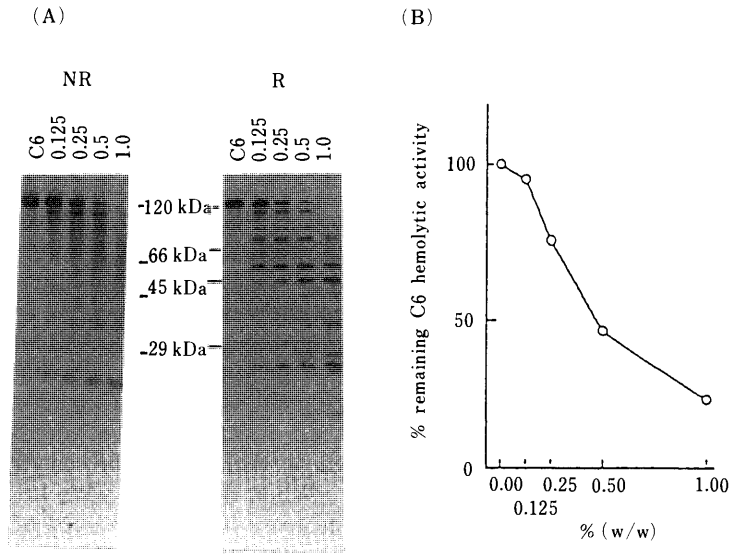

Fig. 3. Trypsin Digestion of C6

C6 (23 μg) was incubated with the indicated amount (% w/w) of trypsin in 23 μl of VBS for 5 min at 37 °C, and 27 μl of ice-cold VBS was added. Two 20-μl portions of each sample were taken and immediately added to 20 μl of Laemmli's slab gel buffer with 2-mercaptoethanol (2-ME) (R) or without 2-ME (NR) and analyzed on a 15% polyacrylamide gel (A). A 5-μl portion of each sample was supplied with a 2-molar excess of SBTI and diluted 1 : 400 in SGVB^{++} and assayed for the remaining C6 hemolytic activity as described in Experimental (B).

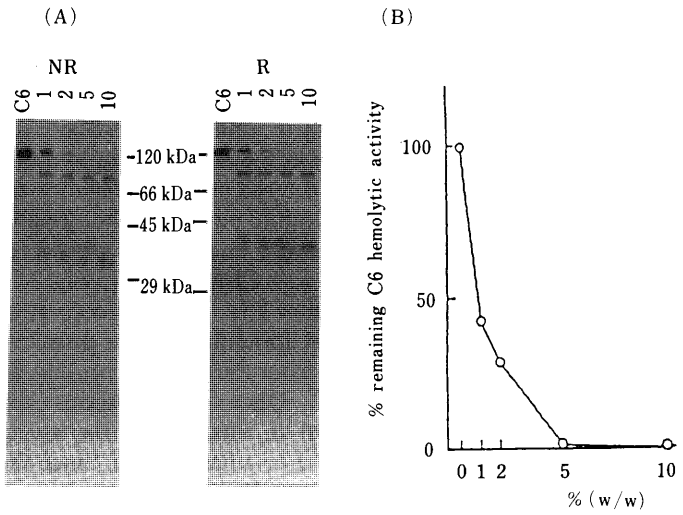

Fig. 4. V8 Protease Digestion of C6

C6 (23 μg) was incubated with the indicated amount (% w/w) of V8 protease in a total volume of 23 μl of 50 mM ammonium acetate, pH 4.0 for 20 min at 37 °C and treated as described in Fig. 3, except that no inhibitor was added after proteolysis.

sensitivity of C6 to proteolytic digestion has not been elucidated well, C6 was treated with several proteases to determine the functional domains. The proteases used were trypsin, plasmin, thrombin, lysyl endopeptidase, and V8 protease. Trypsin gave only a few fragments on SDS-PAGE under nonreducing conditions, but much more under reducing conditions (Fig. 3). Nearly 50% of the activity of C6 remained even after a 0.5% (w/w) trypsin treatment, whereas less than 10% of intact C6 remained (Fig. 3). These findings indicate that major tryptic fragments remain disulfide-bonded to retain the steric conformation of C6. In the cleavage of C6, plasmin was similar to, but less effective, than trypsin (data not shown). Yamamoto also reported that plasmin cleaved less effectively to C6 in the complex C5b, 6.[19] C6 was highly resistant to thrombin. Treatment of C6 with lysyl endopeptidase yielded only a fragment of 100 kilodaltons (kDa) on SDS-PAGE under nonreducing conditions, and significant C6 activity remained even after C6 completely disappeared (data not shown). V8 protease was distinct in that a similar fragment profile was observed on SDS-PAGE under both reducing and nonreducing conditions (Fig. 4). Thus, C6 may be divided into some structural domains which can be separated without disruption of its disulfide bonds. We chose V8 protease for further analysis. At first, [^{3}H]DFP-labeled C6 was digested with V8 protease. Major fragments detected by Coomassie blue staining were 74, 53, 38, 37.5, 35 and 26.4 kDa. Fragments 38 and 37.5 kDa were mainly labeled with [^{3}H]DFP, and fragments 74, 53 and 26.4 kDa were also weakly labeled, but fragment 35 kDa wasn't labeled at all (Fig. 2). These results indicate that C6 reacts with DFP within the fragments 38 and 37.5 kDa.

Interaction of C5 with C6 and Its Fragments C5 and C6 reversibly interact in their native forms as demonstrated by zone ultracentrifugation.[20] When C6 was mixed with C5 and subjected to ultracentrifuge, C6 was found in the range of fraction 12 to 18 while C5 in the range of fraction 14 to 22 (Fig. 5). When C6 alone was centrifuged, C6 was found in the range of fraction 8 to 10; the fraction range of C5 did not change in the absence of C6. Thus, C6 in the presence

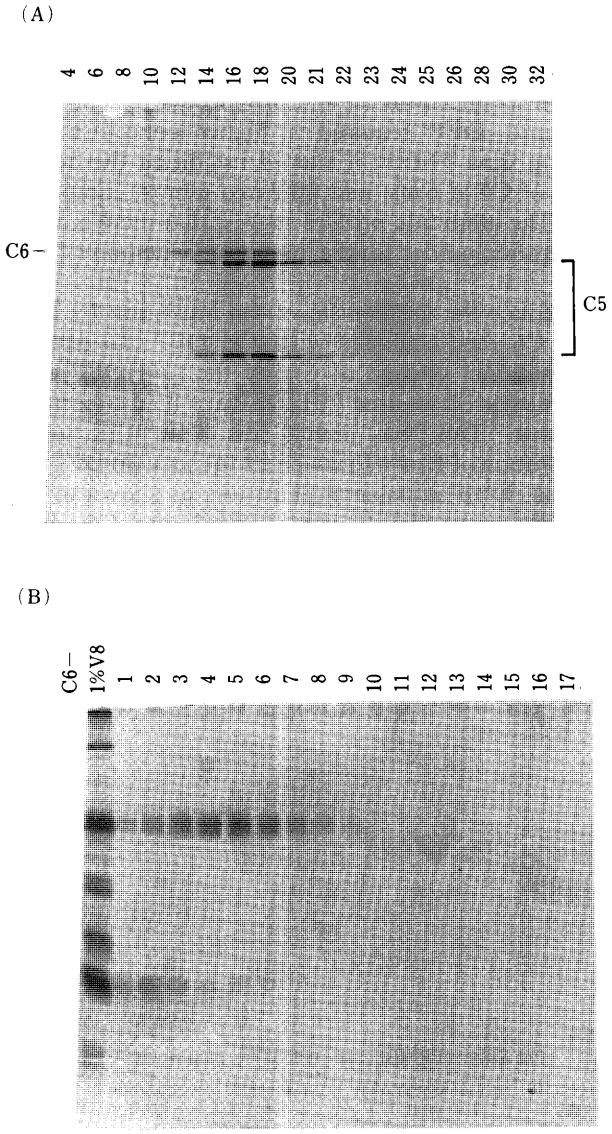

Fig. 5. Sedimentation Behavior of C6 with C5 and of C6 Treated with 1% (w/w) of V8 Protease

(A) 90 μg of C5 and 45 μg of C6 in 0.1 ml were mixed and treated as described in Experimental. Ultracentrifugation was performed at 25000 rpm for 41 h in a 5 to 25% sucrose density gradient. Fractions were analyzed on a 7.5% polyacrylamide gel under reducing conditions and detected by silver staining. (B) 70 μg of C6 treated with 1% (w/w) of V8 protease in 0.1 ml was treated as (A), and analyzed on a 15% polyacrylamide gel under nonreducing conditions and detected by silver staining.

of C5 behaved as larger molecule than C6 alone, confirming the interaction of C5 with C6. Using this technique, we tried to determine C6-domains responsible for the interaction with C5. When V8 protease digest of C6 alone was centrifuged, all the fragments were localized in the range of fractions 1 to 8 according to their molecular weights (Fig. 5). Since those fragments behaved as smaller molecules than intact C6, it was obvious that they dissociated from each other during the centrifuge.

When the digests with 1% (w/w) and 10% (w/w) of V8 protease were centrifuged after the addition of C5, small but significant amounts of fragments 53, 38, 35 and 27.5 kDa were found in the range of fractions 12 to 17 (Fig. 6A and 6C). Those fragments in fractions 12 to 17 could be more clearly detected by an immunoblotting technique using the anti-C6 antibody (Fig. 6B and 6D). In contrast, fragment

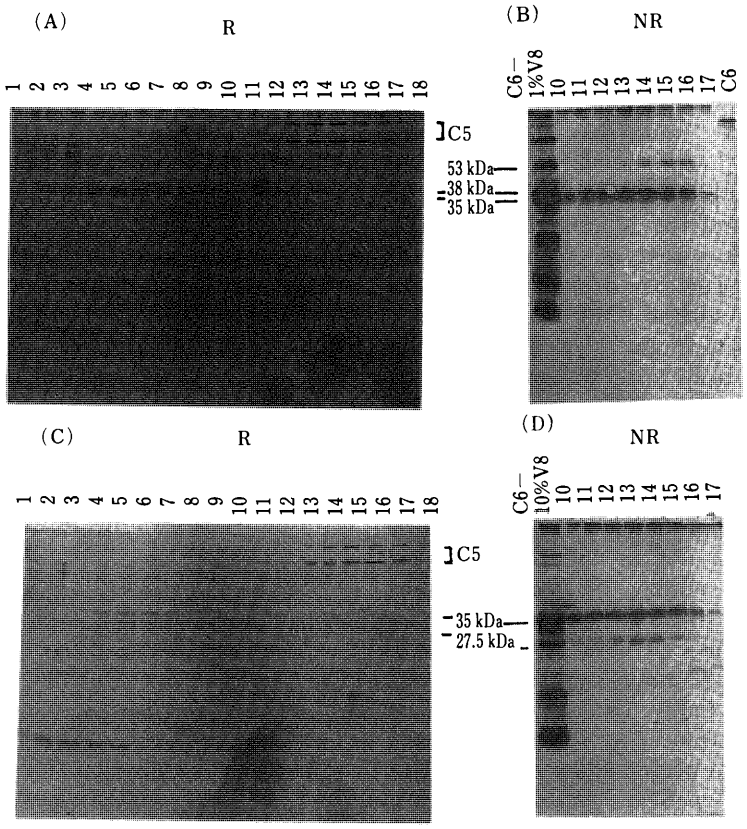

Fig. 6. Interaction of C6 Fragments with C5

90 μg C5 and 70 μg C6 treated with 1% (w/w) of V8 protease were mixed and examined as in Fig. 5. Fractions were electrophoresed in a 15% polyacrylamide gel and detected by silver staining (A) and immunoblotting with rabbit anti-C6 serum (B). The same experiments were done with C6 treated with 10% (w/w) of V8 protease. (C) is the gel which was detected by siliver staining and (D) by immunoblotting. R, reducing conditions; NR, nonreducing conditions.

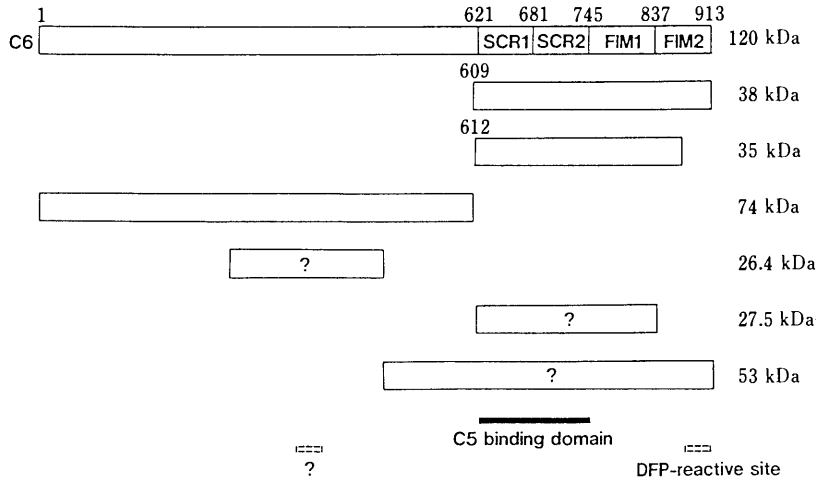

Fig. 7. Schematic Representation of C6 Fragments Produced with V8 Protease

The assignments of fragments 38 kDa and 35 kDa are based on sequence analyses and the cDNA sequence data of C6.[10,11] The other fragments are tentatively positioned considering DFP incorporation and the ability to interact with C5.

26.4 kDa and smaller fragments didn't interact with C5. Therefore, it can be concluded that fragments 53, 38, 35 and 27.5 kDa have a weak binding site to C5. The hemolytic activity of C6 was inhibited by DFP treatment. This may be due to a defectiveness to interact with C5, so DFP-treated C6 and its digests with V8 protease were tested also. They produced the same result which means that the DFP incorporation doesn't disturb the interaction of C6 with C5 (data not shown).

Discussion

More than 6 mM DFP or 1 mM PMSF was needed to inactivate C6. This finding is consistent with the results reported by Kolb *et al.*[7,12] as well as by DiScipio and Gagnon.[8] The concentration of inhibitors required for inactivation of C6 was much higher than that required for inactivation of ordinary serine proteases. Presumably those inhibitors inactivate C6 differently from the way they inhibit serine proteases. As shown in Fig. 2, DFP-reactive sites

were mainly located in fragment 38 kDa produced by the V8 protease digestion of C6, which indicates the existence of a DFP-reactive site. When the amino-terminal sequences of fragment 38 and 35 kDa were analyzed, that of 38 kDa was Met–Lys–Glu–Val–Asp··· and that of 35 kDa was Val–Asp–Leu–Pro–Glu···. From the cDNA sequence of C6,[10,11] 38 and 35 kDa were located in one third of the carboxyl-terminal of C6, and the *N*-terminal of 35 kDa started from the 4th amino acid of 38 kDa (Fig. 7). Fragment 35 kDa, which appears to be derived from 38 kDa, didn't contain [^{3}H]DFP, so the DFP-reactive site is probably located in the 3 kDa fragment released from the C-terminal end of 38 kDa. It likely resides in the complement control factor I module 2 (FIM2) of the C-terminal end of C6. In FIM2, there are two Ser rich sequences which contain 3 Ser in 4 to 5 amino acids. One or more Ser of those might be the target of DFP and PMSF.

C6 was subjected to limited proteolytic digestion in order to obtain functional domains. At an initial stage of this study, trypsin seemed to be suitable for limited digestion because it cleaved several sites of C6 without drastic damage of C6 activity (Fig. 3). But major tryptic fragments could not be separated unless disulfide-bonds were disrupted; and the disruption would eventually damage the tertiary structures of the fragments. Hence, we sought a protease which gave a similar fragment profile under both reducing and nonreducing conditions on SDS-PAGE. V8 protease gave two major fragments, 74 and 38 kDa from C6. The fragments were not associated each other by a disulfide bond, as shown in Fig. 6. Although it was evident that neither of the two fragments carried the hemolytic activity of C6 (Fig. 4), those fragments might retain C5-binding activity, which is another important function of C6 to be characterized.[19,21] We examined the C5-binding activity of those fragments by the method described by Arroyave and Müller-Eberhard.[20] As shown in Fig. 6, fragments 53, 38, 35 and 27.5 kDa interacted weakly but significantly with C5. Haefliger *et al.*[11] also reported that C5b binds to the carboxyl-terminal domain of C6. In that study, they fixed V8 protease-cleaved C6 fragments to nitrocellulose filter strips by electroblotting after SDS-PAGE. The filter strips were incubated in zymosan-containing serum and bound C5b were detected by specific mouse monoclonal ab. against C5b. Their C5b binding fragment, 34 kDa, is identical to our fragment 35 kDa from the amino acid sequences. The yields of fragment 53 kDa and 27.5 kDa were very poor and we couldn't obtain satisfying sequence data. But again, from the cDNA sequence data[10,11] and the pattern of [^{3}H]DFP incorporation, this interaction domain with C5 resided in two SCR (short consensus repeat) modules. C6 has two FIM after SCR modules. In factor I, FIM is supposed to help in recognizing the protease substrate C3b. In C6, DFP incorporation in the second FIM didn't change the binding activity with C5, so the defect of hemolytic activity must have been caused by chemical modification of another domain with DFP. C5 and C7 interact without C6 in their native forms, as demonstrated by zone ultracentrifugation.[22] The C6 modified with DFP might have a conformational change which would disturb the binding of C7 to C5b.

References

1) H. J. Müller-Eberhard, *Ann. Rev. Immunol.*, **4**, 503 (1986).
2) T. E. Hugli and H. J. Müller-Eberhard, *Adv. Immunol.*, **26**, 1 (1978).
3) R. G. DiScipio, C. A. Smith, H. J. Müller-Eberhard and T. E. Hugli, *J. Biol. Chem.*, **258**, 10629 (1983).
4) E. R. Podack, G. Biesecker, W. P. Kolb and H. J. Müller-Eberhard, *J. Immunol.*, **121**, 484 (1978).
5) P. J. Lackmann, E. R. Munn and G. Weissmann, *Immunology*, **19**, 983 (1970).
6) E. R. Podack, W. P. Kolb, A. F. Esser and H. J. Müller-Eberhard, *J. Immunol.*, **123**, 1071 (1979).
7) W. P. Kolb, L. M. Kolb and J. R. Savary, *Biochemistry*, **21**, 294 (1982).
8) R. G. DiScipio and J. Gagnon, *Mol. Immunol.*, **19**, 1425 (1982).
9) D. N. Chakravarti, B. Chakravarti, C. A. Parra and H. J. Müller-Eberhard, *Proc. Natl. Acad. Sci. U.S.A.*, **86**, 2799 (1989).
10) R. G. DiScipio and T. E. Hugli, *J. Biol. Chem.*, **264**, 16197 (1989).
11) J-A. Haefliger, J. Tschopp, N. Vial and D. E. Jenne, *J. Biol. Chem.*, **264**, 18041 (1989).
12) W. P. Kolb, L. M. Kolb and J. R. Savary, *Mol. Immunol.*, **19**, 1381 (1982).
13) C. H. Hammer, G. H. Wirtz, L. Renfer, H. D. Gresham and B. F. Tack, *J. Biol. Chem.*, **256**, 3995 (1981).
14) A. Dessauer and U. Rother, *Immunobiology*, **164**, 370 (1983).
15) E. R. Podack, W. P. Kolb and H. J. Müller-Eberhard, *J. Immunol.*, **116**, 263 (1976).
16) K. Hong, T. Kinoshita and K. Inoue, *J. Immunol.*, **127**, 109 (1981).
17) U. K. Laemmli, *Nature* (London), **227**, 680 (1970).
18) D. N. Chakravarti and H. J. Müller-Eberhard, *J. Biol. Chem.*, **263**, 18306 (1988).
19) K. Yamamoto, *J. Immunol.*, **125**, 1745 (1980).
20) C. M. Arroyave and H. J. Müller-Eberhard, *J. Immunol.*, **111**, 536 (1973).
21) E. R. Podack and H. J. Müller-Eberhard, *J. Immunol.*, **124**, 332 (1980).
22) W. P. Kolb, J. A. Haxby, C. M. Arroyave and H. J. Müller-Eberhard, *J. Exp. Med.*, **138**, 428 (1973).

Transcellular Transport of Low Density Lipoprotein through Cultured Newborn Rat Skin Epidermal Cell Monolayer

Kazuto OHKURA and Hiroshi TERADA*

Faculty of Pharmaceutical Sciences, University of Tokushima, Shomachi-1, Tokushima 770, Japan. *Received August 2, 1990*

Epidermal cells from newborn rat skin were cultured on type IV collagen-coated Millipore filter, and the transport of low density lipoprotein (LDL) labeled with Rhodamine B isothiocyanate (RB-LDL) through the cultured cell layer was examined. The transport of RB-LDL was dependent on temperature and biological energy. The transport was low at 17 °C, but above 20 °C, it became high with increase in temperature up to 37 °C. The transport was markedly inhibited by the energy inhibitors 2-deoxyglucose and NaN_3. Furthermore, the transport was saturable at the RB-LDL concentration of about 300 μg/ml and the activation energy of the transport was determined as 104.6 kJ/mol. No degradation product of LDL (apoprotein B) was observed during LDL transport through the cultured cell layer. The transport of RB-LDL through skin epidermal cells in culture is suggested to be mediated by transcytotic vesicles, but not by endocytosis and exocytosis *via* the lysosomal system, nor through cellular junctions.

Keywords skin; epidermal cell; cell culture; lipoprotein transport

Introduction

In skin dermis fibroblasts, low density lipoprotein (LDL) binds to its receptor, which is localized in specialized regions of plasma membrane called coated pits.[1] On binding with LDL, the receptor rapidly invaginates into the cell and is pinched off to form coated endocytotic vesicles, in which the LDL bound to its receptor is involved. The coated vesicles migrate through the cytoplasm until they are fused into cellular lysosomes. In lysosomes, the proteins in LDL are hydrolyzed to amino acids, and the cholesteryl esters in the core of LDL are also hydrolyzed and the liberated cholesterol is used to form cell membranes.[2] This transport is important for lipid metabolism and accumulation concerning with lipoidoses such as xanthomatosis.[3]

Transport of LDL in the cultured cell system is of interest. Cultured porcine hepatocytes contain the LDL binding site that mediates uptake and degradation of LDL.[4] LDL is reported to be transported through cultured porcine endothelial cell monolayer *via* transcytotic vesicles in temperature and energy dependent ways, but not through cellular junctions nor by endocytosis and exocytosis *via* the lysosomal system.[5] Although the transport of LDL was examined in several cultured cells,[4,5] it had not been studied with skin epidermal cells.

Skin epidermal cells have been cultured by various methods: on type I collagen film, on extracellular matrices and with 3T3 cells.[6] Recently we developed the method for obtaining a confluent monolayer of skin epidermal cells cultured on a type IV collagen-coated Millipore filter.[7] Although the viability of cells cultured on type I collagen film was less than that on type IV collagen film, it was improved by addition of ascorbic acid in culture medium to the level of a type IV collagen.[7] The cultured cells on type IV collagen film, and those on type I collagen in the presence of ascorbic acid were found to cover confluently the whole surface of the Millipore filter coated with collagen film, and bioactive compounds such as nitrophenols permeated through the cell monolayer according to their physicochemical properties.[8] In this study we examined the transcellular transport of LDL using a cultured epidermal cell monolayer.

Materials and Methods

Reagents Sources of the reagents used in this study were as follows: Eagle's minimum essential medium (MEM), Flow Laboratories, McLean, Scotland; Fetal bovine serum (FBS), Whittaker M.A. Bioproducts, Inc. Walkersville, MD, U.S.A.; dispase, Godo-Shusei Co., Tokyo, Japan; Millicell-CM (12-mm diameter, pore size, 0.4 μm), Millipore Products Co., Bedford, MA, U.S.A.; anti-type IV collagen serum (rabbit), Medac Co., Hamburg, Germany; human plasma LDL, Chemicon Inc. Temecula, CA, U.S.A.; and Rhodamine B isothiocyanate, Sigma Chemical Co., St. Louis, MO, U.S.A.

Preparation and Culture of Epidermal Cells Cell culture was performed as described previously.[7] The skin epidermis removed from 3 d old Wistar rats was digested with dispase (1000 u/ml), and washed with Ca^{2+}- and Mg^{2+}-free phosphate buffered saline (PBS) and incubated in 0.25% trypsin–0.02% ethylenediaminetetraacetic acid (EDTA) solution. The epidermal cells were suspended in Eagle's MEM buffered at pH 7.2 with 23.8 mM sodium bicarbonate and 20 mM Hepes, supplemented with 10% FBS. A volume of 500 μl of this suspension was seeded on type IV collagen-coated Millipore filter at an initial density of 1.2×10^6cells per well and cells were incubated at 37 °C for 20 h in a CO_2 incubator.

Coating of Millipore Filter with Collagen Type IV collagen was obtained from bovine kidney cortex as reported previously.[9] The purity of collagen, judged by sodium dodecylsufate polyacrylamide gel electrophoresis (SDS-PAGE) and Western immunoblotting with anti-type IV collagen serum,[10] was more than 99%. Type IV collagen dissolved in 0.1 M acetic acid at 3 mg/ml was diluted with ethanol to a final concentration of 0.06% (w/v). The solution was applied to 12-mm Millipore filters (300 μl/well), and the filters were dried at room temperature under ultraviolet (UV)-irradiation.

Labeling of LDL LDL was labeled with Rhodamine B isothiocyanate (RB) as reported previously.[11] The LDL solubilized in 0.5 M $NaHCO_3$ buffer (pH 9.3) at 1 mg protein/ml was mixed with 10 mg/ml of RB in dimethylsulfoxide in a ratio of 5 : 1. The mixture was kept at 4 °C for 24 h, and then applied to a Sephadex G-50 column to eliminate free RB. The number of RB incorporated to LDL molecules was determined from the optical absorbance according to the relation of $A_{545} = 80000\,M^{-1}\,cm^{-1}$.[11] Protein contents of LDL was determined by the method of Lowry *et al.*[12]

Transport of RB-LDL Transport of RB-LDL was examined with a permeation chamber as described previously.[7] Amount of transported RB-LDL through the cultured cell layer was monitored by fluorescence intensity of Rhodamine B at 578 nm excited at 553 nm in a Hitachi Fluorescence Spectrophotometer, model 650-60. We used the serum and phenol red depleted MEM in examination of the transport.

Detection of Apoprotein by Fluorometry An aliquot of the solution in the receiver in the permeation chamber after transport study of RB-LDL was concentrated up to about 250 fold with a Millipore molcut II (Millipore Ltd., Bedford, U.S.A.). The concentrated solution was subjected to SDS-PAGE, and RB-LDL was detected from the fluorescence of RB-LDL with a Transilluminator, model TS-20 (Ultraviolet Inc., Tokyo, Japan).

Results

Effects of Temperature and Inhibitors of Energy-Transduction on Transport of RB-LDL Figure 1 shows rat epi-

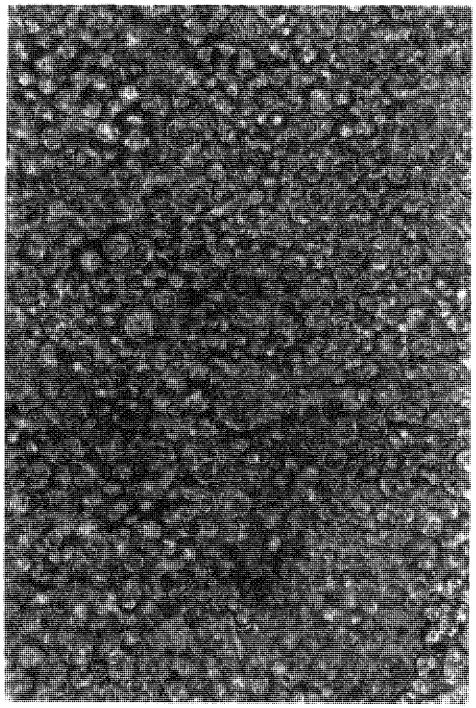

Fig. 1. Phase-Contrast Micrograph of Epidermal Cells Cultured on Type IV Collagen-Coated Millipore Filter for 20 h

Magnification: ×750.

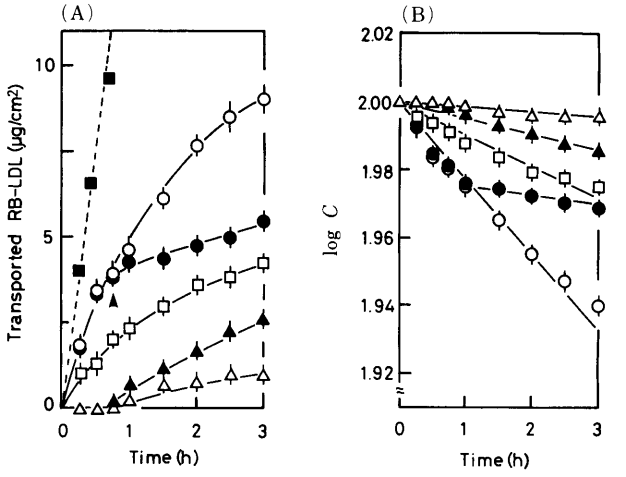

Fig. 2. Time Courses (A) and First-Order Kinetics (B) of RB-LDL Transport through Epidermal Cell Monolayer

Transport at 37 °C (○), 25 °C (□), and 10 °C (△) and 10 °C by changing temperature from 37 °C at the time indicated by an arrowhead (●). ▲: Transport in the presence of 50 mM 2-deoxyglucose and 10 mM NaN_3 at 37 °C. ■: Transport through the collagen-coated Millipore filter without a cell layer. *C*: The concentration (μg protein/ml) of RB-LDL in the donor phase of permeation cell. Results are means (±S.E.) for three determinations.

dermal cells cultured for 20 h on type IV collagen-coated Millipore filter. Cells covered confluently the whole surface of the Millipore filter coated with type IV collagen. The 500 μl RB-LDL solution at 100 μg protein/ml in MEM was applied to the cultured epidermal cell monolayer, and amount of the permeated RB-LDL to the receiver cell that contained 50 ml of MEM was determined. RB-LDL passed freely through a type IV collagen-coated Millipore filter without cell monolayer (*cf.* Fig. 2A, closed squares). The transport of RB-LDL with time was hyperbolic at 10 °C

Table I. Rate Constants of RB-LDL Transport across Rat Skin Epidermal Cell Layer at Various Temperatures

	k_{temp} (h^{-1})	k_{temp}/k_{10}
k_{10}	3.1×10^{-3}	1.0
k_{25}	2.2×10^{-2}	7.1
k_{37}	5.1×10^{-2}	16.5
k_{37-10} [a]	3.5×10^{-3}	1.1
k_{37} (inhibitor) [b]	1.0×10^{-2}	3.2

The apparent rate constant k_{temp} was determined from the results in Fig. 2. *a*) Rate constant by changing the temperature from 37 °C to 10 °C. *b*) Transport at 37 °C in the presence of 2-deoxyglucose and NaN_3.

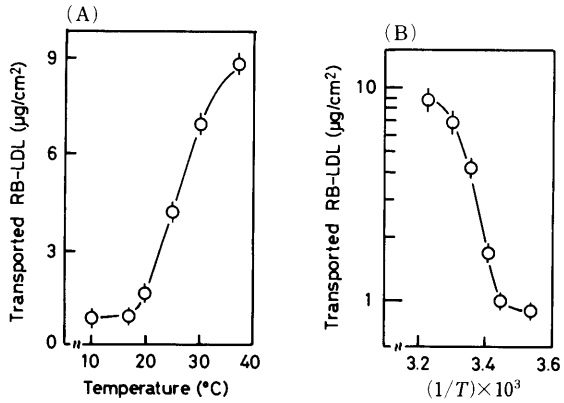

Fig. 3. Temperature Dependence of RB-LDL Transport through Epidermal Cell Monolayer (A) and Arrhenius-Plot (B) of the Transport

T: Absolute temperature. Results are means (±S.E.) for three determinations.

(open triangles), 25 °C (open squares) and 37 °C (open circles), as shown in Fig. 2. The permeation was greater with increase in temperature. After 3 h, amounts of the transported RB-LDL at 10 °C, 25 °C and 37 °C were 0.92, 4.24 and 8.88 μg protein/cm^2, respectively, in the ratio of 1.0:4.6: 9.7. When the temperature was decreased to 10 °C from 37 °C at the time indicated by the arrowhead in Fig. 2, the transport was decreased greatly (closed circles). Furthermore, transport of RB-LDL at 37 °C was markedly inhibited by the inhibitors of energy-transduction 2-deoxyglucose (50 mM) and NaN_3 (10 mM) (Fig. 2A, closed triangles). These results indicate that the transport of RB-LDL through the cell layer was temperature and energy dependent.

As shown in Fig. 2B, the transport of RB-LDL obeyed first-order rate kinetics and the apparent rate constants k_{temp}(the subscript indicates the experimental temperature) were determined as k_{10}, $3.1 \times 10^{-3}\,h^{-1}$; k_{25}, $2.2 \times 10^{-2}\,h^{-1}$; and k_{37}, $5.1 \times 10^{-2}\,h^{-1}$. When the temperature was decreased from 37 °C to 10 °C, k_{37-10} became almost the same as k_{10}. These values are summarized in Table I.

To know the dependence of RB-LDL transport on the temperature more precisely, we next determined the amount of RB-LDL that had been transported in 3 h over a wide range of temperature, and the results are shown in Fig. 3A. Transport of RB-LDL was very low, below 17 °C, but it was increased greatly above 20 °C. The transport seemed to reach a plateau at a temperature slightly higher than 40 °C. The Arrhenius-plot was sigmoidal, as shown in Fig. 3B, and activation energy of the transport was determined as 104.6 kJ/mol, from the straight portion of the curve.

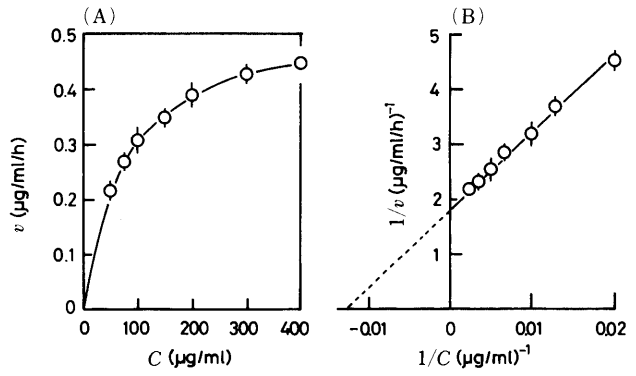

Fig. 4. Concentration Dependence of RB-LDL Transport at 37 °C (A) and Double-Reciprocal Plot of the Transport (B)

C: Concentration (μg protein/ml) of RB-LDL in the donor phase. *v*: Rate of RB-LDL transport (μg protein/ml/h). Results are means (±S.E.) for three determinations.

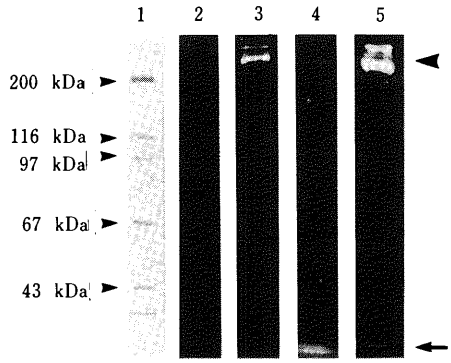

Fig. 5. SDS-PAGE Analysis of Transported RB-LDL

1 and 2: Marker proteins for molecular mass stained by Coomassie brilliant blue R-250 and their fluorogram, respectively. 3 and 4: Fluorograms of RB-LDL transported at 37 °C and 10 °C, respectively. 5: Fluorogram of standard RB-LDL. Arrowhead indicates the apoprotein B (about 250 kDa), and arrow indicates top of the electrophoresis.

Effect of RB-LDL Concentration Next, we examined the effect of RB-LDL concentration on its transport at 37 °C. The rate of RB-LDL transport (v) was increased with increase in the RB-LDL concentration (C) in a hyperbolic way, reaching a plateau at about 300 μg protein/ml (Fig. 4A). The double-reciprocal plots gave a linear relationship between $1/v$ and $1/C$, and values of K_m and V_{max} were determined as 76.9 μg protein/ml and 0.56 μg/ml/h, respectively (Fig. 4B).

Detection of Apoprotein by Fluorogram It would be very important to know whether LDL is degradated or not by transport through the cultured epidermal cell layer. We performed SDS-PAGE of the transported LDL, and fluorescence of the labeled Rhodamine B was monitored. As shown in Fig. 5, a fluorescent band at 250 kDa was detected for the transported protein at 37 °C. This molecular mass was exactly the same as that of apoprotein B of LDL (*cf.* the arrowhead of lane 3),[13] and no degradation product was observed. In the case of the transport at 10 °C, a band corresponding to that of apoprotein B was also observed, but its intensity was much weaker than that at 37 °C, as reflected by the lower permeability (*cf.* lane 4). These results indicate that LDL was transported through the cell layer keeping its original molecular mass without any degradation.

Discussion

In skin dermis fibroblasts, LDL is incorporated into the cells by the receptor-mediated pathway and it is digested to cholesterol and amino acids in lysosome.[2] Fibroblasts of familial hypercholesterolemia (FH) patients can not express LDL receptors.[14] Due to their receptor defect, these cells are unable to take up and degrade LDL, and content of cholesterol in plasma is increased. In hepatocytes, most of the degraded LDL is taken up by an LDL-specific mechanism that is suggested to be similar to the transport in fibroblasts mediated by the receptor.[4]

In this study, we examined the transport of RB-LDL through the confluent skin epidermal cell monolayer in culture. Transport of RB-LDL was greatly dependent on the temperature: less than 17 °C, the rate of transport was very small, but it became progressively larger above 20 °C with increase in temperature. This transport was completely inhibited by the biological energy inhibitors 2-deoxyglucose and NaN_3. The activation energy of the transport determined from the Arrhenius plot was 104.6 kJ/mol, being in agreement with 102.1 kJ/mol determined with the cultured porcine endothelial cell monolayer.[5] Furthermore, no degradation products of apoprotein B of LDL was observed. This suggests that LDL is not digested by the lysosomal system. Thus, the transport of LDL through the skin epidermal cells is possibly based on the same mechanism as that through a cultured endothelial cell layer, where the transport was temperature and energy dependent and no degradation product of LDL was observed.[5] The marked dependence of the transport on the temperature and the inhibition by the energy inhibitors suggest that the transport is mediated by a carrier system supported by biological energy. The transport of bovine serum albumin and insulin through endothelial cells, and thyroglobulin from the inside to the outside of thyroid follicles and vesicular stomatitis virus G protein from the apical to basal plasma membrane of MDCK cells are reported to be temperature dependent.[15]

We found that the transport of RB-LDL was dependent on its concentration, and the transport was saturated at the RB-LDL concentration of 300 μg protein/ml at 37 °C. The K_m value was determined as 76.9 μg protein/ml (Fig. 4B). LDL (apoprotein B) concentration in rat plasma and interstitial fluid were reported to be 204 μg protein/ml and about 20 μg protein/ml, respectively.[16] The K_m value of LDL transport through the skin epidermal cell layer is intermediate to the concentrations in plasma and in interstitial fluid, although the physiological meaning of this K_m value is not apparent at present.

It is noteworthy that in the present study the LDL transport through the cultured skin epidermal cell layer is suggested not to be mediated by the lysosomal system as observed in the cultured endothelial cells.[5] However, all mammalian cells require free cholesterol for their plasma membrane.[17] It has recently been shown that mammalian cells in culture cannot survive unless they can acquire cholesterol either from a usable exogenous source or as a result of *de novo* synthesis in cells.[18] The LDL receptor has not yet been identified in the skin epidermal cell, but LDL receptors in dermal fibroblasts are characterized.[14] Thus, it is expected that skin epidermal cells have LDL receptors and LDL transport is mediated by the lysosomal system. Further study is necessary to examine the existence of LDL

receptors in intact rat skin epidermal cells. If the receptor is identified, it would be important to know why LDL transport in the cultured cells is not mediated by the lysosomal system.

References

1) J. L. Goldstein, M. S. Brown, R. G. W. Anderson, D. W. Russel, and W. J. Schneider, *Ann. Rev. Cell Biol.*, **1**, 1 (1985).
2) J. L. Goldstein and M. S. Brown, *Ann. Rev. Biochem.*, **46**, 897 (1977).
3) J. Tappeiner and P. Wodniansky, "Dermatologie u. Venerologie III," vol. 2, ed. by H. A. von Gottron and W. Schonfeld, Georg Thieme, Stuttgart, 1959, pp. 1115–1194.
4) P. S. Bachorik, F. A. Franklin, D. G. Virgil, and P. O. Kwiterovich, Jr., *Biochemistry*, **21**, 5675 (1982).
5) R. Hashida, C. Anamizu, J. Kimura, S. Ohkuma, Y. Yoshida, and T. Takano, *Cell Struct. Funct.*, **11**, 31 (1986).
6) *a*) K. Yoshizato, A. Nishikawa, and T. Taira, *J. Cell Sci.*, **91**, 491 (1988); *b*) E. Tinois, M. Faure, P. Chatelain, P. Vollier, and D. Schmitt, *Arch. Dermatol. Res.*, **279**, 241 (1987); *c*) J. G. Rheinwald and H. Green, *Cell*, **6**, 331 (1975).
7) K. Ohkura, T. Fujii, R. Konishi, and H. Terada, *Cell Struct. Funct.*, **15**, 143 (1990).
8) K. Ohkura, K. Iwamoto, and H. Terada, *Chem. Pharm. Bull.*, **38**, 2788 (1990).
9) T. F. Kresina and E. J. Miller, *Biochemistry*, **18**, 3089 (1979).
10) *a*) U. K. Laemmli, *Nature* (London), **227**, 680 (1970); *b*) H. Towbin, T. Staehelin, and J. Gordon, *Proc. Natl. Acad. Sci. U.S.A.*, **76**, 4350 (1979).
11) Y. Shechter, J. Schlessinger, S. Jacobs, K. Chang, and P. Cuatrecasas, *Proc. Natl. Acad. Sci. U.S.A.*, **75**, 2135 (1978).
12) O. H. Lowry, N. J. Rosebrough, A. L. Farr, and R. J. Randall, *J. Biol. Chem.*, **193**, 265 (1951).
13) M. S. Brown, P. T. Kovanen, and J. L. Goldstein, *Recent Prog. Horm. Res.*, **35**, 215 (1979).
14) M. S. Brown and J. L. Goldstein, *Science*, **232**, 34 (1986).
15) *a*) C. C. C. O'Morchoe, W. R. Jones III, H. M. Jarosz, P. J. O'Morchoe, and L. M. Fox, *J. Cell Biol.*, **98**, 629 (1984); *b*) G. L. King and S. M. Johnson, *Science*, **29**, 1583 (1985); *c*) V. Herzog, *J. Cell Biol.*, **97**, 607 (1983); *d*) M. Pesonen, W. Ansorge, and K. Simons, *ibid.*, **99**, 796 (1984).
16) G. L. Mills and C. E. Taylaur, *Comp. Biochem. Physiol. B*, **40**, 489 (1971).
17) R. J. Harel, *Ann. N.Y. Acad. Sci.*, **348**, 16 (1980).
18) *a*) M. S. Brown and J. L. Goldstein, *J. Biol. Chem.*, **249**, 7306 (1974); *b*) H. W. Chem, A. A. Kaudutsh, and C. Waymouth, *Nature* (London), **251**, 419 (1974).

Structural Features of Ukonan C, a Reticuloendothelial System-Activating Polysaccharide from the Rhizome of *Curcuma longa*

Ryōko GONDA and Masashi TOMODA*

Kyoritsu College of Pharmacy, Shibakōen, Minato-ku, Tokyo 105, Japan. *Received August 20, 1990*

The structural features of ukonan C, the polysaccharide having remarkable reticuloendothelial system-potentiating activity obtained from the rhizome of *Curcuma longa* L., were investigated by methylation analysis, carbon-13 nuclear magnetic resonance, periodate oxidation and enzymic degradation studies. It is mainly made up of arabino-3,6-galactan type and 4,6-branched glucan type structural units. Degradation with α-amylase followed by the elimination of 1,4-linked glucan side chains resulted in a marked decrease of its immunological activity.

Keywords *Curcuma longa*; rhizome; ukonan C; reticuloendothelial system; immunological activity; polysaccharide structure; methylation analysis; enzymic degradation

Recently, we isolated and characterized three polysaccharides, ukonan A, ukonan B and ukonan C, from the rhizome of *Curcuma longa* L.,[1] having remarkable activity on the reticuloendothelial system (RES). The dried rhizome of this plant is a well-known crude drug under the name of turmeric. The structural features of ukonan B and ukonan A have been elucidated by us.[1,2] Among these three substances, ukonan C is a characteristic glucose-rich acidic polysaccharide having the value of 9×10^3 for its molecular mass. It contains 94.4% polysaccharide and 5.6% peptide moieties. The polysaccharide is composed of L-arabinose, D-xylose, D-galactose, D-glucose, L-rhamnose and D-galacturonic acid in the molar ratio of 8:3:6:14:2:3.[1] The present paper describes methylation analysis and partial degradation studies of it, and presents structural features of the polysaccharide.

Materials and Methods

Isolation of Polysaccharide This was performed as described in a previous report.[1] The yield of ukonan C was 315 mg from 1 kg of the material rhizomes.

Determination of Components Neutral sugars were analyzed by gas chromatography (GC) after conversion of the hydrolysate into alditol acetates as described previously.[3] Galacturonic acid was determined by the *m*-hydroxybiphenyl method.[4] Peptide determination was performed by the method of Lowry *et al.*[5]

Nuclear Magnetic Resonance (NMR) NMR spectrum was recorded on a JEOL JNM-GX 270 FT NMR spectrometer in heavy water containing sodium 2,2-dimethyl-2-silapentane-5-sulfonate as an internal standard at 70 °C.

Reduction of Carboxyl Groups This was carried out with 1-cyclohexyl-3-(2-morpholinoethyl)carbodiimide metho-*p*-toluenesulfonate and sodium borohydride as described previously.[6] The reduction was repeated three times under the same conditions. Yield was 32.6 mg from 50.3 mg of ukonan C.

Methylation This was performed with powdered sodium hydroxide and methyl iodide in dimethyl sulfoxide as described in a previous report.[7] Yields were 7.0 mg from 9.7 mg of ukonan C, 7.2 mg from 10.0 mg of its carboxyl-reduced product, 6.1 mg from 10.5 mg of degraded ukonan C (DUC)-I, and 3.2 mg from 4.8 mg of DUC-II and -III each.

Analysis of Methylated Products The products were hydrolyzed with dilute sulfuric acid in acetic acid, then reduced and acetylated in the manner described in a previous report.[8] The partially methylated alditol acetates obtained were analyzed by gas chromatography–mass spectrometry (GC-MS) using a fused silica capillary column (0.32 mm i.d. × 30 m) of SP-2330 (Supelco Co.) with a programmed temperature increase of 4 °C per min from 160 to 220 °C at a helium flow of 1 ml per min. GC-MS was performed with a JEOL JMS-GX mass spectrometer. The relative retention times of the products with respect to 1,5-di-*O*-acetyl-2,3,4,6-tetra-*O*-methyl-D-glucitol in GC and the main fragments in MS are listed in Table I.

Periodate Oxidation Periodate oxidation followed by reduction with sodium borohydride was performed as described previously.[1] The yield of the product was 6.0 mg from 11.5 mg of ukonan C. Determination of the surviving components was carried out as described above.

Enzymic Degradation and Isolation of the Products Ukonan C (102 mg)

TABLE I. Relative Retention Times on GC and Main Fragments in MS of Partially Methylated Alditol Acetates

	Relative retention time[a]	Main fragments (*m/z*)
1,4-Ac_2-2,3,5-Me_3-L-Arabinitol	0.69	43, 45, 71, 87, 101, 117, 129, 161
1,3,5-Ac_3-2,4-Me_2-L-Arabinitol	1.04	43, 87, 113, 117, 233
1,4,5-Ac_3-2,3-Me_2-L-Arabinitol	1.13	43, 87, 101, 117, 129, 189
1,2,4,5-Ac_4-3-Me-L-Arabinitol	1.51	43, 87, 129, 189
1,4,5-Ac_3-2,3-Me_2-D-Xylitol	1.21	43, 87, 101, 117, 129, 189
1,3,4,5-Ac_4-2-Me-D-Xylitol	1.54	43, 117, 261
1,5-Ac_2-2,3,4-Me_3-L-Rhamnitol	0.64	43, 101, 117, 131, 175
1,2,5-Ac_3-3,4-Me_2-L-Rhamnitol	0.95	43, 89, 129, 131, 189
1,2,4,5-Ac_4-3-Me-L-Rhamnitol	1.28	43, 87, 101, 129, 143, 189, 203
1,5-Ac_2-2,3,4,6-Me_4-D-Galactitol	1.09	43, 45, 71, 87, 101, 117, 129, 145, 161, 205
1,3,5-Ac_3-2,4,6-Me_3-D-Galactitol	1.36	43, 45, 87, 101, 117, 129, 161
1,4,5-Ac_3-2,3,6-Me_3-D-Galactitol	1.44	43, 45, 87, 99, 101, 113, 117, 233
1,5,6-Ac_3-2,3,4-Me_3-D-Galactitol	1.60	43, 87, 99, 101, 117, 129, 161, 189
1,2,4,5-Ac_4-3,6-Me_2-D-Galactitol	1.75	43, 45, 87, 99, 113, 129, 189, 233
1,3,5,6-Ac_4-2,4-Me_2-D-Galactitol	2.01	43, 87, 117, 129, 189
1,5-Ac_2-2,3,4,6-Me_4-D-Glucitol	1.00	43, 45, 71, 87, 101, 117, 129, 145, 161, 205
1,4,5-Ac_3-2,3,6-Me_3-D-Glucitol	1.49	43, 45, 87, 99, 101, 113, 117, 233
1,4,5,6-Ac_4-2,3-Me_2-D-Glucitol	1.92	43, 101, 117, 261

a) Relative to 1,5-di-*O*-acetyl-2,3,4,6-tetra-*O*-methyl-D-glucitol. Abbreviations: Ac = acetyl; Me = methyl (*e.g.*, 1,4-Ac_2-2,3,5-Me_3- = 1,4-di-*O*-acetyl-2,3,5-tri-*O*-methyl-).

was dissolved in 0.05 M acetate buffer (pH 5.0, 5 ml) and α-amylase preparation (25 μl, Sigma Co.) was added. The solution was incubated with a few drops of toluene at 37 °C for 6 h. After heating in a boiling water bath for 5 min, it was applied to a column (5 × 85 cm) of Sephadex G-25. The column was eluted with water, and fractions of 20 ml were collected and analyzed by the phenol-sulfuric acid method.[9] The eluates obtained from the column were divided into four groups: Frac. 1, tubes 32 to 36; frac. 2, tubes 38 to 41; frac. 3, tubes 60 to 61; frac. 4, tubes 63 to 66. The yields were 38.4 mg for frac. 1, and 14.1 mg for frac. 2. For the removal of a salt in low molecular weight fractions, fracs. 3 and 4 were each treated with a column (1 × 18 cm) of Dowex 50W-X8 (H^+) and the eluates with water were evaporated to dryness. Then the yields were 14.6 mg for frac. 3, and 18.0 mg for frac. 4. DUC-I was obtained from frac. 1. Frac. 2 was dissolved in water and applied to a column (2.6 × 95 cm) of Sephacryl S-200. The column was equilibrated and eluted with 0.1 M Tris–HCl buffer (pH 7.0), and fractions of 10 ml were collected and analyzed by the phenol–sulfuric acid method. The eluates obtained from tubes 56 to 62 were combined, dialyzed, concentrated and applied to a column (2.6 × 95 cm) of Sephadex G-25. The column was eluted with water, and fractions of 10 ml were collected and analyzed as described above. DUC-II was obtained from tubes 24 to 28, and DUC-III from tubes 29 to 32; their yields were 4.2 and 4.7 mg.

Analysis of Degradation Products Molecular weights were estimated by the method of Park *et al.*[10] compared with the value of glucose. Thin-layer chromatography (TLC) was performed on Merck precoated Kieselgel 60 plates using *n*-butanol–acetic acid–water (2 : 1 : 1, v/v) as a developing solvent. Detection was done by spraying 0.2% orcinol in 20% sulfuric acid followed by heating at 110 °C for 5 min. *Rf* values of maltose and glucose were 0.50 and 0.59. The high-performance liquid chromatography (HPLC) system used consisted of a Hitachi L-6200 intelligent pump, a Shodex SE-51 RI monitor and a Hitachi D-2000 chromatointegrator. The analysis was carried out using a column (0.46 × 25 cm) of Asahipak NH 2P-50 with acetonitrile–water (3 : 1, v/v) as an eluent at a flow rate of 1 ml per min at room temperature. Retention times of glucose and maltose were 9.14 and 15.37.

Phagocytic Activity This was measured as described in a previous report.[3] The sample and a positive control, zymosan (Tokyo Kasei Co.), were each dissolved and suspended in physiological saline and dosed i.p. (5 mg/kg body weight) once a day. The phagocytic index, *K*, was calculated by means of the following equation:

$$K=(\ln OD_1-\ln OD_2)/(t_2-t_1)$$

where OD_1 and OD_2 are the optical densities at times t_1 and t_2, respectively. Results were expressed as the arithmetic mean ± S.D. of five male mice (ICR-SPF). The comparison of results was performed by means of Student's *t*-test.

Results

The crude polysaccharide fraction obtained from the rhizome of *Curcuma longa* was applied to a column chromatography of diethylaminoethyl (DEAE)-Sephadex A-25. The eluate with 0.2 M ammonium carbonate was subjected to affinity chromatography on Con A-Sepharose. The passed-through fraction was applied to gel chromatography on a Sephacryl S-300 column. Ukonan C was isolated from the relatively low molecular weight fraction.[1]

The polysaccharide was composed of L-arabinose, D-xylose, D-galactose, D-glucose, L-rhamnose and D-galacturonic acid in the molar ratio of 8 : 3 : 6 : 14 : 2 : 3.[1] The glucan moiety in ukonan C was degraded by treatment with α-amylase followed by gel chromatography with Sephadex G-25. Five products were obtained, and two of them were identified as glucose and maltose by TLC and HPLC analysis. The residual three fractions are tentatively designated as DUC-I, DUC-II and DUC-III. In both DUC-II and DUC-III, glucose was the only component sugar. DUC-I, the highest molecular weight fraction in the enzymic degradation products, contained 26.9% arabinose, 9.8% xylose, 24.7% galactose, 12.2% glucose, 7.0% rhamnose, 13.8% galacturonic acid and 6.4% peptide moiety. The molar ratio of these component sugars was 8 : 3 : 6 : 3 : 2 : 3. DUC-I had $[\alpha]_D^{24}$ −10.6° (H_2O, $c=0.1$). Determination of the reducing powers gave values of 6000, 1300 and 830 for the molecular weights of DUC-I, DUC-II and DUC-III, respectively.

The carbon-13 NMR (^{13}C-NMR) spectrum of ukonan C gave no good result on anomeric signals. However, the ^{13}C-NMR spectrum of DUC-I showed seven signals due to anomeric carbons at δ 100.48, 100.94, 102.55, 104.33, 105.36, 105.87 and 111.19 ppm. The signals at δ 100.94 and 102.55 ppm were assigned to the anomeric carbons of α-D-galactopyranosyluronic acid and α-L-rhamnopyranose, respectively.[11] The signals at δ 100.48, 104.33 and 105.36 ppm were assigned to the anomeric carbons of α-D-glucopyranose, β-D-xylopyranose and β-D-galactopyranose, respectively.[12] The signals at δ 105.87 and 111.19 ppm were assigned to the anomeric carbons of α-L-arabinopyranose and α-L-arabinofuranose.[13]

The carboxyl groups of galacturonic acid residues in

Table II. Methylation Analysis of Ukonan C and Its Carboxyl-Reduced Derivative

Methylated sugars (as alditol acetates)	Molar ratios	
	Original	Carboxyl-reduced
2,3,5-Me_3-L-Arabinose	9	9
2,4-Me_2-L-Arabinose	5	5
2,3-Me_2-L-Arabinose	1	1
3-Me-L-Arabinose	1	1
2,3-Me_2-D-Xylose	2	2
2-Me-D-Xylose	4	4
2,3,4-Me_3-L-Rhamnose	1	1
3,4-Me_2-L-Rhamnose	2	2
3-Me-L-Rhamnose	1	1
2,3,4,6-Me_4-D-Galactose	2	2
2,4,6-Me_3-D-Galactose	1	1
2,3,6-Me_3-D-Galactose	1	7
2,3,4-Me_3-D-Galactose	2	2
3,6-Me_2-D-Galactose	1	1
2,4-Me_2-D-Galactose	5	5
2,3,4,6-Me_4-D-Glucose	2	2
2,3,6-Me_3-D-Glucose	24	24
2,3-Me_2-D-Glucose	2	2

Table III. Methylation Analysis of the Enzymic Degradation Products of Ukonan C

Methylated sugars (as alditol acetates)	Molar ratio		
	DUC-I	DUC-II[a]	DUC-III[a]
2,3,5-Me_3-L-Arabinose	9	–	–
2,4-Me_2-L-Arabinose	5	–	–
2,3-Me_2-L-Arabinose	1	–	–
3-Me-L-Arabinose	1	–	–
2,3-Me_2-D-Xylose	2	–	–
2-Me-D-Xylose	4	–	–
2,3,4-Me_3-L-Rhamnose	1	–	–
3,4-Me_2-L-Rhamnose	2	–	–
3-Me-L-Rhamnose	1	–	–
2,3,4,6-Me_4-D-Galactose	2	–	–
2,4,6-Me_3-D-Galactose	1	–	–
2,3,6-Me_3-D-Galactose	1	–	–
2,3,4-Me_3-D-Galactose	2	–	–
3,6-Me_2-D-Galactose	1	–	–
2,4-Me_2-D-Galactose	5	–	–
2,3,4,6-Me_4-D-Glucose	—	+	+
2,3,6-Me_3-D-Glucose	6	+	+

a) Precise molar ratios of the products were not obtained.

ukonan C were reduced to give the corresponding neutral sugar residues.[14] Both the original polysaccharide and the carboxyl-reduced derivative were methylated with solid sodium hydroxide and methyl iodide in dimethyl sulfoxide.[15] The methylated products were hydrolyzed, then converted into the partially methylated alditol acetates. The hexuronic acid methyl ether was removed from the hydrolysis products of the methylated polysaccharide by treatment with an anion-exchange resin. Analysis by GC-MS[16] gave the results shown in Table II. The methylation analyses of DUC-I, DUC-II and DUC-III were performed in the similar manner to that of ukonan C, and the results were shown in Table III.

Ukonan C was subjected to periodate oxidation followed by reduction. The maximal value of periodate consumption was 0.6 mol per mol of anhydrosugar unit. The component sugar analysis of the product showed that three-eighths of the arabinose units, two-thirds of the xylose units, seven-twelfths of the galactose units and a quarter of the rhamnose units survived after periodate oxidation. All the glucose and the galacturonic acid residues were completely destroyed by this treatment.

These results indicated that the minimal unit of ukonan C is composed of eighteen kinds of component sugar units, as shown in Chart 1.

(nine)[a] α-L-Ara*f* 1→
(one)[a] →5 α-L-Ara*f* 1→
(one)[a] →5 α-L-Ara*f* 1→
2
↑
(five)[a] →3 α-L-Ara*p* 1→
(two)[a] →4 β-D-Xyl*p* 1→
(four)[a] →4 β-D-Xyl*p* 1→
3
↑
(two)[a] β-D-Gal*p* 1→
(one)[a] →3 β-D-Gal*p* 1→
(one)[a] →4 β-D-Gal*p* 1→
(two)[a] →6 β-D-Gal*p* 1→
↓
6
(five)[a] →3 β-D-Gal*p* 1→
(one)[a] →4 β-D-Gal*p* 1→
2
↑

(two)[a] α-D-Glc*p* 1→
(twenty-four)[a] →4 α-D-Glc*p* 1→
↓
6
(two)[a] →4 α-D-Glc*p* 1→
(one)[a] α-L-Rha*p* 1→
(two)[a] →2 α-L-Rha*p* 1→
↓
4
(one)[a] →2 α-L-Rhap 1→
(six)[a] →4 α-D-Gal*p*A 1→

Chart 1. Component Sugar Residues in the Minimal Unit in the Structure of Ukonan C

a) Number of residues. Ara*f*, arabinofuranose; Ara*p*, arabinopyranose; Xyl*p*, xylopyranose; Gal*p*, galactopyranose; Glc*p*, glucopyranose; Rha*p*, rhamnopyranose; Gal*p*A, galactopyranosyluronic acid.

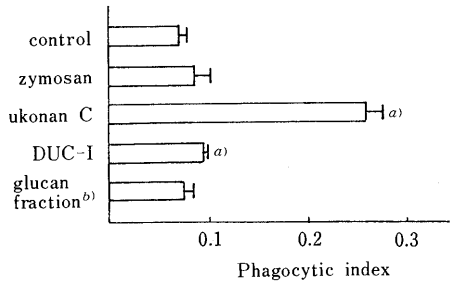

Fig. 1. Effects of Ukonan C, DUC-I and Glucan Fraction on Carbon Clearance Index in ICR Mice

Significantly different from the control, *a*) $p<0.001$. *b*) The glucan fraction is composed of DUC-II and -III in a ratio of 1.0:1.1.

The effects of ukonan C, DUC-I and the fraction containing DUC-II and -III on the RES were demonstrated by a modification[3] of the *in vivo* carbon clearance test[17] using zymosan as a positive control. As shown in Fig. 1, DUC-I showed significant activity. However, the value was much lower than that of ukonan C. The fraction containing DUC-II and -III showed no RES activity.

Discussion

We have already reported remarkable RES activities of ukonan A, ukonan B and ukonan C, the three acidic polysaccharides obtained from the rhizome of *Curcuma longa*.[1] These substances are commonly composed of L-arabinose, D-xylose, D-galactose, D-glucose, L-rhamnose, D-galacturonic acid and a peptide moiety. Both ukonan A and ukonan B possess the same fourteen kinds of component sugar residues, though the two substances are different in the ratios of these sugar units.[1,2] Ukonan A and ukonan B are mainly made up of an arabino-3,6-galactan type structure with additional α-1,3-linked L-arabinopyranosyl, β-3,4-branched D-xylosyl, α-1,4-linked D-glucosyl and α-2,4-branched L-rhamno-D-galacturonan units. In both ukonan A and ukonan B, glucose is a quite minor component. In contrast to these substances, glucose is the major component sugar in ukonan C.

The structural features of ukonan C are more complicated than those of ukonan A and ukonan B. The polysaccharide has nineteen kinds of component sugar units. All the kinds of component sugar units in ukonan A and ukonan B are also found in ukonan C with the other additional five units, those are, α-2,5-branched L-arabinosyl, β-1,4-linked D-galactosyl, β-2,4-branched D-galacyosyl, α-4,6-branched D-glucosyl and terminal α-L-rhamnosyl residues. After treatment with α-amylase, ukonan C lost about 80% of its glucose units. As a result of this enzymic degradation, RES activity of the main product, DUC-I, composed of the residual acidic polysaccharide moiety was more markedly decreased than that of the original substance. This fact showed that the presence of component glucose units contributes to the activity of ukonan C. The degradation products composed of only glucose showed no RES activity. Methylation analysis of DUC-I revealed only 1,4-linked units as its glucose linkage. So is conceivable that side chains of branched glucose units in ukonan C were lost by the enzymic degradation.

As other examples of RES-activating polysaccharides from Oriental crude drugs, sanchinan-A isolated from the root of *Panax notoginseng*,[18] and tochibanan-A and -B from the rhizome of *Panax japonicus*[19] have been reported. Sanchinan-A possesses an α-L-arabino-β-3,6-branched D-galactan type structure, and tochibanan-A and -B belong to β-1,4-linked D-galactan and partially 2,3,6-branched β-1,4-linked D-galactan, respectively.

In addition, we have reported the RES activities and structural features of saposhnikovans A and C from the root and rhizome of *Saposhnikovia divaricata*,[3,20] MVS-IIIA, -IVA and -VI from the seed of *Malva verticillata*,[7,21,22] cinnaman AX from the bark of *Cinnamomum cassia*,[23] glycyrrhizans UA, UB and UC from the root of *Glycyrrhiza uralensis*,[24,25] and of eucomman A from the bark of *Eucommia ulmoides*.[26] Saposhnikovan A has an α-1,4-linked D-galacturonan backbone bearing α-1,5-

linked L-arabino-β-3,6-branched D-galactan side chains, and saposhnikovan C possesses a rhamnogalacturonan type backbone with α-3,5-branched L-arabinan and β-3,4-branched D-galactan side chains. Both MVS-IIIA and MVS-IVA are mainly made up of an α-1,5-linked L-arabino-β-3,6-branched D-galactan structure. MVS-VI, the main acidic polysaccharide in the material seed, has similar arabinogalactan moieties as its main part, though the ratio of these moieties in the components is lower than those of MVS-IIIA and -IVA. The backbone of cinnaman AX is a β-1,4-linked D-xylan mostly bearing α-L-arabinofuranosyl-(1→3)-β-L-arabinopyranose side chains. The main part of glycyrrhizan UA is occupied by α-1,5-linked L-arabino-β-3,6-branched D-galactan. Glycyrrhizan UB is a polysaccharide basically similar to glycyrrhizan UA, though α-2,4-branched rhamnogalacturonan units occupy its major part. Glycyrrhizan UC also possesses many arabino-3,6-galactan units, and besides these factors, this neutral polysaccharide is rich in β-1,4-linked D-galactan and α-1,4-linked D-glucan moieties. Eucomman A has similar arabinogalactan and branched rhamnogalacturonan units to those in glycyrrhizan UB.

Thus, most of the RES-activating polysaccharides obtained by us possess α-1,5-linked L-arabino-β-3,6-branched D-galactan moieties as their major parts, though cinnaman AX is a new structural type of RES-activating substance. Among them, ukonan C and glycyrrhizan UC are characteristically rich in α-1,4-linked D-glucose units. In the present work, the participation of glucan side chains in the RES activity was found in ukonan C.

Acknowledgement This work was supported in part by the Sasagawa Scientific Research Grant.

References

1) R. Gonda, M. Tomoda, N. Shimizu and M. Kanari, *Chem. Pharm. Bull.*, **38**, 482 (1990).
2) M. Tomoda, R. Gonda, N. Shimizu, M. Kanari and M. Kimura, *Phytochemistry*, **29**, 1083 (1990).
3) N. Shimizu, M. Tomoda, R. Gonda, M. Kanari, N. Takanashi and N. Takahashi, *Chem. Pharm. Bull.*, **37**, 1329 (1989).
4) N. Blumenkrantz and G. Asboe-Hansen, *Anal. Biochem.*, **54**, 484 (1973).
5) O. H. Lowry, N. J. Rosebrough, A. L. Farr and R. J. Randall, *J. Biol. Chem.*, **193**, 265 (1951).
6) M. Tomoda and M. Ichikawa, *Chem. Pharm. Bull.*, **35**, 2360 (1987).
7) R. Gonda, M. Tomoda, M. Kanari, N. Shimizu and H. Yamada, *Chem. Pharm. Bull.*, **38**, 2771 (1990).
8) M. Tomoda, K. Shimada, Y. Saito and M. Sugi, *Chem. Pharm. Bull.*, **28**, 2933 (1980).
9) M. Dubois, K. A. Gilles, J. K. Hamilton, R. A. Rebers and F. Smith, *Anal. Chem.*, **28**, 350 (1952).
10) J. T. Park and M. J. Johnson, *J. Biol. Chem.*, **181**, 149 (1949).
11) N. Shimizu and M. Tomoda, *Chem. Pharm. Bull.*, **33**, 5539 (1985).
12) K. Bock, C. Pedersen and H. Pedersen, "Advances in Carbohydrate Chemistry and Biochemistry," Vol. 42, ed. by R. S. Tipson and D. Horton, Academic Press, Inc., Orland, 1984, pp. 193—214.
13) J.-P. Joseleau, G. Chambat, M. Vignon and F. Barnoud, *Carbohydr. Res.*, **58**, 165 (1977).
14) R. L. Taylor and H. E. Conrad, *Biochemistry*, **11**, 1383 (1972).
15) I. Cincanu and F. Kerek, *Carbohydr. Res.*, **131**, 209 (1984).
16) H. Björndall, B. Lindberg and S. Svensson, *Carbohydr. Res.*, **5**, 433 (1967).
17) G. Biozzi, B. Benacerraf and B. N. Halpern, *Br. J. Exp. Pathol.*, **34**, 441 (1953).
18) K. Ohtani, K. Mizutani, S. Hatono, R. Kasai, R. Sumino, T. Shiota, M. Ushijima, J. Zhou, T. Fuwa and O. Tanaka, *Planta Medica*, **53**, 166 (1987).
19) K. Ohtani, S. Hatono, K. Mizutani, R. Kasai and O. Tanaka, *Chem. Pharm. Bull.*, **37**, 2587 (1989).
20) N. Shimizu, M. Tomoda, R. Gonda, M. Kanari, Aki. Kubota and Ake. Kubota, *Chem. Pharm. Bull.*, **37**, 3054 (1989).
21) M. Tomoda, M. Kanari, R. Gonda and N. Shimizu, *Phytochemistry*, **28**, 2609 (1989).
22) R. Gonda, M. Tomoda, N. Shimizu and M. Kanari, *Planta Medica*, **56**, 73 (1990).
23) M. Kanari, M. Tomoda, R. Gonda, N. Shimizu, M. Kimura, M. Kawaguchi and C. Kawabe, *Chem. Pharm. Bull.*, **37**, 3191 (1989).
24) M. Tomoda, N. Shimizu, M. Kanari, R. Gonda, S. Arai and Y. Okuda, *Chem. Pharm. Bull.*, **38**, 1667 (1990).
25) N. Shimizu, M. Tomoda, M. Kanari, R. Gonda, A. Satoh and N. Satoh, *Chem. Pharm. Bull.*, **38**, 3069 (1990).
26) R. Gonda, M. Tomoda, N. Shimizu and M. Kanari, *Chem. Pharm. Bull.*, **38**, 1966 (1990).

Effects of Glucose and Ascorbic Acid on Absorption and First Pass Metabolism of Isoniazid in Rats

Yōko MATSUKI,*,[a] Yoshimitsu KATAKUSE,[a] Hiroshi MATSUURA,[a] Hiroshi KIWADA[a] and Tsuyoshi GOROMARU[b]

Faculty of Pharmaceutical Sciences, University of Tokushima,[a] Shomachi 1-chome, Tokushima 770, Japan, and Faculty of Pharmacy and Phamaceutical Sciences, University of Fukuyama,[b] Higashimuracho 985, Fukuyama 729–02, Japan. *Received July 6, 1990*

We examined the effect of glucose (Glu) and ascorbic acid (AA) on absorption and metabolism of isoniazid (INAH). After *p.o.* administration of INAH with or without Glu or AA, plasma concentration and urinary excretion of INAH and its metabolites, acetyl INAH (AcINAH), acetyl hydrazine (AcHy) and hydrazine (Hy), were determined by means of gas chromatography–mass spectrometry using stable isotope labeled compounds as internal standard. The combined administration of INAH with Glu or AA led to a significant decrease in the excretion of INAH and Hy, and a significant increase in the excretion of AcINAH and AcHy. The absorption amount of INAH was reduced to about one-half by the addition of Glu and the absorption rate of INAH markedly decreased in the case of co-administration of AA. Comparing the oral case with the results of i.v. administration, Glu and AA only affect the absorption process containing the first pass metabolism of INAH.

Keywords isoniazid; absorption; first pass metabolism; hydrazine; co-administration; glucose; ascorbic acid; hydrazone

Isoniazid (INAH) has been used as a primary drug for the treatment of tuberculosis. In our previous work,[1] we studied the effect of ascorbic acid (AA), which has recently been used more frequently in high dosage, on the urinary excretion of INAH and its metabolites, and have found that the combined use of AA with INAH led to a significant increase in the excretion of acetyl INAH (AcINAH), the major metabolite of INAH, and a marked decrease in the excretion of free hydrazine (Hy). The decrease in Hy excretion due to the combined use of AA is of interest in view of the fact that Hy has been reported to have close relations with hepatic injury caused by INAH.[2] Glucose (Glu),which has been used in various formulas, is known to form a hydrazone with INAH.[3]

Therefore, the effects of Glu on the metabolic fate of INAH are interesting. The present study focuses on the effect of Glu and AA on the concentrations of INAH and its metabolites, including AcINAH, acetyl hydrazine (AcHy) and Hy, in plasma and urine.

Experimental

Materials INAH, AA, hydrazine sulfate (Hy-sulfate) and Glu were purchased from Wako Pure Chemical Ind., Ltd. AcHy was obtained from Tokyo Chemical Ind., Co., Ltd. AcINAH was synthesized by the method of Fox *et al.*[4] 1-Isonicotinoyl-2-glucosylhydrazine was prepared according to the method of Zinner *et al.*[5]

Deuterium-labeled INAH (INAH-d_2, 95.2 atom%D) was synthesized from deuterated isonicotinic acid ethylester produced by the protium–deuterium exchange reaction, as described in our previous report.[6] Deuterated AcINAH (AcINAH-d_3, 97.9 atom%D) was prepared by acetylation of INAH with deuterated acetic acid (E. Merck, 99 atom%D) and deuterated acetic anhydride (MSD, 99 atom%D), according to the method of Fox *et al.*[4] Deuterated AcHy (AcHy-d_3, 97.1 atom%D) was prepared by acetylation of hydrazine hydrate (Wako Pure Chemical Ind., Ltd.) with deuterated acetic acid (CEA, 99.4 atom%D), followed by conversion into fumarate by method of Nelson *et al.*[7] ^{15}N-labeled hydrazine sulfate (^{15}N-Hy, 99 atom%D) was purchased from MSD. These stable isotope-labeled compounds were used as an internal standard in gas chromatographic–mass spectrometric (GC-MS) determination.

Animal Experiments Male Wistar rats weighing 170—220 g were used after fasting for 24 h prior to the experiments. An aqueous solution containing INAH (100 mg/kg) with or without Glu (656.8 mg/kg) or AA (642 mg/kg) was orally administered to rats. Those amounts of Glu and AA are equivalent to fivefold molar amount of INAH. Blood samples were taken from heart at 15, 30, 60, 120, 180, 240 and 300 min after administration, followed by the separation of plasma. Urine was collected for 24 h after dosing of the same solution. In addition, an isotonic solution containing Hy-sulfate (19 mg/kg) alone or with AA (fivefold molar amount of Hy) was injected via the femoral vein of rats, and urine was collected for 24 h.

To examine the formation of hydrazone in the rat stomach, INAH (100 mg/kg) and Glu (fivefold molar amount of INAH) were administered to rats, and 0.2 ml of gastric juice was collected by using a cannule at 30 and 60 min after administration.

Extraction of INAH and its Metabolites from Plasma and Urine a) INAH: As described in the previous paper,[6] 40 μg of INAH-d_2 was added to 0.5 ml of plasma. Then 20 ml of CH_3CN was added and the plasma sample was shaken for 30 min and centrifuged. The upper CH_3CN layer was separated and evaporated. The residue was dissolved in 5 ml of 0.2 N acetate buffer (pH 5.0), and this solution was shaken for 30 min after the addition of ethanolic benzaldehyde solution (0.05 ml/ml), resulting in the formation of 1-isonicotinoyl-2-benzylidene-hydrazine (IBH) and IBH-d_2. The formed derivatives were extracted with 20 ml of dichloromethane. The organic layer was dried over anhydrous sodium sulfate and evaporated. The residue was dissolved in 30 μl of *N*,*N*-dimethylformamide and *tert*-butyldimethyl-silylation (TBDMS) of IBH was performed by treatment with 20 μl of *N*-(*tert*-butyldimethylsilyl)-*N*-methyltrifluoroacetamide (Tokyo Chemical Ind.).

b) AcINAH: AcINAH-d_3 (15 μg) was added to 0.5 ml of plasma. The plasma was treated with CH_3CN by means similar to the INAH. The sample was dissolved in 5 ml of water. The solution was supersaturated with ammonium sulfate and extracted with 20 ml of ethyl acetate. The extract was derivatized to *tert*-butyldimethyl-silylated-AcINAH.

c) AcHy: AcHy-d_3 (6.4 μg) was added to 0.5 ml of plasma. The plasma was treated with CH_3CN. After the formation of Schiff base with benzaldehyde, the sample was extracted with 20 ml of ethyl acetate. The extract was dissolved in 20 μl of pyridine and derivatized to a trimethylsilyl derivative of 1-acetyl-2-benzylidene-hydrazine with 20 μl of bis-trimethylsilylacetamide.

d) Hy: ^{15}N-Hy (1.6 μg) was added to 0.5 ml of plasma. Then, 2 ml of water, 1 ml of ethanol and 3.5 g of ammonium sulfate were added and the mixture was shaken for 30 min and centrifuged. The supernate was separated and added in 3 ml of 0.2 N acetate buffer solution (pH 5.0) containing benzaldehyde. After condensation, resultant benzalazine and $^{15}N_2$-benzalazine were extracted with 20 ml of ethyl acetate. The extract

TABLE I. GC-MS Conditions for Measurement of INAH and Its Metabolites

Condition	INAH	AcINAH	AcHy	Hy
Column	1.5% OV-1	1.5% OV-1	1.5% OV-17	1.5% OV-17
Column temperature	230 °C	230 °C	150 °C	200 °C
Injection temperature	280 °C	280 °C	250 °C	250 °C
Monitoring ion	*m/z* 282 *m/z* 284 $(M-57)^+$	*m/z* 350 *m/z* 353 $(M-57)^+$	*m/z* 219 *m/z* 222 $(M-15)^+$	*m/z* 208 *m/z* 210 M^+

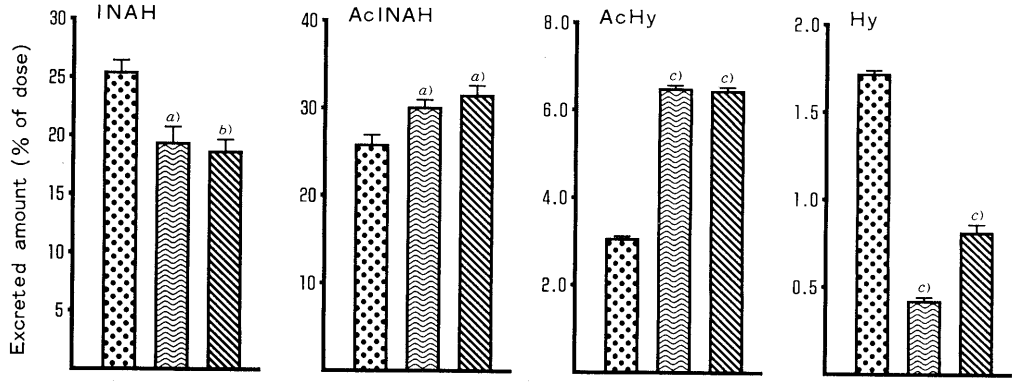

Fig. 1. Urinary Excretion of INAH and Its Metabolites for 24 h after Oral Administration of INAH (100 mg/kg) with or without Glucose (656.8 mg/kg) and Ascorbic Acid (642 mg/kg)

⁘, INAH alone; ≋, with glucose; ▨, with ascorbic acid. Mean ± S.E. ($n=5$). *a*) $p<0.05$, *b*) $p<0.01$, *c*) $p<0.001$.

was dissolved in 30 μl of pyridine.

To determine urinary excretion of INAH and its metabolite, the entire amount of urine collected for 24 h was diluted with water up to 50 ml. Two ml aliquots of the urine sample were subjected to the same treatment as for plasma described above. The labeled internal standards, however, were used in twofold amounts in the case of plasma.

Quantitative Determination of INAH and its Metabolites The concentration of INAH and its metabolites in plasma and urine were determined by isotope dilution analysis using labeled compounds as the internal standard. The analysis was performed by GC-MS. GC-MS was carried out in a JEOL D-300 GC-MS computer system. Helium gas flow rate, 20 ml/min; accelerating voltage, 3 kV; ionizing energy, 20 eV. The column condition and the selected monitoring ions were as listed in Table I. Working curves were prepared with blank plasma and blank urine containing known amounts of INAH, AcINAH, AcHy and Hy-sulfate. The GC-MS peak area ratio of non-labeled to labeled compound was proportional to the molar ratio of non-labeled to labeled compound, the correlation coefficient obtained by regression analysis being 0.9996, 0.9989, 0.9918 and 0.9998 for INAH, AcINAH, AcHy and Hy, respectively, in the sample prepared using plasma.

Quantitative Determination of 1-Isonicotinoyl-2-glucosylhydrazine (Glu-INAH) For quantitative determination of the hydrazone formed from INAH and Glu, 0.2 ml of gastric juice was dissolved in a 250-fold volume of high performance liquid chromatography (HPLC) mobile phase solvent. In the case of plasma, 10 ml of CH_3CN was added to 0.25 ml of plasma and the sample was shaken for 30 min and centrifuged. The upper CH_3CN layer was separated and evaporated. The residue was dissolved in 1 ml of the mobile phase. The solution was filtered through a 0.2 nm membrane filter and subjected to quantitative determination by HPLC according to the condition of Butterfield *et al.*[8] HPLC was carried out in a TRI ROTAR Japan Spectroscopic Co., Ltd.) and a Finepak SIL CN column (5 μm, 250 mm × 4.6 mm i.d.) was used at a flow rate of 1 ml/min. The mobile phase was aqueous 0.01 M acetate buffer (pH 3.7)–acetonitrile (95 : 5 v/v). The absorbance was measured at 254 nm and a 100 μl loop injector was used to inject the samples.

Results and Discussion

Urinary excretion of INAH and its metabolites (AcINAH, AcHy and Hy) after oral administration of INAH with or without Glu or AA is shown in Fig. 1. It is noticeable that the combined administration of INAH with Glu or AA led to a significant decrease in the excretion of INAH and a significant increase in the excretion of AcINAH. Furthermore, the excretion of AcHy increased more than twofold as compared with that after single administration. Co-administration of Glu and AA gave rise to a significant reduction of the excretion of Hy. In particular the excretion of Hy after INAH administration with Glu decreased significantly to less than one-third of that after INAH alone.

Concerning the single administration of INAH, excretion

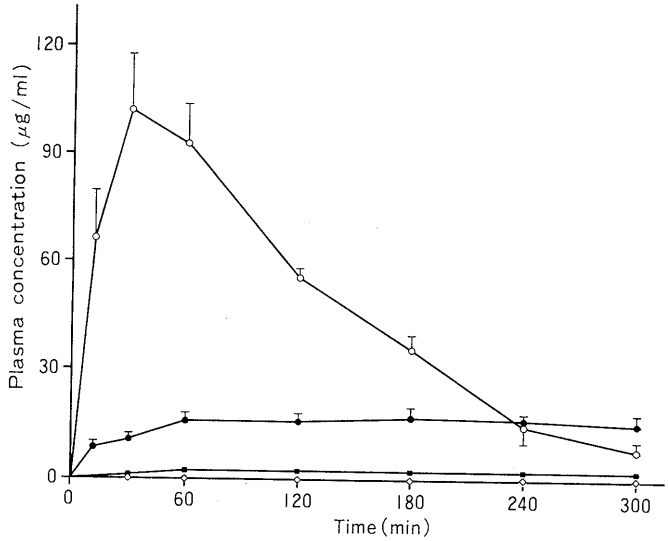

Fig. 2. Plasma Concentration *versus* Time Profile for INAH and Its Metabolites in Rats after Administration of INAH (100 mg/kg, *p.o.*)

○, INAH; ●, AcINAH; ■, AcHy; ◇, Hy. Mean ± S.E. ($n=3$).

of intact INAH in this study was about four times as high as in our previous work.[1] It is known that the acetylation rate of INAH varies among rats even in the same strain. The difference between the previous and present results of INAH excretion, therefore, might be attributed to lower ability of acetylation in rats used here.

The plasma concentration of INAH and its metabolites are shown in Fig. 2—4. The co-administration of Glu or AA caused a significant decrease in INAH level. The maximum level of INAH was observed within 30 ml in the cases of single administration and co-administration of Glu, while over 60 min in the case of co-administration of AA. *AUC* (area under the blood concentration–time curve) from 0 to 300 min after administration with Glu or AA were 50.31% and 84.48%, respectively, of that in the case of single administration. These observations indicate that the absorption amount of INAH was reduced to about one-half by the addition of Glu and the absorption rate of INAH markedly decreased in the case of co-administration of AA. Glu appears to have no effect on the excreted amount of AcINAH, while AA causes a significant increase in the AcINAH level as compared with INAH alone ($p<0.05$ using Student *t*-test, at 180 min after administration). In

TABLE II. Elimination Rate Constant of INAH and Urinary Excretion of INAH and AcINAH for 24 h after i.v. Administration of INAH (100 mg/kg) with or without Glucose (656.8 mg/kg) or Ascorbic Acid (642 mg/kg) to Rats

Condition	Kel[a] of INAH (h^{-1})	Excreted amout (% of dose) INAH	AcINAH
INAH alone	0.468±0.036 (n=6)	27.57±1.73	31.93±1.39 (n=3)
With glucose	0.498±0.096 (n=7)	24.85±1.46	34.28±3.40 (n=3)
With ascorbic acid	0.492±0.042 (n=3)	22.60±1.65	35.72±0.99 (n=3)

Mean±S.E. *a*) Calculated from plasma concentration of INAH by using least-squares method.

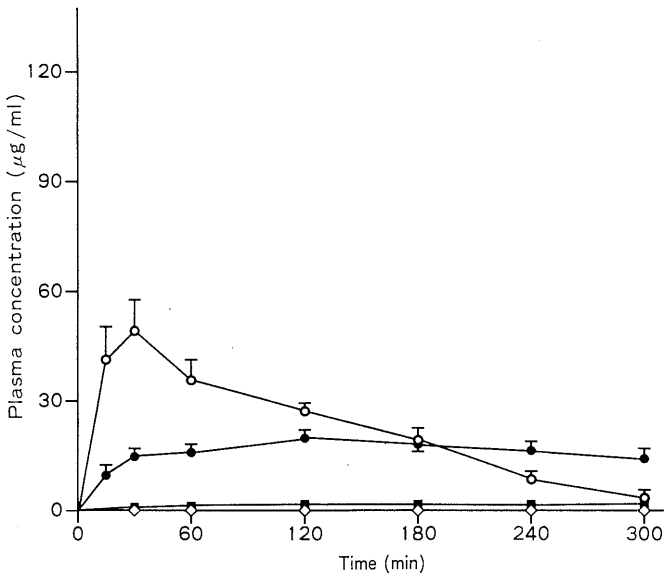

Fig. 3. Plasma Concentration *versus* Time Profile for INAH and Its Metabolites in Rats after Administration of INAH (100 mg/kg, *p.o.*) with Glucose (656.8 mg/kg, *p.o.*)

○, INAH; ●, AcINAH; ■, AcHy; ◇, Hy. Mean±S.E. (n=3).

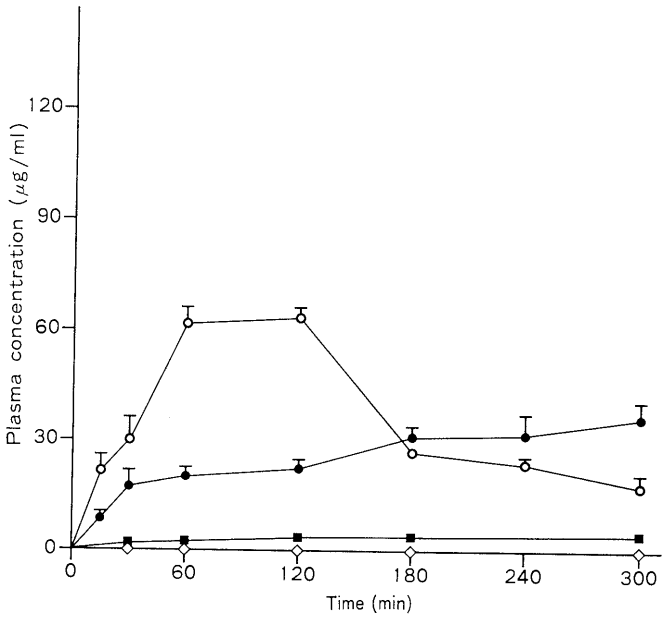

Fig. 4. Plasma Concentration *versus* Time Profile for INAH and Its Metabolites in Rats after Administration of INAH (100 mg/kg, *p.o.*) with Ascorbic Acid (642 mg/kg, *p.o.*)

○, INAH; ●, AcINAH; ■, AcHy; ◇, Hy. Mean±S.E. (n=3).

any case, the concentration of AcHy and Hy were extremely low, therefore, the effect of Glu and AA on these metabolites could not be confirmed in plasma concentration.

To discuss the effect on elimination process of INAH, the concentration of INAH and AcINAH in plasma and urine were determined after i.v. administration of INAH with or without Glu or AA. From results shown in Table II, Glu and AA have no effects on the elimination of INAH and on the excretion of INAH and AcINAH, confirming that Glu and AA do not affect the metabolism, distribution and elimination process of INAH.

As mentioned previously, Glu and AA only affect the absorption process of INAH. From the fact that urinary excretion of INAH and its metabolites varied with the co-adminstration, the first pass metabolism is presumed to be influenced by the absorption rate. The percentages of the urinary excretion of INAH and AcINAH for 24 h after the oral administration of various doses of INAH are summarized in Table III. With increase of dose, the percentages of INAH excretion increase, while those of AcINAH excretion decrease. The ratios of excretion of AcINAH to that of INAH indicate a marked tendency for the acetylation of INAH to saturate. This saturation phenomenom may contribute to the change of metabolic rate of INAH, therefore, the decrease in absorption rate of INAH results in the increase of urinary excretion of AcINAH.

TABLE III. Urinary Excretion of INAH and AcINAH for 24 h after Oral Administration of Various Dose of INAH to Rats

Dose of INAH (mg/kg)	Excreted amount (% of dose) INAH	AcINAH	AcINAH/INAH
50	15.06±0.85	39.83±0.98	2.65
100	25.23±1.51	25.77±1.13	1.02
200	37.55±0.96	19.51±1.21	0.52

Mean±S.E. (n=5).

It has been reported[9] that INAH reacted with sugar to form hydrazone in acidic solution, therefore, the hydrazone might be formed in the stomach after dosing INAH with Glu. The concentration of the hydrazone was determined in gastric juice and plasma after oral administration of INAH and Glu by HPLC. Typical HPLC-grams of gastric juice are shown in Fig. 5. As summarized in Table IV, a large portion of INAH remained in the gastric juice as the hydrazone form and the hydrazone was also detected from the plasma. Kakemi *et al.*[10] reported that the hydrazone would not be absorbed in an intact form. However, the formation and the degradation of the Glu-INAH hydrazone did not occur in neutral medium such as plasma.[9] In addition, no hydrazone was found in the plasma after i.v. administration of INAH with Glu. These observations

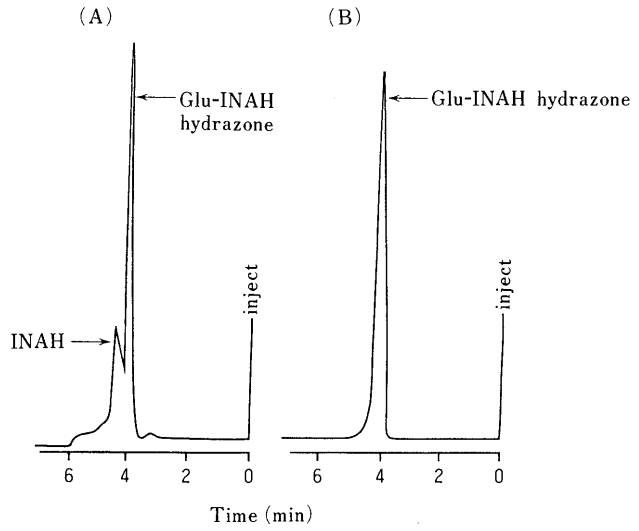

Fig. 5. High Performance Liquid Chromatogram of Gastric Fluid after Administration of INAH (100 mg/kg, *p.o.*) with Glucose (656.8 mg/kg, *p.o.*)
A, 30 min; B, 60 min.

TABLE IV. Glu-INAH and INAH Concentration in Gastric Fluid and Plasma after Administration of INAH (100 mg/kg, *p.o.*) with Glucose (656.8 mg/kg, *p.o.*) to Rats

Compound	Time after administration (min)	Concentration Gastric fluid (μg/0.2 ml)	Plasma (μg/ml)
Glu-INAH	30	1785.6±153.5	4.1±1.1
	60	1449.5±155.7	7.5±2.2
INAH	30	513.9± 21.3	29.5±4.4
	60	N.D.	23.1±6.1

Mean±S.E. ($n=3$).

indicate the possibility of the absorption as the intact hydrazone. The formation of the hydrazone which has lower absorbability than free INAH, causes the decrease of the plasma concentration of INAH after the co-administration. In the case of AA, the reason for the decrease in absorption rate of INAH has not been clarified.

In our previous report,[1] we found that AA reacted with Hy in pH 7.4 phosphate buffer solution. After incubation of Hy (23 μg/ml) with AA (636 μg/ml) in control plasma at 37 °C, the concentration of Hy decreased linearly with the incubation time, reaching 50% of the initial concentration after 2 h, while no decrease of Hy was observed in the case of without AA. It can therefore be presumed that similar reaction of Hy with AA occurs *in vivo*. Urinary excretion of Hy was 22.3% of dose for 24 h after i.v. dosing of Hy-sulfate only, while it decreased to 2.7% of dose when AA was co-administered. This result indicates that AA reacts with Hy and remarkably affect *in vivo* behavior of Hy.

The present study reveals that Glu and AA have remarkable effects on the absortion process of INAH and on the excretion of the harmful metabolites, such as AcHy and Hy. However, the mechanism of AA in the decrease of absorption rate of INAH and in the reaction with Hy have not been clarified. Further investigation is required to reveal the effect of AA on the *in vivo* behaviour of INAH and Hy.

References

1) Y. Matsuki, T. Goromaru and H. Matsuura, *Yakugaku Zasshi*, **103**, 1219 (1983).
2) *a*) L. Severi and C. Biancifiori, *J. Natl. Cancer*, **41**, 331 (1968); *b*) A. Noda, T. Sendo, K. Ohno, H. Noda and S. Goto, *Chem. Pharm. Bull.*, **35**, 2538 (1987).
3) *a*). H. H. Fox, *J. Org. Chem.*, **18** 990 (1953); *b*) M. B. Devani, C. J. Shishoo, M. A. Patel and D. D. Bhalara, *J. Pharm. Sci.*, **67**, 661 (1978).
4) H. H. Fox and J. T. Gibas, *J. Org. Chem.*, **18** 1375 (1953).
5) H. Zinner and W. Bock, *Chem. Ber.*, **89**, 1124 (1957).
6) Y. Matsuki, Y. Katakuse, M. Katashima, H. Matsuura and T. Goromaru, *Chem. Pharm. Bull.*, **37**, 1637 (1989).
7) S. D. Nelson, J. A. Hinson and J. R. Mitchell, *Biochem. Biophs. Res. Comm.*, **69**, 900 (1976).
8) A. G. Butterfield, E. G. Lovering and R. W. Sears, *J. Pharm. Sci.*, **69**, 222 (1980).
9) M. B. Devani, C. J. Shishoo, K. J. Doshi and H. B. Patel, *J. Pharm. Sci.*, **74**, 427 (1985).
10) K. Kakemi, T. Arita, H. Sezaki and N. Takasugi, *Chem. Pharm. Bull.*, **13**, 551 (1965).

Percutaneous Absorption of Elcatonin and Hypocalcemic Effect in Rat

Taro OGISO,* Masahiro IWAKI, Isako YONEDA, Mina HORINOUCHI and Katsuaki YAMASHITA

Faculty of Pharmaceutical Sciences, Kinki University, Kowakae 3-4-1, Higashi-Osaka 577, Japan. *Received June 27, 1990*

The percutaneous absorption of elcatonin (EC), a hypocalcemic peptide, was investigated. A transdermal dosage form of EC was produced using a gel base, absorption enhancer and protease inhibitor, and applied to rats for 24 h. The combination of bile salt such as taurocholate and glycocholate, and *n*-octyl-β-D-glucoside or *n*-octyl-β-D-thioglucoside (OTG) exerted the potent enhancing effect on the absorption of EC, and a potent hypocalcemic effect was shown for 24 h or longer. The least level of plasma calcium was obtained 6 h or longer after application, suggesting the relatively rapid absorption of EC. The apparent bioavailability of EC in system 5 was 4.6%, this value being noteworthy in the percutaneous absorption of peptides. When the enhancing effect of taurocholate and OTG was separately measured, both agents acted additively on the absorption of EC. An EC ointment maintained the hypocalcemin effect after storage for 15 d at 40 °C. The transdermal dosage form has the potential to be an efficient drug delivery system for Paget's disease and osteoporosis.

Keywords elcatonin; percutaneous absorption; hypocalcemic effect; absorption enhancer; bile salt; octyl glucoside; octyl thioglucoside; rat

Calcitonin, a hypocalcemic peptide hormone, has been used for the treatment of Paget's disease as well as certain types of osteoporosis.[1] Elcatonin (EC), synthetic [Asu^{1,7}]-eel calcitonin, also inhibits osteoclastic bone resorption stimulated by bone resorptive factors.[2] Recently, there is growing evidence that EC action can stimulate osteoblastic bone formation.[3] Peptides, such as EC, are given effectively only by injection, because, when taken orally, they are digested by the proteolytic enzymes in the gastrointestinal tract and metabolized by the liver. In addition, it has been generally considered difficult for a peptide hormone to be absorbed through the intestinal mucosa. Furthermore, calcitonin therapy is inconvenient because the drug must be injected subcutaneously or intramuscularly. More simple or convenient administration may be favorable as a dosage route for EC and calcitonin. This is an important problem for patients who are unable to have injections or are in need of long-term therapy.

The rectal administration of EC is reported as a dosage route.[4,5] However, the bioavailability and the ability to lower serum calcium levels after rectal administration are relatively small.[4,5]

The transdermal route of administration is useful for drugs with low bioavailability after oral dosing. Drug administration *via* skin has the advantage of bypassing the hepatogastrointestinal "first-pass" metabolism associated with oral administration. It may also be useful for short-acting drugs since transdermal absorption tends to be slow, and prolonged effects may be realized.

It is reported that the absorption of human calcitonin through rat's gingiva is enhanced by the coadministration of sodium cholate,[6] and that bile salts will inhibit the degradation of the peptide in oral mucosa supernatant.[7] In addition, the absorption of thyrotropin-releasing hormone through rat skin is shown to be enhanced by *n*-octyl-β-D-glucoside (OG).[8] These observations led to our interest in the percutaneous (p.c.) absorption of EC based on the combined use of the enhancers.

The present study was designed to evaluate the p.c. absorption of EC and the effect of various absorption promotors and protease inhibitors, in addition to maintaining the prolonged effect after the transdermal application.

Experimental

Materials [Asu^{1,7}]-eel calcitonin (6400 U/mg, Toyo Jozo Co., Ltd.), a synthetic analogue of eel calcitonin in which the disulfide bridge between the first and seventh amino acids in the eel calcitonin molecule is replaced by a $-CH_2CH_2-$ bridge[9] was used throughout this study. Hiviswako 104 and Carbopol 934 (Carbopol), gel bases, were obtained from Wako Pure Chemical Industries and Kishida Chemical Co., Ltd., respectively. Gabexate mesilate and bestatin were obtained from Ono Pharmaceutical Industry Co. and Sigma Chemical Co. (St. Louis, MO, U.S.A.), respectively. Bile salts, *n*-octyl-β-D-thioglucoside (OTG) and OG were reagent grade commercial products. Gentamycin solution (5 mg/ml) was purchased from Boehringer Mannheim Co. Male Wistar rats (Japan SLC Inc.), weighing 270—300 g, were used throughout this experiment.

Preparation of Gel Ointments The pH value of Carbopol was adjusted to 6.5 with 10% NaOH. EC dissolved in a mixture of water and propylene glycol was mixed with the gel base and was followed by the addition of other additives. In one ointment (Rp. 10), Hiviswako 104 was vigorously

TABLE I. Composition of Elcatonin Gel Ointment and Absorption Enhancer and Protease Inhibitor Used

Rp. 1—9		Rp.	Additive I	Additive II		Rp. 10	
Carbopol 934	2.0 g	1	OG	Bestatin	5.0 mg	Glycerin	93.1 g
Elcatonin	25.0 mg	2	OG	Taurocholate	1.0 g	Hiviswako 104	1.0 g
Propylene glycol	10.0 g	3	OTG	Bestatin	5.0 mg	Elcatonin	25.0 mg
Gentamycin sol.	2.0 g	4	OTG	Gabexate	20.0 mg	Triethanolamine	1.37 g
Additive I	1.5 g	5	OTG	Taurocholate	1.0 g	Gentamycin sol.	2.0 g
Additive II	—	6	OTG	Deoxycholate	1.0 g	OTG	1.5 g
Purified water ad.	100.0 g	7	OTG	Glycocholate	1.0 g	Taurocholate	1.0 g
		8	OTG	—			
		9	—	Taurocholate	1.0 g		

OG, *n*-octyl-β-D-glucoside; OTG, *n*-octyl-β-D-thioglucoside.

mixed with glycerin heated at 65 °C and, after cooling, EC dissolved in gentamycin solution was added to the base. Details of the ointment composition are listed in Table I.

Intravenous (i.v.) Administration On the day before the experiment, the rat jugular vein was cannulated with a silicon tubing[10,11] and rats were fasted for 16 h prior to the experiment. EC dissolved in saline was administered intravenously at 40 or 80 U/rat. After administration, blood samples were collected periodically through the tubing. The plasma was separated immediately by centrifugation and stored frozen until assay.

***In Vivo* p.c. Absorption Experiment** On the day before the experiment, the rat jugular vein was cannulated with a silicon tubing[10,11] and the hair of the abdominal area was carefully removed with an electric clipper and an electric razor to prevent damage to the stratum corneum. The animals were fasted for 16 h prior to the experiment, but water was given freely. The transdermal therapeutic system (TTS) which was prepared using a corresponding gel ointment described in Table I, as depicted in Fig. 1, was fixed on the shaved abdominal skin (0.5 g ointment/4 cm^2/rat) with an adhesive (Aronalpha, Konishi Co.) and immediately occluded with an adhesive tape. The application of system to rat was done for 24 h and then the remaining ointment was wiped off with absorbent cotton soaked in warm water. The fast was broken at this time. Blood samples from the cannulated jugular vein were collected periodically for 48 h after dosing.

Determination of Plasma Calcium Concentration The plasma calcium concentration was determined by the *o*-cresolphthalein complexone method using the Calcium C-Test Wako (Wako Pure Chemical Industries) and 0.01 ml plasma.

Pharmacokinetic and Statistical Analyses The area under the plasma calcium concentration–time curve (the difference in the area between the EC-dosing group and control group, *AUC*) after i.v. administration and topical application of EC was calculated by the trapezoidal method up to 24 h. The area under the first moment curve (*AUMC*) and the mean residence time (*MRT*) were calculated by means of the following equations[12]:

$$AUMC=\int_0^{24} t\cdot C_p dt$$

$$MRT=AUMC/AUC$$

where C_p is the difference in plasma calcium concentration between EC-dosing and control rats at time, t.

The apparent bioavailability was calculated by the following equation:

$$\text{apparent bioavailability}=\frac{AUC_{p.c.}\,Dose_{i.v.}}{AUC_{i.v.}\,Dose_{p.c.}}\times 100$$

where $AUC_{p.c.}$ and $AUC_{i.v.}$ are *AUC* after p.c. and i.v. (40 U/rat) administrations, respectively. The bioavailability was calculated from AUC_{0-24}, because the ingestion of diet enhanced the calcium level in the plasma.

The means of all data are presented with their standard deviation (mean ± S.D.). One-way analysis of variance (ANOVA) with Scheffe's multiple comparison procedure was used to compare each data, and a p value of 0.05 or less was considered to be significant.

Results

Plasma Calcium Concentration after Single i.v. Administration The plasma calcium concentrations after i.v. administration of EC (40 or 80 U/rat) are shown in Fig. 2. The plasma calcium levels decreased rapidly in both dosing and a significant hypocalcemic effect was obtained 3—24 h after administration, although the effect declined 30 h after dosing. The AUC_{0-24} values were 57.89 ± 7.48 and 73.87 ± 6.19 mg·h/dl for the 40 U and 80 U dosing, respectively.

Plasma Calcium Concentration after Single p.c. Administration The plasma calcium concentrations during a single p.c. application of TTS are shown in Figs. 3 and 4. The pharmacokinetic parameters calculated are listed in Table

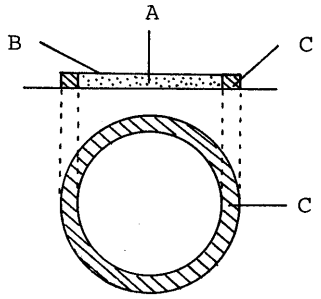

Fig. 1. Sectional View of Transdermal Therapeutic System
A, ointment; B, aluminum foil; C, silicon rubber (2.26 cm i.d., 1.0 mm thickness).

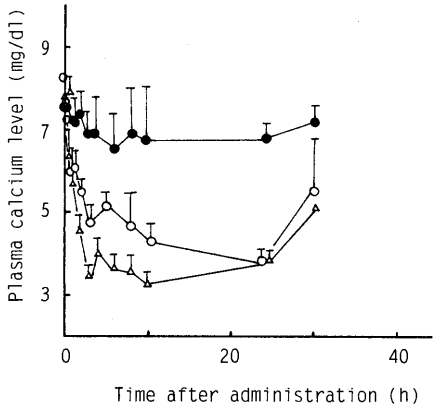

Fig. 2. Changes in Plasma Calcium Concentrations Following i.v. Administration of EC
○, 40 U/rat; △, 80 U/rat; ●, saline.

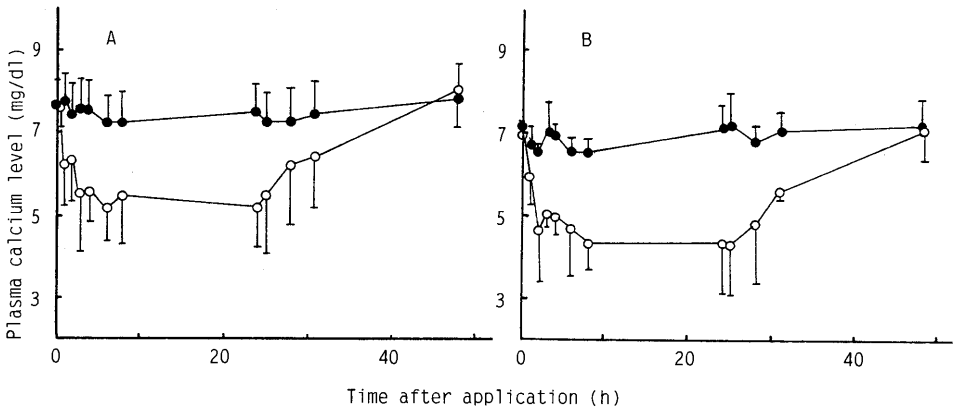

Fig. 3. Changes in Plasma Calcium Concentrations Following p.c. Application of Systems 2 and 5
Each point represents the mean ± S.D. (n = 4—9). A, system 2; B, system 5. ●, placebo (control) system; ○, EC system.

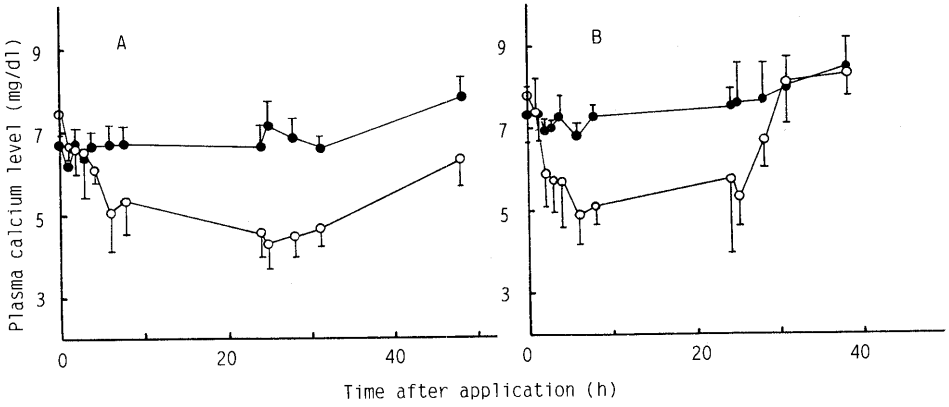

Fig. 4. Changes in Plasma Calcium Concentrations Following p.c. Application of Systems 6 and 7

Each point represents the mean ± S.D. (n=4—7). A, system 6; B, system 7. ●, placebo system; ○, EC system.

TABLE II. Pharmacokinetic Parameters Calculated by the Moment Method after Percutaneous Application of Elcatonin Systems

System No.	*AUC* (mg·h/dl)	*AUMC* (mg·h²/dl)	*MRT* (h)	Apparent bioavilability (%)
1	30.99±11.75	371.41±159.80	12.06±1.99	2.68
2	46.25±19.25[a)]	623.71±233.74	13.81±2.36	3.99
3	36.13±21.93	445.49±249.06	12.83±1.68	3.12
4	17.25±10.07	271.52±106.34	18.16±6.19	1.49
5	53.50±14.96[b)]	752.04±298.40	13.66±3.46	4.62
6	31.97±17.89	505.37±238.24	16.32±2.35	2.76
7	40.85±20.01	513.32±292.53	12.34±2.37	3.53
8	26.40±20.66	341.64±271.20	13.91±3.02	2.28
9	35.02±16.72	433.42±114.39	13.37±3.60	3.02
10	35.23±33.53	490.35±444.31	16.31±6.88	3.04

Each value represents the mean ± S.D. of 4—9 experiments. The system was prepared using the corresponding gel ointment (0.5 g) described in Table I. The applied dose of elcatonin was 800 U/4 cm². *a*) Significantly different from No. 1, 3, 4 and 6—10, $p<0.05$. *b*) Significantly different from No. 1—4 and 6—10, $p<0.05$.

II. The calcium levels decreased relatively rapidly and the least level was obtained 6 h or longer after application. The calcium levels were gradually increased after the cessation of application, probably due to the ingestion of calcium (diet).

The application of the preparation without the enhancer and/or inhibitor listed in Table I failed to reduce the plasma calcium level (data not shown). Therefore, it is suggested that the enhancers and inhibitors used would significantly promote the absorption of EC through rat skin. System 5 showed an excellent hypocalcemic effect, giving the highest bioavailability among the systems applied ($p<0.05$).

Systems 2 and 7 also showed higher hypocalcemic effects than those of other preparations, although the difference in the values of the latter system did not reach statistical significance. These preparations contained taurocholate or glycocholate and OG or OTG as an enhancer, suggesting that they are effective enhancers. The system containing gabexate, a protease inhibitor, however did not exert a significantly hypocalcemic effect. There was not a significant difference in *MRT* values between all systems.

Enhancing Effect of Taurocholate and OTG Individually on p.c. Absorption In order to clarify whether or not taurocholate and OTG exert a synergetic or additive effect, the system (No. 8 and 9) containing each agent alone was prepared and applied to rat. The *AUC* value was shown in Table II. The sum of *AUC* for No. 8 and No. 9 roughly approximated that for system 5 which contained both taurocholate and OTG. Thus, it appears that both agents might not act synergetically on the enhancing effect.

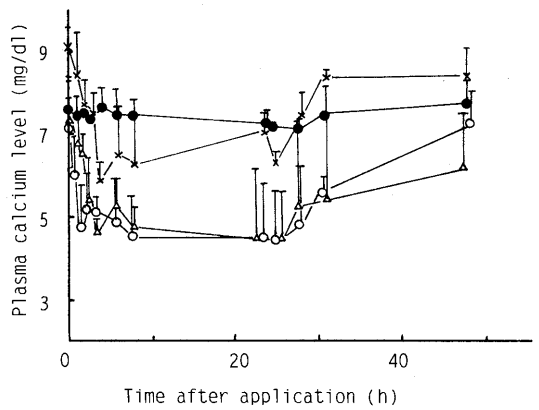

Fig. 5. Changes in EC Activity in Ointment in the Course of Time

Rp. 5 ointment was stored at 40 °C for 15 (△) and 30 d (×). ●, placebo ointment; ○, immediately after preparation.

Stability of EC in Ointment Rp. 5 ointment was stored in a polystylene microtube with a cap at 40 °C for 15 or 30 d and then a system prepared was applied to rat. The hypocalcemic effect is shown in Fig. 5. The hypocalcemic action was still as exerted after storage for 15 d as immediately after preparation, but the effect was extremely decreased after 30 days' storage.

Discussion

The p.c. absorption of peptides including calcitonin is

reported by Muranishi *et al.*[8] They estimated the effect of Azone on the *in vitro* penetration, but not *in vivo*, and show that the enhancer increases the absorption of calcitonin.[8] To date, however no quantitative data are available concerning the p.c. absorption of EC.

The lower limit for molecular weight for which p.c. absorption becomes a limiting factor is assumed to be 5000.[13] But the quantities of compounds in the skin expressed as moles exhibit a disproportionate decrease with increasing molecular weight.[13] Since the molecular weight of EC is 3363.8,[9] it is assumed that EC may be partly absorbed through the skin. Consequently, the assumption was clearly demonstrated by our experiments using absorption promoters.

It now seems that the dominant path for polar molecules is the polar region of the intercellular lipid (the intercellular route) in the stratum corneum and the appendages, *e.g.* the hair follicles and the sweat ducts (the shunt route).[14] At short times, the flux through the shunts is much larger than that through the stratum corneum.[14] The relatively shorter lag time, observed in this experiment (Figs. 3 and 4), suggests the transport of EC, at least partly, through the routes. The diffusional resistance of the stratum corneum is reduced when the skin is occluded, due to the existence of free water[15] and pathways develop in the stratum corneum in which water molecules diffuse more easily.[16] Many absorption enhancers will interact with the polar head groups of the lipid *via* hydrogen bonding and ionic interactions.[17,18] The consequent disturbance of the lipids and alterations in head group interactions will upset the packing at the head region.[17] OG, OTG and bile salts might also interact with the head groups. These enhancers used thus might increase the volume of the aqueous layer so that more water enters the tissue. This swelling provides a greater cross-sectional area for polar diffusion and a larger fractional volume of free water. Consequently, the major absorption pathway of EC would be *via* shunt routes and intercellular channels.

Below the stratum corneum is the viable epidermal layer, the most metabolically active layer in skin.[19,20] Metabolism, being mainly hydrolysis, of EC may reduce the amount of drug systemically available and pharmacologic activity. The high hypocalcemic activity after p.c. administration of EC indicated that the additives such as bile salts might largely inhibit the hydrolytic enzyme activity in the viable tissues. It is shown that bile salts significantly inhibit the degradation of human calcitonin in oral mucosa homogenate, thus suggesting the inhibition of peptidases in the mucosa.[7] Therefore, bile salts used would act as the absorption enhancer and protease inhibitor in this study.

When taurocholate was used in combination with OTG, they showed an apparently additive effect on p.c. absorption of EC (Table II), although the conclusive evidence must await further studies, *e.g.* the direct determination of the peptide in serum. Our results suggest that taurocholate probably increased skin permeability by a different mechanism than that for OTG.

The bioavailability, calculated based on the *AUC* of 40 U/rat (i.v.), of EC following p.c. application of system 5 was 4.62%. This value was much more than that (0.8%) after rectal administration in rats, and the hypocalcemic effect was maintained much longer than in the rectal administration.[4] As a result, the transdermal system of EC has the potential to be an efficient drug delivery system. System 4, containing gabexate, did not produce a significant effect. A possible mechanism involved in the decreased effect is unclear. However, a likely explanation is that the protease inhibitor might not penetrate through the cell membrane, owing to the highly water-soluble property, and therefore EC penetrated into viable skin might be partly hydrolyzed by the proteases.

The reason why the ability to lower serum calcium levels was not proportional to the doses (40 and 80 U/rat) may be that the doses used were much larger than the dose for the adequate response (*e.g.* 10 or 40 U/man, twice weekly), and thus the ability to lower the levels attained nearly a maximum at these doses. Yamaguchi *et al.* report that bone calcium content is increased significantly by the presence of 10 and 100 ng EC/ml in the *in vitro* experiment, but the increased extent is not proportional to the doses.[21]

When the hypocalcemic effect was compared with that after the i.v. injection of EC (40 or 80 U/rat), the administration by p.c. route showed an equivalent effect to the i.v. injection, although a much higher dose of EC was required in the p.c. dosing. The hypocalcemic effect after p.c. administration may be maintained over a more prolonged period, if the system is applied more than a day.

The study on changes of EC activity in the system in the course of time revealed a significant decrease in the hypocalcemic effect after 30 days' storage at 40 °C, but not after 15 d. This may be mainly due to the decline in the antibacterial activity of gentamycin (10 mg/100 g ointment) added as an antiseptic. If a more effective antiseptic is used, the changes would probably be prevented.

These systems produced no erythema and no edema during application for 24 h. Therefore, these systems appear not to have irritant effects on the skin. The negligible irritant effect may make the formulation acceptable for clinical use.

In conclusion, the present results lead us to postulate that the drug delivery system of EC gave a constant decrease in plasma calcium levels over a prolonged period. The transdermal system has the potential to be an efficient drug delivery system for Paget's disease and osteoporosis. Our data present an evidence of p.c. absorption of peptide, EC.

References

1) J. C. Stevenson and I. M. A. Evans, *Drugs*, **21**, 257 (1981).
2) M. E. Holtrop, L. G. Raisz and H. A. Simmons, *J. Cell Biol.*, **60**, 346 (1974).
3) J. R. Farley, N. M. Tarbaux, S. L. Hall, T. A. Linkhart and D. J. Baylink, *Endocrinology*, **123**, 159 (1988).
4) K. Morimoto, H. Akatsuchi, R. Aikawa, M. Morishita and K. Morisaka, *J. Pharm. Sci.*, **73**, 1366 (1984).
5) K. Morimoto, H. Akatsuchi, K. Morisaka and A. Kamada, *J. Pharm. Pharmacol.*, **37**, 759 (1985).
6) Y. Nakada, Y. Ikuta and N. Awata, *Yakuzaigaku*, **49**, 166 (1989).
7) Y. Nakada, N. Awata, C. Nakamichi and I. Sugimoto, *Yakuzaigaku*, **47**, 217 (1987).
8) N. Yamashita, M. Murakami, H. Yoshikawa, H. Takada and M. Muranishi, Abstracts of Papers, 4th Yakuzai Gakkai, Fukuoka, September, 1988, pp. 187—188.
9) T. Morikawa, E. Munekata, S. Sakakibara, T. Noda and M. Otani, *Experientia*, **32**, 1104 (1976).
10) R. A. Upton, *J. Pharm. Sci.*, **64**, 112 (1975).
11) S. K. Bakar and S. Niazi, *J. Pharm. Sci.*, **72**, 1027 (1983).
12) K. Yamaoka, T. Nakagawa and T. Uno, *J. Pharmacokinet. Biopharm.*, **6**, 547 (1978).
13) R. C. Wester and H. I. Maibach, "Percutaneous Absorption,

Mechanisms-Methodology-Drug Delivery," ed. by R. L. Bronaugh and H. I. Maibach, Marcel Dekker Inc., New York, 1983, pp. 107—123.
14) B. W. Barry (ed.), " Dermatological Formulations, Percutaneous Absorption," Marcel Dekker Inc., New York and Basel, 1983, pp. 95—126.
15) S. A. Akhter and B. W. Barry, *J. Pharm. Pharmacol.*, **37**, 27 (1985).
16) I. H. Blank, "Percutaneous Absorption," ed. by R. L. Bronaugh and H. I. Maibach, Marcel Dekker Inc., New York and Basel, 1985, pp. 97—105.
17) B. W. Barry, "Drug Delivery Systems," ed. by P. Johnson and J. G. Lloyd-Jones, Ellis Horwood, Chichester, England, 1987, pp. 208—212.
18) B. W. Barry, *J. Controlled Release*, **6**, 85 (1987).
19) O. D. Laerum, *J. Invest. Dermatol.*, **52**, 204 (1969).
20) R. H. Chapman, M. D. Rawlins, S. Rogers and S. Shuster, *Br. J. Clin. Pharmacol.*, **4**, 393p (1977).
21) M. Yamauchi, M. Uto and R. Matsui, *J. Pharmacobio-Dyn.*, **12**, 708 (1989).

Chem. Pharm. Bull. **39**(2) 454—457 (1991) Vol. 39, No. 2

Studies on the Photolysis and Hydrolysis of Furosemide in Aqueous Solution[1)]

Naomi YAGI,* Harumi KENMOTSU, Hitoshi SEKIKAWA and Masahiko TAKADA

Faculty of Pharmaceutical Sciences, Higashi-Nippon-Gakuen University, Ishikari-Tobetsu, Hokkaido 061-02, Japan. *Received July 9, 1990*

Photolysis and hydrolysis of furosemide were studied in buffere solutions (pH between 1.2 and 12.0). Photolysis experiments were made at room temperature under a Daylight lamp® or fluorescent lamps as artificial light sources and direct and indirect sunlight as natural light sources by changing the strength of illumination. The photolysis of furosemide was found to follow apparent first-order kinetics under both artificial and natural light sources. In acidic media, the rate of photolysis of furosemide was larger than those in neutral or alkaline media. The pH-rate profile for the photolysis of furosemide indicated that the rate of photolysis of unionized furosemide was much larger than that of ionized furosemide. A hydrolysis experiment of furosemide was made at 37 °C in the darkened room. The hydrolysis of furosemide was also found to follow apparent first-order kinetics. Furosemide was stable in neutral or alkaline solutions. In acidic media below pH 3, hydrolysis of furosemide was found to be catalyzed by hydrogen ion with an acid catalyzed rate constant of 0.893 $M^{-1} \cdot h^{-1}$.

Keywords furosemide; photolysis; photodegradation; hydrolysis; pH-rate profile; HPLC assay

Furosemide, 4-chloro-*N*-furfuryl-5-sulfamoylanthranilic acid, is a potent diuretic agent of pharmacokinetic/pharmacodynamic interest in humans.[2,3)] Pharmacokinetic parameters in the literatures have varied much in different groups in spite of the development of high performance liquid chromatography (HPLC) methods for furosemide assay.[3,4)] A difference in assay methods of furosemide in biological specimens might be one of the reasons for variations, as some of the groups did not notice that furosemide was an unstable compound. Furosemide is hydrolyzed in acidic media to form 4-chloro-5-sulfamoylanthranilic acid (CSA).[5)] Extraction of furosemide into organic solvents from strongly acidified biological specimens prior to the assay was reported in several papers. In such cases, the concentration of furosemide extracted might be lower than the actual concentration. Further, CSA has been misunderstood as the metabolite of furosemide in plasma or urine. Although furosemide is recognized as a photosensitive drug, protection of the biological specimens from light has not been taken into consideration in several reports. In these cases, the concentration of furosemide might also be lower. Sekikawa *et al.*[6)] reported on the photodegradation of furosemide and furosemide glucuronide in aqueous solution under direct or indirect sunlight as light sources.

In this study, the authors made comparative studies of photodegradation and hydrolysis of furosemide in aqueous solution. Photodegradation of furosemide was made under several conditions, such as light sources, strengths of illumination, or pHs, to obtain information prior to the kinetic studies in furosemide assays.

Experimental

Materials Furosemide (lot. No. 263 D210) was supplied by Hoechst Japan Ltd., Tokyo. CSA was obtained from U.S. Pharmacopeia (Rockville, MD). Acetonitrile was HPLC grade from Wako Pure Chemicals Ind., Ltd., Osaka. Piretanide (lot No. 700 L023), supplied by Hoechst Japan, was dissolved in phosphate buffer at pH 7.4 and used as an internal standard for furosemide assay. All other chemicals were of reagent grade.

Photodegradation Studies Irradiative sources employed were as follows; direct (illumination; between 10000 and 30000 lux) and indirect sunlight (illumination; between 75 and 8000 lux) were used as natural light sources. As an artificial light source, Daylight lamp® D400[7)] with the stabilizer 4MT-105H-AE (400 W, Toshiba Electric Co., Ltd., Tokyo) was used in the darkened room. The maximun relative intensity was found to be around 500 nm. The strength of the illumination was controlled by changing the distances of the samples from the lamp. The Daylight lamp® was stabilized enough prior to the study. "Fluorescent lightings" referred to setting the test solutions on a bench in the dark about 1.4 m below naked fluorescent lamps (40 W × 2, 340 ± 20 lux, white type, Mitsubishi, Tokyo) as artificial light sources. The strengths of illumination were measured using a lux meter of Maris® (A-BS type, Tokyo Maekawa Science Co., Japan).

Furosemide was dissolved in redistilled water containing a small volume of 0.1 N NaOH, and the solution was used as a stock solution (100 μg/ml). A test solution (10 μg/ml) was made by dilution with buffer solutions of various pHs (pH 1.2—12.0). The buffer systems used ($\mu = 0.2$) were pH 1.2—2, 0.2 M KCl–0.2 M HCl; pH 3—5, 0.1 M CH_3COOH–0.1 M CH_3COONa; pH 6—9, 0.1 M KH_2PO_4–0.05 M $Na_2B_4O_7$; pH 10—12, 0.1 M NaOH–0.1 M $Na_2B_4O_7$. The test solutions were put into test tubes (15 cm × 15 mm i.d.) and light sources described above were irradiated. At appropriate time intervals, portions of the test solutions were removed and put into the test tubes, mixed with the internal standard solution, and transferred into glass inserts and assayed by HPLC for automatic assay. Temperatures were not controlled and varied between 24 ± 3 °C. All of the analytical conditions were carefully protected from light.

Hydrolysis Studies The solutions were put into light-resistant flasks, and were shaken (50 strokes/min) at 37 ± 0.1 °C in an incubator. Portions of the solutions were removed at the appropriate time and assayed as described in photodegradation studies.

Assay Procedure for Furosemide The assay procedure for furosemide was based on the previous study.[6)]

HPLC was performed on a Shim-pack CLC-ODS, with a 5 μm reversed-phase column (150 × 6 mm i.d.) and a Shim-pack CLC-ODS, with 30 μm guard column (50 × 2.1 mm i.d.) from Shimadzu Co., Kyoto. The columns were maintained at 40 ± 0.5 °C in the column oven (CTO-6A, Shimadzu). A fluorescence spectrophotometer Model RF-535 (Shimadzu) was used as a detector. Excitation and emission wave lengths, respectively, were 345 and 415 nm. The mobile phase used was 40% acetonitrile containing phosphoric acid (0.1%, pH 3.5). The flow rate was 1.0 ml/min. Samples were automatically injected onto HPLC using a SIL-6A auto injector (Shimadzu) and a LC-6A pump (Shimadzu) with a run time of 12 min using a SCL-6A system controller (Shimadzu). A C-R6A computing injector (Shimadzu) was used to obtain the area of the peaks of the chromatogram. In the chromatogram, peaks of furosemide and an internal standard were observed at 6.0 and 9.6 min, respectively.

Identification of Photodegradation Product After the irradiation of indirect sunlight to furosemide aqueous suspension, the major photodegradation product was separated using an Intersil PREP-ODS, 10 μm column (20.0 × 250 mm i.d.) from Gasukuro Kogyo Inc. The mobile phase was 40% acetonitrile containing acetic acid (0.3%, pH 4.0). The flow rate was 3.0 ml/min. The elute of the fraction was collected. Acetonitrile in the elute was removed *in vacuo*. The organic phase was washed with water after the solution was extracted into ethylacetate. Then ethylacetate was evaporated *in vacuo* using a rotary evaporator at 40 °C. The molecular weight of the residue was determined by a GCMS 9100-MK (Shimadzu) and a GCMSPAC 1500 (Shimadzu) mass data system. Proton nuclear magnetic resonance (^{1}H-NMR) spectrum [$CD_3OD + CD_3COCD_3$ (δ)]: 8.37 (1H, s), 7.49 (1H, m), 6.32—6.42 (3H, m), 4.48 (2H, s). FAB-MS

m/z: 313 ($M^+ + 1$).

Results and Discussion

Photodegradation Studies Figure 1 shows the time course of the photodegradation of furosemide with different lights at pH 5. The degradation of furosemide was found to follow apparent first-order kinetics. Under the direct sunlight (20000 lux) and indirect sunlight (1600 lux), half-lives ($t_{1/2}$) were about 18 and 290 min, respectively. These results indicate the possible loss of furosemide in solution if the sample is not protected from natural light sources in daytime.

The use of curtains or window shades may be one of the ways to protect the sample solutions from natural light sources. Figure 1 also shows the effects of plastic window shades on the photodegradation of furosemide. Using plastic window shades on a sunny day (220 ± 30 lux) and a cloudy day (75 ± 25 lux), the apparent first-order rate constants for the degradation were 3.60×10^{-2} and $3.20 \times 10^{-3}\,h^{-1}$, respectively. The results show that the apparent reductions in the degradation of furosemide were made by the window shades, however, significant decreases of the concentration of furosemide were observed within the experimental period. The apparent degradation rate constant was $5.12 \times 10^{-3}\,h^{-1}$ when fluorescent lightings (340 ± 20 lux) were used. The half-life of the degradation was 135 h. This value was much larger than that reported by Kerremans *et al.* (5 h)[8] though the experimental conditions were different. Sekikawa *et al.*[6] found no degradation of furosemide at pH 5 by irradiation of fluorescent lights covered with a translucent plastic frame (260 lux) for 4 h. The plastic frame might cut the light at wave lengths that caused the photodegradation of furosemide. The results suggested that the effect of irradiation on the photodegradation was not due to the illumination but to the wave lengths contained in the light sources.

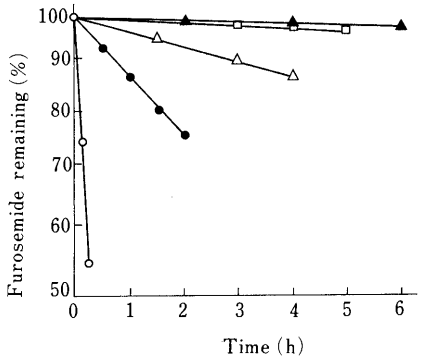

Fig. 1. Apparent First-Order Plots for the Photolysis of Furosemide at pH 5.0 with Different Light Sources

○, direct sunlight (20000 ± 1000 lux); ●, indirect sunlight (1600 ± 200 lux); △, indirect sunlight shut off by a plastic window shade on a sunny day (220 ± 30 lux); ▲, indirect sunlight shut off by a plastic window shade on a cloudy day (75 ± 25 lux); □, fluorescent lamp (340 ± 20 lux). Each point represents the mean of four determinations. All standard deviations were within 3%.

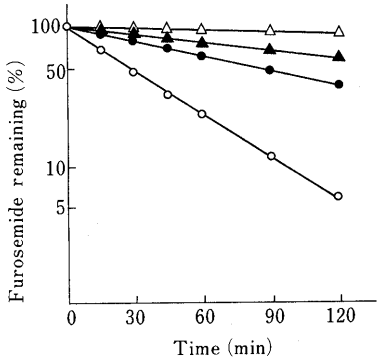

Fig. 2. Apparent First-Order Plots for the Photolysis of Furosemide under Indirect Sunlight (3500 ± 300 lux)

○, pH 1.2; ●, pH 4.0; △, pH 6.0; ▲, pH 12.0.

Figure 2 shows the time course of the photodegradation of furosemide in solutions with different pHs (pH 1.2—12.0) under indirect sunlight (3500 ± 300 lux). The photodegradation of furosemide in all solutions was found to follow apparent first-order kinetics. Degradation rates of furosemide in acidic regions were much larger than those in neutral and alkaline solutions. This tendency was in agreement with the result by Bundgaard *et al.*[9] although they did not indicate the illumination value when furosemide solutions were exposed to normal laboratory light (furosemide solutions in test tubes were placed beside the laboratory window) or diffused daylight (furosemide solutions in test tubes were placed on a laboratory table in normal laboratory light and with diffused daylight entering the room from the window). The half-lives of the degradation at pHs 5, 6 and 7 were 4.2, 6.8 and 11 h, respectively. The pH of urine from a normal subject ranges between 5 and 8. A range between 2000 and 4000 lux is considered to be the usual lighting conditions in the laboratory in daytime without any care taken to alter the lighting conditions. In these cases, 5% of the concentration will be lost within 20 min.

Furosemide glucuronide is the major metabolite excreted in human urine. For the assay of furosemide and furosemide glucuronide simultaneously, urine must be acidified appropriately to prevent the intramolecular acyl migration of furosemide glucuronide.[10] In such cases, a rapid photodegradation of furosemide ($t_{1/2}$ was about 30 min at pH 3, 3500 ± 300 lux) might be noticed.

Using sunlight as the light source is important for photodegradation studies of drugs, because it provides information about the degradation rates of drugs naturally occurring in the laboratory, the rooms for collection of biological specimens or the rooms for analysis. However, interday and intraday variations of the illumination are considerably large, and the experimental time periods are limited. In studies of the photodegradation of drugs; fluorescent lights, mercury lamps or other artificial lamps were utilized as the light sources. In this study, the authors used a Daylight lamp® as the light source. The wave lengths of the light from the Daylight lamp® developed by Toshiba Electronics are similar to those of sunlight. The spectral radiation energy of the Daylight lamp® was reported by Matsuda and Masahara.[7]

Figure 3 shows the time course the photodegradation of furosemide in solutions of different pHs under irradiation of the Daylight lamp® (10000 lux). The illumination was constant during the study. A similar tendency to those observed in the photodegradation study of furosemide under indirect sunlight (Fig. 2) was obtained. In the acidic region at pHs 1.2, 2 and 3, rapid degradation was obtained. In the neutral region at pHs 6, 7, 8 and 9, the degradation

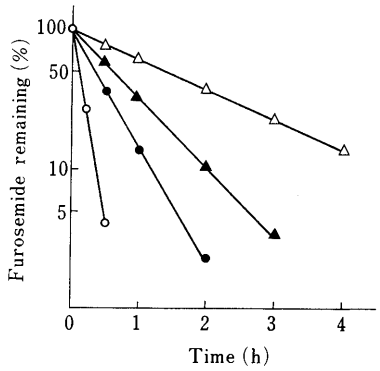

Fig. 3. Apparent First-Order Plots for the Photolysis of Furosemide under the Daylight Lamp® (10000±500 lux)

Symbols are same as Fig. 2.

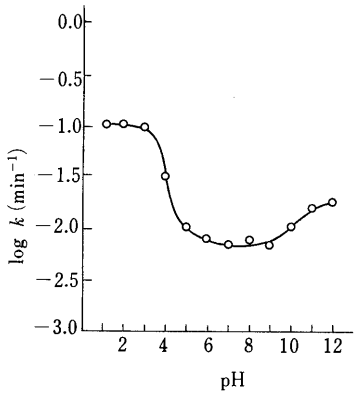

Fig. 4. pH-Rate Profile for the Photolysis of Furosemide under the Daylight Lamp® (10000±500 lux)

rate constants were smaller than those obtained in the acidic region. The degradation rate constants obtained in the neutral region had similar values. The pH-rate profile is shown in Fig. 4. The pK_a of furosemide is 3.8.[11] At lower pHs 1.2, 2 and 3, the molecule of furosemide exists mostly unionized. At pHs 6, 7, 8 and 9, the molecule of furosemide exists mostly ionized. The result indicates that the photodegradation rate constants of unionized furosemide are about ten times larger than those of the ionized form. At higher pHs (pH 10—12), photodegradation rate constants larger than those at neutral pHs were obtained. Rowbotham *et al.*[5] reported on the photodegradation of furosemide in solution after irradiation by ultraviolet light. They found a degradation product in alkaline solution as 4-chloro-5-sulphoanthranilic acid. Moore *et al.*[12,13] estimated a chlorine ion after irradiation of furosemide with ultraviolet light and some chlorine-containing drugs in aqueous or methanol solution. They suggested that these drugs correlated with their abilities to photosensitive oxidation by the free radical reaction. We ascertained the photodegradation product by fast atom bombardment mass spectrum (FAB-MS) and ^{1}H-NMR spectrum described above. From these results the major photodegradation product was determined to be 4-hydroxy-*N*-furfuryl-5-sulfamoylanthranilic acid (HFSA). Chart 1 shows the structure of the photodegradation product. Sekikawa *et al.*[6] reported on the photodegradation of furosemide in aqueous solution. By the photodegradation of furosemide, the first product (HFSA) was found. After that, several peaks in the

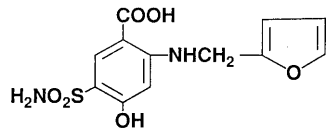

Chart 1. Structure of Photodegradation Product of Furosemide

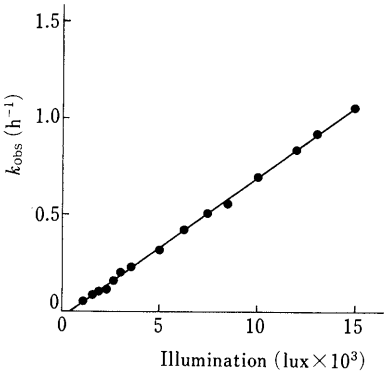

Fig. 5. Apparent First-Order Rate Constant of the Photodegradation of Furosemide and Illumination by the Daylight Lamp®

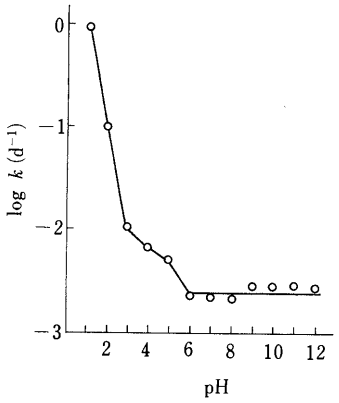

Fig. 6. pH-Rate Profile for the Hydrolysis of Furosemide at 37 °C

HPLC chromatogram were observed after the photodegradation of HFSA. Further study concerning the identification of these photodegradation products may clarify the total degradation process of furosemide in a solution with different pHs.

Figure 5 shows the relation between the rate constants of the photodegradation of furosemide at pH 5 and the strength of illumination by the Daylight lamp®. Good correlation was observed between the illumination and the rate constants of photodegradation with $Y=7.20\times10^{-5}X-0.027$, $r=0.9989$. The result indicated that the rate constants of photodegradation were proportional to the strength of illumination, if the light source was the same.

When the light source was sunlight, however, such a proportional relation was not observed. Distribution of the wave lengths contained in direct or indirect sunlight might be different with different conditions.

Hydrolysis Studies Hydrolysis of furosemide was found to follow apparent first-order kinetics. Figure 6 shows the pH-rate profile for the hydrolysis of furosemide at 37 °C. Similar studies were reported by Cruz *et al.*[14] or Bundgaard *et al.*[9] From Fig. 6, the apparent rate constant of hydrolysis may be described by:

$$k_{obs}=k_{H^+}[H^+]+k_{H_2O} \quad (1)$$

where k_{obs} is the apparent degradation rate constant, k_{H^+} is the specific acid catalytic rate constant and k_{H_2O} is the rate constant by water molecule. In the acidic pH region below 3, where the furosemide molecule is mostly unionized, the contribution of k_{H_2O} is considerably small, and the slope of the pH-rate profile indicated specific hydrogen ion catalysis. In this region, the pH-rate profile may be described approximately by:

$$k_{obs}=k_{H^+}[H^+] \quad (2)$$

or

$$\log k_{obs}=\log k_{H^+}-\mathrm{pH} \quad (3)$$

According to Eq. 3, the slope was -1.15 with an intercept ($\log k_{H^+}$) of 1.33 ($k_{H^+}=0.893\,\mathrm{M}^{-1}\cdot\mathrm{h}^{-1}$).

By these parameters, the half-life of furosemide at pH 1.0 and 37 °C may be calculated as 7.76 h. Cruz *et al.*[14] and Bundgaard *et al.*[9] calculated the half-life at pH 1.0 and 37 °C as 2.97 and 17.2 h, respectively. The value of our result was almost intermediate compared to these workers. Cruz *et al.*[14] calculated this half-life by extrapolation from the rate constants of hydrolysis obtained between 60 and 80 °C. Probably, at those temperatures, actual concentrations of hydrogen ion presented in the solution might be different from those at room temperature at which buffer solutions were prepared.

Under those conditions, furosemide would hydrolyze to an extent of approximately 4, 0.4 and 0.04% if it remained at pHs 1.2, 2 and 3 for 1 h at 37 °C, respectively. Sekikawa *et al.*[6] found furosemide and furosemide glucuronide in urine and plasma after the oral administration of furosemide tablets and intravenous administration of furosemide in ten male subjects. They also found no detectable CSA in any of the urine or plasma samples. Furosemide is practically insoluble in water. After the disintegration of the tablet in the stomach, furosemide may not dissolve rapidly. The furosemide fraction that would hydrolyze during passing through the stomach may be very little. Thus, the hydrolysis of furosemide would be negligible under physiological conditions in the stomach.

Between pHs 3 and 6, the slope was not -1 because the molecule of furosemide is partially ionized. Above pH 6, the furosemide molecule present may be mostly ionized. In this region, the contribution of k_{H^+} is negligible and the rate constant of the hydrolysis of ionized furosemide may be described approximately as:

$$k_{obs}=k_{H_2O} \quad (4)$$

Due to the difference of the component of the buffer solution, the values of k_{H_2O} were between $2.5\times10^{-3}\,\mathrm{d}^{-1}$ (KH_2PO_4–$Na_2B_4O_7$ system) and $3.1\times10^{-3}\,\mathrm{d}^{-1}$ (NaOH–$Na_2B_4O_7$ system).

In some reports,[15–18] CSA was considered to be one of the photodegradation products. During the photodegradation study, CSA was not detectable in the HPLC chromatogram even when the pH of the solution was 1.2 under indirect sunlight (3200 to 3800 lux) or direct sunlight (20000 to 25000 lux). The rate constants of photodegradation were much larger than that of hydrolysis at room temperature ($k_{obs}=174\times10^{-3}\,\mathrm{d}^{-1}$, pH 1.2, and 23 ± 0.5 °C).

Concentrated hydrochloric acid was used to acidify the biological specimen prior to the organic solvent extraction. In such a case, the pH of the solution might decrease below 1. CSA might be produced as the artifact during the assay.[19] However, CSA could not be the photodegradation product.

For the assay of furosemide in biological specimens, sufficient care must be taken during the collection, storage or analysis of biological specimens to protect the photodegradation of furosemide and its metabolite, glucuronic acid conjugate, which was more photosensitive than furosemide.[3,6]

Acknowledgment We are deeply grateful to Dr. Akiyo Sakushima for his helpful suggestions concerning the confirmation of the photodegradation product. Thanks are also given to Mr. Koji Matsubara, Hideki Matsumoto and Katsuhiko Oda for their assistance in the experimental work.

References

1) A part of this study was presented at the 107th Annual Meeting of the Pharmaceutical Society of Japan, Kyoto, April, 1987.
2) L. Z. Benet, *J. Pharmacokinet. Biopharm.*, **7**, 1 (1979).
3) M. Hammarlund and L. Z. Benet, *J. Pharmacokinet. Biopharm.*, **17**, 1 (1989).
4) E. S. Waller, S. F. Hamilton, J. W. Massarella, M. A. Sharanevych, R. V. Smith, G. J. Yakatan and J. T. Doluisio, *J. Pharm. Sci.*, **71**, 1105 (1982).
5) P. C. Rowbotham, J. B. Stanford and J. K. Sugden, *Pharm. Acta Helv.*, **51**, 304 (1976).
6) H. Sekikawa, E. T. Lin and L. Z. Benet, *Pharmaceut. Res.*, submitted.
7) Y. Matsuda and R. Masahara, *Yakugaku Zasshi*, **100**, 953 (1980).
8) A. L. M. Kerremans, Y. Tan, C. A. M. Van Ginneken and F. W. J. Gribnau, *J. Chromatogr.*, **229**, 129 (1982).
9) H. Bundgaard, T. Nørgaard and N. M. Nielsen, *Int. J. Pharm.*, **42**, 217 (1988).
10) H. Sekikawa, T. Mizuma, E. T. Lin and L. Z. Benet, *Pharmaceut. Res.*, submitted.
11) Y. Orita, A. Ando, S. Urakabe and H. Abe, *Arzneim.-Forsch.*, **26**, 11 (1976).
12) D. E. Moore and S. R. Tamat, *J. Pharm. Pharmacol.*, **32**, 172 (1980).
13) D. E. Moore and V. Sithipitaks, *J. Pharm. Pharmacol.*, **35**, 489 (1983).
14) J. E. Cruz, D. D. Maness and G. J. Yakatan, *Int. J. Pharm.*, **2**, 275 (1979).
15) I. Steiness, J. Christiansen and E. Steiness, *J. Chromatogr.*, **164**, 241 (1979).
16) J. M. Neil, A. F. Fell and G. Smith, *Int. J. Pharm.*, **22**, 105 (1984).
17) J. Szemán, Á. Stadler-Szöke, M. Vikmon and J. Szejtli, "Chromatography," H. Kalász and L. S. Ettre, Ed., Akadémiai Kiadó, Budapest, 1986, p. 323.
18) A. M. Yahya, J. C. McElnay and P. F. D'Arcy, *Int. J. Pharm.*, **31**, 65 (1986).
19) D. E. Smith, E. T. Lin and L. Z. Benet, *Drug Metab. Dispos.*, **8**, 337 (1980).

Chem. Pharm. Bull. **39**(2) 458—464 (1991) Vol. 39, No. 2

Controlled Release of 5-Fluoro-2′-deoxyuridine by the Combination of Prodrug and Polymer Matrix

Hirotaka ENDOH, Takeo KAWAGUCHI,* Toshinobu SEKI, Tetsuya HASEGAWA and Kazuhiko JUNI

Faculty of Pharmaceutical Sciences, Josai University, 1–1 Keyakidai, Sakado, Saitama 350–02, Japan. *Received July 13, 1990*

Poly(L-lactic acid) (L-PLA) microspheres containing 5-fluoro-2′-deoxyuridine (FUdR) or its ester prodrugs with saturated aliphatic acids (FUdR-C*n*, *n*=2, 3, 4, 5, 6, 8, 10 and 12) were prepared. The physicochemical and biological properties and antitumor activity of the L-PLA microspheres were studied. The lipophilicity of FUdR-C*n* was increased by prolonging its acyl-promoieties. FUdR-C5, FUdR-C6, FUdR-C8, FUdR-C10 and FUdR-C12 showed almost complete incorporation into the microspheres, while incorporation of hydrophilic FUdR and FUdR-C2 was poor. The sustained release of FUdR from the microspheres containing FUdR-C4, FUdR-C5 and FUdR-C6 was obtained in the presence of esterase, and higher antitumor activity against P388 leukemia was observed *in vivo*. On the other hand, the release rates of FUdR from the microspheres containing FUdR-C10 and FUdR-C12 were very small, and their antitumor activity was much smaller than that of the free prodrug suspension. Effects of the susceptibility to enzymatic hydrolysis and the physicochemical properties of prodrugs on the release profiles of FUdR from spheres were discussed.

Keywords poly(L-lactic acid); microsphere; 5-fluoro-2′-deoxyuridine; prodrug; sustained release; enzymatic hydrolysis; P388 leukemia

In cancer chemotherapy, it is important to control the pharmacokinetic behavior of antitumor drugs for effective treatment. Various approaches for delivering drugs to tumor tissues have been studied. Microspheres containing anticancer agents have been successfully employed for the treatment of carcinomas in the kidney, urinary bladder, and liver.[1] Though many biodegradable polymers such as gelatin,[2] albumin,[3] polyhydroxybutyric acid[4] and polylactic acid[5] have been investigated as matrices of the microspheres, their compatibility with anticancer agents have not always been sufficient. Many anticancer drugs, therefore, are poorly entrapped in microspheres and/or show rapid release from the spheres. Chemical modification of drug molecules in order to develop adequate physicochemical properties can be a promising approach to improving the drug's incorporation efficiency and release profiles. 5-Fluoro-2′-deoxyuridine (FUdR), one of the active metabolites of 5-fluorouracil (FU), shows as much as 100 times higher activity than FU against several tumor lines *in vitro*,[6–9] but it has been reported to be less effective than FU *in vivo*.[10,11] The reason for the low activity of FUdR in animal studies may be attributable to its rapid metabolism in the body,[12] since the cytotoxicity of FUdR is time-dependent or requires long retention *in vivo*.[13] To overcome the above problems, 3′,5′-diesters of FUdR with various acyl-moieties were synthesized,[8] and their antitumor activity,[8,14] susceptibility to enzymatic hydrolysis[15,16] and retention in mice[14] has been investigated. The esters were chemically very stable, so their hydrolysis rates depended strictly on their enzymatic reactivity.[15] Since these ester prodrugs of FUdR show a wide range of physicochemical properties, the compatibility, release profiles and antitumor activity of the microspheres containing the prodrugs are of interest. In the present study, eight 3′,5′-diester-FUdR with saturated aliphatic acids and poly(L-lactic acid) (L-PLA) were used to prepare the microspheres. The physicochemical and biological properties and the applicability of the L-PLA microspheres have been investigated.

Experimental

Materials FUdR was a gift from Yamasa Shoyu Co. (Chiba, Japan). 3′,5′-Diester-FUdR with aliphatic acid (FUdR-C*n*) was synthesized according to the procedure described by Nishizawa *et al.*[8]; acetyl (*n*=2), propionyl (*n*=3), butyryl (*n*=4), pentanoyl (*n*=5), hexanoyl (*n*=6), octanoyl (*n*=8), decanoyl (*n*=10), and dodecanoyl (*n*=12) esters of FUdR were so prepared. The compounds were identified by elemental analysis, nuclear magnetic resonance (NMR) and mass spectrum (MS). All the esters were more than 98% pure, as shown by one major peak by high-performance liquid chromatography (HPLC). L-PLA, with an average molecular weight of 6000, was supplied by Mitsui Toatsu Chemical Co. (Tokyo, Japan). Gelatin was a gift from Nitta Gelatin Co. (Osaka, Japan). Porcine liver esterase was purchased from Sigma Chemical Co. (St. Louis, Mo. U.S.A.). The esterase suspension (2600 units/ml) in 3.2 M $(NH_4)_2SO_4$ solution was diluted with 0.1 M phosphate buffer (pH 7.4) to give a final concentration of 100 units/ml; the resultant solution was then filtered though a membrane filter (0.45 μm, Toyo Roshi Co., Ltd., Tokyo). The esterase preparation was stored at 4 °C until use. Albumin (bovine) was purchased from Wako Pure Chemical Industries Ltd. (Osaka). All other chemicals were commercial reagent grade products.

Measurement of Melting Points Melting points of the drugs were determined on a Yanagimoto MPS-3 micro melting apparatus.

Measurement of Partition Coefficients Apparent partition coefficients of the drugs were determined in an *n*-octanol/0.1 M phosphate buffer system (pH 7.0) and a chloroform/0.1 M phosphate buffer system at 25 °C.

Measurements of Solubilities The solubilities of the drug in water and a saline solution containing 0.01% Tween 80 were determined by the following method. An excess amount of each drug was added to a flask filled with one of the test solvents (20 ml). The flask was immersed in a shaker bath maintained at 37 °C and shaken horizontally. After equilibrium, aliquots of the supernatant were withdrawn to determine the concentration of the drug.

Preparation of L-PLA Microspheres L-PLA microspheres were prepared by the solvent-evaporation method similar to that reported previously.[17] A weighed amount of each FUdR-C*n* (20 mg) was dissolved or dispersed (in the case of FUdR) in a 5% solution of L-PLA in methylene chloride (2 ml). The organic solution was then dispersed in a 100 ml gelatin solution (1%) under stirring at 500 rpm by means of a three-bladed propeller. The stirring was continued for 35 min at room temperature. The microspheres were collected by filtration through a glass filter (3G4, Sibata Scientific Technology Ltd., Tokyo), washed with water, and dried under reduced pressure at room temperature.

Determination of Drug Contents and Sizes of Microspheres A weighed amount of microspheres containing each FUdR-C*n* was dissolved in chloroform, and the drug concentration was determined spectrophotometrically at 268 nm. Drug contents of the microspheres (weight ratio, drug/microspheres) were then calculated. The drug content of microspheres containing FUdR was determined spectrophotometrically at 268 nm after the following extraction process. First, chloroform (2 ml) was added to a weighed amount of microspheres to dissolve the polymer. Then water (2 ml) was further added to the organic solution, which was shaken for 15 min to extract the drug. The aqueous layer was then used for the spectrophotometric determination.

The Green diameters of the microspheres were measured by an optical microscope (BH-2, Olympus Kogaku Co., Tokyo).

Release Studies Weighed amounts of microspheres in a flask were suspended in a saline solution containing 0.01% Tween 80, which works as a surfactant to complete the wetting of the spheres. The flask was immersed in a shaker bath maintained at 37 °C and shaken horizontally. At fixed time intervals, an aliquot of the solution was withdrawn and an appropriate volume of fresh medium was added to the release medium to maintain a sink condition, in which the concentration of each drug in the release medium was less than 10% of its solubility. The amount of the drug released was calculated from spectrophotometric determination of the aliquot solution at 268 nm.

Effect of Esterase and Albumin on Drug Release from Microspheres *in Vitro* In order to study the effect of esterase and albumin on drug release from microspheres *in vitro*, release studies in a 0.1 M phosphate buffer (pH 7.4) containing porcine liver esterase or albumin were carried out by the following method. Microspheres containing FUdR-C4, FUdR-C5 or FUdR-C6 were suspended in the release medium containing bovine albumin in a flask. The flask was immersed in a shaker bath maintained at 37 °C. At fixed time intervals, an aliquot of the solution was withdrawn, and an appropriate volume of fresh medium was added to the release medium to maintain the sink condition. The aliquot was subjected to an HPLC assay for both the esters and FUdR. A protein-free 0.1 M phosphate buffer (pH 7.4) was used as the release medium for the control study.

Release studies in a 0.1 M phosphate buffer (pH 7.4) containing esterase were carried out for FUdR-C4, FUdR-C5, FUdR-C6, FUdR-C8, FUdR-C10 and FUdR-C12 by the same method described above.

HPLC Assay Except for spectrophotometric determination, concentration of FUdR and FUdR-C*n* were measured by the use of an HPLC system (LC-6A, Shimadzu, Kyoto, Japan) equipped with a variable wavelength detector (SPD-6A, Shimadzu). The stationary phase was a Nucleosil $5C_{18}$ packed stainless steel column (4.6 × 250 mm, Macherey Nagel, Germany). The mobile phases were water : acetonitrile : acetic acid (95 : 5 : 0.1) for FUdR, a mixture of 0.02 M acetate buffer (pH 4.0) and methanol: (30 : 70) for FUdR-C4, (20 : 80) for FUdR-C5, (15 : 85) for FUdR-C6, (10 : 90) for FUdR-C8, (5 : 95) for FUdR-C10, and (2 : 98) for FUdR-C12, with a flow rate of 1.0 ml/min.

Evaluation of Antitumor Activity Female CDF_1 mice were purchased from Shizuoka Agricultural Cooperative Association for Laboratory Animals (Shizuoka, Japan). Five mice (weighing 20—23 g) for each group were inoculated intraperitoneally with 1×10^6 P388 leukemia cells. The drug suspension was given intraperitoneally either on day 1 only, or on days 1, 2, 3, 4 and 5 starting 24 h after the inoculation. Microspheres were also given intraperitoneally on day 1 only. The antitumor activities were indicated as *T*/*C* (%), the ratio of the mean survival time of the treated group (*T*) to that of the control group (*C*). To check side effects, the body weight of each group was measured on the day of onset and on day 5. The side effects were evaluated by the decrease in body weight from days 0—5.

Results and Discussion

Physicochemical Properties of Drugs and Microspheres Table I shows the physicochemical properties of the drugs and the microspheres containing each drug. The partition coefficients of 3′,5′-diester-FUdR in both systems increased when the alkyl chain length of acyl-promoieties was prolonged. On the other hand, FUdR showed very high hydrophilicity compared to the diesters. The solubility of the diesters in water and in a saline solution containing 0.01% Tween 80 tended to decrease with the prolongation of the alkyl chain length of acyl promoieties. But FUdR-C3 showed higher solubility compared to FUdR-C2, and FUdR-C5 also showed a higher solubility compared to FUdR-C4. The relatively higher solubility of FUdR-C3 and FUdR-C5 would be related to the low melting points of these compounds.

The drug contents in microspheres increased as a result of prolonging the alkyl chain length of acyl-promoieties of the diesters. As Bodmeier *et al.* reported,[18] the reason could be that partitioning of the drug occurred between the organic phase and the aqueous phase during the preparation process. Therefore, the successful entrapment of the prodrugs into the microspheres seems to depend on the higher lipophilicity of the prodrugs. On the other hand, the drug contents of hydrophilic drugs, such as FUdR and FUdR-C2, were very low because a large amount of the drugs were moved into the aqueous phase during the solvent-evaporation process and then removed with water during the washing step. The physicochemical properties of the drugs had little influence on the diameter of the microspheres containing the drugs. The average diameter of the microspheres was about 100 μm.

Drug Release from the Microspheres Figure 1 shows the release profiles of FUdR and diester-FUdR in a saline solution containing 0.01% Tween 80 from the microspheres.

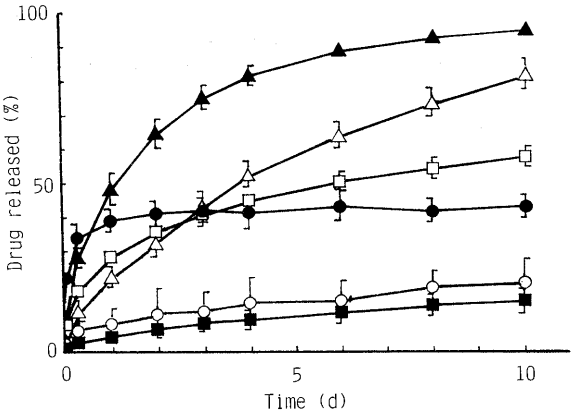

Fig. 1. Release Profiles of Drug from the Microspheres in Saline Containing 0.01% Tween 80

●, FUdR; ○, FUdR-C2; ■, FUdR-C3; □, FUdR-C4; ▲, FUdR-C5; △, FUdR-C6. Each value represents the mean ± S.D. ($n = 3$). In each case of microspheres containing the prodrug, the prodrug itself was determined.

TABLE I. Physicochemical Properties of the Drugs and the Microspheres

Compd.	mp (°C)	Partition coefficient		Solubility (μg/ml)		Diameter of sphere (μm)[d]	Drug content (%)
		log P[a]	log P[b]	Water	Saline[c]		
FUdR	150	−1.53	−3.89	>70000	>70000	85±46	0.45
FUdR-C2	152	−0.34	1.02	3900	4300	79±34	0.17
FUdR-C3	77	0.79	2.26	5700	5100	113±45	1.60
FUdR-C4	117	1.90	3.49	100	95	101±45	9.83
FUdR-C5	59	2.72	4.19	140	115	118±39	14.2
FUdR-C6	38	4.25	5.34	20	—	104±36	15.4
FUdR-C8	Oil	6.05	5.85	1.7×10^{-2}	—	97±59	16.5
FUdR-C10	34	—	—	3.5×10^{-4}	—	108±54	15.8
FUdR-C12	63	—	—	—	—	102±50	15.9

a) *n*-Octanol: 0.1 M phosphate buffer (pH 7.0). *b*) Chloroform: 0.1 M phosphate buffer (pH 7.0). *c*) Saline containing 0.01% Tween 80. *d*) Mean ± S.D.

In the microspheres containing FUdR, the release of the drug was very slow after an initial burst. The release rates of FUdR-C2 or FUdR-C3 from their microspheres were very small, and only 10 to 30% of each drug was released during 10 d. On the other hand, the release of FUdR-C4, FUdR-C5 and FUdR-C6 from each of their microspheres was more rapid than those of FUdR-C2 and FUdR-C3. The comparative release rates were FUdR-C4 < FUdR-C6 < FUdR-C5. We reported previously that the lower the drug content in the microspheres, the slower the drug release.[19] The slow release rates of FUdR-C2 and FUdR-C3 from the spheres, though their solubility was high, would be attributable to their low drug content in the spheres. No structural changes in the microspheres' surface containing FUdR-C6 were observed after the release study in the scope of a scanning electron microscope (SEM; Type S-430, Hitachi, Tokyo) (Fig. 2). In all other microspheres, structural changes in the surface were not observed.

Effect of Esterase and Albumin on Drug Release We reported previously on the mechanism of the *in vitro* drug release from L-PLA microspheres containing diester-FUdR.[19] In the paper, we concluded that the dispersed drug in the microspheres would dissolve in an aqueous medium which had penetrated through pores formed within the microspheres, and would pass through the pores to an external medium.

Considering the above mechanism of *in vitro* drug release from the microspheres, we expected that drug release from the microspheres is influenced by various species existing in the release medium (*i.e.* enzyme, proteins and other surface-

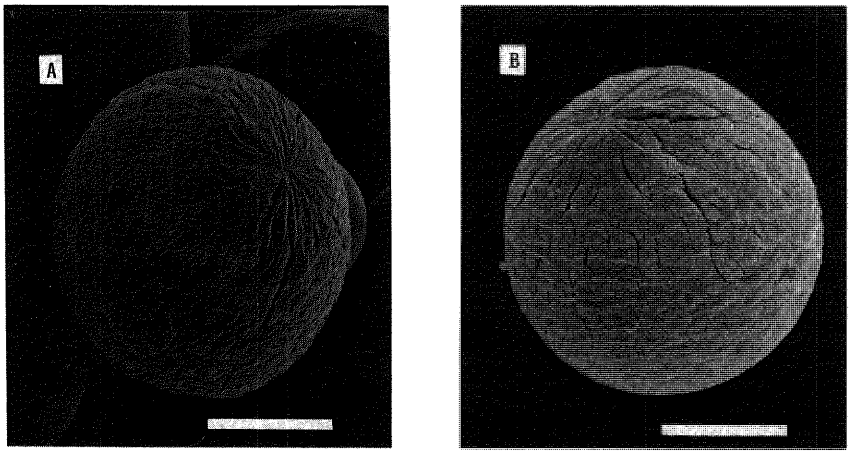

Fig. 2. Scanning Electron Photomicrographs of Microspheres Containing FUdR-C6 before and after Drug Release
A, before; B, after, Bar = 50 μm.

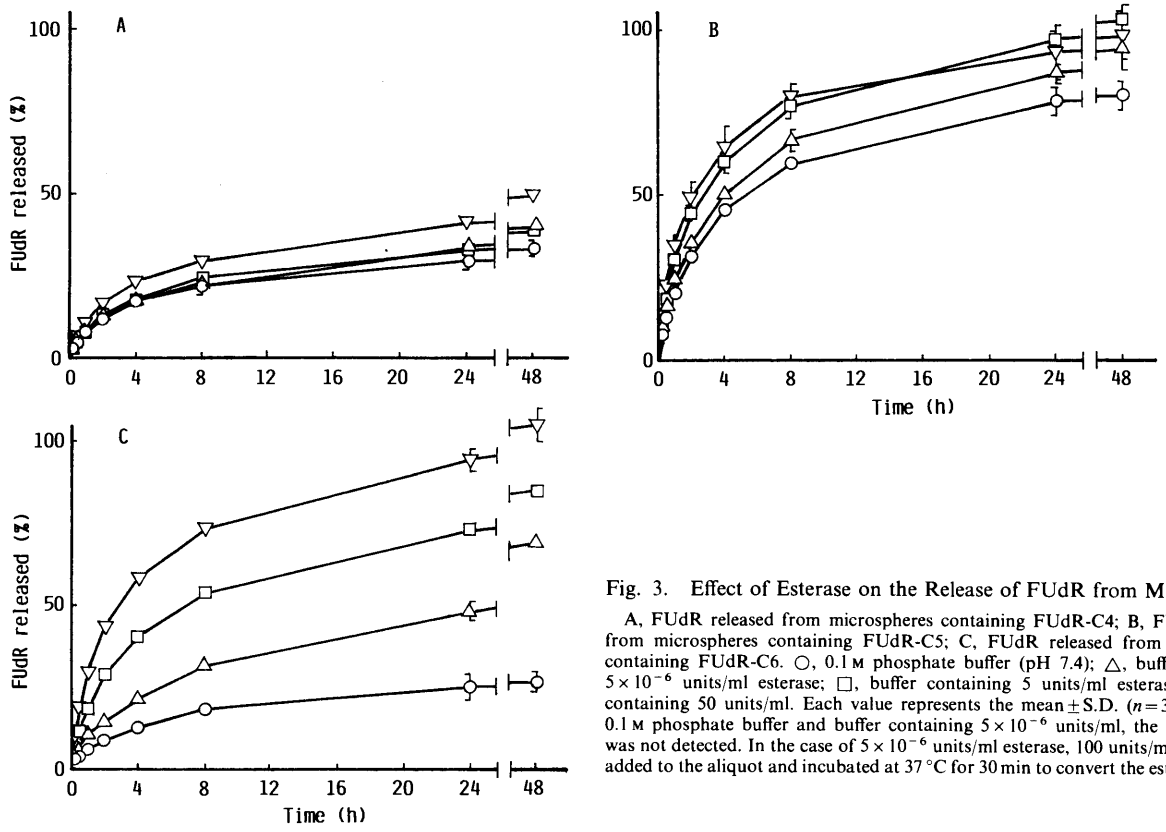

Fig. 3. Effect of Esterase on the Release of FUdR from Microspheres
A, FUdR released from microspheres containing FUdR-C4; B, FUdR released from microspheres containing FUdR-C5; C, FUdR released from microspheres containing FUdR-C6. ○, 0.1 M phosphate buffer (pH 7.4); △, buffer containing 5×10^{-6} units/ml esterase; □, buffer containing 5 units/ml esterase; ▽, buffer containing 50 units/ml. Each value represents the mean ± S.D. ($n = 3$). Except for 0.1 M phosphate buffer and buffer containing 5×10^{-6} units/ml, the prodrug itself was not detected. In the case of 5×10^{-6} units/ml esterase, 100 units/ml esterase was added to the aliquot and incubated at 37 °C for 30 min to convert the esters to FUdR.

active materials), so that release patterns of the drug from microspheres may differ from those *in vivo*. Therefore, in order to study the influence of body fluid components on the drug release from the microspheres *in vitro*, porcine liver esterase, an ubiquitous enzyme involved in the body's catalyzing the hydrolysis of diester-FUdR, to FUdR and albumin, which is expected to act as a surfactant, were selected as additives for these experiments.

The effects of esterase on the drug release from the microspheres containing FUdR-C4, FUdR-C5 or FUdR-

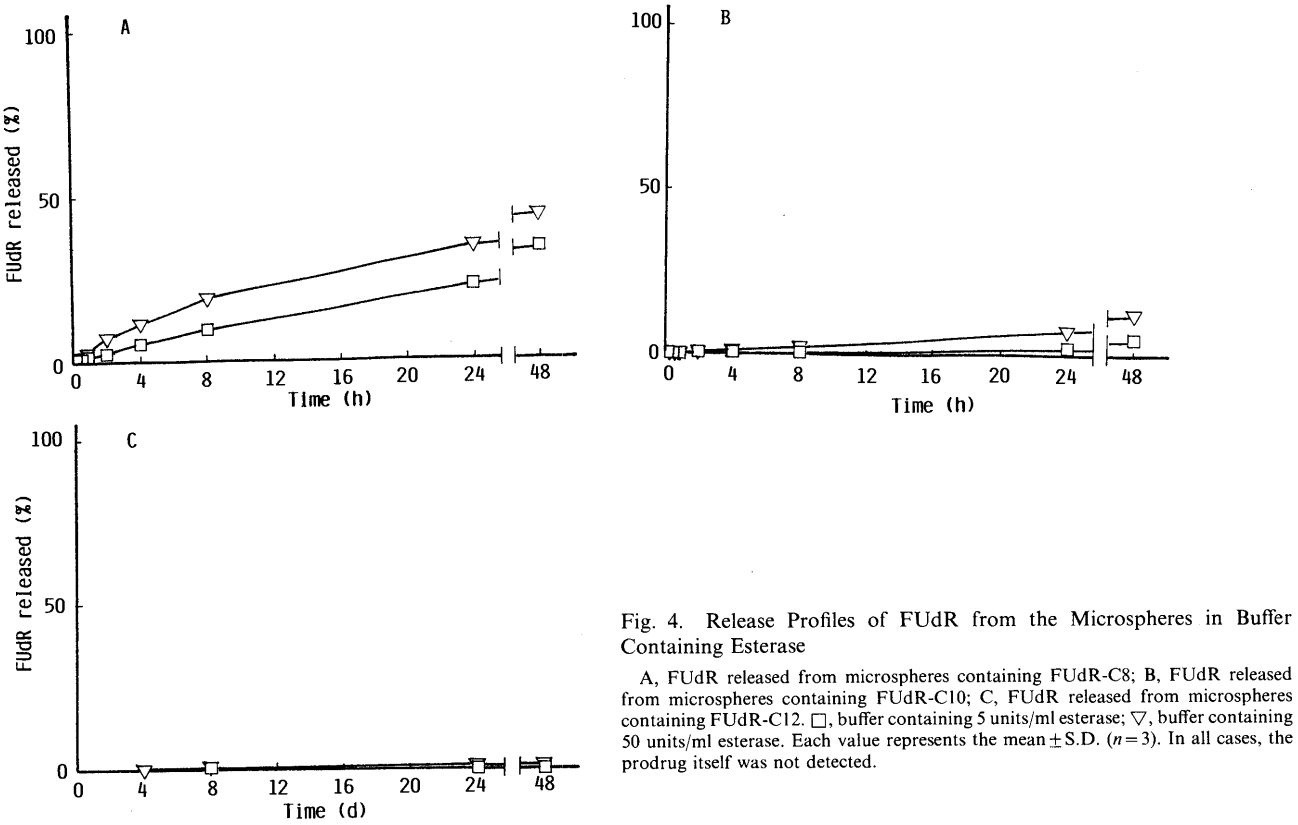

Fig. 4. Release Profiles of FUdR from the Microspheres in Buffer Containing Esterase

A, FUdR released from microspheres containing FUdR-C8; B, FUdR released from microspheres containing FUdR-C10; C, FUdR released from microspheres containing FUdR-C12. □, buffer containing 5 units/ml esterase; ▽, buffer containing 50 units/ml esterase. Each value represents the mean ± S.D. ($n=3$). In all cases, the prodrug itself was not detected.

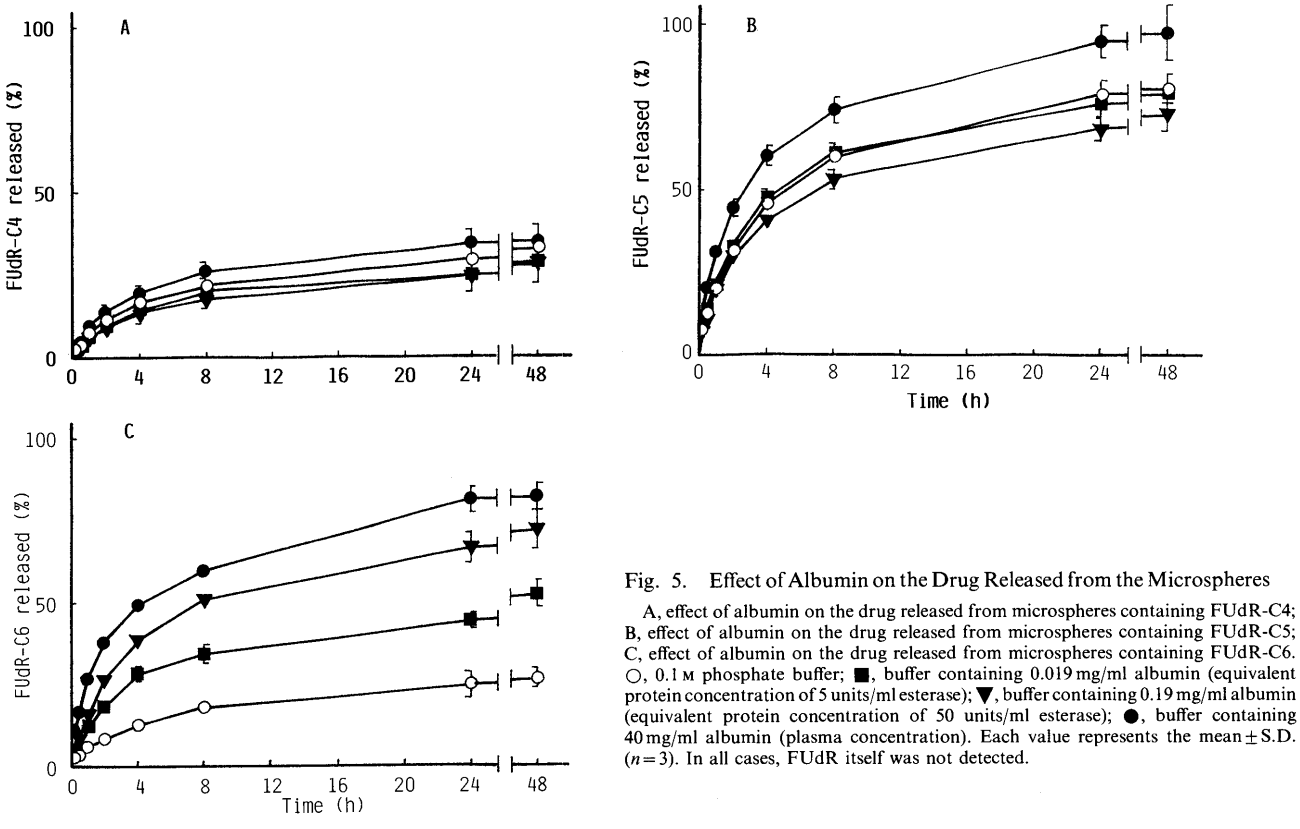

Fig. 5. Effect of Albumin on the Drug Released from the Microspheres

A, effect of albumin on the drug released from microspheres containing FUdR-C4; B, effect of albumin on the drug released from microspheres containing FUdR-C5; C, effect of albumin on the drug released from microspheres containing FUdR-C6. ○, 0.1 M phosphate buffer; ■, buffer containing 0.019 mg/ml albumin (equivalent protein concentration of 5 units/ml esterase); ▼, buffer containing 0.19 mg/ml albumin (equivalent protein concentration of 50 units/ml esterase); ●, buffer containing 40 mg/ml albumin (plasma concentration). Each value represents the mean ± S.D. ($n=3$). In all cases, FUdR itself was not detected.

C6 are shown in Fig. 3. Although the release study for microspheres containing FUdR-C8, FUdR-C10 or FUdR-C12 could not be carried out because of their very low solubility in saline, the release in the presence of esterase could be carried out because the lipophilic prodrugs were converted to hydrophilic FUdR by enzymatic hydrolysis, and the results are shown in Fig. 4. In the case of the microspheres containing FUdR-C6, it is evident that the greater the concentration of esterase in the release medium, the more rapidly the drug is released. On the other hand, the effect on drug release from microspheres containing FUdR-C5, FUdR-C8 and FUdR-C10 was smaller than those of FUdR-C6. The release enhancing effect of the esterase was not evident in microspheres containing FUdR-C4 and FUdR-C12. The enhancing effect of esterase on drug release from the microspheres containing diester-FUdR may be related to their reactivity to porcine liver esterase, because insoluble diester-FUdR would be converted to very soluble FUdR by the enzymatic hydrolysis during the drug release process from the microspheres. As reported previously,[15] the reactivity of diester-FUdR to porcine liver esterase increased as the acyl chains were lengthened up to dioctanoyl (-C8), but a further increase in the acyl chain length resulted in a sharp decrease in reactivity. Therefore, a larger enhancing effect by esterase could be observed in the highly reactive FUdR-C6 and FUdR-C8, and the effect of esterase on the drug release from microspheres was small in the less reactive FUdR-C10 and FUdR-C12. Although the reactivity of FUdR-C8 to porcine liver esterase was higher than that of FUdR-C6, the release of FUdR-C8 from the microspheres was slower than that of FUdR-C6 in the same concentration of esterase. This discrepancy may be partly attributable to the very low solubility of FUdR-C8.

The effect of albumin on the drug release from the microspheres is shown in Fig. 5. A similar effect to that of esterase on drug release was observed. In the case of microspheres containing FUdR-C6, it is evident that the greater the concentration of albumin in the release medium, the more rapidly was the drug released. The effect of albumin on the microspheres containing FUdR-C4 or FUdR-C5 was smaller than that for FUdR-C6. Since FUdR-C4 and FUdR-C5 show considerable intrinsic solubilities, the effect of albumin as a surfactant to increase apparent solubility of the esters can be limited. Under the same protein concentration (0.019 and 0.19 mg/ml), the effect of esterase on FUdR-C6 release from the microspheres (Fig. 3) was greater than that of albumin, which shows no esterase activity for the FUdR esters. No structural changes in the microspheres' surface were observed during the course of this study in the scope of SEM analysis (data not shown). These results suggest that the release rate of the drug, especially FUdR-C6 and FUdR-C8, depends on the concentration of esterase, albumin and other materials, and that

Table II. Antitumor Activity of Single Injection of FUdR and Its Diesters

Compd.	Dose[a] (mg/kg)	Weight change (0—5 d, g/mouse)	Survival time ($n=5$, d±SEM)	T/C (%)	Control[b]
FUdR-C3	250	+0.9	10.8±0.4	102	A
	50	+1.8	10.2±0.2	96	A
	25	+0.8	11.0±0.8	104	A
FUdR-C4	250	+0.4	11.2±0.4	115	B
	50	+1.4	10.2±0.2	105	B
	25	+1.7	10.6±0.2	106	C
FUdR-C5	250	+1.6	10.2±0.4	104	D
	50	+2.6	9.8±0.2	100	D
	25	+1.5	10.2±0.2	104	D
FUdR-C6	250	+1.1	11.0±1.0	113	B
	50	+2.9	10.2±0.2	105	B
	25	+1.9	9.6±0.2	104	E
FUdR-C8	250	−1.4	11.8±0.5	116	F
	50	−0.4	10.8±0.6	106	F
	25	−0.1	11.8±0.4	118	C
FUdR-C10	250	−3.2	11.2±1.3	106	A
	50	−1.8	13.8±0.7	130	A
	25	−1.2	13.4±0.5	126	A
FUdR-C12	250	−3.1	10.0±0.8	100	C
	50	−1.9	13.0±0.0	130	C
	25	−1.4	13.6±0.5	136	C
	5	+0.4	13.8±1.4	147	G
	2.5	+1.4	9.6±0.4	114	G
FUdR	250	+1.3	11.2±0.4	114	D
	50	+1.7	10.2±0.6	105	B

a) Dose of diester-FUdR mg/kg or FUdR mg/kg. *b*) Control groups were not treated. The survival time of control groups; A, 10.6±0.2; B, 9.7±0.2; C, 10.0±0.3; D, 9.8±0.2; E, 9.2±0.2; F, 10.2±0.5; G, 9.4±0.4. The weight changes of control groups were A = +1.7, B = +2.3, C = +2.5, D = +1.6, E = +2.4, F = +1.2 and G = +2.7.

Table III. Antitumor Activity of Five Injections (day 1, 2, 3, 4 and 5) of FUdR and Its Esters.

Compd.	Dose[a] (mg/kg/d)	Weight change (0—5 d, g/mouse)	Survival time ($n=5$, d±SEM)	T/C (%)	Control[b]
FUdR-C3	225	0	12.2±0.2	122	A
	75	−0.5	11.2±0.2	112	A
	22.5	+0.4	10.4±0.2	104	A
FUdR-C4	225	−6.7	12.4±2.3	123	B
	75	−2.7	13.2±1.6	131	B
	22.5	−2.0	12.6±0.4	125	B
FUdR-C5	750	−2.4	9.2±0.2	94	C
	225	−2.5	14.6±0.2	146	A
	75	−1.2	13.4±0.2	134	A
	22.5	−0.7	12.4±0.4	124	A
FUdR-C6	750	−1.5	10.0±0.5	102	C
	225	−1.5	13.6±0.9	135	B
	75	−1.5	12.2±0.9	121	B
	22.5	−0.6	12.0±1.3	119	B
FUdR-C8	750	−2.8	9.0±0.0	92	C
	225	−2.0	12.6±0.2	125	B
	75	−2.9	12.2±1.7	121	B
	22.5	−2.7	11.8±1.6	117	B
FUdR-C10	225	−2.6	11.8±0.2	118	A
	75	−2.9	13.4±1.0	134	A
	22.5	+0.4	14.4±0.5	144	A
	7.5	+0.8	12.3±0.9	131	D
	2.25	+1.2	10.5±0.9	112	D
FUdR-C12	225	−2.9	10.4±0.5	102	E
	75	−1.6	13.2±1.0	129	E
	22.5	−0.1	14.6±0.4	143	E
	7.5	−0.7	14.4±0.2	144	A
	2.25	+1.3	12.8±0.6	128	A
FUdR	750	−3.0	9.4±0.4	96	C
	225	−2.1	15.4±0.4	157	C
	75	−0.1	13.0±0.0	133	C
	22.5	+0.8	11.8±1.1	120	C

a) Dose of diester-FUdR mg/kg or FUdR mg/kg. *b*) Control groups were not treated. The survival time of control groups; A, 10.0±0.0; B, 10.1±0.2; C, 9.8±0.2; D, 9.4±0.4; E, 10.2±0.2. The weight changes of the control groups were A = +2.0, B = +2.9, C = +1.6, D = +2.7 and E = +2.3.

these are ubiquitous in the injection sites of microspheres. Thus, the release pattern of drugs from microspheres containing FUdR-C4, FUdR-C5, FUdR-C10 or FUdR-C12 may not undergo such a large change in the body.

***In Vivo* Antitumor Activity** The antitumor effects of FUdR or diester-FUdR were measured by a single injection of a saline solution or suspension to mice bearing P388 leukemia (Table II).

Diester-FUdR, with shorter alkyl chains (FUdR-C3—FUdR-C6), showed a poor effect ($T/C=96$—115%), and only an increase in the body weight was observed. In contrast, diester-FUdR with longer alkyl chains showed a significant effect (130 and 147% at 50 mg/kg FUdR-C10, 5 mg/kg FUdR-C12, respectively) compared to that of unesterified FUdR (114 and 105% at 250, 50 mg/kg, respectively).

Table III shows the antitumor effect of FUdR and diester-FUdR given five times at 1, 2, 3, 4 and 5 d after inoculation.

Higher effects have been observed compared to those by single injection, in the shorter esters, which were expected to show a short retention in the body.[17] These results reconfirm the fact that the cytotoxicity of FUdR is time-dependent or requires long retention *in vivo*.

The effects of a single injection of the microspheres containing diester-FUdR on the survival of mice bearing P388 leukemia are shown in Table IV.

TABLE IV. Antitumor Activity of Single Injection of Microspheres

Compd.	Dose[a] (mg/kg)	Weight change (0—5 d, g/mouse)	Survival time ($n=5$, d±SEM)	T/C (%)	Control[b]
FUdR-C3	24 (1500)[c]	−3.8	11.2±1.9	110	A
	8.0 (500)	−3.3	13.0±0.8	127	A
	2.4 (150)	−2.1	11.2±0.3	110	A
	0.80 (50)	−1.3	11.4±0.9	112	A
FUdR-C4	145 (1500)	−3.8	11.6±0.9	120	B
	49.0 (500)	−3.3	14.2±0.8	146	B
	14.5 (150)	−0.5	11.4±0.2	118	B
	4.90 (50)	+0.6	10.8±0.4	111	B
FUdR-C5	225 (1500)	−3.1	10.4±0.5	106	C
	75 (500)	−3.3	14.2±0.8	146	C
	22.5 (150)	−1.3	12.4±0.4	127	C
	7.5 (50)	−0.1	12.0±0.0	122	C
FUdR-C6	225 (1500)	−3.4	12.0±1.2	124	B
	75 (500)	−4.0	14.8±0.3	153	B
	22.5 (150)	−3.3	13.6±0.3	140	B
	7.5 (50)	−0.2	11.4±0.2	118	B
FUdR-C8	225 (1500)	−4.1	11.8±2.1	118	A
	75 (500)	−3.3	13.6±0.9	133	A
	22.5 (150)	−1.2	12.0±0.6	111	A
	7.5 (50)	+0.8	11.0±0.4	108	A
FUdR-C10	225 (1500)	−2.6	9.8±1.2	97	D
	75 (500)	−3.5	12.0±1.3	119	D
	22.5 (150)	−0.1	11.2±0.4	111	D
	7.5 (50)	−1.9	11.2±0.5	111	D
FUdR-C12	225 (1500)	−0.4	12.0±0.3	119	D
	75 (500)	+1.2	10.6±0.4	105	D
	22.5 (150)	+3.1	10.2±0.2	101	D
	7.5 (50)	+3.2	10.0±0.3	99	D
Spheres[d]	(900)	+1.8	9.2±0.2	94	C

a) Dose of content drug in the microspheres. *b*) Control groups were not treated. The survival time of control groups; A, 10.2±0.5; B, 9.7±0.2; C, 9.8±0.2; D, 10.1±0.2. The weight changes of the control groups were A = +1.2, B = +2.3, C = +1.6 and D = +2.9. *c*) In parentheses, dose of microspheres mg/kg. *d*) The microspheres did not contain the drug.

The optimal dose of microspheres was in the range of 8—75 mg/kg except for the FUdR-C12-sphere, and the microspheres containing FUdR-C4, FUdR-C5 or FUdR-C6 showed significant effects ($T/C>140\%$). The microspheres containing FUdR-C6 showed the maximal effect ($T/C=153\%$) at the dose of 75 mg/kg. The higher activity of microspheres containing FUdR-C4, FUdR-C5 or FUdR-C6 may be attributable to their moderate release rates of the drug from the microspheres (Fig. 1, 3 and 5). Although the suspension of free FUdR-C12 showed high activity, and its optimal dose was low (Tables II and III), the microspheres containing FUdR-C12 showed a poor effect. This may be because the release rate of FUdR-C12 from the microspheres is too small (Fig. 4), the microspheres at the highest dose, therefore, showed the highest effect as well as a decrease in body weight.

As compared to the single administration of the suspensions at about the same dose (Table II), the effect of microspheres containing FUdR-C4, FUdR-C5 or FUdR-C6 was evidently higher. The effects of microspheres containing FUdR-C4, FUdR-C5 or FUdR-C6 were at least equal to or greater than those of the drug suspensions given by consecutive injection (5 times). These results suggested that in spite of the single administration and low dose of drugs, microspheres containing FUdR-C4, FUdR-C5 or FUdR-C6 are more potent than the suspensions of free drugs.

In conclusion, the combination of chemical modification and polymeric carrier devices seems to be a promising means to control the *in vivo* fate and increase the therapeutic efficacy of anticancer agents. In order to accomplish this purpose, the prodrug should be designed to be efficiently incorporated into carriers and to supply the drug sufficiently at an adequate rate. In this study, diester-FUdR with saturated aliphatic acids were shown with various physicochemical properties, and the drug contents in L-PLA microspheres were improved by prolonging the alkyl chain length of acyl groups of diester-FUdR. The microspheres containing FUdR-C4, FUdR-C5 or FUdR-C6 showed higher antitumor activity, though the prodrug suspensions did not show the advantage of prodrug over the parent drug, compared to those containing FUdR-C10 or FUdR-C12, which showed high activity when administered as free drug suspensions.

In the future, the determination of release of FUdR from the microspheres *in vivo* and the kinetic behavior of the released FUdR are required to clarify the mechanism of the action. Since the microspheres also are more useful than an aqueous solution or suspension in targeting therapy, the microspheres containing diester-FUdR may be applicable to cancer chemotherapy.

References

1) T. Kato, R. Nemoto, H. Mori, M. Takahashi, Y. Tamakawa and M. Harada, *J. Am. Med. Assoc.*, **245**, 1123 (1981).
2) T. Yoshioka, M. Hashida, S. Muranishi and H. Sezaki, *Int. J. Pharmaceut.*, **81**, 131 (1981).
3) Y. Morimoto, K. Sugibayashi and Y. Kato, *Chem. Pharm. Bull.*, **29**, 1433 (1981).
4) K. Juni, M. Nakano and M. Kubota, *J. Controlled Release*, **4**, 25 (1986).
5) K. Juni, J. Ogata, N. Matsui, M. Kubota and M. Nakano, *Chem. Pharm. Bull.*, **33**, 1609 (1985).

6) J. H. Burchenal, *Ann. N. Y. Acad. Sci.*, **255**, 202 (1975).
7) J. D. Laskin, E. F. Jordan, L. N. Kenny, D. Sugg, A. Y. Divecal and M. T. Hakala, *Proc. Am. Assoc. Cancer Res.*, **17**, 71 (1978).
8) Y. Nishizawa, J. E. Casida, S. W. Anderson and C. Heidelberger, *Biochem. Parmacol.*, **14**, 1605 (1965).
9) M. A. Rich, J. L. Bolaffi, J. E. Knoll, L. Cheong and M. L. Eidinoff, *Cancer Res.*, **18**, 730 (1958).
10) J. H. Burchenal, E. A. D. Holmberg, J. J. Fox, S. C. Hemphill and J. A. Reppert, *Cancer Res.*, **19**, 494 (1959).
11) C. Heidelberger, L. Grieshach, O. Cruz, R. J. Schnitzer and E. Grunberg, *Prog. Soc. Exp. Biol. Med.*, **97**, 470 (1958).
12) W. M. Williams, B. S. Warren and F. Lin, *Anal. Biochem.*, **147**, 478 (1985).
13) F. Kanzawa, A. Hoshi and K. Kuretani, *Eur. J. Cancer*, **16**, 1087 (1980).
14) F. Kanzawa, A. Hosi, K. Kuretani, M. Saneyoshi and T. Kawaguchi, *Cancer Chemother. Pharmacol.*, **6**, 19 (1981).
15) T. Kawaguchi, Y. Suzuki, Y. Nakahara, N. Nambu and T. Nagai, *Chem. Pharm. Bull.*, **33**, 301 (1985).
16) T. Kawaguchi, S. Fukushima, Y. Hayashi and M. Nakano, *Pharm. Res.*, **5**, 741 (1988).
17) N. Wakiyama, K. Juni and M. Nakano, *Chem. Pharm. Bull.*, **30**, 2621 (1982).
18) R. Bodmeier and J. W. McGinity, *Pharm. Res.*, **4**, 465 (1987).
19) T. Seki, T. Kawaguchi, H. Endoh, K. Ishikawa, K. Juni and M. Nakano, *J. Pharm. Sci.*, **79**, 985 (1990).

Application of the Solid Dispersion Method to Controlled Release of Medicine. I. Controlled Release of Water Soluble Medicine by Using Solid Dispersion[1)]

Hiroshi YUASA,*[,a] Tetsuya OZEKI,[a] Yoshio KANAYA,[a] Katsutoshi OISHI[b] and Tadashi OYAKE[c]

Tokyo College of Pharmacy,[a] 1432–1 Horinouchi, Hachioji, Tokyo 192–03, Japan, Nihon Pharmaceutical Industry Co., Ltd.,[b] 2–12–12 Honkomagome, Bunkyo-ku, Tokyo 113, Japan and Kanto Teishin Hospital,[c] 5–9–22 Higashigotanda, Shinagawa-ku, Tokyo 141, Japan. *Received July 19, 1990*

The release of medicine from solid dispersion which was prepared by evaporation after dissolving or suspending water-soluble medicine into an organic solvent was studied. Oxprenolol hydrochloride was used as a water soluble medicine. Eudragit RS, methylcellulose, ethylcellulose, polyvinylpyrrolidone, hydroxy propyl cellulose and pullulane were used as the polymers. These polymers and oxprenolol hydrochloride were suspended in or dissolved into ethanol under heating, and the ethanol in these solutions was evaporated to solid dispersion. Solid dispersion granules were prepared by grounding and sieving the solid dispersions obtained. The dissolution behavior of oxprenolol hydrochloride was studied by the dissolution test (JP XI).

As a result, it was clarified that in a solid dispersion granule composed of 25% oxprenolol hydrochloride, 70% ethylcellulose and 5% hydroxypropyl cellulose, the dissolution behavior of oxprenolol hydrochloride from this granule was of a leaching type for the matrix and was not affected by pH. Furthermore, various dissolution behaviors could be obtained by changing the particle size and the ratio of the polymer in the granule. These results suggest that this granulating method by the evaporation of the solvent is useful in preparing a sustained release preparation.

Keywords solid dispersion; evaporation; polymer; granule; sustained release; matrix

For the development of preparations of sustained release or controlled release, addition of or coating with wax or water-insoluble cellulose has generally been adopted.[2–6)] We conducted the following experiment to investigate the utility of a solid dispersion prepared by evaporation of the solution or suspension composed of a water soluble medicine, a polymer and an organic solvent.

Experimental

Materials Oxprenolol hydrochloride (OXP, known as a β-receptor inhibitor, one g of which dissolves in less than 2 ml of water at 37 °C) was supplied by Nihon Pharmaceutical Industry Co., Ltd., Tokyo. Acrylic resin (Eudragit® RS, EU) and pullulane (PULL) were provided by Higuchi Oil Co., Ltd., Tokyo. Methyl cellulose 25cp (MC), ethyl cellulose 45cp (EC) and polyvinylpyrrolidone K-30 (PVP) were purchased from Wako Pure Chemical Industries, Ltd., Osaka. Hydroxypropyl cellulose L grade (HPC) was obtained from Nippon Soda Co., Ltd., Tokyo.

Preparation of Granules One or two of the polymers mentioned above and OXP were suspended in or dissolved into ethanol under heating at 50 °C, and the ethanol in the suspensions or solutions was evaporated to solid dispersion. The solid dispersions were ground and sieved. The fractions of 18—20, 24—28 and 32—42 mesh were collected as granule sizes of L, M and S, respectively.

Observation of Dissolution Profile of OXP from Granule The dissolution profile of OXP from the granule was observed with a dissolution tester (FREUND-JASCO, DT-300), following the paddle method (JP XI), using 900 ml of the dissolution medium at 37 + 0.5 °C and a rotating paddle at 100 rpm. The quantity of OXP was determined with the absorbance at 273 nm by a spectrophotometer (JASCO, Ubest-30). Distilled water (pH 5.8), buffer solutions composed of NaCl and HCl of pH 1.2, KH_2PO_4 and Na_2HPO_4 of pH 5.5, KH_2PO_4 and NaOH of pH 6.8, H_3PO_3, KCl and NaOH of pH 9.0 and Na_2HPO_4 and NaOH of pH 11.0 were used for the dissolution medium.

Results and Discussion

Solid Dispersion Granule Composed of OXP and One Kind of Polymer Figure 1 shows the dissolution behavior of OXP from the solid dispersion granule composed of OXP and one kind of ethanol soluble polymer. The granule size was L. It is thought that EC is the most suitable polymer for controlling OXP dissolution, since the dissolved percentage of OXP in the cases of HPC and EU reached 100% after about 10 min from the start in the so-called the initial burst phenomenon.

Figure 2 shows the dissolution behavior of OXP with varied contents of EC in the solid dispersion granule. After 24 h of the dissolution test, the percentage of dissolved OXP decreased as the content of EC in the granule was increased. The dissolution rate from the start up to 5 min in Fig. 2 is shown in Fig. 3, and the rate after 12 to 24 h is shown in

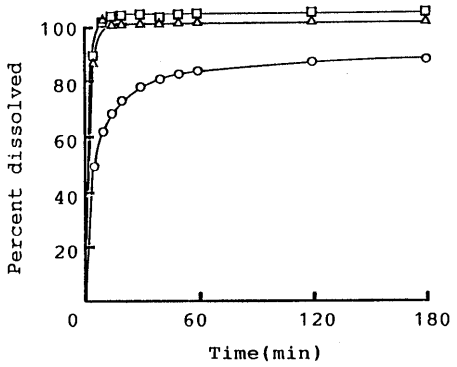

Fig. 1. Dissolution Behavior of OXP from Solid Dispersion Granule Composed of OXP and One Kind of Ethanol Soluble Polymer

□, composed of 25% OXP and 75% EU; △, composed of 25% OXP and 75% HPC; ○, composed of 25% OXP and 75% EC.

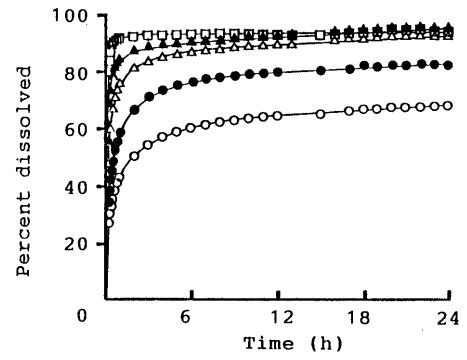

Fig. 2. Effect of Composition Ratio of OXP and EC in Solid Dispersion Granule on Dissolution Behavior of OXP

Percent of EC to OXP: □, 200%; ▲, 300%; △, 400%; ●, 500%; ○, 700%.

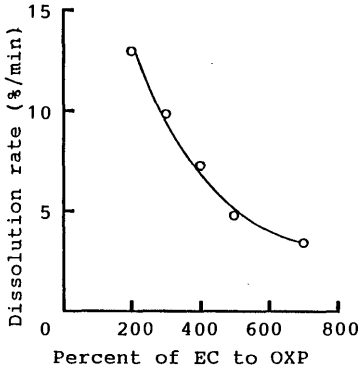

Fig. 3. Effect of Composition Ratio of OXP and EC in Solid Dispersion Granule on Initial Dissolution Rate of OXP

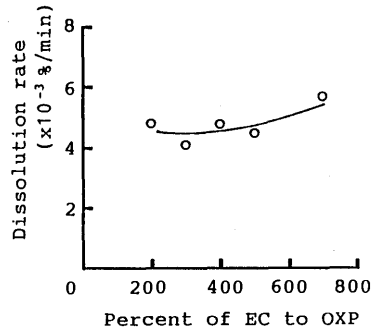

Fig. 4. Effect of Composition Ratio of OXP and EC in Solid Dispersion Granule on Last Dissolution Rate of OXP

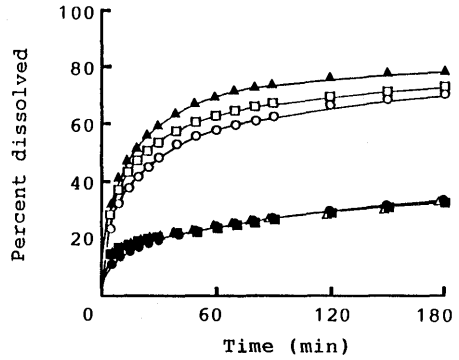

Fig. 5. Effect of Addition of Water Soluble Polymer to Granule Composed of OXP and EC on Dissolution Behavior of OXP

Added polymer: ▲, PULL; □, MC; ●, EU; ■, PVP; △, HPC; ○, 500% of EC to OXP (composed of OXP and EC).

Fig. 4. When the content of EC increased, the initial dissolution rate of OXP decreased, but the later dissolution rate was about the same. It is speculated that all of these results can be attributed to the decreased exposure of OXP to the surface of the granule with a larger content of EC in the granule.

Addition of Water Soluble Polymer to the Granule Composed of OXP and EC The later dissolution rate and the dissolved percentage of OXP could not be controlled, although these could be controlled initially by varying the content of EC. So, an attempt was made to form a channel in the granule by the addition of a water soluble polymer to the granule composed of OXP and EC.

The dissolution behavior of OXP from the granules which received additions of MC, PULL, PVP, HPC or EU

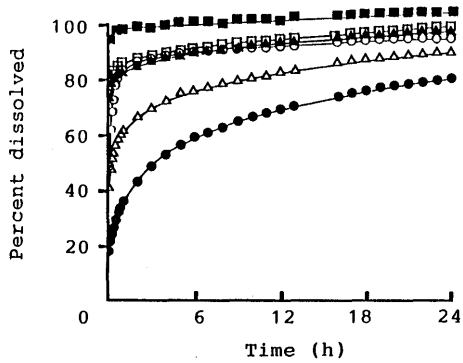

Fig. 6. Effect of Composition Ratio of OXP, EC and HPC in Solid Dispersion Granule on Dissolution Behavior of OXP

Percent of EC and HPC: ■, 30% and 45%; □, 40% and 35%; ▲, 50% and 25%; △, 60% and 15%; ●, 70% and 5%;○, 75% of EC.

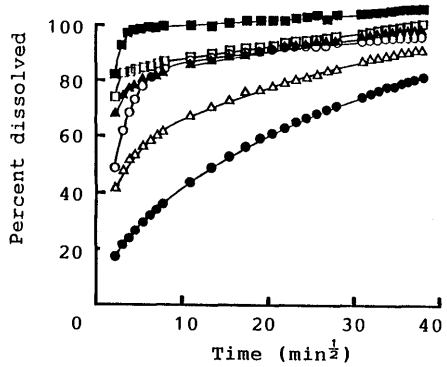

Fig. 7. Figure of Abscissa in Fig. 6 Converted to Square Root of Time

Percent of EC and HPC: ■, 30% and 45%; □, 40% and 35%; ▲, 50% and 25%; △, 60% and 15%; ●, 70% and 5%; ○, 75% of EC.

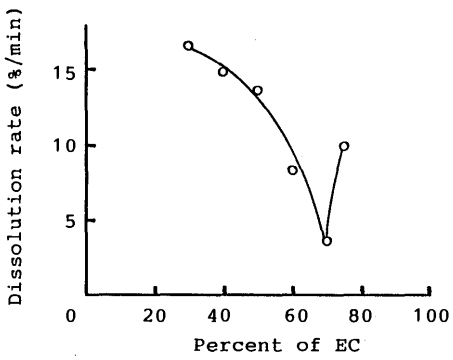

Fig. 8. Effect of Composition Ratio of OXP, EC and HPC on Initial Dissolution Rate of OXP

is shown in Fig. 5. Each granule was composed of OXP, EC and the polymer at the ratio of 100, 450 and 50, respectively. The initial dissolution rates in the granules of OXP–EC–PVP, OXP–EC–HPC and OXP–EC–EU markedly decreased compared to the rate of the OXP–EC granule, though the reason is not yet clarified. The dissolution behavior in the granules of OXP–EC–MC and OXP–EC–PULL was the same as that in the OXP–EC granule. This is probably because there were large MC and PULL particles in the OXP–EC–MC and OXP–EC–PULL granules; MC and PULL did not dissolve, but were suspended in ethanol when these granules were prepared. The parts of these granules, except for the suspended MC or PULL particles,

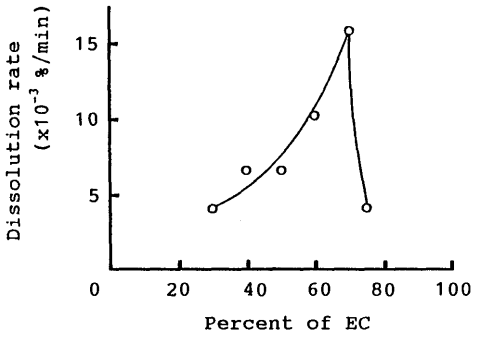

Fig. 9. Effect of Composition Ratio of OXP, EC and HPC on Last Dissolution Rate of OXP

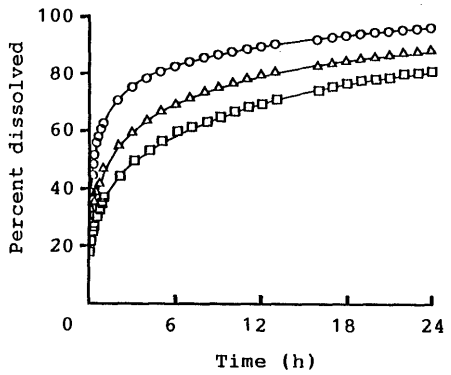

Fig. 10. Effect of Particle Size of Solid Dispersion Granule on Dissolution Behavior of OXP

□, L; △, M; ○, S.

were of the same composition ratio as the OXP–EC granule. In this report, the OXP–EC–HPC granule was dealt with.

Figure 6 shows the dissolution behavior of OXP from the granule composed of 25% OXP and 75% of the mixture with varied ratios of EC and HPC. The abscissa in Fig. 6 was converted to the square root of time and is shown in Fig. 7. Since the dissolution curve of the granule composed of 25% OXP, 70% EC and 5% HPC has the highest linearity, it was thought that the dissolution profile from the granule of this composition ratio was the most approximate for that of the leaching type for the matrix presented by T. Higuchi.[7]

The initial and later dissolution rates in Fig. 6 are shown in Figs. 8 and 9, respectively. The granule composed of 25% OXP, 70% EC and 5% HPC showed a minimum level in the initial dissolution rate and a maximum level in the later rate, though the reason is not yet clear. Anyway, it is speculated that OXP, EC and HPC formed a homogeneous matrix granule, that is to say, a solid dispersion granule, and channels were formed homogeneously in the granule after the dissolution of the water soluble HPC; OXP in the EC was diffused and dissolved into the dissolution medium in the channels. It is thought that the channels formed by the dissolving of HPC corresponded to openings, cracks and intergranular spaces in the matrix granule showing the leaching type dissolution profile, as the granule of this composition ratio showed the same dissolution profile.

Effect of the Particle Size of Granule on Dissolution Behavior The dissolution behavior of OXP from the granules composed of 25% OXP, 70% EC and 5% HPC of L, M and S sizes is shown in Fig. 10. The initial dissolution rate increased with a reduction of the particle size of granule. It is thought that the reduction of the granule particle size caused an increase in the specific surface area of the granules and in the exposure of OXP on the surface of the granule. However, the dissolution rates from about 6 h from the start of the test were much the same regardless of granule size. This suggests that the dissolution rates or the diffusion rates of OXP from the internal granules were the same.

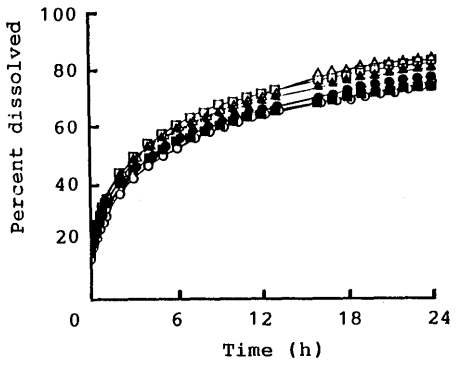

Fig. 11. Effect of pH of Dissolution Medium on Dissolution Behavior of OXP

■, pH 1.2; □, pH 5.5; ▲, pH 5.8 (distilled water); △, pH 6.8; ●, pH 9.0; ○, pH 11.0.

Effect of pH on Dissolution Behavior Figure 11 shows the dissolution behavior under varied pH of the dissolution medium with the L size granule composed of 25% OXP, 70% EC and 5% HPC. Although there was a slight difference in the dissolved percentage after 24 h, pH scarcely affected the dissolution behavior of OXP from the granule.

Conclusion

It has been clarified that a solid dispersion granule composed of 25% OXP, 70% EC and 5% HPC is a sustained release granule of the matrix type, and the dissolution behavior of OXP from this granule was not affected by pH. Furthermore, it has been found that various dissolution behaviors can be obtained by varying the particle size and the ratio of the polymer in the granule. These results suggest that this granulating method by evaporation of the solvent is useful as a preparation method for the sustained release of medicine.

References

1) A part of this study was presented at the 109th Annual Meeting of the Pharmaceutical Society of Japan, Nagoya, April 1989.
2) Y. Seta, F. Higuchi, Y. Kawahara, K. Nishimura and R. Okada, *Int. J. Pharm.*, **41**, 245 (1988).
3) A. Dakkuri, L. D. Butler and P. D. Patrick, *J. Pharm. Sci.*, **67**, 350 (1978).
4) A. Dakkuri, L. D. Butler and P. D. Patrick, *J. Pharm. Sci.*, **67**, 354 (1978).
5) A. Dakkuri, L. D. Butler and P. D. Patrick, *J. Pharm. Sci.*, **67**, 357 (1978).
6) Ch. R. Kowarski, R. M. Schachere, C. T. Agostini and A. L. Friedman, *Pharm. Acta Helv.*, **50**, 91 (1975).
7) T. Higuchi, *J. Pharm. Sci.*, **52**, 1145 (1963).

Interaction of Pentoxifylline with Human Erythrocytes. III. Comparison of Fluidity Change of Erythrocyte Membrane Caused by *S*-Adenosyl-L-methionine with That by Pentoxifylline

Yukio SATO,*[,a] Tadayoshi MIURA[b] and Yasuo SUZUKI[a]

Pharmaceutical Institute, Tohoku University,[a] Aobayama, Aoba-ku, Sendai 980, Japan and Sendai Teishin Hospital,[b] Chuo 4–5–1, Aoba-ku, Sendai 980, Japan. *Received August 1, 1990*

The change in fluidity by adding pentoxifylline to erythrocyte membranes was compared with that caused by *S*-adenosyl-L-methionine (SAM) by the method of electron spin resonance (ESR) spectroscopy. When SAM or pentoxifylline was added externally to the erythrocyte suspension (outside), the fluidity of the membrane bilayer was increased after incubation at 37 °C. However, the fluidity change in the inner part of the bilayer was relatively small compared to that in its outer part. These fluidity changes were dependent on the incubation time and the temperature. When the erythrocyte suspension was preincubated overnight at 4 °C in the presence of durgs (inside), the fluidity of the inner part of the membrane changed significantly. Nevertheless, that of the outer part of the lipid bilayer was not affected. Such an asymmetric fluidity change in the lipid bilayer was not observed by the addition of other xanthine derivatives such as caffeine, theophylline and theobromine. *S*-Adenosyl-L-homocysteine suppressed and $MgCl_2$ enhanced the increase of the membrane fluidity by SAM or pentoxifylline. Furthermore, the effects of SAM and pentoxifylline on erythrocyte deformability were determined by a filtering technique method. In increasing order the additive effects of SAM and pentoxifylline on the erythrocyte filterability were SAM (outside) < pentoxifylline (inside) < pentoxifylline (outside) < SAM (inside). These results suggest that pentoxifylline also affects the membrane fluidity through the enzymatic methylation of phospholipids.

Keywords erythrocyte; pentoxifylline; *S*-adenosyl-L-methionine; ESR spectrum; spin label; membrane fluidity; deformability

It is well known that pentoxifylline, 3,7-dimethyl-1-(5-oxohexyl)xanthine, can improve erythrocyte deformability and decrease blood viscosity.[1] There are many reports explaining the effects of pentoxifylline on membrane fluidity. Stefanovich[2] reported a significant increase in red cell adenosine triphosphate (ATP) content after the oral administration of pentoxifylline in rats. Also, the change of erythrocyte deformability was explained in terms of the elevation of ATP concentrations.[3] Rahmani-Jourdheuil *et al.*[4] pointed out that pentoxifylline had disturbing effects on the metabolism of polyphosphoinositide and thus controlled the membrane fluidity. This mechanism is related to the activation of protein kinase, which is known to be affected by pentoxifylline. On the other hand, pentoxifylline increases the surface charge on erythrocytes resulting in a rise in mobility.[5] However, other xanthine derivatives such as caffeine and theophylline, which have no significant effect on erythrocyte deformability, also change the surface charge. These derivatives bind the membrane phosphodiesterase active site, leading to an increase in cyclic adenosine monophosphate (c-AMP) concentration.[6]

We reported that the fluidity of acyl chains near the phospholipid head groups in the erythrocyte bilayer was increased by externally added pentoxifylline and suggested that some biological processes are related in the enhancement of membrane fluidity.[7] Membrane fluidity is closely correlated to molecular ordering of the fatty acyl chains in phospholipids and depends also on the type of polar head groups.[8] In this connection, it is well known that enzymatic methylations of phosphatidylethanolamine (PE) to form phosphatidylcholine (PC) are associated with many biological processes.[9] Hirata *et al.*[10] found that the enzymatic methylation of PE in erythrocyte membranes increased its fluidity. The methylation of PE to PC proceeds stepwisely with *S*-adenosyl-L-methionine (SAM) and the fluidity changed mainly in the formation of phosphatidyl-*N*-monomethylethanolamine (PME). PME affects the asymmetric distribution of phospholipids in the membrane and results in a change of membrane microviscosity. This information prompted us to examine the relationship between the fluidizing effect of erythrocyte membranes and phospholipid methylation in the presence of pentoxifylline.

Experimental

Materials Pentoxifylline was a gift from Hoechst Japan Ltd. Caffeine, theobromine and theophylline were from Nacalai Tesque, Inc. SAM was purchased from Sigma Chemical Co. *S*-Adenoxyl-L-homocysteine (SAH) was obtained from Seikagaku Kogyo Co., Ltd. The fatty acid spin labels, 5-doxyl stearic acid and 16-doxyl stearic acid, were purchased from Aldrich Chem. Co. Water was doubly distilled from an all-glass system. All other chemicals used were of analytical grade purity.

Electron Spin Resonance (ESR) Measurements Fresh heparinized human blood was obtained from Miyagi Prefectural Red Cross Blood Center. Red cells were washed with 0.9% NaCl to remove the buffy coat and further washed three times with sodium phosphate buffer, 310 ideal milliosmolarity (mosM), pH 7.4. Preparation of spin-labeled erythrocytes for ESR measurements were the same as previously reported.[7] The spin-labeled erythrocytes were incubated with pentoxifylline or SAM under various conditions (hematocrit of about 45%) and packed in a hematocrit capillary tube (Hyland Co., 1.1 mm i.d.). The ESR spectra were recorded by the JEOL JES-FE ESR spectrometer with a field intensity of 3290 G (100 G field sweep) equipped with a variable temperature accessory. The microwave power was kept at 4 mW at which no power saturation effect was observed.

Introduction of SAM into Erythrocytes SAM was incorporated into erythrocytes according to the procedure of Hirata and Axelrod[10b] without modification. Three milliliters of packed erythrocytes were suspended in 3 ml of phosphate buffer, pH 7.4, containing 2 mM of SAM and incubated overnight (approximately 16 h) at 4 °C. Before use, the erythrocytes were washed with 10 volumes of the phosphate buffer. The washed erythrocytes were incubated for 30 min at 4 °C with the spin labels which were previously formed as a thin film on the wall of the flask. Pentoxifylline was incorporated into erythrocytes in a similar manner as SAM.

Erythrocyte Filterability Measurement The deformability of erythrocytes was measured by a filtration method. An apparatus for measuring erythrocyte filerability was assembled according to Reid *et al.*[11] The erythrocyte suspension filled in a 6 ml syringe was connected onto a membrane holder equipped with a cleaned membrane filter (Cellulose Nitrate, 5 μm pore and 25 mm diameter, Toyo Roshi, Ltd.). The suspensions were passed through the membrane filter using a negative

pressure of 20 cm of water. The rate of flow was measured at least in triplicate on each erythrocyte sample. The erythrocyte suspension used was of about 0.045% hematocrit. The measurement was performed at room temperature.

Results

Effects of SAM Addition on Erythrocyte Membrane Figure 1 shows representative ESR spectra of the erythrocyte membranes labeled with 5-doxyl stearic acid and/or 16-doxyl stearic acid used in this study. 5-Doxyl stearic acid has a nitroxide radical close to the polar groups whereas that in 16-doxyl stearic acid locates in the hydrophobic end.

Previously, we reported the increase of fluidity near the head groups in the bilayer by incubating the erythrocytes with pentoxifylline added externally (pentoxifylline (outside)).[7] Also, the fluidity near the terminal methyl groups, hydrophobic end, was reduced or showed little change. These changes could be estimated by calculating a variation of order parameter, h_{+1}/h_0, where h_{+1} and h_0 represent the peak-to-trough amplitudes in the low field line and central line, respectively. The peak height is influenced by (i) the rate of axial rotation of the spin-label moiety, (ii) the rate of tumbling motion of the rotational axis, and (iii) the augular amplitude of the tumbling motion. Thus, h_{+1}/h_0 can be used as an empirical parameter of the membrane fluidity.[12]

In the present study, we first examined the effects of SAM added externally on erythrocyte membranes (SAM (outside)) at 37 °C. In Fig. 2, the changes of the parameter of each spin label were plotted as a function of incubation time.

As can be seen in the figure, the fluidity of the bilayer, both near the phospholipid head groups and the hydrophobic end, increased by the addition of SAM. The parameter increased with incubation time and then gradually decreased to reach the original values. The change of the fluidity near the hydrophobic end, however, was smaller than that near the head groups. These fluidity changes were not observed below 10 °C.

Figure 3 shows the changes of the parameter when SAM was previously incorporated into the inside of the erythrocytes (SAM (inside)). A large difference in fluidity change was observed between the hydrophobic end and near the head group in the lipid bilayer. The latter was not significantly influenced by SAM. The parameter for the former increased with incubation time and then gradually decreased to reach the original value which was larger than that of the control. The change of the parameter was dependent on the temperature and could not be observed below 10 °C (data not shown).

The results shown in Fig. 3 seem to reflect the methylation of PE in the cytoplasmic side of the membrane.[10] In the conversion of PE to PC, two methyltransferases asymmetrically distributed in the membranes are actively involved. The increase of the membrane fluidity shown in Fig. 2 may also be explained successively by the methylation with the two methyltransferases. It should be noticed that the maximal values of the parameter were observed at about 30 min of incubation. It can be said that a time-independent interaction also contributes to

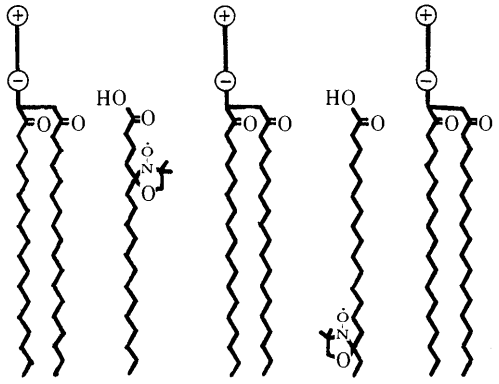

spin labels used in this study with their relative lengths and positions in membrane

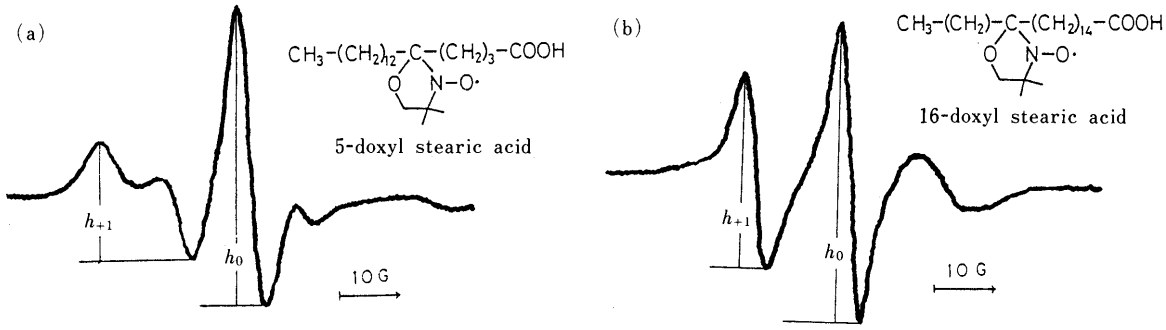

Fig. 1. ESR Spectra of 5-Doxyl Stearic Acid (a) and 16-Doxyl Stearic Acid (b) in Erythrocyte Membranes

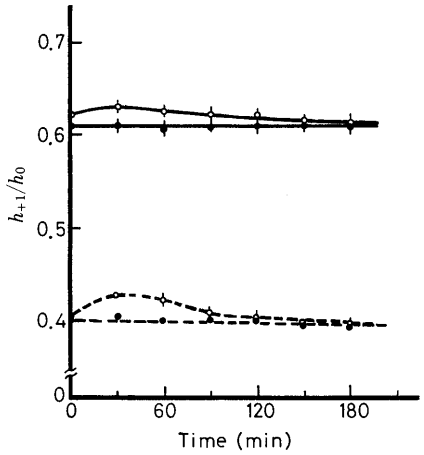

Fig. 2. Variation of h_{+1}/h_0 of Spin Labeled Erythrocytes as a Function of Incubation Time at 37 °C in the Presence of SAM

5-Doxyl stearic acid: --●--, control; --○--, in the presence of SAM. 16-Doxyl stearic acid: —●—, control; —○—, in the presence of SAM. [SAM] = 5×10^{-5} M (initial). Each point represents the mean ± S.D. of 3 experiments.

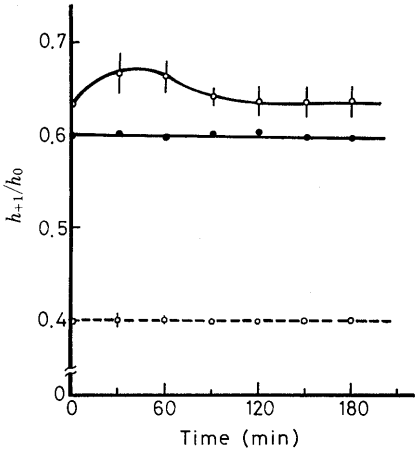

Fig. 3. Variation of h_{+1}/h_0 of Spin Labeled Erythrocytes as a Function of Incubation Time at 37 °C

The erythrocytes were preincubated with SAM overnight at 4 °C. 5-Doxyl stearic acid: --○--, pre-treated with SAM (be identical with control). 16-Doxyl stearic acid: —●—, control; —○—, pre-treated with SAM. [SAM] = 1×10^{-3} M (initial). Each point represents the mean ± S.D. of 3 experiments.

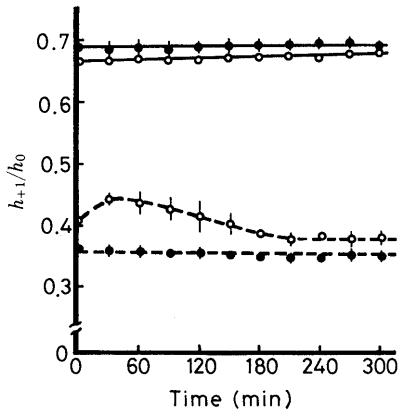

Fig. 4. Variation of h_{+1}/h_0 of Spin Labeled Erythrocytes as a Function of Incubation Time at 37 °C in the Presence of Pentoxifylline

5-Doxyl stearic acid: --●--, control; --○--, in the presence of pentoxifylline. 16-Doxyl stearic acid: —●—, control; —○—, in the presence of pentoxifylline. [pentoxifylline] = 5×10^{-5} M (initial). (The data are the same as those in Figs. 2 and 3 in ref. 7.)

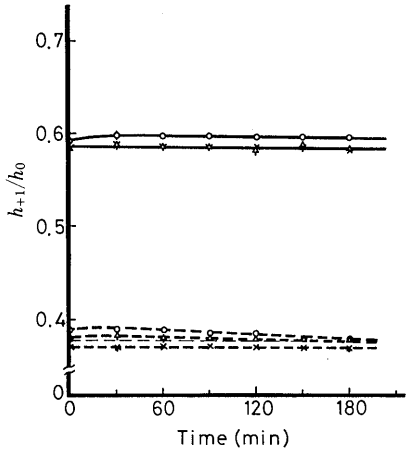

Fig. 5. Variation of h_{+1}/h_0 of Spin Labeled Erythrocytes as a Function of Incubation Time at 37 °C in the Presence of Xanthine Derivatives

5-Doxyl stearic acid: --○--, caffeine; --△--, theophylline; --×--, theobromine; a broken line corresponds to the control for theophylline. 16-Doxyl stearic acid: —○—, caffeine; —△—, theophylline; —×—, theobromine. [xanthine derivative] = 5×10^{-5} M (initial). Each point represents the mean ± S.D. of 2 experiments.

the fluidity change.[7] However, Hirata and Axelrod[10b] reported that negligible methylation of phospholipids occurred when SAM was added externally to the membrane. The details of the changes in fluidity caused by the external SAM are now uncertain.

Change of Membrane Fluidity by Xanthine Derivatives We compared the effects of pentoxifylline with other xanthine derivatives on membrane fluidity.

Figure 4 represents plots in the change of the parameter as a function of incubation time when pentoxifylline was added externally to the erythrocyte suspension and incubated at 37 °C. The fluidity of the bilayer near the phospholipid head groups showed a similar change to that observed in the SAM–erythrocyte system. The fluidity near the hydrophobic end seemed to be decreased. On the other hand, when caffeine, theobromine or theophylline was added externally to erythrocyte suspensions, the fluidities both at hydrophobic end and near the head group in bilayer were little affected by the addition of these drugs (Fig. 5). These results are consistent with the facts that the xanthine derivatives, except for pentoxifylline, have no significant effect on erythrocyte deformability[13] and that pentoxifylline interacts specifically with erythrocyte membranes.[14] The characteristic effect of pentoxifylline on membrane fluidity originates from the amphiphilic 5-oxohexyl side chain.[13b,14] Throughout these experiments, the absolute values of the parameters were not always constant. This seems to be due to the differences in donors and storage conditions. However, the degree of relative change of the parameters was kept almost constant by incubating the erythrocytes with SAM or pentoxifylline.

When erythrocytes were incubated overnight at 4 °C in the presence of pentoxifylline and then incubated at various temperatures (pentoxifylline (inside)), the changes in the parameters could be observed (Fig. 6).

The change of fluidity was dependent on temperature and restricted to the hydrophobic end in the bilayer. The time courses shown in Fig. 6 were similar to those observed for SAM (Fig. 3). The same experiment was tested for other xanthine derivatives. However, they did not show any

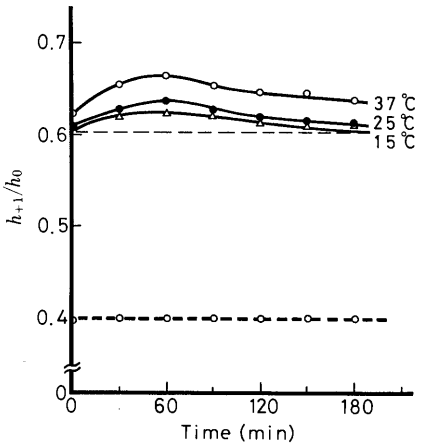

Fig. 6. Variation of h_{+1}/h_0 of Spin Labeled Erythrocytes as a Function of Incubation Time

The erythrocytes were preincubated with pentoxifylline overnight at 4 °C. 5-Doxyl stearic acid: --○--, pre-treated with pentoxifylline (identical with control). 16-Doxyl stearic acid: —△—, at 15 °C; —●—, at 25 °C; —○—, at 37 °C. [pentoxifylline] = 1×10^{-3} M (initial). A broken line corresponds to the control at 15 °C. The controls at 25 °C and 37 °C shifted slightly upper from that at 15 °C, which were omitted because of crowding.

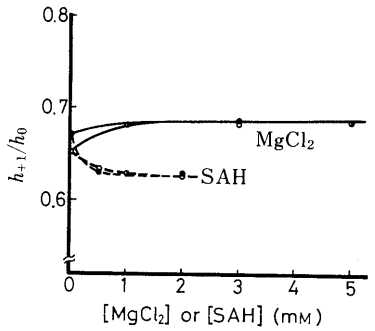

Fig. 7. Change of h_{+1}/h_0 by in the Presence of SAH or $MgCl_2$

The values of h_{+1}/h_0 were estimated after 30 min incubation at 37 °C for the erythrocytes labeled with 16-doxyl stearic acid. ●, preincubated in the presence of SAM; ○, preincubated in the presence of pentoxifylline. [SAM] = 1×10^{-3} M (initial); [pentoxifylline] = 1×10^{-3} M (initial).

fluidizing effect on the erythrocyte membranes. The change in membrane fluidity caused by pentoxifylline or SAM is asymmetric with respect to the lipid bilayer when they were added either externally or internally to the erythrocyte suspension. Although the time dependent fluidity change near the hydrophobic end was observed when SAM was added externally to the erythrocyte suspension, pentoxifylline did not show such an effect (Figs. 2 and 4). This discrepancy may come from differences in the enzymatic reactivity of the two drugs and/or in adsorptivity to the erythrocyte membranes through hydrophobic interaction.[14]

Effects of SAH and $MgCl_2$ on the Interaction of Pentoxifylline with Erythrocyte Membranes The change of membrane fluidity by pentoxifylline at the hydrophobic end of the bilayer was examined in the presence of SAH or $MgCl_2$ (Fig. 7). The erythrocyte suspension in the phosphate buffer was preincubated overnight at 4 °C with pentoxifylline and SAH or $MgCl_2$ of appropriate concentrations and washed with 10 volumes of the same buffer, then followed with spin labeling. SAH, a competitor of SAM, acted as the inhibitor of pentoxifylline. On the other hand, Mg^{2+}, a cofactor for methyltransferase, acted as the stimulator of pentoxifylline.

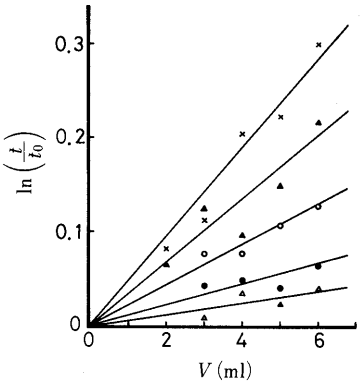

Fig. 8. Effect of Pentoxifylline or SAM on the Erythrocyte Filterability

Erythrocyte concentration was about 0.045% hematocrit. The erythrocytes were incubated for 30 min at 37 °C and then diluted to 0.045% hematocrit. Each point represents the mean value of 2 experiments for different batches of erythrocytes. —×—, control; —▲—, in the presence of SAM (5×10^{-5} M), SAM (outside); —△—, pre-treated with SAM overnight at 4 °C (1×10^{-3} M, initial), SAM (inside); —●—, in the presence of pentoxifylline (5×10^{-5} M), pentoxifylline (outside); —○—, pre-treated with pentoxifylline overnight at 4 °C (1×10^{-5} M, initial), pentoxifylline (inside).

TABLE I. Filterability Coefficients of Erythrocytes at Various Conditions

	λ (ml^{-1})
Control	0.05
SAM (outside)	0.03
SAM (inside)	0.005
Pentoxifylline (outside)	0.01
Pentoxifylline (inside)	0.02

Erythrocyte concentration: about 0.045% hematocrit. A negative pressure (20 cm water) was applied across a cellulose nitrate filter (5 μ pore size). The details of the preparation of SAM- or pentoxifylline-treated erythrocytes are noted in the text.

The same results were obtained when the fluidizing effect of SAM was examined in the presence of SAH or $MgCl_2$. Thus, in the erythrocyte membranes pentoxifylline may act in a similar manner as SAM.

Effects of Pentoxifylline and SAM on Erythrocyte Deformability The effect of pentoxifylline or SAM on erythrocyte filterability was determined. The experimental data were expressed as[15,16]

$$v = v_0 \exp(-\lambda V) \quad (1)$$

where v is the rate of volume flow in milliliters per second at volume V and v_0 an initial flow rate, which may be replaced by that of the buffer. λ is an occlusion parameter, which has a positive correlation with the concentration of cells, is inversely proportional to the applied pressure and is related to the erythrocyte deformability. By assuming $v = dV/dt = \Delta V/\Delta t$ and measuring flow time at a constant volume, Eq. 1 reduces to

$$\ln v_0/v = \ln \Delta t/\Delta t_0 = \lambda V \quad (2)$$

Here Δt_0 and ΔV_0 are replaced by values of the buffer. Eq. 2 indicates the linearity of the $\ln t/t_0$ *vs.* V plot. Figure 8 shows $\ln t/t_0$ of erythrocytes as a function of V at various conditions.

Table I summarizes the λ values of a series of experiments calculated from the data of Fig. 8. The λ values of pentoxifylline- or SAM-treated erythrocytes are smaller

than that of intact erythrocytes. From these results, it is obvious that both pentoxifylline and SAM can enhance erythrocyte deformability. In the increasing order, the fluidizing effects of SAM and pentoxifylline on the erythrocyte membranes are SAM (outside) < pentoxifylline (inside) < pentoxifylline (outside) < SAM (inside).

Discussion

Change of the Membrane Fluidity The plasma membrane must provide passive flexibility, elasticity and a certain degree of plasticity. ATP acts on erythrocyte deformability through several biochemical and biophysical changes including internal viscosity, intracellular ionic concentrations, hemoglobin binding activity to the membrane, phosphorylations of membrane proteins and inhibition of transglutaminases.[17] Glycolysis is the most probable source of ATP supply in erythrocytes. Actually, pentoxifylline had an increasing effect on the permeability of the cell membranes for glucose.[18] It seems that the improvement on erythrocyte deformability by pentoxifylline may also be explained as the secondary effect of this primary event. Since in the present experiment, however, there is no glucose supplement for glycolysis, an alternative explanation is needed for the fluidizing effect of the lipid bilayer by pentoxifylline.

As methylxanthines including pentoxifylline are potent inhibitors of cyclic nucleotide phosphodiesterase, these chemicals increase the c-AMP level in erythrocytes and indirectly stimulate the c-AMP-dependent phosphorylation.[6,19] However, the participation of this inhibitory effect of pentoxifylline may also be excluded in the present study, because the other xanthine derivatives did not increase the fluidity (Fig. 5).

It has been shown that pentoxifylline affects polyphosphoinositides metabolism.[17] However, as other xanthine derivatives also can disturb polyphosphoinositide metabolism, the participation of this metabolism in the deformability change of erythrocytes by pentoxifylline cannot be the assumed explanation of the change in the membrane fluidity. On the basis of the present study, it is reasonable to presume that pentoxifylline can affect the membrane properties by a mechanism different from polyphosphoinositide metabolism. Hirata and Axelrod[10c] used 1,6-diphenyl-1,3,5-hexatriene as a fluorescent probe for the measurement of microviscosity change in the membranes. By using this probe, Giraud and Claret[20] reported the lack of effect of pentoxifylline on the membrane lipid order in erythrocytes. This probe does not seem to fully reflect the time dependent change of a local physical state of lipids caused by pentoxifylline. The change of lipid order caused by pentoxifylline may be smaller than that by SAM. This corresponds to the results of the filtration experiment.

According to Hirata and Axelrod,[10b,c] the change in the membrane fluidity by SAM is due to methylation of PE by two methyltransferases (PMT) asymmetrically distributed in the membranes. One of them (PMT-I), catalyzing PE to PME, is localized on the cytoplasmic side of the membrane whereas the second enzyme (PMT-II), catalyzing PME to PC, faces the outside of the erythrocyte. PME in the membrane (inner PME) leads to the change of membrane fluidity, and the flip–flop of the methylated phospholipids soon follows enzymatically. The changes of the ESR parameter caused by SAM are very similar to those caused by pentoxifylline. Therefore, it seems that pentoxifylline can affect membrane fluidity also through the enzymatic methylation of phospholipids. In the present study, the change of the membrane fluidity was observed when pentoxifylline was preincubated overnight with the erythrocyte suspension at 4 °C, following incubation at 37 °C. The fluidizing effect on the interior of the bilayer may result from pentoxifylline penetrated into the erythrocytes. Stefanovich *et al.*,[18] however, said that pentoxifylline itself apparently does not permeate into erythrocytes after incubation for 2.5 h at 37 °C. The discrepancy between our result and theirs comes from a difference in incubating conditions. Bilto *et al.*[13b] reported that pentoxifylline more effectively improved the filterability of nystatin-treated erythrocytes after 1 h of incubation at 4 °C than at 25 °C. This result may also support our finding. However, as shown in Fig. 8 and Table I, the significant effect of pentoxifylline on erythrocyte deformability is due to both the penetrated molecules and the outside molecules.

Kinetics of the Fluidity Change Next, we will consider the kinetics of the fluidity change of erythrocyte membranes when the drugs were incorporated into erythrocytes and 16-doxyl stearic acid was used as the spin probe.

The change of the phospholipids in the cytoplasmic side of the membranes can be simplified as follows

$$A \xrightarrow{k_1} B \underset{k_3}{\overset{k_2}{\rightleftarrows}} C \tag{3}$$

where A, B and C correspond to a concentration of PE, inner PME and outer PME and/or PC in membranes, respectively, and k_1, k_2 and k_3 are rate constant. Since in this study, the concentration of the spin-label is constant and the experimental condition is the same, the value of h_{+1}/h_0 is mainly dependent on the membrane fluidity or organization. It was observed that the fluidity change was dependent of the incubation time and temperature. The membrane fluidity is exclusively influenced by the inner PME, so that the change of the ESR parameter reflects the inner PME.[10c] Therefore, the value of h_{+1}/h_0 is directly proportional to the inner PME concentration. From Eq. 3, $[B]$ is as follows

$$[B]=\frac{k^3}{k_2+k_3}[A]_0\{1-\exp(-(k_2+k_3)t)\} + \frac{k_1-k_3}{k_2+k_3}[A]_0\{\exp(-k_1t)-\exp(-(k_2+k_3)t)\} \tag{4}$$

If the value of h_{+1}/h_0 is used instead of the inner PME concentration, the relative values of the rate constant in Eq. 4 can be determined so as to give the smallest mean-square error between the observed and theoretical values. Figure 9 represents a computer fitting of the parameter changes in the SAM-treated erythrocytes (inside) at various temperatures. The values of h_{+1}/h_0 at 37 °C compared are those in Fig. 3. The parameter changes can be explained well by Eq. 4.

Table II shows the relative values of the rate constants in the SAM (inside)- or pentoxifylline (inside)-treated erythrocytes. These values are comparable to each other, indicating similar changes of the lipid order in both systems. At 37 °C, the values of k_1 and k_2 in the SAM–erythrocyte

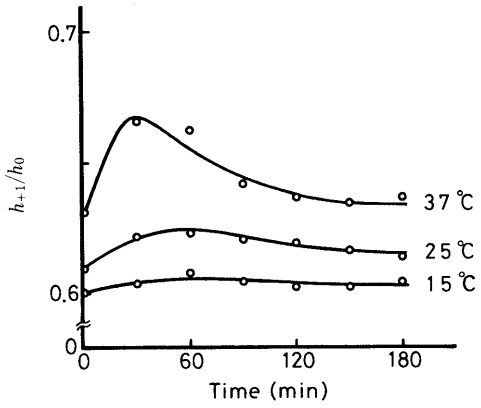

Fig. 9. Time Course of the Change of h_{+1}/h_0 of Spin Labeled Erythrocytes Pre-treated with SAM at Various Temperatures

The solid lines are the best fitted curves for the observed values. The observed values at 37 °C are the same as those in Fig. 3.

TABLE II. Relative Values of Rate Constants in the SAM- or Pentoxifylline-Treated Erythrocyte System

Addition	°C	k_1 (h^{-1})	k_2 (h^{-1})	k_3 (h^{-1})
SAM	15	1.39	1.43	*ca.* 0
(inside)	25	0.92	1.09	*ca.* 0
	37	1.79	3.27	0.03
Pentoxifylline	15	1.30	1.58	*ca.* 0
(inside)	25	1.00	1.39	*ca.* 0
	37	1.56	1.92	0.08

The values were obtained from the most fitted curves by the use of Eq. 4 in the text.

system are larger than those in the pentoxifylline–erythrocyte system. This indicates that the fluidity change by SAM is more effective than that by pentoxifylline, being consistent with the results in Fig. 8. At the lower temperatures, the values of k_3 are very small. This implies that the vectoral rearrangement of the methylated phospholipids is irreversible in practice. The values of the rate constant at 25 °C are smaller than those at 15 °C, reflecting nonlinear Arrhenius plots. It is well known that there are a number of examples in the literature of nonlinear Arrhenius plots for enzyme-catalyzed reactions.[21] Silvius and McElhaney[22] proposed that when two alternate reaction pathways with different activation enthalpies catalyze the reaction observed, an Arrhenius plot will concave upward. It seems that the enzymatic phospholipid translocation corresponds to this case.

On the other hand, when 5-doxyl stearic acid was used as the spin probe, the spectrum was characteristic of the anisotropic motion (Fig. 1). In this case, it seems that the empirical parameter h_{+1}/h_0 is not adequate for discussion of the kinetics, though this parameter can be used as a relative measurement of membrane fluidity.[23]

In the present study, the physical properties of membrane in the presence of pentoxifylline is explicable by the methylation of phospholipids. Membrane fluidity is closely related to biological and biochemical processes such as the transport of chemicals, cell fusion, and protein rotation and diffusion. The fluidity change caused by pentoxifylline seems to also trigger other membrane events such as enhancement of ATP concentration.

References

1) A. M. Ehrly, *Med. Welt*, **26**, 2300 (1975); R. Smud, B. Sermukslis and D. Kartin, *Pharmatherapeutica*, **1**, 229 (1976); H.-G. Grigoleit, E. Porsche, V. Stefanovich, G. Jacobi and A. Lahham, *ibid.*, **1**, 241 (1976); A. M. Ehrly, *Curr. Med. Res. Opin.*, **5**, 608 (1978).
2) V. Stefanovich, *Med. Welt*, **26**, 1882 (1975); *idem*, *Res. Commun. Chem. Pathol. Pharmacol.*, **10**, 747 (1975).
3) A. M. Ehrly, *Angiology*, **27**, 188 (1976); H.-G. Grigoleit and H. Leonhardt, *Pharmatherapeutica*, **1**, 642 (1977); R. Muller, *J. Med.*, **10**, 307 (1979).
4) D. Rahmani-Jourdheuil, I. Juhan-Vague, C. Roul, Y. Mourayre, Z. Mishal, J. le Petit and P. Vague, *Eur. J. Clin. Pharmacol.*, **31**, 725 (1987).
5) Y. O. Luk, S. L. Law and F. L. Chu, *J. Pharm. Pharmacol.*, **37**, 646 (1985).
6) S. Hayashi and H. Ozawa, *Chem. Pharm. Bull.*, **22**, 587 (1974); S. Hayashi, T. Sakaguchi and H. Ozawa, *Jpn. J. Pharmacol.*, **26**, 117 (1976); V. Stefanovich, *Res. Commun. Chem. Pathol. Pharmacol.*, **5**, 655 (1973).
7) Y. Sato, T. Miura and Y. Suzuki, *Chem. Pharm. Bull.*, **38**, 555 (1990).
8) J. Seelig, H. Limacher and P. Bader, *J. Am. Chem. Soc.*, **94**, 6364 (1972).
9) G. A. Scarborough and J. F. Nye, *J. Biol. Chem.*, **242**, 238 (1967).
10) *a*) F. Hirata, O. H. Viveros, E. J. Diliberto, Jr. and J. Axelrod, *Proc. Natl. Acad. Sci. U.S.A.*, **75**, 1718 (1978); *b*) F. Hirata and J. Axelrod, *ibid.*, **75**, 2348 (1978); *c*) *Idem*, *Nature* (London), **275**, 219 (1978); *d*) F. Hirata, W. J. Strittmatter and J. Axelrod, *Proc. Natl. Acad. Sci. U.S.A.*, **76**, 368 (1979); *e*) F. Hirata and J. Axelrod, *Science*, **209**, 1082 (1980).
11) H. L. Reid, A. J. Barnes P. J. Lock, J. A. Dormandy and T. L. Dormandy, *J. Clin. Pathol.*, **29**, 855 (1976).
12) K. Takeshita, H. Utsumi and A. Hamada, *Biophys. J.*, **52**, 187 (1987); B. Sato, K. Nishikida, L. T. Samuels and F. H. Tyler, *J. Clin, Invest.*, **61**, 251 (1978).
13) *a*) H. M. Thao Chan, E. Franzini and M. Thao Chan, *Clin. Hemorheol.*, **8**, 17 (1988); *b*) Y. Y. Bilto, M. Player and J. Stuart, *ibid.*, **8**, 213 (1988).
14) Y. Sato, T. Miura and Y. Suzuki, *Chem. Pharm. Bull.*, **38**, 552 (1990).
15) M. I. Gregersen, C. A. Bryant, W. E. Hammerle, S. Usami and S. Chien, *Science*, **157**, 825 (1967).
16) K. Shirahama, S. Kubota and J. T. Yang, *Hemoglobin*, **4**, 149 (1980).
17) P. Boivin, *Clin. Hemorheol.*, **7**, 25 (1987).
18) V. Stefanovich, E. Porsche and E. Müller, *Arzneim.-Forsch.*, **29**, 757 (1979).
19) V. Stefanovich, P. Jarvis and H.-G. Grigoleit, *Int. J. Biochem.*, **8**, 359 (1977); M. I. Argel, L. Vittone, A. O. Grassi, L. E. Chiappe, G. E. Chiappe and H. E. Cingolani, *J. Mol. Cell. Cardiol.*, **12**, 939 (1980); M.-C. Lecomte and P. Boivin, *Scand. J. Clin. Lab. Invest.*, **41**, 291 (1981).
20) F. Giraud and M. Claret, *Scand. J. Clin. Lab. Invest.*, **41**, Suppl. 156 (1981).
21) V. Massey, B. Curti and H. Ganther, *J. Biol. Chem.*, **241**, 2347 (1966).
22) J. R. Silvius and R. N. MeElhaney, *J. Theor. Biol.*, **88**, 135 (1981).
23) S. R. Wassall, T. M. Phelps, M. R. Albrecht, C. A. Langsford and W. Stillwell, *Biochim. Biophys. Acta*, **939**, 393 (1988).

Effects of Protopine on Blood Platelet Aggregation. III.[1] Effect of Protopine on the Metabolic System of Arachidonic Acid in Platelets

Hidemi SHIOMOTO,* Hideaki MATSUDA and Michinori KUBO

Faculty of Pharmaceutical Sciences, Kinki University, 3-4-1, Kowakae, Higashiosaka, Osaka 577, Japan. *Received October 11, 1990*

The mode of action of protopine on blood platelet aggregation was investigated in the metabolic system of arachidonic acid and in liberation of platelet activating factor using *in vitro* experimental models. Protopine inhibited the releases of arachidonic acid and platelet activating factor from platelet membrane phospholipids. Protopine also inhibited the conversion of prostaglandin G_2 to thromboxane A_2, as well as carboxyheptyl imidazole, a thromboxane synthetase inhibitor.

These results indicated that protopine functions both as a phospholipase inhibitor and a thromboxane synthetase inhibitor. It is expected that protopine can be applied for treatment of thrombosis as an antiplatelet drug.

Keywords Corydalis tuber; protopine; phospholipase; thromboxane A_2; platelet activating factor; platelet aggregation

In the preceding paper,[1] we reported that the effect of protopine against platelet aggregation is attributed not only to the activation of adenylate cyclase in the conversion of adenosine triphosphate (ATP) to cyclic adenosine 3′,5′-monophosphate (AMP), but also involves some other mode of action. The purpose of the present investigation was therefore to study the effects of protopine on the metabolic system of arachidonic acid and the release of platelet activating factor from membrane phospholipids in platelets.

Experimental

Materials Protopine was isolated from Corydalis tuber (*Corydalis turtschaninovii* BESSER *forma yanhusuo* Y. H. CHOU *et* C. C. HSU) by the method of Kaneko and Naruto.[2] The sources of materials were as follows: arachidonic acid, bovine serum albumin (BSA), essentially fatty acid-free BSA (eff BSA) and hemoglobin (Sigma Chemical Co., U.S.A.), [1-^{14}C]-arachidonic acid (2.07 GBq/mM) and thromboxane B_2 (TXB_2)-[^{125}I] assay system (Amersham International plc, U.K.), thrombin (Mochida Pharmaceutical Co., Ltd., Japan), platelet activating factor C_{18} (PAF, Boehringer Mannheim GmbH, Germany), PAF-[^{125}I] radioimmunoassay kit (Daiichi Pure Chemicals Co., Ltd., Japan), carboxyheptyl imidazole (CHI, Molecular Biologische Technologie GmbH, Germany), sheep seminal vesicular gland microsomes (Eldan Technologies Co., Inc., U.S.A.), acetylsalicylic acid (ASA), *p*-bromophenacyl bromide (*p*-BPB), *N*-2-hydroxyethylpiperazine-*N*′-2-ethanesulfonic acid (HEPES), imidazole, indomethacin, *o*-phthalaldehyde, tris(hydroxymethyl)nitromethane (Tris) and tryptophan (Nacalai Tesque, Inc., Japan).

Animals Male Kwl: JW strain rabbits (2.0—2.5 kg) were used for the experiments. They were maintained in an air-condition room with lighting from 7 a.m. to 7 p.m. The room temperature (about 23 °C) and humidity (about 60%) were controlled automatically. A laboratory pellet chow (Labo R Stock, Nihon Nosan Kogyo K.K., Japan) and water were given freely.

Preparation of Platelet-Rich or -Poor Plasma (PRP or PPP) Whole blood samples were collected from the heart of pentobarbital-anesthetized rabbits. Nine ml of the blood and 1 ml of sodium citrate (3.8%) were transferred into a plastic tube and centrifuged at 200 *g* at room temperature for 10 min to obtain PRP (3.0×10^8 platelets/ml). The PRP was removed with a siliconized pipet and stored in a plastic test tube. The remaining red cell precipitate of the blood samples was further centrifuged at 1800 *g* for 30 min to give PPP.

Preparation of Washed Platelet Suspension (WPS) The PRP was resuspended in a buffered mixture [1.5 mM ethylenediaminetetraacetic acid (EDTA), 25 mM Tris–HCl, 130 mM NaCl and 5.5 mM glucose; pH 6.8], and was centrifuged at 1800 *g* at 4 °C for 10 min. The resulting platelet pellet was washed twice with the same buffered mixture. The washed platelet was resuspended in HEPES buffer (137 mM NaCl, 2.7 mM KCl, 1.0 mM $MgCl_2$, 3.75 mM NaH_2PO_4, 11.9 mM $NaHCO_3$, 5.5 mM glucose and 5.0 mM HEPES; pH 7.35) containing 0.35% BSA to give the suspention at 5.0×10^8 platelets/ml. This suspension was referred to as WPS.

Preparation of Labelled Platelet Suspension (Labelled-WPS) The labelled-WPS was prepared according to the method of Billah *et al.*[3] [1-^{14}C]-Arachidonic acid (74 kBq) was added to 20 ml of PRP and incubated at 37 °C for 120 min under shaking with 45 cycles/min. To the incubated suspention was added 20 ml of the buffered mixture (2.0 mM EDTA, 25 mM Tris–HCl, 130 mM NaCl, 5.5 mM glucose and 0.25% eff BSA; pH 6.8), and it was then centrifuged at 1800 *g* at 4 °C for 10 min. The resulting labelled platelet pellet was washed twice with the same buffered mixture. The washed platelet was resuspended in HEPES buffer containing 0.25% eff BSA to give the suspention at 5.0×10^8 platelets/ml. This suspension was referred to as labelled-WPS.

Arachidonic Acid Release from Platelet Membrane Phospholipids To 400 μl of labelled-WPS preincubated at 37 °C for 2 min was added 50 μl of test solution [dissolved in 10% dimethyl sulfoxide (DMSO)/HEPES buffer solution]. After incubation for 5 min, 50 μl of thrombin (1.0 U/ml) was added to the incubated mixture and incubated for 5 min. The reaction stopping solvent, chloroform–methanol (2 : 1, v/v; 2.4 ml), was added to the incubated mixture and shaken. The extraction procedure of lipids in platelets was performed according to the method of Bligh and Dyer.[4] The lipid extract obtained was subjected on thin layer chromatography [Silica gel 60 plate (Merck, Germany)] using chloroform–methanol–acetic acid–water (45 : 20 : 6 : 1, v/v). The separated phospholipids [phosphatidylcholine (PC), phosphatidylethanolamine (PE) and phosphatidylinositol plus phosphatidylserine (PI + PS)] and free fatty acids (FFA; arachidonic acid and its metabolites) were located on the chromatogram and exposed to an iodine vapor, and the radioactivity in each spot was determined by liquid scintillation counting.

TXB_2 Formation by Thrombin, Arachidonic Acid and PAF in Platelets To 200 μl of WPS preincubated at 37 °C for 2 min was added 25 μl of the test solution (dissolved in 10% DMSO/HEPES buffer solution) and the mixture was incubated for 5 min. To the incubated mixture was added 25 μl of thrombin (1.0 U/ml), arachidonic acid (0.25 mM) or PAF (0.1 μM) and each mixture was incubated, respectively. To the incubated mixture was added 250 μl of the reaction stopping solution [20 mM potassium-phosphate buffered solution (PBS; pH 7.35) containing 10 mM EDTA·2Na, 0.1 mM indomethacin and 15 mM imidazole to stop the reaction 10 min after the addition of thrombin, or 3 min after in the cases of the addition of arachidonic acid or PAF. The resulting TXB_2 in the incubated mixture was measured by radioimmunoassay.

TXB_2 Formation by Prostaglandin G_2 (PGG_2) in Platelets A mixture of 150 μl of an enzyme solution containing 15 mg sheep seminal vesicular gland microsomes (cyclooxygenase) per 1.0 ml of 25 mM Tris–HCl buffer (pH 8.0) containing 7.0 mM tryptophan and 3.0 μM hemoglobin, and 50 μl of 5.0 mM arachidonic acid in ethanol was incubated at 30 °C for 1.5 min; then, 50 μl of 0.1 mM indomethacin (dissolved in 25 mM PBS) was added to stop the reaction. The ice-cold reaction mixture was used as a PGG_2 solution. Assay of TXB_2 in the incubated mixture was performed in the same manner as described in the case of the addition of arachidonic acid or PAF.

Correlation between Percentages of Thrombin- and Arachidonic Acid-Induced Platelet Aggregation and Quantity of the Resulting TXB_2 The operation for thrombin- and arachidonic acid-induced platelet aggregation and TXB_2 formation was carried out in the same manner as described previously, in this paper. Using thrombin as a stimulant, a WPS suspension was used, while a PRP suspension was used when arachidonic acid was the stimulant. When the aggregation reached its maximum, 250 μl

of the reaction stopping solution was added to the incubated mixture to stop the formation of TXB_2. Percentages of platelet aggregation on each sample were calculated. TXB_2 in the incubated mixture was measured by radioimmunoassay.

PAF Release from Platelets To 200 μl of WPS preincubated at 37 °C for 2 min was added 25 μl of the test solution (dissolved in 10% DMSO/HEPES buffer solution) and the mixture was incubated for 5 min. To the incubated mixture was added 25 μl of thrombin (1.0 U/ml) and this was incubated for 10 min. To the incubated mixture was added 50 μl of an ice-cold buffered mixture (30 mM EDTA·2Na, 25 mM Tris–HCl and 65 mM NaCl; pH 7.35) to stop the reaction. The resulting mixture was then centrifuged at 1800 *g* at 4 °C for 10 min. The extraction procedure of lipids from the supernatant layer was performed according to the method of Pinckard *et al.*[5] to give a chloroform fraction containing PAF. The chloroform fraction was evaporated to dryness under a N_2-stream. The PAF in the chloroform was measured by radioimmunoassay.

Platelet Aggregation Test The platelet aggregation test was performed according to the method described previously.[1] WPS suspended in a HEPES buffer and in a HEPES buffer containing 1.0 mM $CaCl_2$, were used in thrombin concentrations of 1.0 U/ml and 0.1 U/ml, respectively. PRP was used, in the cases of LASS (labile aggregation-stimulating substance) and PAF. LASS was prepared according to the method of Hamberg *et al.*[6] The mixture of 50 μl of platelet suspension (1.0×10^9 platelets/ml) in Krebs–Henseleit bicarbonate medium (118 mM NaCl, 4.7 mM KCl, 1.2 mM $MgSO_4$, 2.5 mM $MgCl_2$, 25 mM $NaHCO_3$, 12 mM KH_2PO_4 and 11.0 mM glucose; pH 7.35) and 50 μl of 2.0 mM arachidonic acid (dissolved in 10% ethanolic saline) was incubated at 37 °C for 30 s. The reaction mixture obtained was referred to as LASS. Platelet aggregation was induced by the addition of 10 μl of LASS into 200 μl of preincubated PRP containing indomethacin (15 μM). The inhibitory effects on platelet aggregation were represented by a concentration of 50% inhibition (IC_{50}) according to the Litchfield–Wilcoxon method.

Serotonin Release from Platelets To 200 μl of WPS preincubated at 37 °C for 2 min was added 25 μl of the test solution (dissolved in 10% DMSO/HEPES buffer solution) and the mixture was incubated for 5 min. To the incubated mixture was added 25 μl of thrombin (1.0 U/ml or 0.1 U/ml), arachidonic acid (0.25 mM) or PAF (0.1 μM) and these were incubated, respectively. To the incubated mixture was added 250 μl of ice-cold buffered mixture (10 mM EDTA·2Na, 25 mM Tris–HCl and 65 mM NaCl; pH 7.35) to stop the reaction 10 min after the addition of thrombin, or 3 min after in the cases of the addition of arachidonic acid or PAF. The reaction mixture was centrifuged at 1800 *g* at 4 °C for 10 min to obtain a supernatant layer (*A*) and a deposited platelet pellet (*B*). Serotonin in the supernatant layer and in the deposited platelet pellet was determined according to the method of Drummond and Gordon[7] as described below; into a test tube containing 100 μl of H_2O was added 400 μl of the supernatant layer. The platelet pellet was lysed in 500 μl of H_2O. To the supernatant layer and to the lysed platelet pellet solution were added a 100 μl portion of 200% (w/v) trichloroacetic acid solution, and each mixture was centrifuged at 2000 *g* at 4 °C for 20 min. To each of the defecated supernatant with the removal of protein was added 1.0 ml of a 0.05% *o*-phthalaldehyde solution (0.5% *o*-phthalaldehyde-ethanol solution–8 N HCl (1 : 9, v/v)), and the resulting mixture was heated in boiling water for 10 min. After cooling, each reaction mixture was washed with 2 ml of chloroform. The fluorescence of each aqueous layer was measured by a fluorometer with activation and emission wavelengths of 360 and 475 nm, respectively. Percentage of serotonin release from platelets were calculated by the formula presented below;

$$\text{serotonin release } (\%) = [A/(A+B)] \times 100$$

A: serotonin content in supernatant layer
B: serotonin content in deposited platelet pellet

Statistical Analysis The experimental data was tested for statistically significant differences by means of the Student's *t* test.

Results

Effect of Protopine on Arachidonic Acid Release from Membrane Phospholipids in Thrombin-Stimulated Labelled Platelets As shown in Table I, 26.0 ± 1.3% of arachidonic acid were released from phospholipids (PC, PE and PI + PS) in thrombin-stimulated platelets (control), in comparison with non-stimulation. Arachidonic acid release was inhibited dose-dependently by protopine as compared to those of the control. *p*-BPB also significantly inhibited arachidonic acid release at a concentration of 0.1 mM.

Effects of Protopine on TXB_2 Formation from Thrombin-, Arachidonic Acid-, PGG_2- and PAF-Stimulated Platelets As shown in Table II, protopine dose-dependently inhibited TXB_2 formation in all platelets stimulated by thrombin, arachidonic acid, PGG_2 and PAF. ASA significantly inhibited TXB_2 formation in thrombin-, arachidonic acid- and PAF-stimulated platelets, but was ineffective in PGG_2-stimulated platelets. CHI also inhibited significantly TXB_2 formation in all of the platelets used.

Correlation between Percentages of Thrombin-Induced Platelet Aggregation and Quantity of the Resulting TXB_2 As shown in Fig. 1, the quantity of the resulting TXB_2 was directly proportional to the percentages of platelet aggregation in additional groups of protopine with $r^2 = 0.732$, $p < 0.01$. Although *p*-BPB, a positive control, strongly inhibited platelet aggregation, it was ineffective on TXB_2 formation.

Correlation between Percentages of Arachidonic Acid-Induced Platelet Aggregation and Quantity of the Resulting TXB_2 The quantity of the resulting TXB_2 was directly proportional to the percentages of platelet aggregation in additional groups of protopine with $r^2 = 0.829$, $p < 0.01$. The same correlation ($r^2 = 0.737$, $p < 0.01$) was also observed by

TABLE I. Effect of Protopine on Arachidonic Acid Release from Membrane Phospholipids in Thrombin-Stimulated [1-^{14}C]-Arachidonic Acid-Labelled Platelets

Treatment	Concentration (mM)	Radioactivity (% dpm)			
		FFA	PC	PE	PI+PS
Non-stimulation		1.7±0.1[b]	40.4±1.0[b]	36.6±1.2[a]	21.4±0.5[b]
Thrombin-stimulation (control)		26.0±1.3	29.4±0.6	32.6±0.7	12.2±0.7
Protopine	0.01	26.1±0.9	30.4±0.9	32.2±1.3	11.3±0.6
	0.05	16.1±0.8[b]	33.2±0.6[a]	33.9±0.9	17.0±0.9[a]
	0.25	11.2±0.7[b]	34.8±0.8[b]	35.0±0.7[a]	19.0±1.1[b]
	1.0	7.3±0.5[b]	37.4±1.1[b]	34.5±1.1[a]	20.3±0.9[b]
p-BPB	0.1	7.5±0.3[b]	38.1±1.1[b]	36.8±0.9[a]	17.6±0.7[b]
ASA	0.5	21.2±1.0[a]	30.4±0.9	34.5±0.6	13.8±0.9
CHI	0.1	18.8±1.7[a]	32.3±1.2	35.0±1.1	13.9±0.6

FFA, free fatty acid (arachidonic acid and its metabolites); PC, phosphatidylcholine; PE, phosphatidylethanolamine; PI + PS, phosphatidylinositol plus phosphatidylserine; *p*-BPB, *p*-bromophenacyl bromide; ASA, acetylsalicylic acid; CHI, carboxyheptyl imidazole. Labelled platelets treated with protopine, *p*-BPB, ASA or CHI were stimulated by 1.0 U/ml thrombin. After extraction and separation of lipids from platelets, the radioactivity in each lipid spot was determined. For details, see Experimental. Each value represents the mean ± S.E. of 3 experiments. Significantly different from the control, *a*) $p < 0.05$, *b*) $p < 0.01$.

TABLE II. Effects of Protopine on TXB_2 Formation in Thrombin-, Arachidonic Acid-, PGG_2- and PAF-Stimulated Platelets

Treatment	Concentration (mM)	TXB_2 (pmol/10^9 platelets)			
		Thrombin	Arachidonic acid	PGG_2	PAF
Control		421.7±12.1	1342±76	1009±86	242.6±22.3
Protopine	0.01	409.2±28.3	1062±75	925±64	233.9±15.4
	0.05	286.4±14.1[b]	839±63[b]	774±87	118.1±18.2[a]
	0.25	8.4±1.3[b]	619±83[b]	609±59[a]	17.1±2.9[b]
	1.0	2.2±0.6[b]	391±78[b]	441±48[b]	2.0±0.2[b]
p-BPB	0.1	21.7±3.3[b]	414±83[b]	875±31	159.5±17.4[a]
ASA	0.5	2.4±0.5[b]	18±3[b]	1024±25	2.9±0.8[b]
CHI	0.1	9.7±1.7[b]	47±11[b]	177±27[b]	28.9±7.6[b]

Abbreviations are the same as those described in the legend to Table I. Platelets treated with protopine, *p*-BPB, ASA or CHI were stimulated by 1.0 U/ml thrombin, 0.25 mM arachidonic acid, PGG_2 (enzymatically synthesized substance from arachidonic acid) or 0.1 μM PAF. The resulting TXB_2 was measured. For details, see Experimental. TXB_2 was not detected in non-stimulated platelets. Each value represents the mean±S.E. of 3 experiments. Significantly different from the control, *a*) $p<0.05$, *b*) $p<0.01$.

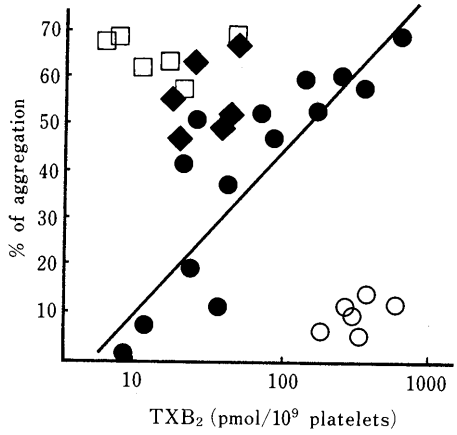

Fig. 1. Correlation between Percentages of Thrombin-Induced Platelet Aggregation and Quantity of the Resulting TXB_2

●, protopine; ○, *p*-bromophenacyl bromide (*p*-BPB); □, acetylsalicylic acid (ASA); ◆, carboxyheptyl imidazole (CHI). Aggregation and TXB_2 formation in platelets treated with protopine, *p*-BPB, ASA or CHI were induced by 1.0 U/ml thrombin. For details, see Experimental. Percentage of platelet aggregation and TXB_2 content in control were 70.6±7.4% and 478.3±83.5 pmol/10^9 platelets, respectively. Each point represents a single observation. The correlation line of protopine represents the data by means of linear regression analysis ($r^2=0.732$, $p<0.01$).

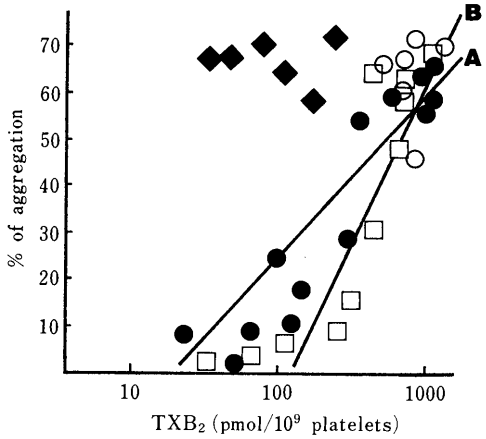

Fig. 2. Correlation between Percentages of Arachidonic Acid-Induced Platelet Aggregation and Quantity of the Resulting TXB_2

All symbols are the same as those described in the legend to Fig. 1. Aggregation and TXB_2 formation in platelets treated with protopine, *p*-BPB, ASA or CHI were induced by 0.2 mM arachidonic acid. For details, see Experimental. Percentage of platelet aggregation and TXB_2 content in control were 72.0±6.3% and 1146±128 pmol/10^9 platelets, respectively. Each point represents a single observation. The correlation line of protopine or ASA represents the data by means of linear regression analysis (A line; protopine, $r^2=0.829$, $p<0.01$, B line; ASA, $r^2=0.737$, $p<0.01$).

TABLE III. Effect of Protopine on PAF Release from Thrombin-Stimulated Platelets

Treatment	Concentration (mM)	PAF (ng/10^9 platelets)
Control		14.53±2.10
Protopine	0.01	14.75±3.42
	0.05	11.65±5.24
	0.25	7.16±1.31[a]
	1.0	5.03±1.43[a]
p-BPB	0.1	5.62±1.76[a]
ASA	0.5	15.20±4.33
CHI	0.1	14.85±3.98

Abbreviations are the same as those described in the legend to Table I. Platelets treated with protopine, *p*-BPB, ASA or CHI were stimulated by 1.0 U/ml thrombin. After extraction of lipids, PAF was measured. For details, see Experimental. PAF was not detected in non-stimulated platelets. Each value represents the mean±S.E. of 3 experiments. Significantly different from control, *a*) $p<0.05$.

TABLE IV. Effects of Protopine on Thrombin-, LASS- and PAF-Induced Platelet Aggregation

Treatment	IC_{50}[a] (mM)			
	Thrombin		LASS	PAF
	1.0 U/ml	0.1 U/ml		
Protopine	0.13	0.89	0.12	0.13
p-BPB	0.071	0.040	0.77	0.85
ASA	>1.0	>1.0	>1.0	>1.0
CHI	>1.0	>1.0	>1.0	>1.0

Abbreviations are the same as those described in the legend to Table I. Platelet aggregation was induced by 1.0 or 0.1 U/ml thrombin, LASS (enzymatically synthesized substance from arachidonic acid) or 0.1 μM PAF. *a*) Concentration required to inhibit platelet aggregation by 50 percent, Litchfield-Wilcoxon method. Maximal sample concentration used was 1.0 mM.

additional groups of ASA, but CHI had no correlation (Fig. 2).

Effect of Protopine on PAF Release from Thrombin-Stimulated Platelets Protopine significantly inhibited PAF release in concentrations of 0.25 and 1.0 mM. *p*-BPB also exhibited an inhibitory effect on PAF release (Table III).

Effects of Protopine on Thrombin-, LASS- and PAF-Induced Platelet Aggregation As shown in Table IV, the inhibitory effect of protopine on 1.0 U/ml thrombin-induced platelet aggregation (IC_{50}; 0.13 mM) was superior to that of protopine on 0.1 U/ml thrombin-induced platelet aggregation (IC_{50}; 0.89 mM). Protopine showed strong

TABLE V. Effects of Protopine on Serotonin Release from Thrombin- and PAF-Stimulated Platelets

Treatment	Concentration (mM)	% serotonin release		
		Thrombin		PAF
		1.0 U/ml	0.1 U/ml	
Control		91.6±2.4	97.9±0.3	69.4±3.4
Protopine	0.01	91.9±0.6	96.9±1.2	67.9±2.1
	0.05	90.3±0.7	93.3±1.7	59.5±2.8
	0.25	59.8±3.8[a)]	90.3±1.2	27.3±3.3[a)]
	1.0	24.7±1.6[a)]	49.0±2.1[a)]	15.4±1.7[a)]
p-BPB	0.1	3.3±1.4[a)]	97.0±0.6	7.7±3.4[a)]
ASA	0.5	86.8±2.1	95.6±1.7	68.0±0.9
CHI	0.1	85.7±1.9	95.8±1.9	65.8±2.2

Abbreviations are the same as those described in the legend to Table I. After platelets treated with protopine, *p*-BPB, ASA or CHI were stimulated by 1.0 or 0.1 U/ml thrombin or 0.1 μM PAF, serotonin released from platelets was measured. For details, see Experimental. % serotonin release from non-stimulated platelets was less than 1.0%. Each value represents the mean±S.E. of 3 experiments. Significantly different from the control, *a*) $p<0.01$.

inhibitory effects compared with those of *p*-BPB, ASA and CHI on platelet aggregation induced by LASS and PAF.

Effects of Protopine on Serotonin Release from Thrombin- and PAF-Stimulated Platelets As shown in Table V, protopine dose-dependently inhibited the release of serotonin from thrombin- and PAF-stimulated platelets. The inhibitory effect of protopine on serotonin release from 1.0 U/ml thrombin-stimulated platelets was superior to that of protopine on serotonin release from 0.1 U/ml thrombin-stimulated platelets. *p*-BPB also inhibited the release of serotonin from 1.0 U/ml thrombin- and PAF-stimulated platelets.

Discussion

We have previously reported that one mode of action of protopine on the inhibition of platelet aggregation is based upon the metabolic system of cyclic AMP; that is, the activation of adenylate cyclase and elevation of cyclic AMP accumulation in platelets. In this work, the study attempted to reveal another mode of inhibition of platelet aggregation. Thus, the effect of protopine on the metabolic system of arachidonic acid was investigated, including its effect on the release of PAF, a mediator of platelet aggregation, as well as, on TXA_2 or adenosine diphosphate (ADP). When platelets are stimulated by various stimulants, such as thrombin and collagen *etc.*, phospholipase A_2 and phospholipase C are activated, and arachidonic acid is released into the cytoplasm from membrane phospholipids consisting of PC, PE, PI and PS *etc.* The decomposed reaction of phospholipids which occur with this stimulation is recognized to be a rate-determining step in the metabolic system of arachidonic acid. Protopine dose-dependently inhibited the release of arachidonic acid from the membrane phospholipids in labelled platelets stimulated with thrombin. It can therefore be inferred that besides the participation of the metabolic system of cyclic AMP, protopine directly inhibits activation of phospholipase A_2 and phospholipase C, which participate in a metabolic system of arachidonic acid in platelets. Protopine resulted in the inhibition of the liberation of arachidonic acid from the membrane phospholipids. Arachidonic acid released in platelets is converted into PG endoperoxides (PGG_2) by cyclooxygenase, followed by TXA_2 with TX synthetase. These unstable PG endoperoxides and TXA_2 are non-enzymatically hydrolyzed to produce finally stable TXB_2, a non-bioactive metabolite. Protopine inhibited the formation from arachidonic acid to TXA_2 in platelets containing additional arachidonic acid and from PGG_2 to TXA_2 in platelets containing additional PGG_2. ASA, a cyclooxygenase inhibitor,[8)] inhibited the formation of arachidonic acid-induced TXA_2, but was ineffective on the formation of PGG_2-induced TXA_2. On the other hand, CHI, a TX synthetase inhibitor,[9)] inhibited both the formation of arachidonic acid- and PGG_2-induced TXA_2. The pattern of inhibition of protopine resembled that of CHI. Accordingly, the inhibitory effect of protopine on the formation of arachidonic acid to TXA_2 would seem to be closely dependent on the inhibition of TX synthetase activity. As shown in Figs. 1 and 2, there was correlation between the inhibitory effects of protopine on platelet aggregation and on the quantity of the resulting TXB_2 in platelets, while this was not observed with CHI.

Protopine strongly inhibited the platelet aggregation induced in a high concentration of thrombin (1.0 U/ml) in addition to having an inhibitory effect on phospholipase activity. From these results and the report[10)] that platelet aggregation induced in a high concentration of thrombin is mainly derived from PAF rather than TXA_2, it was expected that protopine would inhibit the release of PAF from membrane phospholipids. Protopine showed an inhibitory effect of PAF release from thrombin-stimulated platelets similar to that of *p*-BPB, a phospholipase A_2 inhibitor.[11)] It is considered that protopine inhibits the liberation both of TXA_2 and PAF.

Protopine inhibited platelet aggregation induced by LASS (solution containing mainly TXA_2) and PAF. Consequently, it has become apparent that protopine also possesses an inhibitory effect on secondary platelet aggregation.

These results on protopine are consistent with the fact that crude drugs containing protopine, such as Corydalis tuber, are now used for treatment of Oketsu-syndrome in the traditional Chinese system of medicine. It will be expected that protopine can eventually be applied for treatment of thrombosis as an antiplatelet drug.

References

1) Part II: H. Shiomoto, H. Matsuda and M. Kubo, *Chem. Pharm. Bull.*, **38**, 2320 (1990).
2) H. Kaneko and S. Naruto, *J. Org. Chem.*, **34**, 2803 (1969).
3) M. M. Billah, E. G. Lapetina and P. Cuatrecasas, *J. Biol. Chem.*, **255**, 10217 (1980).
4) E. G. Bligh and W. J. Dyer, *Can. J. Biochem. Physiol.*, **37**, 911 (1959).
5) R. N. Pinckard, R. S. Farr and D. J. Hanahan, *J. Immunol.*, **123**, 1847 (1979).
6) M. Hamberg, J. Svensson and B. Samuelsson, *Proc. Natl. Acad. Sci. U.S.A.*, **72**, 2994 (1975).
7) A. H. Drummond and J. L. Gordon, *Thrombos. Diathes. Haemorrh.* (Stuttg.), **31**, 366 (1974).
8) G. J. Roth and P. W. Majerus, *J. Clin. Invest.*, **56**, 624 (1975).
9) L. J. Grimm, D. R. Knapp, D. Senator and P. V. Halushka, *Thromb. Res.*, **24**, 307 (1981).
10) B. B. Vargaftig, M. Chignard and J. Benveniste, *Biochem. Pharmacol.*, **30**, 263 (1981).
11) B. B. Vargaftig, *J. Pharm. Pharmac.*, **29**, 222 (1977).

Binding Characteristics of a Thyroid Hormone Metabolite, 3,3'-Diiodo-L-thyronine, to Bovine Serum Albumin as Measured by Fluorescence

Nobuo OKABE* and Misa HOKAZE

Faculty of Pharmaceutical Sciences, Kinki University, Kowakae 3-4-1, Higashiosaka, Osaka 577, Japan. *Received August 7, 1990*

The interaction between a thyroid hormone metabolite, 3,3'-diiodo-L-thyronine(3,3'-T_2) and bovine serum albumin (BSA) was investigated by the fluorescence method. The apparent binding constants and thermodynamic parameters were obtained assuming the equivalence and independence of the binding sites on the BSA molecule. The maximum binding was attained at near pH 8.5 and the apparent binding constant at pH 8.5 was 2.7 (0.2) $\times 10^5 M^{-1}$. The standard free energy change, enthalpy change and entropy change were -7.36 (0.02) kcal mol^{-1}, -7.75 kcal mol^{-1} and -1.51 e.u., respectively.

Keywords thyroid hormone metabolite; thyroid hormone; hormone binding; 3,3'-diiodo-L-thyronine; bovine serum albumin; serum albumin binding; binding constant; thermodynamic parameter; fluorescence

Introduction

Thyroid hormone, 3,5,3',5'-tetraiodo-L-thyronine (T_4) and 3,5,3'-triiodo-L-thyronine (T_3) are well known as being the hormonogenically active forms.[1-3] The binding characteristics of these active hormones with serum albumin have been investigated extensively by fluorescence, equilibrium dialysis and circular dichroism measurements.[4-9] Contrasting with these hormonogenically active forms, little is known about the binding properties of the thyroid hormone metabolite, 3,3'-diiodo-L-thyronine (3,3'-T_2). 3,3'-T_2, it is the main deiodinated metabolite of T_3 and 3,3',5'-triiodo-L-thyronine (r-T_3), has an extremely high metabolic clearance rate relative to other iodothyronines, and is contained at about 9—28 ng/dl in serum.[9] Although the physiological functions of 3,3'-T_2 are not yet clear, it is important to clear its binding characteristics with serum albumin in order to obtain information about the transport of the deiodinated thyroid hormone metabolites through blood serum. In this study, the interaction between 3,3'-T_2 and bovine serum albumin (BSA) was investigated by fluorescence measurements at various pH's and temperatures.

Materials and Methods

BSA (Lot No. 9365) was obtained from Sigma Chemical Co. 3,3'-T_2 (Lot No. 12100) was from Reinstsubstanzen Henning Berlin. Other reagents were of the highest quality available and obtained from Nakarai Chemicals, Ltd.

Fluorescence measurements were performed with a Hitachi 850 spectrofluorometer. The temperature of the sample was controlled by the use of a hollow cell holder through which water from a constant temperature bath regulated within 0.1 °C was circulated and measured directly by using a Takara thermister D641. The fluorescence excitation and emission wavelengths were 280 nm and 340 nm, respectively. In a typical experiment, aliquots (0.5—1.0 μl) of 1 mM 3,3'-T_2 were added to 200 μl of a 1 μM BSA solution in 0.1 M of sodium phosphate buffer in a $0.5 \times 0.5\,cm^2$ quartz micro cuvette under stirring. The observed relative intensity was corrected for dilution of the albumin. The BSA concentration was determined spectrophotometrically using, $E^{1\%}_{1\,cm}=6.54$ at 280 nm[10] and the molecular weight of 66300[11] in 0.1 M sodium phosphate buffer, pH 7.5. The apparent binding constants and the number of binding sites were evaluated from the fluorescence quenching titration of BSA with 3,3'-T_2 according to Attallah and Lata[12] assuming the equivalence and independence of the binding sites.

$$K=\frac{Q_f}{(1-Q_f)(T_t-nQ_fP_t)} \quad (1)$$

$$Q_f=\frac{f_0-f_m}{f_0-f_r} \quad (2)$$

where K is the apparent binding constant, Q_f is the ratio of quenching at a point on the quenching curve to the maximum quenching, T_t is the total concentration of 3,3'-T_2 added, P_t is the total BSA concentration, n is the number of 3,3'-T_2 bound to a BSA molecule, f_0 is the fluorescence intensity of the albumin solution without added 3,3'-T_2, f_m is the measured fluorescence intensity of the sample added 3,3'-T_2, and f_r is the rest of the fluorescence intensity not quenchable with 3,3'-T_2. pH measurements were made with a TOA pH meter HM-20 and ultraviolet absorption measurements were in a Hitachi 557 double-beam spectrophotometer.

Results and Discussion

The pK of the phenolic hydroxyl group of 3,3'-T_2 was determined as 8.40 from the pH titration of the absorbance at 325 nm (data, not shown). This value is nearly the same as the pK of 8.45 for T_3.[13] In many reports, the importance of the contribution of the phenolic hydroxyl group of T_4 or T_3 to their binding to carrier proteins in serum, nuclear thyroid hormone receptor or iodothyronine mono deiodinase has been pointed out,[2,14] because the phenolic hydroxyl group could act as a hydrogen bond donor or an acceptor. Further, the anionic phenolate group could be involved in electrostatic interaction between thyroid hormones and their carrier proteins.[6,15] By this reason, the binding ability of 3,3'-T_2 to BSA was investigated at various pH's. Figure 1 shows the typical fluorescence quenching titration curve of BSA with 3,3'-T_2. The tryptophanyl fluorescence intensity of BSA was decreased by the addition of 3,3'-T_2 as a radiationless energy transfer,[6] while only

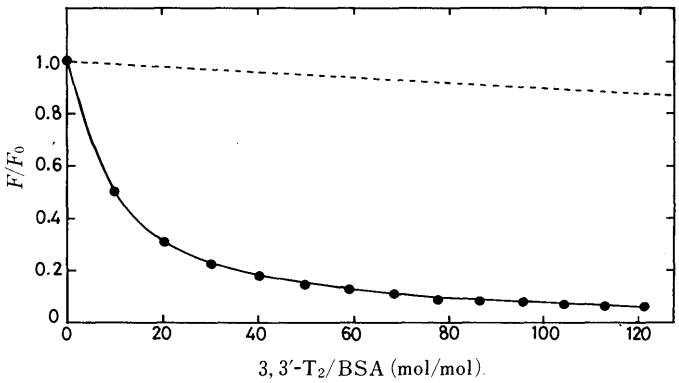

Fig. 1. Relative Fluorescence Intensity of BSA *vs.* Molar Ratios of 3,3'-T_2 to BSA in 0.1 M Sodium Phosphate Buffer, pH 8.0 at 25 °C

BSA concentration was 1.80 μM. Dotted line indicates the titration of the amino acid, tryptophan (1.80 μM) with 3,3'-T_2. Fluorescence excitation and emission wavelengths were 280 nm and 340 nm, respectively.

TABLE I. Parameters of Binding of 3,3′-T_2 to BSA at Various pH's at 25 °C

pH	Binding constant K (S.D.) $\times 10^{-5}$ (M^{-1})	Binding sites n (S.D.)
5.0	1.3 (0.1)	30 (5)
6.0	1.1 (0.1)	27 (6)
7.0	1.4 (0.1)	23 (6)
7.5	2.4 (0.2)	38 (6)
8.0	2.5 (0.1)	43 (9)
8.5	2.7 (0.2)	17 (5)
9.0	1.3 (0.2)	25 (8)

Standard deviations (S.D.) were obtained from ten times the fluorescence titrations at each pH.

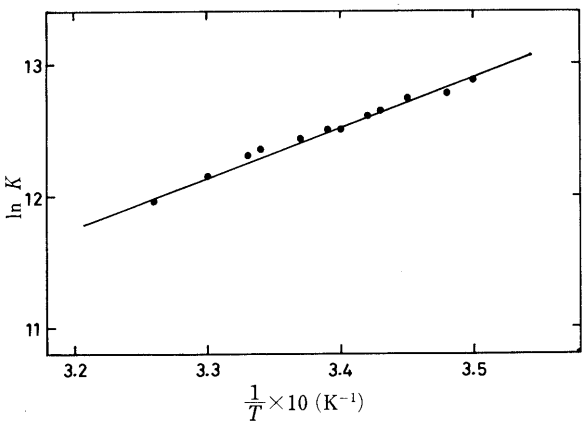

Fig. 2. Van't Hoff Plot of the Apparent Binding Constants at pH 8.0
Conditions were the same as in Fig. 1.

the fluorescence of tryptophan was not affected. Although it is clear that there are multiple binding sites for given ligands having different binding affinities on the BSA molecule,[16-18] it is extremely difficult to determine each binding parameter from the fluorescence curves. Therefore, in this study, we calculated the apparent binding constants and the numbers of binding sites based on the assumption of the equivalence and independence of the binding sites. The calculated apparent binding constants and the number of the binding sites are summarized in Table I. These values are of the same order of magnitude within the pH range studied. A small increase of the apparent binding constant could be observed with increasing pH values and reached maximum at near pH 8.5. This pH is near the pK of the phenolic hydroxyl group of 3,3′-T_2 (pK=8.4). This result resembles the result that T_4, T_3 bound to human serum albumin (HSA) maximally at pHs corresponding to the pKs of their phenolic hydroxyl group of T_4 (pK=6.73) and T_3 (pK=8.5).[15] In the case of r-T_3 and 3-monoiodo-L-thyronine (T_1) binding to BSA,[19,20] binding also reached its maximum near the pKs of r-T_3 (pK=7.4) and 3-T_1 (pK=9.67), respectively. These results suggest that iodination of the 4′-hydroxyl group of the outer ring of the thyroid hormone metabolites plays an important role in strengthening the binding of these on the albumin molecule. The apparent binding constant of $2.4(0.06)\times 10^5\,M^{-1}$ at pH 7.4 is about one-eighth lower than the value of $1.16\ (0.4)\times 10^6\,M^{-1}$ at pH 7.4 for T_4. It resembles the value of $3.8\ (0.14)\times 10^5\,M^{-1}$ at pH 8.6 for T_3 or $4.43\ (0.15)\times 10^5\,M^{-1}$ at pH 7.4 for r-T_3, and is higher than the value of $8.85\ (1.07)\times 10^4\,M^{-1}$ at pH 7.4 for 3-T_1. A large number of binding sites on an albumin molecule for 3,3′-T_2 is considerably different from a few binding sites for T_4, T_3 or r-T_3[15,19] and resemble about 24 binding sites for 3-T_1.[20] This result suggests the existence of a large number of non-specific binding pockets on the BSA molecule which fit the size for outer ring deiodinated or mono iodinated thyronine metabolites. The decrease of the binding constants above pH 8.5 could be explained by some alkaline conformational change of BSA.[21] The thermodynamic parameters for 3,3′-T_2 binding to BSA were also obtained at pH 8.0 by measuring the temperature dependence of the binding constant at a temperature range of 10—35 °C. The binding constant decreased with increasing temperature from $3.9\ (0.1)\times 10^5\,M^{-1}$ at 12.5 °C to $1.6\ (0.2)\times 10^5\,M^{-1}$ at 34.0 °C. The Van't Hoff plot is shown in Fig. 2. $\ln K$ is linearly related to $1/T$ in this temperature range. The enthalpy change, ΔH^0, was evaluated from the slope of the linear line as -7.75 kcal mol^{-1} at 25 °C. The free energy change, ΔG^0, was $-7.36\ (0.02)$ kcal mol^{-1} at 25 °C at pH 8.0 and the entropy change, ΔS^0, was -1.51 e.u. at 25 °C. The free energy change of $-7.3\ (0.02)$ kcal mol^{-1} resembles that of $-8.44\ (0.15)$ kcal mol^{-1} for the binding of T_4 to BSA at pH 7.4 at 24 °C[6] or $-7.7\ (0.09)$ kcal mol^{-1} for the binding of r-T_3 to BSA.[19] The principal contribution to the free energy binding of 3,3′-T_2 to BSA is derived from the large increase in the enthalpy term. The small decrease of the entropy is, however, very different from its large increase in T_4 binding to HSA (21—25 e.u.)[16] or r-T_3 binding to BSA (10.4 e.u.),[19] in which the entropy term is the main contribution to the free energy change for T_4 or r-T_3 bindings. The large negative enthalpy change and small negative entropy change could be partly explained by assuming rather hydrated water molecules on the 3,3′-T_2 bound BSA molecule, because the large increase of the entropy in T_4 binding to HSA could be accounted for by the release of water molecules from both HSA and T_4 molecules.[16]

References

1) J. Robbins, S. Y. Cheng, M. C. Gershengorn, D. Glinoer, H. J. Cahnman and H. Edelhoch, *Recent Prog. Horm. Res.*, **34**, 477 (1978).
2) I. J. Chopra, D. H. Solomon, U. Chopra, S. Y. Wu, D. A. Fisher and Y. Nakamura, *Recent Prog. Horm. Res.*, **34**, 521 (1978).
3) V. Cody, *Endocr. Rev.*, **1**, 140 (1980).
4) N. Okabe, N. Manabe, R. Tokuoka and K. Tomita, *J. Biochem.* (Tokyo), **77**, 181 (1975).
5) R. Tokuoka, N. Okabe and K. Tomita, *J. Biochem.* (Tokyo), **87**, 1729 (1980).
6) R. F. Steiner, J. Roth and J. Robbins, *J. Biol. Chem.*, **241**, 560 (1966).
7) K. Sterling, *J. Clin. Invest.*, **43**, 1721 (1964).
8) M. Tabachnick, *J. Biol. Chem.*, **242**, 1646 (1967).
9) B. G. Jenkins and R. B. Lauffer, *J. Clin. Endocrinol. Metab.*, **45**, 339 (1977).
10) W. H. Pealman and I. F. F. Fong, *J. Biol. Chem.*, **247**, 8078 (1972).
11) R. G. Reed, F. W. Putnum and T. Peter, Jr., *Biochem. J.*, **191**, 867 (1980).
12) N. A. Attallah and G. F. Lata, *Biochim. Biophys. Acta*, **168**, 321 (1968).
13) C. L. Gemmill, *Arch. Biochem. Biophys.*, **54**, 359 (1955).
14) J. Koehrle, M. Auf'mkolk, H. Rokos, R. D. Hesch and V. Cody, *J. Biol. Chem.*, **261**, 11613 (1986).
15) M. Tabachnick, *J. Biol. Chem.*, **239**, 1242 (1964).

16) B. G. Jenkins and R. B. Lauffer, *Mol. Pharmacol.*, **37**, 111 (1990).
17) T. Peters, Jr., *Adv. Protein Chem.*, **37**, 161 (1985).
18) D. C. Carter, X.-Y. He, S. H. Munson, O. D. Twigg, K. M. Gernert, M. B. Broom and T. Y. Miller, *Science*, **244**, 1195 (1989).
19) N. Okabe, N. Mano and S. Tahira, *Biochim. Biophys. Acta*, **990**, 303 (1989).
20) N. Okabe and E. Takimoto, *J. Biochem.* (Tokyo), **97**, 1317 (1985).
21) W. J. Leonard, Jr., K. K. Vijai and J. F. Foster, *J. Biol. Chem.*, **238**, 1984 (1963).

Synthesis of (−)-Patchoulipyridine and Related Compounds

Junko KOYAMA,*[,a] Teruyo OKATANI,[a] Tamaki OGURA,[a] Kiyoshi TAGAHARA,[a] and Hiroshi IRIE[b]

Kobe Women's College of Pharmacy,[a] Kobe 658, Japan and Faculty of Pharmaceutical Sciences,[b] Nagasaki University, Nagasaki 852, Japan.
Received June 27, 1990

Synthesis of optically active sesquiterpene alkaloids, patchoulipyridine and related compounds, was accomplished by application of a method for constructing cycloalkenopyridines by thermal rearrangement of *O*-2-butenyloximes.

Keywords sesquiterpene alkaloid; (−)-patchoulipyridine; thermal rearrangement; *O*-2-butenyloxime

Sesquiterpene alkaloids, patchoulipyridine (**1**) and epiguaipyridine (**2**), were isolated from the essential oil of *Pogostemon patchouli* Pellet. by Büchi and his co-workers[1] and syntheses of these alkaloids have been completed by several groups.[1-5]

In this paper, we report the synthesis of optically active patchoulipyridine (**1**) and related compounds by using a synthetic method for constructing cycloalkenopyridines by thermal rearrangement of oxime *O*-allyl ethers.[6]

(+)-(1*S*,5*R*)-1,8,8-Trimethylbicyclo[3.2.1]octan-3-one (**3**), which was synthesized from (+)-10-camphorsulfonic acid monohydrate according to Lightner and his co-workers,[7] was treated with *O*-2-butenylhydroxylamine[6] (**4**) in ethanol in the presence of sodium acetate to give the corresponding oxime (**5**) as an oil in 87% yield. Thermolysis of the oxime (**5**) in a sealed glass tube at 180 °C (bath temperature) for 24 h under air gave a mixture of cycloalkenopyridines, which were separated in pure form by preparative thin layer chromatography (PTLC) on silica gel (20% recovery of the starting material). The least polar one was 2,8-dimethyl-(5,8-dimethylmethano)cyclohepta[*b*]-pyridine (**6**) (24.5%). The middle one was patchoulipyridine (**1**) (7.8%), and the most polar one was 4,8-dimethyl-(5,8-dimethylmethano)cyclohepta[*b*]pyridine (**7**) (2.5%). The structures of **6** and **7** were revealed by their proton nuclear magnetic resonance (^{1}H-NMR) spectra. Thus, **6** showed no signal due to the α-proton of the pyridine ring, while **7** showed the α-proton signal at δ 8.19. No detectable amount of the regioisomeric cycloalkenopyridine (**8**) was obtained. This might be due to the subtle steric effect of a methyl group on the bicyclooctane framework during the course of the cyclization reaction.[6] The specific optical rotation of synthetic patchoulipyridine (**1**) was $[\alpha]_D^{25}$ −27.3° (*c*=0.5, EtOH) (natural patchoulipyridine, $[\alpha]_D^{28}$ −31.3° (*c*=5.06, EtOH)[1]) and its spectral properties showed good agreement with those described in the literature.[1] The synthetic patchoulipyridine was purified by recrystallization of its di-*p*-toluoyl-D-tartrate followed by regeneration, $[\alpha]_D^{25}$ −34.9° (*c*=0.57, EtOH). The enantiomer of (−)-patchoulipyridine was synthesized from (−)-(1*R*,5*S*)-1,8,8-trimethylbicyclo[3.2.1]octan-3-one (**9**), $[\alpha]_D^{25}$ −29° (*c*=0.75, heptane) by the same reaction sequence as used for (−)-patchoulipyridine; its infrared (IR), mass (MS), and ^{1}H-NMR spectra were identical with those of (−)-(**1**) and its specific rotation was $[\alpha]_D^{25}$ +16.9° (*c*=1.22, EtOH). It is likely that the low rotation value was due to the low optical purity of the starting material. Further purification of the enantiomeric patchoulipyridine has not been performed so far.

Experimental

Melting points were determined on a Yanagimoto micro-melting point apparatus and are uncorrected. IR spectra were measured on a Hitachi 270-30 spectrophotometer. ^{1}H- and ^{13}C-NMR spectra were determined in $CDCl_3$ with Me_4Si as the internal reference on NEVA NV-21 and

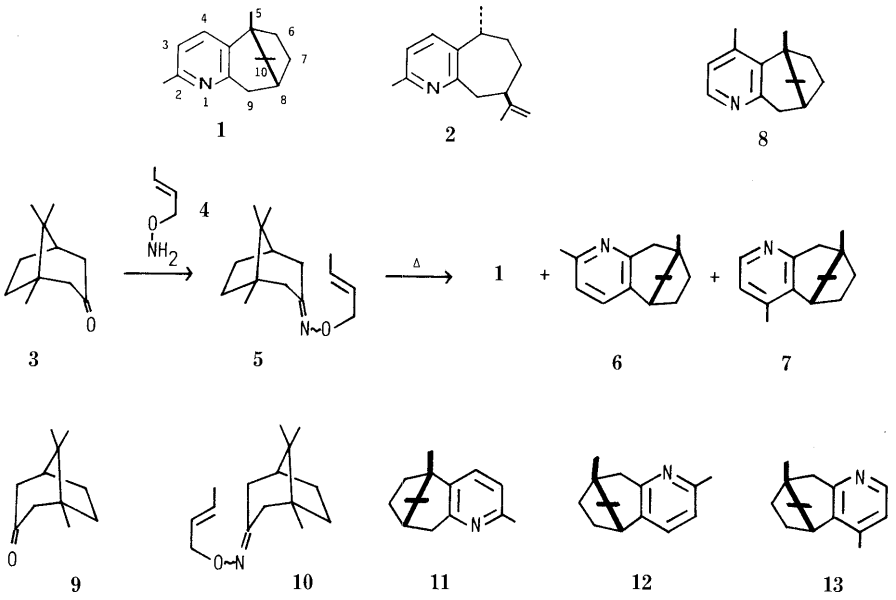

Chart 1

Varian VXR-500 spectrometers. MS spectra were recorded on a JEOL JMS-O1SG spectrometer. Specific rotations were measured with a JASCO DIP-181 polarimeter. PTLC was carried out on Kiesel gel $60F_{254}$ (Merck) with appropriate solvents.

(+)-(1*S*,5*R*)-1,8,8-Trimethylbicyclo[3.2.1]octan-3-one (3)[7] IR $\nu_{max}^{CHCl_3}$ cm^{-1}: 1710 (C=O). ^{1}H-NMR ($CDCl_3$) δ: 0.92 (3H, s, CH_3), 1.00 (3H, s, CH_3), 1.12 (3H, s, CH_3), 1.21—2.75 (9H, m). MS *m/z*: 166.1355 (M^+, Calcd for $C_{11}H_{18}O$, 166.1356). $[\alpha]_D^{25}$ +37.2° (*c*=0.6, heptane) (lit.[7] $[\alpha]_D^{25}$ +39.5° (*c*=0.2, heptane)).

(−)-(1*R*,5*S*)-1,8,8-Trimethylbicyclo[3.2.1]octan-3-one (9) The IR, MS, and ^{1}H-NMR spectra of this sample were identical with those of (+)-(**3**). $[\alpha]_D^{25}$ −29° (*c*=0.75, heptane).

(+)-1,8,8-Trimethylbicyclo[3.2.1]octan-3-one *O*-2-Butenyloxime (5) A solution of bicyclo[3.2.1]octanone (**3**) (0.5 g), *O*-2-butenylhydroxylamine (**4**) (0.8 g), and anhydrous NaOAc (1 g) in EtOH (20 ml) was refluxed for 20 h. After evaporation of the solvent, the residue was extracted with $CHCl_3$. The $CHCl_3$ layer was washed with water, dried ($MgSO_4$), and evaporated to dryness to give bicyclo[3.2.1]octanone oxime (**5**) as an oil. Yield, 0.61 g (87%). IR $\nu_{max}^{CHCl_3}$ cm^{-1}: 1640 (C=N). ^{1}H-NMR ($CDCl_3$) δ: 0.89 (6H, s, $CH_3\times2$), 0.98 (3H, s, CH_3), 1.72 (3H, d like, =CH–CH_3), 4.47 (2H, m, O–CH_2), 5.71 (2H, m, CH=CH). MS *m/z*: 235.1930 (M^+, Calcd for $C_{15}H_{25}NO$, 235.1934). $[\alpha]_D^{25}$ +55.9° (*c*=1.1, EtOH).

(−)-1,8,8-Trimethylbicyclo[3.2.1]octan-3-one *O*-2-Butenyloxime (10) The IR, MS and ^{1}H-NMR spectra were identical with those of (+)-(**5**). $[\alpha]_D^{25}$ −42° (*c*=1.2, EtOH).

Thermolysis of the (+)-*O*-2-Butenyloxime (5) Heating of the oxime (**5**) (300 mg) in a sealed glass tube under air at 180 °C (bath temperature) for 24 h gave a brown oil (275 mg). The crude product was separated by PTLC ($CHCl_3$: MeOH = 50 : 1) to give 2,8-dimethyl-(5,8-dimethylmethano)cyclohepta[*b*]pyridine (**6**) (67 mg) (24.5%), patchoulipyridine (**1**) (21.5 mg) (7.8%), 4,8-dimethyl-(5,8-dimethylmethano)cyclohepta[*b*]pyridine (**7**) (7 mg) (2.5%), and the starting material (**5**) (60 mg) (20%).

Thermolysis of the (−)-*O*-2-Butenyloxime (10) The (−)-oxime was subjected to thermolysis in the same manner as described for the (+)-oxime to give a mixture of (−)-(**12**) (17.5%), (+)-(**11**) (7.1%), and (−)-(**13**) (3.4%).

(+)-2,8-Dimethyl-(5,8-dimethylmethano)cyclohepta[*b*]pyridine (6) IR $\nu_{max}^{CHCl_3}$ cm^{-1}: 1600, 1590. ^{1}H-NMR ($CDCl_3$) δ: 0.79 (3H, s, CH_3), 1.02 (6H, s, $CH_3\times2$), 1.42—2.23 (4H, m, 6 and 7-H_2), 2.48 (3H, s, 2-CH_3), 2.54 (1H, d, *J*=6 Hz, 5-H), 2.67 (1H, d, *J*=18 Hz, 9-H), 2.89 (1H, dd, *J*=18 and 2 Hz, 9-H), 6.86 (1H, d, *J*=7.5 Hz, 3-H), 7.13 (1H, d, *J*=7.5 Hz, 4-H). MS *m/z*: 215.1689 (M^+, Calcd for $C_{15}H_{21}N$, 215.1673). $[\alpha]_D^{25}$ +77.54° (*c*=0.5, EtOH).

(−)-2,8-Dimethyl-(5,8-dimethylmethano)cyclohepta[*b*]pyridine (12) The IR, MS, and ^{1}H-NMR spectra were identical of those of (+)-(**6**). $[\alpha]_D^{25}$ −31° (*c*=1, EtOH).

(−)-Patchoulipyridine (1) IR $\nu_{max}^{CHCl_3}$ cm^{-1}: 1600. ^{1}H-NMR ($CDCl_3$) δ: 0.81 (3H, s, 10-CH_3), 1.04 (3H, s, 10-CH_3), 1.26 (3H, s, 5-CH_3), 1.43 (1H, m, 7-H), 1.67 (1H, m, 6-H), 1.90 (1H, m, 6-H), 2.05 (2H, m, 7 and 8-H), 2.48 (3H, s, 2-CH_3), 2.78 (1H, d, *J*=18 Hz, 9-H), 3.23 (1H, dt, *J*=18 and 3 Hz, 9-H), 6.91 (1H, d, *J*=8 Hz, 3-H), 7.39 (1H, d, *J*=8 Hz, 4-H). ^{13}C-NMR ($CDCl_3$) δ: 15.9 (CH_3-5), 19.1 (CH_3-10), 23.7 (CH_3-2), 24.1 (CH_3-10), 28.6 (C-7), 40.7 (C-9), 41.7 (C-6), 42.6 (C-10), 44.3 (C-8), 46.6 (C-5), 120.4 (C-3), 131.8 (C-4), 139.4 (C-2), 154.2 (C-9a), 155.4 (C-4a). MS *m/z*: 215.1694 (M^+, Calcd for $C_{15}H_{21}N$, 215.1673). $[\alpha]_D^{25}$ −27.3° (*c*=0.5, EtOH). (ref.[1]) $[\alpha]_D^{28}$ −31.3° (*c*=5.06, EtOH)).

Patchoulipyridine Hydroperchlorate: mp 279—283 °C (MeOH–Et_2O) (ref.[1]) mp 276—279 °C). Patchoulipyridine was purified by using di-*p*-toluoyl-D-tartaric acid in ether. Patchoulipyridine di-*p*-toluoyl tartrate: mp 187—188 °C (Et_2O). $[\alpha]_D^{25}$ +72.1° (*c*=0.58, EtOH). A 5% Na_2CO_3 solution (5 ml) was added to patchoulipyridine tartrate (30 mg) in $CHCl_3$ (20 ml) under stirring. The $CHCl_3$ layer was separated and the Na_2CO_3 solution was extracted with $CHCl_3$. The combined $CHCl_3$ fraction was washed with water, dried ($MgSO_4$), and evaporated to give free patchoulipyridine (9 mg, 84%). $[\alpha]_D^{25}$ −34.9° (*c*=0.57, EtOH).

(+)-Patchoulipyridine (11) The IR, MS, and ^{1}H-NMR spectra were identical of those of (−)-(**1**). $[\alpha]_D^{25}$ +16.9° (*c*=1.22, EtOH).

(+)-4,8-Dimethyl-(5,8-dimethylmethano)cyclohepta[*b*]pyridine (7) IR $\nu_{max}^{CHCl_3}$ cm^{-1}: 1600. ^{1}H-NMR ($CDCl_3$) δ: 0.79 (3H, s, CH_3), 1.03 (3H, s, CH_3), 1.05 (3H, s, CH_3), 1.34—2.20 (4H, m, 6 and 7-H_2), 2.24 (3H, s, 4-CH_3), 2.67 (1H, d, *J*=18 Hz, 9-H), 2.81 (1H, d, *J*=7 Hz, 5-H), 2.94 (1H, dd, *J*=18 and 2.5 Hz, 9-H), 6.86 (1H, d, *J*=5 Hz, 3-H), 8.19 (1H, d, *J*=5 Hz, 2-H). MS *m/z*: 215.1684 (M^+, Calcd for $C_{15}H_{21}N$, 215.1673). $[\alpha]_D^{25}$ +129.5° (*c*=0.28, EtOH).

(−)-4,8-Dimethyl-(5,8-dimethylmethano)cyclohepta[*b*]pyridine (13) The IR, MS, and ^{1}H-NMR spectra were identical with those of (+)-(**7**). $[\alpha]_D^{25}$ −40.5° (*c*=0.1, EtOH).

References

1) G. Büchi, I. M. Goldman, and D. W. Mayo, *J. Am. Chem. Soc.*, **88**, 3109 (1966).
2) M-C. Gren, G. Defaye, and M. Fetizon, *Bull. Soc. Chim. Fr.*, **1970**, 3020.
3) A. van der Gen, L. M. van der Linde, and J. G. Witteveen, *Recl. Trav. Chim. Pays-Bas.*, **91**, 1433 (1972).
4) T. Okatani, J. Koyama, K. Tagahara, and Y. Suzuta, *Heterocycles*, **26**, 595 (1987).
5) J. Koyama, T. Okatani, K. Tagahara, Y. Suzuta, and H. Irie, *Heterocycles*, **26**, 925 (1987).
6) J. Koyama, T. Sugita, Y. Suzuta, and H. Irie, *Chem. Pharm. Bull.*, **31**, 2601 (1983).
7) B. V. Crist, S. L. Rodgers, and D. A. Lightner, *J. Am. Chem. Soc.*, **104**, 6040 (1982).

Studies on the Constituents of *Osmanthus* Species. VII.[1] Structures of Lignan Glycosides from the Leaves of *Osmanthus asiaticus* NAKAI

Masataka SUGIYAMA and Masao KIKUCHI*

Tohoku College of Pharmacy, 4–4–1 Komatsushima Aoba-ku, Sendai-shi 981, Japan. *Received July 4, 1990*

A new lignan glycoside, named isoeucommin A (I), and four known lignan glucosides, (+)-syringaresinol-*O*-*β*-D-glucopyranoside (II), phillyrin (III), (−)-olivil-4″-*β*-D-glucopyranoside (IV) and pinoresinol-*O*-*β*-D-glucopyranoside (V), were isolated from the leaves of *Osmanthus asiaticus* NAKAI (Oleaceae). The structure of I was determined to be (+)-medioresinol-4″-*O*-*β*-D-glucopyranoside on the basis of chemical and spectral data.

Keywords Oleaceae; *Osmanthus asiaticus*; lignan glycoside; isoeucommin A; (+)-medioresinol-4″-*O*-*β*-D-glucopyranoside; NMR

We have already reported the isolation of phenylpropanoid glycosides from *Osmanthus* (*O.*) *asiaticus* NAKAI (Oleaceae).[1] We now wish to report the isolation and structure elucidation of a new lignan glycoside, named isoeucommin A (I), as well as the isolation of four lignan glycosides, (+)-syringaresinol-*O*-*β*-D-glucopyranoside (II), phillyrin (III), (−)-olivil-4″-*β*-D-glucopyranoside (IV) and (+)-pinoresinol-*O*-*β*-D-glucopyranoside (V).

The fresh leaves of *O. asiaticus* NAKAI (Japanese name; Ginmokusei) were extracted with MeOH and the MeOH extract was suspended in a small excess of water. This suspension was extracted with $CHCl_3$, Et_2O, AcOEt and *n*-BuOH, successively. The AcOEt-soluble fraction was chromatographed on silica gel to give six fractions (frs. 1—6). After repeated chromatography (silica gel and Sephadex LH-20) of these fractions, five lignan glycosides (I—V) were isolated.

Isoeucommin A (I) was isolated as an amorphous powder. On acetylation with acetic anhydride and pyridine, I gave a pentaacetate (I_a), which gave a peak at *m/z* 910 $(M+H+TEA^{2)})^+$ on fast atom bombardment mass spectrometry (FAB-MS). The infrared (IR) spectrum of I suggested the presence of hydroxyl (3600—3000 cm^{-1}) and aromatic (1600, 1505 cm^{-1}) moieties. The proton nuclear magnetic resonance (^{1}H-NMR) spectrum of I showed the signals of three methoxyl groups [δ 3.84 (6H, s), 3.87 (3H, s)], five aromatic protons [δ 6.65 (2H, s), 6.92 (1H, dd, J=8.0, 2.0 Hz), 7.02 (1H, J=2.0 Hz), 7.14 (1H, d, J=8.0 Hz)] and other protons. Hydrolysis of I with *β*-glucosidase gave an aglycone (I_b) as an amorphous powder, $[\alpha]_D^{22}$ +62.5° ($CHCl_3$), whose ^{1}H-NMR and IR spectra and thin-layer chromatography (TLC) behavior were identical with those of (+)-medioresinol.[3] The presence of glucose in the hydrolysate was detected by paper chromatography (PC). The above result and the carbon-13 nuclear magnetic resonance (^{13}C-NMR) spectrum suggested that I is (+)-medioresinol monoglucopyranoside and that a glucosyl group is attached to a phenolic hydroxyl group at the 4′ or 4″ position. The position of the glucosyl linkage in I was investigated as follows. In a nuclear Overhauser effect (NOE) experiment, irradiation at δ 4.86 (1-H of the *β*-glucopyranosyl moiety) enhanced the intensity of the signal at δ 7.14 (5″-H) (11%), suggesting that the glucosyl group is attached to 4″-OH. The ^{13}C-NMR spectrum (Table I) of I_a was compared with those of the acetates of four known lignan glucopyranosides, (+)-syringaresinol-*O*-*β*-D-glucopyranoside (II_a),[3] (+)-pinoresinol-*O*-*β*-D-glucopyranoside (V_a),[4] liriodendrin ((+)-syringaresinol-di-*β*-D-glucopyranoside) (VI_a)[5] and (+)-medioresinol-di-*β*-D-glucopyranoside (VII_a).[5] It was apparent that the glucosyl group was attached to 4″-OH.

On the basis of the above-mentioned evidence, the structure of isoeucommin A was determined to be (+)-medioresinol-4″-*O*-*β*-D-glucopyranoside (I).

Compound II was purified as the pentaacetate (II_a). The ^{1}H-NMR spectrum of II_a showed the signals of four alcoholic acetoxyl groups [δ 2.02, 2.03, 2.04, 2.05 (each 3H, s)], a phenolic acetoxyl group [δ 2.34 (3H)] and four methoxyl groups [δ 3.83 (12H, s)]. From the above-mentioned evidence and the ^{13}C-NMR spectrum, II_a was

TABLE I. ^{13}C-NMR Chemical Shifts (15 MHz, $CDCl_3$)

Carbon	I_a	II_a	V_a	VI_a	VII_a
1	54.4	54.6	54.4	54.6	54.4
2	86.0	86.0	85.7	86.0	86.0
4	72.1	72.2	72.0	72.2	72.2
5	54.6	54.5	54.5	54.6	54.4
6	85.7	86.0	85.7	86.0	85.7
8	72.1	72.2	72.0	72.2	72.2
1′	140.0	134.4	140.5	134.4	134.3
2′	102.5	103.5	110.2	103.6	103.5
3′	152.7	153.5	151.6	153.6	153.5
4′	123.0	138.3	139.5	138.4	138.4
5′	152.7	153.5	123.0	153.6	153.5
6′	102.5	103.5	118.1	103.6	103.5
1″	138.1	140.0	138.1	134.4	138.1
2″	110.9	102.5	110.9	103.6	110.9
3″	151.2	152.7	151.2	153.6	151.2
4″	145.9	123.0	145.9	138.4	145.9
5″	120.4	152.7	120.4	153.6	120.4
6″	118.4	102.5	118.4	103.6	118.3
OCH_3	56.3	56.4	56.3	56.6	56.3
		56.6			56.6
Glc 1	101.0	101.5	101.0	101.5	101.0
					101.5
Glc 2	71.8	72.2	71.5	72.2	71.5
Glc 3	72.9	73.3	72.8	73.3	72.8
					73.3
Glc 4	68.7	68.8	68.7	68.9	68.7
Glc 5	72.1	72.2	72.0	72.2	72.2
Glc 6	62.1	62.6	62.2	62.6	62.6
					62.1
$\underline{C}H_3COO$	20.6	20.7	20.6	20.7	20.6
$CH_3\underline{C}OO$	169.1	169.1	169.3	169.6	169.7
	169.7	169.8	169.6	169.8	170.5
	170.6	170.9	170.5	170.7	170.8
	170.9		170.8	170.9	

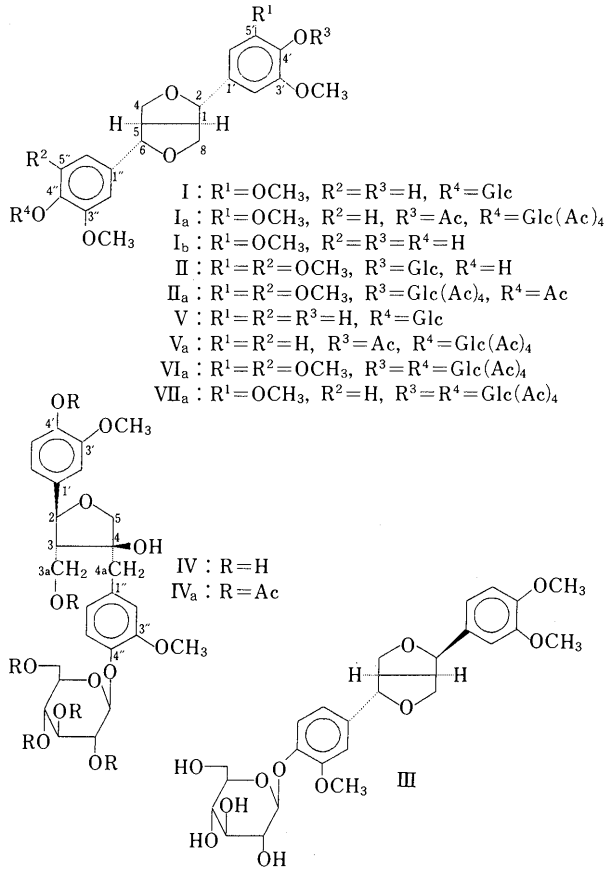

Chart 1

suggested to be (+)-syringaresinol-*O*-*β*-D-glucopyranoside pentaacetate. This identification was confirmed by comparison of II_a with an authentic sample[5] ($[\alpha]_D$, TLC, ^1H- and ^{13}C-NMR). Thus, II was proved to be (+)-syringaresinol-*O*-*β*-D-glucopyranoside.

Compound III was isolated as colorless needles, mp 154—155 °C. The IR spectrum suggested the presence of hydroxyl groups (3600—3000 cm^{-1}) and aromatic rings (1590, 1510 cm^{-1}). The ^1H-NMR spectrum of III showed the signals of three methoxyl groups [δ 3.75, 3.76, 3.77 (each 3H, s)]. From the above-mentioned evidence, III was suggested to be phillyrin. This identification was confirmed by comparison of III with an authentic sample[6] ($[\alpha]_D$, TLC, ^1H- and ^{13}C-NMR).

Compound IV was purified as the hexacetate (IV_a). The ^1H-NMR spectrum of IV_a showed the signals of five alcoholic acetoxyl groups [δ 2.03 (9H, s) and 2.08 (6H, s)], a phenolic acetoxyl group [δ 2.29 (3H)], two methoxyl groups [δ 3.76 (3H, s) and 3.82 (3H, s)] and six aromatic protons [δ 6.69—7.45 (6H, m)]. From the above-mentioned evidence, IV_a was suggested to be (−)-olivil-4″-*β*-D-glucopyranoside hexaacetate. This identification was confirmed by comparison of IV_a with an authentic sample[7] ($[\alpha]_D$, TLC, ^1H- and ^{13}C-NMR). Thus, IV was proved to be (−)-olivil-4″-*β*-D-glucopyranoside.

Compound V was isolated as an amorphous solid. The IR spectrum suggested the presence of hydroxyl groups (3600—3000 cm^{-1}) and aromatic rings (1600, 1510 cm^{-1}). The ^1H-NMR spectrum of V showed the signals of two methoxyl groups [δ 3.85, 3.87 (each 3H, s)], 2-H [δ 4.71 (1H, d, J=4.8 Hz)], 6-H [δ 4.76 (1H, d, J=4.8 Hz)] and six aromatic protons [δ 6.75—7.15 (6H, m)]. From the above-mentioned evidence and the ^{13}C-NMR spectrum, V was suggested to be (+)-pinoresinol-*O*-*β*-D-glucopyranoside. This identification was confirmed by comparison of V with an authentic sample[7] ($[\alpha]_D$, TLC, ^1H- and ^{13}C-NMR).

Experimental

Melting points were determined on a Yanagimoto MP-S3 micro-melting point apparatus and are uncorrected. Optical rotations were determined with a JASCO DIS-360 digital polarimeter. IR spectra were recorded with a Shimadzu IR-430 infrared spectrophotometer. ^1H-NMR and ^{13}C-NMR spectra were recorded with a JEOL JMX-GSX 400 (400 and 100 MHz, respectively) or JEOL FX-60 (60 and 15 MHz, respectively) spectrometer. Chemical shifts are given on a δ (ppm) scale with tetramethylsilane as an internal standard (s, singlet; d, doublet; dd, double doublet; m, multiplet; br, broad). Mass spectra (MS) were recorded on a JEOL JMS-DX 300 mass spectrometer. Column chromatography was carried out on Kieselgel 60 (Merck; 70—230 and 230—400 mesh) and Sephadex LH-20 (Pharmacia Fine Chemical). TLC was carried out with precoated Kieselgel 60 plates (Merck) and detection was achieved by spraying 50% H_2SO_4 followed by heating.

Isolation Fresh leaves of *O. asiaticus* (2.2 kg), collected in October 1988, in Sendai, Japan, were extracted with MeOH at room temperature for one month. The MeOH extract was concentrated under reduced pressure and the residue was suspended in a small excess of water. This suspension was extracted with $CHCl_3$, Et_2O, AcOEt and *n*-BuOH, successively. The AcOEt-soluble fraction was concentrated under reduced pressure to afford the residue (17.4 g). This residue was chromatographed on a silica gel column using $CHCl_3$–MeOH–H_2O (30 : 10 : 1) and the eluate was separated into six fractions (frs. 1—6).

Fraction 2 was rechromatographed on a Sephadex LH-20 column using MeOH–H_2O (1 : 1) to give III (50 mg). The ^1H-NMR spectrum of fraction 2-2 showed no acetyl group signals. Fraction 2-2 was acetylated with acetic anhydride in pyridine and purified by chromatography on silica gel with AcOEt–*n*-hexane (3 : 2) to give the pentaacetate (II_a) (15 mg).

Fraction 3 was rechromatographed on a Sephadex LH-20 column using MeOH–H_2O (1 : 1) to give I (50 mg). I (15 mg) was acetylated with acetic anhydride in pyridine and purified by chromatography on silica gel with acetone–*n*-hexane (2 : 3) to give the pentaacetate (I_a) (12 mg).

Fraction 4 was rechromatographed on a Sephadex LH-20 column using MeOH–H_2O (1 : 1) and the eluate was separated into six fractions. The ^1H-NMR spectrum of fraction 4-1 showed no acetyl group signals. Fraction 4-1 was acetylated with acetic anhydride in pyridine and purified by chromatography on silica gel with acetone–*n*-hexane (2 : 3) to give the hexaacetate (IV_a) (20 mg). Fraction 4-3 was rechromatographed on a silica gel column using $CHCl_3$–MeOH–H_2O (30 : 10 : 1) to give V (30 mg).

Isoeucommin A (I) An amorphous powder (from EtOH), mp 110—113 °C. $[\alpha]_D^{23}$ 0.0° (c=0.6, MeOH). UV λ_{max}^{MeOH} nm: 229.5, 274.5. IR ν_{max}^{Nujol} cm^{-1}: 3600—3000, 1600, 1505. ^1H-NMR (400 MHz, CD_3OD) δ: 3.13 (2H, br s, 1-H and 5-H), 3.84 (6H, s, 2 × OCH_3), 3.87 (3H, s, OCH_3), 4.71 (1H, d, J=4.4 Hz, 2-H), 4.76 (1H, d, J=4.4 Hz, 6-H), 6.65 (2H, s, 2′-H and 6′-H), 6.92 (1H, dd, J=8.0, 2.0 Hz, 6″-H), 7.02 (1H, d, J=2.0 Hz, 2″-H), 7.14 (1H, d, J=8.0 Hz, 5″-H). ^{13}C-NMR (400 MHz, CD_3OD) δ: 55.6 (1 and 5), 56.8 (OCH_3), 56.9 (2 × OCH_3), 62.6 (6‴), 71.4 (4‴), 72.8 (4 and 8), 75.0 (2‴), 77.9 (3‴), 78.3 (5‴), 87.1 (6), 87.7 (2), 102.9 (1‴), 104.6 (2′ and 6′), 111.7 (2″), 118.1 (5″), 119.8 (6″), 133.2 (1′), 137.5 (1″ and 4′), 147.6 (3″), 149.4 (3′ and 5′), 151.0 (4″).

Enzymatic Hydrolysis of I A solution of I (30 mg) in water (3 ml) was incubated with *β*-glucosidase (30 mg, Sigma Chemical Company) at 37 °C overnight, then evaporated under reduced pressure, and the residue was extracted with MeOH. The extractive was fractionated by silica gel column chromatography (solvent: $CHCl_3$–MeOH–H_2O = 8 : 2 : 0.2) into the aglycon (I_b, 10 mg) and glucose (6 mg). (+)-Medioresinol (I_b): an amorphous powder, $[\alpha]_D^{22}$ +62.5° (c=1.0, $CHCl_3$). IR ν_{max}^{KBr} cm^{-1}: 3480, 1616, 1520. ^1H-NMR (60 MHz, $CDCl_3$) δ: 2.90—3.20 (2H, m, 1-H and 5-H), 3.80—4.40 (4H, m, 4-H and 8-H), 3.88 (9H, s, 3 × OCH_3), 4.64—4.80 (2H, m, 2-H and 6-H), 6.57 (2H, s, 2′-H and 6′-H), 6.72—6.93 (3H, m, arom. protons). D-Glucose: a syrup, $[\alpha]_D^{22}$ +51.5° (c=0.5, H_2O). PC (paper, Toyo Roshi No. 51; solvent, BuOH–AcOH–H_2O (4 : 1 : 2); visualizing agent, aniline hydrogen phthalate), Rf=0.24 (glucose).

Isoeucommin A Pentaacetate (I_a) An amorphous powder (from EtOH), mp 82—84 °C, $[\alpha]_D^{23}$ −3.3° (c=0.9, $CHCl_3$). IR $\nu_{max}^{CHCl_3}$ cm^{-1}: 1745, 1600,

1500. FAB-MS *m/z*: 910 $(M+H+TEA)^+$. ^{1}H-NMR (400 MHz, $CDCl_3$) δ: 2.04, 2.08 (each 6H, CH_3COO), 2.33 (3H, CH_3COO), 3.08 (2H, m, 1-H and 5-H), 3.82, 3.83, 3.84 (each 3H, s, OCH_3), 4.77 (2H, m, 2-H and 6-H), 4.94 (1H, d, $J=7.7$ Hz, 1‴-H), 6.60 (2H, s, 2′-H and 6′-H), 6.82 (1H, br d, $J=8.4$ Hz, 6″-H), 6.93 (1H, br s, 2″-H), 7.09 (1H, d, $J=8.4$ Hz, 5″-H). ^{13}C-NMR (15 MHz, $CDCl_3$): Table I.

(+)-Syringaresinol-*O*-*β*-D-glucopyranoside Pentaacetate (II_a) An amorphous powder (from EtOH), $[\alpha]_D^{22}$ $-11.2°$ ($c=0.8$, $CHCl_3$), mp 87—90 °C. IR $\nu_{max}^{CHCl_3}$ cm^{-1}: 1600, 1505. ^{1}H-NMR (400 MHz, $CDCl_3$) δ: 2.02, 2.03, 2.04, 2.05 (each 3H, s, CH_3COO), 2.34 (3H, CH_3COO), 3.09 (2H, m, 1-H and 5-H), 3.83 (12H, s, $4\times OCH_3$), 6.56 (2H, s, arom. protons), 6.59 (2H, s, arom. protons). ^{13}C-NMR (15 MHz, $CDCl_3$): Table I.

Phillyrin (III) Colorless needles (from MeOH), $[\alpha]_D^{23}$ $+48.5°$ ($c=0.5$, MeOH), mp 154—155 °C. IR ν_{max}^{Nujol} cm^{-1}: 3600—3000, 1590, 1510. ^{1}H-NMR (400 MHz, DMSO-d_6) δ: 3.75, 3.76, 3.77 (each 3H, s, OCH_3), 6.85—7.10 (6H, m, arom. protons).

(−)-Olivil-4″-*β*-D-glucopyranoside Hexaacetate (IV_a) An amorphous powder (from EtOH), $[\alpha]_D^{20}$ $-34.6°$ ($c=2.2$, $CHCl_3$), mp 109—110 °C. IR $\nu_{max}^{CHCl_3}$ cm^{-1}: 1745, 1600, 1500. ^{1}H-NMR (60 MHz, $CDCl_3$) δ: 2.03 (9H, s, $2\times CH_3COO$), 2.08 (3H, s, CH_3COO), 2.29 (3H, s, CH_3COO), 3.76 (3H, s, OCH_3), 3.82 (3H, s, OCH_3), 6.69—7.45 (6H, m, arom. protons).

(+)-Pinoresinol-*O*-*β*-D-glucopyranoside (V) An amorphous solid (from EtOH), $[\alpha]_D^{21}$ $+10.8°$ ($c=1.0$, MeOH). IR ν_{max}^{KBr} cm^{-1}: 3600—3000, 1600, 1510. ^{1}H-NMR (400 MHz, CD_3OD) δ: 3.85, 3.87 (each 3H, s, OCH_3), 4.71 (1H, d, $J=4.8$ Hz, 2-H), 4.76 (1H, d, $J=4.8$ Hz, 6-H), 6.75—7.15 (6H, m, arom. protons).

Acknowledgment The authors are grateful to Dr. K. Hisamichi of Tohoku College of Pharmacy for NMR measurements.

References and Notes

1) M. Sugiyama and M. Kikuchi, *Chem. Pharm. Bull.*, **38**, 2953 (1990).
2) TEA: triethanolamine.
3) T. Deyama, T. Ikawa and S. Nishibe, *Chem. Pharm. Bull.*, **33**, 3651 (1985).
4) M. Kikuchi and Y. Yamauchi, *Yakugaku Zasshi*, **104**, 535 (1984).
5) M. Kikuchi and Y. Yamauchi, *Yakugaku Zasshi*, **105**, 542 (1985).
6) M. Chiba, S. Hisada, S. Nishibe and H. Thieme, *Phytochemistry*, **19**, 335 (1980).
7) M. Kikuchi and Y. Yamauchi, *Yakugaku Zasshi*, **104**, 390 (1984).

Studies on *as*-Triazine Derivatives. XVI.[1] Reaction of 1,2,4-Triazinecarbonitriles with Carbanions

Setsuya OHBA, Shoetsu KONNO, and Hiroshi YAMANAKA*

Pharmaceutical Institute, Tohoku University, Aobayama, Sendai 980, Japan. *Received July 25, 1990*

A cyano group in 1,2,4-triazines, regardless of its position, acted as an effective leaving group in reactions with carbanions. Thus, the reactions gave the corresponding substituted products in place of the compounds formed by addition reaction of carbanions to the cyano group. Grignard reaction of these carbonitriles is also described.

Keywords active methylene compound; addition; carbanion; cyano group; Grignard reagent; ketone; substitution; 1,2,4-triazine

Like Grignard reagents, enolate anions, in principle, add to cyano groups in π-electron-deficient *N*-heteroaromatic nuclei, and this represents a versatile method for the preparation of *N*-heteroaromatic enaminoketones.[2] A typical example is the reaction of 2,6-dimethylpyrimidine-4-carbonitrile with these reagents, as shown in Chart 1.

On the other hand, it is also known that 4-quinazolinecarbonitrile (**1**) reacts with Grignard reagents to give 4-alkyl (or 4-aryl) quinazoline (**2**) and that the reaction with methylketones gives rise to the formation of 4-quinazolyl-

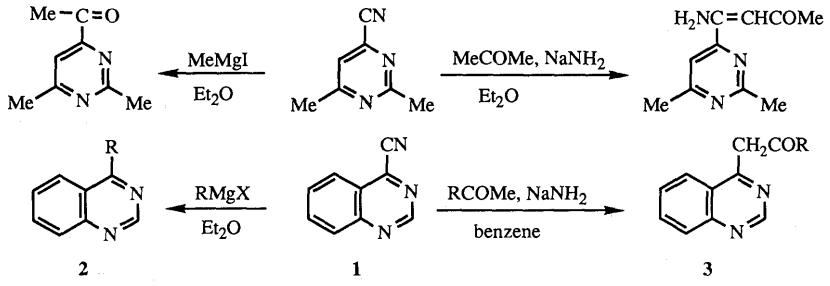

Chart 1

TABLE I. Reactions of **4**, **6**, and **8** with Active Methylene Compounds or with Ketones

Substrate Compd. No.	Nucleophile X-CH-Y X	Y	Reaction conditions Temp.[a]	Time (h)	Product Compd. No.	Yield (%)	mp (°C)	Recryst. solvent
4	H	COPh	B	10	**5a**	47	128—130[b]	Ethyl acetate
	$-CO(CH_2)_4-$		B	10	**5b**	51	170—172[c]	Ethyl acetate
	CN	CN	R	18	**5c**	73	219—220 (dec.)[d]	Acetone
	CN	CO_2Et	B	3	**5d**	51	231(dec.)[e]	Ethyl acetate
	CO_2Et	CO_2Et	B	10	**5e**	21	65—66	Hexane
6	H	COPh	B	5	**7a**	61	192—194[f]	Ethyl acetate
	$-CO(CH_2)_4-$		B	5	**7b**	61	135—136	Ether
	CN	CN	R	18	**7c**	76	261—263 (dec.)[g]	Acetone
	CN	CO_2Et	R	18	**7d**	68	181—183[h]	Ethyl acetate
	CO_2Et	CO_2Et	B	3	**7e**	63	95—97	Hexane
8	H	COPh	B	18	**9a**	51	178—180	Ethyl acetate
	$-CO(CH_2)_4-$		B	18	**9b**	36	120—121	Ether
	CN	CN	B	6	**9c**	71	265—267 (dec.)	Acetone
	CN	CO_2Et	B	24		0 (76)[i]		
	CO_2Et	CO_2Et	B	24		0 (71)[i]		

a) B: boiling point of tetrahydrofuran. R: room temperature. *b*) Lit.[5] mp 130—132 °C. *c*) Lit.[5] mp 172—173 °C. *d*) Lit.[6] mp 220 °C. *e*) Lit.[5] mp 235 °C (dec.). *f*) Lit.[7] mp 192—194 °C. *g*) Lit.[8] mp 261—263 °C. *h*) Lit.[7] mp 181—183 °C. *i*) The figures in parentheses show the recoveries of substrates.

TABLE II. Reactions of **4**, **6**, and **8** with Grignard Reagents

Substrate No.	Temp.	Reagent	Product No.	Yield (%)	mp (°C)	Recryst. solvent
4	R[a]	MeMgI	**10a**	62	162—163[b]	Ethyl acetate
4	R[a]	PhMgBr	**10b**	70	130—132	Ethyl acetate
6	0 °C	MeMgI	**11a**	41	123—125[c]	Ethyl acetate
6	0 °C	PhMgBr	**11b**	46	144—146[d]	Ethyl acetate
8	R[a]	PhMgBr	**12**	66	115—116	Ethyl acetate

a) Room temperature. *b*) Lit.[9] mp 159.5—161.5 °C. *c*) Lit.[10] mp 122—124 °C. *d*) Lit.[11] mp 145—146 °C.

methyleneketones (**3**).[3] Such abnormal behavior of **1** is caused by the extraordinary susceptibility of the C_4–N_3 double bond in the quinazoline ring to nucleophilic reagents, and a few examples in this category have been reported in fused pyrimidine ring systems.[4]

In this paper, we describe the reactions of three positional isomers of 1,2,4-triazinecarbonitriles with various carbanion, in which the cyano group at the 3-, 5- or 6-position acts as an efficient leaving group, together with ketone formation from the 3-cyano and 6-cyano derivatives by means of Grignard reactions.

As listed in Table I, the reaction of diphenyl-1,2,4-triazinecarbonitriles (**4**, **6**, **8**) with acetophenone, cyclohexanone, or active methylene compounds under basic conditions gave the substituted products (**5**, **7**, **9**) corresponding to **3**. Reactions of 3, 5-diphenyl-1,2,4-triazine-6-carbonitrile (**8**) with ethyl cyanoacetate and with diethyl malonate are exceptional, and most of **8** was recovered unchanged. In all cases, no formation of the addition compound(enaminoketone) was detected.

On the other hand, the reactions of **4**, **6**, and **8** with Grignard reagents gave somewhat mixed results as regards the subsitution and addition reactions. The reactions of the 3-carbonitrile (**4**) and the 6-carbonitrile (**8**) with Grignard reagents under traditional conditions, like that of the pyrimidinecarbonitrile, yielded the corresponding ketones (**10a**, **b** and **12**), whereas the reaction of the 5-carbonitrile (**6**) with Grignard reagents gave the substitution products (**11a** and **11b**) corresponding to **2**. The results of these reactions illustrated in Chart 3 are summarized in Table II.

The observations in the present investigation suggest that the chemical properties of the 5-position of 1,2,4-triazine resemble those of the 4-position of quinazoline, while pyrimidine-like character still remains at the 3- and 6-positions of 1,2,4-triazines.

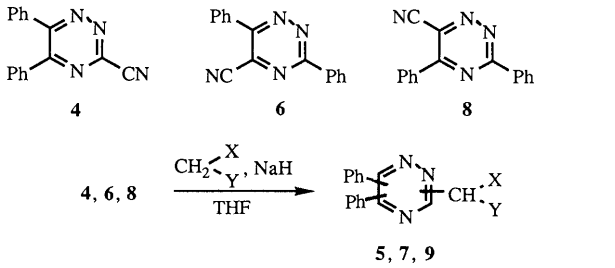

Chart 2

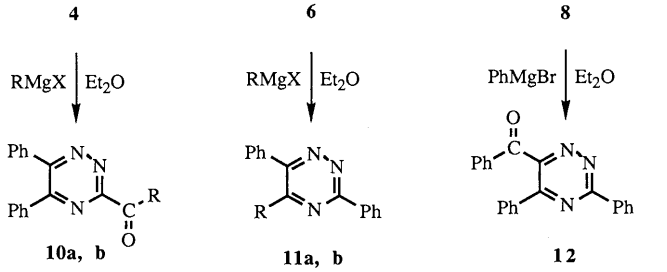

Chart 3

Experimental

All melting points were determined by the capillary method and are uncorrected. Proton nuclear magnetic resonance (^{1}H-NMR) spectra were recorded at either 60 MHz on a JEOL JNM-PMX 60 spectrometer or 100 MHz on a JEOL FX-100 spectrometer. Chemical shifts are quoted in δ values (ppm) with tetramethylsilane (TMS) or 2,2-dimethyl-2-silapentanesulfonic acid sodium salt (DSS) as an internal standard, and coupling constants (J) are given in hertz (Hz). The following abbreviations are used: s = singlet, d = doublet, t = triplet, q = quartet, m = multiplet, and br = broad. Infrared (IR) spectra were obtained on a JASCO IR 810 spectrophotometer.

General Procedure for the Reaction of 1,2,4-Triazinecarbonitriles with Active Methylene Compounds or with Ketones A 50% oil dispersion of NaH (0.12 g, 2.5 mmol) was washed with hexane and the oil-free NaH was suspended in dry tetrahydrofuran (THF) (10 ml). A solution of an active methylene compound or a ketone (2.5 mmol) in dry THF (10 ml) was added to the above suspension and the mixture was stirred at room temperature (in the case of phenylacetonitrile; refluxed) for 15 min. Then, a triazinecarbonitrile (0.53 g, 2 mmol) in dry THF (10 ml) was added, and the whole was stirred at an appropriate temperature. After removal of the solvent under reduced pressure, the residue was dissolved in H_2O and neutralized with diluted HCl. The mixture was extracted with $CHCl_3$ (in the case of malononitrile, precipitated crystals were collected by suction and washed with H_2O). The $CHCl_3$ solution was washed with saturated NaCl solution, dried over Na_2SO_4, and evaporated. The product was pu-

TABLE III. Spectral Data for the Products of the Reaction of **4**, **6**, and **8** with Carbanions

Compd. No.	IR ($CDCl_3$) ν (C≡N, C=O; cm^{-1})	^{1}H-NMR ($CDCl_3$) δ (ppm)
5a	1690	14.3—13.4 (br, 1H), 8.3—7.9 (m, 2H), 7.8—7.3 (m, 13H), 6.54 (s, 1H)
5b	1710	13.7—13.4 (br, 1H), 7.7—7.2 (m, 10H), 2.9—2.5 (m, 8H)
5c	2220, 2200[a]	9.1—8.8 (br, 1H), 7.6—7.1 (m, 10H)[b]
5d	2200, 1650	14.0—13.8 (br, 1H), 7.7—7.2 (m, 10H), 4.35 (q, J=8, 2H), 1.39 (t, J=8, 3H)
5e	1735	7.8—7.2 (m, 10H), 5.34 (s, 1H), 4.32 (q, J=7, 4H), 1.31 (t, J=7, 6H)
7a	1620	16.0—15.8 (br, 1H), 8.6—8.3 (m, 2H), 8.0—7.2 (m, 13H), 6.39 (s, 1H)
7b	1720	8.9—8.5 (m, 2H), 7.8—7.3 (m, 8H), 4.2—3.9 (m, 1H), 2.9—1.4 (m, 8H)
7c	2220, 2200[a]	8.3—8.0 (m), 7.9—7.3 (m)[b,c]
7d	2200, 1650	15.0—14.7 (br, 1H), 8.4—7.9 (m, 2H), 7.9—7.3 (m, 8H), 4.35 (q, J=7, 2H), 1.37 (t, J=7, 3H)
7e	1760	8.8—8.5 (m, 2H), 7.8—7.4 (m, 8H), 5.13 (s, 1H), 4.21 (q, J=7, 4H), 1.23 (t, J=7, 6H)
9a	1615	15.1—15.0 (br, 1H), 8.8—8.4 (m, 2H), 8.1—7.3 (m, 13H), 6.38 (s, 1H)
9b	1720	8.9—8.5 (m, 2H), 7.8—7.3 (m, 8H), 4.3—4.0 (m, 1H), 2.9—1.5 (m, 8H)
9c	2220, 2190[a]	8.2—8.0 (m), 7.8—7.4 (m)[b,c]
10a	1720	7.8—7.2 (m, 10H), 2.95 (s, 3H)
10b	1680	8.5—8.2 (m, 2H), 8.0—7.3 (m, 13H)
11a		8.8—8.5 (m, 2H), 7.9—7.3 (m, 8H), 2.63 (s, 3H)
11b		8.8—8.6 (m, 2H), 7.8—7.3 (m, 13H)
12	1675	8.9—8.5 (m, 2H), 8.2—7.2 (m, 13H)

a) KBr disc. *b*) DMSO-d_6. *c*) The integration ratio is 1:4.

TABLE IV. Analytic Data for the New Compounds

No.	Formula	Analysis (%) Calcd (Found)			No.	Formula	Analysis (%) Calcd (Found)		
		C	H	N			C	H	N
5e	$C_{22}H_{21}N_3O_4$	67.51	5.41	10.74	**9a**	$C_{23}H_{17}N_3O$	78.61	4.88	11.96
		(67.37	5.22	10.85)			(78.38	4.68	11.77)
7a	$C_{23}H_{17}N_3O$	78.61	4.88	11.96	**9b**	$C_{21}H_{19}N_3O$	76.57	5.81	12.76
		(78.75	4.92	11.85)			(76.35	5.73	12.59)
7b	$C_{21}H_{19}N_3O$	76.57	5.81	12.76	**9c**	$C_{18}H_{11}N_5$	72.72	3.73	23.56
		(76.40	5.80	12.74)			(72.60	3.56	23.26)
7e	$C_{22}H_{21}N_3O_4$	67.51	5.41	10.74	**10b**	$C_{22}H_{15}N_3O$	78.32	4.48	12.45
		(67.56	5.19	10.69)			(78.55	4.49	12.56)
8	$C_{16}H_{10}N_4$	74.40	3.90	21.70	**12**	$C_{22}H_{15}N_3O$	78.32	4.48	12.45
		(74.56	4.16	21.59)			(78.05	4.32	12.19)

rified by recrystallization from an appropriate solvent.

General Procedure for the Reaction of 1,2,4-Triazinecarbonitriles with Grignard Reagents A solution of a carbonitrile (0.52 g, 2 mmol) in dry Et_2O (20 ml) was added to a solution of a Grignard reagent in Et_2O, prepared from a halide (2.2 mmol) and metallic magnesium (0.06 g, 2.4 mmol) in dry Et_2O (20 ml). The mixture was vigorously stirred for 2 h and poured into ice-HCl solution. The ethereal phase was separated, washed with H_2O, and dried over $MgSO_4$. After evaporation of the solvent, the residue was recrystallized from AcOEt to give the product.

5,6-Diphenyl-1,2,4-triazine-3-carbonitrile[12] **(4)** $KMnO_4$ (6.4 g, 40 mmol) was added to a solution of 3-methylthio-5,6-diphenyl-1,2,4-triazine[13] (5.6 g, 20 mmol) in AcOH (20 ml) and acetone (200 ml) under cooling in an ice bath. The mixture was stirred for 2 h at room temperature, decolorized by addition of $NaHSO_3$ and H_2O, then poured into H_2O (2.5 l). The separated solid was collected by suction, washed well with H_2O, and dissolved in $CHCl_3$. The $CHCl_3$ solution was dried over Na_2SO_4 and evaporated. After removal of $CHCl_3$, the residue was recrystallized from AcOEt to give 3-methylsulfonyl-5,6-diphenyl-1,2,4-triazine as pale yellow prisms (5.8 g, 93%). mp 140—141 °C (lit.[5] mp 139—140 °C). A solution of the above methylsulfonyl derivative (1.24 g, 4 mmol) in dimethylformamide (DMF) (5 ml) was added in one portion to a solution of NaCN (0.22 g, 4.5 mmol) in DMF (5 ml) under cooling in an ice bath. The mixture was stirred at room temperature for 1 h, diluted with H_2O, and extracted with benzene. The benzene solution was washed well with H_2O, dried over Na_2SO_4, and evaporated. The residue was recrystallized from AcOEt to give yellow needles (0.80 g, 78%), mp 158—159 °C (lit.[5] mp 154—155 °C).

3,6-Diphenyl-1,2,4-triazine-5-carbonitrile[12] **(6)** Compound **6** was prepared according to our previous report.[7]

3,5-Diphenyl-1,2,4-triazine-6-carbonitrile[12] **(8)** 6-Methylthio-3,5-diphenyl-1,2,4-triazine[1] (5.6 g, 20 mmol) was treated with $KMnO_4$ (6.4 g, 40 mmol) as described for the preparation of the 3-methylsulfonyl derivative. Recrystallization from AcOEt gave 6-methylsulfonyl-3,5-diphenyl-1,2,4-triazine as pale yellow prisms (5.8 g, 93%), mp 148—149 °C (lit.[1] mp 150—152 °C). The above methylsulfonyl derivative (1.24 g, 4.0 mmol) was treated with NaCN (0.22 g, 4.5 mmol) as described for the preparation of **4**. Recrystallization from AcOEt gave yellow prisms (0.73 g, 71%), mp 117—119 °C. ^{1}H-NMR ($CDCl_3$–TMS): 8.9—8.7 (m), 8.5—8.3 (m), 8.0—7.6 (m); the integration ratio is 1 : 1 : 3.

References and Notes

1) Part XV: M. Sagi, K. Wada, S. Konno, and H. Yamanaka, *Heterocycles*, **30**, 1009 (1990).
2) Reaction with enolate anions; T. Honma and Y. Tada, *Heterocycles*, **6**, 1985 (1977); M. Yamakawa, T. Kubota, Y. Terui, T. Honma, and Y. Tada, *Bull. Chem. Soc. Jpn.*, **51**, 3059 (1978). Reaction with Grignard reagents; positions 2 and 4 of pyridine: T. Kato, Y. Goto, and T. Chiba, *Yakugaku Zasshi*, **86**, 1022 (1966); position 3 of pyridine: F. B. LaForge, *J. Am. Chem. Soc.*, **50**, 2477 (1928); position 4 of pyridine: Y. Suzuki, *Yakugaku Zasshi*, **81**, 152 (1961); position 2 of quinoline: A. Kaufmann, P. Dandliker, and H. Burkhardt, *Ber.*, **46**, 2932 (1913); position 4 of quinoline: A. Kaufmann, M. Kunker, and H. Peyer, *Ber.*, **46**, 60 (1913); position 1 of isoquinoline: A. Kaufmann, P. Dandliker, and H. Burkhardt, *Ber.*, **46**, 2935 (1913); position 3 of pyridazine: G. Helnish and T. Huber, *J. Heterocycl. Chem.*, **26**, 1787 (1989); position 2 of pyrimidine: W. Klotzer, *Monatsh. Chem.*, **87**, 526 (1956); position 4 of pyrimidine: H. Yamanaka, *Chem. Pharm. Bull.*, **6**, 638 (1958); position 2 of pyrazine: V. K. Smith and S. Kushner, U. S. Patent 2677686 (1954) [*Chem. Abstr.*, **49**, 6322*a* (1955)].
3) T. Higashino, *Chem. Pharm. Bull.*, **10**, 1043, 1048, 1052 (1962).
4) E. Hayashi, T. Higashino, and S. Suzuki, *Yakugaku Zasshi*, **98**, 891 (1978); **T**. Higashino, T. Katori, S. Yoshida, and E. Hayashi, *Chem. Pharm. Bull.*, **28**, 255 (1980).
5) S. Konno, M. Yokoyama, A. Kaite, I. Yamatsuta, S. Ogawa, M. Mizugaki, and H. Yamanaka, *Chem. Pharm. Bull.*, **30**, 152 (1982).
6) R. M. A.-Rahman, *Indian J. Chem., Sect. B*, **25B**, 815 (1986).
7) S. Konno, S. Ohba, M. Agata, Y. Aizawa, M. Sagi, and H. Yamanaka, *Heterocycles*, **26**, 3259 (1987).
8) H. Yamanaka and S. Ohba, *Heterocycles*, **31**, 895 (1990).
9) S. Konno, S. Fujimura, and H. Yamanaka, *Heterocycles*, **22**, 2245 (1984).
10) S. Konno, M. Sagi, E. Takaharu, S. Fujimura, K. Hayashi, and H. Yamanaka, *Chem. Pharm. Bull.*, **36**, 1721 (1988).
11) H. Neunhoeffer, H.-W. Fruhauf, H. Henning, and M. Mutterer, *Tetrahedron Lett.*, **1969**, 3147.
12) The IR spectra of **4**, **6**, and **8** did not show any absorption band due to the cyano group. This is compatible with the reported absence of the absorption band of a cyano group located at a π-deficient position in condensed pyrimidine ring systems: T. Higashino, T. Katori, H. Kawaraya, and E. Hayashi, *Chem. Pharm. Bull.*, **28**, 337 (1980) and references cited therein.
13) W. W. Paudler and **T**.-K. Chen, *J. Heterocycl. Chem.*, **7**, 767 (1970).

Synthesis of Functionalized Indoles by Diels–Alder Reaction Utilizing the Diene Generated by the Alkylation of *N*-Methyl-3-thioacetylpyrrole

Masayuki MURASE, Shinya YOSHIDA, Toshihiro HOSAKA, and Seisho TOBINAGA*

Showa College of Pharmaceutical Sciences, Machida, Tokyo 194, Japan. *Received September 7, 1990*

Cycloaddition reaction of 3-vinylpyrroles, generated by the alkylation of 1-methyl-3-thioacetylpyrrole, with dienophiles provided functionalized indoles.

Keywords cycloaddition; 3-vinylpyrrole; 1-methyl-3-thioacetylpyrrole; alkylation; dienophile; indole

Recently, we reported that functionalized carbazoles can be synthesized by Diels–Alder reaction of the sulfur substituted 3-vinylindoles **2**, generated by the alkylation of thioacetylindole (**1**), with several dienophiles.[1] We also found that such behavior is observed in thioacetylpyrroles. This paper describes the synthesis of indoles having various substituents by means of Diels–Alder reactions of the sulfur substituted 3-vinylpyrrole **7**, generated *in situ* by the

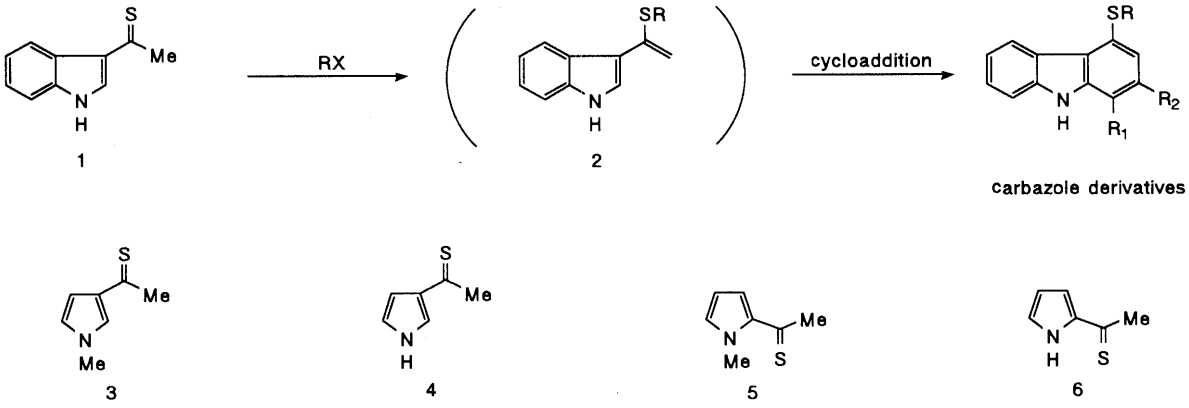

Chart 1

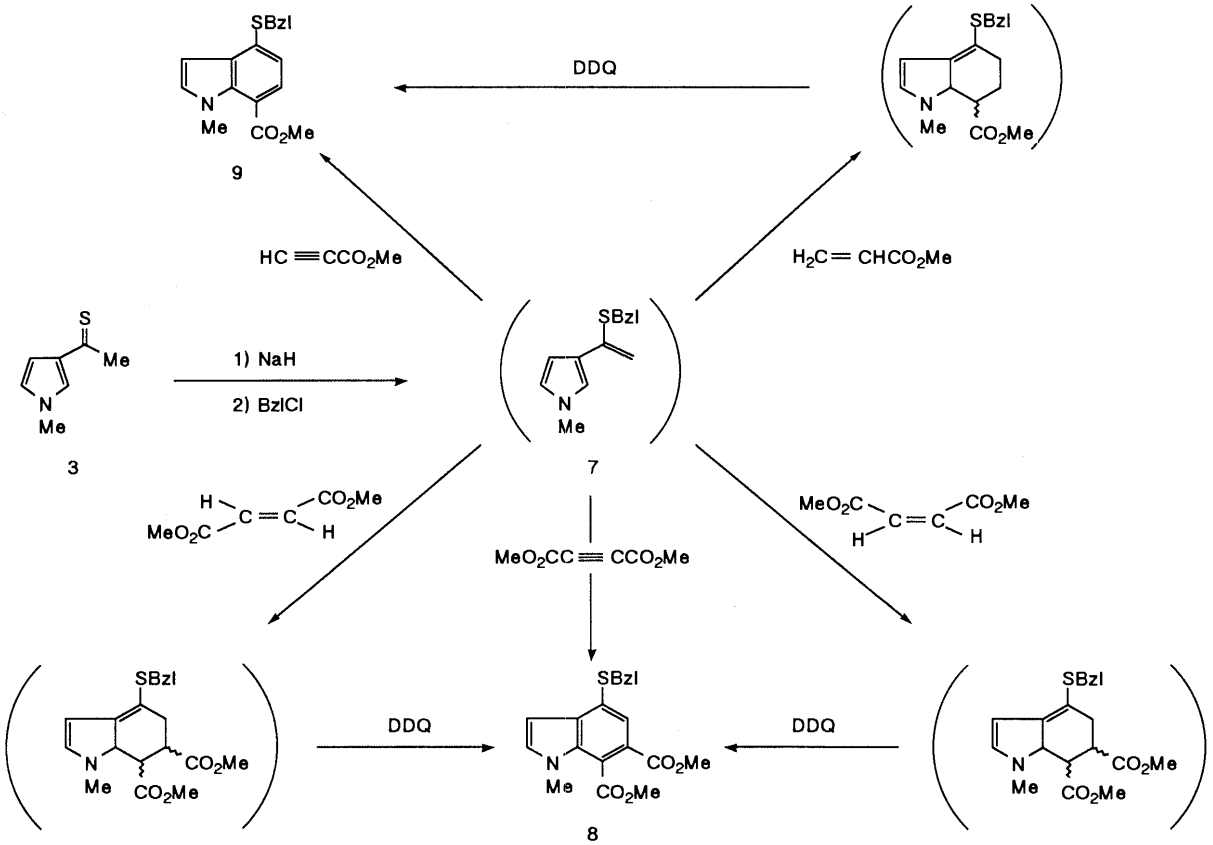

Chart 2

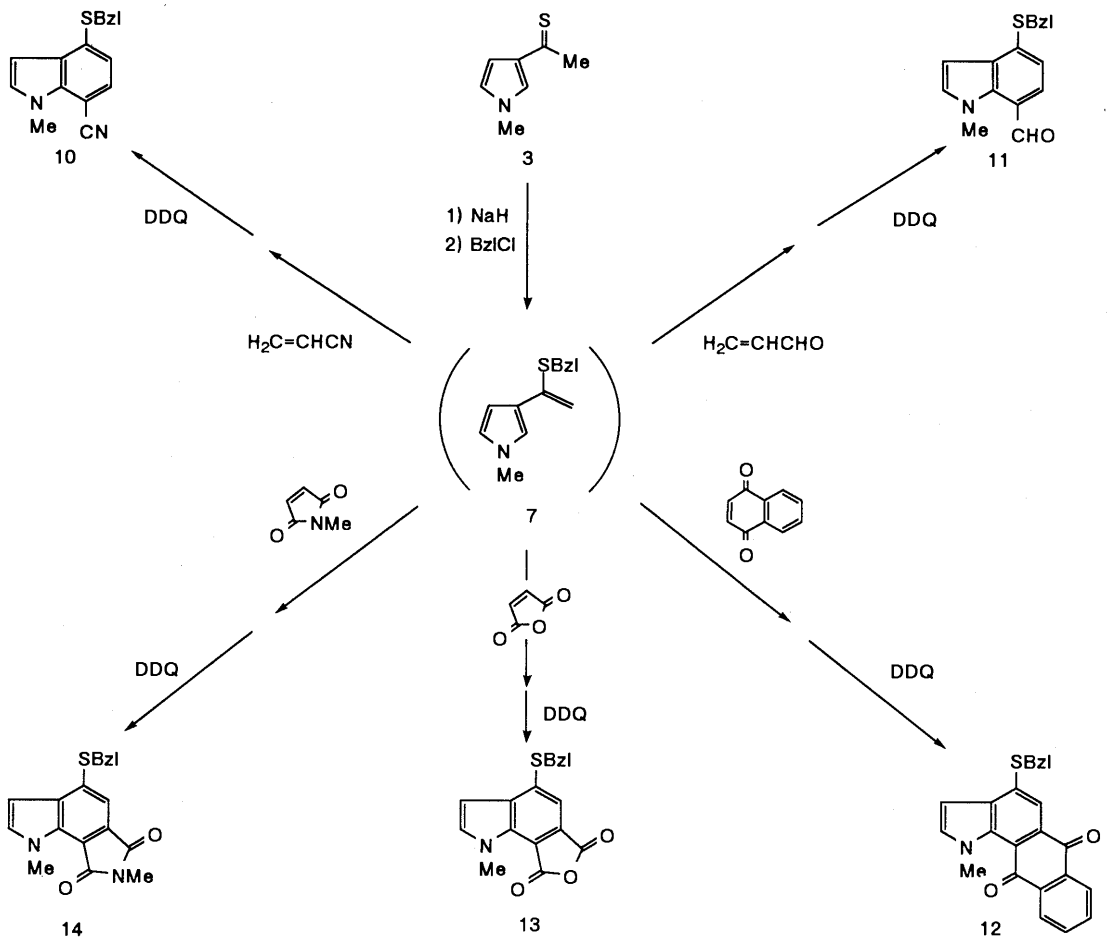

Chart 3

alkylation of the 3-thioacetylpyrrole **3**, with dienophiles.

First, the thioacetylpyrroles **3**, **4**, **5**, and **6** were synthesized by the reaction of corresponding acetylpyrroles with Lawesson's reagent, 2,4-bis(4-methoxyphenyl)-1,3-dithia-2,4-diphosphetane-2,4-disulfide,[2] to examine their reactivity. A preliminary study was done on the reaction of the 3-vinylpyrrole **7**, generated *in situ* by the reaction of 1-methyl-3-thioacetylpyrrole (**3**) with benzyl chloride, with dimethyl acetylenedicarboxylate in tetrahydrofuran (THF). The indole **8** was obtained in 30.5% overall yield from 3-acetyl-1-methylpyrrole. In general, the cycloaddition reactions of the vinylpyrrole **7** with dienophiles were carried out in a fused glass tube at 100 °C in THF or MeCN under a nitrogen atmosphere for an appropriate time, and the results are summarized in Charts 2 and 3 and Table I.

Among the cycloadducts, products of the reactions of the diene **7** with dimethyl maleate, dimethyl fumarate, methyl acrylate, acrylonitrile, acrolein, 1,4-naphthoquinone, maleic anhydride, and *N*-methylmaleinimide were directly transformed to the corresponding indoles by treatment with 2,3-dichloro-5,6-dicyano-1,4-benzoquinone (DDQ), though the products were not purified because of their instability. In these reactions, we also observed significant changes of the cycloadduct yields in the reactions with dimethyl acetylenedicarboxylate, methyl propiolate, and acrolein (Table I).

Although the reactivities of the thioacetylpyrroles **4**, **5**, and **6** for cycloaddition were investigated, in addition to that of **3**, the results were unsatisfactory. That is, the reaction of dimethyl acetylenedicarboxylate with the solution obtained from the reaction of **4** with NaH followed by the treatment with benzyl chloride gave only a trace amount of

Table I. Cycloaddition Reaction of the Diene 7 with Dienophiles

Dienophile	Time (h)	Product	Solvent	Yield (%)[a]
$MeO_2CC{\equiv}CCO_2Me$	24	8	THF	30.5
			MeCN	10.0
MeO_2C, H, $C{=}C$, H, CO_2Me	48	8[b]	THF	29.7
H, $C{=}C$, CO_2Me, MeO_2C, H	48	8[b]	THF	16.7
$HC{\equiv}CCO_2Me$	24	9	THF	10.4
			MeCN	31.4
$H_2C{=}CHCO_2Me$	48	9[b]	THF	13.6
$H_2C{=}CHCN$	48	10[b]	THF	19.6
$H_2C{=}CHCHO$	48	11[b]	THF	Trace
			MeCN	20.4
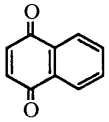	48	12[b]	THF	21.1
	48	13[b]	THF	8.0
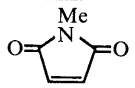	48	14[b]	THF	15.7

a) Overall yield from 3-acetyl-1-methylpyrrole. b) Obtained by the oxidation of the cycloaddition product without purification.

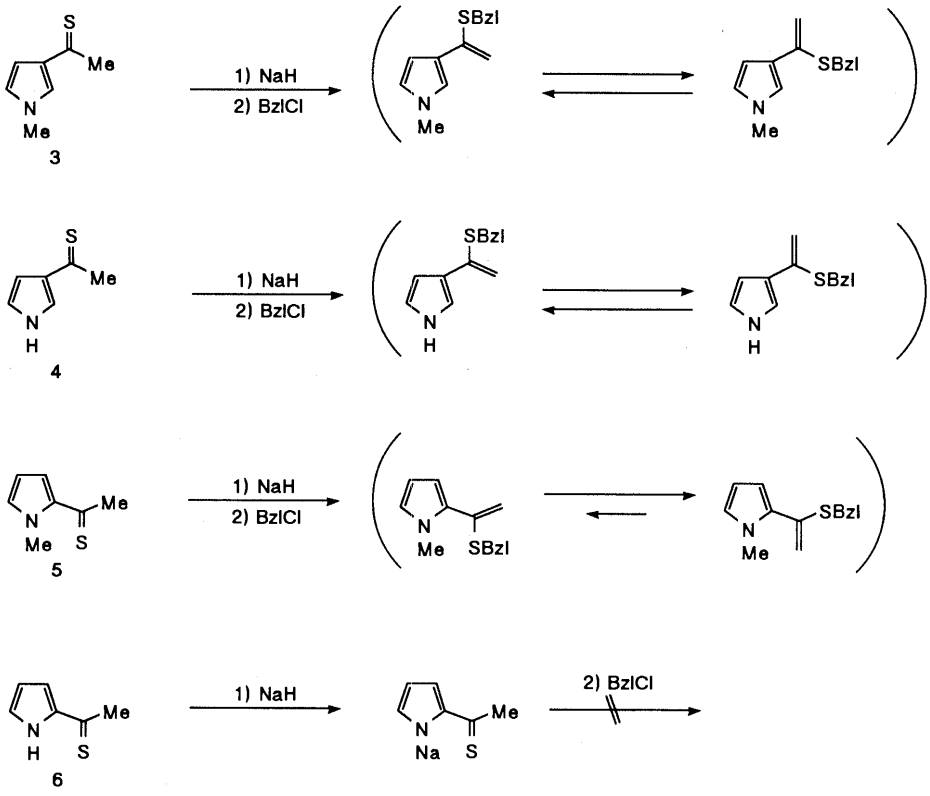

Chart 4

the cycloadduct (not investigated further). The poor result in this reaction may be due to the lability of the vinylpyrrole produced from **4**. Similar treatment of an anion from **5** with benzyl chloride followed by reaction with dimethyl acetylenedicarboxylate did not afford any cycloaddition product. The inertness of the vinylpyrrole generated from **5** to cycloaddition may be due to the predominance of the transoid form of the diene in the solution owing to steric interaction between the N–Me and S-benzyl groups. Further, the reaction of benzyl chloride with an anion derived from the thioacetylpyrrole **6** by treatment with NaH did not give any alkylation product.

Experimental

All melting points are uncorrected. Infrared (IR) spectra were recorded with a Hitachi 260-10 or a JASCO IR-700 spectrometer, ^{1}H-nuclear magnetic resonance (^{1}H-NMR) spectra with a JEOL JNM-GX 270 or a JEOL JNM-EX 90 or a Varian T-60 spectrometer with tetramethylsilane as an internal standard, and mass spectra (MS) with a JEOL JMS-d 300 spectrometer. Elementary analyses were done by Ms. A. Sakamoto and Ms. S. Okamura, Kissei Pharmaceutical Company Ltd., Matsumoto, Japan. Wako Silica gel C-200 (200 mesh) and Merck Kieselgel 60 F_{254} were used for column chromatography and thin layer chromatography (TLC), respectively.

1-Methyl-3-thioacetylpyrrole (3) Lawesson's reagent (2425 mg, 6 mmol) was slowly added to a solution of 3-acetyl-1-methylpyrrole (615 mg, 5 mmol) in THF (15 ml) and the whole was stirred at room temperature under a nitrogen atmosphere with shielding from light for 30 min. Hexane (24 ml) was added to the reaction mixture and the insoluble precipitate was filtered off. The filtrate was poured into water and extracted with hexane. The organic layer was washed with saturated aqueous $NaHCO_3$ and brine, and then dried and concentrated. The residue was used without purification for the synthesis of the diene **7**. An analytic sample was obtained by silica gel column chromatography of the above residue to give 605 mg (87%) of **3** from the chloroform–hexane (1 : 1) eluate as deep red plates (petroleum ether), mp 42—44 °C. ^{1}H-NMR (acetone-d_6) δ: 2.84 (3H, s, Me), 3.72 (3H, s, N–Me), 6.70 (2H, m, pyrrole H), 7.59 (1H, m, pyrrole H). MS *m/z* Calcd for C_7H_9NS (M^+): 139.0456. Found: 139.0468.

3-Thioacetylpyrrole (4) Lawesson's reagent (484 mg, 1.2 mmol) was slowly added to a solution of 3-acetylpyrrole (109 mg, 1 mmol) in THF (5 ml) and the whole was stirred at room temperature under a nitrogen atmosphere with shielding from light for 1 h. The reaction mixture was poured into water and extracted with ether. The organic layer was washed with saturated aqueous $NaHCO_3$ and brine, and then dried and concentrated. The residue was subjected to silica gel column chromatography to yield **4** from the benzene eluate in a quantitive yield as orange plates, mp 74—75 °C (benzene–hexane). ^{1}H-NMR (acetone-d_6) δ: 2.90 (3H, s, Me), 6.73 (2H, m, pyrrole H), 7.67 (1H, m, pyrrole H), 10.80 (1H, br, NH). MS *m/z* Calcd for C_6H_7NS (M^+): 125.0298. Found: 125.0288.

1-Methyl-2-thioacetylpyrrole (5) Lawesson's reagent (967 mg, 2.4 mmol) was slowly added to a solution of 2-acetyl-1-methylpyrrole (246 mg, 2 mmol) in THF (10 ml) and the whole was stirred at room temperature under a nitrogen atmosphere with shielding from light for 3 h. *n*-Pentane was added to the reaction mixture and the insoluble precipitate were filtered off. The filtrate was poured into water and extracted with *n*-pentane. The organic layer was washed with saturated aqueous $NaHCO_3$ and brine, then dried and concentrated carefully at low temperature. The residue was subjected to silica gel column chromatography with *n*-pentane as an eluent to give 228 mg (82%) of **5** as deep red needles, mp 37—38 °C (petroleum ether). ^{1}H-NMR (acetone-d_6) δ: 2.93 (3H, s, Me), 4.03 (3H, s, NMe), 6.15 (1H, m, pyrrole H), 7.17 (2H, m, pyrrole H). MS *m/z* Calcd for C_7H_9NS (M^+): 139.0456. Found: 139.0435.

2-Thioacetylpyrrole (6) Lawesson's reagent (484 mg, 1.2 mmol) was slowly added to a solution of 2-acetylpyrrole (109 mg, 1 mmol) in 1,2-dimethoxyethane (5 ml) and the whole was stirred at room temperature under a nitrogen atmosphere with shielding from light for 1 h. The reaction mixture was poured into water and extracted with ether. The organic layer was washed with saturated aqueous $NaHCO_3$ and brine, then dried and concentrated. The residue was subjected to silica gel column chromatograhy to give **6** as a red oil from the chloroform eluate in a quantitative yield. ^{1}H-NMR (acetone-d_6) δ: 2.87 (3H, s, Me), 6.35 (1H, m, pyrrole H), 7.10 (1H, m, pyrrole H), 7.38 (1H, m, pyrrole H), 10.73 (1H, br, NH). MS *m/z* Calcd for C_6H_7NS (M^+): 125.0298. Found: 125.0323.

Preparation of the Diene 7 A solution of 1-methyl-3-thioacetylpyrrole (**3**) (695 mg, 5 mmol) in MeCN or THF (5 ml) was added to a suspension of 60% NaH (200 mg, 5 mmol) and benzyl chloride (696 mg, 5.5 mmol) in MeCN or THF (35 ml) with stirring at −15 °C under a nitrogen

atmosphere and the whole was stirred at room temperature for 24 h to give the diene **7**, which was used without purification for the reaction with dienophiles under the conditions described in Table I.

General Procedure for the Cycloaddition Reaction of the Diene 7 with Dienophiles A solution of the diene **7** prepared by the reaction of **3** (5 mmol) with benzyl chloride in the presence of NaH was heated with a dienophile (7.5 mmol) in a fused glass tube under a nitrogen atmosphere under the appropriate conditions (Table I). The reaction mixture was poured into water and the whole was extracted with ethyl acetate or chloroform. The organic layer was washed with brine, and then dried and concentrated. The residue was subjected to silica gel column chromatography using the appropriate solvent.

General Method for DDQ Oxidation of the Cycloadducts A benzene solution (50 ml) of the residue, obtained by applying the general procedure for the reaction of the diene **7** with dienophiles, was treated with DDQ (1.183 mg, 5 mmol) and the whole was stirred at room temperature for 1 h, then concentrated. CH_2Cl_2 (50 ml) was added to the residue and insoluble materials were filtered off. The filtrate was concentrated and subjected to silica gel column chromatography using an appropriate solvent.

4-Benzylthio-6,7-dimethoxycarbonyl-1-methylindole (8) The residue obtained from the reaction of the diene **7** with dimethyl acetylenedicarboxylate in THF by the general procedure in ethyl acetate was subjected to silica gel column chromatography to yield 562 mg (30.5% overall yield from 3-acetyl-1-methylpyrrole) of **8** from the chloroform–hexane (1 : 1) eluate as colorless needles (ether), mp 140—142 °C. IR (Nujol) cm^{-1}: 1720, 1705. ^{1}H-NMR (acetone-d_6) δ: 3.82 (3H, s, NMe or CO_2Me), 3.86 (3H, s, NMe or CO_2Me), 3.96 (3H, s, NMe or CO_2Me), 4.34 (2H, s, benzyl H), 6.64 (1H, d, J=3.18 Hz, C-3 H), 7.20—7.33 (3H, m, aromatic H), 7.37—7.42 (2H, m, aromatic H), 7.50 (1H, d, J=3.18 Hz, C-2 H), 7.69 (1H, s, C-5 H). MS m/z: 369 (M^+). *Anal.* Calcd for $C_{20}H_{19}NO_4S$: C, 65.02; H, 5.18; N, 3.79. Found: C, 64.82; H, 5.28; N, 3.65.

The residue obtained from the reaction of the diene **7** with dimethyl maleate in THF by the general procedure was oxidized with DDQ by the general method in ethyl acetate. The residue was subjected to silica gel column chromatography to yield 308 mg (16.7% overall yield from 3-acetyl-1-methylpyrrole) of **8** from the chloroform–hexane (1 : 1) eluate.

Reaction of the diene **7** with dimethyl fumarate in the same manner as described for the reaction with dimethyl maleate afforded 548 mg (29.7% overall yield from 3-acetyl-1-methylpyrrole) of **8**.

4-Benzylthio-7-methoxycarbonyl-1-methylindole (9) The residue obtained from the reaction of the diene **7** with methyl propiolate in MeCN by the general procedure in ethyl acetate was subjected to silica gel column chromatography to give 488 mg (31.4% overall yield from 3-acetyl-1-methylpyrrole) of **9** from the chloroform–hexane (1 : 1) eluate as colorless needles (ether), mp 122—122.5 °C. IR ($CHCl_3$) cm^{-1}: 1700. ^{1}H-NMR (acetone-d_6) δ: 3.90 (3H, s, NMe or CO_2Me), 3.92 (3H, s, NMe or CO_2Me), 4.37 (2H, s, benzyl H), 6.61 (1H, d, J=3.18 Hz, C-3 H), 7.11 (1H, d, J=7.81 Hz, C-5 H or C-6 H), 7.24—7.34 (4H, m, C-2 H and aromatic H), 7.42—7.45 (2H, m, aromatic H), 7.56 (1H, d, J=7.81 Hz, C-5 H or C-6 H). MS m/z: 311 (M^+). *Anal.* Calcd for $C_{18}H_{17}NO_2S$: C, 69.43; H, 5.50; N, 4.50. Found: C, 69.40; H, 5.40; N, 4.48.

The residue obtained from the reaction of the diene **7** with methyl acrylate in THF by the general procedure was oxidized with DDQ by the general method in ethyl acetate. The residue was subjected to silica gel column chromatography to give 211 mg (13.6% overall yield from 3-acetyl-1-methylpyrrole) of **9** from the chloroform–hexane (1 : 1) eluate.

4-Benzylthio-7-cyano-1-methylindole (10) The residue obtained from the reaction of the diene **7** with acrylonitrile in THF by the general procedure was oxidized with DDQ by the general method in ethyl acetate. The residue was subjected to silica gel column chromatography to yield 272 mg (19.6% overall yield from 3-acetyl-1-methylpyrrole) of **10** from the chloroform–hexane (2 : 1) eluate as colorless plates (ether), mp 112—114 °C. IR (KBr) cm^{-1}: 2210. ^{1}H-NMR (acetone-d_6) δ: 4.11 (3H, s, NMe), 4.40 (2H, s, benzyl H), 6.60 (1H, d, J=3.29 Hz, C-3 H), 7.14 (1H, d, J=7.91 Hz, C-5 H or C-6 H), 7.25—7.52 (7H, m, C-2 H, C-5 H or C-6 H and aromatic H). MS m/z: 278 (M^+). *Anal.* Calcd for $C_{17}H_{14}N_2S$: C, 73.35; H, 5.07; N, 10.06. Found: C, 73.22; H, 4.98; N, 9.91.

4-Benzylthio-7-formyl-1-methylindole (11) The residue obtained from the reaction of the diene **7** with acrolein in MeCN by the general procedure was oxidized with DDQ by the general method in ethyl acetate. The residue was subjected to silica gel column chromatography to give 286 mg (20.4% overall yield from 3-acetyl-1-methylpyrrole) of **11** from the chloroform–hexane (1 : 1) eluate as yellow needles (ether), mp 112—114 °C. IR ($CHCl_3$) cm^{-1}: 1685. ^{1}H-NMR (acetone-d_6) δ: 4.15 (3H, s, NMe), 4.44 (2H, s, benzyl H), 6.62 (1H, d, J=3.17 Hz, C-3 H), 7.24 (1H, d, J=7.81 Hz, C-5 H or C-6 H), 7.26—7.37 (4H, m, C-2 H and aromatic H), 7.48—7.51 (2H, m, aromatic H), 7.70 (1H, d, J=7.81 Hz, C-5 H or C-6 H), 10.23 (1H, s, CHO). MS m/z: 281 (M^+). *Anal.* Calcd for $C_{17}H_{15}NOS$: C, 72.57; H, 5.37; N, 4.98. Found: C, 72.47; H, 5.50; N, 4.77.

4-Benzylthio-1-methylnaphth[2,3-*g*]indole-6,11-quinone (12) The residue obtained from the reaction of the diene **7** with 1,4-naphthoquinone in THF by the general procedure was oxidized with DDQ by the general method in chloroform. The residue was subjected to silica gel column chromatography to yield 404 mg (21.1% overall yield from 3-acetyl-1-methylpyrrole) of **12** from the chloroform–hexane (1 : 1) eluate as red needles (CH_2Cl_2–ether), mp 170—172 °C. IR (KBr) cm^{-1}: 1665. ^{1}H-NMR ($CDCl_3$) δ: 4.04 (3H, s, NMe), 4.42 (2H, s, benzyl H), 6.65 (1H, d, J=3.18 Hz, C-3H), 7.22—7.48 (6H, m, C-2 H and aromatic H), 7.68—7.75 (2H, m, aromatic H), 7.99 (1H, s, C-5H), 8.11—8.24 (2H, m, aromatic H). MS m/z: 383 (M^+). *Anal.* Calcd for $C_{24}H_{17}NO_2S$: C, 75.17; H, 4.47; N, 3.65. Found: C, 75.22; H, 4.59; N, 3.58.

4-Benzylthio-1-methylindole-6,7-dicarboxylic Anhydride (13) The residue obtained from the reaction of the diene **7** with maleic anhydride in THF by the general procedure was oxidized with DDQ by the general method in ethyl acetate. The residue was subjected to silica gel column chromatography to yield 129 mg (8% overall yield from 3-acetyl-1-methylpyrrole) of **13** from the chloroform–hexane eluate as yellow needles (ether), mp 184—186 °C. IR (KBr) cm^{-1}: 1821, 1759. ^{1}H-NMR (acetone-d_6) δ: 4.31 (3H, s, NMe), 4.60 (2H, s, benzyl H), 6.79 (1H, d, J=3.29 Hz, C-3 H), 7.30—7.50 (5H, m, aromatic H), 7.56 (1H, s, C-5 H), 7.66 (1H, d, J=3.29 Hz, C-2 H). MS m/z: 323 (M^+). *Anal.* Calcd for $C_{18}H_{13}NO_3S$: C, 66.86; H, 4.05; N, 4.33. Found: C, 66.67; H, 3.75; N, 4.28.

1,7-Dimethyl-4-benzylthiopyrrolo[3,4-*g*]indole-6,8-dione (14) The residue obtained from the reaction of the diene **7** with *N*-methylmaleinimide in THF by the general procedure was oxidized with DDQ by the general method in chloroform. The residue was subjected to silica gel column chromatography to yield 264 mg (15.7% overall yield from 3-acetyl-1-methylpyrrole) of **14** from the chloroform–hexane (1 : 1) eluate as yellow needles (CH_2Cl_2–ether), mp 187—189 °C. IR (KBr) cm^{-1}: 1753, 1697. ^{1}H-NMR ($CDCl_3$) δ: 3.16 (3H, s, NMe), 4.28 (3H, s, indole NMe), 4.35 (2H, s, benzyl H), 6.68 (1H, d, J=3.3 Hz, C-2 H), 7.23—7.45 (5H, m, aromatic H), 7.46 (1H, s, C-5 H). MS m/z: 336 (M^+). *Anal.* Calcd for $C_{19}H_{16}N_2O_2S$: C, 67.84; H, 4.79; N, 8.33. Found: C, 67.80; H, 4.73; N, 8.30.

References

1) M. Murase, T. Hosaka, T. Koike, and S. Tobinaga, *Chem. Pharm. Bull.*, **37**, 1999 (1989).
2) M. C. Cava and M. I. Levinson, *Tetrahedron*, **22**, 5061 (1985).

Synthesis of Mannich Bases of 5-Hydroxynaphthalene-1,8-carbolactone as Potential Antifungal or Antitumor Agents

Houda FILLION,*,[a] Monique PORTE,[b] Marie-Hélène BARTOLI,[c] Zouhair BOUAZIZ,[a] Maryse BERLION,[c] and Jean VILLARD[b]

Laboratoire de Chimie Organique,[a] Laboratoire de Mycologie,[b] Institut des Sciences Pharmaceutiques et Biologiques, Université Claude Bernard, 8 Avenue Rockefeller, 69373 Lyon Cedex 08, France and Laboratoire de Physiologie et Pharmacologie I,[c] Faculté de Pharmacie, Université Joseph Fourier, Domaine de La Merci, 38700 La Tronche, France. *Received July 6, 1990*

Mannich bases of 5-hydroxynaphthalene-1,8-carbolactone 1 were prepared from various secondary amines or bulky primary amines and formaldehyde.

They were isolated in almost all cases as hydrochlorides. These derivatives were submitted to *in vitro* antifungal and cytotoxic assays. The antifungal assays were performed against three strains of yeasts and five strains of human pathogenic fungi. Two of the tested compounds, 2i and 2j, exhibited interesting antifungal activities against *Candida albicans* and *Candida tropicalis*. The cytotoxic activity was evaluated towards L 1210 leukemia cells. Almost all of the Mannich bases had shown significant activity against this tumor cell line as values of $IC_{50} \leqslant 4\,\mu g/ml$ are considered interesting. Only one derivative 2 developed better cytotoxicity than the parent compound 1.

Keywords aminomethylation; Mannich base; naphthalenecarbolactone; antifungal activity; cytotoxic activity; L 1210 leukemia cell

Mannich bases exhibit several pharmacological properties. Yet, although many substituted aminomethyl derivatives of α,β-unsaturated ketones are known as anticancer[1-4] or antifungal agents,[5] Mannich bases of phenols or naphthols have not yet been described for these biological activities.

In a precedent work,[6] we have reported the *in vitro* antifungal and antitumor activities of 5-hydroxynaphthalene-1,8-carbolactone (**1**). In order to check whether aminomethylation of **1** would ameliorate the pharmacological response, we planned to synthesize and to submit a series of Mannich bases **2** to biological assay.

Synthesis Mannich bases **2a—h** were prepared by reaction of 5-hydroxynaphthalene-1,8-carbolactone **1** with various secondary amines and formaldehyde in ethanol at room temperature. Compound **2i** or **2j** was obtained under the same conditions from *tert*-butylamine or cyclohexylamine, while **2k** resulted from the treatment of the aziridinyl derivative **2d** with concentrated hydrochloric acid. Almost all of the derivatives were isolated as hydrochlorides except **2c** and **2d**, which were obtained as free bases.

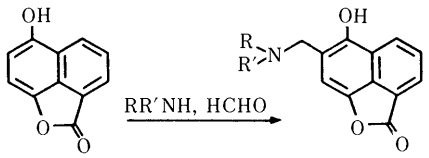

1 2

	R	R′
2a	CH_3	CH_3
2b	C_2H_5	C_2H_5
2c	CH_2CH_2Cl	CH_2CH_2Cl
2d	$-(CH_2)_2-$	
2e	$-(CH_2)_4-$	
2f	$-(CH_2)_5-$	
2g	$-(CH_2)_2-N(CH_3)-(CH_2)_2-$	
2h	$-(CH_2)_2-O-(CH_2)_2-$	
2i	H	$C(CH_3)_3$
2j	H	C_6H_{11}
2k	H	CH_2CH_2Cl

Chart 1

Pharmacology **1) *In Vitro* Antifungal Assays** The antifungal assays were performed *in vitro* against three strains of yeasts and five strains of human pathogenic fungi (3 moulds and 2 dermatophytes).

2) *In Vitro* Cytotoxicity towards L 1210 Leukemia Cells The cytotoxic activity was evaluated towards L 1210 leukemia cells. Dose effect relationships of the various compounds tested were determined from the regression line in a plot of percent cell growth inhibitions as a function of the logarithm of the dose. From these curves, the dose of drug reducing the cell growth by 50% after 48 h as compared to the controls (IC_{50}) was estimated. Cytotoxicity of the Mannich bases **2** is summarized in Table I.

Conclusion

We have prepared a series of Mannich bases **2a—k** derived from 5-hydroxynaphthalene-1,8-carbolactone. Compounds **2a—k** were submitted to *in vitro* antifungal and cytotoxic assays. Two of the tested compounds, **2i** and **2j**, exhibited interesting antifungal activities against two yeasts: *Candida albicans* and *Candida tropicalis*. In addition, almost all of the Mannich bases showed significant cytotoxic activity against L 1210 leukemia cells as values of $IC_{50} \leqslant 4\,\mu g/ml$ are considered to be interesting.

TABLE I. Effect of the Mannich Bases **2** on the Growth of L 1210 Cells

Compound	IC_{50}	
	$\mu g/ml$	μM
Mitomycin C	0.0298	0.0925
1	0.38	2.04
2a	1.69	6.05
2b	3.37	10.97
2c	0.35	1.029
2d	0.92	3.81
2e	2.85	9.35
2f	4.27	13.28
2g	1.44	4.30
2h	0.76	2.37
2i	1.216	3.95
2j	1.75	5.25
2k	0.63	2.006

Only one derivative, **2c**, developed a higher cytotoxicity than the parent compound **1**, while the activity of **2k** was the same ($IC_{50} = 2\ \mu M$). This data indicates that the *in vitro* cytotoxic activity towards L 1210 leukemia cells seems to be enhanced by the alkylating ability of the nitrogen mustard group.

Experimental

Melting points were measured on a Kofler apparatus. The infrared (IR) spectra (KBr discs) were recorded on a Perkin-Elmer 1310 spectrophotometer. The proton nuclear magnetic resonance (^{1}H-NMR) spectra were recorded at 300 MHz on a Bruker AM 300 apparatus. Chemical shifts are reported in ppm (δ) from tetramethylsilane (TMS) as an internal reference. The mass spectra (MS) were obtained by direct ionization (EI at 70 eV) on an AE 1 MS 902 apparatus. Elemental analysis was made at the Centre de Microanalyse du CNRS at Solaise.

All the amines were freshly distilled before use. Aziridine was prepared according to the literature.[7,8] Compound **1** was initially prepared in a two-step path[9] from the adduct[10] of *p*-benzoquinone and (*E*)-2,4-pentadienoic acid. Better yields of **1** are obtained from the same adduct through a modified one-pot synthesis.[11]

Preparation of 5-Hydroxy-6-dialkylaminomethylnaphthalene-1,8-carbolactone (2a—h) (General Procedure) An aqueous solution of 37% formaldehyde (0.2 ml, 2.5 mmol) was added to a stirred and cooled solution (0 °C) of the appropriate secondary amine (2.5 mmol) in ethanol. After 30 min, a solution of compound **1** (0.186 g, 1 mmol) was added and the mixture was stirred at room temperature for a variable time, the course of the reaction being followed by thin layer chromatography (TLC).

The hydrochlorides were obtained by bubbling hydrogen chloride through the ethanolic solution.

5-Hydroxy-6-dimethylaminomethylnaphthalene-1,8-carbolactone Hydrochloride (2a) Compound **2a** was recrystallized from ethanol (70% yield). mp 246 °C. IR (KBr): 3420 (ν OH), 2700 (ν $\overset{+}{N}$H), 1780 (ν CO) cm^{-1}. ^{1}H-NMR (DMSO-d_6) δ: 8.81 to 7.79 (3H, m, H aromat.), 7.47 (1H, s, H_7), 4.44 (2H, s, CH_2), 3.4 (1H, br, $\overset{+}{N}$H), 2.73 (6H, s, CH_3). MS *m/z*: 243 (M^+, 1), 198 (81.5), 170 (12.2), 142 (23), 114 (100). *Anal.* Calcd for $C_{14}H_{14}ClNO_3 \cdot 0.66\ H_2O$: C, 57.64; H, 5.30; Cl, 12.15; N, 4.80. Found: C, 57.65; H, 4.98; Cl, 12.20; N, 4.88.

5-Hydroxy-6-diethylaminomethylnaphthalene-1,8-carbolactone Hydrochloride (2b) Compound **2b** was recrystallized from ethanol (40% yield). mp 176 °C. IR (KBr): 3440 (ν OH), 2780, 2730, 2690 (ν $\overset{+}{N}$H), 1780 (ν CO) cm^{-1}. ^{1}H-NMR (DMSO-d_6) δ: 10.98 (1H, br, OH), 8.7 to 7.85 (3H, m, H aromat.), 7.64 (1H, s, H_7), 4.49 (2H, s, CH_2), 3.2 (1H, br, $\overset{+}{N}$H), 3.16 (4H, q, CH_2), 1.32 (6H, t, CH_3). MS *m/z*: 271 (M^+, 0.2), 198 (83), 170 (12), 142 (20), 114 (100). *Anal.* Calcd for $C_{16}H_{18}ClNO_3$: C, 62.44; H, 5.85; Cl, 11.55; N, 4.55. Found: C, 62.47; H, 5.77; Cl, 11.59; N, 4.59.

5-Hydroxy-6-[*N*,*N*-bis(2-chloroethyl)aminomethyl)]naphthalene-1,8-carbolactone (2c) Compound **2c** was prepared at −15 °C. It was crystallized from ethanol (95% yield). mp 130 °C. IR (KBr): 3430 (ν OH), 1770 (ν CO) cm^{-1}. ^{1}H-NMR ($CDCl_3$) δ: 10.44 (1H, br, OH), 8.41 to 7.76 (3H, m, H aromat.), 6.82 (1H, s, H_7), 4.07 (2H, s, CH_2), 3.71 (4H, t, CH_2), 3.08 (4H, t, CH_2). MS *m/z*: 198 (36.5), 170 (5.3), 142 (9.9), 114 (48.5). *Anal.* Calcd for $C_{16}H_{15}Cl_2NO_3$: C, 56.47; H, 4.41; Cl, 20.88; N, 4.12. Found: C, 56.29; H, 4.41; Cl, 20.91; N, 4.20.

5-Hydroxy-6-aziridinylmethylnaphthalene-1,8-carbolactone (2d) Compound **2d** was recrystallized from benzene (10% yield). mp 140 °C. IR (KBr): 3480 (ν OH), 1780 (ν CO) cm^{-1}. ^{1}H-NMR ($CDCl_3$) δ: 8.40 to 7.74 (3H, m, H aromat.), 6.70 (1H, s, H_7), 3.76 (2H, s, CH_2), 2.04 (2H, m, CH_2), 1.48 (2H, m, CH_2). MS *m/z*: 241 (M^+, 4), 198 (100), 170 (10.5), 142 (17), 114 (76). *Anal.* Calcd for $C_{14}H_{11}NO_3$: C, 69.71; H, 4.56; N, 5.81. Found: C, 69.76; H, 4.71; N, 5.77.

5-Hydroxy-6-pyrrolidinylmethylnaphthalene-1,8-carbolactone Hydrochloride (2e) Compound **2e** was recrystallized from ethanol (64% yield). mp 182 °C. IR (KBr): 3520 (ν OH), 2730, 2580, 2500 (ν $\overset{+}{N}$H), 1770 (ν CO) cm^{-1}. ^{1}H-NMR (DMSO-d_6) δ: 10.77 (1H, br, OH), 8.85 to 7.85 (3H, m, H aromat.), 7.58 (1H, s, H_7), 4.56 (2H, s, CH_2), 3.32 (5H, br, 2 CH_2 and $\overset{+}{N}$H), 1.98 (4H, br, CH_2). MS *m/z*: 269 (M^+, 0.9), 198 (100), 170 (22.3), 142 (33.6), 114 (24.3). *Anal.* Calcd for: $C_{16}H_{16}ClNO_3$, 0.66 H_2O: C, 60.50; H, 5.46; Cl, 11.19; N, 4.41. Found: C, 60.89; H, 5.58; Cl, 11.10; N, 4.27.

5-Hydroxy-6-piperidinylmethylnaphthalene-1,8-carbolactone Hydrochloride (2f) Compound **2f** was recrystallized from ethanol (53% yield). mp 190 °C. IR (KBr): 3460 (ν OH), 2680, 2580, 2550 (ν $\overset{+}{N}$H), 1780 (ν CO) cm^{-1}. ^{1}H-NMR (DMSO-d_6) δ: 9.55 (1H, br, OH), 8.77 to 7.79 (3H, m, H aromat.), 7.54 (1H, s, H_7), 4.41 (2H, s, CH_2), 3.4 (1H, br, $\overset{+}{N}$H), 3.16 (4H, m, CH_2), 1.74 (6H, m, CH_2). MS *m/z*: 283 (M^+, 1.4), 198 (72.6), 170 (9.4), 142 (15.9), 114 (61.7). *Anal.* Calcd for $C_{17}H_{18}ClNO_3 \cdot 1H_2O$: C, 60.45; H, 5.97; Cl, 10.50; N, 4.15. Found: C, 60.54; H, 5.85; Cl, 10.51; N, 4.03.

5-Hydroxy-6-[4′-methyl(piperazinylmethyl)]naphthalene-1,8-carbolactone (2g) Compound **2g** was recrystallized from ethanol (60% yield). mp 240 °C. IR (KBr): 3370 (ν OH), 2720, 2660, 2600 (ν $\overset{+}{N}$H), 1780 (ν CO) cm^{-1}. ^{1}H-NMR (DMSO-d_6) δ: 9.90 (1H, br, OH), 8.82 to 7.85 (3H, m, H aromat.), 7.57 (1H, s, H_7), 4.54 (2H, s, CH_2), 3.55 (4H, m, CH_2), 3.45 (5H, m, CH_2 and $\overset{+}{N}$H), 2.82 (3H, s, CH_3). MS *m/z*: 298 (M^+, 0.6), 198 (87), 170 (12), 142 (20), 114 (100). *Anal.* Calcd for $C_{17}H_{20}Cl_2N_2O_3 \cdot 2.5\text{-}H_2O$: C, 49.04; H, 6.00; Cl, 17.06; N, 6.73. Found: C, 49.07; H, 5.87; Cl, 16.99; N, 6.68.

5-Hydroxy-6-morpholinylmethylnaphthalene-1,8-carbolactone Hydrochloride (2h) Compound **2h** was recrystallized from ethanol (48% yield). mp 192 °C. IR (KBr): 3600 (ν OH), 2710, 2700, 2640 (ν $\overset{+}{N}$H), 1770 (ν CO) cm^{-1}. ^{1}H-NMR (DMSO-d_6) δ: 10.25 (1H, br, OH), 8.77 to 7.80 (3H, m, H aromat.), 7.55 (1H, s, H_7), 4.51 (2H, s, CH_2), 3.84 (4H, m, CH_2), 3.24 (5H, m, CH_2 and $\overset{+}{N}$H). MS *m/z*: 285 (M^+, 1.8), 198 (66.4), 170 (9), 142 (17.6), 114 (100). *Anal.* Calcd for $C_{16}H_{16}ClNO_4 \cdot 1H_2O$: C, 56.56; H, 5.34; Cl, 10.40; N, 4.12. Found: C, 56.60; H, 5.26; Cl, 10.64; N, 3.98.

5-Hydroxy-6-*tert*-butylaminomethylnaphthalene-1,8-carbolactone Hydrochloride (2i) An aqueous solution of 37% formaldehyde (0.05 ml, 0.54 mmol) was added to a stirred and cooled solution of *tert*-butylamine (0.058 ml, 0.54 mmol) in dichloromethane (10 ml). After 30 min of continued stirring, a solution of compound **1** (0.1 g, 0.54 mmol) in dichloromethane (25 ml) was added and the mixture was stirred at room temperature for 1.5 h. After evaporation of the solvent, the oily residue was dissolved in anhydrous ether (5 ml) and treated by concentrated hydrochloric acid until a yellow solid precipitated. Then, the hydrochloride **2i** was recrystallized from anhydrous ethanol (55% yield). mp 230 °C. IR (KBr): 3340 (ν OH), 2780, 2630, 2400 (ν $\overset{+}{N}H_2$), 1780 (ν CO) cm^{-1}. ^{1}H-NMR (DMSO-d_6) δ: 8.80 to 7.75 (3H, m, H aromat.), 7.5 (1H, s, H_7), 4.2 (2H, s, CH_2), 3.3 (2H, br, $\overset{+}{N}H_2$), 1.4 (9H, s, CH_3). MS *m/z*: 198 (100), 170 (12.5), 142 (18.8), 114 (87.5). *Anal.* Calcd for $C_{16}H_{18}ClNO_3$: C, 62.44; H, 5.90; Cl, 11.52; N, 4.55. Found: C, 62.57; H, 6.07; Cl, 11.54; N, 4.73.

5-Hydroxy-6-cyclohexylaminomethylnaphthalene-1,8-carbolactone Hydrochloride (2j) Compound **2j** was prepared as described for **2i**. Yield: 65%. mp 160 °C. IR (KBr): 3400 (ν OH), 2600, 2460, 2380 (ν $\overset{+}{N}H_2$), 1780 (ν CO) cm^{-1}. ^{1}H-NMR (DMSO-d_6) δ: 8.80 to 7.80 (3H, m, H aromat.), 7.52 (1H, s, H_7), 4.3 (2H, s, CH_2), 3.2 (2H, br, $\overset{+}{N}H_2$), 2.11 to 1.24 (11H, m, C_6H_{11}). MS *m/z*: 297 (M^+, 0.5), 198 (7.4), 170 (0.7), 114 (3.3). *Anal.* Calcd for $C_{18}H_{20}ClNO_3$: C, 64.77; H, 6.04; Cl, 10.62; N, 4.20. Found: C, 64.67; H, 6.05; Cl, 10.86; N, 4.05.

5-Hydroxy-6-[*N*-(2-chloroethyl)aminomethyl]naphthalene-1,8-carbolactone Hydrochloride (2k) Anhydrous hydrochloric acid was bubbled through a solution of compound **2d** (0.3 g, 1.25 mmol) in anhydrous dichloromethane (60 ml) until a yellow solid precipitated. Then, the precipitate was filtered and recrystallized from anhydrous dichloromethane. Yield: 80%. mp 212 °C. IR (KBr): 3450 (ν OH), 2800, 2670, 2450 (ν $\overset{+}{N}H_2$), 1770 (ν CO) cm^{-1}. ^{1}H-NMR (DMSO-d_6) δ: 8.73 to 7.94 (3H, m, H aromat.), 7.45 (1H, s, H_7), 4.38 (2H, s, CH_2), 3.94 (2H, t, CH_2), 3.3 (2H, t, CH_2). MS *m/z*: 314 [(M, HCl)$^+$, 2], 277 (M^+, 4.5), 198 (32.7), 170 (14.9), 142 (7), 114 (15.8).

***In Vitro* Antifungal Assays** The following species, from the Mycological Laboratory of the Claude Bernard University of Lyon, were used for the *in vitro* screening tests.

Human pathogenic fungi (*Candida albicans*, *Candida tropicalis*, *Torulopsis glabrata*, *Aspergillus niger*, *Aspergillus fumigatus*, *Scopulariopsis brevicaulis*, *Microsporum canis*, *Trichophyton rubrum*) were isolated from infected persons.

For the cultures, Sabouraud or malt agar were used. The compounds were dissolved in a solution of 5% DMSO in water, the ratio of volume of solvent to weight (ml/mg) 1/10. The tests were carried out using agar-well diffusion methanol in Petri plates. Each compound solution was deposited in a well dig in agar at about 1 cm of the fungical culture. The plates were

incubated at 24—25 °C in obscurity. A well full of the solvent was used as the control. The compounds diffused in agar with a decrease of concentration around the well. A compound was considered active if the fungical growth stopped at a minimum of 3 mm around the well, and performed in triplicate.

***In Vitro* Cytotoxic Activity towards L 1210 Leukemia Cells** The *in vitro* cytotoxic testing methods of L 1210 leukemia cells have been previously described.[12] The Mannich bases are tested as hydrochlorides except for **2c** and **2d**. All compounds were dissolved in DMSO (final concentration of DMSO = 0.2%).

Acknowledgments We thank the University Claude Bernard for its financial support on a high field NMR program and Prof. M. Daudon for useful discussions.

References and Notes

1) J. R. Dimmoch and W. G. Taylor, *J. Pharm. Sci.*, **64**, 241 (1975).
2) C. B. Nyathi, V. S. Gupta, and J. R. Dimmock, *J. Pharm. Sci.*, **68**, 1383 (1979).
3) J. R. Dimmock, S. K. Rhaghavan, B. M. Logan, and G. E. Bigam, *Eur. J. Med. Chem.*, **18**, 248 (1983).
4) J. R. Dimmock, S. K. Rhaghavan, and G. E. Bigam, *Eur. J. Med. Chem.*, **23**, 111 (1988).
5) P. Cagniant, G. Kirsch, M. Wierzbicki, F. Lepage, D. Cagniant, D. Loebenberg, R. Parmegiani, and M. Sherlock, *Eur. J. Med. Chem.*, **15**, 439 (1980).
6) R. Steiman, M. Berlion, F. Seigle-Murandi, H. Bériel, and H. Fillion, *Pharmazie*, **44**, 632 (1989).
7) P. A. Leighton, W. A. Perkins, and M. L. Renquist, *J. Am. Chem. Soc.*, **69**, 1540 (1947).
8) W. A. Reeves, G. L. Drake, and G. L. Hoffpanir, *J. Am. Chem. Soc.*, **73**, 3522 (1951).
9) C. Laharotte, Z. Bouaziz, A. Rougny, and H. Fillion, *Pharmazie*, **41**, 142 (1986).
10) R. B. Woodward, F. E. Bader, H. Bickel, A. J. Frey, and R. W. Kierstead, *Tetrahedron*, **2**, 1 (1958).
11) R. Sabie, H. Fillion, M. Daudon, and H. Pinatel, *Synth. Commun.*, **20**, 1713 (1990).
12) M. Chigr, H. Fillion, A. Rougny, M. Berlion, J. Riondel, and H. Bériel, *Chem. Pharm. Bull.*, **38**, 688 (1990).

Oleanene Glycosides from *Crotalaria albida*[1)]

Yi DING,[a] Jun-ei KINJO,[a] Chong-Ren YANG[b] and Toshihiro NOHARA*,[a]

Faculty of Pharmaceutical Sciences, Kumamoto University,[a] Oe-Honmachi 5–1, Kumamoto 862, Japan and Kunming Institute of Botany, Chinese Academy of Science,[b] Kunming, China. *Received August 20, 1990*

Two new oleanene glycosides 4 and 7 were isolated by treatment with CH_2N_2 during a separation procedure from the methanolic extract of *Crotalaria albida* HEYNE, and their structures were characterized as 3-*O*-β-D-xylopyranosyl (1→2)-β-D-galactopyranosyl (1→2)-6-*O*-methyl-β-D-glucuronopyranosyl sophoradiol and 3-*O*-α-L-rhamnopyranosyl (1→2)[β-D-glucopyranosyl(1→6)]-β-D-galactopyranosyl (1→2)-6-*O*-methyl-β-D-glucuronopyranosyl soyasapogenol B, respectively. Other compounds 1, 2, 3, 5 and 6 were identified as the uronic acid methyl esters of kaikasaponins I, III and III monomethyl ether, and soyasaponins III and I, respectively.

Keywords *Crotalaria albida*; sophoradiol; soyasapogenol B; oleanene glycoside; glucoronic acid

Crotalaria albida is distributed in the south of China. The whole plants of *C. albida* are used in traditional Chinese medicine for the treatment of coughs and phlegmy asthma.[2)] Regarding its chemical constituents, a kind of alkaloid, croalbidine, has been characterized. As part of continuing studies on the ingredients in leguminous plants,[1)] we have investigated the glycosidic constituents of the title plant. The methanol extract of the whole plant of *C. albida* was separated by normal and reversed phase column chromatographies to give four sophoradiol glycosides (**1**—**4**) and three soyasapogenol B glycosides (**5**—**7**), among which compounds **4** and **7** were obtained as new compounds. Compounds **1**, **2**, **3**, **5** and **6** were identified with the uronic acid methyl esters of kaikasaponin I,[3)] kaikasaponin III,[3)] kaikasaponin III monomethyl ether, soyasaponin III[4)] and soyasaponin I,[4)] respectively, according to carbon-13 nuclear magnetic resonance (^{13}C-NMR) spectrum and *Rf* values on thin layer chromatography (TLC).

Compound **3**, a white powder, showed peaks due to $[M-H]^-$, at *m/z* 953, which is 14 mass units higher than that of kaikasaponin III methyl ester (**2**), and also a fragment ion peak due to $[M-H-\text{rhamnose}]^-$ at *m/z* 807 in the negative fast atom bombardment mass spectrum (FAB-MS). Acid hydrolysis yielded sophoradiol as a sapogenol. The proton (^{1}H)-NMR spectrum of **3** disclosed the appearance of eight methyl groups and three anomeric proton signals at δ 4.89 (1H, d, *J*=8.1 Hz), 5.64 (1H, d, *J*=8.1 Hz), 6.28 (1H, br s). By comparing ^{13}C-NMR spectrum of **3** with that of **2**, a signal due to an alcholic methoxy group at δ 59.1 newly occurred, and a signal ascribable to the C-6 of the galactosyl moiety showed a lower field shift into δ 72.2 in **3**. From the above evidence, the structure of **3** was assumed to be a 6-*O*-methylated ether derivative in the part of the galactosyl moiety of kaikasaponin III (**2**). The ^{13}C-NMR signals due to the sugar moiety could be assigned reasonably as shown in Table I. The methyl group attached to the galactosyl moiety of **3** might be introduced during CH_2N_2 methylation.[5)]

Compound **4** was obtained as a white powder, $[\alpha]_D$ +161.8° (MeOH). The negative FAB-MS spectrum of **4** exhibited peaks due to $[M-H]^-$ at *m/z* 925 and a $[M-H-\text{pentose}]^-$ at *m/z* 793. The ^{1}H-NMR spectrum of the **4**-peracetate exhibited three anomeric proton signals at δ 4.24 (1H, d, *J*=7.3 Hz), 4.59 (1H, d, *J*=7.7 Hz) and 4.70 (1H, d, *J*=7.6 Hz). The electron impacting mass spectrum (EI-MS) of its acetate revealed fragment ion peaks at *m/z* 547 $[(\text{hexosyl-pentosyl-})Ac_6]^+$ and 259 $[(\text{terminal pentosyl-})Ac_3]^+$. On acid hydrolysis, **4** yielded a sapogenol identical to sophoradiol. This evidence indicated that **4** should be constituted of one mole each of sophoradiol, pentose, hexose and glucuronic acid methyl ester. On the basis of a detailed ^{1}H–^{1}H correlation spectroscopy (COSY) NMR study, all signals due to the sugar moiety could be assigned as shown in the experimental section, namely, the structure of sugar moiety was constructed as β-D-xylopyranosyl (1→2)-β-D-galactopyranosyl (1→2)-6-*O*-

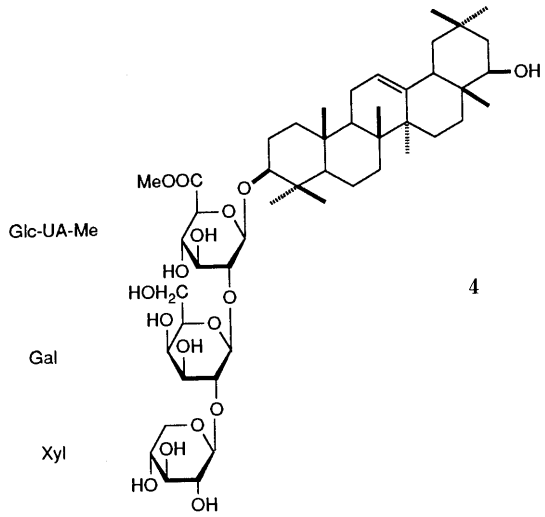

4

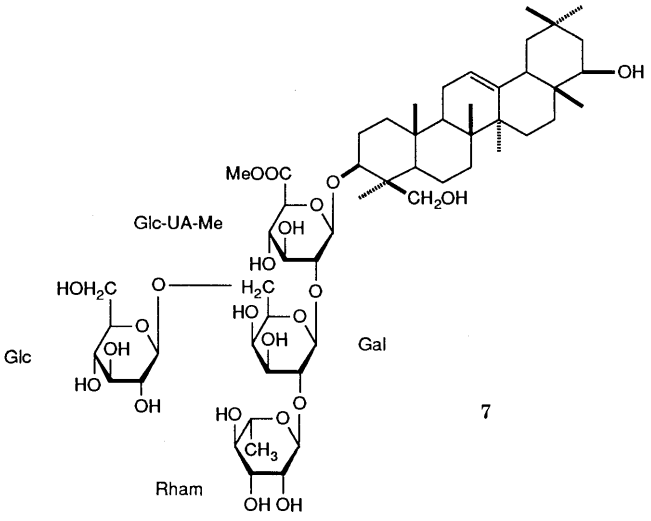

7

TABLE I. ^{13}C-NMR Chemical Shifts of Compounds **1**—**7** (Pyridine-d_5)

	1	2	3	4	5	6	7
C-1	38.9	38.9	38.8	38.9	38.5	38.7	38.6
C-2	26.7[a]	26.5[a]	26.5[a]	26.6[a]	26.6[a]	26.6[a]	26.7[a]
C-3	89.3	90.0	89.9	89.4	90.7	91.3	91.4
C-4	39.7[b]	39.7[b]	39.6[b]	39.6[b]	43.8	43.9	43.8
C-5	55.8	56.0	55.9	55.9	56.1	56.2	56.1
C-6	18.5	18.6	18.5	18.5	18.6	18.5	18.5
C-7	33.2	33.2	33.2	33.2	33.2	33.3	33.2
C-8	40.0[b]	40.1[b]	40.0[b]	40.0[b]	39.8	40.0	39.9
C-9	48.0	48.0	47.9	47.9	47.7	47.8	47.8
C-10	36.9	36.9	36.4	36.8	36.4	36.5	36.4
C-11	23.9	23.9	23.8	23.8	24.0	24.0	24.0
C-12	122.5	122.6	122.5	122.5	122.3	122.3	122.3
C-13	144.8	144.8	144.8	144.9	144.8	144.8	144.8
C-14	42.4	42.5	42.4	42.4	42.2	42.4	42.2
C-15	26.5[a]	26.4[a]	26.5[a]	26.5[a]	26.4[a]	26.4[a]	26.4[a]
C-16	28.7	28.8	28.7	28.7	28.6	28.7	28.6
C-17	38.0	38.1	37.9	38.0	38.0	38.0	38.0
C-18	45.4	45.4	45.3	45.3	45.2	45.3	45.2
C-19	46.8	46.8	46.7	46.8	46.7	46.8	46.7
C-20	30.9	30.9	30.8	30.9	30.8	30.8	30.9
C-21	42.4	42.4	42.3	42.3	42.2	42.3	42.3
C-22	75.6	75.6	75.6	75.6	75.5	75.6	75.5
C-23	23.6	23.0	28.7	28.5	28.6	23.0	23.0
C-24	15.8	15.8	15.7	15.8	63.4	63.5	63.5
C-25	16.8	16.8	16.8	16.9	15.7	15.8	15.8
C-26	17.2	17.2	17.2	17.2	16.9	17.0	16.9
C-27	25.8	25.7	25.7	25.8	25.7	25.6	25.6
C-28	28.2	28.7	28.4	28.2	28.6	28.6	28.6
C-29	33.3	33.2	33.3	33.3	33.2	33.2	33.3
C-30	21.2	21.1	21.2	21.2	21.1	21.0	21.1
G-UA							
1	104.9	105.2	105.2	104.9	105.3	105.4	105.5
2	83.2	79.4	79.4	83.3	80.7	78.1	78.6
3	77.0	76.1[c]	76.2[c]	76.9[c]	77.2	76.7[c]	76.4[c]
4	74.7	73.0	74.3	72.3	73.6	74.3	74.3
5	77.5	76.3[c]	76.8[c]	77.9	77.9	77.6	77.6
6	170.6	170.6	170.6	170.4	170.3	170.2	170.6
COOMe	52.1	51.9	52.1	52.1	52.1	52.0	52.1
Gal							
1	107.2	101.9	102.0	104.0	104.9	101.8	102.5
2	72.8	78.5	78.5	83.1	72.7	76.4[c]	77.0
3	75.0	76.6[c]	76.3[c]	76.0[c]	75.4	76.5[c]	75.0
4	69.6	70.5	70.4	69.1	71.0	71.1	71.5
5	76.7	76.7[c]	75.9	76.5[c]	76.9	76.8[c]	76.0[c]
6	62.0	62.0	72.2	61.4	62.6	61.7	68.1
CH_2OMe			59.1				
Rham							
1		102.8	102.7			102.2	101.6
2		72.3[d]	72.3[d]			72.2[d]	72.3[d]
3		72.6[d]	72.7[d]			72.6[d]	72.7[d]
4		73.0	73.1			73.4	73.7
5		69.4	69.4			69.2	69.3
6		18.9	18.9			18.8	18.9
Xyl							
1				106.7			
2				75.1			
3				77.8			
4				70.6			
5				67.4			
Glc							
1							105.3
2							75.0
3							78.3
4							70.5
5							78.1
6							62.7

a—*d*) In each vertical column may be changeable.

methyl-β-D-glucuronopyranoside. The ^{13}C-NMR spectrum of **4** (Table I) showed a downfield shift at C-3 in the sapogenol moiety compared to that of sophoradiol, indicating the sugar chain to be attached to the C-3 of sophoradiol.[6] In the ^{13}C-NMR spectrum of sugar moiety (Table I), signals due to C-2 of both glucuronic acid and galactose were down-shifted to δ 83.3 ppm and δ 83.1 ppm, respectively, the result of which is consistent with the evidence of the ^{1}H-NMR spectrum. Therefore, the structure of **4** could be represented as 3-*O*-β-D-xylopyranosyl (1→2)-β-D-galactopyranosyl (1→2)-6-*O*-methyl-β-D-glucuronopyranosyl sophoradiol.

Compound **7**, a yellowish powder, $[\alpha]_D$ −11.1° (MeOH), on acid hydrolysis provided soyasapogenol B as sapogenol. The negative FAB-MS spectrum showed peaks due to [M + *p*-nitrobenzylalcohol (NBA) − H]$^-$ at *m/z* 1270 and [aglycone moiety]$^-$ at *m/z* 457, suggesting the occurrence of four sugars including one methyl pentose, two hexose and one glucuronic acid methyl ester. On the other hand, the EI-MS revealed the appearance of a peracetylated terminal hexosyl cation at *m/z* 331 and a peracetylated terminal methyl pentosyl cation at *m/z* 273. On partial acid hydrolysis, **7** provided prosapogenins, two of which were identical with soyasaponin I methyl ester (**6**) and soyasaponin III methyl ester (**5**). The other main compound, P-1, was characterized as a trisaccharide glycoside, in which the terminal rhamnose was removed from **7**, according to the ^{13}C-NMR spectrum. That is, the carbon signals originating from the sugar part indicated the presence of a β-D-glucopyranosyl(1→6)-β-D-galactopyranosyl(1→2)-6-*O*-methyl-β-D-glucuronopyranosyl moiety. Moreover, in the ^{13}C-NMR spectrum (Table I) of **7**, a carbon signal at C-3 showed a downshift to δ 91.4 ppm. Therefore, the structure of **7** was concluded as shown in the formula.

Experimental

Optical rotations were measured on a JASCO DIP-360 automatic digital polarimeter. The ^{1}H- and ^{13}C-NMR spectra were measured with a JEOL JNM-GX 400 NMR spectrometer, and chemical shifts are given on a δ (ppm) scale with tetramethylsilane as an internal standard. The FAB- and EI-MS were recorded with a JEOL DX-300 spectrometer. Column chromatography was carried out with MCI gel CHP 20P (75—100 μm, Mitsubishi Chem. Ind. Co., Ltd.) and Kieselgel 60 (70—230 and 230—400 mesh, Merck). TLC was conducted on a precoated Kieselgel 60 F_{254} plate (0.2 mm, Merck), and detection was achieved by spraying it with 10% H_2SO_4 followed by heating.

Extraction and Separation The dried aerial parts (1.1 kg) of *Crotalaria albida* (Leguminosae) collected in the Yunnan province were extracted with MeOH and the extract (74 g) was partitioned between 1-BuOH and H_2O. The 1-BuOH layer (31 g) was refluxed with *n*-hexane. The *n*-hexane insoluble portion (20 g) treated with AcOH was subjected to MCI gel CHP 20P column chromatography using 30% MeOH→MeOH to give fractions 1 to 14. Fractions 10, 11 and 12 were respectively treated with excess diazomethane followed by column chromatography over silica gel using $CHCl_3$–MeOH–H_2O (9:1:0.1→8:2:0.2), to provide compounds **1** (21 mg), **2** (41.8 mg), **3** (34.1 mg), **4** (24.1 mg), **5** (34 mg), **6** (220 mg) and **7** (71 mg).

Compound 1 Colorless needles, $[\alpha]_D^{29}$ +14.8° (*c*=0.43, MeOH). Negative FAB-MS (*m/z*): 793 [M−H]$^-$. Identified with kaikasaponin I methyl ester.

Acetylation of 1 A solution of **1** (5 mg) in Ac_2O–pyridine (1:1) was heated at 80 °C on a water bath for 2 h. The reaction mixture was evaporated under a N_2 gas and then chromatographed on silica gel using *n*-hexane–acetone (3:1), giving **1**-Ac, a white powder. ^{1}H-NMR ($CDCl_3$) δ: 0.81, 0.85, 0.90, 0.94, 0.97, 1.00, 1.08, 1.14 (each 3H, s, 8×CH_3), 4.51 (1H, d, *J*=7.7 Hz), 4.66 (1H, d, *J*=7.7 Hz).

Compound 2 A white powder, $[\alpha]_D^{29}$ −4.9° (*c*=0.44, MeOH). ^{1}H-NMR

(pyridine-d_5) δ: 0.89, 0.99, 1.02, 1.14, 1.21, 1.25, 1.27, 1.37 (each 3H, s, $8 \times CH_3$), 1.72 (3H, d, $J=5.9$ Hz, CH_3), 4.99 (1H, d, $J=7.3$ Hz), 5.61 (1H, d, $J=7.3$ Hz), 6.22 (1H, br s). Identified with kaikasaponin III methyl ester.

Compound 3 A white powder. Negative FAB-MS (m/z): 953 $[M-H]^-$. 807 $[M-H-rham]^-$. ^{1}H-NMR (pyridine-d_5) δ: 0.75, 0.96, 1.00, 1.23, 1.26, 1.27, 1.29, 1.42 (each 3H, s, $8 \times CH_3$), 1.73 (3H, d, $J=5.9$ Hz, CH_3), 4.98 (1H, d, $J=8.1$ Hz), 5.64 (1H, d, $J=8.1$ Hz), 6.28 (1H, br s).

Compound 4 A white powder, $[\alpha]_D^{29}$ +161.8° ($c=0.51$, MeOH). Negative FAB-MS (m/z): 925 $[M-H]^-$, 793 $[M-H-pentose]^-$.

Acetylation of 4 A solution of **4** (8 mg) in Ac_2O–pyridine (1 : 1) was heated at 80 °C on a water bath for 2 h. The reaction mixture was worked up as described above to give **4**-Ac, a white powder. EI-MS (m/z): 547 $[(pen\text{-}hex\text{-})Ac_6]^+$, 259 $[(terminal\ pen\text{-})Ac_3]^+$. ^{1}H-NMR ($CDCl_3$) δ: 0.81, 0.84, 0.89, 0.95, 0.97, 1.00, 1.04, 1.14 (each 3H, s, $8 \times CH_3$), 3.13 (1H, dd, $J=4.8$, 11.7 Hz, H-3), 3.37 (1H, dd, $J=7.0$, 12.5 Hz, xyl H-5'), 3.76 (1H, dd, $J=7.7$, 10.3 Hz, gal H-2), 3.81 (1H, m, gal H-5), 3.88 (1H, t, $J=7.7$ Hz, UA H-2), 4.07 (2H, m, gal H-6,6'), 4.16 (1H, d, $J=9.5$ Hz, UA H-5), 4.24 (1H, dd, $J=5.1$, 12.5 Hz, xyl H-5), 4.57 (1H, d, $J=7.0$ Hz, UA H-1), 4.59 (1H, d, $J=7.7$ Hz, gal H-1), 4.64 (1H, br t, H-22), 4.71 (1H, d, $J=6.6$ Hz, xyl H-1), 4.91 (1H, dd, $J=3.3$, 6.6 Hz, gal H-3), 4.93 (1H, t, $J=6.6$ Hz, xyl H-2), 5.04 (1H, m, xyl H-4), 5.15 (1H, t, $J=5.9$ Hz, xyl H-3), 5.18 (1H, t, $J=9.5$ Hz, UA H-4), 5.24 (1H, t, $J=8.4$ Hz, UA H-3), 5.25 (1H, br t, H-12), 5.26 (1H, t, $J=3.3$ Hz, gal H-4).

Compound 5 A white powder, $[\alpha]_D^{29}$ +15.4° ($c=0.52$, MeOH). Identified soyasaponin III methyl ester.

Compound 6 Colorless needles, $[\alpha]_D^{29}$ −7.2° ($c=0.47$, MeOH). ^{1}H-NMR (pyridine-d_5) δ: 0.73, 0.97, 0.99, 1.20 (each 3H, s, $4 \times CH_3$), 1.26 (6H, s, CH_3), 1.43 (3H, s, CH_3), 1.72 (3H, d, $J=5.9$ Hz, CH_3), 4.91 (1H, d, $J=7.3$ Hz), 5.68 (1H, d, $J=7.3$ Hz), 6.19 (1H, br s). Identified with soyasaponin I methyl ester.

Compound 7 A yellowish powder, $[\alpha]_D^{29}$ −11.1° ($c=0.57$, MeOH). Negative FAB-MS (m/z): 1270 $[M+NBA-H]^-$, 1117 $[M-H]^-$, 457 $[aglyconemoiety]^-$.

Acetylation of 7 A solution of **7** (5 mg) in Ac_2O–pyridine (1 : 1) was heated and then purified by silica gel column chromatography using *n*-hexane–acetone (2 : 1) to give **7**-Ac, a white powder. EI-MS (m/z): 331 $[(terminal\ hex\text{-})Ac_4]^+$, 273 $[(terminal\ rham\text{-})Ac_3]^+$. ^{1}H-NMR ($CDCl_3$) δ: 0.82, 0.90, 0.97, 1.00, 1.13, 1.24, 1.26 (each 3H, all s, $7 \times Me$), 3.18 (1H, dd, $J=4.4$, 11.4 Hz, H-3), 3.73 (2H, m, gal H-5 and glc H-5), 3.77 (3H, m, UA H-2 and gal-H-6,6'), 3.98 (1H, t, $J=9.3$ Hz, gal H-2), 4.05 (1H, ABq, $J=10.6$ Hz, H-24), 4.06 (1H, d, $J=9.9$ Hz, UA H-5), 4.12 (1H, q, rham H-5), 4.19 (1H, dd, $J=2.0$, 12.1 Hz, glc H-6), 4.28 (1H, dd, $J=4.4$, 12.1 Hz, glc H-6'), 4.41 (1H, d, $J=7.3$ Hz, UA H-1), 4.42 (1H, ABq, $J=10.6$ Hz, H-24'), 4.59 (1H, d, $J=7.7$ Hz, gal H-1), 4.64 (1H, t, $J=3.7$ Hz, H-22), 4.67 (1H, d, $J=8.1$ Hz, glc H-1), 4.88 (1H, dd, $J=3.3$, 10.3 Hz, gal H-3), 4.96 (1H, br s, rham H-1), 4.99 (1H, t, $J=8.6$ Hz, glc H-2), 5.02 (1H, t, $J=8.1$ Hz, UA H-4), 5.06 (1H, t, $J=8.1$ Hz, rham H-4), 5.13 (1H, t, $J=9.5$ Hz, glc H-4), 5.18 (1H, d, $J=2.2$ Hz, rham H-2), 5.20 (2H, t, $J=9.3$ Hz, UA H-3 and glc H-3), 5.23 (1H, d, $J=9.5$ Hz, rham H-3), 5.27 (1H, br t, H-12), 5.31 (1H, d, $J=3.3$ Hz, gal H-4).

Partial Hydrolysis of 7 Compound **7** (30 mg) was heated on a hot water bath with 0.2 N HCl–MeOH for 20 min. The reaction mixture was evaporated to dryness and chromatographed over silica gel with $CHCl_3$–MeOH–H_2O (8 : 2 : 0.2), to afford prosapogenins P-3 (soyasaponin III), P-2 (soyasaponin I) and P-1 (main compound).

P-1 A white powder. FAB-MS (m/z): 971 $[M-H]^-$, 457 [aglycone moiety]$^-$. ^{13}C-NMR (pyridine-d_5) δ: 38.7, 26.7, 90.8, 43.9, 56.1, 18.7, 33.3, 39.9, 47.7, 36.5, 24.0, 122.4, 144.8, 42.3, 26.4, 28.6, 38.0, 45.2, 46.7, 30.9, 42.3, 75.5, 22.6, 63.3, 15.7, 16.9, 25.7, 28.6, 33.2, 21.1 (C 1—30), 104.6, 78.7, 77.1, 73.4, 77.8, 170. 5, 52.1 (UA 1—6 and Me), 105.1, 72.9, 75.1, 70.2, 75.5, 68.7 (gal 1—6), 105.2, 75.1, 78.3, 71.5, 78.5, 62.7 (glc 1—6).

Acetylation of P-1 P-1 was acetylated as above, giving a white powder after purification with silica gel column chromatography. EI-MS (m/z): 619 $[(hex\text{-}hex\text{-})Ac_7]$, 331 $[(terminal\ hex\text{-})Ac_4]$. ^{1}H-NMR ($CDCl_3$) δ: 0.81, 0.90, 0.96, 0.97, 1.00, 1.14, 1.25 (each 3H, all s, $7 \times Me$), 3.75 (3H, m, gal H-5 and gal-H 6,6'), 3.77 (1H, m, glc H-5), 3.78 (1H, dd, $J=4.8$, 11.7 Hz, H-3), 3.80 (1H, t, $J=7.7$ Hz, UA H-2), 3.97 (1H, d, $J=9.9$ Hz, UA H-5), 4.04 (1H, ABq, $J=10.9$ Hz, H-24), 4.21 (1H, dd, $J=2.0$, 12.5 Hz, glc H-6'), 4.27 (1H, dd, $J=4.4$, 12.5 Hz, glc H-6), 4.44 (1H, ABq, $J=10.9$ Hz, H-24'), 4.46 (1H, d, $J=7.3$ Hz, UA H-1), 4.60 (1H, d, $J=7.7$ Hz, gal H-1), 4.65 (1H, t, $J=3.7$ Hz, H-22), 4.66 (1H, d, $J=8.4$ Hz, glc H-1), 4.89 (1H, dd, $J=3.3$, 10.6 Hz, gal H-3), 4.99 (1H, t, $J=8.6$ Hz, glc H-2), 5.01 (1H, t, $J=9.9$ Hz, UA H-4), 5.04 (1H, t, $J=7.7$ Hz, gal H-2), 5.13 (1H, t, $J=9.9$ Hz, glc H-4), 5.20 (2H, t, $J=9.3$ Hz, UA H-3 and glc H-3), 5.26 (1H, br t, H-12), 5.30 (1H, d, $J=3.7$ Hz, gal H-4).

Acknowledgement We are grateful to Dr. S. Yahara, Mr. K. Takeda and Mr. T. Iriguchi in this Faculty for measurements of NMR spectra and MS and for their valuable suggestions.

References and Notes

1) Part XX in a series of studies of the constituents of leguminous plants.
2) Chiang Su New Medical College (ed.), "Dictionary of Chinese Crude Drugs," Shanghai Scientific Technologic Publisher, Shanghai, 1977, p. 2071.
3) I. Kitagawa, T. Taniyama, W. W. Hong and M. Yoshikawa, *Yakugaku Zasshi*, **108**, 538 (1988).
4) *a*) M. Yoshikawa, H. K. Wang, H. Kayakiri, T. Taniyama and I. Kitagawa, *Chem. Pharm. Bull.*, **33**, 4267 (1985); *b*) J. Kinjo, T. Takeshita, Y. Abe, N. Terada, H. Yamashita, M. Yamasaki, K. Takeuchi, K. Murakami, T. Tomimatsu and T. Nohara, *ibid.*, **36**, 1174 (1988).
5) M. Aritomi and T. Kawasaki, *Chem. Pharm. Bull.*, **18**, 677 (1970).
6) *a*) R. Kasai, M. Suzuo, J. Asakawa and O. Tanaka, *Tetrahedron Lett.*, **1977**, 195; *b*) K. Tori, S. Seo, Y. Yoshimura and H. Arita, *ibid.*, **1977**, 179.

Solid-Phase Enzyme-Immunoassay of Anti-Insulin Antibodies: Effect of Labeling Site in Insulin and of Labeled Number of Horseradish Peroxidase on the Assay Sensitivity

Kiyoshi ZAITSU, Masao NAKAYAMA, Masahiko NANAMI and Yosuke OHKURA*

Faculty of Pharmaceutical Sciences, Kyushu University, 62, Maidashi, Higashi-ku, Fukuoka 812, Japan. *Received June 25, 1990*

Three horseradish peroxidase (HRP)-labeled porcine insulins which have definite labeling site(s) were compared regarding sensitivity in a solid-phase enzyme-immunoassay (EIA) of anti-insulin antibodies. The standard curves obtained with Lys^{B29}–HRP–insulin and Gly^{A1}–HRP–insulin were steeper than that with Gly^{A1},Lys^{B29}–diHRP–insulin for both polyclonal and monoclonal antibodies. Thus, the mono-HRP–labeled insulins can afford higher sensitivities in the EIA. The importance of the HRP-labeling site in insulin and of the number of labeled HRP was first demonstrated by using HRP–labeled insulins having definite labeling site(s).

Keywords enzyme-immunoassay; solid-phase antigen; anti-insulin antibody; monoclonal antibody; enzyme-labeling; horseradish peroxidase–insulin conjugate; labeling site; sensitivity

A solid-phase enzyme-immunoassay (EIA) of an anti-insulin antibody using an enzyme-labeled insulin has been reported[1]: the antibody was sandwiched between insulin covalently attached to albumin-coated silicone lod and β-galactosidase-labeled insulin. This type of EIA is valuable for the assay of antibodies of all immunoglobulin classes. However, little is known about the effect of enzyme-labeled insulins having definite enzyme-labeling site(s) on the EIA. To improve the above mentioned assay system, it is necessary first to know the assay sensitivities of some enzyme-labeled insulins with definite labeling site(s).

Recently, we prepared horseradish peroxidase (HRP; EC 1.11.1.7)-labeled porcine insulin conjugates (HRP–insulins), which have definite labeling site(s): Gly^{A1}–HRP–insulin, Lys^{B29}–HRP–insulin and Gly^{A1},Lys^{B29}–diHRP–insulin.[2] These HRP–insulins were used in a competitive EIA of human insulin. Thus, the assay sensitivity was dependent on the number of enzymes on the insulin molecule.[3]

The aim of this paper is to investigate the effects of the labeled number of enzymes and the enzyme-labeling site in insulin on the sensitivity in the solid-phase assay of anti-insulin antibodies. The HRP activities were measured fluorometrically by using 3-(*p*-hydroxyphenyl)propionic acid (HPPA) as a fluorogenic substrate.[4]

Experimental

Chemicals Bovine serum albumin fraction V (BSA; purified by the method of Chen[5]) and glutaraldehyde solution (70%, biochemical grade) were obtained from Wako (Osaka, Japan). HPPA was obtained from Dojindo (Kumamoto, Japan). Lyophilized porcine insulin was prepared[6] from a porcine insulin solution (Monocomponent Insulin Novo Actrapid; Novo Ind., Copenhagen, Denmark). Other reagents were of analytical-reagent grade. Deionized water was passed through a Milli-QII system (Japan Millipore, Tokyo, Japan) and used throughout this study.

Antibodies A guinea pig anti-porcine insulin serum was obtained from Medical & Biological Laboratories (lot 0274; Nagoya, Japan). A guinea pig anti-human insulin polyclonal antibody immunoglobulin G (IgG) solution (lot AI-11; 2.7 mg IgG/ml in 100 mM Na–K phosphate buffer (pH 7.5)) and a mouse anti-human insulin monoclonal antibody IgG solution (lot AIEB-01; recognizes the A8-A10 loop determinant of insulin; 2.2 mg IgG/ml in 100 mM Na–K phosphate buffer (pH 7.5)) were supplied by Dainabot (Tokyo, Japan). For the preparation of standard curves, these antibody solutions were diluted with a 10 mM Na–K phosphate buffer (pH 7.0) containing 100 mM NaCl and 0.1% (w/v) BSA.

Insulin-BSA-Coated Polystyrene (PS) Balls The two-step glutaraldehyde method[1] was employed to prepare the immobilized insulin with some modifications. Four hundred pieces of PS balls (6.35 mm diameter; Sekisui Chemical Co., Osaka, Japan) were washed with 1% (w/v) Scat 20X-N (Daiichi Kogyo Seiyaku Co., Tokyo, Japan) and rinsed thoroughly with water. The balls were soaked in 160 ml of a 0.1% (w/v) BSA solution in a 10 mM Na–K phosphate buffer (pH 7.0) containing 100 mM NaCl and 1 mM $MgCl_2$ (BSA solution) at 4 °C for 24 h. The BSA-coated balls were soaked in 150 ml of a 0.5% (w/v) glutaraldehyde solution in the dark at 20 °C for 1 h. Excess glutaraldehyde was removed by washing the balls with water at 4 °C. To 100 pieces of glutaraldehyde activated BSA-coated balls was added 100 ml of 0.2 mg/ml porcine insulin solution in 250 mM Na–K phosphate buffer (pH 7.5) containing 0.032% (w/v) BSA, and the mixture was allowed to stand at 4 °C for 18 h. The resulting insulin-BSA-coated PS balls were washed with water at 4 °C and kept in the BSA solution for more than 16 h at 4 °C, then used for the assay.

HRP–Insulin Solutions Gly^{A1}–HRP–insulin, Lys^{B29}–HRP–insulin and Gly^{A1},Lys^{B29}–diHRP–insulin were prepared as previously reported.[2] The HRP–insulins were dissolved in 100 mM Na–K phosphate buffer (pH 7.5) containing 1% (w/v) BSA to obtain 1 μM of the following solutions: Gly^{A1}–HRP–insulin and Lys^{B29}–HRP–insulin solutions, both with absorbances at 403 nm (1-cm optical path length) 0.102, and a Gly^{A1},Lys^{B29}–diHRP–insulin solution with that of 0.204 were prepared. The molar absorptivity of HRP at 403 nm was taken as $1.02 \times 10^5\ M^{-1}\ cm^{-1}$.[7] The solutions were stored at 4 °C and diluted with the BSA solution to 10 nM before use.

Preparation of Calibration Curves To an insulin-BSA-coated PS ball placed in a disposable glass culture tube (75 × 12 mm i.d., Corning Glass Works, New York, U.S.A.) was added a mixture of 100 μl of an anti-insulin antibody solution diluted with the BSA solution and 200 μl of the BSA solution, or 300 μl of the BSA solution for the blank. The mixture was incubated at 4 °C for 18 h and the solution was removed by aspiration. The ball was washed twice, using 2 ml of ice-cold water each time. The ball was transferred into 300 μl of a 10 nM solution of an HRP–insulin placed in another culture tube, and the mixture was again incubated at 4 °C for 3 h. After removal of the solution, the ball was washed in the same way as above. The HRP activity on the ball was measured as follows[8]: the ball was added to a mixture of 700 μl of 150 mM Tris–HCl buffer (pH 8.5) and 350 μl of 60 mM HPPA solution, and the enzyme reaction was initiated by adding 70 μl of 40 mM H_2O_2 with mixing. The mixture was incubated at 30 °C for exactly 30 min with gentle shaking. The reaction was stopped by adding 70 μl of 10% (w/v) Na_2SO_3. The fluorescence intensities were measured at an excitation wavelength of 320 nm and an emission wavelength of 404 nm with a Hitachi MPF-4 spectrofluorometer in quartz cells. The slitwidths in the excitation and emission monochromators were set at 2 and 10 nm, respectively. Duplicate assays were conducted. Fluorescence intensities were plotted against the concentrations of an anti-insulin antibody on a semi-log graph.

Results and Discussion

In a preliminary test for the preparation of the calibration curve, a normal guinea pig serum and its IgG were subjected to control tests to evaluate non-specific binding. Both 100 μl of a BSA solution containing 10 μl of the normal serum, and 100 μl of a BSA solution containing 50 μg of the normal guinea pig IgG, gave almost the same fluorescence intensity as that of the blank obtained under Preparation of

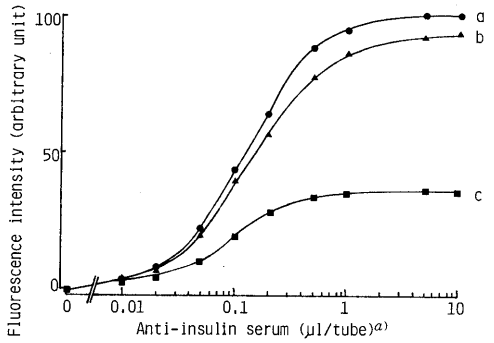

Fig. 1. Standard Curves for Anti-Porcine Insulin Serum with HRP–Insulins

Curves: a, Lys^{B29}–HRP–insulin; b, Gly^{A1}–HRP–insulin; c, Gly^{A1}, Lys^{B29}–diHRP–insulin. *a*) 0.01—10 μl/tube, correspond to 30000—30-fold dilution of anti-serum.

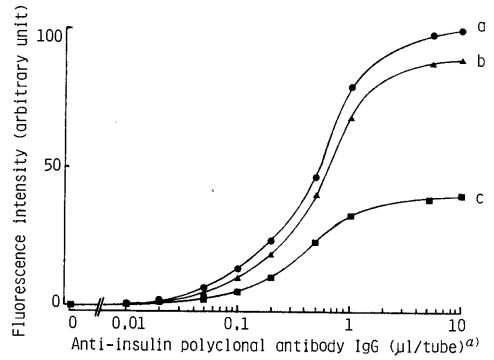

Fig. 2. Standard Curves for Anti-Human Insulin Antibody IgG with HRP–Insulins

For curves a, b and c, see Fig. 1. *a*) 0.01—10 μl/tube, correspond to 27 ng—27 μg of the IgG/tube.

Calibration Curve. Thus, a procedure for the control experiment was omitted in the preparation of standard curves. The HRP-labeling site(s) and the number on the insulin molecule affected the slopes of the standard curves. Sigmoidal standard curves were observed for the anti-insulin polyclonal antibodies (guinea pig anti-porcine insulin serum and guinea pig anti-human insulin antibody IgG) (Figs. 1 and 2). On the other hand, quasi-linear curves were obtained from the anti-insulin monoclonal antibody (mouse anti-human insulin antibody IgG) (Fig. 3). For the polyclonal antibodies, the standard curves obtained with Lys^{B29}–HRP–insulin (curves a in Figs. 1 and 2) were steeper than those with Gly^{A1}–HRP–insulin (curves b in Figs. 1 and 2), and much steeper than those with Gly^{A1},-Lys^{B29}–diHRP–insulin (curves c in Figs. 1 and 2). For the monoclonal antibody, the standard curve obtained with Lys^{B29}–HRP–insulin (curve a in Fig. 3), was similar to that with Gly^{A1}–HRP–insulin (curve b in Fig. 3), and much steeper than that with Gly^{A1},Lys^{B29}–diHRP–insulin (curve c in Fig. 3). A range of relative average deviations of the duplicate assays was 0.2—4.6%. The results obtained with the monoclonal antibodies indicate that mono-HRP–labeled insulins are preferable in attaining higher sensitivities in the

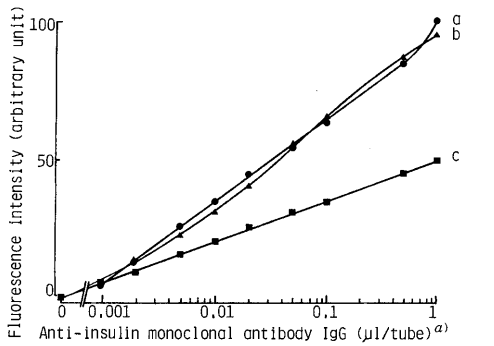

Fig. 3. Standard Curves for Anti-Human Insulin Monoclonal Antibody IgG with HRP–Insulins

For curves a, b and c, see Fig. 1. *a*) 0.001—1 μl/tube, correspond to 2.2 ng—2.2 μg of the IgG/tube.

EIA of anti-insulin antibodies which recognize the A-chain loop determinant, the A8—A10 residue of porcine insulin. Also, the mono-HRP–labeled insulins afford higher sensitivities in the assay of the polyclonal antibodies. The advantage of the mono-HRP–labeled insulins in sensitivity may be derived from the fact that the affinity of the monoclonal antibodies for the A-chain loop determinant of mono-HRP–labeled insulin was larger than that for the diHRP–labeled insulin. Two HRP molecules on the Gly-A1 and Lys-B29 amino groups of the insulin may cause an undesirable effect, which reduces the affinity. The distance between the Gly-A1 and Lys-B29 amino groups is short,[9] thus a lump of HRP molecule may be constructed on the insulin molecule. This lump may disturb access of the A8—A10 region of diHRP–labeled insulin to the monoclonal antibodies. The above assumption may be compatible with the case in the assay of polyclonal antibodies. Therefore, the use of insulin with a suitable labeling site of HRP should be taken into consideration to develop highly sensitive assay methods of anti-insulin antibodies.

Acknowledgement We wish to thank Dainabot Co. Ltd. for the generous gift of the antibodies. This work was supported in part by a Grant-in-Aid for Scientific Research from the Ministry of Education, Science and Culture of Japan (63571022).

References

1) K. Kato, Y. Haruyama, Y. Hamaguchi and E. Ishikawa, *J. Biochem.* (Tokyo), **84**, 93 (1978).
2) K. Zaitsu, M. Nakayama and Y. Ohkura, *Chem. Pharm. Bull.*, **36**, 1425 (1988).
3) M. Nakayama, K. Zaitsu and Y. Ohkura, *Jpn. J. Clin. Chem.*, **18**, 95 (1989).
4) K. Zaitsu and Y. Ohkura, *Anal. Biochem.*, **109**, 109 (1980).
5) R. F. Chen, *J. Biol. Chem.*, **242**, 173 (1967).
6) K. Zaitsu, H. Hosoya, Y. Hayashi, H. Yamada and Y. Ohkura, *Chem. Pharm. Bull.*, **33**, 1159 (1985).
7) G. R. Schonbaum and S. Lo, *J. Biol. Chem.*, **247**, 3353 (1972).
8) K. Zaitsu, K. Nakashima, S. Akiyama and Y. Ohkura, *Chem. Pharm. Bull.*, **30**, 4114 (1982).
9) J. A. Schroer, T. Bender, R. J. Feldman and K. J. Kim, *Eur. J. Immunol.*, **13**, 693 (1983).

High Levels of Cholesteryl Esters, Progesterone and Estradiol in the Testis of Aging Male Fischer 344 Rats: Feminizing Leydig Cell Tumors

Hirokazu KONISHI, Haruo OKAJIMA, Youji OKADA, Hiroshi YAMAMOTO, Kouji FUKAI and Hiroshi WATANABE*

School of Health Sciences, Kyorin University, Miyashita-cho, Hachioji, Tokyo 192, Japan. *Received July 20, 1990*

The levels and fatty acid composition of cholesteryl esters (CEs), and the levels of steroid hormones in the testis of aging Fischer 344 (F344) rats were studied in comparison with those of 6-month-old rats without Leydig cell tumors (controls). The total lipid content in the testis increased as Leydig cell tumors developed: in 23-month-old rats, the content increased to five times higher than that of the controls. The CE level reached about 300 times higher than that of the controls and comprised 57.5% of the total lipid of the testis. The fatty acid composition of the CEs in the tumor compared to the normal tissue from the controls was characterized by a marked increase in 22:4 (*n*-6) and a decrease in 22:5 (*n*-6), a characteristic acid in rat testis lipids. Testicular progesterone levels considerably increased with the development of tumors (23-month-old rats, 2870 ng/wet wt; controls, 7 ng/g wet wt). Also, levels of estradiol showed striking increments (23-month-old rats, 2205 pg/g wet wt; controls, 153 pg/g wet wt). On the other hand, testosterone levels decreased (23-month-old rats, 13 ng/g wet wt; controls, 50 ng/g wet wt).

These results suggest that Leydig cell tumors in aging F344 rats resemble the ovary tissue of rats in the levels and fatty acid composition of the CEs, and in the levels of steroid hormones. This is supported by the observation that the two kinds of cells found in the tumor tissue resemble cells of the corpus luteum and granulosa cells of the follicles, respectively, in the ovary of rats. In conclusion, the study shows that Leydig cell tumors in aging male F344 rats have a tendency towards feminization.

Keywords Fischer 344 rat; Leydig cell tumor; cholesteryl ester; docosatetraenoic acid; progesterone; estradiol

Introduction

It is known that long-term breeding (more than 2 years) of laboratory animals such as rats and mice causes the spontaneous development of tumors in various organs.[1] Male Fischer 344 (F344) rats are characterized by a very high incidence (more than 98% in 24-month-old rats) of Leydig cell (testicular interstitial cell) tumors,[2] when compared with other strains of rats[3] and mice.[4] In humans, Leydig cell tumor, a nongerminal cell tumor,[5a] is relatively rare, accounting for only 2 to 3% of all testicular tumors.[5b] There have been several reports on Leydig cell tumors in male F344 rats,[2] but relatively few on the biochemical findings.[6]

Turek and Desjardins reported on the relationship between Leydig cell tumorigenesis and age-related changes in the synthesis and/or secretion of gonadal adenohypophyseal hormone,[6a] and Amador *et al.* studied the influence of spontaneous Leydig cell tumors on changes in testicular LH receptors and serum steroid hormone levels.[6b] However, these authors did not describe the testicular lipid compositions and testicular steroid hormone levels in aging F344 rats with Leydig cell tumors.

As a part of our biochemical studies on spontaneous Leydig cell tumors in aging male F344 rats, we have studied the testicular levels and fatty acid composition of cholesteryl esters (CEs), which function as precursors of steroid hormones in steroidogenic tissues, and the testicular levels of steroid hormones. The data presented here suggest that Leydig cell tumors in aging F344 rats resemble the ovary tissue of rats with respect to lipid components, their fatty acid compositions, and steroid hormone production.

Materials and Methods

Animals Male F344/DuCrj rats, aged 5 weeks, obtained from Charles River Japan Inc. were maintained on a basal diet (pellet CE-2, Cler Japan Inc.) and tap water. The animals were housed two to a plastic cage and kept under a 14-h light: 10-h dark cycle at 23 ± 2 °C with a relative humidity of 55 ± 5%. Body weights were recorded every week.

Assays of Steroid Hormones Radioimmunoassays (RIAs): RIAs of testosterone (T), progesterone (P), and estradiol (E_2) in serum and in testis were carried out in Special Reference Laboratory (Tokyo), as previously described.[7]

High Performance Liquid Chromatography (HPLC): HPLC analysis of P and T in the tissue was carried out according to the method of Laganà *et al.*[8]

Lipid Extraction, Lipid Fractionation and Preparation of Fatty Acid Methyl Esters The total lipids of tissue were extracted by the method of Folch *et al.*[9] Fractionation of the total lipids and preparation of fatty acid methyl esters were performed by the methods previously reported.[10]

Determinations of the Concentrations of CEs The concentrations of CEs were estimated colorimetrically after chromatographic separation.[11] These values were essentially identical with those determined by an enzymatic method.[12]

Gas Chromatography (GC) and Gas Chromatography-Mass Spectrometry (GC-MS) GC and GC-MS analyses of fatty acid methyl esters from each lipid class[10] and GC analysis of free sterols in the mixture obtained by alkaline hydrolysis of CE[13] were carried out according to the procedures previously described.

Results and Discussion

Light Microscopic Examination of Testes Light microscopy in 6-month-old rats used as controls indicated that the testes consisted of only normal cells (Fig. 1A). In contrast, all five 12-month-old rats had some hyperplasias of Leydig cells, which can progress to a tumor.[14] The testes in all five rats at 18 and 23 months of age and in all four rats at 21 months of age contained tumors in addition to Leydig cell hyperplasias (Fig. 1B). The tumors were composed of two kinds of cells: relatively large cells with clear cytoplasm ("a" in Fig. 1B) and uniform polyhedral cells with nuclei rich in chromatins ("b" in Fig. 1B).[6a] They exhibited distinct boundaries with the remaining tissue consisting mostly of normal and hyperplastic tissue. In the 18-, 21-, and 23-month-old rats, the tumor tissues, which were macroscopically separated from the remaining tissue, occupied 8, 50, and 88% (by weight) of the whole testis, respectively.

Testicular Weights Testicular weights remained unchanged in 6- and 12-month-old rats, but increased after 18 months of age (Table I). The weight in 23-month-old

TABLE I. Weights, Lipid Contents and Cholesteryl Ester (CE) Levels of Testis in Aging Fischer 344 Rats

Age (months)	Wet weight (g/a rat)	Lipid content (% of wet weight)		CE level (mg/g wet weight)	
		Total[a]	Tumor[b]	Total[a]	Tumor[b]
6	3.16±0.04	2.2±0.1	—	0.2±0.1	—
12	3.20±0.10	2.0±0.1	—	0.1±0.1	—
18	3.56±0.12	2.4±0.1	5.8±0.3	3.7±0.2	32.8±0.5
21	4.12±0.30	4.3±0.2	6.6±0.4	17.5±0.5	27.1±0.6
23	5.14±0.24	10.6±0.8	11.7±0.8	60.9±2.5	68.1±2.7

Values are expressed as the mean±SEM of individual determinations in five rats for all groups, except the 21-month-old group (four animals). *a*) Total testis tissue. *b*) Isolated tumor tissue.

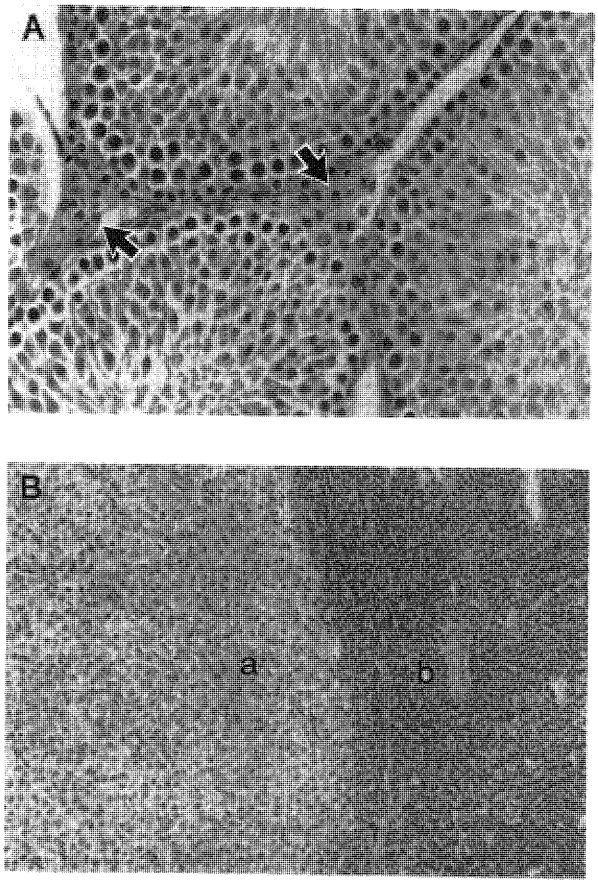

Fig. 1. Light Microscopic Appearance of Leydig Cells from Aging Fischer 344 Rats

A) Normal Leydig cells (arrows) from 6-month-old rats (hematoxylin–eosin; ×200). B) Leydig cell tumors from 23-month-old rats (hematoxylin–eosin; ×100). Two kinds of cells ("a" and "b") found in the tumor tissue resemble cells of the corpus luteum and granulosa cells of the follicle, respectively, of rats.

rats was 1.6 times greater than that in the controls.

Lipid Content of Testes The lipid content of the testes increased after 18 months of age, coinciding with the first appearance of the tumors (Table I). For example, the content of 23-month-old rat testes was five times higher than that in the controls (6-month-old rats). The tumor tissue isolated from the testes of 23-month-old rats contained higher amounts of lipids than did the remaining tissue (2.4% of wet wt). This indicates that the high lipid contents in 18-, 21-, and 23-month-old rat testes were attributed to the tumors. Thus, spontaneous Leydig cell tumors in aging F344 rats were characterized by their high lipid content.

TABLE II. Fatty Acid Composition of Cholesteryl Esters in Normal[a] and Tumor[b] Tissues of Aging Fischer 344 Rat Testes

Fatty acid	Normal	Tumor
16:0	14.45±0.74	8.08±0.28
16:1	4.52±0.78	1.33±0.09
18:0	1.61±0.21	3.74±0.16
18:1	7.58±0.70	18.90±0.33
18:2 (*n*-6)	12.22±1.01	6.04±0.16
18:3 (*n*-6)	0.44±0.04	0.20±0.07
20:0	0.23±0.04	0.32±0.03
20:1	1.99±0.09	4.93±0.34
20:2 (*n*-6)	1.40±0.14	9.48±0.56
20:3 (*n*-3)	0.78±0.03	7.38±0.06
20:4 (*n*-6)	20.46±0.84	6.82±0.28
20:5 (*n*-3)	0.38±0.12	0.39±0.09
22:4 (*n*-6)	1.58±0.13	17.88±0.46
22:5 (*n*-6)	15.04±0.72	1.07±0.12
22:5 (*n*-3)	0.36±0.04	4.08±0.32
22:6 (*n*-3)	2.89±0.32	12.13±0.26
24:4 (*n*-6)	2.34±0.12	1.66±0.12
24:5 (*n*-6)	3.81±0.16	0.32±0.02
Others	7.92±0.63	3.25±0.23

The values are the mean±SEM of five groups (two rats in each) and expressed as weight percentages of total fatty acids. *a*) Testes from 6-month-old rats. *b*) Isolated tumor tissue from testes of 23-month-old rats.

Levels of CEs in Rat Testes The CE increased remarkably with the development of tumors (Table I). Though to a lesser extent, levels of free cholesterol, followed by triacylglycerol and phospholipid, also increased (data not shown). For example, in 23-month-old rat testes the level of CEs increased to 60.9 mg/g wet wt, which comprised 57.5% of the total lipids of the testes, whereas in the controls the concentration was only 0.2 mg/g wet wt. The isolated tumor tissues from the testes of 18-, 21-, and 23-month-old rats accumulated considerable amounts of CEs as shown in Table I. GC analysis of the mixture obtained by alkaline hydrolysis of CE fraction indicated that cholesterol was the only sterol present. In testes,[15] ovaries,[16] and adrenals,[17] CEs serve as a source of cholesterol for steroid hormone synthesis. Perhaps CEs play a similar role in Leydig cell tumors of F344 rats, since Leydig cell tumors can actively produce the steroid hormones, as will be described.

High levels of total lipids and CEs, as in Leydig cell tumors of F344 rats, have been observed in the ovary of most species.[18] Carney and Walker reported that the rat ovary contains relatively high concentrations of total lipids

(12.5% of wet wt) and CEs (about 15 mg/g wet wt), stored as lipid droplets within the cell,[19] as in the Leydig cell tumors of F344 rats.

Fatty Acid Composition of CEs of Leydig Cell Tumors Testicular lipids in some species are unique in that the content of 22-carbon polyunsaturated fatty acids is high.[20] Rats are characterized by relatively high levels (10 to 14%) of 22 : 5 (*n*-6) in the testis lipids.[21] Table II shows the fatty acid composition of CEs in the isolated tumor tissue of 23-month-old rat testes in comparison with that in the testes of the controls (6 month-old rats). The fatty acid composition in the tumor, as well as in the control tissue, was remarkable for the amount of 22-carbon polyunsaturated species. However, Leydig cell tumor contained a pronouncedly decreased level of 22 : 5 (*n*-6), which is a characteristic acid of the rat testes, and an increase in 22 : 4 (*n*-6), compared to the controls. This characteristic acid, 22 : 4 (*n*-6), in Leydig cell tumor tissue of F344 rats, has been observed as a major acid in the CE fraction of ovaries (15 to 20%).[16,19,22]

Thus, Leydig cell tumors of aging F344 rats resemble ovaries, as Leydig cell tumors contain a high level of total lipids and CEs, and a tetraene fatty acid, 22 : 4 (*n*-6), a major one in the fatty acid composition of CE.

Testicular Levels of Steroid Hormones Turek and Desjardins[6a] and Amador *et al.*[6b] independently reported the changes in serum steroid hormone levels during aging in F344 rats with spontaneous Leydig cell tumors, but they did not deal with the changes in testicular steroid hormone levels that accompany the development of Leydig cell tumors. To examine resemblances in steroid hormone levels between Leydig cell tumors and ovary tissue, we studied the changes in the testicular levels of progesterone (P), testosterone (T) and estradiol (E_2) in aging F344 rats. The measurements of P and T were carried out by both RIA and HPLC, and the results obtained by the two different methods agreed with each other.

The testicular levels of P markedly increased with the development of the tumors (after 18 months of age) (Fig. 2A). For example, in 23-month-old rat testes the total level of P was more than 400 times higher than that in the controls (2870 *vs.* 7 ng/g wet wt). The isolated tumor tissue in 23-month-old rats also cntained higher levels of P, compared with the remaining tissue (3240 *vs.* 156 ng/wet wt), suggesting that the Leydig cell tumor can actively synthesize P.

The testicular levels of E_2 increased with the development of the tumor as well. The level of E_2 in 23-month-old rats increased to 14 times that of the controls (2205 *vs.* 153 pg/g wet wt) (Fig. 2B). The isolated tumor tissue also accumulated a higher level of E_2 compared with that in the remaining tissue (2407 *vs.* 722 pg/g wet wt). This suggests that the high level of E_2 in the testes of F344 rats is mostly due to E_2 production by the tumor tissue itself.

On the other hand, the testicular levels of T remained almost unchanged between 6 (controls) and 12 months of age (40 to 50 ng/g wet wt), but at 18 months of age they markedly increased by about three times that of the controls (147 ng/g wet wt) (Fig. 2C). Then at 23 months of age they decreased to one-fourth of that of the controls (13 ng/g wet wt). This increase at 18 months of age may be due to the compensatory action of the hyperplasia, as suggested by

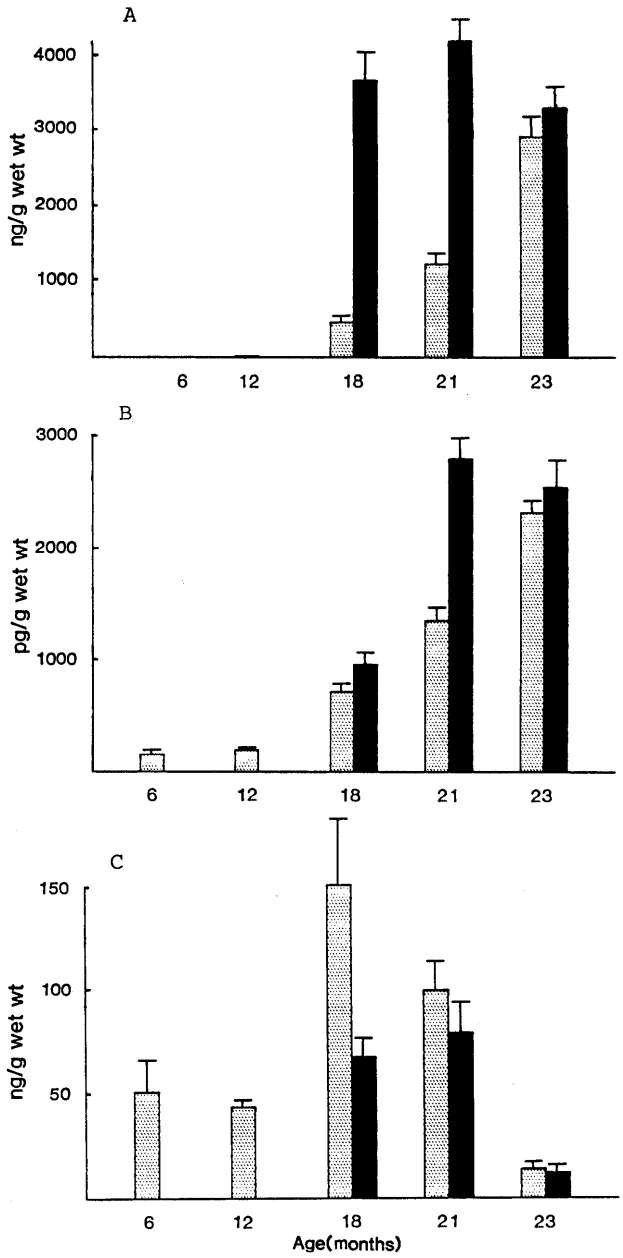

Fig. 2. Testicular Levels of Progesterone, Estradiol and Testosterone in Aging Fischer 344 Rats

A, progesterone; B, estradiol; C, testosterone. ▨, total; ■, tumor. Each value (by RIA method) represents the mean ± SEM (vertical bars) of individual determinations for five rats in all groups, except the 21-month-old group (four rats).

Amador *et al.*[6b] In the isolated tumors, the levels of T were almost constant between 18 and 21 months (66 to 77 ng/g wet wt) (Fig. 2C), but suddenly decreased to one-fourth of that of the controls (12 ng/g wet wt) at 23 months of age, coinciding with the decrease in the level of T in the whole testes. This suggests that the ability of the tumor cells to synthesize T was lower than that of normal cells (from controls), a finding that is different from the results for P and E_2. Sweeny *et al.* reported a similar situation: spontaneous Leydig cell tumors in CDF rats produced less T *in vitro* than did normal cells.[23]

Leydig cell tumors in F344 rats are characterized by high levels of P and E_2 as described, though normal Leydig cells are generally considered to be the main site for the

production of T. The main functions of the corpus luteum and the follicle in the ovary are the syntheses of progestins and estrogens, respectively. Therefore, the data described above suggest that Leydig cell tumors in aging F344 rats resemble ovary tissue with respect to the high levels of P and E_2 as well as the high levels and fatty acid composition of CEs. In addition, the two kinds of cells (indicated by "a" and "b" in Fig. 1B) found in the tumor tissue resemble cells of the corpus luteum and granulosa cells of the follicle, respectively, in the ovary of rats, in appearance on hematoxylin–eosin staining. It is concluded that the study shows that Leydig cell tumors in aging male F344 rats have a tendency towards feminization.

References

1) A. Maekawa, H. Takizawa and Y. Hayashi, *Henigen To Dokusei* (in Japanese), **4**, 22 (1981).
2) *a*) D. G. Goodmann, J. M. Ward, R. A. Squire, K. C. Chu and M. S. Linhart, *Toxicol. Appl. Pharmacol.*, **48**, 237 (1979); *b*) A. Maekawa, H. Onodera, H. Tanigawa, K. Furuta, Y. Komada, S. Horiuchi and Y. Hayashi, *Jpn. J. Cancer Res. (Gann)*, **74**, 36 (1983); *c*) S. F. Stinson, H. M. Schuller and G. K. Reznik (ed.), "Atlas of Tumor Pathology of the Fischer Rat," CRC Press, Boca Raton, 1990, pp. 409—414.
3) *a*) S. W. Thompson, R. A. Huseby, M. A. Fox, C. L. Davis and R. D. Hunt, *J. Natl. Cancer Inst.*, **27**, 1037 (1961); *b*) R. C. Crain, *Am. J. Pathol.*, **34**, 311 (1958).
4) L. M. Ward, D. G. Goodmann, R. A. Squire, K. C. Chu and M. S. Linhart, *J. Natl. Cancer Inst.*, **63**, 849 (1979).
5) *a*) H. Czernobilsky, B. Czernobilsky, H. G. Schneider, W. W. Franke and R. Ziegler, *Cancer*, **56**, 1667 (1985); *b*) F. K. Mostofi and E. B. Price, Jr., "Tumors of the Male Genital System," ed. by Armed Forces Institute of Pathology, 2nd ser, fasc 8, Armed Force Institute of Pathology, Washington DC, 1973, pp. 86—99.
6) *a*) F. W. Turek and C. Desjardins, *J. Natl. Cancer Inst.*, **63**, 969 (1979); *b*) A. Amador, R. W. Steger, A. Bartke, A. Johns, T. M. Siler-Khodr, R. Parker, Jr. and A. M. Shepherd, *J. Androl.*, **6**, 61 (1985).
7) *a*) Y. Arai, *Hormone To Rinsho* (in Japanese), **27**, 527 (1979); *b*) S. Kurano, M. Nakayama and M. Kusuda, *ibid.*, **25**, 331 (1977); *c*) A. Suzuki, K. Koide, Y. Kido, T. Tumosaka and M. Saito, *ibid.*, **27**, 449 (1979).
8) A. Laganà, d'Ascenzo and A. Marino, *Chromatographia*, **23**, 796 (1987).
9) J. Folch, M. Lees and G. H. S. Stanley, *J. Biol. Chem.*, **226**, 497 (1957).
10) *a*) K. Ishii, H. Okajima, T. Koyamatsu, Y. Okada and H. Watanabe, *Lipids*, **23**, 694 (1988); *b*) K. Ishii, H. Okajima, Y. Okada and H. Watanabe, *J. Biochem.* (Tokyo), **103**, 836 (1988); *c*) K. Ishii, H. Okajima, Y. Okada, H. Konishi and H. Watanabe, *Chem. Pharm. Bull.*, **37**, 1564 (1989).
11) D. Watson, *Clin. Chim. Acta*, **5**, 637 (1960).
12) S. E. Carlson and S. Goldfarb, *Clin. Chim. Acta*, **79**, 575 (1977).
13) J. Roviros, O. Munoz and A. S. Martin, *Lipids*, **18**, 570 (1983).
14) G. A. Boorman, M. H. Hamlin II and S. L. Eustis, "Genital System," ed. by T. C. Jones, U. Mohr and R. D. Hunt, Springer Verlag, New York, 1987, pp. 200—204.
15) J. D. Pokel, W. R. Moyle and R. O. Greep, *Endocrinology*, **91**, 323 (1972).
16) J. F. Strause III, L. A. Schuler, M. F. Rosenblum and T. Tanaka, *Adv. Lipid Res.*, **18**, 99 (1981).
17) W. W. Davis and L. P. Garren, *Biochem. Biophys. Res. Commun.*, **24**, 805 (1966).
18) *a*) D. T. Armstrong and A. P. F. Flint, *Biochem. J.*, **134**, 399 (1973); *b*) R. C. Tuckey and P. M. Stevenson, *Biochim. Biophys. Acta*, **575**, 46, (1979); *c*) H. W. Deane, M. F. Hay, R. M. Moor, L. E. A. Rowson, and R. V. Short, *Acta Endocrinol.* (Copenhagen), **51**, 245 (1966); *d*) L. Claesson, *Acta Physiol. Scand.*, **31** (suppl. 113), 53 (1954).
19) J. M. Carney and B. L. Walker, *Comp. Biochem. Physiol.*, **41B**, 137 (1972).
20) J. Bieri and E. L. Prival, *Comp. Biochem. Physiol.*, **15**, 275 (1965).
21) A. D. Johnson, "The Testis," Vol. 2, ed. by A. D. Johnson, W. A. Gomes and N. L. Vandemark, Academic Press, New York, 1970, pp. 193—253.
22) J. F. Straus III, E. Seifter, E. L. Lien, D. B. P. Goodman and R. L. Stambaugh, *J. Lipid Res.*, **18**, 246 (1977).
23) C. Sweeney, D. Castracane, P. Doherry and A. Bartke, *J. Androl*, **4**, 34 (1983).

Participation of Lipid Peroxidation in Rat Pertussis Vaccine Pleurisy. III. Thiobarbituric Acid (TBA) Reactant and Lysosomal Enzyme

Yasukatsu YUDA,*[,a] Junko TANAKA,[a] Fumiya HIRANO,[a] Kazuei IGARASHI,[b] and Tetsuo SATOH[b]

Pharmaceutical Research Center, Meiji Seika Kaisha, Ltd,[a] Morooka-cho, Kohoku-ku, Yokohama 222, Japan and Faculty of Pharmaceutical Sciences, Chiba University,[b] 33, Yayoi-cho, 1-chome, Chiba 260, Japan. *Received August 15, 1990*

Activity of lysosomal enzymes, such as *N*-acetyl-β-D-glucosaminidase (NAG), was assayed in exudate on a rat model of Bordetella pertussis vaccine pleurisy. Thiobarbituric acid (TBA)-reactive substance (TBA·R) and superoxide dismutase (SOD) activity were then monitored in the exudate on the acute phase response in this inflammatory model.

Retention of the exudate in the pleural space increased rapidly after the challenge, and the exudate volume at 24 h reached about three times the volume at 6 h.

The activity of NAG showed high levels at 6 h after the challenge, and then increased slightly at 24 h. This activity correlated with the retention of exudate and TBA·R levels.

The activity of SOD at 6 h was shown to be higher than that at 24 h after the challenge, thus showing negative correlations with TBA·R levels and exudate volume. The levels of TBA·R rapidly increased and reached maximum values at 24 h. It was concluded that the above three parameters correlate to the acute phase response in this inflammatory model.

Keywords pertussis vaccine pleurisy; *N*-acetyl-β-D-glucosaminidase; thiobarbituric acid-reactive substance; superoxide dismutase; lipid peroxidation

Introduction

After the discovery and characterization of lysosomes by de Duve and his coworkers,[1] evidence has been accumulated on the role of these subcellular particles in mediating connective tissue injury, such as carrageenin-induced pleurisy and adjuvant-induced arthritis.

The leakage of lysosomal contents, especially from leukocytes, is considered generally to be a key step in bringing about various inflammatory reactions. The mechanism of the anti-inflammatory action of drugs has been explained by this concept, at least in part. On the other hand, an increase in thiobarbituric acid (TBA)-reactive substance (TBA·R) has been known to occur during intoxication of ethanol and carbon tetrachloride, after exposure to ionizing irradiation, and also as a result of aging and acute or chronic inflammation, such as carrageenin paw edema and arthritis.

Biomembranes and subcellular organelles are the major sites of lipid peroxidation damage. Of importance to cellular damage is the lability of lysosomal membranes to rupture, followed by the concurrent release of an array of hydrolytic enzymes, which initiate intracellular digestion and catabolism. Tappel and his coworkers[2] showed that isolated lysosomes underwent the peroxidation of lipids less rapidly than mitochondrial and microsomal fractions, and showed that lysosomes peroxidized at one-third the rate of mitochondria and one-tenth the rate of the microsomal fractions. Yet, release of lysosomal enzymes occurred relatively rapidly, and initiates further damage to the structural and functional parts of the cell.

In this study, in order to prove the relationship between the inflammatory process and lipid peroxidation, and also to manifest the change of the superoxide dismutase (SOD) activity in the inflammatory process, we examined the level of TBA·R, the activity of SOD, the activity of lysosomal enzymes such as *N*-acetyl-β-D-glucosaminidase (NAG) and the retention of exudate in the pleural space on the acute phase response in a rat inflammatory model of Bordetella pertussis vaccine pleurisy.

Experimental

Animals Five female Fischer rats (SPF), 11 weeks old and weighing 160—180 g were used. The animals were obtained from Charles River Japan, Kanagawa.

Materials Bordetella pertussis vaccine was obtained from Chiba Serum Institute, Chiba. Freund's complete adjuvant was obtained from Iatron, Tokyo. Phenyl-β-*N*-acetyl-glucosaminide, 4-amino antipyrine and potassium ferricyanide were obtained from Nakarai Chemicals, Kyoto. TBA was obtained from BDH Chemicals, Poole, England. The other chemicals were of a reagent grade and were used without purification.

Induction of Pertussis Vaccine Pleurisy Female Fischer rats were used, and pertussis vaccine pleurisy was induced as described in the preceding paper.[3] Animals were sacrificed at 6 and 24 h after induction by bleeding from the carotid artery. The other procedures were the same as described in the previous report.[3]

Determination of Lipid Peroxidation The levels of TBA·R in the pleural exudate supernatants were measured according to the method of Yagi.[4] Lipids and lipids containing peroxides were precipitated by treating the exudate with phosphotungstic acid, followed by the addition of TBA. The reaction product was then assayed spectrophotometrically (532 nm). The results were expressed as nmol of malondialdehyde formed.

Measurements of NAG Activity The activities of NAG in the exudate were assayed according to the modified method of Walker and his coworkers.[5] Phenyl-β-*N*-acetyl-glucosaminide was dissolved in 0.05 M citrate buffer pH 4.3, to provide a 5 mM solution. A test sample (0.1 ml) and the substrate solution (1.5 ml) was mixed and incubated at 37 °C for 30 min. The reaction was stopped by the addition of 1 M borate buffer (pH 8.8, 0.5 ml). The liberated phenol was measured by reading the optical density at 510 nm with a spectrophotometer. The enzyme activity was expressed as μg of liberated phenol during 30 min.

Measurement of SOD-like Activity The activity of O_2^- scavengers was assayed according to the nitrite method described by Oyanagui.[6] To a tube containing 0.2 ml of buffer solution (final concentrations of 13 mM KH_2PO_4 and 7 mM $Na_2B_4O_7$) which contained 0.5 mM ethylenediaminetetraacetic acid, disodium salt (EDTA-2Na) (pH 8.2), the following were added and mixed: 0.5 mM hypoxanthine (0.2 ml), 10 mM hydroxylamine plus 8.85 mM hydroxylamine *O*-sulfonic acid solution (0.1 ml), 0.1 ml of the sample, and 0.2 ml of water. The reaction was started by adding 0.2 ml of 1 mU/ml xanthine oxidase (XOD). This mixture (1.0 ml) was incubated for 30 min at 37 °C. To this solution was added 2.0 ml of a coloring reagent which contained 30 μM *N*-1-naphthylethylenediamine, 3 mM sulfanilic acid and 25% acetic acid. The optical absorption was measured at 550 nm.

Measurements of Protein The amount of protein was determined by the method of Lowry *et al.*[7]

Statistical Method The results are expressed as mean values ± standard deviation (mean ± S.D.) and the probability for significance of the differences was determined by analysis of variance.

TABLE I. Levels of TBA Reactant and Enzyme Activities in the Exudate of Rat Pertussis Vaccine Pleurisy

Time (h)	Volume (ml)	Concentration in exudate				Amount of per g protein in exudate		
		TBA·R	NAG	SOD	Protein	TBA·R	NAG	SOD
6	0.70±0.24	1.50±0.35	1.38±0.15	6.62±1.57	42.4±4.2	36.3±13.2	32.9± 6.1	156.0±25.8
24	2.05±0.35[a)]	2.19±0.39[b)]	1.68±0.77	5.50±1.57	41.0±6.0	55.5±14.7[b)]	42.6±24.0	132.0±23.2

Each value represents the mean±S.D. of 5 rats; TBA·R, TBA reactants are shown as nmol of malondialdehyde (MDA)/ml or nmol/g protein. NAG activities are shown as μg/ml or μg/g protein. SOD activities are shown as U/ml or U/g protein. Protein amounts are shown as mg. TBA·R were measured spectrophotometrically according to the method of Yagi. *a*) Significant difference from 6 h after challenge at $p<0.001$. *b*) Indicates $p<0.05$.

Results

Bordetella pertussis vaccine injected into the pleural cavity of sensitized rats was found to bring about a remarkable inflammatory reaction, which is characterized by retention of exudate and a transient increase of TBA·R in the exudate. The results are summarized in Table I.

The exudate retention volume increased promptly. Six hours after the challenge, 0.70±0.24 ml (S.D.) of the exudate was collected from the pleural cavity, and at 24 h the exudate level reached about three times as high as at 6 h. The levels of TBA·R in the exudate increased transiently, and reached to about 55.5 nmol/g protein at 24 h.

The activity of SOD in the exudate achieved a maximum value at 6 h, and then decreased significantly. This activity changed in an opposite manner to the variation of the level of TBA·R, and shows a negative correlation with the exudate volume (−0.656), the level of TBA·R (−0.714) and NAG activity (−0.716).

The activity of NAG in the exudate reached its high level at 6 h (1.38 μg/ml), and then increased slightly at 24 h. The variation of this activity correlated with the retention of exudate (0.638) and the level of TBA·R (0.800).

The concentration of protein in the exudate exhibited no remarkable change throughout the experiments.

Discussion

Increase of lipid peroxidation in the inflammatory site, such as synovial fluids of rheumatoid arthritis and synovia of rats with adjuvant arthritis, were reported by Yoshikawa and his coworkers.[8)] These increases implied a significant correlation with the activities of lysosomal enzymes.

We used a pertussis vaccine in the present experiments, and studied the level of TBA·R and the activities of SOD and NAG in the acute phase response of pertussis vaccine pleurisy in rats. The levels of TBA·R in the exudate increased transiently and reached maximum values at 24 h. By contrast, the activity of SOD showed high levels of activity at 6 h and decreased slightly, then reached minimum values at 24 h. From the above facts we conclude that the increase of lipid peroxidation may be caused by diminution of SOD activity or the generation of a superoxide by leucocytes which migrated into the pleural space.[9)] Yoshikawa *et al.* used a TBA reactant to examine the damage induced by lipid peroxidation and the protection by SOD (from bovine liver: Orgotein) in rat adjuvant arthritis. It was reported that the TBA reactant was reduced significantly by the injection of SOD.[10)] There are few papers, however, which describe the variation in the activity of SOD at inflammatory sites.

The activity of a lysosomal enzyme such as NAG in the exudate exhibited a high value at 6 h and increased slightly at 24 h; this correlated with the level of TBA·R. The results suggest that the increase of lipid peroxidation caused the release of a lysosomal enzyme; this agrees with the results reported by Yoshikawa and his coworkers in the case of adjuvant arthritis.

From the above results, we suggest that the changes in TBA·R level and SOD activity reflect the acute phase reactions; the increase of NAG activity may be caused secondarily by the increase of lipid peroxidation. So, we conclude that the determination of the level of lipid peroxides and activity of SOD are useful in investigating the inflammatory process.

References

1) C. de Duve, B. C. Pressman, R. Gianetta, R. Watteaux, and F. Appelmaus, *Biochem. J.*, **60**, 604 (1955).
2) H. V. Tappel, P. L. Sawant, and S. Shibko, "Lysosomes," ed. by A. V. S. de Reuck and M. P. Cameron, Churchill, London, 1963, p. 78.
3) Y. Yuda, J. Tanaka, F. Hirano, and H. Kitagawa, *Chem. Pharm. Bull.*, **36**, 2691 (1988).
4) K. Yagi, *Biochem. Med.*, **15**, 212 (1976).
5) P. G. Walker, M. E. Woolen, and D. Pugh, *J. Clin. Path.*, **13**, 353 (1960).
6) Y. Oyanagui, *Anal. Biochem.*, **142**, 290 (1984).
7) O. H. Lowry, N. J. Rosenbrough, A. L. Farr, and R. J. Randall, *J. Biol. Chem.*, **193**, 269 (1951).
8) T. Yoshikawa, N. Yokoe, S. Takemura, H. Kato, K. Hosokawa, and M. Kondo, *Jpn. J. Med.*, **18**, 199 (1979).
9) Y. Yuda, J. Tanaka, F. Hirano, and H. Kitagawa, *Chem. Pharm. Bull.*, **36**, 2490 (1988).
10) Y. Yoshikawa, H. Tanaka, and M. Kondo, *Biochem. Med.*, **33**, 320 (1985).

Changes in the Plethysmogram Patterns of Finger Reactive Hyperemia in Nutritional (Alcoholic) Liver Disease Patients with Increased Serum Monoamine Oxidase Activities

Atsushi HIRAOKA* and Isao MIURA

Kyorin University School of Health Sciences, 476 Miyashita-cho, Hachioji, Tokyo 192, Japan. *Received August 15, 1990*

The activity levels of serum monoamine oxidase in nutritional (alcoholic) liver disease patients were elevated beyond the upper normal limit, while those of other subjects without pathologically accelerated fibrosis ranged within normal values. Capillaroscopic and plethysmographic studies on finger reactive hyperemia revealed that two characteristic changes in the blood microcirculation, which indicated an ocurrence of increased fibritic process in the capillary wall and skin tissues, were observed only in the nutritional (alcoholic) liver disease patients with the elevated serum monoamine oxidase levels. These results suggested that nutritional (alcoholic) liver disease is not a disease restricted to liver tissues, but to a disorder creating pathological fibrosis in the whole-body.

Keywords serum monoamine oxidase; nutritional (alcohoilic) liver disease; fibrosis; blood micro-circulation; reactive hyperemia

Enzymes called monoamine oxidase (MAO; E.C. 1.4.3.4 and/or 1.4.3.6) catalyze oxidative deamination of a variety of biogenic amines. Among them, an enzyme in mammalian blood plasma is immunologically identical with that contained in highest concentration in connective tissues.[1] In the field of human clinical biochemistry, elevation of serum MAO activity levels has been known as a marker of pathological conditions accompanying accelerated collagen biosynthesis in the body (*e.g.* liver,[2-4] vascular wall[5] and skin[6] *etc.*). Therefore, measurement of its activity is considered to be one of the variable laboratory tests for diagnosis of hepatic fibrosis in nutritional (alcoholic) liver disease (NLD) and liver cirrhosis.[7-9] These results also suggest that the actions of the enzyme in tissues and/or blood plasma are connected with fibritic processes, although the precise physiological and/or pathophysiological roles are presently unclear.

Blood micro-circulation is a very delicate process effected by various physiological and/or pathophysiological changes in blood capillaries and tissues around them. One of the important reactions as a stimulation to the blood capillaries is reactive hyperemia (RH), which is a local and transient acceleration of capillary permiability after release of the arterial occlusion. It has been revealed that RH consists of two parts, vasodulation due to arterio-venous anatomosis (AVA) and transfer of fluid from blood capillaries into tissues followed by re-absorption from the tissues into the blood capillaries and that the normal plethysmogram pattern indicates a well-balanced transfer of fluid between the blood capillaries and the skin tissues (the dotted line in Fig. 1).[10] It has also been known that pathological conditions caused by various inflammatory disorders including acute hepatitis give changes in the finger plethysmogram patterns due to argmented penetration of the plasma proteins,[10] but changes in NLD have not been studied.

Therefore, in this investigation, in order to elucidate the relation between blood micro-circulation and MAO in the blood plasma and/or tissues, changes in the serum levels of MAO activity and in the plethysmogram patterns of finger RH were studied in subjects including NLD patients.[11]

Subjects and Methods

Subjects Fifty patients from 15—86 years of age, who were admitted to Nagashima Hospital and Institute (Akikawa, Tokyo 193, Japan), included 6 NLD cases (49—64 year-olds) having slightly or moderately increased serum aspartate aminotransferase (AST) and alanine aminotransferase (ALT) activities (AST: 59.2 ± 17.6 IU/l, ALT: 62.0 ± 20.4 IU/l, as Mean $\pm$ S.D., $n=6$) in routine laboratory examinations, while the upper normal limits of these serum hepatic enzymes were 35 IU/l together. The other patients were suffering from various non-NLD diseases such as acute hepatitis, renal disturbance, transient ischemic attack, cerebral infarction, diabetic mellitus, essential hypertension, *etc.* Among them, an acute hepatitis patient had highly elevated levels of serum AST (953 IU/l) and ALT (1490 IU/l) suggesting that liver functions in this case were more largely disturbed than in the NLD cases.

Determination of the Serum MAO Levels Fifty sera prepared from venous blood samples taken from the above described subjects were stored at -20 °C up to 5 d until assayed. The MAO activities were measured by the previously reported method using allylamine as the substrate.[12]

Examinations of the Blood Micro-Circulation The papilla and the patent capillaries in a hand finger were observed capillaroscopically, and a finger plethysmogram expressing successive changes in finger volume during the RH process were drawn by using the apparatus shown in Fig. 2. The details of these experiments, as well as the physiological aspects of this investigation, are reported elsewhere.[13]

Results and Discussion

The MAO activities of 6 of the NLD patients examined were 1.97, 1.64, 1.26, 1.23, 1.19 and 1.15 IU/l, respectively (1.41 ± 0.30 IU/l, as mean $\pm$ S.D., $n=6$), while the highest value in the other 44 cases with various diseases other than NLD was only 0.89 IU/l which was smaller than the upper normal limit, 1.08 IU/l.[14] An acute hepatitis case mentioned in Subjects and Methods had a low serum MAO activity of 0.36 IU/l in contrast with the extremely elevated AST and ALT levels. These results agreed with earlier workers who reported that the serum MAO activity levels (with benzylamine as the substrate) in NLD and liver cirrhosis patients were significantly higher than in acute hepatitis and normal control subjects and that changes in the serum MAO activities were largely independent of those in the serum AST and ALT levels.[2-4]

Capillaroscopic and plethysmographic observations revealed occurrence of the two following characteristic changes in the blood micro-circulation, only in the above described 6 NLD patients with increased serum MAO activities; (1) AVA formation was not detected by capillaroscopy, and (2) the plethysmograms of RH, as illustrated with the solid line of Fig. 1, indicated that the release of arterial occlusion resulted in a decrease in finger volume and that the fluid translocated from blood capillaries

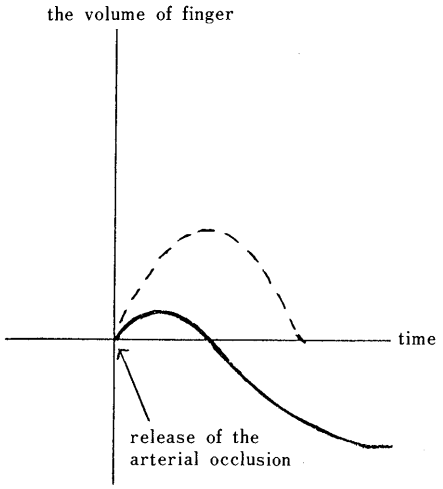

Fig. 1. The Finger Plethysnogram Patterns of Reactive Hyperemia Obtained in Examined Alcholic Liver Disease Patients (Solid Line) and the Normal Pattern (Dotted Line)

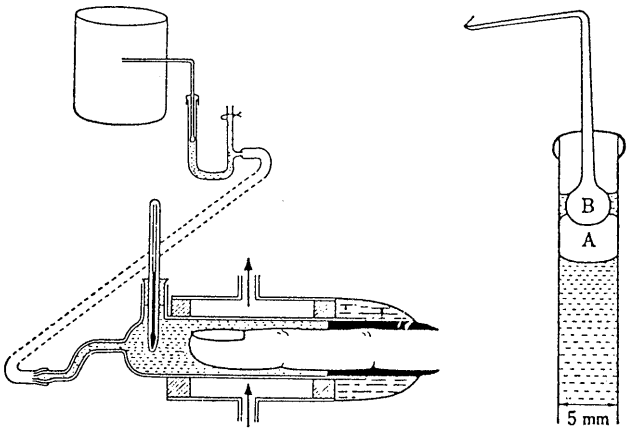

Fig. 2. Measurement of the Finger Plethysmogram

The left and right pictures are the whole of an apparatus and the recorder part, respectively. The portion B in the latter is the sphere part of a glass-ball recorder, and the portion A is the air-layer surrounded by a manometer and the portion B. Changes in the water level in the manometer due to an increase or decrease of the finger volume immediately gives changes in the volume of A, and the successive changes of the A volume are recorded.

into the skin tissues was more abundant than that finally absorbed into the capillaries, although no statistically significant correlation was found between the serum MAO activities and the physiological index such as maximum finger volume and the time required for the finish of RH. It was noteworthy that such changes in blood microcirculation were never detected in patients with any other diseases (including acute hepatitis) so far examined in this investigation[13] and studied by earlier investigators.[10]

MAO in blood plasma is not a releasing enzyme such as AST and ALT, but an enzyme which expresses the activities of the tissues in which it was synthesized. Therefore, it is considered that elevation of the serum MAO activity levels, namely, an increase of the MAO molecules circulating in the blood plasma, reflects an accelerated synthesis of the enzyme molecules in the tissues from which they are derived. In the case of human plasma MAO, this means an advancement of the fibritic processes within the connective tissues in which they originate.[2-6] It is undoubted that such tissues in NLD patients are present mainly in the liver, as pointed out naturally by earlier workers who elucidated the positive correlation between the degree of hepatic fibrosis and the serum MAO levels.[4] However, MAO is also virtually contained in vascular wall and skin tissues,[15] as well as in the liver,[16] and indeed, in advanced arteriosclerosis[5] and acromegaly,[6] *etc.*, the serum MAO levels were raised, although not so often as in NLD and liver cirrohsis. On the other hand, the above-mentioned specific changes in the blood micro-circulation in the examined NLD cases showed that the pathological sclerosis occurred in the capillary wall (no formation of AVA) and that the skin tissues around the blood capillaries had a tendency to lose the fluid (the plethysmograms of RH), thus suggesting an occurrence of accelerated fibrosis in the tissues of both the capillary wall and the skin. It is considered, from these findings, that the increased plasma MAO in NLD originates at least partly in tissues other than liver, such as blood capillary walls and skin, and that NLD is not a disease restricted to liver tissues, as is acute hepatitis which gives no increase of serum MAO activities, but a disorder of pathological fibrosis in the whole body. The mechanisms of the acceleration of fibrosis in tissues other than liver in NLD are unclear, although it is assumed that several hormones stimulate the collagen metabolism accompanied fibrosis, as in the case of hyperthyroidism.[17] However, the capillaroscopic and plethysmographic data have not been obtained on patients with hyperthyroidism (serum MAO is increased),[18] as well as on those with cancers including hepatoma (serum MAO is not increased).[19] In order to elucidate a more detailed relation between MAO and blood micro-circulation in liver diseases and other various disorders, further investigations are needed.

Acknowledgement The authors express their sincere gratitude to Drs. Chosetsu Nagashima and Nobumasa Yamamoto of Nagashima Hospital and Institute for the capillaroscopic and plethysmographic measurement of changes in the blood micro-circulation.

References

1) P. B. Rucker and B. L. O'Dell, *Biochem. Biophys. Acta*, **235**, 32 (1972).
2) C. M. McEwen, Jr. and D. O. Castell, *J. Lab. Clin. Med.*, **70**, 36 (1967).
3) J. P. Kirchner and D. O. Castell, *Gastroenterology*, **62**, 771 (1972).
4) K. Ito, H. Nakano and M. Fukuse, *Digestion*, **4**, 98 (1971).
5) N. Tryding, *J. Clin. Lab. Invest.*, **23**, 76 (1969).
6) H. Nakano and Y. Yamamoto, *Rinshokensa*, **32**, 1394 (1988).
7) A. W. M. Lin and D. O. Castel, *Biochem. Med.*, **9**, 373 (1974).
8) H. Nakano and K. Ito, *Clin. Chim. Acta*, **88**, 315 (1978).
9) Y. Yamamoto, *Rinsho Byori*, **43**, 121 (1981).
10) C. Nagashima, "Physiology of Circulation, Japanese Handbook of Physiology," Vol. III, ed. by K. Masuda, Igaku Shoin, Tokyo, 1967, p. 660.
11) A. Hiraoka, I. Miura, C. Nagashima and N. Yamamoto, *Seikagaku*, **62**, 922 (1990). The summary of this study was presented at the 63rd Annual Meeting of the Japan Biochemical Society, September 1990, Osaka.
12) A. Hiraoka, J. Ohtaka, M. Koike, S. Tsuchikawa, Y. Tsuboi and I. Miura, *Chem. Pharm. Bull.*, **36**, 3027 (1988).
13) N. Yamamoto, Proceedings of the 15th Congress of Micro-Circulation, Akita, April 1990, in press.
14) H. Nakano, K. Tsujii and H. Nakabayashi, *Nihon Rinsho*, **598**, 334 (1989).
15) W. Lovemberg, *Biochem. Pharmacol.*, **17**, 1117 (1968).
16) R. Lewinsohn, *Biochem. Pharmacol.*, **27**, 1857 (1978).
17) G. Asboe-Hansen, *Physiol. Rev.*, **38**, 446 (1958).
18) S. E. Nelson, *Acta Med. Scand.*, **184**, 105 (1968).
19) R. Lewinsohn, *Clin. Chim. Acta*, **81**, 247 (1977).

In Vitro Percutaneous Transport of Sodium Diclofenac and Diclofenac from Oleaginous Vehicle

Koichi TAKAHASHI,*[,a] Satoko TAMAGAWA,[a] Toyoshi KATAGI,[a] Hironori YOSHITOMI,[b] Akira KAMADA,[c] J. Howard RYTTING,[d] Toshiaki NISHIHATA,[d] and Nobuyasu MIZUNO[a]

Faculty of Pharmaceutical Sciences, Mukogawa Women's University,[a] 11–68 Koshien Kyuban-cho, Nishinomiya, Hyogo 663, Japan, Faculty of Pharmaceutical Sciences, Fukuyama University,[b] 985 Sanzo, Higashimuracho, Fukuyama, Hiroshima 727–02, Japan, Faculty of Pharmaceutical Sciences, Osaka University,[c] 1–6 Yamadaoka, Suita, Osaka 565, Japan, and Pharmaceutical Chemistry Department, University of Kansas,[d] 2065 Constant Avenue, Lawrence, Kansas 66046, U.S.A. *Received May 28, 1990*

The penetration enhancement of sodium diclofenac and diclofenac by alcohols with various alkyl chains (C_8 to C_{14}) was evaluated by the steady state flux of diclofenac through rat abdominal skin. Decanol showed the greatest effect in this series. A more remarkable enhancing effect of the alcohols was observed in sodium diclofenac than in diclofenac. Diclofenac can penetrate through the ethylene–vinyl acetate membrane as a lipoid model membrane, but sodium diclofenac can not. Decanol enhanced the penetration of phenol red being dependent on its concentration in the vehicle. Therefore, decanol may interact with lipoid components of the skin and increase the aqueous pathway in the skin. These results indicate that sodium diclofenac and diclofenac may be penetrated through partially different pathways.

Keywords percutaneous permeation; sodium diclofenac; diclofenac; enhancer; primary alcohol; oleaginous vehicle; phenol red

The stratum corneum provides the principal barrier to the percutaneous penetration of topically applied substances.[1] Only a few materials which tend to be extremely lipophilic and have low melting points are easily transported to the underlying viable aqueous tissue. It is therefore important to enhance the penetration of many drugs through the stratum corneum. A number of compounds, such as surfactants,[2,3] organic solvents[4] and azone[5,6] have been reported as penetration enhancers.

Sodium diclofenac, which is a strong anti-inflammatory agent,[7] has been reported as not easily absorbed by transdermal application.[8] In the present study, we investigated the effects of primary alcohols on the transdermal penetration of this drug from an oleaginous vehicle. We also compared the transport of sodium diclofenac with diclofenac, because it is generally considered that an unionized form with greater lipophilicity is easily transported in comparison with an ionized form. As this study was performed as a preliminary study for the transdermal formulation of diclofenac, either sodium diclofenac or diclofenac was dissolved in the oleaginous vehicle to avoid a possible change of the crystal form of the drug in the formulation used.

Experimental

Materials Sodium diclofenac and diclofenac were supplied by Ciba Geigy Japan (Takarazuka, Japan). Squalane was supplied by Nikko Chemicals Co., Ltd., (Tokyo, Japan). An ethylene–vinyl acetate copolymer (EVA) membrane (composition, ethylene : vinyl acetate = 90 : 10; thickness, 40 μm) obtained from Tamapoly Co., Ltd., (Tokyo, Japan) was used. Other reagents used were of analytical grade.

Preparation of Test Vehicles 25 mg of sodium diclofenac or 23 mg of diclofenac was mixed with the 10 g of the combined solvent composed of 10% ethanol, 5% primary alcohol and 85% squalane. The mixture was agitated until a clear solution was obtained. The resulting vehicle solution was used in the *in vitro* penetration study. In the experiment using phenol red, 25 mg of phenol red was mixed in a suspension form with 10 g of the combined solvent which was composed of squalane containing 10% ethanol and various concentrations of decanol (Table II).

***In Vitro* Penetration Study** After the removal of hair by an electric clipper, abdominal skin was excised from a rat (male Wistar, 250 to 300 g) just prior to the experiment. The excised skin was placed on a Franz type diffusion cell. In the present study, 10 ml of 0.1 M sodium phosphate buffer (pH 7.2) was used as a receptor medium and 1 g of the test vehicle was placed on the donor side.

Aliquotes (0.1 ml in diclofenac or 0.2 ml in phenol red) of the receptor medium were collected periodically for 12 h. Just after each collection, 0.1 or 0.2 ml of the buffer was added to the receptor medium. During the experiments, the medium in the receptor was agitated by a magnetic stirrer at 37 °C.

Transport of the drug across the EVA membrane was also performed according to the method described above.

Solubility Study An excess amount of sodium diclofenac, diclofenac or sodium phenol red was added to the test vehicle and was agitated for 24 h at 23 ± 2 °C. The suspension was filtrated through a membrane filter (0.45 μm) to obtain a clear solution, and the concentration of sodium diclofenac and diclofenac was measured by high performance liquid chromatography (HPLC). Phenol red was photometrically measured at 560 nm after extraction with 0.01 N NaOH solution.

Assay The determination of diclofenac was carried out by HPLC as described by Yaginuma *et al.*[9] The concentration of phenol red was photometrically determined at 560 nm after the addition of 0.01 N NaOH solution.

Results and Discussion

Effect of Primary Alcohols on Percutaneous Transport of Diclofenac Figure 1 shows the transport profiles of diclofenac and its sodium salt through the excised skin from the vehicle containing various primary alcohols. After a lag time, a steady state transport of diclofenac after application of either sodium diclofenac or diclofenac was observed. The steady state flux and apparent lag time can be calculated from the straight line plotted in Fig. 1 and summarized in Table I. The flux rates of sodium diclofenac and diclofenac were affected with a primary alcohol, and the apparent lag time seemed to increase with the decrease of flux. When the vehicle prepared with squalane and 10% ethanol without other primary alcohol was applied, the flux rates were below 0.5 nmol/cm^2/h in sodium diclofenac and 25.89 ± 0.80 nmol/cm^2/h in diclofenac. These results suggested that diclofenac easily penetrates from the vehicle uncontained enhancer through the rat skin, but sodium diclofenac does not.

As shown in Fig. 2, the marked increase in the steady state flux of diclofenac was observed in sodium dicofenac when the alcohol with a carbon number of C_{10} was added to the vehicle. Thereafter, an increase in the carbon number of the alcohol in the vehicle decreased the steady state flux of diclofenac. On the other hand, in diclofenac, the same fluxes of diclofenac were observed with C_8 and C_{10}. The greater flux in diclofenac was observed when sodium

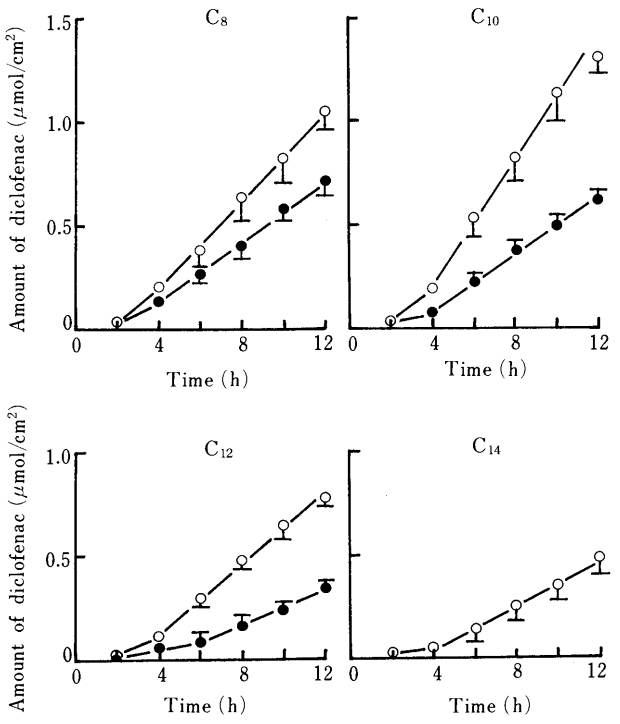

Fig. 1. Permeation Profiles of Sodium Diclofenac and Diclofenac through Rat Skin from Vehicles Containing Various Primary Alcohols

○, sodium diclofenac; ●, diclofenac. Each value represents the mean ± S.D. ($n=4$ to 6).

TABLE I. Effect of Alcohol on the Transport Parameter of Sodium Diclofenac (DCNa) and Diclofenac (DC) through Rat Skin

Carbon number	DCNa		DC	
	Lag time (h)	Flux (nmol/cm²/h)	Lag time (h)	Flux (nmol/cm²/h)
C_8	2.2±0.4	106.0±10.2	2.2±0.4	71.7±6.9
C_{10}	2.8±0.2	158.4±18.7	2.8±0.3	68.8±4.2
C_{12}	2.7±0.4	89.8± 2.8	3.7±0.3	41.0±1.2
C_{14}	3.4±0.8	52.9± 6.1	No experiment	

Each value represents the mean ± S.D. ($n=4$ to 6). The steady state flux and lag time were calculated from the straight line plotted in Fig. 1.

diclofenac was used, in comparison to that when only diclofenac was used.

The primary alcohols may play two possible roles in the permeation enhancement observed in this study. First, the primary alcohols may affect the release of sodium diclofenac or diclofenac from the vehicle. Second, the primary alcohols may interact with the lipid components in the stratum corneum and act as a plasticizer. In this study, sodium diclofenac did not penetrate through the rat skin without the enhancer. Also, the solubility of sodium diclofenac and diclofenac to the vehicle containing 5% primary alcohol (C_8 to C_{14}) was almost constant (its value is about 10 mM in sodium diclofenac and 17 mM in diclofenac). From these results, it is considered that the effect of primary alcohols in increasing permeability of skin epithelium is mainly due to their action as a plasticizer. The low enhancing effect of alcohol with an increase in carbon number (C_{12} and C_{14}) may be due to the low action as a plasticizer.

There are many compounds, such as surfactant[3] including fatty acid and azone,[5,6] which have been reported as penetration enhancers. The transport of water soluble compounds was enhanced to a greater extent by these enhancers compared with the lipophilic compounds.[10] In this study, the greater enhancing effect of primary alcohols was observed in sodium diclofenac rather than in diclofenac as described above.

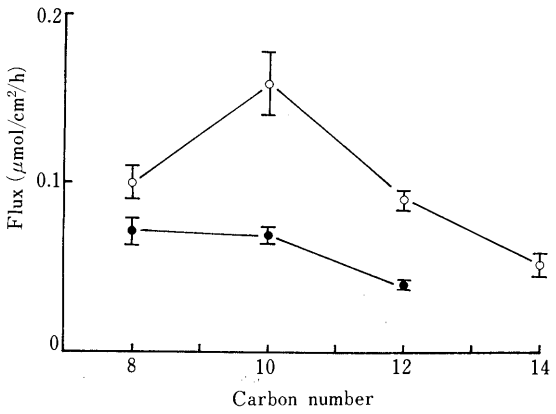

Fig. 2. Relationship between Permeation Rate and Carbon Number of Alcohols

○, sodium diclofenac; ●, diclofenac.

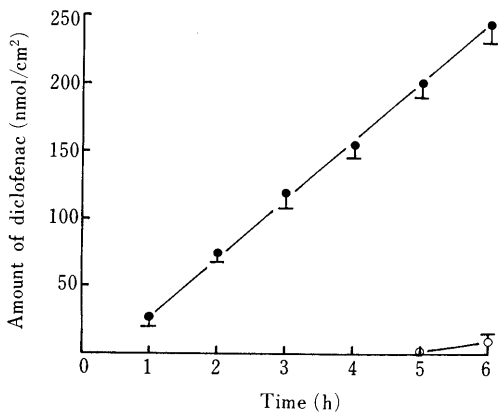

Fig. 3. Permeation Profiles of Sodium Diclofenac and Diclofenac through the EVA Membrane

○, sodium diclofenac; ●, diclofenac.

TABLE II. Effect of Decanol Concentration on the Transport Parameter of Phenol Red through Rat Skin

Concn. (%)	Solubility[a] (μg/ml)	Flux (μg/cm²/h)	Pe[b] (cm/h)
5	12.0	4.0±1.3	0.33±0.09
10	13.3	4.6±1.1	0.37±0.08
20	19.4	16.2±1.6	0.84±0.08
40	30.0	36.9±1.2	1.23±0.04

Each value represents the mean ± S.D. ($n=4$ to 6). *a*) Solubility of phenol red in the vehicle was measured at 23±2 °C. *b*) The permeability rate constant (Pe) was calculated from the flux and initial concentration in the donor.

Percutaneous penetration may occur in two possible pathways; an aqueous pathway which allows for the penetration of water soluble compounds and a lipoidal pathway which allows for the penetration of lipophilic compounds.[11] An EVA membrane which is used as a model membrane for the transdermal study by Kondo *et al.*[12] is a lipophilic membrane and is known to be permeable to

TABLE III. Effect of Decanol Concentration on the Transport Parameter of Sodium Diclofenac (DCNa) and Diclofenac (DC) through Rat Skin

Concn. (%)	DCNa			DC		
	Lag time (h)	Flux (nmol/cm^2/h)	Solubility[a] (mM)	Lag time (h)	Flux (nmol/cm^2/h)	Solubility[a] (mM)
5	2.8±0.2	158.4±18.7	12.3	2.8±0.3	68.8± 4.2	17.1
10	2.4±0.5	134.0±16.9	19.5	3.4±0.3	61.0± 8.4	24.0
20	2.4±0.4	86.5± 3.7	26.5	4.1±0.4	55.7±10.2	31.4
40	3.3±0.6	68.2± 3.3	45.4	3.9±0.7	47.0± 5.2	45.1

Each value represents the mean±S.D. (n=4 to 6). *a*) Solubility of sodium diclofenac and diclofenac in the vehicle was measured at 23±2 °C.

nonionic molecules. Diclofenac penetrated across an EVA membrane from an oily vehicle, but sodium diclofenac did not (Fig. 3). This observation suggests that different pathways through the skin epithelium are involved in the transport of both diclofenac and sodium diclofenac.

Effect of Decanol Concentration in the Vehicle on the Percutaneous Transport Because a decanol provided a greater effect on the transport of both diclofenac and sodium diclofenac than other alcohols, the effect of decanol concentration on percutaneous transport was investigated.

To investigate the effect of decanol on the aqueous pathway, the effect of decanol concentration in the vehicle on the transport of phenol red was examined. It is known that phenol red is a water-soluble compound and is not absorbed from the gastrointestinal tract without an enhancer.[13,14] Also, phenol red is often used as an indicator for measurement of water flux.[15] As shown in Table II, decanol enhanced the transport of phenol red along with an increase in decanol concentration in the vehicle. Since the solubility of phenol red also increased with the concentration of decanol in the vehicle, the permeability rate constant (*Pe*) was calculated from the flux and the initial concentration in the donor. Since the value of *Pe* for phenol red increased along with an increase in the decanol concentration (Table II), it is possible that the aqueous pathway is accentuated by interactions of the alcohol with the lipid components of the skin epithelium.

However, as shown in Table III, the penetration rate of sodium diclofenac which was markedly enhanced from the vehicle containing 5% decanol, decreased with an increase in decanol concentration. On the other hand, the penetration of diclofenac was almost constant (perhaps a slight decrease with an increase of the concentration) in all concentrations of decanol in the vehicle examined. The solubilities of sodium diclofenac and diclofenac increased along with an increase in the decanol concentration (Table III). From these results, the decrease in the sodium diclofenac (and diclofenac) transport along with the increase in the decanol concentration may be due to a change in physicochemical properties of the vehicle with respect to the drug rather than an effect of decanol on the transport route for the drug across the skin epithelium; *i.e.*, the release of sodium diclofenac might be reduced by an increase in decanol concentration. However, a greater enhancing effect of alcohol was observed when sodium diclofenac was used, in comparison to that when diclofenac was used. To clarify the detailed mechanism of alcohol on the permeation of the drug further studies are needed. But, from the results of this study, it is considered that sodium diclofenac and diclofenac are penetrated through partially different pathways; *i.e.*, a lipoid pathway for diclofenac and an aqueous pathway mainly for sodium diclofenac.

References

1) R. J. Scheuplein, *J. Invest. Dermatol.*, **67**, 672 (1976).
2) P. Ashoton, J. Hadgraft, and K. A. Walters, *Pharm. Acta Helv.*, **61**, 2281 (1986).
3) B. J. Aungst, N. J. Rogers, and E. Shefter, *Int. J. Pharm.*, **33**, 225 (1986).
4) N. Tsuzuki, O. Wong, and T. Higuchi, *Int. J. Pharm.*, **46**, 19 (1988).
5) R. B. Stoughton, *Arch. Dermatol.*, **118**, 474 (1982).
6) K. Sugibayashi, K. Hosoya, Y. Morimoto, and W. I. Higuchi, *J. Pharm. Pharmacol.*, **36**, 1519 (1986).
7) W. Riess, *Scand. J. Rheumatol.*, **22**, 17 (1978).
8) T. Nishihata, K. Kotera, Y. Nakano, and M. Yamazaki, *Chem. Pharm. Bull.*, **35**, 3807 (1987).
9) H. Yaginuma, T. Nakata, H. Toya, T. Murakami, M. Yamazaki, and A. Kamada, *Chem. Pharm. Bull.*, **29**, 2974 (1981).
10) B. W. Barry and S. L. Bennett, *J. Pharm. Pharmacol.*, **39**, 535 (1986).
11) R. L. Bronough and H. I. Maibach (eds.), "Percutaneous Absorption," Marcell Dekker Inc., New York and Basel, 1985, p. 107.
12) S. Kondo and I. Sugimoto, *J. Pharmacobio-Dyn.*, **10**, 587 (1987).
13) K. Higaki, N. Takechi, M. Kato, M. Hashida, and H. Sezaki, *J. Pharm. Sci.*, **79**, 334 (1990).
14) T. Nishihata and T. Higuchi, *Life Science*, **34**, 419 (1984).
15) S. Kitazawa, H. Ito, and H. Sezaki, *Chem. Pharm. Bull.*, **23**, 1856 (1975).

Further Metabolism of 3,5-Di-*tert*-butyl-4-hydroxybenzoic Acid, a Major Metabolite of Butylated Hydroxytoluene, in Rats

Kenji YAMAMOTO,*[,a] Kazuo TAJIMA,[a] Mari TAKEMURA[a] and Tamio MIZUTANI[b]

School of Pharmacy, Hokuriku University,[a] Kanazawa 920-11, Japan and Faculty of Living Science, Kyoto Prefectural University,[b] Sakyo-ku, Kyoto 606, Japan. *Received July 9, 1990*

The metabolic pathway of butylated hydroxytoluene (BHT) to the ring-oxygenated metabolites 2,6-di-*tert*-butylhydroquinone (BHQ) and 2,6-di-*tert*-butyl-*p*-benzoquinone (BBQ) was examined in rats. After intraperitoneal administration of 3,5-di-*tert*-butyl-4-hydroxybenzoic acid (BHT-acid), which had been regarded as one of the major metabolic endproducts of BHT, 2,6-di-*tert*-butylphenol (DBP) and BBQ were identified in the feces by gas chromatography and gas chromatography–mass spectrometry (GC-MS). The biliary excretion of BBQ, BHQ glucuronide and BHT-acid glucuronide was also confirmed by GC-MS and high-performance liquid chromatography methods. The excretion rate of BHQ glucuronide for 24 h after dosing with BHT-acid was about 9-fold higher than that after dosing with BHT. In addition, the formation of BBQ was confirmed in the urine after dosing with DBP. These results suggest that BHT is metabolized to BHQ and BBQ through DBP formed by decarboxylation of BHT-acid.

Keywords butylated hydroxytoluene; 3,5-di-*tert*-butyl-4-hydroxybenzoic acid; metabolism; ring-oxygenated metabolite; 2,6-di-*tert*-butylhydroquinone; 2,6-di-*tert*-butyl-*p*-benzoquinone; 2,6-di-*tert*-butylphenol

Several reviews[1] of the metabolism of butylated hydroxytoluene (3,5-di-*tert*-butyl-4-hydroxytoluene, BHT), an antioxidant, have shown that BHT is metabolized in rats mainly through oxidation of the ring-methyl group to a carboxylic derivative (BHT-acid) followed by conjugation with glucuronic acid. In addition, it is known that BHT-acid glucuronide undergoes an enterohepatic circulation in rats.[2] We previously identified 2,6-di-*tert*-butylhydroquinone (BHQ) and 2,6-di-*tert*-butyl-*p*-benzoquinone (BBQ) in the urine and feces,[3] and then BBQ[4] and BHQ glucuronide[5] as biliary metabolites after intraperitoneal (i.p.) administration of BHT to rats. In the present study, we found 2,6-di-*tert*-butylphenol (DBP) in the feces of rats after dosing with BHT-acid. The purpose of this study was to account for the *in vivo* metabolic pathway of BHT-acid to BHQ and BBQ *via* DBP in rats.

Experimental

Materials BHT-acid and BBQ were purchased from Aldrich Chemical Co. (Milwaukee, U.S.A.), and DBP from Nacalai Tesque Inc. (Kyoto, Japan). BHQ[6] and BHQ glucuronide[5] were synthesized by known methods. As described previously,[5] BHT-acid glucuronide was isolated from the bile of rats dosed with BHT.

Administration of Materials Male Wistar rats weighing about 250 g were dosed intraperitoneally with BHT-acid (200 mg/kg) or DBP (200 mg/kg) dissolved in 0.5 ml of a 1 : 5 emulsion of dimethyl sulfoxide and olive oil. Feces and urine were collected for 5 d after dosing with BHT-acid and for 3 d after dosing with DBP, respectively. Bile was collected from rats cannulated as previously described[4] for 24 h after dosing with BHT-acid (200 mg/kg).

Isolation of Metabolite Fractions The feces, previously dried over P_2O_5, were extracted with CH_2Cl_2. The extract was fractionated by a silica gel dry column with $CHCl_3$ as described previously.[3] The urine was adjusted to pH 4 with AcOH, and extracted with peroxide-free ether. This extract was treated in a similar manner as described above for the fecal extract. To analyze conjugated metabolites, the bile collected after dosing with BHT-acid was purified on a SEP-PAK C_{18} cartridge (Waters Associates, Milford, U.S.A.) with MeOH as described previously.[5] The MeOH eluate was divided into two fractions, fractions 1 (10.7—11.5 min) and 2 (13.5—15 min), under high-performance liquid chromatography (HPLC) conditions shown in the caption of Fig. 2. After being lyophilized, fraction 1 was trimethylsilylated directly, but fraction 2 was trimethylsilylated after being esterified with CH_2N_2 for gas chromatography–mass spectrometry (GC-MS) analysis. To analyze unconjugated metabolites, bile was extracted with CH_2Cl_2 and the extract was subjected to instrumental analysis without purification.

Instrumental Analysis The unconjugated metabolites were analyzed by gas chromatography (GC) with a flame-ionization detector (FID) and GC-MS as described previously.[4] GC conditions are shown in the caption of Fig. 1. GC-MS conditions were as follows: 2% OV-1 on Chromosorb W, 1 m × 2 mm i.d.; column temperature, 120 °C; carrier gas, He 0.24 kg/cm^2; ionizing energy, 22 eV. The conjugated metabolites, after dosing with BHT-acid, were analyzed by HPLC and GC-MS as described previously.[5] HPLC conditions are shown in the caption of Fig. 2, and GC-MS conditions were as follows: 1.5% SE-30 on Chromosorb W, 1 m × 2 mm i.d.; column temperature, 250 °C; carrier gas, He 0.25 kg/cm^2, ionizing energy, 22 eV.

Results and Discussion

Two peaks (**a** and **b**) were found in the gas chromatogram of the extract from feces after i.p. administration of BHT-acid (Fig. 1). The mass spectrum of peak **a** (Table I) showed a molecular ion at *m/z* 206 with a base peak at *m/z* 191 ($[M-CH_3]^+$) and fragment ions at *m/z* 175 ($[M-CH_3-CH_4]^+$) and 163 ($[M-CH_3-C_2H_4]^+$). The molecular ion was 44 mass units smaller than that of the parent BHT-acid.[3] This data suggested the presence of a decarboxylated metabolite of BHT-acid, DBP. Peak **a** was

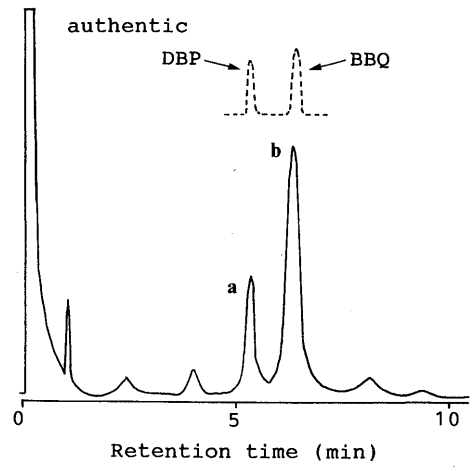

Fig. 1. Gas Chromatogram of the Fecal Extract Obtained during 5 d after Intraperitoneal Administration of BHT-Acid to Rats

Conditions: column, 2% OV-1 on Chromosorb W, 1 m × 3 mm i.d.; column temp., 110 °C; carrier gas, N_2 60 ml/min; detection, FID.

TABLE I. GC-MS Comparison of Metabolites **a** and **b** and Authentic DBP and BBQ

Compound	t_R (min)	Mass spectrum (m/z)[a]
a	4.4	206 (M^+, 32), 191 (100), 175 (10), 163 (19)
b	5.2	220 (M^+, 98), 205 (52), 192 (30), 177 (100)
DBP	4.4	206 (M^+, 25), 191 (100), 175 (10), 163 (19)
BBQ	5.2	220 (M^+, 90), 205 (41), 192 (30), 177 (100)

a) Numbers in parentheses refer to relative intensities.

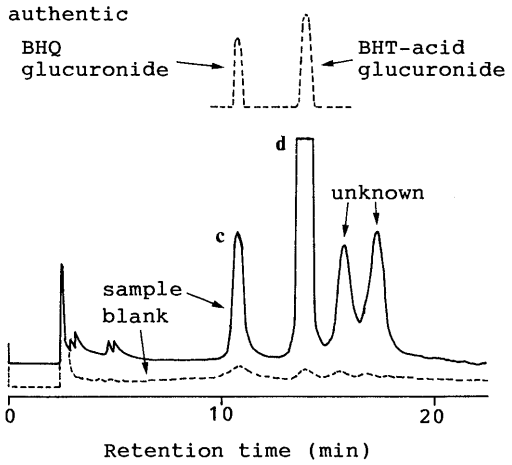

Fig. 2. High-Performance Liquid Chromatogram of the Biliary Extract Obtained during 8 h after Intraperitoneal Administration of BHT-Acid to Rats

Conditions: column, Nucleosil 10 C_{18}, 30 cm × 4 mm i.d.; mobile phase, MeOH–0.1 M $NH_4H_2PO_4$ (52 : 48, v/v); flow rate, 1.0 ml/min; detection, UV 280 nm, 0.08 absorbance unit full scale.

TABLE II. GC-MS Comparison of Metabolites **c** and **d** and Authentic BHQ Glucuronide (BHQ-G) and BHT-Acid Glucuronide (BHT-acid-G)

Compound[a]	t_R (min)	Mass spectrum (m/z)[b]
c	5.3	686 (M^+, 1), 671 (1), 375 (41), 294 (100)
d	9.2	656 (M^+, 1), 641 (1), 407 (10), 233 (100)
BHQ-G	5.3	686 (M^+, 1), 671 (1), 375 (33), 294 (100)
BHT-acid-G	9.2	656 (M^+, 1), 641 (1), 407 (8), 233 (100)

a) Metabolite **c** and BHQ-G were analyzed after being converted to trimethylsilylated derivatives. Metabolite **d** and BHT-acid-G were analyzed after being converted to methylated-trimethylsilylated derivatives. *b*) Numbers in parentheses refer to relative intensities.

proven to be consistent with authentic DBP by GC and GC-MS comparisons (Table I). Peak **b** was identified as BBQ, a known metabolite of BHT,[3] by comparison with the authentic sample (Table I). The fecal excretion rates of DBP and BBQ were 0.06 and 0.26%, respectively, of the dose for 5 d after dosing with BHT-acid.

As shown in Fig. 2, two peaks (**c** and **d**) occurred with two unknown peaks in the HPLC of the fraction of conjugated metabolites in the bile after dosing with BHT-acid. Peaks **c** and **d** showed retention times similar to those of known metabolites of BHT, BHQ glucuronide and BHT-acid glucuronide,[5] respectively. Peak **c**, previously purified by HPLC, was converted to a trimethylsilylated derivative and identified as BHQ glucuronide through GC-MS comparison (Table II) to the authentic sample.[5]

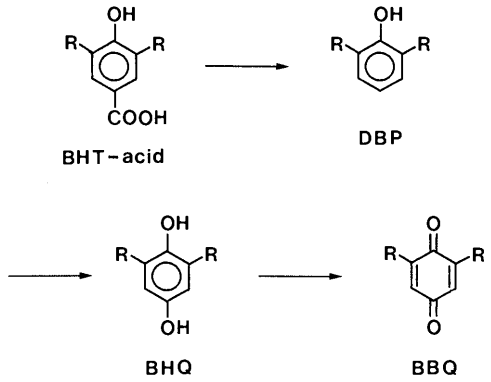

Fig. 3. Proposed Metabolic Pathway of BHT-Acid in Rats
R represents *tert*-butyl group.

Peak **d** was converted to a methylated-trimethylsilylated derivative and identified as BHT-acid glucuronide by GC-MS comparison (Table II) to an authentic sample. The authentic sample of BHT-acid glucuronide was isolated from a biliary fraction of conjugated metabolites of BHT in rats.[5] The excretion rates of BHQ glucuronide in bile after i.p. administration of BHT-acid were 10.51 ± 1.04 and 3.27 ± 2.68 (mean ± S.D. of 4 rats) of the dose during 0—8 and 8—24 h, respectively. The excretion rate of BHQ glucuronide for 24 h after dosing with BHT-acid was about 9-fold higher than that after dosing with BHT.[5] BHT-acid glucuronide, however, was not determined because a sufficient amount of authentic BHT-acid glucuronide was not available.

On the other hand, BBQ was detected in the biliary fraction of unconjugated metabolites after dosing with BHT-acid, although DBP was not detected. The biliary excretion rate of BBQ was 0.04% of the dose during the 24 h after administration. Futhermore, the occurrence of BBQ was confirmed in the urine after i.p. administration of DBP.

In summary, DBP, BBQ, BHQ glucuronide and BHT-acid glucuronide were identified in the feces and bile after i.p. administration of BHT-acid to rats in this study. As shown in Fig. 3, these results suggest that BHT-acid, which has been regarded as a main metabolic endproduct of BHT,[1] is subsequently metabolized to BHQ and BBQ *via* DBP formed by decarboxylation with rat liver enzyme systems. To our knowledge, there has been no example of decarboxylation of xenobiotic benzoic acids by tissue enzyme(s).[7] The metabolic fate of BHT-acid to BHQ and BBQ *via* DBP, however, resembles the biosynthesis pathway of ubiquinone: a 4-hydroxybenzoate with a polyprenyl side-chain at the 3-position undergoes decarboxylation to give a polyprenylphenol derivative, which is further *p*-hydroxylated and oxidized to ubiquinone.[8] The formation of BBQ has also been shown in both the urine and feces after i.p. administration of 2,6-di-*tert*-butyl-4-hydroperoxy-4-methyl-2,5-cyclohexadienone, a ring-oxygenated metabolite of BHT,[9] in rats.[3] An alternative route for the formation of BBQ has been suggested to involve a homolysis reaction of the O–O bond of the hydroperoxide catalyzed by rat liver cytochrome P-450.[10]

References

1) A. L. Branen, *J. Am. Oil Chem. Soc.*, **52**, 59 (1975); H. Babich,

Environ. Res., **29**, 1 (1982); D. M. Conning and J. C. Phillips, *Food Chem. Toxicol.*, **24**, 1145 (1986); H. Witschi, A. M. Malkinson and J. A. Thompson, *Pharmacol. Ther.*, **42**, 89 (1989).
2) L. G. Ladomery, A. J. Ryan and S. E. Wright, *J. Pharm. Pharmacol.*, **19**, 388 (1967); G. M. Holder, A. J. Ryan, T. R. Watson and L. I. Wiebe, *ibid.*, **22**, 832 (1970).
3) K. Yamamoto, K. Tajima and T. Mizutani, *J. Pharmacobio-Dyn.*, **2**, 164 (1979).
4) K. Tajima, K. Yamamoto and T. Mizutani, *Chem. Pharm. Bull.*, **29**, 3738 (1981).
5) K. Tajima, K. Yamamoto and T. Mizutani, *Chem. Pharm. Bull.*, **31**, 3671 (1983).
6) D. H. R. Barton, P. G. Gordon and D. G. Hewitt, *J. Chem. Soc.* (*C*), **1971**, 1206.
7) J. Caldwell, "Metabolic Basis of Detoxication," ed. by W. B. Jakoby, J. R. Bend and J. Caldwell, Academic Press Inc., New York, 1982, pp. 273—274.
8) B. L. Trumpower, R. M. Houser and R. E. Olson, *J. Biol. Chem.*, **249**, 3041 (1974).
9) Y.-S. Shaw and C. Chen, *Biochem. J.*, **128**, 1285 (1972); C. Chen and Y.-S. Shaw, *ibid.*, **144**, 497 (1974).
10) M. D. Wand and J. A. Thompson, *J. Biol. Chem.*, **261**, 14049 (1986).

Reaction of Malonaldehyde with Nucleic Acid. IV.[1,2] Formation of Pyrimido[1,2-*a*]purin-10(3*H*)-one Nucleoside by Thermal Decomposition of Diastereomers Containing Oxadiazabicyclononene Residues Linked to Guanosine

Hiroshi SETO,* Takako SETO, Tomoko OHKUBO and Ikue SAITOH

Tokyo Metropolitan Research Laboratory of Public Health, Hyakunincho 3-24-1, Shinjuku-ku, Tokyo 169, Japan. *Received May 11, 1990*

The reaction of 1,1,3,3-tetraethoxypropane with guanosine under strongly acidic conditions resulted in the formation of diastereomeric oxadiazabicyclononene residues linked to guanine base. The diastereomers were decomposed by heat, giving changed pyrimido[1,2-*a*]purin-10(3*H*)-one nucleoside (3) in a good yield. A convenient method for the preparation of 3, which includes the thermal decomposition process of the diastereomers, was developed.

Keywords malonaldehyde; guanosine; pyrimidopurine; 1,1,3,3-tetraethoxypropane; lipid peroxidation; diastereomeric adduct; thermal decomposition

Malonaldehyde (**1**), a product of lipid peroxidation and prostaglandin biosynthesis,[3] is not only mutagenic[4] but also carcinogenic.[5] Exposure of humans to **1** may be considerable because of the abundance of **1** as a product of normal metabolism and in a variety of foodstuffs. Malonaldehyde is reactive toward amino groups of proteins[6] and nucleic acids,[7] even *in vivo*. Fluorescent adducts, pyrimido[1,2-*a*]purin-10(3*H*)-one homologues, have been separated from the reaction mixture of **1** with guanosine (**2**)[8] or RNA[9] under mild conditions (pH 4.5). The adduct, pyrimido[1,2-*a*]purin-10(3*H*)-one nucleoside (**3**), may have some biological activities. The yield of this adduct was very low (1.4%)[8]; however, the amount of the compound preparable was insufficient for pharmacological and biological tests. The reaction conditions were investigated in order to improve the yield, and the diastereomeric products (**4a**, **4b**) by the reaction of **2** with 1,1,3,3-tetraethoxypropane as a generator of **1** were obtained. Each adduct, **4a** and **4b** was identical with 5,6,7,8-tetrahydro-11-formyl-3(β-D-ribofuranosyl)-6,8-epoxyethenopyrimido[1,2-*a*]purin-10(3*H*)-one which was reported by Marnett *et al.*[10] Both **4a** and **4b** are decomposed by heat, yielding **3** in a good yield. This is a simple and effective method for the preparation of **3**.

This paper describes the preparation of the diastereomers (**4a**, **4b**) and the straightforward preparation of **3** through the thermal decomposition process of **4a** and **4b**.

Experimental

Apparatus Melting points are uncorrected. Optical rotations were measured with a JASCO DIP 181 polarimeter. IR, UV and CD spectra were recorded on Perkin-Elmer 1640, Shimadzu UV 240 and JASCO J-40A spectrophotometers, respectively. NMR spectra were obtained on a JEOL FX-270 spectrometer with 1,4-dioxane as an internal standard in D_2O or with TMS in DMSO-d_6 at room temperature. FAB mass spectra (glycerol matrix) were recorded on a JEOL DX 303 mass spectrometer. Analytical HPLC was carried out with a JASCO 880PU equipped with a three-dimensional detector (Hewlett-Packard HP 1040M) on a Nucleosil 7C18 (Nagel, 4.6 i.d. × 250 mm) column (the mobile phase was 7% (v/v) acetonitrile/water). Preparative HPLC was carried out with a Milton Roy Constametric III pump equipped with a UV detector (Oyobunko Kiki Uvilog II, cell length 1 mm).

Synthesis and Isolation of 3, 4a and 4b All reagents were purchased from commercial sources. Guanosine (**2**) (5.56 g, 0.02 mol) was dissolved in 100 ml of 0.05 M HCl at 50 °C. 1,1,3,3-Tetraethoxypropane (11.0 g, 0.05 mol) was added to the guanosine solution. The reaction mixture was kept at 50 °C with stirring for 2 h, then concentrated to about 50 ml at 35 °C. It was subjected to polyamide column chromatography (Wako Pure Chemicals C-200, 50 i.d. × 350 mm) and eluted with 500 ml of water. The eluate was concentrated to about 50 ml. The solution was injected little by little to a Lichroprep RP-18 (Merck, 22 i.d. × 300 mm) HPLC column and chromatographed with 7% (v/v) acetonitrile/water as the eluent. The fractions of **3**, **4a** and **4b** were collected and concentrated to about 50 ml. The solution was applied little by little to an Inertsil ODS-2 column (Gasukuro Kogyo, 5 μm, 7.6 i.d. × 250 mm, 3% (v/v) acetonitrile/water). The final chromatography was carried out repeatedly more than 500 times. Each product solution was evaporated to dryness *in vacuo*.

Compound **3** (p3): mp > 195 °C (dec.). UV $\lambda_{max}^{H_2O}$ nm (ε): 250 (13000), 308 (2770), 319 (3100), 348 (2700). EI MS *m/z*: 535 ($C_{13}H_{10}N_5O_5(TMS)_3$ M^+). ^{1}H-NMR (D_2O) δ: 3.89 (2H), 4.24 (1H), 4.45 (1H), 4.76 (1H), 6.02 (1H, d, *J* = 5.3 Hz), 7.34 (1H, dd, *J* = 4.0, 7.30 Hz), 8.31 (1H), 8.98 (1H, dd, *J* = 2.1, 3.8 Hz), 9.22 (1H, dd, *J* = 2.0, 7.3 Hz). Yield, 35 mg.

Compound **4a** (p1): mp > 160 °C (dec.); $[\alpha]_D$ −140° (*c* = 0.4, water). UV $\lambda_{max}^{H_2O}$ nm (ε): 249 (20100). IR (KBr): 3329, 1700, 1620, 1560 cm^{-1}. High-resolution FAB MS: Calcd for $C_{16}H_{18}N_5O_7$ ($M+H^+$) *m/z*: 392.1206. Found *m/z*: 392.1185. CD (*c* = 0.11 mM, water) $[\theta]^{22}$ (nm): 0 (310), −45500 (282), 0 (269), +116000 (256), 0 (246), −102000 (237), 0 (219). ^{1}H-NMR (D_2O) δ: 2.14 (1H, d, *J* = 14.5 Hz), 2.28 (1H, d, *J* = 14.5 Hz), 3.81 (2H, m), 4.17 (1H, m), 4.39 (1H, m), 4.70 (1H, m), 5.87 (1H, d, *J* = 5.9 Hz), 5.97 (1H, m), 6.15 (1H, m), 7.78 (1H, s), 7.97 (1H, s), 9.15 (1H, s). ^{13}C-NMR (DMSO-d_6) δ: 23.5 (t), 33.6 (d), 61.2 (t), 70.3 (d), 73.4 (d), 76.2 (d), 85.1 (d), 86.2 (d), 117.0 (s), 119.8 (s), 136.3 (d), 148.5 (s), 148.6 (s), 153.8 (s), 163.7 (d), 188.2 (d). Yield, 200 mg.

Compound **4b** (p2): mp > 160 °C (dec.); $[\alpha]_D$ +111° (*c* = 0.4, water). UV $\lambda_{max}^{H_2O}$ nm (ε): 249 (19800). IR (KBr): 3287, 1701, 1618, 1561 cm^{-1}. High-resolution FAB MS Calcd for $C_{16}H_{18}N_5O_7$ ($M+H^+$) *m/z*: 392.1206. Found *m/z*: 392.1190. CD (*c* = 0.11 mM, water) $[\theta]^{22}$ (nm): 0 (310), +43200 (282), 0 (269), −118000 (256), 0 (246), +114000 (237), 0 (219). ^{1}H-NMR (D_2O) δ: 2.14 (1H, d, *J* = 14.5 Hz), 2.27 (1H, d, *J* = 14.5 Hz), 3.80 (2H, m), 4.18 (1H, m), 4.37 (1H, m), 4.67 (1H, m), 5.85 (1H, d, *J* = 5.6 Hz), 5.97 (1H, m), 6.14 (1H, m), 7.76 (1H, s), 7.97 (1H, s), 9.14 (1H, s). ^{13}C-NMR (DMSO-d_6) δ: 23.6 (t), 33.6 (d), 61.3 (t), 70.3 (d), 73.8 (d), 76.2 (d), 85.2 (d), 86.3 (d), 116.9 (s), 119.8 (s), 136.1 (d), 148.5 (s), 148.7 (s), 153.8 (s), 163.7 (d), 188.2 (d). Yield, 200 mg.

Reaction of Malonaldehyde with Pyrimido[1,2-*a*]purin-10(3*H*)-one Nucleoside (3) Malonaldehyde sodium salt[11] (1 mg) and **3** (1 mg) were dissolved in 0.2 ml of 0.05 M HCl. The reaction mixture was maintained for 1 h at 50 °C. The mixture was neutralized by 0.05 M NaOH. Product analysis of the mixture was carried out by the HPLC method. The product (**4a**, **4b**) was identified by both the UV spectrum and the retention time.

Thermal Decomposition of 4a and 4b A mixture of the diastereomers (**4a**, 5 mg and **4b**, 5 mg) in a glass test tube was heated at 160 °C in an oil bath for 1 h. The product was dissolved in water (1 ml). An aliquot of the solution was chromatographed repeatedly on the Inertsil ODS-2 column with 5% (v/v) acetonitrile/water as the eluent. The fractions including **3** were collected and dried *in vacuo*. Yield, 5 mg (60%). The UV spectrum obtained was identical to that of authentic **3**.

Simplified Method for Preparation of 3 from Guanosine The mixture of guanosine (**2**) (56 mg) and 1,1,3,3-tetraethoxypropane (110 mg) in 5 ml of 0.05 M HCl was stirred at 50 °C for 3 h. The solution was neutralized with 1 M NaOH. The neutral solution was applied to a polyamide gel column (20 i.d. × 300 mm, water as the eluent). The eluate (20—150 ml) was evaporated to dryness *in vacuo*. The mixture of dry materials in a flask was heated at 160 °C in an oil bath for 1 h. The product (**3**) was extracted

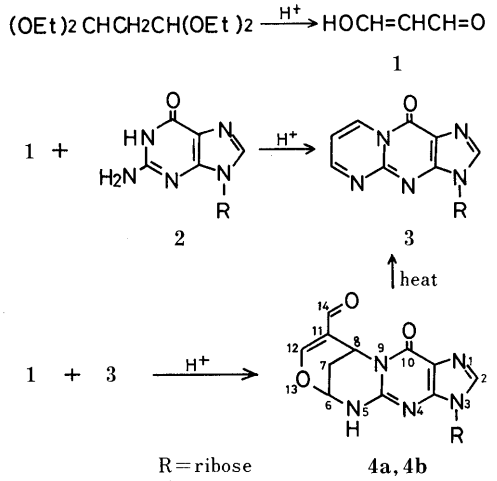

Chart 1

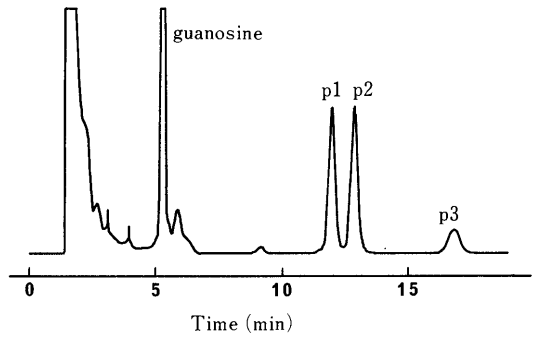

Fig. 1. HPLC Chromatogram of Guanosine–malonaldehyde Reaction Mixture

Column, Nucleosil 7C18 (4.6 i.d. ×250 mm); mobile phase, 7% (v/v) acetonitrile/water 1 ml/min; detector, 254 nm.

from the residue with 5 ml of hot water (60 °C). The extract was cleaned on a polyamide column (13 i.d. × 60 mm, water as the eluent). The eluate (0—20 ml) was concentrated to 5 ml. The solution was subjected to a Lichroprep RP-18 column and chromatographed with 7% (v/v) acetonitrile/water as the eluent (Fig. 2). The fractions of **3** (50—70 min) were collected and evaporated to dryness *in vacuo*. Yield 16 mg.

Results and Discussion

Preparation of the Diastereomers (4a and 4b) Figure 1 shows an HPLC chromatogram of a reaction mixture of guanosine with 1,1,3,3-tetraethoxypropane as a generator of malonaldehyde. The least polar adduct (p3) was identified as **3** by spectroscopic analyses. p1 and p2 showed a UV maximum at 249 nm. These adducts were separated by repeated chromatography. Though the formation of the compounds (p1, p2) proceeded only in strongly acidic media, the adduct (**3**) seems most likely to be formed *in vivo*. In fact, detection and identification of pyrimido[1,2-*a*]purin-10(3*H*)-one (aglycone of the adduct (**3**)) actually formed *in vivo* has been carried out by Draper's group.[12]

Adducts p1 and p2 were isolated as a white solid and 200 mg of each (purity 99%, HPLC) were obtained. They were not fluorescent and possessed UV, NMR, MS and CD spectral properties indicating the presence of oxadiazabicyclononene residues linked to guanosine, as reported by Marnett *et al.*[10] Each adduct, p1 (**4a**) and p2 (**4b**) was deduced to 5,6,7,8-tetrahydro-11-formyl-3(β-D-ribofuranosyl)-6,8-epoxyethenopyrimido[1,2-*a*]purin-10(3*H*)-one

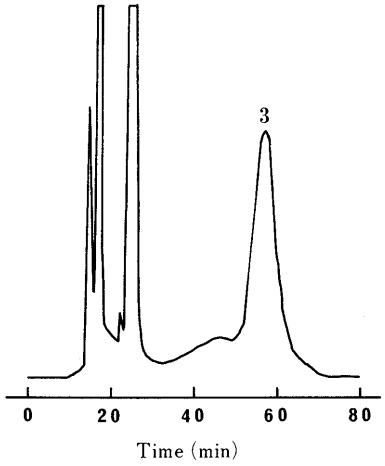

Fig. 2. Preparative HPLC Chromatogram of the Solution Containing **3**

Column, Lichroprep RP-18 (22 i.d. × 300 mm); mobile phase, 7% (v/v) acetonitrile/water 5 ml/min; detector, 254 nm. Details about the sample are described in the text.

(Chart 1). There were two isomers, namely (6*R*,8*R*)- and (6*S*,8*S*)-. Since spectroscopic details about p1 and p2 were not exhibited in a distinguishable form,[10] we listed the data in the experimental section. As shown in Chart 1, the isomers were formed by the addition of a second molecule of **1** to **3** and were easily cleaved by alkali (0.01 M NaOH) into **1** and **2** (data not shown).

Formation of Pyrimido[1,2-*a*]purin-10(3*H*)-one Nucleoside (3) by Thermal Decomposition of 4a and 4b Both **4a** and **4b** were decomposed by heat, yielding **3**. Heating of 10 mg of the isomers at 160 °C for 1 h gave **3** in a 60% yield. The product (**3**) was isolated (5 mg) by HPLC and identified by means of UV spectral comparison.

Based on these results, we proposed a convenient method which includes a thermal decomposition process of **4a** and **4b** for the preparation of **3**.

Preparation of 3 from 2 by the Proposed Method Including the Thermal Decomposition Process of 4a and 4b The product (**3**) was obtained in a 25% yield (16 mg of **3** from 56 mg of **2**) by use of the proposed method in this work (Fig. 2). When the preparation of **3** was carried out without the heating process, only 4 mg (6%) of product (**3**) was obtained. The heating process for the decomposition of **4a** and **4b** is necessary to improve the yield of **3**. In contrast, the reaction of **1** with **2** under a higher pH condition (pH 4.5) produced **3** in only a 1.4% yield.[8]

The rate of formation of 7-alkyl pyrimido[1,2-*a*]purin-10(3*H*)-one on the reaction of 2-alkyl malonaldehyde with guanine was high in a low pH medium.[13] However, as the pH lowered (0.05 M HCl) in the reaction of non-substituted malonaldehyde (**1**) with guanosine (**2**), formation of **4a** and **4b** seemed to be dominant compared to that of **3** (Fig. 1). Our results showed that **3** was the intermediate, and **4a** and **4b** the ultimate, products in the successive reaction. Fortunately, it is possible to obtain **3** in a good yield by use of the thermal decomposition process of **4a** and **4b**. In addition, it took 10 d for a reaction in the previous work.[8] Our proposed method requires only 3 h for the liquid phase reaction and 1 h for the heating process.

The proposed method, which includes the thermal decomposition process of **4a** and **4b**, is rapid and effective for the preparation of **3**.

Acknowledgements We are grateful to Mr. K. Matsuura, JEOL Ltd., for measurements of FAB MS. We also thank Mr. Y. Hiraoka and Mr. R. Inomata for excellent technical assistance.

References and Notes

1) Part III: H. Seto, T. Seto, T. Takesue and T. Ikemura, *Chem. Pharm. Bull.*, **34**, 5079 (1986).
2) Abbreviations used are as follows: RNA, ribonucleic acid; HPLC, high-performance liquid chromatography; UV, ultraviolet; NMR, nuclear magnetic resonance; MS, mass spectrometry; CD, circular dichroism; FAB, fast atom bombardment; EI, electron impact; TMS, tetramethylsilane; DMSO, dimethyl sulfoxide
3) W. A. Pryor, "Free Radicals in Biology," Vol. 1 and Vol. 4, Academic Press, New York, 1976.
4) *a*) F. H. Mukai and B. D. Goldstein, *Science*, **191**, 868 (1976); *b*) A. K. Basu and L. J. Marnett, *Carcinogenesis*, **4**, 331 (1983); *c*) P. E. Hartman, *Environ. Mutagen*, **5**, 603 (1983).
5) *a*) R. J. Shamberger, T. L. Andreone and C. E. Willis, *J. Natl. Cancer. Inst.*, **53**, 1771 (1974); *b*) R. P. Bird, H. H. Draper and V. E. O. Valli, *J. Toxicol. Environ. Health*, **10**, 897 (1982).
6) *a*) K. S. Chio and A. L. Tappel, *Biochemistry*, **8**, 2821 (1969); *b*) H. W. Gardner, *J. Agric. Food Chem.*, **27**, 220 (1979); *c*) H. H. Draper, M. Hadley, L. Lissemore, N. M. Laing and P. D. Cole, *Lipids*, **23**, 626 (1988).
7) *a*) U. Reiss, A. L. Tappel and K. S. Chio, *Biochem. Biophys. Res. Commun.*, **48**, 921, (1972); *b*) K. Kikugawa, K. Taguchi and T. Maruyama, *Chem. Pharm. Bull.*, **35**, 3364 (1987).
8) *a*) H. Seto, K. Akiyama, T. Okuda, T. Hashimoto, T. Takesue and T. Ikemura, *Chem. Lett.*, **1981**, 707; *b*) H. Seto, T. Okuda, T. Takesue and T. Ikemura, *Bull. Chem. Soc. Jpn.*, **56**, 1799 (1983).
9) H. Seto, Y. Takesue and T. Ikemura, *Bull. Chem. Soc. Jpn.*, **58**, 3431 (1985).
10) *a*) L. J. Marnett, A. K. Basu, S. M. O'Hara, P. E. Weller, A. F. M. Maqsdur Rahman and J. P. Oliver, *J. Am. Chem. Soc.*, **108**, 1348 (1986); *b*) A. K. Basu, S. M. O'Hara, P. Vallandier, K. Stone, O. Mols and L. J. Marnett, *Chem. Res. Toxicol.*, **1**, 53 (1988).
11) L. J. Marnett and M. A. Tuttle, *Cancer Res.*, **40**, 276 (1980).
12) M. Hadley and H. H. Draper, *Lipid*, **25**, 82 (1990).
13) R. C. Moschel and N. J. Leonald, *J. Org. Chem.*, **41**, 294 (1976).

SYNTHESIS OF THE SEQUENCE OF HEPT-(α1→5)-KDO-(α2→6)-D-GLUCOSAMINE-4-PHOSPHATE OF LIPOPOLYSACCHARIDE[1)]

Seijiro AKAMATSU, Kiyoshi IKEDA, and Kazuo ACHIWA*
School of Pharmaceutical Sciences, University of Shizuoka, 395 Yada, Shizuoka 422, Japan

We have synthesized Hept-(α1→5)-KDO-(α2→6)-D-glucosamine-4-phosphate (1), which is located in the inner core and lipid A regions of lipopolysaccharide. Compound 1 was mitogenic.

KEYWORDS glucosamine-4-phosphate; KDO; heptose; lipid A; LPS; mitogenicity

Lipopolysaccharide (LPS) isolated from the cell walls of various Gram-negative bacteria, is composed of four structural regions: O-polysaccharide, outer core, inner core, and a lipophilic portion of LPS, lipid A.[2)] The inner core region of LPS consists of 3-deoxy-D-manno-2-octulosonic acid (KDO) and L-glycero-D-manno-heptose. Lipid A consists as a central backbone of a 1,6-linked β-D-glucosamine disaccharide substituted by phosphate groups and by ester- and amide-bound fatty acids.[3)] The KDO region of LPS is bound to lipid A through (α2→6) linkage, and the heptose region is bound to KDO through (α1→5) linkage, as shown in chart 1. The KDO as a ketosidic component in LPS plays a biologically important role in being mitogenic and in amplifying the antitumor activity of lipid A.[4)] The heptose region in the inner-core oligosaccharide seems to be an inducer in immunological reactions,[5)] although its biological roles in LPS are not entirely clear.[6)]

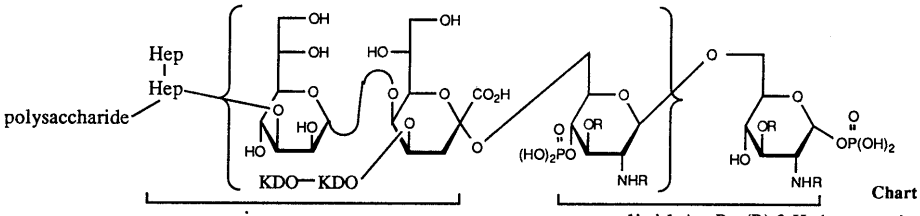

Chart . 1

In the course of investigations[7)] on the relationship between the molecular structure and the biological activity of the nonreducing-sugar subunit analogs of lipid A, we demonstrated that some α(2→6)-linked KDO-acylated 4-O-monophosphorylglucosamine derivatives have mitogenic activity comparable to that of lipid A.[7c,d,e)] Also, it is strongly suggested that the heptosyl-KDO linkage is necessary for the expression of the common LPS specifity.[5b)] Here we wish to report the synthesis of Hept-(α1→5)-KDO-(α2→6)-D-glucosamine-4-phosphate (1), in order to examine the biological significance of KDO and heptose residues in the inner-core region of bacterial lipopolysaccharide.

To synthesize KDO-(α2→6)-GlcN derivative (8), the hydroxyl groups of KDO·NH_3 were treated with chloroacetic anhydride, pyridine, and 4-dimethylaminopyridine in CH_3CN to give the per-O-chloroacetylated compound (2) [39%, mp 121-124℃, $[\alpha]_D^{24}$ +50.2° (c=0.99, $CHCl_3$)]. The carboxyl group of 2 was esterified with phenyldiazomethane to give the fully protected compound (3) [53%, syrup, $[\alpha]_D^{21}$ +51.5° (c=0.99, $CHCl_3$)]. Treatment of 3 with titanium tetrabromide in CH_2Cl_2-AcOEt(10:1) gave the 2-bromo compound (4) in nearly quantitative yield. The unstable bromide (4) was used for the subsequent glycosylation without further purification. Glycosylation of the glycosyl acceptor (5), prepared from benzyl 2-amino-2-deoxy-4,6-O-isopropylidene-β-D-glucopyranoside in 5 steps,[7d,f)] with the glycosyl donor 4 in the presence of $Hg(CN)_2$, $HgBr_2$ and Molecular Sieves 4A in CH_2Cl_2 at room temperature for 48 h gave the desired α-linked disaccharide containing KDO (6) [40%, syrup, $[\alpha]_D^{20}$ +5.1° (c=0.99, $CHCl_3$)]. The α-D-anomeric configuration of the KDO residue was ascertained by the chemical shift value (δ 5.44) of the signal attributable to H-4, which is indicative of the α-D-anomeric configuration of per-O-chloroacetylated KDO derivatives.[8)] Selective removal of the

chloroacetyl groups of 6 was carried out with hydrazinedithiocarbonate[9] in 2,6-lutidine-AcOH (3:1) at 0° for 2 h and then treated with 2-methoxypropene[10] in the presence of a catalytic amount of p-toluenesulfonic acid in DMF to give the isopropylidene compound (7) [52%, syrup, $[\alpha]_D^{21}$ +5.5° (c=1.00)]. An equatorially oriented hydroxyl group of the C-4 of the KDO moiety of 7 was regioselectively protected with benzyloxymethyl chloride and pyridine in CH_2Cl_2 to give the benzyloxymethyl compound (8) [84%, syrup, $[\alpha]_D^{20}$ +6.1° (c=1.40, $CHCl_3$)]. Coupling of 8 and the suitably blocked L-glycero-D-manno-heptose derivative (9)[11] was carried out in the presence of a catalytic amount of p-toluenesulfonic acid to give the α-linked trisaccharide (10) as a single anomer [55%, $[\alpha]_D^{20}$ +7.7° (c=1.66, $CHCl_3$), ^{1}H-NMR:δ 5.26 (1H, br s, H-1 of heptose moiety), and ^{13}C-NMR:δ 100.5 (C-1 of heptose moiety)]. After the cleavage of the isopropylidene group of 10 with 95% trifluoroacetic acid[12] at 0°C, hydrogenolytic removal of the benzyl and phenyl groups was achieved with palladium and Adams' platinum catalysts in MeOH solution to give the heptose-containing trisaccharide (1) [52%, mp 148-150℃ , $[\alpha]_D^{20}$ +4.3° (c=0.24, MeOH)] as the free acid form. In the positive fast atom bombardment mass spectrometry (FAB-MS), 1 revealed an $(M+H)^+$ ion at m/z 1449 and an $(M+Na)^+$ ion at m/z 1471. Compound 1 gave a positive test with the specific spray-reagent for phosphate.[13]

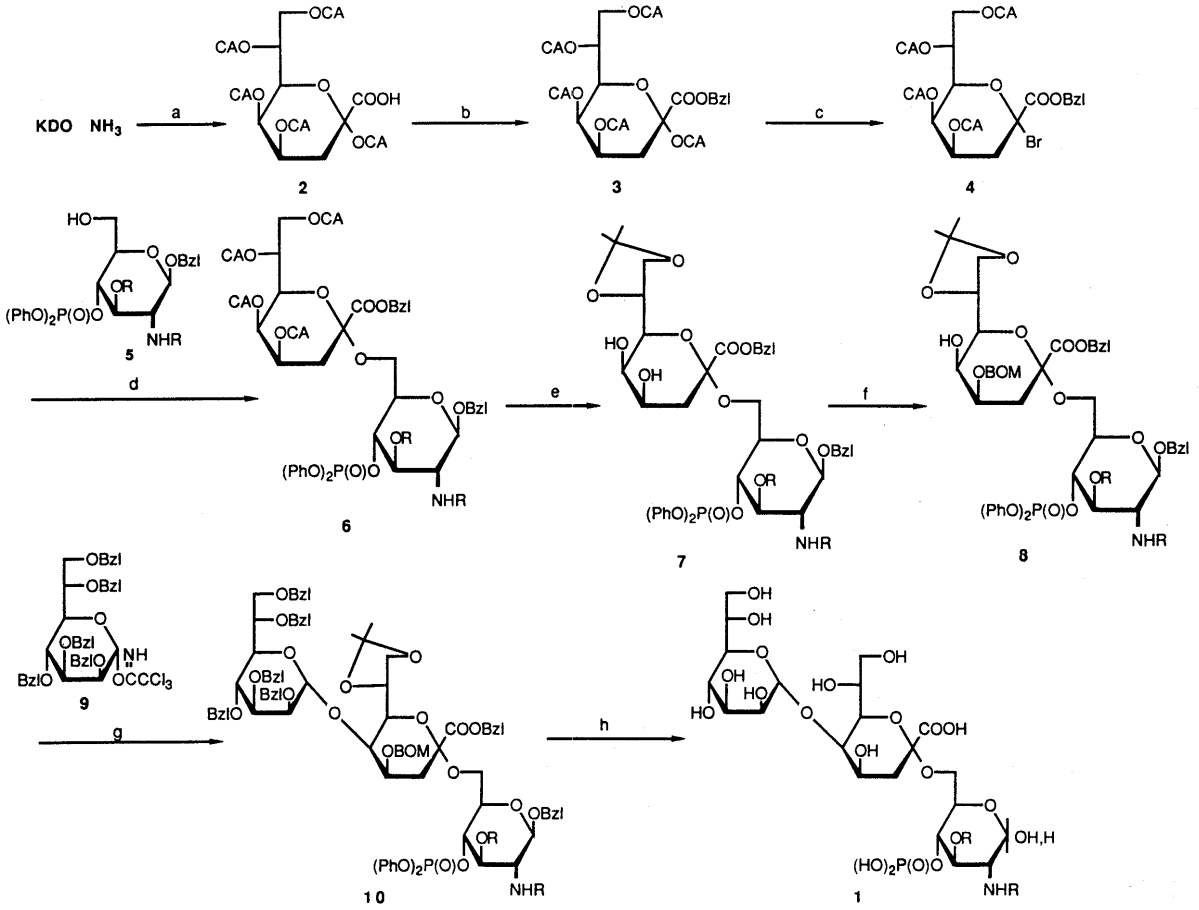

R= $-C_{14}OC_{14}$: $CH_3(CH_2)_{10}\overset{(R)}{C}HCH_2CO-$ CA : $ClCH_2CO-$, BOM : $PhCH_2OCH_2-$
$CH_3(CH_2)_{12}C(O)O$

Reagents: a) CA_2O, pyridine, DMAP, in CH_3CN r.t. 48h, b) $PhCHN_2$, in CH_2Cl_2 r.t. 30min
c) $TiBr_4$, in CH_2Cl_2-AcOEt (10:1) r.t. 24h, d) $Hg(CN)_2$, $HgBr_2$, in CH_2Cl_2 r.t. 48h
e) i) HDTC, in 2,6-lutidine-AcOH (3:1) 0°C 2h, ii) $CH_3C(OCH_3)=CH_2$, PTSA, in DMF r.t. 12h
f) BOM-Cl, pyridine, in CH_2Cl_2 r.t. 24h ; g) **9**, PTSA, in CH_2Cl_2 r.t. 24h
h) i) 95%CF_3COOH, in CH_2Cl_2 0°C 15min, ii) $Pd(OH)_2/H_2$, in MeOH r.t. 3h, iii) PtO_2/H_2, in MeOH r.t. 6h

Preliminaly examination of the biological activity showed that compound 1 has the same level of mitogenicity and lethal toxicity as that of the parent D-glucosamine-4-phosphate.

ACKNOWLEDGMENT This work was supported in part by Grant-in-Aid for Encouragement of Young Scientists from the Ministry of Education, Science and Culture, Japan, and by Research Aid of TERUMO life Science Foundation.

REFERENCES AND NOTES

1) Part XXV of "Lipid A and Related Compounds." For Part XXIV: See, S. Akamatsu, K. Ikeda, and K. Achiwa, Chem. Pharm. Bull., in press.
2) a) O. Westphal, and O. Lüderitz, Angew. Chem., 66, 407 (1954); b) O. Lüderitz, C. Galanos, V. Lehmann, H. Mayer, E. T. Rietschel, and J. Weckesser, Naturwissenschaften, 65, 578 (1978).
3) a) K. Takayama, N. Qureshi, and P. Mascagni, J. Biol. Chem., 258, 12801 (1983); b) M. Imoto, S. Kusumoto, T. Shiba, H. Naoki, T. Iwashita, E. Th. Rietschel, H.- W. Wollenweber, C. Galanos, and O. Lüderitz, Tetrahedron Lett., 24, 4017 (1983); c) U. Seydel, B. Lindner, H. -W. Wollenweber, and E. T.Rietschel, Eur. J. Biochem., 145, 505 (1984).
4) a) K. Amano, H. Fujita, T. Sato, H. Sasaki, Y. Yoshida, and K. Fukushi, Jpn. J. Bacteriol., 40, 775 (1985); b) K. Kamamoto and J. Y. Homma, J. Biochem., 741 (1982).
5) a) K. Dziewiszek and A. Zamojsky, Carbohydr. Res., 145, C5 (1987); b) H. Brade and C. Galanos, Infect. Immun., 42, 250 (1983).
6) A. Gamian and E. Romanowska, Eur J. Biochem., 129, 105 (1982).
7) a) S. Nakamoto, T. Takahashi, K. Ikeda, and K. Achiwa, Chem. Pharm. Bull., 33, 4098 (1985); b) T. Shimizu, S. Akiyama, T. Masuzawa, Y. Yanagihara, S. Nakamoto, T. Takahashi, K. Ikeda, K. Achiwa, ibid., 33, 4621 (1985); c) T. Shimizu, S. Akiyama, T. Masuzawa, Y. Yanagihara, S. Nakamoto, and K. Achiwa. ibid., 34, 2310 (1986); d) S. Nakamoto and K. Achiwa, ibid., 34, 2302 (1986); e) T. Shimizu, S. Akiyama, T. Masuzawa, Y. Yanagihara, S. Nakamoto, and K. Achiwa, Infect. Immun., 55, 2287 (1987); f) S. Nakamoto and K. Achiwa, Chem. Pharm. Bull., 36, 202 (1988); g) T. Shimizu, T. Masuzawa, Y. Yanagihara, S. Nakamoto, H.Itoh, and K. Achiwa, J. Pharmacobio-Dyn., 11, 512 (1988); h) C. Shimizu, K. Ikeda, and K. Achiwa, Chem. Pharm. Bull., 36, 1772 (1988); i)T. Shimizu, T. Masuzawa, Y. Yanagihara, C. Shimizu, K. Ikeda, and K. Achiwa, FEBS Lett., 228, 99 (1988); j) K. Ikeda, S. Akamatsu, and K. Achiwa, Carbohydr. Res., 189, C1 (1989); k) T. Shimizu, T. Masuzawa, Y. Yanagihara, H. Itoh, S. Nakamoto, and K. Achiwa, Chem. Pharm. Bull., 37, 2535 (1989); l) K. Ikeda, S. Akamatsu, and K. Achiwa, ibid., 38, 279 (1990); m) T. Shimizu, Y. Ohtsuka, T. Masuzawa, Y. Yanagihara, H. Itoh, S.Nakamoto, and K. Achiwa, Mol. Biother, 2, 110 (1990); n) K. Idegami, K. Ikeda, and K. Achiwa, Chem. Pharm. Bull., 38, 1766 (1990).
8) M. Kiso, M. Fujita, M. Tanahashi, Y. Fujishima,Y. Ogawa, A. Hasegawa, and F. M. Unger, Carbohydr. Res., 177, 51 (1988).
9) C. A. A. van Boeckel and T. Beetz, Tetrahedron Lett., 24, 3775 (1983).
10) H. Paulsen, M. Stiem, and F. M. Unger, Justus Liebigs Ann. Chem., 1987, 273.
11) Compound 9 was prepared from Benzyl 2,3,4,7-tetra-O-benzyl-β-L-glycero-D-manno-heptopyranoside[5a)] in 4 steps, i) NaH, BzlBr/Bu_4NI/THF, 83% yield. ii) Ac_2O, H_2SO_4/AcOEt, 61% yield. iii) NH_4OH-MeOH (1:10), 90% yield. iv) Cl_3CCN, NaH/CH_2Cl_2, 73% yield.
12) S. Kusumoto, N. Kusunose, T. Kamikawa and T. Shiba, Tetrahedron Lett., 29, 6325 (1988).
13) J. C. Dittmer and R. L. Lester, J. Lipid Res., 5, 126 (1964).

(Received November 19, 1990)

CYTOTOXIC ACETYLENES FROM *PANAX QUINQUEFOLIUM*[1)]

Yasuo FUJIMOTO,*[a] Mitsuru SATOH,[b] Naoki TAKEUCHI,[b] and Makoto KIRISAWA[a]
College of Pharmacy, Nihon University,[a] 7-7 Narashinodai, Funabashi, Chiba 274, Japan and Showa College of Pharmaceutical Sciences,[b] 3-3165 Higashitamagawagakuen, Machida-Shi, Tokyo 194, Japan

Three new cytotoxic polyacetylenes, PQ-1 (1), PQ-2 (2) and PQ-3 (3), have been isolated from *Panax quinquefolium*. The structures of these acetylenes were determined by analyses of their ^{1}H-^{1}H and ^{1}H-^{13}C COSY spectra. All these compounds exhibited strong cytotoxic activities against leukemia cells (L 1210) in tissue culture.

KEYWORDS *Panax quinquefolium*; Araliaceae; polyacetylene; cytotoxic activity

Panax quinquefolium has been considered as one of the most valuable drugs used by American Indians. Recently, the plant has been cultivated on a large scale in the United States and Canada, and it has been exported to Japan and China. The alcoholic extract of the roots of this plant has been widely used as a tonic in these countries and some people with cancer have used it as an anticancer drug in home treatment.

During the course of our studies on the cytotoxic acetylenes of *panax* species, we reported the isolation and structural elucidation of three acetylenes from the callus of *P. ginseng* C. A. Meyer.[2)] Here we describe the isolation and structural elucidation of three new polyacetylenes, PQ-1(1), PQ-2 (2), PQ-3 (3), along with four known acetylenes, falcalinol (4),[3)] panaxytriol (5),[4)] panaxydol (6),[5)] heptadeca-1,8-diene-4,6-diyne-3,10-diol (7)[6)] from *P. quinquefolium*.

The dried roots (1.2 kg) were powdered in a blender and extracted with EtOAc (2.5 l x 3) under ultrasonication. After concentration of the EtOAc solution, the crude extract was chromatographed on a Diaion HP-20 resin (Nippon Rensui) column (eluted successively with 2.0 l each of H_2O, 20%MeOH, 40%MeOH, 60%MeOH, 80%MeOH, 90%MeOH, MeOH and acetone). The growth inhibition of each fraction was tested against leukemia cells (L 1210) and the 80% and 90%MeOH fractions were found to be active. The 80%MeOH fraction was chromatographed on silica gel (hexane : EtOAc = 1 : 1) followed by high performance liquid chromatography (HPLC) (Senshu pack, silica 4251N, hexane : EtOAc = 2 : 1) to give 2 (8

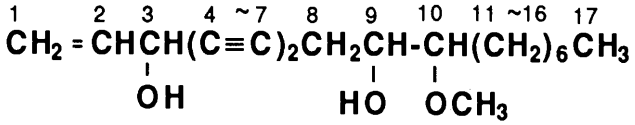

PQ-1 (1)

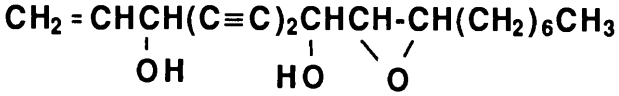

PQ-2 (2)

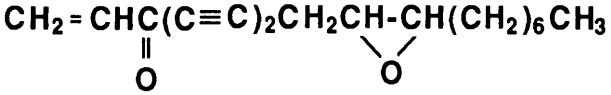

PQ-3 (3)

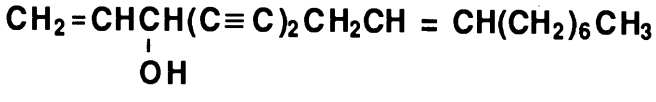

falcalinol (4)

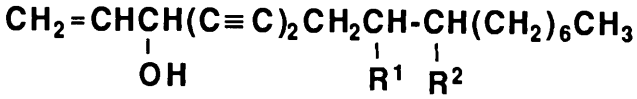

panaxytriol (5) : $R^1 = R^2 = OH$

panaxydol (6) : $R^1, R^2 = >O$

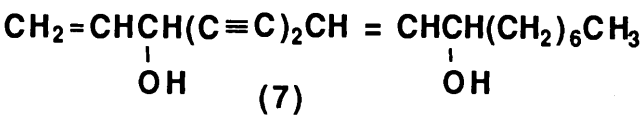

(7)

mg), **6** (114 0 mg) and **5** (71 mg). Similarly, the 90%MeOH fraction was chromatographed on silica gel (hexane : EtOAc = 2 : 1) followed by HPLC (Senshu pack, silica 4251N, hexane : EtOAc = 3 : 1) to afford **1** (91 mg), **3** (35 mg), **4** (670 mg) and **7** (18 mg).

PQ-1 (1),[7] oil, $[\alpha]_D$ -21.7° (MeOH, c=0.58). The high resolution mass spectrum (HR-MS) of **1** indicated the molecular formula $C_{18}H_{28}O_3$ (M^+ 292.2083, calcd. 292.2037). The ^{1}H-NMR spectrum of **1** exhibited the presence of a methyl [δ0.89(t, J=6.6 Hz, H-17)], polymethylene [δ1.25~1.40(10H, brd, W1/2=25 Hz, H-12~H-16)], a methylene [δ1.55(2H, brm, H-11)], nonequivalent methylene [δ2.53(1H, dd, J=6.1, 17.3 Hz) and δ2.60(dd, J=6.3, 17.3 Hz, H-8)], three methine protons [δ3.24(dt, J=4.1, 6.1 Hz, H-10), δ3.71(brq, J=4.1 Hz, H-9) and δ4.92(brd, J=5.4 Hz, H-3)] attached to oxygen-bearing carbons, two hydroxyl [δ2.09 and 2.44(brs, each)],

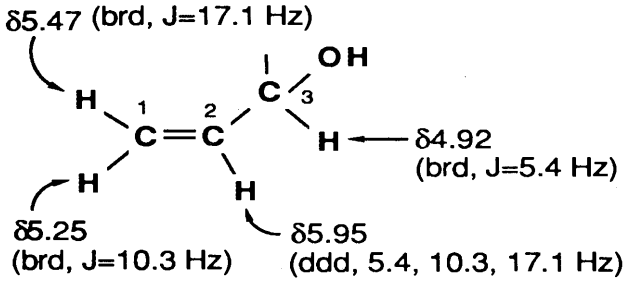

(A)

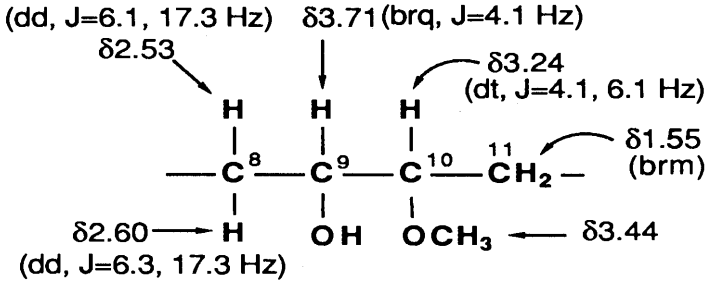

(B)

a methoxyl (δ3.44) and three vinyl protons [δ5.25(brd, J=10.3 Hz, H-1), 5.47(brd, J=17.1 Hz, H-1) and δ5.95(ddd, J=5.4, 10.3, 17.1 Hz, H-2)]. Acetylation of **1** gave a diacetate which exhibited the proton signals due to H-3 (δ5.92) and H-9 (δ5.02) at 1.00 and 1.31 ppm lower field, respectively, as compared with those of **1**. The results of acetylation and ^{1}H-^{1}H COSY spectrum of **1** revealed the partial structures of C-1~C-3 (A), C-8~C-11 (B) and C-12~C-17 sequence. In the ^{13}C-NMR spectrum of **1**, there are four signals (δ66.0, 71.0, 74.5 and 78.4) due to sp carbons which could be assigned to the diacetylene moiety in consideration of the molecular formula. The chemical shifts and the coupling patterns of H-3 and H-8 suggested that the diacetylene moiety should be inserted between C-3 and C-8. Thus, the structure of PQ-1 was confirmed as 10-methoxyheptadeca-1-ene-4,6-diyne-3,9-diol.

PQ-2 (2), oil, $[\alpha]_D$ +86.9° (MeOH, c=0.64). The HR-MS of **2** indicated the molecular formula $C_{17}H_{24}O_3$ (M^+276.1697, calcd. 276.1723). The ^{13}C-NMR spectrum of **2** exhibited the signals due to a methyl (δ14,1), six methylenes (δ22.6, 26.5, 27.5, 29.1, 29.4 and 31.7), four oxygen-bearing carbons (δ57.9, 58.0, 60.7 and 63.4), two sp^2 carbons (δ117.5 and 135.7) and four sp carbons (δ70.1, 70.2, 78.0 and 78.5). The ^{1}H-NMR spectrum of **2** revealed the presence of an allylic alcohol moiety [δ5.96(ddd, J=5.1, 10.3 and 16.9 Hz, H-2), δ5.48 (d, J=16.9 Hz, H-1), δ5.27 (d, J=9.8 Hz, H-1), δ4.95 (brs, H-3)] and a polymethylene sequence from C-11~C-17 [δ0.89(t, J=7.3 Hz, H-17), δ1.2~1.4(brs, H-13~H16), δ1.51 (m, H-12) and δ1.62 (m, H-11)] . The ^{1}H-NMR decoupling experiments on **2** and the chemical shifts of H-8 [δ4.37(brd, J=7.3 Hz)], H-9 [δ3.15(dd, J=4.4, 7.3 Hz) and H-10 [δ3.06(m)] suggested the presence of a hydroxyl group at C-8 and the epoxide ring including C-9 and C-10. The configuration of the epoxide ring was assgined as *cis* from the coupling constant (J=4.4 Hz) between H-9 and H-10. Considering these spectral data and the empirical formula of **2**, the structure of PQ-2 was confirmed as heptadeca-1-ene-9,10-epoxy-4,6-diyne-3,8-diol.

PQ-3 (3),[8] oil, $[\alpha]_D$ -36.9°(MeOH, c=0.68). The HR-MS of **3** showed a molecular ion peak at m/z 258.1620 (calcd. 258.1618 for $C_{17}H_{22}O_2$). The ^{13}C-NMR spectrum of **3** exhibited the signals due to a methyl (δ14.3), seven methylenes (δ20.1, 22.9, 26.7, 27.8, 29.4, 29.7 and 32.0), two oxygen-bearing carbons (δ54.1 and 57.2), four sp carbons (δ65.9, 71.2, 76.7 and 84.8), two sp^2 carbons (δ134.7 and 138.0) and a conjugated carbonyl carbon (δ177.9). The ^{1}H-NMR spectrum of **3** revealed three proton signals [δ6.23(d, J=10.3 Hz, H-1), δ6.41(dd, J=10.3, 16.9 Hz, H-2) and δ6.56(d, J=16.9 Hz, H-1)] due to a terminal

vinyl group. The chemical shifts of these protons were in a rather lower field in comparison with those of PQ-1 or PQ-2. This suggested that the vinyl group should be conjugated with the carbonyl group. On comparison of the ^{1}H-NMR spectrum of **3** with that of panaxydol (6), the coupling pattern and the chemical shifts of the proton signals in 0.8-3.2 ppm region were almost the same, thereby suggesting the presence of the C-7 ~C-17 sequence. Thus, the structure of PQ-3 was confirmed as 3-oxo-9,10-epoxy-heptadeca-1-ene-4,6-diyne (3-oxopanaxydol). All these polyacetylenes completely inhibited the growth of leukemia cells (L 1210) in tissue culture at a concentration of 0.5-1.0 μg/ml.

REFERENCES AND NOTES

1) The contents of this paper were reported briefly on 110th Annual Meeting of the Pharmaceutical Society of Japan, Sapporo, Aug. 1990.
2) a) Y. Fujimoto and M. Satoh, *Phytochemistry*, **26**, 2850 (1987); b) Y. Fujimoto and M. Satoh, *Chem. Pharm. Bull.*, **36**, 4206 (1988).
3) M. Takahashi and K. Isoi, *Yakugaku Zasshi*, **84**, 752 (1964).
4) H. Matsunaga, M. Katano, H. Yamamoto, M. Mori and K. Takata, *Chem. Pharm. Bull.*, **37**, 1279 (1989).
5) J. Poplawski, J. T. Wrobel and T. Glinka, *Phytochemistry*, **19**, 1539 (1980).
6) S. C. Shim, S. Chan, C. W. Hur and C. K. Kim, *Phytochemistry*, **26**, 2849 (1987).
7) ^{13}C-NMR (100 MHz, d, $CDCl_3$): 14.1 (C-17), 22.6 (C-16), 24.6 (C-8), 25.1 (C-12), 29.2 (C-14), 29.8 (C-11 and C-13), 31.8 (C-15), 58.3 (OCH_3), 63.5 (C-3), 70.9 (C-9), 82.0 (C-10), 66.0, 71.0, 74.5 and 78.4 (acetylenic carbons), 117.1 (C-1), 136.1 (C-2).
8) Isolation of this compound from *Panax ginseng* C. A. Meyer was also reported at the 110th Annual Meeting of the Pharmaceutical Society of Japan, Sapporo, Aug. 1990, K. Hirakura, M. Morita, K. Nakajima and H. Mitsuhashi, Abstract Paper, p. 172.

(Received November 30, 1990)

SYNTHESIS OF 2-ARYL-5,6-DIHYDRO-(1)BENZOTHIEPINO[5,4-*C*]PYRIDAZIN-3(2*H*)-ONE BY A NOVEL DEHYDROGENATION REACTION

Tohru NAKAO,* Minoru OBATA, Yuko YAMAGUCHI and Tetsuya TAHARA

Central Research Laboratories, Yoshitomi Pharmaceutical Industries, Ltd., 955, Koiwai, Yoshitomi-cho, Chikujo-gun, Fukuoka, 871, Japan

Treatment of 2-(4-methoxyphenyl)-4,4a,5,6-tetrahydro-(1)benzothiepino[5,4-*c*]pyridazin-3(2*H*)-one 7-oxide (**1a**) in methanesulfonic acid (MSA) gave 2-(4-methoxyphenyl)-5,6-dihydro-(1)benzothiepino[5,4-*c*]pyridazin-3(2*H*)-one (**2a**) in 80% yield. Compound **2a** was also obtained by treating **4a** , a deoxidized compound of **1a**, with dimethylsulfoxide (DMSO) in MSA, trifluoroacetic acid or HBr-AcOH. Apparently this novel dehydrogenation reaction was derived from an acid catalyzed intermolecular redox reaction, that is, a concerted elimination of 4-hydrogen,4a-hydrogen on **1a** or **4a** and sulfinyl oxygen on **1a** or DMSO.

KEYWORDS dehydrogenation reaction; redox reaction; sulfoxide; acid catalyst; (1)benzothiepino[5,4-*c*]pyridazin-3(2*H*)-one; dimethylsulfoxide

Two ways have been reported to prepare 6-arylpyridazin-3(2*H*)-one type compounds by dehydrogenation, i.e., dehydrogenation of the corresponding 6-aryl-4,5-dihydropyridazin-3(2*H*)-ones with either bromine in acetic acid[1,2] or sodium *m*-nitrobenzenesulfonate in aklaline solution.[1b] However, the former is inapplicable to compounds which contain active substituents to bromination on the aromatic rings and the latter is not suitable for compounds which are unstable in alkaline media. In the course of studies on the synthesis of condensed pyridazine derivatives as novel anxiolytics,[2] we obtained information suggesting a novel synthesis pathway which overcomes these limitations.

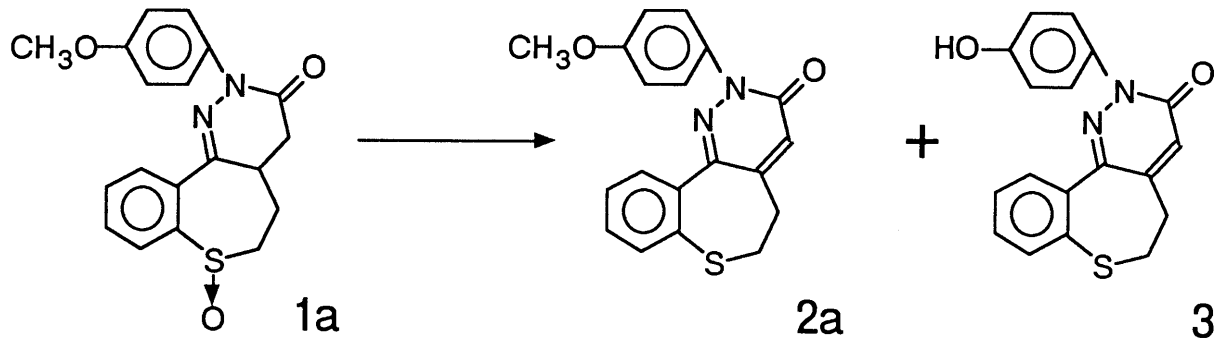

Chart 1

In this study we attempted to remove the *O*-methyl group of 2-(4-methoxyphenyl)-4,4a,5,6-tetrahydro-(1)benzothiepino[5,4-*c*]pyridazin-3(2*H*)-one 7-oxide (**1a**)[3] according to the method reported by Irie et al.[4] Treating **1a** with methionine in methanesulfonic acid (MSA) gave **2a** and **3**.[5] Chart 1 shows the chemical structures of the two compounds which were elucidated mainly by spectral analyses. Moreover, **2a** was obtained exclusively in 80% yield by treating **1a** with MSA in the absence of methionine. Therefore, it appeared that the above reaction consisted of two steps, i. e., an acid-catalyzed redox-reaction in the first step and demethylation from methoxy group in the second. In this context, compound **2a** was derived from **1a** *via* the concerted elimination of the 7-oxgen, 4- and 4a-

hydrogen of **1a** in the first step. Compound **3** was produced at the second stage where methionine plays a role. Furthermore, application of trifluoroacetic acid (TFA) instead of MSA gave **2a** in 73 % yield. Table 1 summarizes the results of these and the following experiments. When a deoxidized compound of **1a** (**4a**)[3] was used, compound **4a** was recovered as an unchanged form even after a solution of **4a** in MSA was stirred at 60-65 °C for 24 h. These results prompted us to investigate the possibility of using DMSO as a source of sulfinyl oxygen (Chart 2).

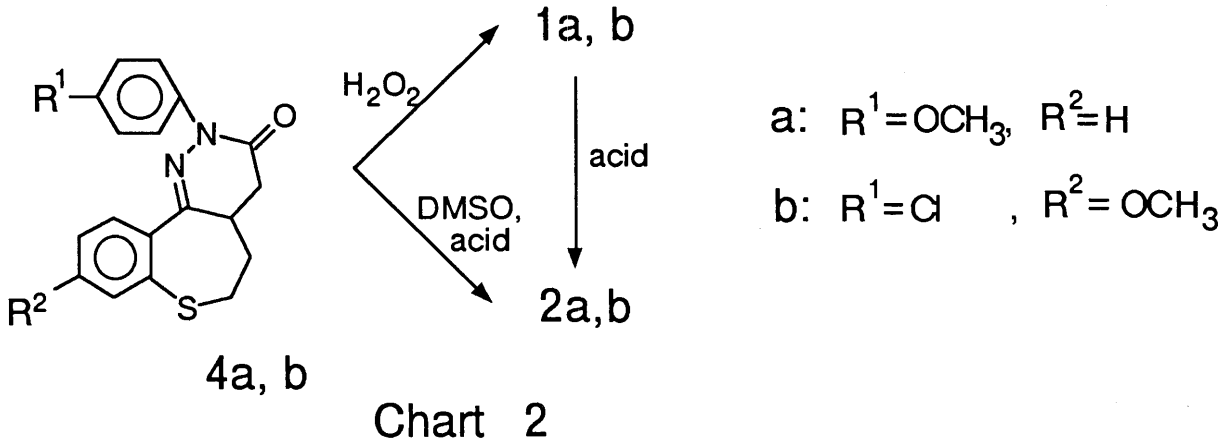

Chart 2

Table I. Synthesis of **2a** or **2b** and the Reaction Conditions

Entry	Substrate	Reaction condition	Product	Yield(%)[a]
1	**1a**	CH_3SO_3H, 60-65°C, 0.5 h	**2a**	80
2	**1a**	CF_3COOH, 60-65°C, 9 h	**2a**	73
3	**4a**	CH_3SO_3H, DMSO, 60-65°C,16 h	**2a**	15
4	**4a**	CF_3COOH, DMSO, 60-65°C,16 h	**2a**	55
5	**4a**	30%HBr-AcOH, DMSO, 20°C,0.5 h	**2a**	95
6	**4a**	Br_2, AcOH, 40-45°C ,0.5 h	**2a**	92[b]
7	**1b**	CH_3SO_3H, 60-65°C, 0.2 h	**2b**	91
8	**4b**	30%HBr-AcOH, DMSO, 20°C,0.5 h	**2b**	86

a) Yield : isolated yield. b) Trace amount of bromine-adduct was detected on mass spectrum.

As shown in Table I, compound **2a** was successfully obtained when DMSO was added to a solution of **4a** in MSA or TFA (entries 3, 4). Moreover, compound **2a** was afforded in good yield by treating **4a** with DMSO in 30 % HBr-AcOH at 20°C for 0.5 h (entry 5). In this reaction, the possibility of forming bromine-adduct[7] on the aromatic moiety activated with substituents, such as methoxy and thio groups, was apparent, excepting the formation of **2a**. But there was no detectable amount of the adduct in the mass spectrum, only compound **2a** was obtained. This may be attributed to the addition of equimolar DMSO in this reaction.

To prepare 2-(4-chlorophenyl)-5,6-dihydro-9-methoxy-(1)benzothiepino[5,4-*c*]pyridazin-3(2*H*)-one (**2b**)[7] from **4b**,[3] a condition using bromine in acetic acid was applied. However, the product was a mixture of **2b** and a corresponding 10-bromine adduct. These were difficult to separate from each other for purification. Also, dehydrogenation of **4b** with sodium *m*-nitrobenzenesulfonate did not provide **2b**, because of the decomposition of the starting material. On the other hand, the target

compound **2b** was successfully prepared from **1b**[3] or **4b** in good yields (Entries 7, 8) under the conditions similar to those in entries 1 or 5.

From these results, it appeared that this dehydrogenation reaction resulted from a concerted elimination of 4- and 4a-hydrogen on 2-aryl-4,4a,5,6-tetrahydro-(1)benzothiepino[5,4-*c*]pyridazin-3(*H*)-ones and sulfinyl oxygen on **1a**, **1b** or DMSO; that is, an acid catalyzed intermolecular redox reaction occured. The detailed mechanism of this reaction is now under investigation. Because of the simplicity of the reaction conditions, this novel reaction would be of use as an alternative method in the preparation of 2-aryl-5,6-dihydro-(1)benzothiepino[5,4-*c*]pyridazin-3(2*H*)-ones. We are now proceeding to apply this method for the preparation of other 6-arylpyridazin-3(2*H*)-one type compounds.

REFERENCES AND NOTES

1) a) E.A. Steck, R.P.Brundage, and L.T. Fletcher, *J, Am. Chem. Soc.*, **75**, 1117 (1953); b) W.V. Curran and A. Ross, *J. Med. Chem.*, **17**, 273 (1974).
2) T. Nakao, M. Kawakami, K. Morita, Y. Morimoto, S. Takehara, and T. Tahara, *Yakugaku Zasshi*, **110**, 561 (1990); T. Nakao, M. Kawakami, K. Morita, M. Obata, Y. Morimoto, S. Takehara, and T.Tahara , *Yakugaku Zasshi*, **110**, 573 (1990).
3) Synthetic methods of **1a**,**b** and **4a**,**b** will be reported elsewhere.
4) H. Irie, N. Fuji, H. Ogawa, H. Yajima, M. Fujino, and S. Shinagawa, *J. Chem. Soc., Chem. Commun.*, **1972**, 922.
5) Compound **2a** and **3** were synthesized as follows: To a solution of **1a** (3.0 g,0.0085 mol) in MSA was added methionine(2.5 g, 0.017 mol) and the mixture was stirred at 60-65 °C for 0.5 h. At this point, the starting compound (**1a**)was undetectable in the reaction mixture, and two spots of new products appeared on TLC. The reaction mixture was poured into ice-water and extracted with $CHCl_3$. The extract was washed with water, dried over $MgSO_4$ and concentrated *in vacuo*. The residue was chromatographed on a silica gel column with $CHCl_3$ to give two fractions. We obtained 1.2 g of **2a** from the first fraction and a 0.6 g of **3** from the second. Physical data of the **2a** and **3**. **2a**: colorless needles mp 134-135 °C. *Anal.* Calcd for $C_{19}H_{16}N_2O_2S$: C,67.88; H,4.80; N,8.33. Found: C,67.89; H,4.97; N,8.25. IRν^{KBr}_{max}cm^{-1}: 1670 (CON). MSm/z: 336 (M^+). ^{1}H-NMR ($CDCl_3$) δ: 2.72 (2H,t, *J*=7Hz, SCH_2CH_2), 3.26 (2H, t,*J*=7Hz, SCH_2CH_2), 3.84 (3H, s, OCH_3), 6.89 (1H, s, C=CHCON), 6.97 (2H, d, *J*=9Hz, ArH), 7.35-7.43 (4H, m, ArH), 7.61(2H, d, *J*=9Hz, ArH). **3**: colorless powder mp 312 °C (dec.). *Anal.* Calcd for $C_{18}H_{14}N_2O_2S$: C,67.06; H,4.38; N,8.69. Found: C,67.12; H, 4.47; N, 8.75. IRν^{KBr}_{max}cm^{-1}: 3130 (OH),1650 (CON). MSm/z:322 (M^+). ^{1}H-NMR (DMSO-d_6) δ:2.63- 2.77 (2H, m), 3.21-3.36 (2H, m), 6.84 (2H, d, *J*=9Hz,ArH), 7.02 (1H, s, C=CHCON), 7.42 (2H, d, *J*=9Hz, ArH), 7.52- 7.68 (4H, m, ArH).
6) H. Gilman and J. Eish, *J. Am. Chem. Soc.*, **77**, 3862 (1955).; H. Gilman and D.R. Swayampqti, *ibid.*, **77**, 5944 (1955); M. Madesclaire, *Tetrahedron*, **44**, 6537 (1988).
7) Physical data of the **2b**: colorless needles mp 131-132°C. *Anal.* Calcd for $C_{19}H_{15}N_2O_2S$: C,61.54; H,4.08; N,7.55. Found: C,61.67; H,4.26; N,7.55. IRν^{KBr}_{max}cm^{-1}: 1670(CON). MSm/z:370(M^+). ^{1}H-NMR ($CDCl_3$) δ: 2.73 (2H, t, *J*=7Hz, SCH_2CH_2), 3.25 (2H, t, *J*=7Hz, SCH_2CH_2), 3.86 (3H, s,OCH_3), 6.87 (1H, s, C=CHCON), 6.97 (1H, dd, *J*=2, 9Hz, ArH), 7.40 (2H, d, *J*=8Hz, ArH), 7.52 (1H, d, *J*=9Hz, ArH), 7.68(2H, d, *J*=8Hz, ArH).

(Received December 3, 1990)

A SYNTHESIS OF 2-*ENDO*-AMINO-2-*EXO*-HYDROXYMETHYLNORBORNENES HAVING INHIBITORY ACTIVITY AGAINST PROTEIN KINASE C

Tameo IWASAKI,* Hiroyoshi YAMAZAKI, Takashi NISHITANI, and Tadashi SATO*
Research Laboratory of Applied Biochemistry, Tanabe Seiyaku Co., Ltd.,
3-16-89 Kashima, Yodogawa, Osaka 532, Japan

2-*endo*-Hexadecylamino-2-*exo*-hydroxymethylnorbornene (**1a**) was synthesized from 2-acetamidonorbornene-2-carboxylic acid methyl ester (**2**) in a good overall yield. 2-*endo*-Hexadecylamino-2,3-*exo*-bis(hydroxymethyl)norbornene (**1b**) was synthesized starting from dimethyl acetamidofumarate based on Diels-Alder strategy. **1a** and **1b** inhibited protein kinase C at the IC_{50} values of 2×10^{-5} M and 1×10^{-5} M, respectively, but not protein kinase A at a concentration of 1×10^{-3} M. The structure-activity relationships are discussed.

KEYWORDS protein kinase C; aminonorbornene; Diels-Alder reaction; amino alcohol

Protein kinase C, a pivotal enzyme in signal transduction and cell regulation, is activated physiologically by diacylglycerol produced by the receptor-mediated turnover of inositol phospholipids.[1] This enzyme is also the principal target of phorbol esters[2] and other tumor promoters.[3] To elucidate the physiological role of protein kinase C and to develop agents that can selectively prevent the effect of tumor promoters, a number of natural[4] and synthetic inhibitors[5] have been investigated. Of these inhibitors, UCN-1028A, isolated from the culture broth of *Cladosporium cladosporioides*, was reported to be a specific inhibitor of this enzyme.[6] Recently, on the other hand, Hannun *et al.*[7] have reported that sphingosin and liso-sphingolipids possessing an amino alcohol skeleton inhibit protein kinase C and may function as endogenous modulators of cell function. In connection with our studies in search of a new compound having intriguing biological activities, we now report a synthesis of 2-*endo*-amino-2-*exo*-hydroxymethylnorbornene derivatives (**1a, 1b**), sterically defined amino alcohols, which inhibit protein kinase C. The critical structural features required for inhibition of protein kinase C for the norbornene derivatives are also be described.

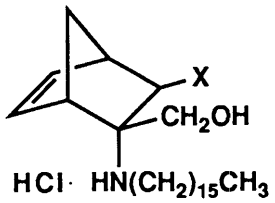

1a, b a: X=H b: X=CH_2OH

In Chart 1 and 2 are shown the synthetic routes of **1a** and **1b**, respectively. **1a**[8] was synthesized in 33% overall yield from 2-*endo*-acetamidonorbornene-2-carboxylic acid methyl ester (**2**)[9] by deacetylation

with the Meerwein's reagent, followed by alkylation with hexadecyl bromide in HMPA in the presence of K_2CO_3 and subsequent $LiAlH_4$ reduction of the resulting hexadecylamino ester (**3**).

1b[8] was synthesized starting from dimethyl acetamidofumarate[10] derived from dimethyl *N*-acetylaspartic acid. Our study began with experiments to evaluate the reactivity of dimethyl acetamidofumarate as a dienophile toward cyclopentadiene. We first examined the reaction of **4** with cyclopentadiene in the absence of a catalyst under the reaction conditions used in the Diels-Alder reaction of *N*-acetyl-α,β-dehydroalaninate with cyclopentadiene.[9] However, no desired Diels-Alder adducts were formed. After an experiments using a number of acidic catalysts, we found that the reaction proceeded smoothly in CH_2Cl_2 with the use of $SnCl_4$ as a catalyst to furnish a mixture of **5** and **6** in 61 % yield. Each isomer was separated by column chromatography on silica gel, the ratio of **5** to **6** being 3:1; the structure of each isomer was unambiguously determined based on the NMR spectrum[11] in which the methyl proton of the acetyl group of **5** shifts to a higher field than that of **6**, due to the shielding effect of the 5,6-double bond.[12] Treating of **5** with NaOMe in MeOH caused the epimerization at the 3-position leading to the formation of **7**, which was converted to **1b** by using the same procedures as those employed in the preparation of **1a**.

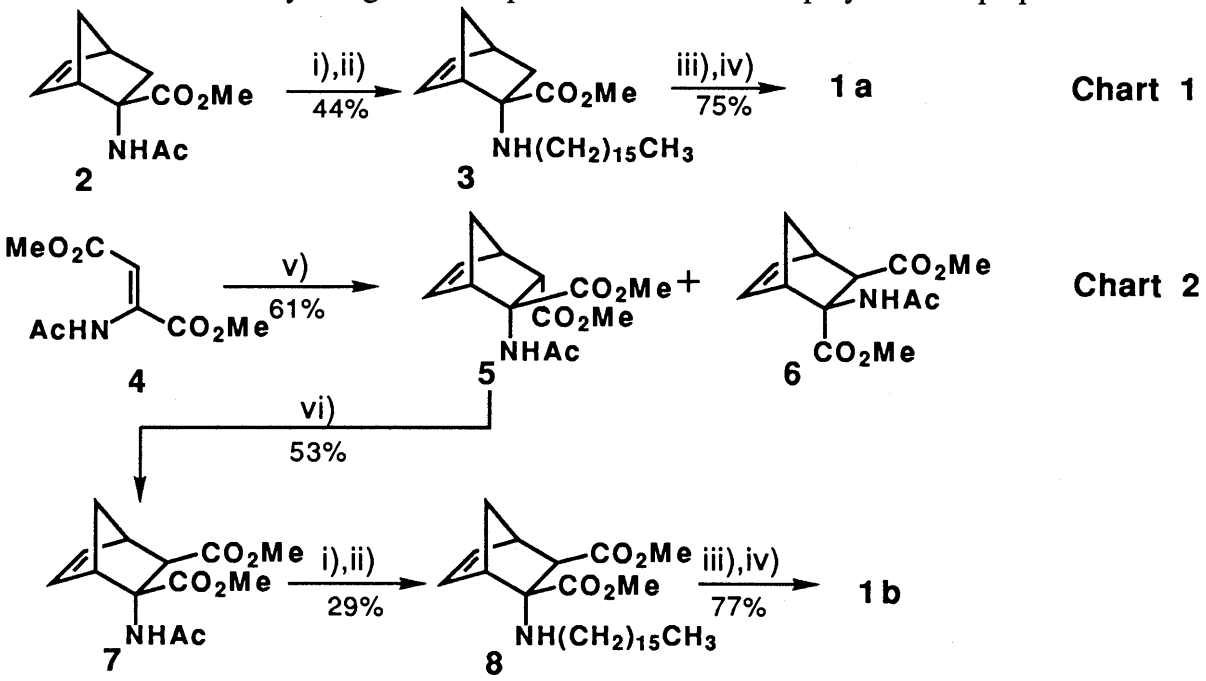

i) a: $Et_3O^+BF_4^-/CH_2Cl_2$, r.t., b: aqueous $NaHCO_3$ solution; ii) $CH_3(CH_2)_{15}Br$, K_2CO_3/ HMPA, r.t.~70°C; iii) $LiAlH_4$/THF, 5°C~r.t.; iv) HCl; v) cyclopentadiene, $SnCl_4/CH_2Cl_2$, r.t.; vi) *N*-NaOMe/ MeOH, r.t.

The inhibitory activity of **1a** and **1b** on protein kinase C prepared from rat brain cytosole was measured under the assay conditions reported by Kikkawa *et al.*[13] **1a** and **1b** inhibited protein kinase C at the IC_{50} values of $2X10^{-5}$ M and $1X10^{-5}$ M, respectively. On the other hand, no inhibitory activities on protein kinase A were observed for **1a** and **1b** at a concentration of $1X10^{-3}$ M. These results indicate that **1a** and **1b** selectively inhibit protein kinase C . We also examined the inhibition of the binding of [^{3}H]-phorbol dibutyl ester (PDBU) to protein kinase C by compound (**1a**) *in vitro* under the assay conditions reported by Blackshear *et al.*[14] **1a** competitively inhibited the [^{3}H]-PDBU binding to protein kinase C at the IC_{50} value of $2X10^{-5}$ M.

To determine the critical structural features of these compounds required for inhibition of protein kinase C for the norbornene derivatives, we further synthesized **9c-d**[15], **10**[15] and **11**[15] starting from **2**, the

stereoisomer of **2**[9] and 2,2-dimethylaminoethanol, respectively. Inhibition of protein kinase C still occurred when the hexadecyl group of **1a** was replaced by the palmitoyl group, the IC_{50} value of **9c** being $5X10^{-5}$ M.

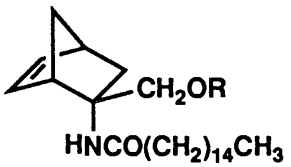

9c, d

c:R=H

d:R=COCH3

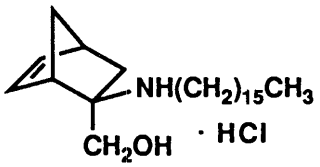

10

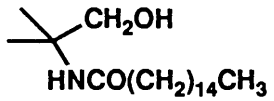

11

No inhibitory activities were observed for **9d** and **10**, strongly indicating that the 2-*exo*-hydroxyl and 2-*endo*-amino groups are crucial for exhibiting the inhibitory activity. Furthermore, the activity of **11** ($IC_{50} = 2X10^{-4}$ M), in which the norbornyl group was replaced by the dimethyl group, was significantly reduced. The result implies the significance of the norbornyl skeleton which is capable of not only forming a rigid hydrophobic region but also sterically defining both the amino and hydroxyl groups.

ACKNOWLEDGEMENT The authors thank Dr. Tetsuya Tosa, Director and Dr. Kazuo Matsumoto, Manager of our research laboratory for their encouragement and interest. We also thank Mr. Yuji Masaki, who evaluated the biological activities.

REFERENCES AND NOTES

1) Y. Nishizuka, *J. Am. Med. Assoc.*, 262, 1826 (1989); and references cited therein.
2) M. Castagna, Y. Takai, K. Kaibuchi, K. Sano, U. Kikkawa, and Y. Nishizuka, *J. Biol. Chem.*, 257, 7847 (1982); J. Yamanishi, Y. Takai, K. Kaibuchi, K. Sano, M. Castagna, and Y. Nishizuka, *Biochem. Biophy. Res. Commun.*, 112, 778 (1983); J. E. Niedel, L. J. Kuhn, and G. R. Vandenvark, *Proc. Natl. Acad. Sci. USA*, 80, 36 (1983).
3) R. Miyake, Y. Tanaka, T. Tsuda, K. Kaibuti, U. Kikkawa, and Y. Nishizuka, *Biochem. Biophy. Res. Commun.*, 121, 649 (1984).
4) T. Tamaoki, H. Nomoto, I. Takahashi, Y. Kato, M. Morimoto, and F. Tomita, *Biochem. Biophy. Res. Commun.*, 135, 397 (1986).
5) T. Mori, Y. Takai, R. Minakuchi, B. Yu, and Y. Nishizuka, *J. Biol. Chem.*, 255, 8378 (1980); L. M. Strawn, R. E. Martell, R. U. Simpson, K. L. Leach, and R. E. Counsell, *J. Med. Chem.*, 32, 2104 (1989); C. J. Marasco, Jr., C. Piantadosi, K. L. Meyer, S. Morris-Natschke, K. S. Ishaq, G. W. Small, and L. W. Daniel, *J. Med. Chem.*, 33, 985, (1990).
6) E. Kobayashi, K. Ando, H. Nakano, T. Tamaoki, *J. Antibiot.* 42, 153 (1989).
7) Y. A. Hannun and R. M. Bell, *Science*, 243, 500 (1989).
8) The melting points (mp) of these compounds are as follows; **1a**, 137-139°C; **1b**, 154-155°C.
9) H. Horikawa, T. Nishitani, T. Iwasaki, Y. Mushika, I. Inoue, and M. Miyoshi, *Tetrahedron Lett.*, 21, 4101 (1980).
10) T. Kolasa, *Synthesis*, 1983, 539.
11) The NMR spectra of **5** and **6** are as follows: **5**, δ ($CDCl_3$) 1.89 (3H,s,$NHCOCH_3$),3.68 (3H,s,C_3-CO_2CH_3), 3.76 (3H,s,C_2-CO_2CH_3); **6**, δ ($CDCl_3$) 1.97 (3H,s,$NHCOCH_3$),3.67 (3H,s,C_3-CO_2CH_3), 3.69 (3H,s,C_2-CO_2CH_3).
12) J. C. Davis, Jr., and T. V. Van Auken, *J. Am. Chem. Soc.*, 87, 3900 (1965).
13) U. Kikkawa, Y. Takai, R. Minakuchi, S. Inohara, and Y. Nishizuka, *J. Biol. Chem.*, 257, 13341 (1982).
14) P. J. Blackshear, L. A. Witlers, P. R. Girard, J. F. Kuo, and S. N. Quamo, *J. Biol. Chem.*, 260, 13304 (1985).
15) The synthetic methods are as follows. **9c** (mp 73-74°C): i) $Et_3O^+BF_4^-/CH_2Cl_2$, rt.; aqueous $NaHCO_3$; ii) $CH_3(CH_2)_{14}COCl$, Et_3N/THF, rt.; iii) $LiAlH_4$/THF. **9d** (syrup) was prepared by acetylation of **9c** with Ac_2O-Et_3N. **10** (mp 66°C) was prepared from the stereoisomer of **2** by the same procedures as described in the preparation of **1a**. **11** (mp 57-58°C) was prepared by acylation of 2,2-dimethylaminoethanol with $CH_3(CH_2)_{14}COCl$-Et_3N.

(Received December 3, 1990)

NOVEL BICYCLIC CHIRAL CROWN ETHERS HAVING A *p*-XYLENEDIOXY UNIT WITH IMPROVED COMPLEX STABILITY AND RATE-ENHANCEMENT IN THE INTRA-COMPLEX THIOLYSIS OF α-AMINO ACID ESTER SALTS

Tatsuro YASUKATA, Shigeki SASAKI,[1] and Kenji KOGA*
Faculty of Pharmaceutical Sciences, University of Tokyo, Hongo, Bunkyo-ku, Tokyo 113, Japan

Novel bicyclic chiral crown ethers having an α, α'-*p*-xylenedioxy unit were synthesized. Crown dithiol **1** with a *p*-xylenedioxy bridge-structure performed intra-complex thiolysis with α-amino acid *p*-nitrophenyl ester HBr salts much faster than the corresponding dithiol **3** without the bridge-structure. A ^{1}H-NMR study suggested that the increased rate of intra-complex thiolysis is due to increased stability of the intermediary complex during the reaction.

KEYWORDS chiral crown ether; intra-complex thiolysis; host-guest complex; pseudo first-order rate constant; stability constant

One of the most important steps in enzyme-catalyzed reactions is the formation of a non-covalent enzyme-substrate complex prior to the reactions.[2] Since the first report by Pedersen, crown ethers have been widely used as artificial hosts for various cations,[3] and applied to the study of enzyme-mimetic reactions.[4] Introduction of bridge-structure to macrocyclic hosts has been undertaken to fix the host cyclic conformation and has realized more stable complex formation.[5] We have already reported enantio-selective thiolysis of D- or L-α-amino acid ester salts (**Fig. 1**) by dithiol-bearing chiral crown ethers[6] and an approach to the enzyme model for the synthesis of peptides.[7] Here, we report novel crown ethers with a *p*-xylenedioxy *bridge-structure*, which form more stable host-guest complexes and perform intra-complex thiolysis faster.

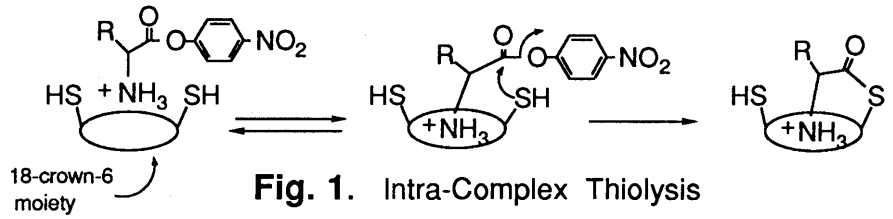

Fig. 1. Intra-Complex Thiolysis

Novel crown ethers **1** and **2** were designed by conceiving that the *p*-xylenedioxy bridge-structure would restrain conformational changes of crown rings and fix the cavity to be more favorable to forming complexes with primary ammonium cations.

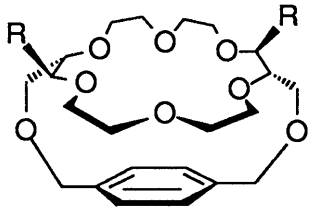

1 : R = -CH_2SH
2 : R = -CH_3

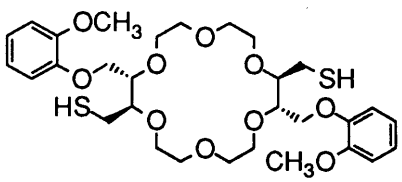

3

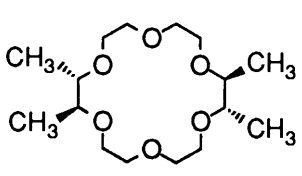

4

Bridged crown ethers **1** and **2** were synthesized as summarized in **Fig. 2**.[8] The crown ether **10**, having the protected hydroxymethyl groups on one face of the crown ring and free hydroxymethyl groups on the other, was chosen as a key intermediate from the preliminary experiments for the introduction of the bridge-structure. A selectively protected chiral threitol derivative **7**, which was readily accessible from alcohol **5**[6] through a cyclic carbonate **6**, was transformed to the crown intermediate **9**. The reaction of introducing the bridge-structure (**10**→**11**) proceeded successfully using **10** and α, α'-dibromo-*p*-xylene in the presence of ^{t}BuOK as a base in THF. Conversions of **11** to **1** and **2** were attained by the conventional method.[6]

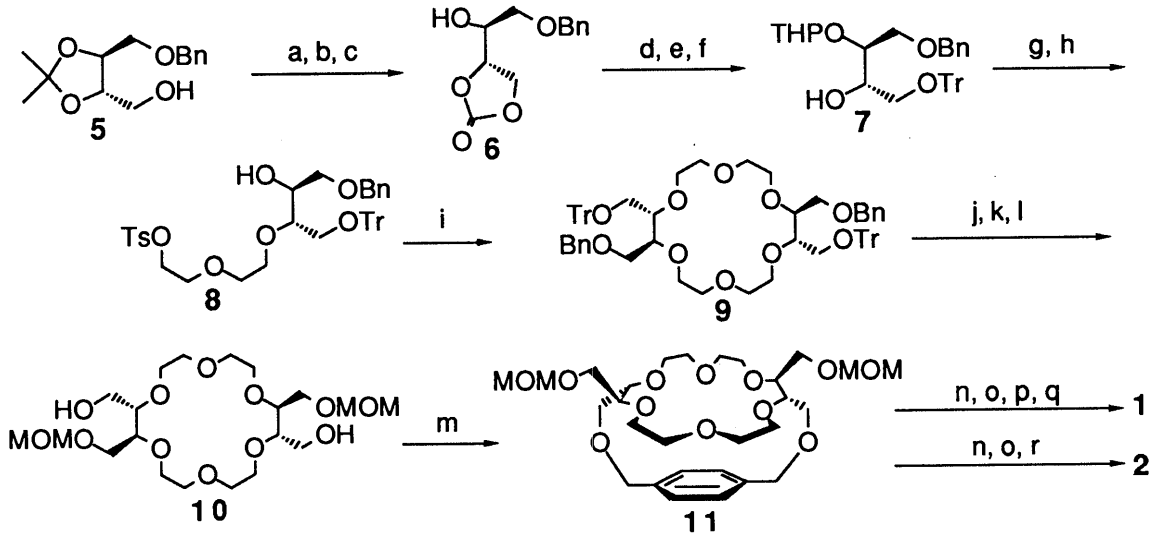

a) PhOCOCl, CH_2Cl_2, pyridine, (quant.); b) 4N-HCl aq., THF; c) K_2CO_3, THF, (69%, 2 steps); d) DHP, PPTS, CH_2Cl_2; e) 1N-NaOH aq., MeOH; f) TrCl, pyridine, (96%, 3 steps); g) $(TsOCH_2CH_2)_2O$, NaH, DMF, (77%); h) PPTS, EtOH, (87%); i) NaH, DMF, (76%); j) c.HCl, MeOH; k) MOMCl, $^{i}Pr_2NEt$, CH_2Cl_2, (92%, 2 steps); l) H_2, 5%-Pd/C, EtOH; m) α, α'-Dibromo-*p*-xylene, ^{t}BuOK, THF, (55%, 2 steps); n) c.HCl, MeOH; o) TsCl, pyridine, (80%, 2 steps); p) PhCOSK, CH_3CN, (78%); q) 4N-NaOH aq., MeOH, THF, (77%); r) $LiAlH_4$, THF, (80%).

Fig. 2. Syntheses of Bridged Crown Ethers **1** and **2**

The intra-complex thiolysis[6,7] of α-amino acid *p*-nitrophenyl ester HBr salts was performed in the presence of **1** or **3** in AcOH-pyridine buffer, and pseudo first-order rate constants of intra-complex thiolysis were obtained by observing the release of *p*-nitrophenol at UV-320 nm. The results are summarized in **Table I**, and the rate using bridged host **1** was compared with that using the corresponding un-bridged **3**. As shown in **Table I** (**1/3** ratio in $k\phi$), bridged host **1** performs the intra-complex thiolysis much faster for all the guests examined than un-bridged **3** does. So the introduction of the bridge-structure greatly enhanced the rate of intra-complex thiolysis. We could not determine the stability of the complex formed during the thiolysis from kinetic experiment by the method previously reported.[6] So we compared the stability of the complexes between the bridged host **2** or un-bridged **4** and primary ammonium salt $^{t}BuNH_3^{+}SCN^{-}$. The stability constants *Ks* were measured by ^{1}H-NMR in CD_3CN, and the results are shown in **Table II**. Bridged host **2** exhibits increased complex stability by a factor of 14 as a result of the introduction of the bridge-structure.

Table I. Pseudo First-Order Rate Constants of Intra-Complex Thiolysis (Fig. 1)

$k\phi$ x10^{-3} [mol/sec]

Crown \ Substrate	Gly	D-Ala	L-Ala	D-Phe	L-Phe	D-Val	L-Val
1	240	530	420	120	27	9.8	3.1
3	26	74	34	12	2.5	2.1	0.24
1/3 Ratio	9.2	7.2	16	10	11	4.8	13

Pseudo first-order rate constants were determined photometrically at 320 nm in 5% EtOH-CH_2Cl_2 buffered with 0.01 M AcOH and 0.02 M pyridine at 25.0°C, using 10^{-4} M α-amino acid ester salts and 5×10^{-3} M dithiol-bearing crown ethers.

Table II. Stability Constants

(Crown • $^tBuNH_3^+SCN^-$)

Host	*Ks* x 10^3 [M^{-1}]
2	84
4	6.2
2/4 Ratio	14

Stability constants were determined by ^{1}H-NMR (400 MHz) in CD_3CN at 30°C, using 0.01-0.06 M $^tBuNH_3^+SCN^-$ in the presence of 0.02 M crown hosts.

Apparently the rate enhancement of intra-complex thiolysis resulting from the introduction of the bridge-structure is due to the increased stability of the intermediary complex, since the reaction proceeds through the complex formed between the crown host and the amino acid substrate[6] (**Fig. 1**). The present study demonstrated an improvement in the efficiency of the enzyme-mimetic reaction, and this methodology can be used to design more efficient enzyme models.

REFERENCES AND NOTES

1) Present address: Faculty of Pharmaceutical Sciences, Kyushu University, 3-1-1, Maidashi, Higashi-ku, Fukuoka 812, Japan.

2) A. L. Lehninger, "Biochemistry," Worth Publishers, Inc., New York, 1975, p. 183.

3) a) C. J. Pedersen, *J. Am. Chem. Soc.*, **89**, 2495 (1967); b) F. de Jong and D. N. Reinhoubt, "Stability and Reactivity of Crown Ether Complexes," Academic Press, London, 1981; c) R. M. Izatt, J. S. Bradshow, S. A. Nielsen, J. D. Lamb, and J. J. Christensen, *Chem. Rev.*, **85**, 271 (1985).

4) a) F. Vögtle and E. Weber (ed.), "Host Guest Complex Chemisty I, II, and III," Springer-Verlag, Berlin, 1984; b) D. J. Cram, "Application of Biochemical Systems in Organic Chemisty," ed. by J. B. Jones, C. J. Sih, and D. Perlman, John Wiley & Sons, New York, 1976, Part II, Chapter V; c) Y. Chao and D. J. Cram, *J. Am. Chem. Soc.*, **98**, 1015 (1976); d) Y. Chao, G. R. Weisman, G. D. Y. Sogah, and D. J. Cram, *ibid.*, **101**, 4948 (1979); e) J. M. Lehn and C. Sirlin, *J. Chem. Soc., Chem. Commun.*, **1978**, 949.

5) For example; J. M. Lehn, *Angew. Chem. Int. Ed. Engl.*, **27**, 89 (1988) and references cited therein.

6) a) T. Matsui and K. Koga, *Chem. Pharm. Bull.*, **27**, 2295 (1979); b) S. Sasaki, M. Kawasaki, and K. Koga, *ibid.*, **33**, 4247 (1985).

7) a) S. Sasaki, M. Shionoya, and K. Koga, *J. Am. Chem. Soc.*, **107**, 3371 (1985); b) K. Koga and S. Sasaki, *Pure Appl. Chem.*, **60**, 539 (1988); c) S. Sasaki and K. Koga, *J. Inclusion Phenomena*, **7**, 267 (1989); d) S. Sasaki and K. Koga, *Chem. Pharm. Bull.*, **37**, 912 (1989); e) S. Sasaki, Y. Takase, and K. Koga, *Tetrahedron Lett.*, **31**, 6051 (1990).

8) Satisfactory spectral and/or analytical data were obtained for all new compounds listed in **Fig. 2**.

(Received December 5, 1990)

ISOLATION AND STRUCTURAL DETERMINATION OF A MUTAGENIC SUBSTANCE IN CREATINE PYROLYSATE

Haruo NUKAYA,*,[a] Hiroki WATANABE,[a] Hitoshi ISHIDA,[a] Kuniro TSUJI,[a] Yoshihide SUWA,[b] Keiji WAKABAYASHI,[c] Minako NAGAO,[c] Takashi SUGIMURA[c] and Takuo KOSUGE[d]

School of Pharmaceutical Science, University of Shizuoka,[a] Yada 395, Shizuoka 422, Japan, Laboratory of Health Science, Institute for Fundamental Research, Suntory Ltd.,[b] 1-1, Wakayamadai 1-chome, Shimamoto-cho, Mishima-gun, Osaka 618, Japan, Carcinogenesis Division, National Cancer Center Research Institute,[c] 1-1, Tsukiji 5-chome, Chuo-ku, Tokyo 104, Japan and Cawthron Institute,[d] 98 Halifax Street, Nelson, New Zealand

The pyrolysis product of creatine showed potent mutagenic activity to *Salmonella typhimurium* TA98 with metabolic activation by S9 mix. One of the mutagenic substances in creatine pyrolysate was isolated and named Cre-P-1. Its structure was determined by X-ray crystallography to be 4-amino-1,6-dimethyl-2-methylamino-1H,6H-pyrrolo[3,4-*f*]benzimidazole-5,7-dione. Cre-P-1 is the first registered mutagenic heterocyclic amine containing oxygen atoms in the molecule, that has been isolated from pyrolysis products.

KEYWORDS creatine; creatine pyrolysate; mutagenic substance; Cre-P-1

Cooked meat and fish contain various kinds of mutagenic and carcinogenic heterocyclic amines.[1] It was proposed that creatine or creatinine is a precursor of an imidazole moiety of the IQ type of heterocyclic amines, aminoimidazoquinoline and aminoimidazoquinoxaline compounds.[2] In fact, some of the IQ type compounds were produced by heating a mixture of creatinine, sugars and amino acids.[3] Moreover, we found that the pyrolysis product of creatine or creatinine alone was also highly mutagenic to *Salmonella typhimurium* TA98 with S9 mix.[4] In this study, we isolated a new mutagenic substance from creatine pyrolysate and determined its chemical structure.

A mutagenicity test was carried out using an improved method of the Ames test.[5] The test material dissolved in dimethyl sulfoxide, bacteria and S9 mix, the S9 of which was prepared from the liver of rats treated with PCB, were preincubated at 37°C for 20 min, and revertant colonies that appeared after 2 days incubation were counted.

Creatine monohydrate (4.0 kg) with sea sand in a flask with a thick side arm was pyrolyzed over a direct gas flame to give a tar (842 g). The tar was purified as shown in Chart 1. First, a basic and neutral mixture (269 g) was obtained by counter current distribution using a solvent system of n-BuOH and ammonia water. This fraction was fractionated by a blue cotton treatment,[6] followed by ODS gel column chromatography, counter current distribution, alternate and repeated gel filtrations by Sephadex LH-20, G-15 and CM-Sephadex C25 and avicel column chromatography. Finally, the active fraction (VI-1) was subjected to preparative HPLC (Fig. 1A) and the purity of the mutagen isolated was confirmed by analytical HPLC (Fig. 1B). The pure compound was recrystallized from methanol to yield yellow needles. The mutagenicity of this compound with S9 mix was 19,000 revertants to TA98 and 400 revertants to TA100/1.0 μg/plate. This mutagenic substance was designated Cre-P-1.

The molecular formula for Cre-P-1 was determined to be $C_{12}H_{13}N_5O_2$ (259.1048, calculated 259.1067) by mass spectroscopy. Its UV spectrum is shown in Fig. 2. The crystal of Cre-P-1 was grown from hydrous methanol to obtain a yellow prism with mp 286–290°C (dec.). X-ray crystallographic analysis of a Cre-P-1 monohydrate crystal 0.5 x 0.05 x 0.05 mm in size, showed that the crystal had cell dimensions of a = 5.808Å, b = 12.237Å, c = 18.164Å and β = 97.44°, and the monoclinic space group $P2_1/c$ with four molecules in a unit cell. The structure was determined by the direct method using the program MULTAN, and refined by the method of block-diagonal matrix least squares. The final R value for the structure, shown as a monohydrate, was 0.057, including anisotropic temperature factors for the non-hydrogen atoms and an isotropic one for the hydrogen atoms. The whole molecule is illustrated in perspective in Fig. 3. The chemical structure was determined to be 4-amino-1,6-dimethyl-2-methylamino-1H,6H-pyrrolo[3,4-*f*]benzimidazole-5,7-dione.

creatine monohydrate 4.0 kg
↓ Pyrolysis (250-400°C)
pyrolysate 842 g (292/50, 492)*
↓ counter current distribution (8.3%NH_3:n-BuOH, n=4)
basic & neutral fraction(r=3-5) 269 g (632/50, 340)*
↓ blue cotton treatment
adsorbate 11.6 g (1375/5, 320)*
↓ ODS gel column chromatography (MeOH-H_2O,1%AcOH)
20/80 MeOH/1%AcOH fraction 5.33 g (1771/5, 189)*
↓ counter current distribution (1N HCl:n-BuOH, n=9)

r=4-10 1.08 g (2772/5, 59.7)*	r=0-3 4.83 g (1186/5, 115)*
↓ Sephadex LH-20 (0.1N HCl:MeOH=1:3)	
fraction I-1 200 mg (10.7)**	fraction I-2 712 mg (43.9)**
↓ Sephadex G-15 (0.1N HCl:MeOH=1:3)	
fraction II-1 122 mg (6.66)**	fraction II-2 63.2 mg (3.02)**
↓ Sephadex LH-20 (0.1N HCl:MeOH=1:3)	
fraction III-1 81.3 mg (6.25)**	fraction III-2 42.7 mg (2.80)**
↓ avicel column chromatography (0.1N HCl)	
fraction IV-1 29.8 mg (2.70)**	fraction IV-2 54.1 mg (3.03)**
↓ Sephadex G-15 (0.1N HCl:MeOH=1:3)	
fraction V-1 12.0 mg (1.99)**	fraction V-2 7.6 mg (0.27)**
↓ CM-Sephadex C25 (0.1N HCl)	
fraction VI-1 3.9 mg (0.54)**	fraction VI-2 12.5 mg (2.87)**
↓ preparative HPLC(ODS, CH_3CN-H_2O,1%AcOH)	
fraction VII-1 0.4 mg (0.27)**	fraction VII-2 4.8 mg (0.24)**
(Cre-P-1)	

( )* : Specific activity revertants/μg, Total activity x10^7 to TA98 with S9 mix.
( )** : Total activity x10^7.

Chart 1. Isolation of Mutagenic Substance from Creatine Pyrolysate

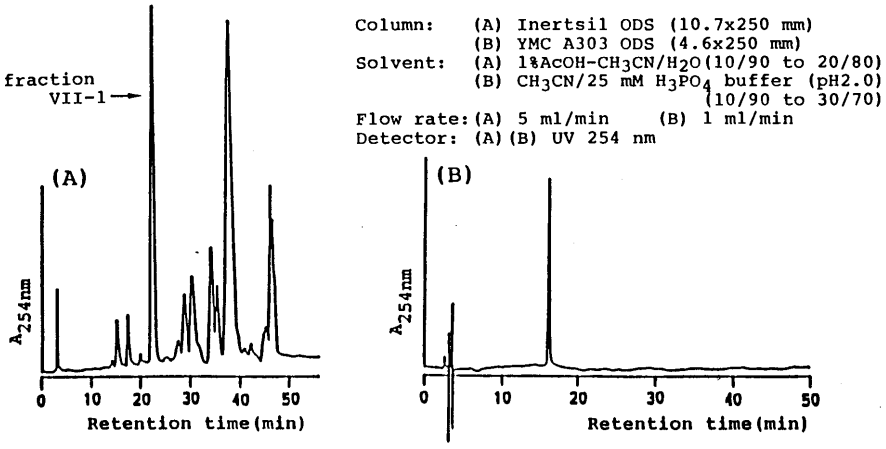

Fig. 1. Separation of Fraction VI-1(A) and Fraction VII-1(B) by HPLC

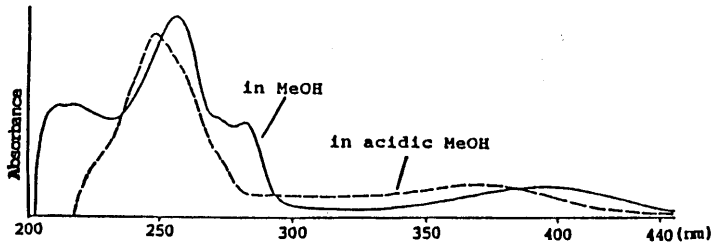

Fig. 2. UV Spectrum of Cre-P-1

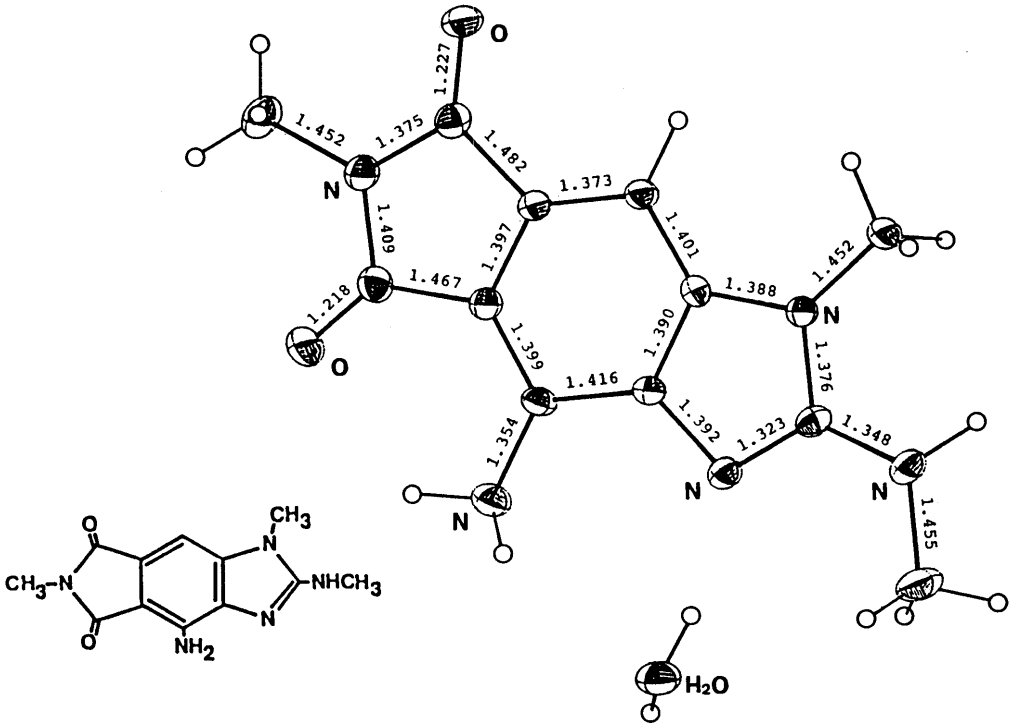

Fig. 3. Chemical Structure of Cre-P-1 and Perspective Drawing Showing Bond Lengths(Å)

Cre-P-1 is a completely flat molecule with three rings, like the other known mutagenic and carcinogenic heterocyclic amines.[1] As shown in Fig. 3, Cre-P-1 has a phthalimide moiety with an imidazole ring. This indicates that by pyrolysis, creatine could provide not only an imidazole but also a benzimidazole. The presence of mutagens containing an oxygen atom in the molecule was suggested in the basic fraction of cooked food,[7] however, their chemical structures have not been elucidated yet. We first report here the presence of a mutagenic heterocyclic amine having oxygen atoms in the pyrolysis product.

It is important to determine whether Cre-P-1 is present in our daily foodstuffs or not and if so, in what amounts it exists in them.

ACKNOWLEDGEMENT This work was supported in part by a Grant-in-Aid for Cancer Research from the Ministry of Health and Welfare of Japan.

REFERENCES AND NOTES

1) T.Sugimura, *Science*, 233, 312 (1986); T.Sugimura, *Trends Pharmacol. Sci.*, 9, 205 (1988).
2) M.Jägerstad, A.Laser Reuterswärd, R.Öste, A.Dahlqvist, S.Grivas, K.Olsson and T.Nyhammar, "The Maillard Reaction in Foods and Nutrition," ACS Symposium Series 215, ed. by G.R.Waller and M.S.Feather, American Chemical Society, Washington, DC, 1983 p. 507.
3) D.Yoshida, Y.Saito and S.Mizusaki, *Agric. Biol. Chem.*, 48, 241 (1984); M.Jägerstad, K.Olsson, S.Grivas, C.Negishi, K.Wakabayashi, M.Tsuda, S.Sato and T.Sugimura, *Mutat. Res.*, 126, 239 (1984); S.Grivas, T.Nyhammar, K.Olsson and M.Jägerstad, *Mutat. Res.*, 151, 177 (1985).
4) T.Kosuge, K.Tsuji, K.Wakabayashi, T.Okamoto, K.Shudo, Y.Iitaka, A.Itai, T.Sugimura, T.Kawachi, M.Nagao, T.Yahagi and Y.Seino, *Chem. Pharm. Bull.*, 26, 611 (1978).
5) T.Sugimura and M.Nagao, "Chemical Mutagens," Vol. 6, ed. by F.J.de Serres and A.Hollaender, Plenum, New York, 1980, p. 41.
6) H.Hayatsu, T.Oka, A.Wakata, Y.Ohara, T.Hayatsu, H.Kobayashi and S.Arimoto, *Mutat. Res.*, 119, 233 (1983).
7) G.Becher, M.G.Knize, I.F.Nes and J.S.Felton, *Carcinogenesis*, 9, 247 (1988).

(Received December 10, 1990)